Valencia, 07 – 10 October 2018

ESTRO School

Advanced Brachytherapy Physics

WWW.ESTRO.ORG/SCHOOL

Advanced Brachytherapy Physics
A Biennial ESTRO Course since 2014

Imitative started in 2008

Formal Submission of Proposal to ESTRO-ETC November 24, 2009:

- **Jack Venselaar**
- **Dimos Baltas**

1st Course in Brussels, Belgium, 18-21 May 2014

Advanced Brachytherapy Physics
07-10 October 2018 | Valencia, Spain

The Faculty of the 3rd Course

Course Director: Dimos Baltas (DE)

Teachers:

Luc Beaulieu (CA)
Nicole Nesvacil (AT)
Panagiotis Papagiannis (GR)
Mark Rivard (USA)

Local Organisers:

Jose Perez-Catalayud
Facundo Ballester

Project Manager:

Alessandra Nappa, ESTRO office (BE)

Advanced Brachytherapy Physics
07-10 October 2018 | Valencia, Spain

- Brachytherapy is the pioneer of extreme hypofractionation that has currently become one of the hot topics in radiation oncology.
- Brachytherapy experiences here an ever broader imitation by external beam methods as is especially demonstrated in the radiation therapy of localized prostate cancer.
- There is an emerging role of advance and dedicated 3D imaging modalities, image guidance techniques and navigation technologies for pre-planning of the implant, for the implantation procedure, for the treatment planning and finally for treatment verification.
- The availability of inverse planning and optimization techniques enforces the demand for individualized implant design, dose prescription and accurate 3D dose calculation.
- All above enable adaptive (4D) treatment planning and adaptive (4D) treatment delivery techniques.
- At the same time raises the demand for deep background knowledge and extended expertise for the involved medical physicists.
- There is a central role assigned for clinical medical physicists and researchers for development, validation and implementation of such advance methods and techniques.

Advanced Brachytherapy Physics
07-10 October 2018 | Valencia, Spain

- Brachytherapy remains a lively and interesting field of clinical and research activities.

- It is well worthwhile for young researchers and medical physicists to get involved in this evolving area of radiation oncology with a strong sense of multidisciplinarity and interdisciplinarity.

- We, the faculty and our local organisers, will do our best to demonstrate *“there is really something going on in the Physics and Technology in Brachytherapy”.*

Participants 1st Course, Brussels, 2014
N = 62 (33 Countries)

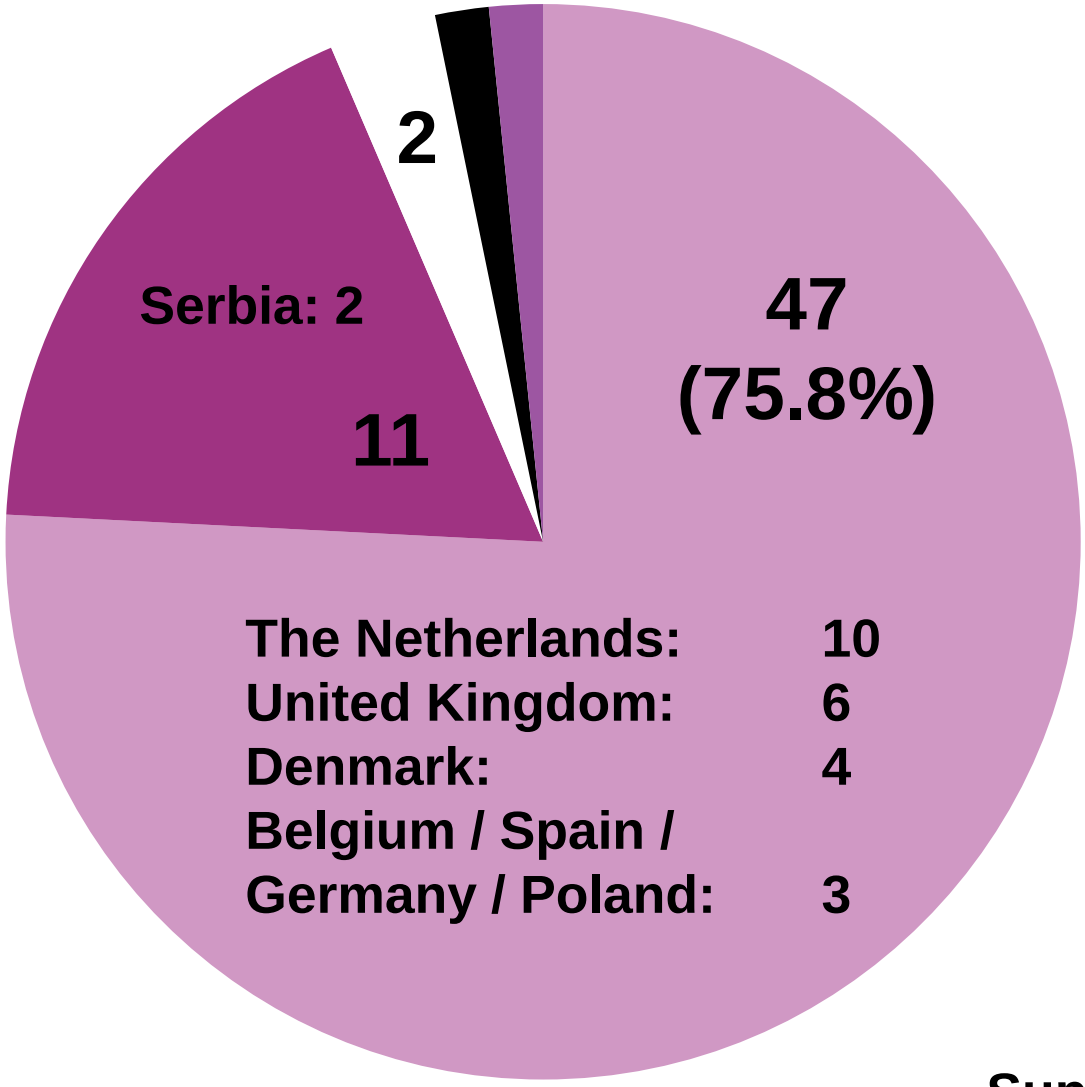

- EU
- Europe - EU
- Asia
- Australia
- Ocenaia (New Zealand)

Support from IAEA: 25 travel grants

Participants 2nd Course, Vienna, 2016
N = 39 (15 Countries)

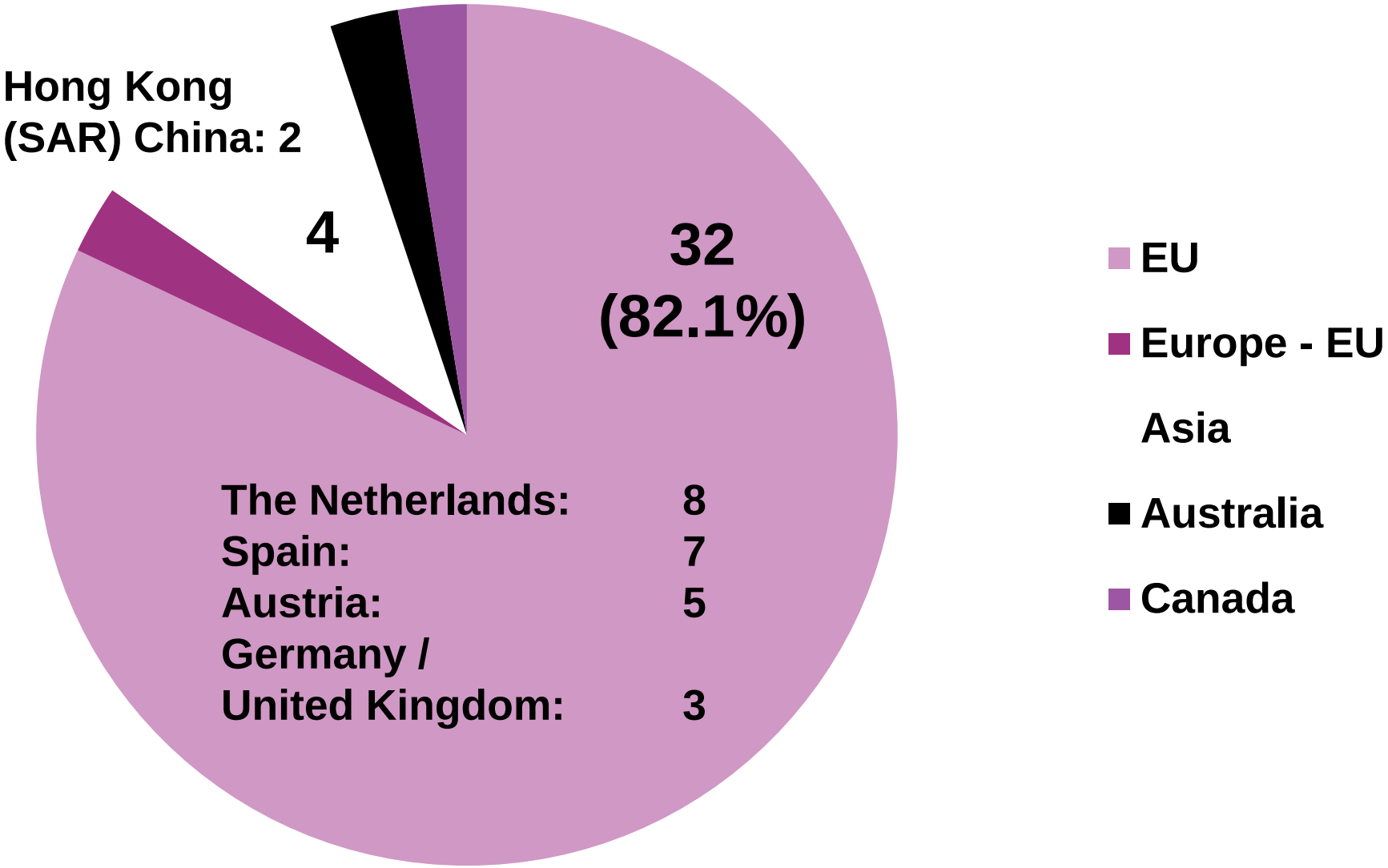

Participants 3rd Course, Valencia, 2018
N = 61 (17 Countries)

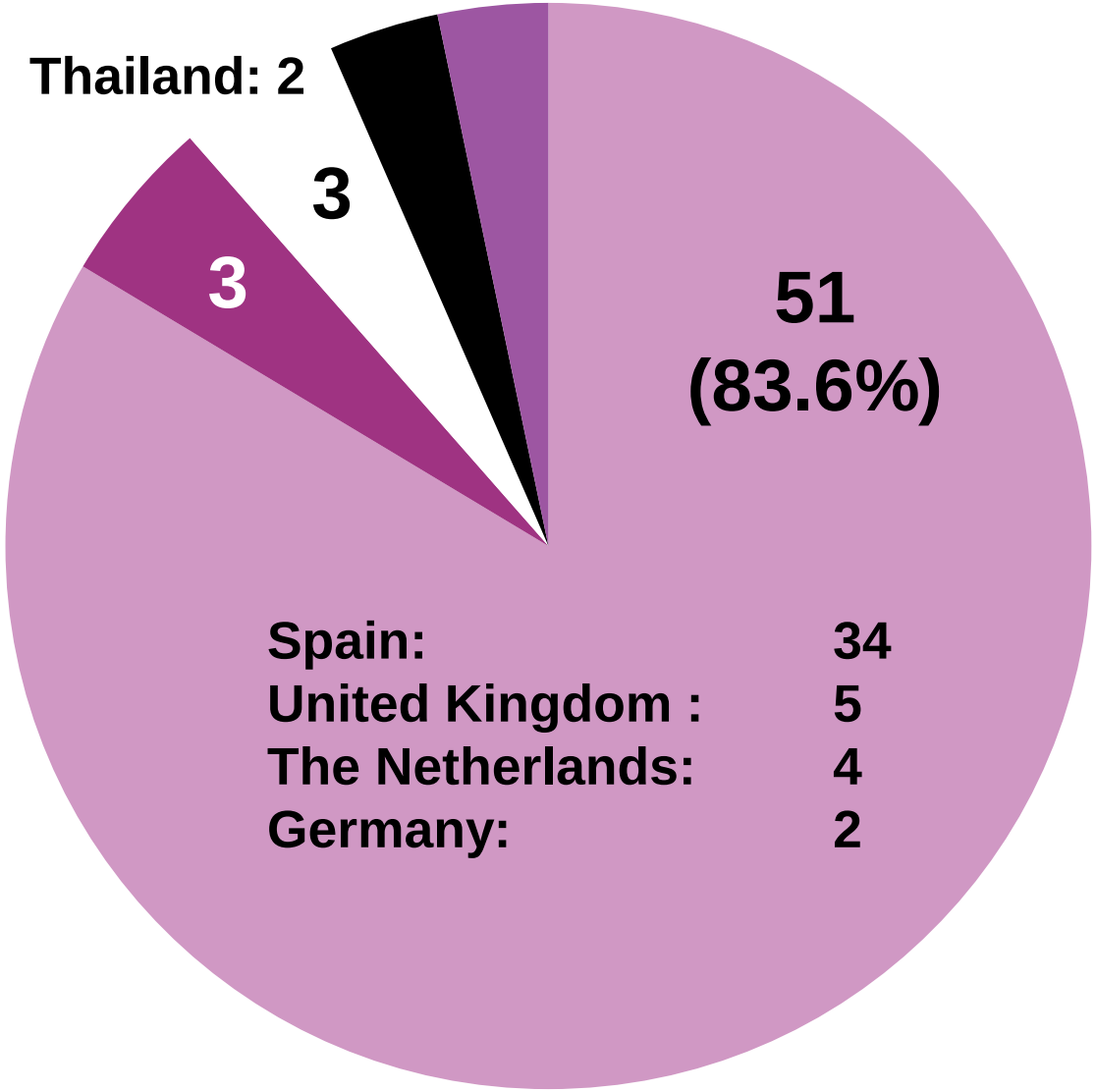

- EU
- Europe - EU
- Asia
- South America
- New Zealand

ESTRO School

WWW.ESTRO.ORG/SCHOOL

ESTRO School

Advanced Brachytherapy Physics

Treatment Delivery Technologies in Brachytherapy

Prof. Mark J. Rivard, Ph.D., FAAPM

Advanced Brachytherapy Physics, 29 May – 1 June, 2016

ESTRO School

Disclosures

The are no conflicts-of-interest to report.

Opinions herein are solely those of the presenter, and are not meant to be interpreted as societal guidance.

Specific commercial equipment, instruments, and materials are listed to fully describe the necessary procedures. Such identification does not imply endorsement by the presenter, nor that these products are necessarily the best available for these purposes.

Learning Objectives

1. Brief history of BT sources and delivery systems
2. LDR BT sources and advancements
3. HDR BT sources and advancements
4. Robotic systems for BT delivery

Manually Delivered LDR BT

[20.4] Radium plaques being applied in the Skin Department, St. Vincent's Hospital, Melbourne, Australia in 1905[19].

image courtesy of Jack Venselaar

ESTRO School

Radium Needles and Tubes

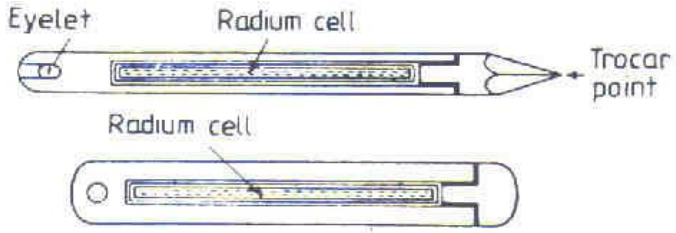

[3.17] Although there was a large range of linear radium sources, tubes and needles, in terms of geometrical and active length and linear activity (milligram radium/cm), the basic design from the early 1920s was essentially that shown in the schematic diagram. Eyelets were used to suture a needle to the patient's tissue to prevent the possibility of its involuntary removal before the end of treatment, or to attach string threads to a tube to enable removal, such as from the uterus or vagina after gynaecological brachytherapy had been completed. Some designs had removeable screw-on ends so that different radium cells could be placed in the outer container, depending on the required treatment. Union Minière du Haut Katanga, the Belgian company, supplied such sources in the 1920s, but by the 1950s the Radiochemical Centre, Amersham (later Amersham International), who were then the major supplier of radium sources, had no screw-on end designs and certainly did not supply any radium cells which, because of their very thin walls, were of a much greater hazard that the sealed sources illustrated here. These are the well known G-tubes which were 2 cm geometrical length, and available with different milligram radium contents

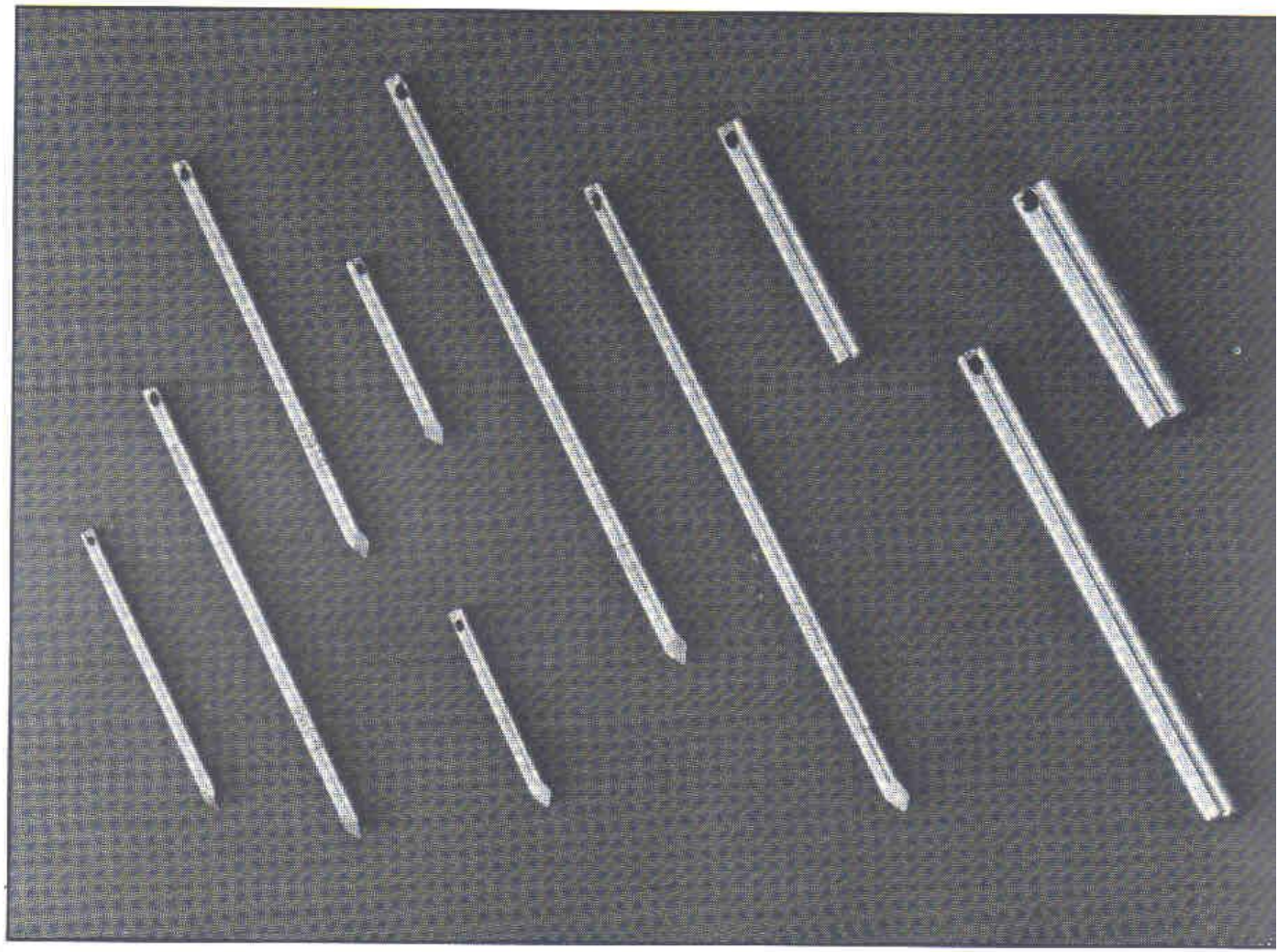

such as 10 mg, 15 mg, 20 mg and 25 mg. When radium was replaced by artificially produced radionuclides, such G-tubes then contained caesium-137 with an actively specified in terms of milligram radium equivalent [20.12, 20.56].

ESTRO School

Sealed Source Configurations

Physical Forms (schematically)

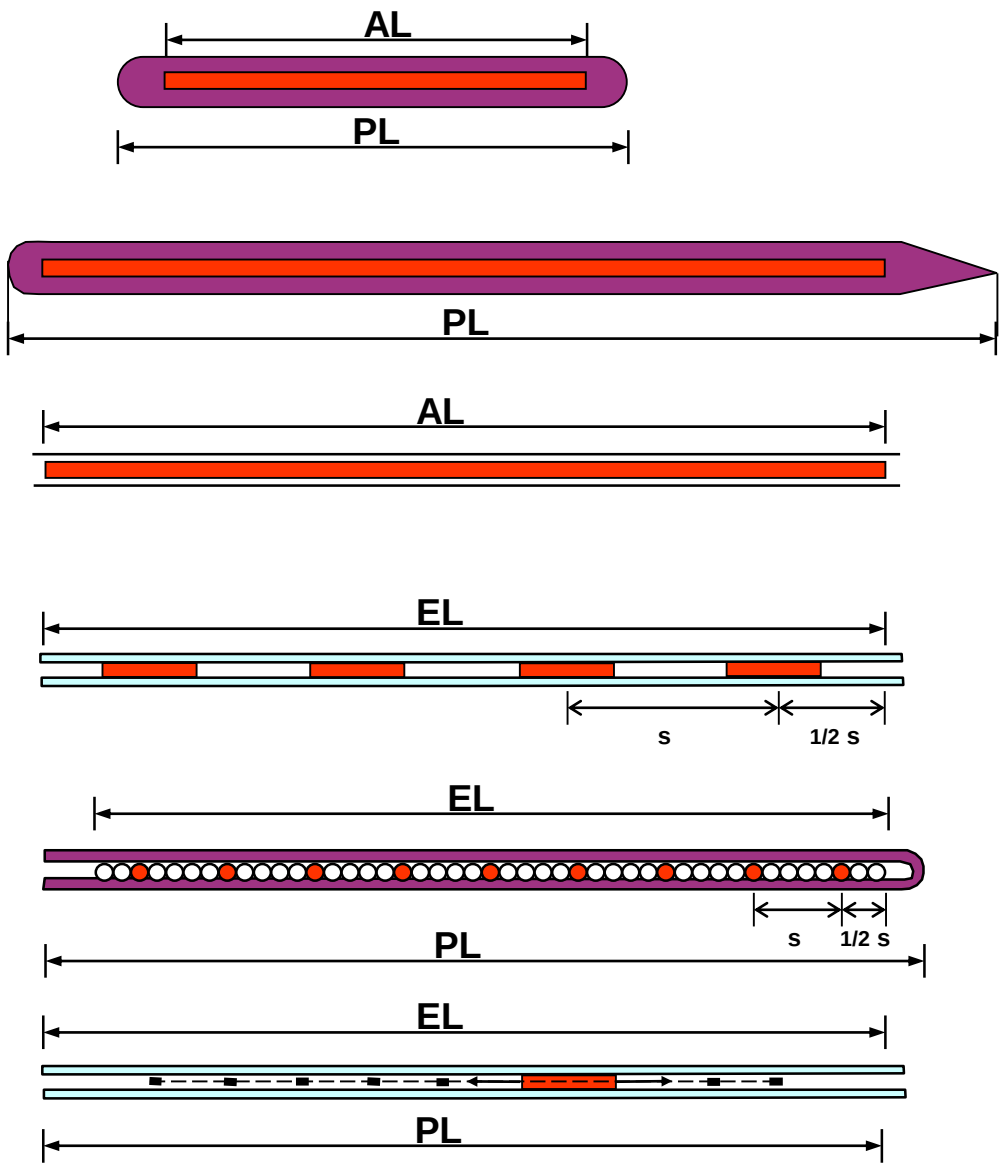

Tube

Needle

Wire

Seed Ribbon

Source Train

Stepping source

ESTRO School

Current LDR Brachytherapy Sources

- Low-energy LDR sources (seeds)
  - ^{125}I and ^{103}Pd most common with ^{131}Cs gaining interest
  - about 4.5 mm long and 0.8 mm diameter copsules
  - treatments either temporary or permanent

    $0.4 < D_{Rx} < 2$ Gy/h

- High-energy LDR sources (increasingly rarely)
  - ^{137}Cs tubes and ^{192}Ir ribbons or wire
  - treatments mainly temporary (^{137}Cs or ^{192}Ir), or permanent (^{192}Ir)

Low-Energy LDR Seeds

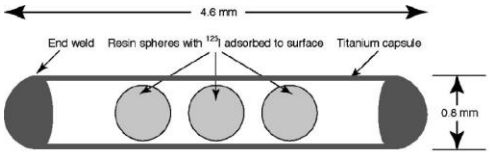

Amersham Health model 6702 source

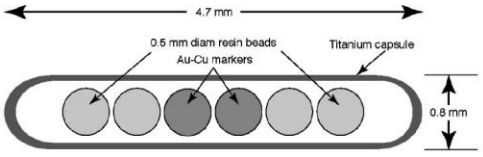

NASI model MED3631-A/M or MED3633 source

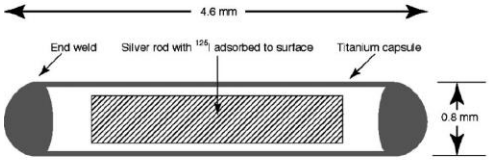

Amersham Health model 6711 source

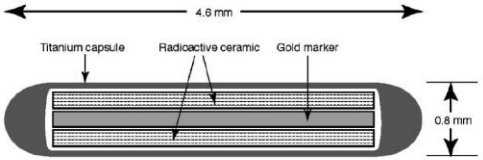

Bebig model I25.S06 source

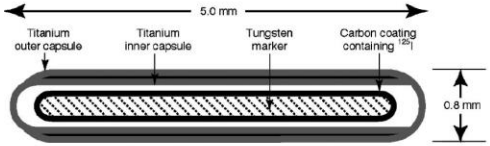

Best model 2301 source

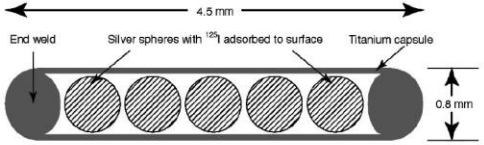

Imagyn model IS-I2501 source

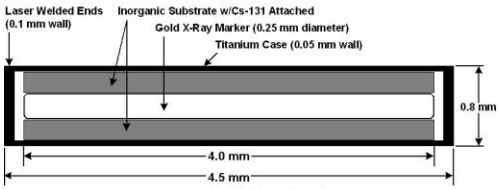

IsoRay model CS-1 Rev2

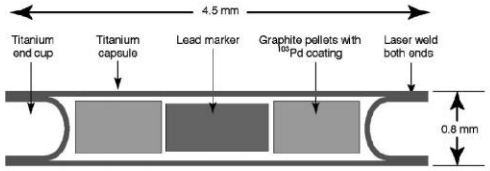

Theragenics model 200 source

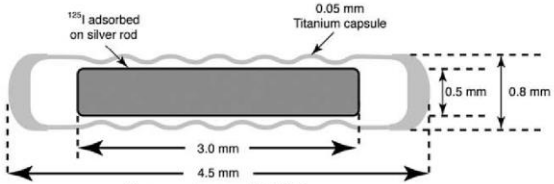

Amersham 6733

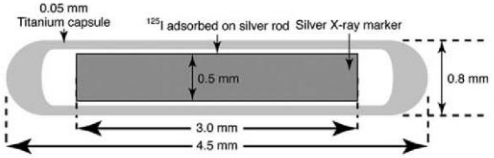

IsoAid Advantage

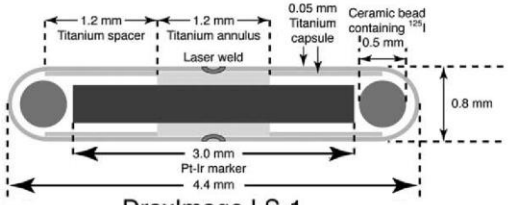

DraxImage LS-1

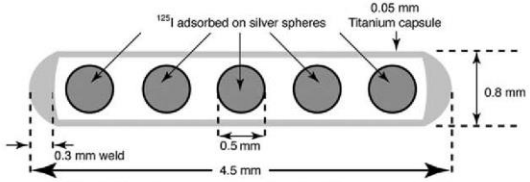

Mills Biopharmaceuticals Prostaseed

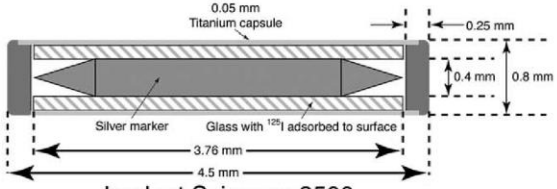

Implant Sciences 3500

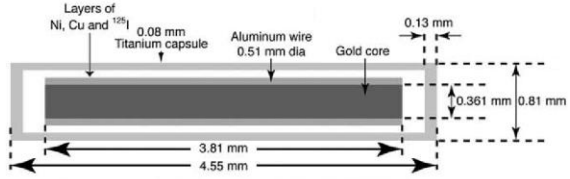

Source Tech Medical STM1251

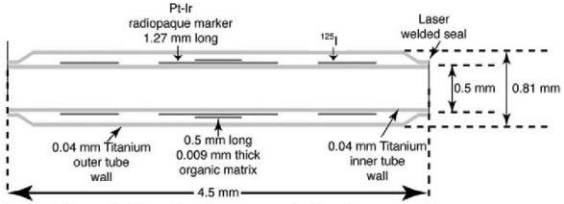

International Brachytherapy InterSource^{125}

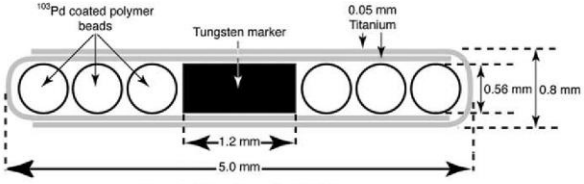

Best Medical 2335

Low-Energy LDR Seeds

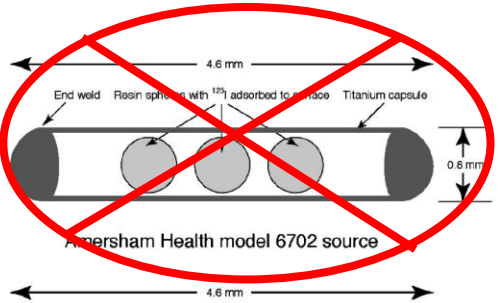

Amersham Health model 6702 source

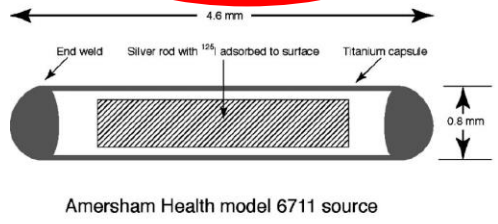

Amersham Health model 6711 source

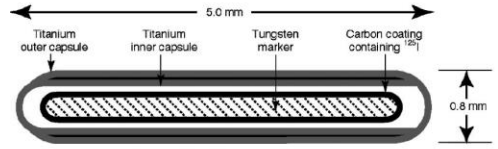

Best model 2301 source

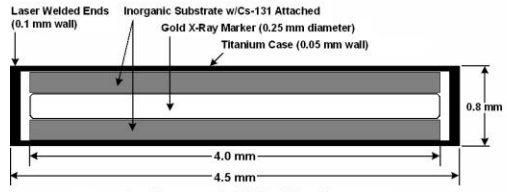

IsoRay model CS-1 Rev2

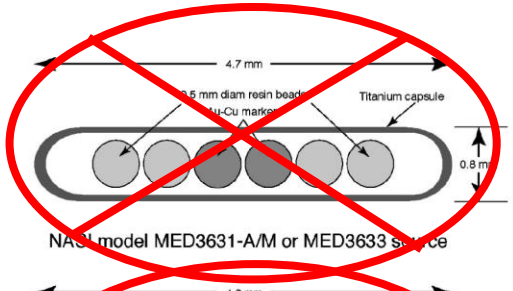

NASI model MED3631-A/M or MED3633 source

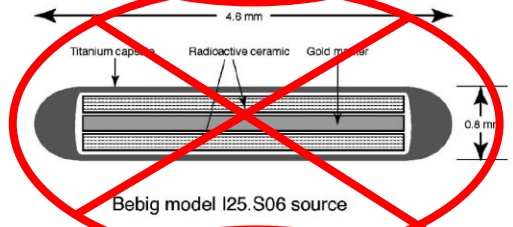

Bebig model I25.S06 source

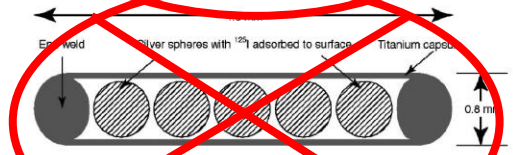

Imagyn model IS-I2501 source

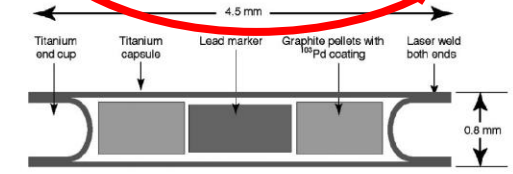

Theragenics model 200 source

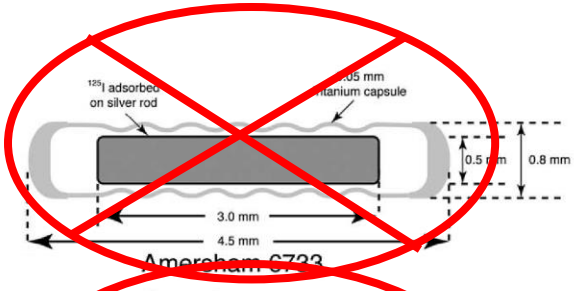

Amersham 6733

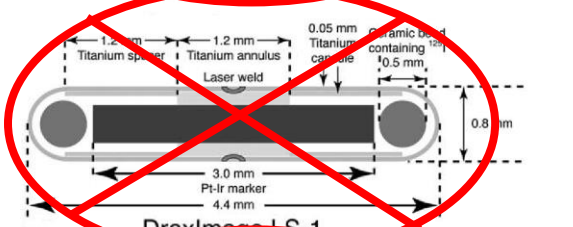

DraxImage LS-1

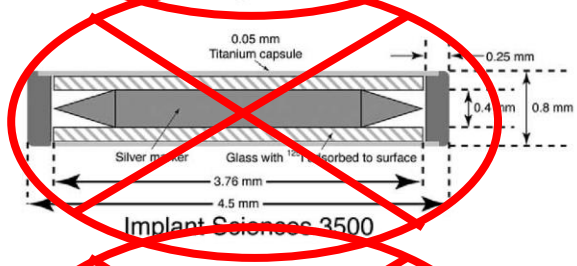

Implant Sciences 3500

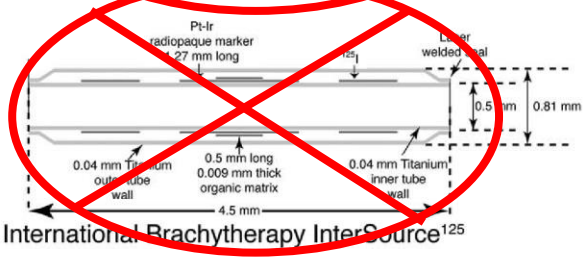

International Brachytherapy InterSource^{125}

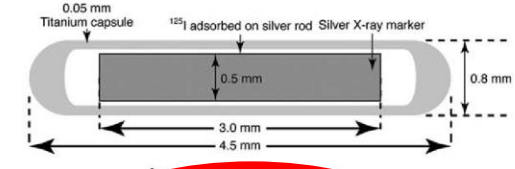

IsoAid Advantage

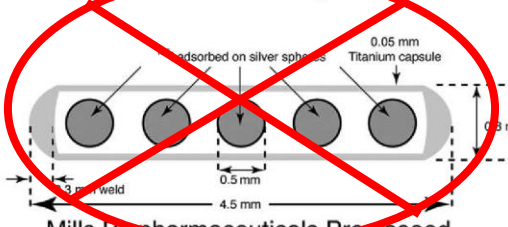

Mills Biopharmaceuticals Prostaseed

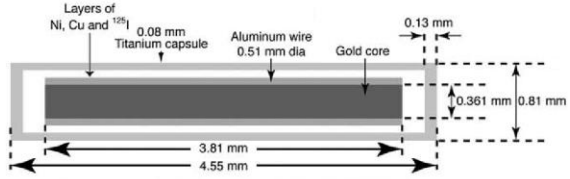

Source Tech Medical STM1251

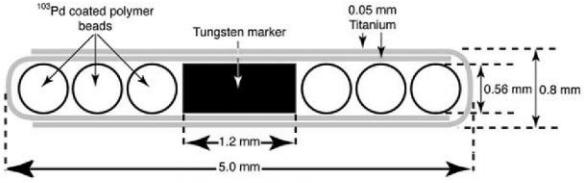

Best Medical 2335

Low-Energy LDR Seeds

Understand the source geometry

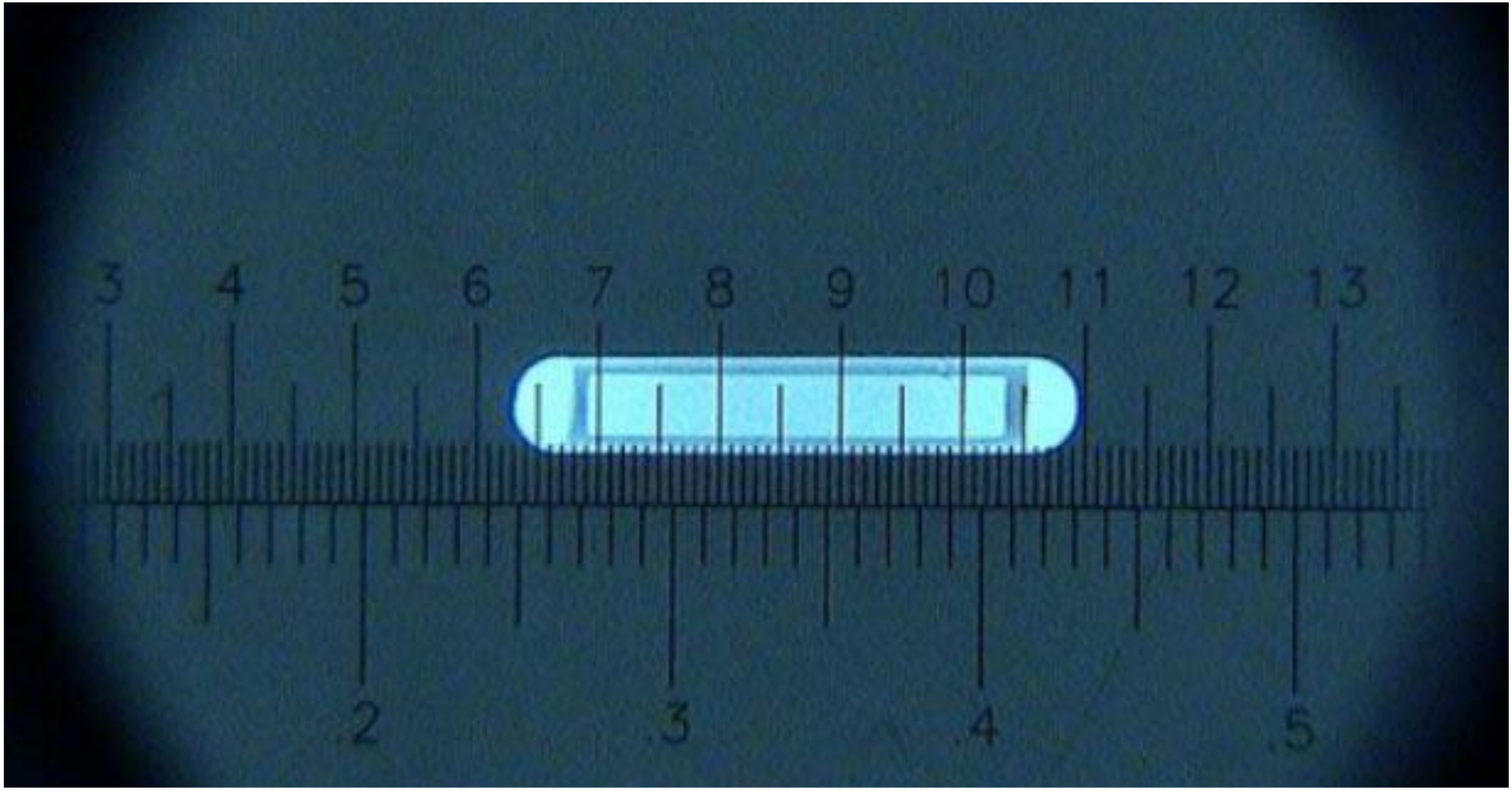

Low-Energy LDR Seeds

Dynamic source orientation influences some dose distributions

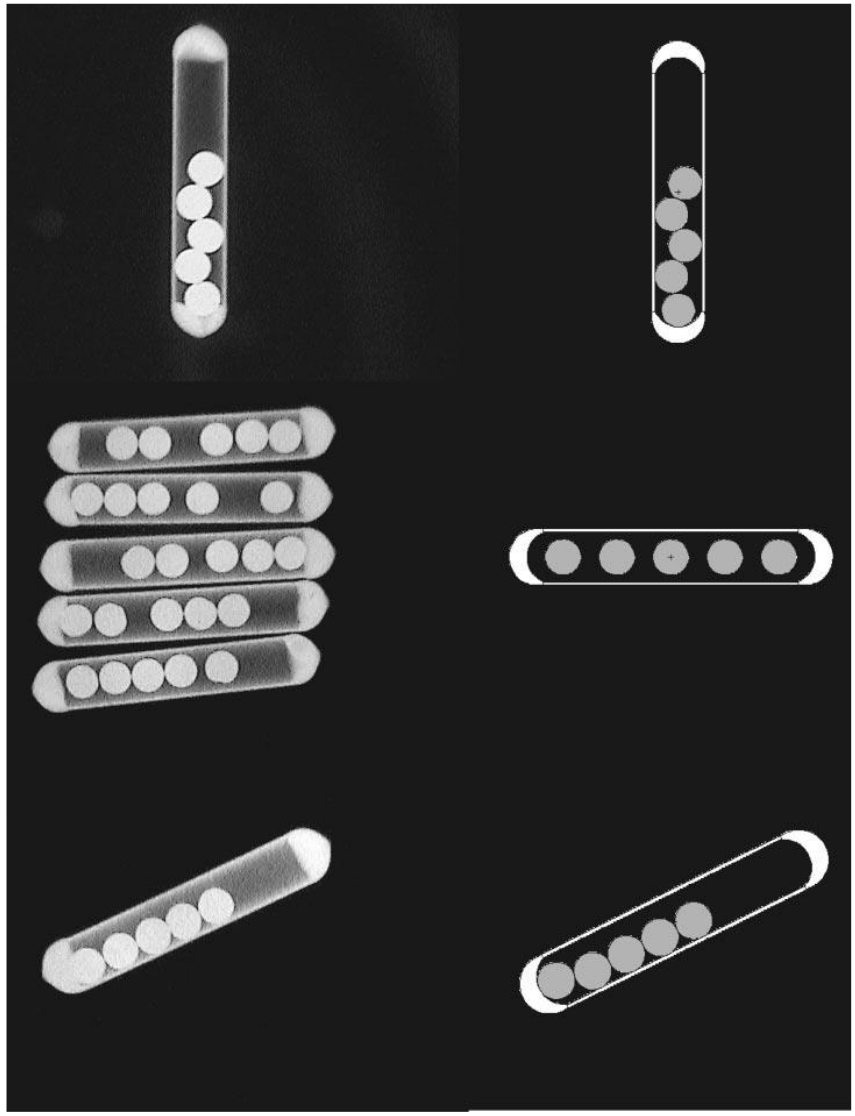

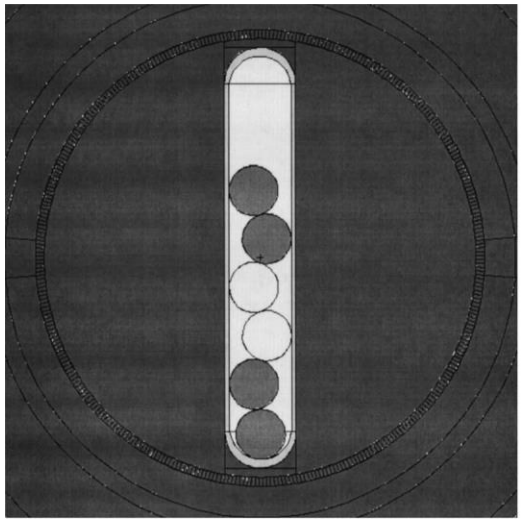

(a)

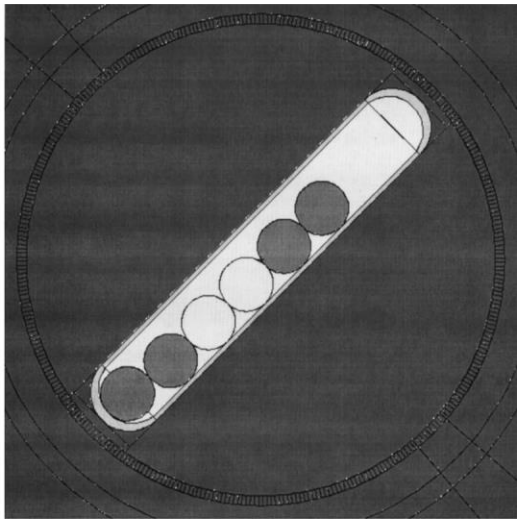

(b)

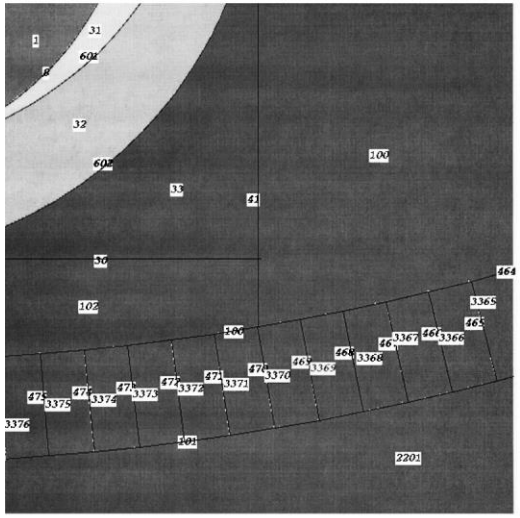

(c)

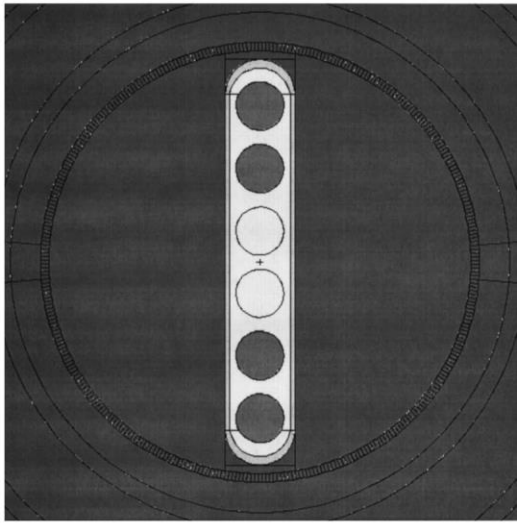

(d)

Low-E HDR Brachytherapy Systems

- Low-energy sources for HDR brachytherapy
  - electronic brachytherapy (eBT) can turn on/off
  - similar dose distributions to HDR ^{125}I source
  - independence from a radioactive materials license
  - diminished shielding/licensing/security required
  - potential to replace radionuclide-based brachytherapy like linacs replaced ^{60}Co

- Vendors for eBT brachytherapy systems
  - Carl Zeiss AG (INTRABEAM)
  - Xoft/iCAD (Axxent)
  - Nucletron/Elekta (esteya)

INTRABEAM System

INTRABEAM X-ray Source

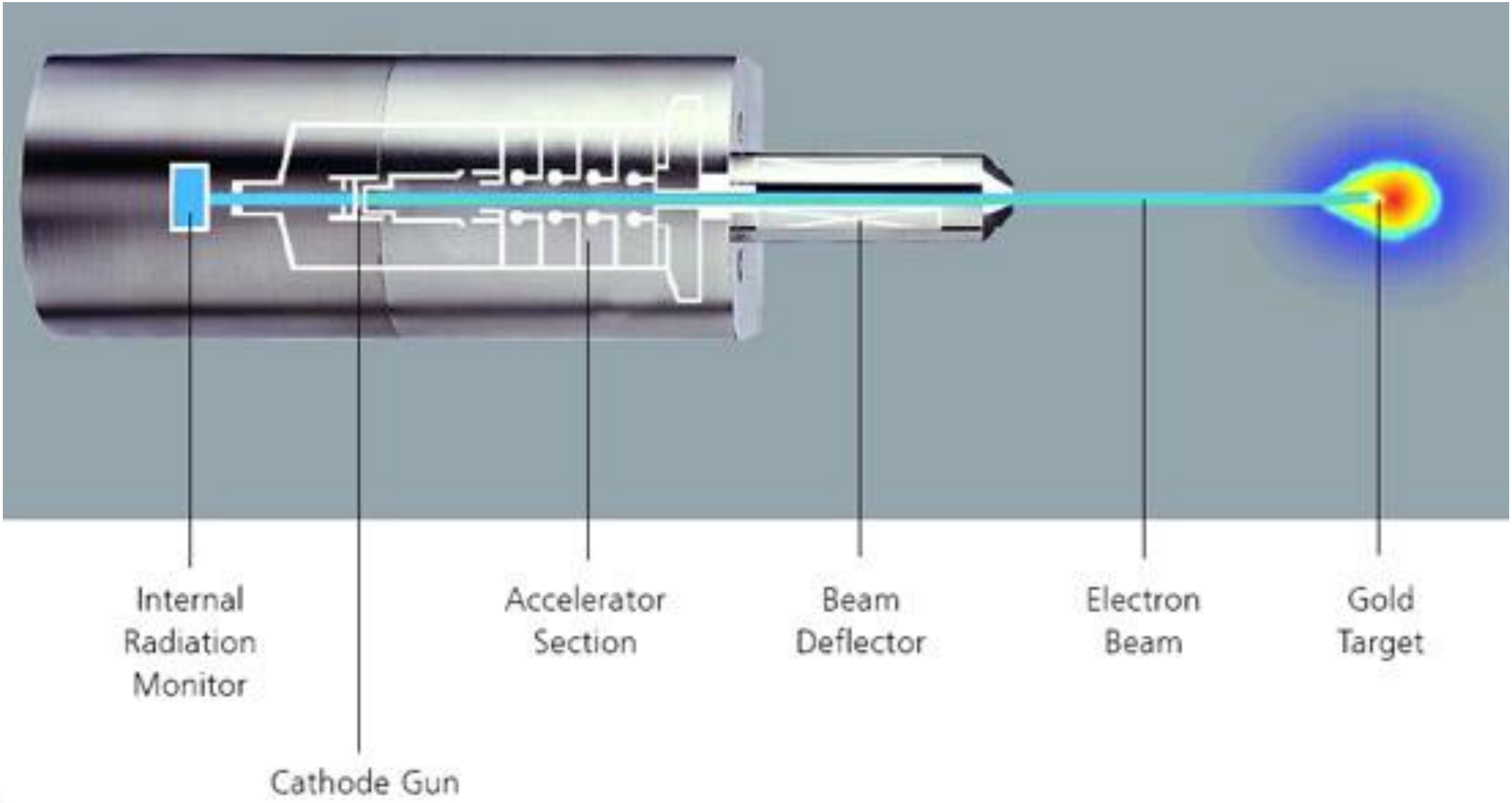

ESTRO School

Axxent Controller

touch screen display

barcode reader

electrometer

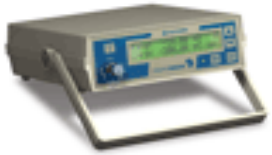

controller pullback arm

USB port

well chamber

ESTRO School

Axxent X-ray Source

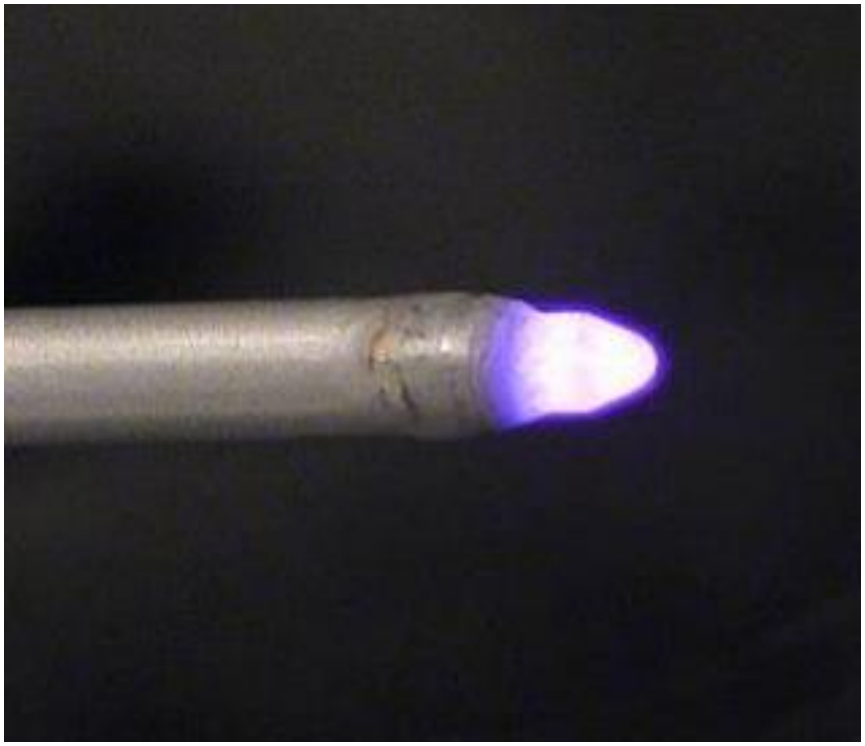

light emission from e^- and x-ray interactions with anode

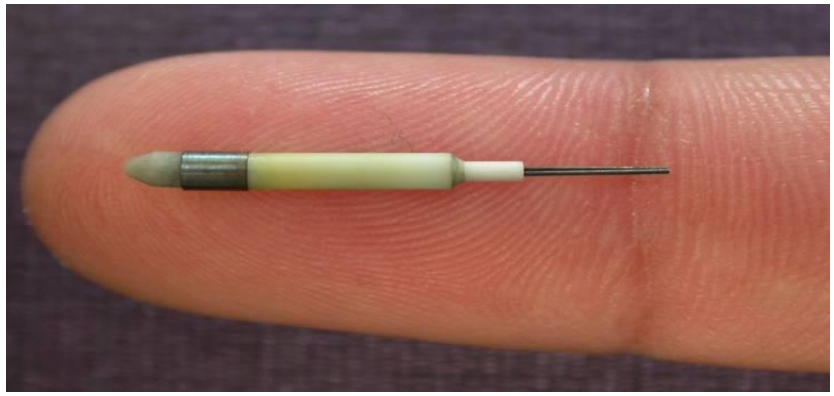

x-ray tube size

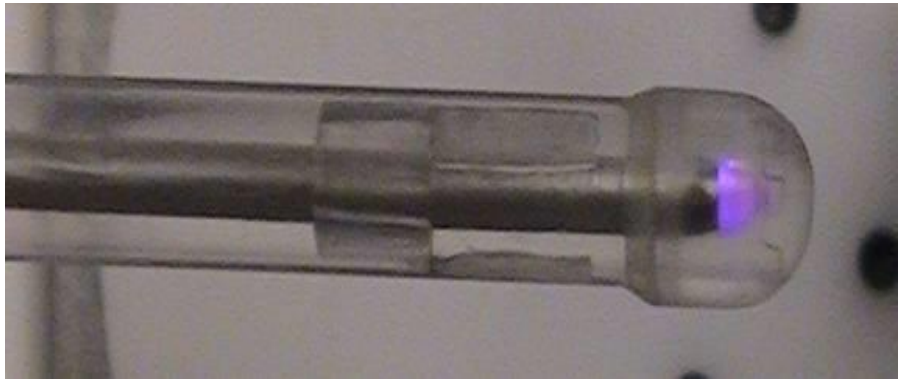

x-ray source in cooling catheter

ESTRO School

esteya System

69.5 kV
10 mm to 30 mm diam.
specific to skin lesions

Medical Physics discussion on eBT

Miniature x-ray tubes will ultimately displace Ir-192 as the radiation sources of choice for high dose rate brachytherapy

Randall W. Holt, Ph.D.
Radiation Oncology Center, Enloe Hospital, Chico, California 95926
(Tel: 530-332-3930, E-mail: randall.holt@enloe.org)

Bruce R. Thomadsen, Ph.D.
Medical Physics, Human Oncology, Engineering Physics and Biomedical Engineering, University of Wisconsin, Madison, Wisconsin 53706
(Tel: 608-263-4183, E-mail: thomadsen@humonc.wisc.edu)

OVERVIEW

Recent advances in the development of miniature x-ray tubes have made electronic brachytherapy a feasible alternative to conventional high dose rate brachytherapy with high activity Ir-192 sources. Because of the obvious radiation safety and security advantages, it is conceivable that the miniature x-ray tube might displace Ir-192 as the source of choice for HDR brachytherapy. This is the proposition debated in this month's Point/Counterpoint.

Arguing for the Proposition is Randall W. Holt, Ph.D. Dr. Holt earned his Ph.D. in Biomedical Engineering at Case Western Reserve University, specializing in 3D-image analysis, after which he received postdoctoral training at the USC Department of Radiation Oncology, specializing in virtual simulation and 3D dosimetry software. Currently Dr. Holt is the Director of Physics for North Valley Radiation Oncology, which provides a broad range of medical physics services to clinics in Northern California. He is board certified by the ABR in radiation therapy physics.

Arguing against the Proposition is Bruce R. Thomadsen, Ph.D. Dr. Thomadsen earned his M.S. and Ph.D. degrees in Medical Physics at the University of Wisconsin—Madison, where he is currently an Associate Professor in the Department of Medical Physics. He is board certified by the ABR in Radiological Physics, by the ABHP in Comprehensive Health Physics, and by the ABMP in Radiation Oncology Physics. His major research interests include all aspects of radiation therapy physics but especially brachytherapy. Dr. Thomadsen currently serves on numerous AAPM committees and task groups and chairs the Radiation Safety Subcommittee and the Special Brachytherapy Modalities Working Group, and is a member of the Board of Editors of *Medical Physics*.

FOR THE PROPOSITION: Randall W. Holt, Ph.D

Opening statement

To displace Ir-192, miniature x-ray sources must deliver therapeutic radiation as well as, or potentially better than, Ir-192, under safer conditions, and with favorable economics.

 0094-2405/2008/35(3)/815/3/$23.00

ESTRO School

High-Energy LDR Sources

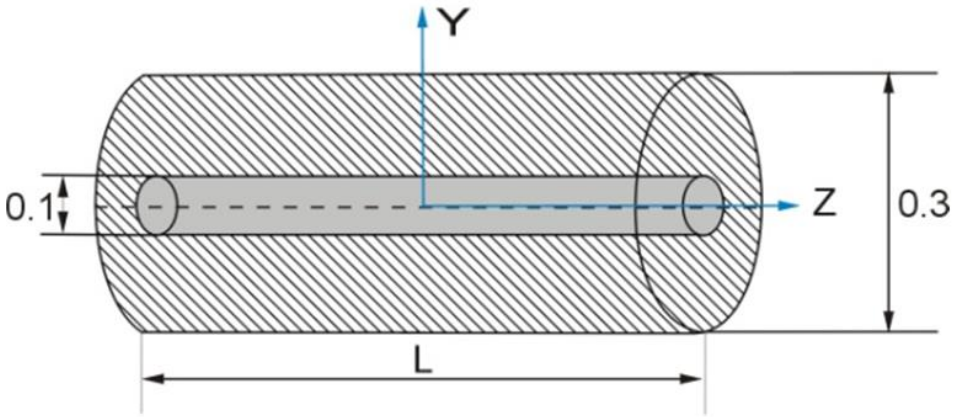

IBt-Bebig LDR ^{192}Ir wires

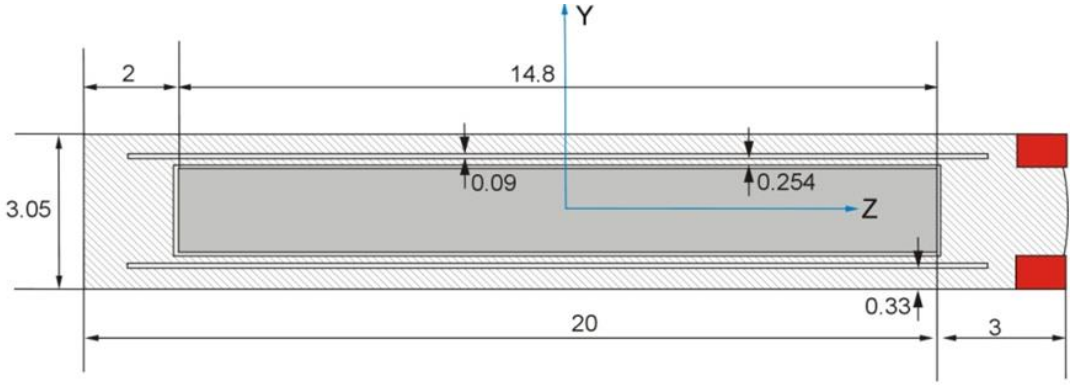

IPL LDR ^{137}Cs model 67-6520 source

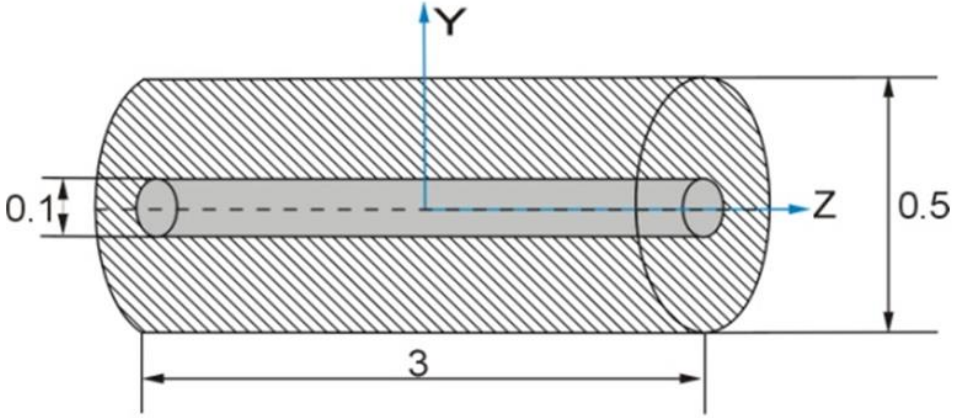

Best Industries LDR ^{192}Ir seed

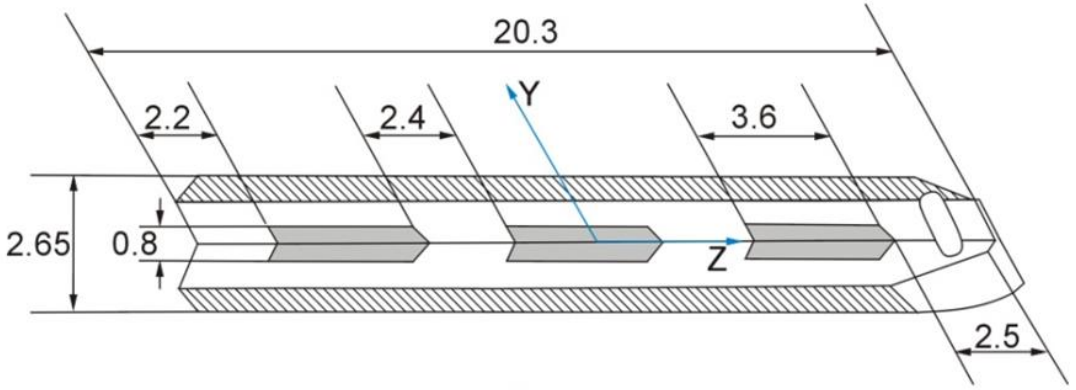

IBt-Bebig LDR ^{137}Cs model CSM3 source

ESTRO School

High-Energy LDR ^{137}Cs Tubes

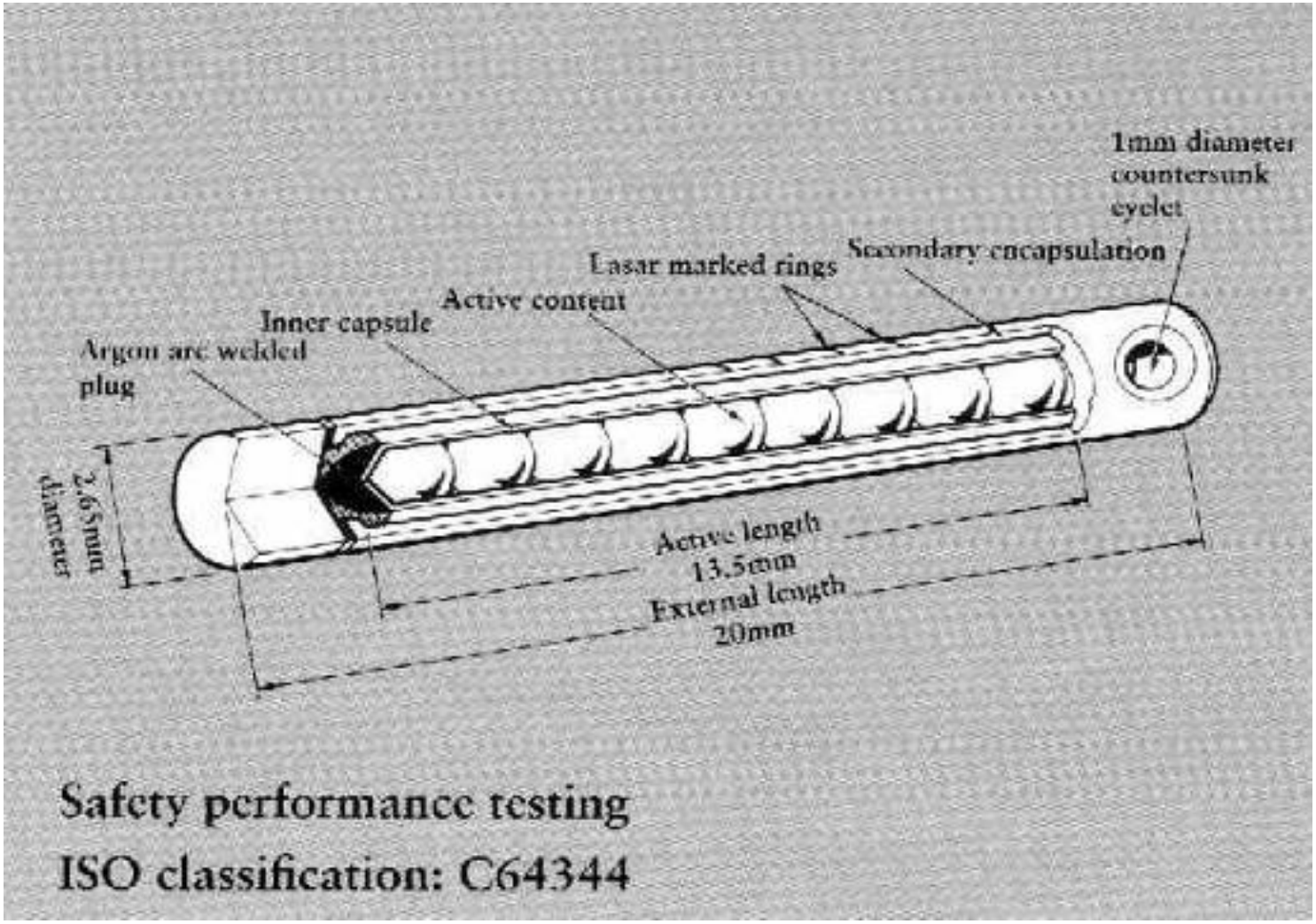

Example of 2 cm tube source

Note difference in active length and external length

ESTRO School

High-Energy LDR ^{192}Ir Hairpins

Special forms of LDR ^{192}Ir sources

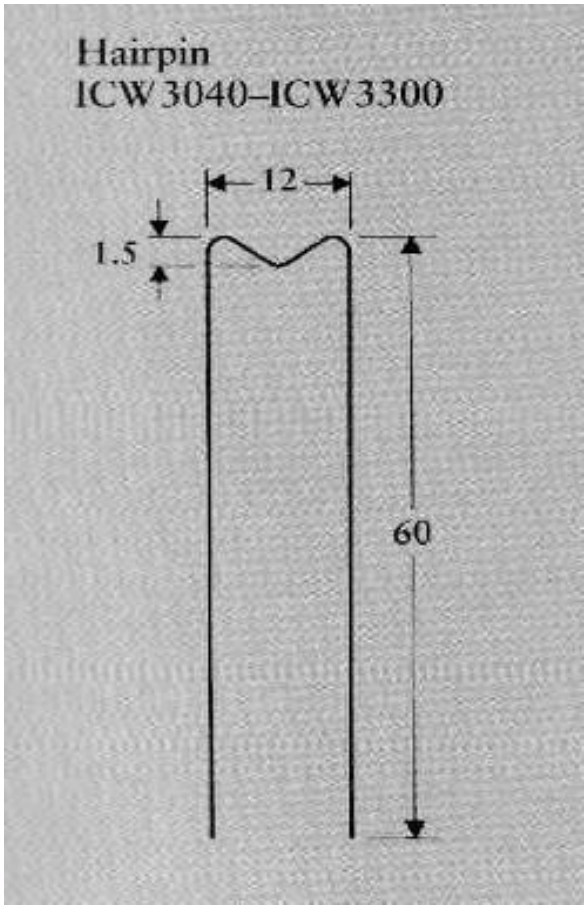

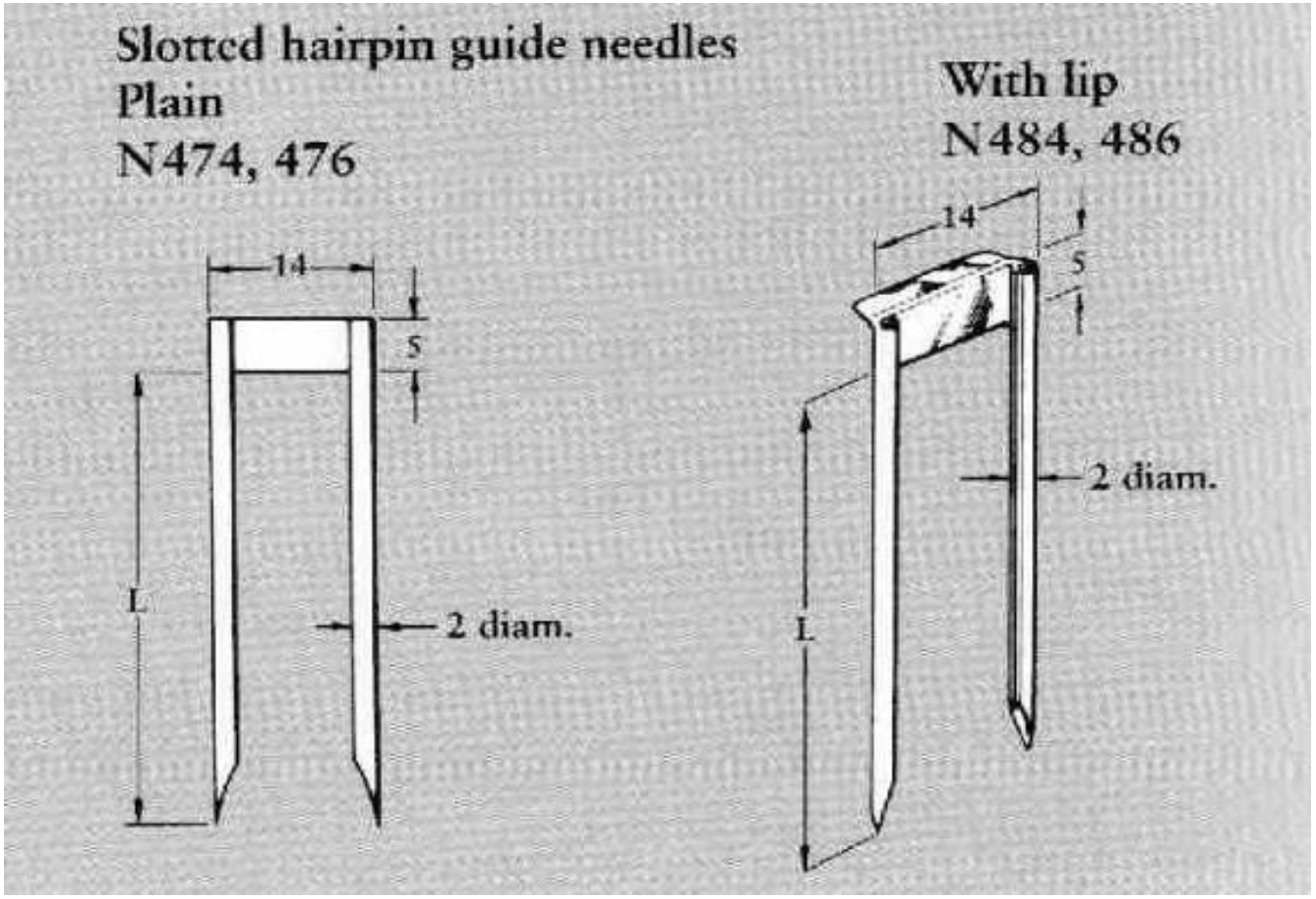

Left: example of a wire-type source, in "hairpin" form, e.g., for tongue implants

Right: guiding needles for "hairpin"

ESTRO School

Remote Afterloading BT

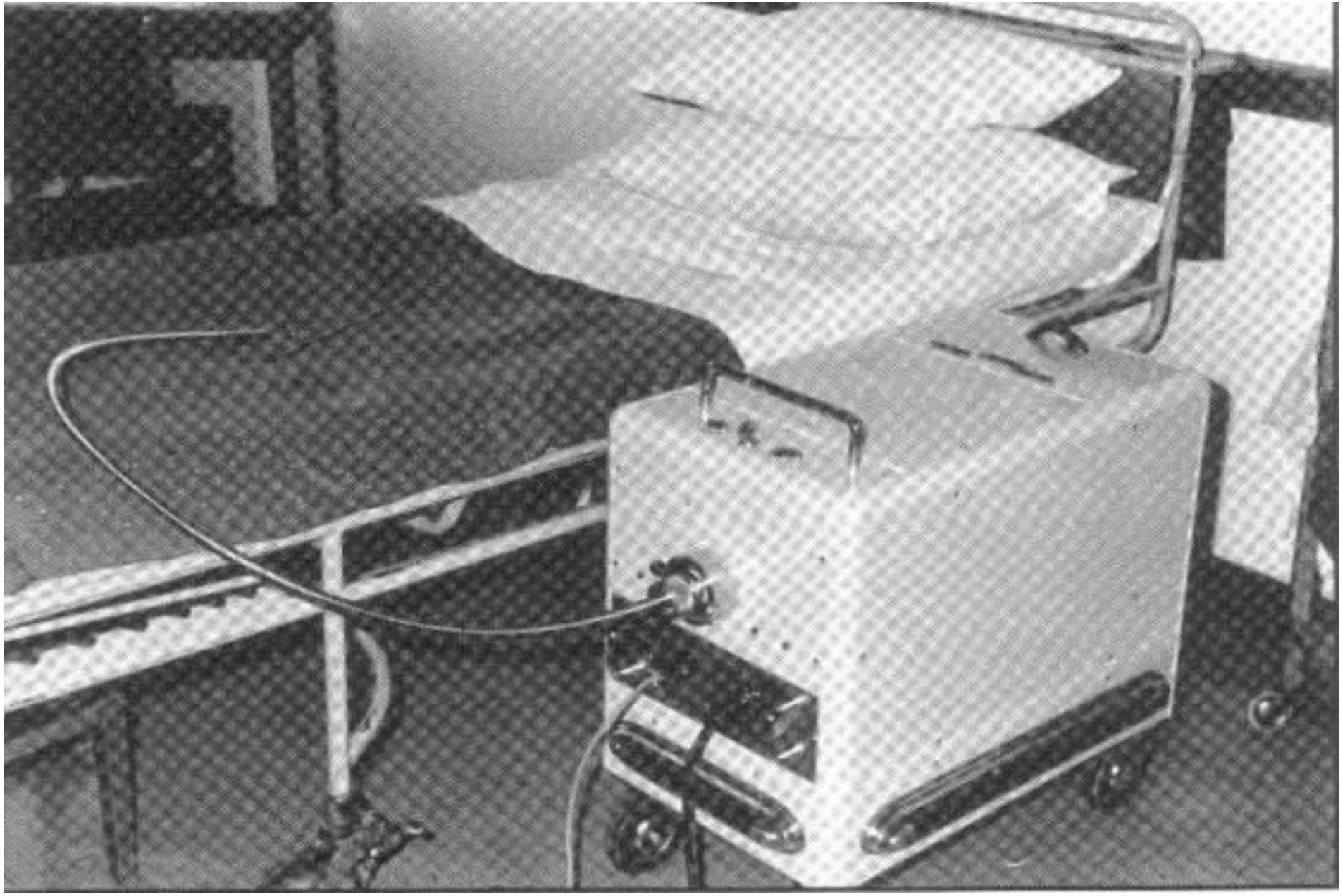

First afterloader ever built

ESTRO School

Selectron LDR ^{137}Cs Pellet Afterloaded

3 or 6 channels

Maximum: 48 sources

(2.5 mm Ø pellets)

ESTRO School

Selectron LDR ^{137}Cs Pellet Afterloaded

Afterloader connected to GYN-applicator set

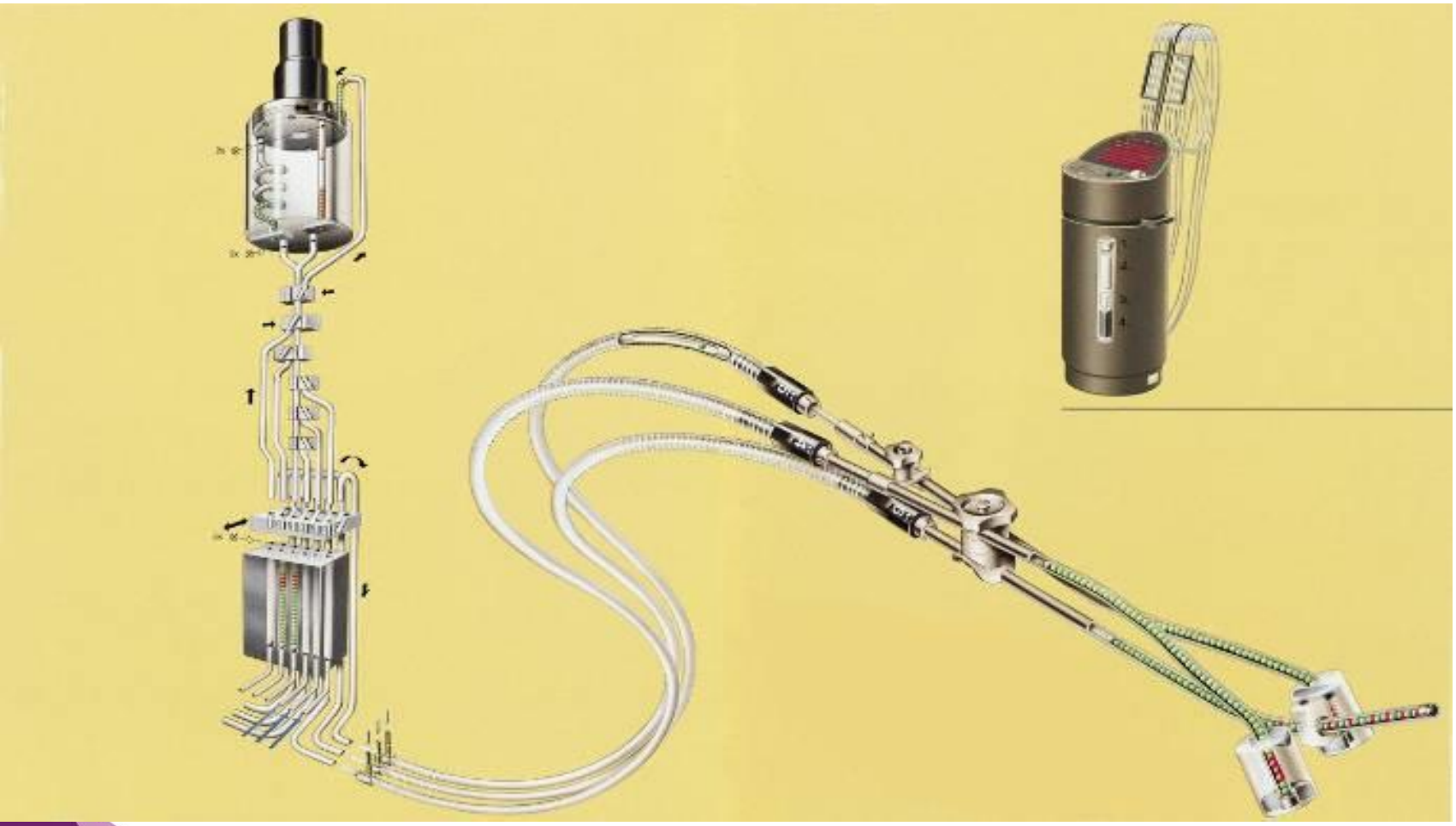

Source pellets pneumatically sorted and driven to applicators

ESTRO School

HDR Brachytherapy Systems

- High-energy sources for HDR brachytherapy
  - ^{192}Ir most common with ^{60}Co under development
  - outer diameter $\leq$ 1 mm
  - treatments from 2 to 20 minutes

    D_{Rx} > 12 Gy/h or > 0.2 Gy/min.
  - regulatory activity 4 to 12 Ci
  - shielding/licensing required

- Vendors for HDR ^{192}Ir brachytherapy RAUs
  - Nucletron/Elekta (microSelectron + Flexitron)
  - Varian (VariSource + GammaMed)
  - BEBIG (MultiSource)

HDR ^{192}Ir Brachytherapy Sources

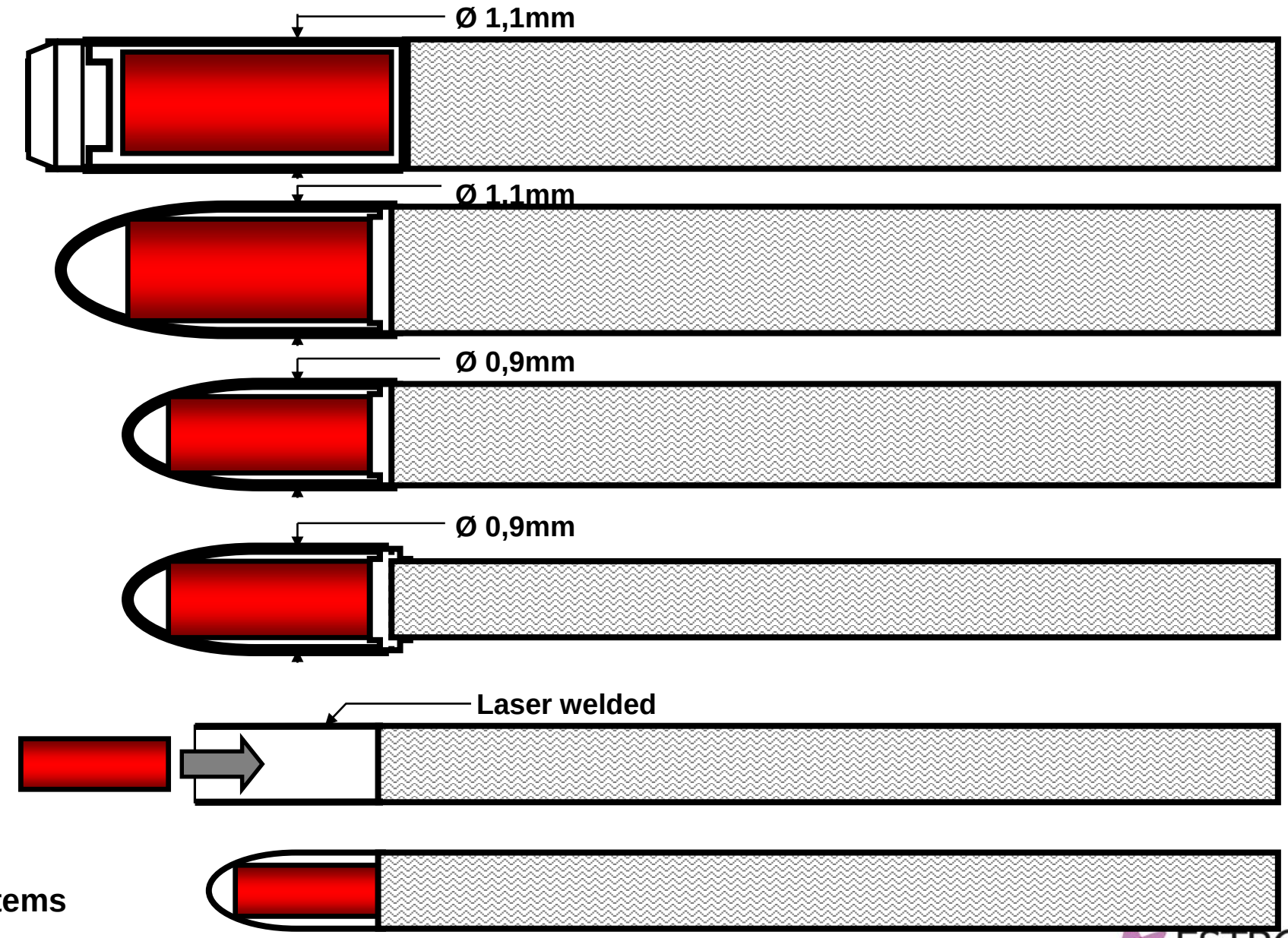

HDR & PDR have identical dimensions

ESTRO School

HDR ^{192}Ir Brachytherapy Sources

Example of miniaturized source welded to the end of a drive cable.

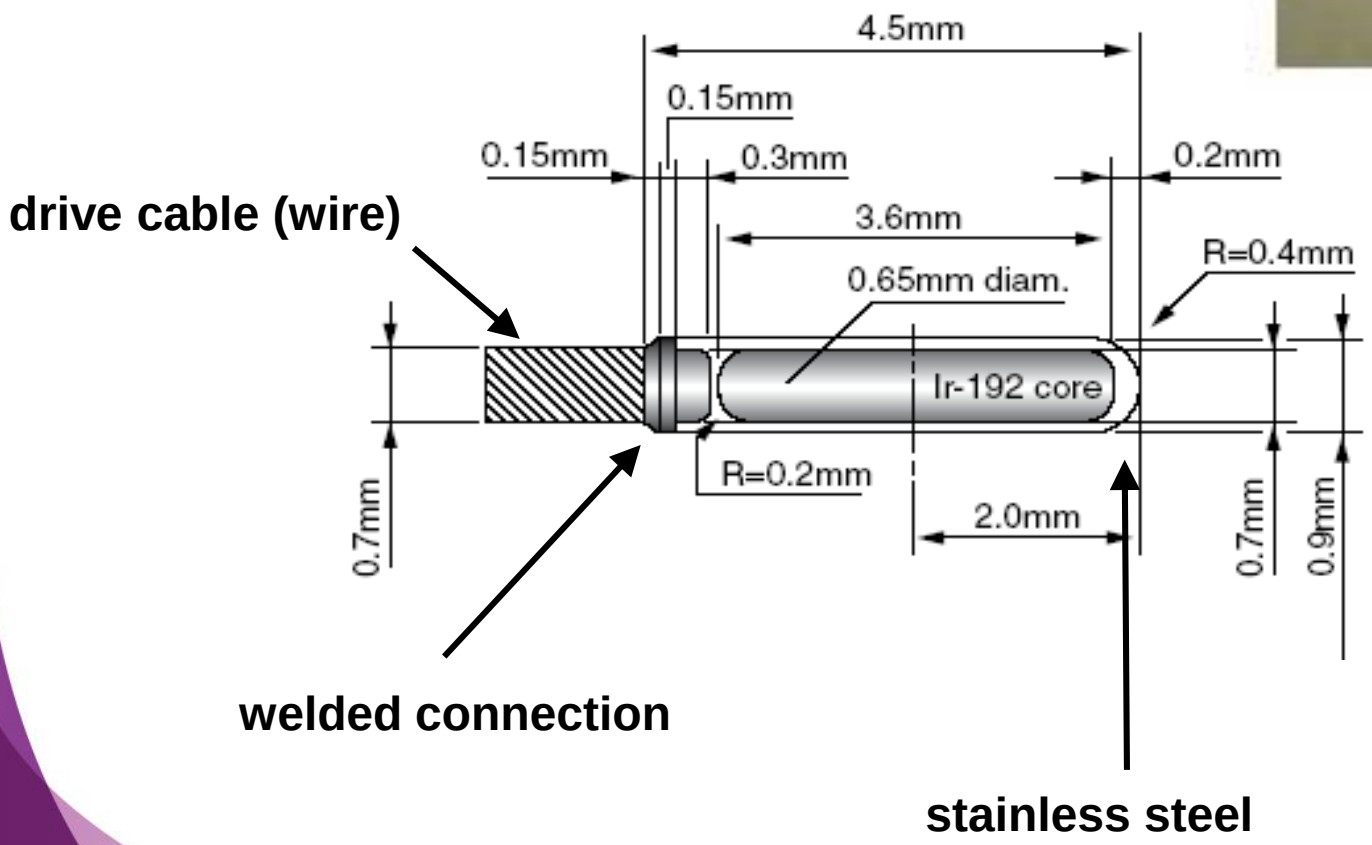

ESTRO School

HDR/PDR ^{192}Ir BT Afterloaders: Overview

Varian, GammaMed Plus

Varian, VariSource

BEBIG, MultiSource

Elekta/Nucletron, microSelectron v3

Elekta/Nucletron, Flexitron

ESTRO School

Nucletron/Elekta microSelectron

3.5 mm long, 0.9 mm diameter ^{192}Ir source

ESTRO School

Varian VariSource

5.0 mm long, 0.59 mm diameter ^{192}Ir source

ESTRO School

Eckert & Ziegler **BEBIG** **MultiSource**

3.5 mm long, 1 mm diameter source

potential for dual HDR ^{192}Ir + ^{192}Ir or HDR ^{192}Ir + ^{60}Co

integrated calibration system for daily verification

ESTRO School

Afterloader Head Mechanism

Nucletron, microSelectron v3

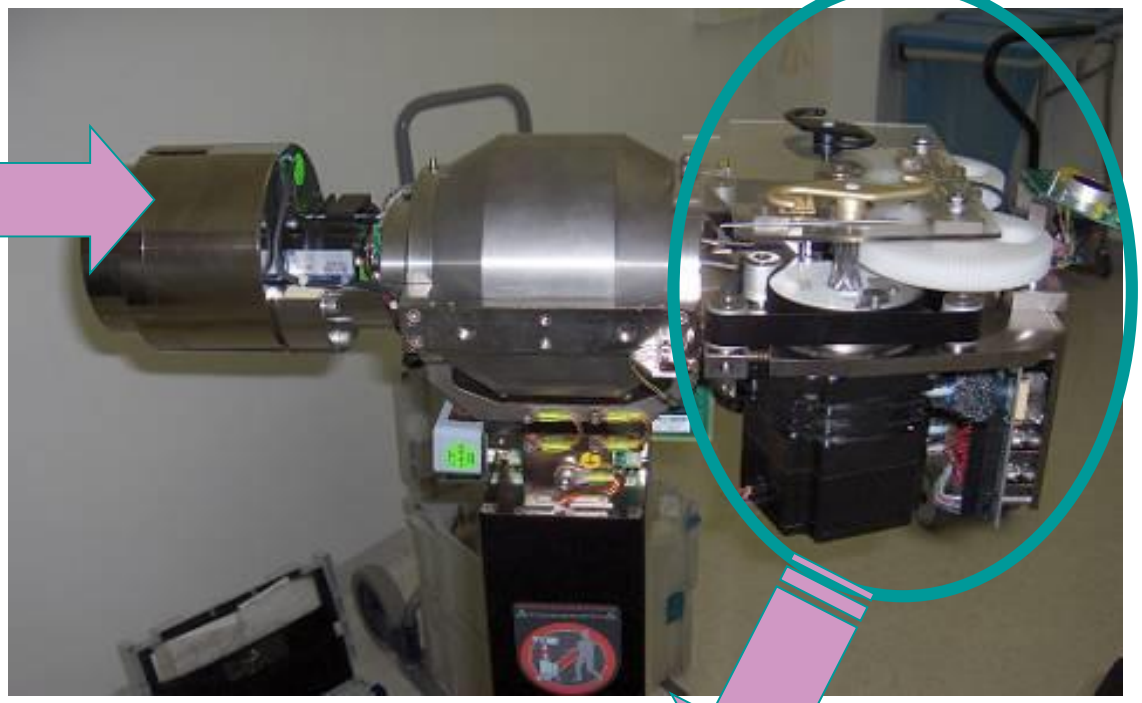

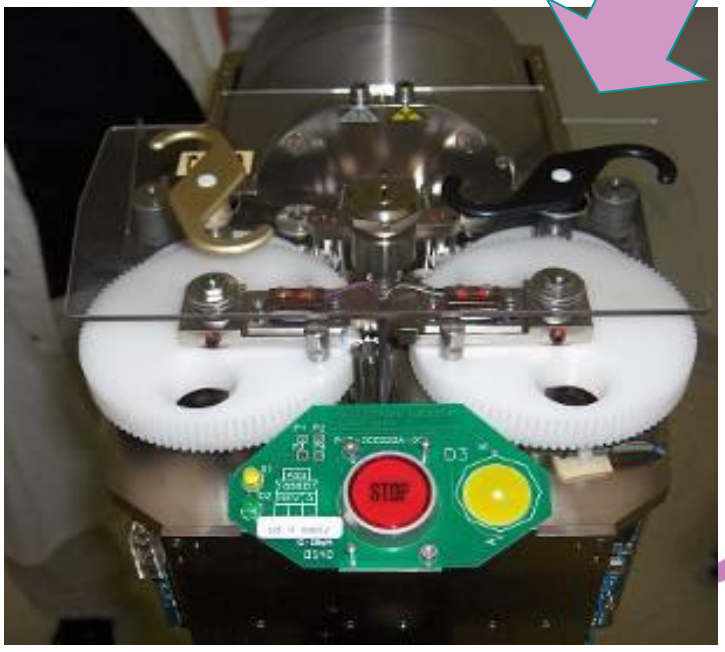

ESTRO School

Afterloader Properties

TABLE 2.1 Features of Modern HDR and PDR Afterloading Equipment

1. Vendor and Product Specification					
Name of Vendor	Nucletron B.V.	Nucletron B.V.	Eckert & Ziegler BEBIG GmbH	Varian Medical Systems Inc.	Varian Medical Systems Inc.
Website	www.nucletron.com	www.nucletron.com	www.ibt-bebig.eu	www.varian.com	www.varian.com
Name of product(s)	microSelectron Digital 6CH - 18CH - 30CH	Flexitron 40CH	MultiSource: 20 channels (extended to 40 channels in 2011) GyneSource: with 5 channels but same specs as MultiSource	Varisource iX	GammaMedplus iX; GammaMedplus iX 3/24 with 3 channels but same specs
Specify capability for use as HDR and/or PDR	HDR and PDR	HDR and PDR	HDR only	HDR only	HDR for iX models, PDR for non iX models
2. Specifications of Source or Sources					
Single or dual source capability	2 drives	3 drives	Single source	Single source	Single source
Possible types of source (radionuclide), available now and/or under development	^{192}Ir	^{192}Ir	Co-60: source type Co0.A86 Ir-192: source type Ir2.A85-2	^{192}Ir	^{192}Ir

(continued)

Refs:

Thomadsen 2000, Achieving Quality in Brachytherapy.

ESTRO Booklet 8 2004, A Practical Guide to QC of Brachytherapy Equipment.

Table taken from Chap. 2 of: Comprehensive Brachytherapy 2013, (Eds. Venselaar, Baltas, Meigooni, Hoskin).

ESTRO School

TABLE 2.1 (Continued) Features of Modern HDR and PDR Afterloading Equipment

2. Specifications of Source or Sources					
Maximum source strength for each possible radionuclide, with approval for marketing by authorities	HDR: 57 mGy.h–1 @ 1m (518 GBq (14Ci) of Ir-192) PDR: 10.2 mGy.h–1 @ 1m (92.5 GBq (2.5 Ci) of Ir-192) Maximum storage source capacity: 518 GBq (14 Ci)	HDR: 49 mGy.h–1 @ 1m (444 GBq (12 Ci) of Ir-192) PDR: 10.2 mGy.h–1 @ 1m (92.5 GBq (2.5 Ci) of Ir-192) Maximum storage capacity: 814 GBq (22 Ci) of Ir192	Co0.A86: 22.6 mGy.h–1 @ 1m (2 Ci, 74 GBq) values + 10 % Ir2.A85-2: 40 mGy.h–1 @ 1m (10 Ci, 370 GBq) values +30 % – 10 %	44.8 mGy.h–1 @ 1m (11 Ci, 407 GBq)	61.1 mGy.h–1 @ 1m (15 Ci, 555 GBq) Local regulations may prohibit to install more than 10 Ci
Source outer dimensions for each of the source types (L = length, OD = outer diameter, in mm)	3.5 mm active length × 0.6 mm diameter Source capsule outer diameter: 0.9mm	3.5 mm active length × 0.6 mm diameter Source capsule outer diameter: 0.86 mm	Co0.A86 1.0(OD) × 5(L) mm Ir2.A85-2 0.9(OD) × 5(L) mm	0.59(OD) × 5(L) mm	HDR: 0.9(OD) × 4.52(L) mm; PDR: 0.9(OD) × 2.97(L) mm
Guarantee for the maximum number of source transfers, or source cycles	25,000 cycles	30,000 cycles	Co0.A86 100,000 (>400.000 tested) Ir2.A85-2 25,000	1,000	5,000
3. Specification of Applicators					
Outside diameter of the applicators (needles and or tubes, in mm)	Needles 1.3 mm Flexibles 4F	Needles 1.3 mm Flexibles 4F	needles 1.5 mm (17G) catheters 1.65mm for both sources	18G (1.27 mm) needles constructed from robust think wall tubing. 4.7F robust thick walled catheters	17G (1.5 mm) needles. 5F catheters.
Minimum curvature of an applicator (plastic loop radius, e.g. for an 180 degree curve, in mm)	13 mm for all applicators with a fixed geometry and an inner diameter of 2.5 mm or larger; 15 mm for flexible applicators with an inner diameter of 1.5 mm or higher; 20 mm for flexible applicators with an inner diameter of 1.3 mm up to 1.5 mm	13 mm for applicators with a fixed geometry; 15 mm for flexible applicators with an inner diameter of 1.2 mm and outer diameter of 1.5mm or higher;	10 mm (loop of 90°) 15 mm (loop of 180°) for both sources	17 mm	13 mm
4. Source to Cable Attachment					
Method of source attachment to cable	Laser welded to ultra flexible drive wire	Laser welded to ultra flexible drive wire, including weld protection	Laser welded	Embedded in the Nitinol (nickel-titanium) source drive wire	Laser welded to ultraflexible drive cable
5. Source Extension and Movement					
Maximum source extension (in mm from the indexer)	1500 mm	1400 mm	1500 mm	1500 mm	1300 mm
Speed of source movement, in seconds over maximum source extension	500 mm/s, typ. outdrive time 4 s for 1500 mm	1400mm in 3.7 sec	300 mm/s 5 s for 1500 mm	600 mm/s	630 mm/s
6. Number of Channels					
Number of hardware applicator channels	30	40	MultiSource: 20 GyneSource: 5	20	iX model: 24; iX 3/24 model: 3
Maximum number of channels that can be used in one plan/treatment	90	40	MultiSource (2011): 40 GyneSource model: 5	unlimited	unlimited

(*continued*)

And 2 pages more……

ESTRO School

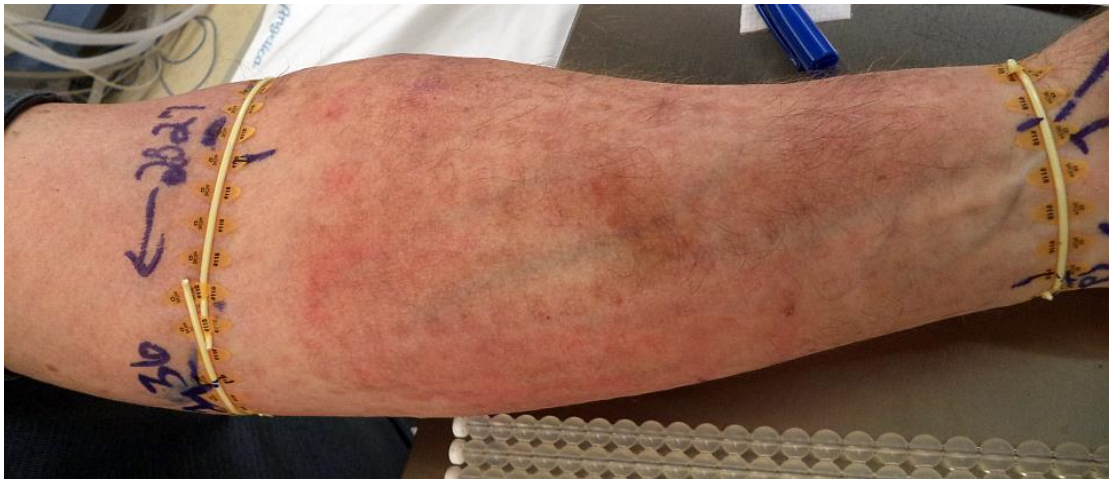

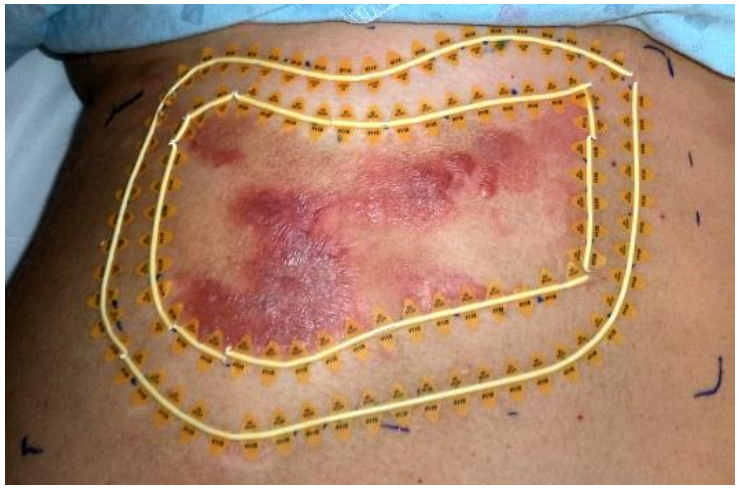

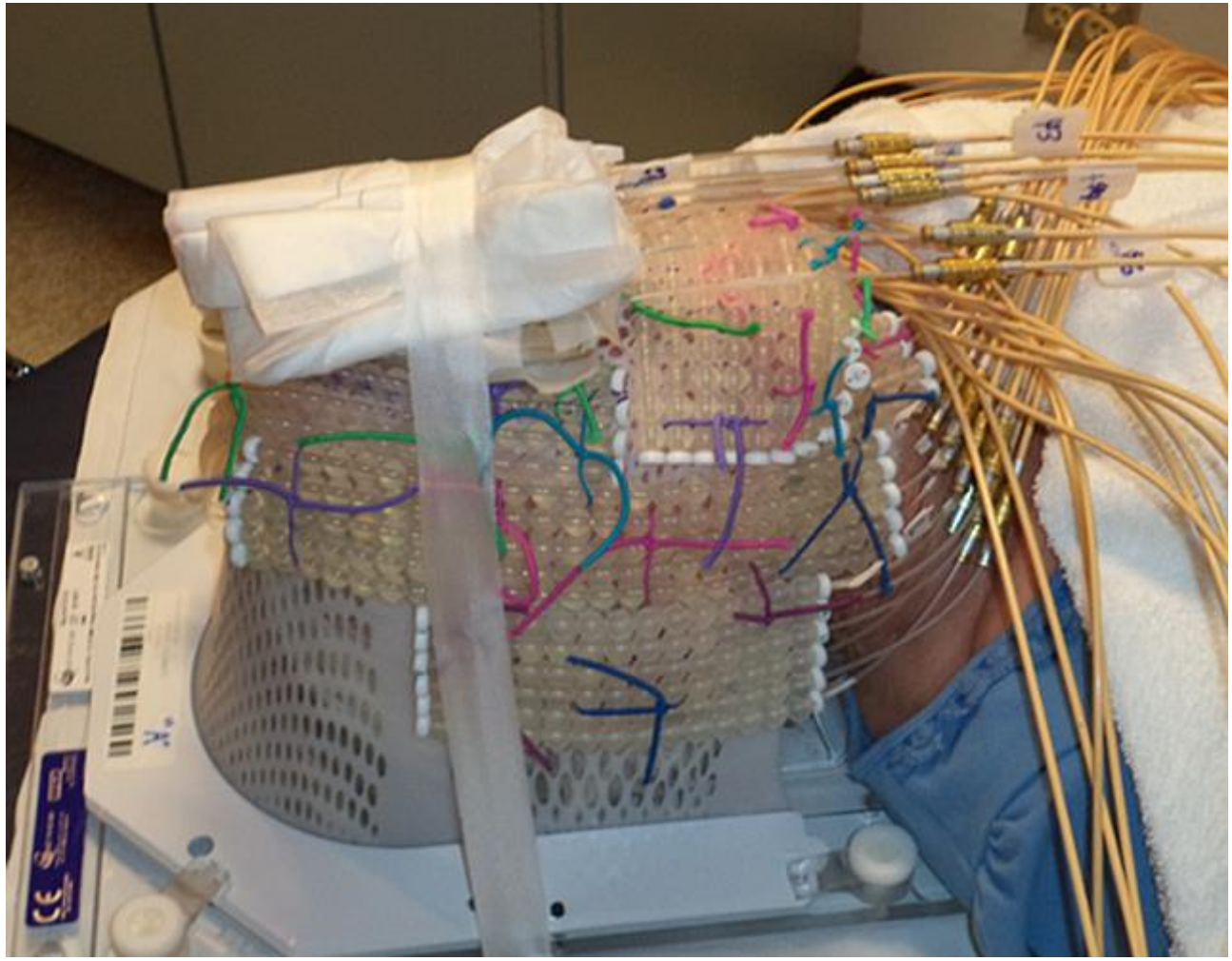

images courtesy of Ivan Buzurovic

ESTRO School

Robotic based Afterloading Technology?

Evolution

Robots!

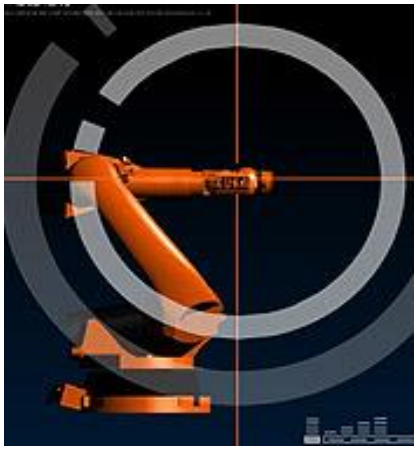

^{192}Ir,
^{60}Co,
eBT,
low-E seeds

ESTRO School

Robot Definition

Robot = a reprogrammable multifunctional manipulator designed to move materials, parts, tools, or specialized devices through variable programmed motions for performance of a variety of tasks.

Robotics Institute of America®

Podder et al, *Med. Phys.* 41, 101501-1-27 (2014)

ESTRO School

Commerically Available LDR Robot

A seed afterloader for prostate BT: Robotic Assisted Seed Delivery

seedSelectron
(by Elekta/Nucletron, The Netherlands)

ESTRO School

Commerically Available LDR Robot

A seed afterloader for prostate BT:
Robotic Assisted Seed Delivery
Principle of loading of a needle

Application of the seed afterloader

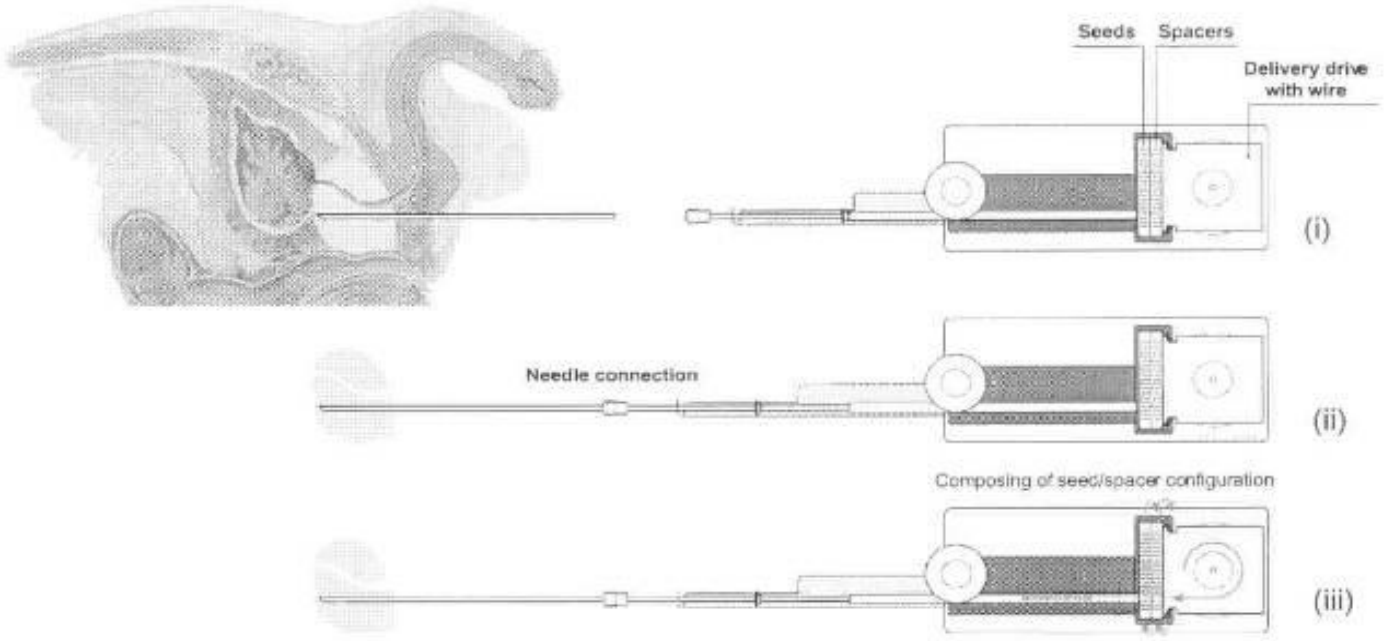

Cassettes with ^{125}I sources and spacers

ESTRO School

AAPM/GEC-ESTRO TG-192 Report: Robotic BT

Medical Physics

AAPM and GEC-ESTRO guidelines for image-guided robotic brachytherapy: Report of Task Group 192

Tarun K. Podder, Luc Beaulieu, Barrett Caldwell, Robert A. Cormack, Jostin B. Crass, Adam P. Dicker, Aaron Fenster, Gabor Fichtinger, Michael A. Meltsner, Marinus A. Moerland, Ravinder Nath, Mark J. Rivard, Tim Salcudean, Danny Y. Song, Bruce R. Thomadsen, and Yan Yu

This is a joint Task Group with the Groupe Européen de Curiethérapie-European Society for Radiotherapy & Oncology (GEC-ESTRO). All developed and reported robotic brachytherapy systems were reviewed. Commissioning and quality assurance procedures for the safe and consistent use of these systems are also provided. Manual seed placement techniques with a rigid template have an estimated in vivo accuracy of 3–6 mm. In addition to the placement accuracy, factors such as tissue deformation, needle deviation, and edema may result in a delivered dose distribution that differs from the preimplant or intraoperative plan. However, real-time needle tracking and seed identification for dynamic updating of dosimetry may improve the quality of seed implantation. The AAPM and GEC-ESTRO recommend that robotic systems should demonstrate a spatial accuracy of seed placement ≤1.0 mm in a phantom. This recommendation is based on the current performance of existing robotic brachytherapy systems and propagation of uncertainties. During clinical commissioning, tests should be conducted to ensure that this level of accuracy is achieved. These tests should mimic the real operating procedure as closely as possible.

Podder et al, *Med. Phys.* 41, 101501-1-27 (2014)

ESTRO School

LDR Seed Robots Under Development

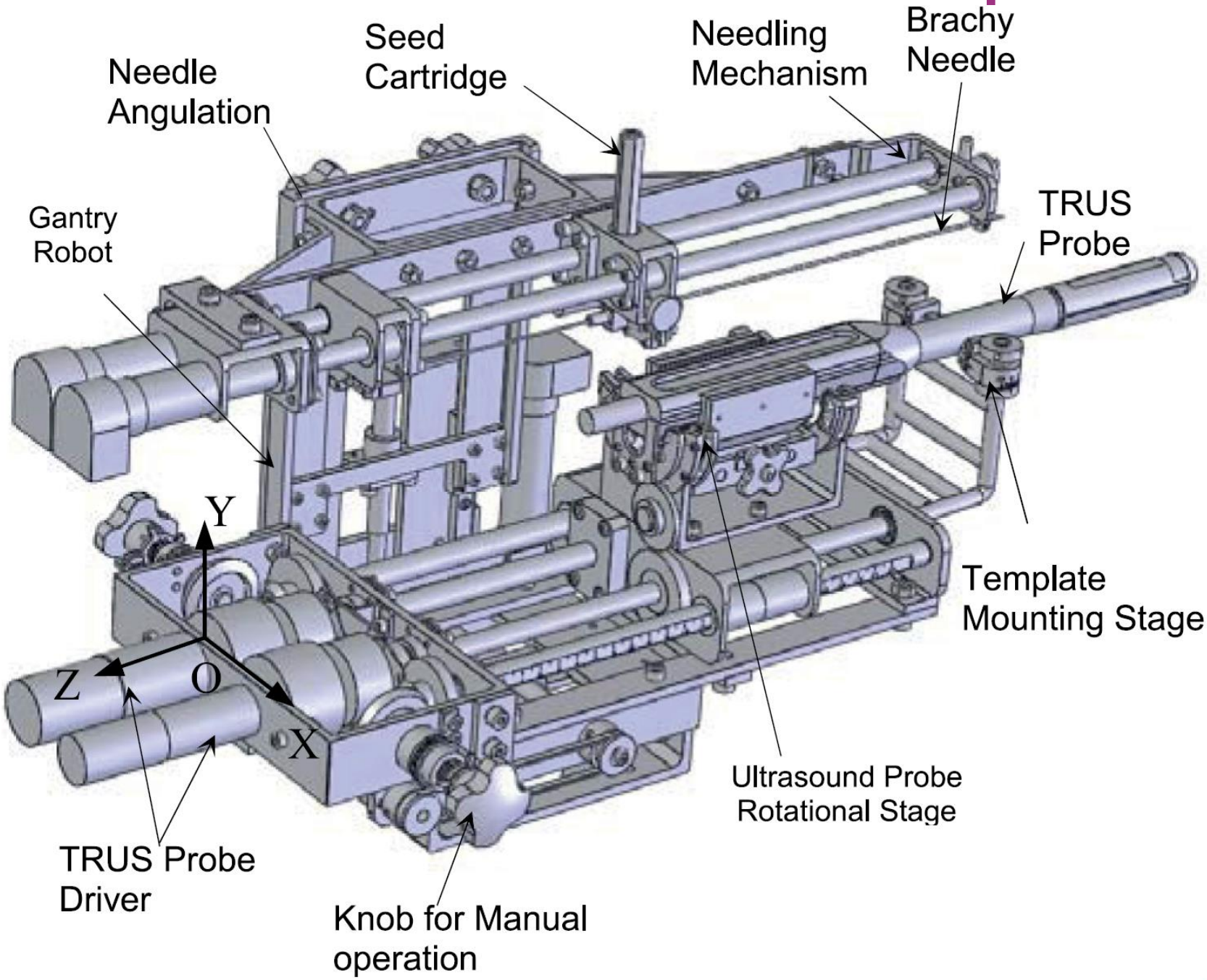

EUCLIDIAN, Thomas Jefferson Univ.

ESTRO School

LDR Seed Robots Under Development

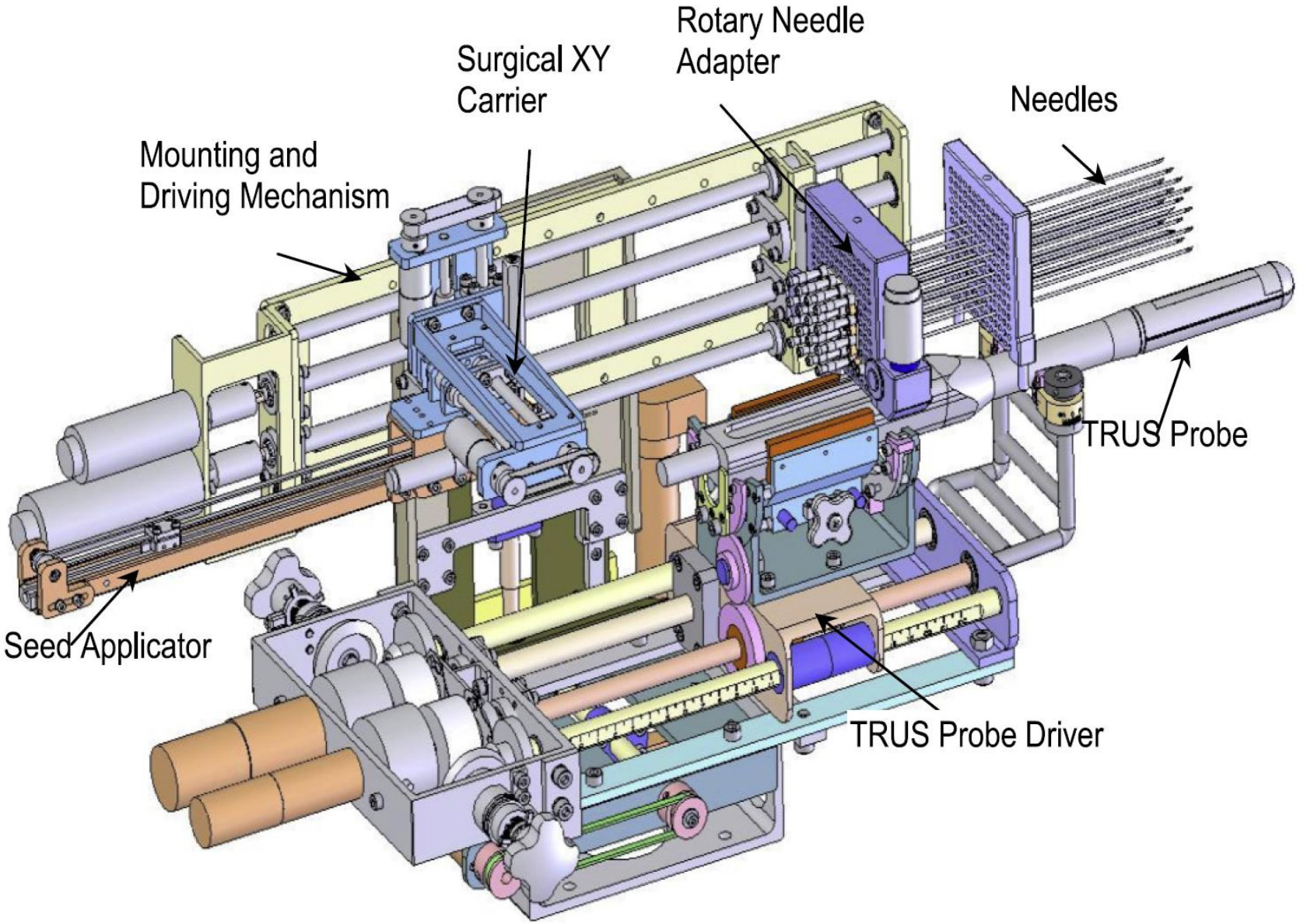

MIRAB, Thomas Jefferson Univ.

ESTRO School

LDR Seed Robots Under Development

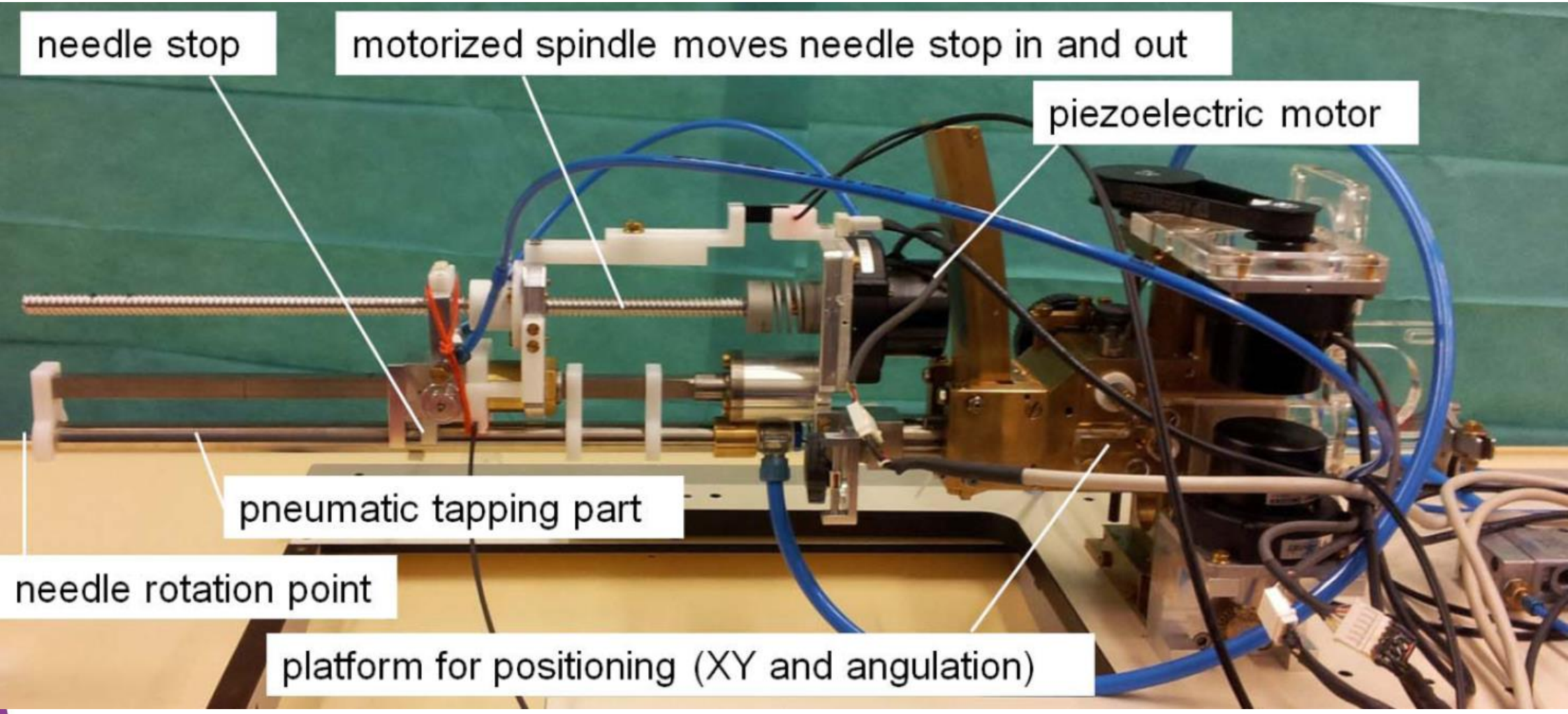

LDR Seed Robots Under Development

Robot-assisted Needle Placement in Open-MRI: System Architecture, Integration and Validation

S.P. DiMaio [a,1], S. Pieper [b], K. Chinzei [c], N. Hata [a], E. Balogh [d], G. Fichtinger [d], C.M. Tempany [a], R. Kikinis [a],

[a] *Brigham and Women's Hospital, Harvard Medical School*

[b] *Isomics Inc.*

[c] *National Institute of Advanced Industrial Science and Technology, Japan*

[d] *Johns Hopkins University*

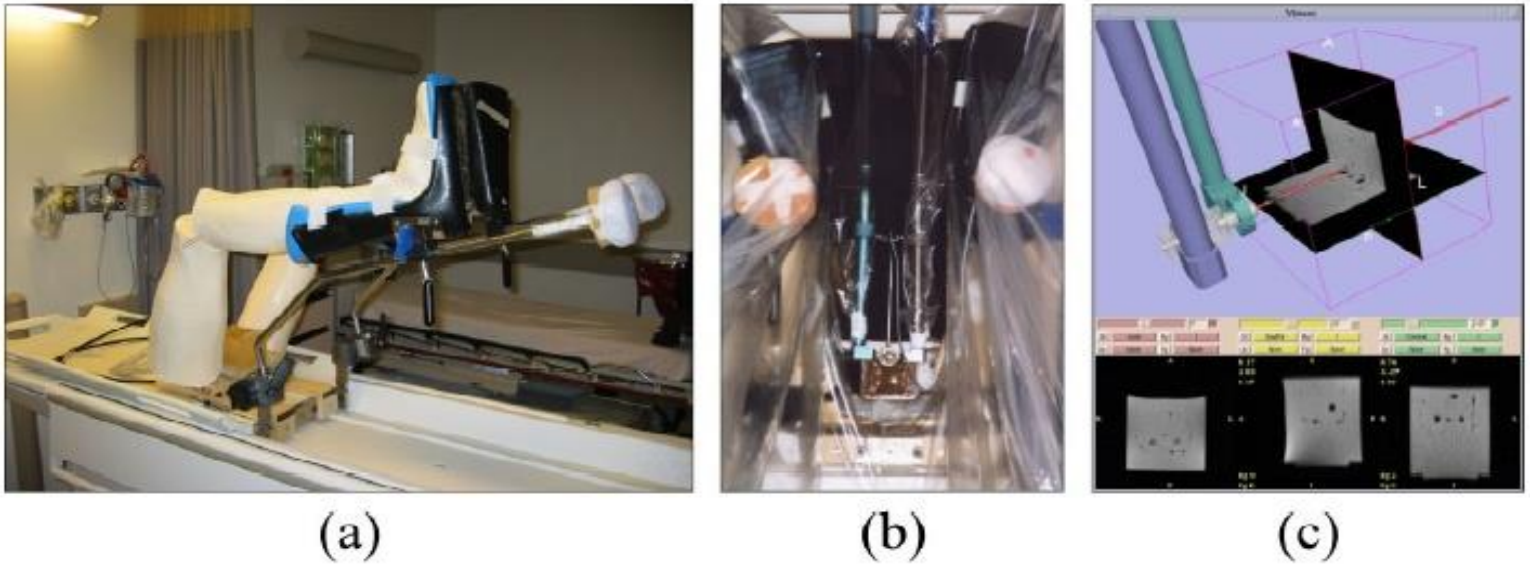

(a) (b) (c)

Figure 3. Phantom experiments: (a) scale models of legs and PVC prostate phantom with embedded targets, (b) patient model and robot placement inside the scanner, with sterile draping, (c)needle trajectories are interactively specified in the planning environment.

MRI-compatible

Johns Hopkins Univ.

ESTRO School

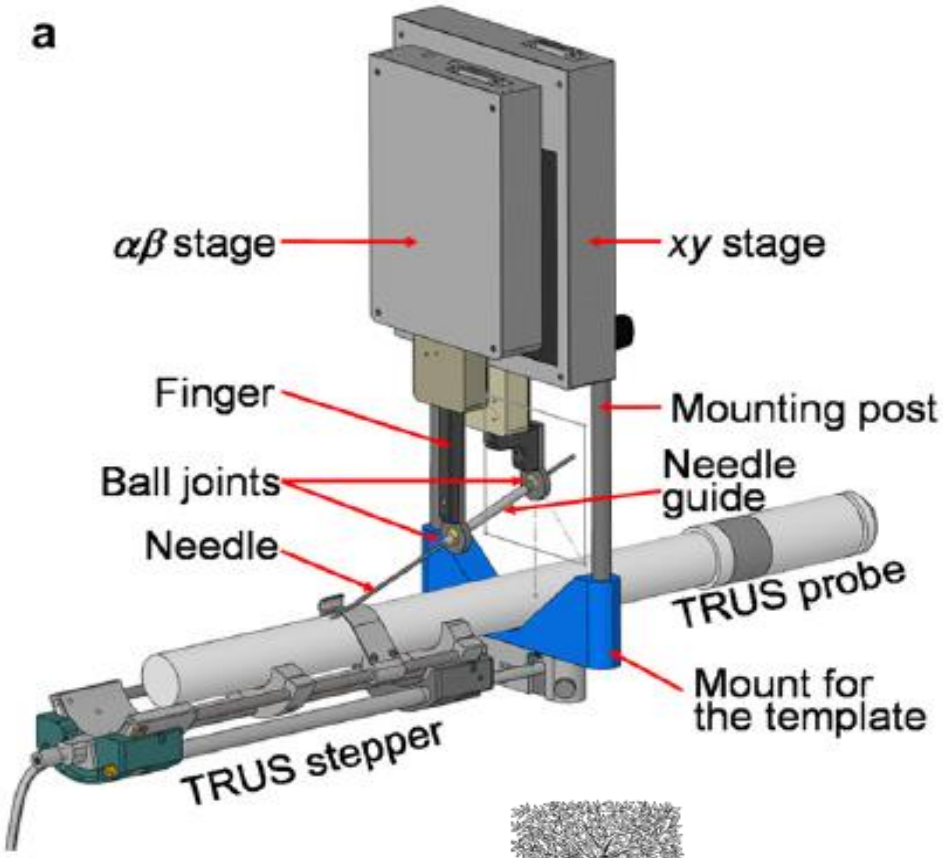

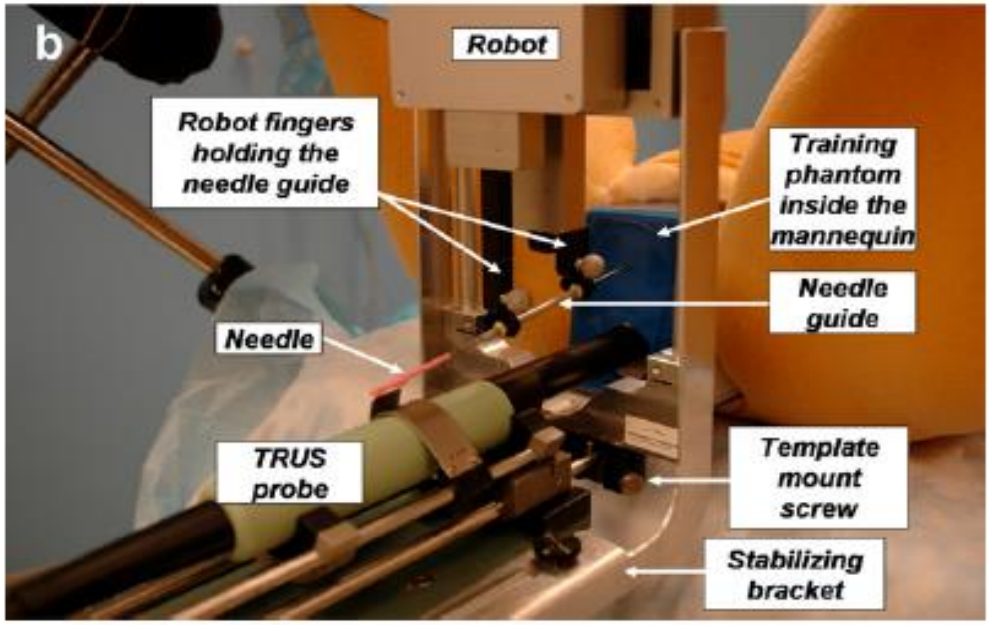

Fig. 1. (a) Computer-generated image of robot positioner mounted onto stepper with ultrasound probe, with depiction of *xy* and *αβ* stages. (b) Photograph of robot positioner on stepper with ultrasound probe in

ELSEVIER

BRACHYTHERAPY

Brachytherapy 10 (2011) 57–63

Robotic needle guide for prostate brachytherapy: Clinical testing of feasibility and performance

Danny Y. Song[1,*], Everette C. Burdette[2,3], Jonathan Fiene[4], Elwood Armour[1], Gernot Kronreif[5], Anton Deguet[3], Zhe Zhang[6], Iulian Iordachita[3], Gabor Fichtinger[3,7], Peter Kazanzides[3]

[1]*Department of Radiation Oncology and Molecular Radiation Sciences, Johns Hopkins University, Baltimore, MD*
[2]*Acoustic Medsystems, Inc., Urbana-Champaign, IL*
[3]*Computer Science, Johns Hopkins University, Baltimore, MD*
[4]*Mechanical Engineering and Applied Mechanics, University of Pennsylvania, Philadelphia, PA*
[5]*Austrian Center for Medical Innovation and Technology, Wiener Neustadt, Austria*
[6]*Oncology Biostatistics, Johns Hopkins University, Baltimore, MD*
[7]*Computer Science, Queen's University, Kingston, Ontario, Canada*

Summary

- Numerous possibilities for LDR and HDR sources
- Discriminate RAL system features across manufacturers
- Diligence needed by medical physicists to remaining tech savvy
- Future BT developments will grow more complicated with technology
- Medical physicist should decide technology for clinic

Acknowledgements

Dimos Baltas, University of Freiburg, Germany
Bruce Thomadsen, University of Wisconsin, USA
Jack Venselaar, Instituut Verbeeten, The Netherlands

Valencia, 07 – 10 October 2018

ESTRO School

Advanced Brachytherapy Physics

WWW.ESTRO.ORG/SCHOOL

The Principles of Imaging based Treatment Planning

Dimos Baltas, Ph.D.

Professor for Medical Physics in Radiation Oncology

Division of Medical Physics
Department of Radiation Oncology, Medical Center - University of Freiburg
Faculty of Medicine, University of Freiburg, Germany
and
German Cancer Consortium (DKTK), Partner Site Freiburg, Germany

E-mail: dimos.baltas@uniklinik-freiburg.de

ESTRO School

List of Content

- BRT *versus* ERT from Dosimetry Point of View
- BRT *versus* ERT from RTP-Workflow Point of View
- Introduction to Localisation
- DVH-Evaluation and Prescription
- Introduction to Dynamic and Adaptive Planning

ESTRO School

Modern Radiation Therapy

BRT *versus* ERT Similarities and Differences

- Dosimetric Kernel
- Delivery Technology
- Dose Distribution

ESTRO School

Modern Radiation Therapy

BRT *versus* ERT Similarities and Differences

The Field / Beam:

ERT

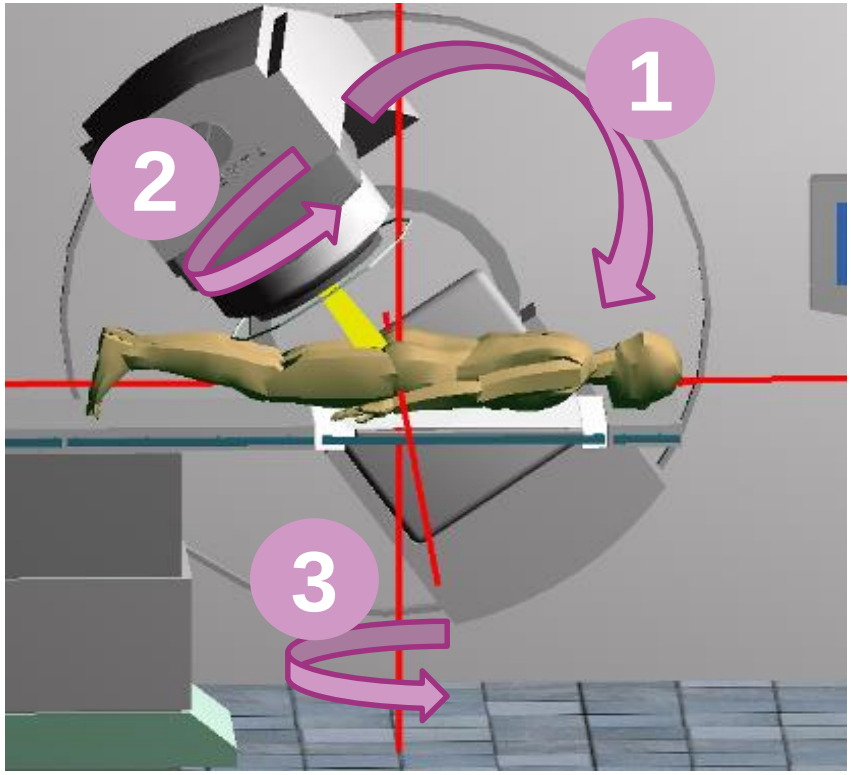

BRT

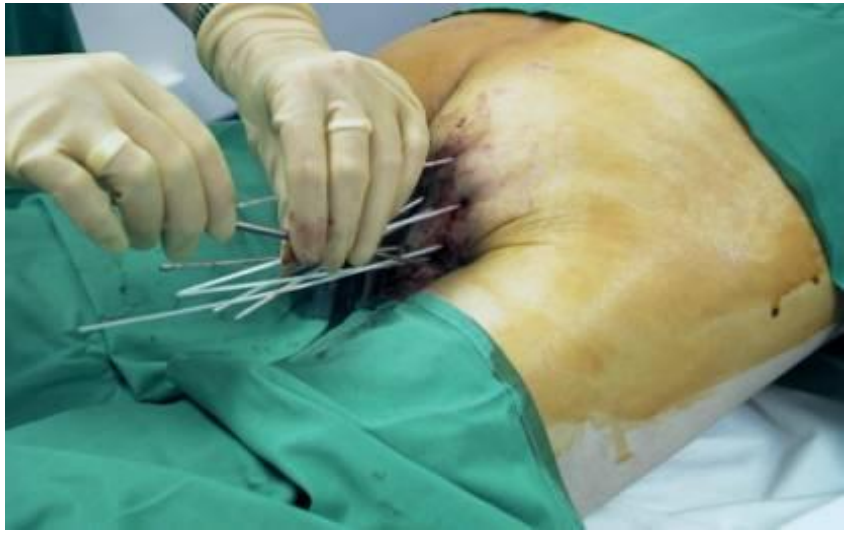

ESTRO School

Modern Radiation Therapy

BRT *versus* ERT Similarities and Differences

Beam Shaping: Plane

Field

MLC

2.5 mm
or
5.0 mm
or
10.0 mm

ERT

Catheter/Needle/Applicator

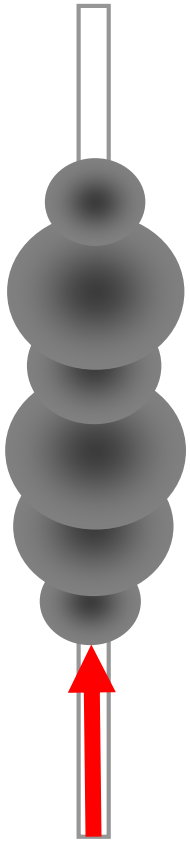

- 1.0 mm
- 2.5 mm
- 5.0 mm
- 10.0 mm
- ?? mm

MSS

BRT

ESTRO School

Modern Radiation Therapy

BRT *versus* ERT Similarities and Differences

Dosimetric Kernel

ERT **10 : 1** **BRT**

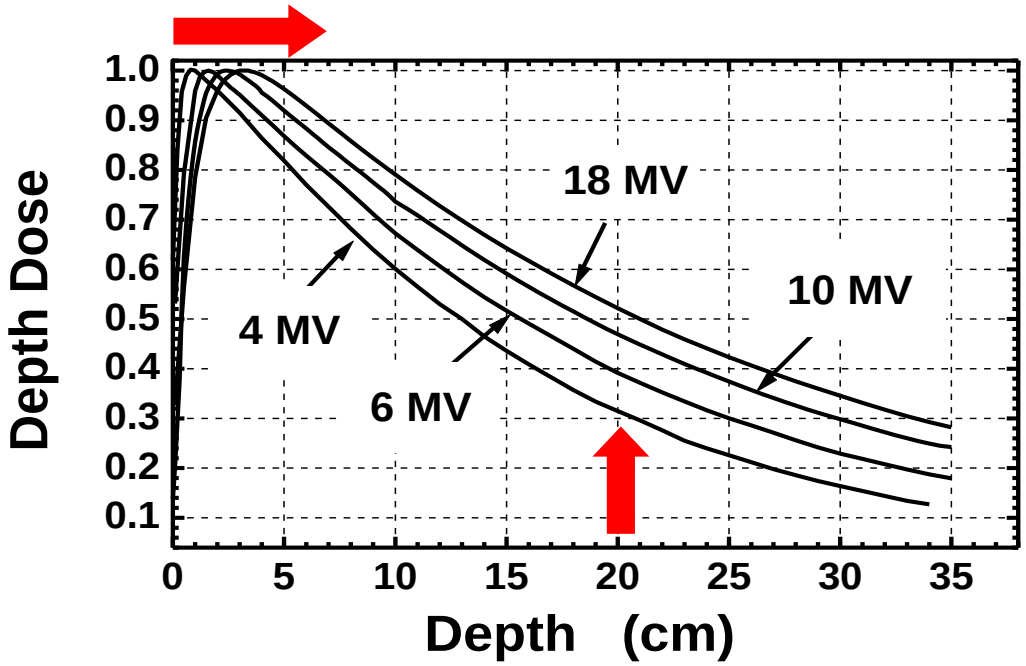

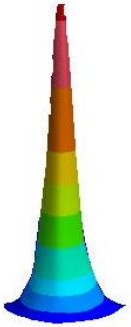

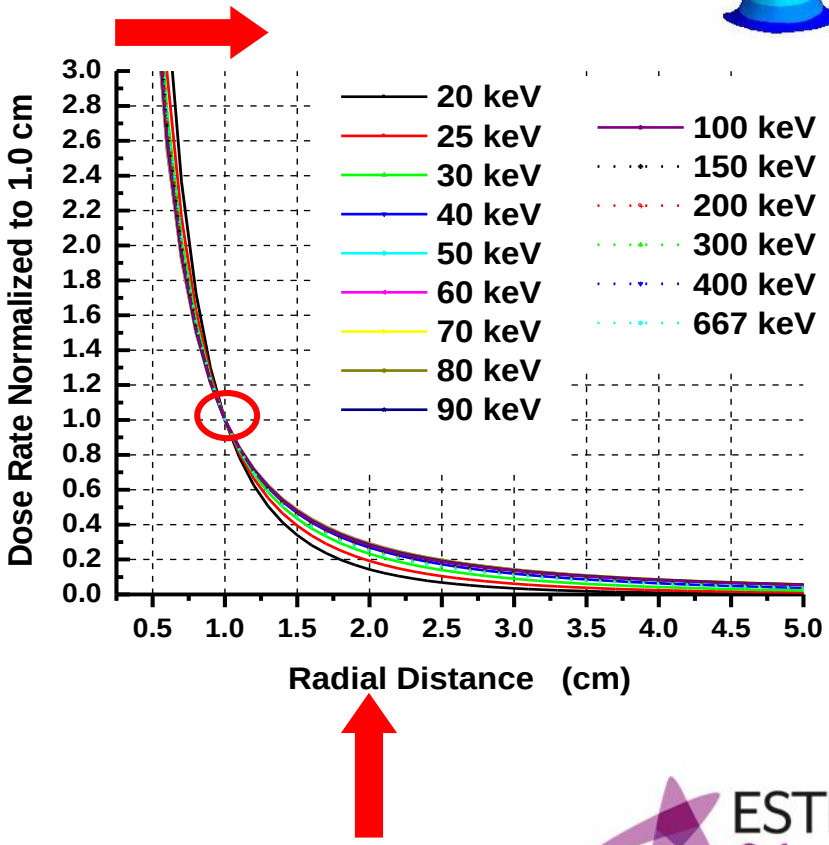

ESTRO School

Modern Radiation Therapy

BRT *versus* ERT Similarities and Differences

Dosimetric Kernel

ERT

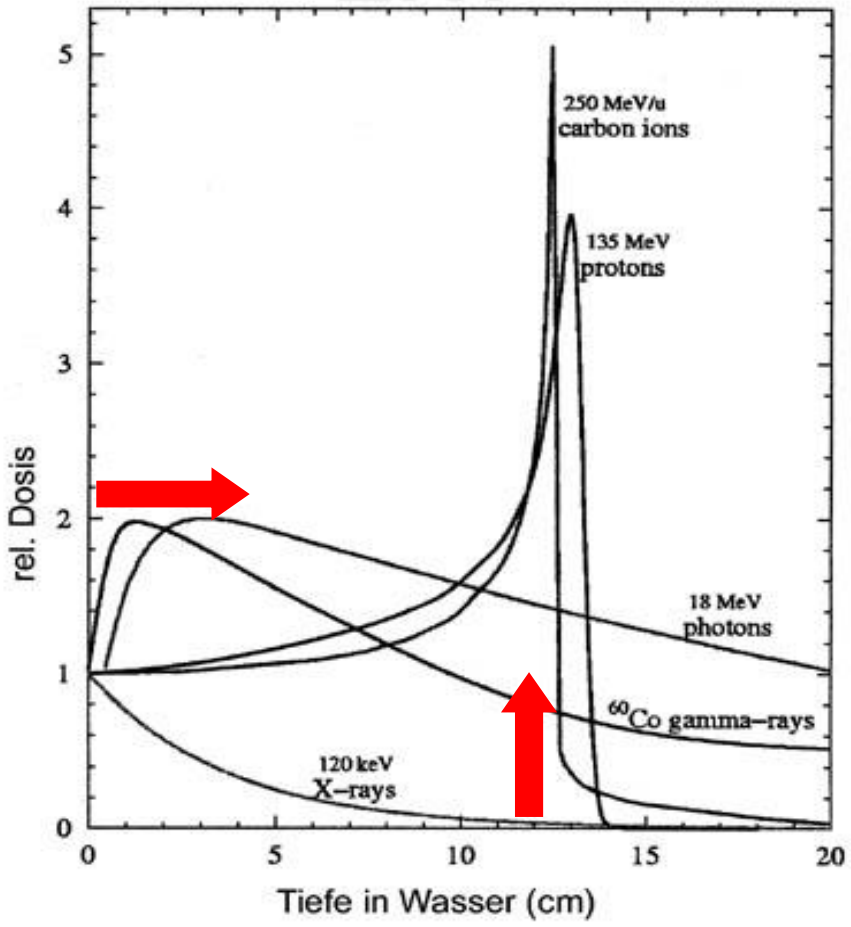

BRT

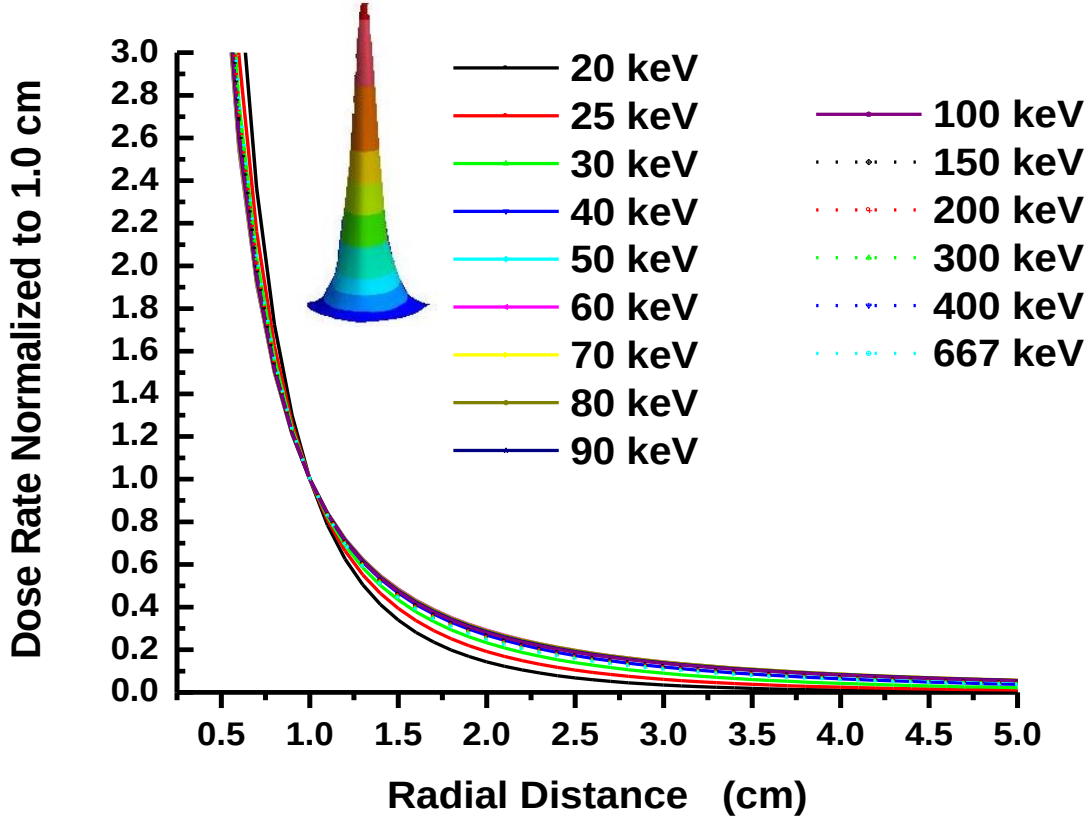

Modern Radiation Therapy

BRT *versus* ERT Similarities and Differences

Dosimetric Kernel

BRT

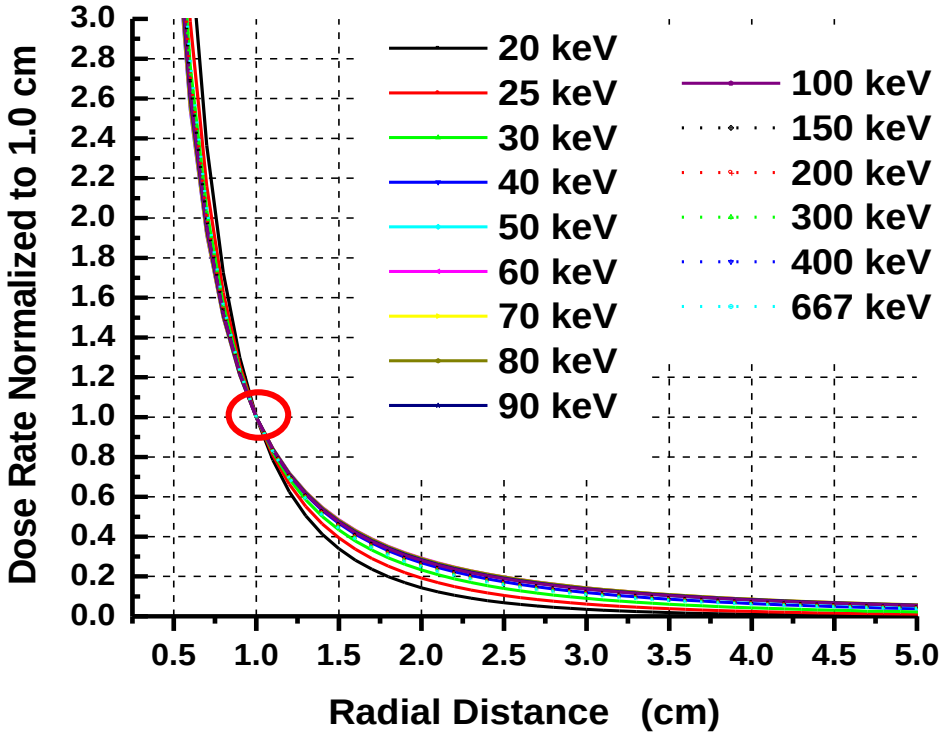

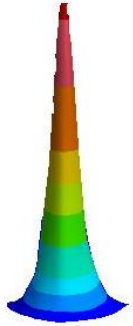

BRT

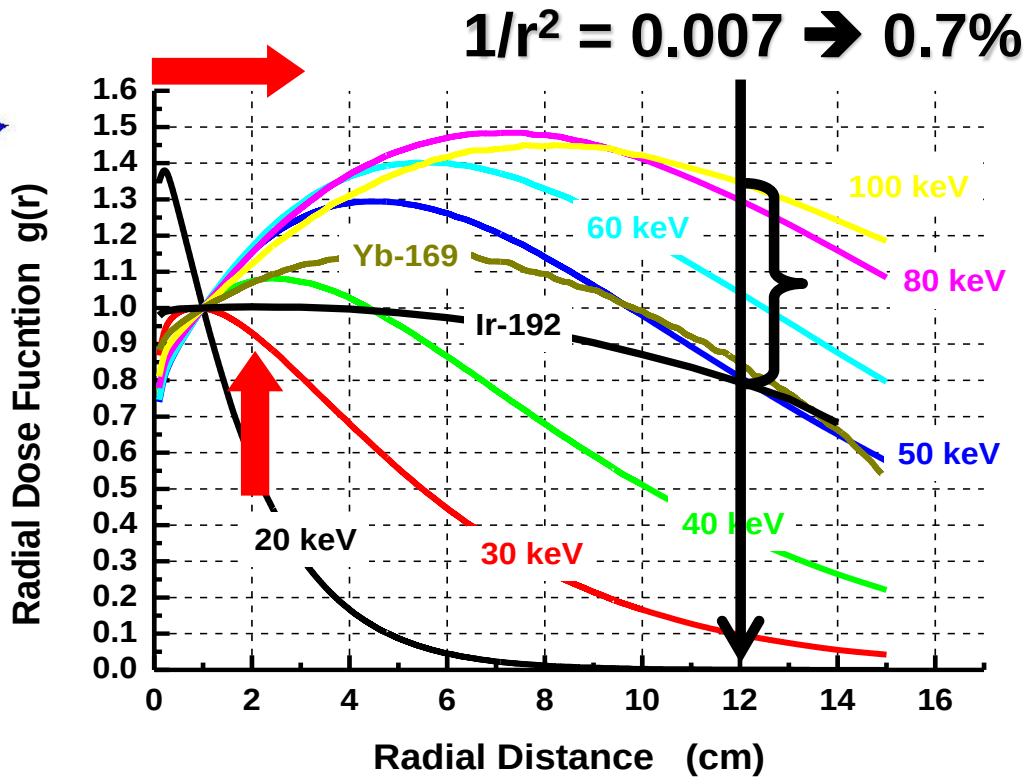

Modern Radiation Therapy

BRT *versus* ERT Similarities and Differences

Delivery Technology: Intensity Modulation (2D)

ERT

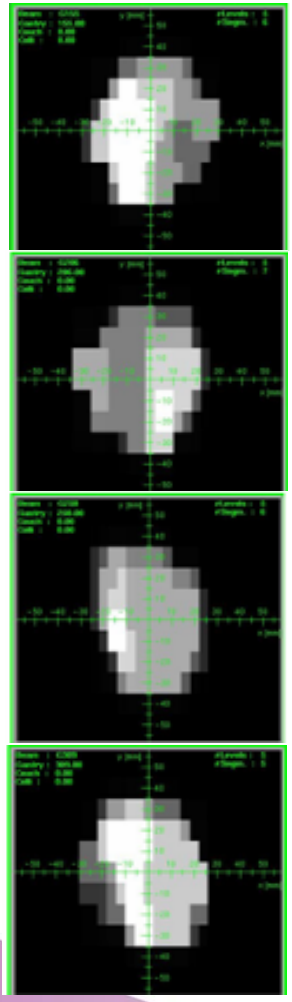

BRT

MSS: Step & Shoot

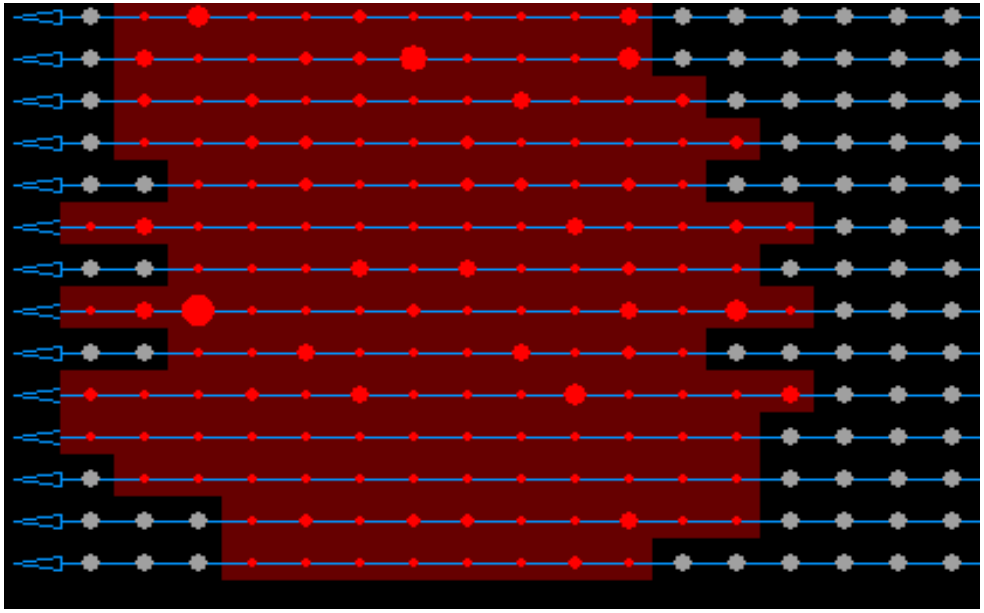

“Bixel” ⇔ Dwell Position

“MUs” ⇔ Dwell Time

ESTRO School

Modern Radiation Therapy

Delivery Technology

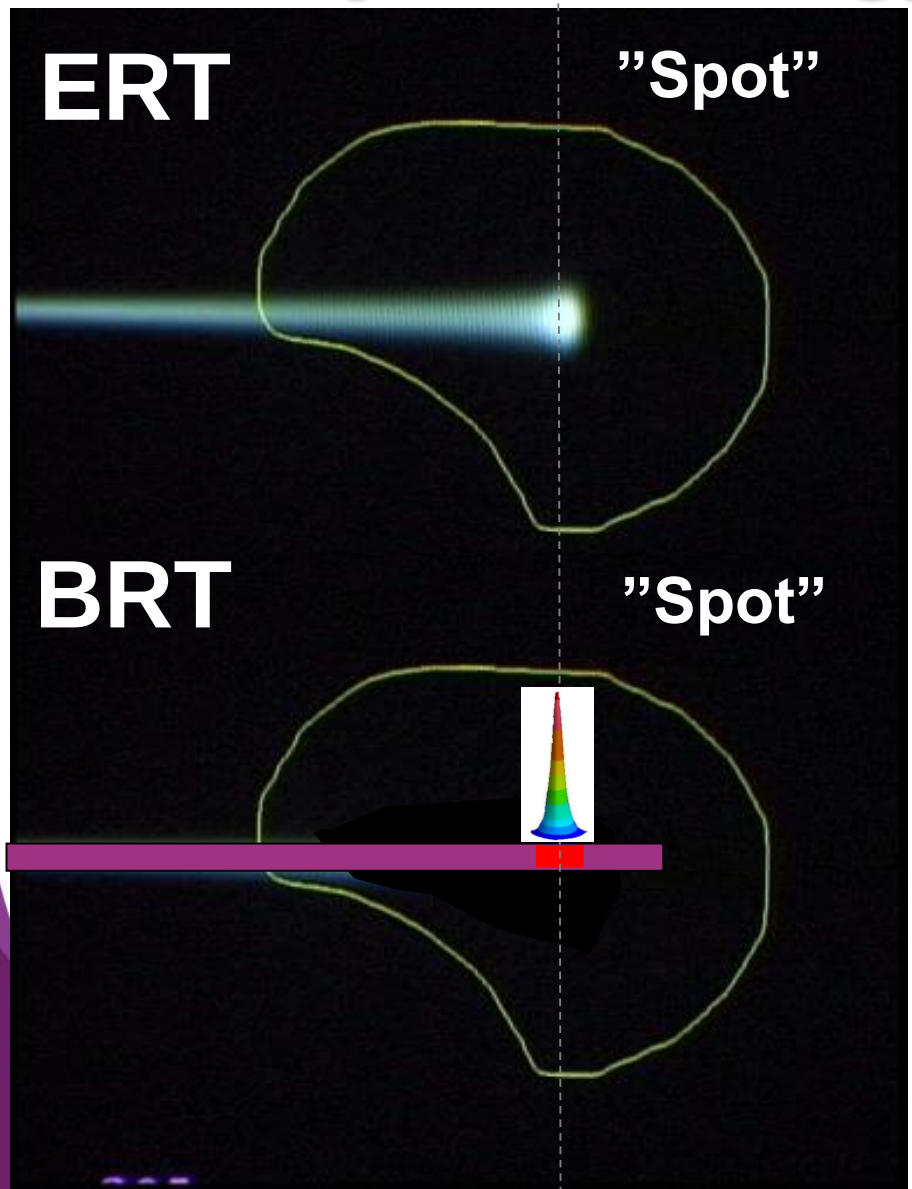

Energy ⇔ Dwell Position (3D)

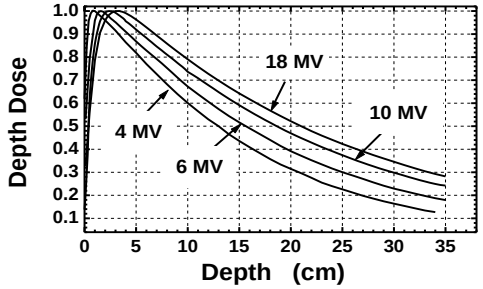

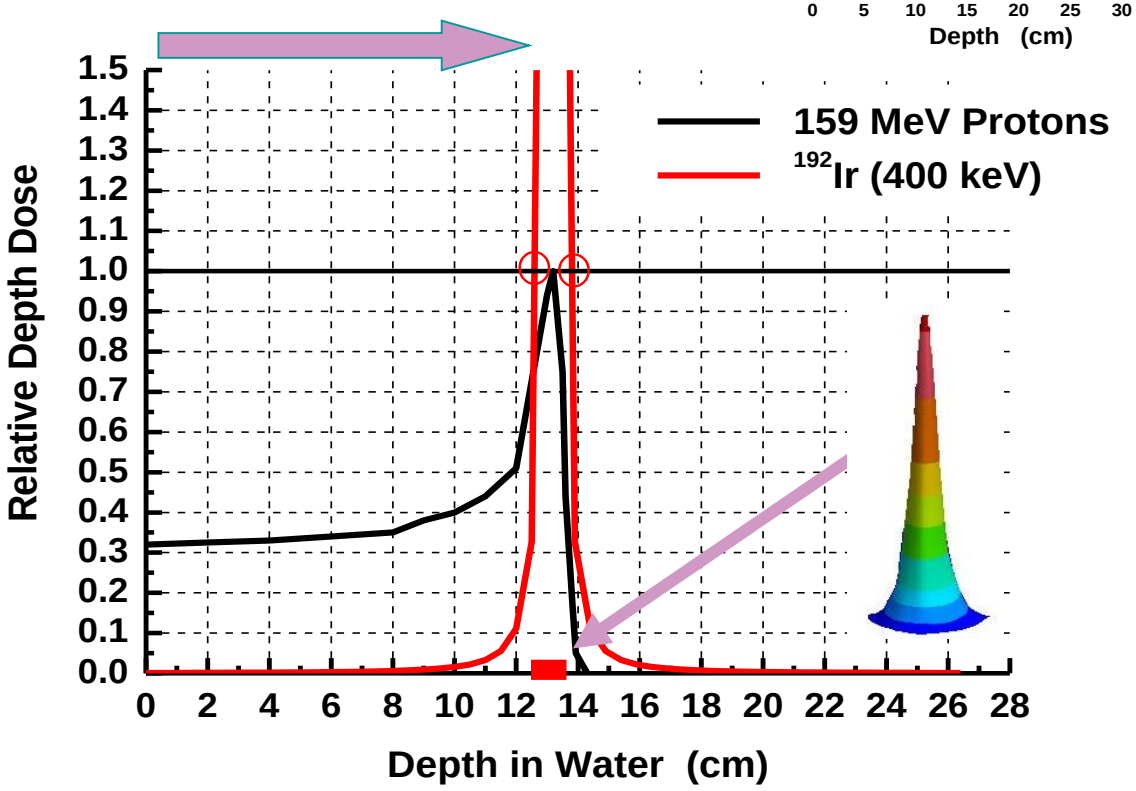

Modern Radiation Therapy

Delivery Technology

Energy ⇔ Dwell Position (3D)

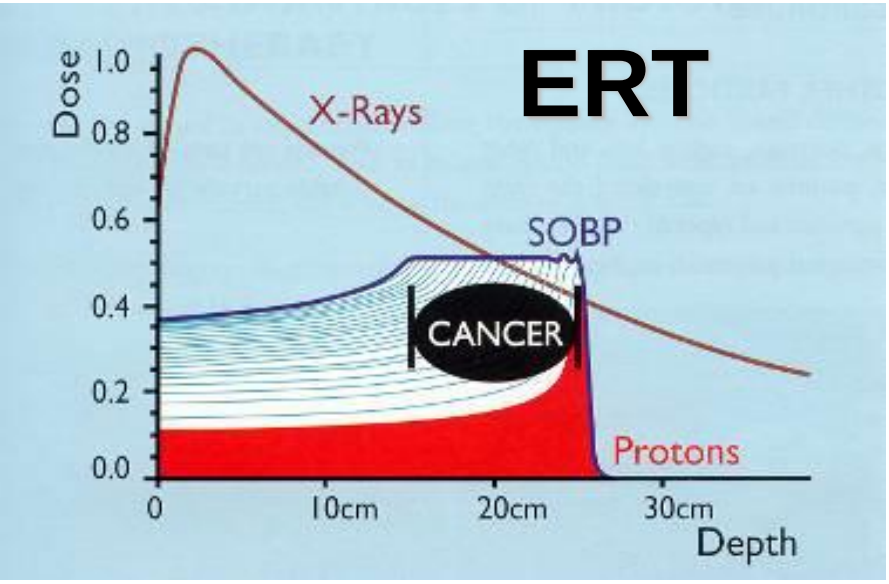

BRT

”Multi-Spots”

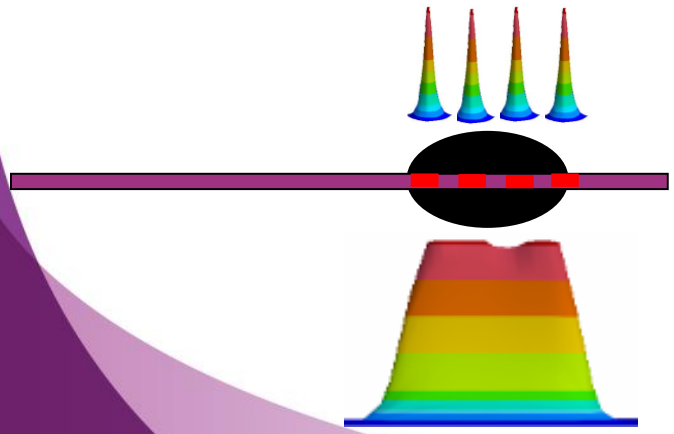

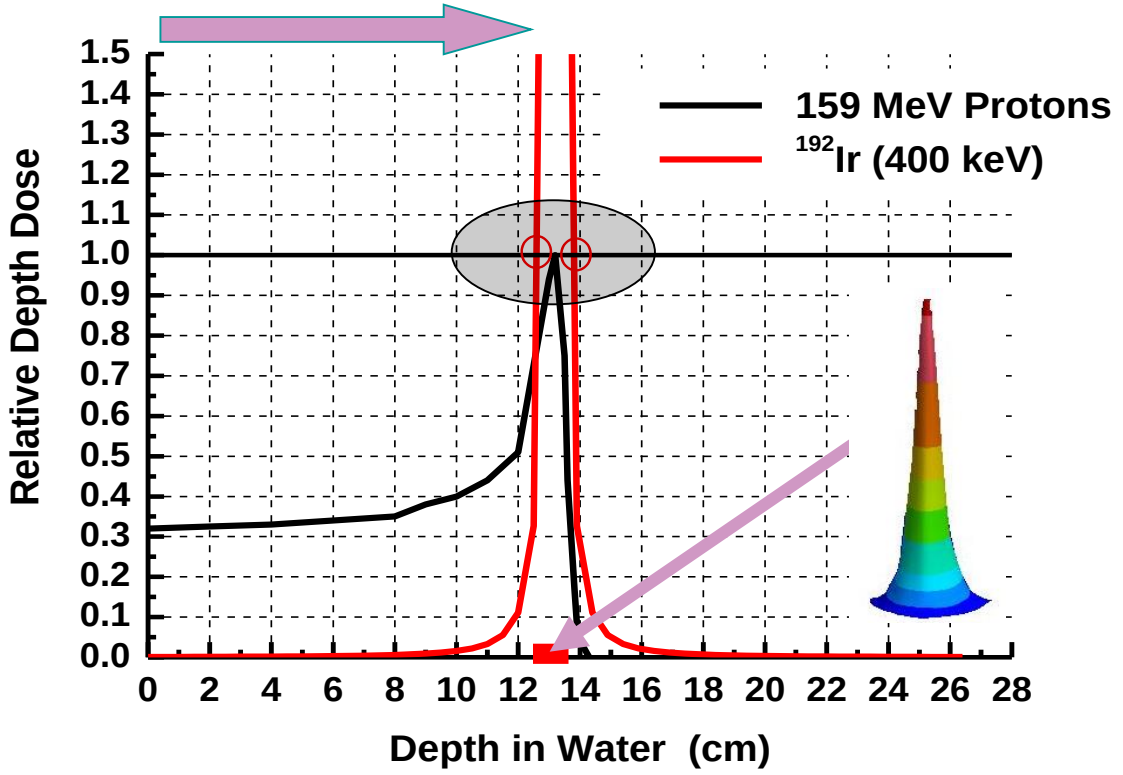

Modern Radiation Therapy

BRT *versus* ERT Similarities and Differences

Summary - I

Dosimetric Kernel → **Particles** ✓
(Spot)

Delivery Technology → **IMRT (X, P)** ✓
(Modulation, Dose-Volume-Prescription)

Dose Distribution → **SRS / SBRT** ?
(Inhomogeneity)

ESTRO School

Modern Radiation Therapy

Dose Distribution: Inhomogeneity

SRS

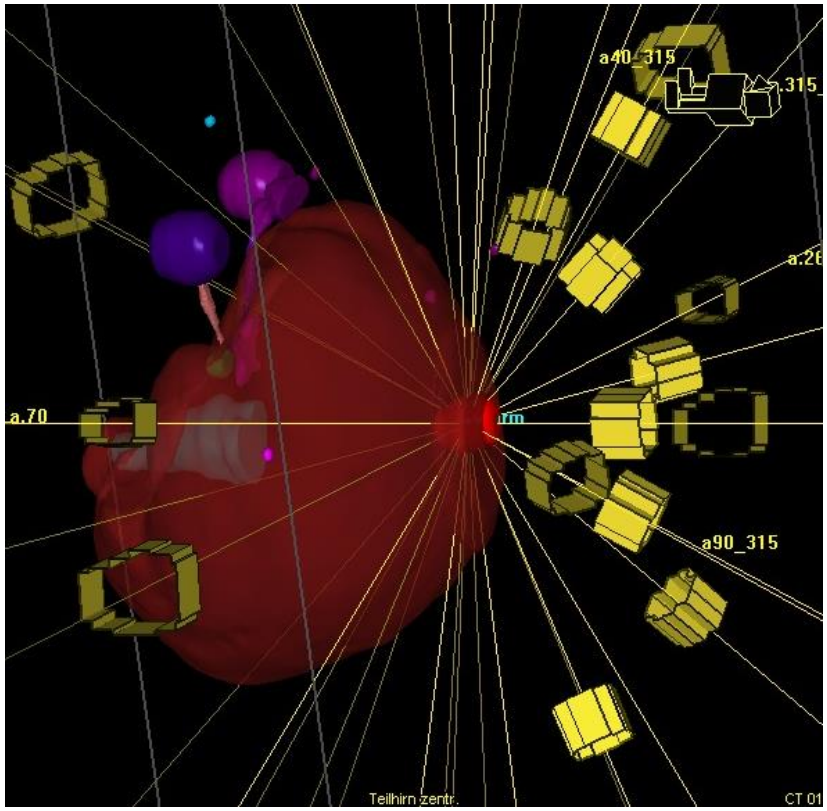

BRT

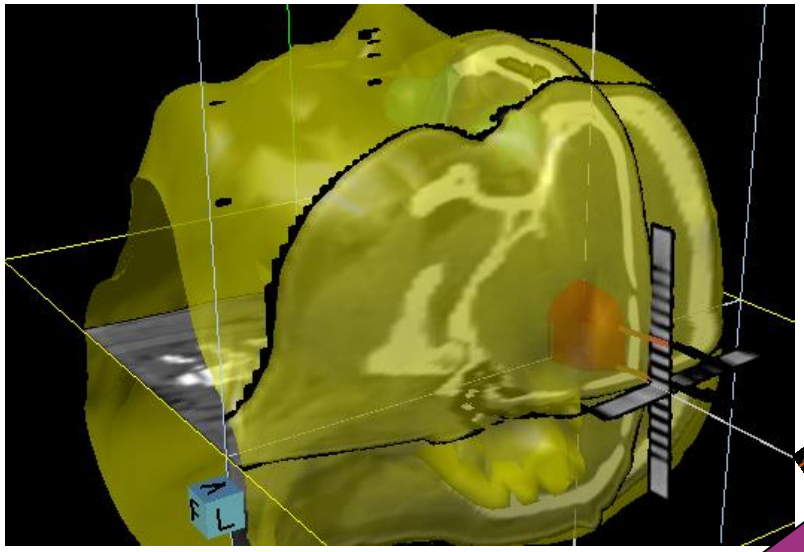

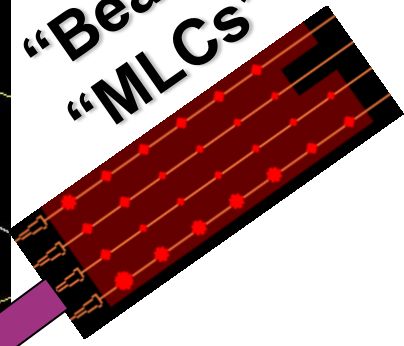

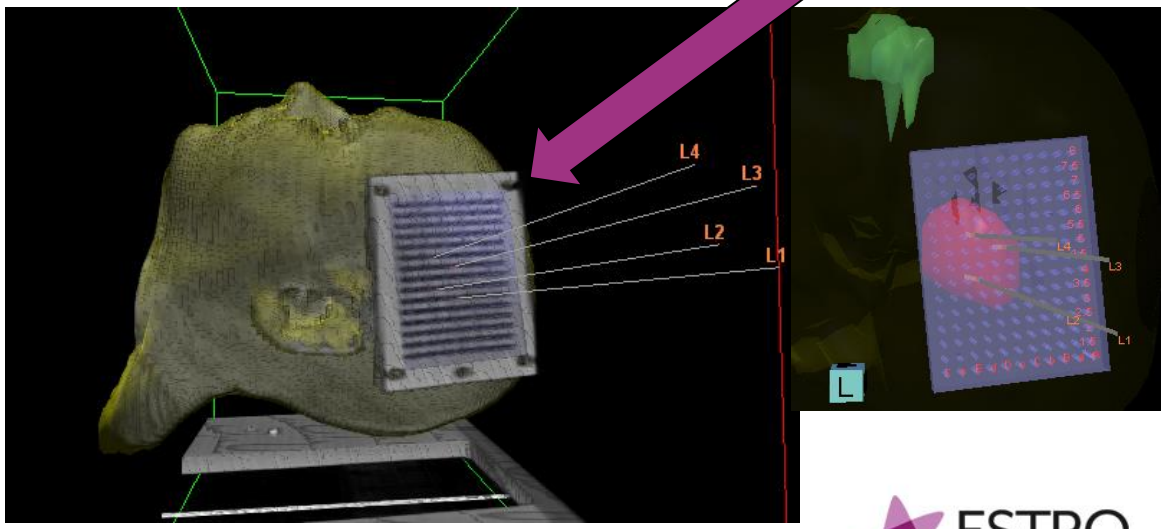

ESTRO School

Modern Radiation Therapy

Dose Distribution: Inhomogeneity

SRS

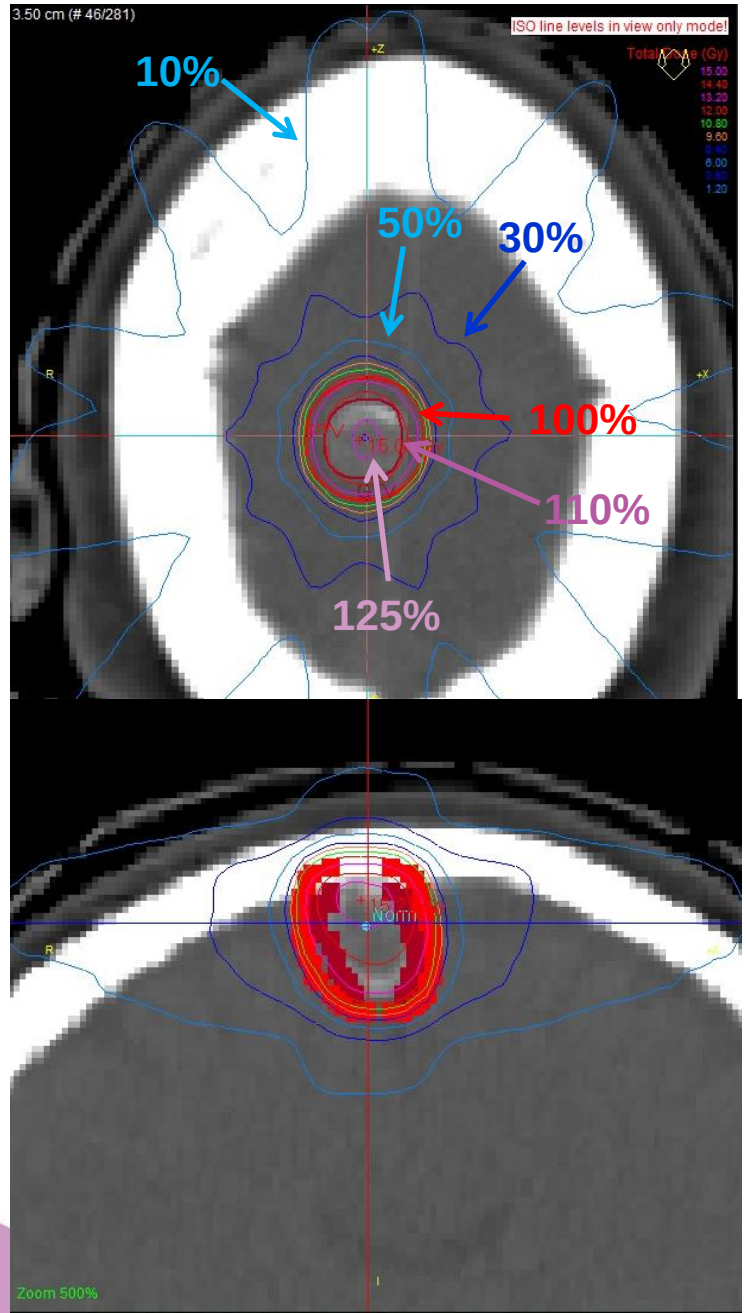

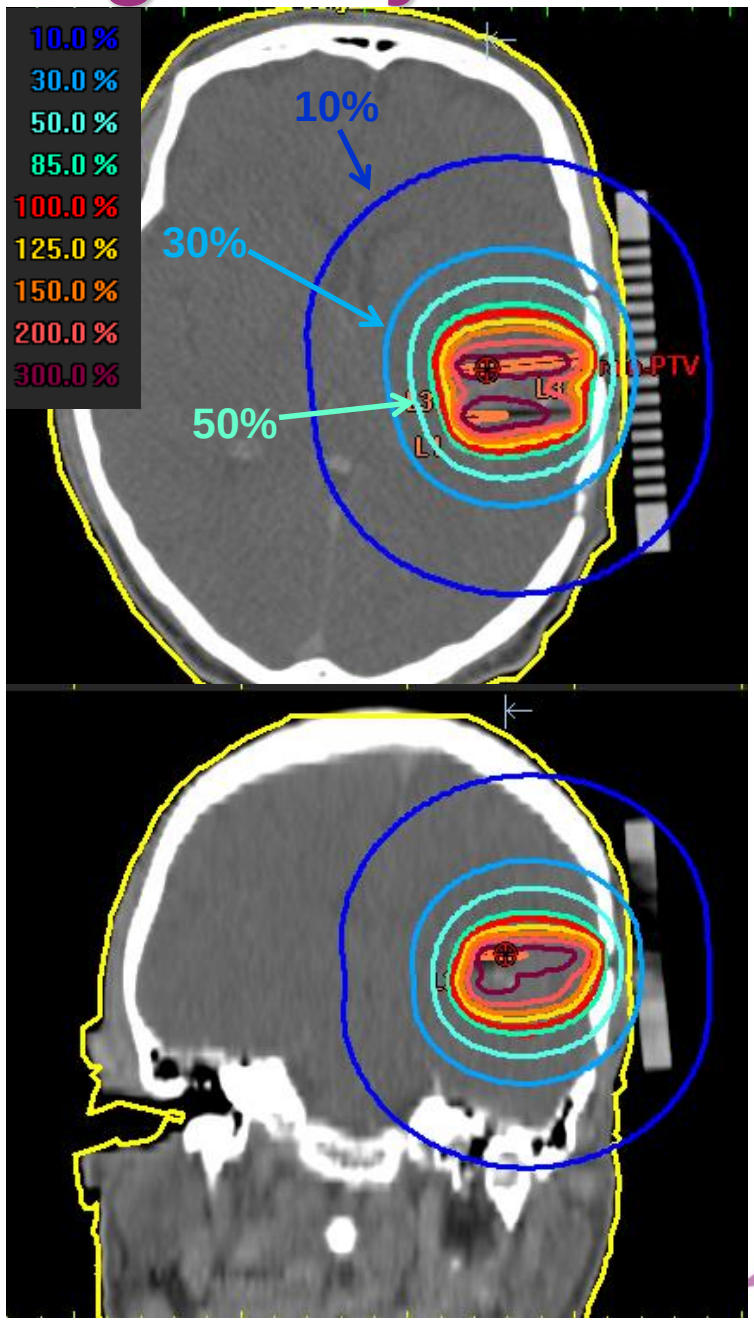

BRT

ESTRO School

Modern Radiation Therapy

Dose Distribution: Inhomogeneity

SRS

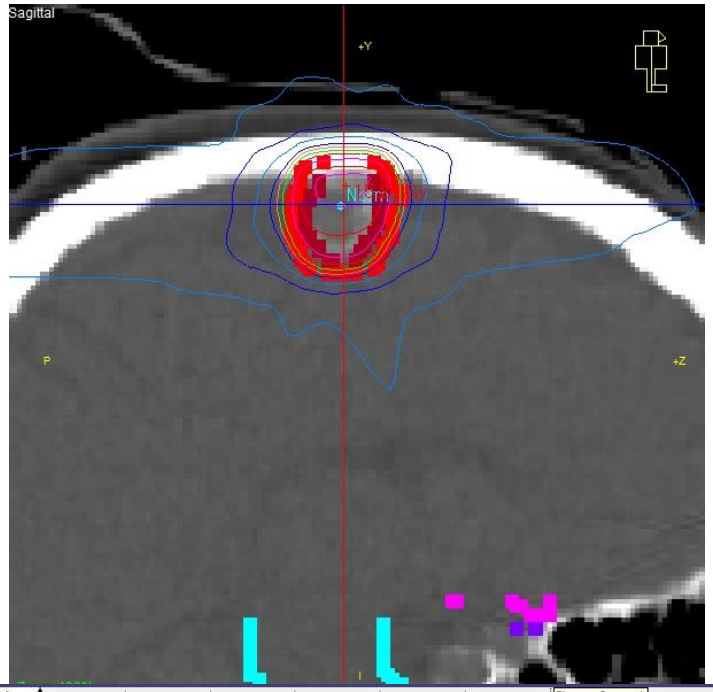

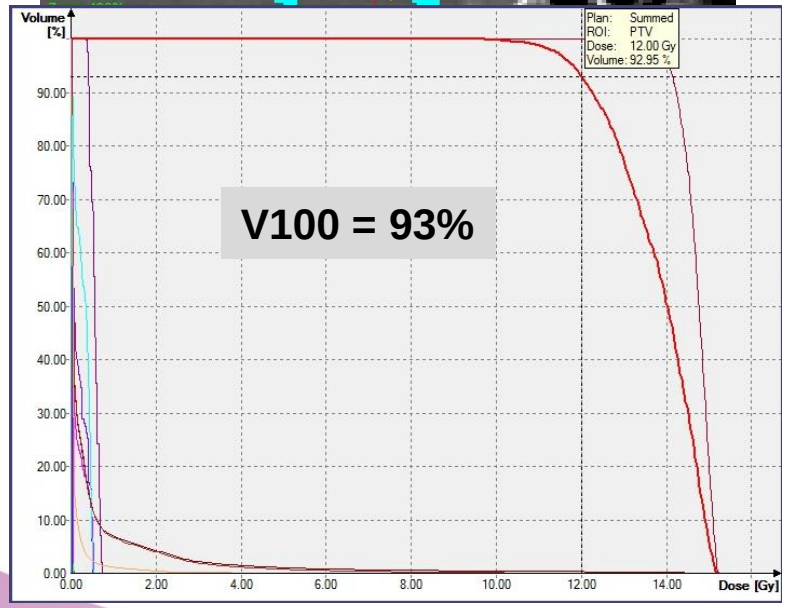

BRT

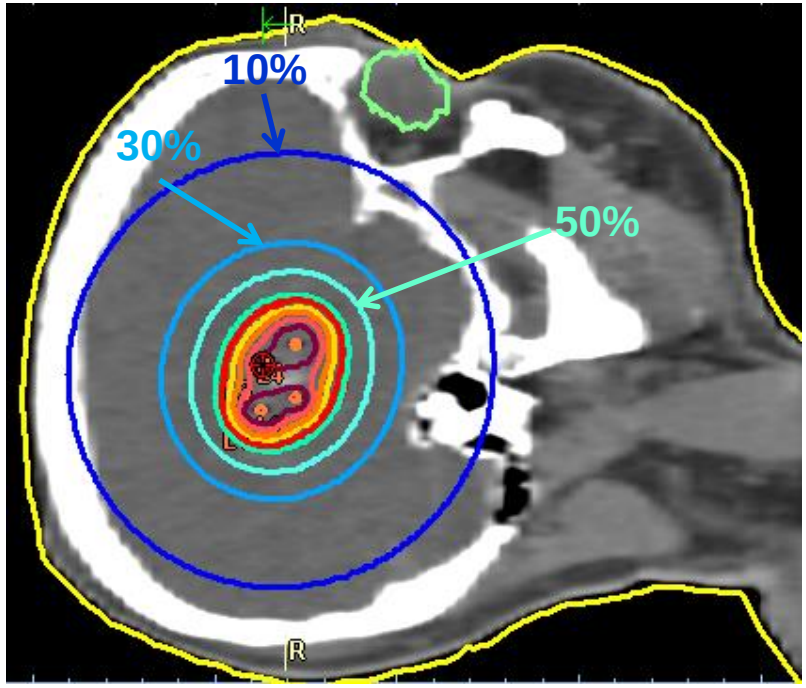

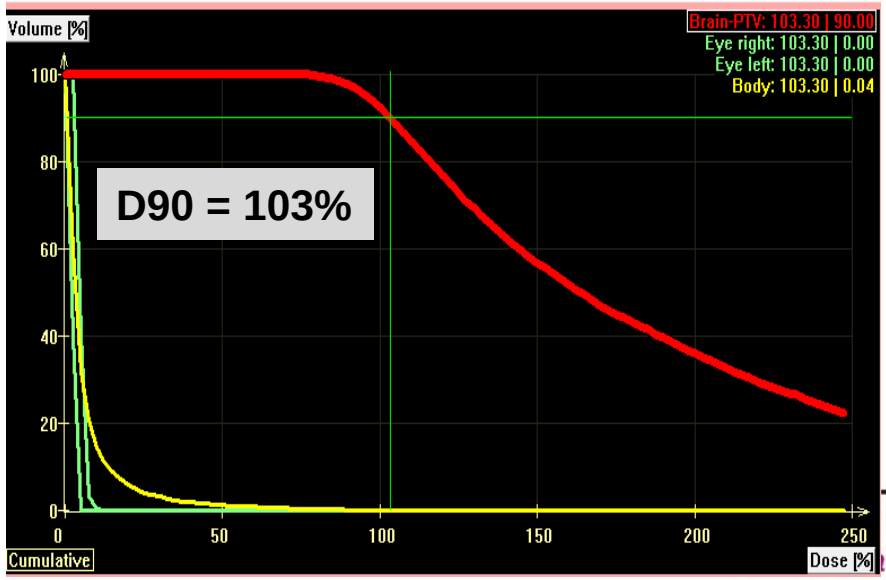

Modern Radiation Therapy: Gradients …

ELSEVIER

CrossMark

BRACHYTHERAPY

Brachytherapy 16 (2017) 884–892

Physics

Iridium-Knife: Another knife in radiation oncology

Natasa Milickovic[1,*,4], Nikolaos Tselis[2,3,4], Efstratios Karagiannis[2,5], Konstantinos Ferentinos[2], Nikolaos Zamboglou[2,6]

[1]*Department of Medical Physics and Engineering, Sana Klinikum Offenbach, Offenbach, Germany*
[2]*Department of Radiation Oncology, Sana Klinikum Offenbach, Offenbach, Germany*
[3]*Department of Radiotherapy and Oncology, J. W. Goethe University, Frankfurt am Main, Germany*

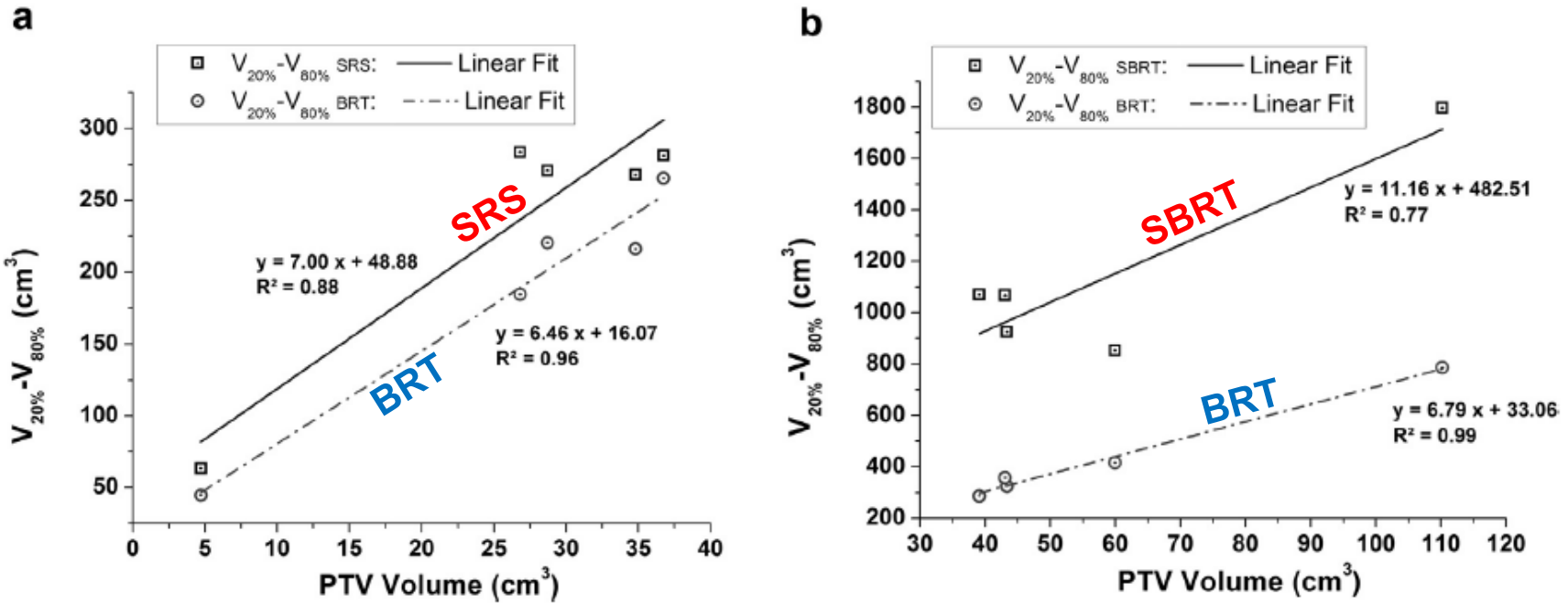

Fig. 2. Comparison of the volume of healthy tissue beyond the PTV covered by dose between the 20% and 80% of prescribed dose between (a) HDR BRT and SRS plans and (b) HDR BRT and SBRT plans. There is no significant difference ($p = 0.397$) between the $V_{20\%}-V_{80\%}$ of SRS and HDR BRT plans. The $V_{20\%}-V_{80\%}$ of SBRT and HDR BRT are significantly different with $p = 0.003$ in favor of HDR BRT. The $V_{20\%}-V_{80\%}$ parameter of HDR BRT plans increases slower with increase of the PTV compared with that of X-Knife. The $V_{20\%}-V_{80\%}$ is expressed in cm^3. PTV = planning target volume; HDR = high-dose-rate; BRT = brachytherapy; SRS = stereotactic radiosurgery; SBRT = stereotactic body radiation therapy.

ESTRO School

Modern Radiation Therapy

BRT *versus* ERT Similarities and Differences

Summary - II

Dosimetric Kernel → **Particles** ✓
(Spot)

Delivery Technology → **IMRT (X, P)** ✓
(Modulation, Dose-Volume-Prescription)

Dose Distribution → **SRS / SBRT** ✓
(Inhomogeneity)

List of Content

- BRT *versus* ERT from Dosimetry Point of View
- BRT *versus* ERT from RTP-Workflow Point of View
- Introduction to Localisation
- DVH-Evaluation and Prescription
- Introduction to Dynamic and Adaptive Planning

ESTRO School

Modern Radiation Therapy

Workflow / Processes in ERT Treatment Planning

- Immobilization
- Positioning
- External Coordinate System
- CT-Acquisition
- 3D-Patient Model
- VOI-Definition
- Prescription
- Beam Configuration
- Fluence Adjustment
- DVH-Evaluation
- Treatment Parameters Transfer

Model-Based

3D-Patient Model

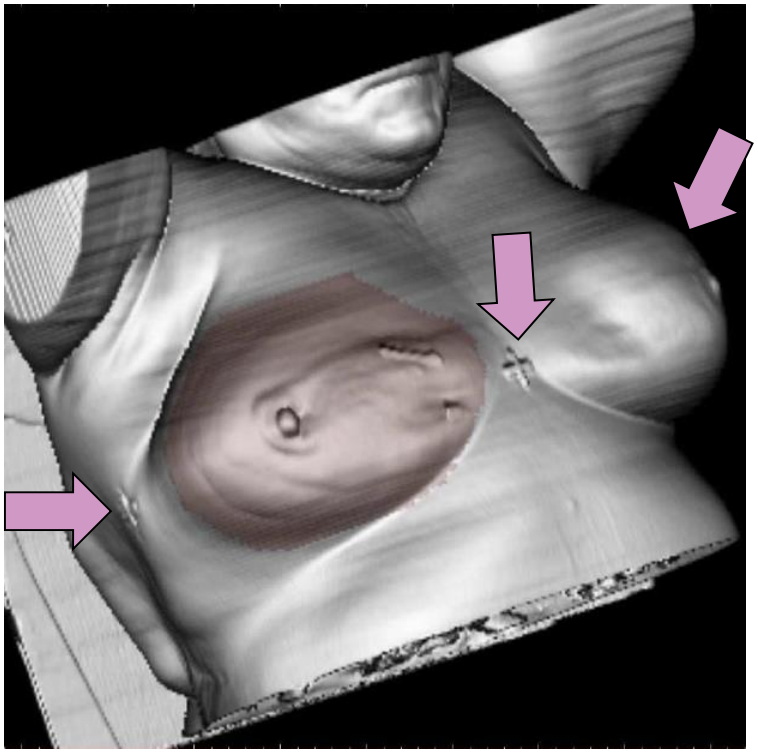

Reference Point / Coordinate System

ESTRO School

Modern Radiation Therapy

BRT *versus* ERT Similarities and Differences

- Immobilization
- Positioning
- External Coordinate System
- Implantation (Catheters = Beams)
- CT-Acquisition
- 3D-Patient Model
- VOI-Definition
- Prescription
- Beam Configuration → Localisation
- Fluence Adjustment
- DVH-Evaluation
- Treatment Parameters Transfer

Model-Based

3D-Patient Model

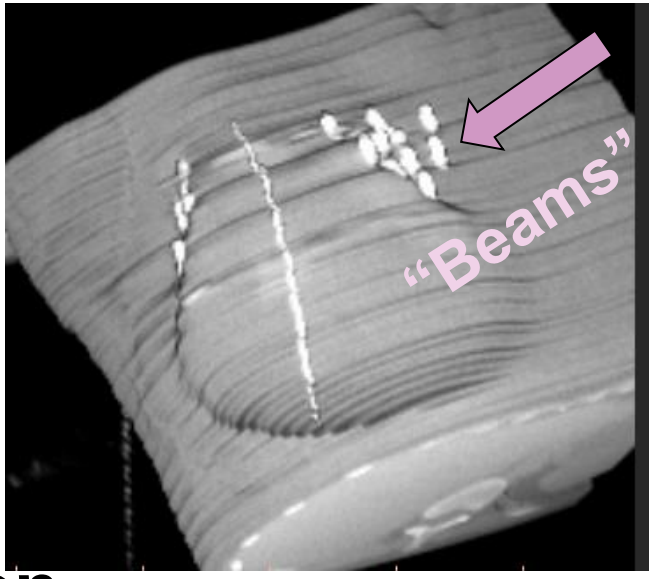

ESTRO School

Modern Radiation Therapy

BRT *versus* ERT Similarities and Differences

3D-Patient Model: Anatomy (VOI) Definition

- GTV, CTV, PTV
- OARs

→ **CT: Artifact Reduction**

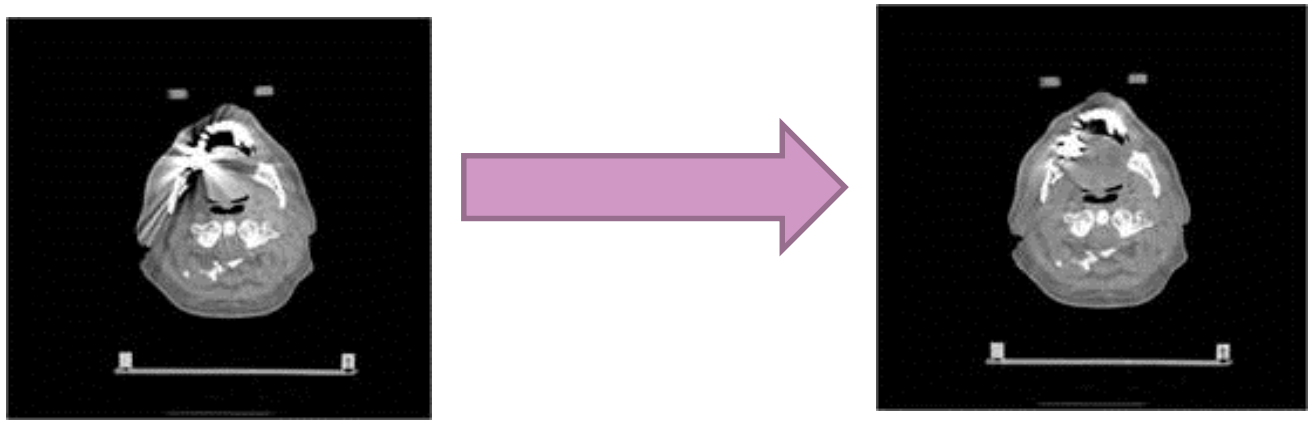

OMAR
By Courtesy of Philips CT Imaging

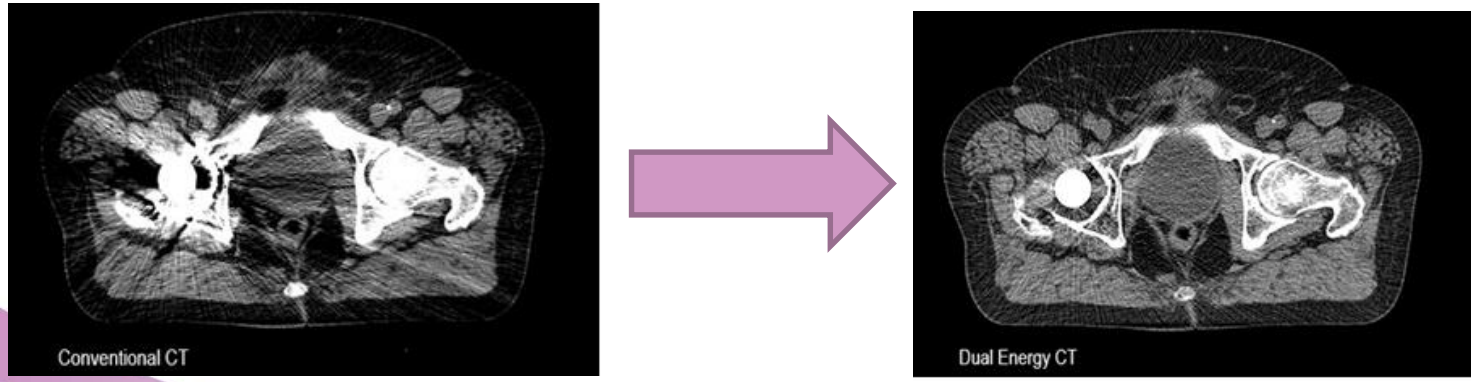

DECT-System by SIEMENS Healthcare, Germany

ESTRO School

Modern Radiation Therapy

BRT *versus* ERT Similarities and Differences

3D-Patient Model: Anatomy (VOI) Definition

- GTV, CTV, PTV
- OARs

→ *with* implanted catheters

CT: Artifact Reduction

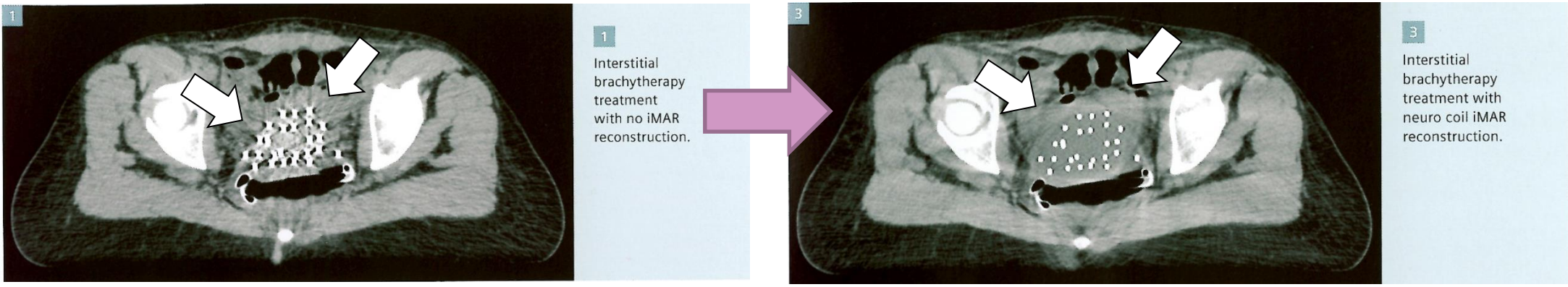

SIEMENS Healthcare, Germany: SOMATOM Definition AS Open – RT Pro edition

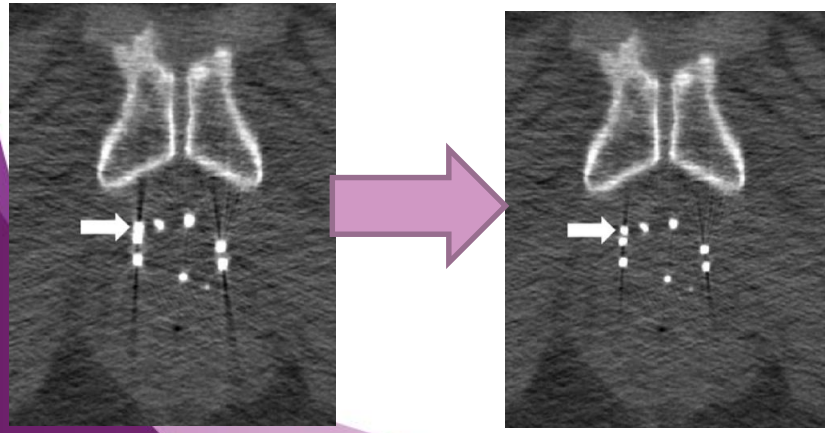

SEMAR, Aquilion ONE/ViSION edition, Toshiba Medical Systems

ELSEVIER
CrossMark
BRACHYTHERAPY
Brachytherapy 15 (2016) 768–773

Physics

Single-energy metal artifact reduction in postimplant computed tomography for I-125 prostate brachytherapy: Impact on seed identification

Yutaka Shiraishi*, Yoshitake Yamada*, Tomoki Tanaka, Takahisa Eriguchi, Shuichi Nishimura, Kayo Yoshida, Takashi Hanada, Toshio Ohashi, Naoyuki Shigematsu, Masahiro Jinzaki
Department of Radiology, Keio University School of Medicine, Tokyo, Japan

Modern Radiation Therapy

BRT *versus* ERT Similarities and Differences

3D-Patient Model: Anatomy (VOI) Definition

- GTV, CTV, PTV
- OARs

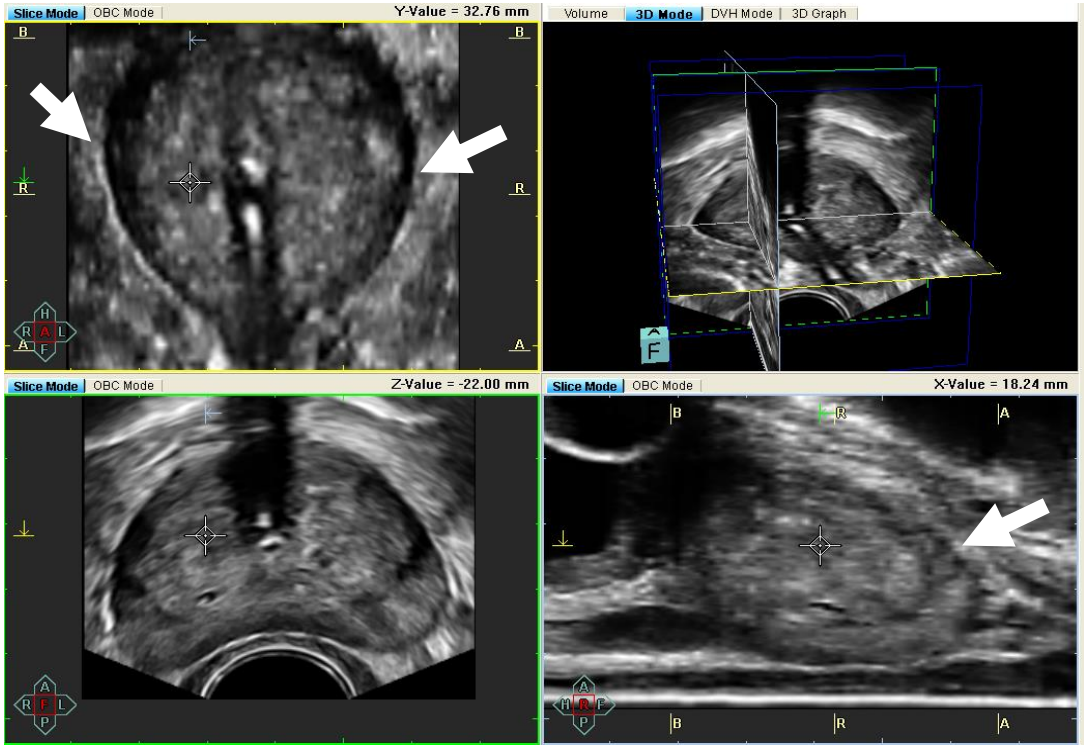

3D-U/S
***w/o* catheters**

Clinical Data and Images by courtesy of Dept. of Radiation Oncology, Offenbach, Germany

ESTRO School

Modern Radiation Therapy

BRT *versus* ERT Similarities and Differences

3D-Patient Model: Anatomy (VOI) Definition

- GTV, CTV, PTV
- OARs

→ ***w*** **implanted catheters**

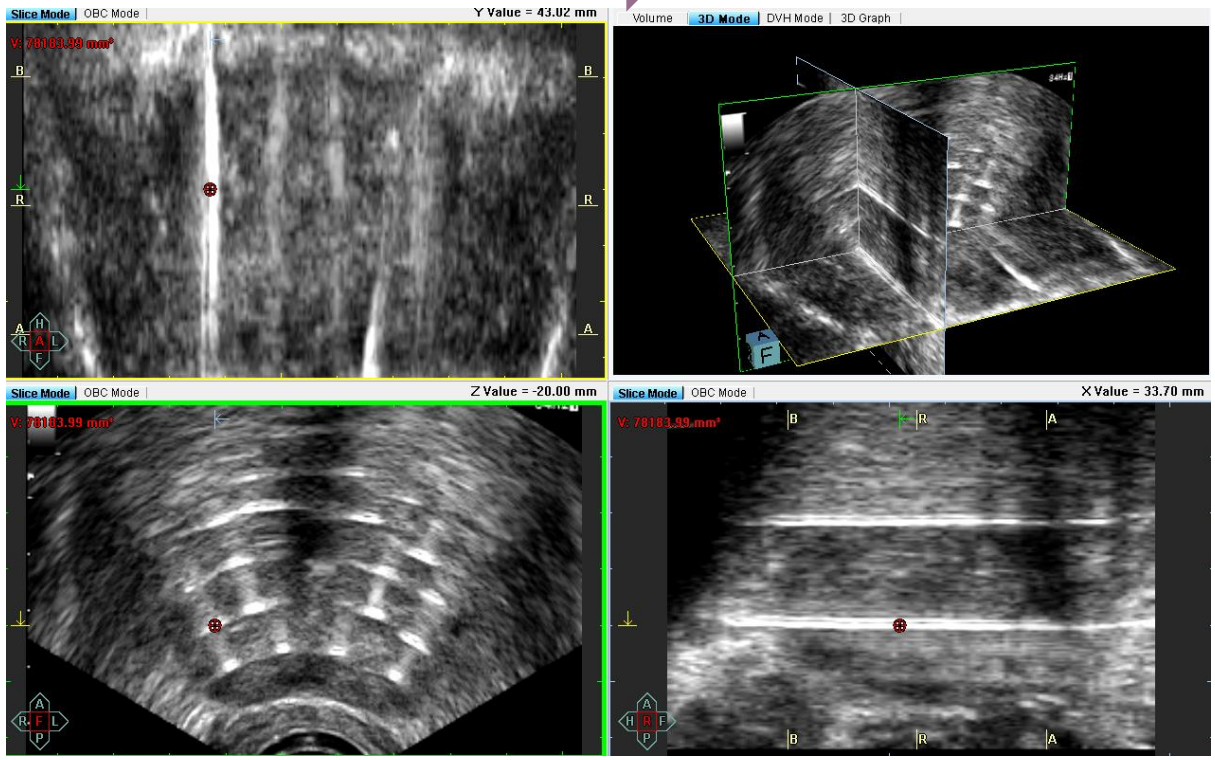

3D-U/S *with* metallic catheters

Clinical Data and Images by courtesy of Dept. of Radiation Oncology, Offenbach, Germany

ESTRO School

Modern Radiation Therapy

BRT *versus* ERT Similarities and Differences

3D-Patient Model: Catheter (Beam) Configuration

- **Localisation of Catheters/Applicators (Beams)**
- **Visual Control (BEV, skin projection)**
- **DRRs**

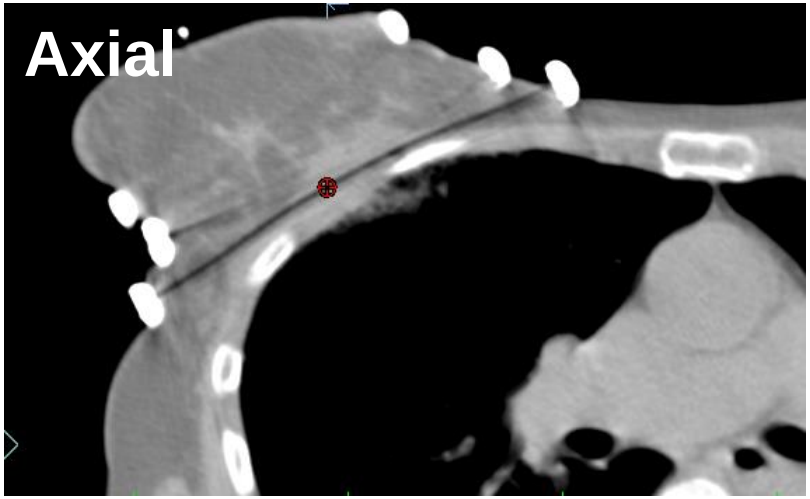

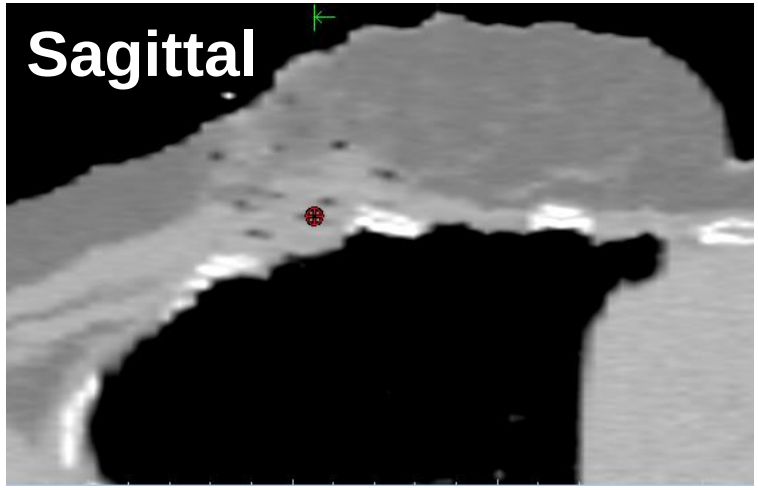

ESTRO School

Modern Radiation Therapy

BRT *versus* ERT Similarities and Differences

3D-Patient Model: Catheter (Beam) Configuration

- **Localisation of Catheters/Applicators (Beams)**
- **Visual Control (BEV, skin projection)**
- **DRRs**

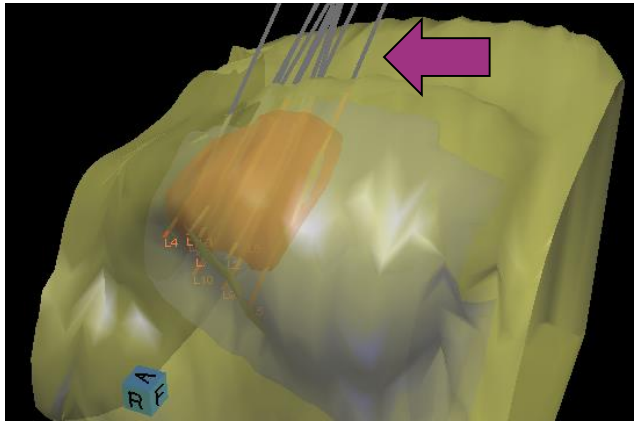

“Beams”

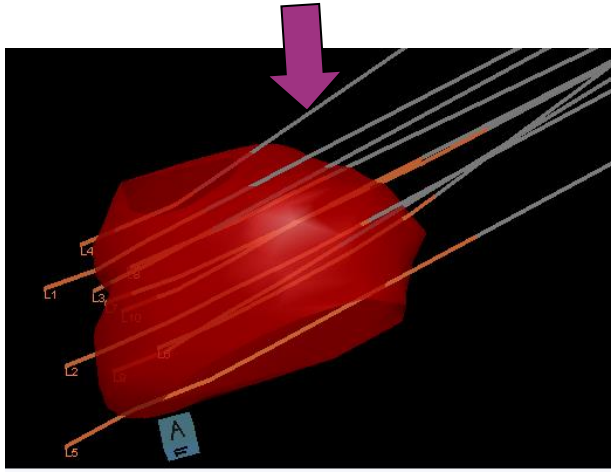

“MLCs”

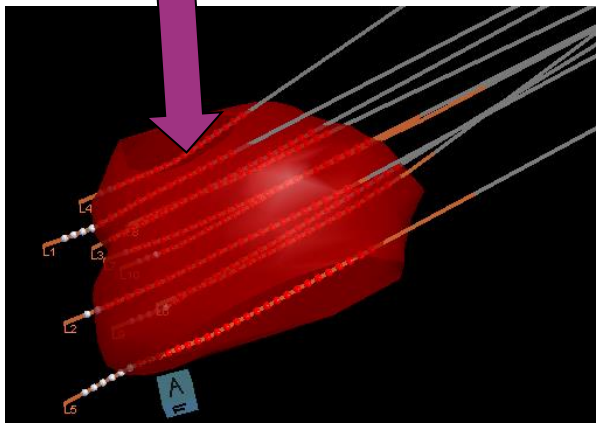

ESTRO School

List of Content

- BRT *versus* ERT from Dosimetry Point of View
- BRT *versus* ERT from RTP-Workflow Point of View
- **Introduction to Localisation**
- DVH-Evaluation and Prescription
- Introduction to Dynamic and Adaptive Planning

ESTRO School

Modern Brachytherapy Treatment Planning

Catheters/Applicators (Sources) Localisation

In contrast to ERT, where the set-up of the real Beams (irradiation) is based on:

- **Immobilization of the patient as in planning process (CT)**
- **(re)Positioning of the patient using the RP and the Machine Coordinate System (Laser Projection of Isocentre)**
  ➔ RP = Laser-Iso
- **Imaging-based (2D/3D, SIG) verification of Anatomy/Target position**
- **Fully automatic move: Plan-Isocenter ➔➔ Machine-Isocenter**
- **Fully automatic set-up of the beams and MLC-configurations**

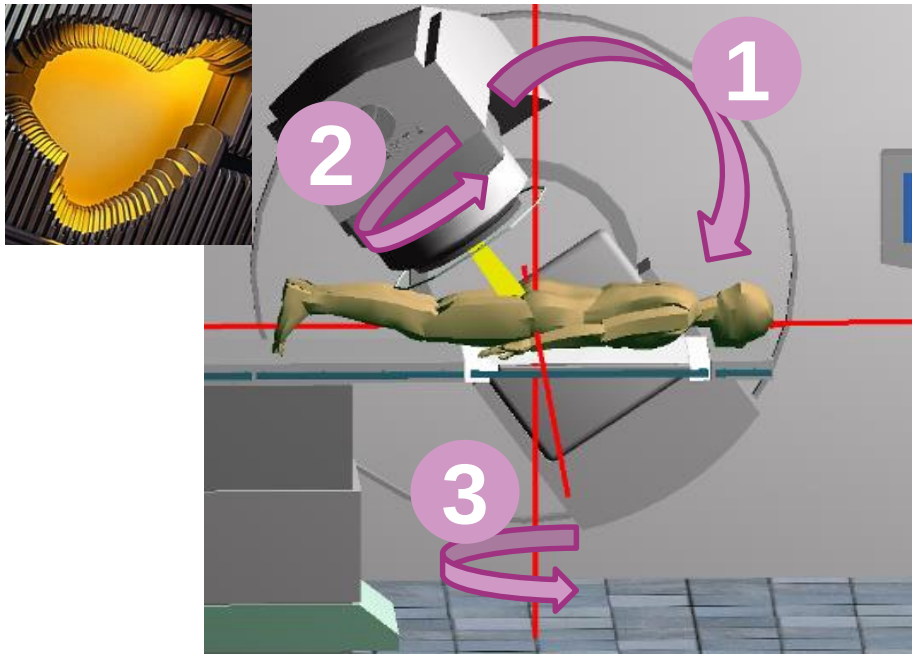

ESTRO School

In contrast to ERT, where the set-up of the real Beams (irradiation) is based on:

- **Immobilization of the patient as in planning process (CT)**

➔ **RP = Laser-Iso**

The Reference Point (RP)

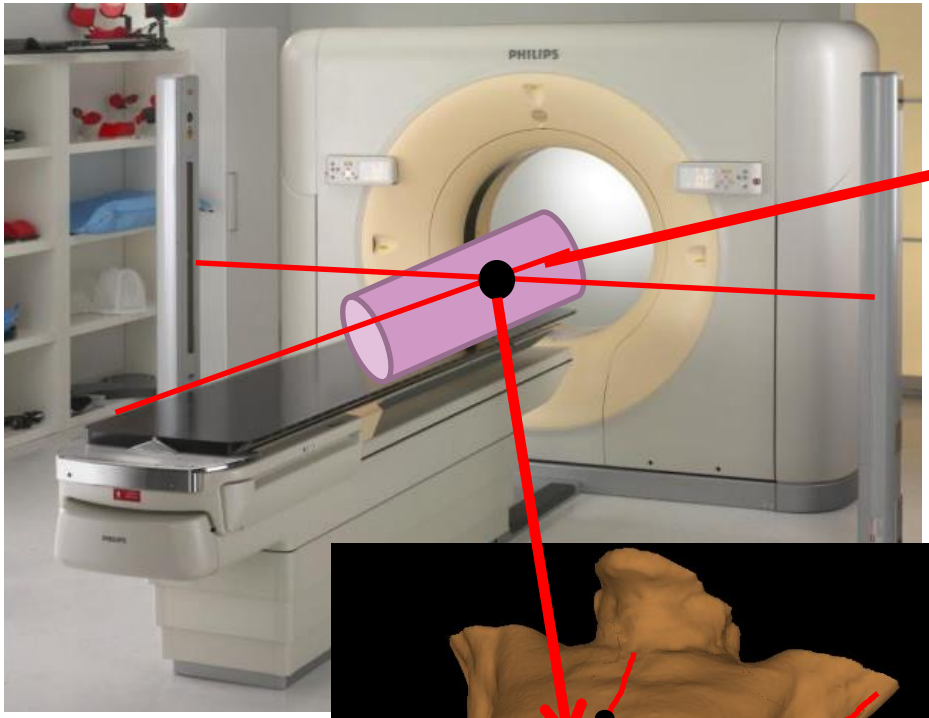

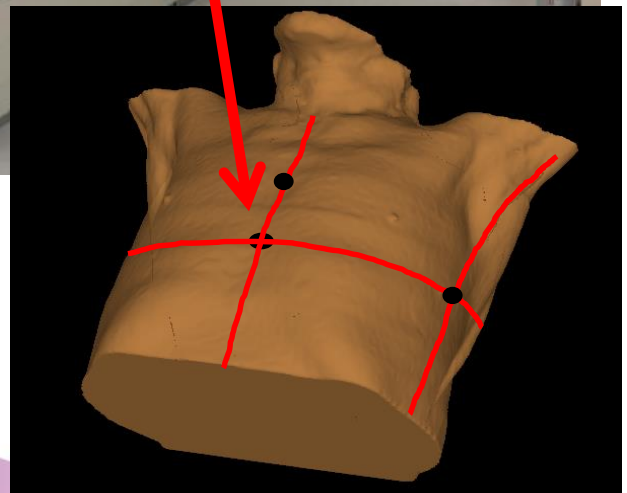

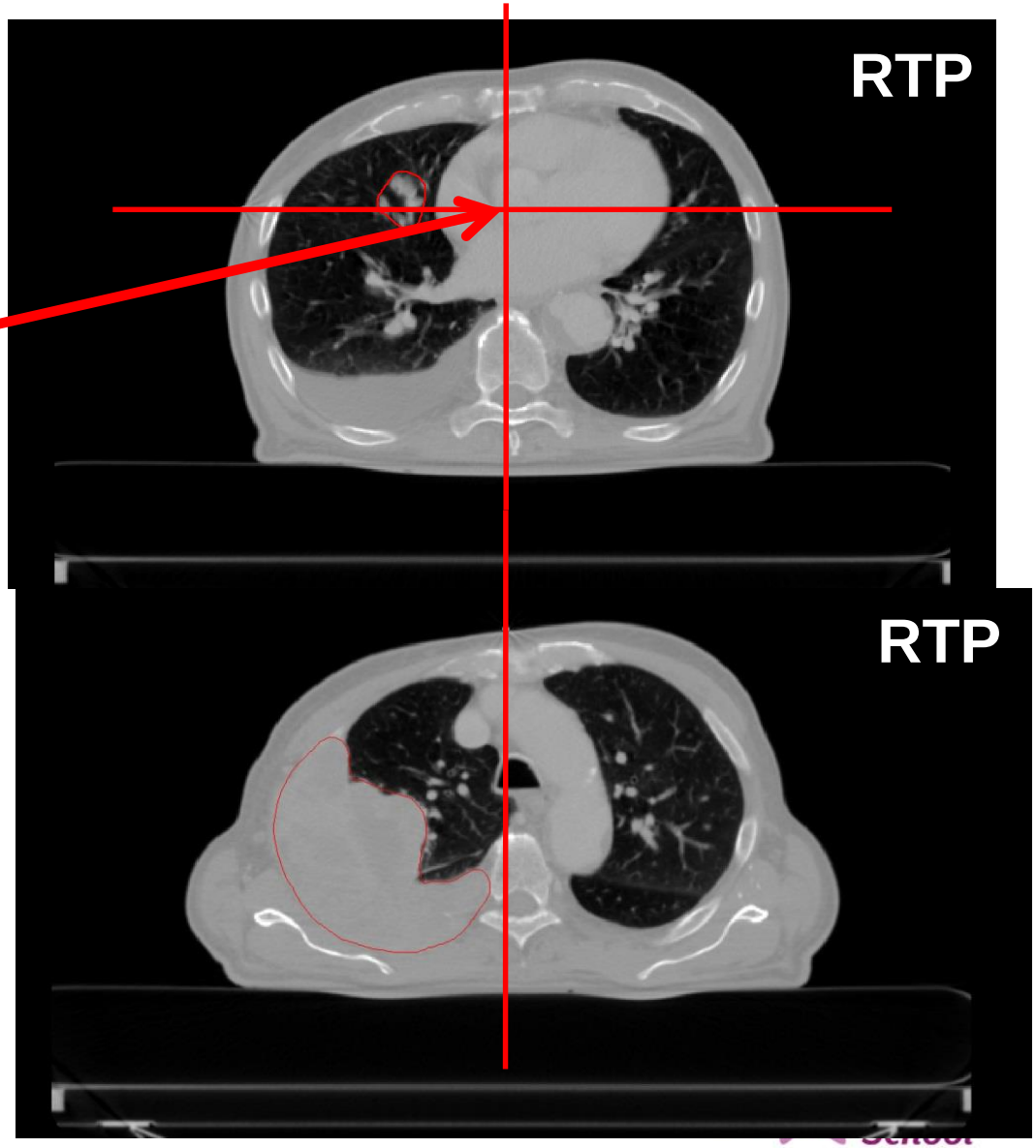

In contrast to ERT, where the set-up of the real Beams (irradiation) is based on:

- **Immobilization of the patient as in planning process (CT)**
- **(re)Positioning of the patient using the RP and the Machine Coordinate System (Laser Projection of Isocentre)**

➔ **RP = Laser-Iso**

The Reference Pont (RP)

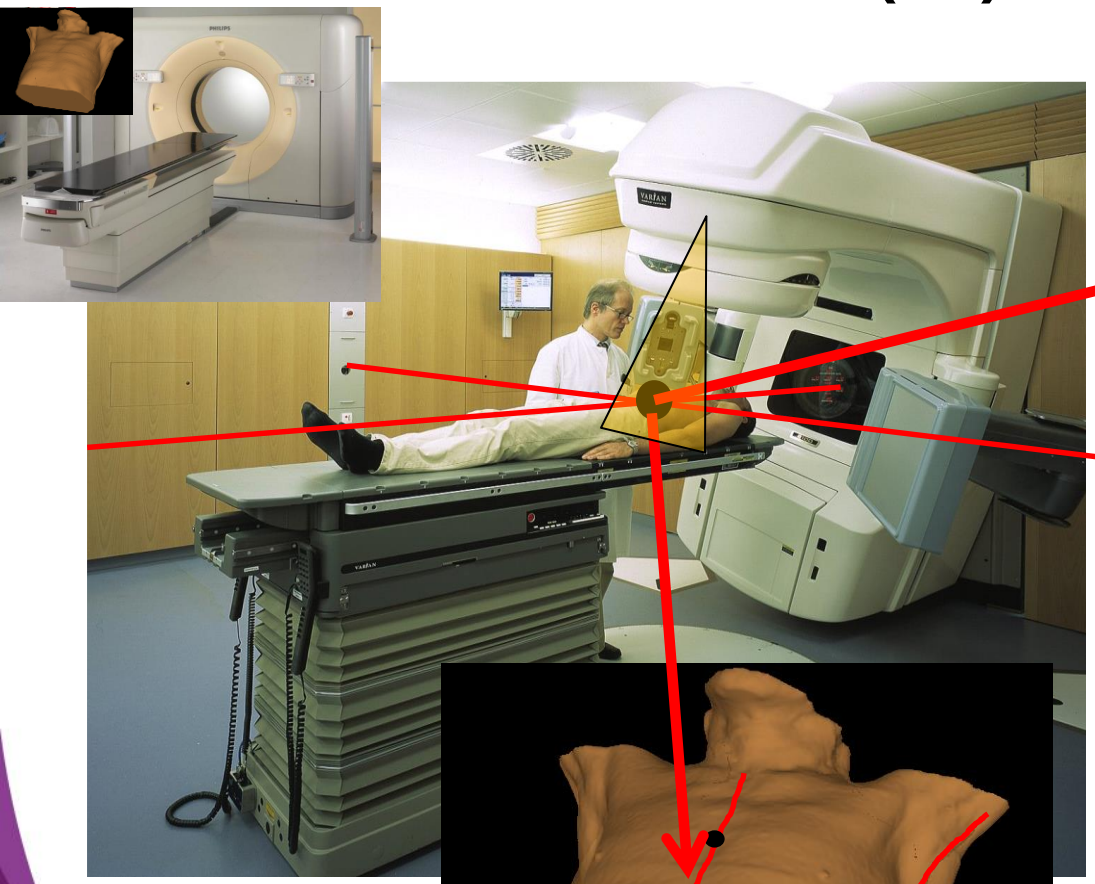

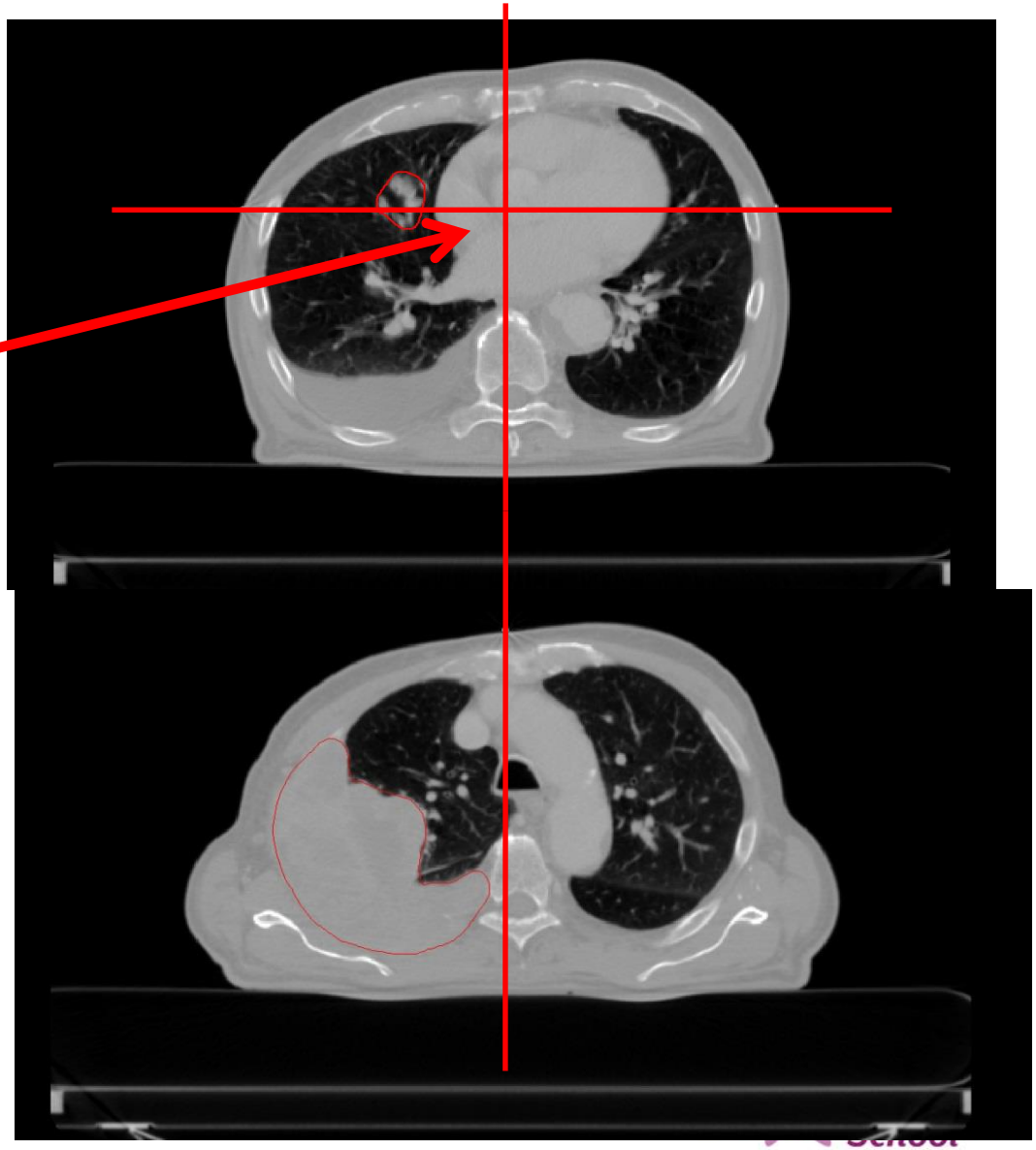

In contrast to ERT, where the set-up of the real Beams (irradiation) is based on:

- **Immobilization of the patient as in planning process (CT)**
- **(re)Positioning of the patient using the RP and the Machine Coordinate System (Laser Projection of Isocentre)**

  ➔ RP = Laser-Isocenter
- **Fully automatic shift: Plan-Isocenter ➔➔ Machine-Isocenter**
- **Imaging-based (2D/3D, SIG) verification of Anatomy/Target position**
- **Fully automatic set-up of the beams and MLC-configurations**

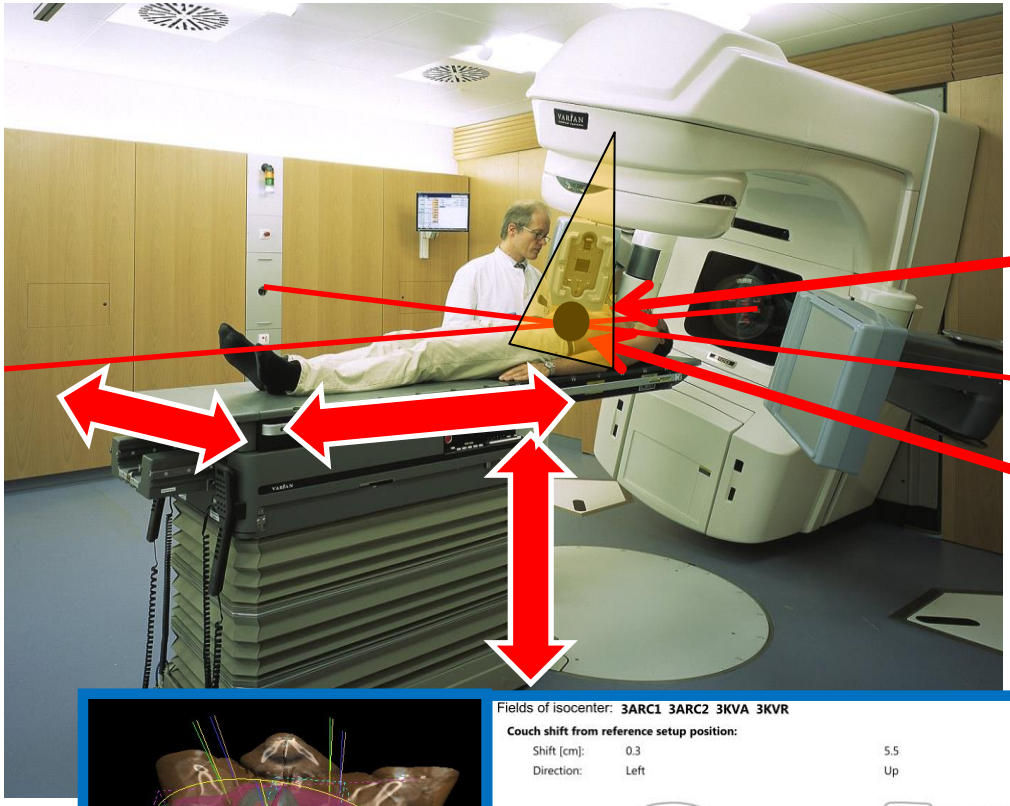

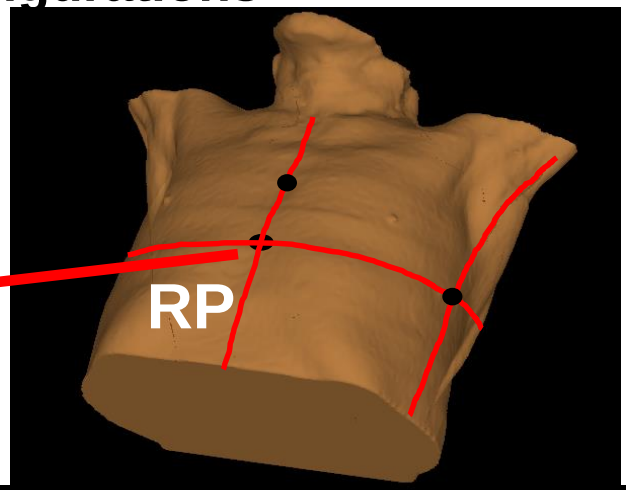

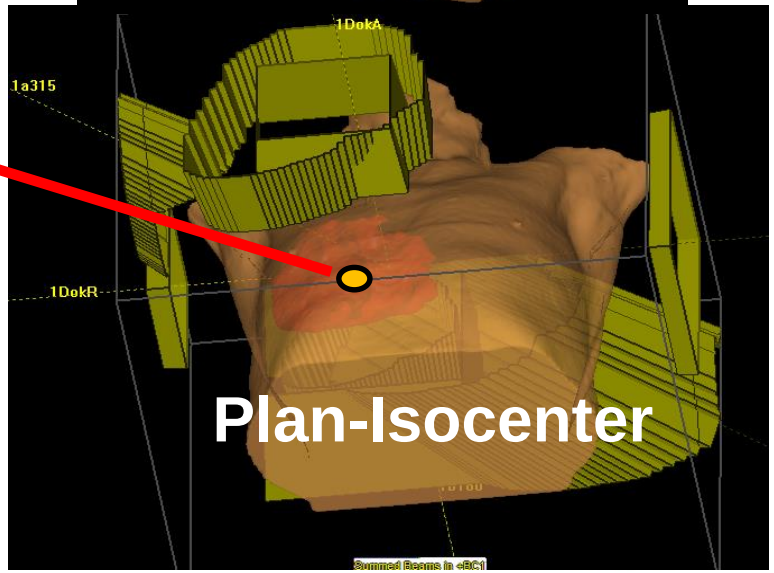

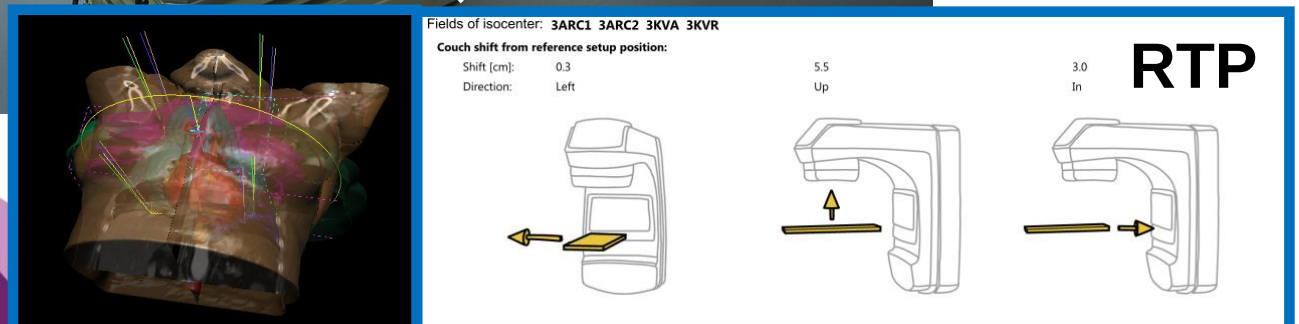

Modern Brachytherapy Treatment Planning

Catheters/Applicators (Sources) Localisation

In contrast to ERT

In BRT the “Beams”, the implanted Catheters/Applicators, have to be firstly localised (reconstructed; definition of their 3D geometry) and registered to the anatomy based on the available imaging data. Exactly this Co-registration of Anatomy ←→ Catheters/Applicators replaces the/corresponds to RP ←→ Laser-Iso Positioning of ERT.

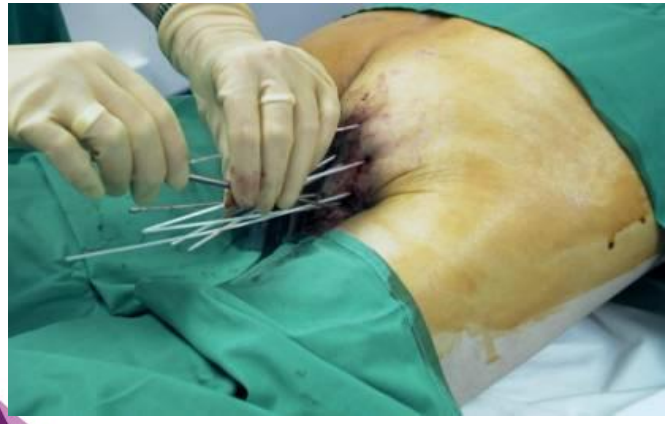

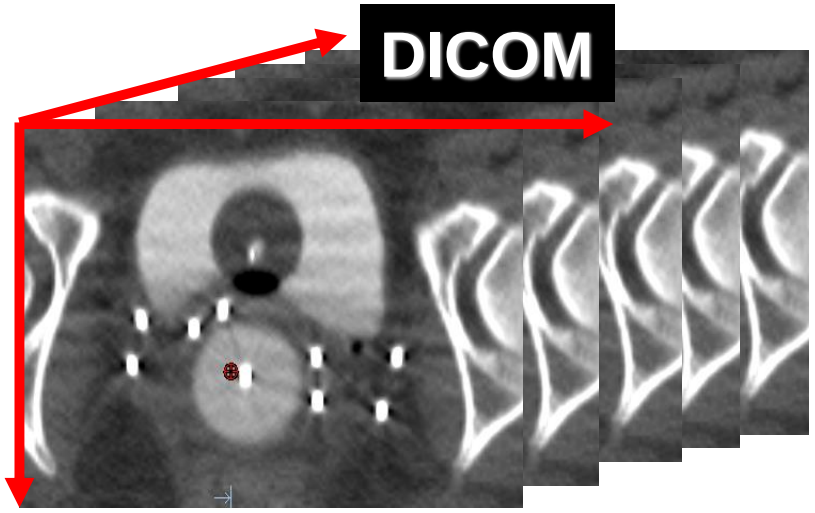

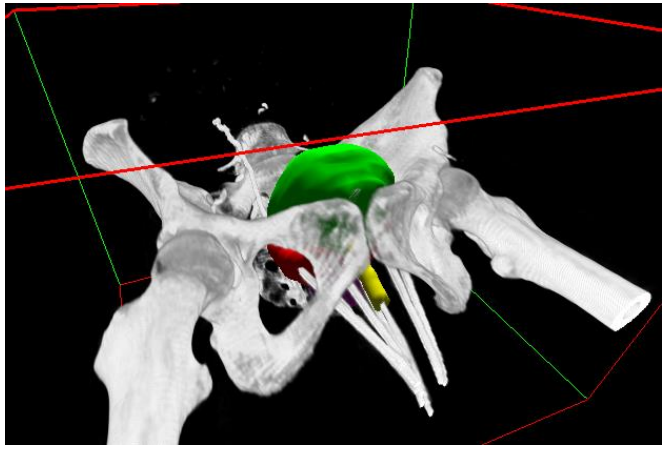

ESTRO School

Modern Brachytherapy Treatment Planning

Catheters/Applicators (Sources) Localisation

The actual aim of the Localisation Process is:

to define the 3D-positions of the sources or of the possible source dwell positions and register these to the relevant anatomy (PTV, OARs).

This presumes:

- **Localisation of the implanted Catheters/Needles/ Applicators and**
- **Knowledge of Afterloader and Catheter/Applicator specific Information/Characteristics.**

ESTRO School

Modern Brachytherapy Treatment Planning

Catheters/Applicators (Sources) Reconstruction

Knowledge of Afterloader and Catheter/Applicator specific Information/Characteristics

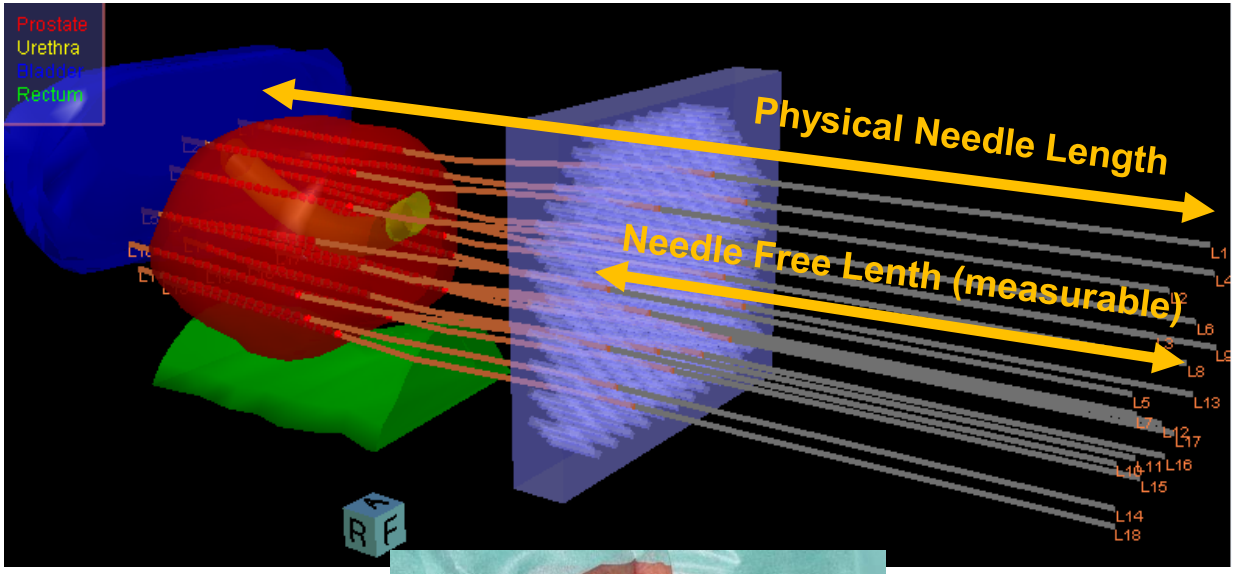

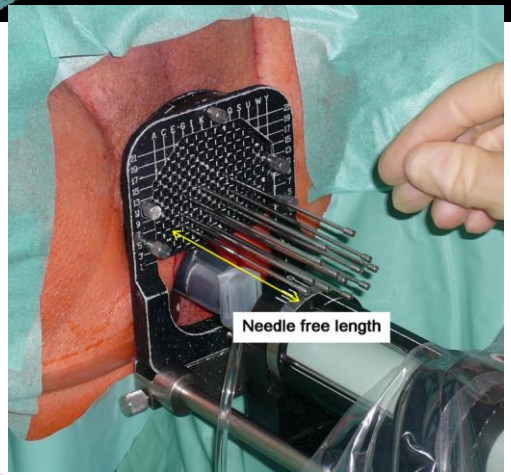

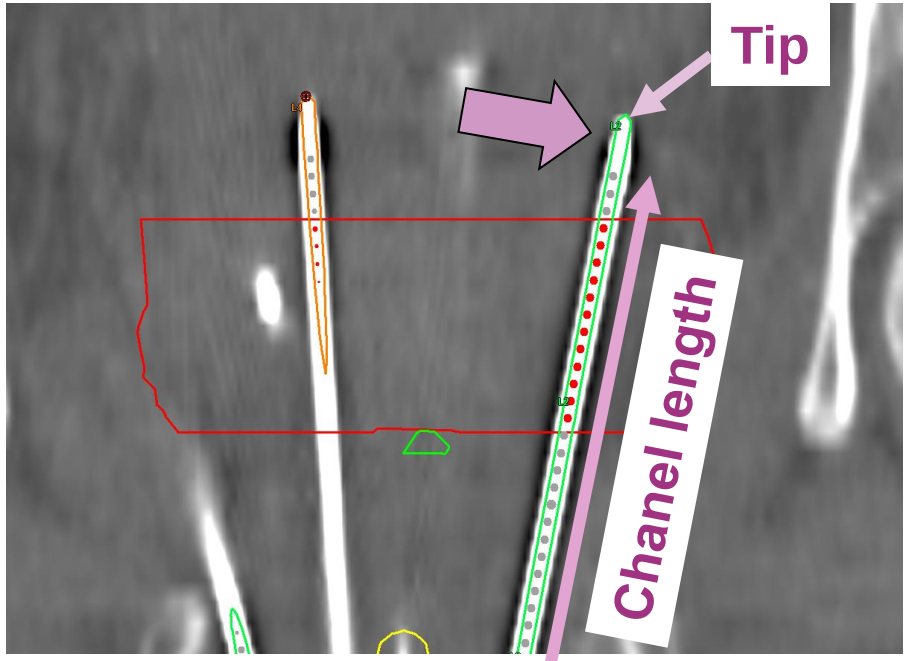

Afterloader

ESTRO School

Modern Brachytherapy Treatment Planning

Catheters/Applicators (Sources) Reconstruction

Knowledge of Afterloader and Catheter/Applicator specific Information/Characteristics

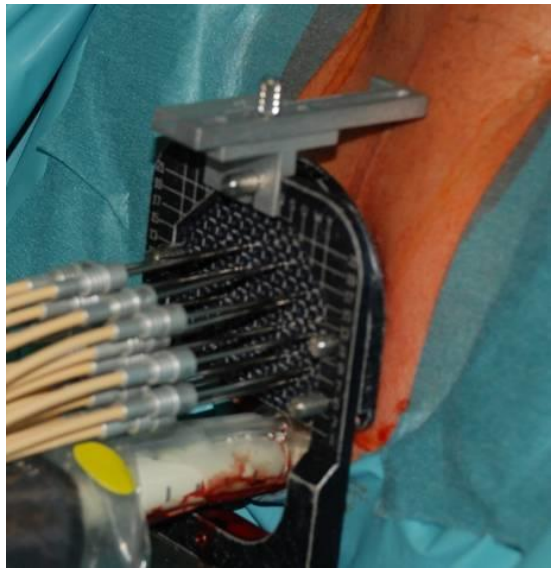

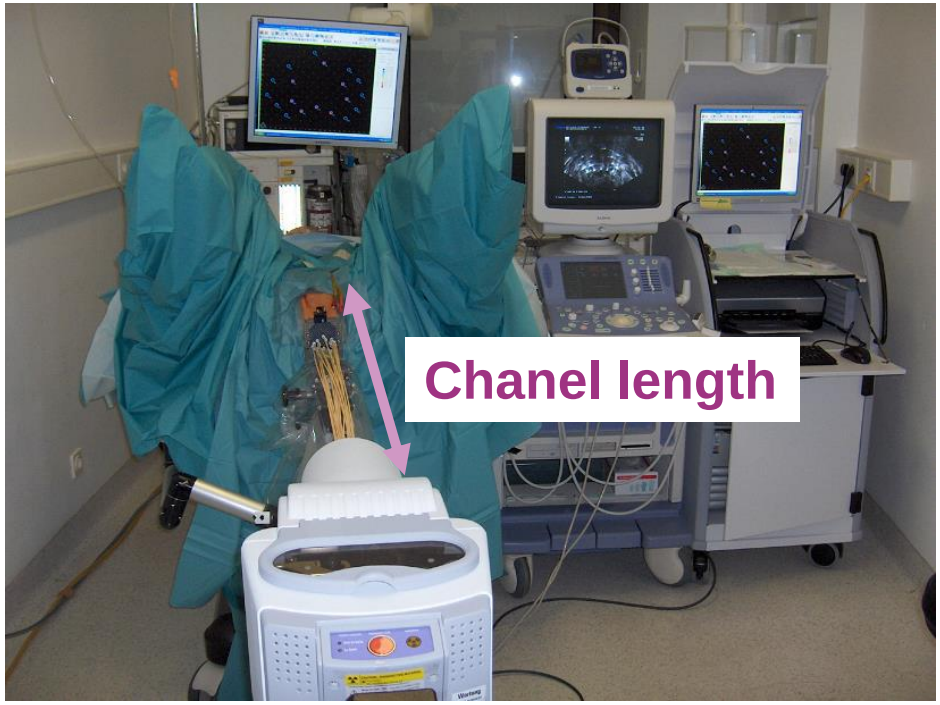

ESTRO School

Modern Brachytherapy Treatment Planning

Catheters/Applicators (Sources) Localisation

In general there are exist two methods for the Localisation of the sources/ possible source dwell positions.

Source Path Method

Here the "*finger-print*" of the individual implanted catheters/ applicators on the acquired images is utilized (interstitial implants, endoluminal and simple endocavitary applicators)

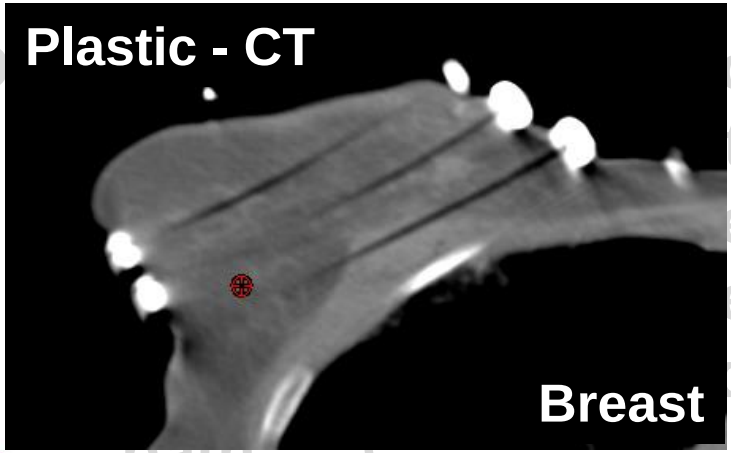

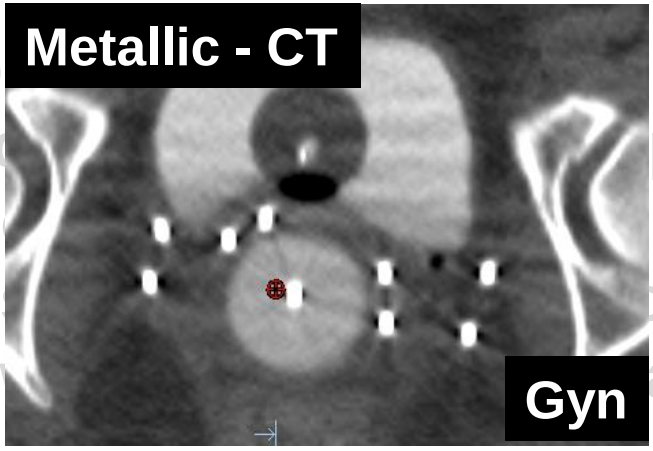

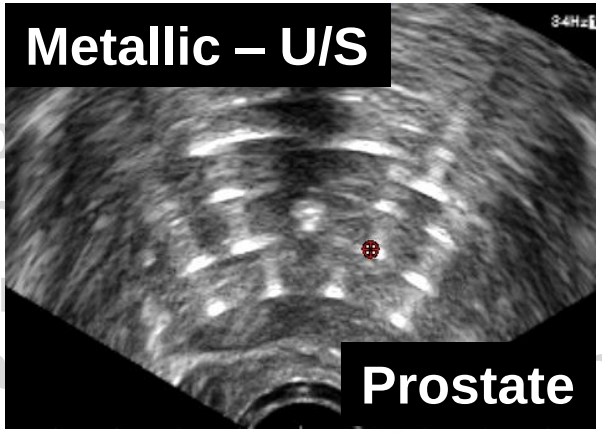

Modern Brachytherapy Treatment Planning

Catheters/Applicators (Sources) Localisation

In genera … of the sources/ … Source P… He… theters/ ap… titial im… icators)

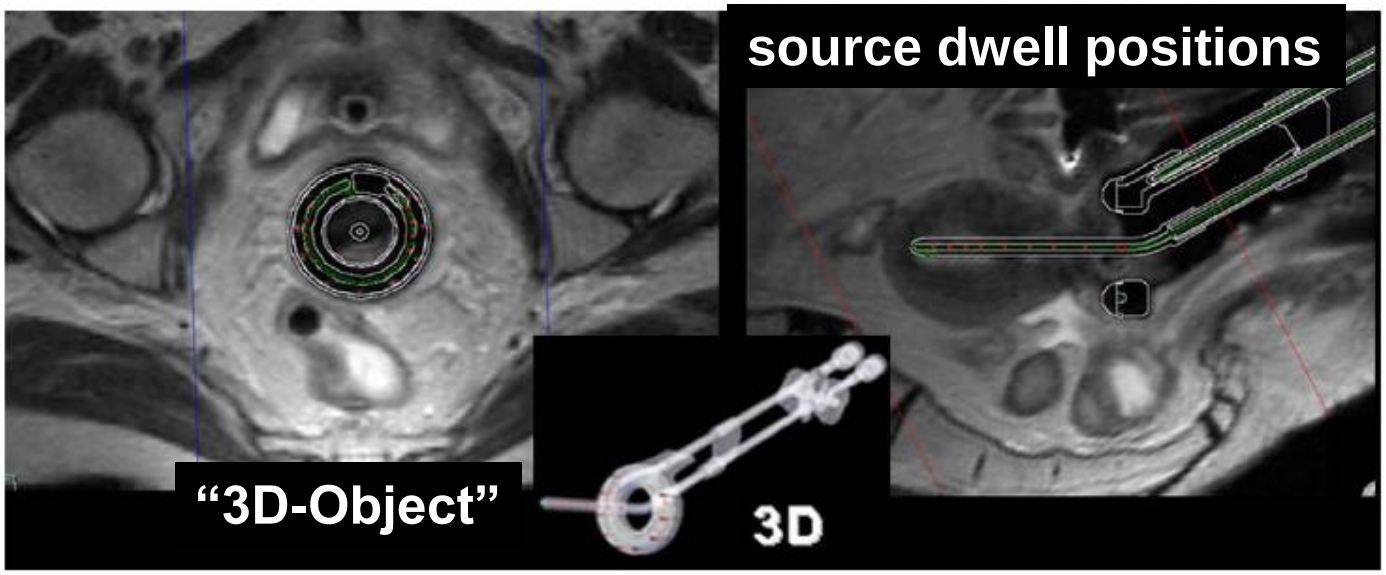

Fig. 7. Position of a library applicator (in the middle) in the transversal (left) and sagittal (right) plane.

3D-Applicator Model Method

Here the 3D Applicator geometry (rigid) is preexisting and stored as a "3D-Object" including all required information for generation of sources/source dwell positions (source paths, all possible source dwell positions and channel length for each path, …)

GEC-ESTRO Recommendations, Hellebust T., Kirisits, C., Berger, D., et al., Rad Oncol 95, 153-160, 2010.

ESTRO School

Modern Brachytherapy Treatment Planning

Catheters/Applicators (Sources) Localisation

The actual aim of the Localisation Process is:

to define the 3D-positions of the sources or of the possible source dwell positions and register these to the relevant anatomy (PTV, OARs).

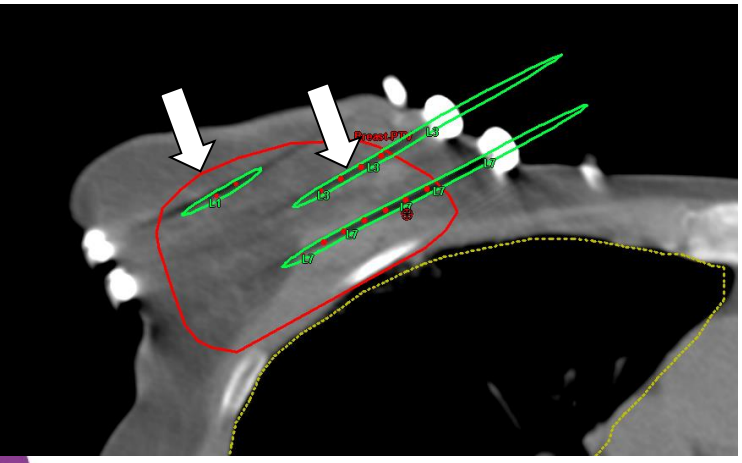

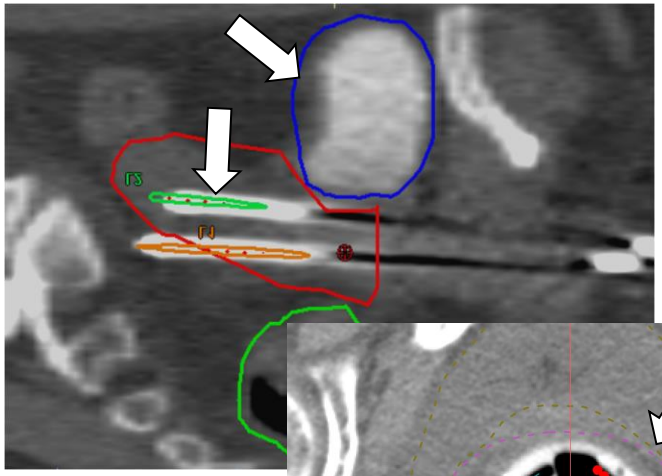

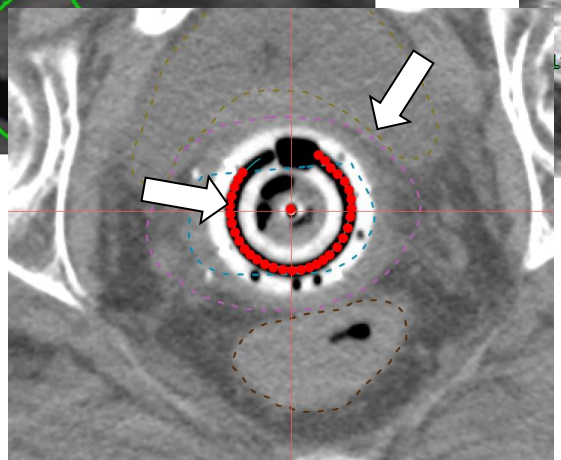

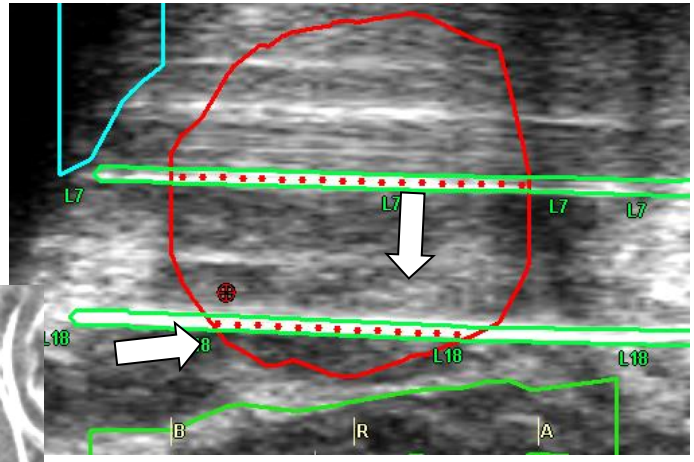

ESTRO School

Modern Brachytherapy Treatment Planning

Catheters/Applicators (Sources) Localisation

Today´s Session on 3D Imaging and Localisation

- **3D imaging modalities and techniques**
  N. Nesvacil

- **Catheter/Applicator and source localisation using 3D imaging**
  N. Nesvacil

ESTRO School

List of Content

- BRT *versus* ERT from Dosimetry Point of View
- BRT *versus* ERT from RTP-Workflow Point of View
- Introduction to Localisation
- DVH-Evaluation and Prescription
- Introduction to Dynamic and Adaptive Planning

ESTRO School

Modern Brachytherapy Treatment Planning

For all further steps in RTP-Workflow in BRT, following is given:

- **3D-Model of the patient anatomy**
  - **Target(s)**
  - **OARs**
- **3D-Model of the implant**
  - **Catheter and/or applicators**
  - **(Possible and) active source dwell positions ASDPs**
- **Their Co-Registration**
  - **DICOM-coordinate system**
- **Dwell times for all ASDPs (Optimization, Inverse/Forward)**

ESTRO School

Modern Brachytherapy Treatment Planning

For all further steps in RTP-Workflow in BRT, following is presumed:

- **Dose-Calculation Engine**
  Monday-Session on Dose Calculation
  L. Beaulieu, P. Papagiannis and M. Rivard

- **DVH-Calculation and Evaluation Methods**
  Tuesday-Session on Optimization and Prescription
  D. Baltas, N. Nesvacil and J. Pérez-Calatayud

ESTRO School

List of Content

- BRT *versus* ERT from Dosimetry Point of View
- BRT *versus* ERT from RTP-Workflow Point of View
- Introduction to Localisation
- DVH-Evaluation and Prescription
- Introduction to Dynamic and Adaptive Planning

ESTRO School

Modern Brachytherapy Treatment Planning

Dynamic and Adaptive Implantation Process

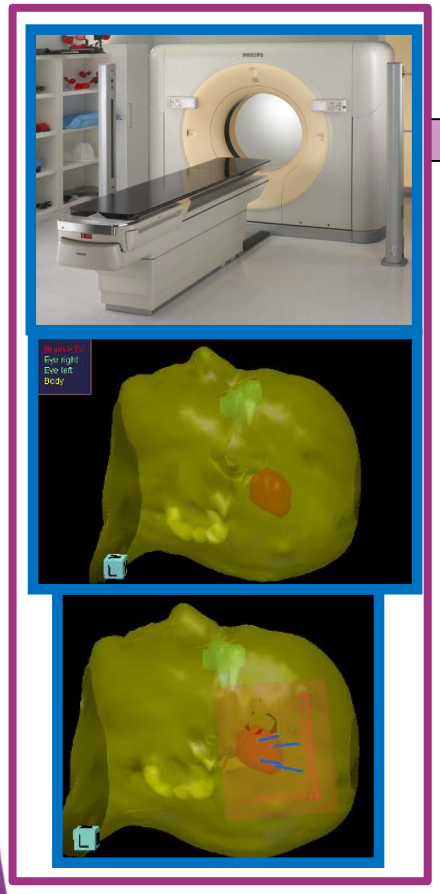

Define "best possible" implant: *Inverse Planning*

Number implanted Catheters < max. Number?

No

FInalise Implantation

Yes

Implant next catheter/needle incl. real time feedback: *Implantation/Navigation/Telemanipulator/ Robotics*

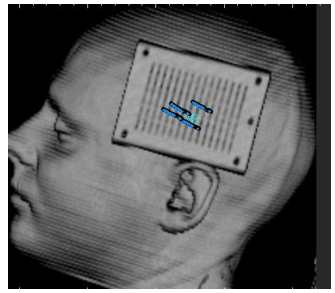

Deviation "planned-implanted" acceptable?

Yes

No

Re-optimisation*

Deviation from "best possible" acceptable?

No

Yes

Adjust "best possible" for remaining catheters/needles

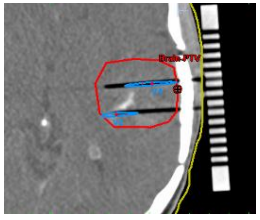

* under consideration of anatomical changes

Modern Brachytherapy Treatment Planning

Define “best-possible” = Inverse Planning

It presupposes the availability of:

- **A complete 3D anatomy model**
  VOIs: Target(s), OARs

  } **Morphology (3D Imaging)**

- **The *Desired/Aimed* Dose Distribution**

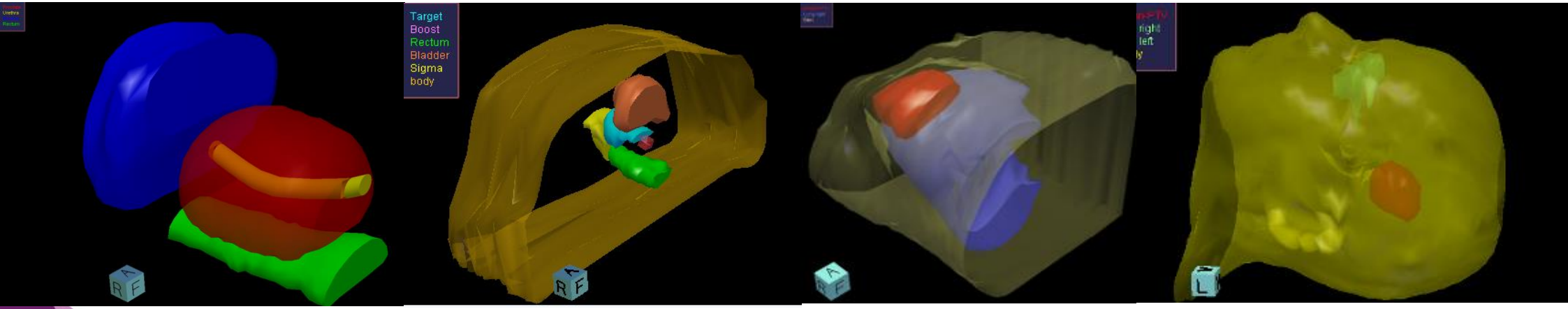

ESTRO School

Modern Brachytherapy Treatment Planning

Inverse Planning:

The automatic placement of an adequate number of catheters/applicators/needles based on dosimetric objectives and constraints. Consideration of (i) *Medical* (ii) *Anatomical* und (iii) *Technical Implantation* demands/presetting. It is solvable in clinically acceptable time only after *discretisation*

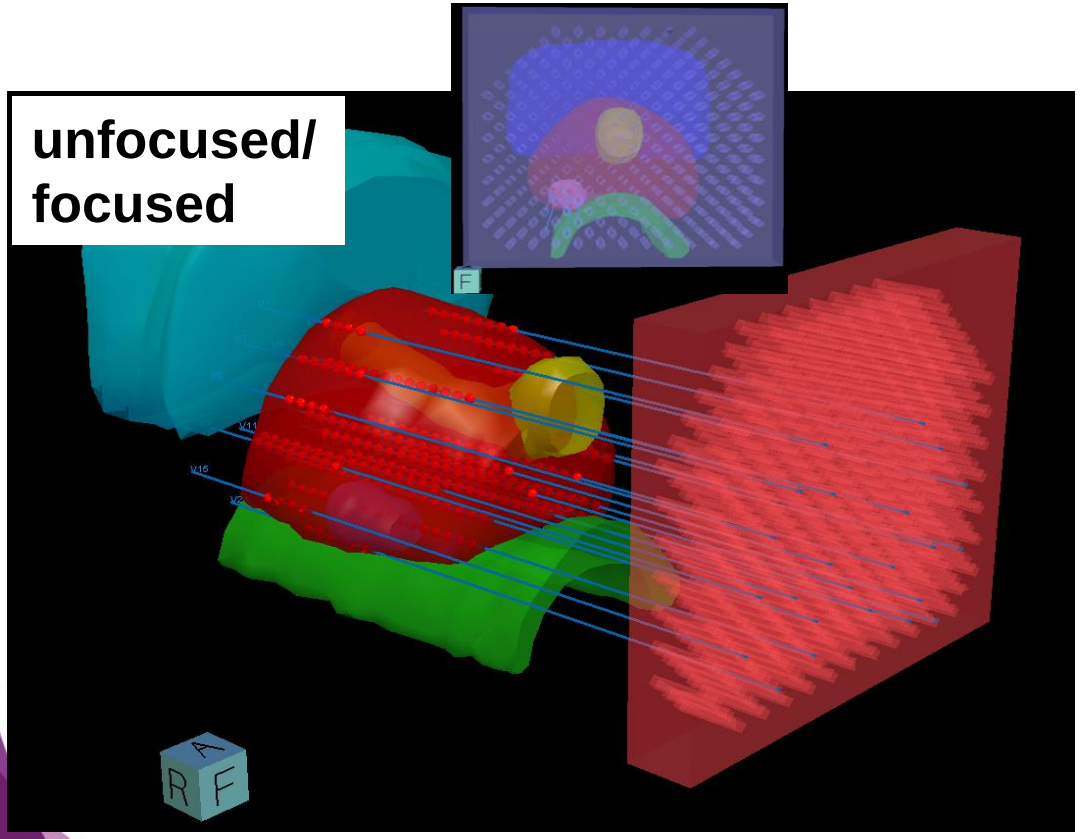

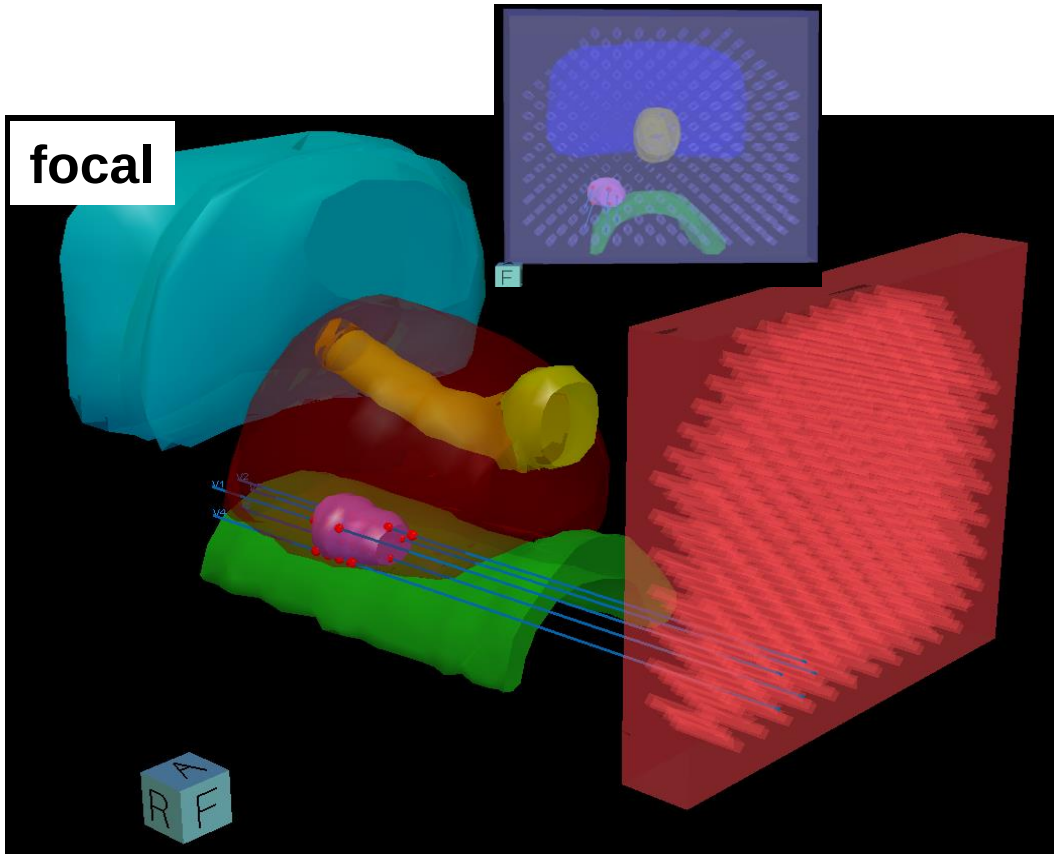

ESTRO School

Modern Brachytherapy Treatment Planning

The Inverse Planning of an adequate number of catheters/applicators / needles based on dosimetric objectives and constraints *is solvable in clinically acceptable time* only after *discretisation*

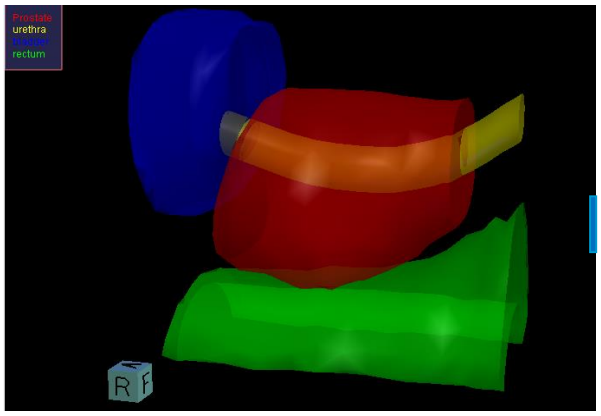

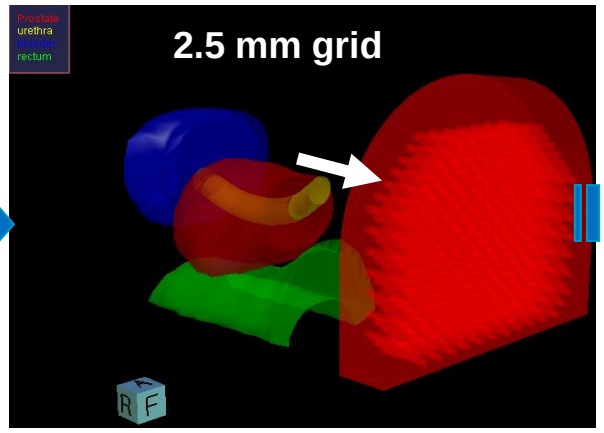

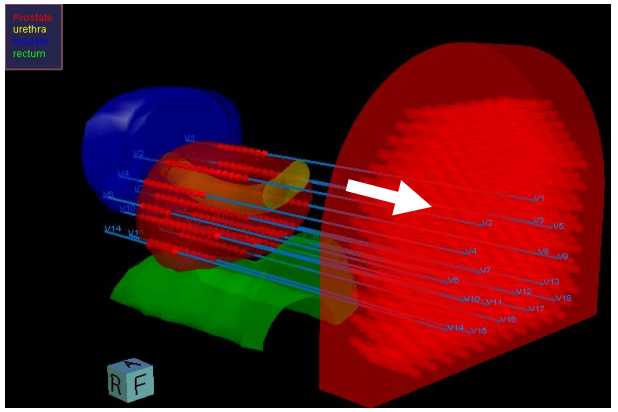

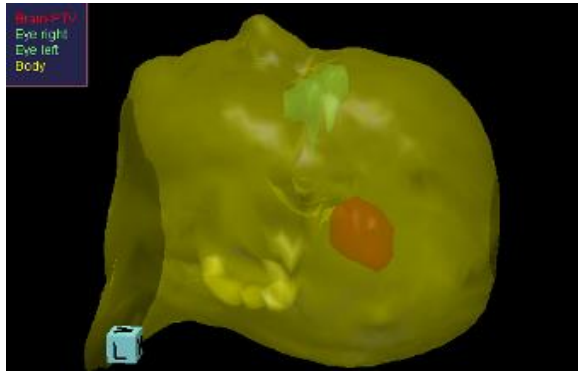

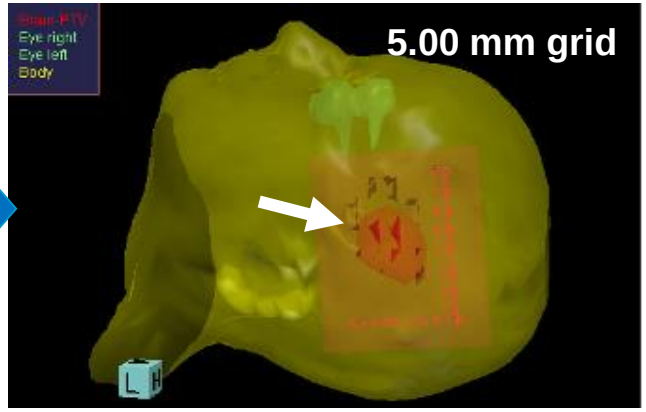

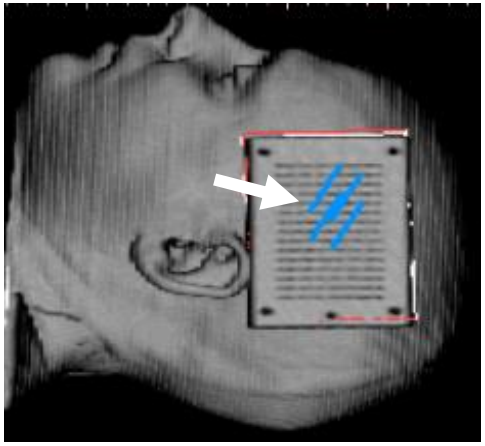

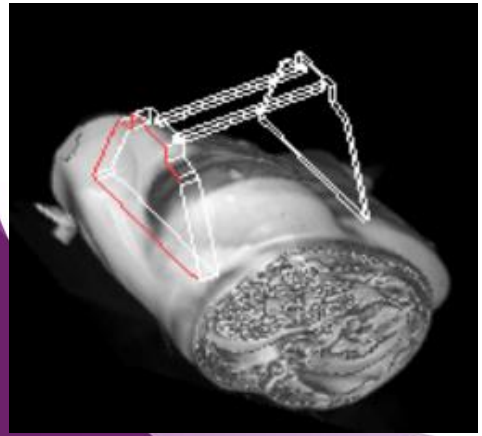

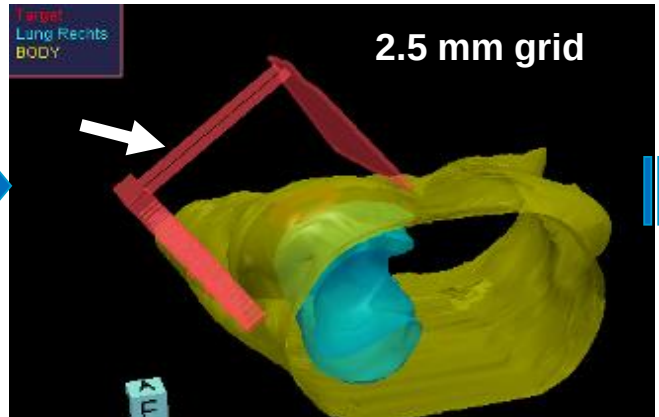

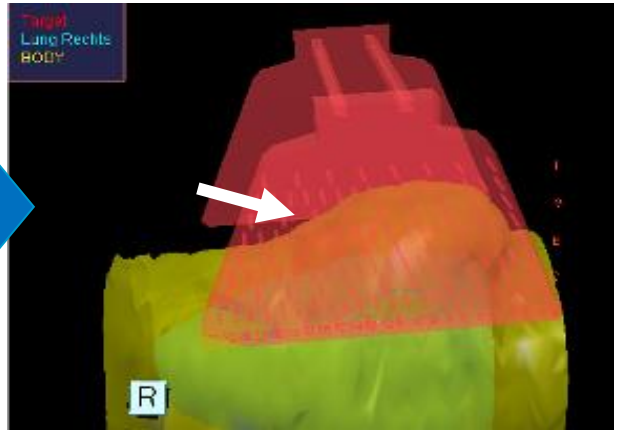

Modern Brachytherapy Treatment Planning

Inverse Planning:

The automatic placement of an adequate number of catheters/applicators/needles based on dosimetric objectives and constraints. Consideration of (i) *Medical* (ii) *Anatomical* und (iii) *Technical Implantation* demands/presetting. It is solvable in clinically acceptable time only after *discretisation*.

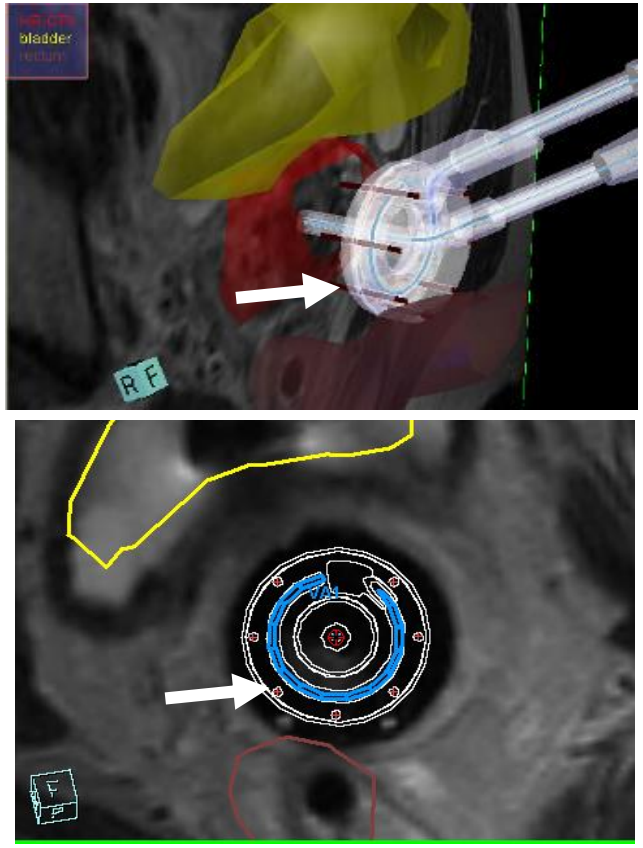

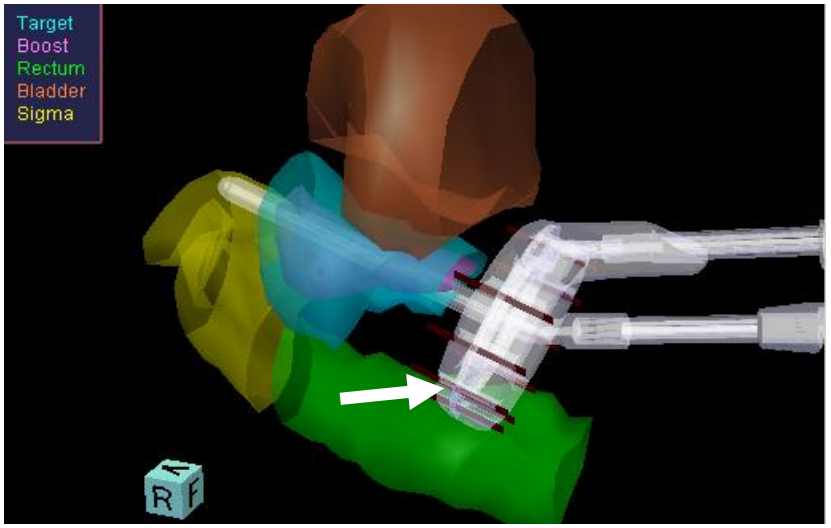

Cervix-Ca: Applicator + Needles
Data by courtesy of University of Vienna

ESTRO School

Modern Brachytherapy Treatment Planning

Dynamic and Adaptive Treatment Delivery

1 … N Fractions

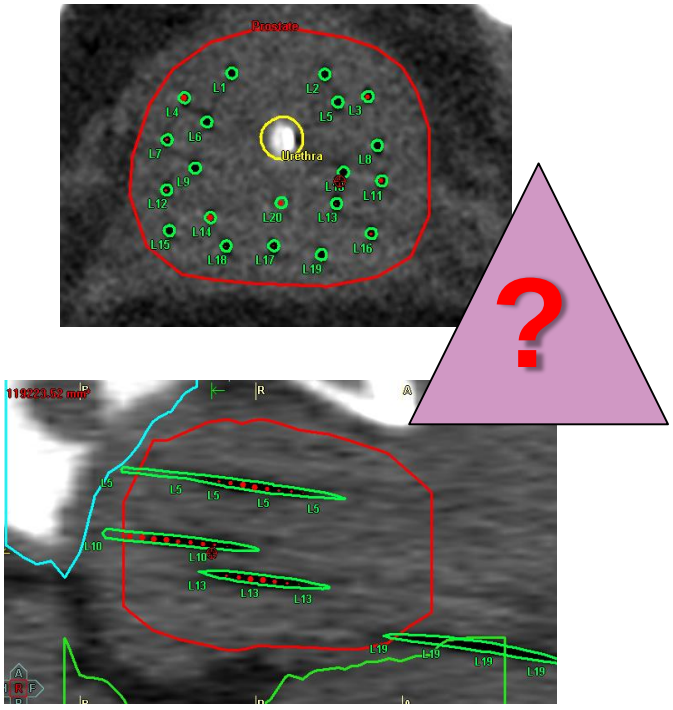

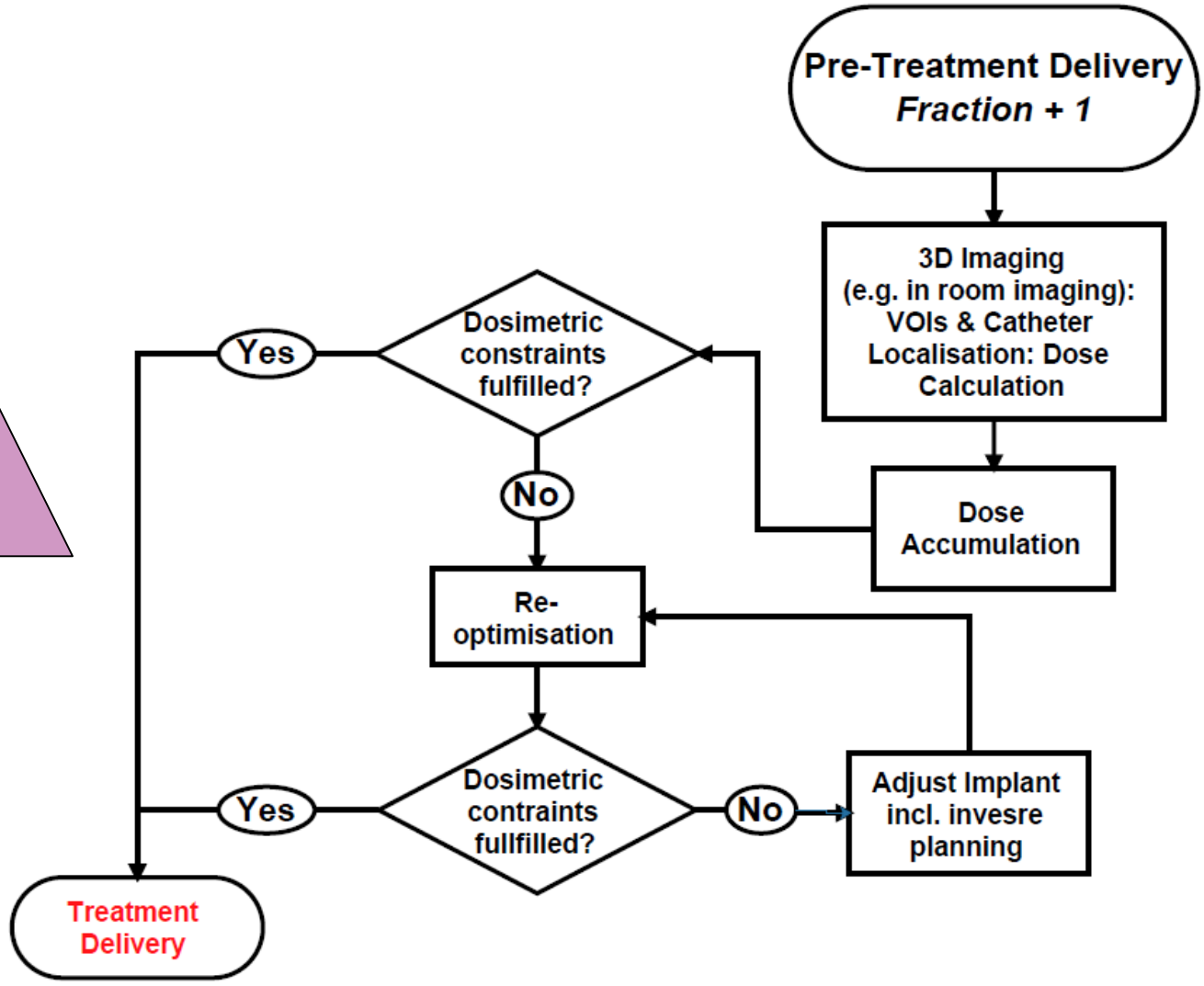

ESTRO School

List of Content

- ✓ BRT *versus* ERT from Dosimetry Point of View
- ✓ BRT *versus* ERT from RTP-Workflow Point of View
- ✓ Introduction to Reconstruction
- ✓ DVH-Evaluation and Prescription
- ✓ Introduction to Dynamic and Adaptive Planning

ESTRO School

ESTRO School

ESTRO School

WWW.ESTRO.ORG/SCHOOL

Tissue segmentation and characterization

Prof. Luc Beaulieu, Ph.D., FAAPM, FCOMP

1- Département de physique, de génie physique et d'optique, et Centre de recherche sur le cancer, Université Laval, Canada

2- Département de radio-oncologie et Centre de recherche du CHU de Québec, CHU de Québec, Canada

Valencia, Spain – Oct 7-10 2018

Disclosures

- None for this section

Learning Objectives

- Provide an understanding of the challenges of tissue segmentation in brachytherapy
- Present and explain the TG-186 recommendations
- Look at DECT has the next step for tissue segmentation in radiation therapy.

Acknowledgements

TG-186

- Luc Beaulieu (Chair)
- Å. Carlsson-Tedgren
- Jean-François Carrier
- Steve Davis
- Firas Mourtada
- Mark Rivard
- Rowan Thomson
- Frank Verhaegen
- Todd Wareing
- Jeff Williamson

Factor-based TG43

	INPUT	CALCULATION	OUTPUT
TG43	Source characterization	Superposition of data from source characterization	$D_{w\text{-}TG43}$

There is no tissue segmentation, only organ contouring

From Åsa Carlsson-Tedgren

Factor-based vs Model-based

TG43

INPUT	CALCULATION	OUTPUT
Source characterization	Superposition of data from source characterization	$D_{w\text{-}TG43}$

MBDC

INPUT	CALCULATION	OUTPUT
Source Characterization + **Tissue/applicator information**	**Model-Based Dose Calculation Algorithms**	$D_{m,m}$ $D_{w,m}$

From Åsa Carlsson-Tedgren

Definition of the scoring medium

$D_{x,y}$

x: dose specification medium

y: radiation transport medium

- *x*,*y*: Local medium (m) or water (w)

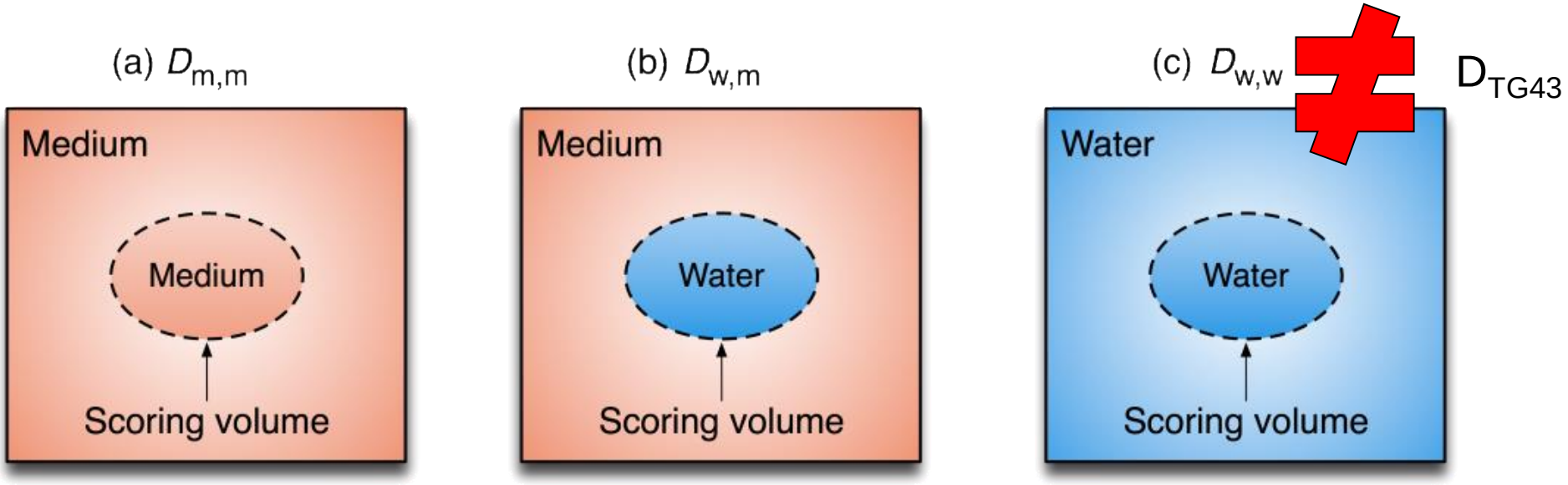

FROM: G Landry, Med Phys 2011

On-going Debate

"Results suggest that cells in cancerous and normal soft tissues are generally not radiologically equivalent to either water or the corresponding average bulk tissue"

Thomson, Carlsson, Williamson. PMB 58 (2013)

Procedure: tissue segmentation

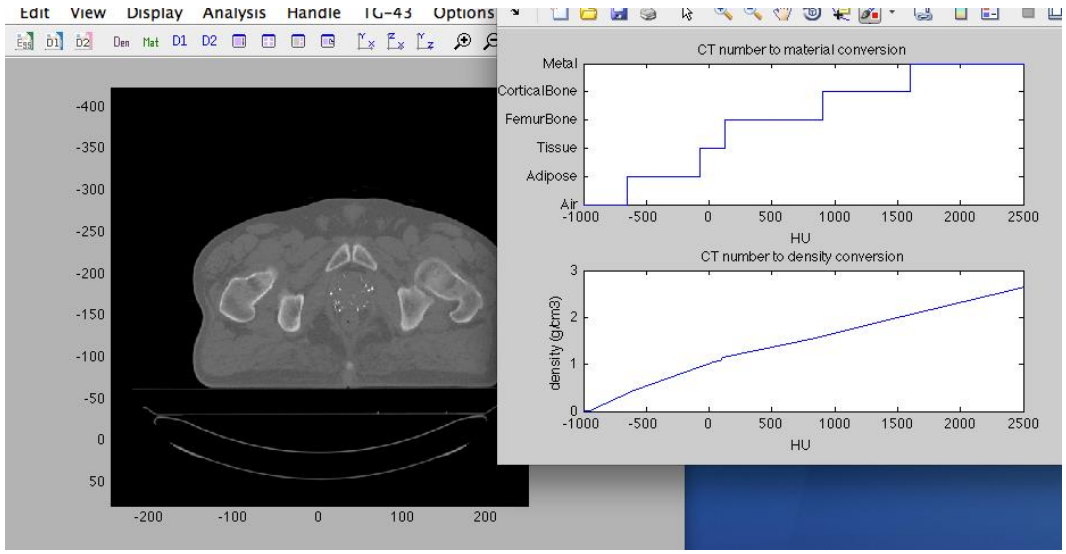

			$(Density)_i$, $(Medium)_i$		

From F. Verhaegen

Cross section assignments (segmentation)

- MDBCA requires assignment of interaction cross section on a voxel-by-voxel basis
- In EBRT one only needs electron densities ρ_e (e^-/cm^3) from CT scan
- In BT (energy range 10-400 keV) the interaction probabilities depend not only on ρ_e but also strongly on atomic number Z

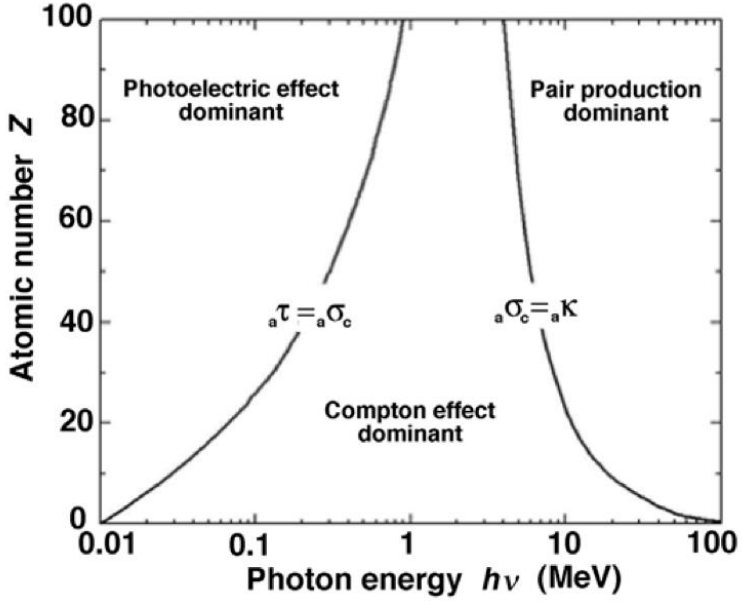

Cross section assignments

- Accurate tissue segmentation, sources and applicators needed: identification (ρ_e ,Z_{eff})
  - e.g. in breast: adipose and glandular tissue have significantly different (ρ_e ,Z_{eff}); dose will be different

- If this step is not accurate ➔ incorrect dose
  - Influences dosimetry and dose outcome studies
  - Influences dose to organs at risk

Large Cavity Theory Cross Section

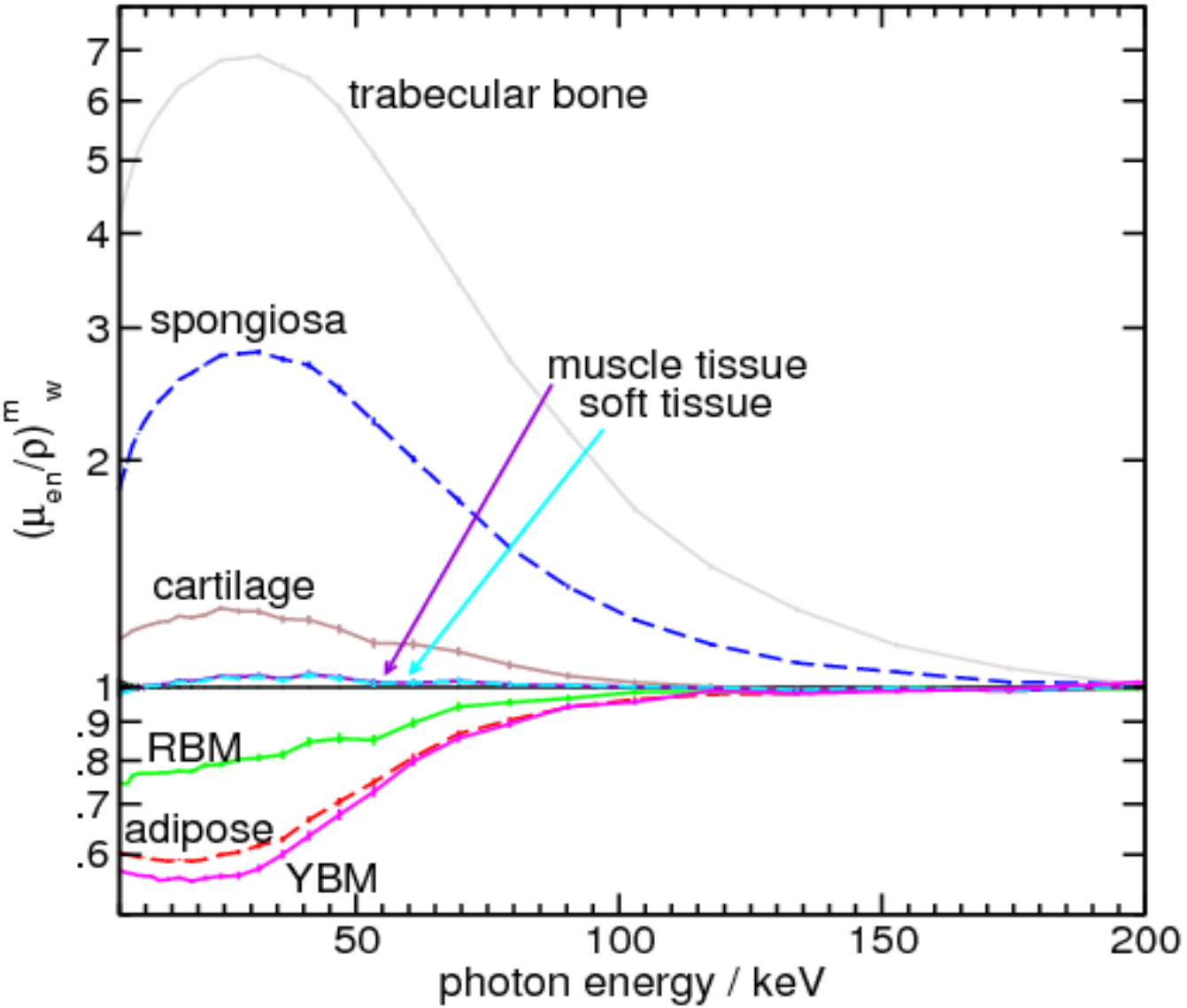

TG-186

TG-186 recommendations

- Consensus material definition
- Material assignment method
- CT/CBCT artifact removal

Recommendations

- Extract electron density from CT calibration (see TG53, TG66 …)
  - Use the density from CT for each voxel
  - Use recommended tissue compositions
    - Organ-based (contoured) assignments
      - Prostate from Woodard et al, BJR 59 (1986) 1209-18
      - All others from ICRU-46 composition
    - From CT calibration: breast, adipose, muscle and bone

TABLE III. Material definitions. Water is given for comparison.

	% mass					Mass density
Tissue	H	C	N	O	Z > 8	g cm^{-3}
Prostate (Ref. 110)	10.5	8.9	2.5	77.4	Na(0.2), P(0.1), S(0.2), K(0.2)	1.04
Mean adipose (Ref. 110)	11.4	59.8	0.7	27.8	Na(0.1), S(0.1), Cl(0.1)	0.95
Mean gland (Ref. 110)	10.6	33.2	3.0	52.7	Na(0.1), P(0.1), S(0.2), Cl(0.1)	1.02
Mean male soft tissue (Ref. 109)	10.5	25.6	2.7	60.2	Na(0.1), P(0.2), S(0.3), Cl(0.2), K(0.2)	1.03
Mean female soft tissue (Ref. 109)	10.6	31.5	2.4	54.7	Na(0.1), P(0.2), S(0.2), Cl(0.1), K(0.2)	1.02
Mean skin (Ref. 109)	10.0	20.4	4.2	64.5	Na(0.2), P(0.1), S(0.2), Cl(0.3), K(0.1)	1.09
Cortical bone (Ref. 109)	3.4	15.5	4.2	43.5	Na (0.1), Mg (0.2), P (10.3), S (0.3), Ca(22.5)	1.92
Eye lens (Ref. 109)	9.6	19.5	5.7	64.6	Na(0.1), P(0.1), S(0.3), Cl(0.1)	1.07
Lung (inflated) (Ref. 109)	10.3	10.5	3.1	74.9	Na(0.2), P(0.2), S(0.3), Cl(0.3), K(0.2)	0.26
Liver (Ref. 109)	10.2	13.9	3.0	71.6	Na(0.2), P(0.3), S(0.3), Cl(0.2), K(0.3)	1.06
Heart (Ref. 109)	10.4	13.9	2.9	71.8	Na(0.1), P(0.2), S(0.2), Cl(0.2), K(0.3)	1.05
Water	11.2			88.8		1.00

Consequences:
Uncertainties associated with this process?

- Limited measurements
  - e.g. 1930s' data of prostate from a specimen of 14 year old boy [1]
- Considerable tissue composition variability
  - e.g. Adipose tissue water content between 23% to 78%[2]
- Patient-specific distribution of tissue types
  - e.g. Breast adipose vs glandular composition: 16% to 68%[3,4]

1) A. H. Neufeld, Canadian Journal of Research 15B, 132-138 (1937).
2) B. Brooksby, B. W. et al., PNAS 103 (23), 8828-8833 (2006).
3) R. A. Geise and A. Palchevsky, Radiology 198 (2), 347-50 (1996)
4) The Myth of the 50-50 breast, MJ Yaffe et al., Med Phys 36 (2009)

Consequences:
Uncertainties associated with this process?

- Human tissues vary from one individual to the other
- Reports (like ICRP 23 or ICRU 44) provides average compositions

(Woodard & White)

Body tissue	Elemental composition (% by mass)					Densities		
						Mass	Electron	
	H	C	N	O	Elements with $Z > 8$	kg m^{-3}	el. kg^{-1} $\times 10^{26}$	el. m^{-3} $\times 10^{26}$
Adipose tissue 1	11.2	51.7	1.3	35.5	Na(0.1), S(0.1), Cl(0.1)	970	3.342	3241
Adipose tissue 2	11.4	59.8	0.7	27.8	Na(0.1), S(0.1), Cl(0.1)	950	3.347	3180
Adipose tissue 3	11.6	68.1	0.2	19.8	Na(0.1), S(0.1), Cl(0.1)	930	3.353	3118

Cross sections

Attenuation

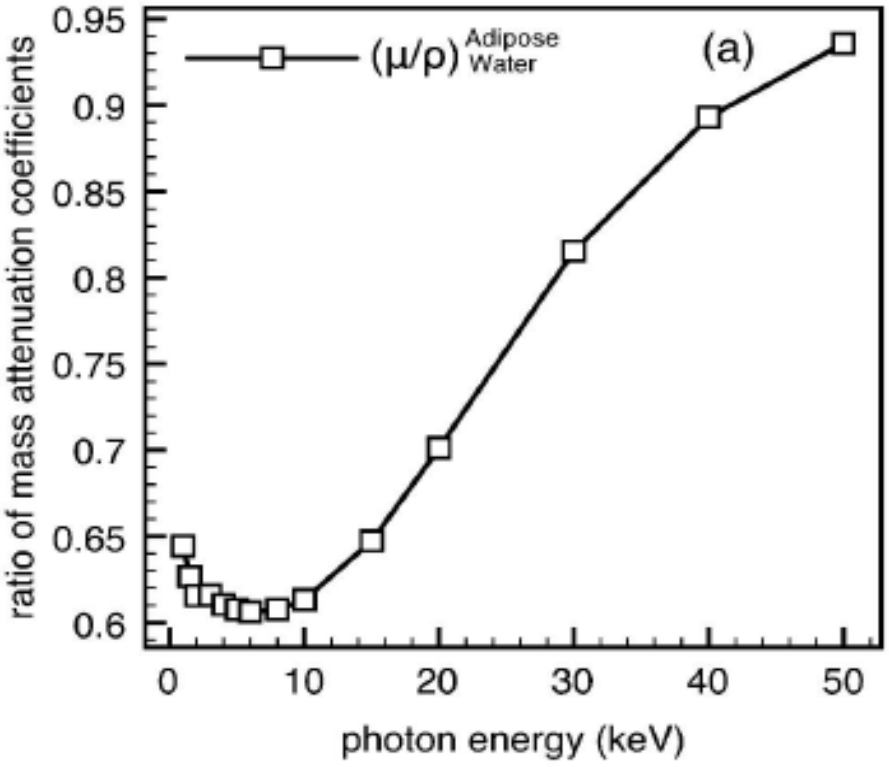

$D_{W,M}$ / $D_{M,M}$

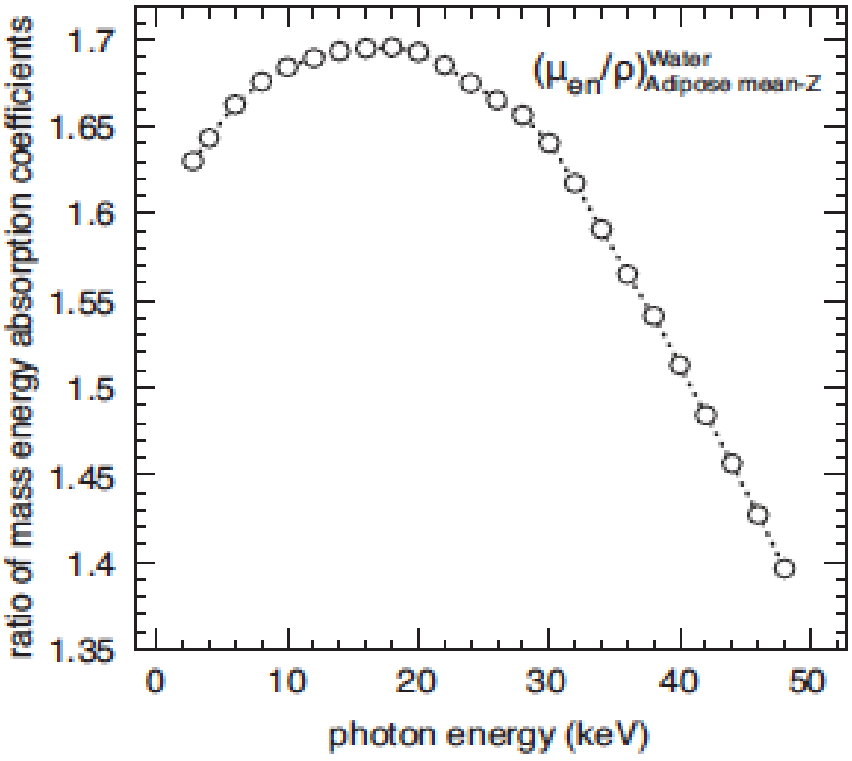

G Landry et al., Med Phys 2010 and Med Phys 2011

Sensitivity Analysis

TABLE VI. Variations of breast PTV D_{90} with various compositions compared to D_{TG-43}.

Dose calculation method	Mean ΔD_{90} (%)	Absolute uncertainty on ΔD_{90} (%)
$MC_{\rho=1}$		
A30/G70 hi-Z	12.6	0.9
A30/G70 mean-Z	22.1	1.4
A50/G50 mean-Z	26.3	1.8
A70/G30 mean-Z	30.4	2.3
A70/G30 lo-Z	39.8	3.2
$MC_{\rho=CT}$		
Water (ρ_{CT})	3.9	1.5
A30/G70 hi-Z	16.3	1.7
A30/G70 mean-Z	25.8	2.0
A50/G50 mean-Z	29.8	2.6
A70/G30 mean-Z	34.1	2.6
A70/G30 lo-Z	42.9	3.1

G Landry et al., Med Phys 2010

Sensitivity Analysis

TABLE VI. Variations of breast PTV D_{90} with various compositions compared to D_{TG-43}.

Dose calculation method	Mean ΔD_{90} (%)	Absolute uncertainty on ΔD_{90} (%)
$MC_{\rho=1}$		
A30/G70 hi-Z	12.6	0.9
A30/G70 mean-Z	22.1	1.4
A50/G50 mean-Z	26.3	1.8
A70/G30 mean-Z	30.4	2.3
A70/G30 lo-Z	39.8	3.2
$MC_{\rho=CT}$		
Water (ρ_{CT})	3.9	1.5
A30/G70 hi-Z	16.3	1.7
A30/G70 mean-Z	25.8	2.0
A50/G50 mean-Z	29.8	2.6
A70/G30 mean-Z	34.1	2.6
A70/G30 lo-Z	42.9	3.1

26%

G Landry et al., Med Phys 2010

Sensitivity Analysis

TABLE VI. Variations of breast PTV D_{90} with various compositions compared to D_{TG-43}.

Dose calculation method	Mean ΔD_{90} (%)	Absolute uncertainty on ΔD_{90} (%)
$MC_{\rho=1}$		
A30/G70 hi-Z	12.6	0.9
A30/G70 mean-Z	22.1	1.4
A50/G50 mean-Z	26.3	1.8
A70/G30 mean-Z	30.4	2.3
A70/G30 lo-Z	39.8	3.2
$MC_{\rho=CT}$		
Water (ρ_{CT})	3.9	1.5
A30/G70 hi-Z	16.3	1.7
A30/G70 mean-Z	25.8	2.0
A50/G50 mean-Z	29.8	2.6
A70/G30 mean-Z	34.1	2.6
A70/G30 lo-Z	42.9	3.1

9%

G Landry et al., Med Phys 2010

Sensitivity Analysis

"If A80/G20 breast is representative of the average breast cancer patient then our A70/G30 breast results indicate that the compositional uncertainty and the use of breast density from CT data translate into **second order effects** [≈±10%] compared to effect of going from water to average breast tissue [≈30%]"

G Landry et al., Med Phys 2010

Sensitivity Study: Prostate

- About 3% D90 difference from TG-43
  - Two compositions found in literature disagree…

    …By 3%
  - Effect of inter-seed attenuation on average also 3-4%

Carrier et al, IJROBP 2007; G. Landry *et al*. Med. Phys. 38 (2011)

Sensitivity Study: ^{192}Ir

- Water vs soft-tissus: almost little effect!

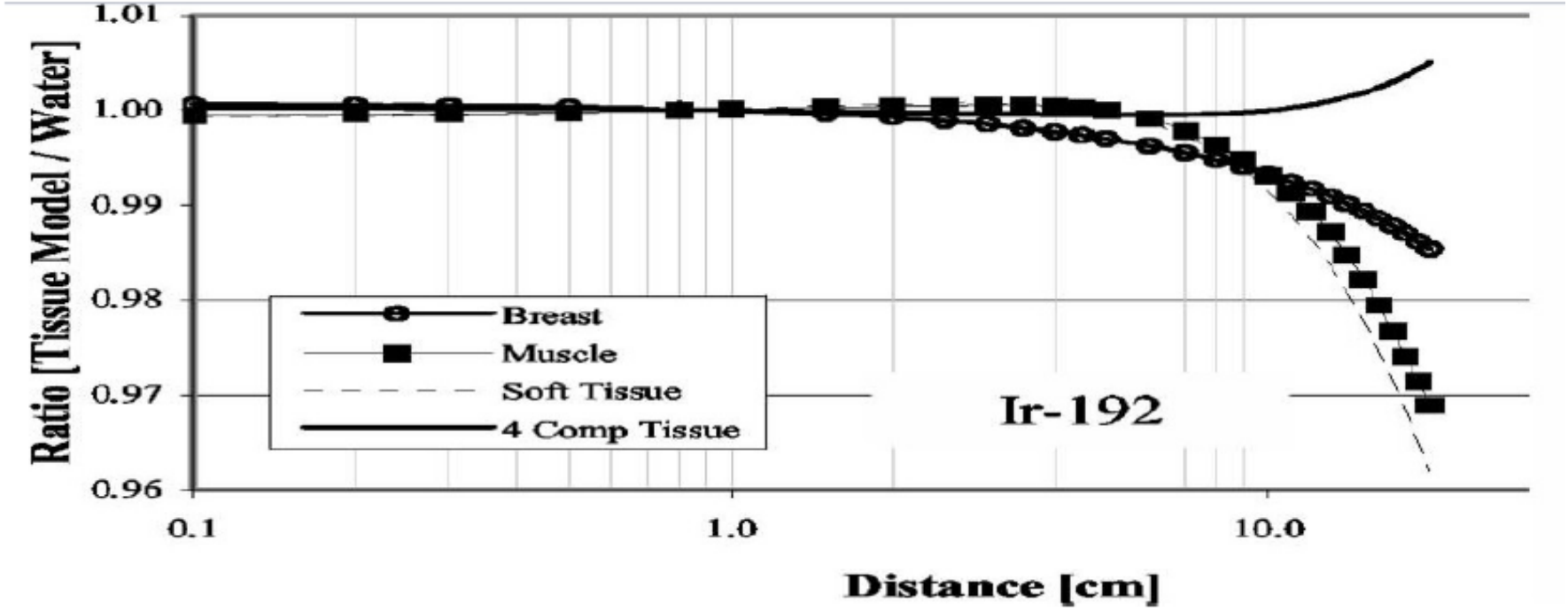

Melhus et al, Med Phys 33 (2006).
From clinical cases: Mikell et al., IJROBP 83 (2012); Desbiens et al, Radiother. Oncol (2013); FA Siebert et al., Brachytherapy 5 (2013)

Recommendations

- If artifacts (e.g. from metals)
  - Override the density using the recommended default organ/tissue density
  - Assign tissue composition based on organ contours

TABLE III. Material definitions. Water is given for comparison.

	% mass					Mass density
Tissue	H	C	N	O	Z > 8	g cm^{-3}
Prostate (Ref. 110)	10.5	8.9	2.5	77.4	Na(0.2), P(0.1), S(0.2), K(0.2)	1.04
Mean adipose (Ref. 110)	11.4	59.8	0.7	27.8	Na(0.1), S(0.1), Cl(0.1)	0.95
Mean gland (Ref. 110)	10.6	33.2	3.0	52.7	Na(0.1), P(0.1), S(0.2), Cl(0.1)	1.02
Mean male soft tissue (Ref. 109)	10.5	25.6	2.7	60.2	Na(0.1), P(0.2), S(0.3), Cl(0.2), K(0.2)	1.03
Mean female soft tissue (Ref. 109)	10.6	31.5	2.4	54.7	Na(0.1), P(0.2), S(0.2), Cl(0.1), K(0.2)	1.02
Mean skin (Ref. 109)	10.0	20.4	4.2	64.5	Na(0.2), P(0.1), S(0.2), Cl(0.3), K(0.1)	1.09
Cortical bone (Ref. 109)	3.4	15.5	4.2	43.5	Na (0.1), Mg (0.2), P (10.3), S (0.3), Ca(22.5)	1.92
Eye lens (Ref. 109)	9.6	19.5	5.7	64.6	Na(0.1), P(0.1), S(0.3), Cl(0.1)	1.07
Lung (inflated) (Ref. 109)	10.3	10.5	3.1	74.9	Na(0.2), P(0.2), S(0.3), Cl(0.3), K(0.2)	0.26
Liver (Ref. 109)	10.2	13.9	3.0	71.6	Na(0.2), P(0.3), S(0.3), Cl(0.2), K(0.3)	1.06
Heart (Ref. 109)	10.4	13.9	2.9	71.8	Na(0.1), P(0.2), S(0.2), Cl(0.2), K(0.3)	1.05
Water	11.2			88.8		1.00

Recommendations

- If relevant, artifacts must be removed prior to dose calculations
- Manual override of tissue composition and density is the simplest approach.
- Advanced approaches: if used, must be carefully documented

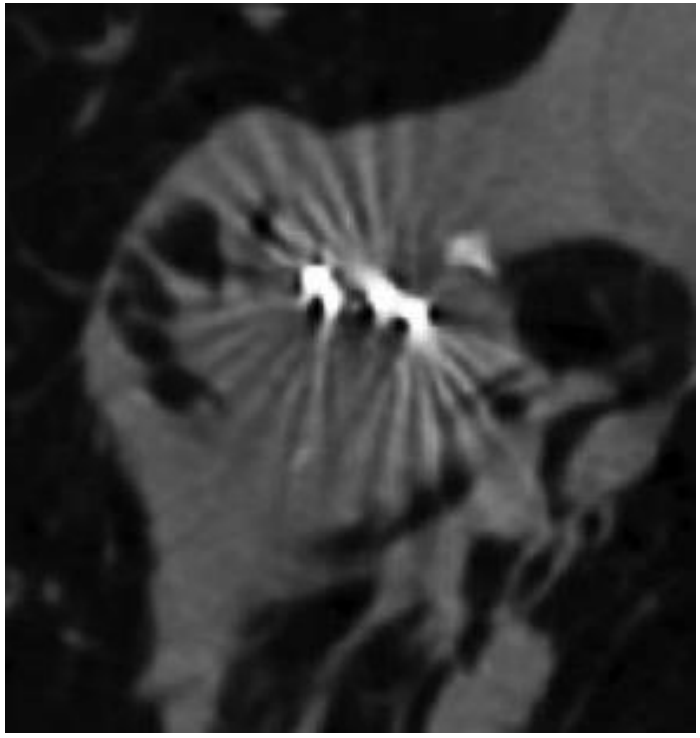

Sutherland et al, Med. Phys. **38**, 4365 (2012)

Recommendations

- If no CT (US and MRI)
  - Use contoured organs with recommended tissue compositions
    - For ^{192}Ir, water is a good approximation for soft tissues only.
    - Air, lung, bone, … should be assigned correctly
      - Could potentially be generated on MRI (Yu et al., IJROBP, In press; DOI: 10.1016/j.ijrobp.2014.03.028)
  - Use accurate source and applicators geometry and composition

About Pseudo-CT?

IRM: prostate avec proton

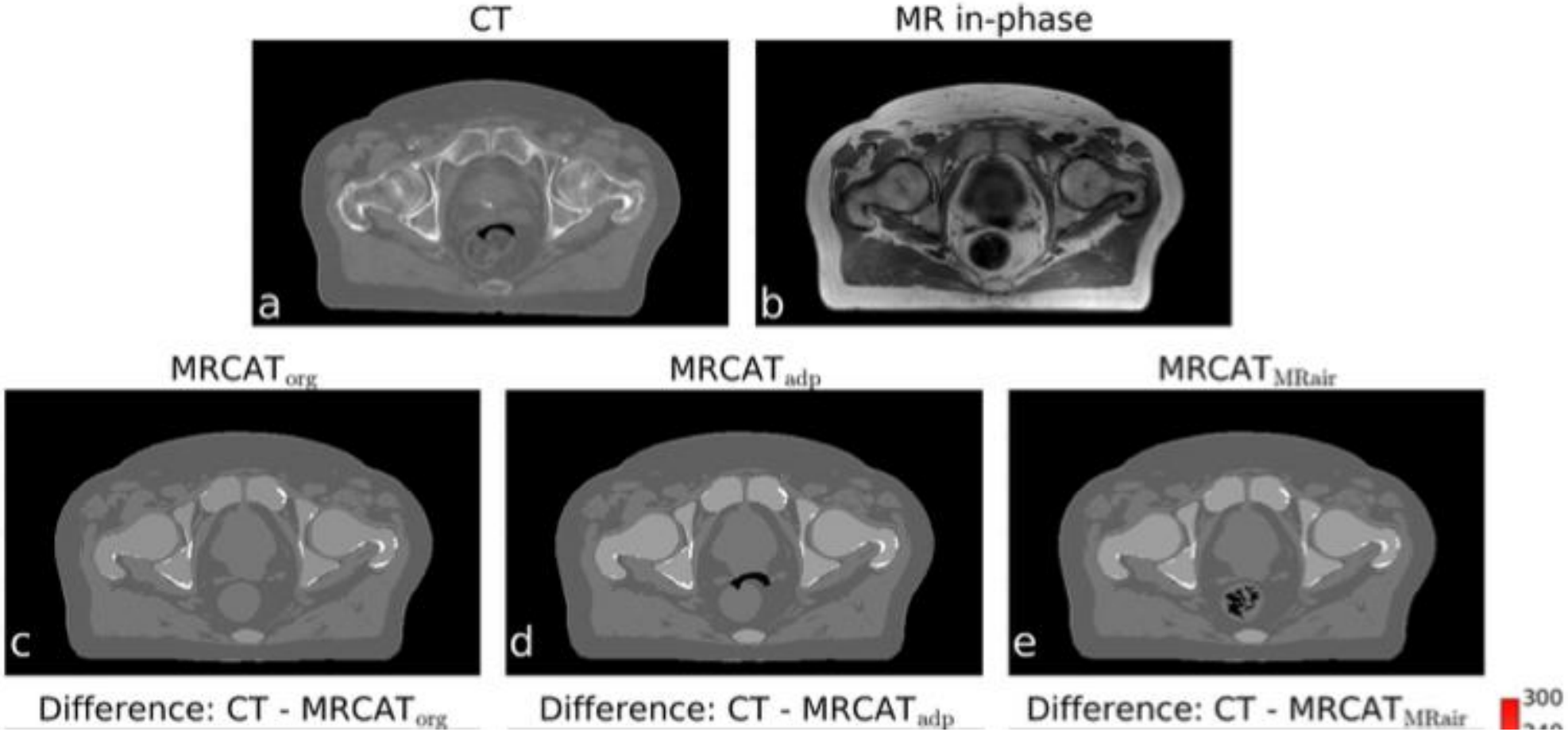

Maspero et al, PMB 62(2017)

IRM: prostate avec proton

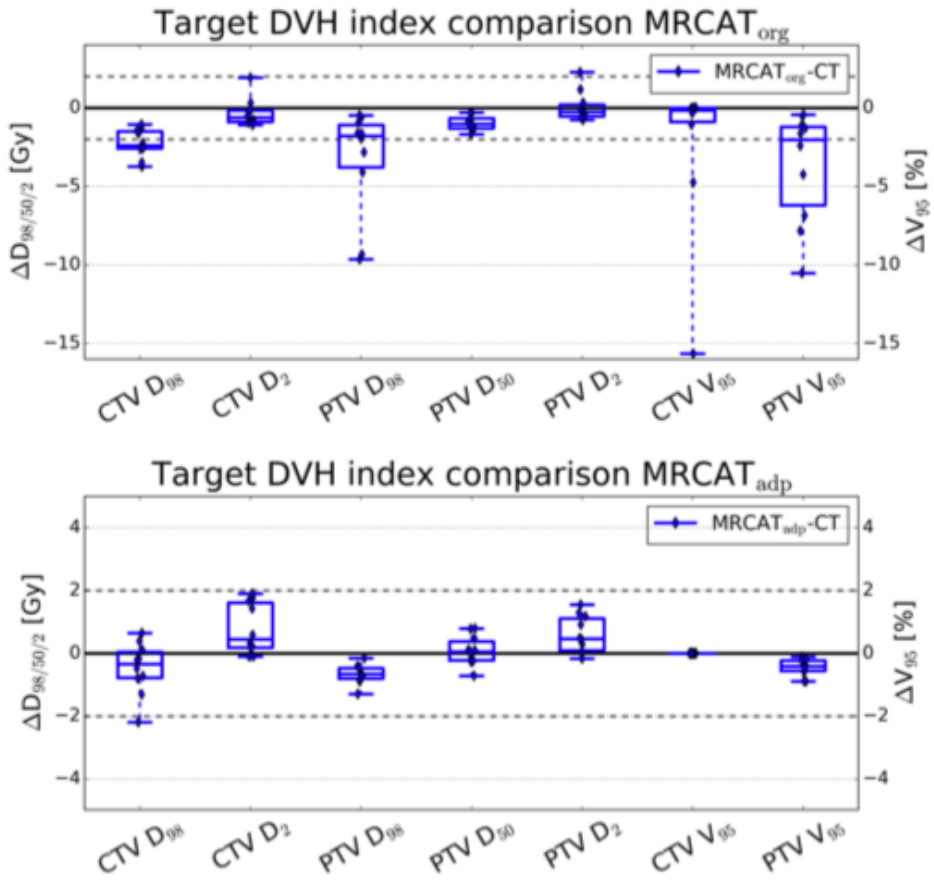

This study shows that accurate MR-based proton dose calculation for prostate cancer treatment could be performed using a commercial solution originally designed for photon radiotherapy, following adaptation of pseudo-HU values. The correct modelling of internal air cavities was found crucial. For this, a novel method to detect air cavities in an MR-only workflow was pro-

Maspero et al, PMB 62(2017)

Recommendations

- Requirements from vendors
  - Accurate geometry (information accessible to users for commissioning)
  - Responsible for providing accurate composition of seeds, applicators and shields.
  - To provide a way for the manufacturers (of the above) or alternatively the end users to input such information into the TPS

  - Poke your favorite vendor, this will be critical

Other issues

What is the problem with this figure?

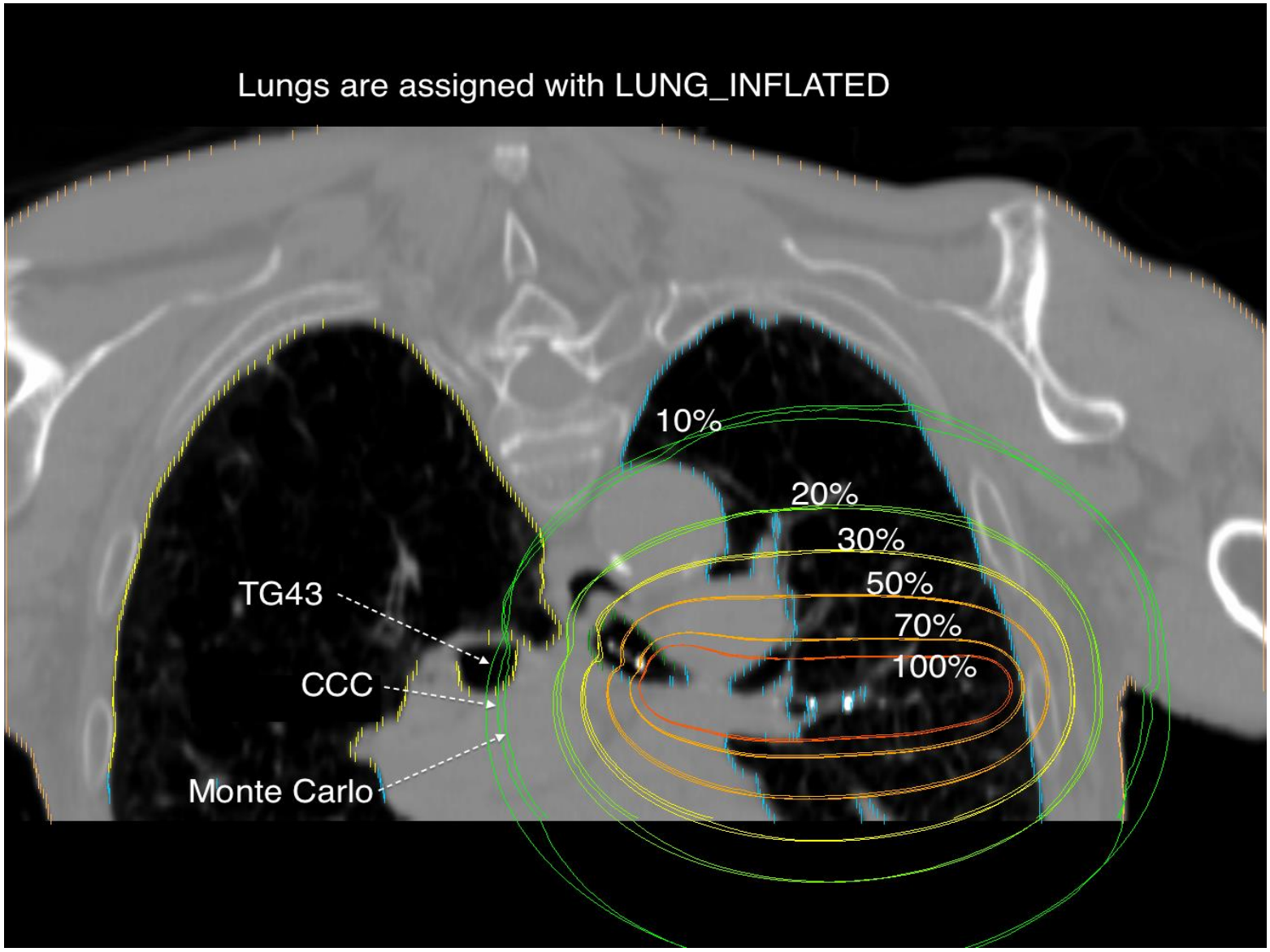

An easier case

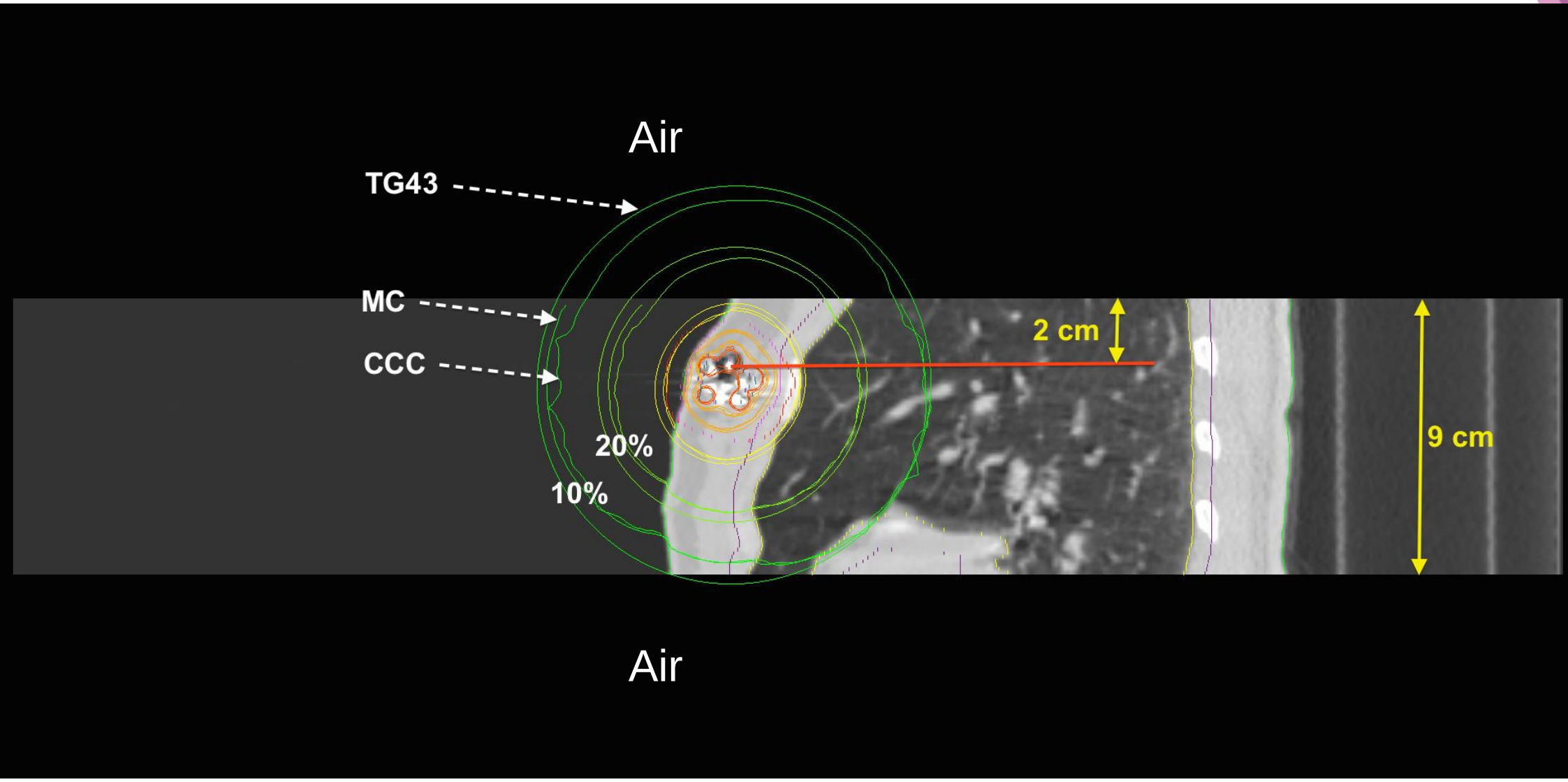

Seed/Applicator Model Accuracy Requirements

- Patient CT grids (>1 mm voxel) are probably not adequate for accurate modeling on the spatial scale of brachytherapy sources and applicators.

- MBDCA vendors should use analytic modeling schemes or recursively specify meshes with 1–10 μm spatial resolution.

- Vendors to disclose their geometry, material assignments, and manufacturing tolerances to both end users and TPS vendors (if responsible for data entry and maintenance)

If TPS Applicator Library provided

- Preferred approach
  - Will ease the verification task.

- Vendor must provide visualization or reporting tools to end user to verify the correctness of each included applicator and source model
  - Ideally against independent design specifications.

- In addition, TPS vendors must disclose sufficient information regarding the model or recursive mesh generation to allow verification of the spatial resolution requirement specified in recommendation (2) in TG-186 Section IV-B

TG-186 Section IV.B: Applicators

- “It is the responsibility of the end-user clinical physicist to confirm that MBDCA dose predictions are based upon sufficiently accurate and spatially resolved applicator and source models, including correct material assignments, to avoid clinically significant dose-delivery error prior to implementing the dose algorithm in the clinic.”

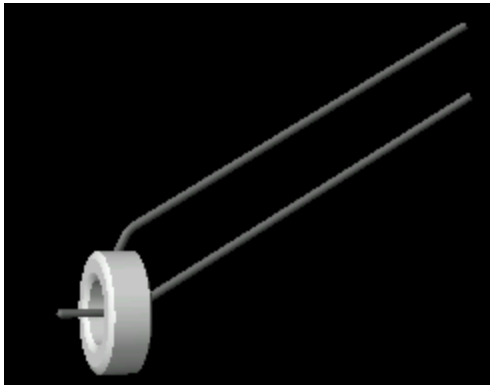

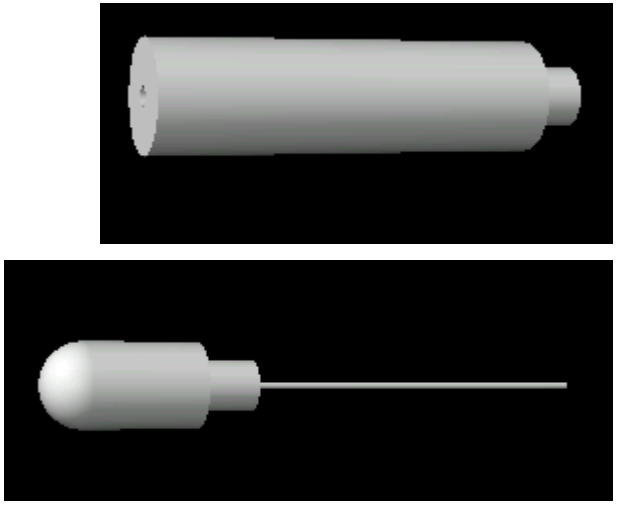

Example: Solid Applicator Models in AcurosBV

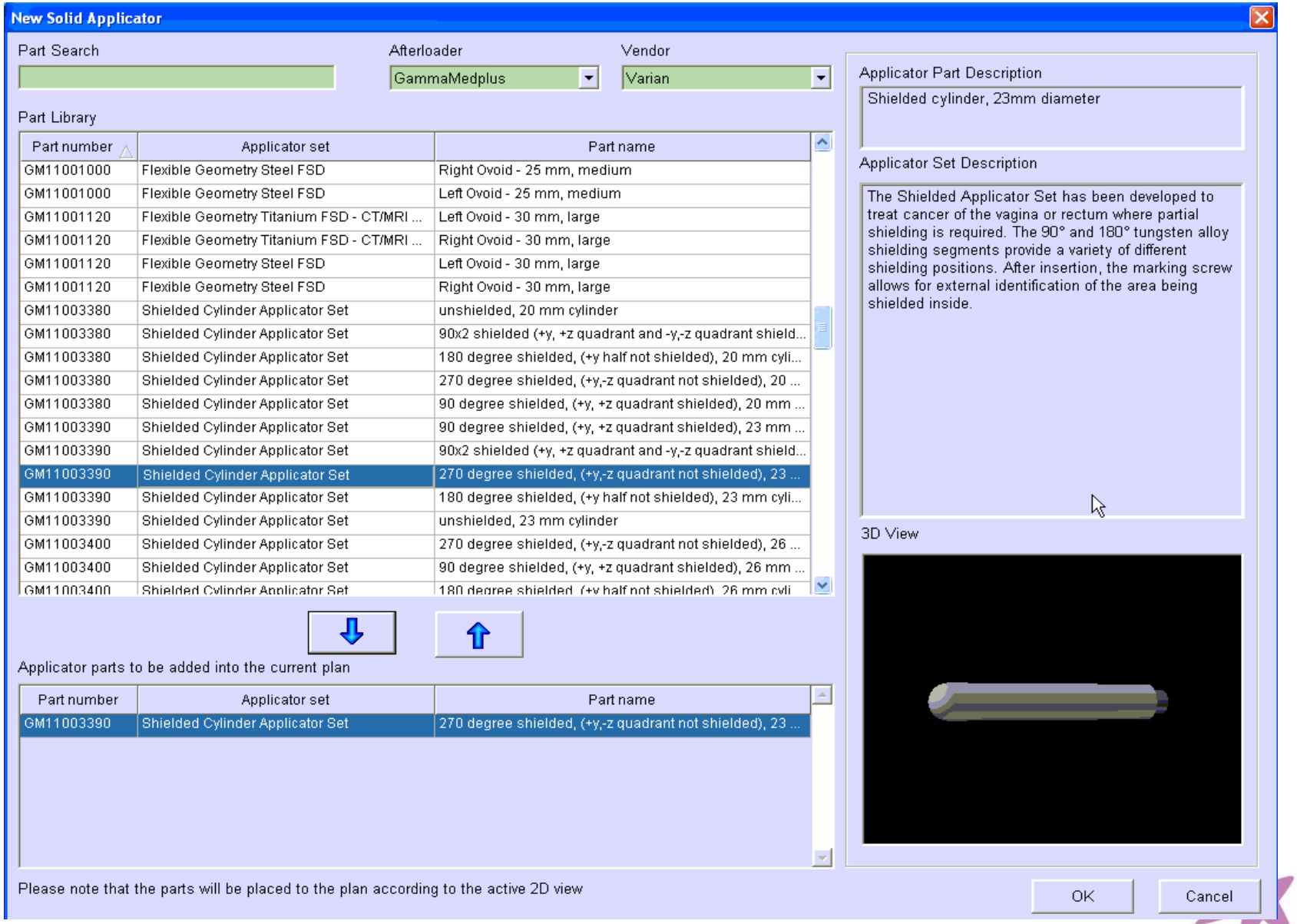

Open Issues: Is there a better approach?

- No simple method to extract Z_{eff} from standard imaging modalities
- Dual/Multi energy CT?

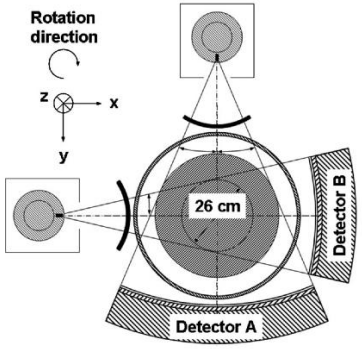

FIG. 1. Technical realization of a DSCT system (SOMATOM Definition, Siemens Healthcare, Forchheim, Germany). One detector (A) covers the entire scan field of view with a diameter of 50 cm, while the other detector (B) is restricted to a smaller, central field of view.

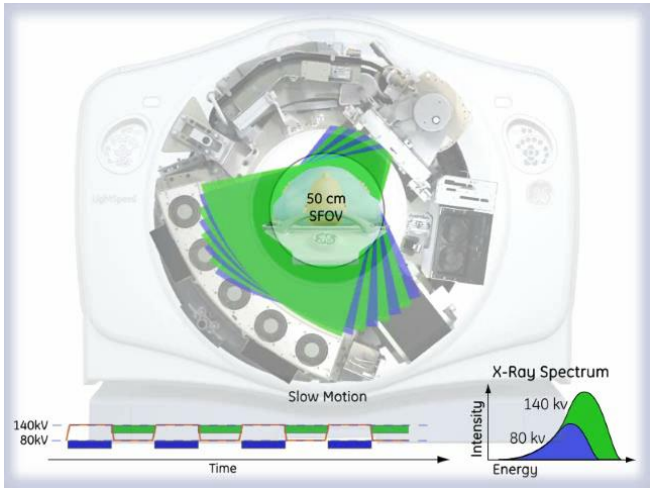

DECT for Brachytherapy and related topics

- Bazalova M et al 2008a Dual-energy CT-based material extraction for tissue segmentation in Monte Carlo dose calculations Phys. Med. Biol. 53 2439–56
- Bazalova M et al 2008b Tissue segmentation in Monte Carlo treatment planning: a simulation study using dual-energy CT images Radiother. Oncol. 86 93–8
- Goodsitt M M et al 2011 Accuracies of the synthesized monochromatic CT numbers and effective atomic numbers obtained with a rapid kVp switching dual energy CT scanner Med. Phys. 38 2222–32
- Heismann B and Balda M 2009 Quantitative image-based spectral reconstruction for computed tomography Med. Phys. 36 4471–85
- Heismann B J et al 2003 Density and atomic number measurements with spectral x-ray attenuation method J. Appl. Phys. 94 2073–9
- Landry G et al 2010 Sensitivity of low energy brachytherapy Monte Carlo dose calculations to uncertainties in human tissue composition Med. Phys. 37 5188–98
- Landry G et al 2011 The difference of scoring dose to water or tissues in Monte Carlo dose calculations for low energy brachytherapy photon sources Med. Phys. 38 1526–33
- Mahnken A H et al 2009 Spectral rhoZ-projection method for characterization of body fluids in computed tomography: ex vivo experiments Acad. Radiol. 16 763–9
- Landry G et al 2011 Simulation study on potential accuracy gains from dual energy CT tissue segmentation for low-energy brachytherapy Monte Carlo dose calculations Phys. Med. Biol. 56 6257–6278
- Bourque AE et al. 2014 A stoichiometric calibration method for dual energy computed tomography. Phys Med Biol. 59 2059-88

- Literature is extensive in radiology and DECT is also of interest in hadron therapy (stopping power)

How does it work?

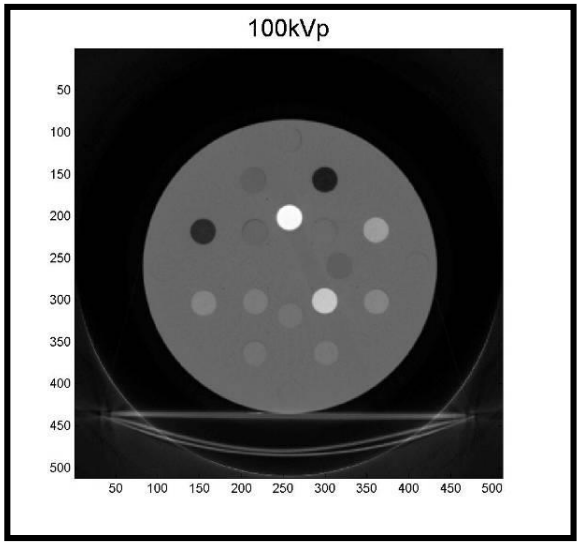

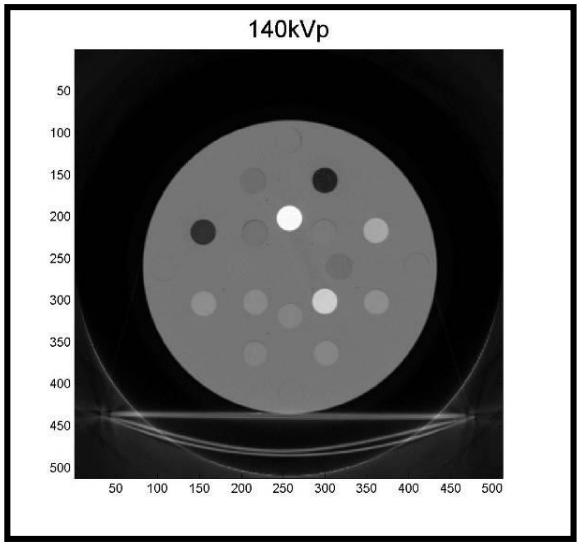

How does it work?

SECT

DECT

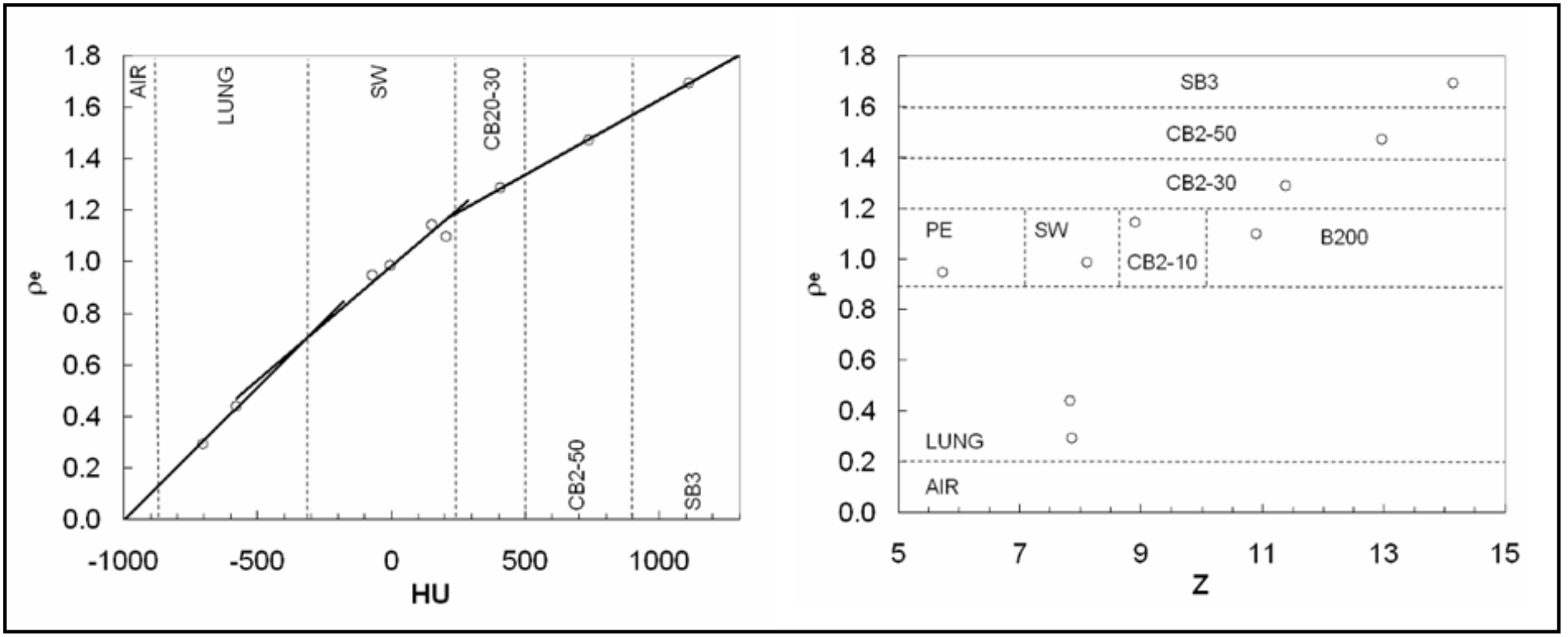

M. Bazalova et al., PMB 53 (2008)

Dual-energy x-ray CT material extraction

- CT images are represented by HU = 1000x(μ/μ_w-1)
  - μ *and* μ_w are the linear attenuation coefficients of a material and of water
- dual-energy material extraction (DECT) is based on
  - Taking CT images at two tube voltages (e.g. 100 kVp and 140 kVp)
  - The farther apart the energy the better!
  - Parameterization of the linear attenuation coefficient results in ρ_e and Z maps

Linear attenuation coefficient

Describes attenuation of a photon beam

Torikoshi *et al*:

$$\mu(E) = \rho_e \left(Z^4 F(E,Z) + G(E,Z) \right)$$

- $\rho_e = \rho Z/A * N_A$ = electron density
- Z = effective atomic number
- $F(E,Z)$ and $G(E,Z)$ are the photoelectric absorption and scattering terms (Rayleigh and Compton) of μ

For polychromatic x-rays:

$$\mu_j = \rho_e \sum_i \omega_{ji} \left[Z^4 F(E_{ji}, Z) + G(E_{ji}, Z) \right]$$

x-ray spectra represented by weights ω_i at E_i

Torikoshi et al, Phys. Med. Biol. 2003; 48: 673-685.
Tsunoo T, et al , NSS Conference Record, IEEE, 2004; 6: 3764-3768

Linear attenuation coefficient

Having the densities the same material measured at two tube voltages, one can solve for Z:

$$\frac{m_1}{m_2} - \frac{\sum_i w_{1i}\left[Z^4 F\left(E_{1i},Z\right)+G\left(E_{1i},Z\right)\right]}{\sum_i w_{2i}\left[Z^4 F\left(E_{2i},Z\right)+G\left(E_{2i},Z\right)\right]} = 0$$

Or, solve for both Z and density simultanetously

$$Z^4 - \frac{\frac{\mu_2}{\mu_{2w}}\sum_i \omega_{2i}\left[Z_w^4 F(E_{2i},Z_w)+G(E_{2i},Z_w)\right]\sum_i \omega_{1i} G(E_{1i},Z) - \frac{\mu_1}{\mu_{1w}}\sum_i \omega_{1i}\left[Z_w^4 F(E_{1i},Z_w)+G(E_{1i},Z_w)\right]\sum_i \omega_{2i} G(E_{2i},Z)}{\frac{\mu_1}{\mu_{1w}}\sum_i \omega_{1i}\left[Z_w^4 F(E_{1i},Z_w)+G(E_{1i},Z_w)\right]\sum_i \omega_{2i} F(E_{2i},Z) - \frac{\mu_2}{\mu_{2w}}\sum_i \omega_{2i}\left[Z_w^4 F(E_{2i},Z_w)+G(E_{2i},Z_w)\right]\sum_i \omega_{1i} F(E_{1i},Z)} = 0$$

M. Bazalova et al., PMB 53 (2008); Bazalova et al Radiother Oncol 86 (2008)

ESTRO School

$F(E,Z)$ and $G(E,Z)$ functions

$$\mu = \mu_{photoeffect} + \mu_{Compton+Rayleigh}$$

- $(\mu/\rho)_p = Z^5 N_A/A * F(E,Z) \Rightarrow \quad \mu_p = \rho_e Z^4 * F(E,Z)$
- $(\mu/\rho)_{C+R} = Z N_A/A * G(E,Z) \Rightarrow \quad \mu_{C+R} = \rho_e * G(E,Z)$

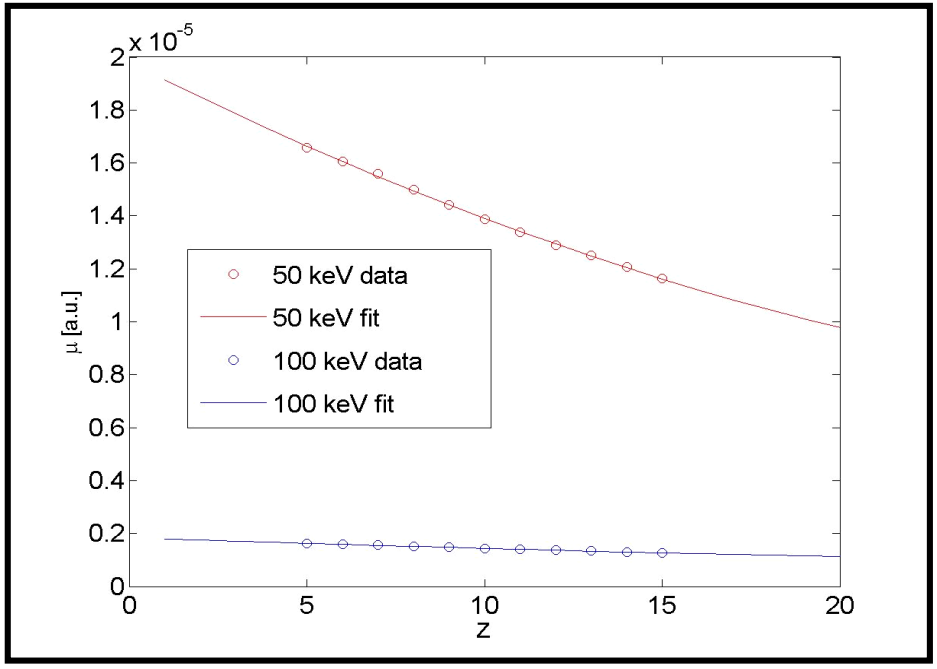

$F(E,Z)$

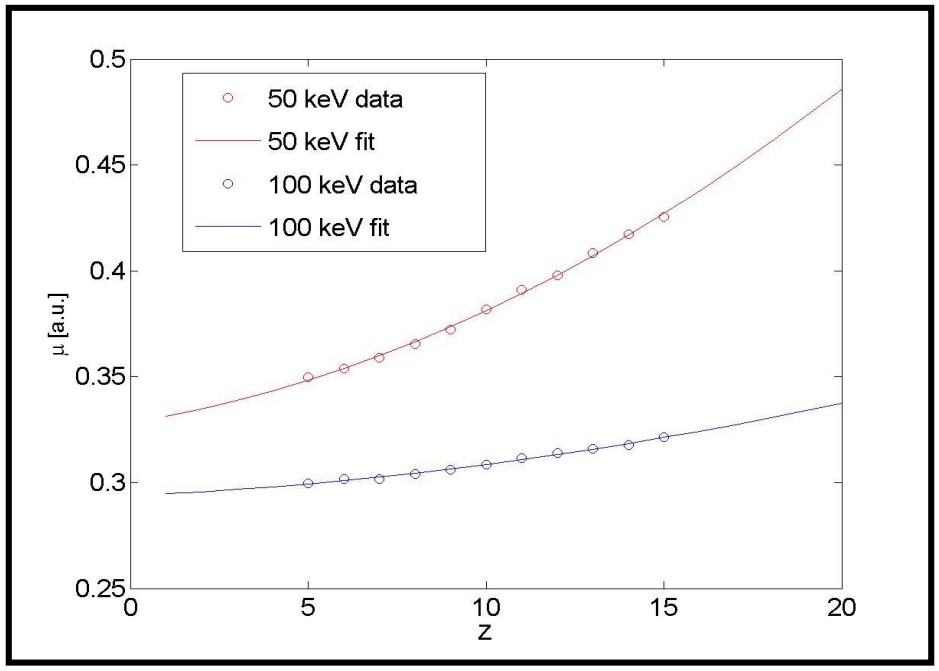

$G(E,Z)$

Putting these equation to practice

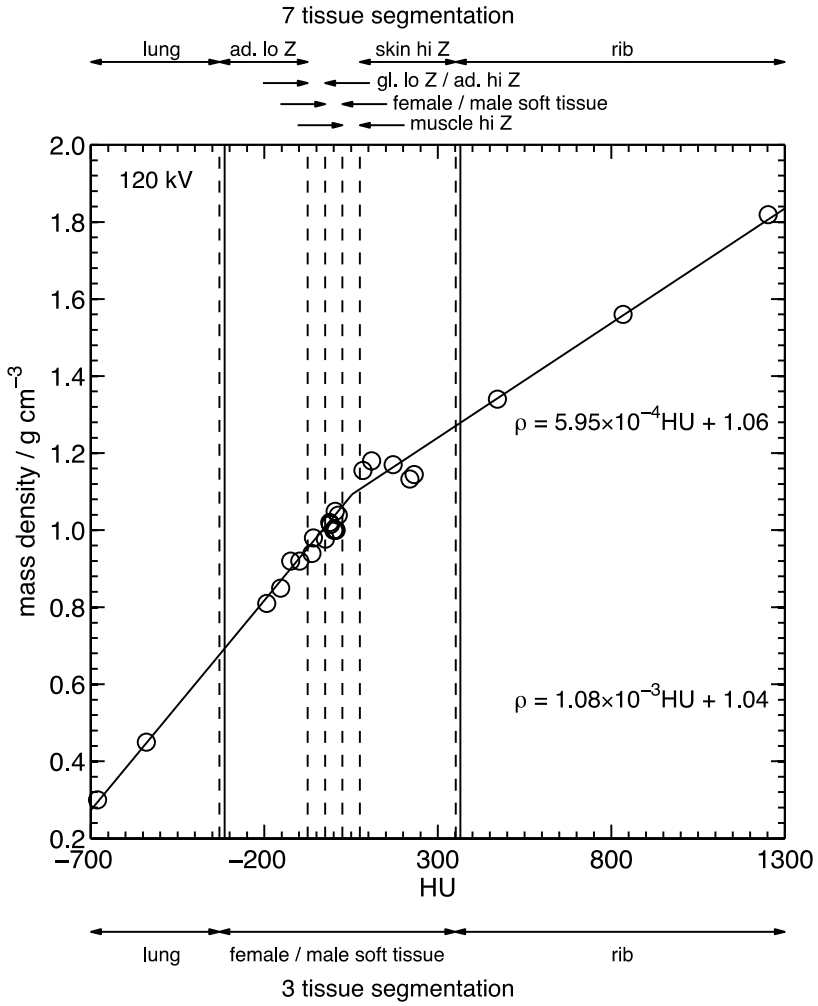

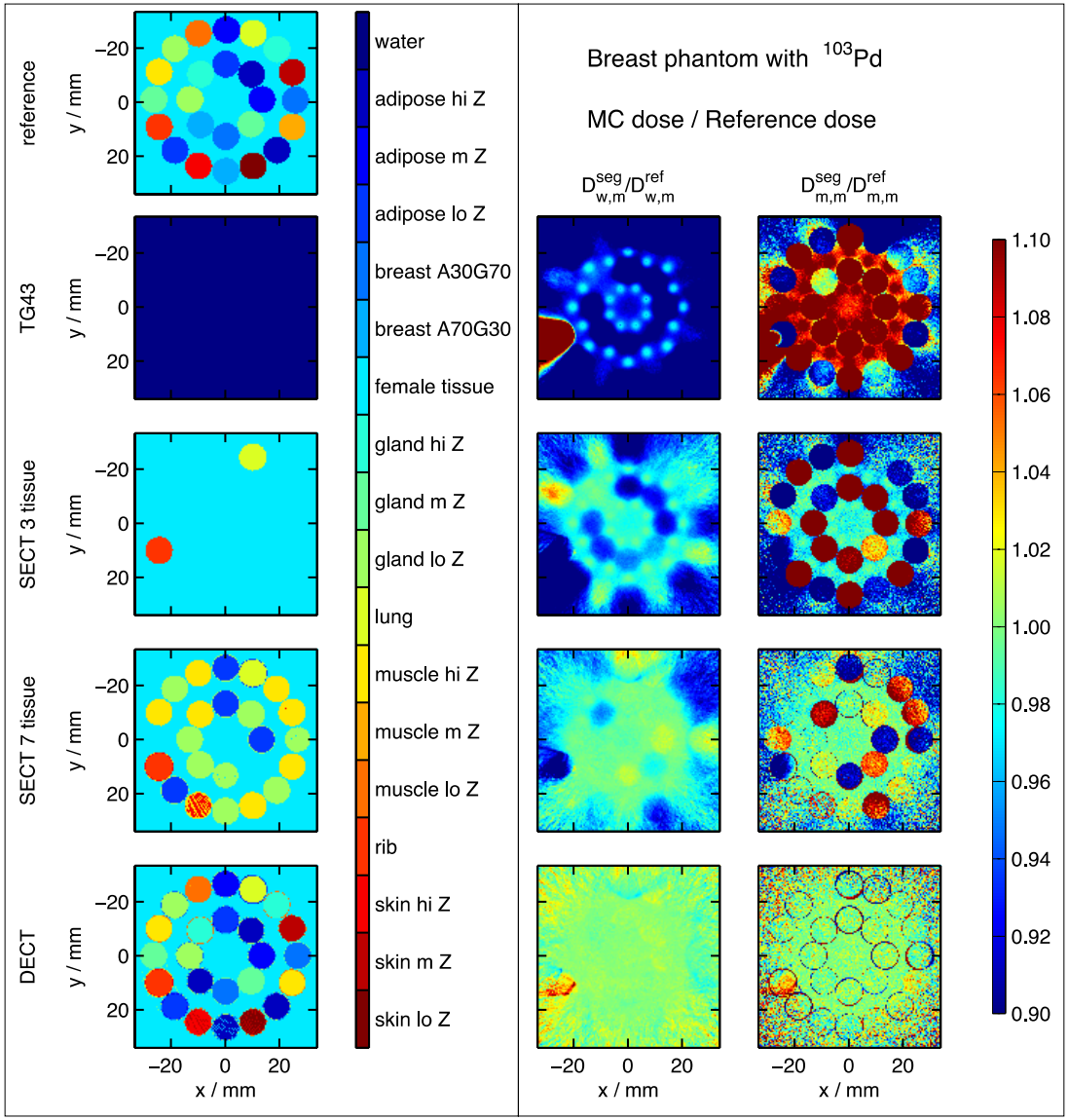

G. Landry et al., PMB 56 (2011)

Putting these equation to practice

Improved tissue assignment using dual-energy computed tomography in low-dose rate prostate brachytherapy for Monte Carlo dose calculation

Nicolas Côté
Département de Physique, Université de Montréal, Pavillon Roger-Gaudry (D-428), 2900 Boulevard Édouard-Montpetit, Montréal, Québec H3T 1J4, Canada

Stéphane Bedwani
Département de Radio-Oncologie, Centre Hospitalier de l'Université de Montréal (CHUM), 1560 Rue Sherbrooke Est, Montréal, Québec H2L 4M1, Canada

Jean-François Carrier[a)]
Département de Physique, Université de Montréal, Pavillon Roger-Gaudry (D-428), 2900 Boulevard Édouard-Montpetit, Montréal, Québec H3T 1J4, Canada and Département de Radio-Oncologie, Centre Hospitalier de l'Université de Montréal (CHUM), 1560 Rue Sherbrooke Est, Montréal, Québec H2L 4M1, Canada

(Received 28 August 2015; revised 9 April 2016; accepted for publication 12 April 2016; published 29 April 2016)

Cote et al, Med Phys 43

Putting these equation to practice

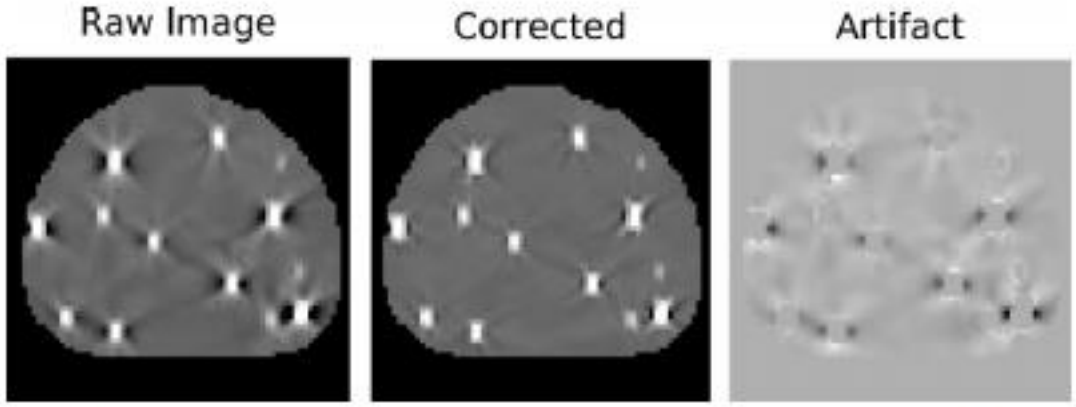

FIG. 3. Raw image at 100 kVp which has been corrected by DECT MAR algorithm. Window level: 461 HU, window width: 1592 HU for both images raw and corrected images. The last image represents the artifact information generated from Eq. (5).

An automatic tissue assignment technique was developed using DECT images. This modality allows for a reduced impact of metallic artifacts, which in turn improves the quality of tissue assignment. Differences in D_{90} were underestimated in the SECT-based approach by up to 2.3% compared with the developed DECT algorithm. Thus, the DECT is a potentially superior method, allowing significant reduction in metallic artifact presentation, and more accurate representation of patient tissue anatomy and density.

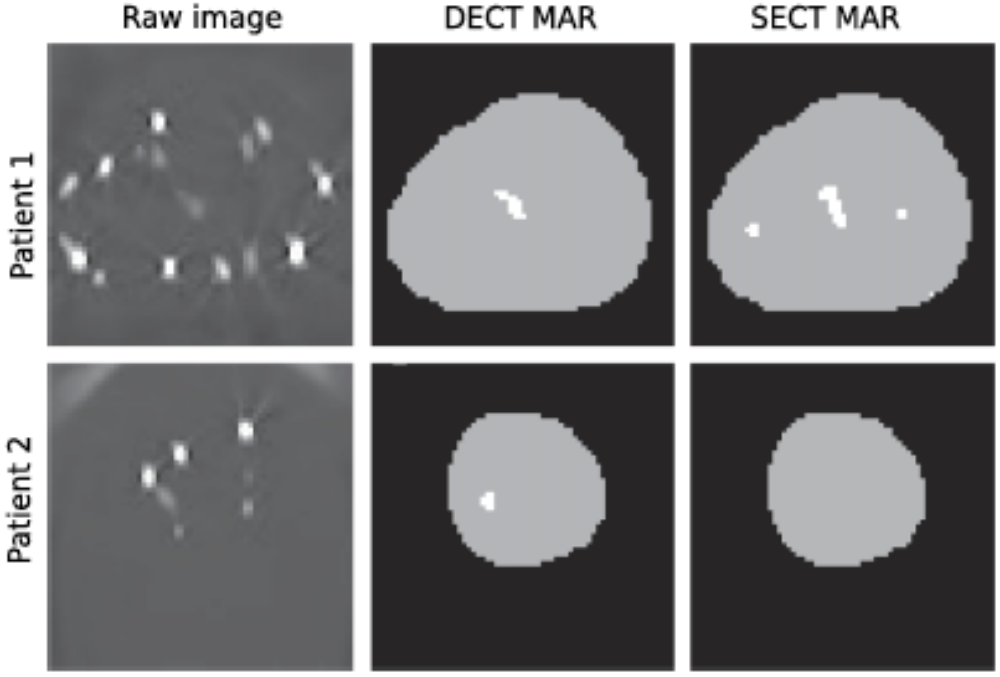

Cote et al, Med Phys 43

Lesson learned?

- DECT calculations for low energy sources within 4% of ground truth
  - 7 tissue bins SECT at <9%; 3 tissue bin (like EBRT) failed!

- DECT very sensitive to noise and motion
  - May make DECT difficult for patient imaging (CT dose / mAs settings)
  - Simultaneous imaging

- Still a very active field of research!

Conclusion

- Voxel-by voxel cross section assignment is a critical step
  - Tissue segmentation; Applicator and source description
  - Follow TG-186 guidelines to ensure centre-to-centre consistency
  - Poke/Question your favorite TPS/Applicator vendor(s)…
- For ^{192}Ir, water is a good representation of soft tissue only
  - Air, bone, metals, … should be segmented and assigned the right material/densitiy
- Dual-Energy/Multi-Energy-CT should be explored actively
  - Potential accurate solution to (ρ_e ,Z_{eff}) assignments
  - Hot research topics

ESTRO School

WWW.ESTRO.ORG/SCHOOL

ESTRO School

La Fe
Hospital Universitari i Politècnic

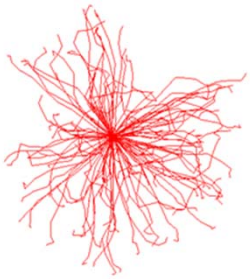

Medical Physics Group
University of Valencia
IRIMED

QA of 3D Imaging in Brachytherapy

Jose Perez-Calatayud

Hospital Universitario y Politecnico La Fe. Valencia.

perez_jos@gva.es

Advanced Brachytherapy Physics. Valencia 7-10 October 2018

ESTRO School

Disclosures

- We are users of Elekta equipment (HDR Ir-192 and LDR I-125)
- Commercial products included in this presentation just for illustrative purposes

Acknowledgments

Frank-André Siebert

Luc Beaulieu

Dimos Baltas

Françoise Lliso

Vicente Carmona

José Gimeno

Rafael García

Nuria Carrasco

Learning Objectives

- To identify the various imaging modalities used in brachytherapy planning
- To give key points to be considered in a efficient QA/QC program and some practical considerations
- To provide some examples of recent and in progress topics to improve accuracy

Imaging modalities for brachy planning

- Contouring + Cath reconstruction + Optimization & calculation
- Most convenient, because of uncertainties, is that all steps on the same image set, avoiding registrations

Imaging modalities for brachy planning

CT

- Head & Neck
- Skin
- Breast
- Lung
- Esophagus
- Keloid
- Gyn.
- ....
- *GENERAL*

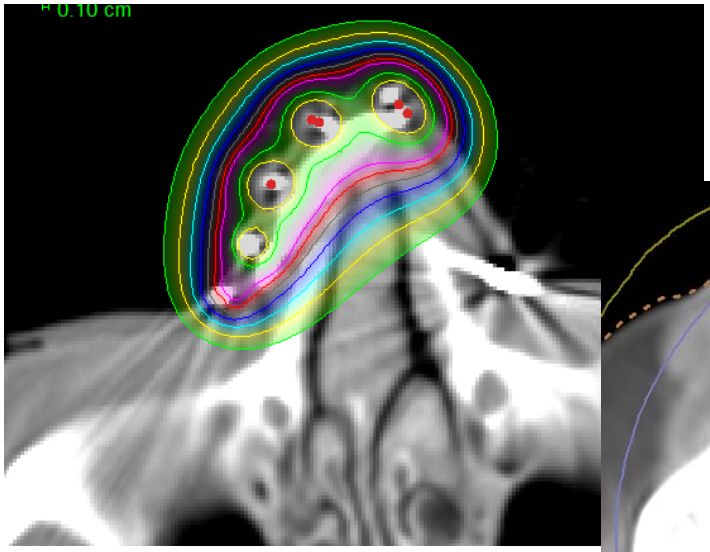

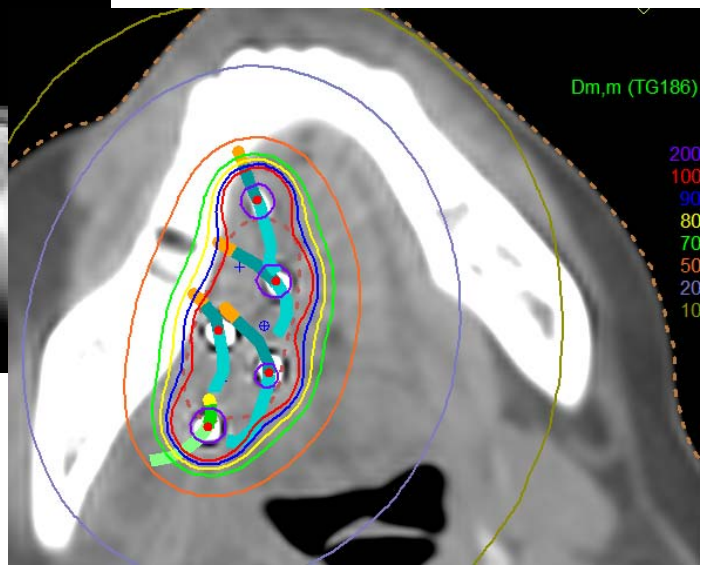

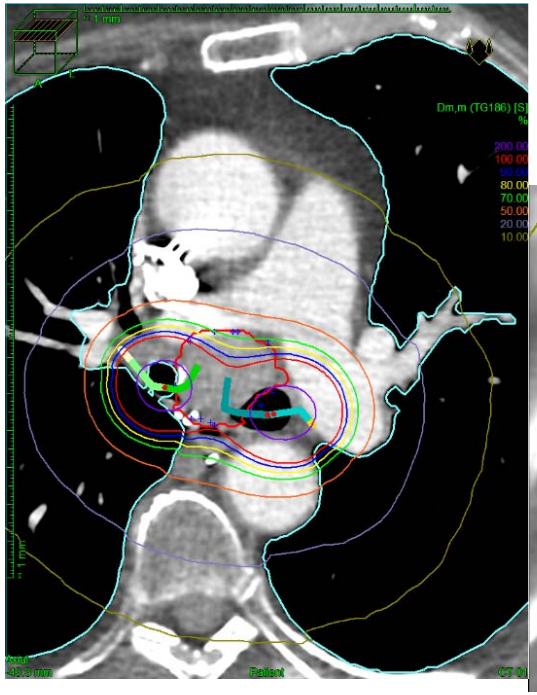

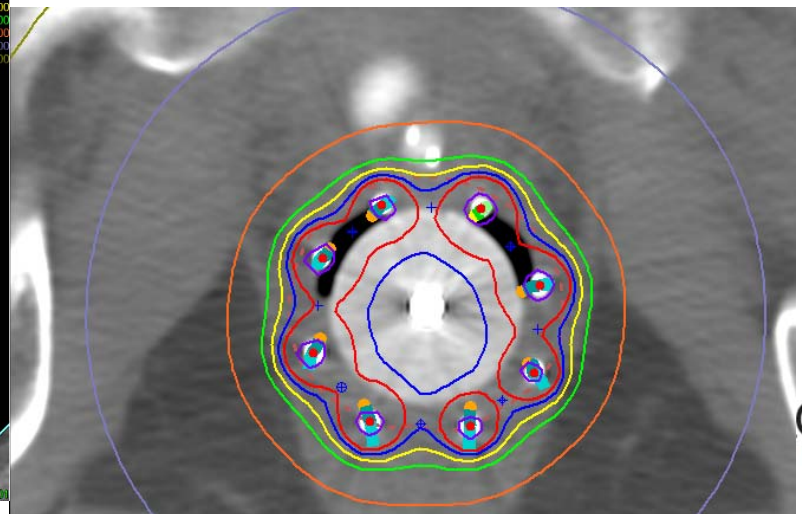

Imaging modalities for brachy planning

- Intraoperative prostate HDR & LDR

TRUS

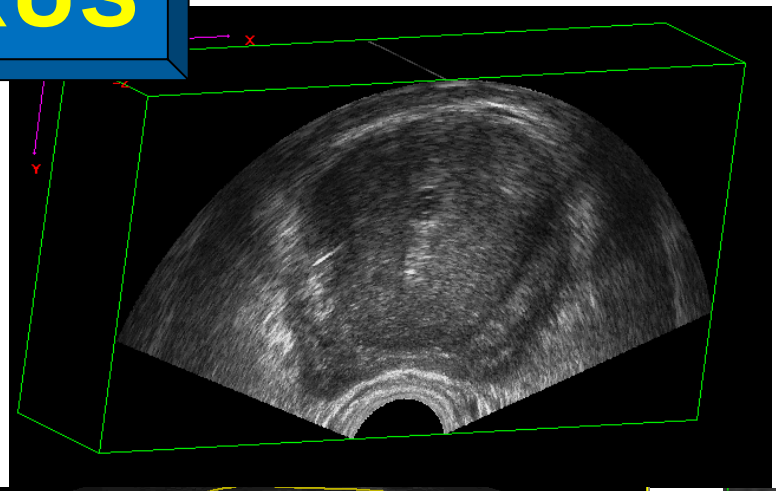

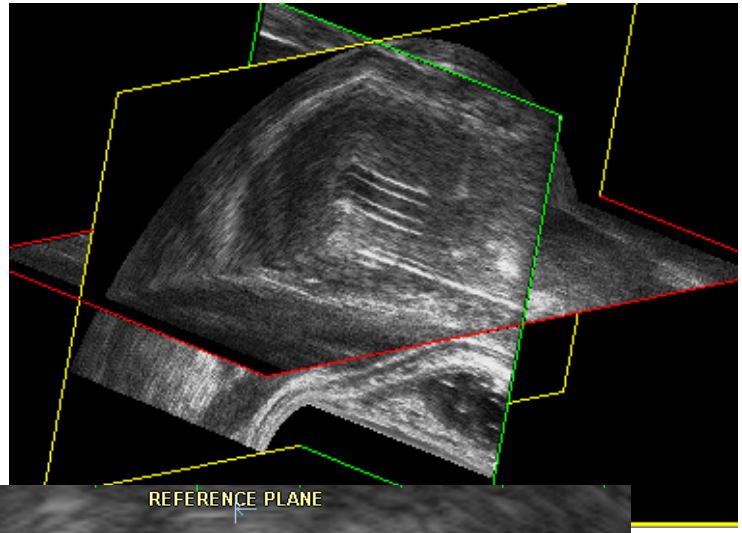

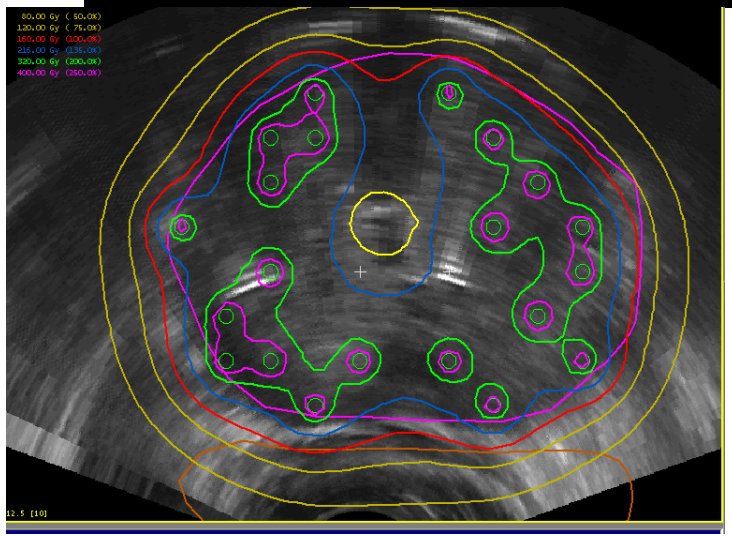

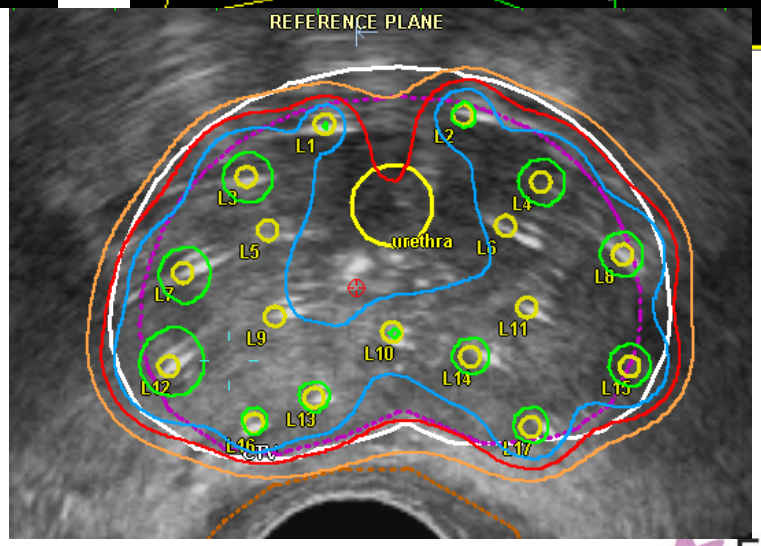

Permanent I-125

HDR Ir-192 or Co-60

ESTRO School

Imaging modalities for brachy planning

MRI T2

- Cervix GYN

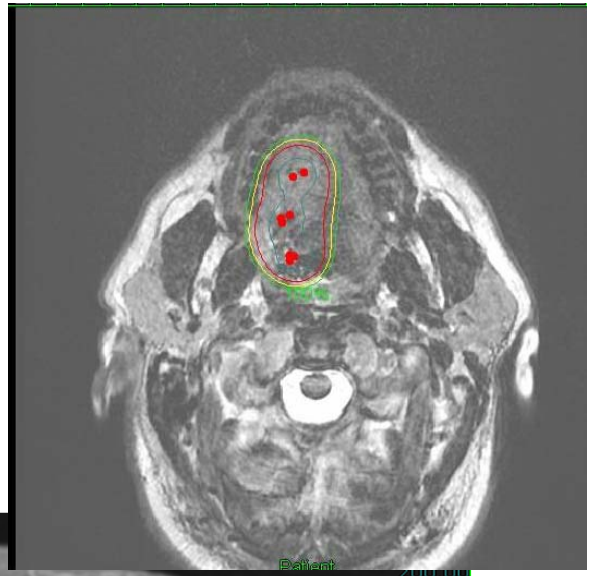

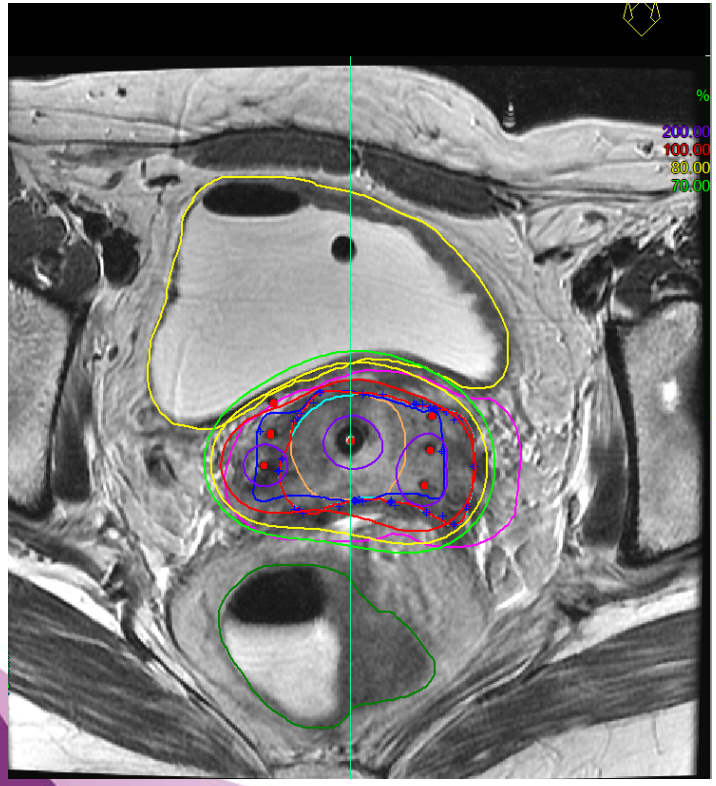

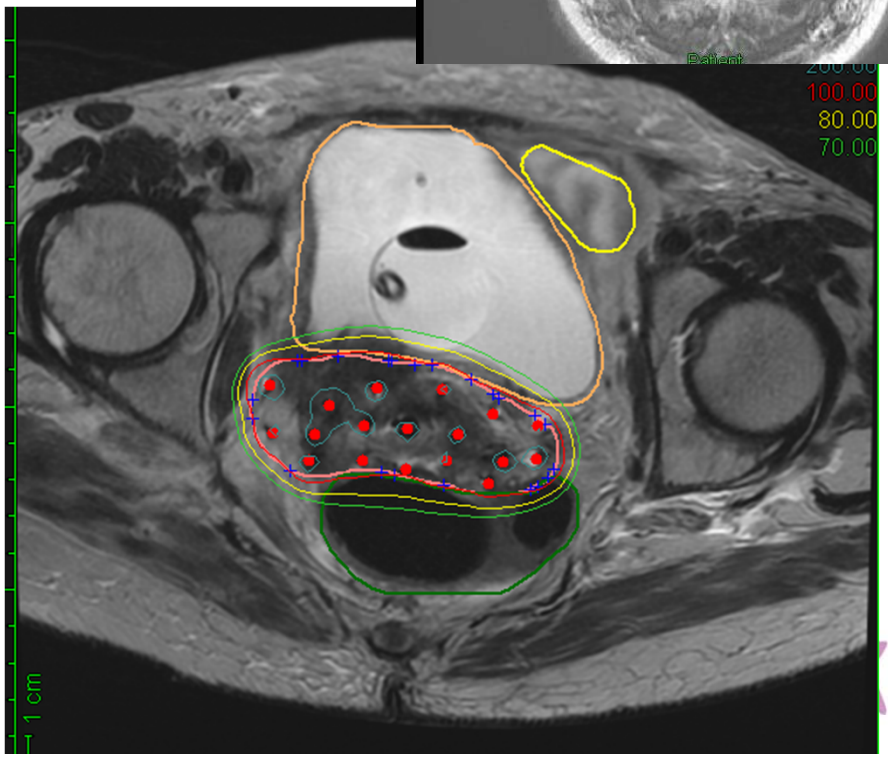

ESTRO School

Imaging modalities for brachy planning

- Prostate LDR Postplan

TRUS + CT + MRI

CT T1 T2

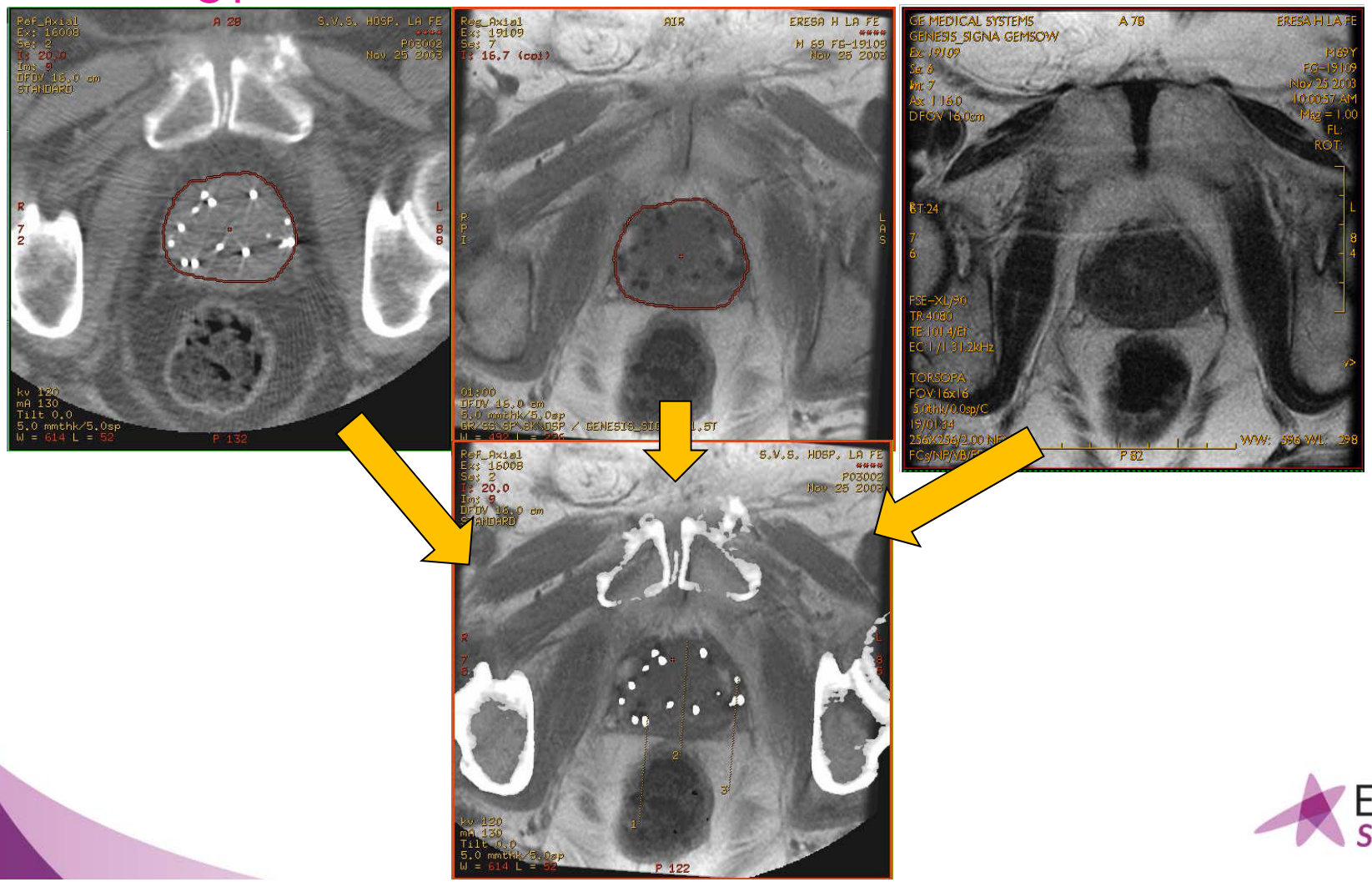

ESTRO School

Imaging modalities for brachy planning

Registration to define GTVs

US

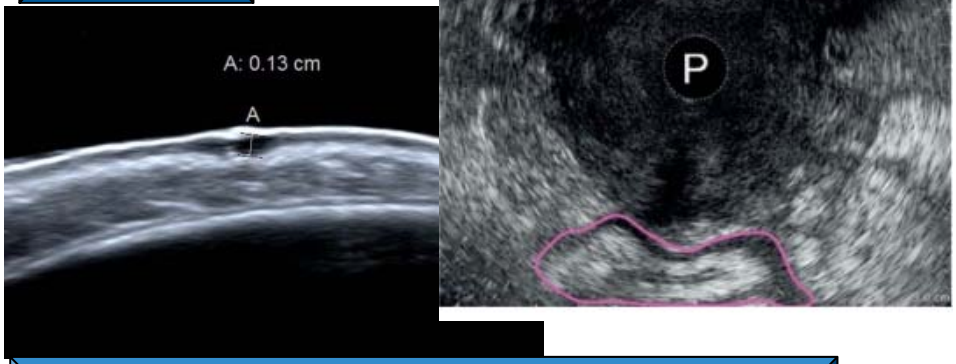

TRAns Cervical Endosonography with rotating transducer (TRACE BT).
Petric 2016

Alternative to T2 MRI ??

mpMRI + TRUS

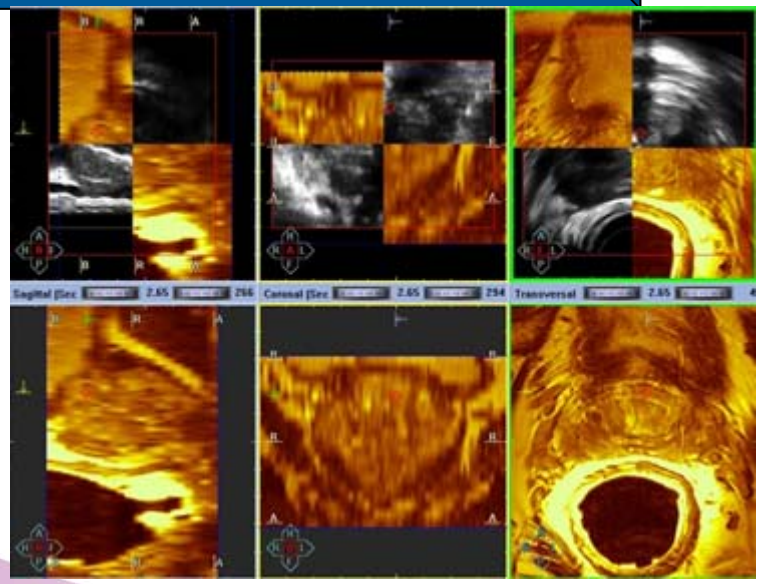

Hybrid Imaging: Example of mP-MR und 3D-U/S (Biology + Morphology)
Courtesy D. Baltas

ESTRO School

Imaging modalities for brachy planning

Registration to define GTVs

PET-CT

MR-US

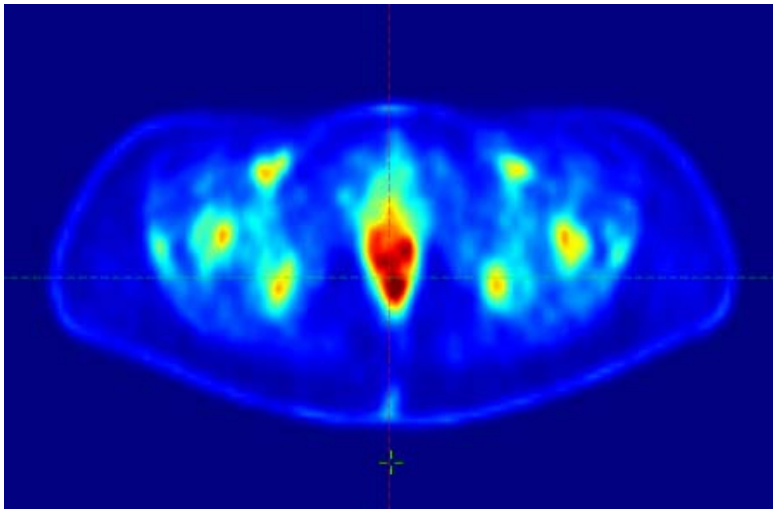

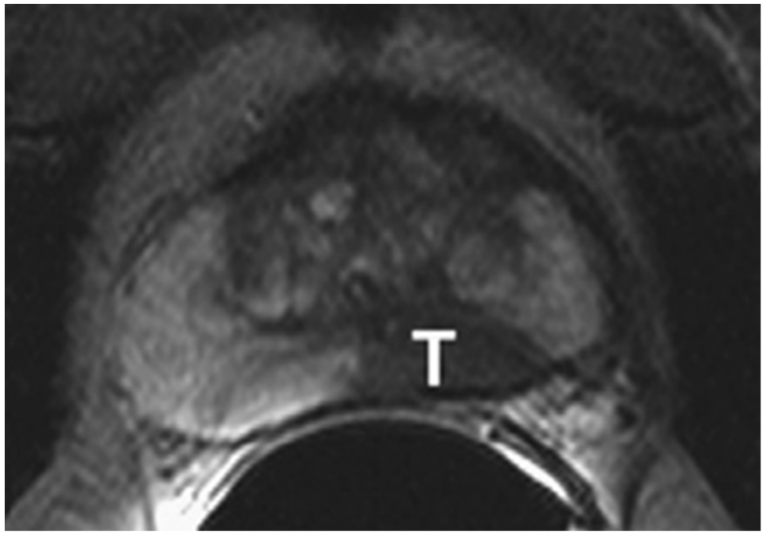

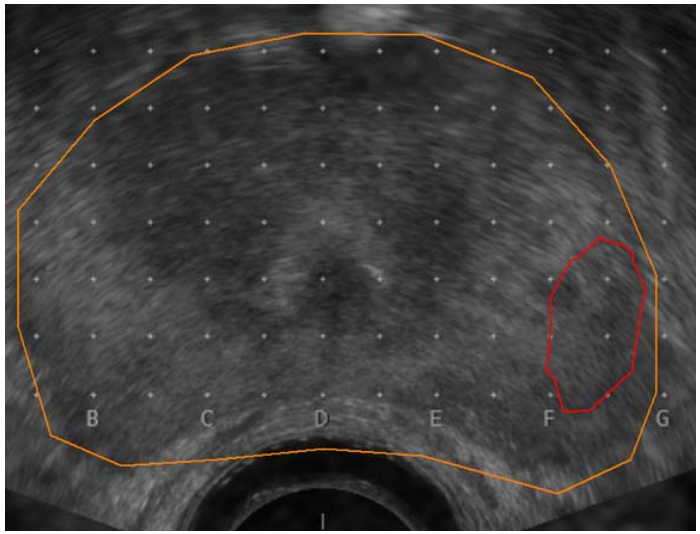

RMN → TRUS

ESTRO School

Imaging modalities for brachy planning

NON-RIGID REGISTRY

MR pre-RT & MR BT

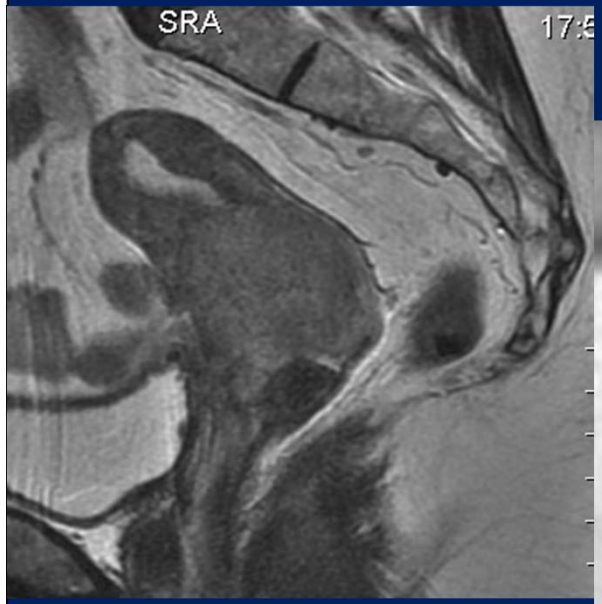

Pre-ERT

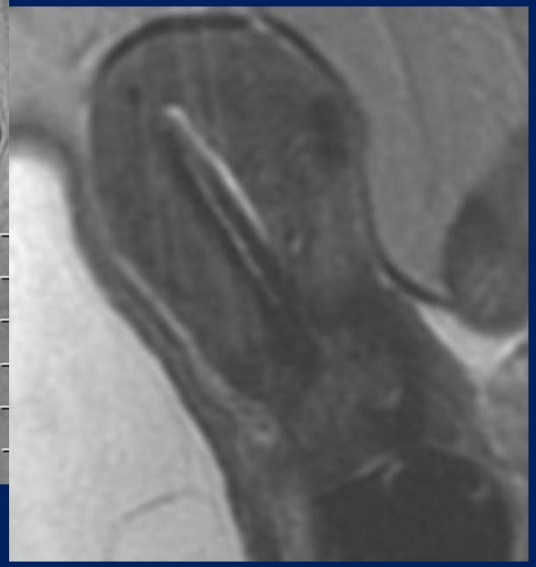

BT-1

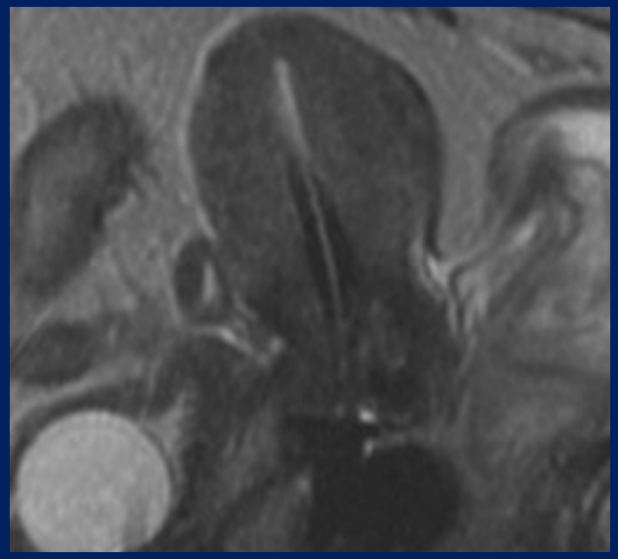

BT-2

Imaging modalities for brachy planning

NON-RIGID REGISTRY

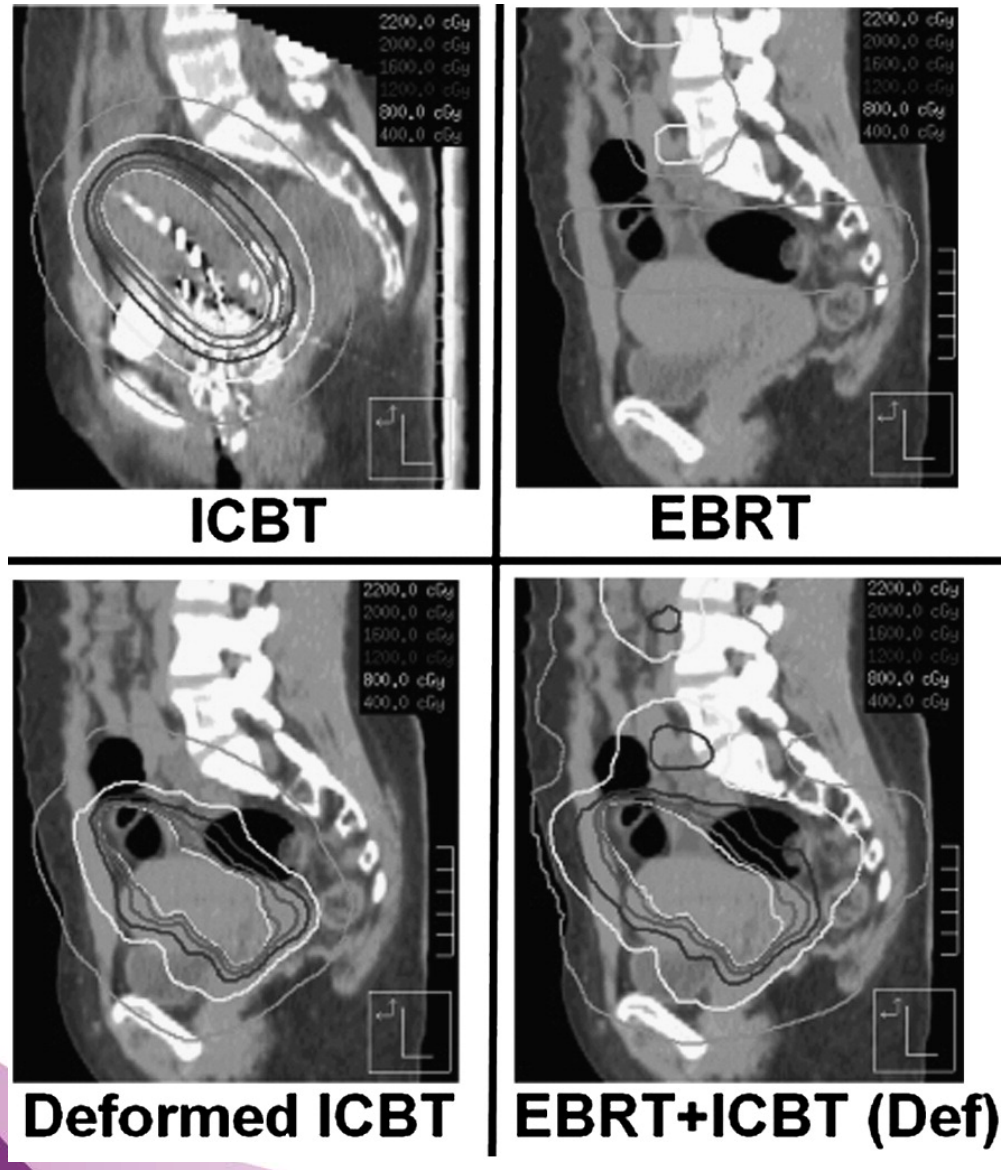

Yu 2011

Uncertainty

Caution

ICRU89 ¡¡¡¡

ESTRO School

Imaging modalities for brachy planning

Most commonly available imaging modality for treatment planning in radiation oncology
Relatively fast
Electronic density can be obtained
Bone, air, bladder, rectum: OK
Excellent resolution in the transverse plane

Resolution limited along the scan axis: needle-cath. tip?
Not very good for soft tissue

Adapted from L. Beaulieu ABP ESTRO Course 2016

ESTRO School

Implants along transversal direction

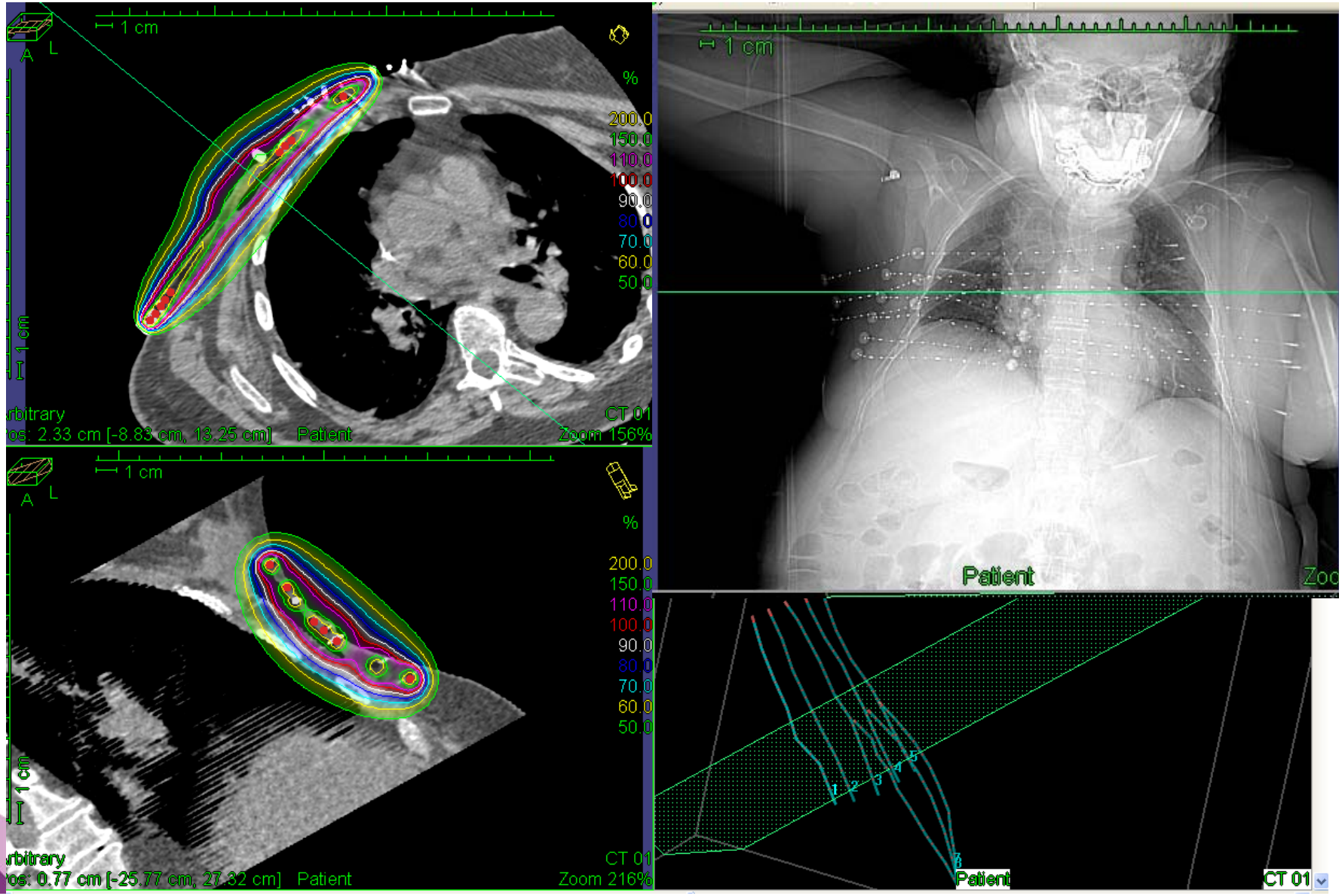

Slice thickness: Catheter tip definition

Use of scout views or scanograms

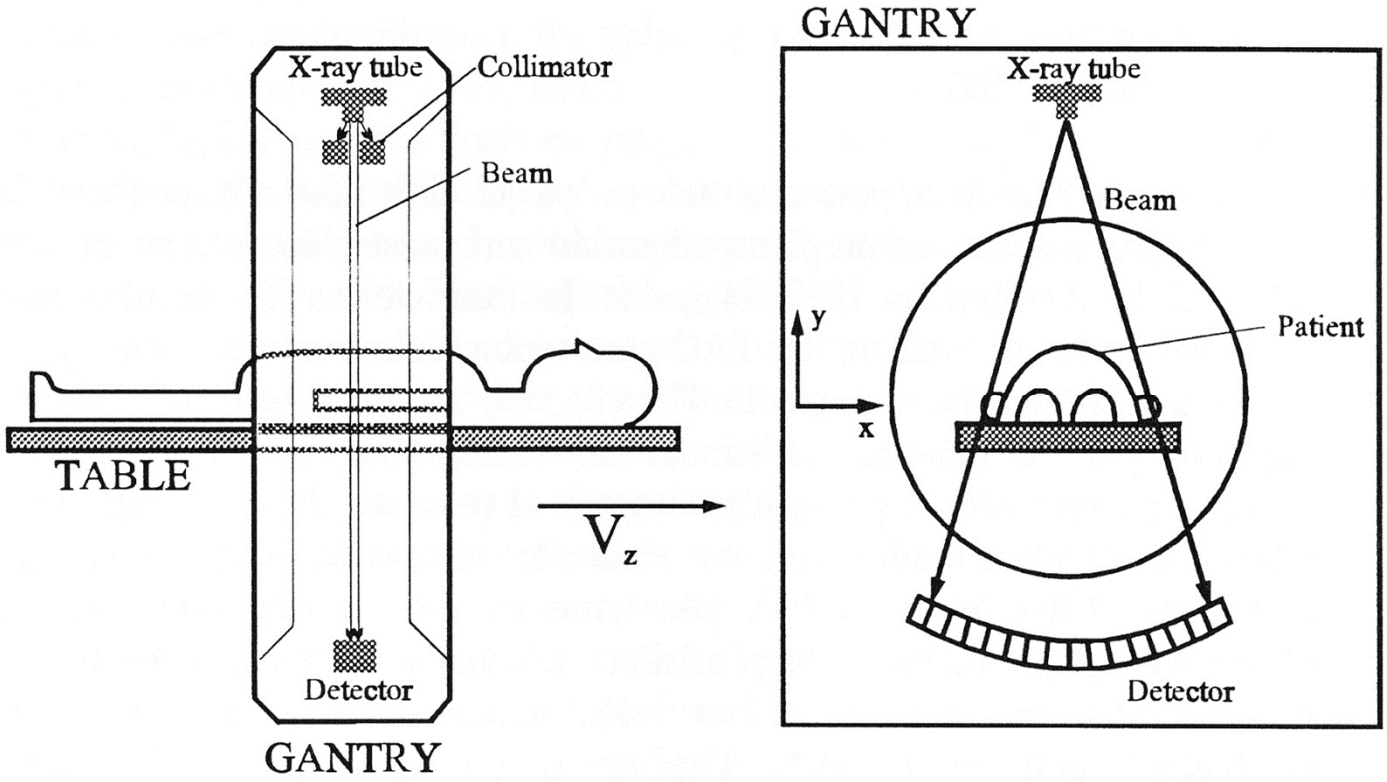

No divergence in longitudinal direction showing real size

ESTRO School

Use of scout views or scanograms

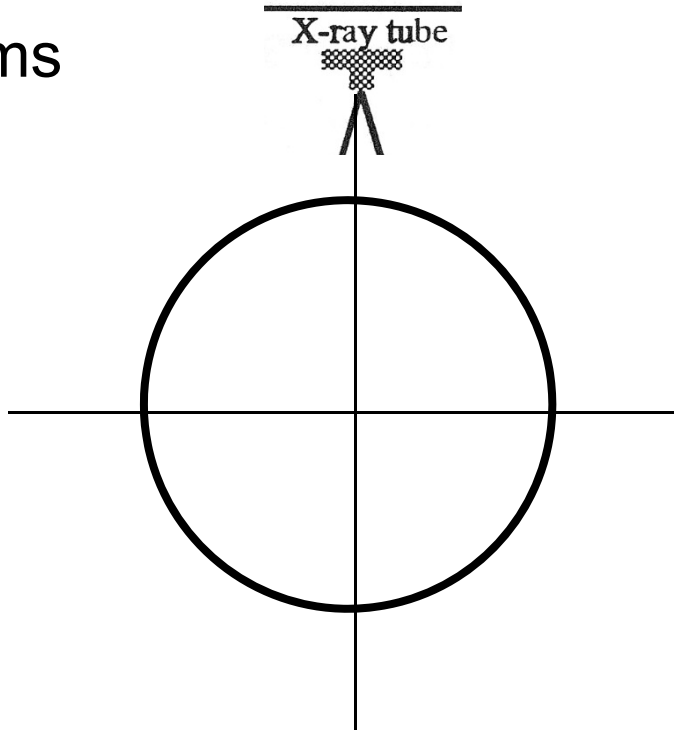

No divergence in longitudinal direction showing real size

ESTRO School

Use of scout views or scanograms

SV a 0º

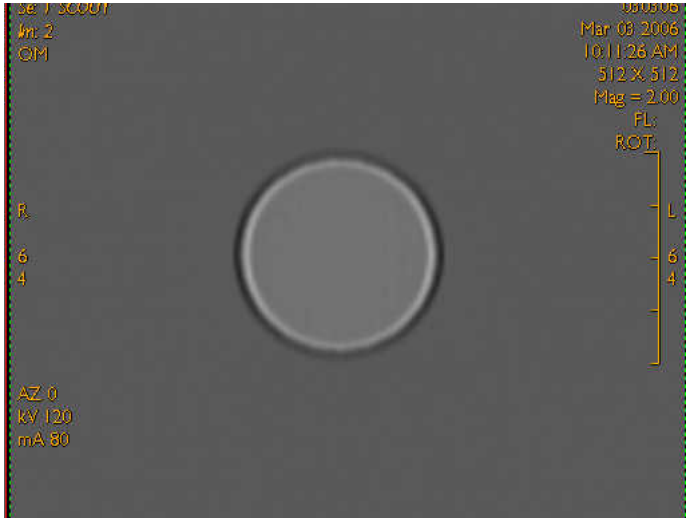

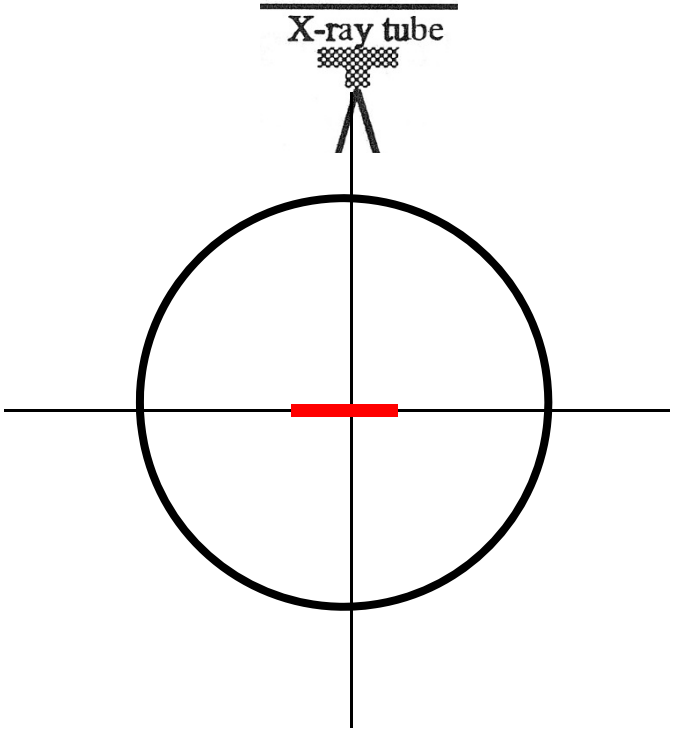

At CT isocenter: Real size in both directions

ESTRO School

Use of scout views or scanograms

SV a 0º

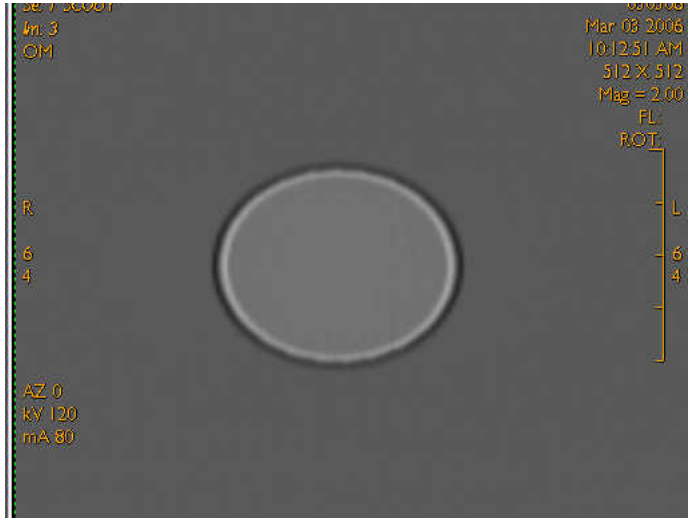

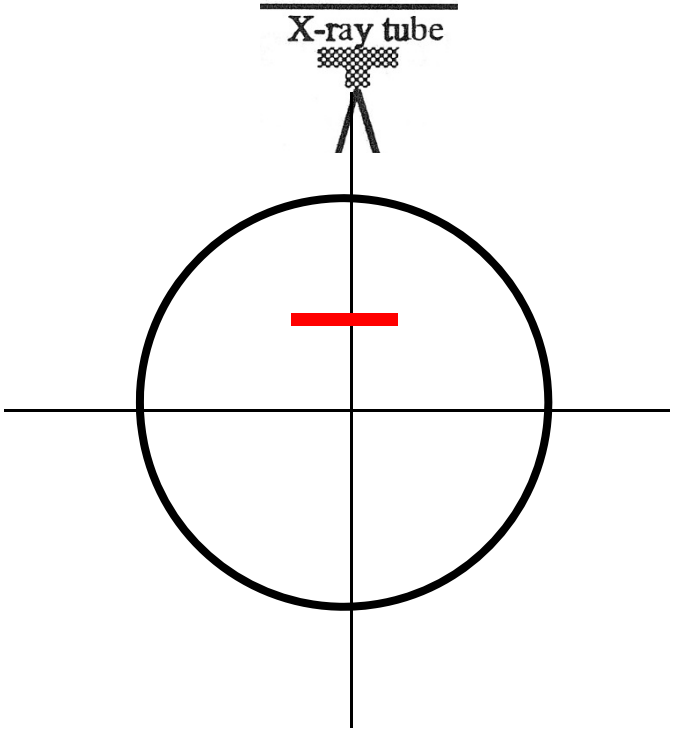

Above isocenter: Real size in long and magnified lat

ESTRO School

Use of scout views or scanograms

SV a 0º

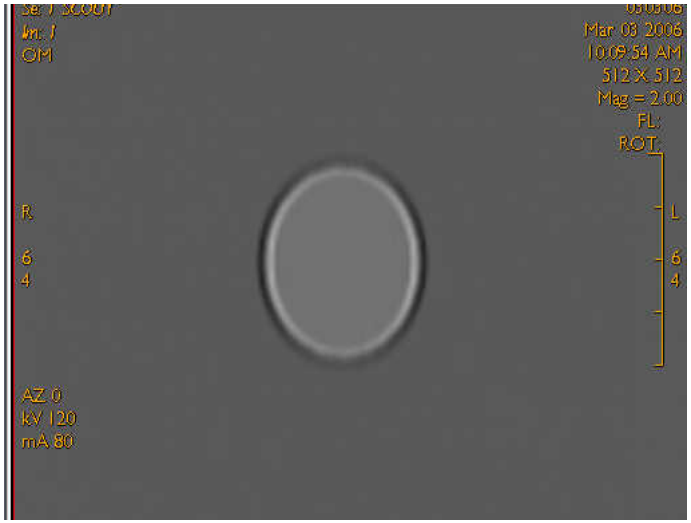

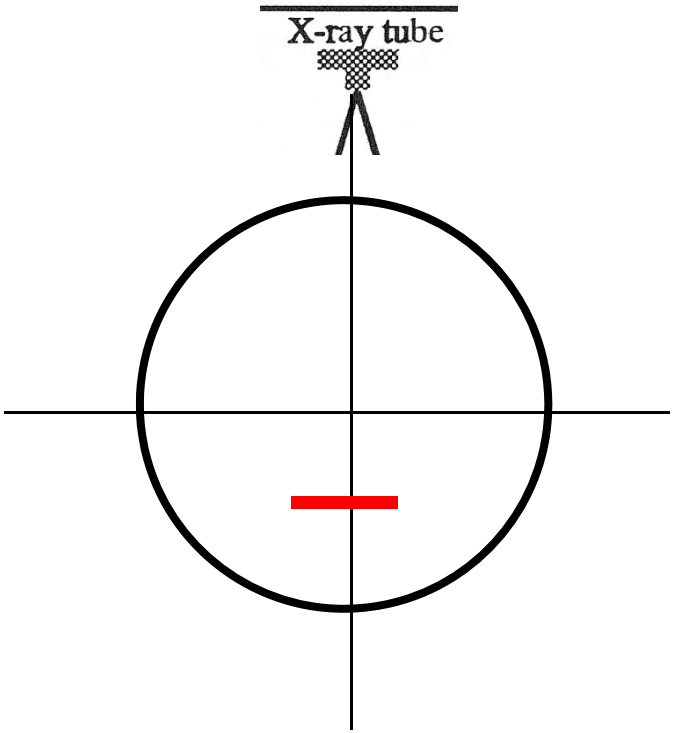

Below isocenter: Real size long and de-magnified lat

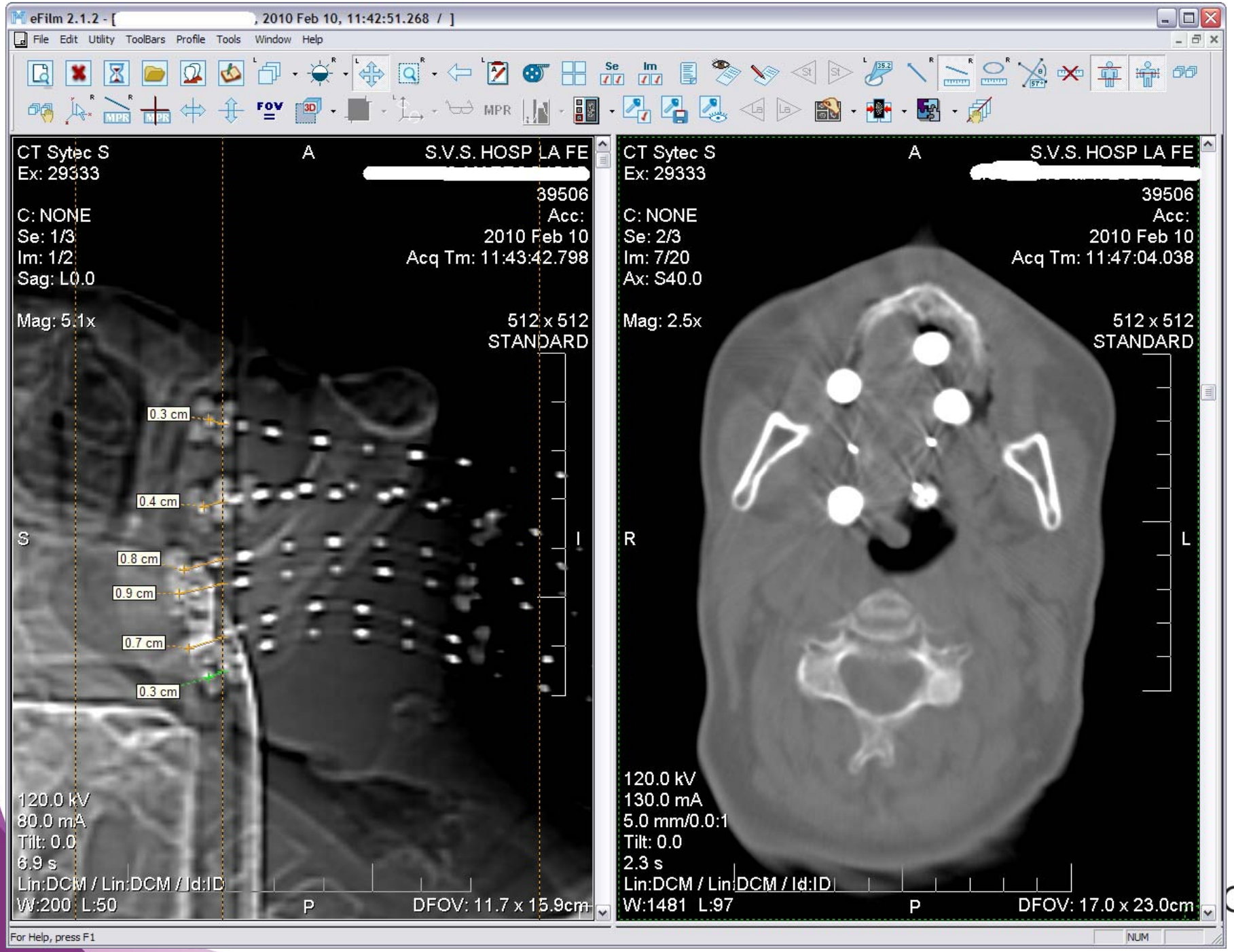
eFilm 2.1.2 - [, 2010 Feb 10, 11:42:51.268 /]
File Edit Utility ToolBars Profile Tools Window Help
CT Sytec S
Ex: 29333
A
S.V.S. HOSP LA FE
39506
Acc:
2010 Feb 10
Acq Tm: 11:43:42.798
C: NONE
Se: 1/3
Im: 1/2
Sag: L0.0
Mag: 5.1x
512 x 512
STANDARD
0.3 cm
0.4 cm
0.8 cm
0.9 cm
0.7 cm
0.3 cm
S
I
120.0 kV
80.0 mA
Tilt: 0.0
6.9 s
Lin:DCM / Lin:DCM / Id:ID
W:200 L:50
P
DFOV: 11.7 x 15.9cm
CT Sytec S
Ex: 29333
A
S.V.S. HOSP LA FE
39506
Acc:
2010 Feb 10
Acq Tm: 11:47:04.038
C: NONE
Se: 2/3
Im: 7/20
Ax: S40.0
Mag: 2.5x
512 x 512
STANDARD
R
L
120.0 kV
130.0 mA
5.0 mm/0.0:1
Tilt: 0.0
2.3 s
Lin:DCM / Lin:DCM / Id:ID
W:1481 L:97
P
DFOV: 17.0 x 23.0cm
For Help, press F1
NUM

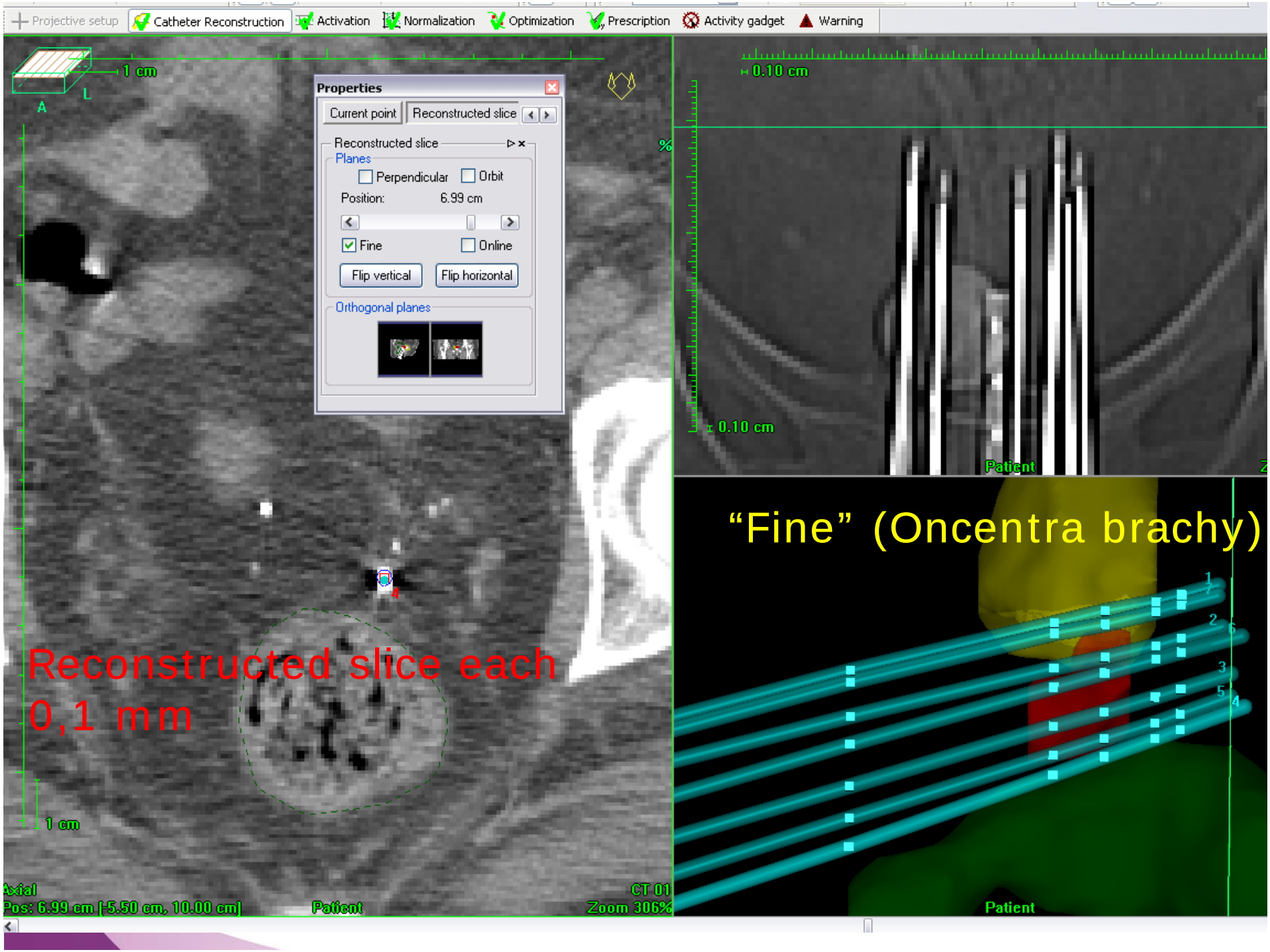
Projective setup
Catheter Reconstruction
Activation
Normalization
Optimization
Prescription
Activity gadget
Warning
1 cm
A
L
Properties
Current point
Reconstructed slice
Reconstructed slice
Planes
Perpendicular
Orbit
Position:
6.99 cm
Fine
Online
Flip vertical
Flip horizontal
Orthogonal planes
0.10 cm
0.10 cm
Patient
"Fine" (Oncentra brachy)
Reconstructed slice each 0,1 mm
1 cm
Axial
Pos: 6.99 cm [-5.50 cm, 10.00 cm]
Patient
CT 01
Zoom 306%
Patient

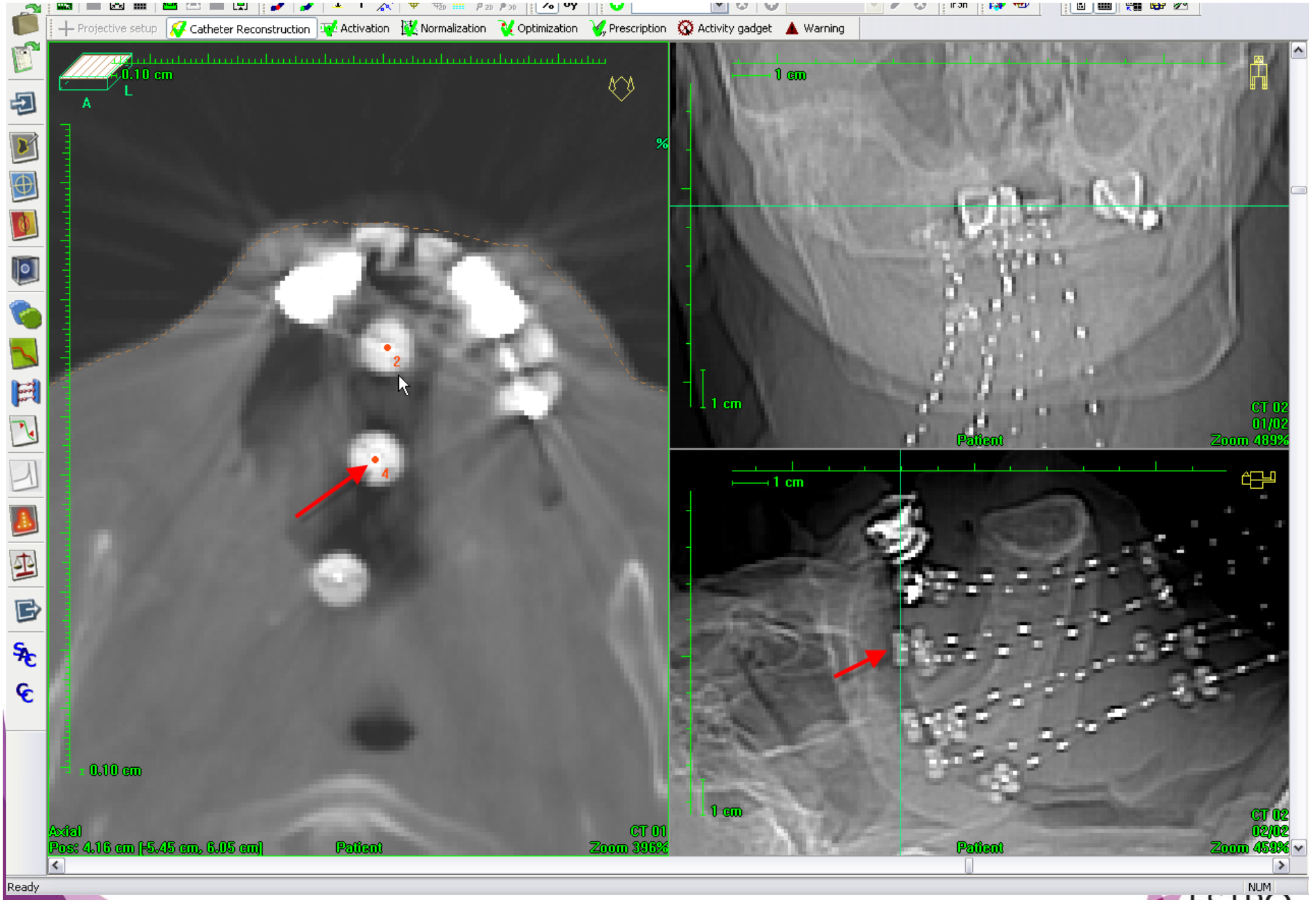
Projective setup
Catheter Reconstruction
Activation
Normalization
Optimization
Prescription
Activity gadget
Warning
0.10 cm
A
L
2
4
0.10 cm
Axial
Pos: 4.16 cm [-5.45 cm, 6.05 cm]
Patient
CT 01
Zoom 396%
1 cm
1 cm
Patient
CT 02
01/02
Zoom 489%
1 cm
1 cm
Patient
CT 02
02/02
Zoom 458%
Ready
NUM

QA CT

Med Phys Sept 2003

Quality assurance for computed-tomography simulators and the computed-tomography-simulation process: Report of the AAPM Radiation Therapy Committee Task Group No. 66

Sasa Mutic[a)]
Department of Radiation Oncology, Washington University School of Medicine, St. Louis, Missouri 63110

Table vertical and longitudinal motion	To verify that the table longitudinal motion according to digital indicators is accurate and reproducible	Monthly	±1 mm over the range of table motion
Table indexing and position	To verify table indexing and position accuracy under scanner control	Annually	±1 mm over the scan range
Gantry tilt accuracy	To verify accuracy of gantry tilt indicators	Annually	±1° over the gantry tilt range
Gantry tilt position accuracy	To verify that the gantry accurately returns to nominal position after tilting	Annually	±1° or ±1 mm from nominal position
Scan localization	To verify accuracy of scan localization from pilot images	Annually	±1 mm over the scan range

ESTRO School

QA CT

Med Phys Sept 2003

Quality assurance for computed-tomography simulators and the computed-tomography-simulation process: Report of the AAPM Radiation Therapy Committee Task Group No. 66

Sasa Mutic[a)]
Department of Radiation Oncology, Washington U

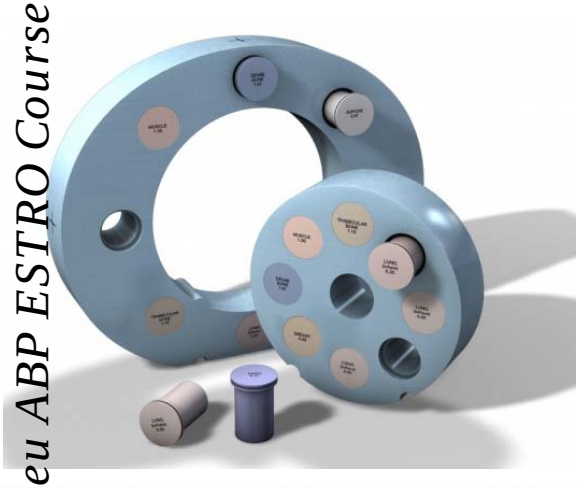

Photos from L. Beaulieu ABP ESTRO Course 2016

Performance parameter	Frequency	Tolerance limits
CT number accuracy	Daily—CT number for water Monthly—4 to 5 different materials Annually—Electron density phantom	For water, 0±5 HU
Image noise	Daily	Manufacturer specifications
In plane spatial integrity	Daily—*x* or *y* direction Monthly—both directions	±1 mm
Field uniformity	Monthly—most commonly used kVp Annually—other used kVp settings	within ±5 HU
Electron density to CT number conversion	Annually—or after scanner calibration	Consistent with commissioning results and test phantom manufacturer specifications
Spatial resolution	Annually	Manufacturer specifications

QA CT

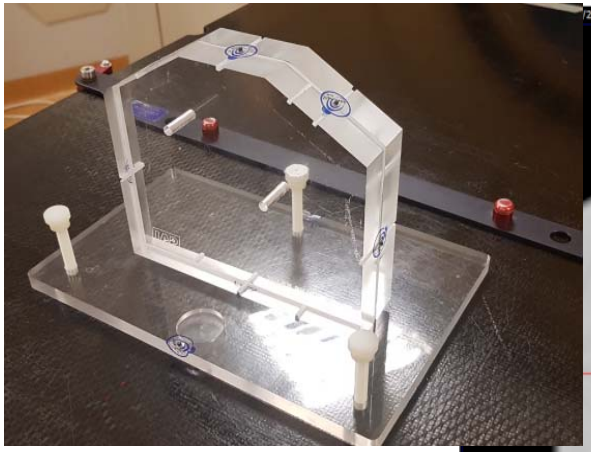

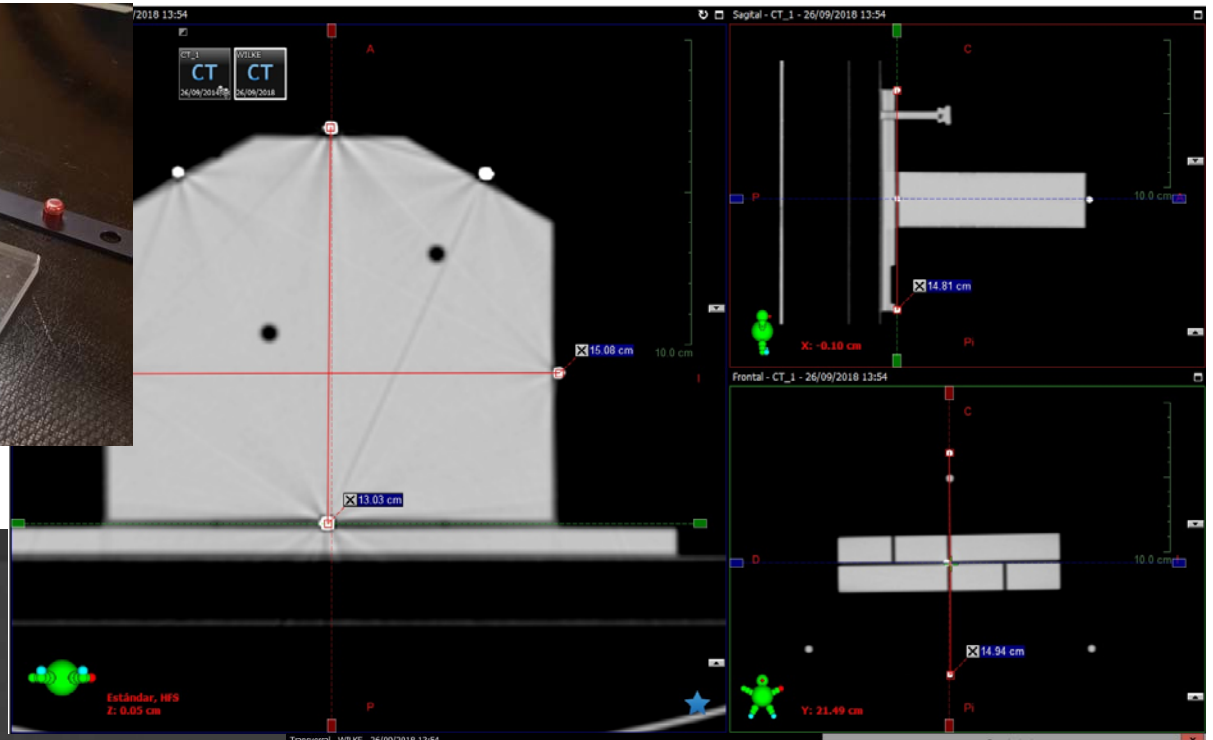
Sagital - CT_1 - 26/09/2018 13:54
Frontal - CT_1 - 26/09/2018 13:54
15.08 cm
13.03 cm
14.81 cm
14.94 cm
X: -0.10 cm
Y: 21.49 cm
Estándar, HFS
Z: 0.05 cm

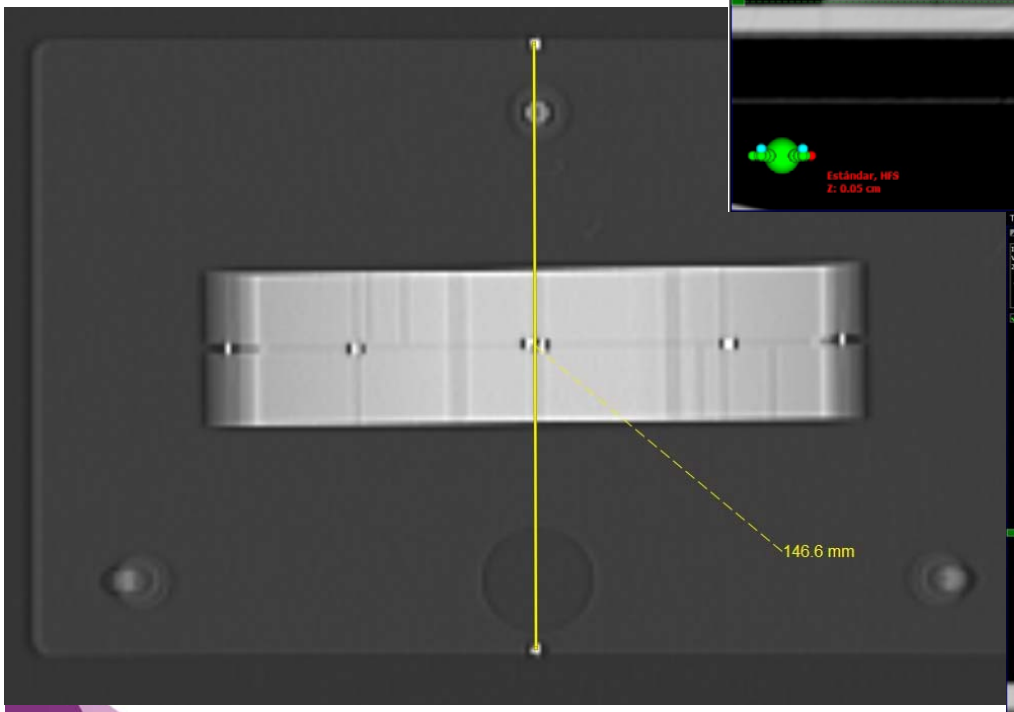
146.6 mm

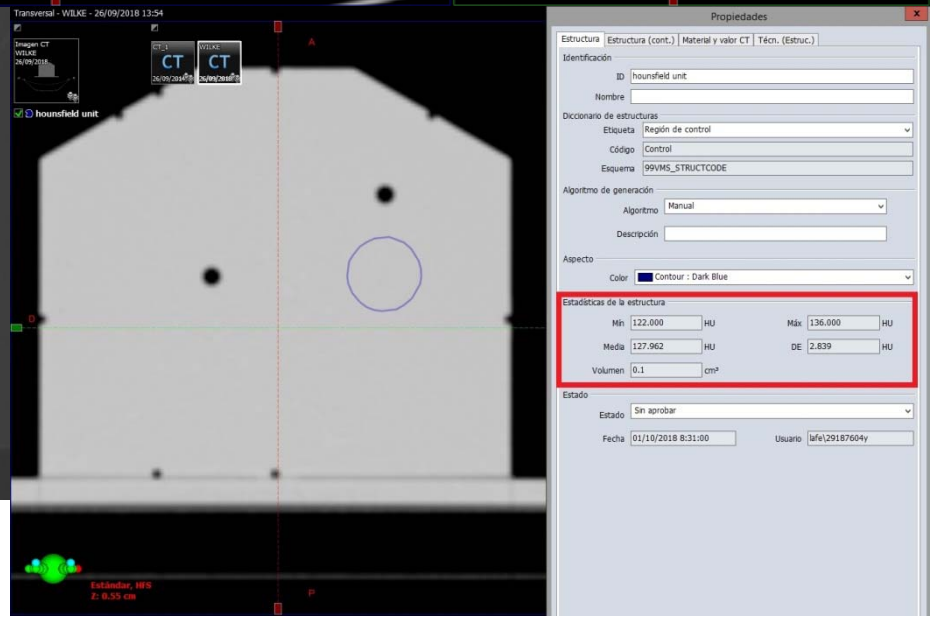
Transversal - WILKE - 26/09/2018 13:54
hounsfield unit
Estándar, HFS
Z: 0.55 cm
Propiedades
Estructura
Estructura (cont.)
Material y valor CT
Técn. (Estruc.)
Identificación
ID
hounsfield unit
Nombre
Diccionario de estructuras
Etiqueta
Región de control
Código
Control
Esquema
99VMS_STRUCTCODE
Algoritmo de generación
Algoritmo
Manual
Descripción
Aspecto
Color
Contour : Dark Blue
Estadísticas de la estructura
Mín
122.000
HU
Máx
136.000
HU
Media
127.962
HU
DE
2.839
HU
Volumen
0.1
cm³
Estado
Estado
Sin aprobar
Fecha
01/10/2018 8:31:00
Usuario
lafe\29187604y

QA CT

Baltas phantom

25 pellets

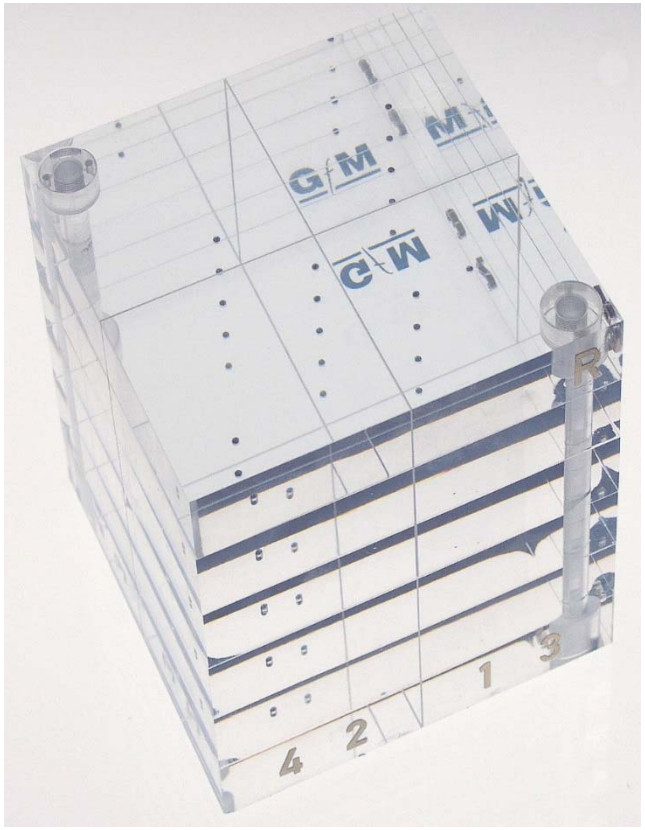

Baltas 1993

Scanograms

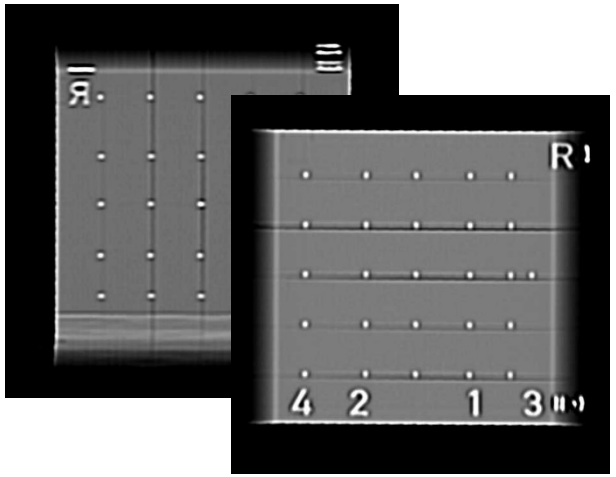

CT

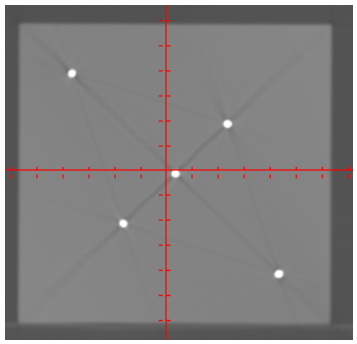

TPS

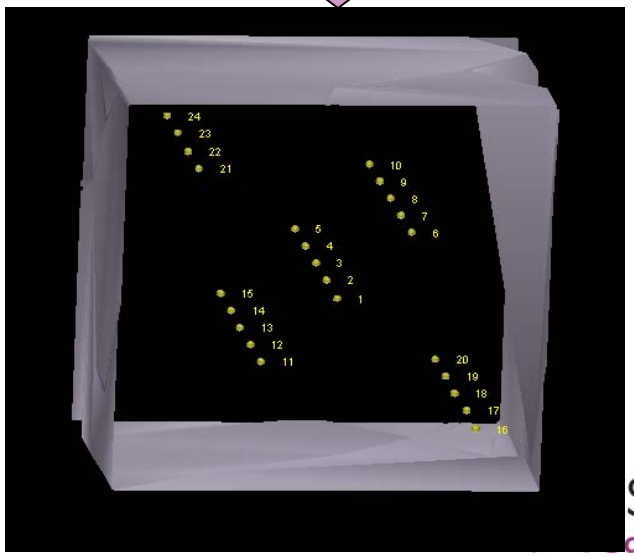

Brachy audits Booklet 8 ESTRO

STRO
chool

Imaging modalities for brachy planning

TRUS

Imaging modality for intraoperative prostate brachytherapy
Prostate, rectum, urethra probe: OK
Imaging reconstruction accuracy is favored by the motorized probe
Needle and catheter visualization

No clear seed & spacing visualization
No electronic density for dose calculation (issue in low energy)
Needle & Cath Tips difficult
Probe motion inducing organ motion or deformation ?

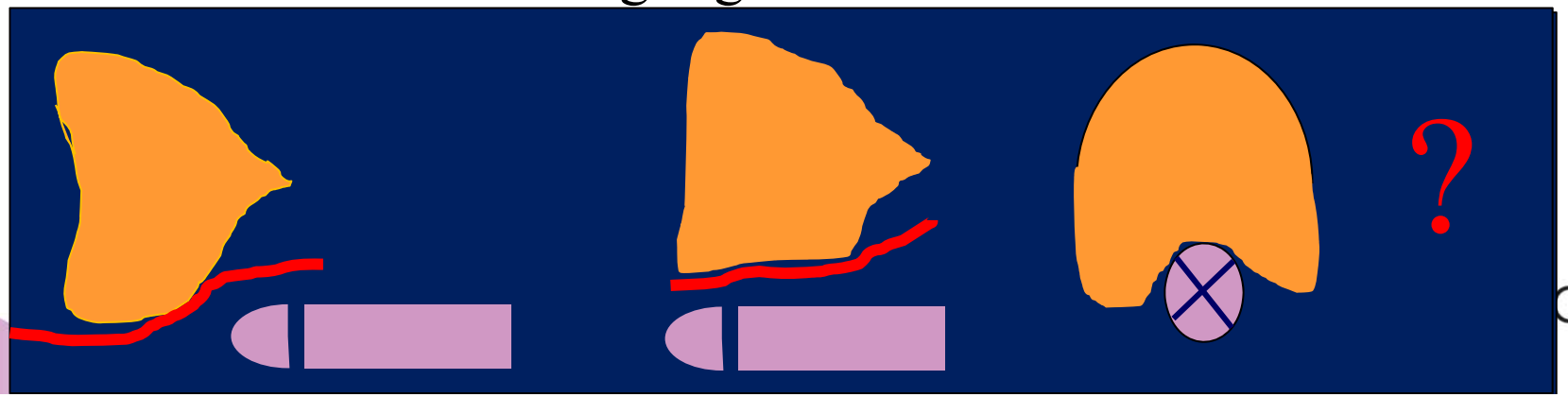

Adapted from L. Beaulieu ABP ESTRO 2016

Use of “free length”

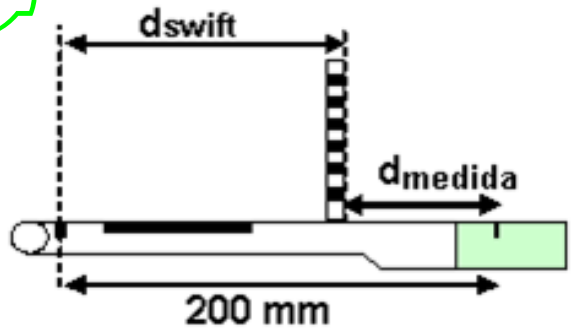

d medida (distancia del template a la marca)
d swift = 200 – d medida
Para agujas metálicas de 200 mm free length = d medida - 10 mm

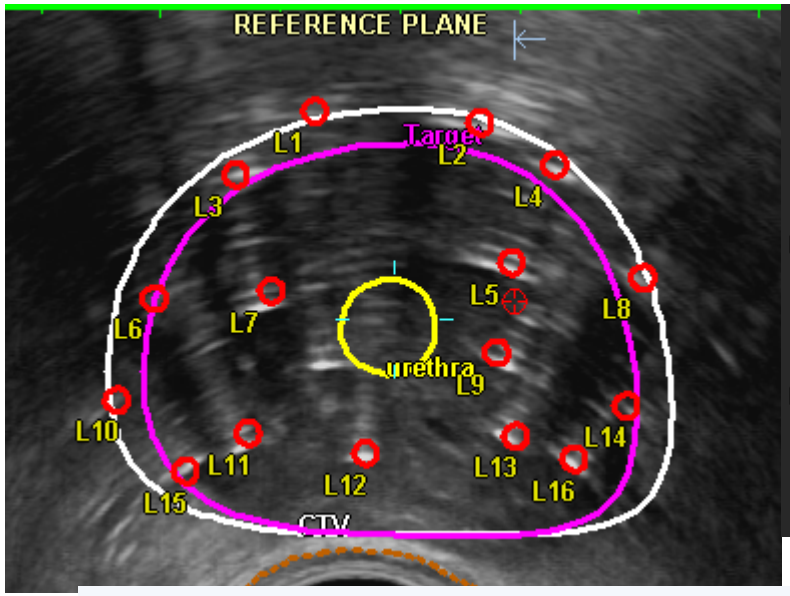

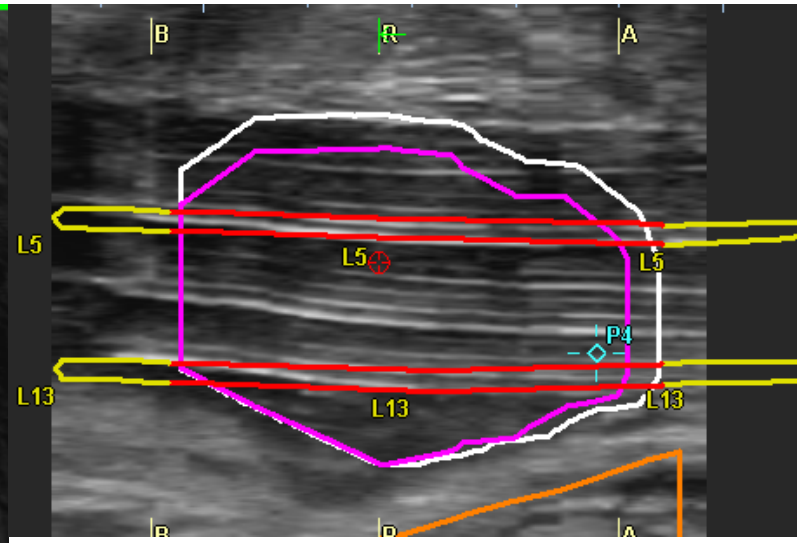

#	Column	Row	Indexer[mm]	Depth[mm]	Free Len.[mm]	Free Len.	Offset[mm]	Tip-1st SDP[mm]	Activation	Dwell Times
L1	c	4	1408.00	9.93	55.00	Unlocked	-0.06	10.00	Unlocked	Unlocked
L2	E	4	1408.00	9.86	55.00	Unlocked	-0.12	10.00	Unlocked	Unlocked
L3	b	3.5	1408.00	9.86	55.00	Unlocked	-0.14	10.00	Unlocked	Unlocked
L4	F	3.5	1408.00	9.85	55.00	Unlocked	-0.15	10.00	Unlocked	Unlocked
L5	C	3	1408.00	9.93	55.00	Unlocked	-0.07	10.00	Unlocked	Unlocked
L6	e	3	1408.00	9.89	55.00	Unlocked	-0.10	10.00	Unlocked	Unlocked
L7	B	2.5	1408.00	9.93	55.00	Unlocked	-0.07	10.00	Unlocked	Unlocked
L8	f	2.5	1408.00	9.85	55.00	Unlocked	-0.11	10.00	Unlocked	Unlocked
L9	C	2	1408.00	9.91	55.00	Unlocked	-0.08	10.00	Unlocked	Unlocked
L10	D	2	1408.00	9.86	55.00	Unlocked	-0.13	10.00	Unlocked	Unlocked

ESTRO School

AAPM Task Group 128: Quality assurance tests for prostate brachytherapy ultrasound systems

Douglas Pfeiffer[a)]
Imaging Department, Boulder Community Foothills Hospital, Boulder, Colorado 80301

Steven Sutlief
Radiation Therapy, VA Medical Center, VA Puget Sound Health Care System, Seattle, Washingon 98108

Wenzheng Feng
Cardiology and Interventional Radiology, William Beaumont Hospital, Royal Oak, Michigan 48073

Heather M. Pierce
CIRS, Inc., Norfolk, Virginia 23513

Jim Kofler
Radiology, Mayo Clinic, Rochester, Minnesota 55905

(Received 26 December 2007; revised 27 August 2008; accepted for publication 6 October 2008; published 12 November 2008)

- QA assessments according to AAPM Task Group 128[1]:
  - Depth of penetration
  - Axial and Lateral Resolution
  - Distance Measurement Accuracy
  - Area Measurements
  - Volume Measurements
  - Geometric Consistency with the treatmentplanning computer

ESTRO School

QA of Ultrasound

Christian-Albrechts-Universität zu Kiel

- TG-128 (**2008**)
  - Prostate, no stepper
- Doyle et al (**2017**): Review
- BRAPHYQS WP12

(**near to be published**)

  - European recommendations

  (includes stepper, TPS, applicator reconstruction, …)

AAPM Task Group 128: Quality assurance tests for prostate brachytherapy ultrasound systems

Douglas Pfeiffer[a)]
Imaging Department, Boulder Community Foothills Hospital, Boulder, Colorado 80301

Steven Sutlief
Radiation Therapy, VA Medical Center, VA Puget Sound Health Care System, Seattle, Washington 98108

Wenzheng Feng
Cardiology and Interventional Radiology, William Beaumont Hospital, Royal Oak, Michigan 48073

Heather M. Pierce
CIRS, Inc., Norfolk, Virginia 23513

Jim Kofler
Radiology, Mayo Clinic, Rochester, Minnesota 55905

(Received 26 December 2007; revised 27 August 2008; accepted for publication 6 October 2008; published 12 November 2008)

Physica Medica 44 (2017) 51–57

Contents lists available at ScienceDirect

Physica Medica

journal homepage: www.elsevier.com/locate/ejmp

Review paper

A review of the recommendations governing quality assurance of ultrasound systems used for guidance in prostate brachytherapy

Andrea Jane Doyle[a], Deirdre M. King[b], Jacinta E. Browne[b,*]

[a] School of Physics & Clinical & Optometric Sciences, Medical Ultrasound Physics and Technology Group, Centre of Industrial Engineering Optics, FOCAS Institute, Dublin Institute of Technology, Ireland
[b] Hermitage Medical Clinic, Dublin, Ireland

Courtesy Frank-André Siebert

QA of Ultrasound

Christian-Albrechts-Universität zu Kiel

BRAPHYQS WP12

- Ultrasound phantoms
- General quality assurance of brachytherapy ultrasound units and TPS
  - Image quality
  - Scaling and volume checks
  - Offset calibration for biplane probes
- Ultrasound for **prostate** treatment
  - Template calibration
  - Stepping device calibration
  - Needle reconstruction
- Ultrasound for **gynaecological** brachytherapy
  - Ultrasound techniques
  - Applicator visualization
- QA sheet example

Courtesy Frank-André Siebert

QA of Ultrasound

Christian-Albrechts-Universität zu Kiel

Scaling in US device and Treatment planning system

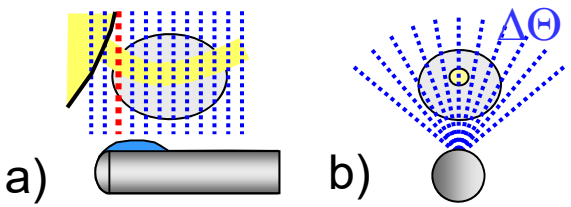

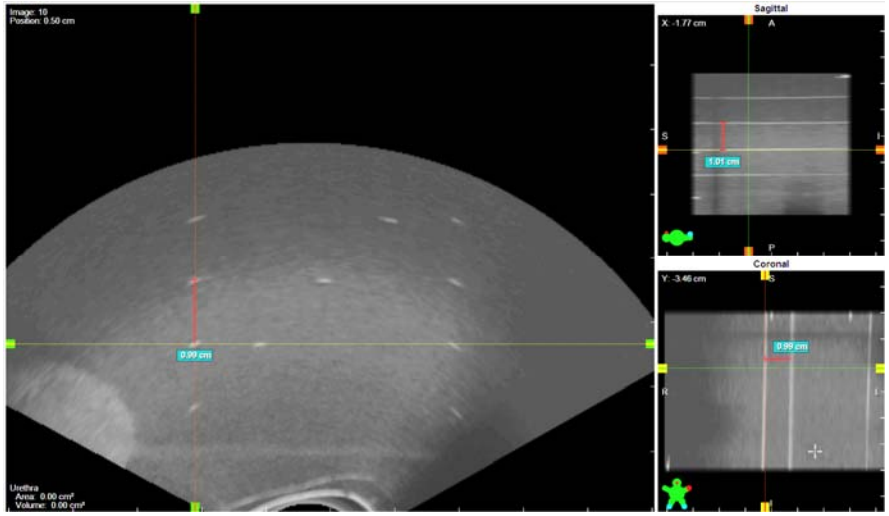

Courtesy Frank-André Siebert

N-shaped pattern in the CIRS phantom (Model 045A).

The scaling is checked in all views in the TPS.

QA of Ultrasound

Christian-Albrechts-Universität zu Kiel

Template calibration

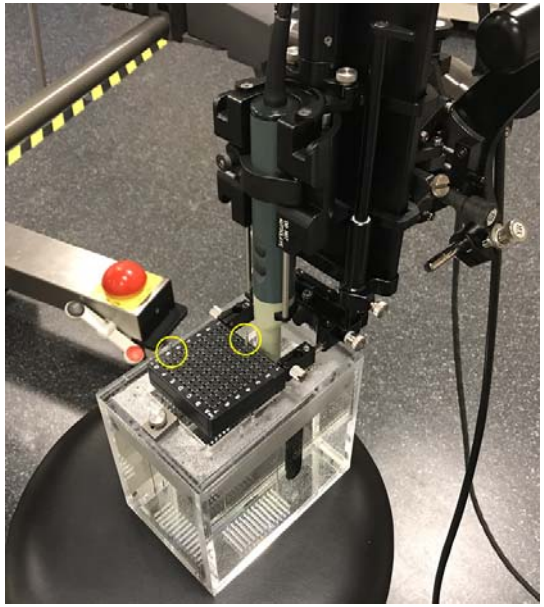

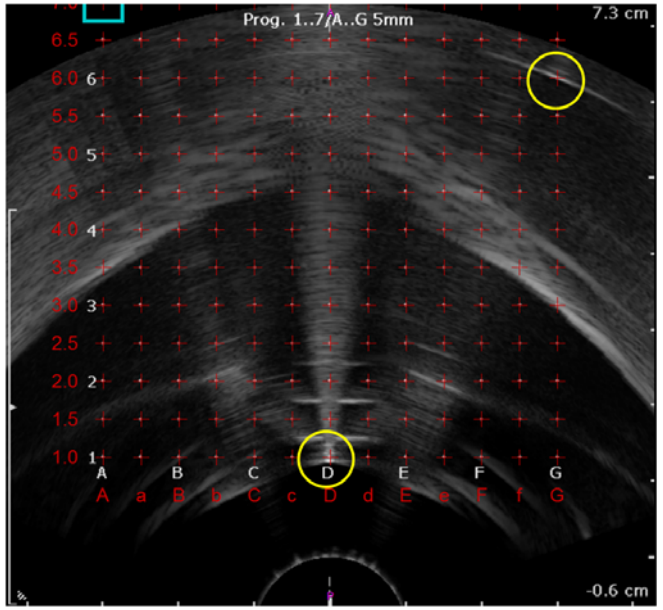

- Needles parallel to probe axis
- Water temperature:
  - 20°C speed of sound: 1480m/s -> 4% error, usage of 48°C reduce this error (integrity of probe ?!)
- All frequencies, depths of penetration used clinically

Courtesy Frank-André Siebert

QA of Ultrasound

Christian-Albrechts-Universität zu Kiel

Needle reconstruction

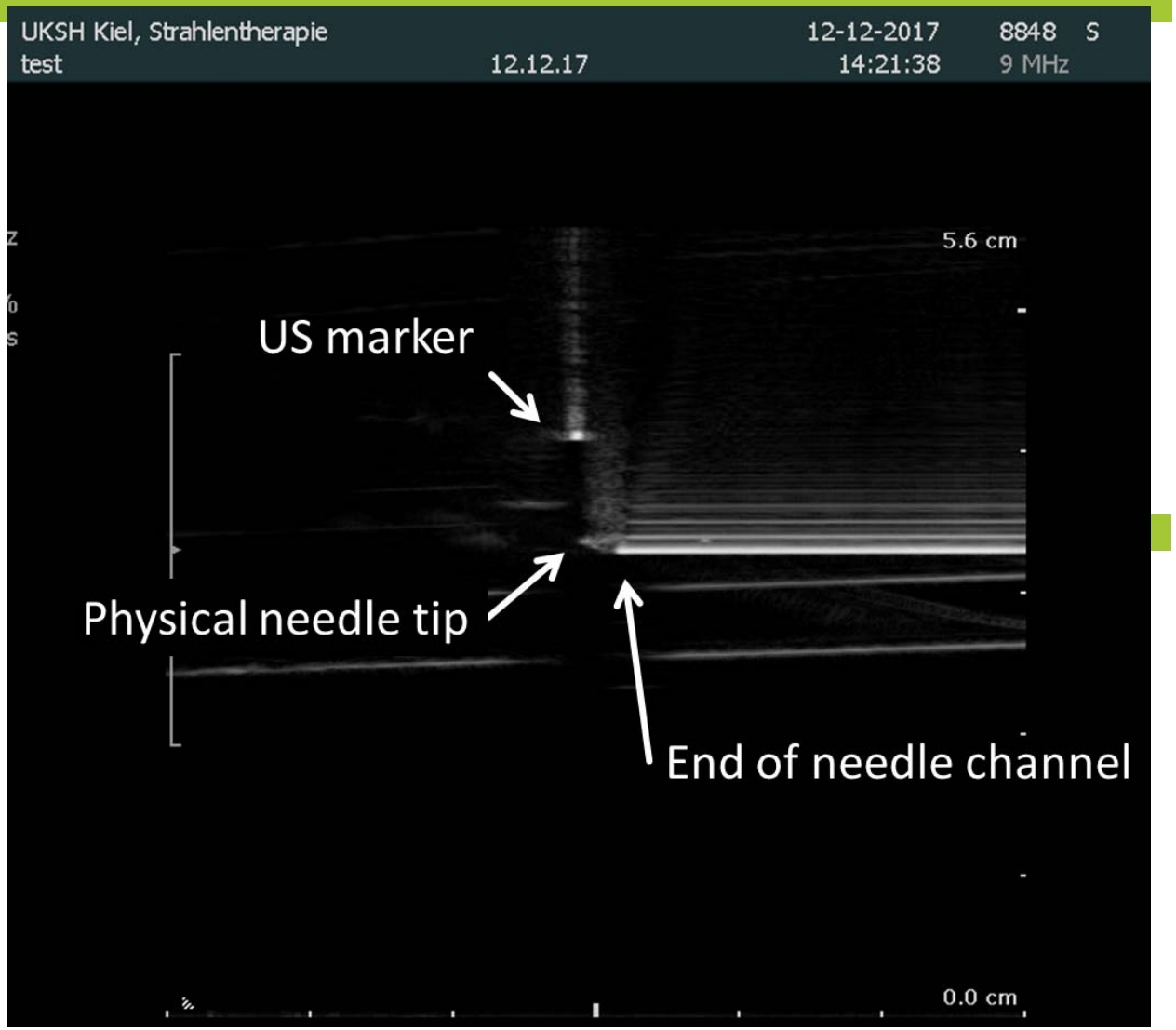

Courtesy Frank-André Siebert

Imaging modalities for brachy planning

MRI

Gold standard for most pelvic sites (T2)
3D image acquisition techniques with good resolution in all planes (isotropic 1 mm voxel size possible!)
Functional MRI possible (specific QA/QC must be implemented)

Must have compatible catheters and applicators
No electron density (might not be an issue for high energy brachytherapy, ^{192}Ir and over (1% deviation *Kirisits 2013*))
Potential distortions
Potential patient motion between or during sequences

Adapted from L. Beaulieu ABP ESTRO Course 2016

ESTRO School

Tabla 2. Parámetros de adquisición recomendados GEC-ESTRO[32] y habituales en distintos hospitales. (Los valores en rojo provienen del Curso de braquiterapia de GEC-ESTRO celebrado en Budapest 2017).

Centro	GEC-ESTRO			H. Ramón y Cajal (Madrid)		H. La Ribera (Alzira)		
Secuencia	T2W	T2W	T2W	T2W	T2W	T2W	T2W	T2W
Orientación	Para axial	Para sag	Para cor	Para axial	3D	Axial	Sag	Cor
ETL, *echo train length* (ms)	4-20	4-20	4-20	18	94	18	18	22
TR, *repetition time* (ms)	2000-5000	2000-5000	2000-5000	4000	2000	17380	14316	9638
TE (*echo time*) (ms)	90-120 (80)	90-120 (80)	90-120 (80)	100	200	120	120	120
Espesor (mm)	3-5 (3)	3-5 (3)	3-5 (3)	3.3	0.9	3	2.5	3
Dirección de la fase	RL	FH	RL	Row	Row	AP	AP	RL
NEX (nº excitaciones)	2 (1)	2 (1)	2 (1)	2	1	1	1	1
FOV (*field of view*) (mm^2)	350x200 (200x200)	350x400 (180x180)	350x200 (200x200)	250x250	200x200	270x219	240x208	240x208
Matriz de Adquisición *Frequency* × *phase*	512x256 (332x276)	512x256 (300x255)	512x256 (332x276)	320x270	220x220	338x215	286x193	300x204
Tamaño de píxel (mm)	0.7x0.8 (0.6x0.7)	0.7x1.6 (0.6x0.7)	0.7x0.8 (0.6x0.7)	0.8x0.9	0.9^3	0.8x1.02	0.84x1.08	0.8x1.02
Bandwidth (Hz)	437.8	438.6	437.8	190	650	137.2	170.1	185.2
Resonancia	0.1-3T			Philips Achieva 1.5T		Philips Achieva 1.5T		

Practical Recommendations of the Spanish Society of Medical Physics in MRI Based Cervix Brachytherapy. Perez-Calatayud, Colmenares, Garcia, Herreros, Pellejero, Richart, Tornero. In press

Tabla 2 (cont.). Parámetros de adquisición recomendados GEC-ESTRO y habituales en distintos hospitales

Centro	H. Clínic Barcelona	Complejo Hospitalario de Navarra (Pamplona)			H. La Fe (Valencia)		H. Clínica Benidorm (Benidorm)	
Secuencia	T2W	T2W	T2W	T2W	T2W	T2W	T2W	3D Cube
Orientación	3D CUBE	Para axial	Para sag	Para cor	Axial	Sag	Axial	3D
ETL, echo train length (ms)	100	28	30	30	16	15	19	90
TR, repetition time (ms)	3000	11296	6683	6148	8500	4480	4000-8000	2000
TE (echo time) (ms)	116.485	93.4	104	106	119	148	66	maximun
Espesor (mm)	2	4	4	4	2.5	2.5	2.5	1.4
Dirección de la fase	AP	inplane	inplane	inplane	col	row	Row	AP
NEX (nº excitaciones)	1	1	1	1	1	2	2	1
FOV (field of view) (mm^2)	240x240	220x220	250x220	250x220	200x200	200x200	200x200	240x240
Matriz Adquisición *Frequency x phase*	288x288	288x288	320x320	320x320	320x320	320x224	256x192	256x256
Tamaño de píxel (mm)	0.83x0.83	0.8x0.8	0.8x0.7	0.8x0.7	0.6x0.6	0.6x0.9	0.8x1.04	0.9x0.9
Bandwidth (Hz)	244.1	325.52	325.52	325.52	122.1	122.1	97.7	50
Modelo Resonancia	G.E. Signa 1.5T	G.E. Signa HDxt 1.5T			G.E. Signa HDxt 3T		G.E. Signa 1.5T	

Practical Recommendations of the Spanish Society of Medical Physics in MRI Based Cervix Brachytherapy. Perez-Calatayud, Colmenares, Garcia, Herreros, Pellejero, Richart, Tornero. In press

ESTRO School

https://www.aapm.org/pubs/reports/RPT_100.pdf

Acceptance Testing and Quality Assurance Procedures for Magnetic Resonance Imaging Facilities

Jackson, Bronskill, Drost, Och, Pooley, Sobol, Clarke

AAPM 2010

Geometric distortion

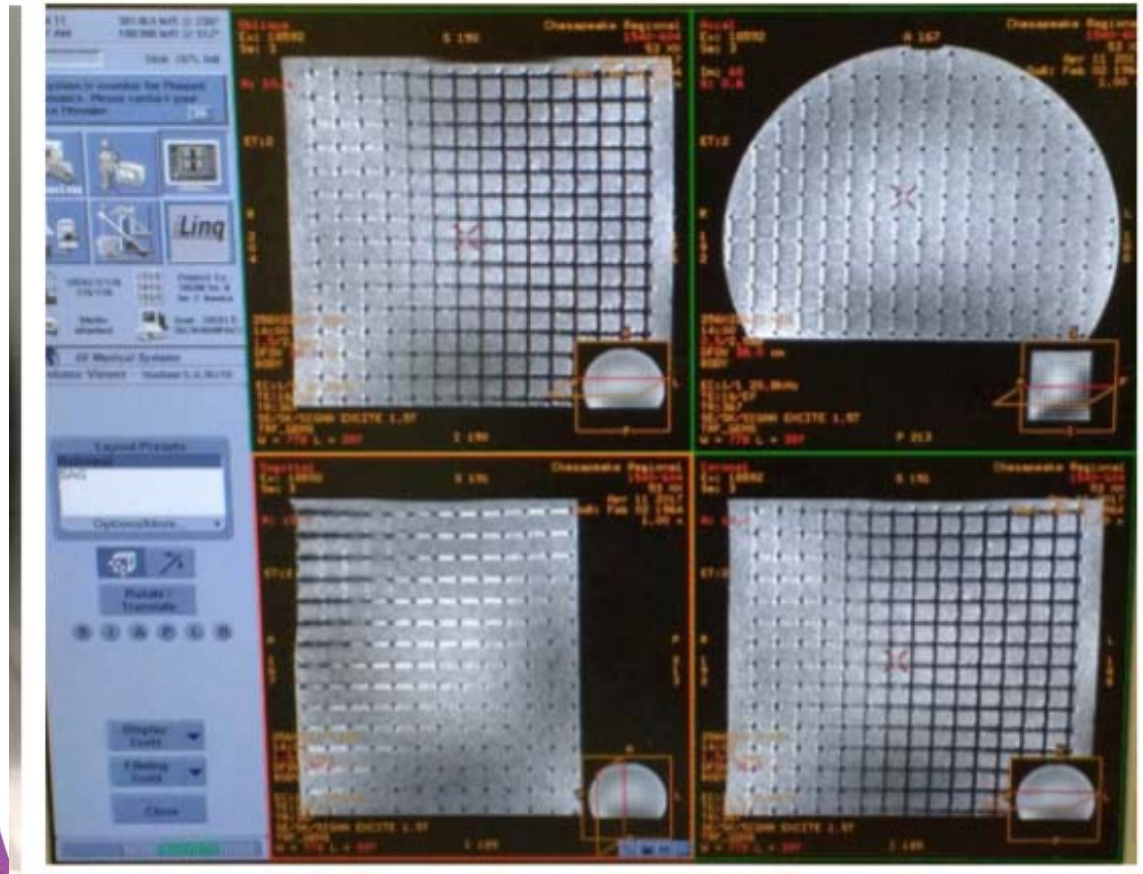

LARGE FIELD MRI DISTORTION PHANTOM
MODEL 604

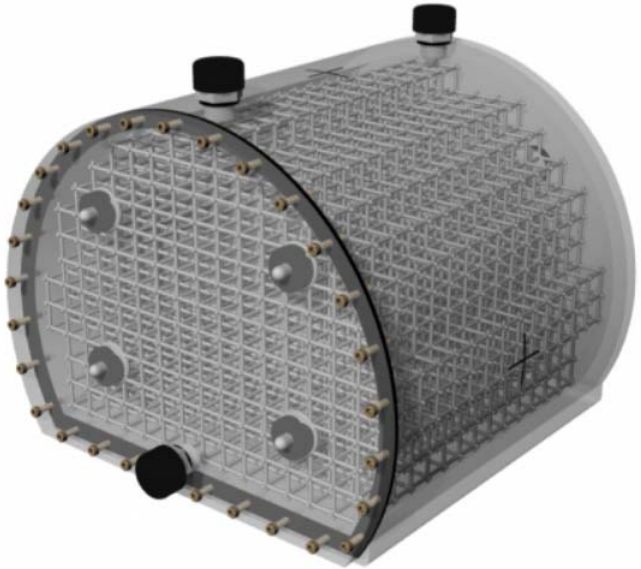

www.cirsinc.com/products/all/118/large-field-mri-distortion-phantom/

ESTRO School

Distortion evaluation

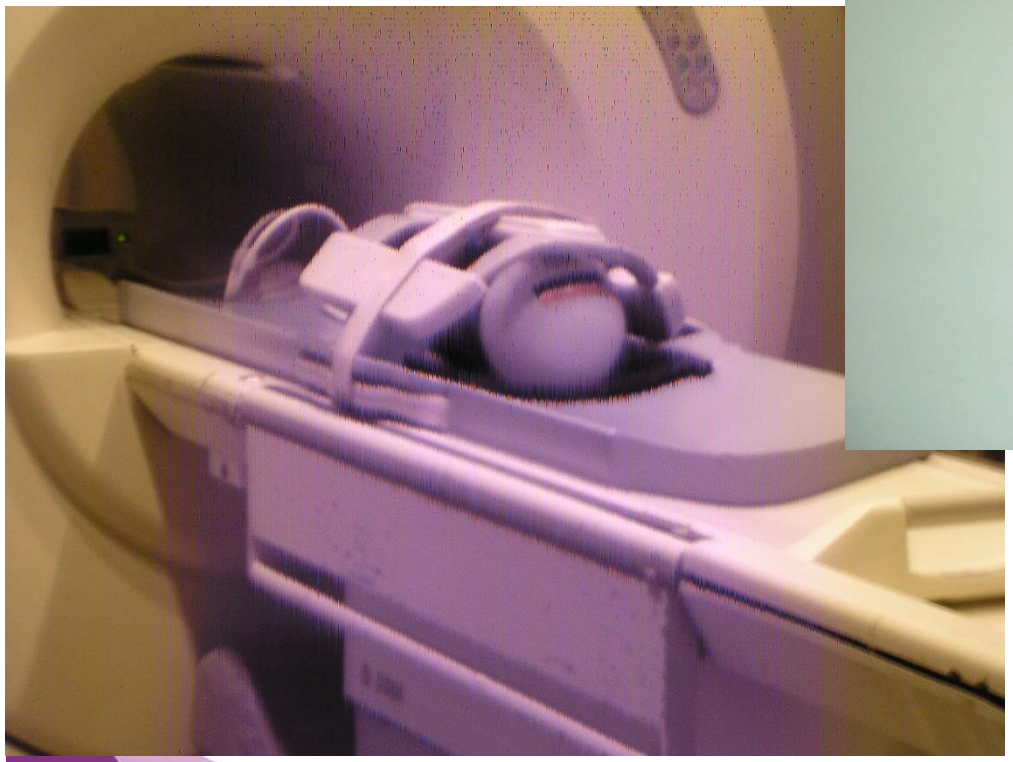

Distortion evaluation

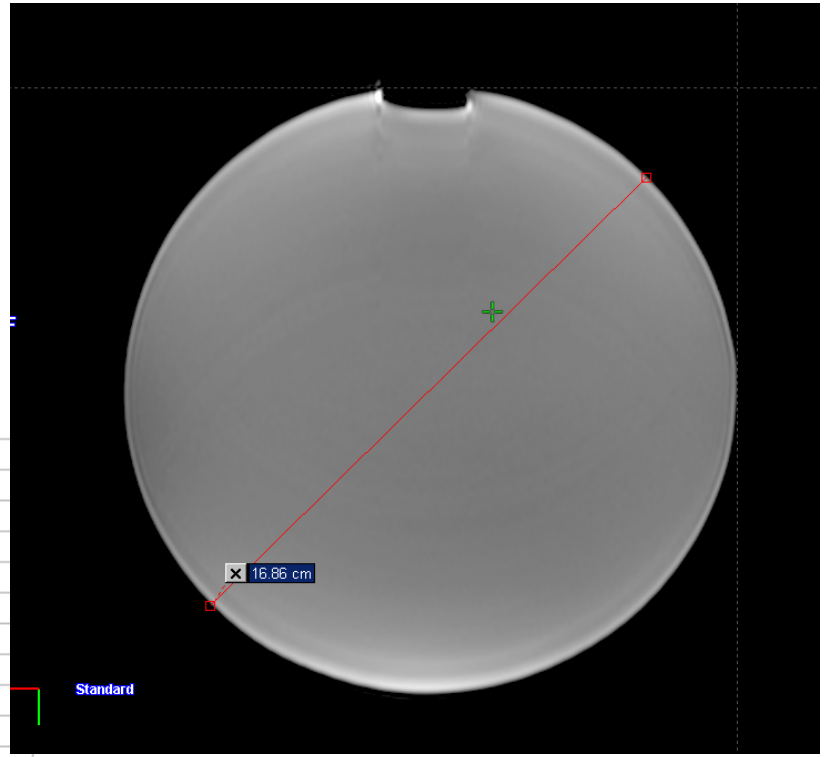

Measured diameters in axial and longitudinal images.
The diameters of each sphere have been measured in 4 directions: horizontal, vertical, 45° and -45°.

The value of the phantom diameters are 169 mm and 99 mm

axial slice (image n° 26 large sphere centred in coil axis) 169 mm

horizontal diameter	168,7	mm
vertical diameter	168,2	mm
45° diameter	169,1	mm
-45° diameter	168,8	mm

axial slice (image n° 70 small sphere offset from coil axis) 99 mm

horizontal diameter	99,7	mm
vertical diameter	98,6	mm
45° diameter	99,3	mm
-45° diameter	99,4	mm

longitudinal slice (image n° 11 large sphere centred in coil axis) 169 mm

horizontal diameter	166,9	mm
vertical diameter	166,1	mm
45° diameter	166,7	mm
-45° diameter	166,8	mm

ESTRO School

3T H. La Fe

Distortion evaluation

3T-MRI images

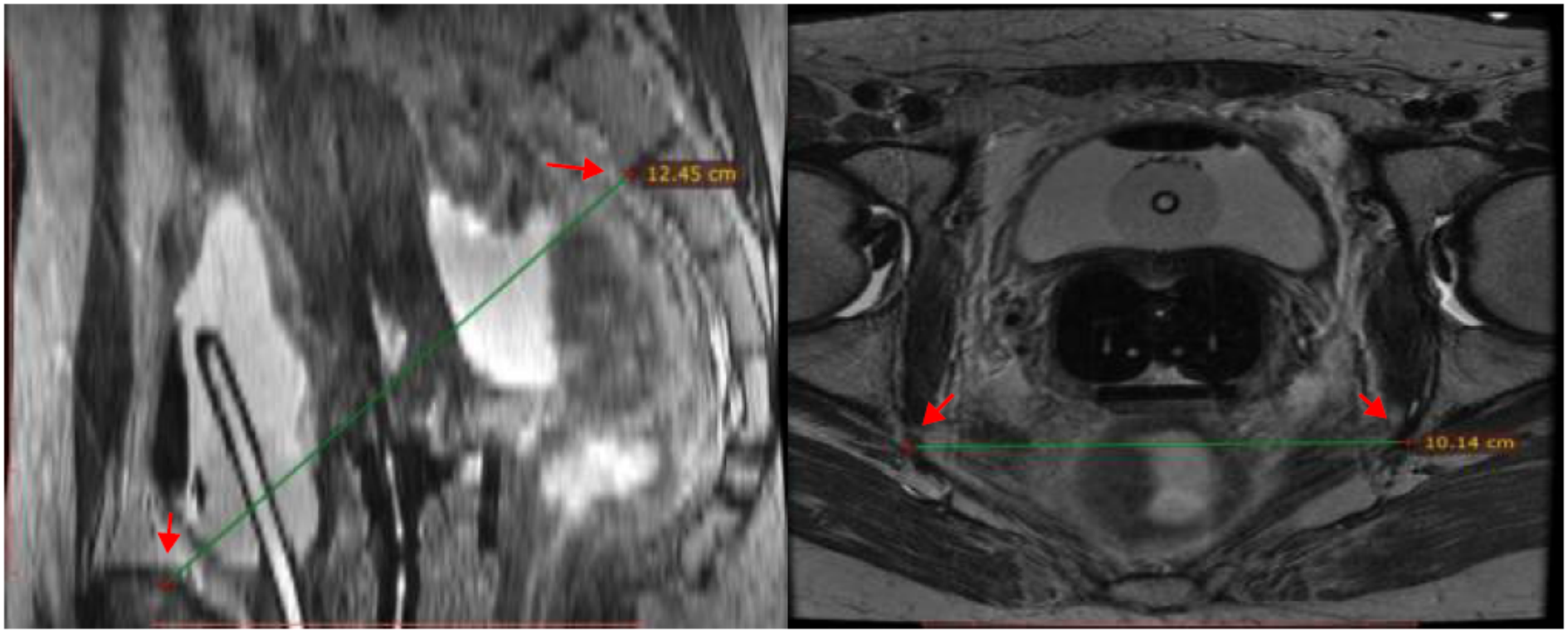

A) B)

Figure 1. A) Sagittal view. Distance from S2-S3 of the sacrum to the posterosuperior part of the pubis
B) Axial view. Interspinous distance at the level of femur's foveae.

"A simple method to evaluate MRI distortion in cervical brachytherapy" C. Domingo, J. Richart, A. Otal, V. Carmona, S. Rodriguez, M. Santos, J. Perez-Calatayud XIX Congreso SEOR 8-10 June 2017 Santander.

ESTRO School

Distortion evaluation

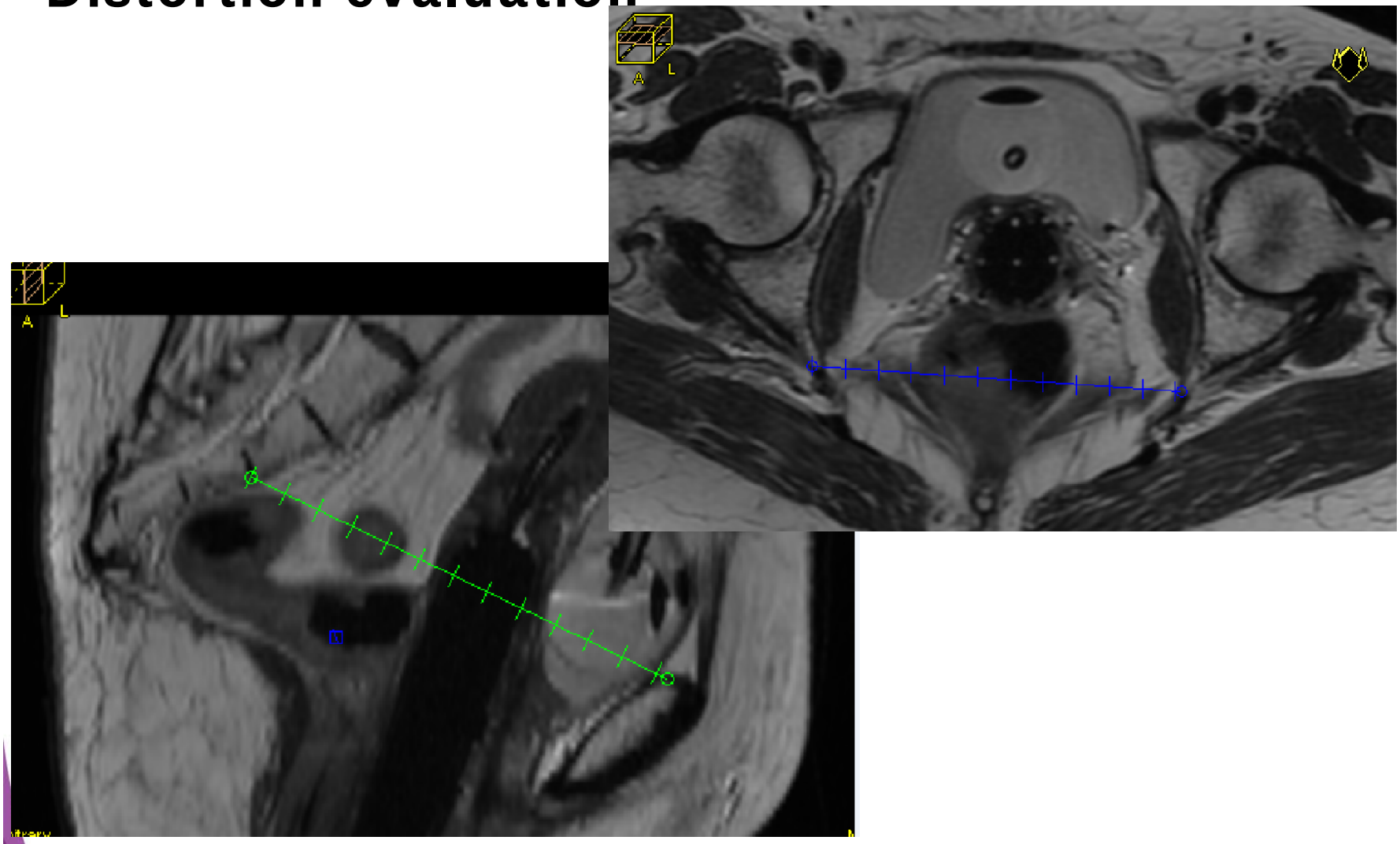

"A simple method to evaluate MRI distortion in cervical brachytherapy" C. Domingo, J. Richart, A. Otal, V. Carmona, S. Rodriguez, M. Santos, J. Perez-Calatayud XIX Congreso SEOR 8-10 June 2017 Santander.

CT

Distortion evaluation

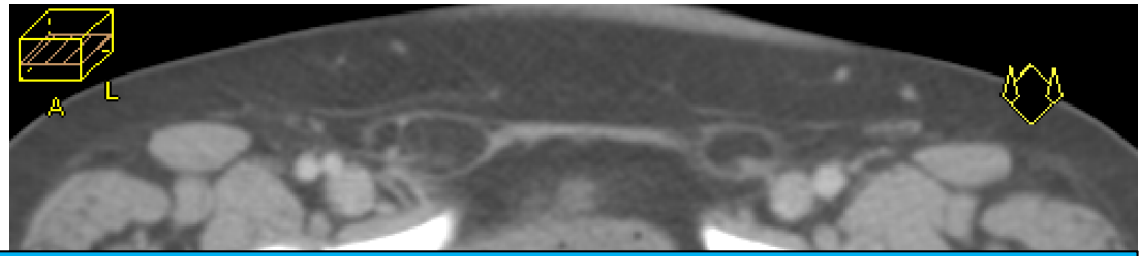

Results: There was no noteworthy difference with measurements done between 1.5T and 3T images, also inter and intra-observer, indicating a substantial agreement. Mean values for statistical analysis were calculated with a 95% confidence interval. There was no significant difference between axial and sagittal measurements. The maximum CT vs MRI deviation mean was 1.6mm ± 0.39 (SD).

"A simple method to evaluate MRI distortion in cervical brachytherapy" C. Domingo, J. Richart, A. Otal, V. Carmona, S. Rodriguez, M. Santos, J. Perez-Calatayud XIX Congreso SEOR 8-10 June 2017 Santander.

ESTRO School

AMERICAN ASSOCIATION of PHYSICISTS IN MEDICINE

Improving Health Through Medical Physics

Home | Directory | Career Services | Continuing Education | BBS | Contact

My AAPM

AAPM

- Staff Contacts
- Mission
- Policies & Procedures
- Association Governance
- **Committees**
- Committee

International

Medical Physicist

Members

Students

AAPM COMMITTEE TREE

Task Group No. 303 - MRI Guidance in HDR - Brachytherapy - Considerations from Simulation to Treatment (TG303)

Chair

- bookmark this page (bookmarks show under "My AAPM" in the menu to left)

Committee Website | **Directory:** Committee | Membership

Email You may send email to this group now using gmail or outlook.
- or -
You may save the address *2018.TG303@aapm.org*
to your local address book. This alias updates hourly from the AAPM Directory.

Charge 1. Develop recommendations for the commissioning, clinical

a. Considerations for brachytherapy-specific image parameters (e.g., frequency of imaging, evaluation of geometric and dosimetric uncertainties, use of contrast, and workflow),

c. MR safety awareness for patient and staff when using HDR applicators and tools,

d. Logistical and economic considerations for initial program development and maintenance.

ESTRO School

Med Phys September 2018

Recent advances on the development of phantoms using 3D printing for imaging with CT, MRI, PET, SPECT, and ultrasound

Valeria Filippou
Institute of Medical and Biological Engineering, Faculty of Mechanical Engineering, University of Leeds, Leeds, LS2 9JT, West Yorkshire, UK

Charalampos Tsoumpas[a)]
Department of Biomedical Imaging Science, School of Medicine, University of Leeds, Leeds, LS2 9NL, West Yorkshire, UK

Conclusions: The development of this field is rapidly evolving and becoming more refined. There is potential to reach the ultimate goal of using 3D phantoms to get feedback on imaging scanners and reconstruction algorithms more regularly. Although the development of imaging phantoms is evident, there are still some limitations to address: One of which is printing accuracy, due to the printer properties. Another limitation is the materials available to print: There are not enough materials to mimic all the tissue properties. For example, one material can mimic one property—such as the density of real tissue—but not any other property, like speed of sound or attenuation.

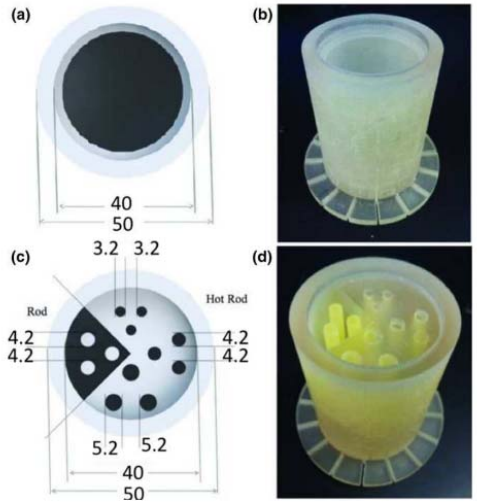

FIG. 11. (a) Diagram and (b) photograph of 3D printed PET/MRI normalization phantom. (c) Diagram and (d) photograph of a 3D printed PET/MRI resolution phantom with hot and cold rods.[10] Figure license: Bieniosek, et al.,

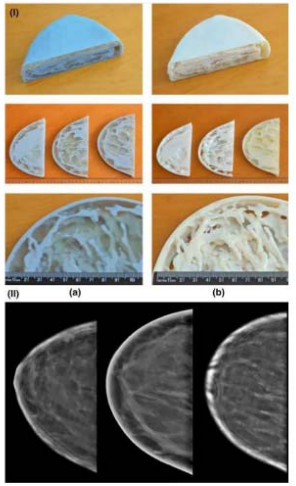

FIG. 8. (I) (a) Singlet, (b) Doublet, (II) Mammogram.[48] Figure license: Kiarashi, et al., 2015, Development of realistic physical breast phantoms matched to virtual breast phantoms based on human subject data. This article is distributed under the terms of the Creative Commons Attribution 4.0 International License (http://creativecommons.org/licenses/by/4.0/)

ESTRO School

Applicators library

Less critical slice thickness selection (most times in direct relation with required image quality for contouring)

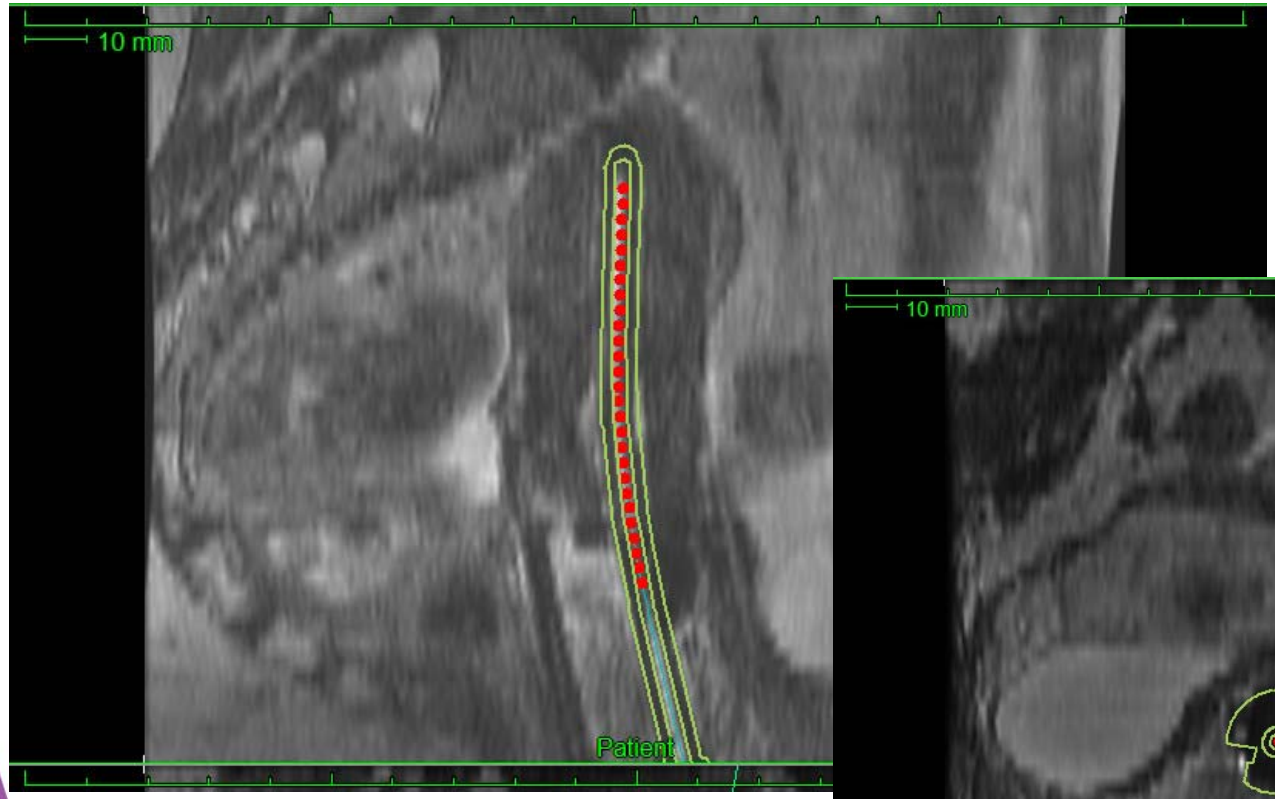

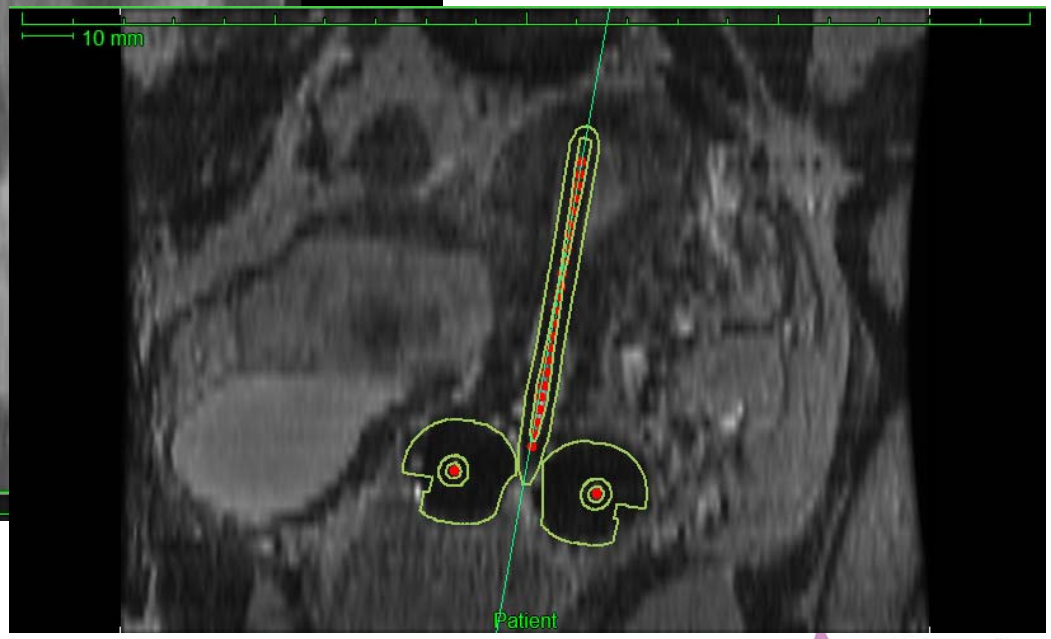

ESTRO School

Applicators library

Not available for intracavitary & interstitial implants

RPOR-659; No. of Pages 15 ARTICLE IN PRESS
REPORTS OF PRACTICAL ONCOLOGY AND RADIOTHERAPY XXX (2018) XXX–XXX

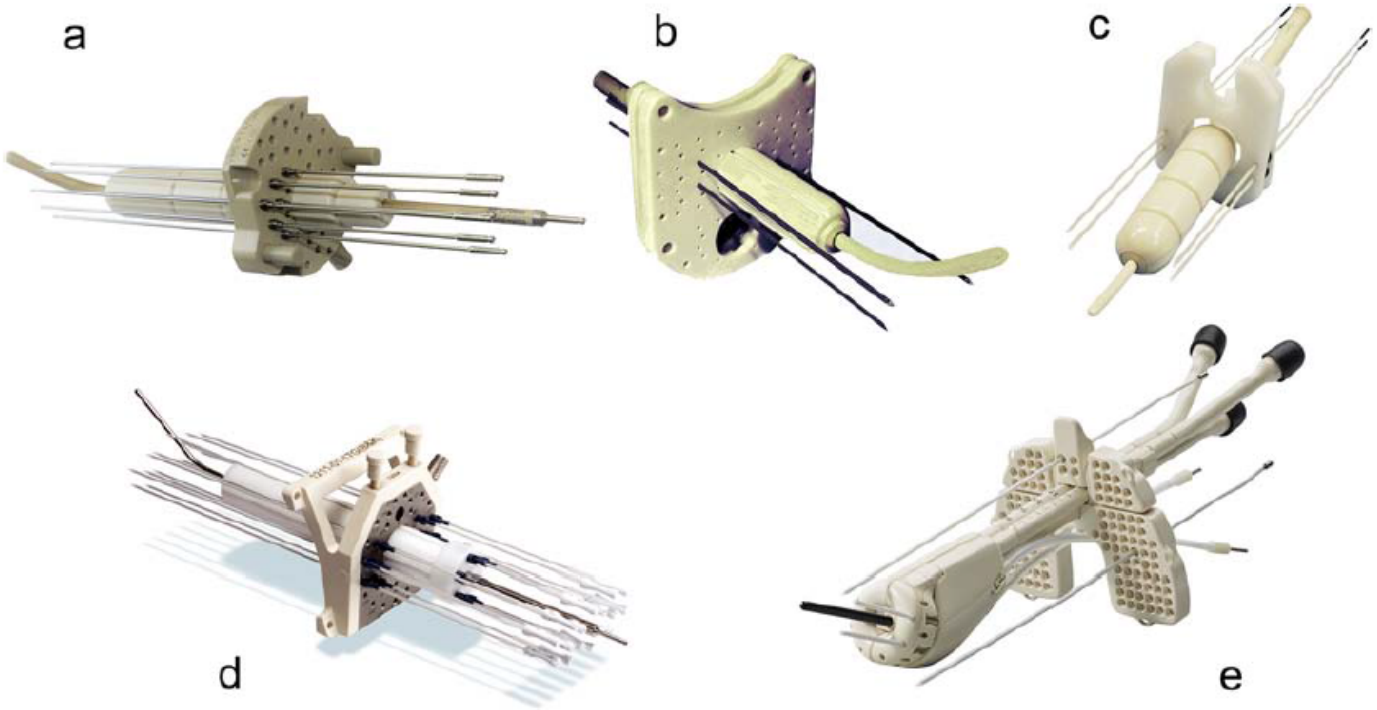

Fig. 1 – Applicators with perineal interstitial component. (a) Kelowna applicator (Varian), (b) Benidorm applicator (Lorca Marín), (c) Pamplona applicator, (d) M.A.C Applicator (Bebig) and (e)Venezia applicator (Elekta).

J Richart, V Carmona, T García, A Herreros, A Otal, S Pellejero, A Tornero, J Pérez-Calatayud Reports of Practical Oncology and Radiotherapy (2018)

Applicators library

Otal et al 2017

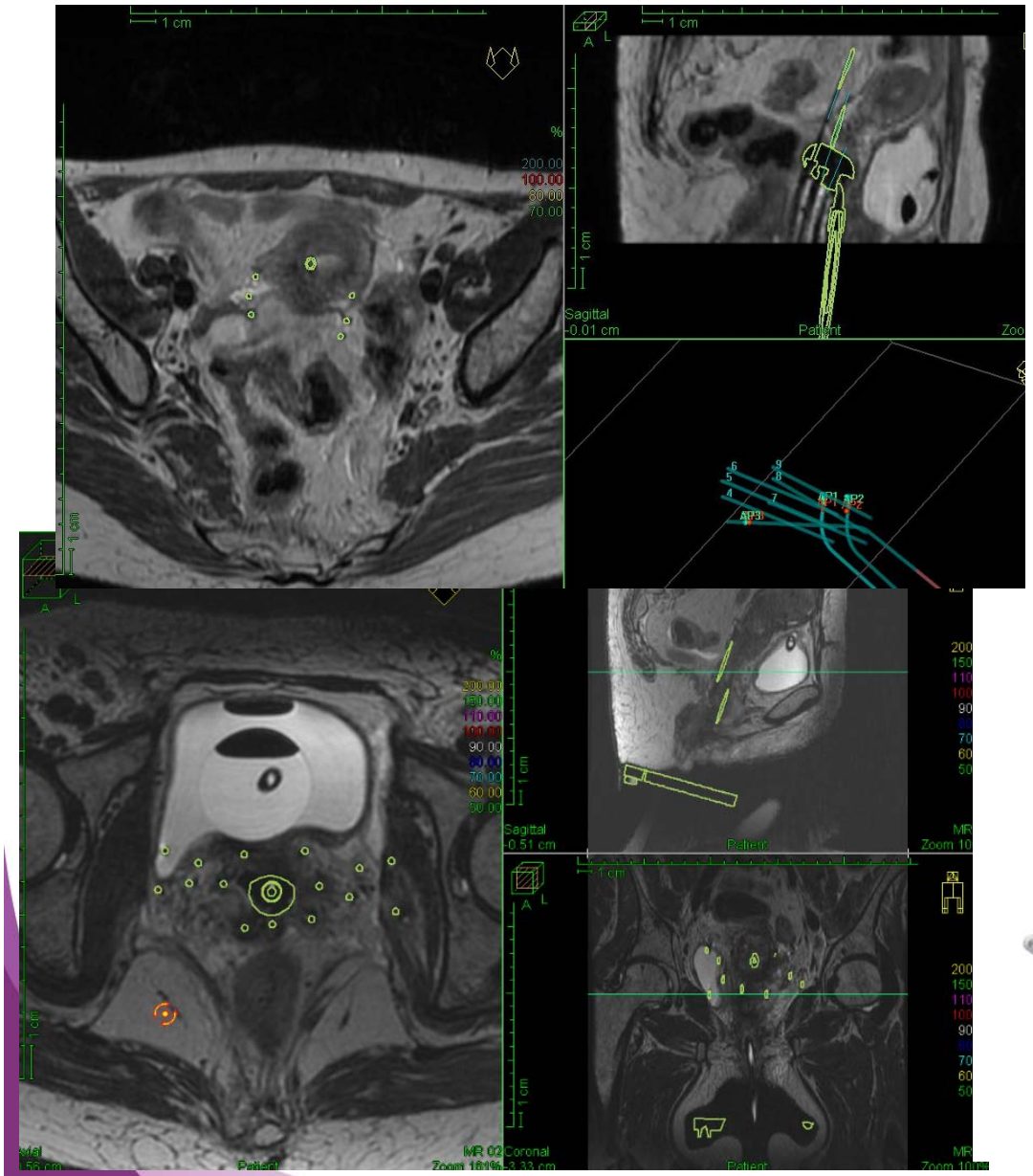

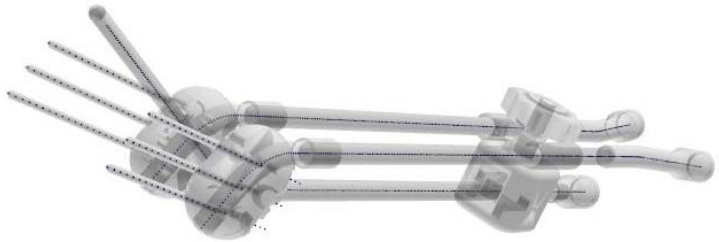

Use with T2

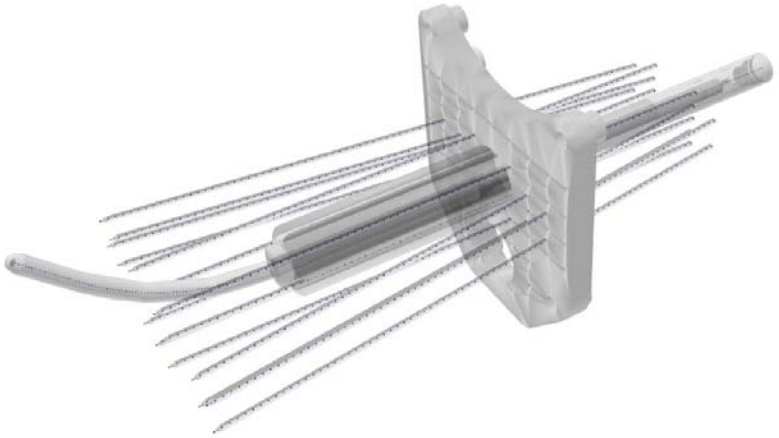

MR markers and free length

Richart et al 2015

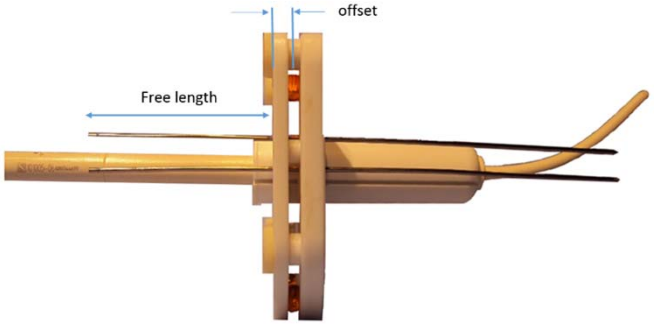

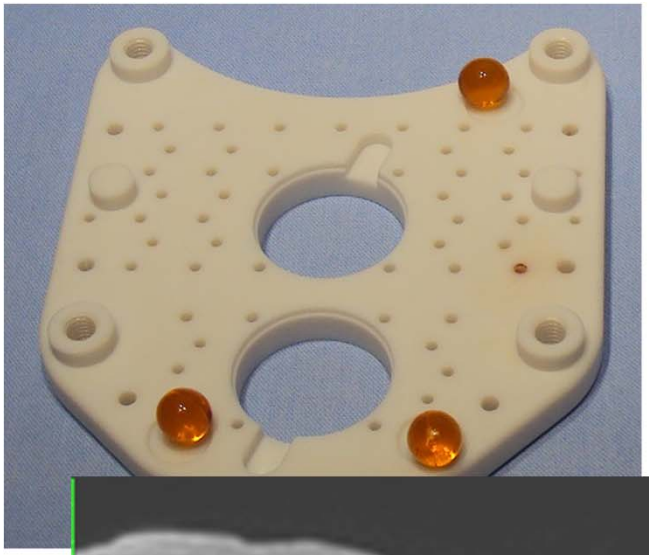

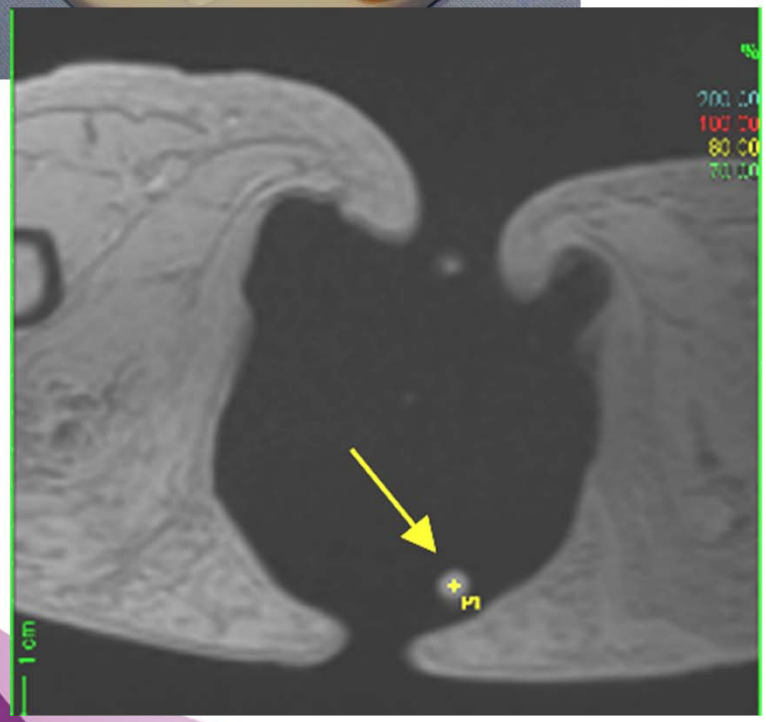

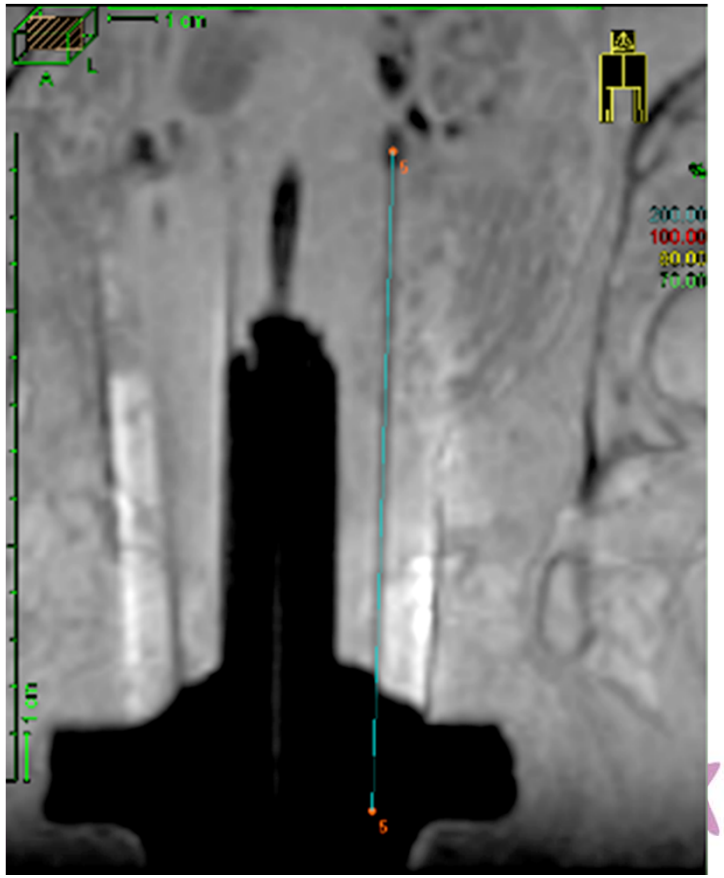

ESTRO School

3D printed MR markers embedded in the applicator

Otal et al 2016

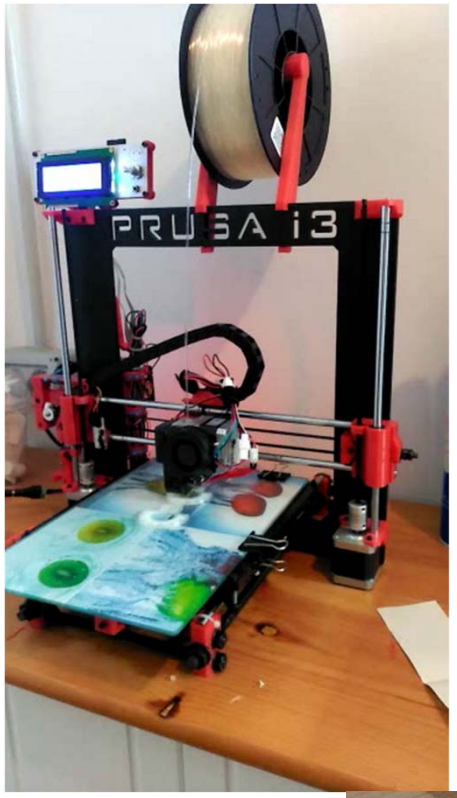

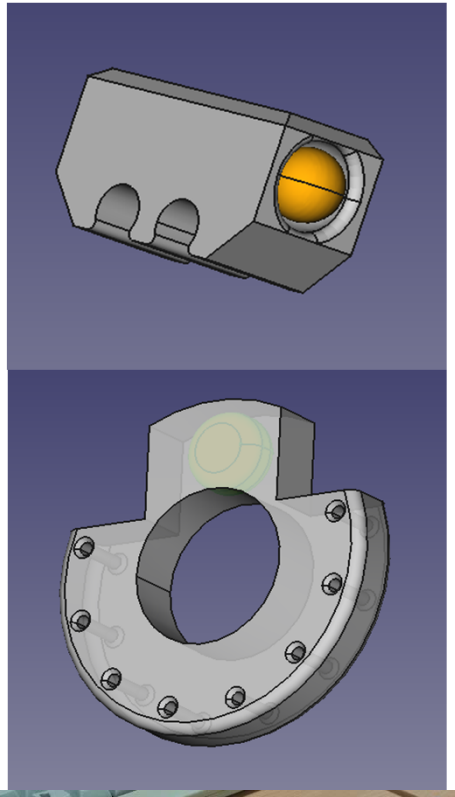

EMT reconstruction

Implant Verification by Electro-Magnetic Tracking

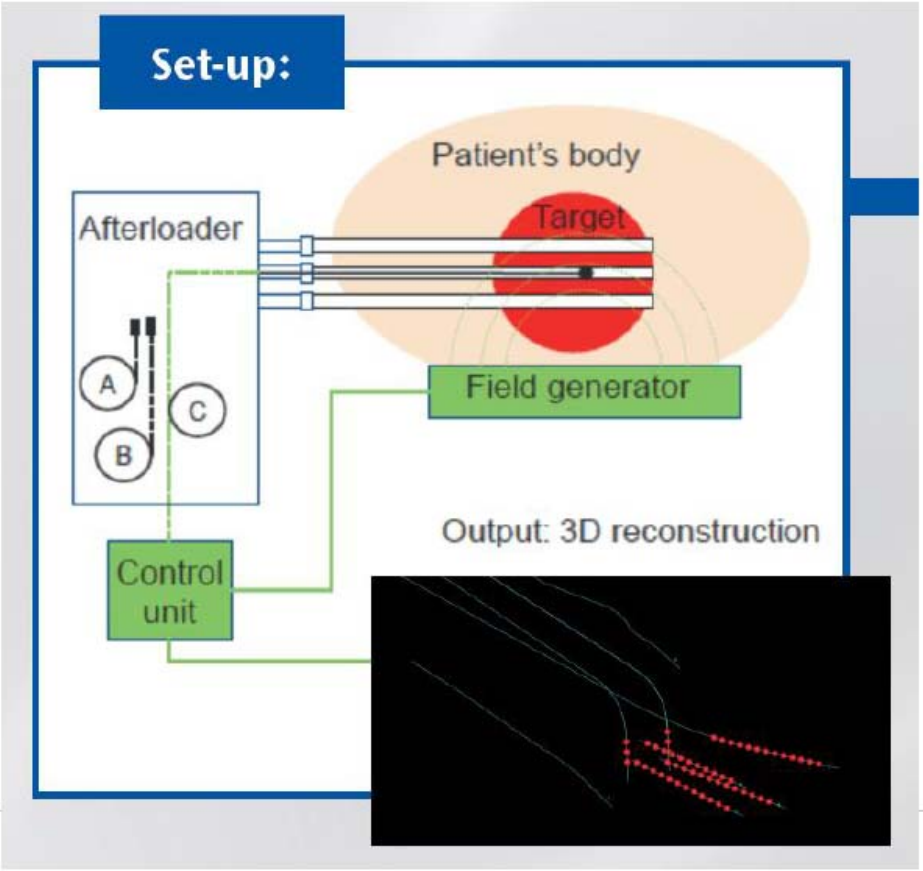

ELEKTA

Courtesy from Elekta

ESTRO School

EMT reconstruction

Pre-treatment verification

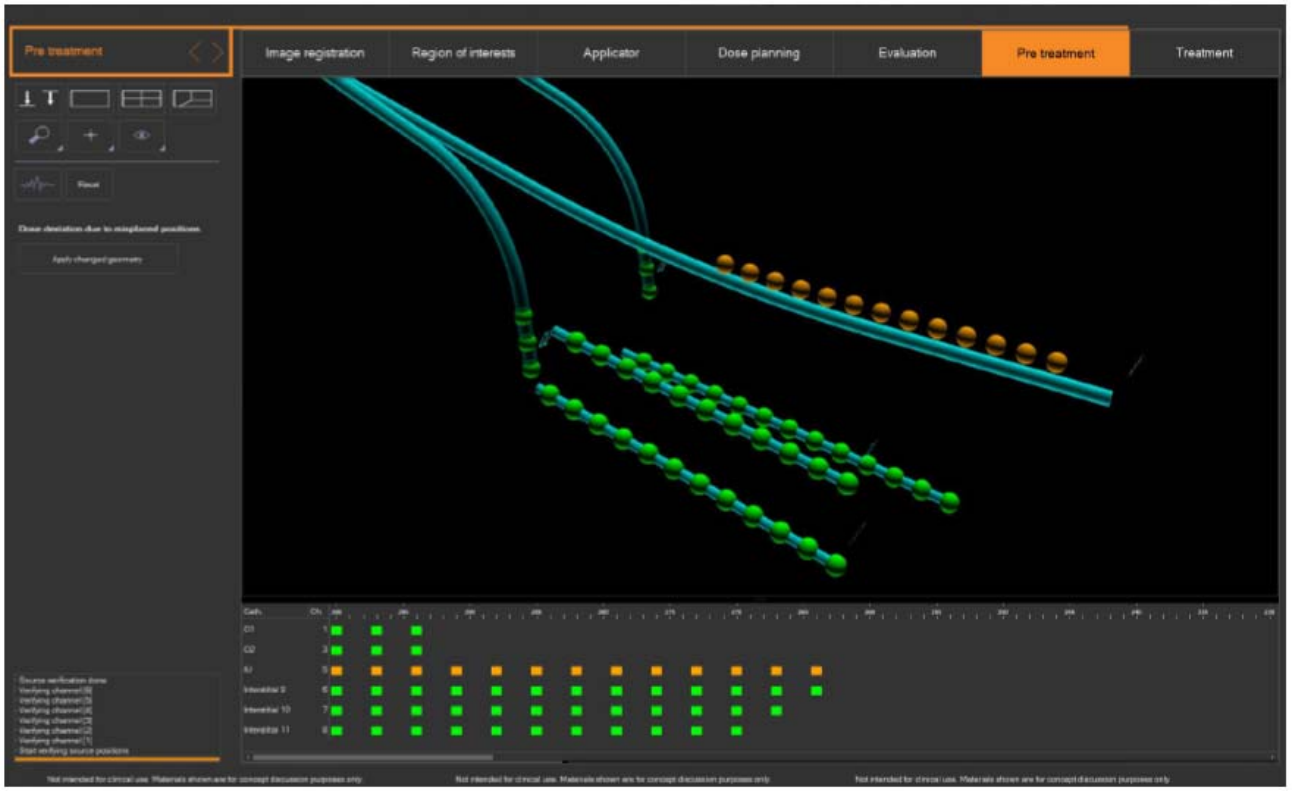

ELEKTA

Courtesy from Elekta

ESTRO School

Conclusions

- **3D** imaging modalities are **essential** for modern brachytherapy.
- Most convenient: contouring, catheter reconstruction and calculation on the **same image set**. Registration (moreover non-rigid one) must be carefully evaluated.
- **CT** is the most available. Caution: the limited **resolution** along the scan axis. Scout views can help with it.
- **TRUS** is mostly used in intraoperative prostate. Caution: needle **tip** definition. “Free length” can help with it.
- **MRI** T2 has excellent soft tissue definition. Caution: **distortion**. Phantoms and CT patient data can verify it.
- **Society Recommendations** are available to perform QA/QC of all these image modalities.
- TPS applicators **libraries and special markers** can help in reconstruction to be less sensitive to image resolution and cath. visibility.

ESTRO School

Thank you

perez_jos@gva.es

Regarding QA imaging in brachytherapy, please point the **wrong** statement

A. Most convenient: contouring, catheter reconstruction and calculation on the same image set.
B. CT, when used in intraoperative prostate, has the problem that the electronic density can not be obtained.
C. MRI has excellent soft tissue definition. The distortion must be evaluated.
D. Society Recommendations are available to perform QA/QC of all these image modalities.

ESTRO School

WWW.ESTRO.ORG/SCHOOL

ESTRO School

Advanced Brachytherapy Physics

Catheter/Applicator and Source Localisation using 3D Imaging

Nicole Nesvacil

Advanced Brachytherapy Physics, Valencia 2018

ESTRO School

Learning Objectives

1. Goal of brachytherapy reconstruction

2. History of reconstruction methods

3. Areas to concern for commissioning

Goal of Brachytherapy Reconstruction

accurately identify position of radiation field relative to tumor (and healthy) tissues

Tasks of Brachytherapy Reconstruction

accurately identify position of sources (markers or applicators) relative to contours

Historical Reconstructions Methods in Brachytherapy

1. Orthogonal x rays

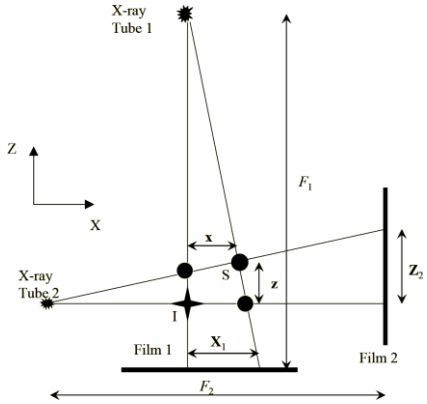

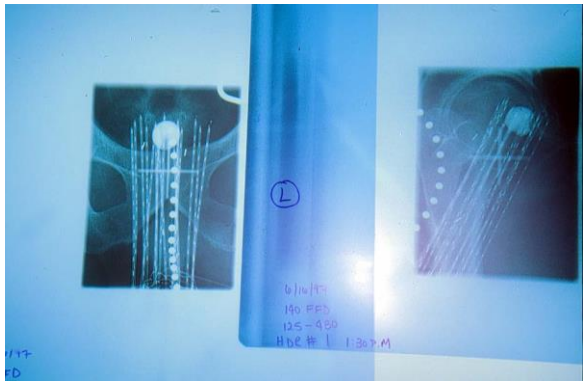

2. Stereo shifts (table/couch or x-ray tube)

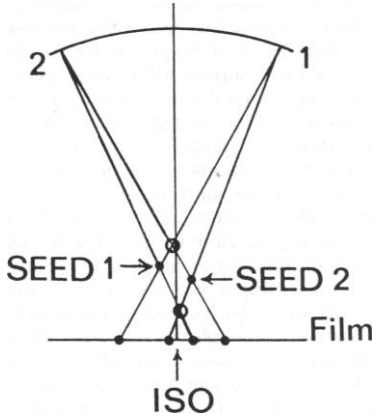

3. Fluoroscopy

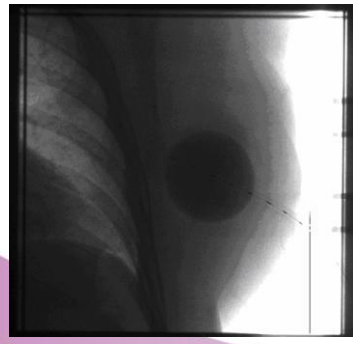

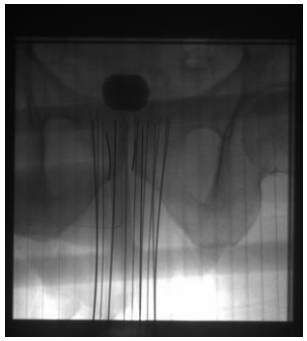

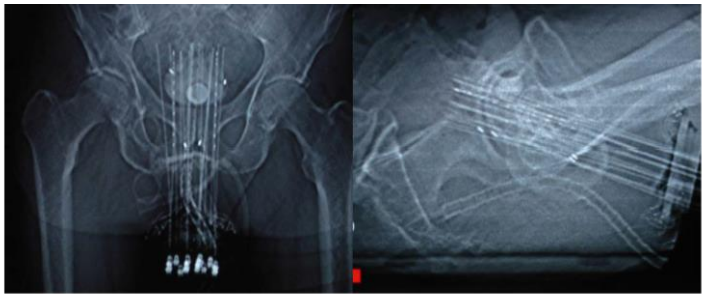

AP LAT

ESTRO School

Historical Reconstructions Methods in Brachytherapy

1. Orthogonal x rays

Strengths	high spatial resolution (< 0.5 mm)
	less susceptible to high-Z artifacts than CT
Weaknesses	not suitable for dozens of seeds
	planar representation of 3D anatomy
	limited by magnification uncertainty

2. Stereo shifts (table/couch or x-ray tube)

Strengths	good spatial resolution (~1 mm)
Weaknesses	highly sensitive to uncertainties in shift direction
	limited perspective

3. Fluoroscopy

Strengths	practical for intraoperative imaging
Weaknesses	crude 3D representation

Tasks of Brachytherapy Reconstruction

accurately identify position of sources (markers or applicators) relative to contours

Assumptions of 3D Brachytherapy Reconstruction

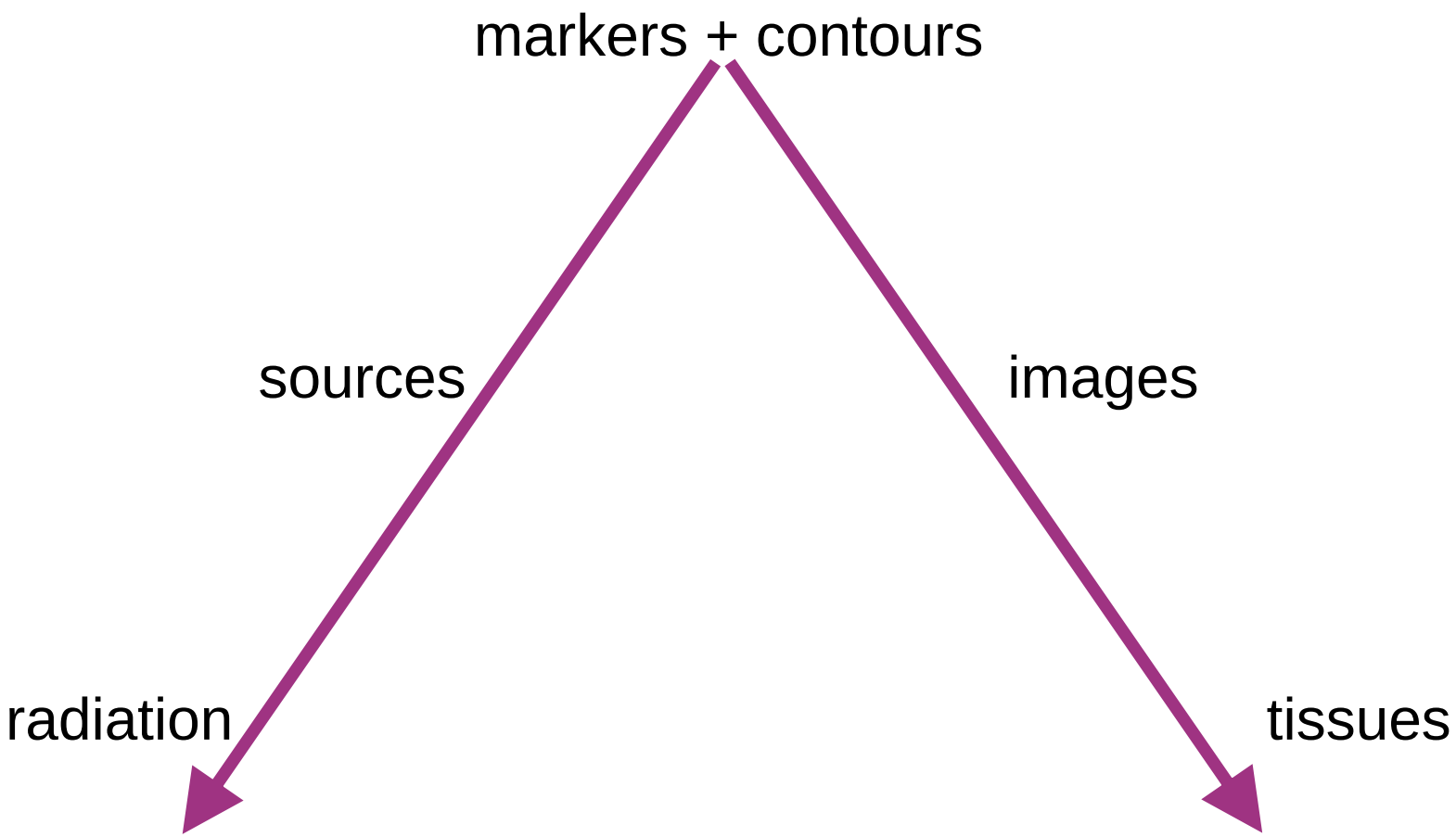

ESTRO School

Assumptions of 3D Brachytherapy Reconstruction

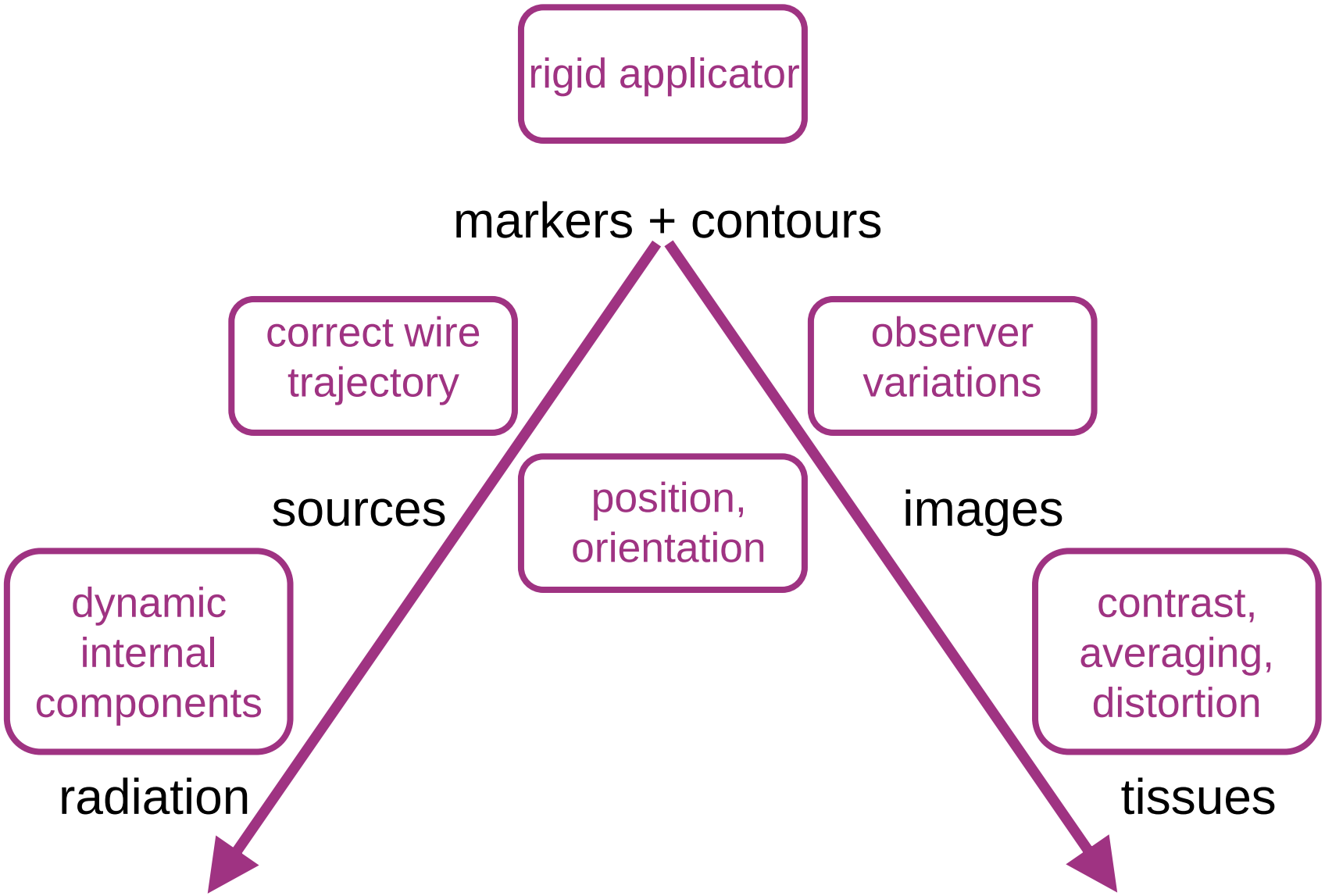

ESTRO School

Seeds

Test Assumptions: Reconstruction Commissioning

- source dynamic internal components
  - > 1 mm for some LDR sources

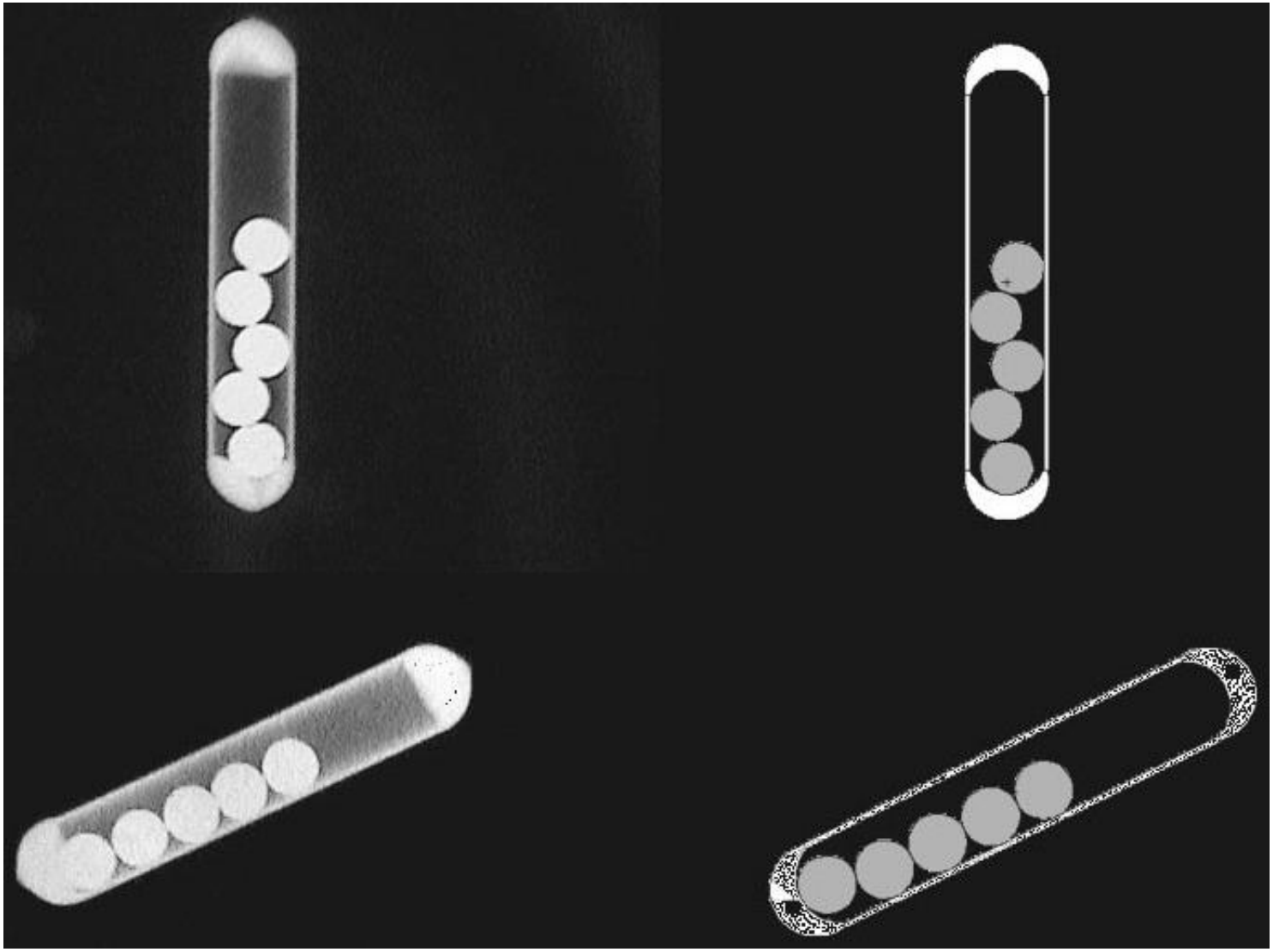

ESTRO School

Automatic Seed Reconstruction: Threshold-Based

Automatic localization of implanted seeds from post-implant CT images

Haisong Liu[1], Gang Cheng[1], Yan Yu[1], Ralph Brasacchio[1], Deborah Rubens[2], John Strang[2], Lydia Liao[2] and Edward Messing[3]

[1] Department of Radiation Oncology, University of Rochester, 601 Elmwood Avenue, Rochester, NY 14642, USA
[2] Department of Radiology, University of Rochester, 601 Elmwood Avenue, Rochester, NY 14642, USA
[3] Department of Urology, University of Rochester, 601 Elmwood Avenue, Rochester, NY 14642, USA

Received 18 December 2002, in final form 5 March 2003
Published 22 April 2003
Online at stacks.iop.org/PMB/48/1191

Abstract

An automatic localization method of implanted seeds from a series of post-implant computed tomography (CT) images is described in this paper. Post-implant CT studies were obtained for patients who underwent prostate brachytherapy. Bright areas were segmented using binary thresholding in each CT slice, and geometrical information on these areas was collected. Large areas (possibly containing two connected seeds) were split into smaller ones by geometry-based filtering in each slice. The area connectivity along the longitudinal direction was analysed using a geometry-based connection search algorithm executed on every area slice by slice, so that the connected areas were combined into one object. The weighted centroid of each object was taken as the seed position. This method was tested on a seed-containing prostate phantom as well as using CT studies from patients. Statistical analysis demonstrates that it can achieve above 99% detection rate with reliable localization accuracy and high speed. It is reliable and convenient for localizing implanted seeds on CT and can be used to assist post-implant dosimetry for prostate brachytherapy.

Liu, et al., *Phys. Med. Phys.* 48, 1191-1203 (2003)

ESTRO School

Automatic Seed Reconstruction: Threshold-Based

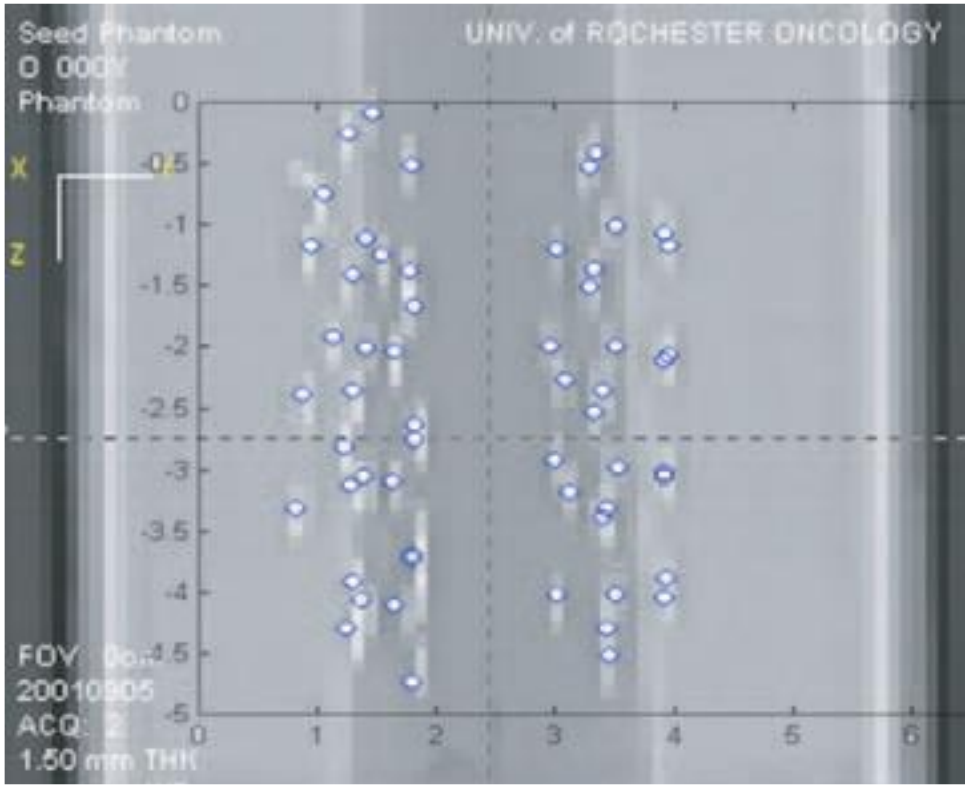

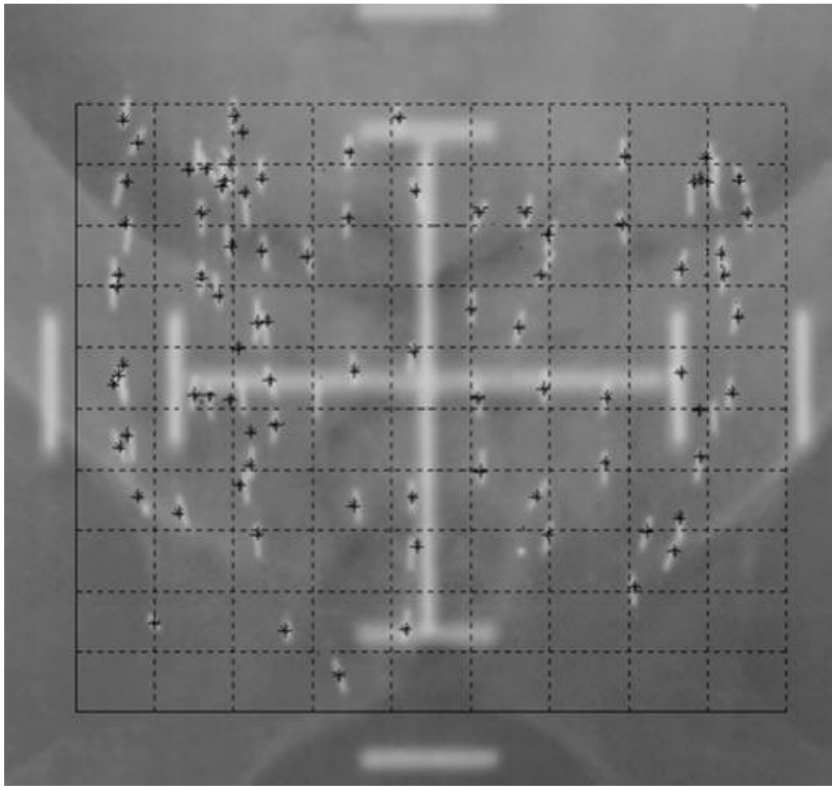

99% seeds identified,
3 mm localization error

Table 1. Distances between corresponding coordinates comparing the two-film technique with the automated method using 1 and 3 mm CT of two patients.

	Minimum (mm)	Maximum (mm)	Average (mm)
1 mm CT vs film (patient 1)	0.17	5.37	2.65
3 mm CT vs film (patient 1)	0.26	6.41	2.99
1 mm CT vs 3 mm CT (patient 1)	0.12	0.32	0.17
3 mm CT vs film (patient 2)	0.26	7.46	3.10

Liu, et al., *Phys. Med. Phys.* 48, 1191-1203 (2003)

ESTRO School

Automatic Seed Reconstruction: Hough Transform

An automatic seed finder for brachytherapy CT postplans based on the Hough transform

E. J. Holupka[a] and P. M. Meskell
Department of Radiation Therapy, Beth Israel Deaconess Medical Center, Harvard Medical School, Boston, Massachusetts 02115

E. C. Burdette
Computerized Medical System, Inc., Corporate Park Centre, 2110 Clearlake Boulevard, Suite 102, Champaign, Illinois 61822

I. D. Kaplan
Department of Radiation Therapy, Beth Israel Deaconess Medical Center, Harvard Medical School, Boston, Massachusetts 02115

(Received 1 August 2003; revised 11 June 2004; accepted for publication 12 June 2004; published 27 August 2004)

Purpose: The purpose of the work is to describe a new algorithm for the automatic detection of implanted radioactive seeds within the prostate. The algorithm is based on the traditional Hough transform. A method of quality assurance is described as well as a quantitative phantom study to determine the accuracy of the algorithm. Methods and Materials: An algorithm is described which is based on the Hough transform. The Hough transform is a well known transform traditionally used to automatically segment lines and other well defined geometric objects from images. The traditional Hough transform is extended to three-dimensions and applied to CT images of seed implanted prostate glands. A method based on digitally reconstructed radiographs is described to quality assure the determined three-dimensional positions of the detected seeds. Two phantom studies utilizing eight seeds and nine seeds are described. All eight seeds form a contiguous a square while the nine seed phantom describes seeds which are placed side-by-side in groups of two and three. The algorithm is applied to the CT scans of both phantoms and the seed positions determined. Results: The algorithm has been commercially developed and used to perform post-surgical dosimetric assessment on approximately 1000 patients. Using the described quality assurance tool it was determined that the algorithm accurately determined the seed positions in all 1000 patients. The algorithm was also applied to the eight seed phantom. The algorithm successfully found all eight seeds as well as their seed coordinates. The average radial error was determined to be 0.9 mm. For the nine seed phantom, the algorithm correctly identified all nine seeds, with an average radial error of 3 mm. Conclusions: The described algorithm is a robust, accurate, automatic, three-dimensional application for CT based seed determination. © *2004 American Association of Physicists in Medicine.* [DOI: 10.1118/1.1778837]

Holupka, et al., *Med. Phys.* 31, 2672-2679 (2004)

ESTRO School

Automatic Seed Reconstruction: Hough Transform

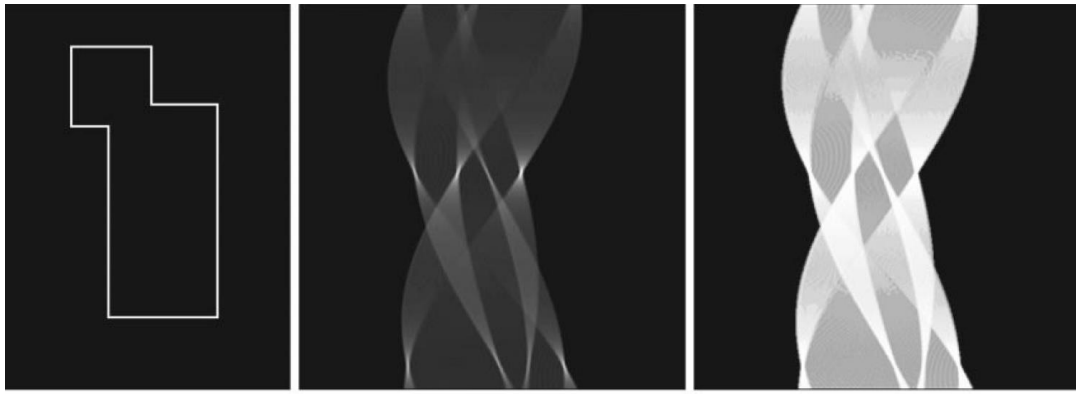

(a) (b) (c)

(a) A simple binary image containing lines.
(b) The Hough transform of the image.
(c) The Hough transform contrasted to display the underlying structure.

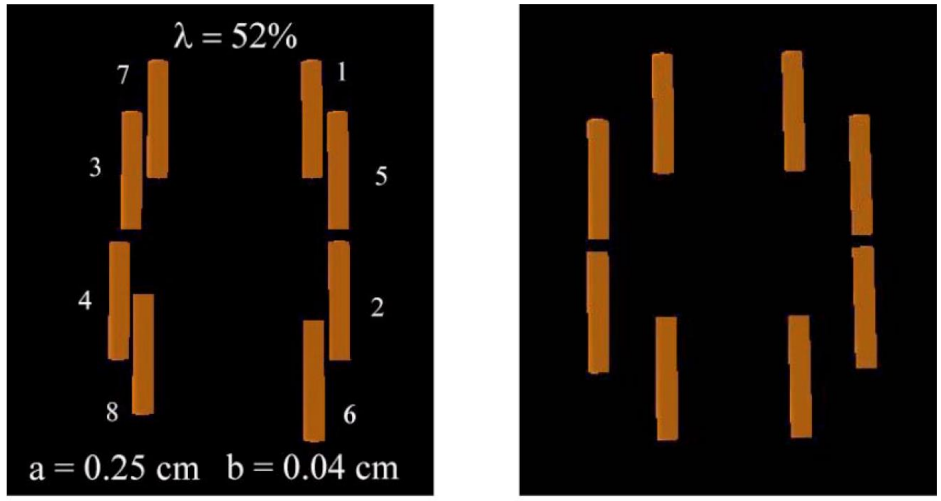

(a) (b)

(a) Seed positions as determined by the described algorithm.
(b) Theoretical seed coordinates. The seeds appear in the inferior to superior direction because the point dose approximation was used and the true orientation is not needed.

seed localization error ranged from 1-3 mm

Holupka, et al., *Med. Phys.* 31, 2672-2679 (2004)

ESTRO School

Seed Reconstruction Uncertainties: CT & MRI

CT- and MRI-based seed localization in postimplant evaluation after prostate brachytherapy

Marisol De Brabandere[1,*], Bashar Al-Qaisieh[2], Liesbeth De Wever[3], Karin Haustermans[1], Christian Kirisits[4], Marinus A. Moerland[5], Raymond Oyen[3], Alex Rijnders[6], Frank Van den Heuvel[1], Frank-André Siebert[7]

[1]*Department of Radiation Oncology, University Hospital Gasthuisberg, Leuven, Belgium*
[2]*Department of Medical Physics and Engineering, St James's Institute of Oncology, Leeds, United Kingdom*
[3]*Department of Radiology, University Hospital Gasthuisberg, Leuven, Belgium*
[4]*Department of Radiotherapy, Medical University of Vienna, Comprehensive Cancer Center, Vienna, Austria*
[5]*Department of Radiation Oncology, University Medical Center Utrecht, Utrecht, The Netherlands*
[6]*Department of Radiation Oncology, Europe Hospitals, Brussels, Belgium*
[7]*University Hospital of Schleswig-Holstein, Clinic of Radiotherapy, Kiel, Germany*

ABSTRACT

PURPOSE: To compare the uncertainties in CT- and MRI-based seed reconstruction in postimplant evaluation after prostate seed brachytherapy in terms of interobserver variability and quantify the impact of seed detection variability on a selection of dosimetric parameters for three postplan techniques: (*1*) CT, (*2*) MRI-T1 weighted fused with MRI-T2 weighted, and (*3*) CT fused with MRI-T2 weighted.

METHODS AND MATERIALS: Seven physicists reconstructed the seed positions on postimplant CT and MRI-T1 images of three patients. For each patient and imaging modality, the interobserver variability was calculated with respect to a reference seed set. The effect of this variability on dosimetry was calculated for CT and CT + MRI-T2 (CT-based seed reconstruction), as well as for MRI-T1 + MRI-T2 (MRI-T1–based seed reconstruction), using fixed CT and MRI-T2 prostate contours.

RESULTS: Averaged over three patients, the interobserver variability in CT-based seed reconstruction was 1.1 mm (1 SD_{ref}, i.e., standard deviation with respect to the reference value). The D_{90} (dose delivered to 90% of the target) variability was 1.5% and 1.3% (1 SD_{ref}) for CT and CT + MRI-T2, respectively. The mean interobserver variability in MRI-based seed reconstruction was 3.0 mm (1 SD_{ref}), and the impact of this variability on D_{90} was 6.6% for MRI-T1 + MRI-T2.

CONCLUSIONS: Seed reconstruction on MRI-T1–weighted images was less accurate than on CT. This difference in uncertainties should be weighted against uncertainties due to contouring and image fusion when comparing the overall reliability of postplan techniques.

De Brabandere, et al., *Brachytherapy* 12, 580-588 (2013)

ESTRO School

Seed visualisation: prostate vs agarose gel

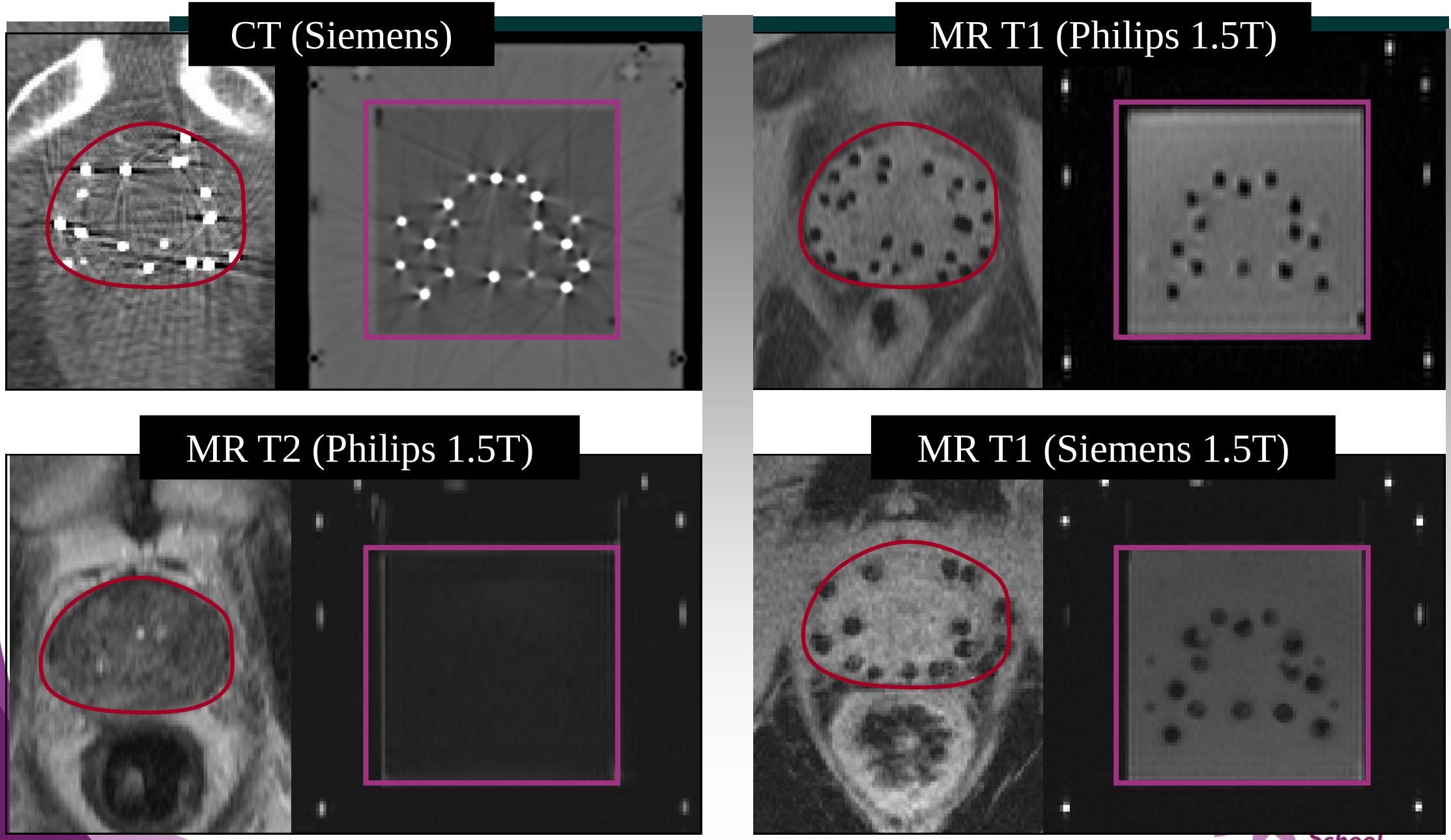

de Brabandere et al. R&O 2006

Seed Reconstruction Uncertainties: CT & MRI

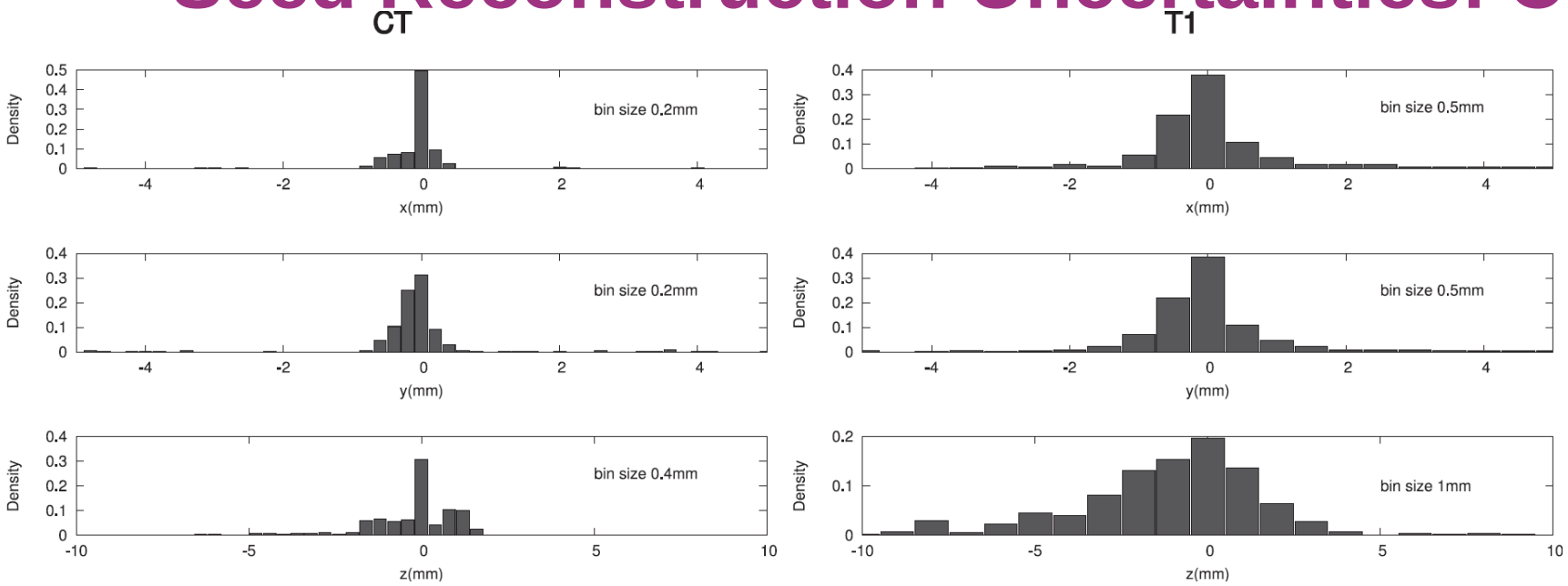

MRI-based seed reconstruction was less accurate than CT, with a mean interobserver variation in seed positioning of 3 mm (1 SD). This resulted in a non-negligible mean interobserver variation in D_{90} of about 7% for T1 + T2.

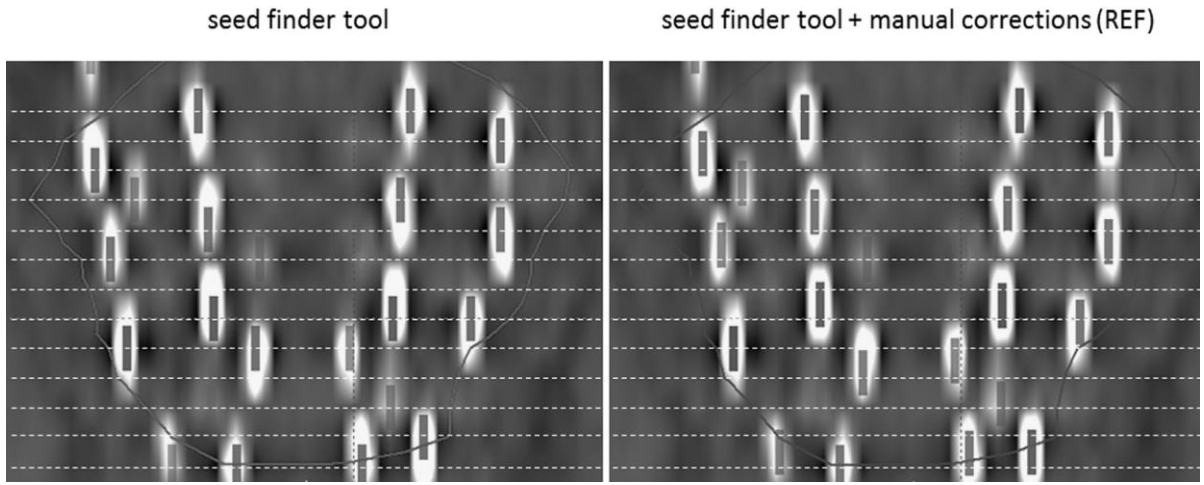

De Brabandere, et al., *Brachytherapy* 12, 580-588 (2013)

ESTRO School

Rigid applicators
GYN

The problem: no visible source channel

How to reconstruct the tandem ring applicator directly on MR Images ?

How to identify the 1st source position of the ring ?

Do we need MR markers to identify the whole source channel (path) ?

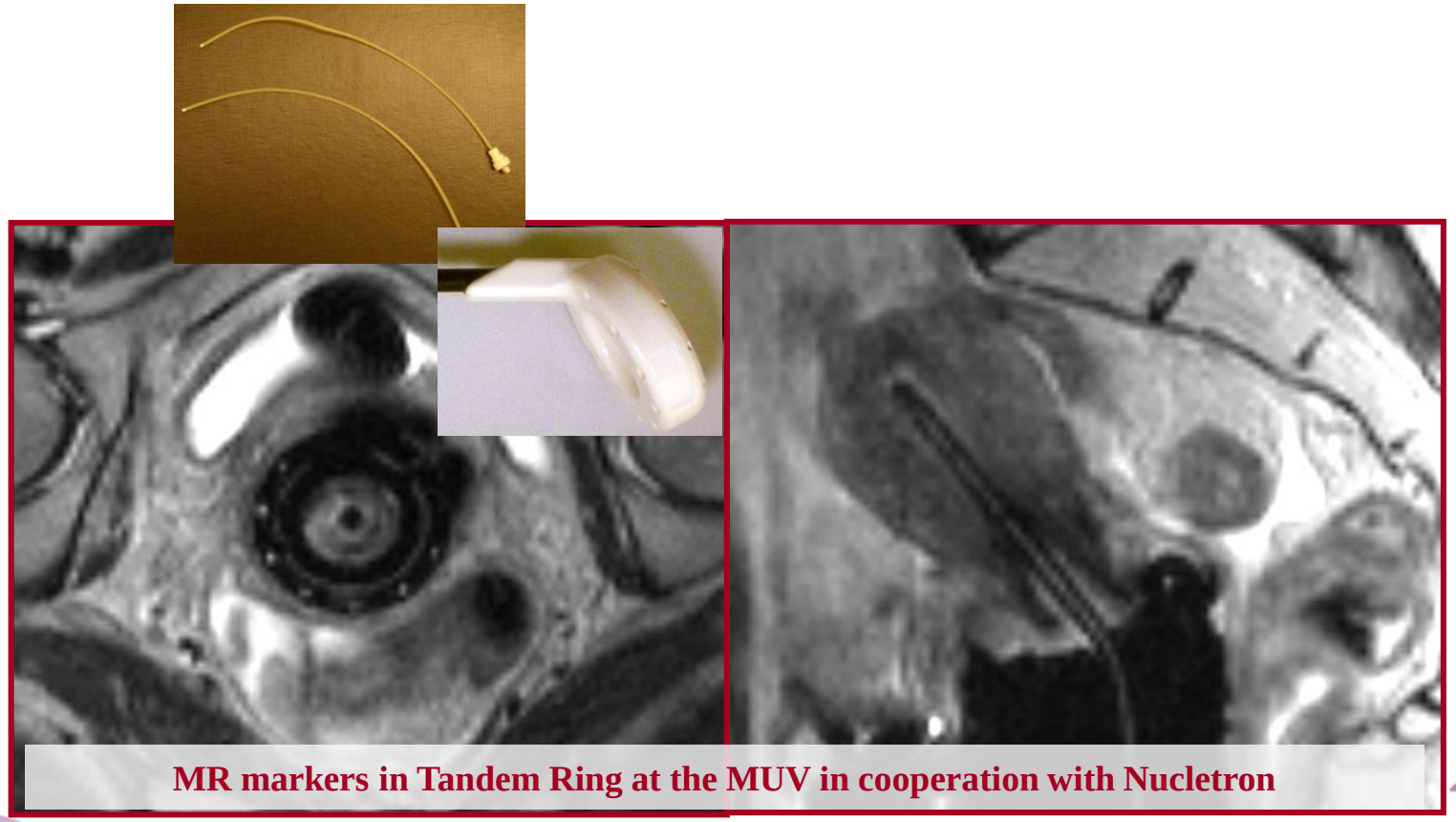

MR markers in Tandem Ring at the MUV in cooperation with Nucletron

ESTRO School

The problem: no visible source channel

How to reconstruct the tandem ovoids applicator directly on MR Images ?

How to identify the 1st source position of the ring ?

Do we need MR markers to identify the whole source channel (path) ?

MR markers in Tandem Ovoids provided by Jamema Swamidas and Umesh Mahantshetty, Mumbai

ESTRO School

The problem: no visible source channel

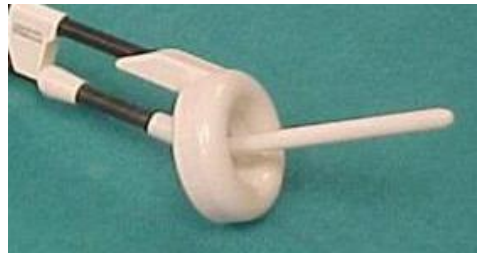

How to reconstruct the tandem ring applicator directly on MR Images ?

How to identify the 1st source position of the ring ?

Do we need MR markers to identify the whole source channel (path) ?

- ***Not necessarily when using the Vienna ring, it helps to provide additional information during the reconstruction process***

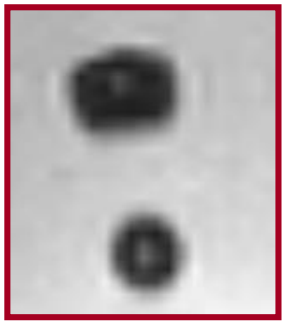

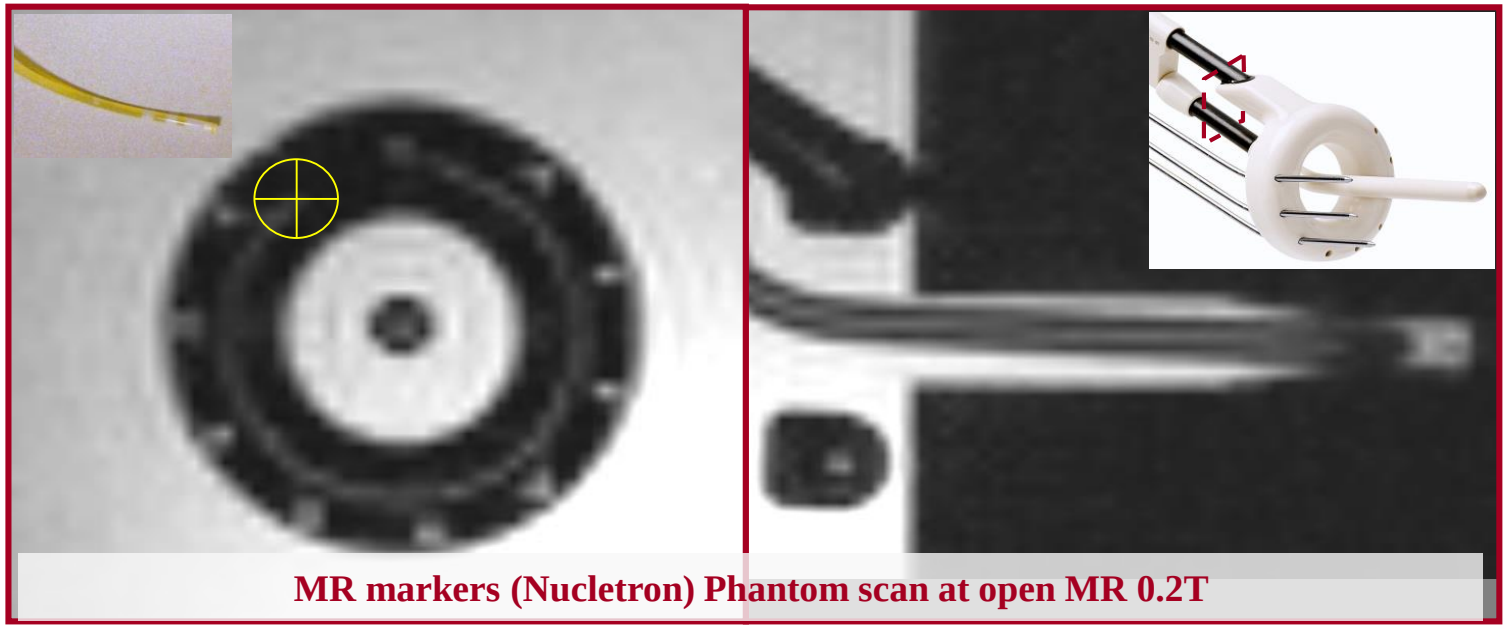

MR markers (Nucletron) Phantom scan at open MR 0.2T

ESTRO School

The problem: no visible source channel

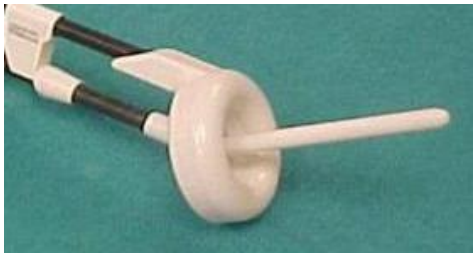

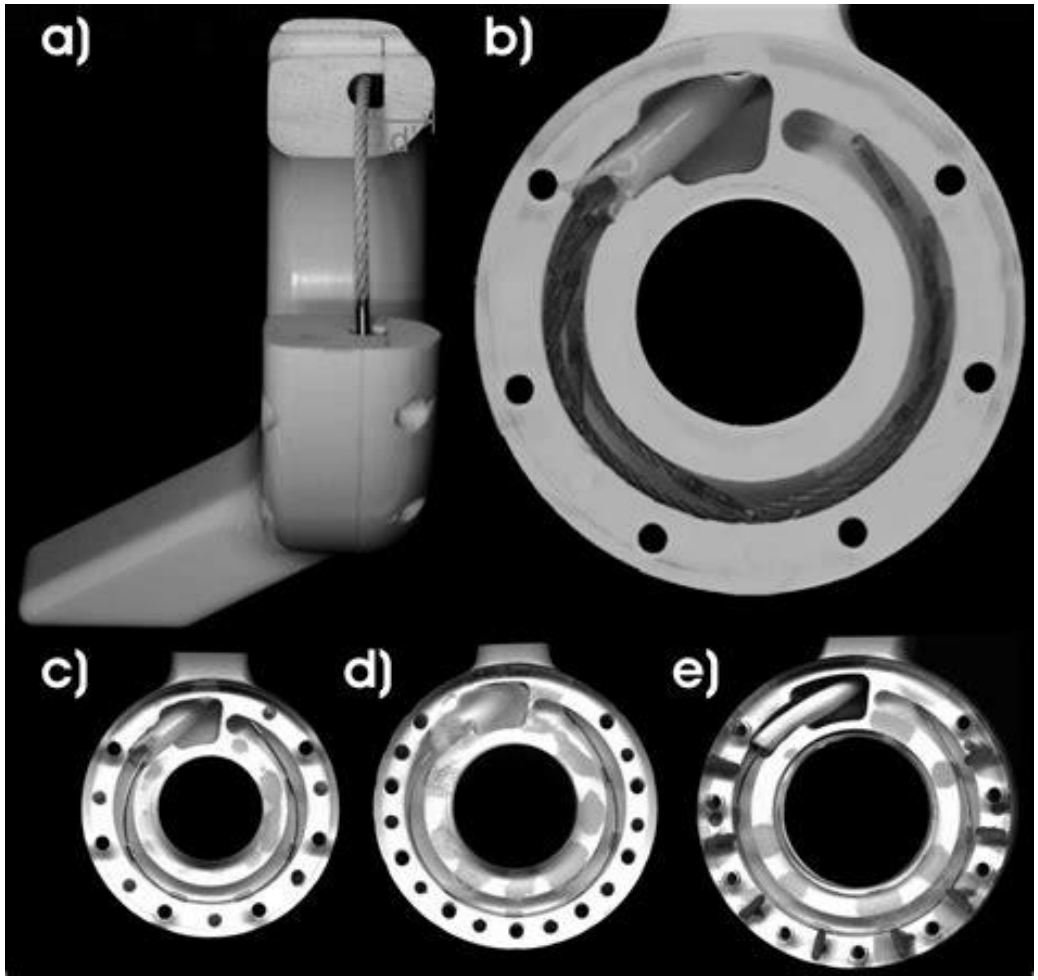

Radiotherapy and Oncology 93 (2009) 347–351

Contents lists available at ScienceDirect

Radiotherapy and Oncology

journal homepage: www.thegreenjournal.com

Cervix cancer brachytherapy

Direct reconstruction of the Vienna applicator on MR images

Daniel Berger *, Johannes Dimopoulos, Richard Pötter, Christian Kirisits

Department of Radiotherapy, Medical University of Vienna, General Hospital of Vienna, Währinger Gürtel, Vienna, Austria

ESTRO School

Test Assumptions: Reconstruction Commissioning

- correct wire trajectory (Vienna ring) courtesy of Christian Kirisits

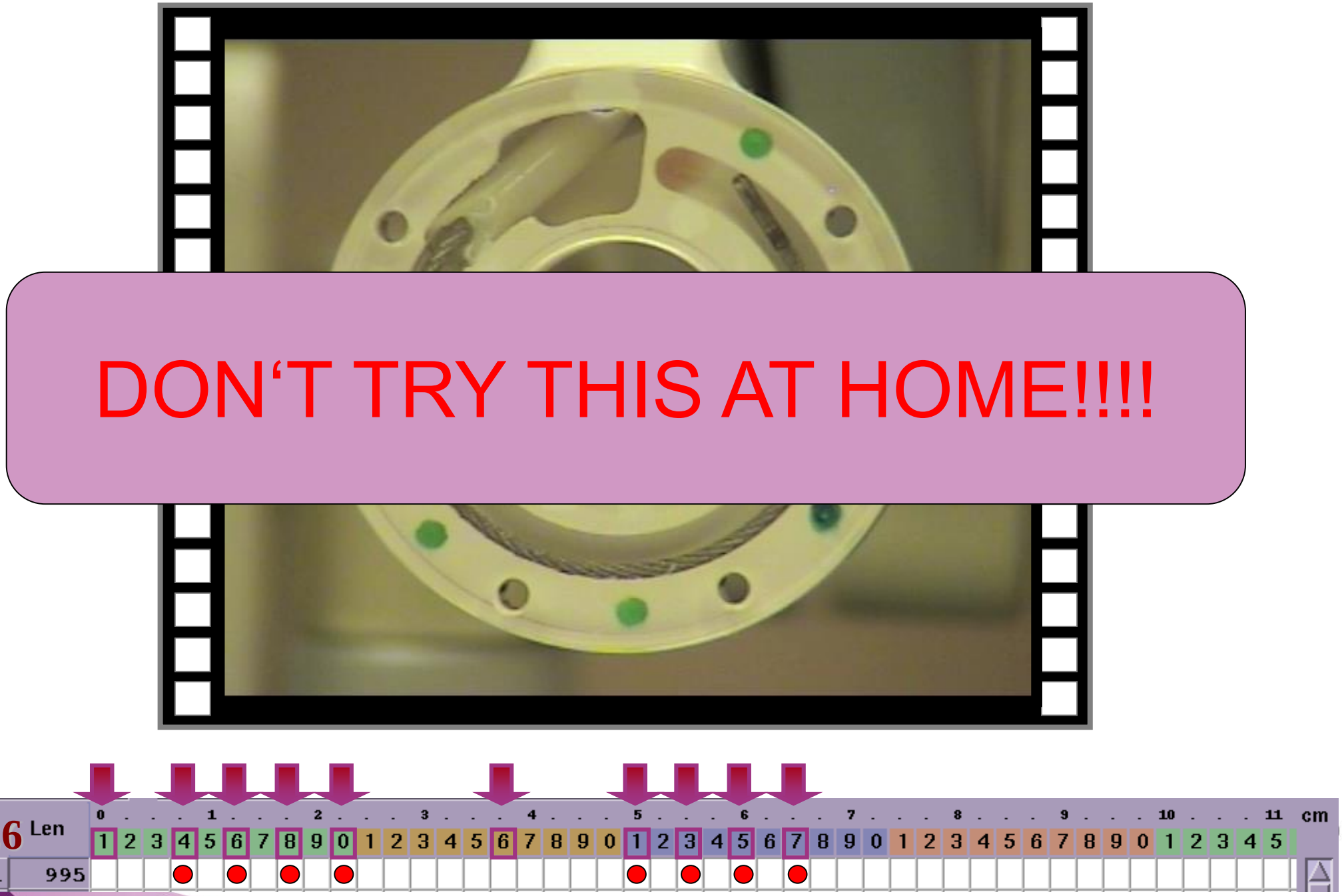

Do acceptance tests and check

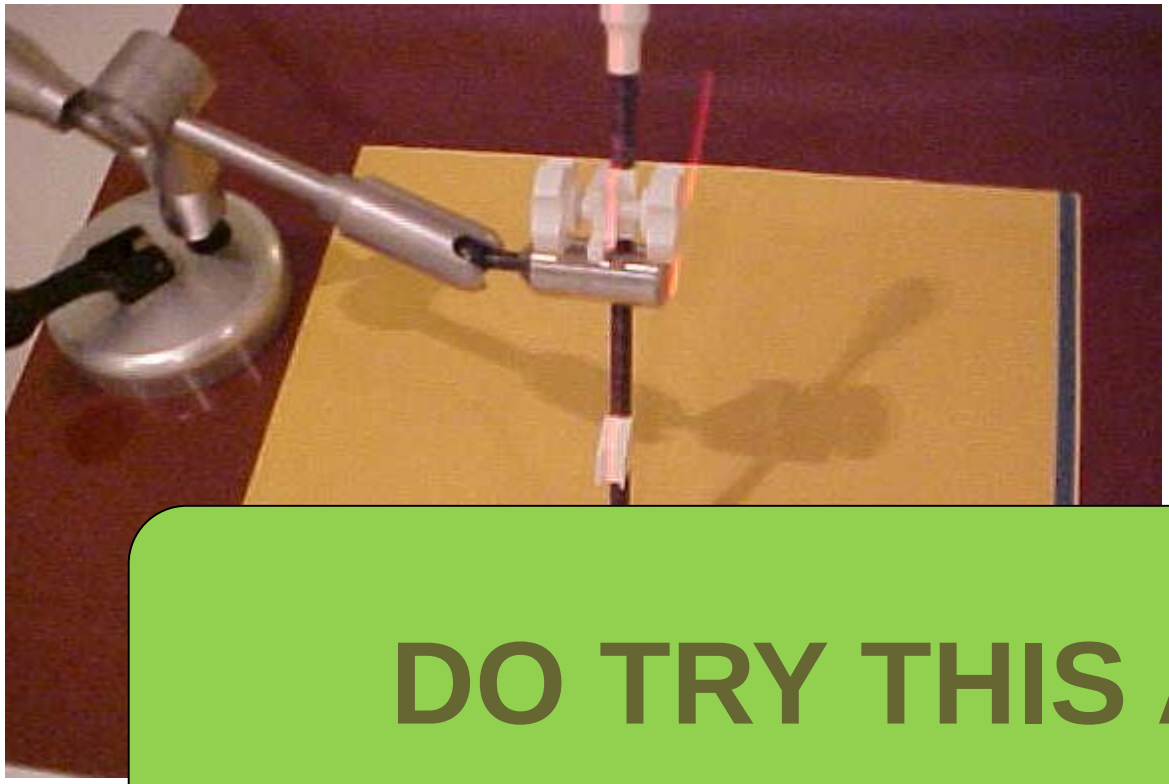

DO TRY THIS AT HOME!

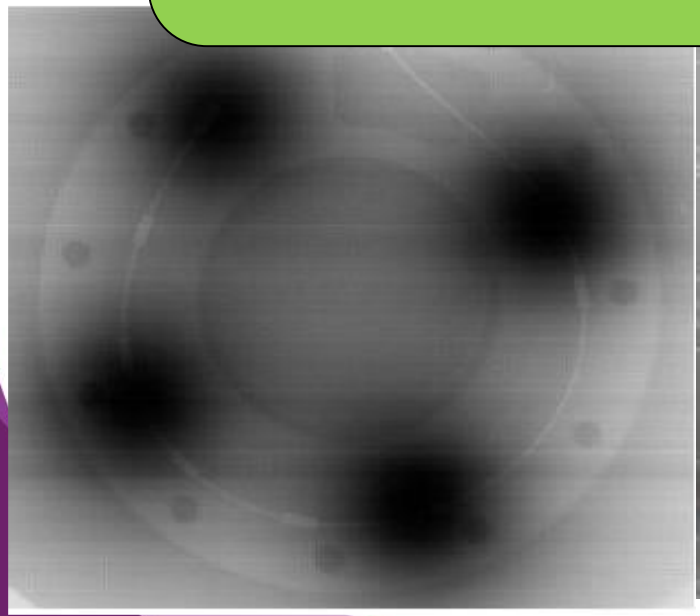

A. De Leeuw *et al.* *Tandem- Ovoids applicator reconstruction on MRI*

Radiographs

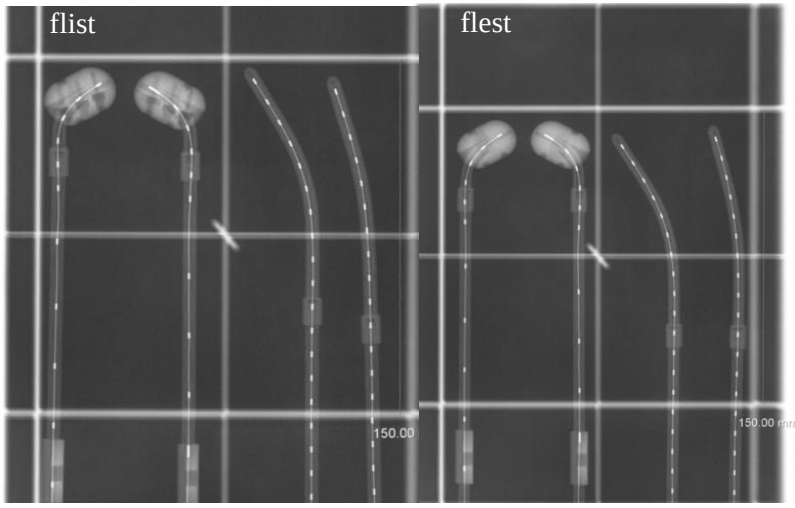

Auto-Radiography

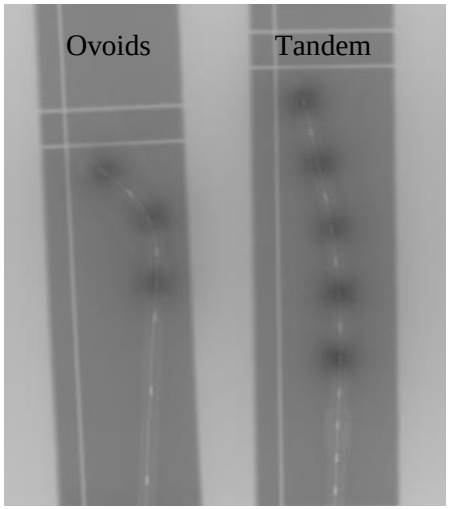

Template for Reconstruction

Ovoids:
Tip-1st dwell position 6 mm
1st dwell position-intersection 19 mm
Angle 120 °

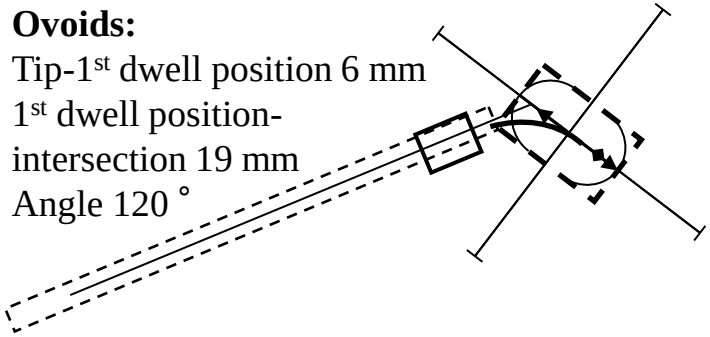

Intrauterine Tandem:
Tip-1st dwell position 7 mm

MR Imaging

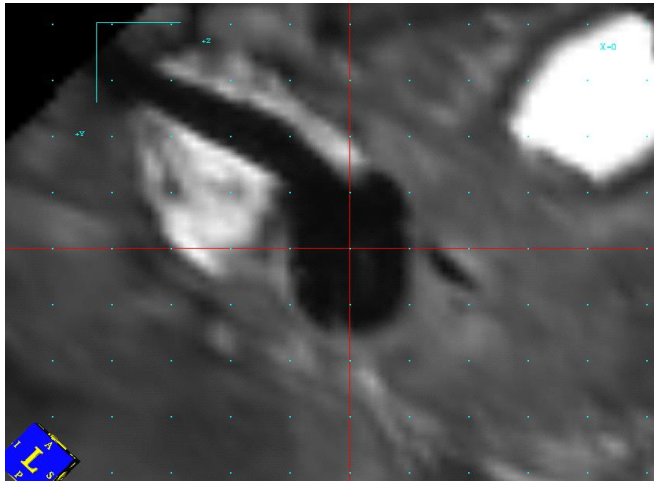

Template in place

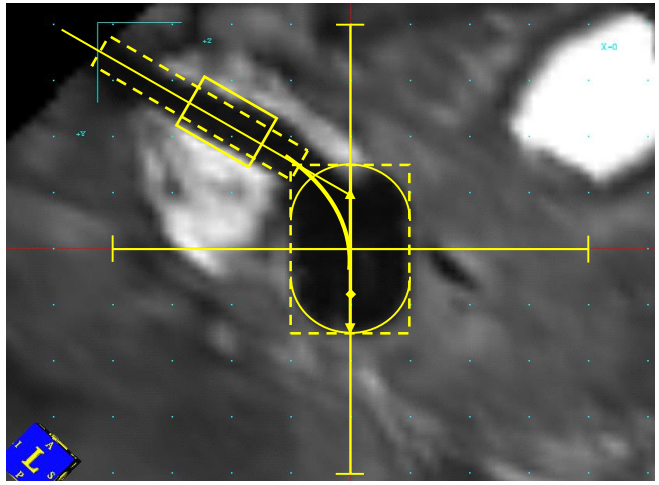

Reconstruction of source path

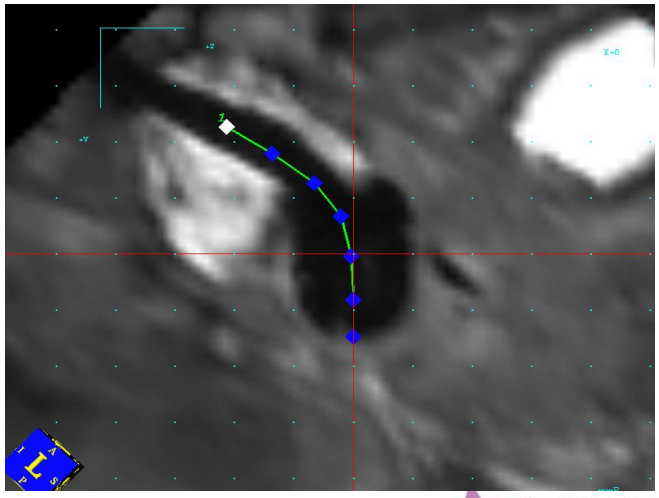

ESTRO School

D. Berger *et al.*

Direct reconstruction of the Vienna applicator on MR images

manual direct	software integrated
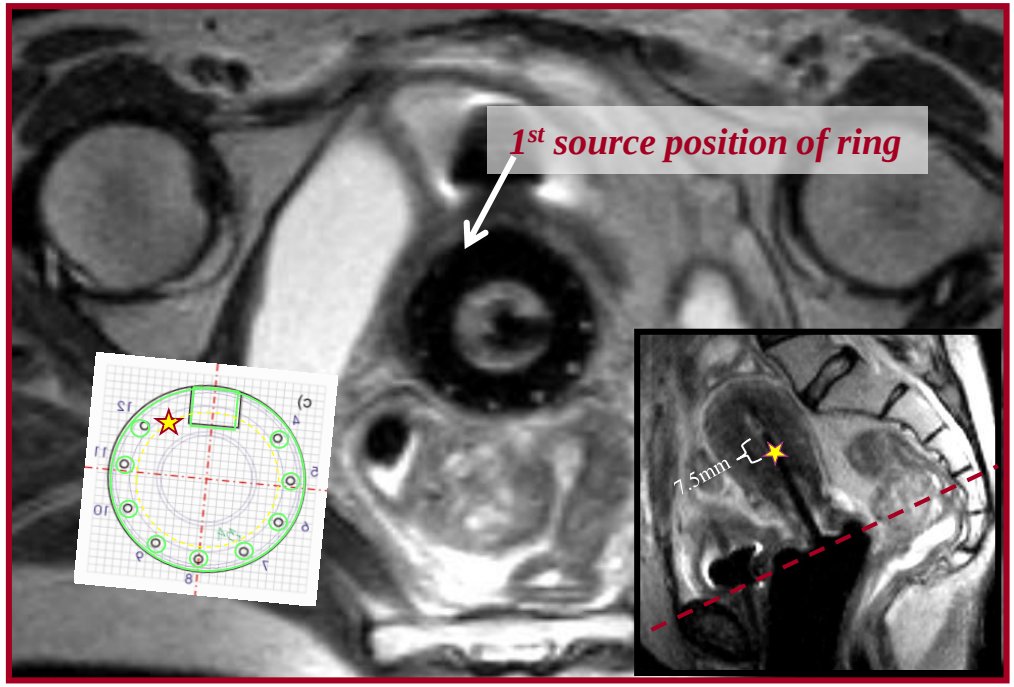	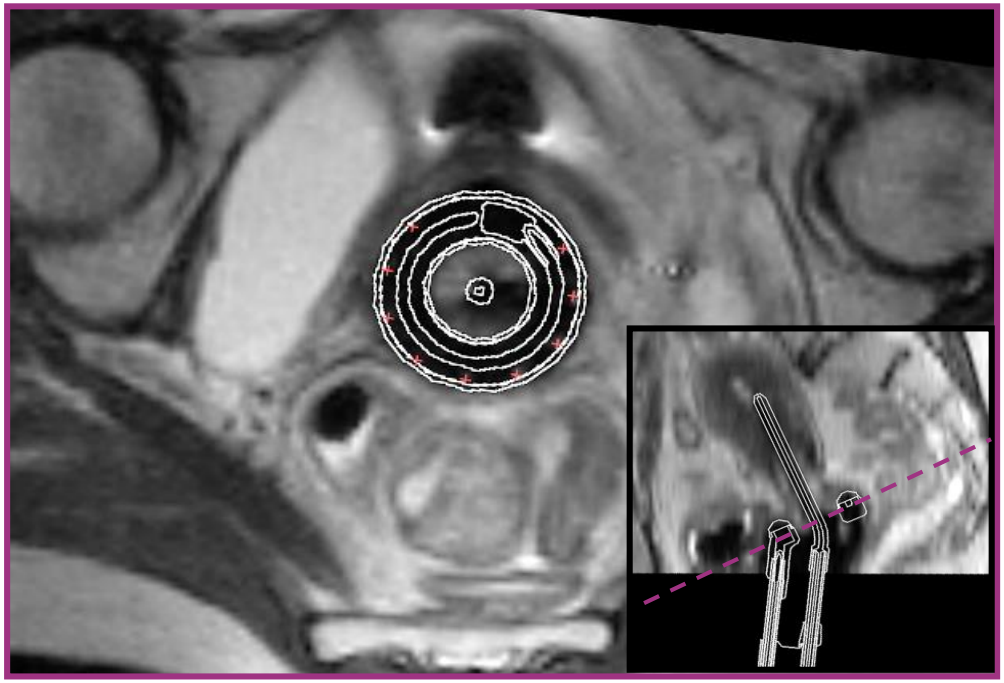
5 – 10 min	less than 5 min

If the relation between applicator shape and the source path is defined once,
the reconstruction process can be performed by directly placing the applicator in the MRI dataset.

ESTRO School

Applicator surface

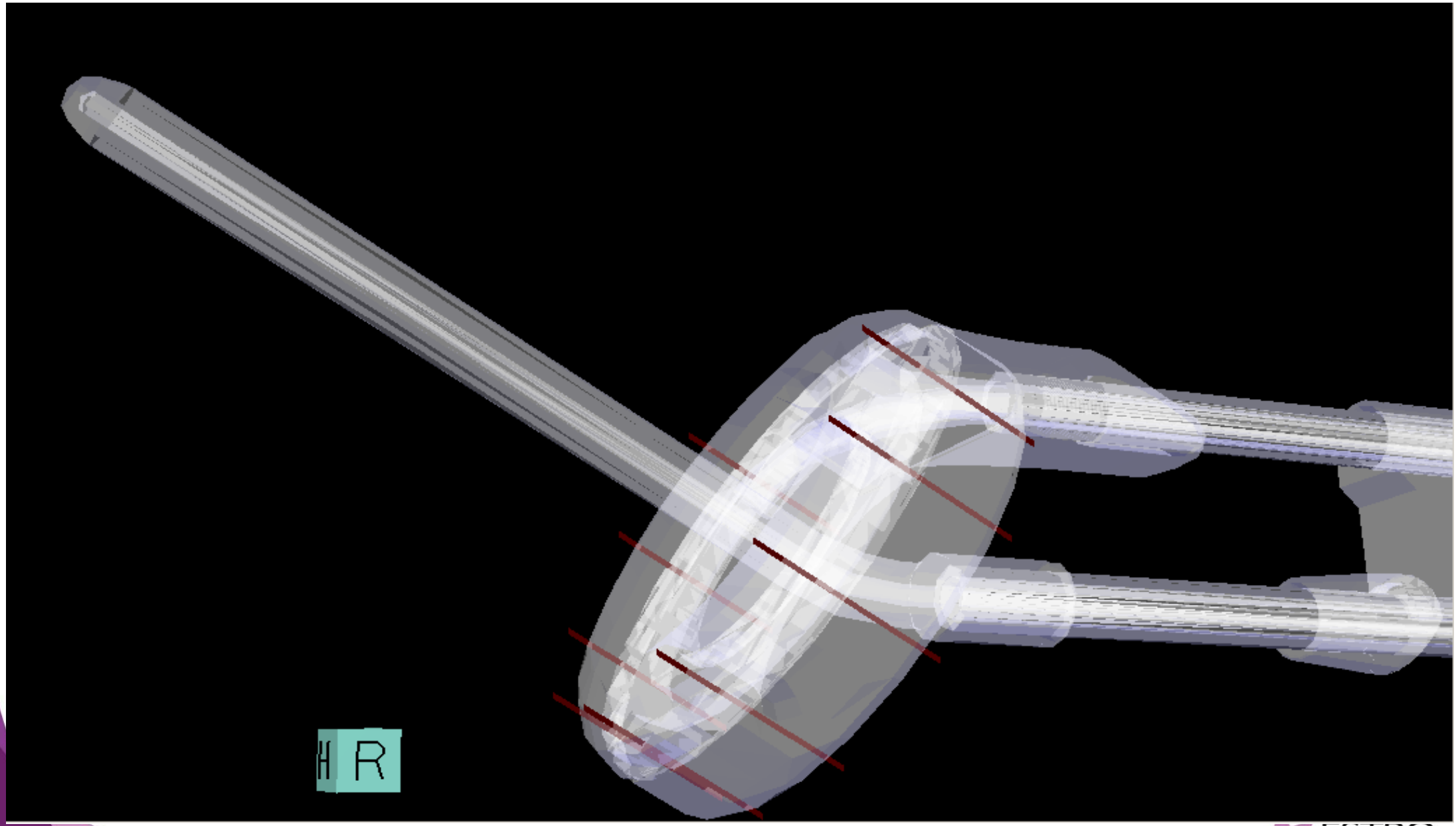

Source path

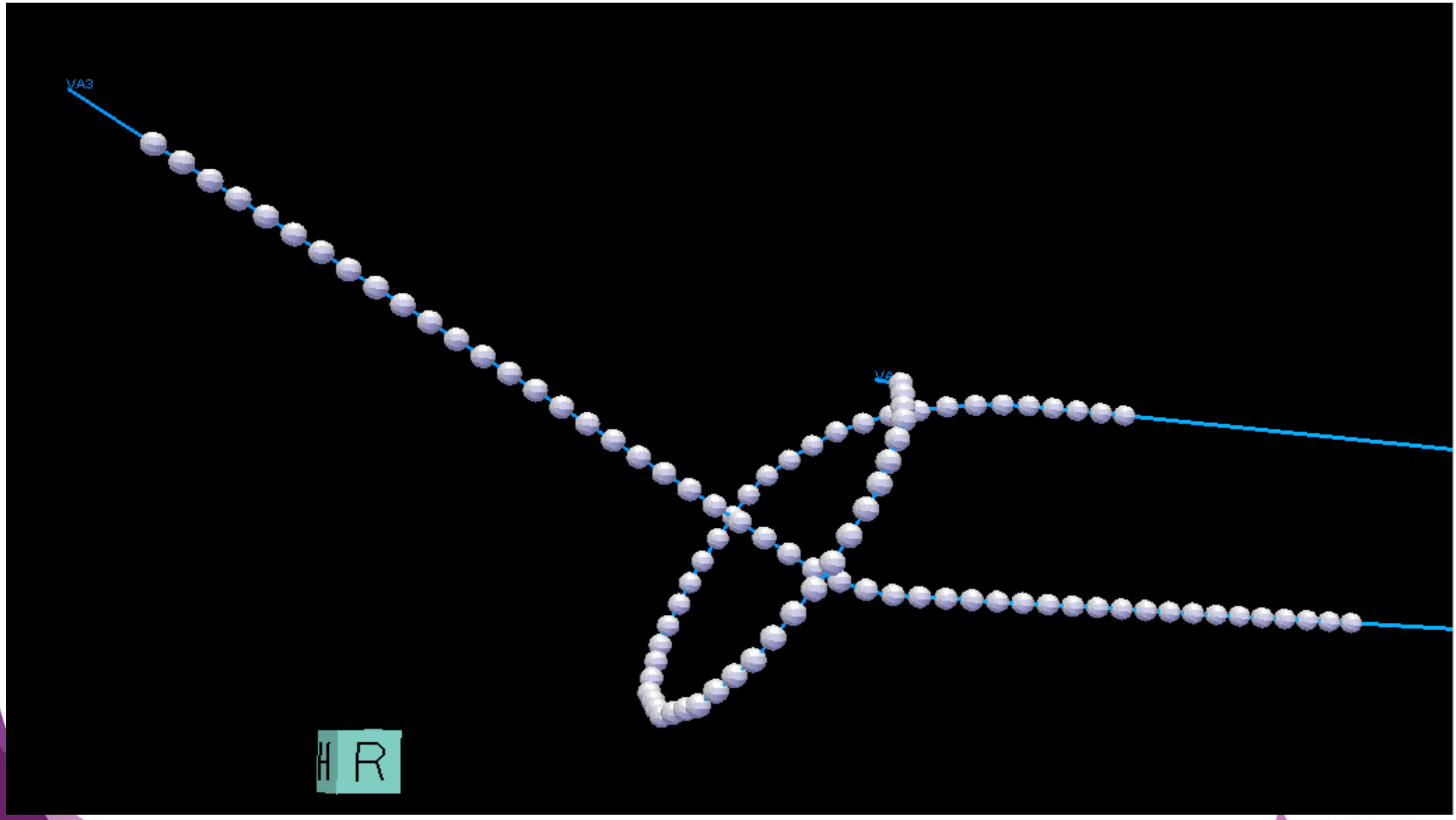

ESTRO School

Applicator + Source path

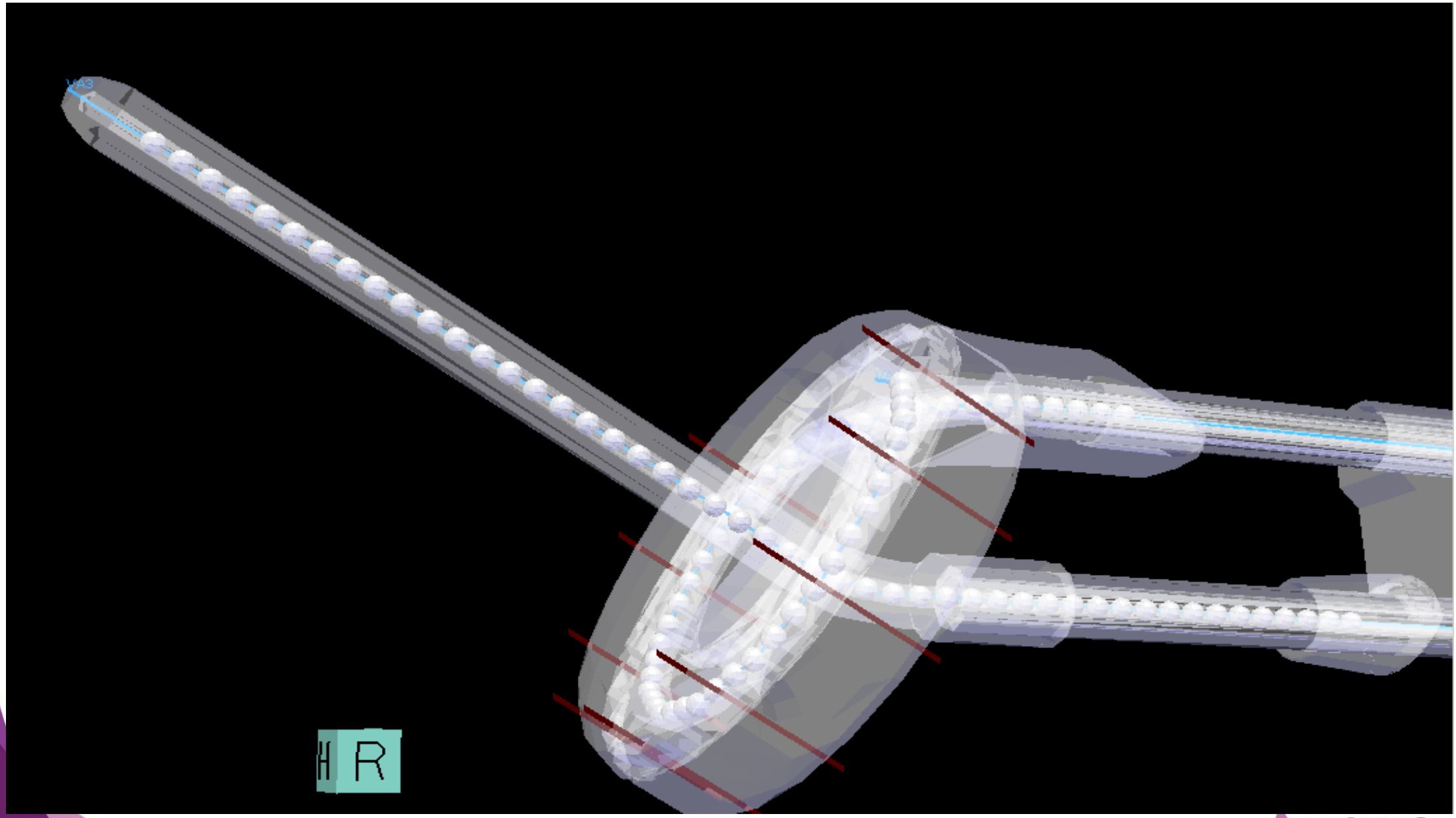

ESTRO School

Reconstruction

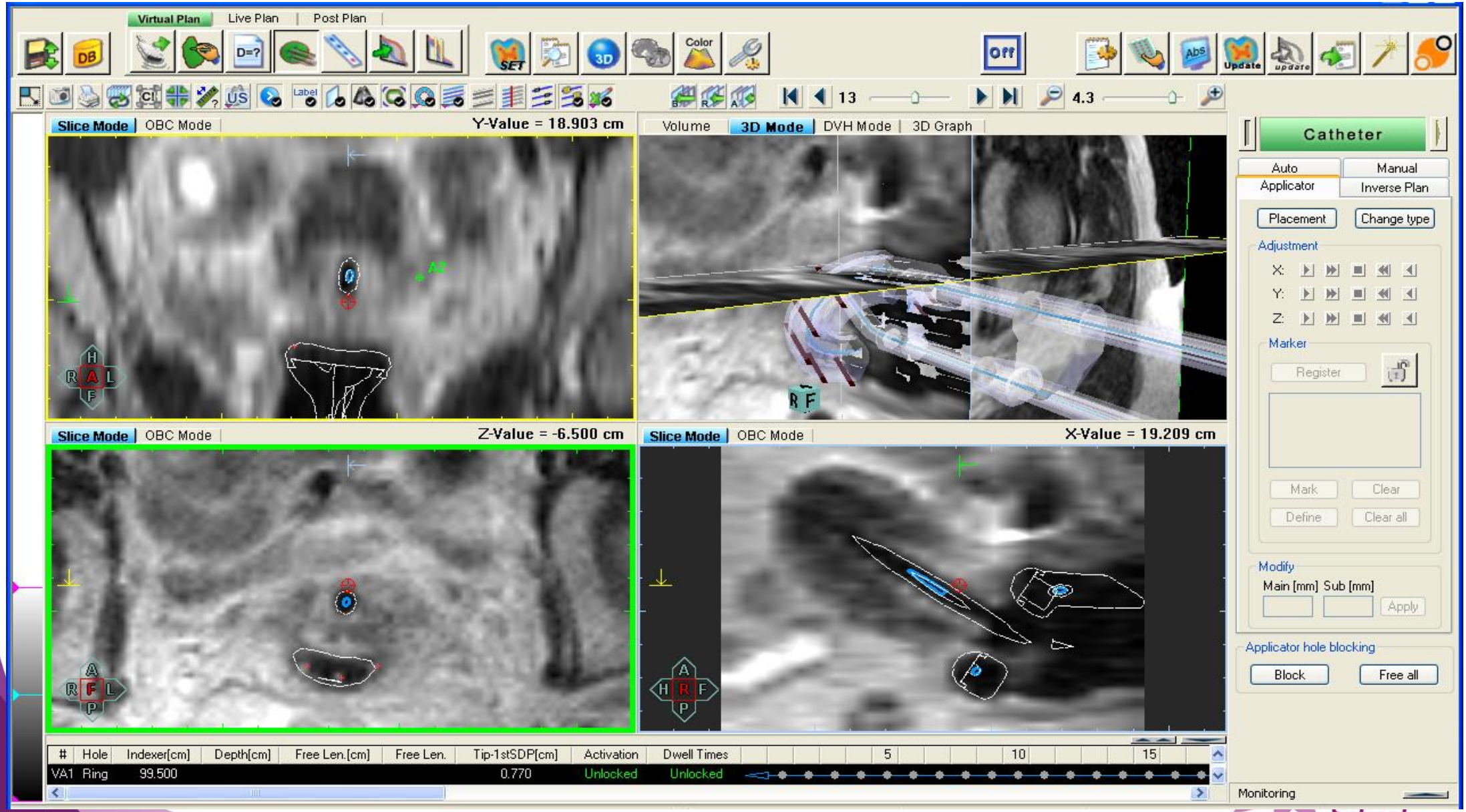

Reconstruction

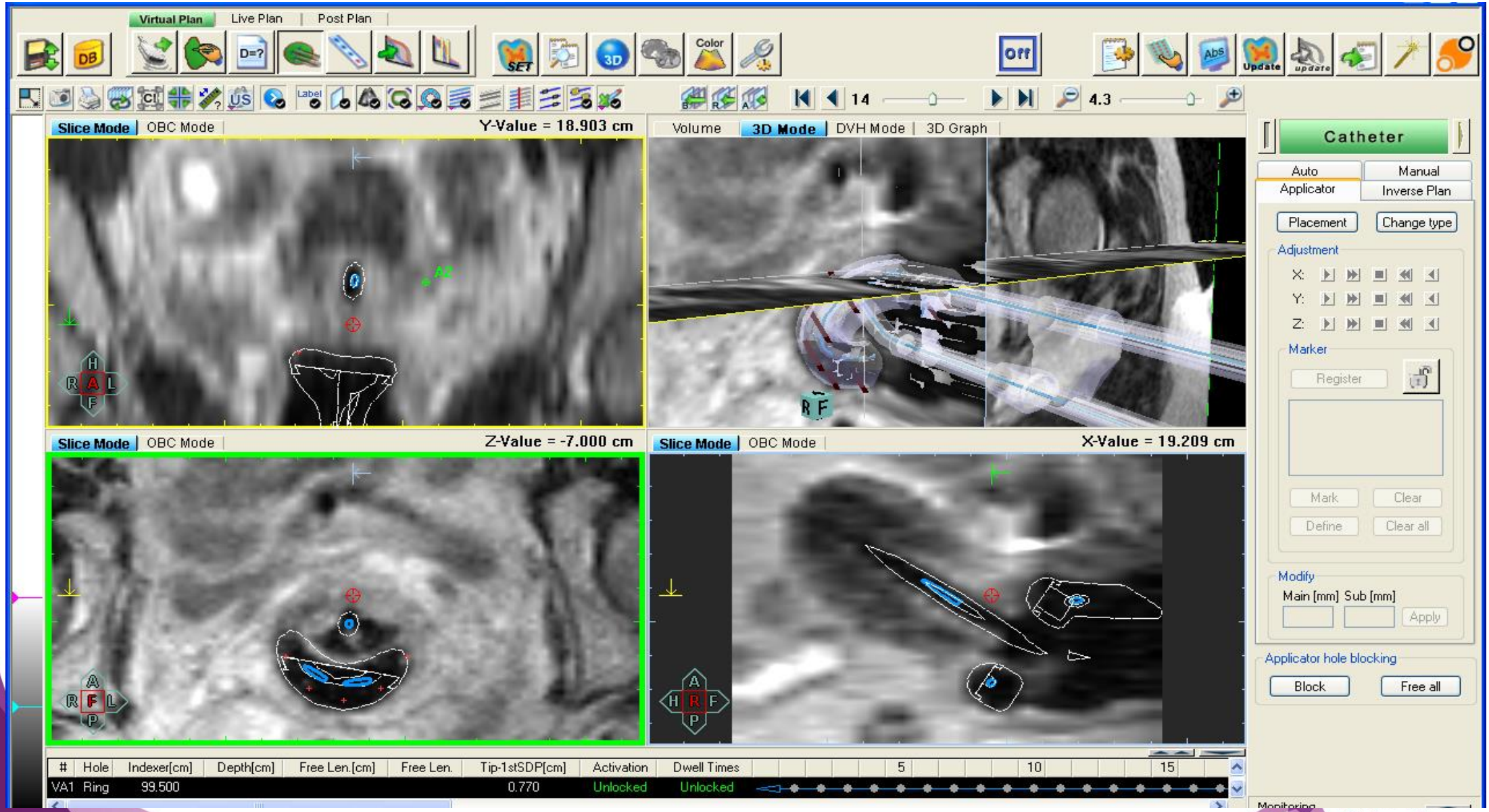

Reconstruction

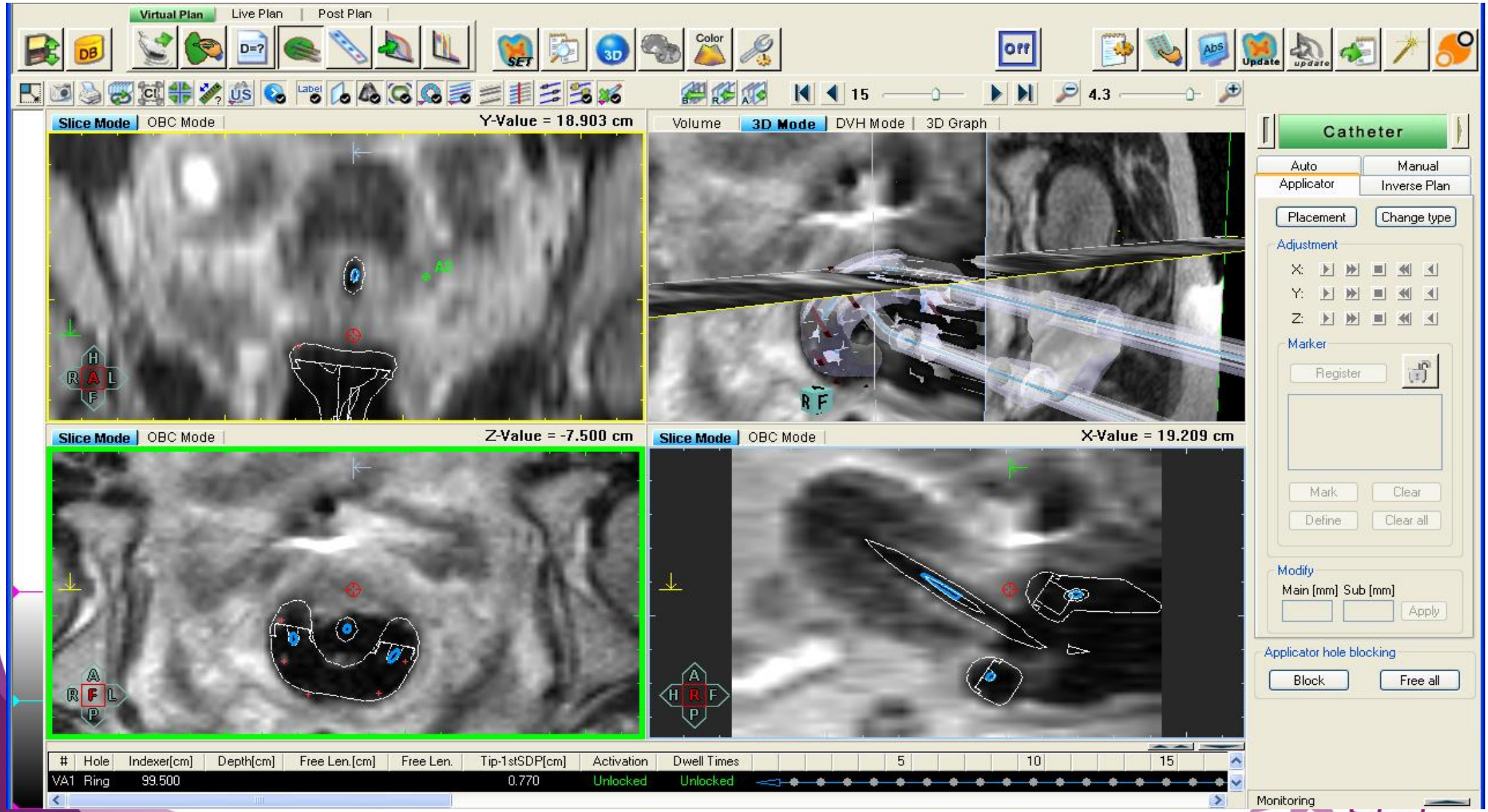

Reconstruction

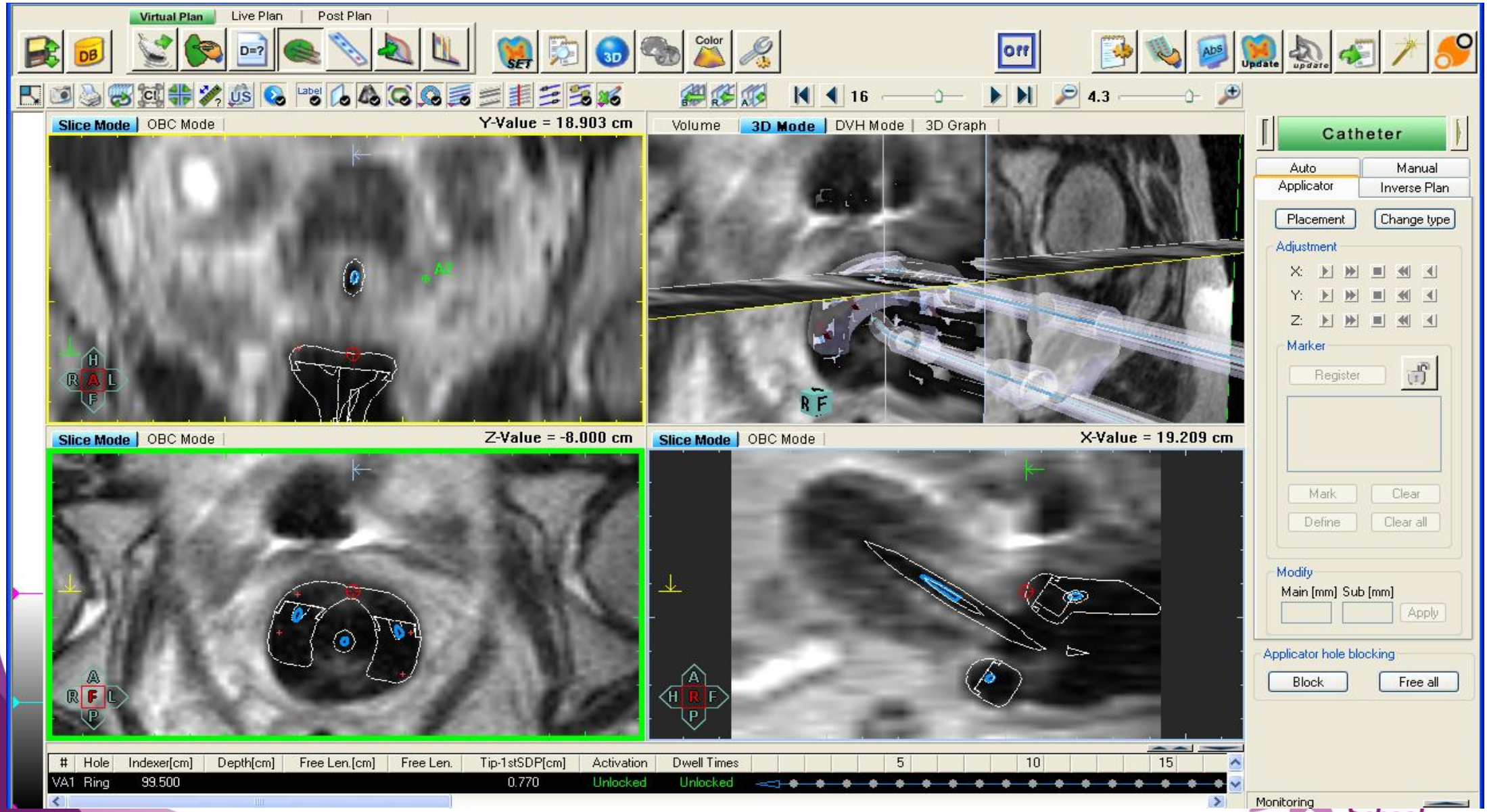

Reconstruction

Reconstruction

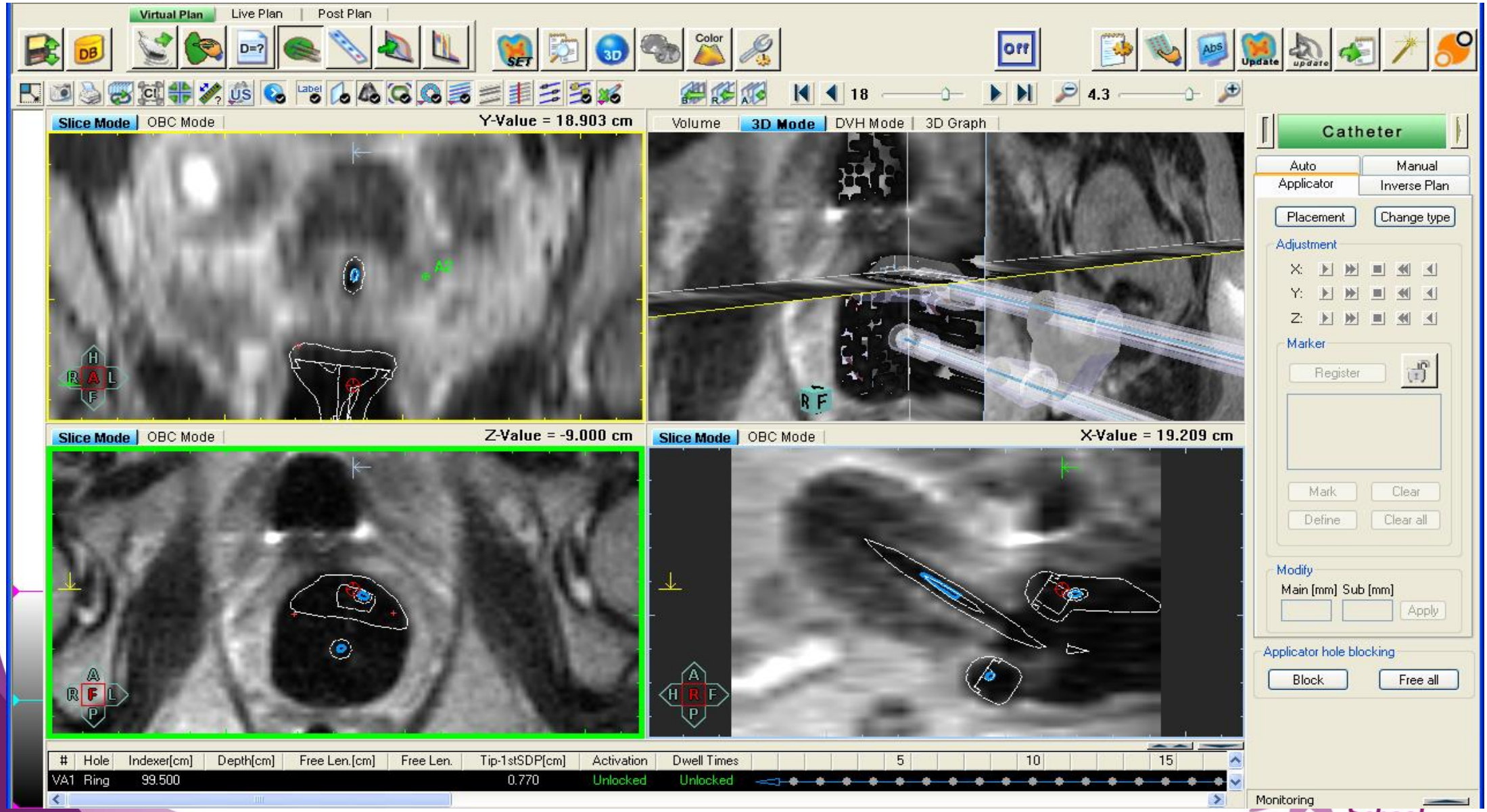

Reconstruction

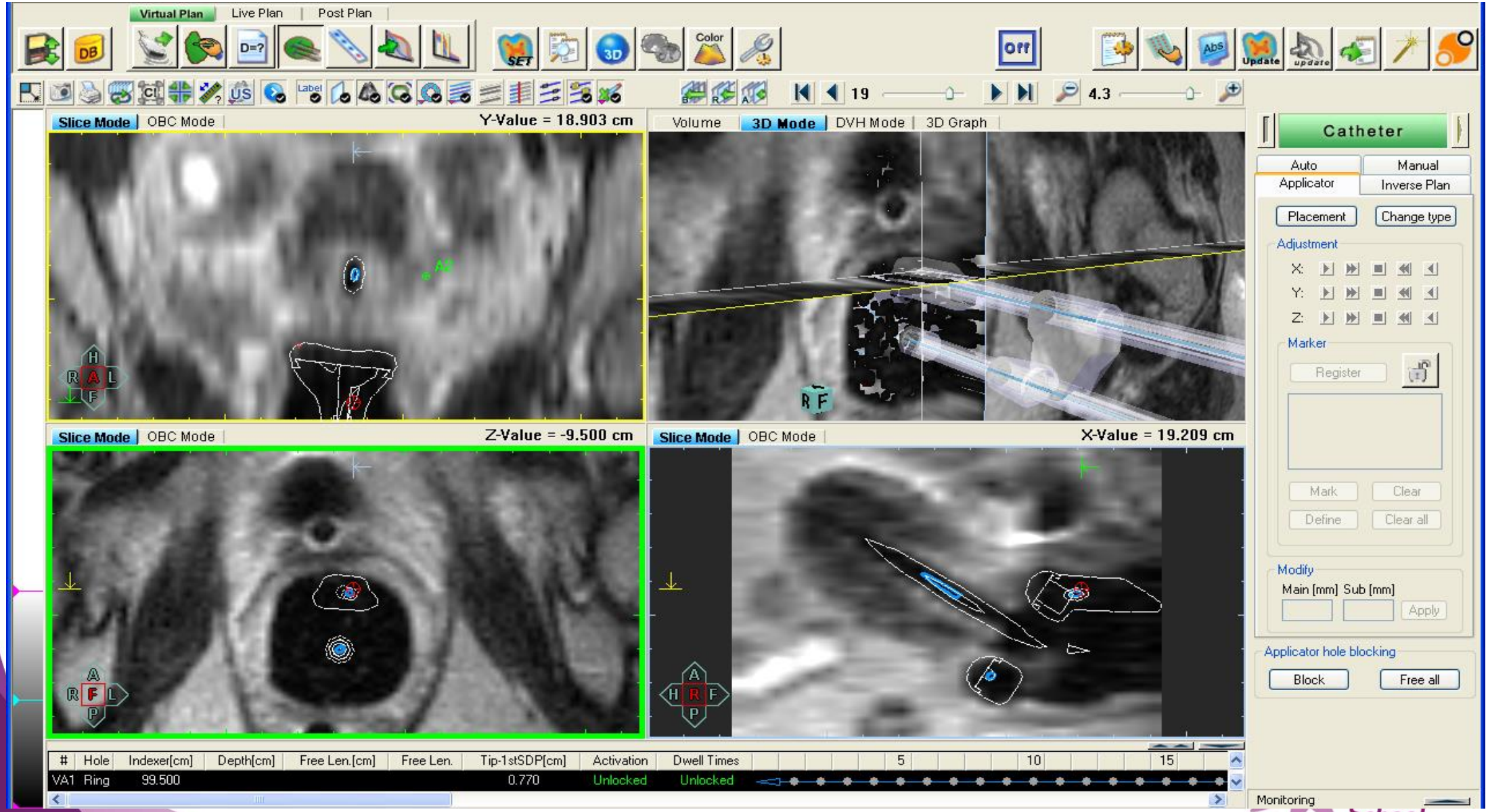

Reconstruction

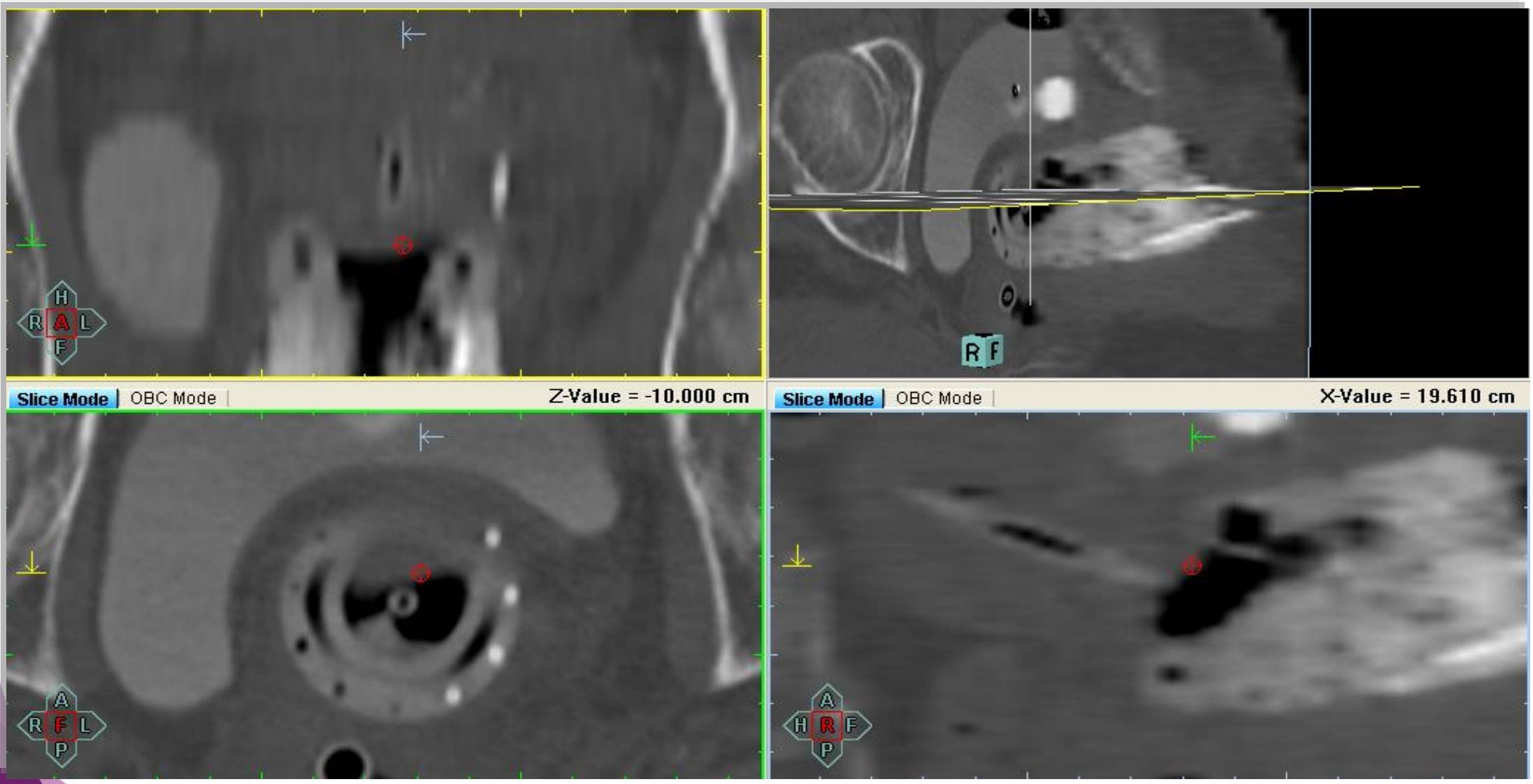

Reconstruction

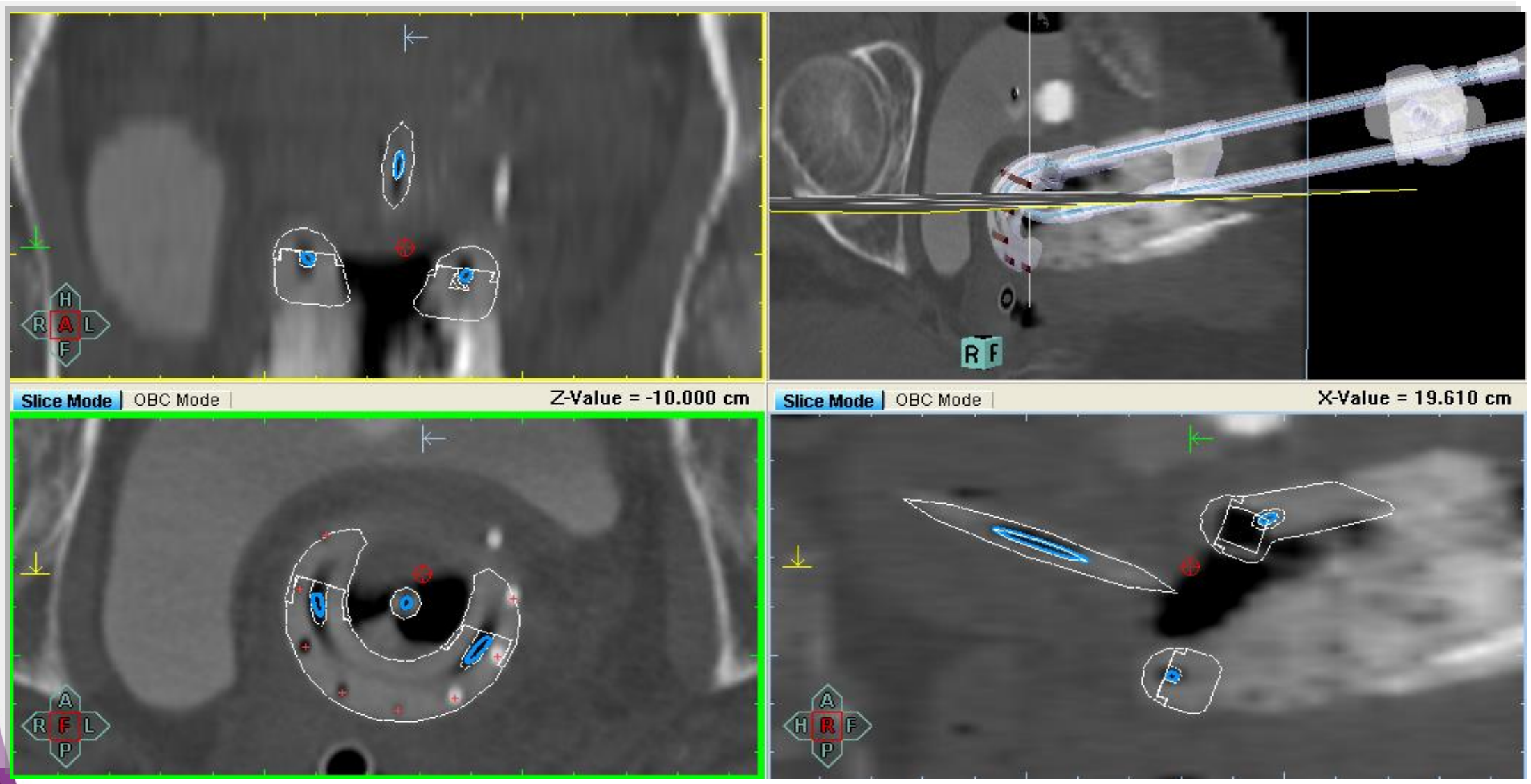

Better accuracy

less time to reconstruct

ESTRO School

Treatment Planning directly on MR

- Import vendor provided archived applicator into planning images
- Can use with 3D SPACE or T2 FSE

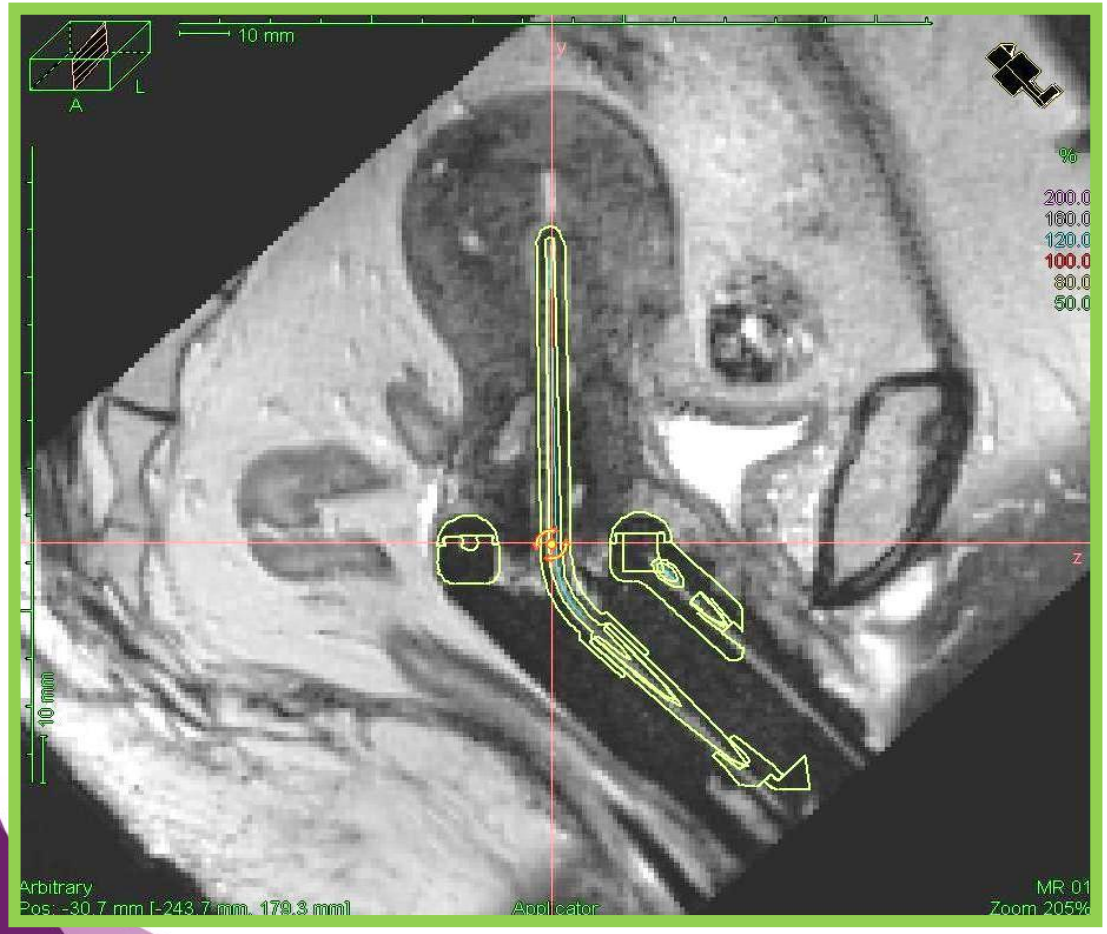

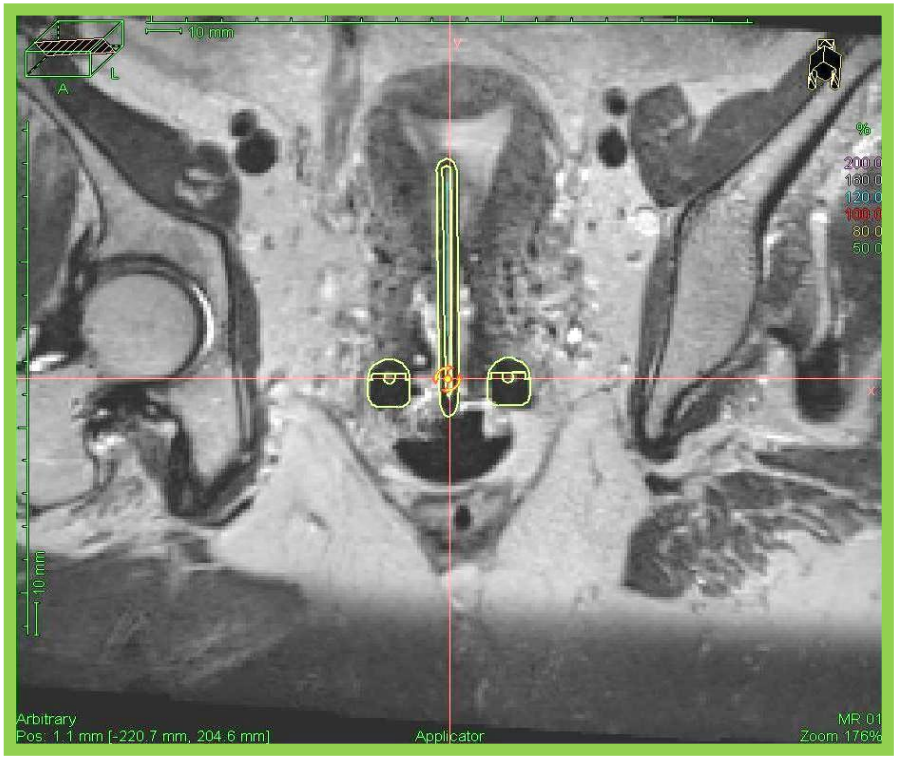

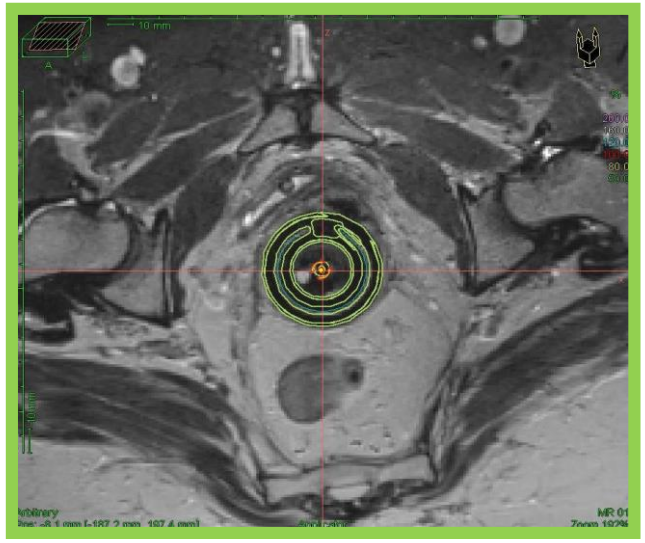

Courtesy
B. Erickson
MCW, USA

ESTRO School

Recommendations III
Applicator reconstruction

Radiotherapy and Oncology 96 (2010) 153–160

Contents lists available at ScienceDirect

Radiotherapy and Oncology

journal homepage: www.thegreenjournal.com

GEC-ESTRO Recommendations

Recommendations from Gynaecological (GYN) GEC-ESTRO Working Group: Considerations and pitfalls in commissioning and applicator reconstruction in 3D image-based treatment planning of cervix cancer brachytherapy

Taran Paulsen Hellebust [a,*], Christian Kirisits [b], Daniel Berger [b], José Pérez-Calatayud [c], Marisol De Brabandere [d], Astrid De Leeuw [e], Isabelle Dumas [f], Robert Hudej [g], Gerry Lowe [h], Rachel Wills [h], Kari Tanderup [i]

- Guidelines for reconstruction of the applicator in 3D image based treatment planning:
  - Applicator commissioning
  - Applicator reconstruction

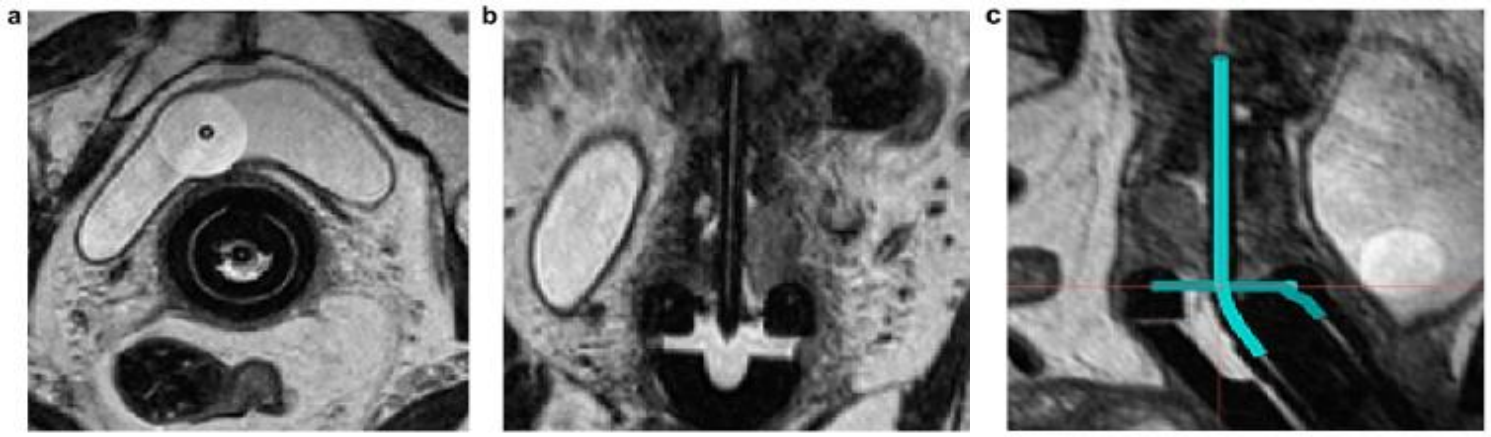

Hellebust et al. Radioth Oncol 2010

ESTRO School

Applicator Reconstruction: ESTRO Recommendations

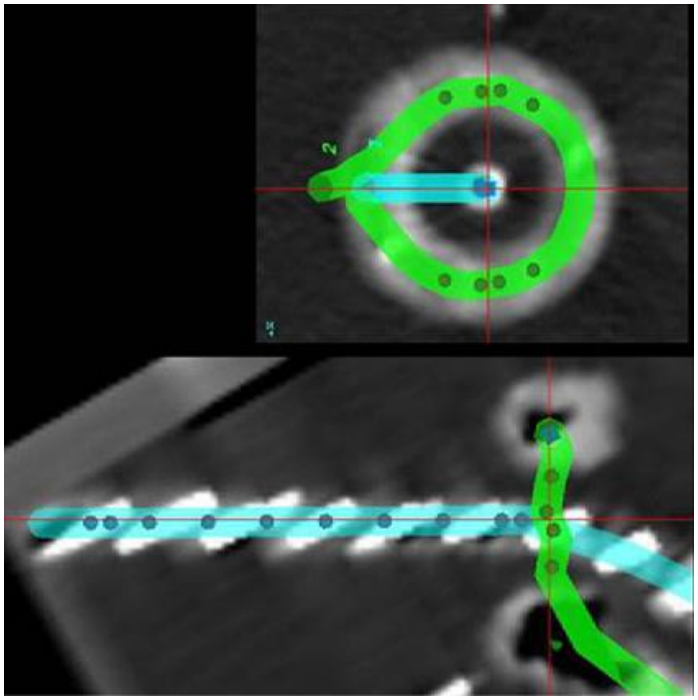

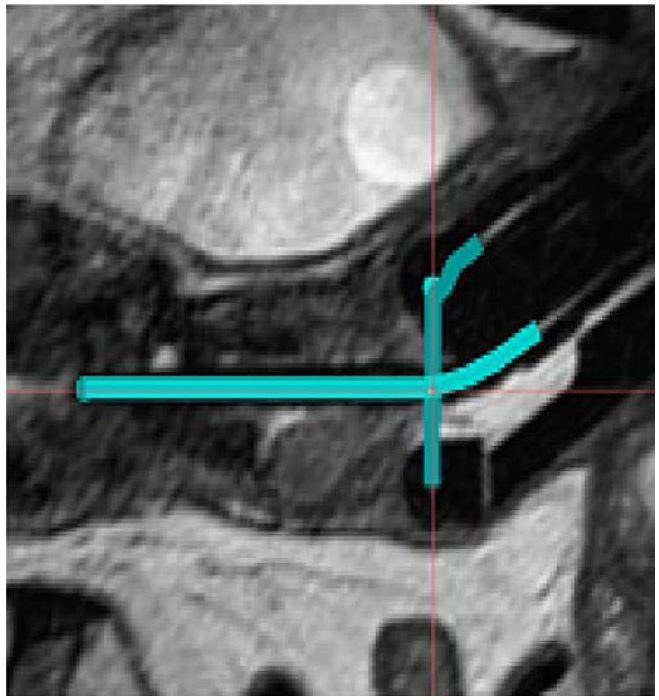

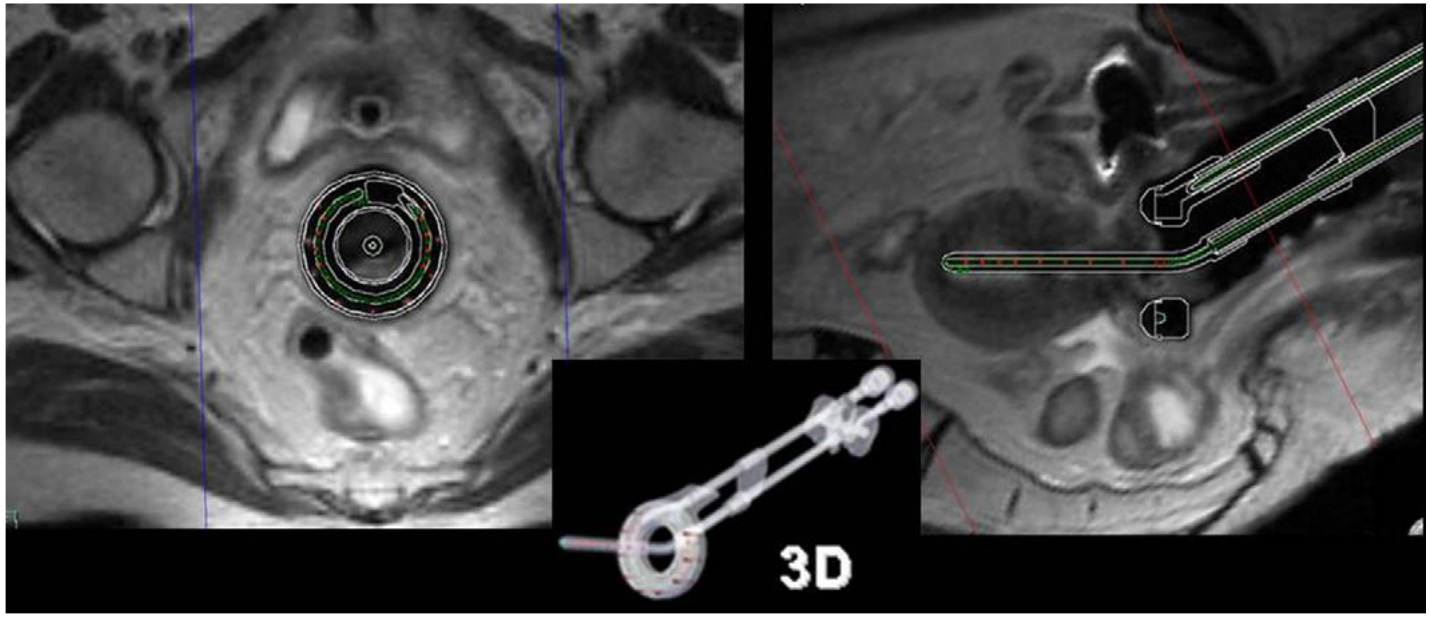

Hellebust, et al., *Radiother. Oncol.* 96, 153-160 (2010)

ESTRO School

Needles

US Needle Reconstruction Uncertainties: Phantom

Imaging of implant needles for real-time HDR-brachytherapy prostate treatment using biplane ultrasound transducers

Frank-André Siebert,[a] Markus Hirt, and Peter Niehoff
Clinic of Radiotherapy, University Hospital of Schleswig-Holstein, Campus Kiel, Kiel 24105, Germany

György Kovács
Interdisciplinary Brachytherapy Unit, University of Lüebeck, Lüebeck 23538, Germany

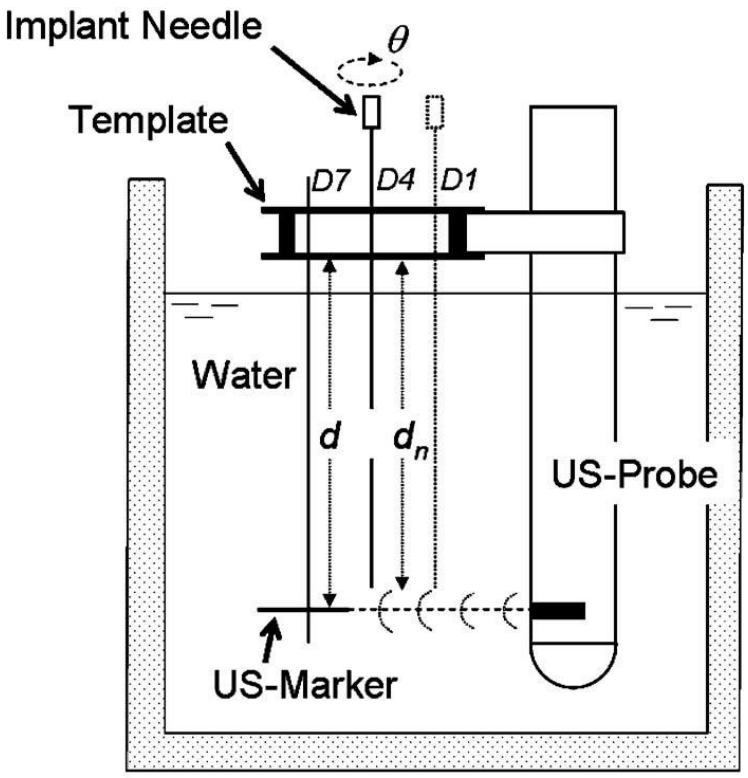

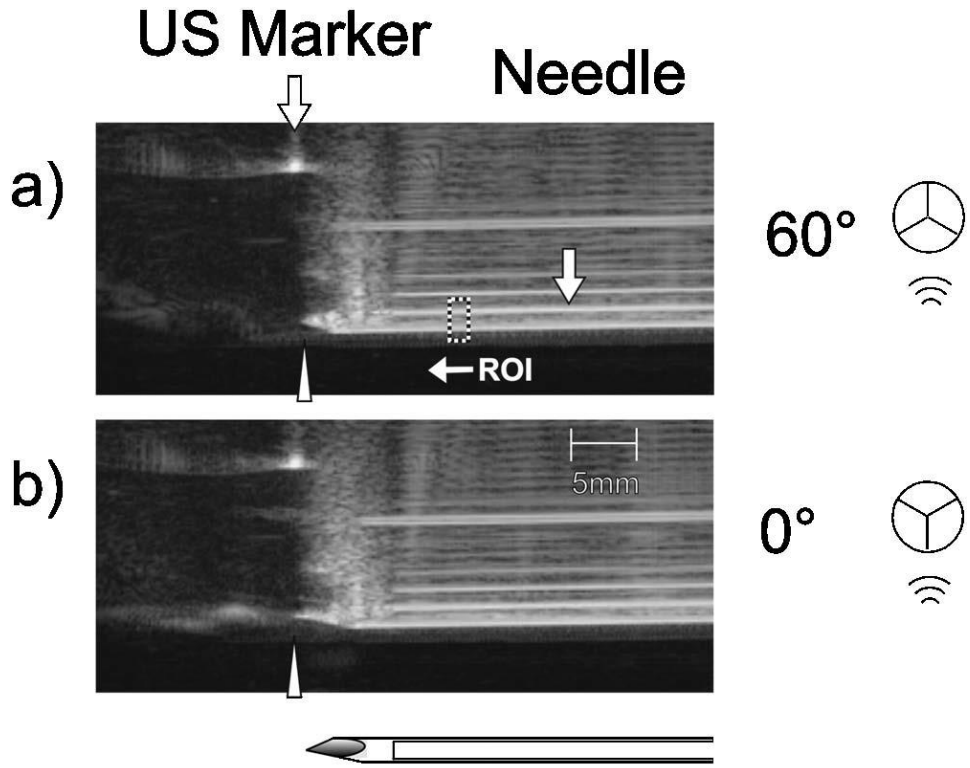

0.5 mm needle tip uncertainty,
better accuracy with lower gain

Siebert, et al., *Med. Phys*. 36, 3406-3412 (2009)

ESTRO School

US Needle Reconstruction Uncertainties: Patient

Validation study of ultrasound-based high-dose-rate prostate brachytherapy planning compared with CT-based planning

Deidre Batchelar, Miren Gaztañaga, Matt Schmid, Cynthia Araujo, François Bachand, Juanita Crook*

Cancer Center for the Southern Interior, British Columbia Cancer Agency, Kelowna, BC, Canada

PURPOSE: The use of transrectal ultrasound (TRUS) to both guide and plan high-dose-rate (HDR) brachytherapy (BT) for prostate is increasing. Studies using prostate phantoms have demonstrated the accuracy of ultrasound (US) needle tip reconstruction compared with CT imaging standard. We have assessed the *in vivo* accuracy of needle tip localization by TRUS using cone-beam CT (CBCT) as our reference standard.

METHODS AND MATERIALS: Needle positions from 37 implants have been analyzed. A median of 16 needles (range, 16–18) per implant were inserted, advanced to the prostate base, and their tips identified using live TRUS images and real-time planning BT software. Needle protrusion length from the template was recorded to allow for reverification before capturing images for planning. The needles remained locked in the template, which was fixed to the stepper, while a set of three-dimensional TRUS images was acquired for needle path reconstruction and HDR-BT treatment planning. Following treatment, CBCT images were acquired for subsequent needle reconstruction using a BT Treatment Planning System. The coordinates of each needle tip were recorded from the Treatment Planning System for CT and US and compared.

RESULTS: A total of 574 needle tip positions have been compared between TRUS and CBCT. Of these, 59% agreed within 1 mm, 27% within 1–2 mm, and 11% agreed within 2–3 mm. The discrepancy between tip positions in the two modalities was greater than 3 mm for only 20 needles (3%).

CONCLUSIONS: The US needle tip identification *in vivo* is at least as accurate as CT identification, while providing all the advantages of a one-step procedure.

Batchelar, et al., *Brachytherapy* 13, 75-79 (2014)

ESTRO School

US Needle Reconstruction Uncertainties: Patient

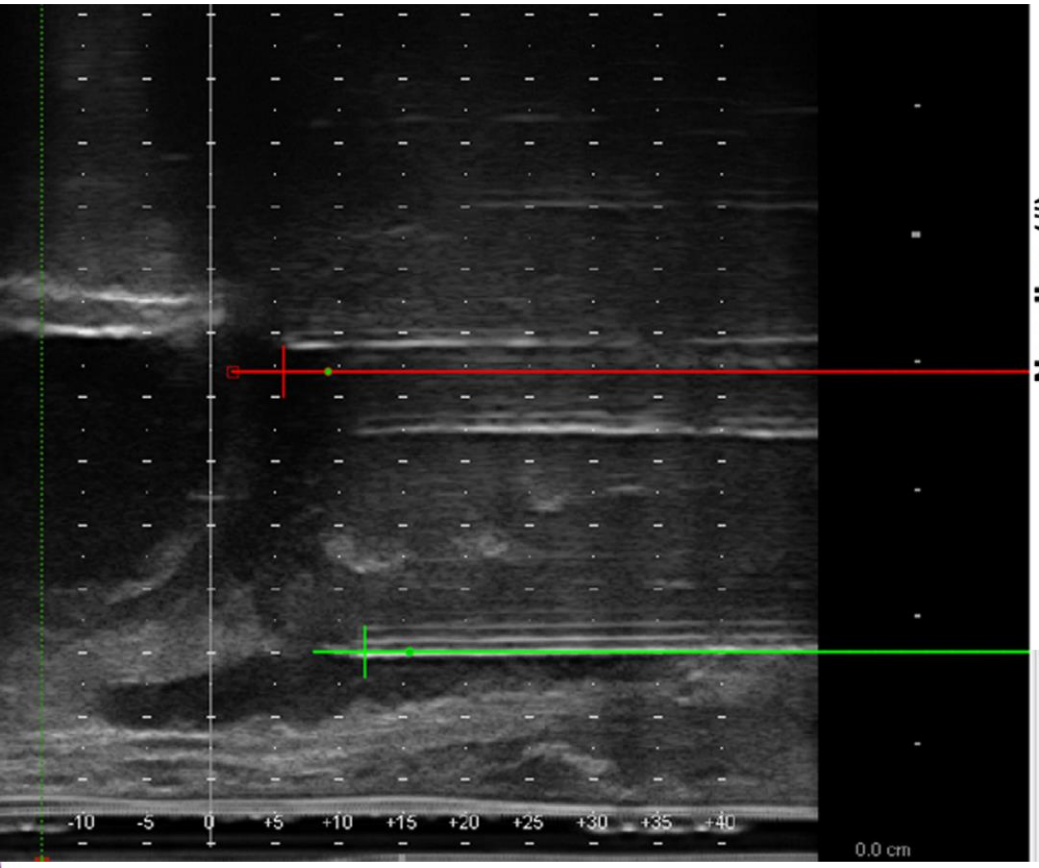

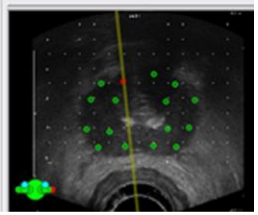

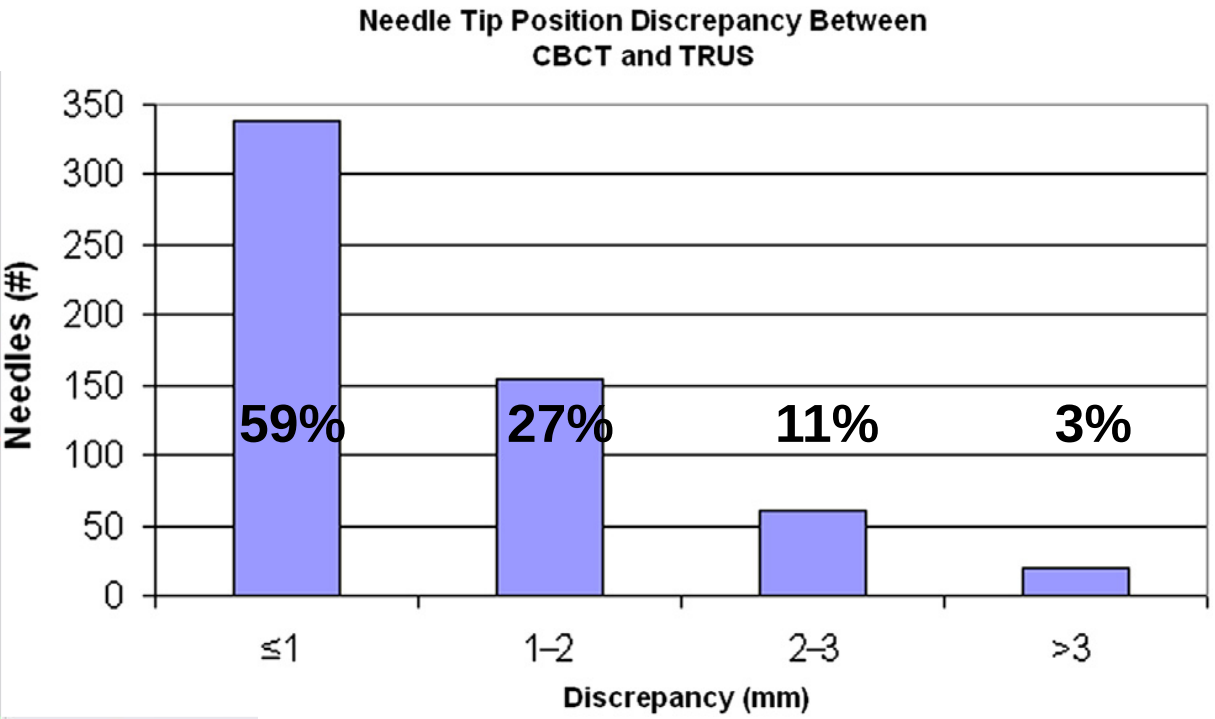

1-3 mm needle tip uncertainty,
comparable accuracy to CT for prostate BT

Batchelar, et al., *Brachytherapy* 13, 75-79 (2014)

ESTRO School

MRI/CT reconstruction accuracy

CT scan 2mm slices 0°	CT scan 2mm slices 45°	CT scan 2mm slices 90°

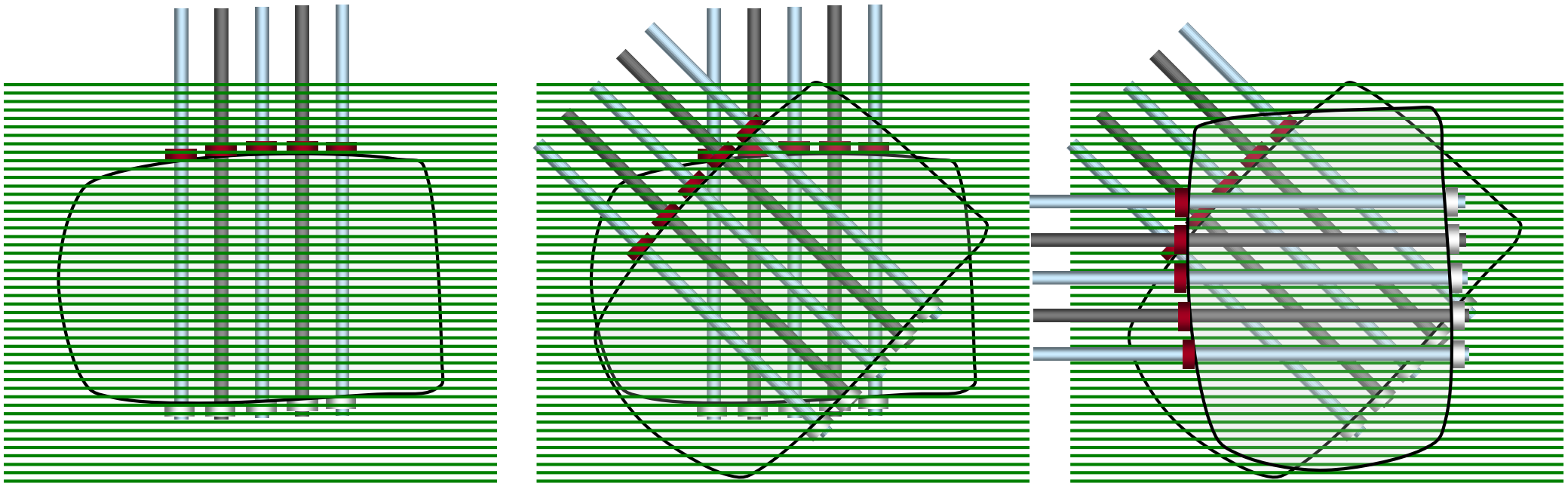

Reconstructed catheter length at the tissue phantom

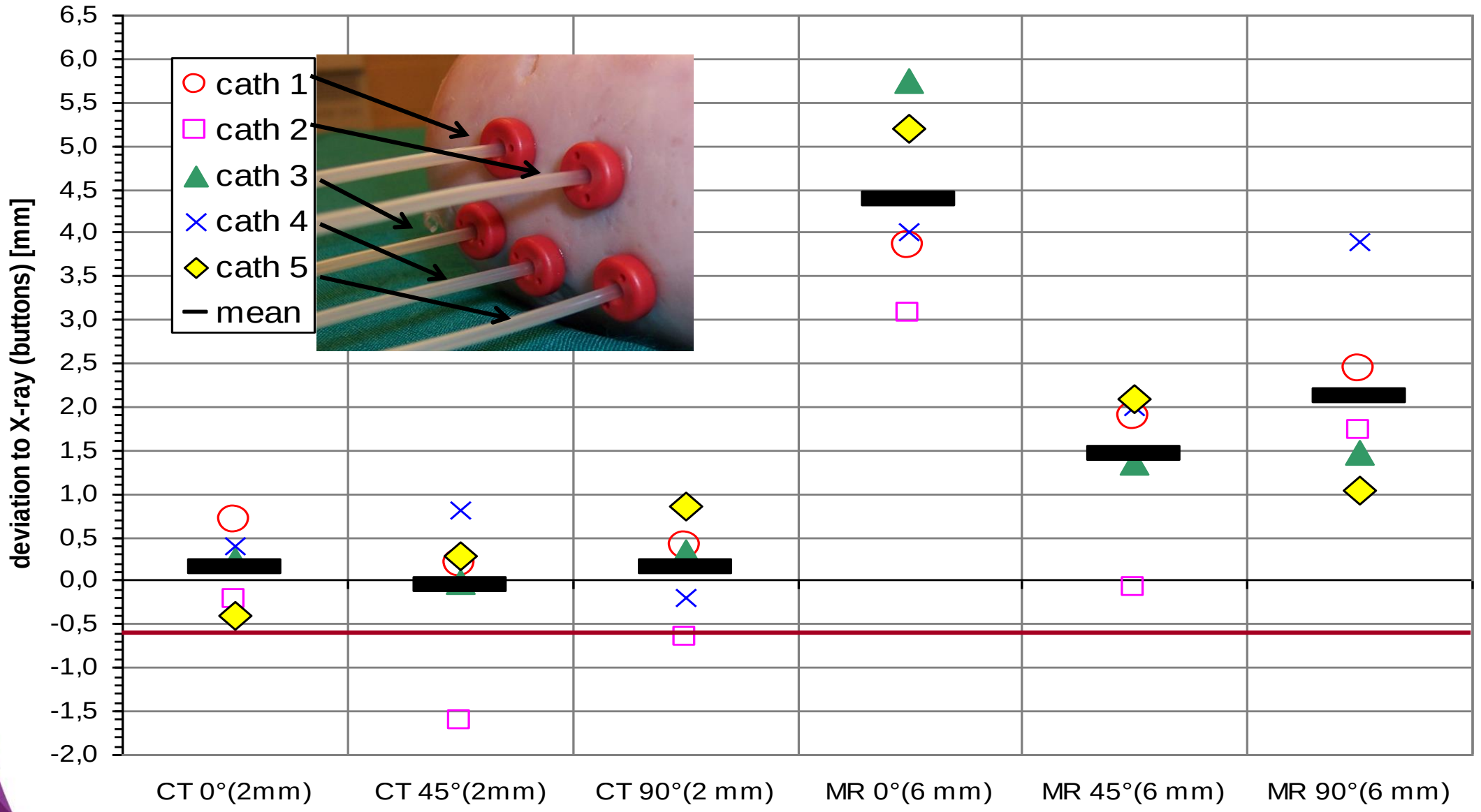

Direct reconstruction by using CT or MR images

the first dwell position problem !

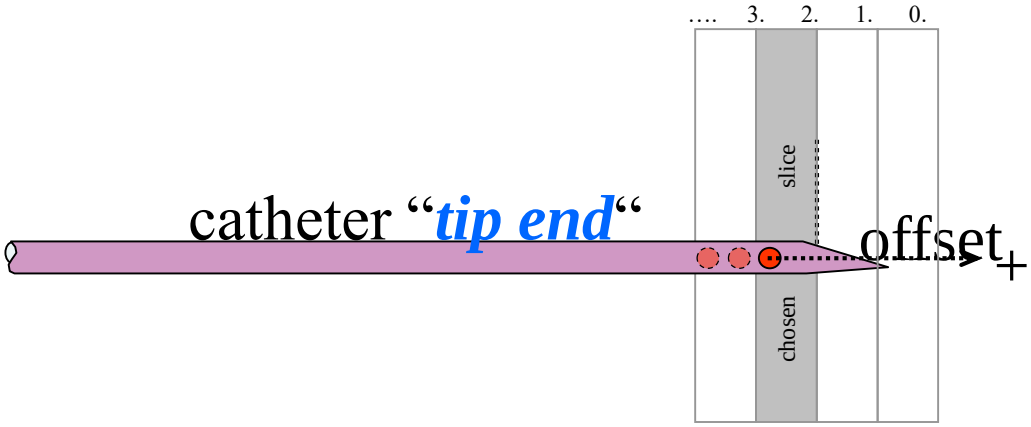

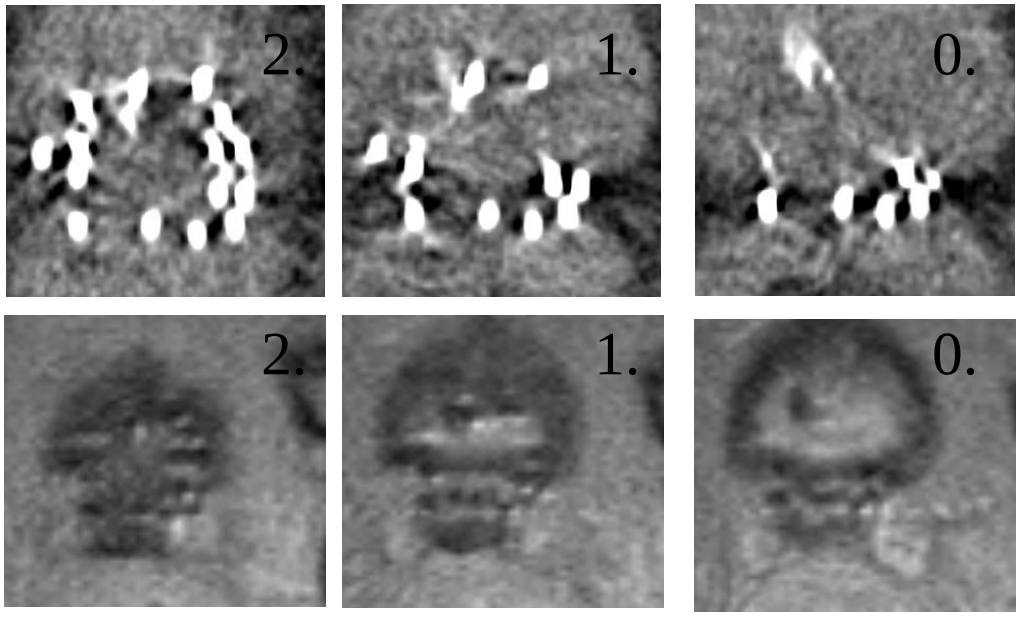

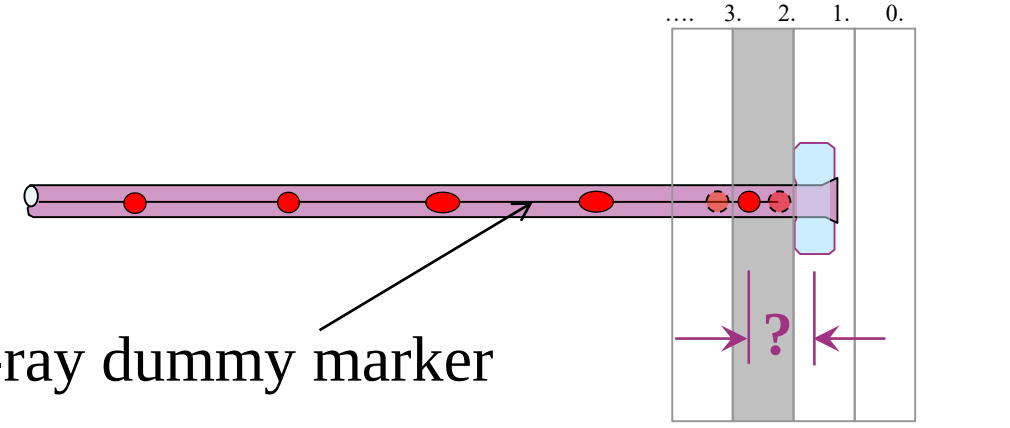

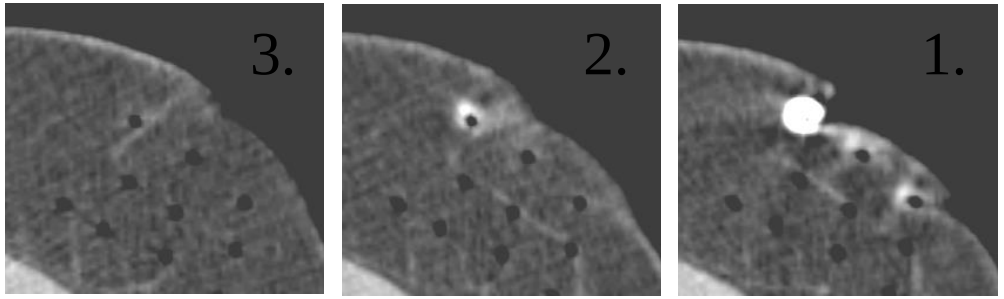

ESTRO School

Interstitial Applicator

Know the tool you are using!

Material

Plastic — flexible

Titanium — rigid

Steel — rigid

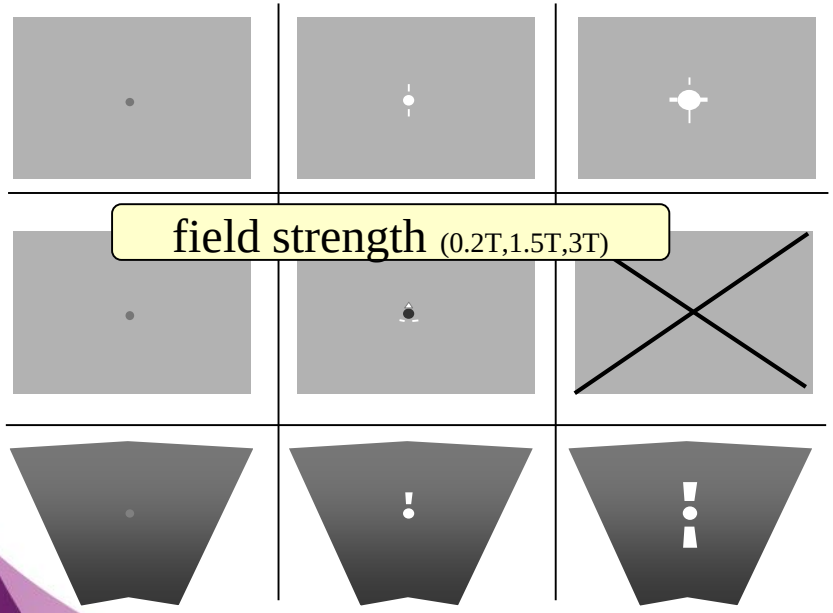

Different materials scanned in 0.2 T open MRI

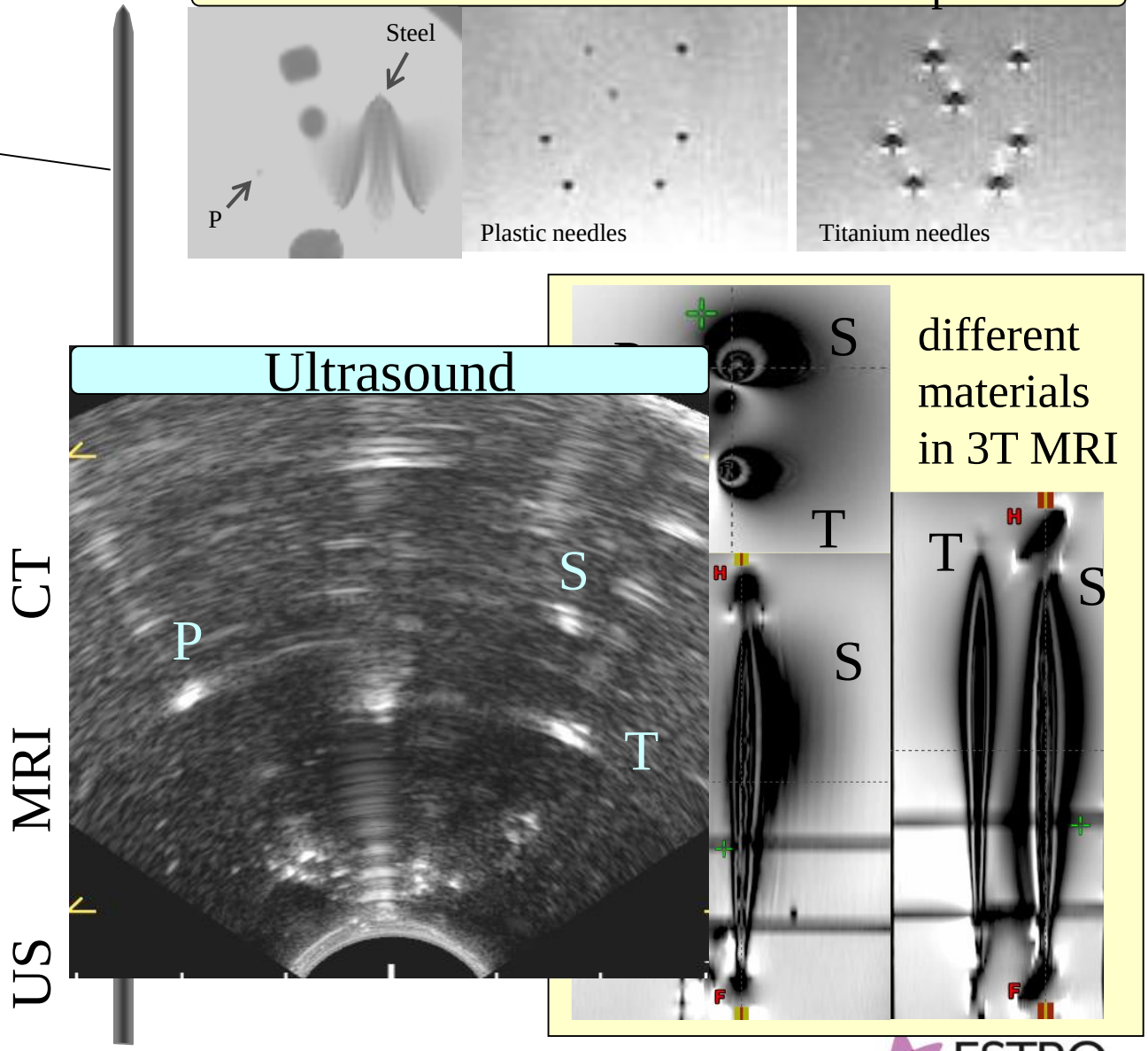

ESTRO School

Test Assumptions: Reconstruction Commissioning

- rigid applicator:

  required approach for source localization using applicator library

  consider flexible catheters (HDR prostate and breast) sim-to-treatment

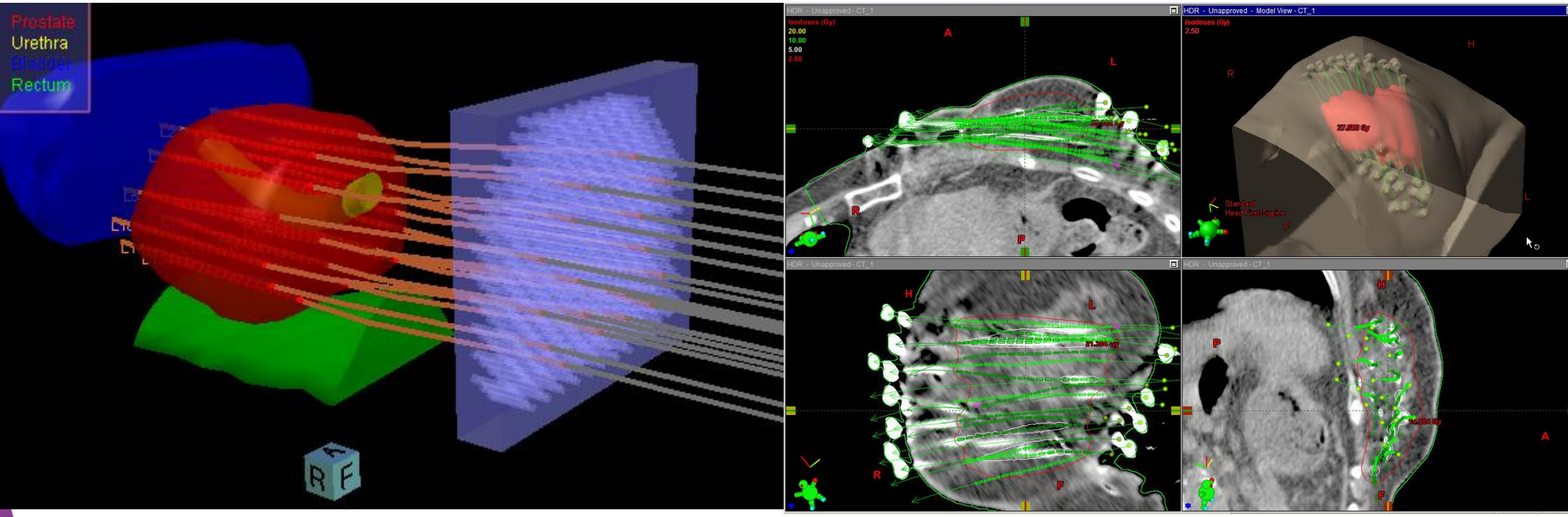

Be aware that aso „rigid“ needles can bend during insertion!

ESTRO School

Stability of DVH

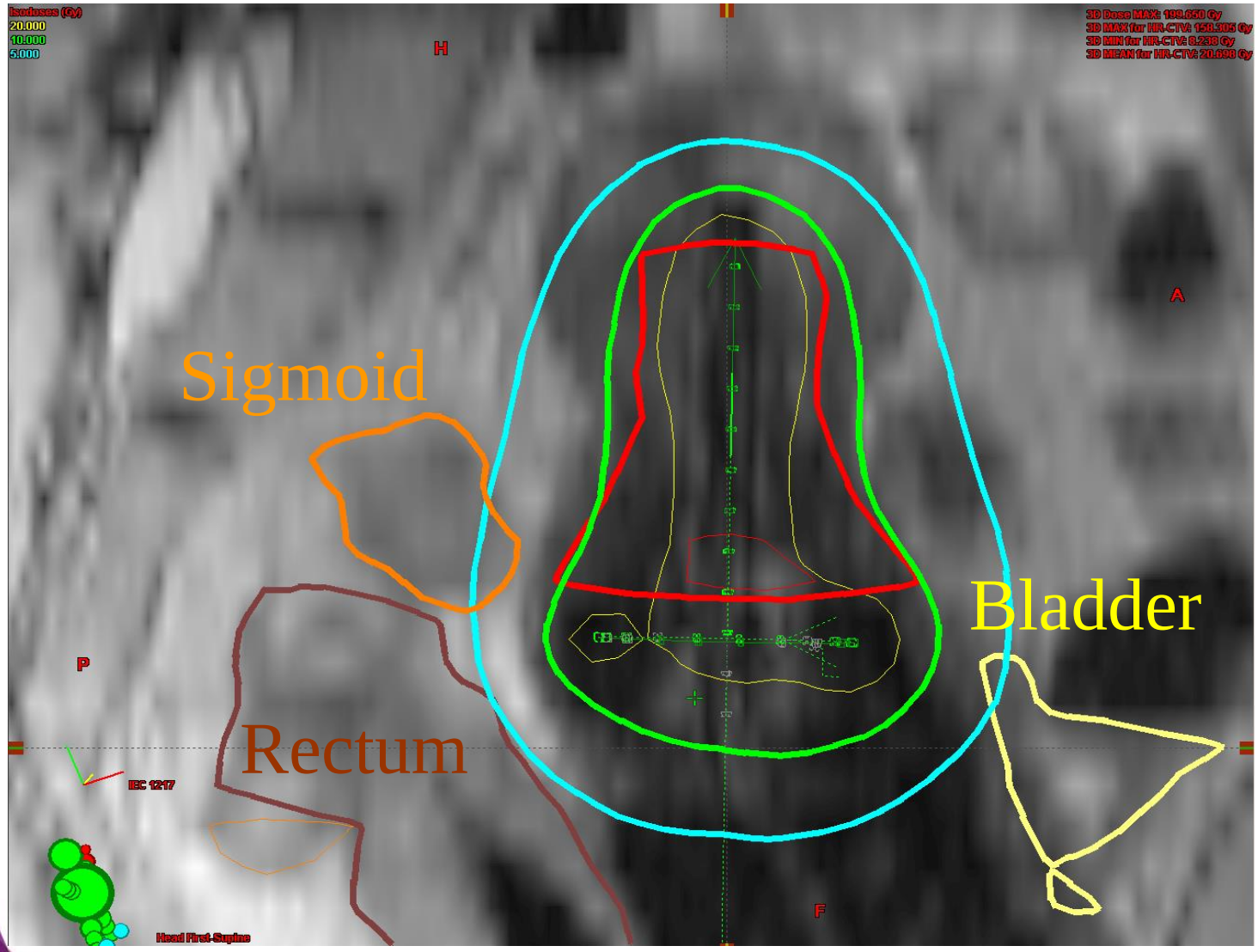

Uncertainty of cranio-caudal applicator positioning

Mean DVH shifts (%)

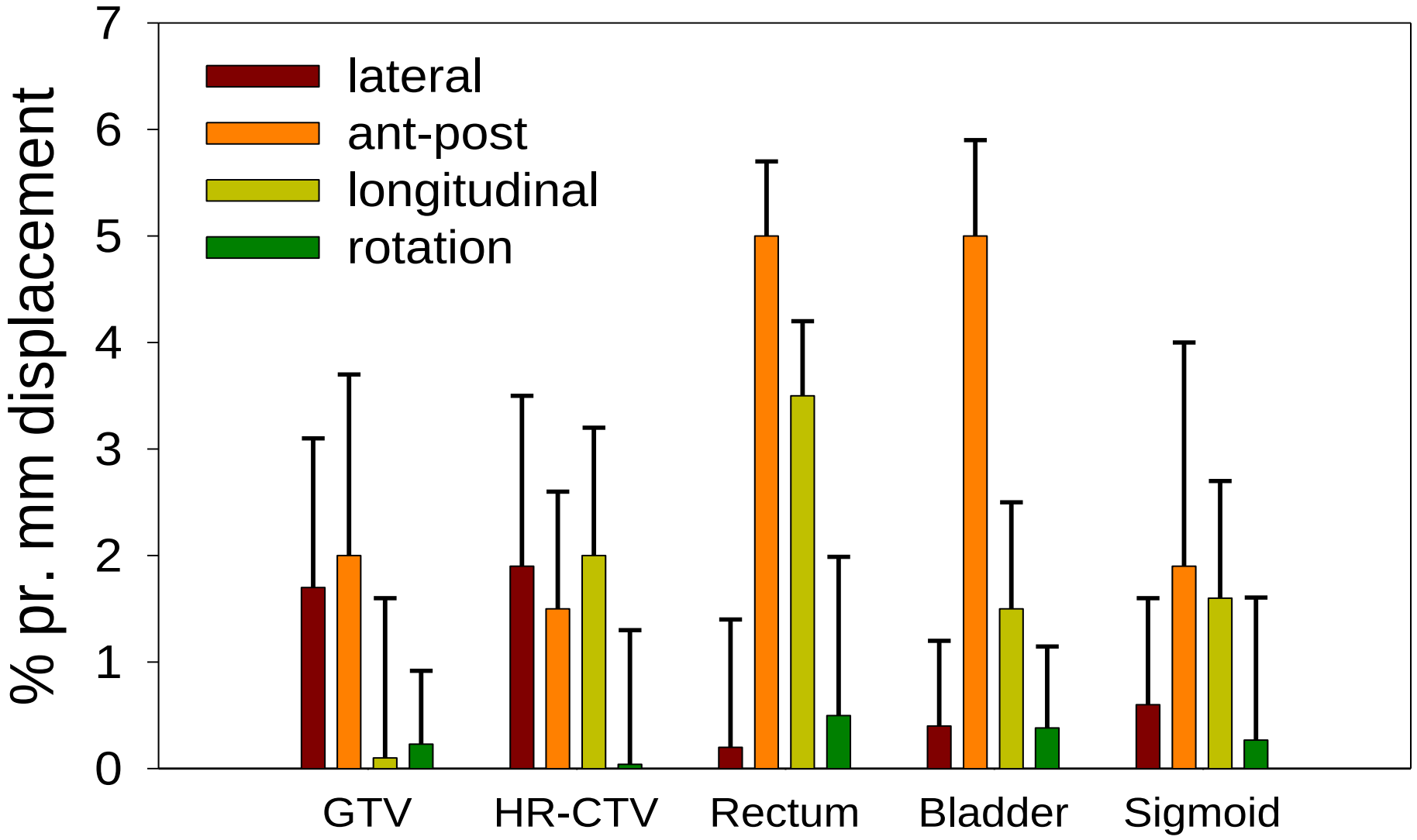

Tanderup et al. R&O 2008

Dosimetric influence of reconstruction errors for T&O plans

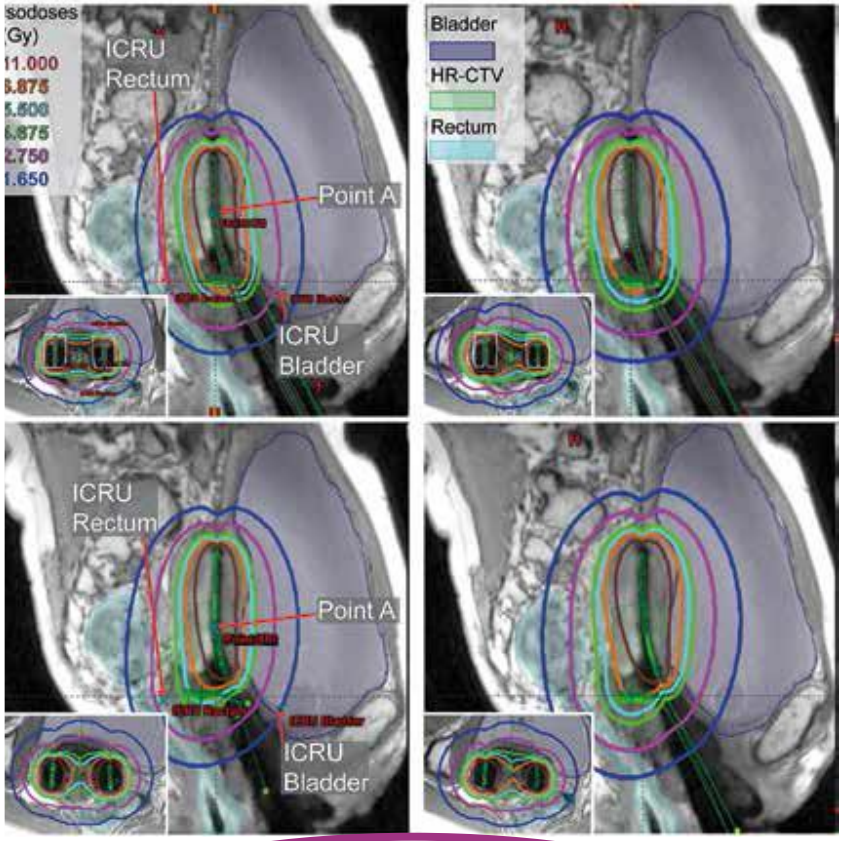

1.5 mm cran/caud reconstruction error changed dose metrics by up to ~5% (rectum)

Table 1. The simulated dosimetric impacts of T&O displacements for MRIG-CBT (20 plans) by virtually shifting whole T&O in a treatment planning system

	Simulated dosimetric impacts [%] of T&O displacements for MRIG-CBT plans													
	Caudal T&O shift							Cranial T&O shift						
	−20 mm	−10 mm	−7.5 mm	−6 mm	−5 mm	−3 mm	−1.5 mm	1.5 mm	3 mm	5 mm	6 mm	7.5 mm	10 mm	20 mm
HR-CTV D_{90} [%]	23 ± 11	9 ± 5	7 ± 4	9 ± 3	5 ± 3	3 ± 2	2 ± 1	1 ± 1	3 ± 2	5 ± 4	7 ± 5	8 ± 6	11 ± 8	21 ± 16
HR-CTV D_{100} [%]	20 ± 9	6 ± 9	7 ± 5	6 ± 4	5 ± 4	3 ± 3	2 ± 2	2 ± 1	4 ± 2	6 ± 3	7 ± 4	9 ± 5	11 ± 7	24 ± 11
Rectum D_{2cc} [%]	136 ± 46	50 ± 13	35 ± 8	27 ± 6	22 ± 5	12 ± 3	6 ± 1	6 ± 1	10 ± 2	16 ± 4	19 ± 4	23 ± 5	29 ± 6	47 ± 10
Badder D_{2cc} [%]	29 ± 10	14 ± 7	11 ± 5	8 ± 5	7 ± 4	4 ± 3	2 ± 1	2 ± 2	5 ± 3	8 ± 6	10 ± 7	13 ± 9	19 ± 13	50 ± 42
Sigmoid D_{2cc} [%]	24 ± 12	12 ± 6	8 ± 5	7 ± 4	5 ± 3	3 ± 2	2 ± 1	1 ± 1	3 ± 2	5 ± 3	5 ± 3	6 ± 4	9 ± 7	13 ± 9
Point A left [%]	28 ± 14	12 ± 8	9 ± 6	7 ± 4	6 ± 4	4 ± 2	2 ± 1	2 ± 1	3 ± 2	5 ± 4	7 ± 4	8 ± 5	11 ± 8	41 ± 31
Point A right [%]	28 ± 17	13 ± 9	10 ± 7	8 ± 5	7 ± 4.5	4 ± 3	2 ± 2	2 ± 2	4 ± 3	8 ± 5	9 ± 7	12 ± 9	17 ± 13	65 ± 53
ICRU rectum [%]	60 ± 53	31 ± 23	23 ± 16	18 ± 12	15 ± 10	9 ± 6	4 ± 3	4 ± 2	8 ± 4	14 ± 6	16 ± 7	20 ± 8	26 ± 9	46 ± 11
ICRU bladder [%]	27 ± 14	14 ± 9	11 ± 6	9 ± 5	7 ± 4	5 ± 3	2 ± 1	3 ± 1	5 ± 3	9 ± 5	10 ± 6	13 ± 8	18 ± 11	35 ± 26

	< 5%	≥ 5%	≥ 10%	≥ 15

Table 4. The simulated dosimetric impacts of T&O reconstruction-uncertainties for conventional planning (20 plans)

	Simulated dosimetric impact [%] of T&O reconstruction-uncertainties for conventional point A plans											
	Caudal tandem shift & Anterior ovoid shift						Cranial tandem shift & Posterior ovoid shift					
	−10 mm	−7.5 mm	−6 mm	−4.5 mm	−3 mm	−1.5 mm	1.5 mm	3 mm	4.5 mm	6 mm	7.5 mm	10 mm
HR-CTV D_{90} [%]	5 ± 5	4 ± 3	4 ± 3	2 ± 2	2 ± 1	2 ± 2	2 ± 2	4 ± 4	5 ± 5	5 ± 5	6 ± 5	7 ± 5
HR-CTV D_{100} [%]	8 ± 9	6 ± 5	5 ± 5	3 ± 2	3 ± 2	4 ± 3	3 ± 3	5 ± 5	6 ± 5	8 ± 6	9 ± 7	10 ± 7
Rectum D_{2cc} [%]	19 ± 10	14 ± 8	13 ± 8	11 ± 6	9 ± 6	5 ± 4	7 ± 4	15 ± 8	23 ± 11	33 ± 15	43 ± 22	65 ± 32
Badder D_{2cc} [%]	10 ± 11	7 ± 6	6 ± 5	5 ± 3	3 ± 3	3 ± 2	2 ± 1	3 ± 2	4 ± 2	5 ± 3	6 ± 4	8 ± 6
Sigmoid D_{2cc} [%]	8 ± 7	7 ± 6	7 ± 7	6 ± 6	5 ± 5	6 ± 6	6 ± 4	8 ± 6	9 ± 6	12 ± 8	12 ± 10	16 ± 13
Point A left [%]	1 ± 1	1 ± 1	2 ± 1	1 ± 2	1 ± 1	1 ± 1	1 ± 1	1 ± 1	1 ± 1	2 ± 2	1 ± 1	2 ± 1
Point A right [%]	1 ± 1	1 ± 1	1 ± 1	1 ± 1	1 ± 1	1 ± 1	1 ± 1	1 ± 1	1 ± 1	2 ± 3	1 ± 1	1 ± 1
ICRU rectum [%]	17 ± 9	12 ± 7	10 ± 7	8 ± 6	6 ± 5	4 ± 4	4 ± 3	9 ± 6	14 ± 7	20 ± 10	25 ± 13	41 ± 26
ICRU bladder [%]	23 ± 23	18 ± 16	14 ± 14	11 ± 10	8 ± 7	5 ± 5	3 ± 3	5 ± 3	7 ± 3	9 ± 4	11 ± 6	15 ± 8

Schindel, et al., *J. Contemp. Brachy*. 5, 250-257 (2013)

ESTRO School

Take Home Message

- BT reconstruction methods have advanced over past 40 years
- 3D imaging datasets permit volumetric rendering not possible with:
  - orthogonal x rays
  - stereo shift planar x rays
  - fluoroscopy
- differing strengths/weaknesses for modern imaging methods
- learn the reconstruction process and datachain
- identify uncertainties at each stage in the reconstruction process

Acknowledgements

Dimos Baltas, University of Freiburg, Germany
Christian Kirisits, Medical University of Vienna, Austria
Frank-André Siebert, University of Kiel, Germany
Mark Rivard, Tufts Medical Center, Boston, USA
Daniel Berger, General Hospital of Vienna, Austria

ESTRO School

ESTRO School

WWW.ESTRO.ORG/SCHOOL

Advanced Brachytherapy Physics

07-10 October 2018 | Valencia, Spain

Monte Carlo simulation

P. Papagiannis, PhD
Medical Physics Laboratory
Medical School
National & Kapodistrian University of Athens

(no conflict of interest to disclose)

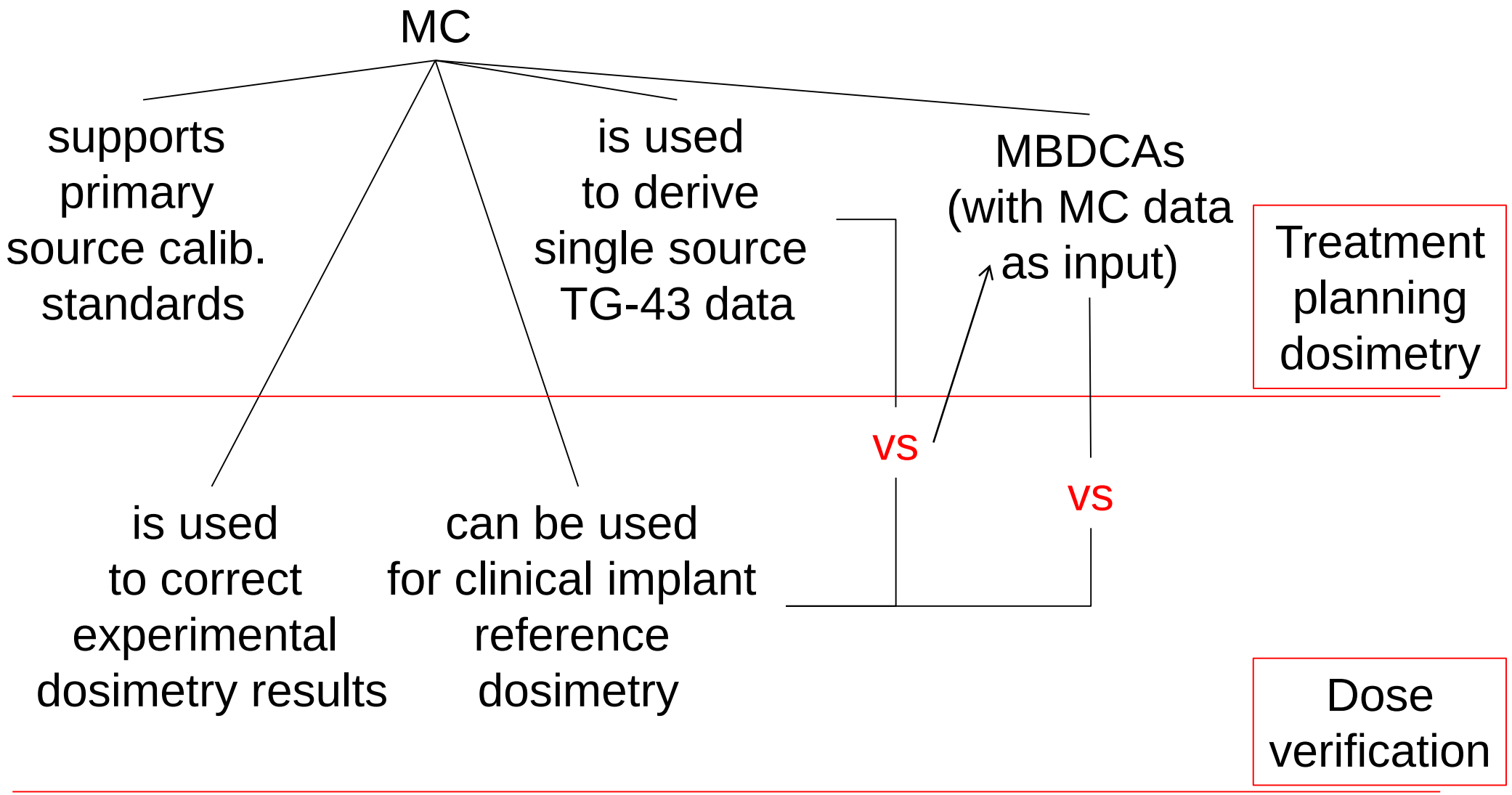
MC
supports primary source calib. standards
is used to derive single source TG-43 data
MBDCAs (with MC data as input)
Treatment planning dosimetry
vs
vs
is used to correct experimental dosimetry results
can be used for clinical implant reference dosimetry
Dose verification

Objectives/Outline:

To :

- review the basic principles of the MC method
- outline its implementation for brachy dosimetry

(and especially type A and type B uncertainties)

so as to identify:

- its potential to provide reference dose distributions
- TG-43 uncertainties
- its potential for clinical implementation

The problem …

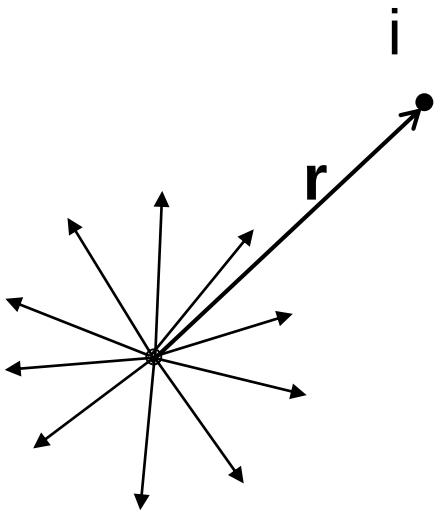

- Let us start from the simplest case (point isotopic monoenergetic photon source in infinite medium of given composition)
- If I know everything there is to know about the source and the medium, can I calculate dose at a point i …?

The problem …

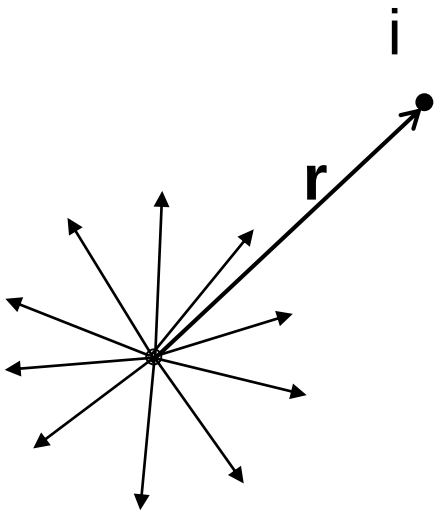

- Let us start from the simplest case (point isotopic monoenergetic photon source in infinite medium of given composition)
- If I know everything there is to know about the source and the medium, can I calculate dose at a point i …?

from intial activity i can calculate the radiant energy rate or the radiant energy over t, R_{pr}

from R i can calculate energy fluence at any point, $\Psi_{pr_i} = \frac{R_{pr}}{4\pi r_i^2} \exp(-\mu r_i)$

from Ψ_i i can calculate the TERMA at any point, $T_i = (\frac{\mu}{\rho})\Psi_{pr_i}$

i can also calculate the fraction of TERMA that is transferred to kinetic energy of charged particles

$\equiv$ KERMA at any point, $K_{pr_i} = (\frac{\mu_{en}}{\rho})\Psi_{pr_i} = (\frac{\mu_{en}}{\mu})T_{pr_i}$

The problem …

For brachytherapy photons:

- secondary e- ranges are small relative to photon m.f.p.
- e- radiative energy loss is negligible
- CPE can be assumed to exist at all points (except close to a source or high Z materials)

Energy [keV]	CSDA-range electrons [g/cm^2]	$\frac{1}{\mu}$ [cm]
30	1.8E-03	2.5
100	1.2E-02	5.6
350	1.1E-01	8.9
1000	4.4E-01	14

Dose to a point can be approximated by collision KERMA throughout a geometry of mm sized voxel elements

In short, to know the dose distribution one needs to know the energy distribution of fluence, Φ_E, at all points of a geometry:

$$D(\boldsymbol{r}) = K(\boldsymbol{r}) = \int_E E\Phi_E(\mathbf{r})[{}^{\mu_{en}(E)}/_{\rho}]\mathrm{d}E$$

Table from: Venselaar, Baltas, Meigooni, Hoskin (Eds), Comprehensive Brachytehrapy: physical and clinical aspects. CRC Press, Taylor & Francis, © 2013

The problem …

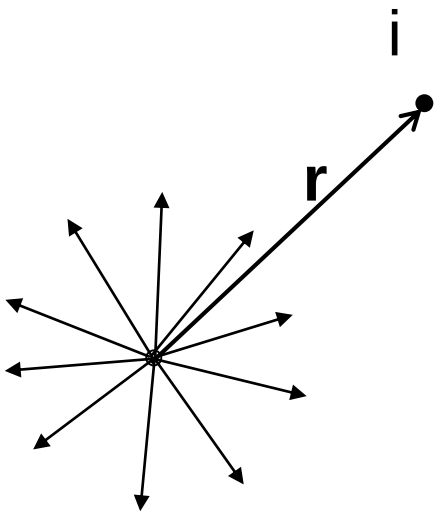

- Let us start from the simplest case (point isotopic monoenergetic photon source in infinite medium of given composition)
- If I know everything there is to know about the source and the medium, can I calculate dose at a point i …?

$$\text{under CPE}: D_{pr_i} \equiv K_{\text{pr}_i} = \left(\frac{\mu_{en}}{\rho}\right)\Psi_{\text{pr}_i}$$

- BUT WHAT ABOUT SCATTER DOSE…?

The problem …

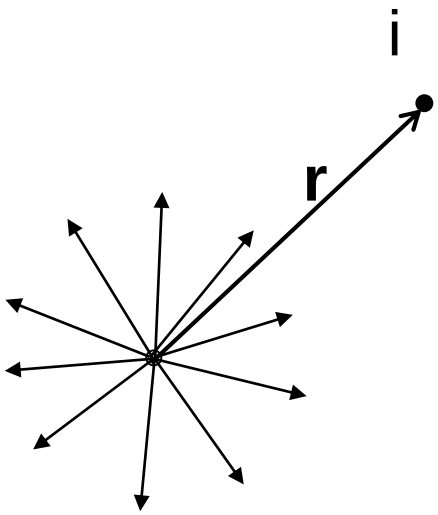

• Point isotopic monoenergetic photon source in infinite medium of given composition

• If I know everything there is to know about the source and the medium, can I calculate dose at a point i …?

$$D_{pr_i} \equiv K_{pr_i} = \left(\frac{\mu_{en}}{\rho}\right)\Psi_{pr_i}$$

For D_{scat} at point i need Ψ_{Esc_i} the depends on:

the probability of a primary photon interacting in one of a number of possible interaction types **at every point of the geometry**,

the probability distribution determining the new direction of a photon and its energy degradation,

the probability this process is repeated due to multiple scattering **at every point of the geometry**

D_{scat} at point i, CANNOT be analytically calculated

NOT because of its stochastic nature, but due to the complexity of the calculation

The problem …

How important is D_{scat} in brachy …?

It depends on ENERGY!

Energy [keV]	CSDA-range electrons [g/cm²]	$\frac{1}{\mu}$ [cm]	$1-\mu_{en}/\mu$
30	1.8E-03	2.5	0.56
100	1.2E-02	5.6	0.85
350	1.1E-01	8.9	0.71
1000	4.4E-01	14	0.58

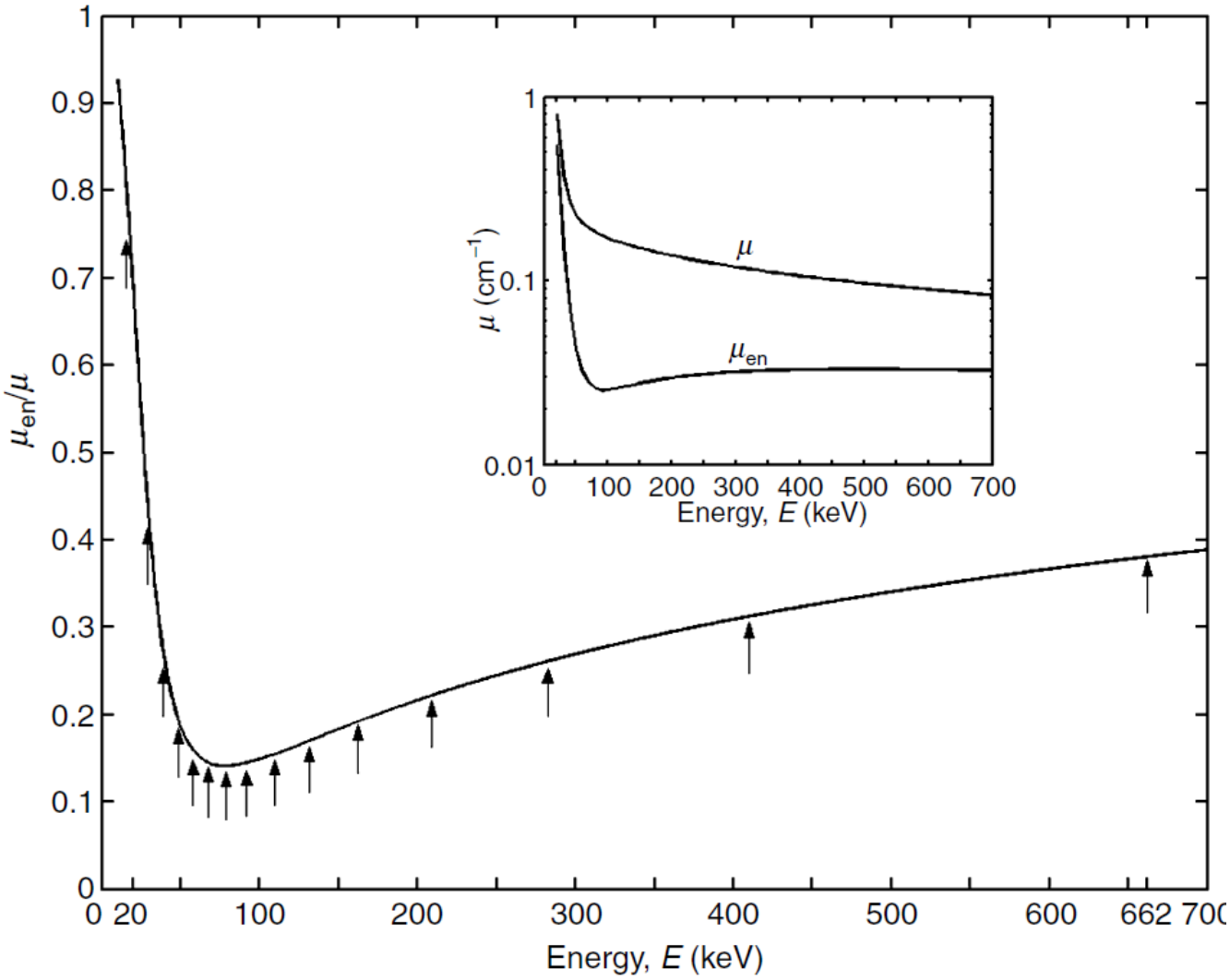

Figure from: Baltas, Sakelliou, Zamboglou (Eds), The Physics of modern brachytherapy for oncology, Taylor & Francis Books Inc, 2006

The problem …

How important is D_{scat} in brachy …?

It depends on distance from source(s)!

Do not forget: in brachy r^2 reigns!!!

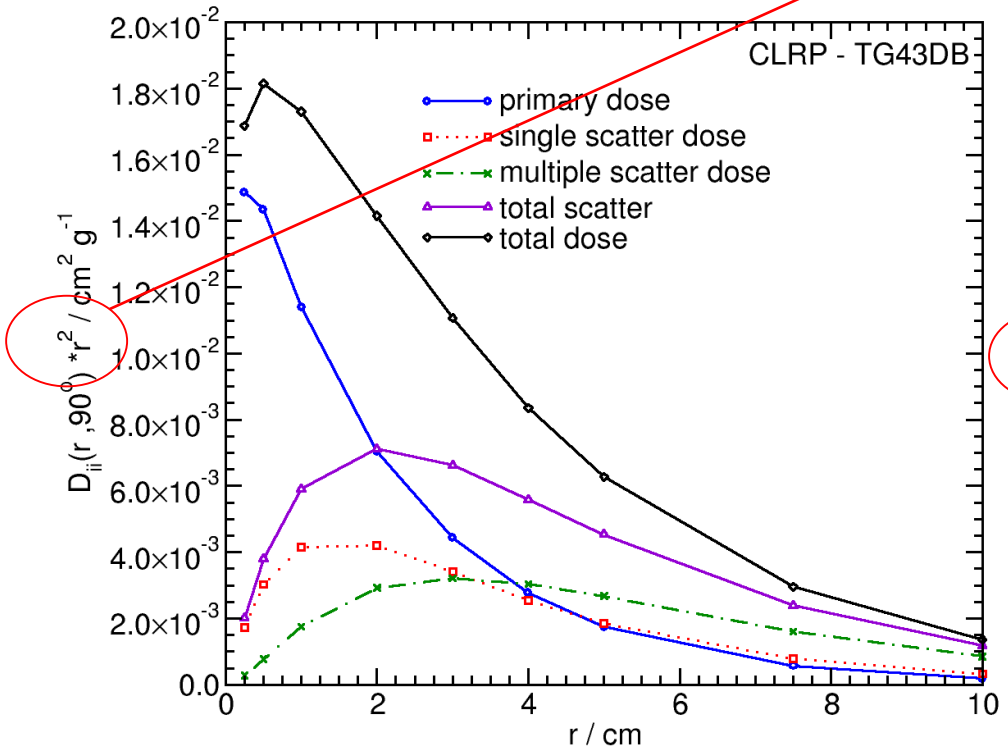

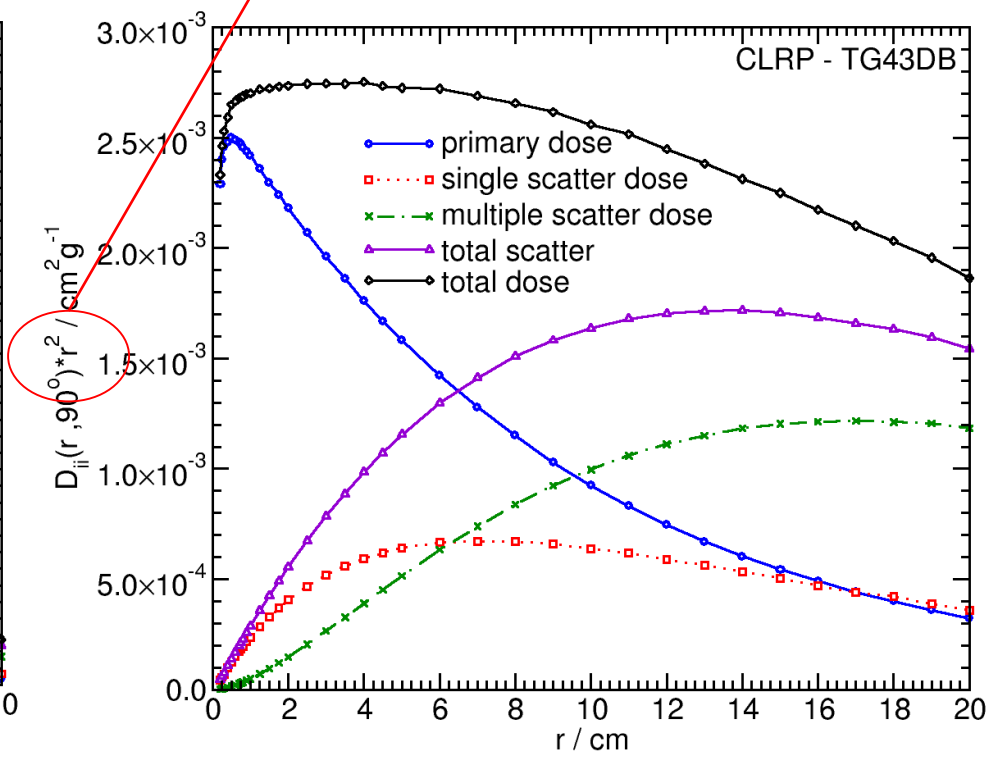

Figures from the Carleton U. TG-43 database available online @:
http://www.physics.carleton.ca/clrp/seed_database

The problem …

How important is D_{scat} in brachy …?

It associates the dose distribution with the entire calculation geometry (ρ, Z, dimensions) rather than just the path from a source to a point.

E.g. for dimensions:

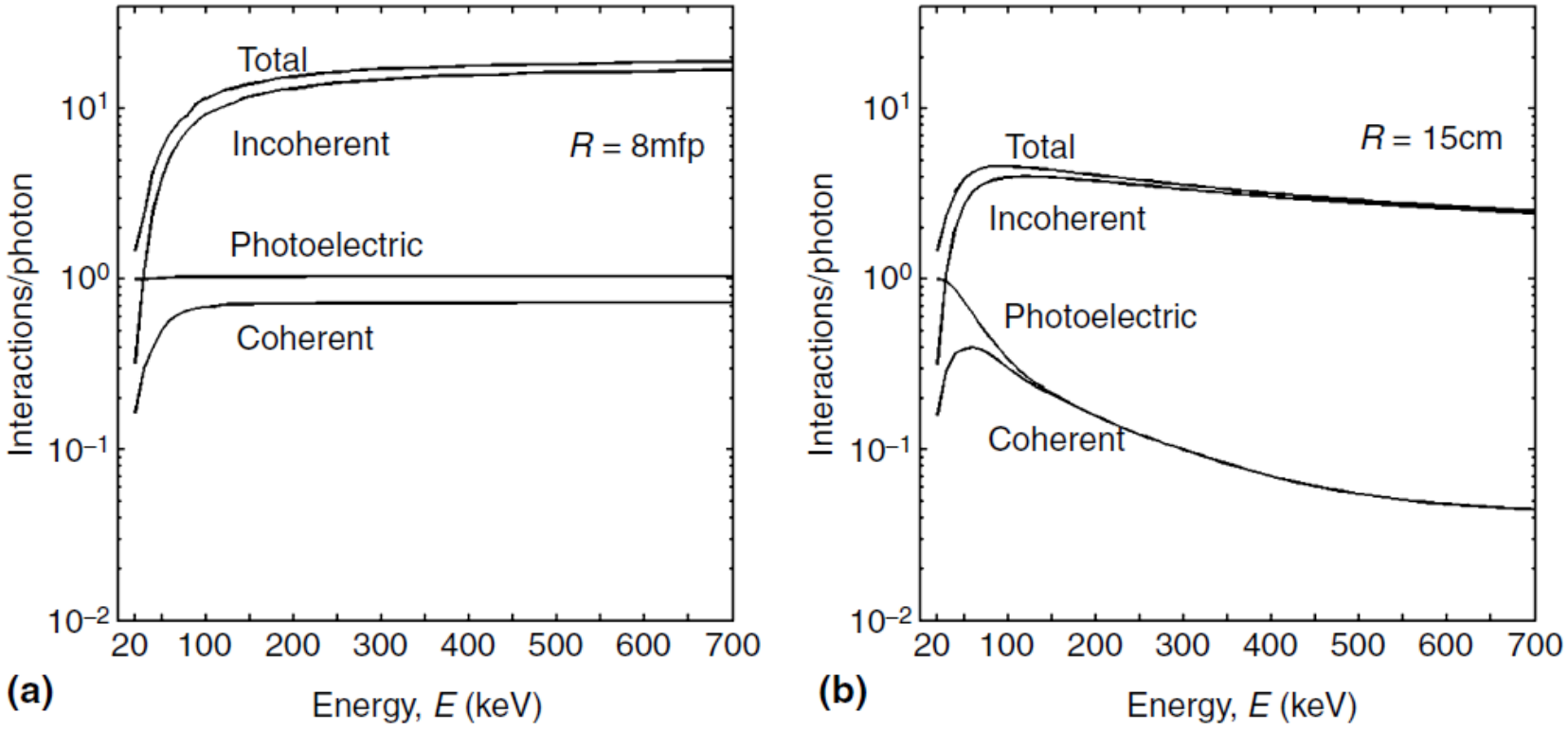

Figure from: Venselaar, Baltas, Meigooni, Hoskin (Eds), Comprehensive Brachytehrapy: physical and clinical aspects. CRC Press, Taylor & Francis, © 2013

The problem …

How important is D_{scat} in brachy …?

It associates the dose distribution with the entire calculation geometry (ρ, Z, dimensions) rather than just the path from a source to a point.

E.g. for dimensions:

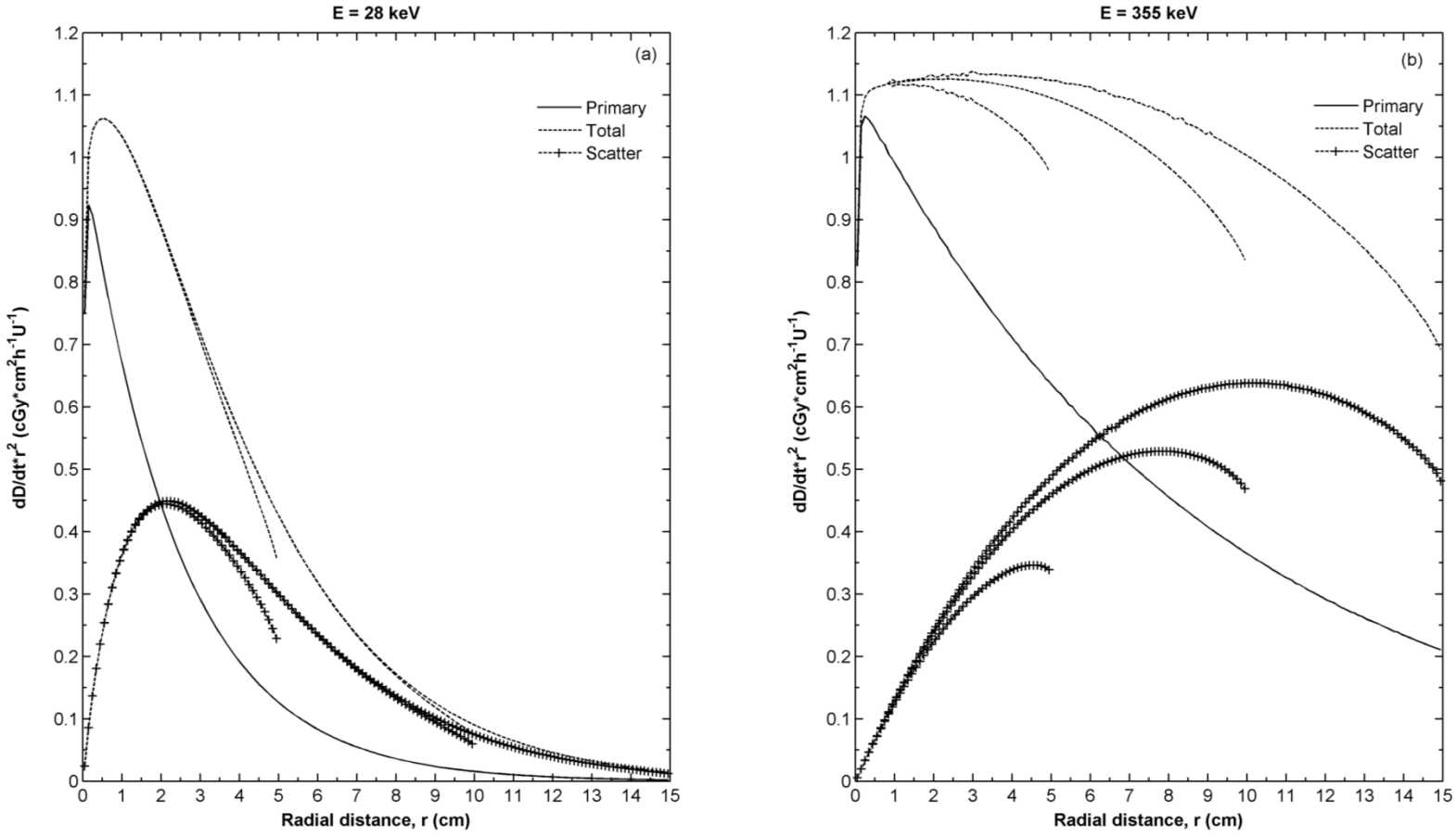

Figures from: Papagiannis, Pantelis, Karaiskos, Br J Radiol (2014) 87: 20140163

The problem …

How important is D_{scat} in brachy …?

It associates the dose distribution with the entire calculation geometry (ρ, Z, dimensions) rather than just the path from a source to a point.

E.g. for materials:

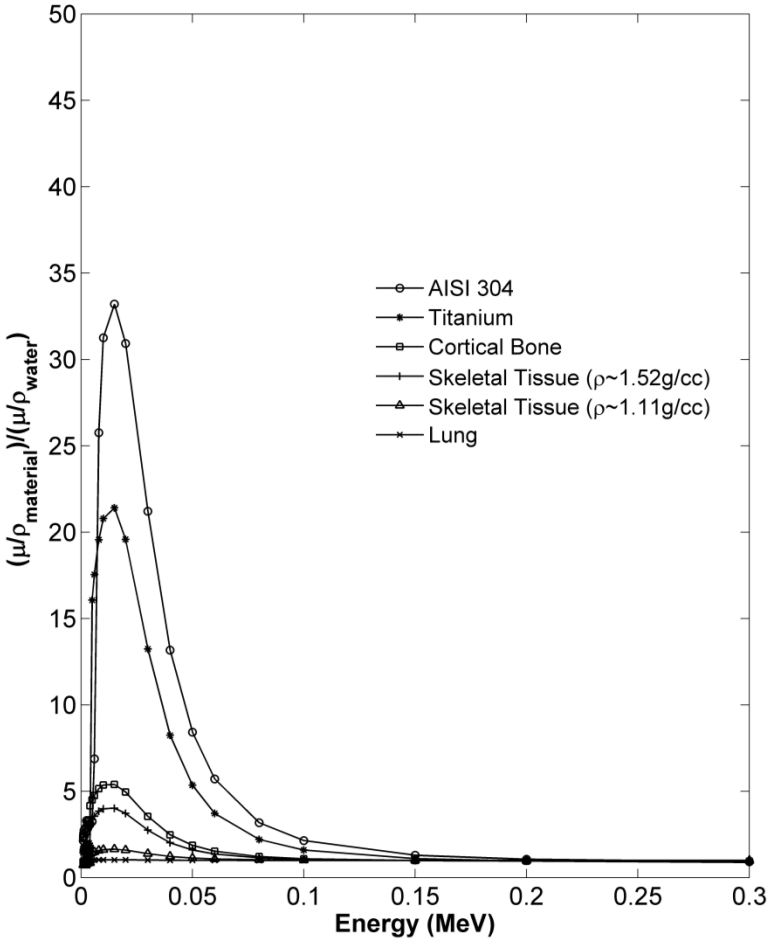

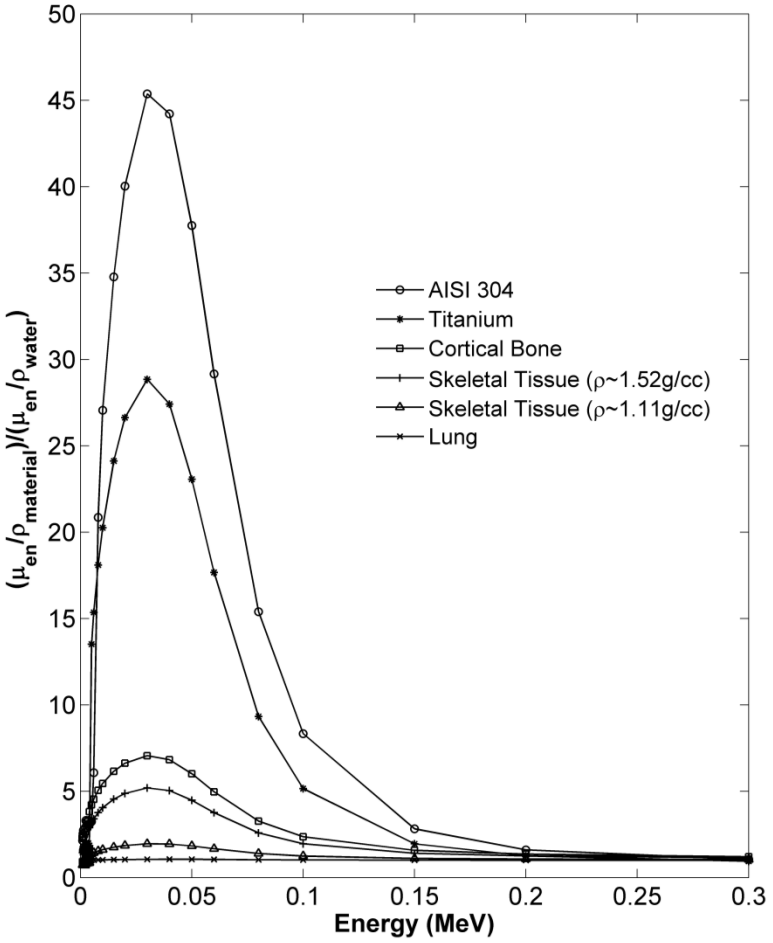

The MC method …

Since we know the Physics underlying radiation transport through matter (probabilities for interaction: site, type and associated energy/direction distributions), can't we reproduce (simulate) all possible photon tracks?

Could I then calculate any related quantity at all points…?

The MC method …

The Central Limit Theorem: the sum of a **large** number of identical, independent random variables is approximately **normally** distributed.

So, if I want to calculate an unknown quantity, m,
and k is a random variable of expectation value E(k)=m and variance Var(k)=b^2.
If $k_1, k_2, \ldots, k_N$ are N RANDOMLY selected values of k,

then: $\sum_{i=1}^{N} k_i$ is normally distributed with E($\sum_{i=1}^{N} k_i$)=Nm and V ($\sum_{i=1}^{N} k_i$)=Nb^2

or equivalently:
$$P(Nm - 3b\sqrt{N} < \sum_{i=1}^{N} k_i < Nm + 3b\sqrt{N}) \approx 0.997$$

or:
$$P(-3b/\sqrt{N} < \frac{1}{N}\sum_{i=1}^{N} k_i - m < 3b/\sqrt{N}) \approx 0.997$$

So, if I want to estimate the photon fluence (or any related quantity) at point r, I can average the contribution of N photon tracks RANDOMLY sampled from the probability distribution of all possible tracks

The MC method …

Do I know the probability distribution of possible tracks?

A photon "moves" from phase space element to phase space element.

A photon track is composed of the sequential phase space elements or photon states, $\mathbf{S}_j(\mathbf{r}_j, E_j, \boldsymbol{\Omega}_j)$ just before each interaction j.

The probability of occurrence of each photon state j only depends on the probability of occurrence of state j-1.

Or in other words: the probability that the photon interacts at r_{j-1}, the probability that a specific kind of interaction occurs and the probability that during this interaction the photon is scattered in direction Ω_j with energy E_j given Ω_{j-1} and E_{j-1}.

These probability distributions are known in Physics….!

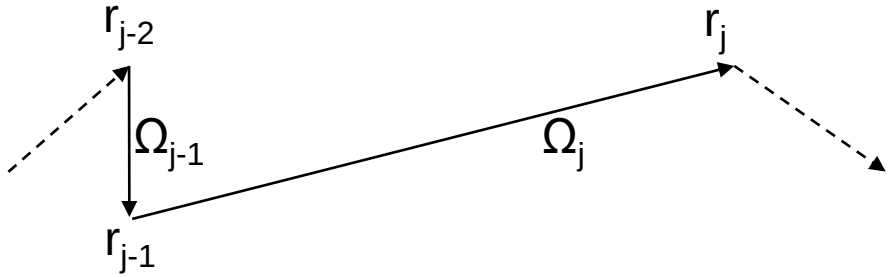

Hence, the only component missing is a method to RANDOMLY sample from the above, known, probability distributions.

The MC method …

How do I sample RANDOMLY from a known probability distribution?

There are numerous mathematical methods. In example:

Inversion theorem

Let x be a continuous random variable distributed over the interval [a, b] with a probability density function f(x) and a cumulative probability distribution function F(x) that is invertible. Given a random number, r, in the interval [0, 1], a value x^* of x can be randomly selected according to:

$$r = F(x^*) = \int_a^{x^*} f(x)dx$$

Let x be a discrete random variable taking N values, x_i of probability, P_i so that: $\sum_{i=1}^{N} P_i = 1$

Given a random number, r, in the interval [0, 1], a value x^* of x can be randomly selected according to:

$x^* = x_j$ where $j = \min\{ : r < \sum_{i=1}^{j} P_i \}$

The MC method …

Simple examples:

Choosing emission direction for a mono-energetic point source.

The emission is isotropic and the probability of emission into a solid angle element dΩ equals the fraction of this solid angle in the 4π geometry so that:

$$p(\theta,\phi)d\theta d\phi = \frac{d\Omega}{4\pi} = \frac{\sin\theta d\theta d\phi}{4\pi}$$

$$p(\theta)d\theta = \frac{\sin\theta d\theta}{2} \quad and \quad r = P(\theta^*) = \int_0^{\theta^*} \frac{\sin\theta d\theta}{2} \Rightarrow r = \frac{1-\cos\theta^*}{2} \Rightarrow \cos\theta^* = 1-2r$$

$$p(\phi)d\phi = \frac{d\phi}{2\pi} \quad and \quad r' = P(\phi^*) = \frac{1}{2\pi}\int_0^{\phi^*} d\phi \Rightarrow \phi^* = 2\pi r'$$

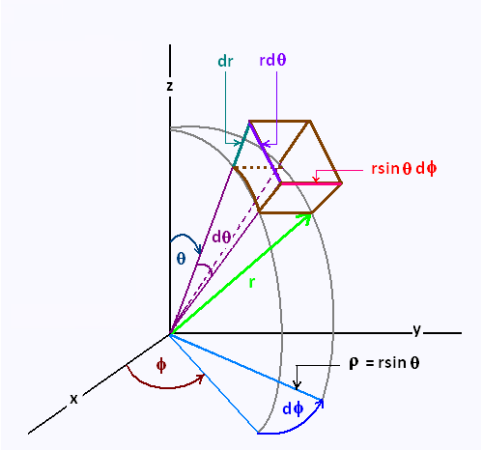

Figure from: Venselaar, Baltas, Meigooni, Hoskin (Eds), Comprehensive Brachytehrapy: physical and clinical aspects. CRC Press, Taylor & Francis, © 2013

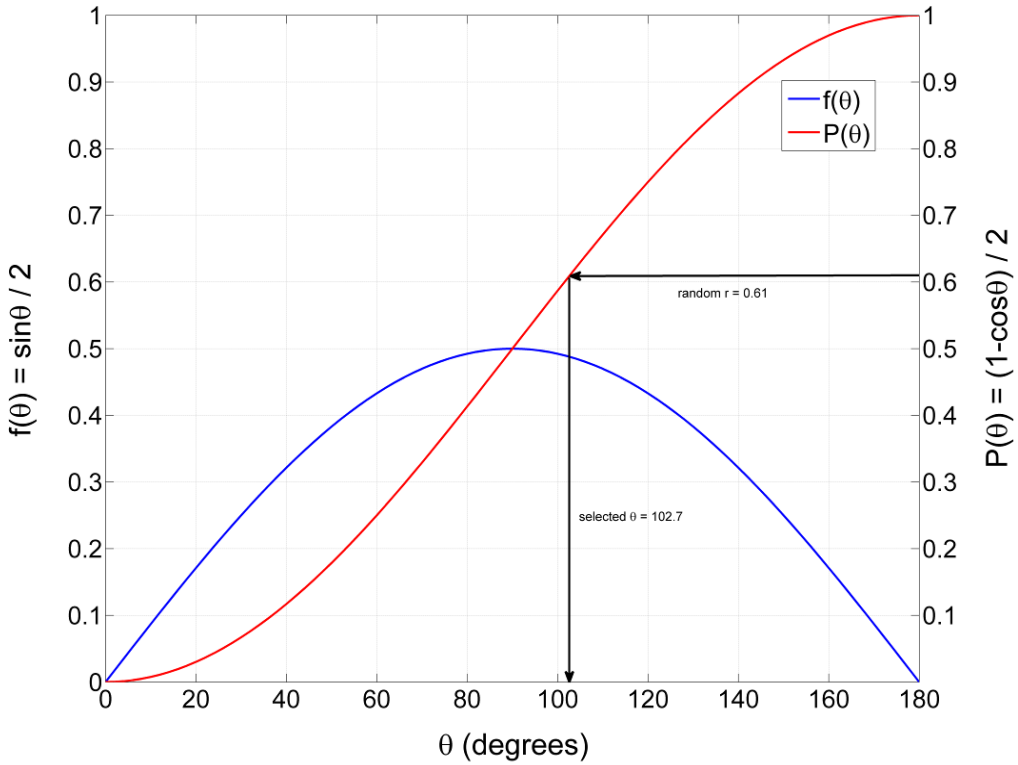

The MC method …

Choosing interaction site.

The probability that a photon interacts within dx after travelling a distance x is μexp(-μx) so that:

$$r = P(x) = \int_0^{x^*} \mu \exp(-\mu x)dx \Rightarrow r = -\exp(-\mu x^*) + 1 \Rightarrow x^* = -\frac{1}{\mu}\ln(1-r) = -\frac{1}{\mu}\ln(r)$$

Choosing interaction type.

Interaction type is a discrete random variable of i values so that $P_i=\mu_i/\mu_{total}$.

So given r, I choose interaction j so that:

$$j = \min\{\ j: r < \sum_{i=1}^{j} P_i \ \}$$

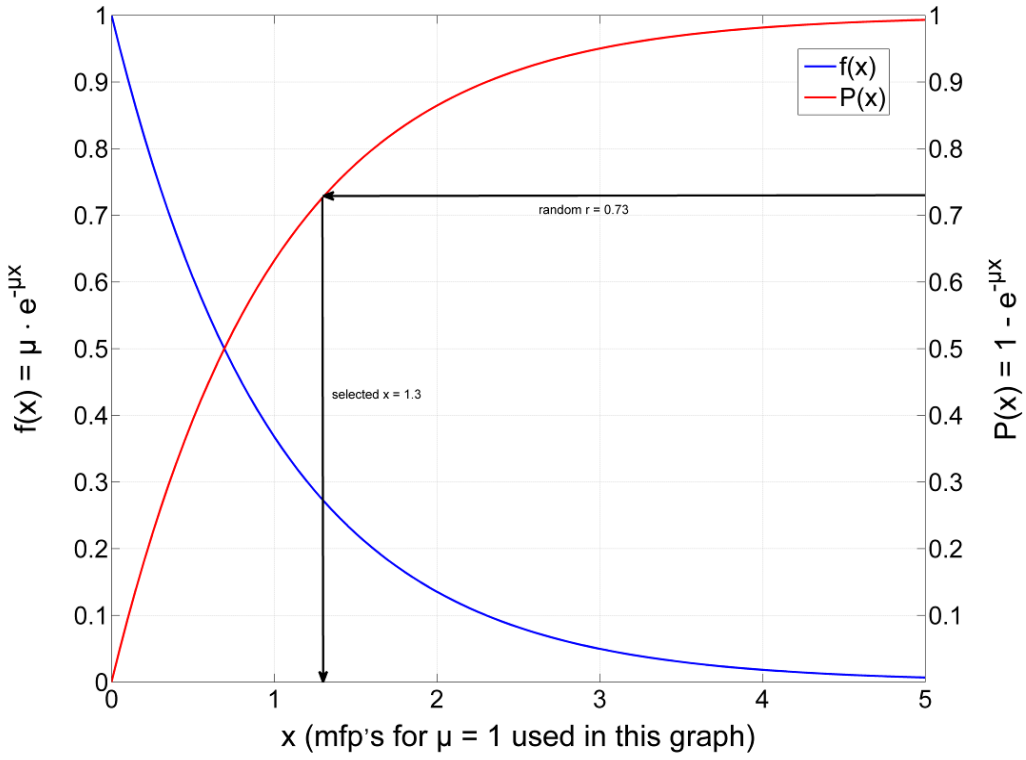

Figure from: Venselaar, Baltas, Meigooni, Hoskin (Eds), Comprehensive Brachytehrapy: physical and clinical aspects. CRC Press, Taylor & Francis, © 2013

The MC method …

- Similar procedures (available in the literature from the 50's) are used for sampling randomly from the probability distributions for every process involved in photon transport.
- MC is a statistical method to approximate dose at all points of a geometry
- The method inherently accounts for real sources, inhomogeneities, and phantom dimensions according to input data.
- The collision KERMA can be calculated within voxels by scoring the energy transferred to charged particles from interactions within the voxel and weighing by voxel mass (dm=ρdV) (analogue MC).
- Alternatively, photon energy fluence can be scored in each voxel and weighed by μen/ρ to obtain collision KERMA (track length estimator).

$$\Phi = \lim_{\substack{N\to\infty \\ V\to 0}} \left\{ \frac{1}{V} \sum_{i=1}^{N} l_i \right\}$$

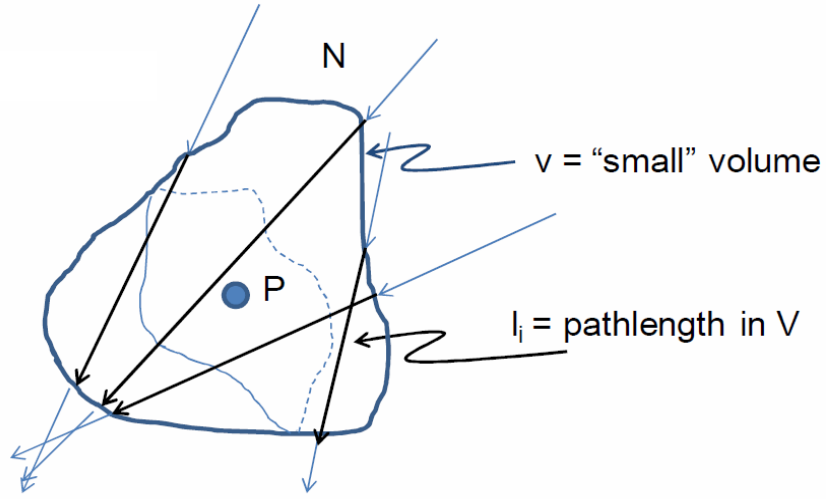

The MC method …

MC simulations for single source dosimetry are ALWAYS a set of **2 MC** simulations

one for the distribution of energy absorbed

at all points of the geometry per starting particle

and

one for the air kerma of the source per starting particle

In multiple source MC dosimetry (e.g. a clinical case) results from single source positions can be weighed by t_i, summed

and multiplied by TRAK ($S_K * t_{tot}$)

The MC method …

The general outline of a MC code is:

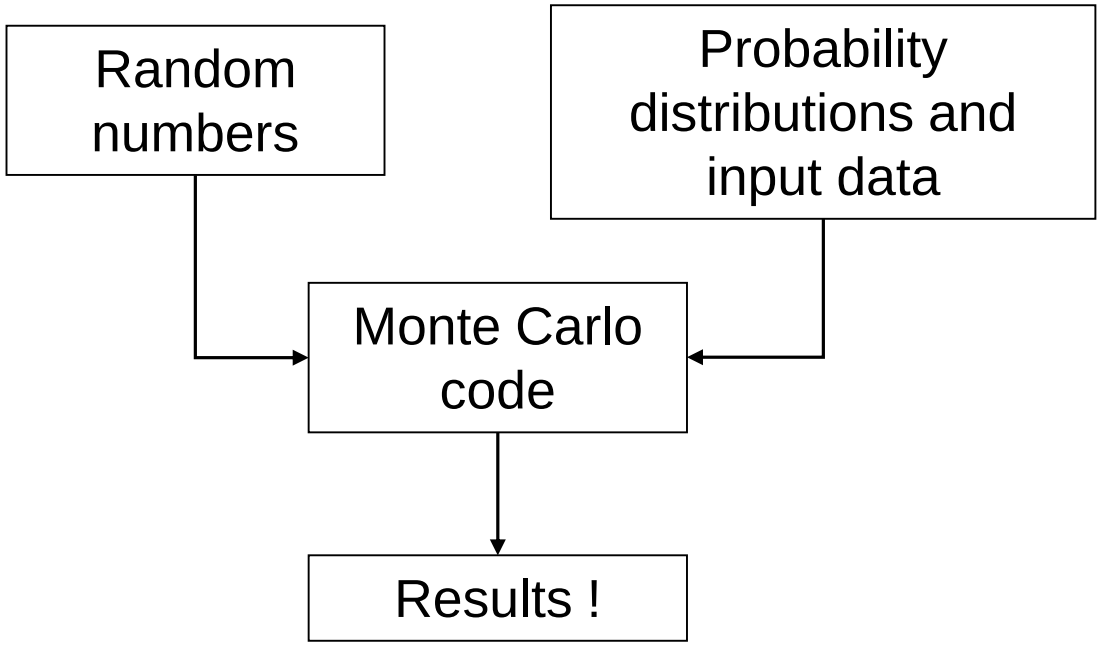

The questions then are:

1. What is the accuracy/precision of the method?
2. How efficient can the method be?

Type A uncertainty

- Recall that : $P(-3b/\sqrt{N} < \frac{1}{N}\sum_{i=1}^{N} k_i - m < 3b/\sqrt{N}) \approx 0.997$

b, the stdev of unknown quantity m is not known but for N>>$\bar{k} = \frac{1}{N}\sum_{i=1}^{N} k_i$ approximates m

and the square root of the variance $Var(k) = \frac{1}{N-1}\sum_{i=1}^{N}(k_i - \bar{k})^2 \approx \overline{k^2} - \bar{k}^2$ approximates b.

$\sqrt{\frac{Var(k)}{N}}$ therefore forms precision confidence interval (k=3) of our tally and it must be as low as possible.

- <u>Type A uncertainty decreases ~ 1/sqrt(N)</u>

- type A uncertainty decreases as voxel size increases for analogue MC (at the expense of volume averaging)

- the only other way to decrease type A would be to reduce Var(k) which is in essence an efficiency gain and will be discussed later

Type A uncertainty

- TG-43 U1* suggests that enough histories, N, should be used to ensure that dosimetry results have relative uncertainties <2% at r<5 cm

- AAPM/ESTRO** recommendations are MC Type A uncertainties (k=1)<0.1% for distances < 5 cm and Type A uncertainties (k=1)<0.2% for distances <10cm

- TG-138 (AAPM/ESTRO)*** suggests MC type A<0.1% when feasible

* Rivard et al., 2004. Update of AAPM Task Group No. 43 Report: A revised AAPM protocol for brachytherapy dose calculations. Med. Phys. 31(3), p.633.
** Perez-Calatayud et al., 2012. Dose calculation for photon-emitting brachytherapy sources with average energy higher than 50 keV: report of the AAPM and ESTRO. Med. Phys. 39(5), p.2904
*** DeWerd et al., 2011. A dosimetric uncertainty analysis for photon-emitting brachytherapy sources: report of AAPM Task Group No. 138 and GEC-ESTRO. Med. Phys. 38(2), pp. 782

Type B uncertainty

All other aspects of the simulation contribute to type B uncertainty

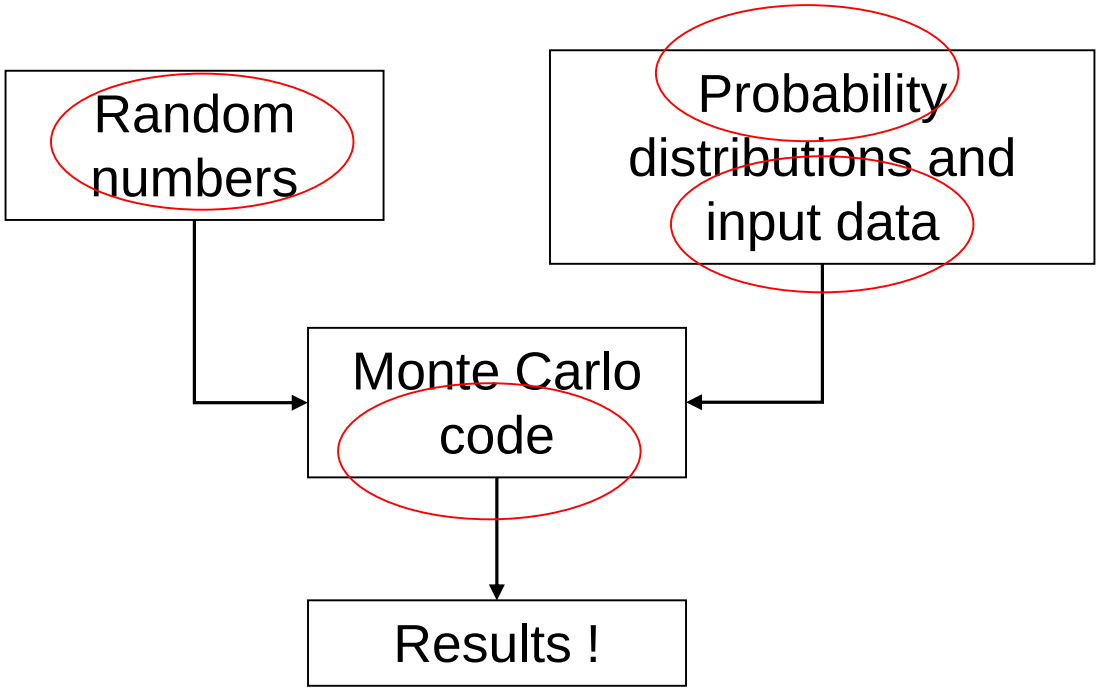

Type B uncertainty … random number generator

Pseudo random number generators are used, e.g. Lehmer type, multiplicative-congruential of the form:

$$r_{n+1}=Br_n \bmod 2^M$$

with B,M and r_o (the "seed" of the sequence) appropriately selected.

- <u>These generators are generally robust in benchmarked and extensively used codes</u>
- These generators are periodic with a period of 2^M. Exceeding this period might underestimate result variance
- If you are using different simulations to estimate Var(k) make sure the seed is different

Type B uncertainty … code

- What MC code should I use? / Should I prepare my own?

- Codes benchmarked and extensively used in the literature:
PTRAN, MCNP, GEANT4, PENELOPE, and EGS.

- TG-43U1*: Monte Carlo codes not previously used in brachytherapy dosimetry, should be more rigorously tested and documented in the peer-reviewed literature before proposing to use their results clinically.

- TG-43U1*: “regardless of the transport code chosen and its pedigree, all investigators should assure themselves that they are able to reproduce previously published dose distributions for at least one widely used brachytherapy source model. This exercise should be repeated whenever new features of the code are explored, upon installing a new code version, or as part of orienting a new user.”

Popular, nonproprietary codes, benchmarked for brachytherapy dosimetry*

Code	Operating System	Availability /License	Applications	Significant features
EGSnrc	All major modern operating systems (portions available for a limited set)	Through NRC web (GitHub) / General Public License for research & education, separate NRC license for commercial use	EGSnrc is a set of functions and subroutines for coupled ph/el transport mainly in Medical Physics. For an application, a user code is required (in Mortran, Fortran, C, C++). Major applications are available, including brachytherapy.	• Accurate condensed history technique implementation for charged particle transport. • More accurate Physics (rel. to its predecessor). • Choice of cross sections tabulation/data. • Faster than other codes for charged particle transport. • General purpose geometry package + utility classes.

*According to material from Appendix D in: W.L. Dunn. J. K. Shultis (Eds), Exploring Monte Carlo Methods. CRC Press, Elsevier B.V. © 2012

Popular, nonproprietary codes, benchmarked for brachytherapy dosimetry*

Code	Operating System	Availability /License	Applications	Significant features
GEANT4	Linux variants, Windows and Mac OS X (verified and supported on specific configurations)	Through CERN web subject to the open-source conditions of the Geant4 license (cannot be included in whole or in part in patented applications)	General purpose simulation of particle transport primarily for high-energy and medical physics Comprehensive geometry and physics modeling capabilities are embedded in a flexible structure base using object-oriented technology and C++ A large number of specialized applications based on GEANT4 are available including one for brachytherapy.	• Users can choose existing components, tailor and adapt them, or create their own. • A choice of physics models is offered for many physics processes with different trade-offs between accuracy and CPU cost. • Tools for optimization of configurations of geometry and physics are also provided. • Combinations of Physical processes for typical applications are recommended in Physics lists. • Powerful geometry module. • Range of visualization options.

*According to material from Appendix D in: W.L. Dunn. J. K. Shultis (Eds), Exploring Monte Carlo Methods. CRC Press, Elsevier B.V. © 2012

Popular, nonproprietary codes, benchmarked for brachytherapy dosimetry*

Code	Operating System	Availability/License	Applications	Significant features
MCNP6	Supported on most operating systems (32/64-bit) including Windows, Mac OS X, Linux, and UNIX-like.	US: through the Radiation Safety Information Computational Center (RSICC) Europe: to members of the Nuclear Energy Agency (NEA) Data Bank Japan: through the Research Organization for Information Science and Technology (RIST). Limited license and export control regulations restrict the distribution of Fortran source code.	General purpose simulation of particle transport primarily for nuclear applications and medical physics.	• Extensive geometry, source definition, and tallying capabilities. • Built in variance reduction techniques. • Straightforward generation of structured input files for specific applications.

*According to material from Appendix D in: W.L. Dunn. J. K. Shultis (Eds), Exploring Monte Carlo Methods. CRC Press, Elsevier B.V. © 2012

Popular, nonproprietary codes, benchmarked for brachytherapy dosimetry*

Code	Operating System	Availability/License	Applications	Significant features
Penelope	Written in FORTRAN and can be run on any computer with FORTRAN 77 (or higher) compiler. Geometry viewers run under Windows.	Through the Nuclear Energy Agency (NEA) Data Bank and the Radiation Safety Information Computational Center (RSICC) as open software.	Simulation of coupled electron-photon transport in material structures consisting of homogeneous bodies limited by quadratic surfaces. Structured as a set of subroutine packages. User should write a steering main program or build upon the generic one provided.	• Particularly well adapted to simulations of electron transport at low and intermediate energies

*According to material from Appendix D in: W.L. Dunn. J. K. Shultis (Eds), Exploring Monte Carlo Methods. CRC Press, Elsevier B.V. © 2012

Type B uncertainty … scoring

- CPE can be assumed and only photons need be simulated

Photon-only simulation introduces errors >2% @ distances at or below 1.6, 3, and 7mm for Ir-192, Cs-137, and Co-60 sources, respectively (Perez-Calatayud et al. 2012) but this is source specific and clinically irrelevant in most cases.

- Scoring cell dimensions are important! See Taylor et al. (2007) for details and Rivard et al. (2004) and Perez-Calatayud et al. (2012) for recommendations

  - For analogue MC increasing voxel size will reduce type A but increase volume averaging

  - For track length estimators reducing voxel thickness while preserving surface will reduce volume averaging without affecting type A

$$\Phi = \lim_{\substack{N\to\infty \\ V\to 0}} \left\{ \frac{1}{V} \sum_{i=1}^{N} l_i \right\}$$

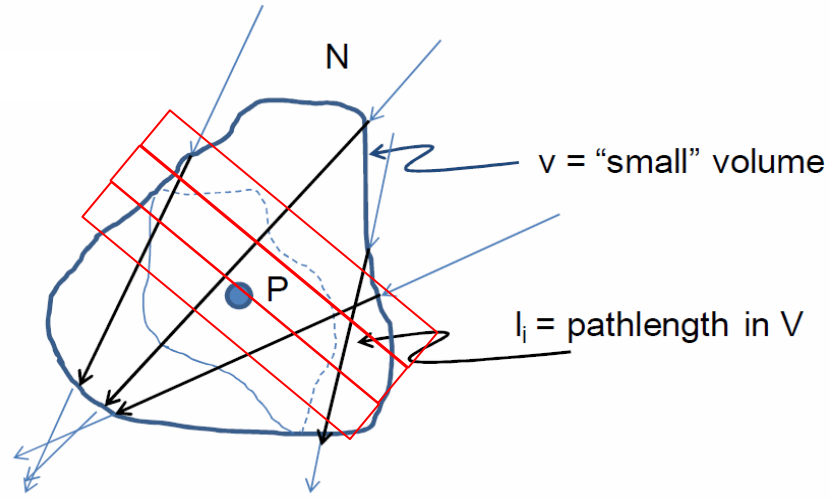

Type B uncertainty … cross sections

- Probability distributions are in the form of a cross section data base.
- Total partial and differential photon cross sections are required including atomic form factors F(x, Z) and incoherent scatter factors S(x, Z)
- These cross sections must be: complete (in terms of E, Z) self-consistent and up to date/accurate.
- Self-consistency is also required with mass energy absorption data used for kerma calculation from energy fluence

- Up to date cross sections are used in all current versions of benchmarked MC codes: EPDL97 (LLNL) in the ENDL or ENDF/B-VI formats or the DLC-146 format (ORNL) or XCOM (NIST) database. Mass energy-absorption coefficients for water by Seltzer and Hubbell (available on line at NIST).
Data readily available online through NIST (http://www.nist.gov/pml/data/xraycoef/)

- TG-138 (AAPM/ESTRO) cites ~1% cross section type B that contributes to dosimetric uncertainty at r=5 cm about 0.76 % (low E) and 0.12% (high E)

Type B uncertainty … input

Source geometry

- Information is required on geometry, materials, density, elemental composition, and dimensions.
- The uncertainty of this information is more crucial for low energy sources
- For reference dosimetry of new sources geometry and dimensions should be verified experimentally in a sample of sources.
- If the source includes parts of non-negligible mobility, MC should be performed for different configurations and results averaged.

e microscopy (6711)

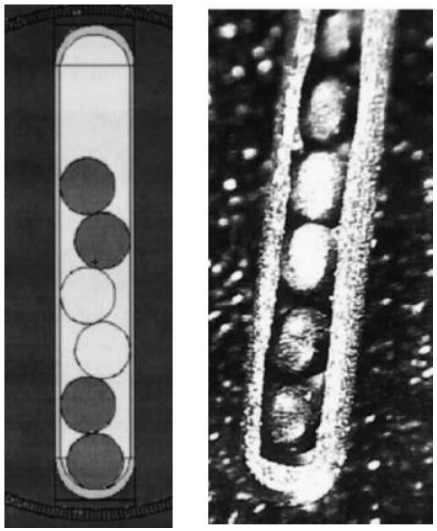

seed cut out view (3631 A/M)

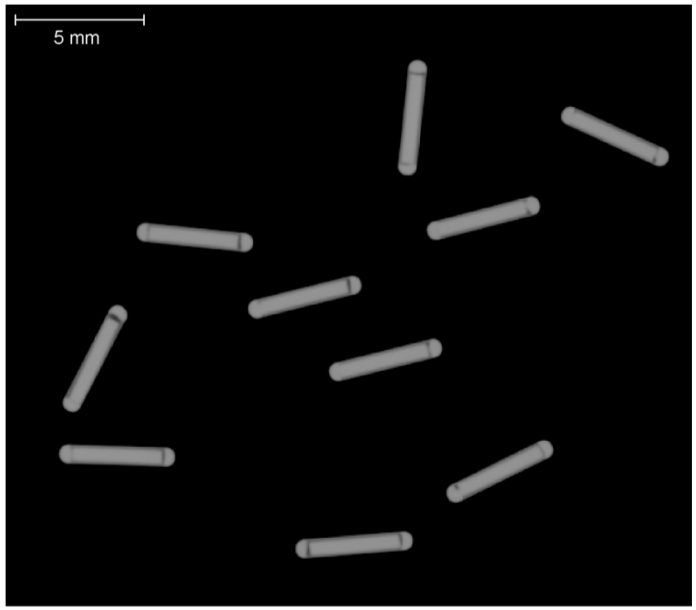

contact tr. radiography (IsoSeed I25.S17plus)

Pics from: Rogers & Cygler (Eds), Clinical dosimetry measurements in radiotherapy (2009 AAPM Summer School), Monograph No. 34, Medical Physics Publishing 2011

Pantelis et al, J Contemp Brachytherapy 5(4), 240 (2013)

Type B uncertainty … input

Source geometry

➢Besides verified, the uncertainty in construction details (tolerances) must be included in the uncertainty budget. In example: uncertainty map for an I-125 seed

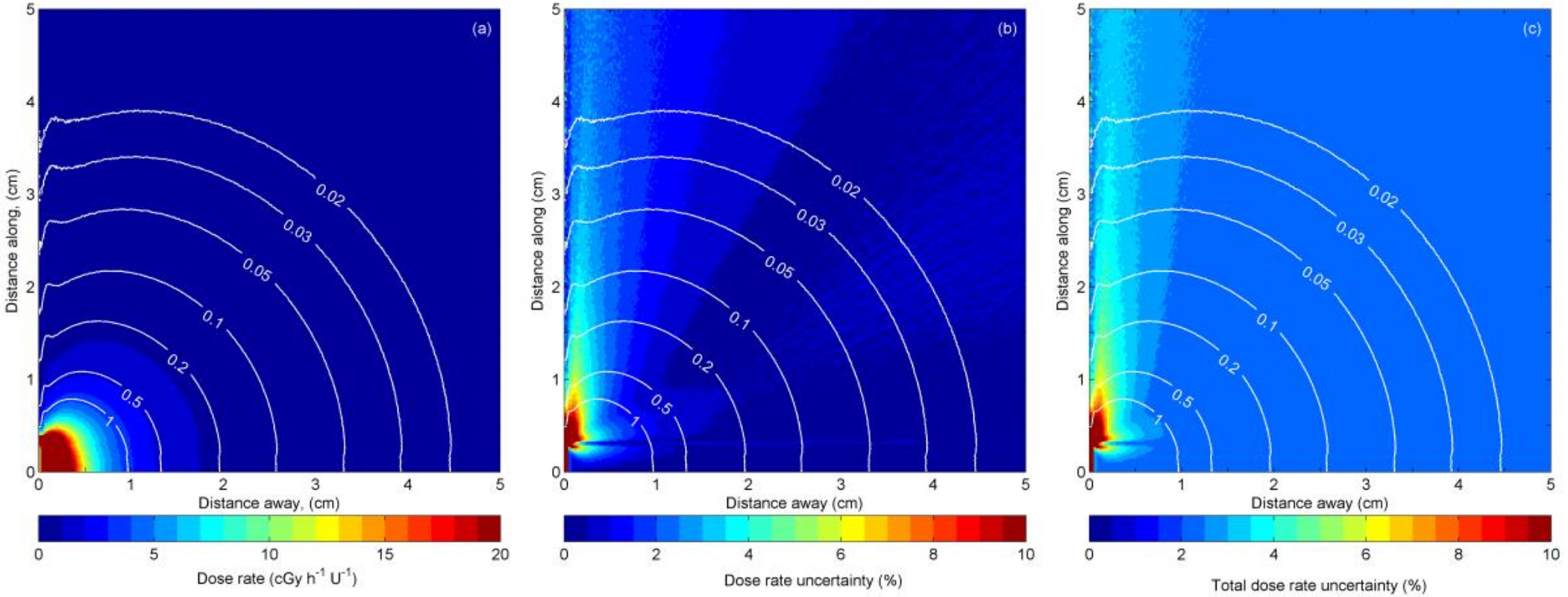

IsoSeed I25.S17plus:

MC dose rate distr. % uncert.: geo. + type A % uncert.: geo. + type A + cross secs.

Pantelis et al, J Contemp Brachytherapy 5(4), 240 (2013)

Type B uncertainty … input

➢ Phantom geometry (for single source dosimetry)

Remember dose from scatter depends on geometry dimensions…!

or patient segmentation and source/applicator position (for patient dosimetry)

➢ Geometry in simulation for S_K (for single source dosimetry)

In order to comply with the definition of S_K :

- Air (point) detector at large distance from the source in vacuo
- Photon emissions of energy lower than δ=5 keV (i.e. characteristic x-rays of Ti encapsulation following photoelectric absorption of 125I photons) must be suppressed.

Geometry for actual measurement of S_K

For low energy sources, simulations must also account for the WAFAC - 7.6° half angle.

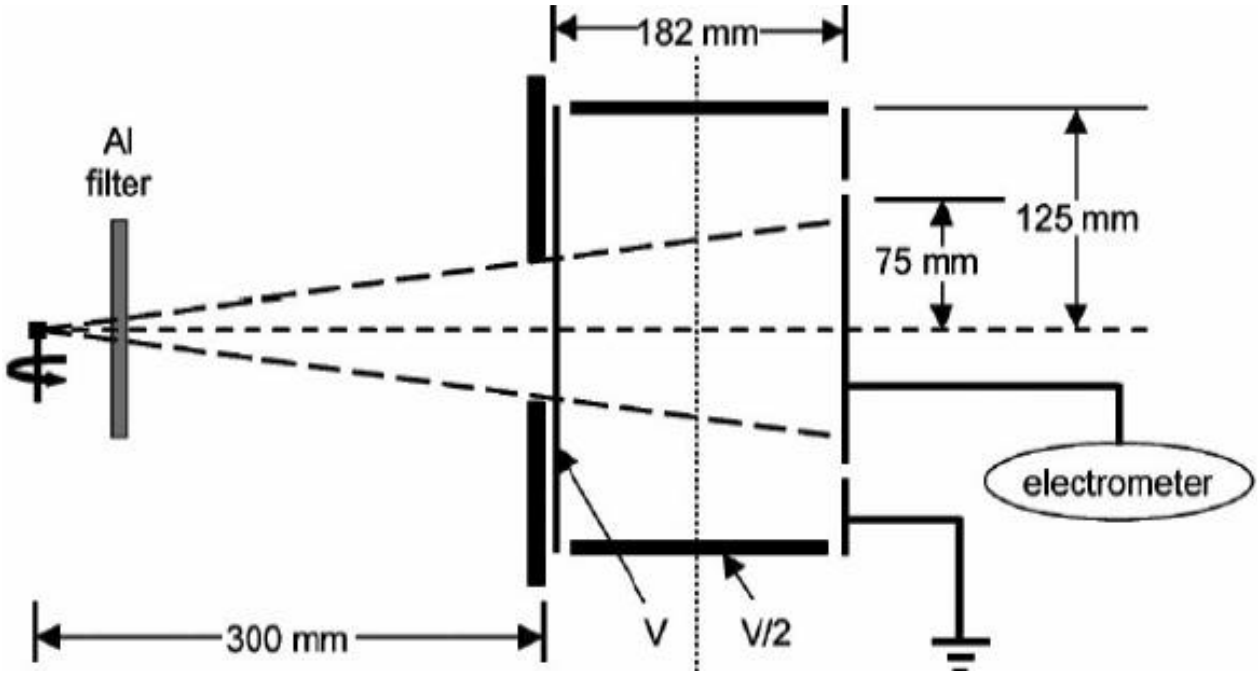

- Due to polar angle averaging, S_K increases for sources with radioactivity distributed over cyl. ends, leading to Λ_{WAFAC} lower than Λ_{point} results.
- This effect depends on the ratio of marker diameter to marker length.
- Differences between Λ_{WAFAC} and Λ_{point} range from non-detectable to 3.5%.

Figure from : J. F. Williamson, Med. Phys. 27 (4) 643 2000

How efficient can MC be …?

Traditionally, MC was said to be too slow for clinical use and therefore reserved for high quality single source dosimetry in reference conditions that was then partitioned to TG-43 quantities and used in TPS for treatment planning purposes.

How efficient can MC be …?

Traditionally, MC was said to be too slow for clinical use and therefore reserved for high quality single source dosimetry in reference conditions that was then partitioned to TG-43 quantities and used in TPS for treatment planning purposes.

- Total t_{CALC} scales with N, which is determined by the level of desired type A uncertainty which is proportional to $\sqrt{Var(k)/N}$

- MC for Brachy enjoys t_{CALC}/N reduction from photon only tracking (20%-70%)

- In brachy however, t_{CALC}/N is large when multiple scattering occurs

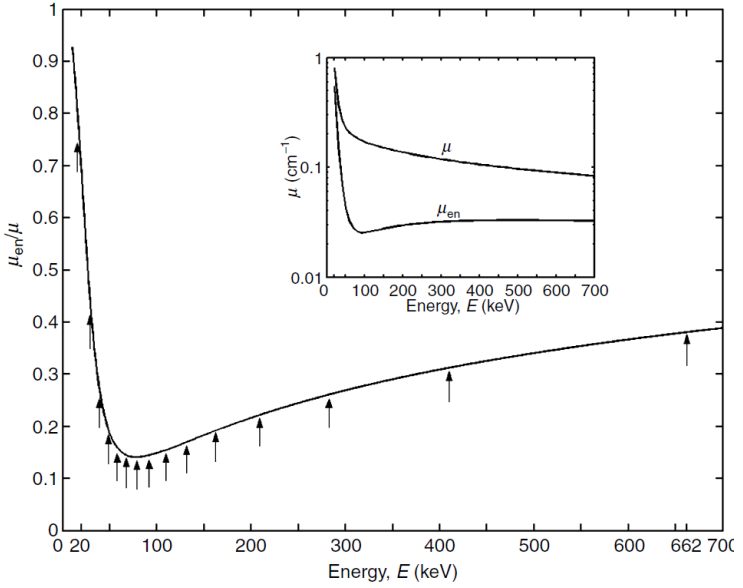

How efficient can MC be …?

t_{CALC} scales with N, type A uncertainty scales with $\sqrt{\frac{Var(k)}{N}}$

➢ The only means to decrease t_{CALC} for a given level of type A uncertainty is variance reduction.

➢ Variance reduction:

• Simple techniques: geom. truncation, E cut off, phase space files*, analytical primary scatter separation (PSS), …

(* Pantelis et al. On source models for 192Ir HDR brachytherapy dosimetry using model based algorithms Phys. Med. Biol. 61, 2016)

• Elaborate techniques**: techniques to bias the sampling distributions while using correction factors to eliminate the biasing effect in the sample mean of the quantity of interest

(** see Sheikh-Bagheri, D., Kawrakow, I., Walters, B., and Rogers, D.W.O. 2006. Monte Carlo simulations: Efficiency improvement techniques and statistical considerations. Integrated New Technologies into the Clinic: Monte Carlo and Image-Guided Radiation Therapy—Proceedings of the 2006 AAPM Summer School)

Monte Carlo for TPS?

- t_{CALC} reductions from: photon only tracking (20%-70%), track length scoring (20-30), pre-calculated source phase space (30%-40%), variance reduction (40-60) + (inherent) parallelization and reduction of t_{CALC}/N from availability of multi-core processors have facilitated clinically viable calculation times :

✓ sub-minute to minutes for LDR applications

MCPI (GEPTS): Chibani & Williamson 2005 Med Phys 32, 3688

BRACHYDOSE (EGSnrc): Thomson et al 2010 Med. Phys. 37, 3910

ALGEBRA (GEANT4): Afsharpour et al. 2012 Phys Med Biol 57, 3273

✓ 2.5–17 minutes for 40^3–140^3 2mm voxels for HDR rectal application

BRACHYGUI (PTRAN) Poon et al 2008 J Phys Conf Ser 102, 012018.

- further reduction of of t_{CALC}/N from GPU implementation :

✓Tian et al, “Monte Carlo dose calculations for high-dose–rate brachytherapy using GPU-accelerated processing,” *Brachytherapy* 15(3), pp. 387 (2016).

Monte Carlo for TPS?

- recent efforts in the literature have focused on GUI functionality and/or further optimization for brachytherapy specific use :
  - ✓ AMIGOBRACHY (MCNP6): Fonseca et al, 2014, Brachytherapy 13, 632
  - ✓BrachyGuide (MCNP6): Pantelis et al 2015 JACMP 16, 208

Freely distributed through www.rdl.gr

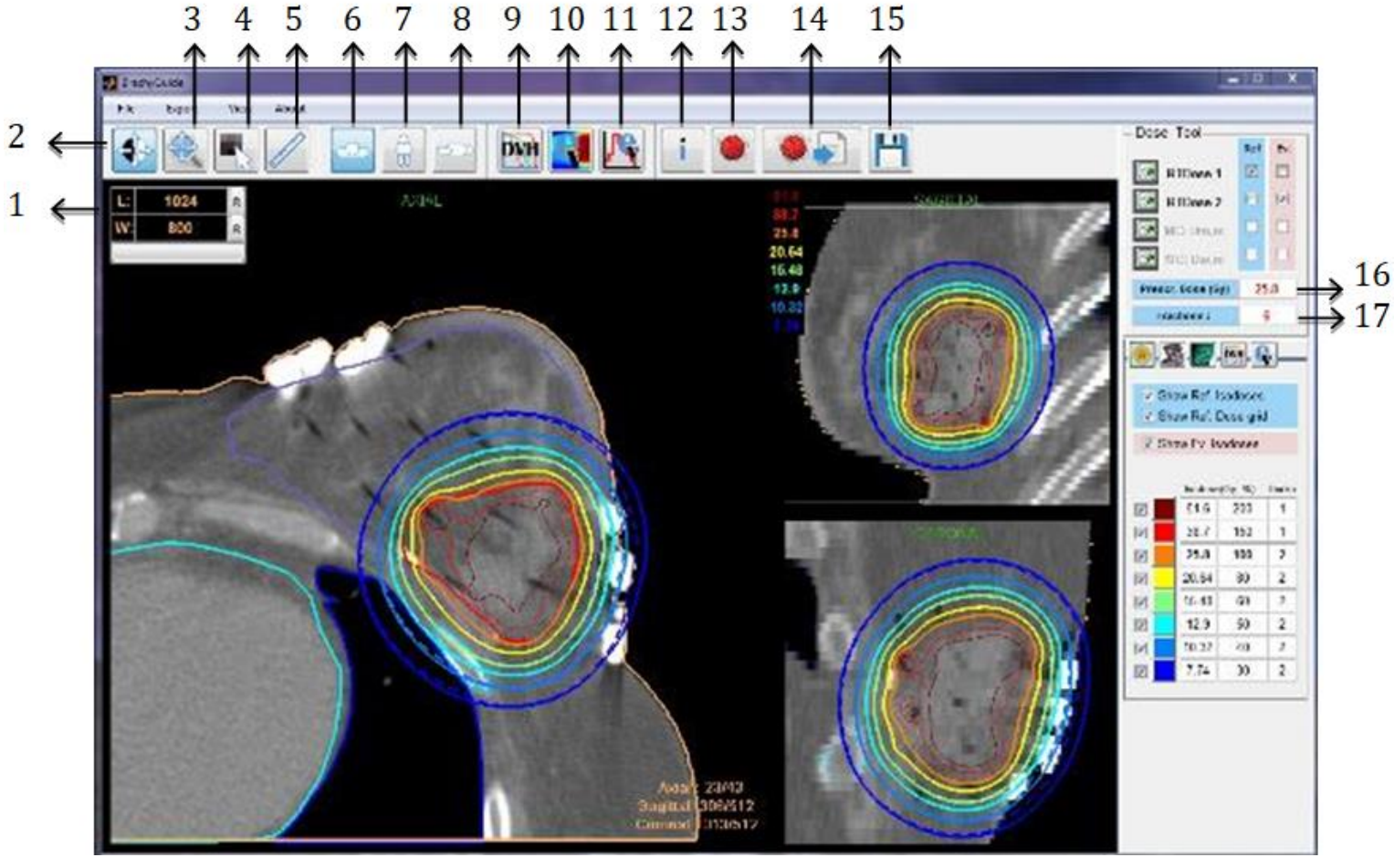

Monte Carlo for TPS?

- recent efforts in the literature have focused on GUI functionality and/or further optimization for brachytherapy specific use :
  - ✓ AMIGOBRACHY (MCNP6): Fonseca et al, 2014, Brachytherapy 13, 632
  - ✓BrachyGuide (MCNP6): Pantelis et al 2015 JACMP 16, 208

Item	Function
File menu	import data (Session, RT Plan, RTSS, CT Scale) and exit
View menu	display VOIs, source dwell positions and isodose lines on patient images, display CT calibration curve
Export menu	save current session and anonymize current data
Tool 1	window and level selection, image series navigation
Tool 2	change image window and level by pressing left mouse button while moving the mouse up/down and/or left/right
Tool 3	image panning and zooming
Tool 4	pixel value tool
Tool 5	Ruler (measure the distance between two points on the image in mm)
Tool 6	main view: axial
Tool 7	main view: coronal
Tool 8	main view: sagittal
Tool 9	display the Dose Volume Histogram (DVH) on the main view of the GUI
Tool 10	display results from the comparison between the reference and the evaluated dose distribution, on the axial, sagittal and coronal images using an appropriate color map
Tool 11	display the relative histogram of the results from the comparison between the reference and the evaluated dose distribution
Tool 12	display imported image series information
Tool 13	create a lattice-based patient geometry model
Tool 14	create the input file for the MCNP code
Tool 15	save the session (i.e., CT images and RT data) for quick loading
Tool 16	define prescription dose (if RTPLAN hasn't been loaded, a prescription dose of 10Gy is used by default)
Tool 17	define number of prescribed fractions (if RTPLAN hasn't been loaded, single fraction is used by default)

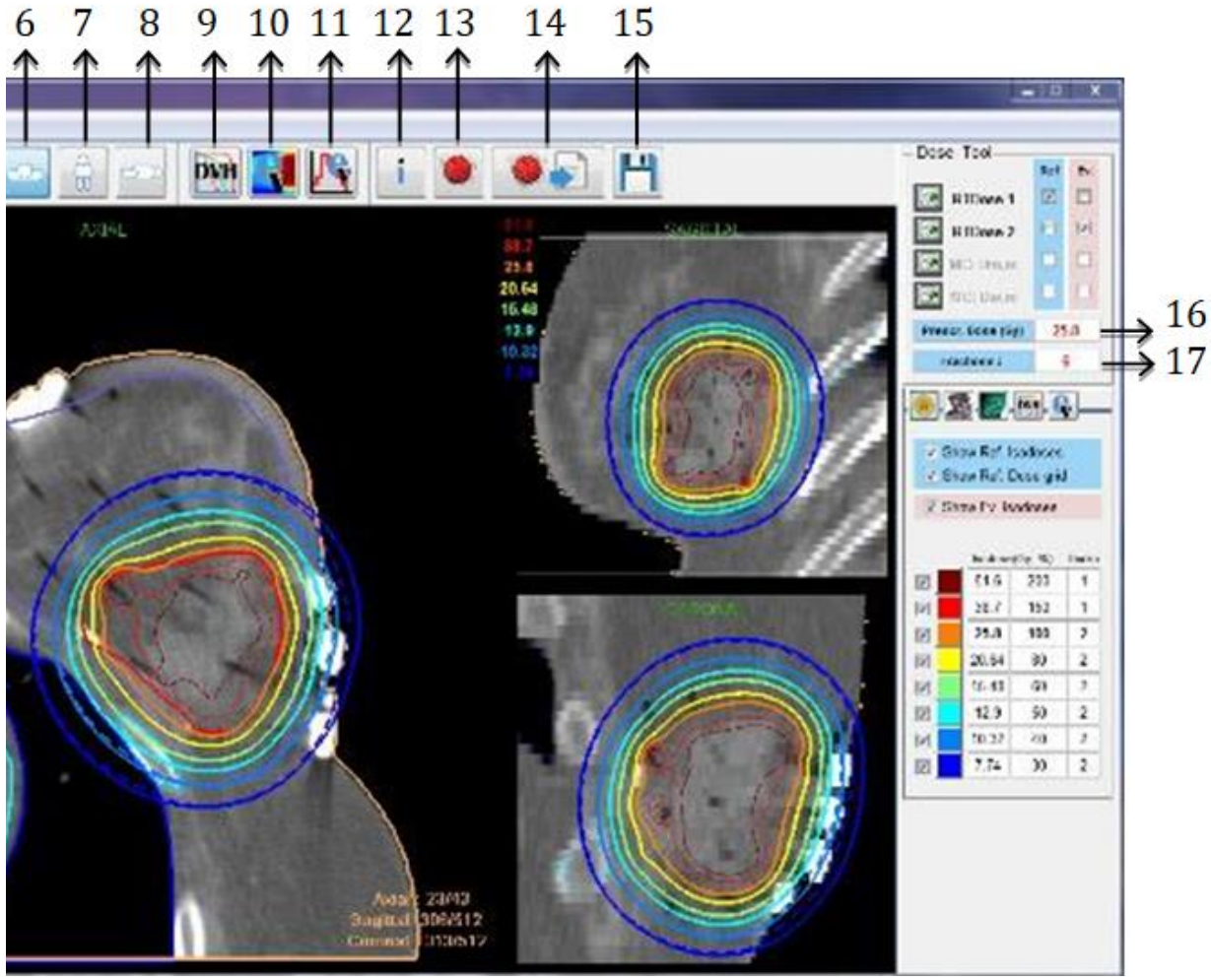

Monte Carlo for TPS?

✓ BrachyGuide (MCNP6): Pantelis et al 2015 JACMP 16, 208

- compatible with the DICOM-RT file format implementation from all three major vendors
- GUI serves as a viewer for all data parsed from DICOM-RT
- GUI also serves as a front end MCNP software tool (no MCNP experience required)
- patient represented by rectangular grid (CT resolution that can be down-sampled)
- individual voxel density from CT data based on generic or custom calibration
- option for density binning using 54 bins (accuracy better than 1%, Peppa et al 2013, Radiother Oncol. 106,S371)
- elemental composition assigned using a look-up table of 23 human tissue composition bins (Schneider et al 2000, Phys Med Biol. 45, 459)
- incorporates RTDose and MCNP output comparison tools (%D.d., isodose, DVH, g-index)
- source represented by its phase space file (no library available)
- no applicator library available
- user must edit the generated input file to employ variance reduction and other speed enhancement techniques

Monte Carlo for TPS?

- recent efforts in the literature have focused on GUI functionality and further optimization for brachytherapy specific use :
  - ✓ egs_brachy (EGSnrc): Chamberland et al 2016 Phys. Med. Biol. 61 8214

• 3868cm^3 water breast model with 30 ^{192}Ir HDR source implant: 2mm^3 scoring in 4cm^3 region with 2% PTV type A uncert. takes 147 s (151 s)
• 13548cm^3 inhomogeneous breast model with 79 ^{192}Ir HDR source implant:
2x2x3mm^3 scoring in 34x34x12cm^3 region takes 102 s (119 s) for 2% PTV type A uncert. and
222 s (238 s) for 2% PTV and 5% skin type A uncert.
(single 2.5 GHz Intel Xeon E5-2680 v3)

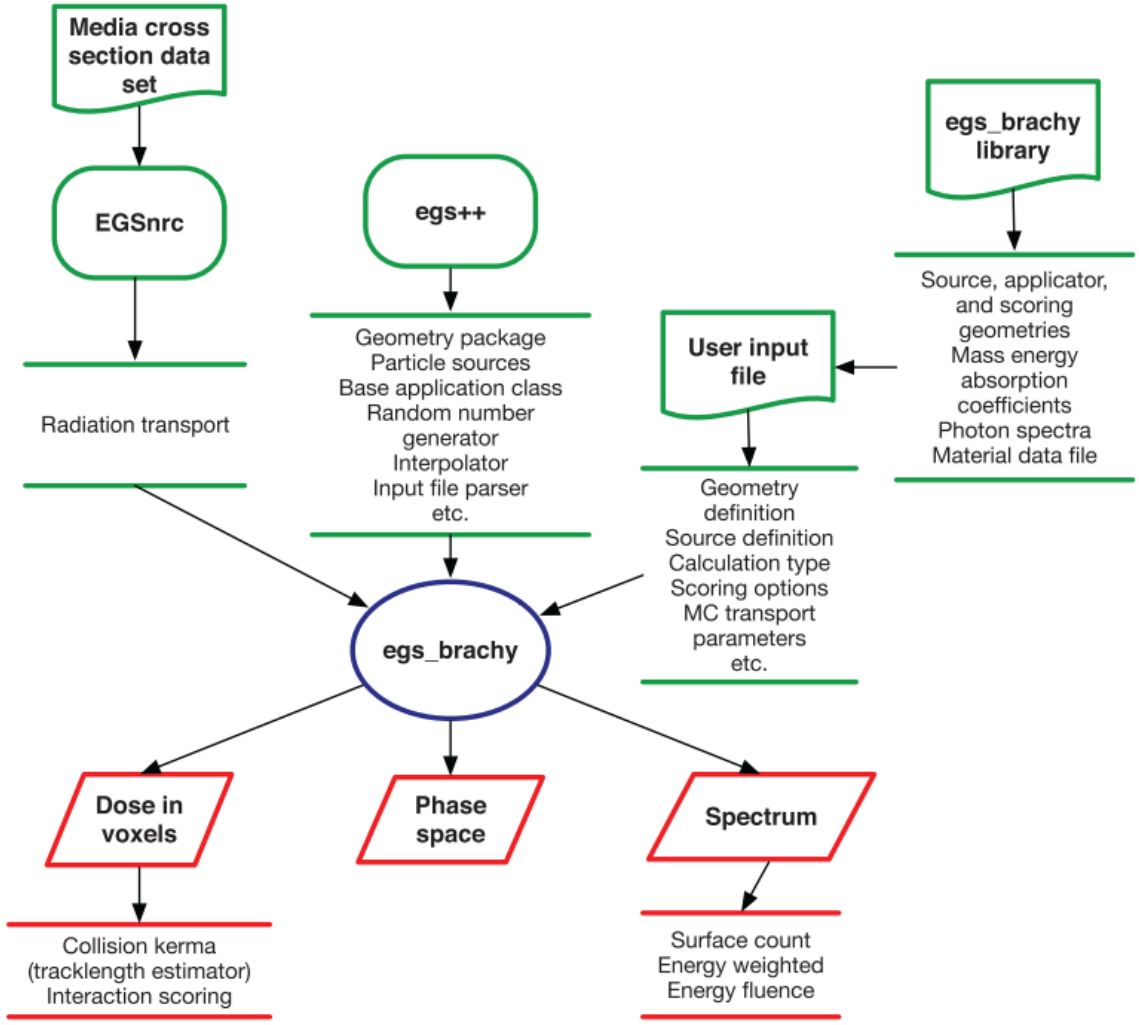

Monte Carlo for TPS?

✓ egs_brachy (EGSnrc): Chamberland et al 2016 Phys. Med. Biol. 61 8214

- includes a library of geometry models for many brachytherapy sources, in addition to eye plaques and applicators
- offers extensive capabilities and options

(comensurate to EGSnrc and its applications e.g.: complex geometries can be modelled using the built-in elementary and composite geometries of egs++, DOSXYZnrc can be used to prepare a rectilinear phantom by a CT dataset in egsphant file format, EGS_AutoEnvelope, can be used to inscribe copies of a source geometry inside a phantom)

but no front end GUI (so experience with EGS is required)

Monte Carlo for TPS?

- recent efforts in the literature have focused on GUI functionality and further optimization for brachytherapy specific use :

✓ RapidBrachyMCTPS (GEANT4): Famulari et al 2018 Phys. Med. Biol. 63 175007

• prostate HDR implant of 144 dwell positions:
2% PTV type A uncert. takes
2.4, 5.1, and 18.2 min
for
3, 2, and 1 mm^3
scoring resolution
(single Intel core from a 2.6 GHz processor)

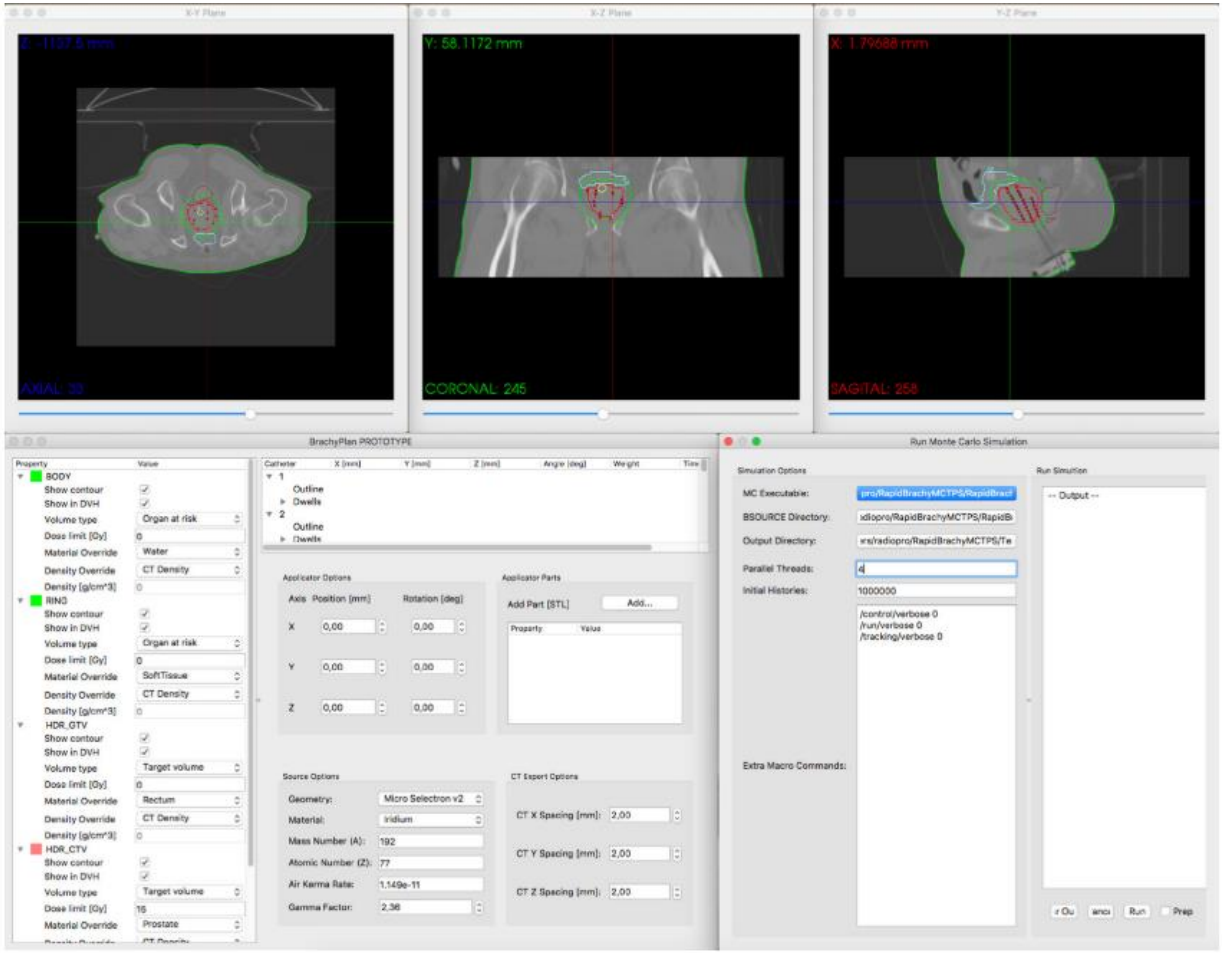

Monte Carlo for TPS?

✓ RapidBrachyMCTPS (GEANT4): Famulari et al 2018 Phys. Med. Biol. 63 175007

- DICOM-RT image data and structure set imported using VTK
- GUI serves as a viewer for all data parsed from DICOM-RT
- GUI also serves as a front end GEANT4 software tool (no GEANT4 experience required)
- source and applicator libraries available through the GUI
- CT numbers converted to density and material for each voxel via user-specified data. Segmentation can also be performed based on the patients structure set
- patient data is saved using the egsphant file format
- the user can change various simulation settings, physics options, and scoring options via the GUI
- the GUI also incorporates some (basic) treatment planning functionalities (simulated annealing-based optimization with dose constraints)

Monte Carlo: summary

- !Monte Carlo based TPS not clinically available for brachytherapy yet!

- MC is the gold standard for single source dosimetry in brachytherapy (TG-43 data)
- Several public domain codes are available that have been extensively benchmarked, and ample literature/experience/recommendations are available
- Type B uncertainties associated with MC results for single source dosimetry are (mainly) user-related
- MC is inherently associated with a level of type A uncertainty

- MC is also used:
  - to support source calibration,
  - to correct experimental dosimetry results,
  - to provide input data to other classes of dose calculation algorithms
  - to provide reference dose distributions for the verification of TPS results

Further reading …

• A. Haghighat, Monte Carlo Methods for Particle Transport, CRC Press, Taylor & Francis, © 2015

• W.L. Dunn. J. K. Shultis (Eds), Exploring Monte Carlo Methods. CRC Press, Elsevier B.V. © 2012

• Venselaar, Baltas, Meigooni, Hoskin (Eds), Comprehensive Brachytehrapy: physical and clinical aspects. CRC Press, Taylor & Francis, © 2013

• Rivard, M.J. et al., 2004. Update of AAPM Task Group No. 43 Report: A revised AAPM protocol for brachytherapy dose calculations. Medical Physics, 31(3), p.633.

• Perez-Calatayud, J. et al., 2012. Dose calculation for photon-emitting brachytherapy sources with average energy higher than 50 keV: report of the AAPM and ESTRO. Medical physics, 39(5), pp.2904–29.

and references therein

• references cited herein

ESTRO School

WWW.ESTRO.ORG/SCHOOL

ESTRO School

Advanced Brachytherapy Physics

Background and Details on TG-43 Based Dosimetry

Prof. Mark J. Rivard, Ph.D., FAAPM

Advanced Brachytherapy Physics, 29 May – 1 June, 2016

ESTRO School

Disclosures

The are no conflicts-of-interest to report.

Opinions herein are solely those of the presenter, and are not meant to be interpreted as societal guidance.

Specific commercial equipment, instruments, and materials are listed to fully describe the necessary procedures. Such identification does not imply endorsement by the presenter, nor that these products are necessarily the best available for these purposes.

Learning Objectives

1. Review need for international BT dosimetry formalism

2. Explore the TG-43 BT dosimetry formalism

3. Example calculations and TPS source commissioning

Why Follow the TG-43 Dose Calculation Formalism?

- Accurate interpolation of dose distribution is achieved because geometric dependence of dose falloff (as function of r and θ) is accounted for. This allows use of a limited dataset while providing robust dose calculation.

- Analytic, uniform approach to brachytherapy dose calculation is readily available, thereby promoting consistent clinical practice worldwide.

Rivard, et al., *Med. Phys.* 31, 633-674 (2004)
Perez-Calatayud, et al., Med. Phys. 38, 2904-2929 (2012)

ESTRO School

Low-Energy BT Dosimetry Report

Medical Physics

Update of AAPM Task Group No. 43 Report:
A revised AAPM protocol for brachytherapy dose calculations

Since publication of the TG-43 protocol in 1995, significant advances have taken place in the field of permanent source implantation and brachytherapy dosimetry. To accommodate these advances, the AAPM deemed it necessary to update this protocol for the following reasons:

(a) eliminate minor inconsistencies and omissions in the original TG-43 formalism and its implementation.

(b) incorporate subsequent AAPM recommendations, addressing requirements for acquisition of dosimetry data as well as clinical implementation. These recommendations, e.g., elimination of A_{app} (see Appendix E) and description of minimum standards for dosimetric characterization of low-energy photon-emitting brachytherapy sources, needed to be consolidated in one convenient document.

(c) critically reassess published brachytherapy dosimetry data for the ^{125}I and ^{103}Pd source models introduced both prior and subsequent to publication of the TG-43 protocol in 1995, and to recommend consensus datasets where appropriate.

(d) develop guidelines for determination of reference-quality dose distributions by experimental and Monte Carlo methods, and promote consistency in derivation of parameters used in TG-43 formalism.

Rivard, et al., *Med. Phys.* 31, 633-674 (2004)

ESTRO School

High-Energy BT Dosimetry Report

Medical Physics

Dose calculation for photon-emitting brachytherapy sources with average energy higher than 50 keV: Report of the AAPM and ESTRO

Purpose: Recommendations of the AAPM and ESTRO on dose calculations for high energy (avg energy > 50 keV) photon-emitting brachytherapy sources are presented, including physical characteristics of specific ^{192}Ir, ^{137}Cs, and ^{60}Co.
Methods: This report was prepared by the High Energy Brachytherapy Source Dosimetry (HEBD) Working Group, and includes considerations for applying the TG-43U1 formalism to high-E photon-emitting sources with particular attention to phantom size effects, interpolation accuracy dependence on dose calculation grid size, and dosimetry parameter dependence on active length.
Results: Consensus datasets for commercially available sources are provided, along with recommended methods for evaluating these datasets. Recommendations on dosimetry characterization methods, mainly using experimental procedures and Monte Carlo, are established and discussed. Included are methodological recommendations on detector choice, detector energy response characterization and phantom materials, and measurement specification methodology. Uncertainty analyses are discussed and recommendations are given for sources without consensus datasets.
Conclusions: Recommended consensus datasets for high-energy sources are derived for sources that were commercially available as of January 2010. Data are presented according to the AAPM TG-43U1 formalism, with modified interpolation and extrapolation techniques of the AAPM TG-43U1S1 report for the 2D anisotropy function and radial dose function.

Perez-Calatayud, et al., *Med. Phys.* 39, 2904-2929 (2012)

ESTRO School

BT Dose Calculation Geometry

reference position

r_0 = 1 cm

θ_0 = 90°

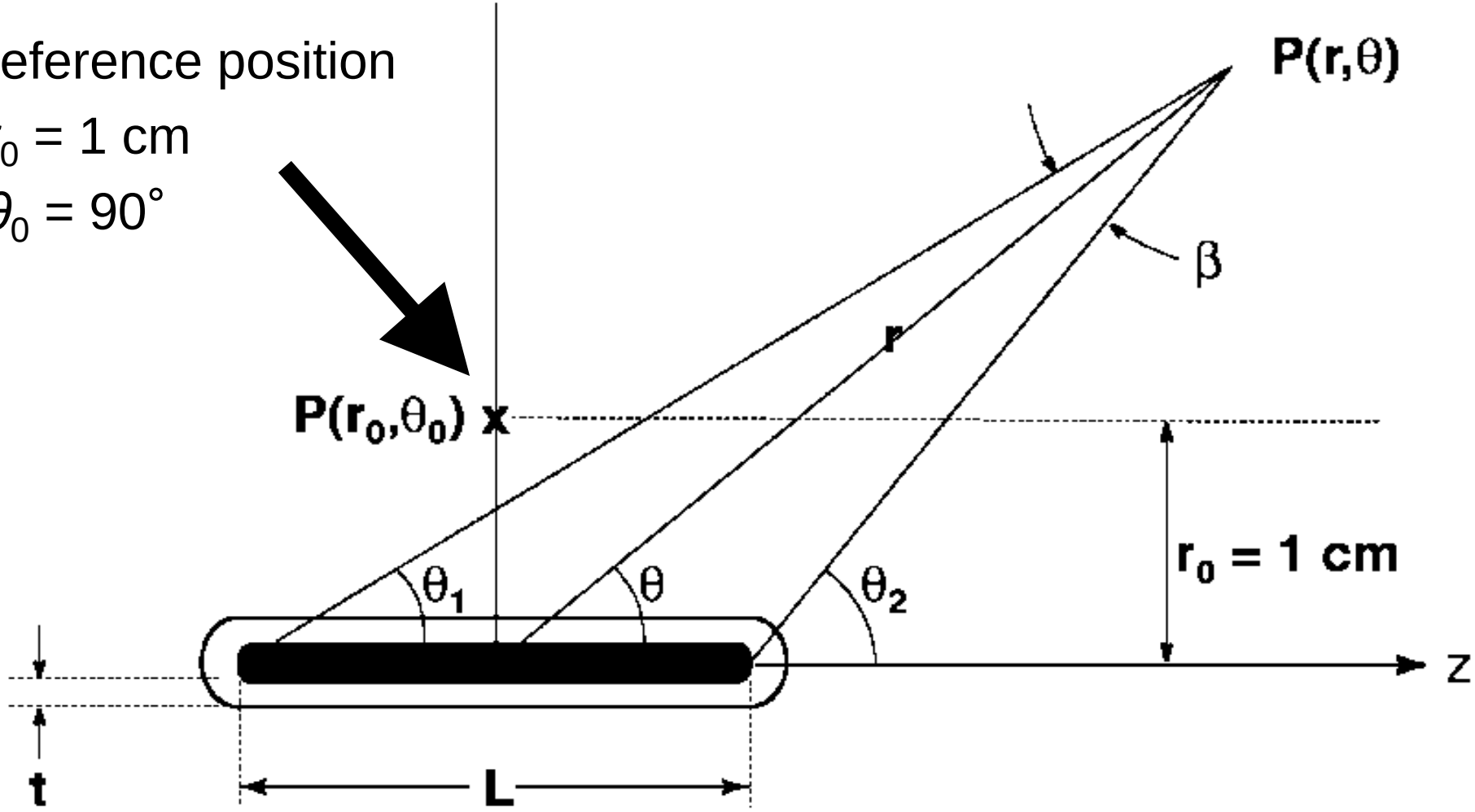

Rivard, et al., *Med. Phys.* 31, 633-674 (2004)

ESTRO School

Origin and Angular Notation

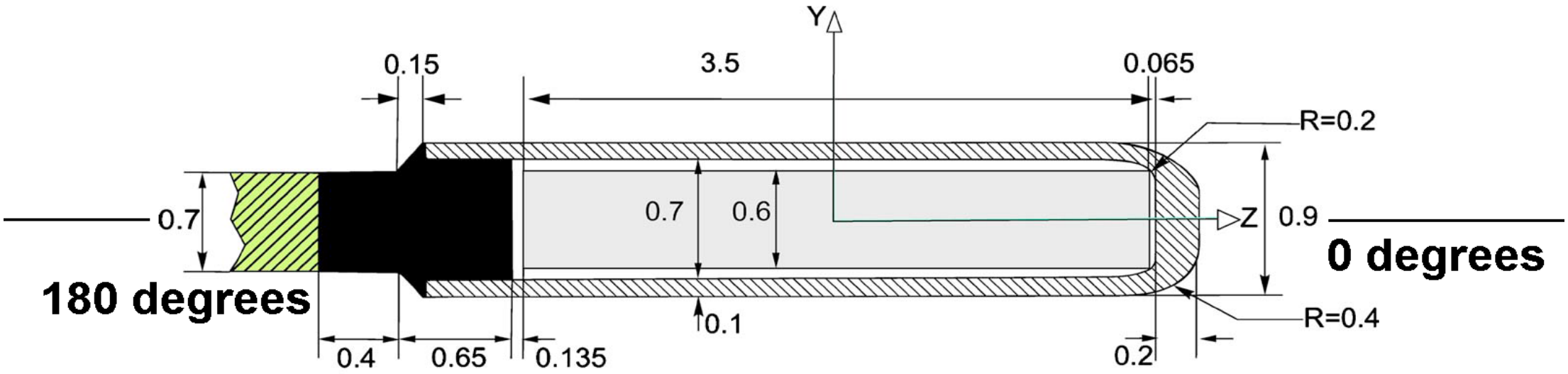

dimensions need to be in centimeters (cm), not millimeters

Perez-Calatayud, et al., *Med. Phys.* 39, 2904-2929 (2012)

ESTRO School

Low-Energy LDR Seeds

Dynamic source orientation influences some dose distributions

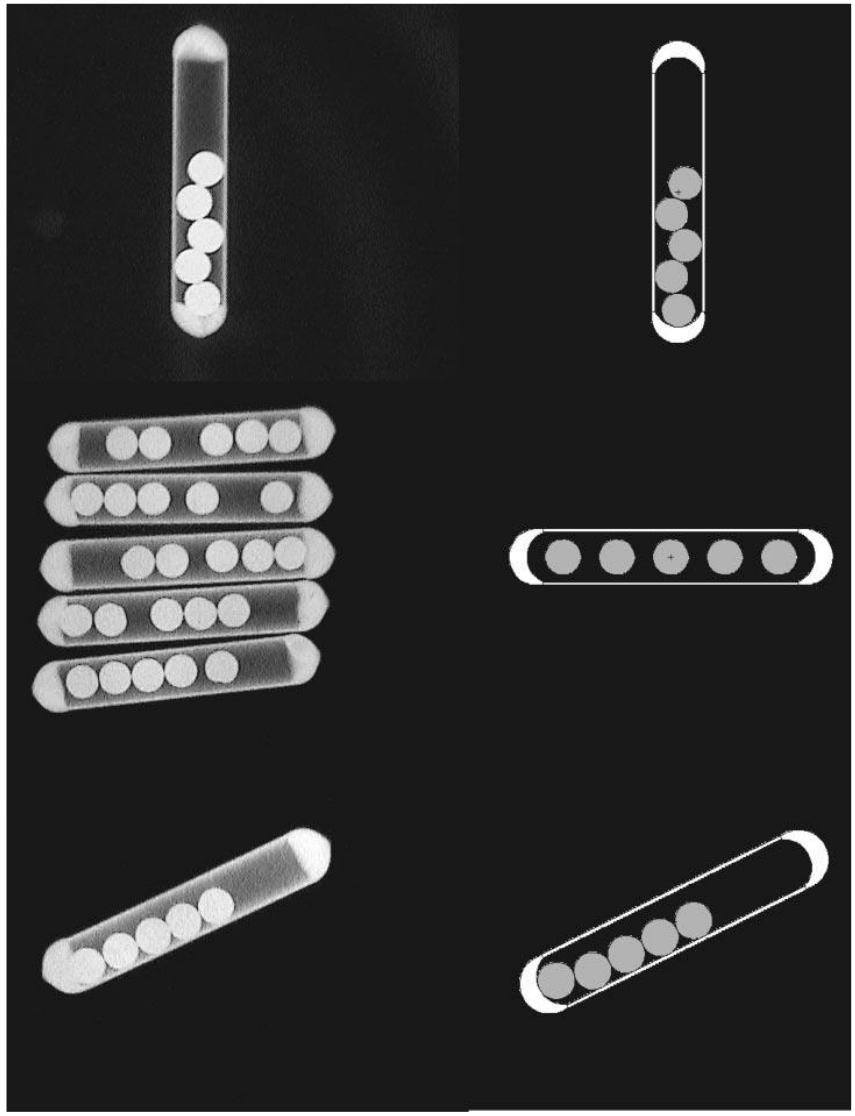

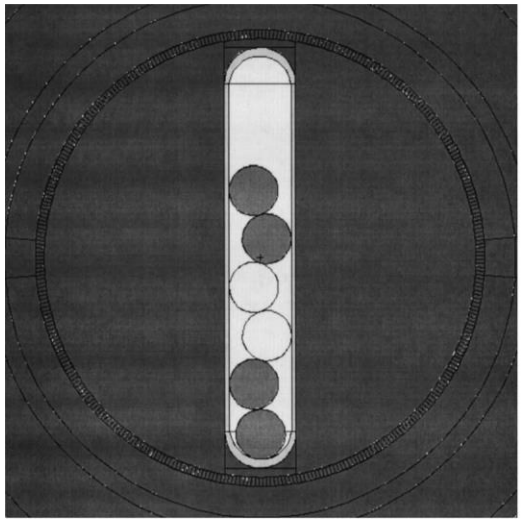

(a)

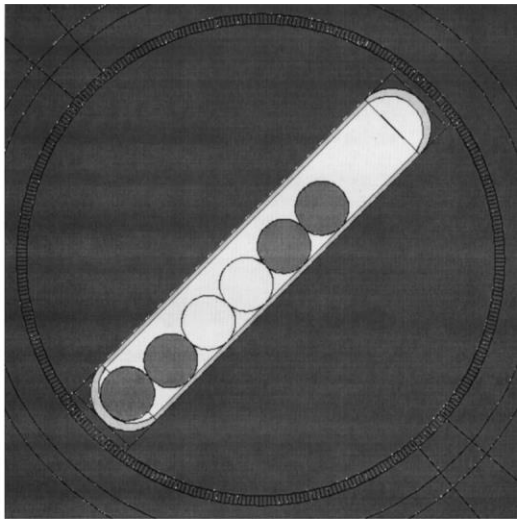

(b)

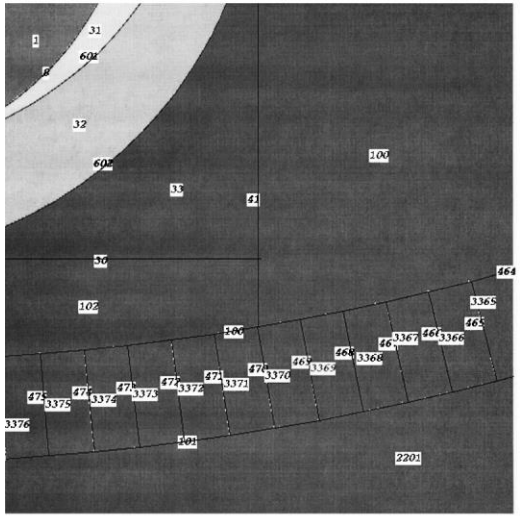

(c)

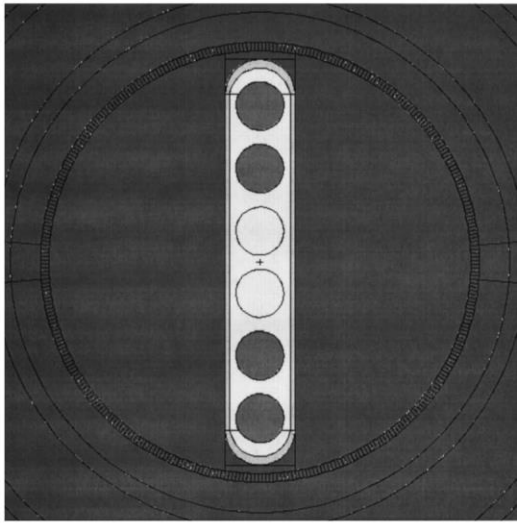

(d)

TG-43 2D Formalism

$$\dot{D}(r,\theta) = S_K \ \Lambda \ \frac{G(r,\theta)}{G(r_0,\theta_0)} \ g_L(r) \ F(r,\theta)$$

$\dot{D}(r,\theta)$	dose rate to water at point P(r,θ)
S_K	air kerma strength
Λ	dose rate constant
$G_L(r,\theta)$	geometry function (line-source approximation)
$g_L(r)$	radial dose function
$F(r,\theta)$	2D anisotropy function

Rivard, et al., *Med. Phys.* 31, 633-674 (2004)

ESTRO School

TG-43 2D Formalism

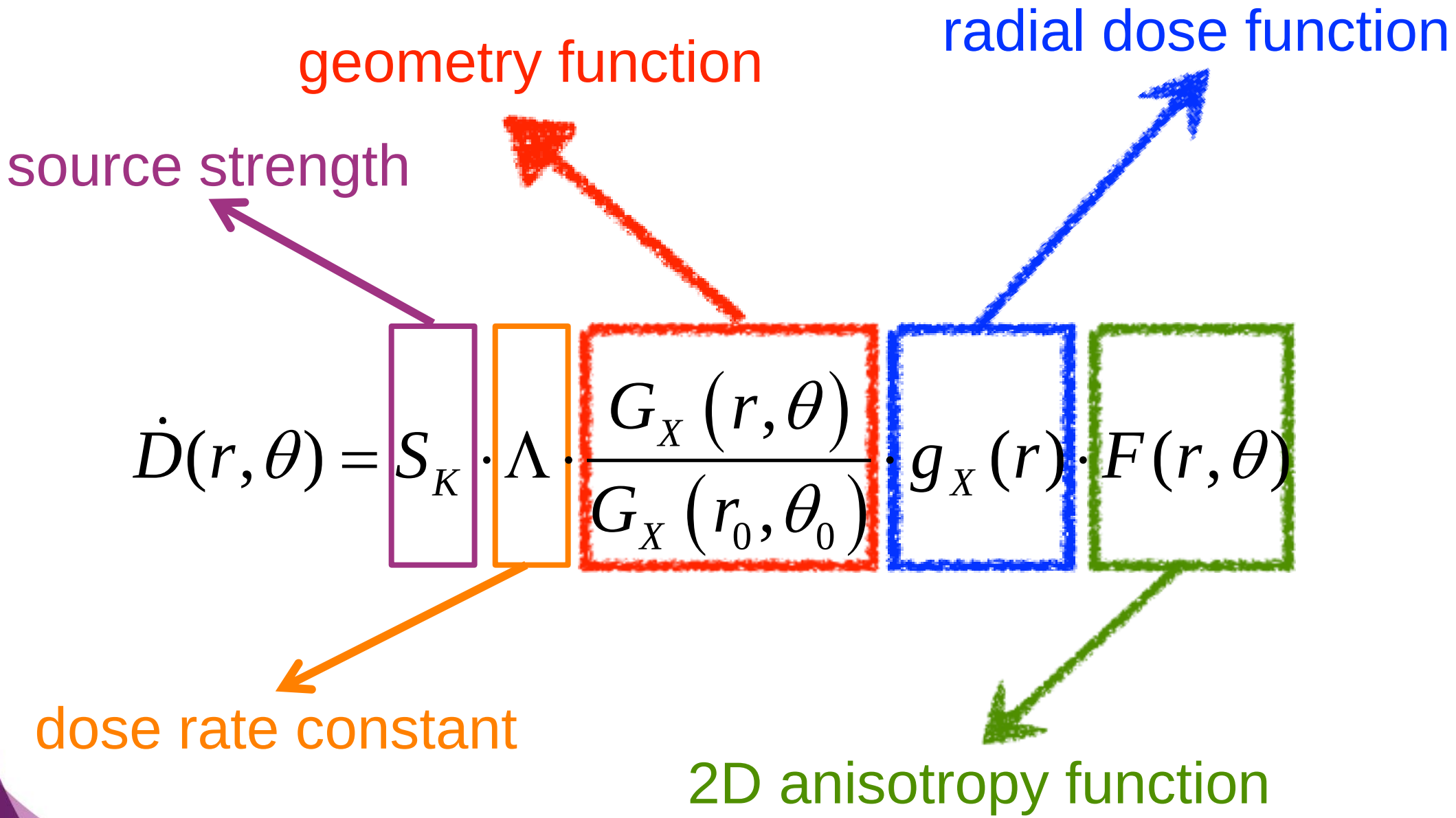

slide adapted from Luc Beaulieu

ESTRO School

TG-43 1D Formalism: Comparisons

BAD $$\dot{D}(r) = S_K \cdot \Lambda \cdot \frac{G_L(r,\theta_0)}{G_L(r_0,\theta_0)} \cdot g_P(r) \cdot \phi_{an}(r)$$

BAD $$\dot{D}(r) = S_K \cdot \Lambda \cdot \left(\frac{r_0}{r}\right)^2 \cdot g_L(r) \cdot \phi_{an}(r)$$

GOOD $$\dot{D}(r) = S_K \cdot \Lambda \cdot \left(\frac{r_0}{r}\right)^2 \cdot g_P(r) \cdot \phi_{an}(r)$$

BEST $$\dot{D}(r) = S_K \cdot \Lambda \cdot \frac{G_L(r,\theta_0)}{G_L(r_0,\theta_0)} \cdot g_L(r) \cdot \phi_{an}(r)$$

ESTRO School

TG-43 1D Formalism

$$\dot{D}(r) = S_K \ \Lambda \left(\frac{r_0}{r} \right)^2 \ g_P(r) \ \phi_{an}(r)$$

$\dot{D}(r)$	dose rate to water at point P(r,θ)
S_K	air kerma strength
Λ	dose rate constant
$1/r^2$	geometry function (point-source approximation)
$g_P(r)$	radial dose function
$\phi_{an}(r)$	1D anisotropy function

Rivard, et al., *Med. Phys.* 31, 633-674 (2004)

ESTRO School

BT Source Strength

$$S_K = \dot{K}_\delta(d)\, d^2$$

$$1\ \mathrm{U} = 1\ \mu\mathrm{Gy\,h^{-1}\,m^2}$$

reference air kerma rate (RAKR)

ICRU 38, ICRU 60

Rivard, et al., *Med. Phys.* 31, 633-674 (2004)

Perez-Calatayud, et al., Med. Phys. 38, 2904-2929 (2012)

ESTRO School

Dose Rate Constant

$$\dot{D}(r_0,\theta_0) = S_K \cdot \Lambda \qquad \frac{\dot{D}(r_0,\theta_0)}{S_K} = \Lambda$$

$$\frac{\Lambda_L}{G_L(r_0,\theta_0)} = \frac{\Lambda_{L_{\mathrm{REF}}}}{G_{L_{\mathrm{REF}}}(r_0,\theta_0)}$$

$$\Lambda_{\text{Ir-192}} = 1.120 \times G_L(r_0,\theta_0)\ [\mathrm{cGy\,h^{-1}\,U^{-1}}]$$

$$\Lambda_{\text{Co-60}} = 1.094 \times G_L(r_0,\theta_0)\ [\mathrm{cGy\,h^{-1}\,U^{-1}}]$$

Perez-Calatayud, et al., *Med. Phys.* 39, 2904-2929 (2012)

ESTRO School

HEBD Dose Rate Constants

Source Name (Manufacturer)	$_{CON}\Lambda$ [cGy·h^{-1}·U^{-1}]	Statistical uncertainty (k = 1)	$_{CON}\Lambda/G_L(r,\theta)$ [cGy·cm^2·h^{-1}·U^{-1}]
mHDR-v1 (Nucletron)	1.116	0.9%	1.127
mHDR-v2 (Nucletron)	1.109	1.1%	1.121
VS2000 (Varian)	1.100	0.6%	1.123
Buchler (E&Z BEBIG)	1.117	0.4%	1.119
GammaMed HDR 12i (Varian)	1.118	0.4%	1.129
GammaMed HDR Plus (Varian)	1.117	0.4%	1.128
GI192M11 (E&Z BEBIG)	1.110	0.4%	1.121
Ir2.A85-2 (E&Z BEBIG)	1.109	1.2%	1.120
M-19 (SPEC)	1.114	0.2%	1.125
Flexisource (Isodose Control)	1.113	1.0%	1.124

Perez-Calatayud, et al., *Med. Phys.* 39, 2904-2929 (2012)

Geometry Function

$$G(r,\theta)=\frac{\arctan\left[L/(2r\sin\theta)+\cot\theta\right]+\arctan\left[L/(2r\sin\theta)-\cot\theta\right]}{Lr\sin\theta}$$

$$G_L(r,\theta)=\begin{cases}\dfrac{\beta}{Lr\sin\theta} & \text{if} \quad \theta\neq 0^\circ \\ (r^2-L^2/4)^{-1} & \text{if} \quad \theta=0^\circ\end{cases}$$

$$G(r,\theta_0)=\frac{2\arctan\left(L/2r\right)}{[Lr]}$$

Rivard, et al., *Med. Phys.* 26, 2445-2450 (1999)
Rivard, et al., *Med. Phys*. 31, 633-674 (2004)

HEBD Radial Dose Functions

	$g_L(r)$									
	Nucletron mHDR-v1	Nucletron mHDR-v2	Varian VS2000	E&Z BEBIG Buchler	Varian GammaMed HDR 12i	Varian GammaMed HDR Plus	E&Z BEBIG GI192M11	E&Z BEBIG Ir2.A85-2	SPEC M-19	Isodose Control Flexisource
r [cm]	$L = 0.35$ cm	$L = 0.35$ cm	$L = 0.5$ cm	$L = 0.13$ cm	$L = 0.35$ cm	$L = 0.35$ cm	$L = 0.35$ cm	$L = 0.35$ cm	$L = 0.35$ cm	$L = 0.35$ cm
0.00	*[0.991]*	*1.276*	*0.986*	*1.023*	*0.992*	*0.998*	*0.990*	*0.990*	*0.993*	*0.991*
0.06		1,276								
0.08		1,199								
0.10		1,110								
0.15		1,018								
0.20	[0.991]	1,001	0.986	1.023	0.992	0.998				
0.25	**[0.992]**	0.995	0.991	**1.018**	**0.992**	**0.997**	0.990	0.990	0.993	0.991
0.50	[0.997]	**0.997**	0.997	**1.002**	**0.994**	**0.996**	0.996	0.996	0.995	0.997
0.75	**[0.999]**	0.998	0.999	**0.999**	**0.997**	**0.998**	0.998	0.998	0.998	0.998
1	1	1	1	1	1	1	1	1	1	1
1.5	[1.002]	1,003	1.005	1.003	1.004	1.003	1.003	1.002	1.001	1.002
2	[1.004]	1,005	1.010	1.004	1.006	1.006	1.004	1.004	1.005	1.004
3	[1.006]	1,008	1.012	1.008	1.008	1.006	1.005	1.005	1.008	1.005
4	[1.006]	1,007	1.013	1.007	1.005	1.004	1.004	1.003	1.003	1.003
5	[1.001]	1,003	1.011	1.002	0.999	0.999	0.999	0.999	0.999	0.999
6	[0.993]	0.996	1.003	0.995	0.991	0.993	0.992	0.991	0.994	0.991
8	[0.970]	0.972	0.982	0.971	0.968	0.968	0.968	0.968	0.969	0.968
10	[0.934]	0.939	0.949	0.941	0.936	0.935	0.935	0.935	0.939	0.935

Perez-Calatayud, et al., *Med. Phys.* 39, 2904-2929 (2012)

ESTRO School

2D Anisotropy Function

$$F(r,\theta) = \frac{\dot{D}(r,\theta)}{\dot{D}(r,\theta_0)} \frac{G_X(r,\theta_0)}{G_X(r,\theta)}$$

- $F(r,\theta)$ is always unity for a perfect point source
- $F(r,\theta) = 1$ at θ_0
- $F(r,\theta)$ accounts for dose-rate variation over angles due to differing attenuation by source capsule, internal components, …
- Must know source orientation use 2D formalism
  - otherwise, use the 1D formalism

slide courtesy of Luc Beaulieu

HEBD 2D Anisotropy Function: HDR ^{192}Ir

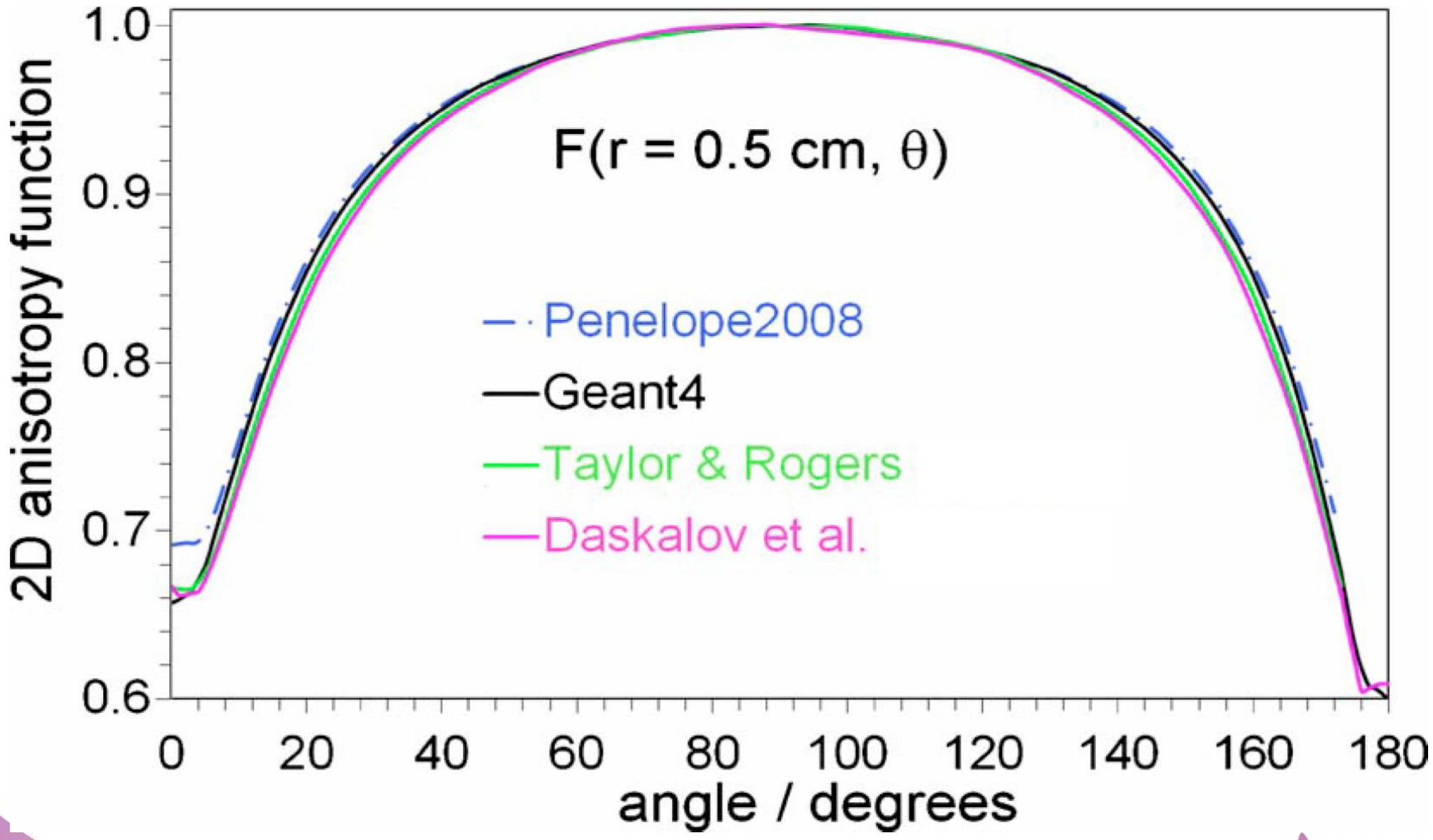

Granero, et al., *Med. Phys.* 38, 487-494 (2011)

ESTRO School

HEBD 2D Anisotropy Function (upper)

	r (cm)									
θ (deg)	0	0.06	0.08	0.10	0.15	0.20	0.25	0.30	0.35	0.40
0	*0.951*	*0.951*	*0.934*	*0.917*	*0.874*	0.831	0.787	0.744	0.714	0.692
2	*0.947*	*0.947*	*0.930*	*0.914*	*0.871*	0.829	0.786	0.744	0.714	0.693
4	*0.944*	*0.944*	*0.927*	*0.910*	*0.869*	0.827	0.785	0.744	0.714	0.694
6	*1.059*	*1.059*	*1.033*	*1.008*	*0.944*	0.881	0.817	0.754	0.721	0.707
8	*0.999*	*0.999*	*0.980*	*0.961*	*0.914*	0.866	0.819	0.772	0.744	0.730
10	*1.007*	*1.007*	*0.989*	*0.971*	*0.927*	0.882	0.837	0.793	0.766	0.755
12	*1.007*	*1.007*	*0.991*	*0.975*	*0.936*	0.897	0.858	0.819	0.791	0.780
14	*1.158*	*1.158*	*1.129*	*1.100*	*1.027*	0.954	0.881	0.830	0.811	0.804
16	*1.269*	*1.269*	*1.230*	*1.192*	*1.094*	0.997	0.900	0.851	0.832	0.825
18	*1.378*	*1.378*	*1.330*	*1.281*	*1.159*	1.037	0.915	0.867	0.850	0.844
20	*1.784*	*1.784*	*1.678*	*1.572*	1.306	1.041	0.933	0.885	0.868	0.861
22	*1.784*	*1.784*	*1.679*	*1.575*	1.313	1.050	0.942	0.893	0.881	0.875
26	*1.704*	*1.704*	*1.610*	*1.516*	1.281	1.046	0.953	0.920	0.906	0.900
30	*1.089*	*1.089*	*1.119*	1.149	1.225	1.049	0.961	0.932	0.923	0.919
32	*1.157*	*1.157*	*1.167*	1.178	1.203	1.039	0.966	0.939	0.931	0.927
36	*1.181*	*1.181*	*1.176*	1.170	1.156	1.023	0.971	0.949	0.944	0.941
40	*0.954*	*0.954*	1.053	1.152	1.109	1.016	0.974	0.961	0.955	0.953
50	*1.037*	*1.037*	1.071	1.104	1.047	0.999	0.981	0.976	0.974	0.973
60	*1.008*	1.008	1.041	1.062	1.013	0.998	0.993	0.987	0.986	0.985
70	*1.078*	1.078	1.023	1.026	1.001	0.997	0.996	0.995	0.994	0.994
80	*1.020*	1.020	1.005	1.007	1.000	1.002	1.003	0.998	0.998	0.998

Perez-Calatayud, et al., *Med. Phys.* 39, 2904-2929 (2012)

HEBD 2D Anisotropy Function (lower)

	r (cm)									
θ (deg)	0	0.06	0.08	0.10	0.15	0.20	0.25	0.30	0.35	0.40
100	1.012	1.012	1.002	1.008	0.996	0.995	0.999	0.999	0.999	0.999
110	1.069	1.069	1.029	1.025	1.006	0.994	0.996	0.995	0.994	0.994
120	1.004	1.004	1.049	1.060	1.020	0.999	0.992	0.988	0.986	0.986
130	1.056	1.056	1.080	1.105	1.047	1.003	0.985	0.976	0.975	0.974
132	1.043	1.043	1.077	1.111	1.058	1.002	0.982	0.974	0.972	0.970
134	1.021	1.021	1.078	1.135	1.068	1.007	0.982	0.971	0.968	0.967
136	1.011	1.011	1.075	1.138	1.076	1.014	0.979	0.967	0.964	0.963
138	1.080	1.080	1.113	1.146	1.098	1.016	0.977	0.963	0.961	0.958
140	0.983	0.983	1.068	1.153	1.113	1.020	0.982	0.961	0.956	0.954
144	1.184	1.184	1.176	1.169	1.151	1.033	0.978	0.951	0.945	0.942
148	1.140	1.140	1.155	1.169	1.204	1.031	0.976	0.942	0.932	0.928
150	1.099	1.099	1.128	1.158	1.232	1.052	0.967	0.930	0.923	0.920
154	1.631	1.631	1.554	1.477	1.285	1.093	0.959	0.914	0.904	0.899
158	1.725	1.725	1.636	1.547	1.324	1.101	0.947	0.896	0.879	0.873
160	1.741	1.741	1.649	1.558	1.329	1.099	0.937	0.880	0.863	0.858
162	1.515	1.515	1.452	1.389	1.230	1.072	0.914	0.862	0.846	0.840
164	1.382	1.382	1.331	1.280	1.153	1.025	0.898	0.843	0.826	0.820
166	1.961	1.961	1.845	1.729	1.439	1.150	0.860	0.819	0.804	0.797
168	1.036	1.036	1.016	0.996	0.946	0.895	0.845	0.794	0.779	0.770
170	0.894	0.894	0.884	0.874	0.850	0.825	0.801	0.776	0.752	0.741
172	0.880	0.880	0.870	0.860	0.835	0.810	0.786	0.761	0.736	0.711
174	0.626	0.626	0.627	0.627	0.628	0.629	0.630	0.631	0.632	0.633
176	0.575	0.575	0.575	0.576	0.577	0.579	0.580	0.582	0.583	0.585
178	0.536	0.536	0.537	0.537	0.539	0.540	0.542	0.543	0.545	0.546
180	0.497	0.497	0.498	0.499	0.500	0.502	0.503	0.504	0.506	0.507

Perez-Calatayud, et al., *Med. Phys.* 39, 2904-2929 (2012)

Example Dosimetry Parameter Dataset

	r [cm]	$g_L(r)$	$g_P(r)$	r [cm]	phi(r)		F(r,8)	0	10	20	30	40	50	60	70	80
1																
2	0.10	0.990	0.582	0.25	1.164		0.05							1.067	0.996	0.985
3	0.25	1.021	0.889	0.5	0.973		0.075					1.050	1.006	0.994	0.996	0.996
4	0.50	1.030	0.998	1.0	0.933		0.1				1.046	0.996	0.990	0.993	0.988	0.999
5	1.00	1.000	1.000	1.5	0.931		0.15			1.039	0.978	0.958	0.977	0.988	0.987	0.996
6	1.50	0.943	0.949	2.0	0.931		0.2		0.987	0.921	0.940	0.960	0.975	0.984	0.988	0.997
7	2.00	0.872	0.879	2.5	0.932		0.25	0.494	0.574	0.785	0.899	0.943	0.967	0.986	0.995	1.000
8	2.50	0.795	0.803	3.0	0.934		0.5	0.610	0.513	0.679	0.808	0.892	0.944	0.974	0.990	0.997
9	3.00	0.717	0.724	3.5	0.935		1	0.580	0.561	0.705	0.813	0.885	0.933	0.967	0.987	0.997
10	3.50	0.643	0.650	4.0	0.937		2	0.652	0.626	0.743	0.830	0.893	0.934	0.967	0.987	0.997
11	4.00	0.573	0.579	4.5	0.938		5	0.690	0.700	0.789	0.854	0.905	0.941	0.968	0.986	0.996
12	4.50	0.508	0.513	5.0	0.938		10	0.709	0.742	0.815	0.872	0.912	0.947	0.972	0.990	0.997
13	5.00	0.448	0.453	6.0	0.939											
14	6.00	0.347	0.351	7.0	0.942		**Λ =**	1.011								
15	7.00	0.265	0.268	10.0	0.948		**L = 3.7 mm or 0.37 cm**									
16	8.00	0.201	0.203													
17	9.00	0.151	0.153													
18	10.00	0.114	0.115													

prefer societal-recommended datasets

otherwise use AAPM/RPC Registry data and original pubs

websites (ESTRO, Univ. Carleton, etc) also post datasets

ESTRO School

HEBD 2D Along-Away QA Table

	y (cm)											
z (cm)	0	0.25	0.5	0.75	1	1.5	2	3	4	5	6	7
7	0.01690	0.01709	0.01724	0.01749	0.01772	0.01800	0.01797	0.01713	0.01564	0.01385	0.01209	0.01044
6	0.0227	0.0231	0.0235	0.0239	0.0243	0.0246	0.0244	0.0226	0.01996	0.01719	0.01455	0.01226
5	0.0320	0.0328	0.0337	0.0345	0.0351	0.0353	0.0345	0.0306	0.0259	0.0213	0.01750	0.01432
4	0.0487	0.0505	0.0524	0.0540	0.0549	0.0542	0.0513	0.0426	0.0338	0.0265	0.0208	0.01656
3	0.0819	0.0886	0.0936	0.0965	0.0967	0.0910	0.0813	0.0604	0.0440	0.0324	0.0244	0.01875
2	0.1776	0.2006	0.214	0.214	0.204	0.1704	0.1360	0.0853	0.0557	0.0384	0.0277	0.0207
1.5	0.311	0.364	0.382	0.362	0.324	0.241	0.176	0.0993	0.0614	0.0410	0.0290	0.0215
1	0.707	0.859	0.818	0.682	0.542	0.340	0.223	0.1124	0.0662	0.0431	0.0301	0.0220
0.5	3.45	3.47	2.19	1.354	0.885	0.446	0.264	0.1219	0.0694	0.0445	0.0308	0.0224
0	[redacted]	15.5	4.29	1.953	1.109	0.497	0.281	0.1254	0.0705	0.0449	0.0310	0.0225
–0.5	2.62	3.47	2.20	1.355	0.885	0.447	0.264	0.1219	0.0694	0.0445	0.0308	0.0224
–1	0.608	0.849	0.816	0.681	0.543	0.340	0.223	0.1124	0.0662	0.0431	0.0301	0.0220
–1.5	0.274	0.355	0.380	0.361	0.323	0.242	0.1764	0.0993	0.0614	0.0410	0.0290	0.0215
–2	0.1587	0.1927	0.212	0.213	0.203	0.1703	0.1361	0.0853	0.0558	0.0384	0.0277	0.0207
–3	0.0745	0.0840	0.0915	0.0955	0.0962	0.0907	0.0812	0.0605	0.0440	0.0324	0.0244	0.01875
–4	0.0422	0.0472	0.0507	0.0531	0.0543	0.0540	0.0512	0.0426	0.0338	0.0265	0.0208	0.01656
–5	0.0279	0.0304	0.0324	0.0337	0.0346	0.0351	0.0343	0.0306	0.0259	0.0213	0.01750	0.01432
–6	0.0200	0.0213	0.0225	0.0233	0.0238	0.0244	0.0242	0.0225	0.01994	0.01717	0.01455	0.01226
–7	0.01500	0.01576	0.01647	0.01697	0.01735	0.01780	0.01786	0.01708	0.01561	0.01384	0.01207	0.01044

Perez-Calatayud, et al., *Med. Phys.* 39, 2904-2929 (2012)

ESTRO School

HEBD Reference Data

	^{192}Ir	^{137}Cs	^{60}Co
Half-life	73.81 days	30.07 yr	5.27 yr
Type of disintegration	β^- (95.1%), EC (4.9%)	β^- (100%)	β^- (100%)
Maximum x-ray energy (keV)	78.6	37.5	8.3
Gamma energy-range (keV)	110.4–1378.2	661.6	1173.2–1332.5
Mean x-ray and gamma energy (keV)	350.0	613.0	1252.9
Maximum β^- ray energies (keV)	81.7 (0.103%) 258.7 (5.6%) 538.8 (41.43%) 675.1 (48.0%)	514.0 (94.4%) 1175.6 (5.6%)	318.2 (99.88%) 1491.4 (0.12%)
Mean β^- ray energy (keV)	180.7	188.4	96.5
Air-kerma rate constant, $\Gamma_{\delta=10\ \mathrm{keV}}$ (μGy m^2 h^{-1} MBq^{-1})	0.1091	0.0771	0.3059
Specific activity (GBq mg^{-1})	341.0	3.202	41.91

NNDC photon spectrum http://www.nndc.bnl.gov/nudat2/

H_2O @ 0.998 g/cm^3 (22˚ C)

dry air (0% humidity)

Perez-Calatayud, et al., *Med. Phys.* 39, 2904-2929 (2012)

ESTRO School

Locale for Dosimetry Parameter Datasets

- HEBD Report (AAPM+GEC-ESTRO) Med. Phys. 2012

- IROC Houston website (Brachytherapy Source Registry) (rpc.mdanderson.org/RPC/BrachySeeds/Source_Registry.htm

- ESTRO website

http://www.estro.org/about/governance-organisation/committees-activities/tg43

- University of Carleton website

http://www.physics.carleton.ca/clrp/seed_database

Data Interpolation/Extrapolation Methods

Parameter	$r < r_{min}$ Extrapolation	$r_{min} < r \leq r_{max}$ Interpolation	$r > r_{max}$ Extrapolation
$g_L(r)$	Nearest neighbor or zeroth-order extrapolation	Linear using datapoints immediately adjacent to the radius of interest	Linear using data of last two tabulated radii
$F(r,\theta)$	Nearest neighbor or zeroth-order extrapolation	Bilinear	Nearest neighbor or zeroth-order extrapolation

Perez-Calatayud, et al., *Med. Phys.* 39, 2904-2929 (2012)

ESTRO School

TG-43 Dataset Resolution

JOURNAL OF APPLIED CLINICAL MEDICAL PHYSICS, VOLUME 16, NUMBER 4, 2015

Brachytherapy treatment planning commissioning: effect of the election of proper bibliography and finite size of TG-43 input data on standard treatments

Christian N. Valdés,[1a] Gustavo H. Píriz,[2] Enrrique Lozano,[3]
Departamento de Física Médica,[1] Centro Oncológico de Antofagasta, Antofagasta, Chile;
Departamento de Física Médica,[2] Centro de Oncología ONCOSUR, Florida, Uruguay;
Departamento de Física Médica,[3] Instituto Nacional del Cáncer, Santiago, Chile
cvalcort@gmail.com

The aim of this work is to evaluate performance of a commercial BT TPS with vendor TG-43 data, analyze possible discrepancies with respect to a proper reference source and its implications for standard treatments, and judge the effectiveness of certain widespread recommended quality controls to find potential errors related with interpolations of TG-43 tables.

Valdés, et al., *J. Appl. Clin. Med. Phys*. 16, 3-17 (2015)

ESTRO School

TG-43 Dataset Resolution

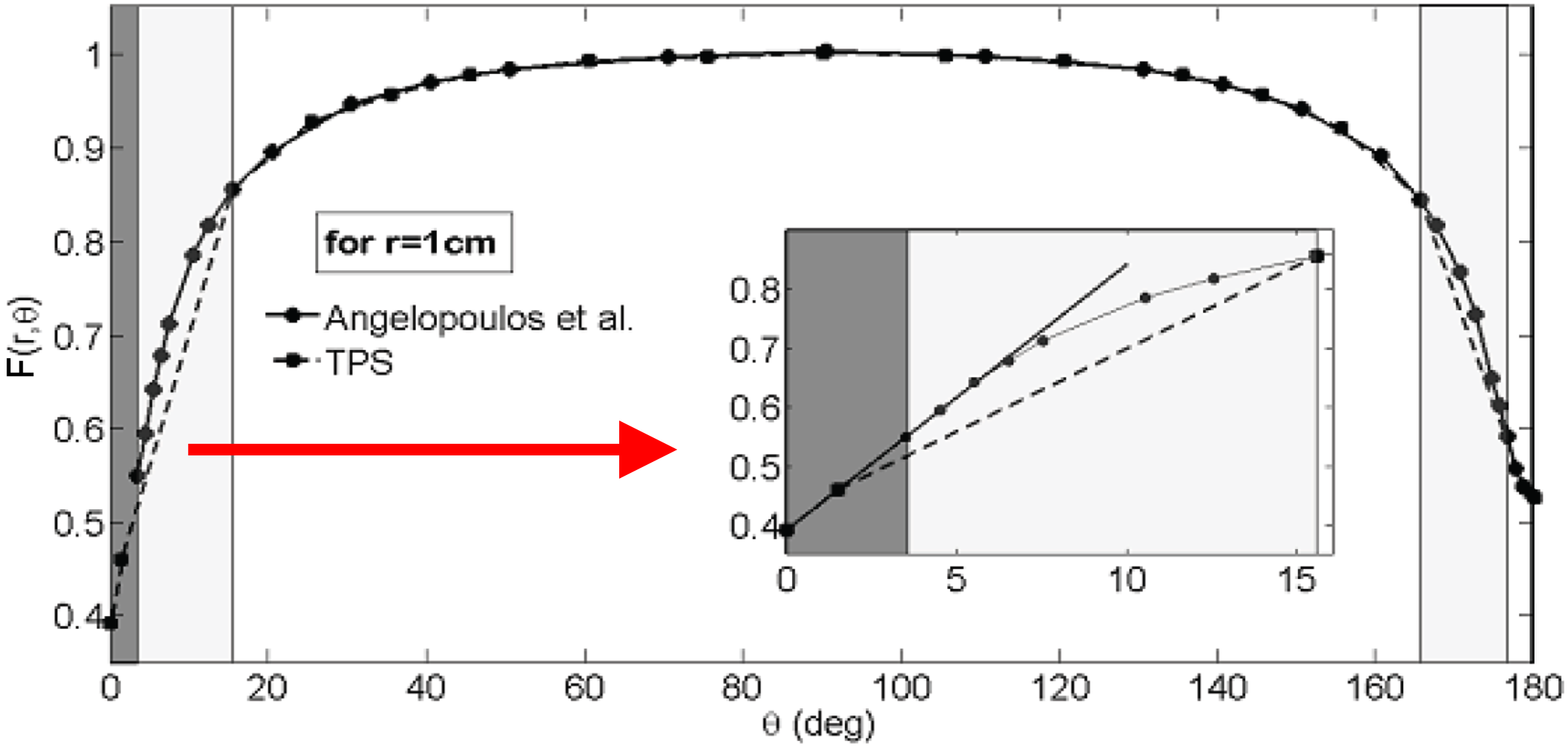

differences > 2% encompassed ~17% of surrounding source volume

Valdés, et al., *J. Appl. Clin. Med. Phys*. 16, 3-17 (2015)

ESTRO School

Monte Carlo Uncertainty Analysis: HDR ^{192}Ir

Component	$\dot{D}(1\ \text{cm}, \theta_0)$		$\dot{D}(5\ \text{cm}, \theta_0)$		s_K	
	Type A	Type B	Type A	Type B	Type A	Type B
Source geometry		0.46%		0.46%		0.46%
Capsule geometry		0.01%		0.01%		0.01%
Dynamic source design		0.4%		0.08%		0.04%
^{192}Ir photon spectrum		1.0%		1.0%		1.0%
MC physics		0.05%		0.05%		0.05%
Phantom composition		0.01%		0.05%		0.01%
Phantom cross sections		0.013%		0.067%		0.001%
Dose calculation (μ_{en}/ρ)		1.0%		1.0%		1.0%
Tally volume averaging		0.2%		0.4%		0.02%
Tally statistics	0.03%		0.03%		0.03%	
Quadrature sum	0.03%	1.54%	0.04%	1.50%	0.03%	1.49%
Total ($k=1$) uncertainty		1.54%		1.50%		1.49%

Granero, et al., *Med. Phys.* 38, 487-494 (2011)

ESTRO School

Example TLD Uncertainty Analysis: ^{125}I

TABLE II. Uncertainty determinations in experimental measurements of dose rate constant.

Component of uncertainty	Type A(%)	Type B(%)
Repetitive TLD measurements	4.6	
TLD dose calibration (including uncertainty in linac calibration)		2.0
Correction for energy dependence of LiF		5.0
Correction for solid water to liquid water conversion factor		3.0
Seed and TLD positioning		1.0
Quadrature combination	4.6	6.2
Total uncertainty (1σ)	7.7	
NIST uncertainty	0.5	
Total combined uncertainty	7.7	

Gearheart, et al., *Med. Phys.* 27, 2278-2285 (2000)

Example MC Uncertainty Analysis: ^{131}Cs

	$\dot{d}(1\text{ cm}, \theta_0)$		$\dot{d}(5\text{ cm}, \theta_0)$		s_K	
Component	A	B	A	B	A	B
Source:capsule geometry		0.16%		0.16%		0.16%
Dynamic internal components		0.02%		0.05%		0.02%
Source radiation spectrum		0.1%		0.7%		0.2%
Phantom composition		0.01%		0.02%		0.01%
Physics of Monte Carlo code		0.3%		0.7%		0.3%
Cross-sections in phantom		0.2%		0.9%		0.2%
μ_{en}/ρ for dose calculation		1.2%		1.2%		1.2%
Tally volume averaging		0.006%		<0.001%		<0.001%
Tally statistics	0.02%		0.04%		0.03%	
Quadrature sum	0.02%	1.3%	0.04%	1.8%	0.03%	1.3%
Total (k=1) uncertainty	1.3%		1.8%		1.3%	

Rivard, *Med. Phys.* 34, 754-762 (2007)

ESTRO School

Brachytherapy Dose Uncertainties (TG-138)

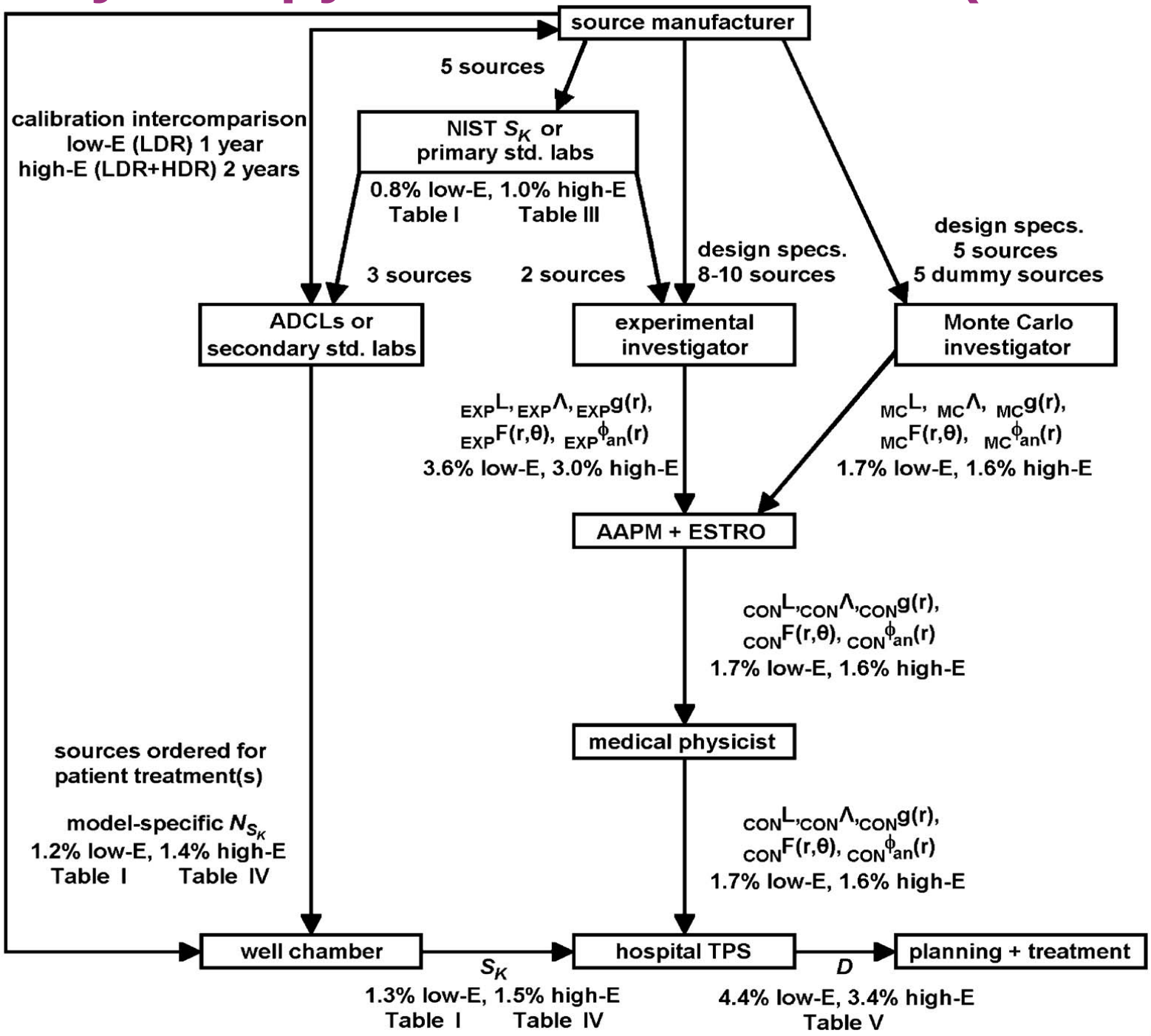

DeWerd, et al., *Med. Phys.* 38, 782-801 (2011)

ESTRO School

Measurement Uncertainty in RAKR and Dose

Measurement description	Quantity (units)	Relative propagated uncertainty (%)
ADCL calibration	$S_{K,\mathrm{NIST}}$ (U)	1.1
ADCL well ion chamber calibration	$S_{K,\mathrm{NIST}}/I_{\mathrm{ADCL}}$ (U/A)	1.2
ADCL calibration of source from manufacturer	$S_{K,\mathrm{ADCL}}$ (U)	1.3
ADCL calibration of clinic well ion chamber	$S_{K,\mathrm{ADCL}}/I_{\mathrm{CLINIC}}$ (U/A)	1.4
Clinic measures source air-kerma strength	$S_{K,\mathrm{CLINIC}}$ (U)	1.5
Expanded uncertainty ($k=2$)	$S_{K,\mathrm{CLINIC}}$ (U)	2.9

Uncertainty component	Relative propagated uncertainty (%) *high-E*
S_K measurements from row 5 of Tables I and IV	1.5
Measured dose	3.0
Monte Carlo dose estimate	1.6
TPS interpolation uncertainties	2.6
Total dose calculation uncertainty	3.4
Expanded uncertainty ($k=2$)	6.8

DeWerd, et al., *Med. Phys.* 38, 782-801 (2011)

ESTRO School

Summary

- BT dosimetry in the clinic generally follows the TG-43 formalism
  - Luc will next show you its limitations and advancements in accuracy

- uniform BT (over time and space) requires standization
  - consistent formalism (and formats)
  - consistent dosimetry parameters
  - consistent reference data
  - consistent TPS approach

- HDR/LDR and HE/LE have different planning approaches

- medical physicist must know the data trail and commission the source(s)

Further Reading

Ballester, et al. Med Phys 2009;36:4250-6.

Beaulieu, et al. Med Phys 2012;39:6208-36.

Butler, et al. Med Phys 2008;35:3860-5.

DeWerd, et al. Med Phys 2011;38:782-801.

Granero, et al. Med Phys 2011;38:487-94.

Kirisits, et al. Radiat Oncol 2014;110:199-212.

Nath, et al. Med Phys 1995;22:209-34.

Perez-Calatayud, et al. Med Phys 2012;39:2904-29.

Rivard, Med Phys 1999;26:2445-50.

Rivard, Appl Radiat Isot 2001;55:755-82.

Rivard, et al. Med Phys 2004;31:633-74.

Rivard, et al. Nuc Sci Engin 2005;149:101-6.

Rivard, et al. Med Phys 2007;34:2187-205.

Rivard, et al. Med Phys 2009;36:1968-75.

Rivard, et al. Med Phys 2009;36:2136-53.

Thomadesn, et al. Med Phys 2008;35:4708-23.

ESTRO School

ESTRO School

WWW.ESTRO.ORG/SCHOOL

Limitations of TG-43 based dosimetry: TG-43 versus the “true” dose distribution

Prof. Luc Beaulieu, Ph.D., FAAPM, FCOMP

1- Département de physique, de génie physique et d’optique, et Centre de recherche sur le cancer, Université Laval, Canada

2- Département de radio-oncologie et Centre de recherche du CHU de Québec, CHU de Québec, Canada

Valencia, Spain – Oct 7-10 2018

Disclosures

- None for this section

Key References

- Comprehensive Brachytehrapy: physical and clinical aspect. JLM Venselaar, D Baltas, AS Meigooni and P.J. Hoskin. CRC Press, Taylor & Francis, 2013.
  - In particular: Chapters 5, 7 and 10
- The physics of modern brachytherapy for oncology. D Baltas, L Sakelliou et N Zamboglou. Taylor & Francis Series in Medical Physics and Biomedical Engineering, 2007.
- The physics of radiation therapy, FM Khan, 4ed, 2009.
- Brachytherapy physics, 2ed, AAPM monograph #31, 2005.
- J. Pouliot and L Beaulieu, Chapter 13, Liebel and Philips Textbook of Radiation Oncology, 3rd Ed, 2010
- Perez-Calatayud JJ, Ballester FF, Das RKR, Dewerd LAL, Ibbott GSG, Meigooni ASA, et al. Dose calculation for photon-emitting brachytherapy sources with average energy higher than 50 keV: Report of the AAPM and ESTRO. Med Phys 2012;39(5):2904–29.
- Rivard MJ, Coursey BM, DeWerd LA, Hanson WF, Saiful Huq M, Ibbott GS, et al. Update of AAPM Task Group No. 43 Report: A revised AAPM protocol for brachytherapy dose calculations. Med Phys 2004;31(3):633–74.

Key References

- Rivard MJ, Venselaar JLM, Beaulieu L. **The evolution of brachytherapy treatment planning**. Med Phys 2009;36:2136–53.

- Beaulieu L, Carlsson Tedgren A, Carrier J-F, Davis SD, Mourtada F, Rivard MJ, et al. **Report of the Task Group 186 on model-based dose calculation methods in brachytherapy beyond the TG-43 formalism: Current status and recommendations for clinical implementation**. Med Phys 2012;39(10):6208–36.

- Papagiannis P, Pantelis E, Karaiskos P. **Current state of the art brachytherapy treatment planning dosimetry algorithms**. Br J Radiol 2014;87(1041):20140163.

- Ma Y, Lacroix F, Lavallée M-C and Beaulieu L. **Validation of the Oncentra Brachy Advanced Collapsed cone Engine for a commercial ^{192}Ir source using heterogeneous geometries**. Brachytherapy 2015;14:939–52

- Ballester F et al. **A generic high-dose rate ^{192}Ir brachytherapy source for evaluation of model-based dose calculations beyond the TG-43 formalism**. *Med. Phys*. 2015;**42**:3048–61

Learning Objectives

- Review the limitations of TG43
- Understand how these limitations translate to clinical tumor sites and brachytherapy procedures (relative to MC)
- Be able to anticipate potential TG43 failures

TG-43: Brachytherapy Dosimetry

Update of AAPM Task Group No. 43 Report: A revised AAPM protocol for brachytherapy dose calculations

$$\dot{D}(r,\theta) = S_K \cdot \Lambda \cdot \frac{G_L(r,\theta)}{G_L(r_0,\theta_0)} \cdot g_L(r) \cdot F(r,\theta)$$

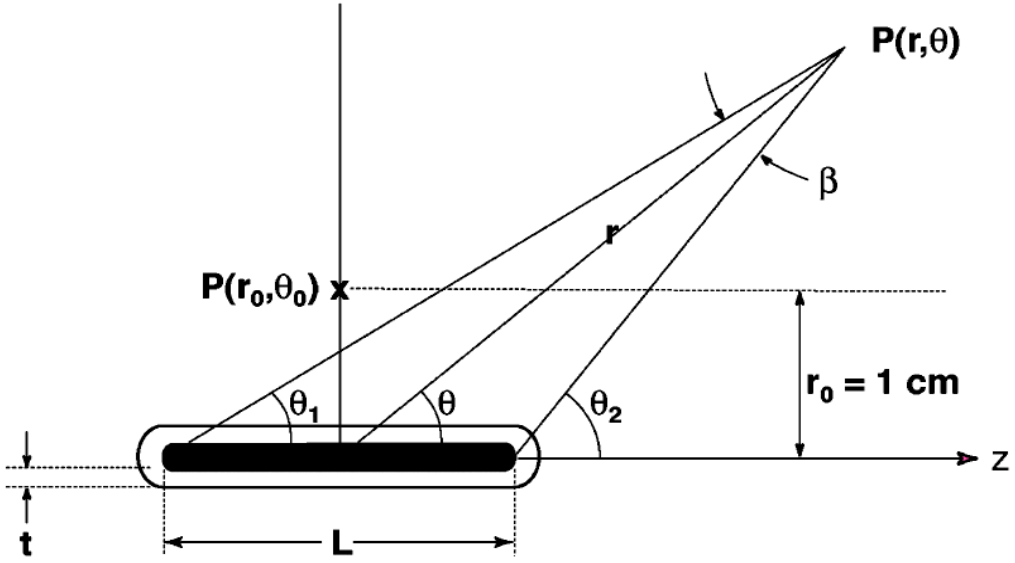

Rivard et al, *Med Phys* 31, 633-674 (2004)

The good!

- Each source model is specifically taken into account
- S_k (and RAKR) link to a primary standard!
- The values of the various parameters are compiled following a rigorous process
  - Process includes a review and consensus by a group of experts
- Analytical formulation leads to fast dose computation
  - Hundreds of thousands of iterations possible in a few seconds

What’s all the fuss about?

TG-43: Brachytherapy Dosimetry

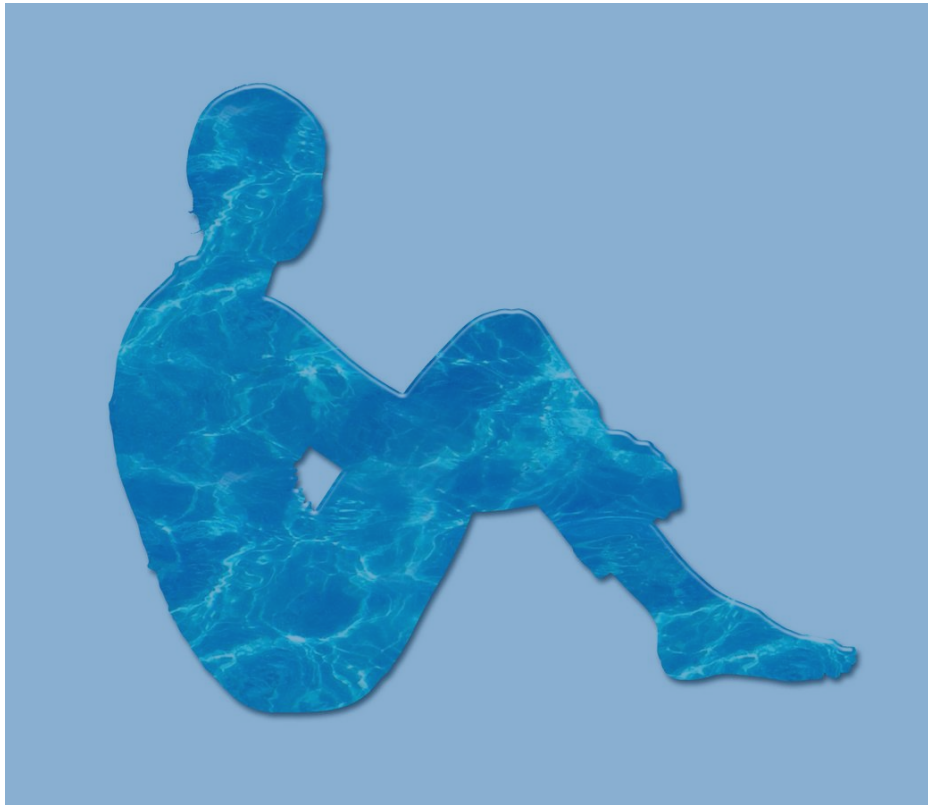

≠

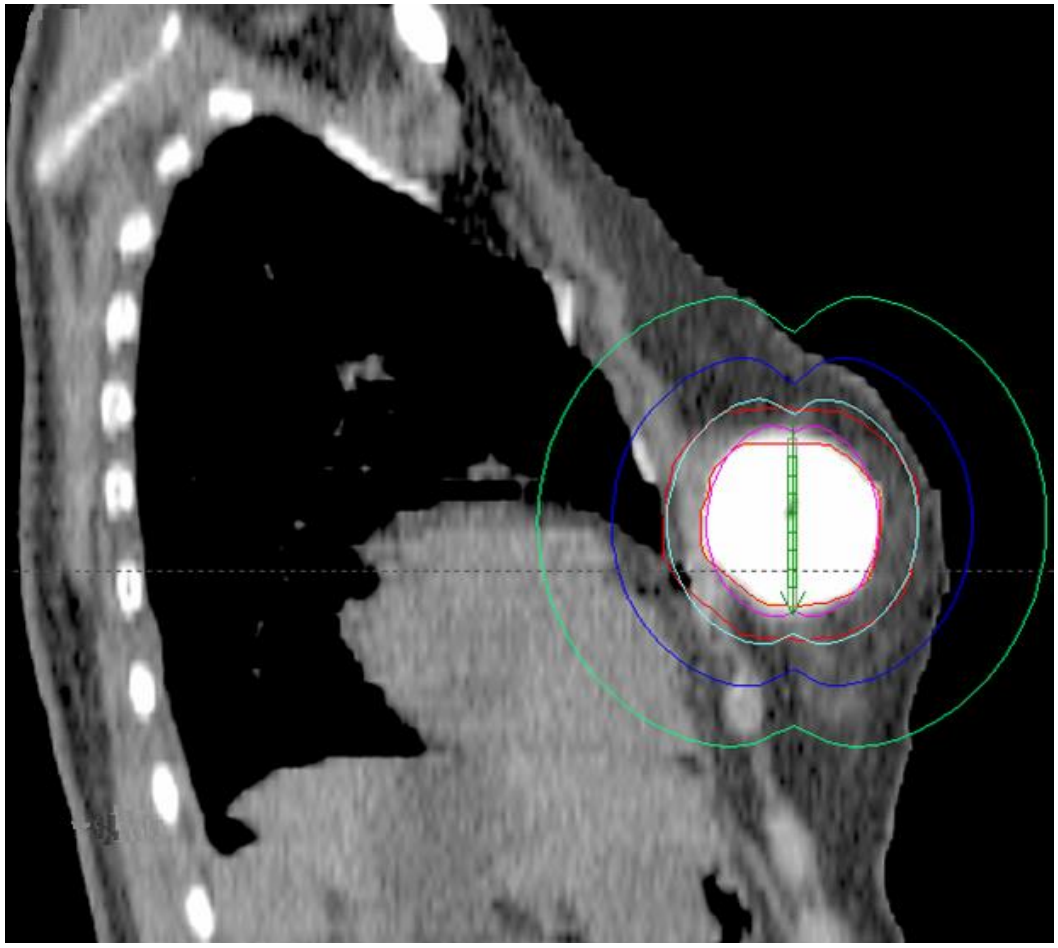

The limitations

- Homogeneous water medium assumed
- Full scatter condition assumed
  - 5 cm beyond the last position of interest for low energy seed (15 cm geometry)
  - 20 cm beyond the last position of interest for E > 50 keV (40 cm radius geometry)
- No electrons (Dose vs Kerma)
  - Dose may not be related to photon fluence close to the source (e.g. ^{60}Co)
- Full 3D source geometry not taken into account
  - Close to the source
  - Extended line sources, …
  - Shielded applicators or directional sources

Why should you care?

Significant dose differences expected

≥ 10% or more relative to TG-43

Dose is the fundamental quantity in RT

Factor-based vs Model-based

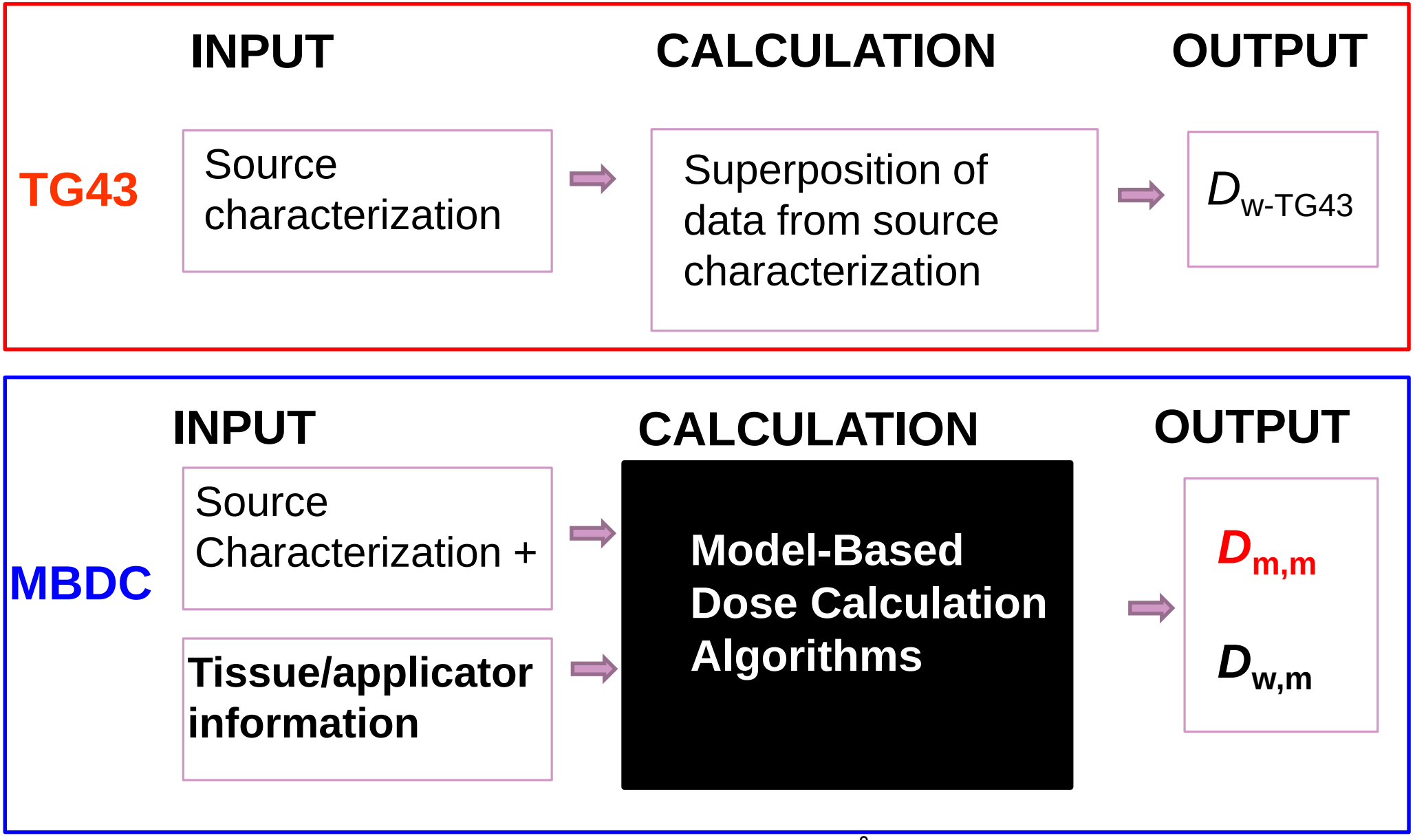

From Åsa Carlsson-Tedgren

Sensitivity of Anatomic Sites to Dosimetric Limitations of Current Planning Systems

anatomic site	photon energy	absorbed dose	attenuation	shielding	scattering	beta/kerma dose
prostate	high					←
	low	XXX	XXX	XXX		
breast	high				XXX	
	low	XXX	XXX	XXX		
GYN	high			XXX		
	low	XXX	XXX			
skin	high			XXX	XXX	
	low	XXX		XXX	XXX	
lung	high				XXX	XXX
	low	XXX	XXX		XXX	
penis	high				XXX	
	low	XXX			XXX	
eye	high			XXX	XXX	XXX
	low	XXX	XXX	XXX	XXX	

Rivard, Venselaar, Beaulieu, *Med Phys* 36, 2136-2153 (2009)

Prostate HDR Brachytherapy

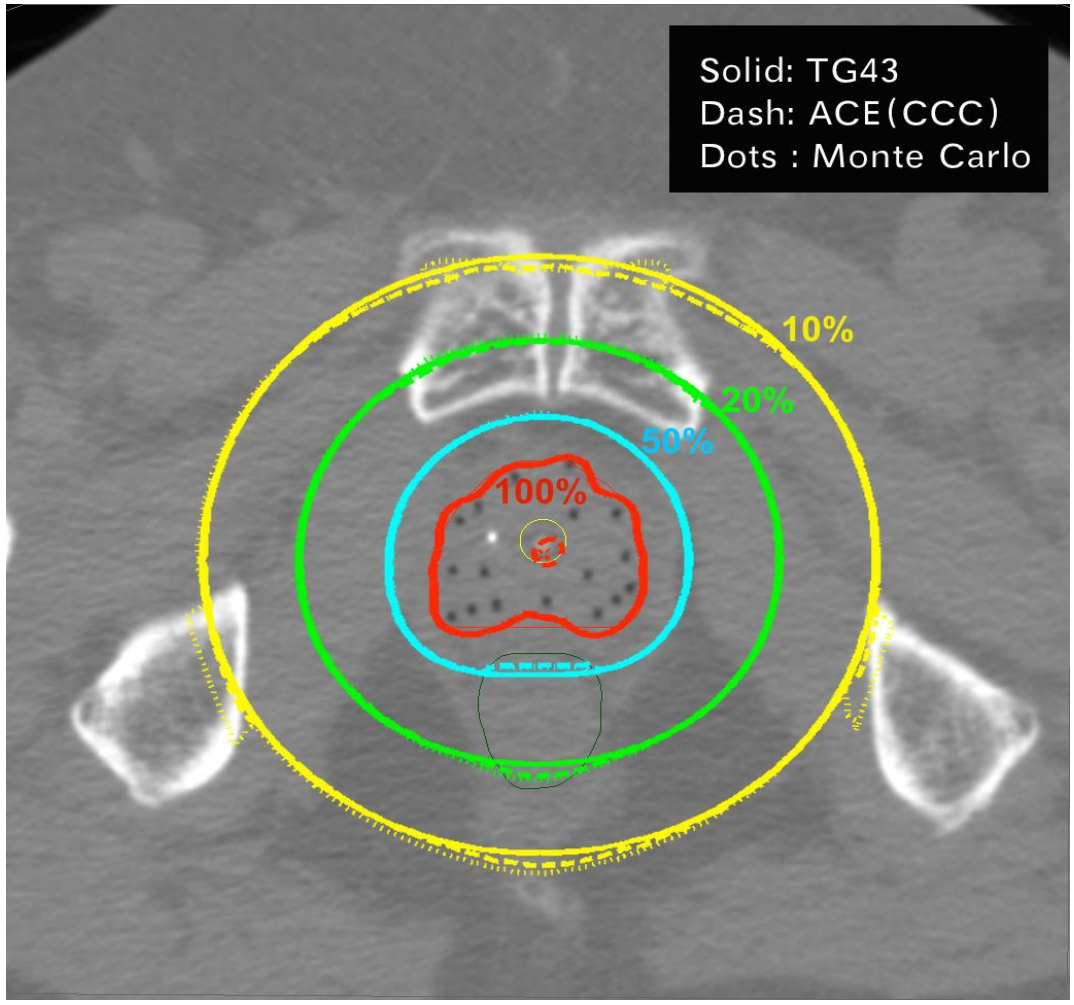

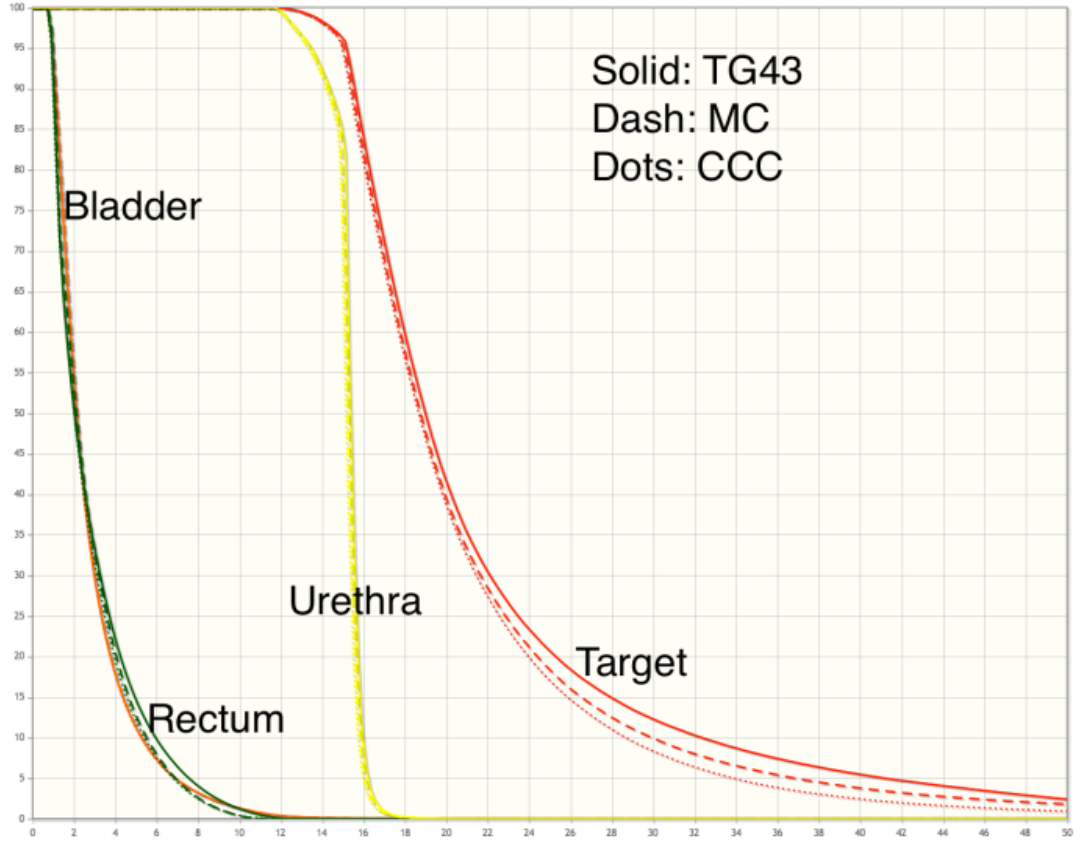

17 catheters; rectum set to air!

Ma et al, Brachytherapy 2015

Prostate LDR Brachytherapy

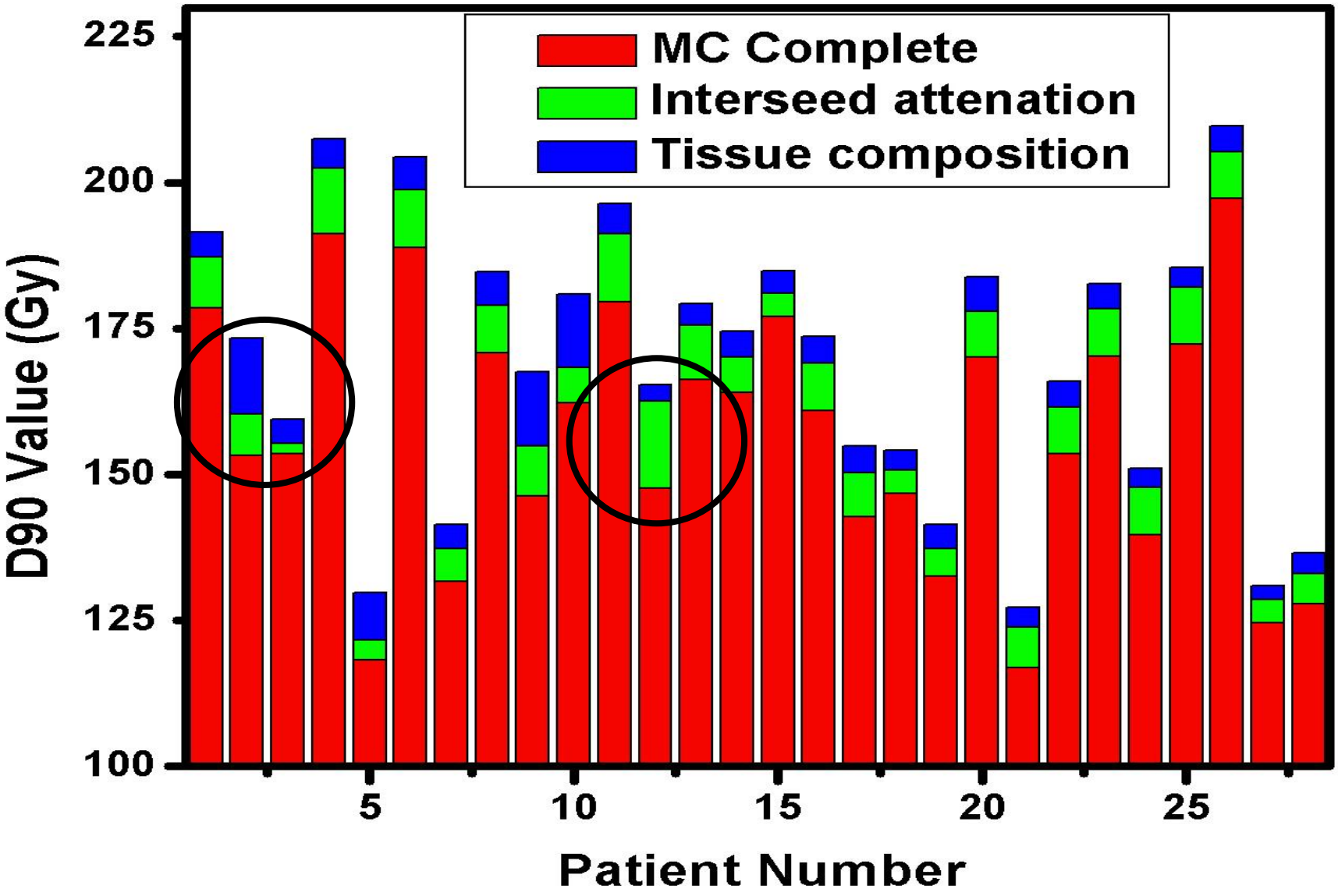

≈ 4% ↓

≈ 3% ↓

JF Carrier et al., IJROBP 2007

The case of calcifications

Calcifications

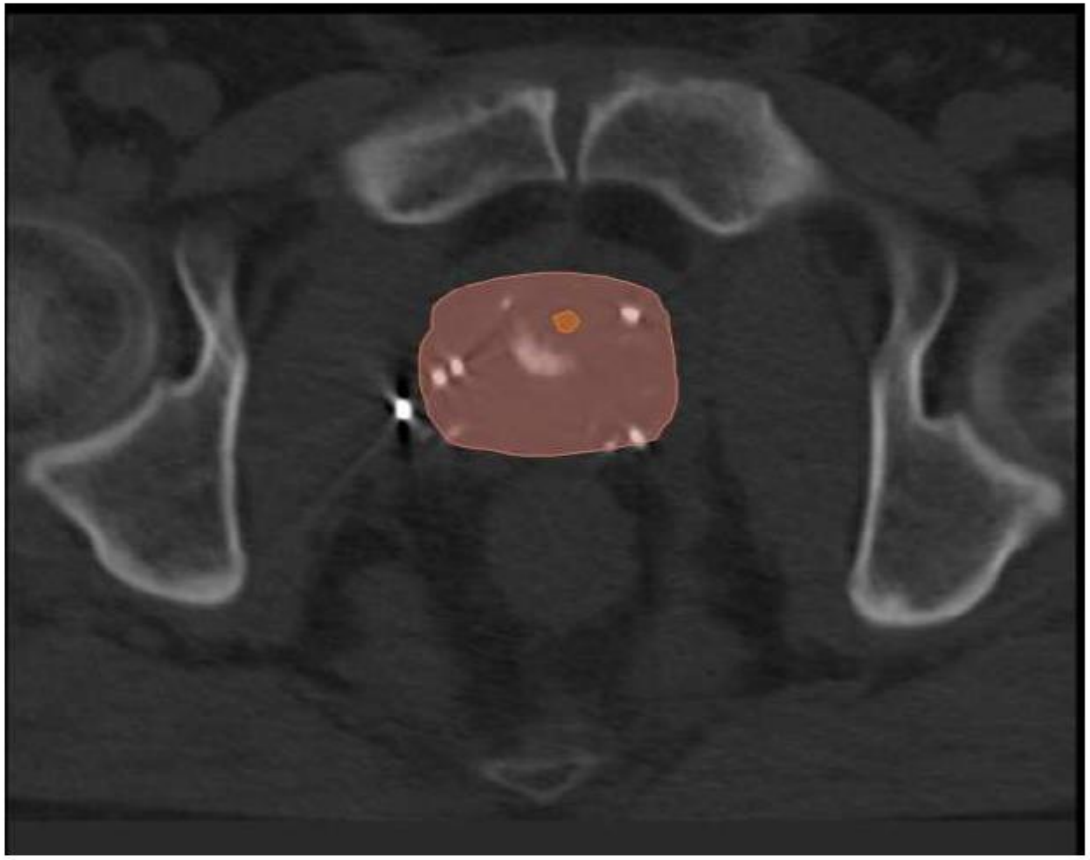

(g) Significant calcification

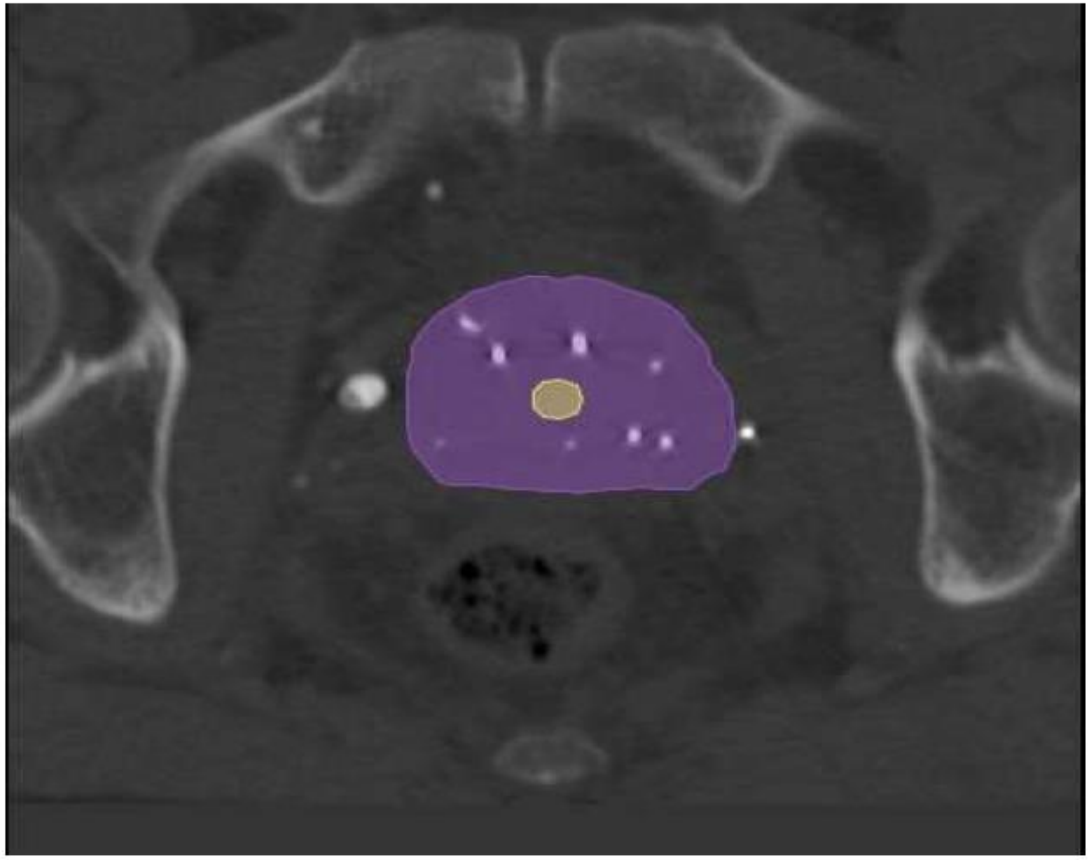

(h) Typical patient

CA Collins-Fekete et al., Radiother Oncol 2014

CALCIFICATIONS

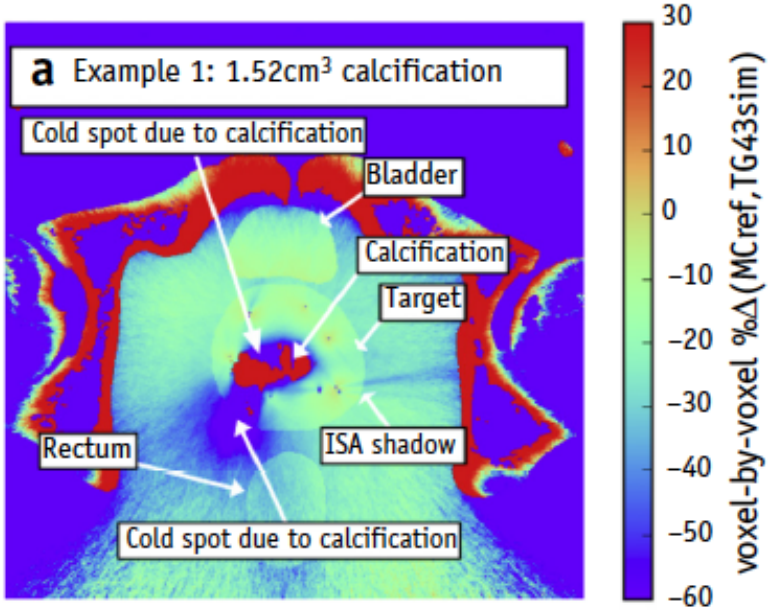

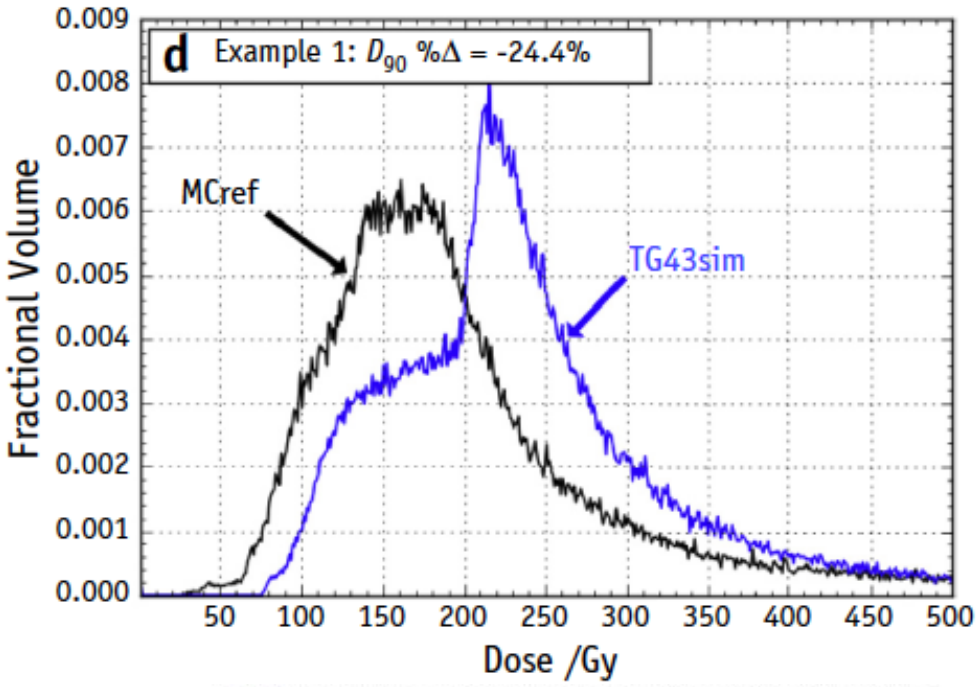

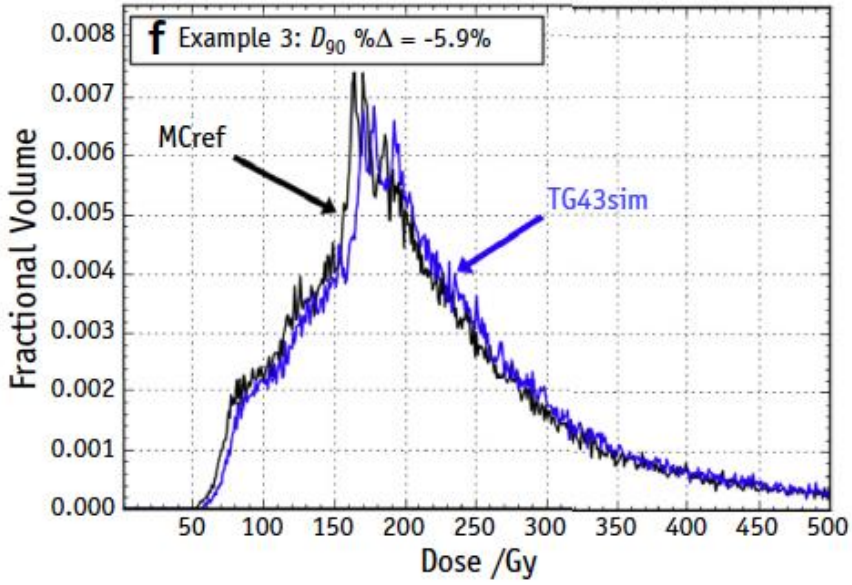

Miksys et al., IJROBP 97 (2017) 606-615

Retrospective Cohort Study

- CHU de Quebec performs seeds implants since 1994
- Needs patients with:
  - post-implant CT
  - DICOM-RT export

- 613 usable cases in the research database out of about 1500

Cohort: Martin *et al*, IJROBP **67** (2007): 334–41; Martell *et al*, IJROBP (2017) In Press.
Physics: Collins-Fekete *et al*, Rad Onc **114** (2015) 339-344; Miksys *et al* IJROBP **97** (2017) 606-615; Miksys *et al*, Med Phys **44** (2017) 4329−4340.

Outcome for this cohort: bRFS

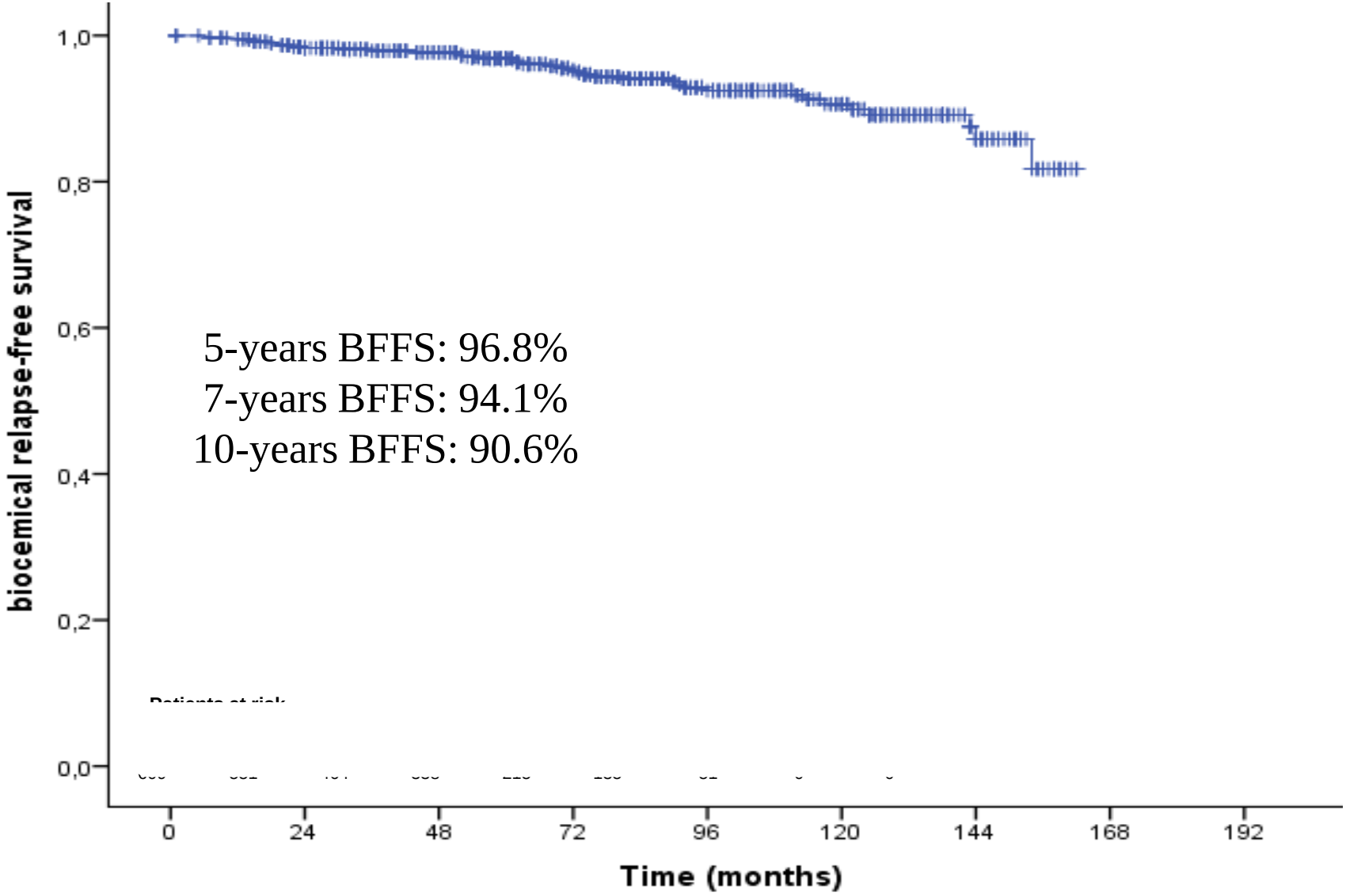

5-years BFFS: 96.8%
7-years BFFS: 94.1%
10-years BFFS: 90.6%

Preliminary results

TABLE: Dosimetric indices differences to TG-43

	D_WATER	D_CALCI	D_FULL_MC
$D_{10\%}$	98.7±0.4	94.8±08.8	92.3±08.4
$D_{90\%}$	98.4±0.4	88.6±12.1	86.8±09.2
$V_{100\%}$	99.6±1.1	93.5±18.4	93.8±17.7
$V_{150\%}$	99.1±0.6	92.1±12.0	90.7±10.2
$V_{200\%}$	97.2±1.1	84.9±13.3	80.8±12.6

CA Collins-Fekete et al., Radiother Oncol 2015

CALCIFICATIONS – Full Cohort

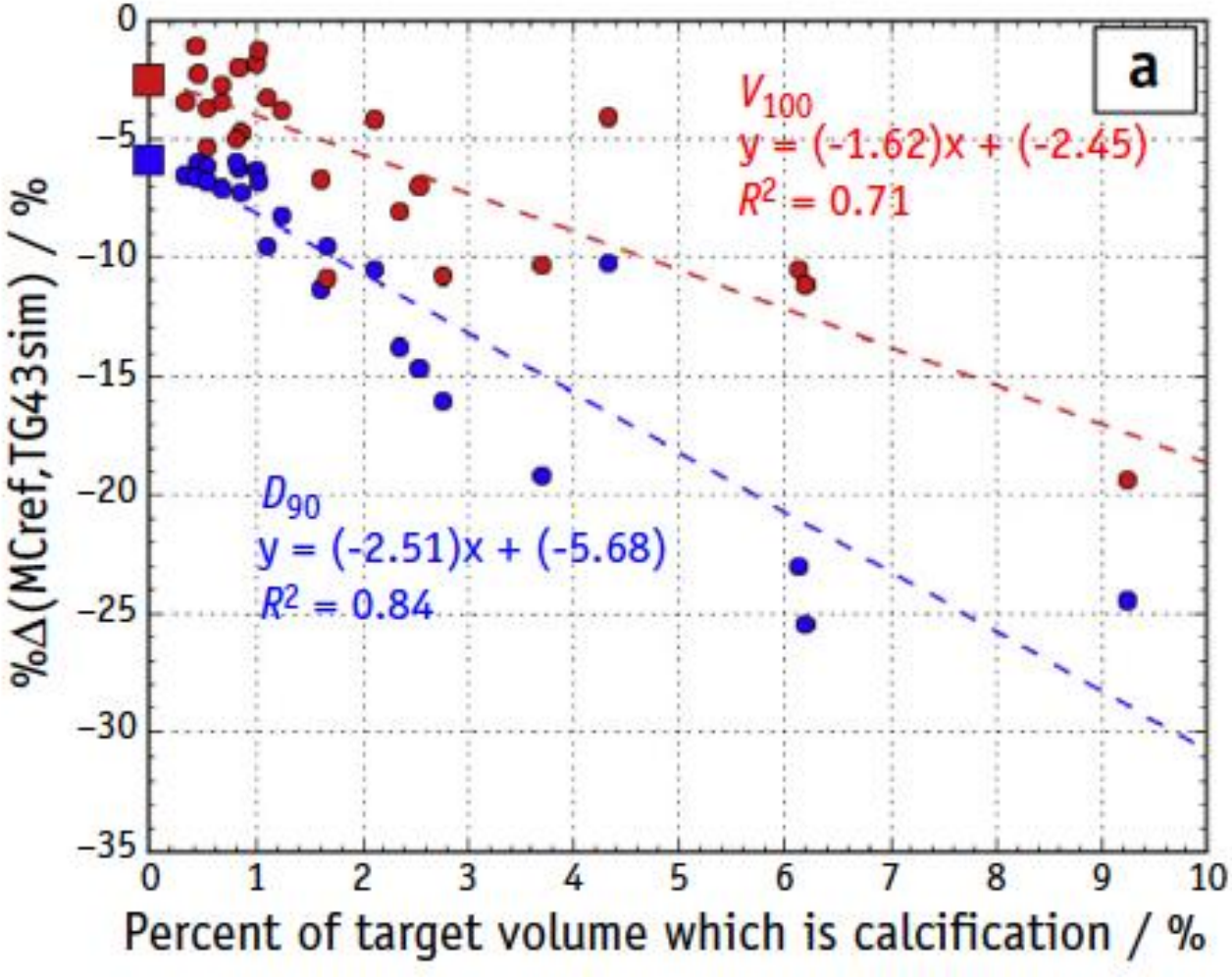

Miksys et al., IJROBP 97 (2017) 606-615

IMPACT ON RADIOBIOLOGICAL DOSE?

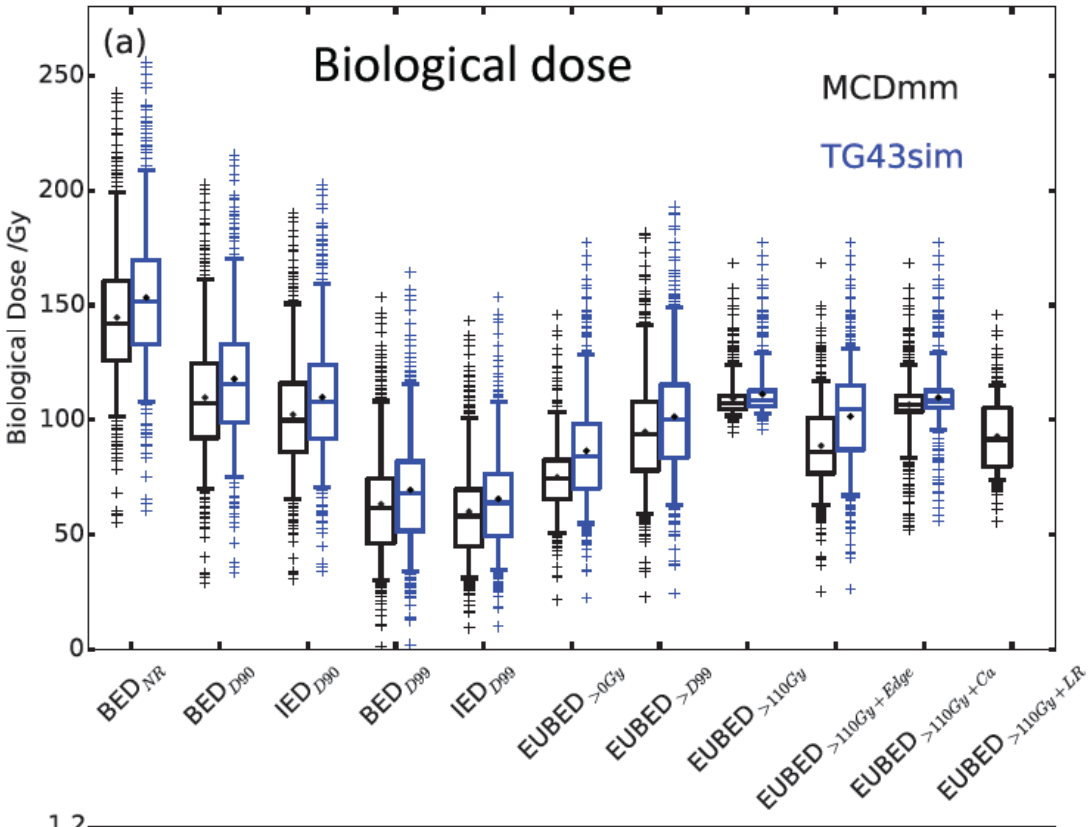

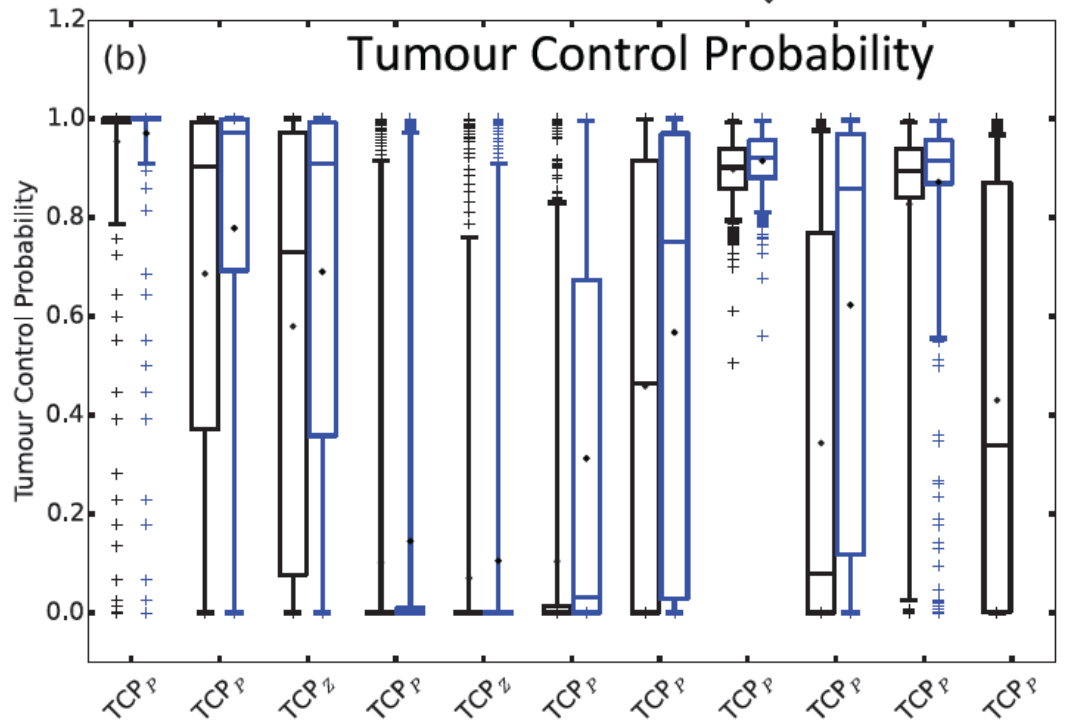

Summary of results

11 biological doses models (varying complexity) and corresponding TCP estimates

Radiobiological doses – also considered IED = Isoeffective dose [Zaider & Minerbo, PMB **45** (2000); Zaider & Hanin, PMB **52**, 6355 (2007)]

Miksys et al, Med Phys 2017

Slide by Rowan Thomson

But in reality, does it make a clinical difference?

Preliminary Results: bRFS

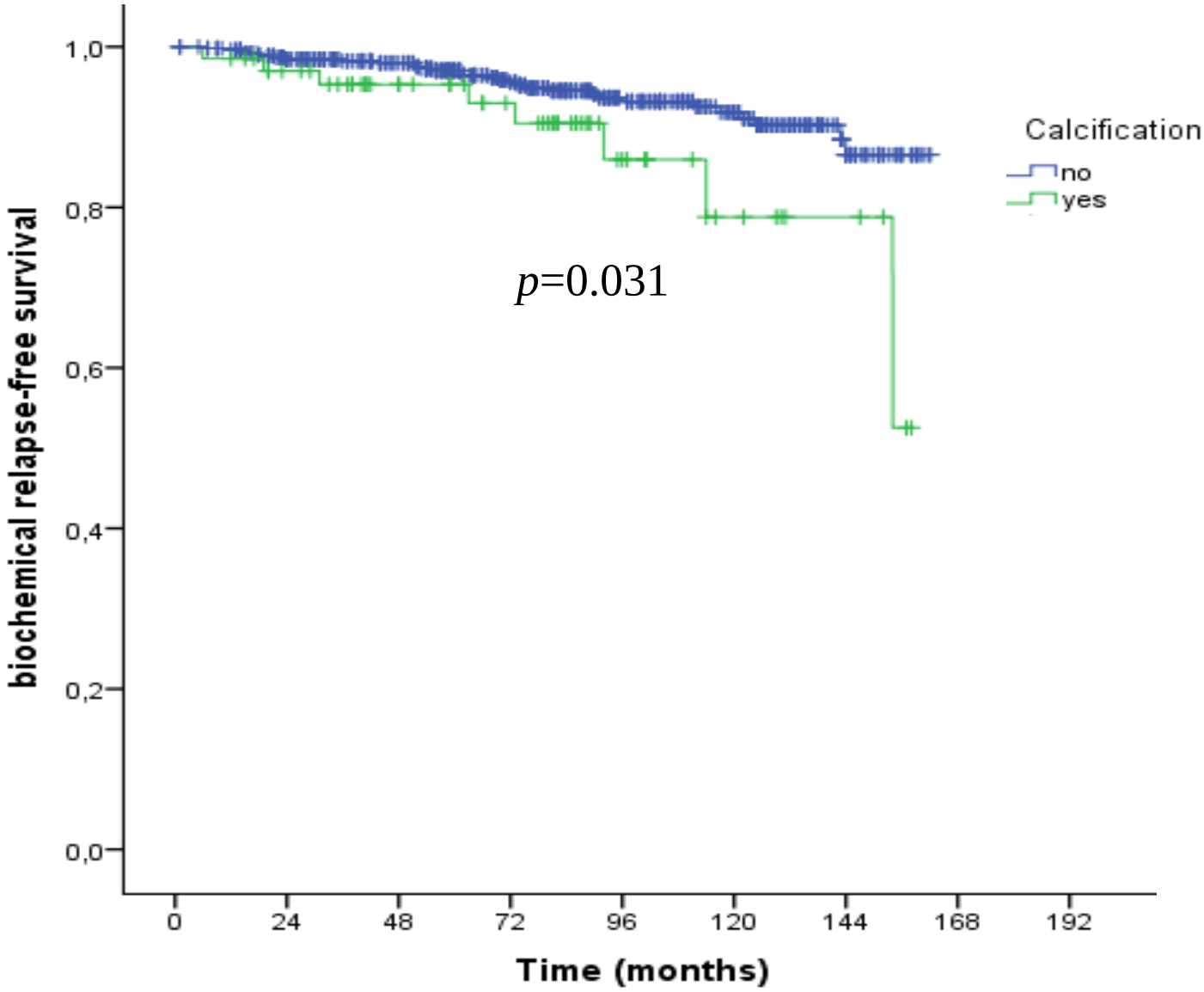

Summary for Prostate Brachytherapy

- Minimal impact for HDR brachytherapy
  - CTV-PTV
  - OARs: rectum, bladder, urethra

- Important effect for seed implants
  - D90: -7% average due to ISA and tissues
  - Calcifications: -10% average on D90 (large std.)

Sensitivity of Anatomic Sites to Dosimetric Limitations of Current Planning Systems

anatomic site	photon energy	absorbed dose	attenuation	shielding	scattering	beta/kerma dose
prostate	high					
	low	XXX	XXX	XXX		
breast	high				XXX	←
	low	XXX	XXX	XXX		
GYN	high			XXX		
	low	XXX	XXX			
skin	high			XXX	XXX	
	low	XXX		XXX	XXX	
lung	high				XXX	XXX
	low	XXX	XXX		XXX	
penis	high				XXX	
	low	XXX			XXX	
eye	high			XXX	XXX	XXX
	low	XXX	XXX	XXX	XXX	

Rivard, Venselaar, Beaulieu, *Med Phys* 36, 2136-2153 (2009)

Various Approaches

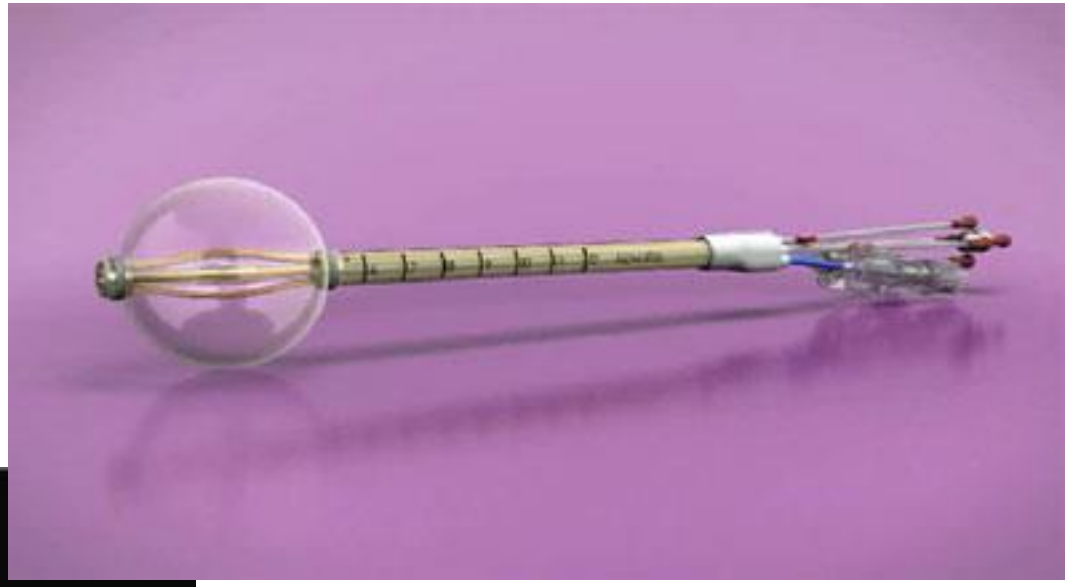

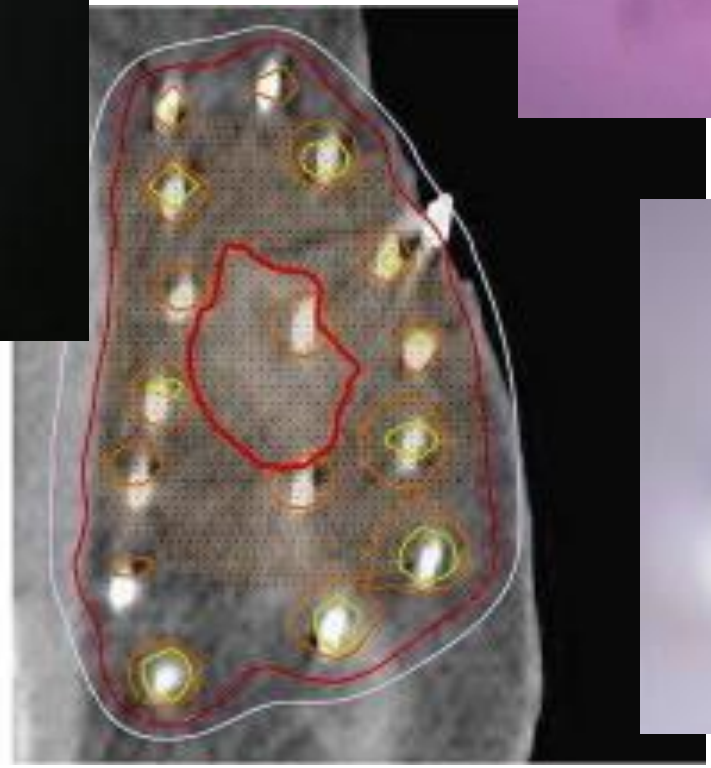

Images Courtesy of: Dr. Firas Mourtada

Various Approaches

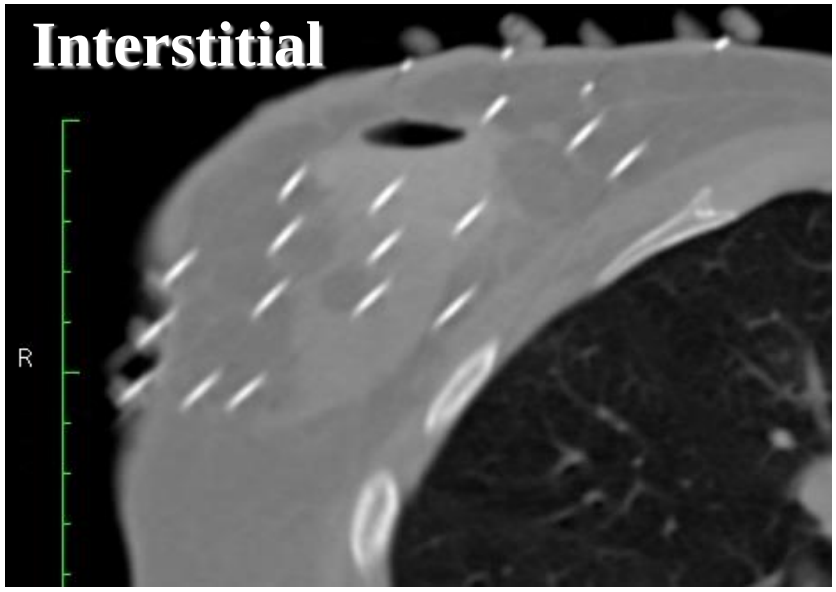

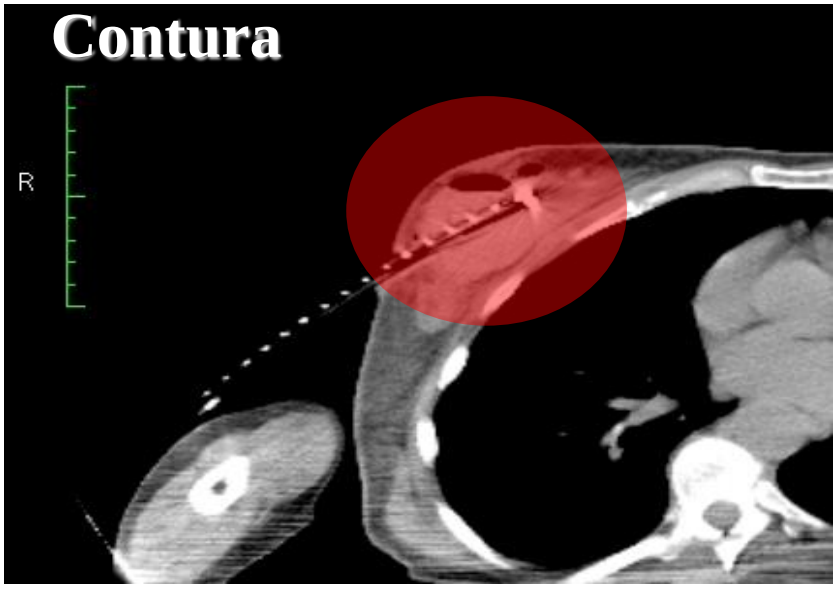

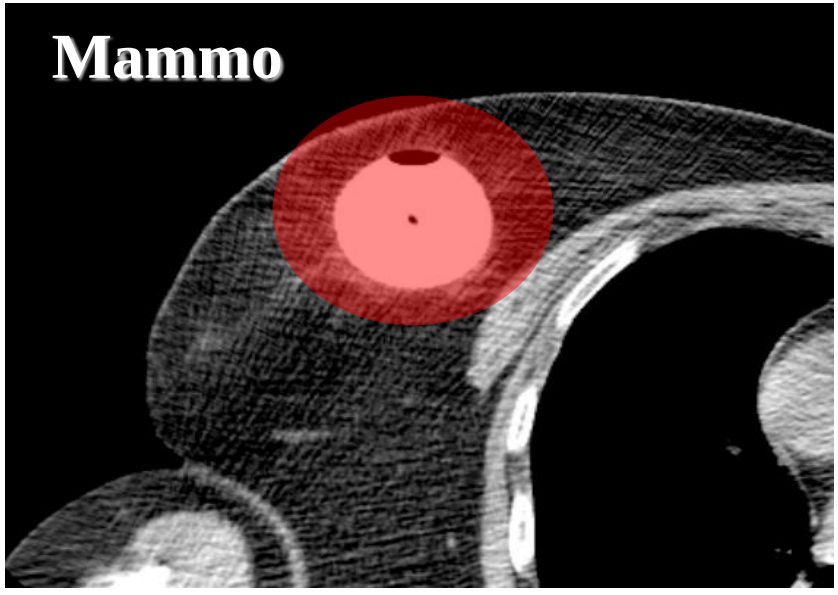

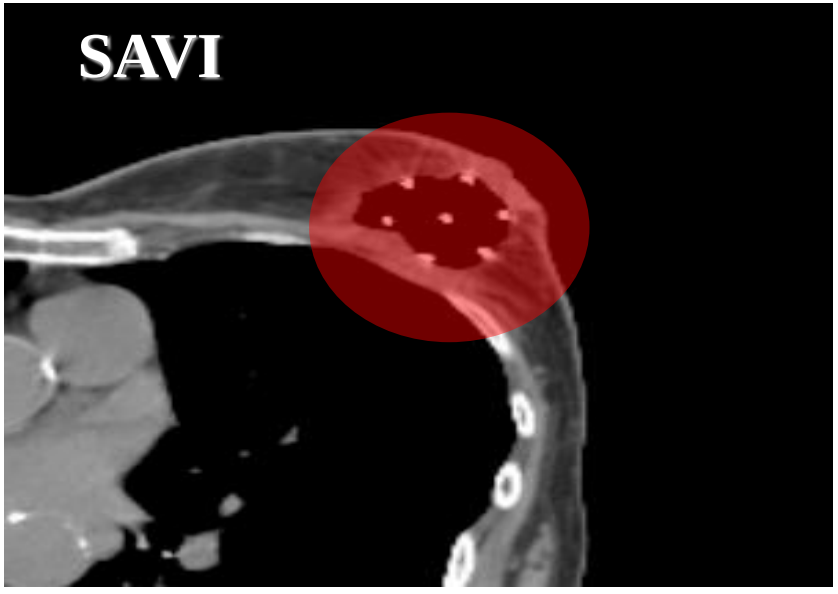

Contrast

TABLE II. Percentage reduction (Δ%) in dose rate at 1 cm from the balloon due to contrast, relative to water, for the various balloon diameters.

Balloon diameter (cm)	Δ%				
	5% contrast	10% contrast	15% contrast	20% contrast	25% contrast
4	−0.8%	−1.6%	−2.4%	−3.2%	−4.0%
5	−1.0%	−1.6%	−2.7%	−3.8%	−4.9%
6	−1.4%	−2.9%	−4.3%	−5.4%	−5.7%

Contrast effects on dosimetry of a partial breast irradiation system

Bassel Kassas,[a] Firas Mourtada, John L. Horton, and Richard G. Lane
The University of Texas MD Anderson Cancer Center, Box 94, 1515 Holcombe Boulevard, Houston, Texas 77030

(Received 24 February 2004; revised 6 April 2004; accepted for publication 22 April 2004; published 17 June 2004)

Papagiannis , Pantelis, Karaiskos, Br J Radiol, 87, 20141063 (2014)

Contrast recommendations were made!

Kassas, Mourtada, Horton, Lane, Med. Phys 31(7),1976-1979 (2004).

Air

Dosimetric effects of an air cavity for the SAVI™ partial breast irradiation applicator

Susan L. Richardson[a)]
Department of Radiation Oncology, Washington University School of Medicine, St. Louis, Missouri 63110

Ramiro Pino
Department of Radiation Oncology, The Methodist Hospital, Houston, Texas 77030 and Texas Cancer Clinic, San Antonio, Texas 78240

(Received 8 July 2009; revised 3 June 2010; accepted for publication 5 June 2010; published 12 July 2010)

Purpose: To investigate the dosimetric effect of the air inside the SAVI™ partial breast irradiation device.
Methods: The authors have investigated how the air inside the SAVI™ partial breast irradiation device changes the delivered dose from the homogeneously calculated dose. Measurements were made with the device filled with air and water to allow comparison to a homogenous dose calculation done by the treatment planning system. Measurements were made with an ion chamber, TLDs, and film. Monte Carlo (MC) simulations of the experiment were done using the EGSnrc suite. The MC model was validated by comparing the water-filled calculations to those from a commercial treatment planning system.
Results: The magnitude of the dosimetric effect depends on the size of the cavity, the arrangement of sources, and the relative dwell times. For a simple case using only the central catheter of the largest device, MC results indicate that the dose at the prescription point 1 cm away from the air-water boundary is about 9% higher than the homogeneous calculation. Independent measurements in a water phantom with a similar air cavity gave comparable results. MC simulation of a realistic multidwell position plan showed discrepancies of about 5% on average at the prescription point for the largest device.
Conclusions: The dosimetric effect of the air cavity is in the range of 3%–9%. Unless a heterogeneous dose calculation algorithm is used, users should be aware of the possibility of small treatment planning dose errors for this device and make modifications to the treatment delivery, if necessary. © *2010 American Association of Physicists in Medicine.* [DOI: 10.1118/1.3457328]

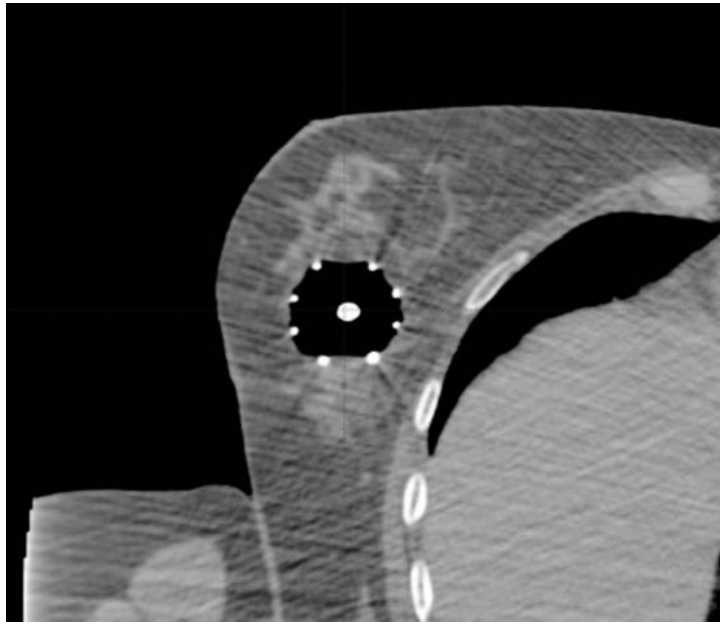

Richardson, Ramino, Med Phys, 37(8), 3919-3926 (2010)

TABLE II. Comparison between MC doses calculated at selected distances from the edge of the device using different sized devices for single and multidwell position plans with and without air cavity present. The treatment planning benchmark is shown for comparison to the MC in water. The percent difference represents the absolute difference between the MC in water and MC in air calculation.

Six-strut device

	Single-dwell positions				Multiple dwell positions			
Distance (cm)	TPS dose	MC water	MC air	Absolute % difference	TPS dose	MC water	MC air	Absolute % difference
1.0	340.2	340.2	352.4	3.6	360.8	369.4	381.2	3.2
1.5	232.6	232.9	241.9	2.7	243.6	245.0	252.6	2.1
2.0	168.8	169.2	177.2	2.3	177.2	178.0	183.9	1.6
3.0	100.0	102.0	106.4	1.3	106.1	106.0	110.7	1.3
4.0	65.6	67.2	70.1	0.9	70.2	71.8	76.5	1.3
5.0	46.0	47.4	49.5	0.6	49.4	51.4	58.2	1.9
10.0	12.3	14.6	15.3	0.2	13.4	14.3	15.5	0.3

0-4%

Eight-strut device

	Single-dwell positions				Multiple dwell positions			
Distance (cm)	TPS dose	MC water	MC air	Absolute % difference	TPS dose	MC water	MC air	Absolute % difference
1.0	340.2	348.8	369.7	6.0	334.1	346.1	362.1	4.6
1.5	249.6	254.8	272.0	4.9	239.6	245.9	259.8	4.0
2.0	190.9	196.8	210.7	4.0	180.2	183.8	194.4	3.1
3.0	121.3	125.7	134.8	2.6	112.6	117.5	118.6	0.3
4.0	83.2	86.6	92.6	1.7	76.6	80.8	83.9	0.9
5.0	60.1	62.8	67.2	1.3	55.1	57.6	60.1	0.7
10.0	17.1	20.2	21.6	0.4	15.6	16.4	21.5	1.5

0-6%

Ten-strut device

	Single-dwell positions				Multiple dwell positions			
Distance (cm)	TPS dose	MC water	MC air	Absolute % difference	TPS dose	MC water	MC air	Absolute % difference
1.0	340.3	345.4	373.9	8.3	371.5	370.8	402.7	8.6
1.5	258.2	263.3	285.7	6.5	265.2	263.2	275.9	3.4
2.0	202.2	208.1	226.6	5.3	201.2	199.2	202.9	1.0
3.0	132.9	137.0	149.5	3.6	128.5	129.8	112.6	4.6
4.0	93.2	96.7	105.8	2.6	89.0	91.6	81.6	2.7
5.0	68.3	71.1	78.0	2.0	64.8	66.1	60.3	1.6
10.0	20.0	23.1	25.2	0.6	18.7	19.8	21.3	0.4

0-9%

Skin Doses: study on 59 patients

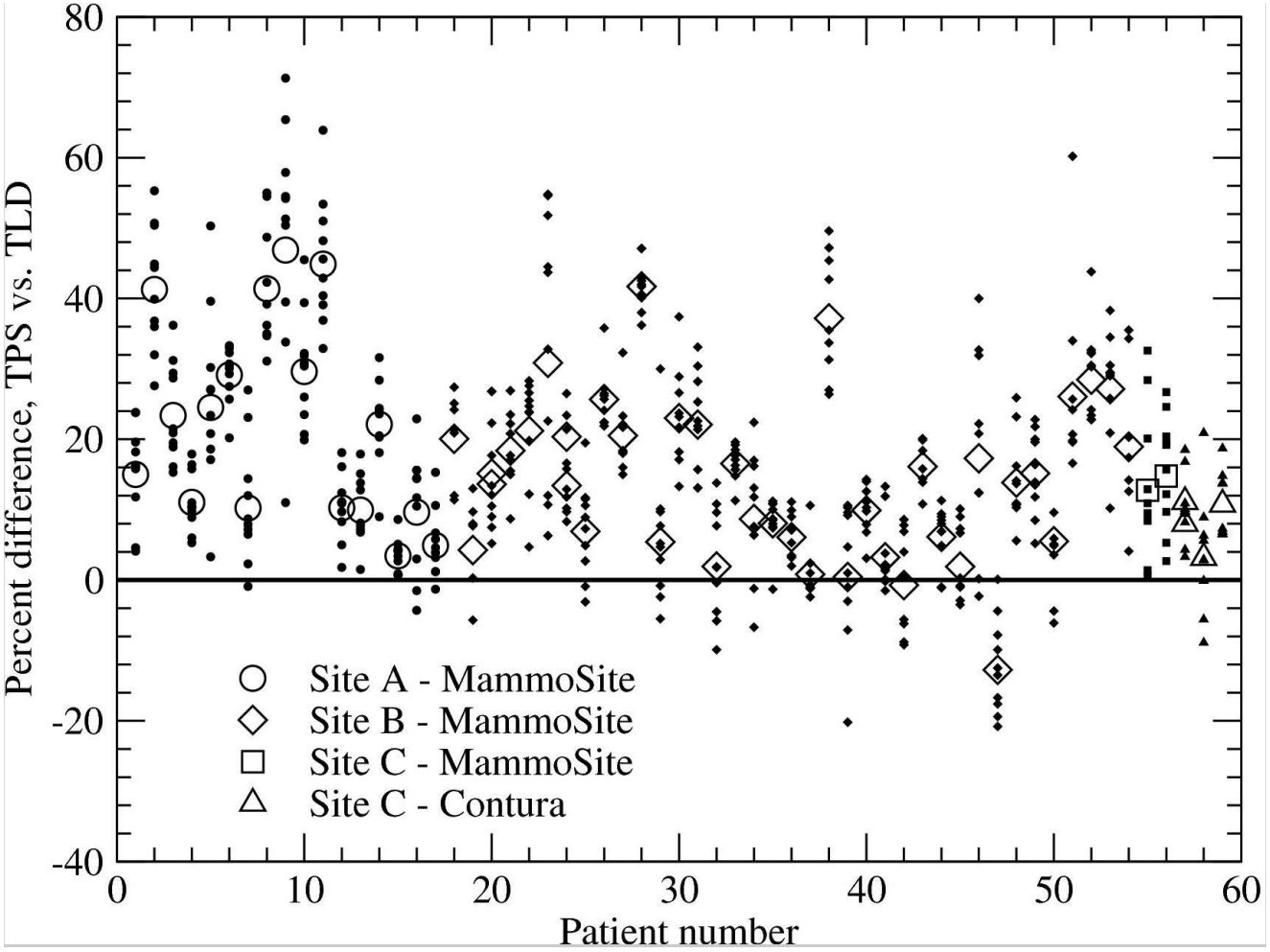

<u>TLD skin dose meas.</u>

- TPS-TLD: -13% to 47%
- Average: 16% overestimation
- MC or Acuros: < 5%

Raffi JA et al, Med. Phys. 37 (2010).

Abstracts / Brachytherapy 10 (2011) S14–S101

Balloon-Based Accelerated Partial Breast Irradiation With Contura™: Comparison Between Conventional TG-43 and Brachyvision Acuros™ Dose Calculation Methods

Ruben Ter-Antonyan, PhD[1], Paul W. Read, MD, PhD[1], Bernard F. Schneider, MD, PhD[1], Anneke T. Schroen, MD, MPH[2], Stanley H. Benedict, PhD[1], Bruce P. Libby, PhD[1]. [1]Radiation Oncology, University of Virginia Health System, Charlottesville, VA; [2]Surgery, University of Virginia Health System, Charlottesville, VA.

- 5 Contura patients

	TG-43	Acuros™	Difference
PTV_eval D95 (cGy)	322.7	311.9	(3.4 ± 0.5) %
PTV_eval D1 (cGy)	816.4	806.6	(1.2 ± 0.6) %
PTV_eval D_{min} (cGy)	238.4	254.1	(-7.1 ± 7.1) %
PTV_eval V150 (cm^3)	26.5	24.0	(9.2 ± 1.3) %
Skin D_{max} (cGy)	439.0	420.1	(4.6 ± 1.2) %
Skin D_{mean} (cGy)	242.8	226.6	(6.7 ± 0.6) %
Skin D_{skin_pt} (cGy)	297.1	278.1	(6.7 ± 1.7) %

courtesy of F. Mourtada

Abstracts / Brachytherapy 9 (2010) S23–S102

Comparison between Two Dose Calculation Methods, Acuros and TG43: Implications for Accelerated Partial Breast Irradiation

Jill P. Heffernan, M.D., Lynn Gilbert, C.M.D., Douglas W. Arthur, M.D., Dorin A. Todor, Ph.D. Radiation Oncology, Virginia Commonwealth University, Richmond, VA.

- 30 patients evaluated $Skin_{max}$, Rib_{max}, D90, V100, V150, V200
- Variety of applicators including interstitial
  - Results for interstitial were within 3% or 3cc
- Balloon based:
  - Skinmax – 8% including >10% if only using central lumen/single dwell
  - Ribmax- 5% on average
  - Target coverage less (3.5% – 8%)
  - Larger balloons had greater differences in V100, etc.

courtesy of F. Mourtada

TG-186 Heterogeneous Model ($D_{m,m}$)

(b) Dose ratio: Heterogenous Model $D_{m,m}$ / TG-43 MC

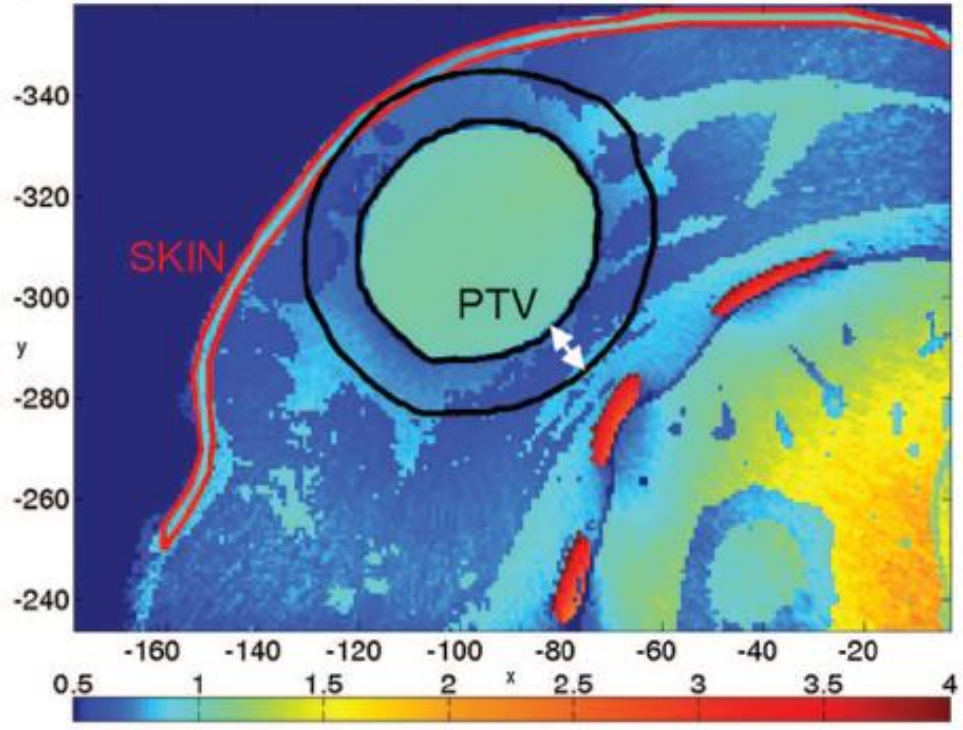

TG-186< TG-43 TG-186> TG-43

DVH	% differences range
D_{90}	-36% to -33%
V_{100}	- 54% to – 29%
V_{200}	- 97% to - 25%
$D_{0.2cc}$ (Skin)	- 19% to 0%

(e) Heterogenous Model

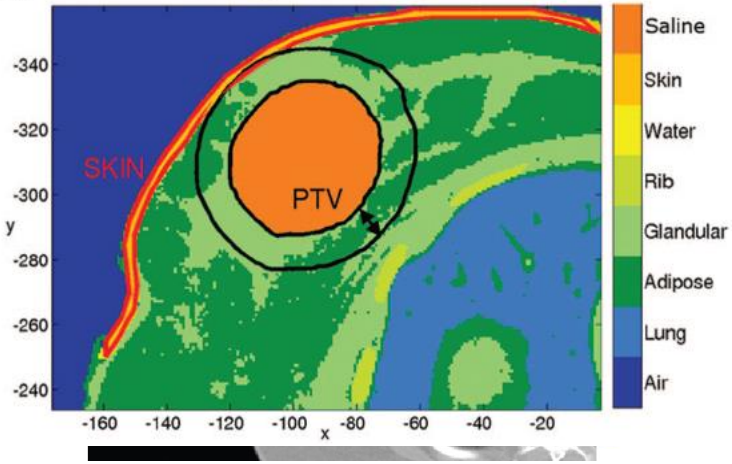

- Large DVH decreases in $D_{m,m}$ compared to TG-43
- Higher calculated rib dose

Shane White *et al* Med Phys 41 (2014)

Summary for Breast Brachytherapy

- The experts agree that in using TG43 for ^{192}Ir procedures:
  - If you are using high levels of contrast – your overall dose is decreased
  - Skin dose is over-estimated (~ 4-10%)
  - Dose to ribs is under-estimated (~ 5 -7%)
  - Dose coverage is probably slightly over-estimated

- If you use seeds or electronic brachytherapy sources
  - Very large effect due to breast composition (adipose and glandular tissues)
  - Very large effect from bones (ribs)

Sensitivity of Anatomic Sites to Dosimetric Limitations of Current Planning Systems

anatomic site	photon energy	absorbed dose	attenuation	shielding	scattering	beta/kerma dose
prostate	high					
	low	XXX	XXX	XXX		
breast	high				XXX	
	low	XXX	XXX	XXX		
GYN	high			XXX		←
	low	XXX	XXX			
skin	high			XXX	XXX	
	low	XXX		XXX	XXX	
lung	high				XXX	XXX
	low	XXX	XXX		XXX	
penis	high				XXX	
	low	XXX			XXX	
eye	high			XXX	XXX	XXX
	low	XXX	XXX	XXX	XXX	

Rivard, Venselaar, Beaulieu, *Med Phys* 36, 2136-2153 (2009)

GYN Standard Applicators too many to list

Fletcher-Williamson T&O

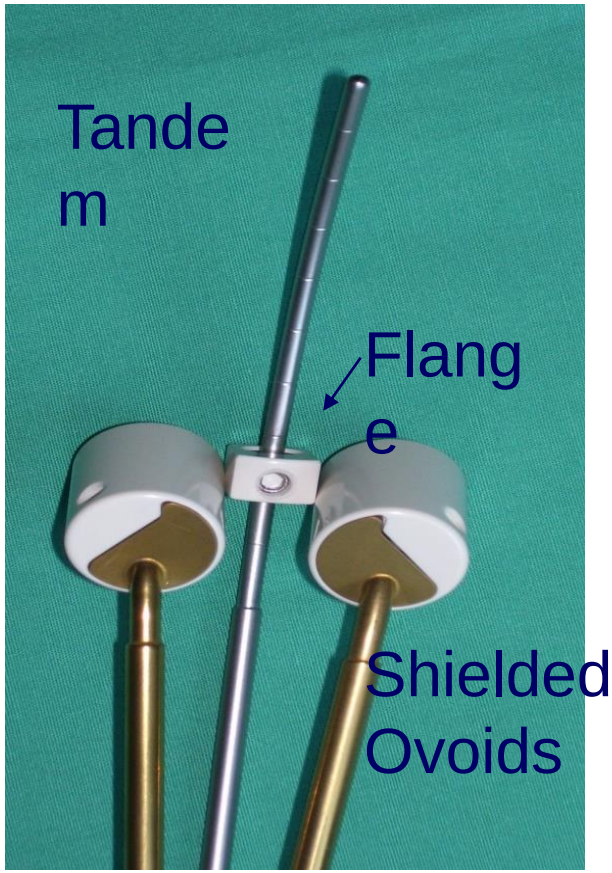

Standard Cylinder
Regular or shielded

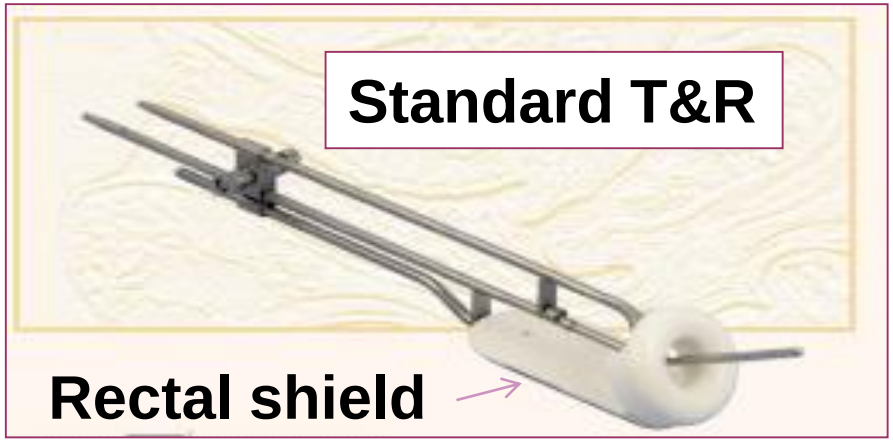

Fletcher Shielded

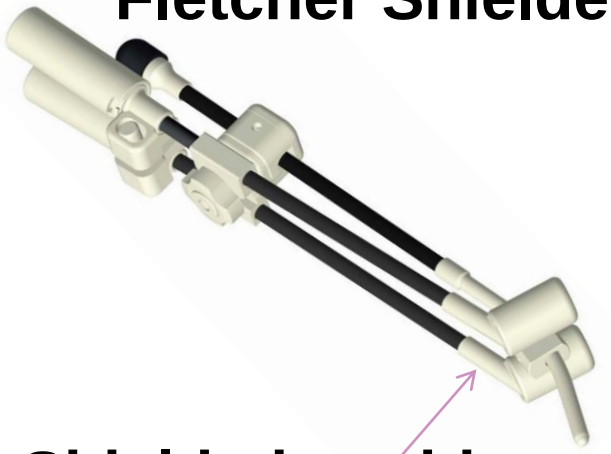

Shielded ovoids

Interstitial

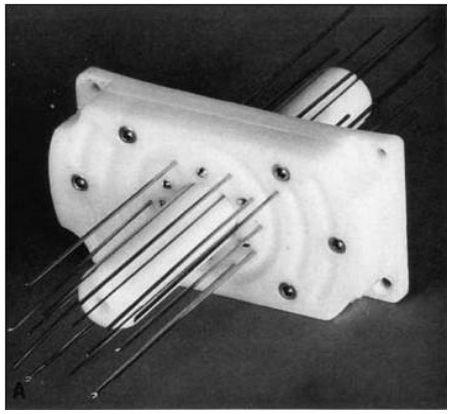

courtesy of F. Mourtada

Shielded applicators with cap

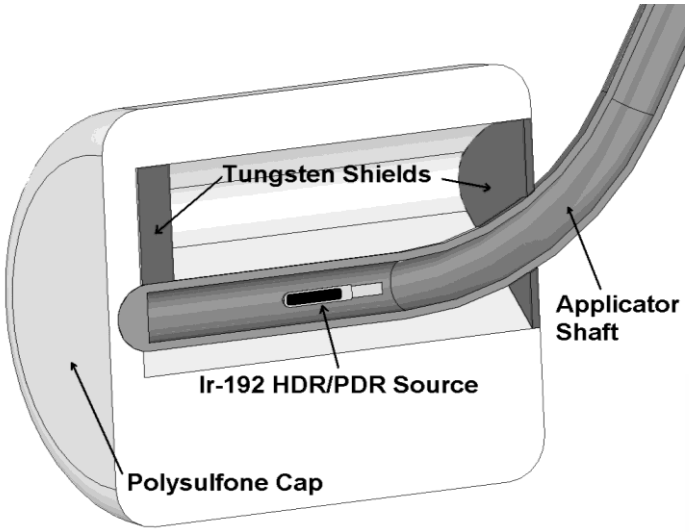

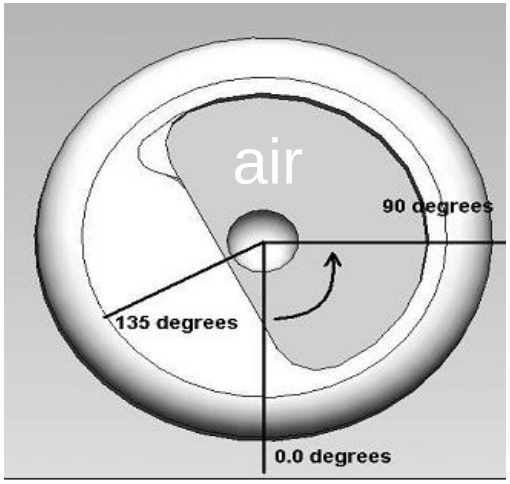

MCNPX 2.5 simulations compared with TG-43 predicted doses (Plato TPS)

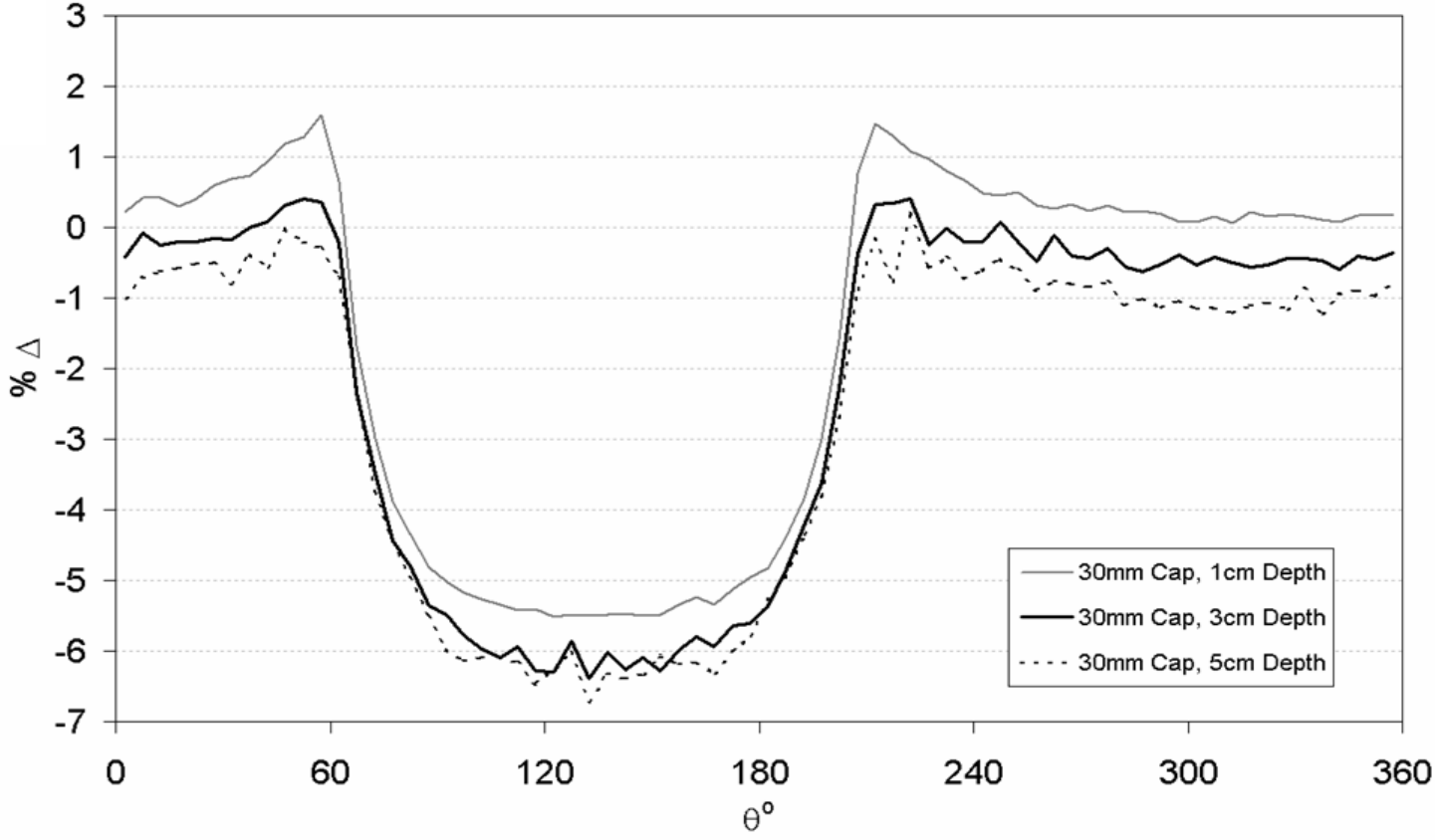

Price, Horton, Eifel, Mourtada, ABS annual meeting, 2007

Attenuation of intracavitary applicators in ^{192}Ir-HDR brachytherapy

Sung-Joon Ye,[a] Ivan A. Brezovich, Sui Shen, Jun Duan, Richard A. Popple, and Prem N. Pareek

Department of Radiation Oncology, University of Alabama School of Medicine, 1824 6th Avenue South, Birmingham, Alabama 35294

TABLE I. Elemental compositions and densities of the ^{192}Ir source and applicator components used in the Monte Carlo simulations.

Component	Material	Atomic composition	Density (g/cm^3)
Active wire	Iridium metal	1.0 Ir	22.42
Encapsulation	Stainless steel	[0.02 Si, 0.18 Cr	8.02
Uterine tube	Stainless steel	0.02 Mn, 0.67 Fe, 0.11 Ni]	8.02
Vaginal cylinder	Polysulfone	0.41 H, 0.5 C, 0.07 O, 0.02 S	1.40

Ye, Brezovich, Shen, Duan, Popple, Pareek, Med Phys, 31 (7), 2097-2106 (2004)

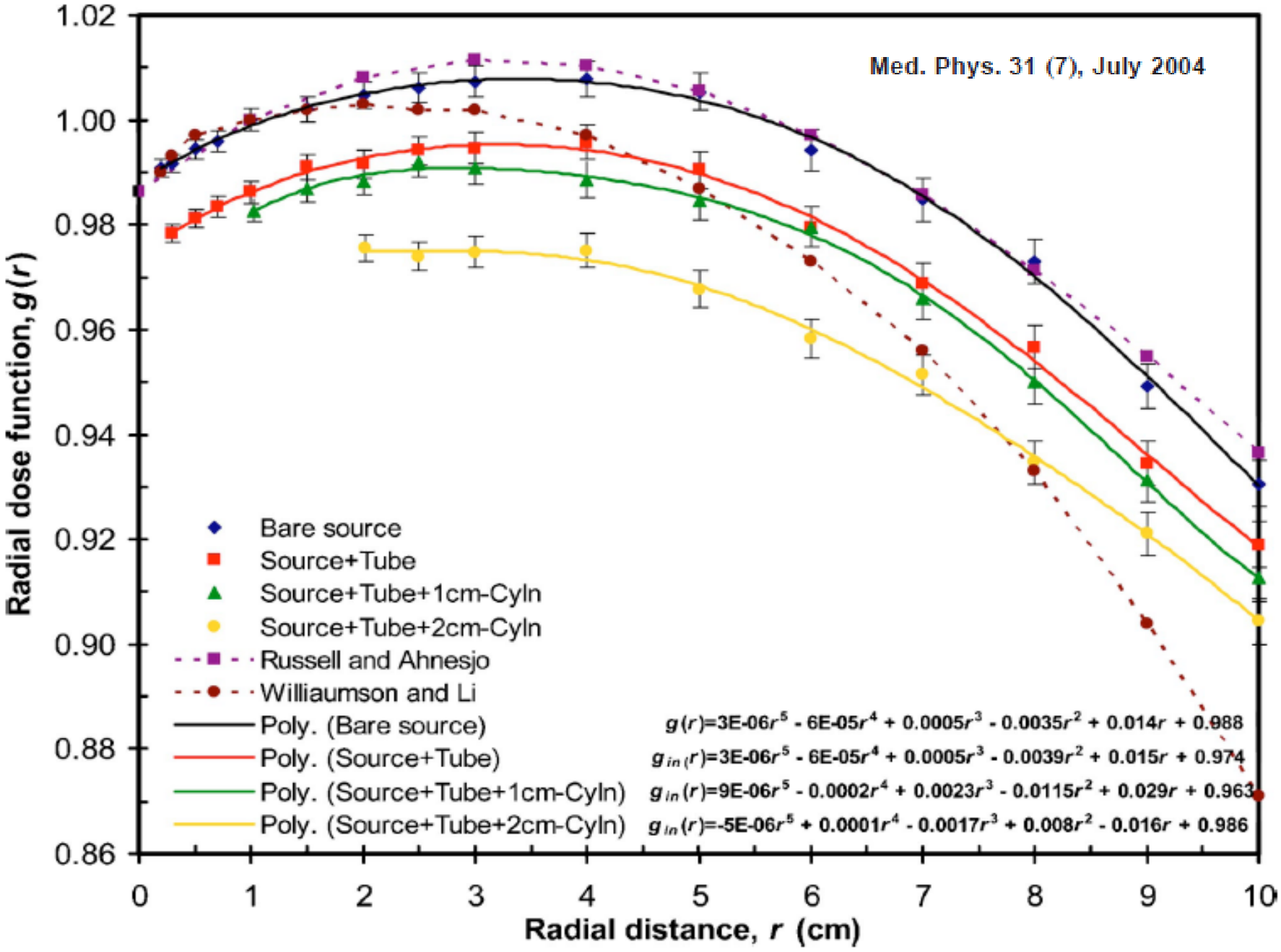

FIG. 5. Radial dose functions calculated for a bare source and a source embedded in various cylindrical applicators and their comparisons to published data. Fifth-order polynomial fittings to our calculated radial dose functions are also presented.

Impact of Heterogeneity-Based Dose Calculation Using a Deterministic Grid-Based Boltzmann Equation Solver for Intracavitary Brachytherapy

Justin K. Mikell, B.S.,[*,‖] Ann H. Klopp, M.D., Ph.D.,[†] Graciela M.N. Gonzalez, M.P.H.,[‡] Kelly D. Kisling, M.S.,[§,‖] Michael J. Price, Ph.D.,[**] Paula A. Berner, B.S.,[*] Patricia J. Eifel, M.D.,[†] and Firas Mourtada, Ph.D.[§,¶,††]

*Departments of *Radiation Physics, †Radiation Oncology, ‡Biostatistics, §Radiation Physics—Patient Care, and ¶Experimental Diagnostic Imaging, The University of Texas MD Anderson Cancer Center, Houston, Texas; ‖University of Texas Graduate School of Biomedical Sciences at Houston, Houston, Texas; **Department of Physics and Astronomy, Louisiana State University and Agricultural and Mechanical College, Baton Rouge, Louisiana, and Mary Bird Perkins Cancer Center, Baton Rouge, Louisiana; and ††Department of Radiation Oncology, Helen F. Graham Cancer Center, Newark, Delaware*

Summary

This study investigated the use of a grid-based Boltzmann solver (GBBS) for cervical cancer patients treated with unshielded CT/MR applicators. The GBBS was found to have minimal impact on clinical dosimetric parameters for these patients. GBBS differences from standard TG-43 dose estimates were mainly due to source, boundary, and applicator model differences. CT-to-material mapping of rectal and balloon contrast did not impact clinical dosimetry. Rectal dose parameters may be affected by incorrectly mapping packing material.

Purpose: To investigate the dosimetric impact of the heterogeneity dose calculation Acuros (Transpire Inc., Gig Harbor, WA), a grid-based Boltzmann equation solver (GBBS), for brachytherapy in a cohort of cervical cancer patients.

Methods and Materials: The impact of heterogeneities was retrospectively assessed in treatment plans for 26 patients who had previously received ^{192}Ir intracavitary brachytherapy for cervical cancer with computed tomography (CT)/magnetic resonance-compatible tandems and unshielded colpostats. The GBBS models sources, patient boundaries, applicators, and tissue heterogeneities. Multiple GBBS calculations were performed with and without solid model applicator, with and without overriding the patient contour to 1 g/cm^3 muscle, and with and without overriding contrast materials to muscle or 2.25 g/cm^3 bone. Impact of source and boundary modeling, applicator, tissue heterogeneities, and sensitivity of CT-to-material mapping of contrast were derived from the multiple calculations. American Association of Physicists in Medicine Task Group 43 (TG-43) guidelines and the GBBS were compared for the following clinical dosimetric parameters: Manchester points A and B, International Commission on Radiation Units and Measurements (ICRU) report 38 rectal and bladder points, three and nine o'clock, and D_{2cm3} to the bladder, rectum, and sigmoid.

Results: Points A and B, D_2 cm^3 bladder, ICRU bladder, and three and nine o'clock were within 5% of TG-43 for all GBBS calculations. The source and boundary and applicator account for most of the differences between the GBBS and TG-43 guidelines. The D_{2cm3} rectum ($n = 3$), D_{2cm3} sigmoid ($n = 1$), and ICRU rectum ($n = 6$) had differences of >5% from TG-43 for the worst case incorrect mapping of contrast to bone. Clinical dosimetric parameters were within 5% of TG-43 when rectal and balloon contrast were mapped to bone and radiopaque packing was not overridden.

Conclusions: The GBBS has minimal impact on clinical parameters for this cohort of patients with unshielded applicators. The incorrect mapping of rectal and balloon contrast does not have a significant impact on clinical parameters. Rectal parameters may be sensitive to the mapping of radiopaque packing.

- ✓ VS-2000 source
- ✓ Applicator part #: AL07334001

IJROBP, vol 83, No 3, pp e414-e422, 2012

ICRU Rectal Point Dose Impact of GBBS relative to TG-43

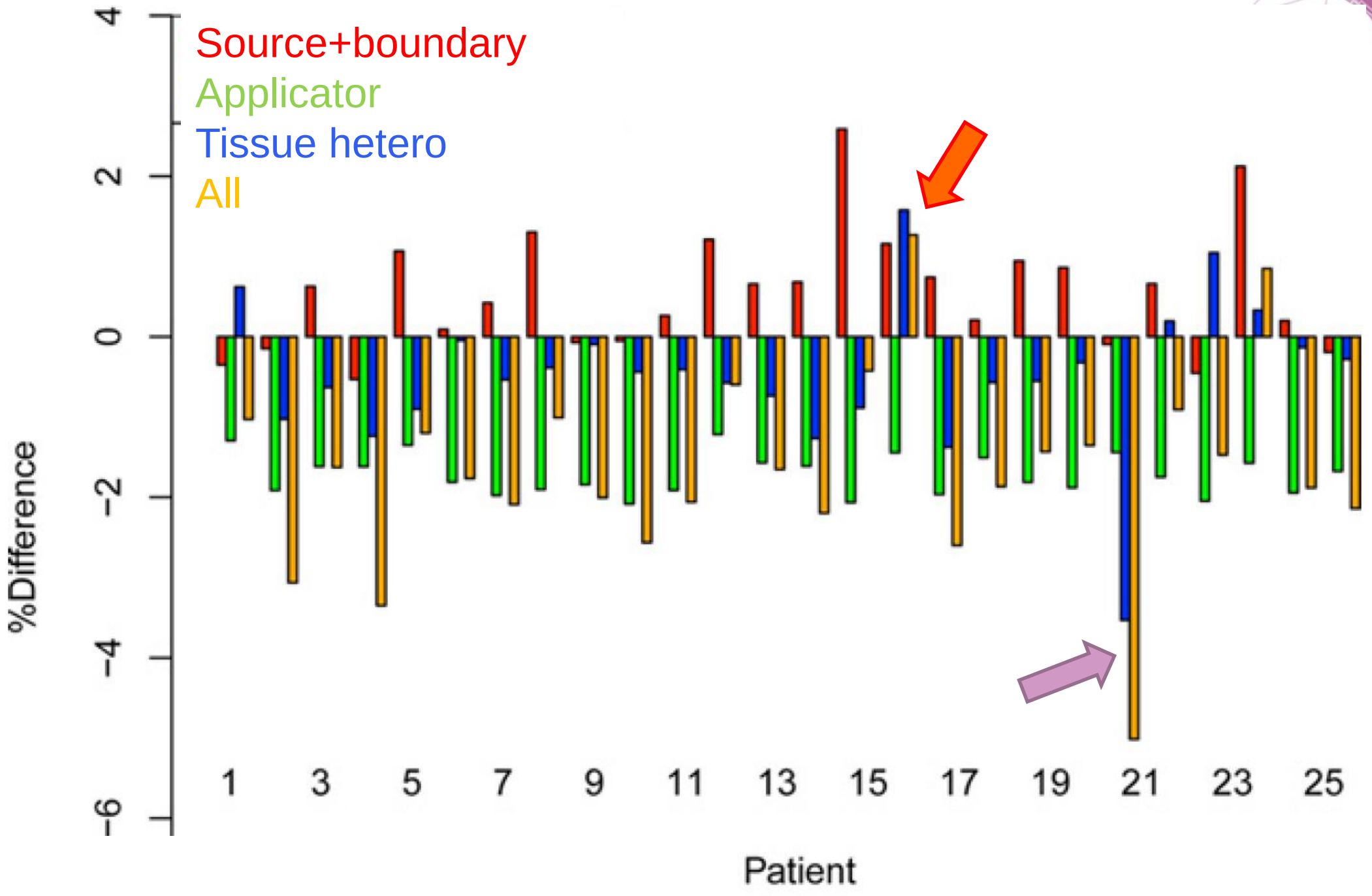

TG43

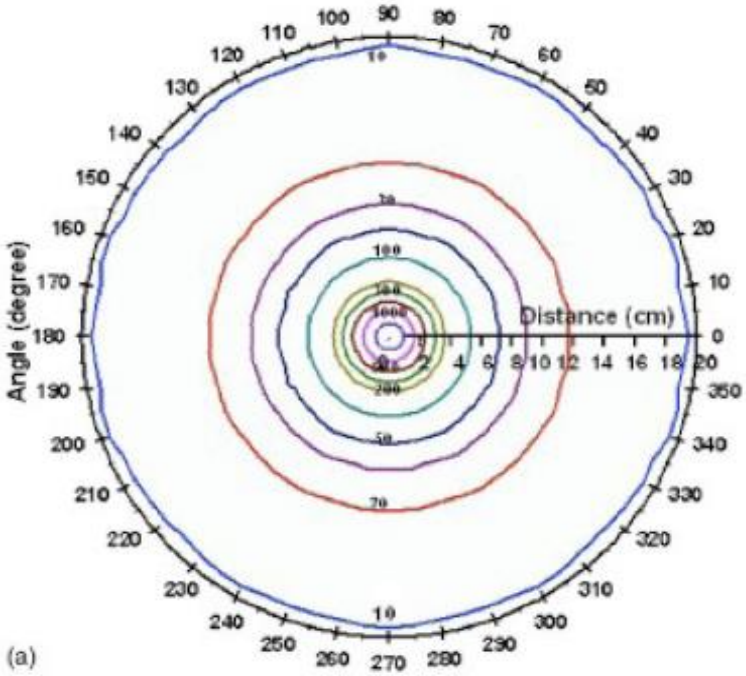

90°

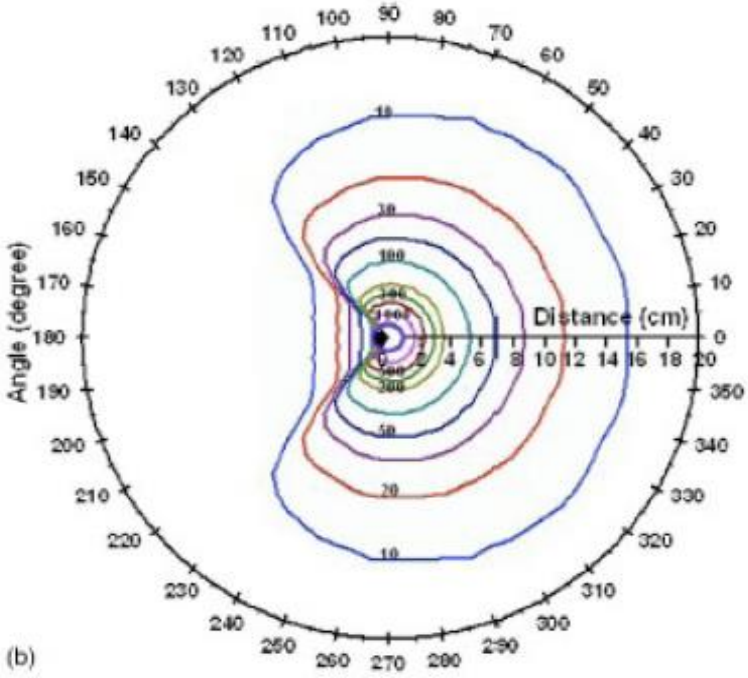

180°

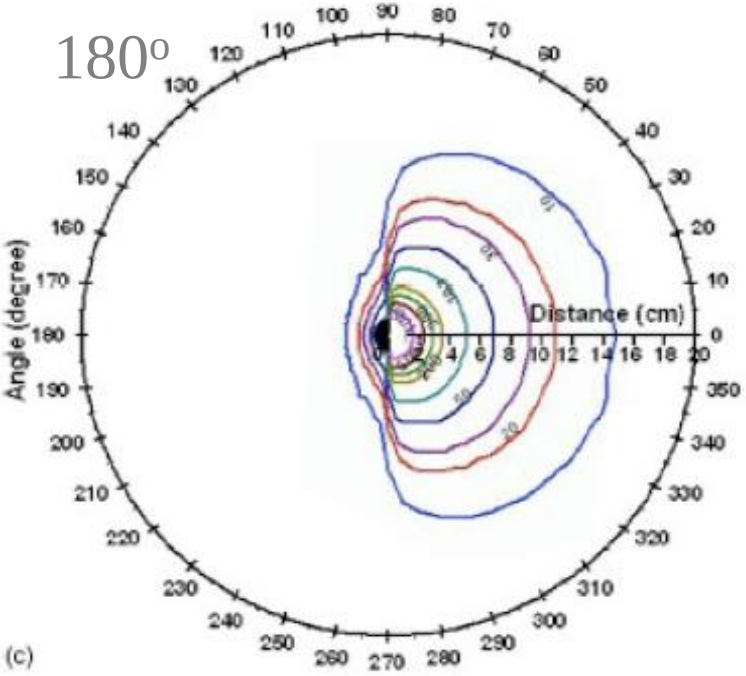

270°

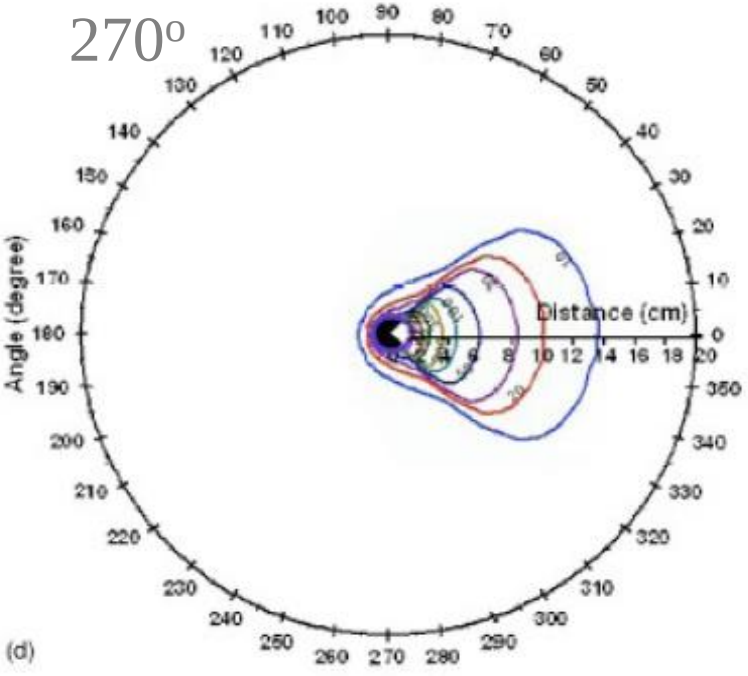

6 : Sureka C S, Aruna P, Ganesan S, « Computation of relative dose distribution and effective transmission around a shielded vaginal cylinder with Ir-192 HDR source using MCNP4B », Med. Phys., 44(6), 2006

Shielded Geometry

Petrokokkinos *et al*., MedPhys 38, 1981-1992 (2011)

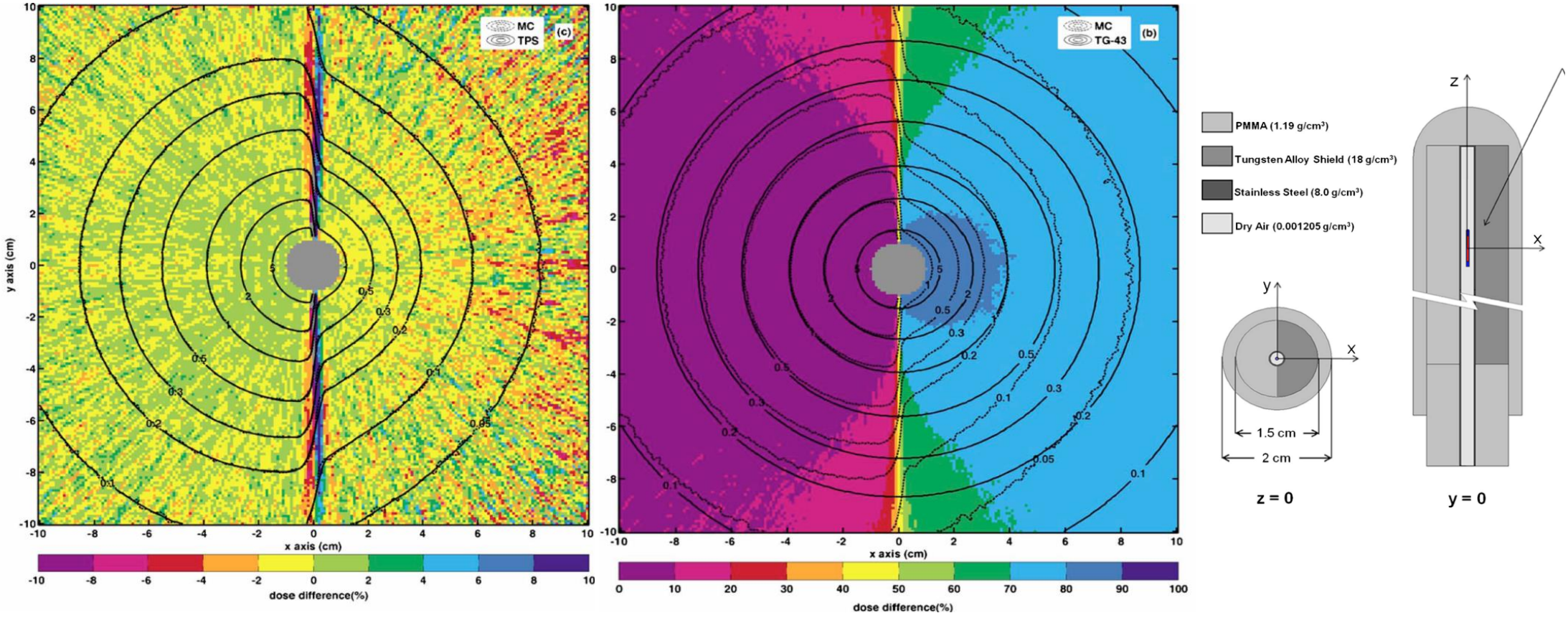

WG Shielded Applicator Test Case

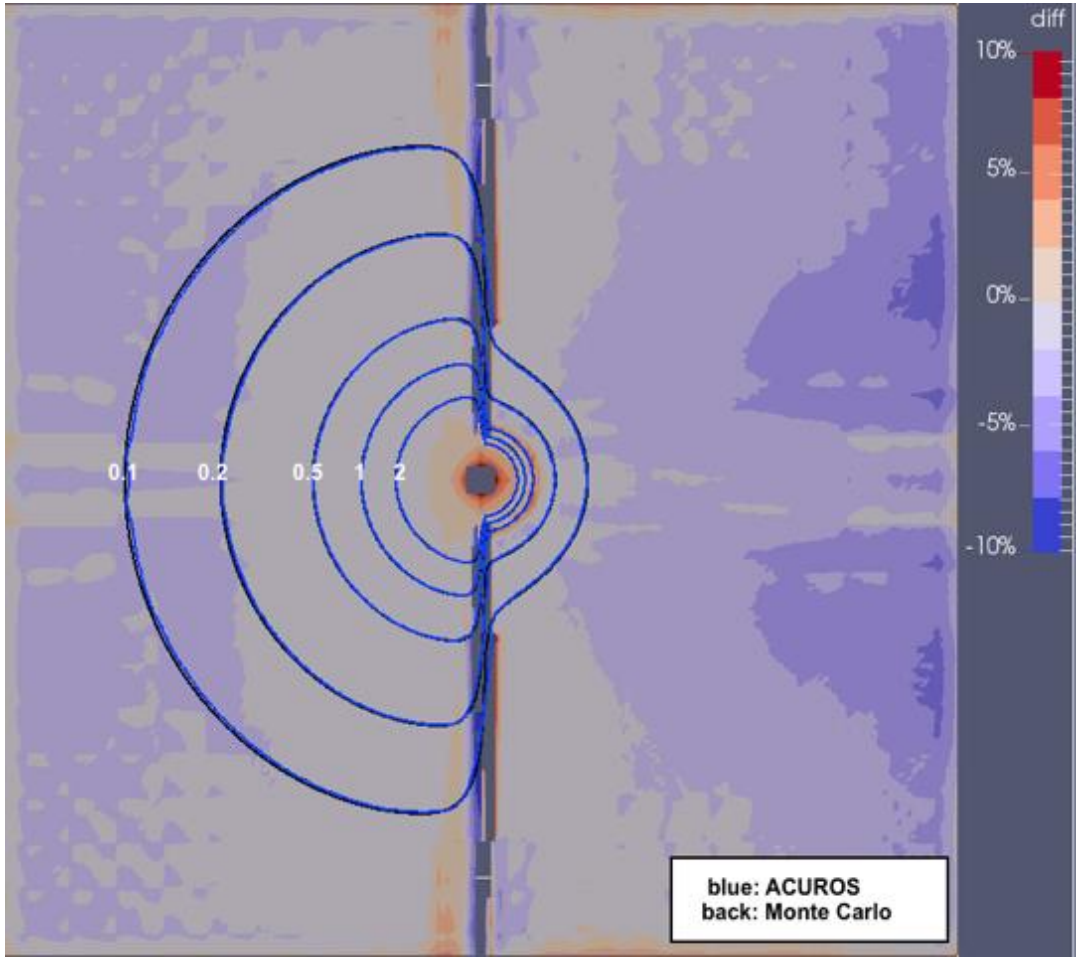

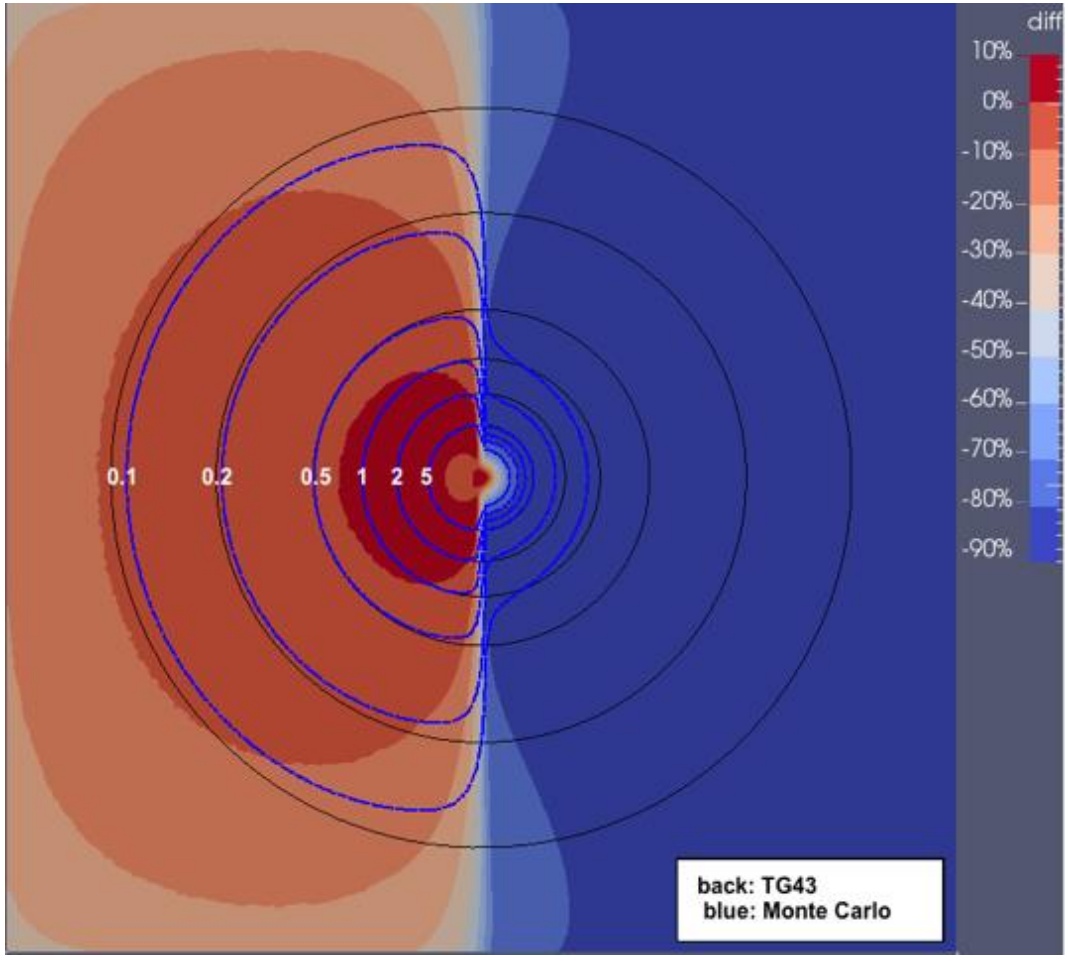

Summary for GYN Brachytherapy

- The new brachy dose calculation algorithms provide more accurate dose distributions for GYN brachytherapy than the standard TG-43.
- Unshielded GYN CT/MR applicators impact is within +/-5%
- Shielded Applicator can significantly reduces dose to OARs

Sensitivity of Anatomic Sites to Dosimetric Limitations of Current Planning Systems

anatomic site	photon energy	absorbed dose	attenuation	shielding	scattering	beta/kerma dose
prostate	high					
	low	XXX	XXX	XXX		
breast	high				XXX	
	low	XXX	XXX	XXX		
GYN	high			XXX		
	low	XXX	XXX			
skin	high			XXX	XXX	←
	low	XXX		XXX	XXX	
lung	high				XXX	XXX
	low	XXX	XXX		XXX	
penis	high				XXX	
	low	XXX			XXX	
eye	high			XXX	XXX	XXX
	low	XXX	XXX	XXX	XXX	

Rivard, Venselaar, Beaulieu, *Med Phys* 36, 2136-2153 (2009)

HDR ^{192}Ir Skin Molds/Flaps

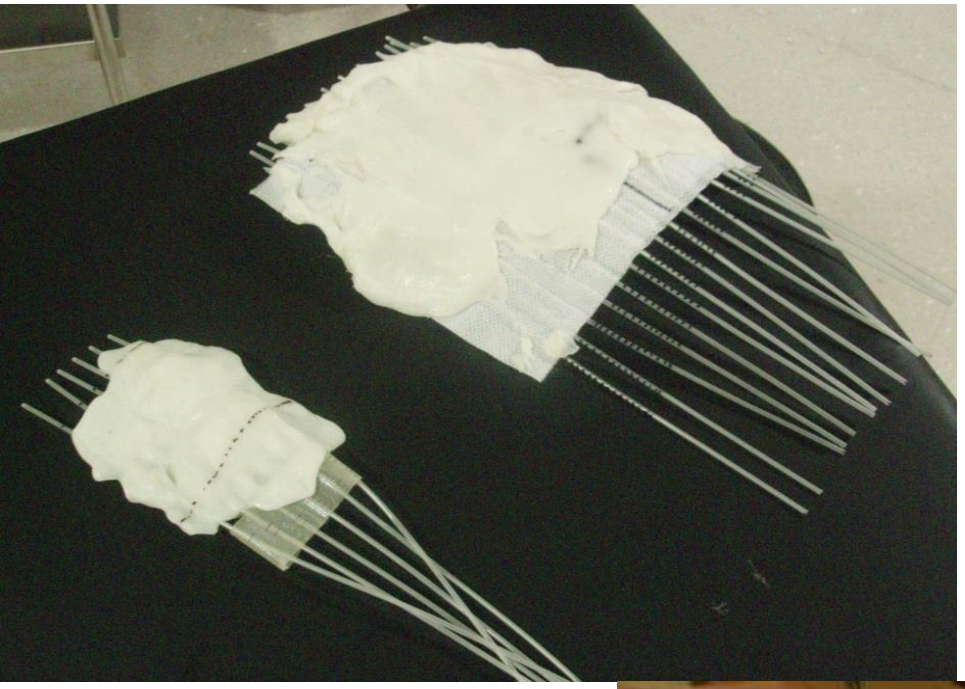

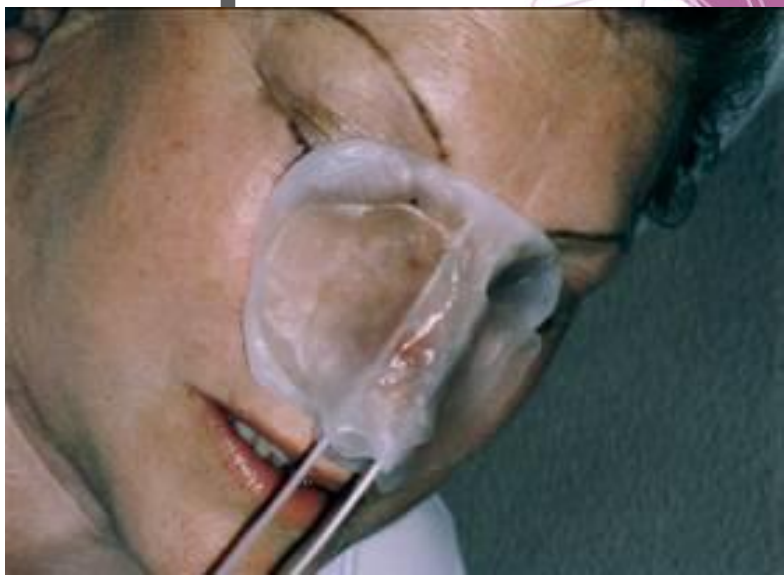

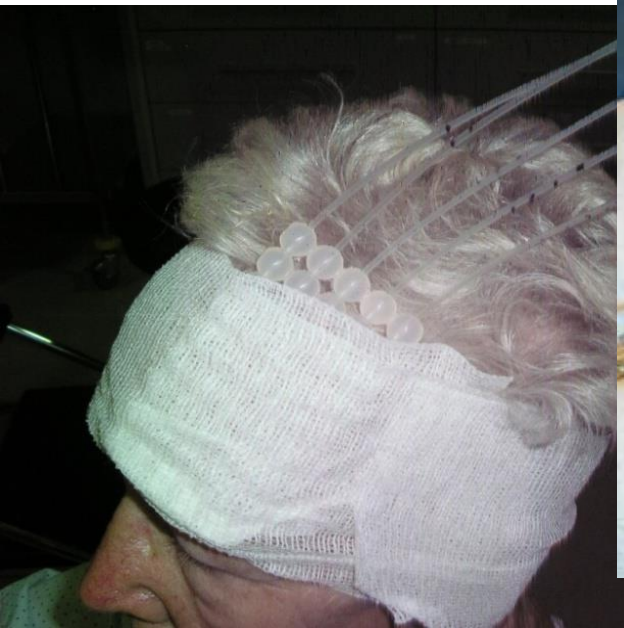

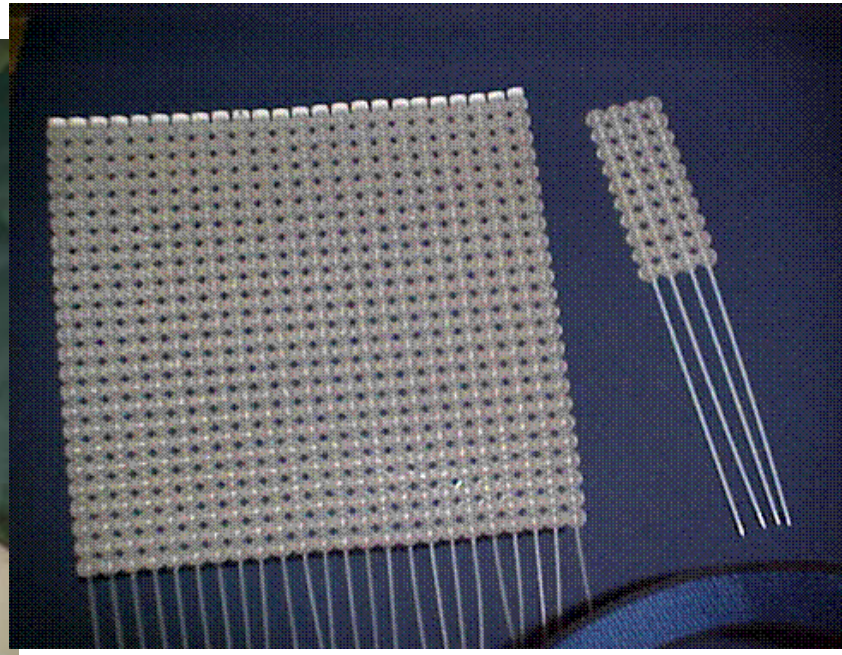

courtesy J. Perez-Calatayud

HDR ^{192}Ir Shielded (Leipzig) Applicators

Cup-shaped of tungsten
Horizontal and Vertical
Diameters 1 cm, 2 cm, 3 cm

Plastic cap 1 mm, to reduce skin dose due to electrons

courtesy J. Perez-Calatayud

Oncentra® ACE TG-43

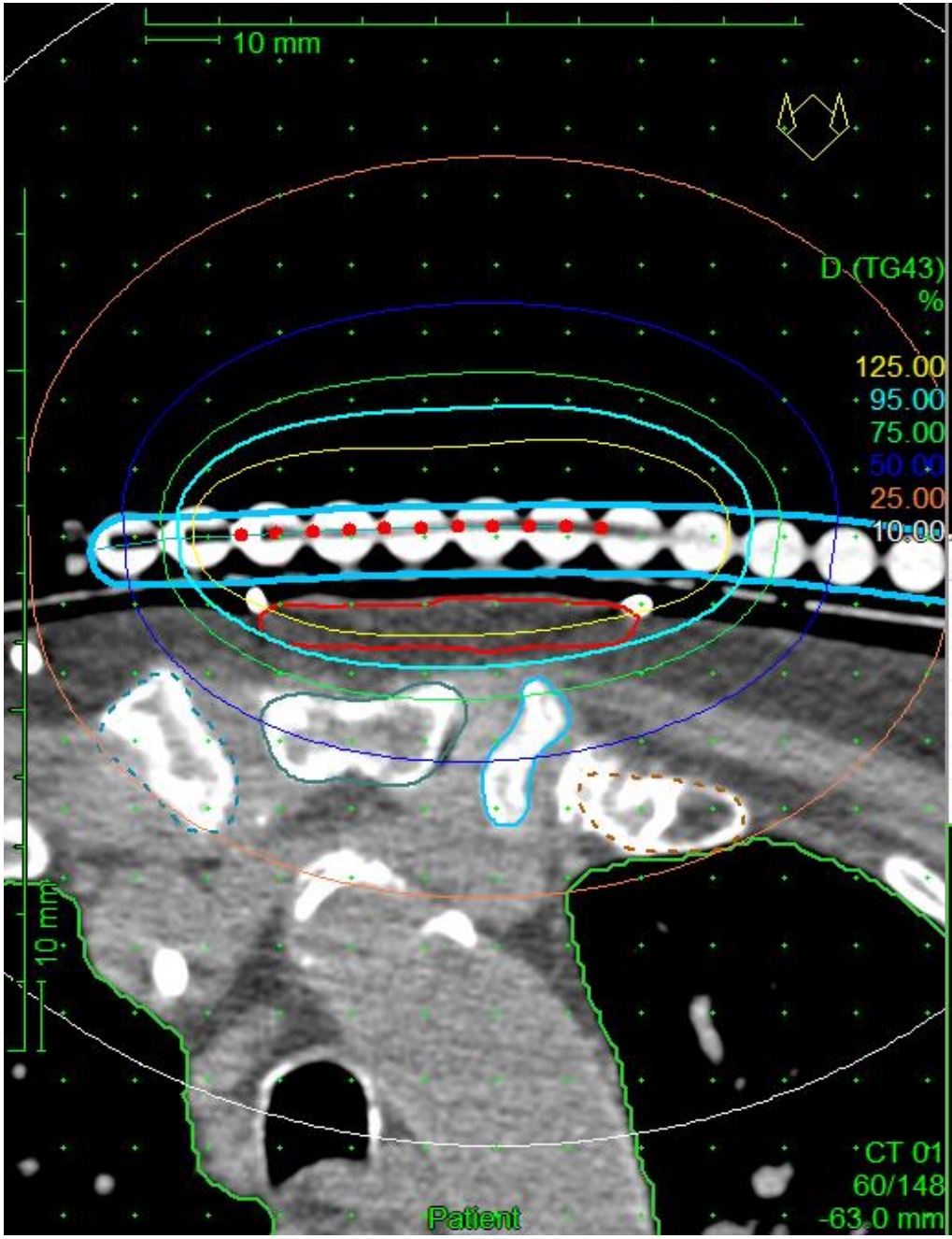

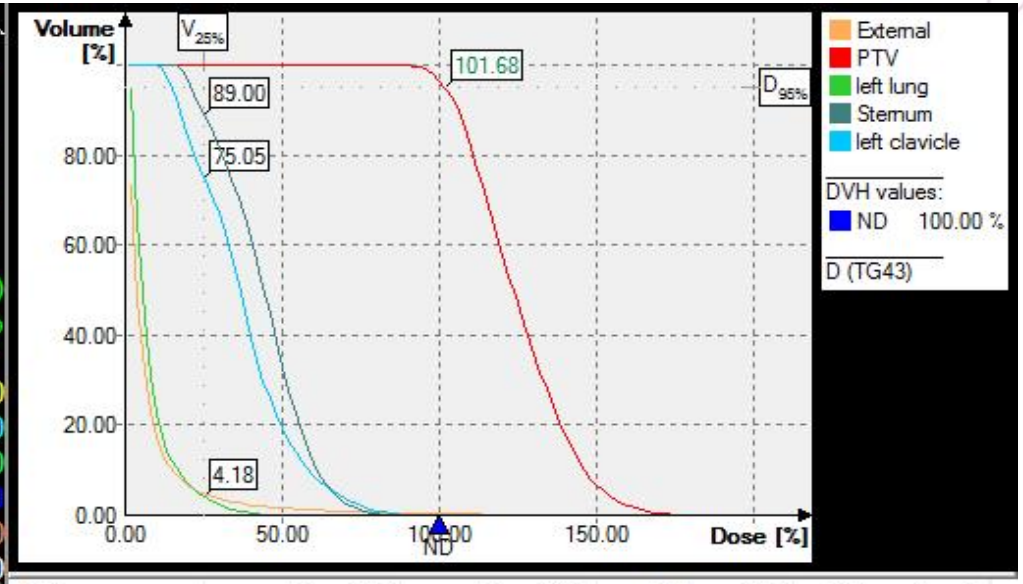

ROI	Dose [%]	Dose [Gy]	Volume [%]	Volume [ccm]
left lung	42.01	1.6804	0.24	**2.00**
Sternum	65.03	2.6011	5.69	**2.00**
left clavicle	48.71	1.9484	21.14	**2.00**
left lung	**25.00**	1.0000	4.18	34.51
Sternum	**25.00**	1.0000	89.00	31.31
left clavicle	**25.00**	1.0000	75.05	7.10
PTV	101.68	4.0673	**95.00**	19.74

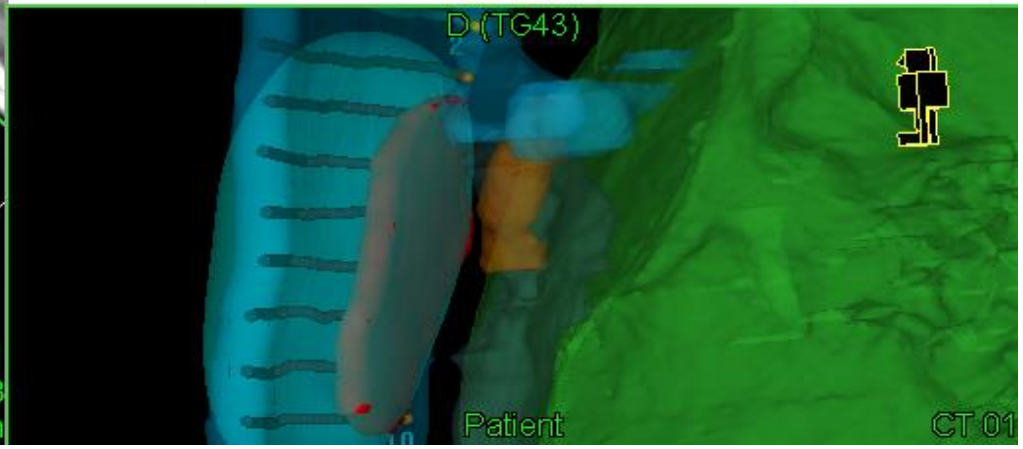

courtesy Y. Niatsetski

Oncentra® ACE TG-186

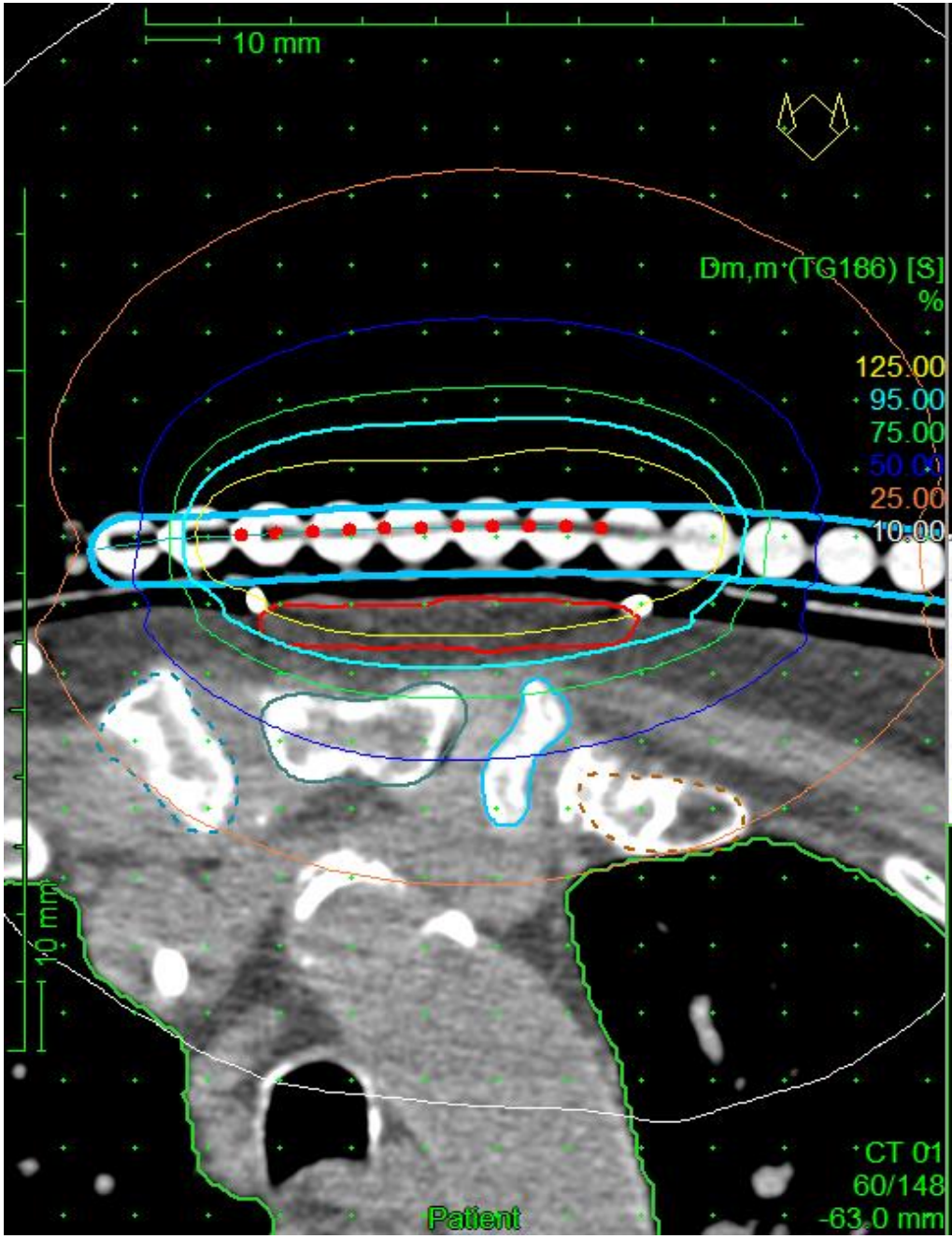

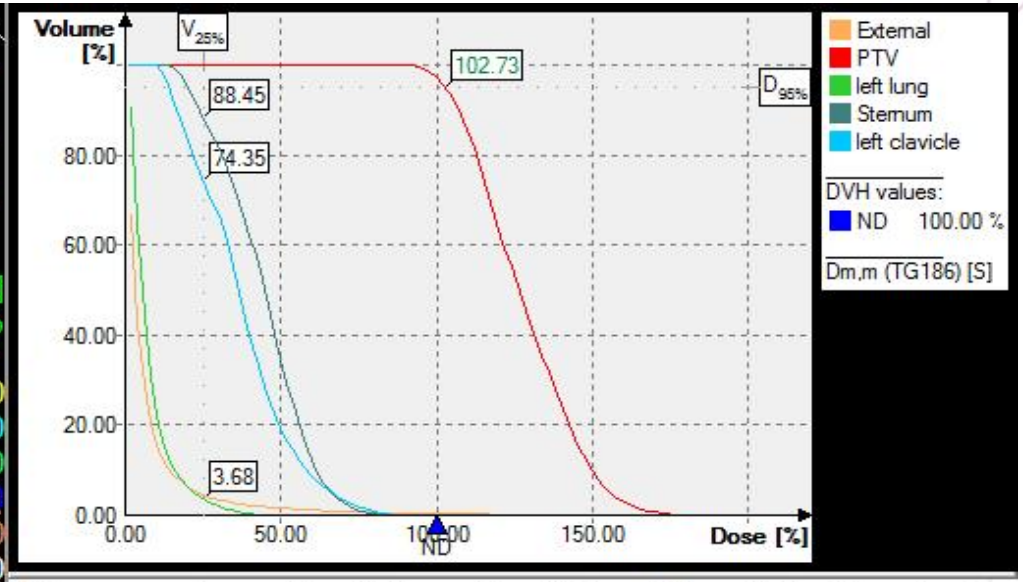

ROI	Dose [%]	Dose [Gy]	Volume [%]	Volume [ccm]
left lung	39.93	1.5970	0.24	**2.00**
Sternum	65.36	2.6145	5.69	**2.00**
left clavicle	48.85	1.9538	21.14	**2.00**
left lung	**25.00**	1.0000	3.68	30.37
Sternum	**25.00**	1.0000	88.45	31.12
left clavicle	**25.00**	1.0000	74.35	7.03
PTV	102.73	4.1093	**95.00**	19.74

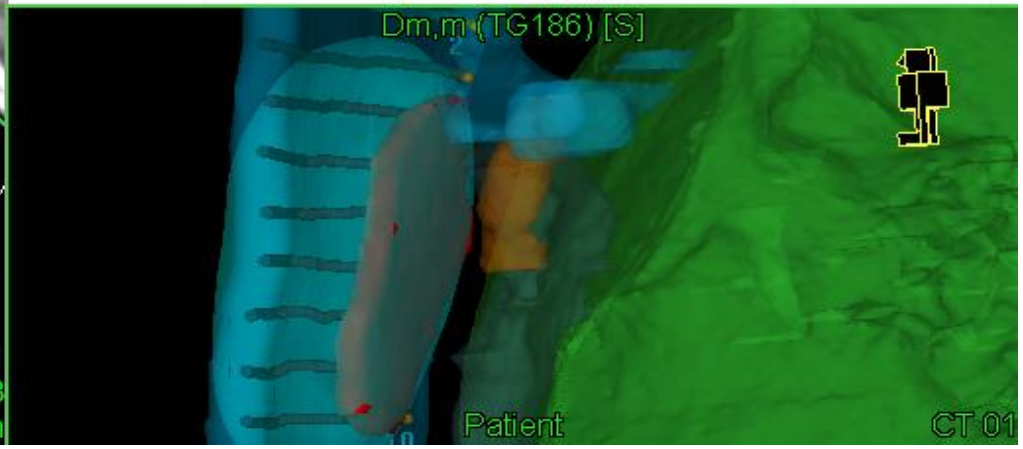

courtesy Y. Niatsetski

Oncentra® ACE Skin Mold Differences

target	TG-43 D_{95} (Gy)	TG-186 D_{95} (Gy)	TG-43 Dose (%)	TG-186 Dose (%)
PTV	**4.07**	**4.11**	**101.7**	**102.7**
no big deal for skin mold				
ROI	TG-43 V_{25} (cm^3)	TG-186 V_{25} (cm^3)	TG-43 V_{25} (%)	TG-186 V_{25} (%)
sternum	**31.31**	**31.12**	**89.00**	**88.45**
clavicle	**7.10**	**7.03**	**75.05**	**74.35**
lung	**34.51**	**30.37**	**4.18**	**3.68**

courtesy of M Rivard

Acuros™ BV TG-43

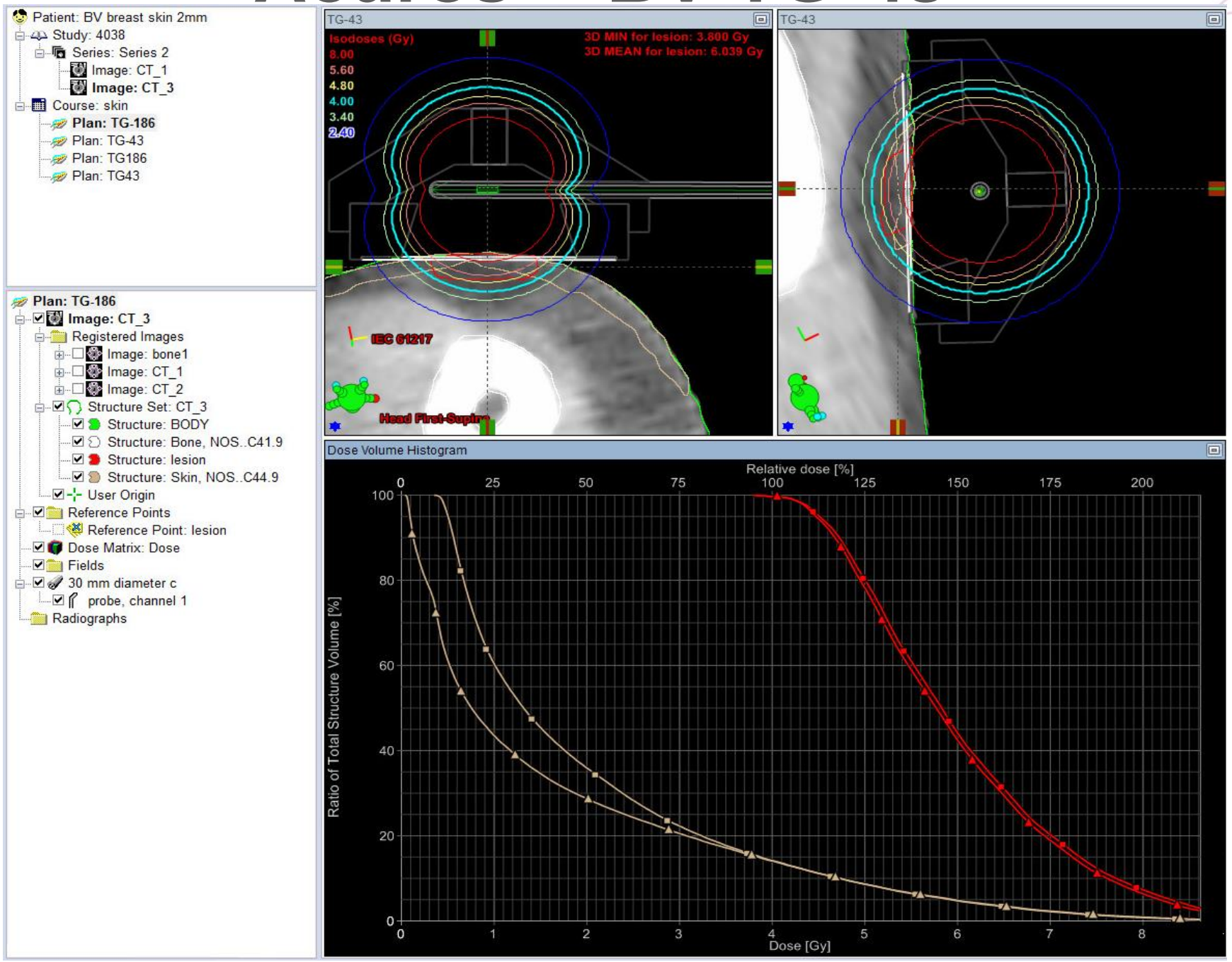

courtesy R. Park

Acuros™ BV TG-186

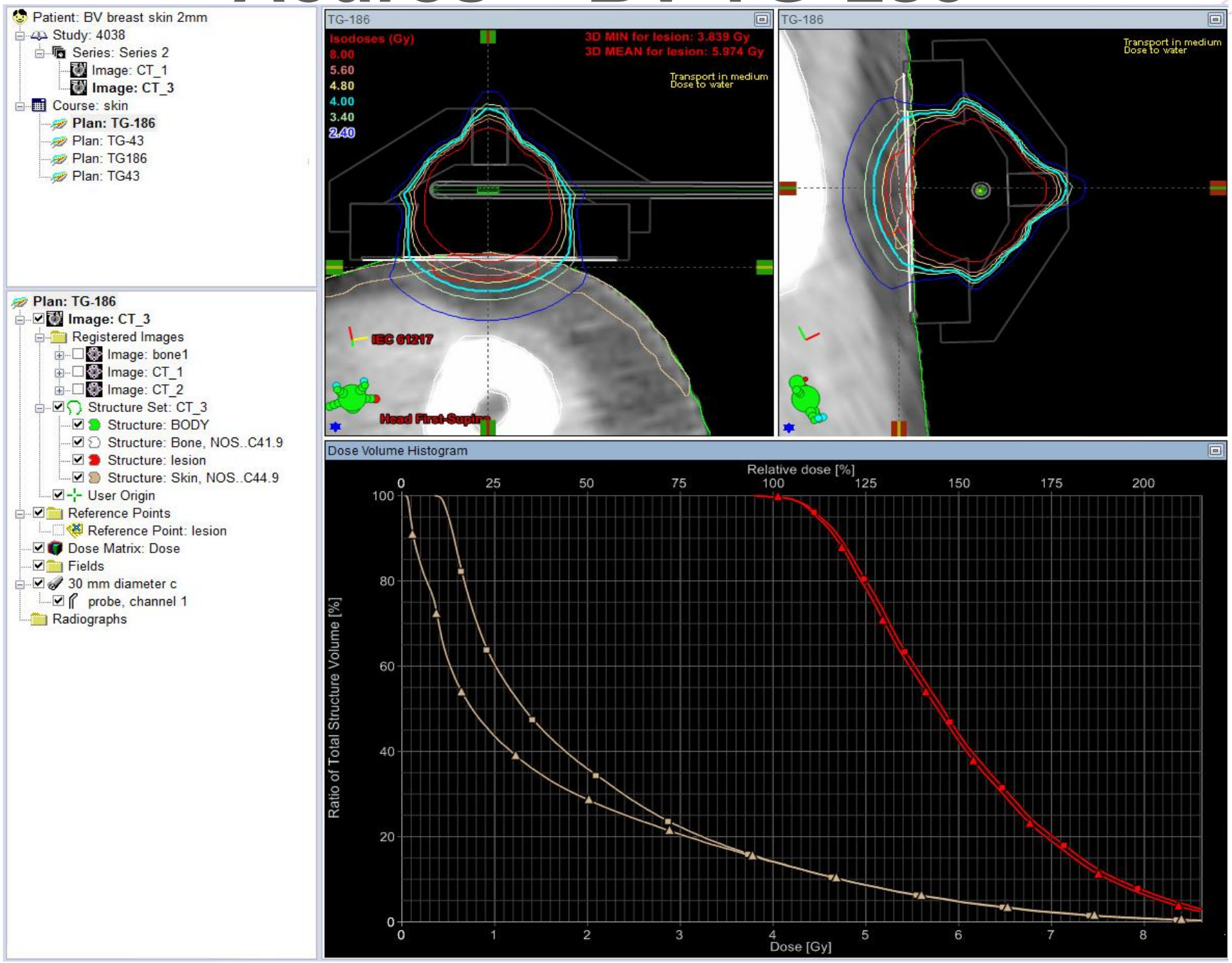

courtesy R. Park

Acuros™ BV Shielded Applicator

target	TG-43 D_{95} (Gy)	TG-186 D_{95} (Gy)	TG-43 Dose (%)	TG-186 Dose (%)
PTV	**4.50**	**4.50**	**100.0**	**100.0**
collimation is important				
ROI	TG-43 V_{25} (cm^3)	TG-186 V_{25} (cm^3)	TG-43 V_{25} (%)	TG-186 V_{25} (%)
skin	**3.97**	**2.88**	**60.1**	**43.7**
bone	**3.32**	**5.85**	**3.88**	**6.83**

courtesy of M Rivard

Comparing TG-43 and MC for Skin BT

Dosimetry comparison between TG-43 and Monte Carlo calculations using the Freiburg flap for skin high-dose-rate brachytherapy

Javier Vijande[1,2,*], Facundo Ballester[1], Zoubir Ouhib[3], Domingo Granero[4], M. Carmen Pujades-Claumarchirant[5], Jose Perez-Calatayud[5]

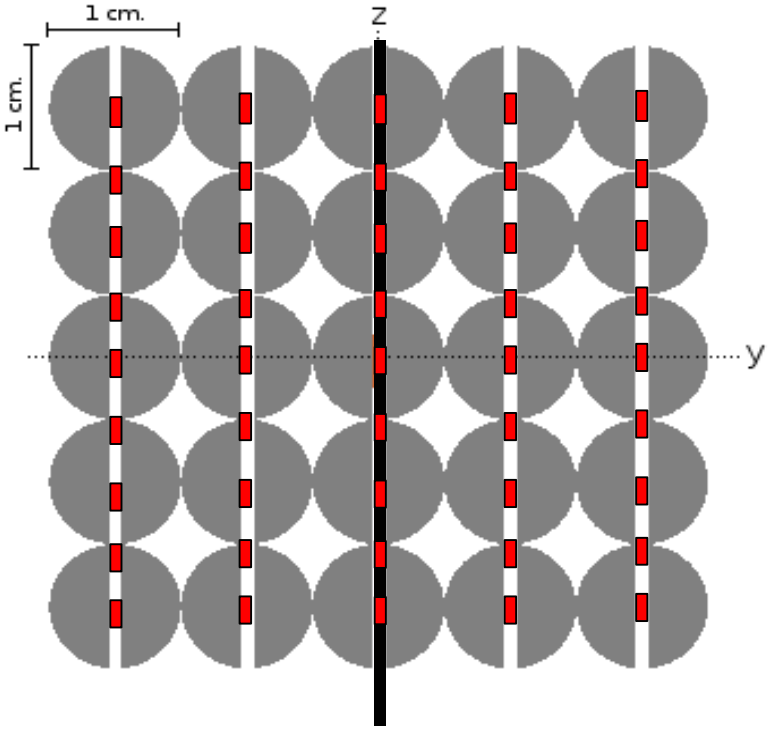

⇨ evaluate scatter defect, air gap

⇨ 5x5 cm^2 clinical mesh

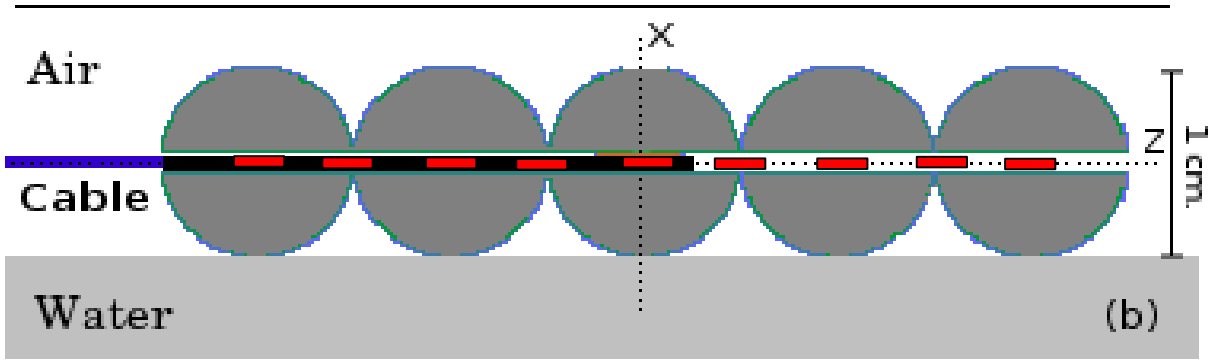

Vijande et al, *J Contemp Brachy* 4, 34-44 (2012) courtesy J. Perez-Calatayud

Comparing TG-43 and MC for Skin BT

Monte Carlo (MCFF) / TG-43

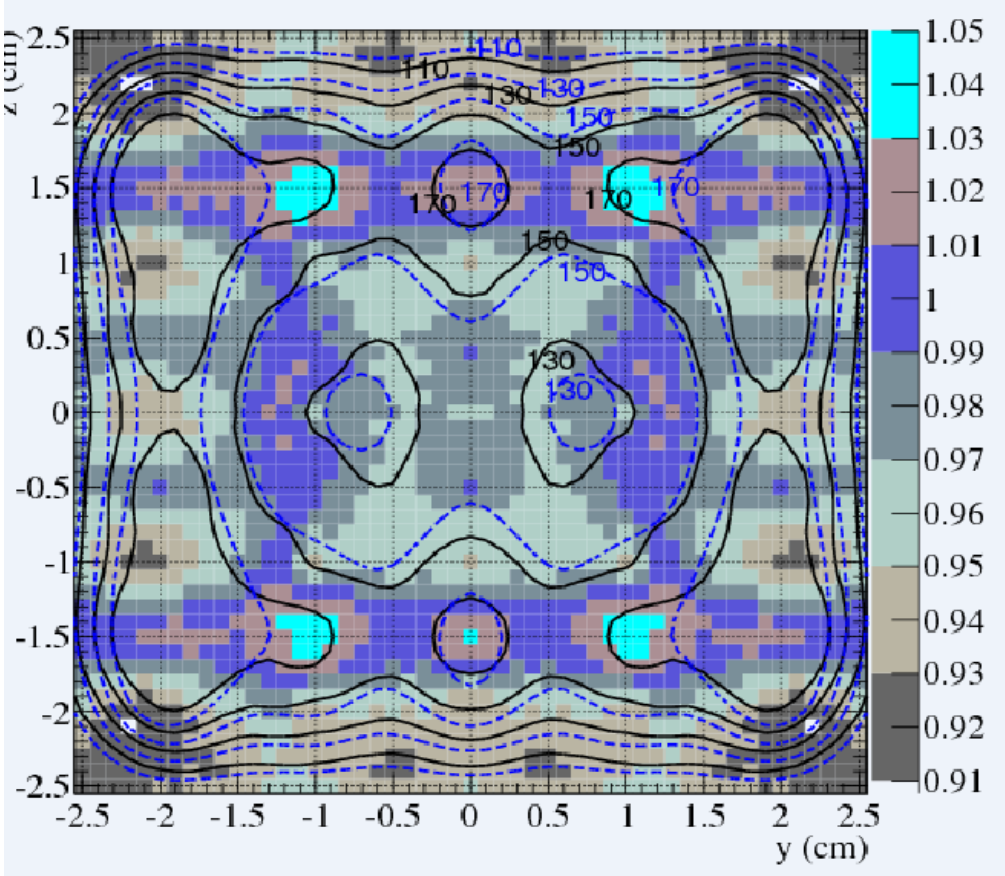

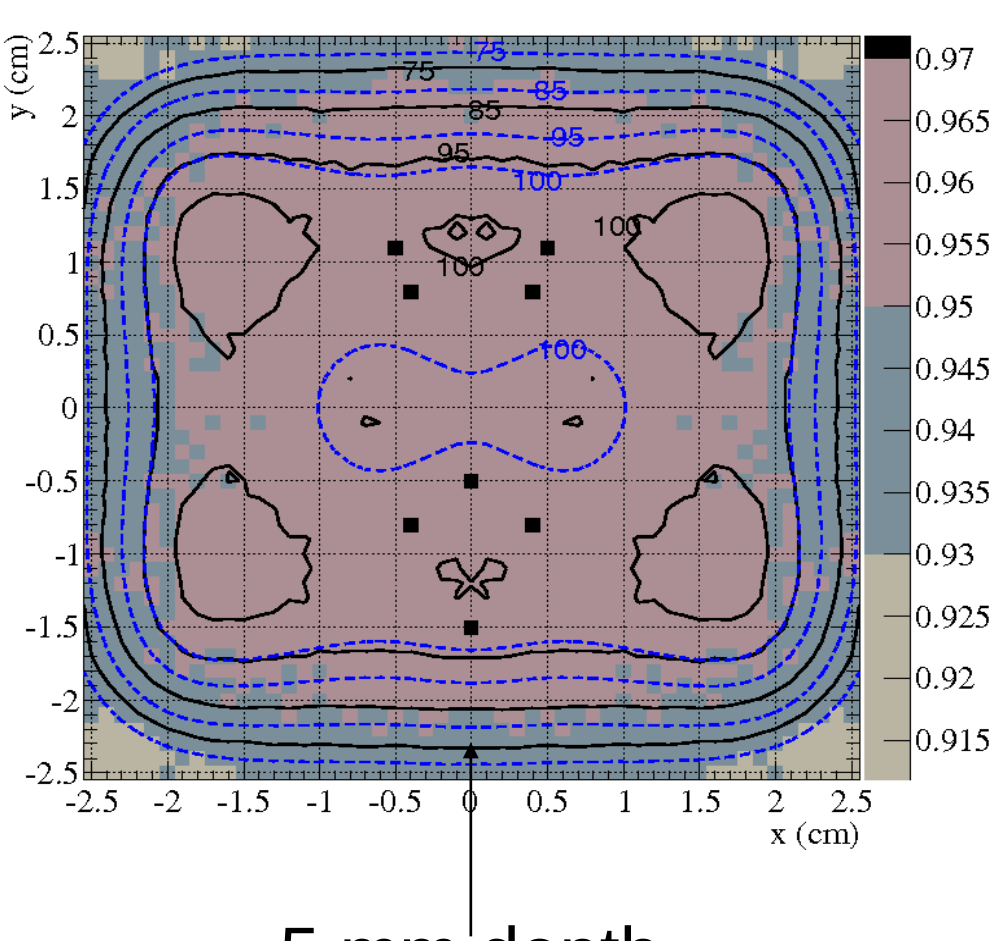

surface

5 mm depth

+5% to -7%

-4% to -7%

over/under dose compensation between adjacent spheres

Vijande et al, *J Contemp Brachy* 4, 34-44 (2012) courtesy J. Perez-Calatayud

Summary for Skin Brachytherapy

- Challenges due to irregular surface
  - Interplay between scatter and shielding effects

- Departure from TG43 calculated dose depends on shielding and/or presence of air gaps
  - Small for PTV with unshielded geometry
  - Need further dose recalculation studies of (large) patient cohorts

Sensitivity of Anatomic Sites to Dosimetric Limitations of Current Planning Systems

anatomic site	photon energy	absorbed dose	attenuation	shielding	scattering	beta/kerma dose
prostate	high					
	low	XXX	XXX	XXX		
breast	high				XXX	
	low	XXX	XXX	XXX		
GYN	high			XXX		
	low	XXX	XXX			
skin	high			XXX	XXX	
	low	XXX		XXX	XXX	
lung	high				XXX	XXX
	low	XXX	XXX		XXX	
penis	high				XXX	←
	low	XXX			XXX	
eye	high			XXX	XXX	XXX
	low	XXX	XXX	XXX	XXX	

Rivard, Venselaar, Beaulieu, *Med Phys* 36, 2136-2153 (2009)

Penil brachytherapy

			PTV						Urethra							
	GTV V100 [SD]		V100 [SD]		V150 [SD]		V200 [SD]		D 1cc [SD]		D 0.5 cc [SD]		D 0.1 cc [SD]		Dmax [SD]	
TG43	99.2	[1.7]	74.3	[15.0]	20.7	[2.8]	8.9	[0.9]	6.9	[2.2]	31.6	[14.1]	76.5	[5.3]	88.8	[9.4]
Monte Carlo	97.0	[3.0]	70.0	[14.1]	18.6	[2.3]	8.7	[1.1]	7.2	[3.1]	36.2	[13.8]	68.5	[4.5]	85.0	[9.0]
MC - TG43 dose difference (Gy)	-2.3		-4.3		-2.0		-0.3		0.4		4.6		-8.1		-3.7	
MC - TG43 dose difference (%)	-2.3		-5.8		-9.7		-2.9		5.1		14.6		-10.6		-4.2	

Carlone et al, World Brachy Congress 2016

Head and Neck?

anatomic site	photon energy	absorbed dose	attenuation	shielding	scattering	beta/kerma dose
prostate	high					
	low	XXX	XXX	XXX		
breast	high				XXX	
	low	XXX	XXX	XXX		
GYN	high			XXX		
	low	XXX	XXX			
skin	high			XXX	XXX	
	low	XXX		XXX	XXX	
lung	high				XXX	XXX
	low	XXX	XXX		XXX	
penis	high				XXX	
	low	XXX			XXX	
eye	high			XXX	XXX	XXX
	low	XXX	XXX	XXX	XXX	

Rivard, Venselaar, Beaulieu, *Med Phys* 36, 2136-2153 (2009)

Geometry

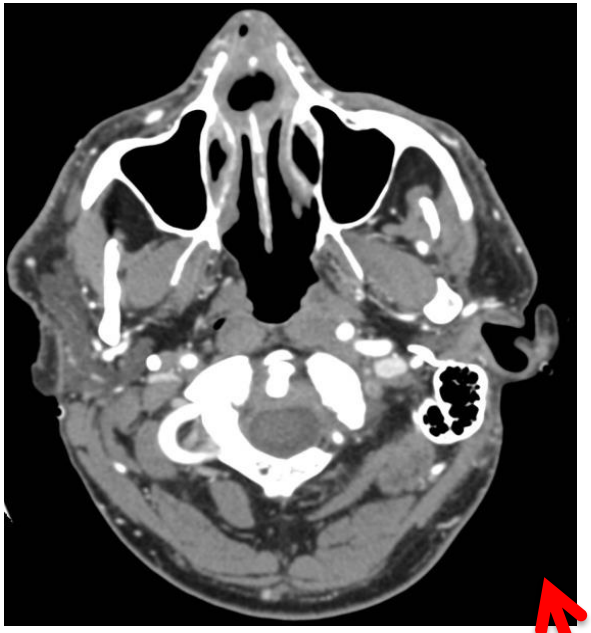

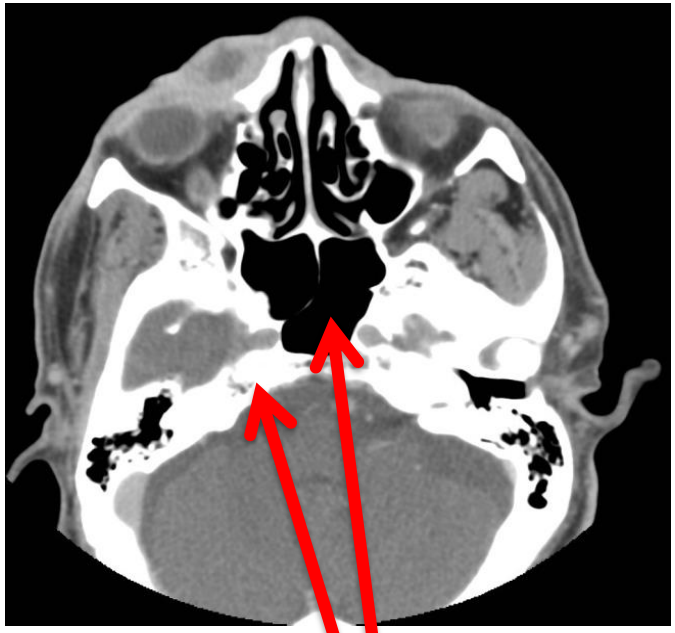

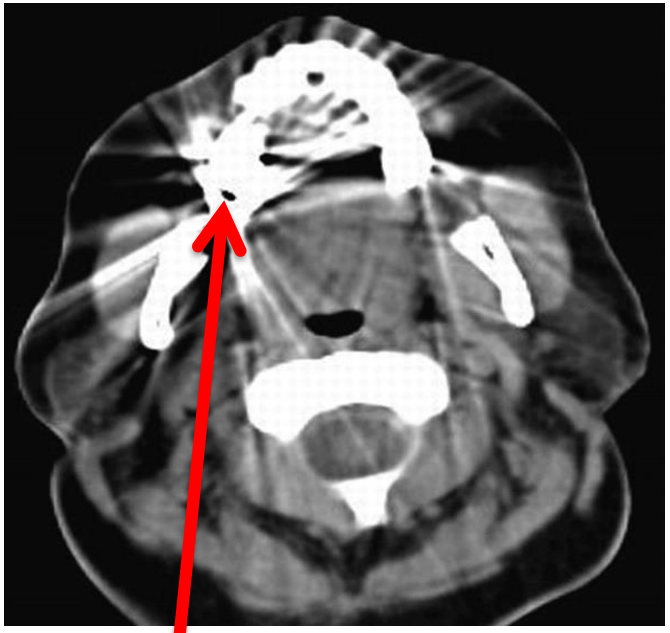

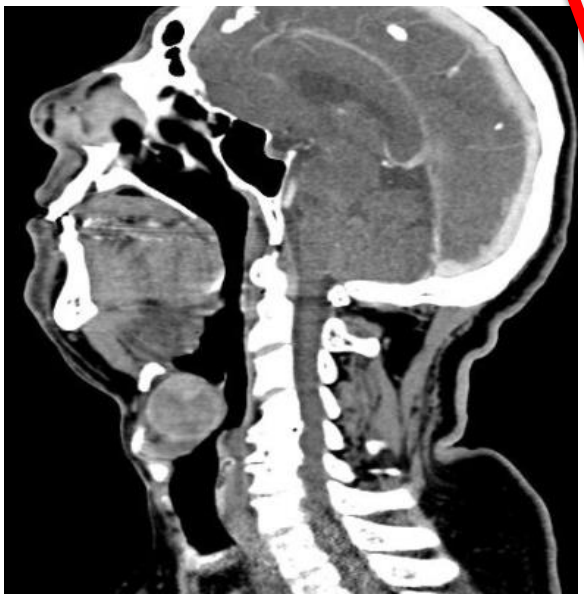

- Tooth filling
- Bone and air cavity
- Scatter condition

TG43 vs MC

Poon *et al*, Med Phys 36 (2009)

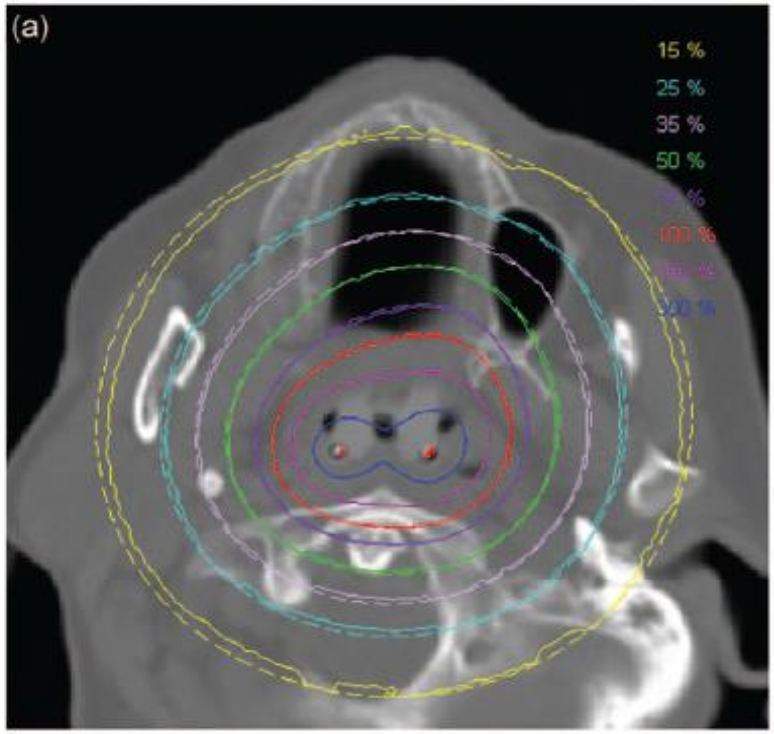

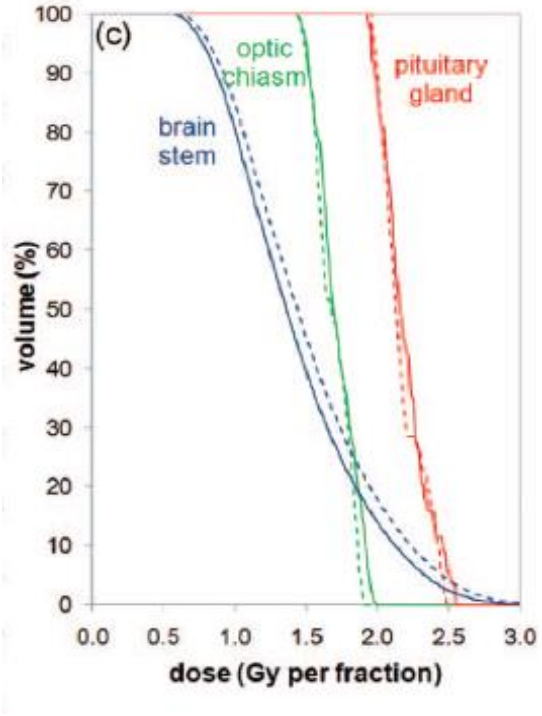

MC = solid lines; TG43= dashed lines

TG43 vs MC

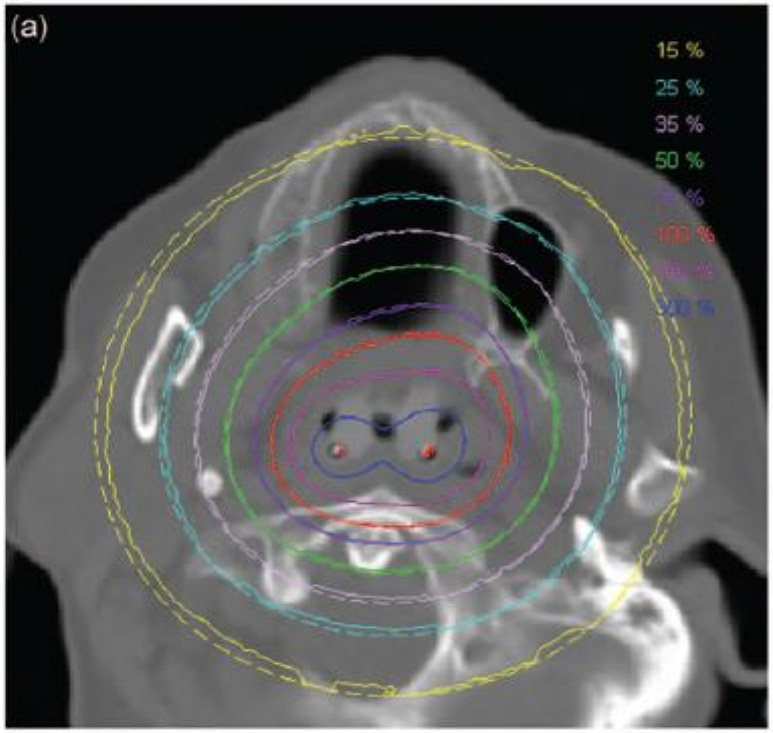

- Target dose unaffected
  - Dominated by primary
- $D_{TG43} > D_{MC}$ brain stem
  - Screening by bones
- $D_{TG43} > D_{MC}$ close to skin

Poon *et al*, Med Phys 36 (2009)

AcurosBV vs TG43

Siebert *et al*, J Contemp Brachytherapy 2013

- 49 consecutive patients, 2001-2009
  - floor of mouth carcinoma
  - larynx carcinoma
  - parotid carcinoma
- 2.5 Gy/Fx
- BV 8.8 and Acuros 1.3.1

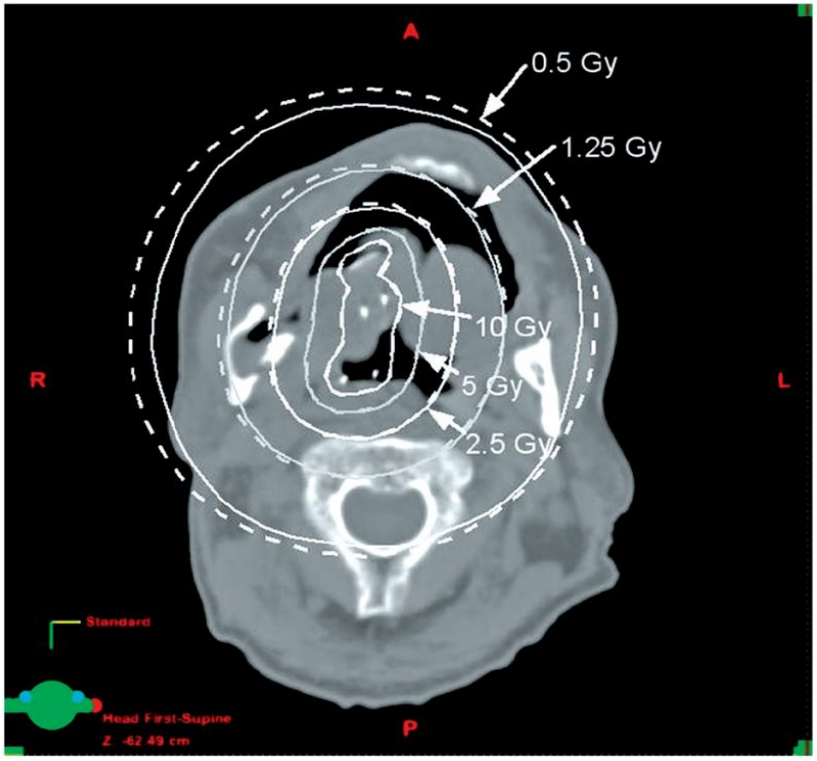

Fig. 1. Transversal CT slice of a patient with mandibular cancer with infiltration of the floor-of-mouth and tongue using a single prescription dose of 2.5 Gy. Dotted isodose lines represent doses of TG-43 formalism, whereas straight lines show isodose lines of computations of the GBBS algorithm

AcurosBV vs TG43

Siebert *et al*, J Contemp Brachytherapy 2013

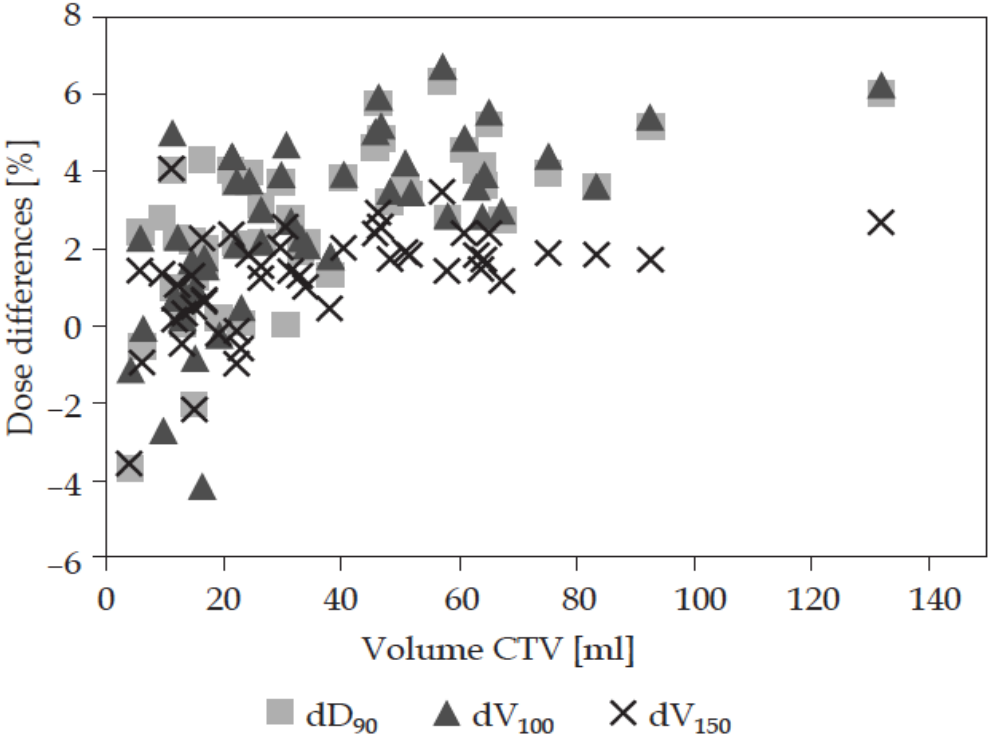

Fig. 2. Dose differences in percent between TG-43 formalism and the GBBS (TG-43 minus GBBS) for D_{90}, V_{100}, and V_{150} of the CTV versus volume of the CTV. A positive dose difference means that TG-43 result was larger than the GBBS results

- $D_{TG43} > D_{MC}$ by ≈ 3%
  - CTV D90 and V100
  - Range -4% to +7%
- Larger volumes lead to larger differences
  - Primary vs scatter contributions to total dose important

MC vs TG43: Study from 22 patients

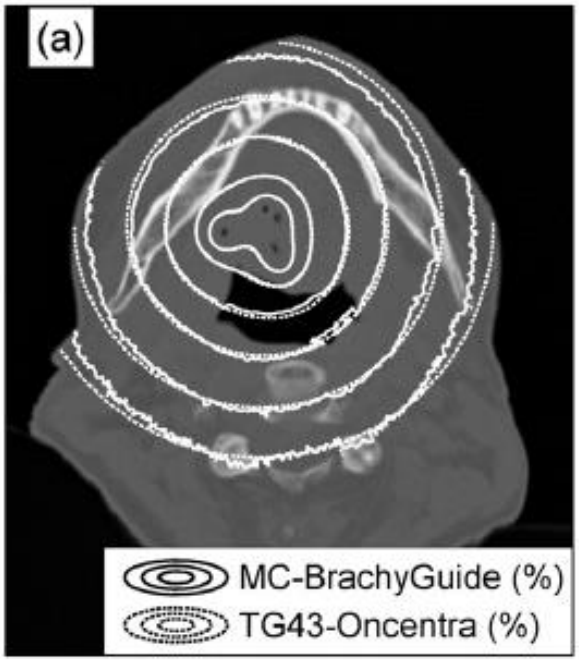

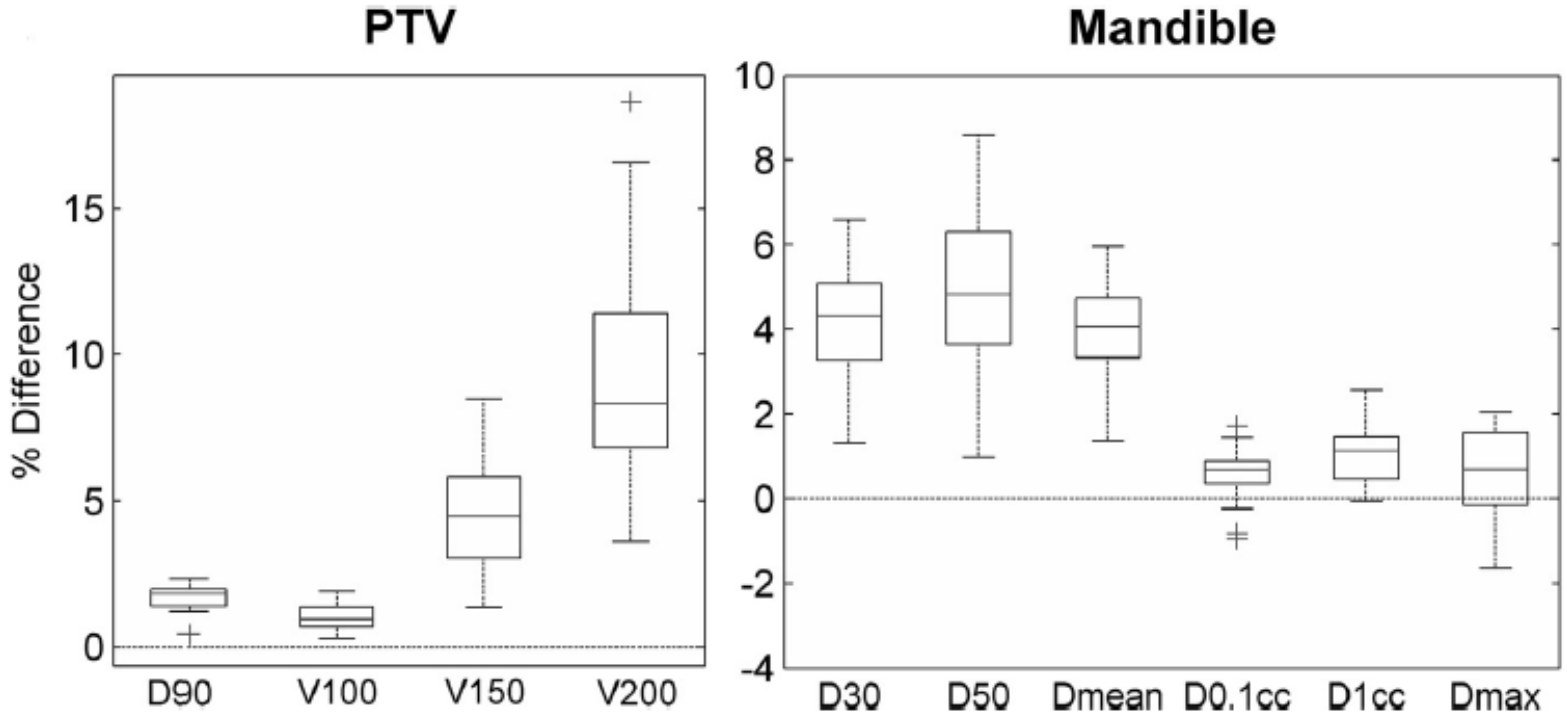

V Peppa et al., Radiother Oncol (2016), In Press

Summary for H&N Brachytherapy

- Differences small on average for CTV/PTV
  - Over and under dosage is patient specific(!)
  - Effects greater at distance from CTV

- OARs
  - Indices statistically different for mandible, parotid, skin, spinal cord.
  - But absolute difference small in most cases.

How Important in the clinic?

Site / Application	Importance
Shielded Applicators	Huge
Eye plaque	-10 to -30% (TG129)
Breast Brachy	-5% to -40%
Prostate Brachy	-2 to -15% on D90
GYN	Depends on applicators
H&N	-4% to +7%

Back to Physics!

Importance of the Physics: Scatter Conditions

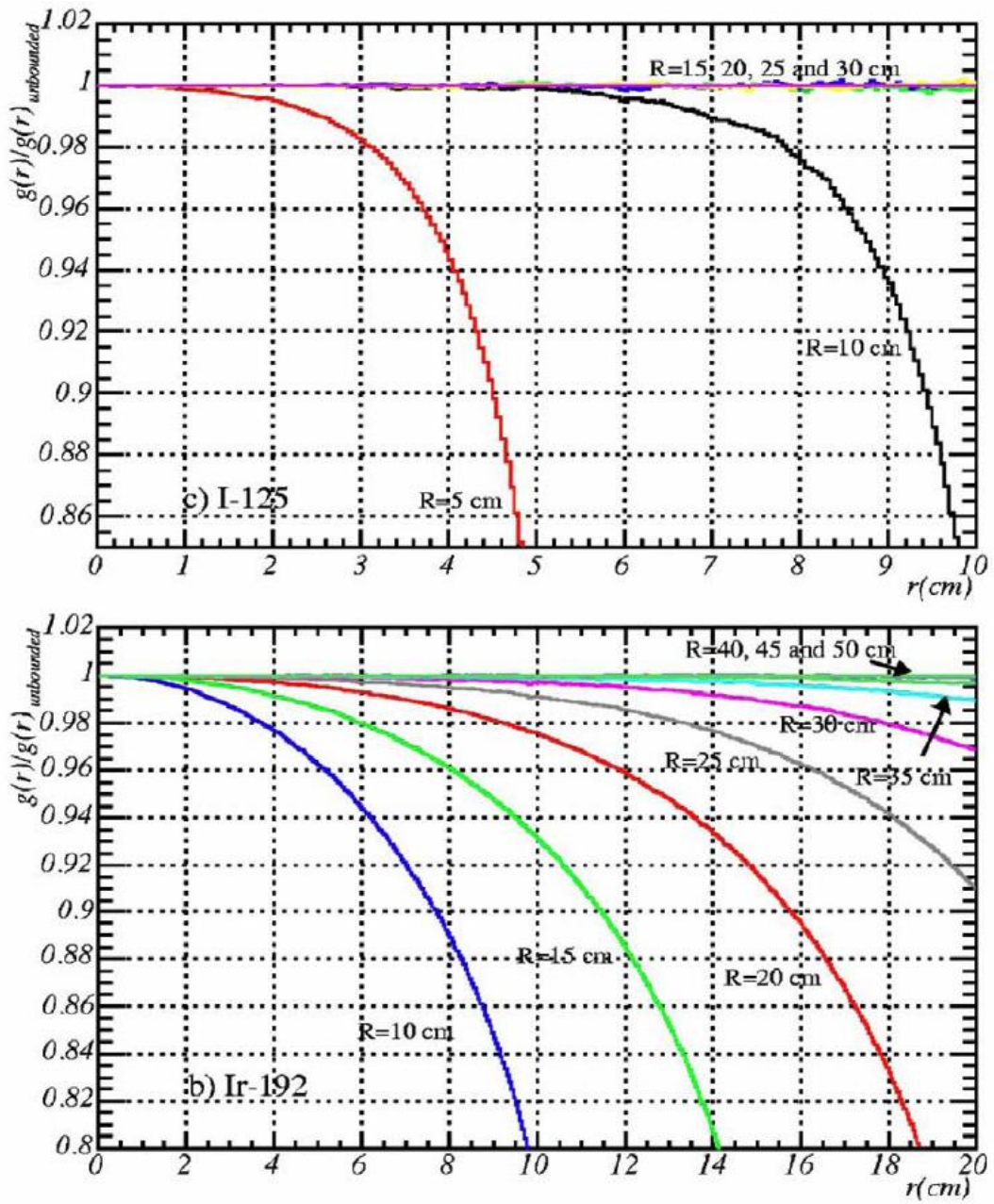

Perez-Calatayud et al, Med Phys 2004

Primary vs. Scatter

Primary dominate total dose for the first 6 cm

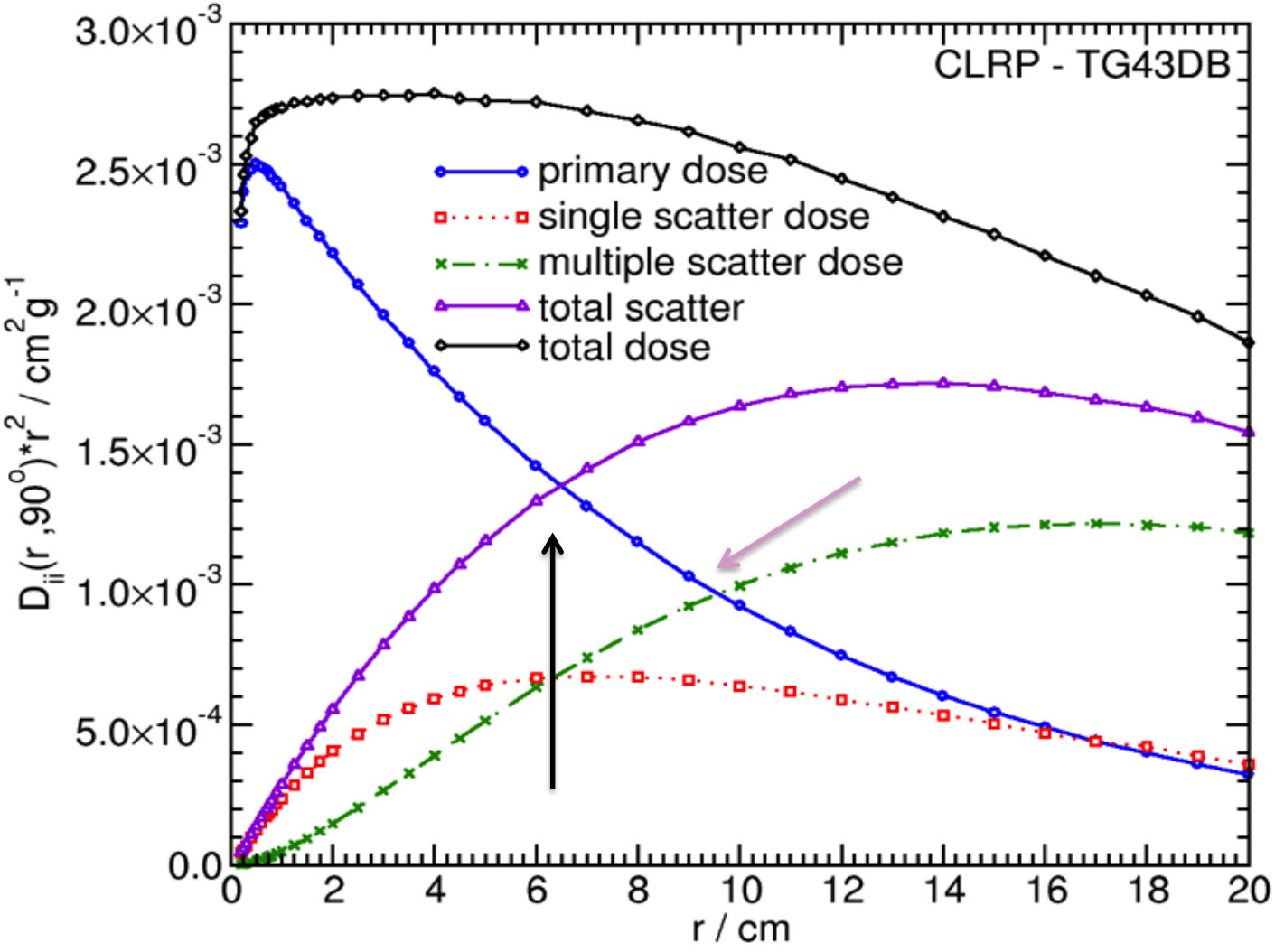

Source: http://www.physics.carleton.ca/clrp

Importance of the Physics: Water vs Tissues

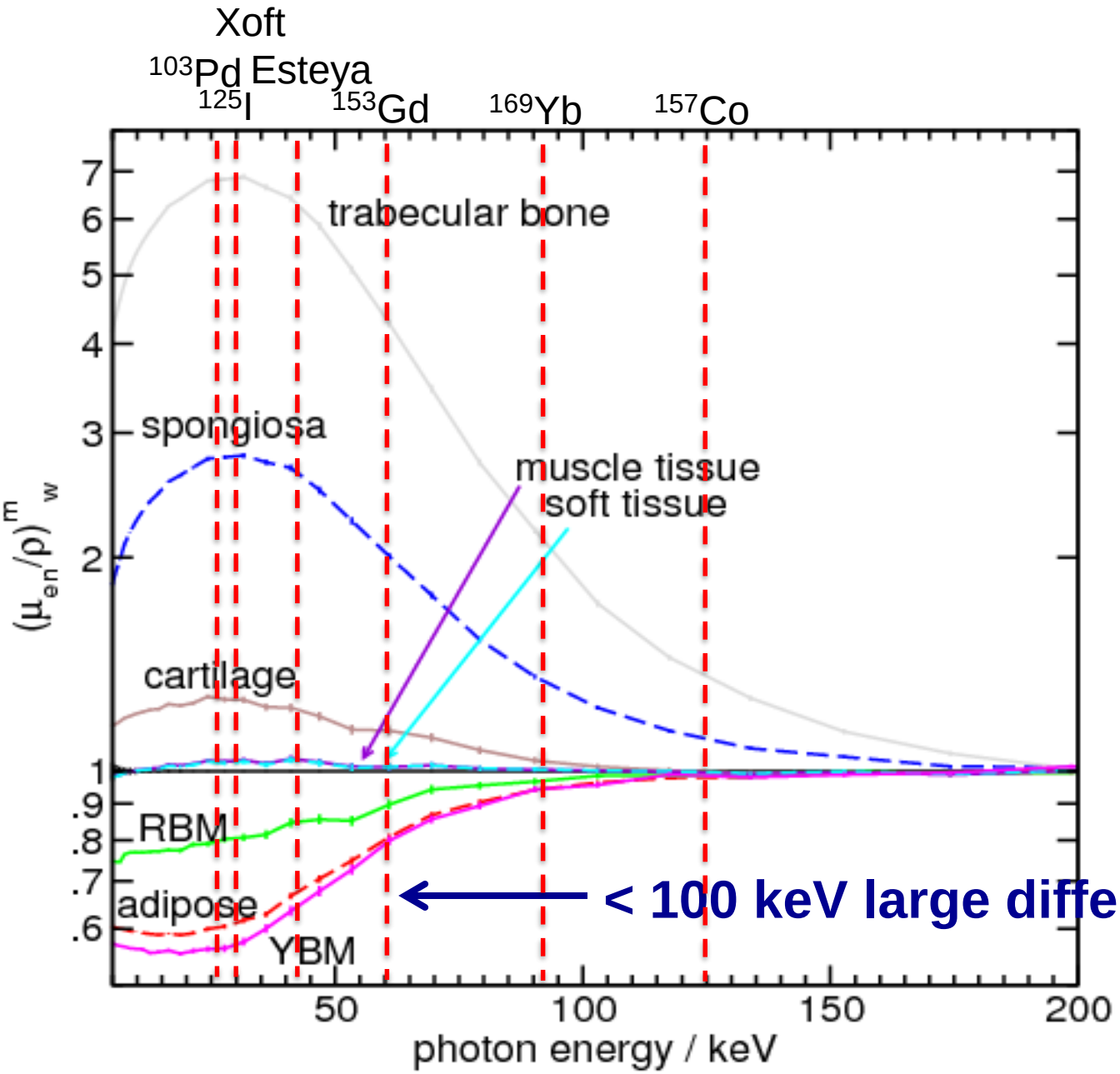

TG-186

< 100 keV large differences

Importance of the Physics: Attenuation by Metals

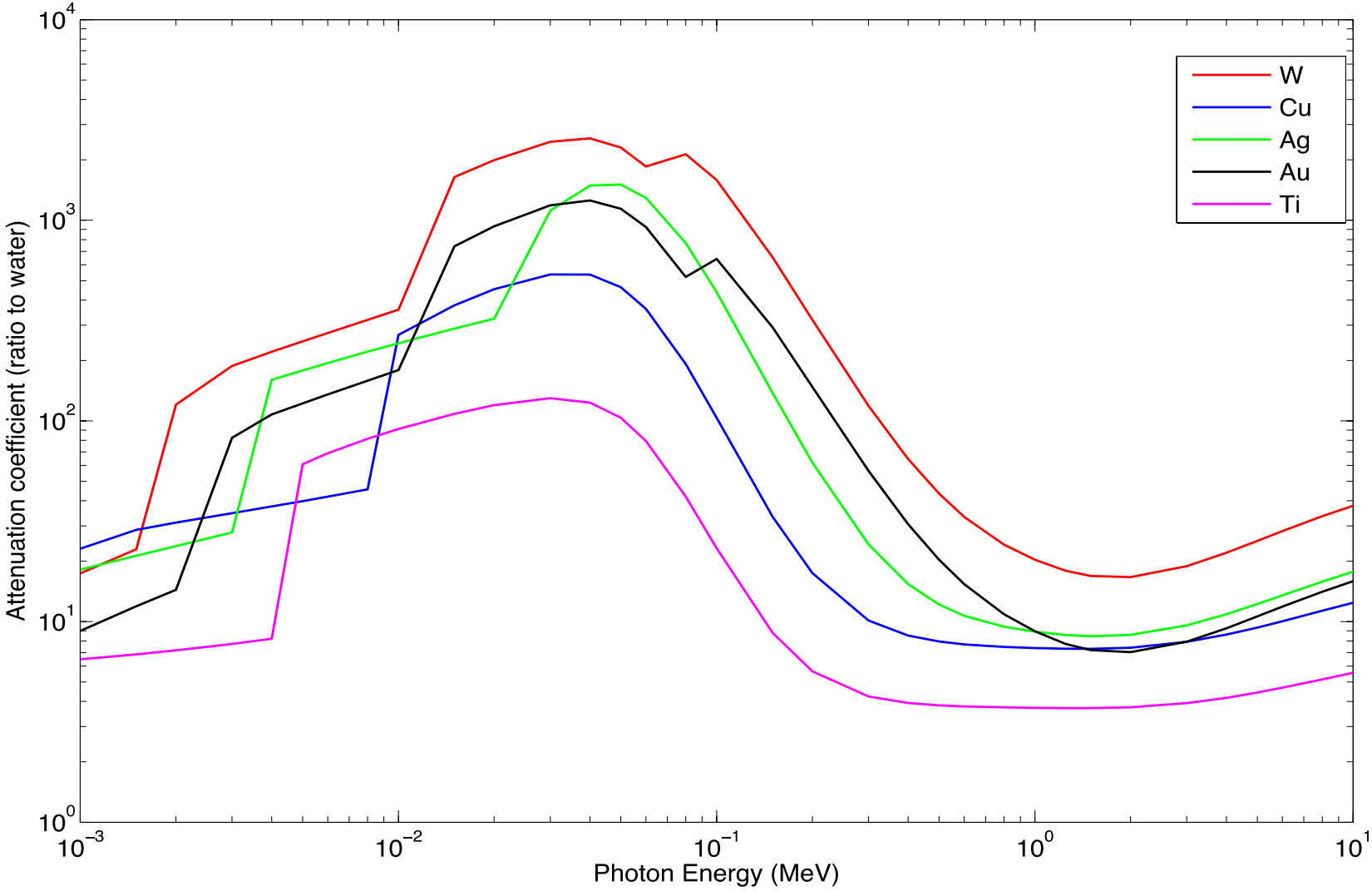

From NIST website

Rule of thumb

Energy Range	Effect
^{192}Ir	Scatter condition
	Shielding (applicator related)
^{103}Pd/^{125}I/eBx	Absorbed dose (μ_{en}/ρ)
	Attenuation (μ/ρ)
	Shielding (applicator, source)

Rivard, Venselaar, Beaulieu, *Med Phys* 36, 2136-2153 (2009)

ESTRO School

Good to know!

- MBDCA are commercially available (for ^{192}Ir and ^{60}Co) – Varian and Elekta
- Starting with the latest release of Varian Brachy TPS, AcurosBV can be used to optimize the dose:

ELSEVIER

Int. J. Radiation Oncology Biol. Phys., Vol. 81, No. 5, pp. 1582–1589, 2011

0360-3016/$ - see front matter

doi:10.1016/j.ijrobp.2010.09.029

PHYSICS CONTRIBUTION

PATIENT-SPECIFIC MONTE CARLO-BASED DOSE-KERNEL APPROACH FOR INVERSE PLANNING IN AFTERLOADING BRACHYTHERAPY

MICHEL D'AMOURS, M.SC.,*† JEAN POULIOT, PH.D.,‡ ANNE DAGNAULT, MD.,*
FRANK VERHAEGEN, PH.D.,§¶ AND LUC BEAULIEU, PH.D.*†

Remember

- TG-43 is still the recommended STD for:
  - Prescription dose levels
  - Dose planning/optimization

- Beyond TG43
  - Follow TG-186 recommendations
    - For tissue assignments
    - For dose reporting
    - ATTN to physics!

Conclusion

- TG43 presents limitation for many clinical sites
  - From a few % to many tens of % for shielded geometries
- Algorithms desperately needed for low energy brachytherapy: seeds or eBx
  - Much larger effects expected
- New approaches depend on going beyond TG43
  - Shielded and directional applicators
  - Directional sources
  - eBx and low energy brachytherapy.

ESTRO School

WWW.ESTRO.ORG/SCHOOL

Advanced Brachytherapy Physics

07-10 October 2018 | Valencia, Spain

Dosimetry using the Advanced Collapsed cone Engine (ACE)

P. Papagiannis, PhD
Medical Physics Laboratory
Medical School
National & Kapodistrian University of Athens

(no conflict of interest to disclose)

Dosimetry using the Advanced Collapsed cone Engine (ACE)

Method used since decades in external beam RT
(for a review see: Ahnesjö and Aspradakis 1999 Phys. Med. Biol. 44(11) R99)

Method for brachy outlined in a series of publications:

✓ Russell KR & Ahnesjö A 1996 Phys Med Biol 41(6):1007
✓Carlsson AK & Ahnesjö A 2000 Med Phys 27(10):2320
✓ Carlsson ÅK & Ahnesjö A 2000 Phys Med Biol 45(2):357–82
✓ Carlsson AK & Ahnesjö A. 2003 Med Phys 30(8):2206.
✓ Russell KR et al 2005 Med Phys 32(9):2739
✓ Carlsson Tedgren A & Ahnesjö A 2008 Med Phys 35(4):1611
✓Ahnesjö A, van Veelen B & Tedgren ÅC 2017 Comput. Meth Prog Biomed 139: 17

and implemented for ^{192}Ir dosimetry in Oncentra Brachy:

✓ user manuals
✓ white paper by Elekta: ACE Advanced Collapsed cone Engine

Objectives/Outline:

To :

- review the basic principles of the method
- outline its implementation

so as to identify:

- strengths and weaknesses
- analogies and differences between (current/future) commercially available MBDCAs
- potential improvements over TG-43
- potential shortcomings relative to reference dose distributions

The method …

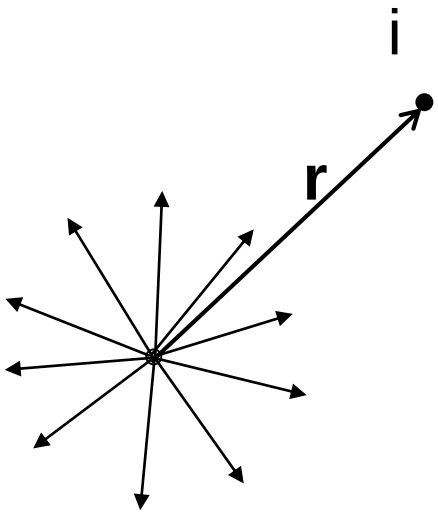

• Let us start again from the simplest case (point isotopic monoenergetic photon source in infinite medium of given composition)

• at any point I know more than D_{prim}:

$$R \rightarrow \Psi_i = \frac{R}{4\pi r_i^2} \exp(-\mu r_i)$$

$$T_i = (\frac{\mu}{\rho})\Psi_i$$

$$\text{under CPE}: D_{prim_i} \equiv K_i = (\frac{\mu_{en}}{\rho})\Psi_i = (\frac{\mu_{en}}{\mu})T_i$$

$$S_i = T_i - K_i = (\frac{\mu - \mu_{en}}{\rho})\Psi_i = (1 - \frac{\mu_{en}}{\mu})T_i = (\frac{\mu}{\mu_{en}} - 1)D_{prim_i}$$

• If I know the spectrum of the source I know the amount of energy per unit mass scattered in first interactions of primary photons, S_{1sc}

The method …

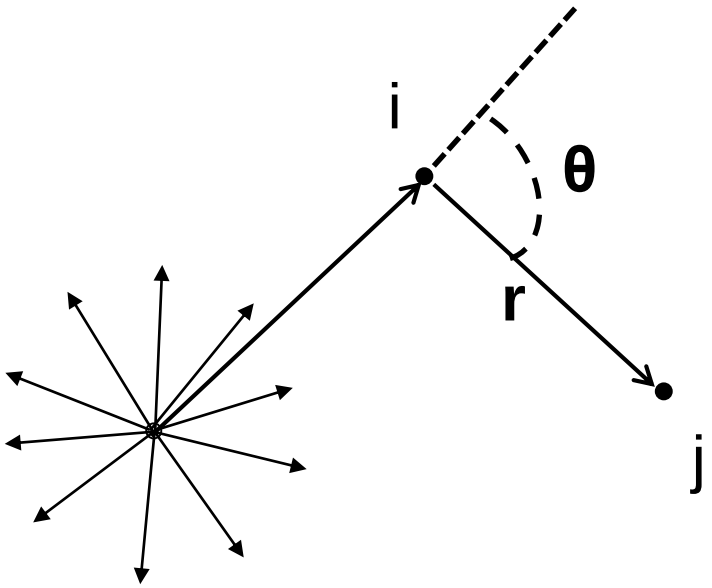

- I know S_{1sc} at each point

$$S_{1sc_i} = T_i - K_i = (\frac{\mu - \mu_{en}}{\rho})\Psi_i = (1 - \frac{\mu_{en}}{\mu})T_i = (\frac{\mu}{\mu_{en}} - 1)D_{prim_i}$$

- I need a way to distribute this energy to all other points …

The method …

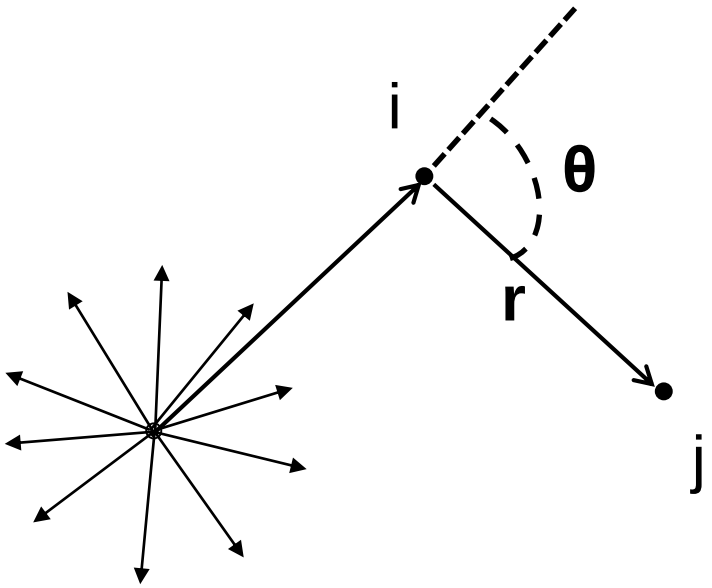

- I know S_{1sc} at each point

$$S_{1sc_i} = T_i - K_i = (\frac{\mu - \mu_{en}}{\rho})\Psi_i = (1 - \frac{\mu_{en}}{\mu})T_i = (\frac{\mu}{\mu_{en}} - 1)D_{prim_i}$$

- I need a way to distribute this energy to all other points …

- Suppose $h_{1sc,j} \equiv h_{1sc}(r,\theta) = \frac{\varepsilon(r,\theta)}{\overline{R}_{1sc}\, dV}$

is the fraction of 1sc energy released at a point (@ the origin) that is absorbed @ (r,θ), per unit of volume

- Can I calculate $h_{1sc}(r,\theta)$ …. ?

- From 1st principles:

$$h_{1sc}(r,\theta) = \frac{\varepsilon(r,\theta)}{\overline{R}_{1sc}\, dV} = \frac{d\sigma(\theta)/d\Omega}{\sigma}\frac{1}{r^2}\exp(-\mu_{1sc,\theta} r)\,\mu en_{1sc,\theta}$$

- Since I know the spectrum of 1sc photons, I can calculate $h_{1sc}(r,\theta)$

The method …

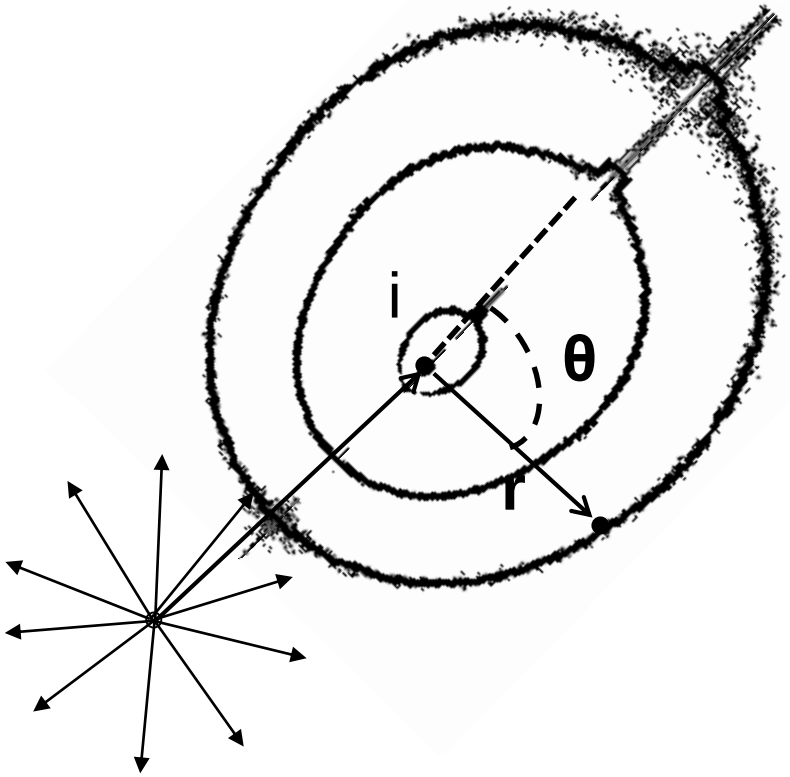

- It is more efficient to use MC to calculate $h_{1sc_i}(r,\theta)$ and fit an analytical expression

$$h_{1sc}(r,\theta) = \frac{\varepsilon(r,\theta)}{\overline{R}_{1sc}\,dV} = \frac{dR_{1sc}(\theta)}{\overline{R}_{1sc}}\frac{1}{r^2 d\Omega}\exp(-\mu_{1sc,\theta}\,r)\,\mu en_{1sc,\theta} =$$

$$= \frac{dR_{1sc}(\theta)}{E(1-\frac{\mu_{en}}{\mu})}\frac{1}{r^2 d\Omega}\exp(-\mu_{1sc,\theta}\,r)\,\mu en_{1sc,\theta} =$$

$$= \frac{B_\theta \exp(-b_\theta\, r)}{r^2}$$

where:

$$B_\theta = \frac{dR_{1sc}(\theta)}{E(1-\frac{\mu_{en}}{\mu})}\frac{1}{d\Omega}\,\mu en_{1sc,\theta}$$

$$b_\theta = \mu_{1sc,\theta}$$

- What material should I choose for the calculation of h…?

The method …is ready!

(and it's convolution/superposition)

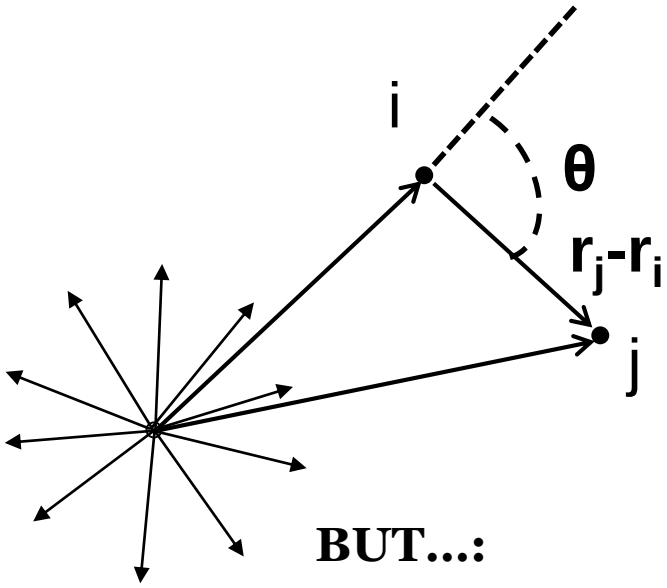

• I can calculate D_{1sc} @ any point from any point, e.g.:

$$D1sc_{i\rightarrow j} = \frac{1}{\rho_j} R_{1sc,i}\, h_j = \frac{1}{\rho_j} S_{1sc,i}\, \rho_i\, dV\, h(\vec{r}_j - \vec{r}_i, \theta) =$$

$$= \frac{\rho_i}{\rho_j} S_{1sc,i}\, h(\vec{r}_j - \vec{r}_i, \theta)\, dV$$

and the total dose to j would be:

$$D1sc_j = \iiint_V \frac{\rho_i}{\rho_j} S_{1sc,i}\, h_j\, dV$$

BUT…:

1. **I need to be efficient** (reduce the # of the N^6 evaluations required) **& work with finite voxels**
2. **I need to account for inhomogeneities**
3. **I need to account for higher order of scatter (D_{2sc}, D_{3sc}, …, D_{msc})**
4. **I need to work with real sources**
5. **I need to account for finite patient dimensions**

1. I need to be efficient

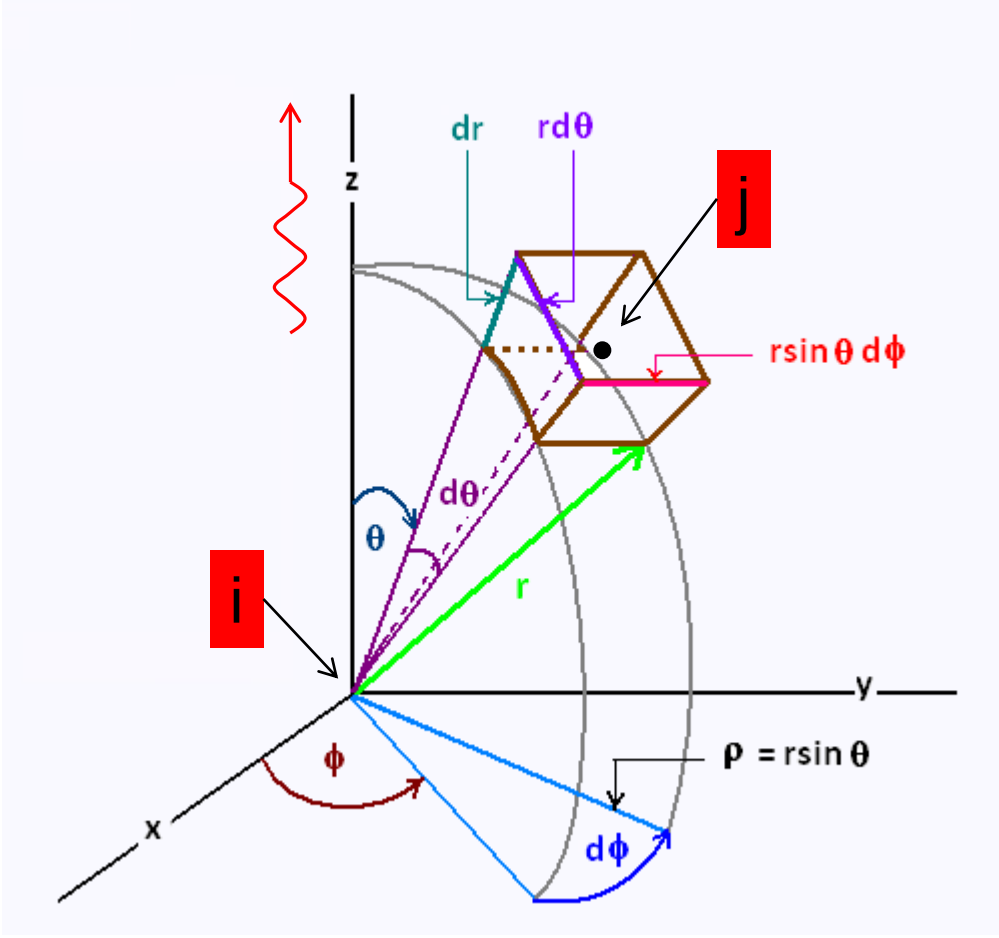

• It is inherently beneficial to work in spherical coordinates to lift the kernel singularity since:
$dV = dS\,dr = r^2\,d\Omega\,dr = r^2 \sin\theta\,d\theta\,d\varphi\,dr$

$$D_{1sc_{i\to j}} = \iiint_V \frac{\rho_i}{\rho_j} S_{1sc,i}\, h_j\, dV =$$

$$\frac{\rho_i}{\rho_j} \int_r \int_\phi \int_\theta S_{1sc,i}\, \frac{B_\theta \exp(-b_\theta r)}{r^2} r^2 \sin\theta\, d\theta\, d\phi\, dr$$

• Instead of evaluating ALL directions around a scerma generating point, I can DISCRETIZE space using a number M of solid angle elements, $\Delta\Omega_M$, defined by $(\theta_o,\varphi_o)_M$, and assume scerma does not vary with θ within ΔΩ (i.e. on dS for a given r)

$$D_{1sc_{i\to j}} = \iint_{\Delta\Omega} \int_r \frac{\rho_i}{\rho_j} S_{1sc,i} B_\theta \exp(-b_\theta r)\, d\Omega\, dr =$$

$$\Delta\Omega \frac{\rho_i}{\rho_j} S_{1sc,i} B_{\theta 0} \int_r \exp(-b_{\theta_0} r)\, dr$$

1. I need to be efficient

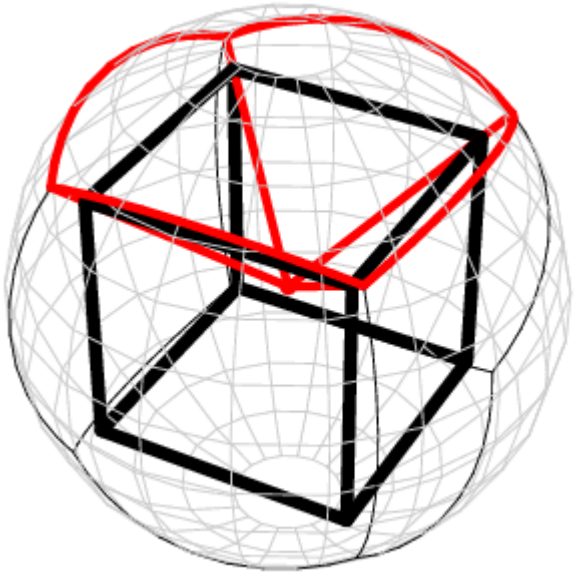

An oversimplified example:
one solid angle element per cubic voxel side

$M=6,\ \Delta\Omega=2\pi/3$

1. I need to be efficient

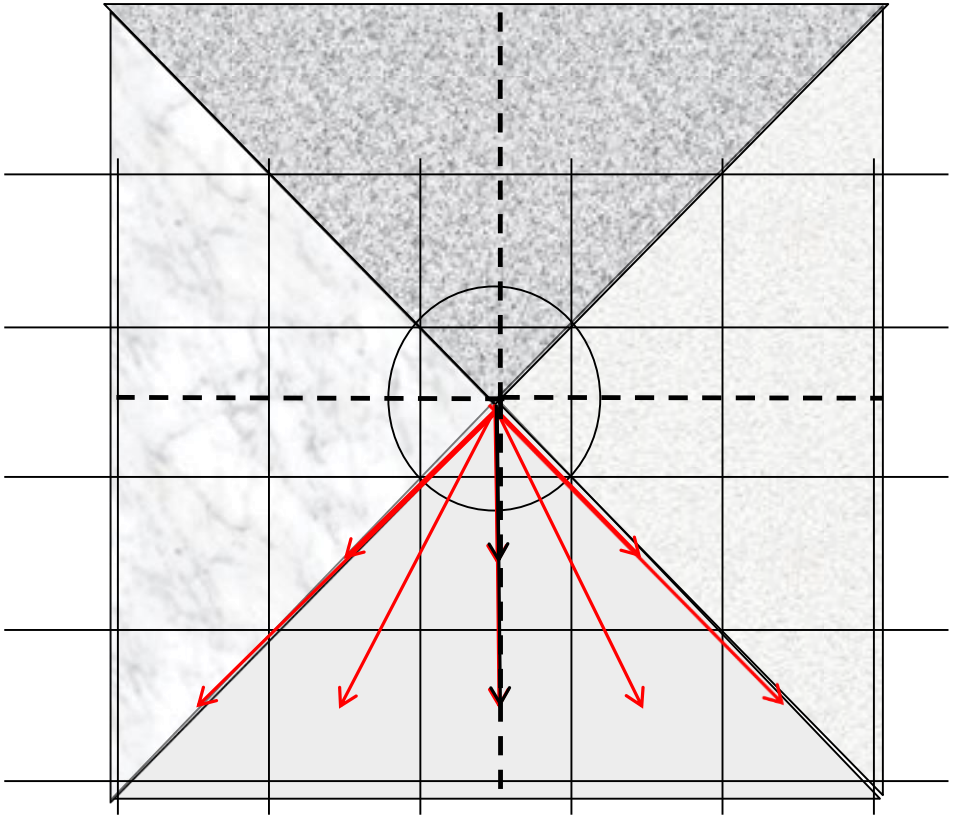

Our oversimplified example on a plane (one array of voxels or one image):

scerma does not vary with θ within ΔΩ → less fitting for B_θ, b_θ

BUT

- I still need to evaluate $D_{i->j}$ for all points j at different radial distance

OR

- I could evaluate $D_{i->j}$ only for j at exactly θ_o, φ_o

Hence each **cone** defined by ΔΩ is **collapsed** to its main axis and scerma from each point is transported along lines defined by the directions from volume discretization in ΔΩ

(order of evaluations required~MN^4)

1. I need to be efficient

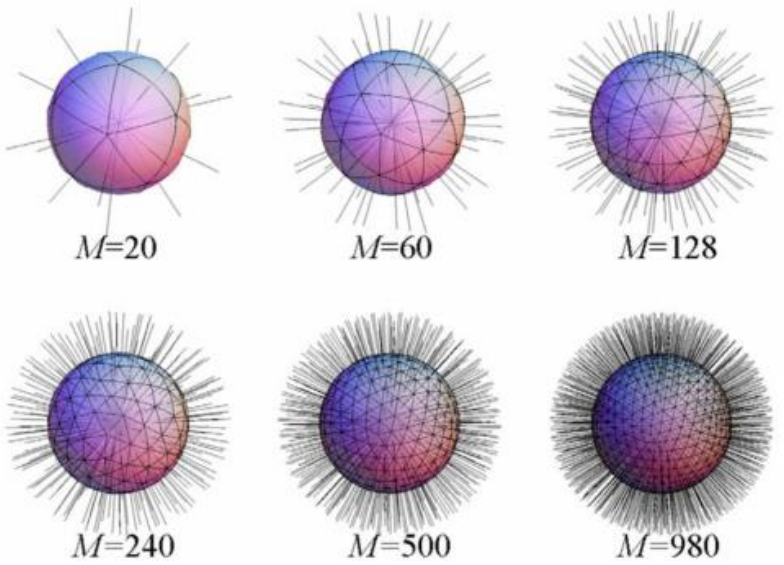

Figure from: Carlsson & Ahnesjö Med. Phys. 35 (4) 1611 (2008)

Can the CC method be both efficient AND accurate…?

- At the limit of fine discretization ($M \rightarrow N^3$, $\Delta\Omega \rightarrow d\Omega$) the collapsed cone method can be exact (but inefficient)

1. I need to be efficient

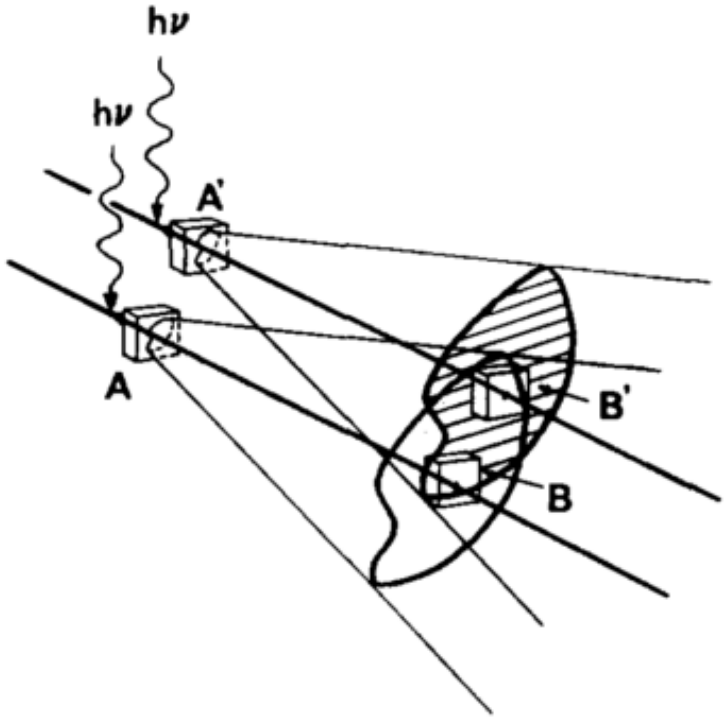

Figure from: Ahnesjö Med. Phys. 16, 577 (1989)

Can the CC method be both efficient AND accurate…?

- I can reduce the number of directions since scerma from voxel A

  not distributed to voxel B'

  due to the CC approximation

  will be compensated by

  scerma from another point A' along the same transport direction

1. I need to be efficient

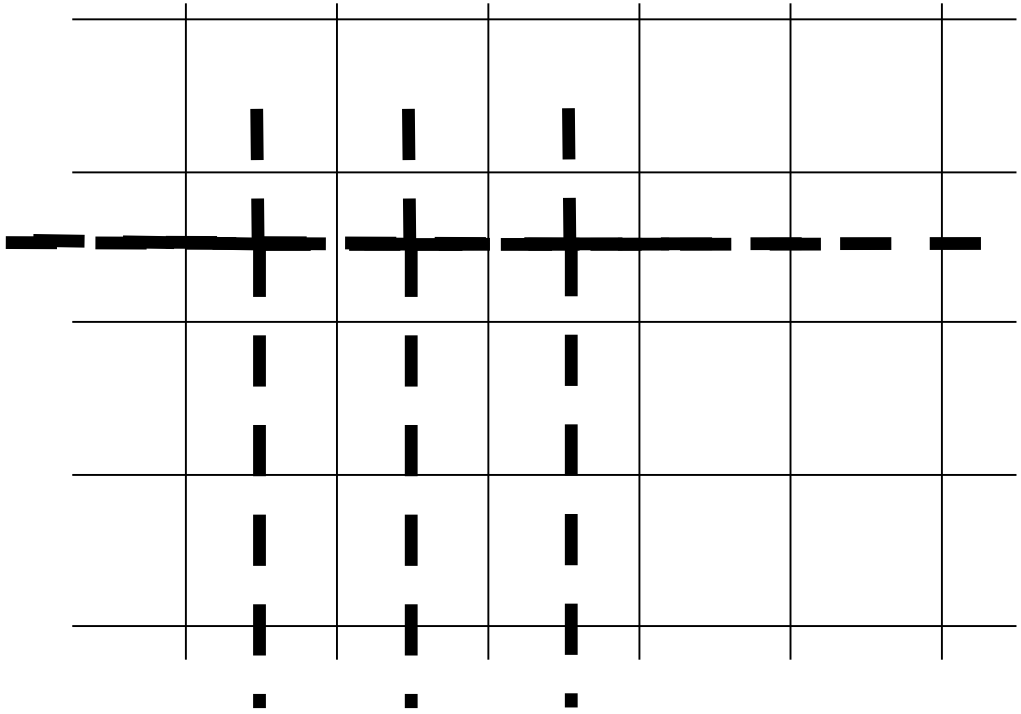

Can the CC method be both efficient AND accurate…?

YES if I optimize the number of directions

- Optimization criterion…?

1. I need to be efficient

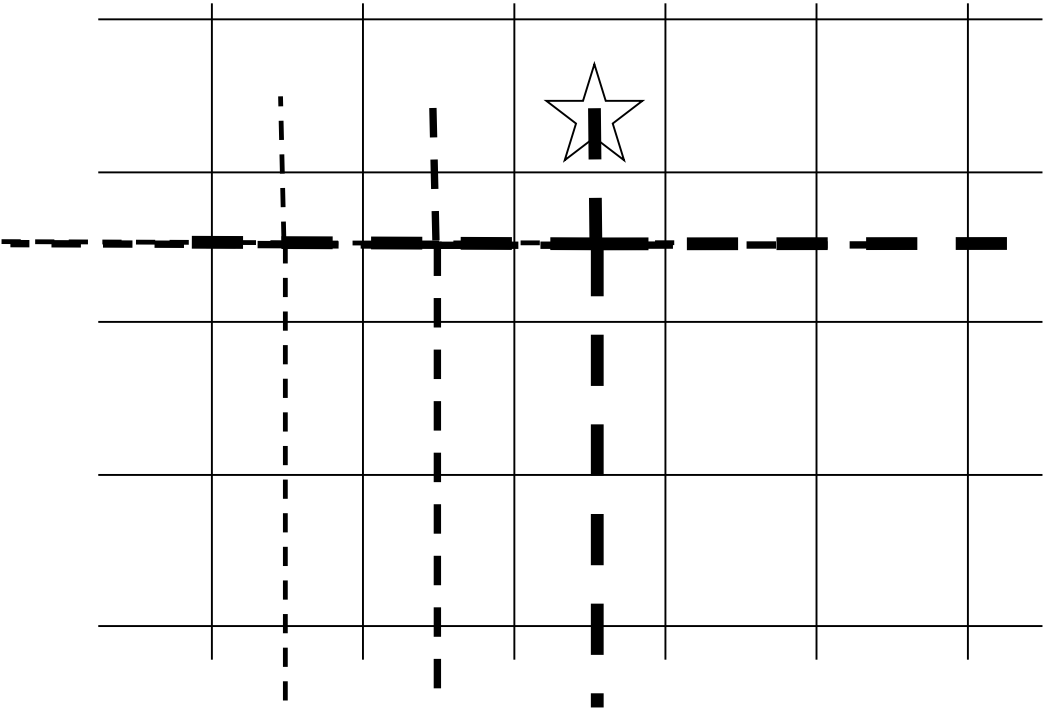

Can the CC method be both efficient AND accurate…?

YES if I optimize the number of directions

Optimization criterion…?

- THE SCERMA GRADIENT!!!

1. I need to be efficient

Can the CC method be both efficient AND accurate…?

The less scerma varies the more I can reduce the number of directions
(increase of efficiency) without a considerable loss of accuracy

Which cases are less/more forgiving…?

1. I need to be efficient

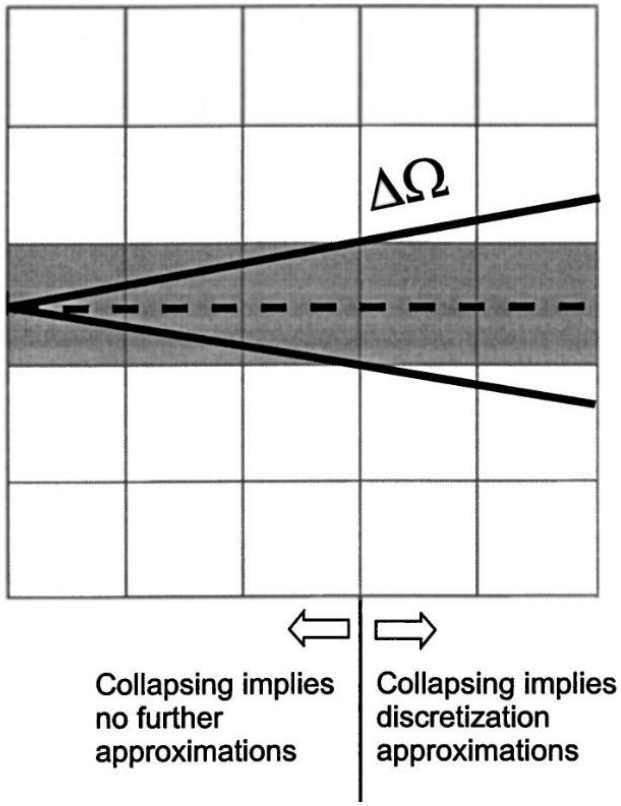

Figure from: Carlsson & Ahnesjö Med. Phys. 27, 2320 (2000)

Can the CC method be both efficient AND accurate...?

The less scerma varies the more I can reduce the number of directions (increase of efficiency) without a considerable loss of accuracy

The approximation by CC that scerma is transported linearly

will only break down

at increased distances where

$r^2\Delta\Omega=\Delta S >>$

so that the cone opening is greater than voxel cross section

1. I need to be efficient

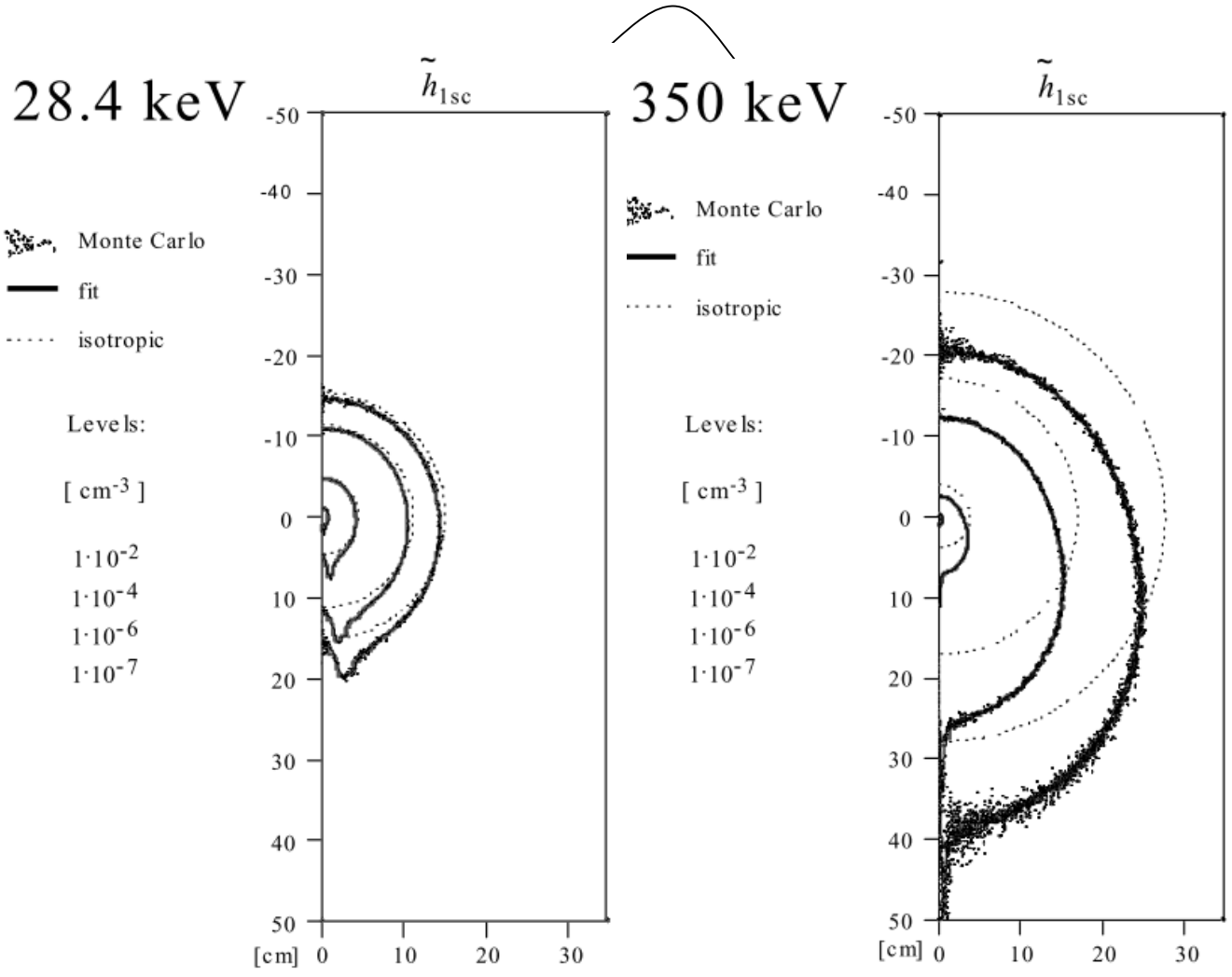

Can the CC method be both efficient AND accurate…?

The less scerma varies the more I can reduce the number of directions (increase of efficiency) without a considerable loss of accuracy

The approximation by CC that scerma is transported linearly will only break down (ray artefacts) at <u>increased</u> distances where $r^2 \Delta\Omega = \Delta S$ >>

Discretization artefacts decrease for:

- coarse voxel resolution (voxel cross section ~ ΔS)
- Rapidly decreasing kernels (lower E)

1. I need to be efficient

All that is missing then is:

- a method to define a grid of transport lines along the discretization directions

and

- a set of recursive equations to calculate stepwise on each transport line and not from point to point

1. I need to be efficient

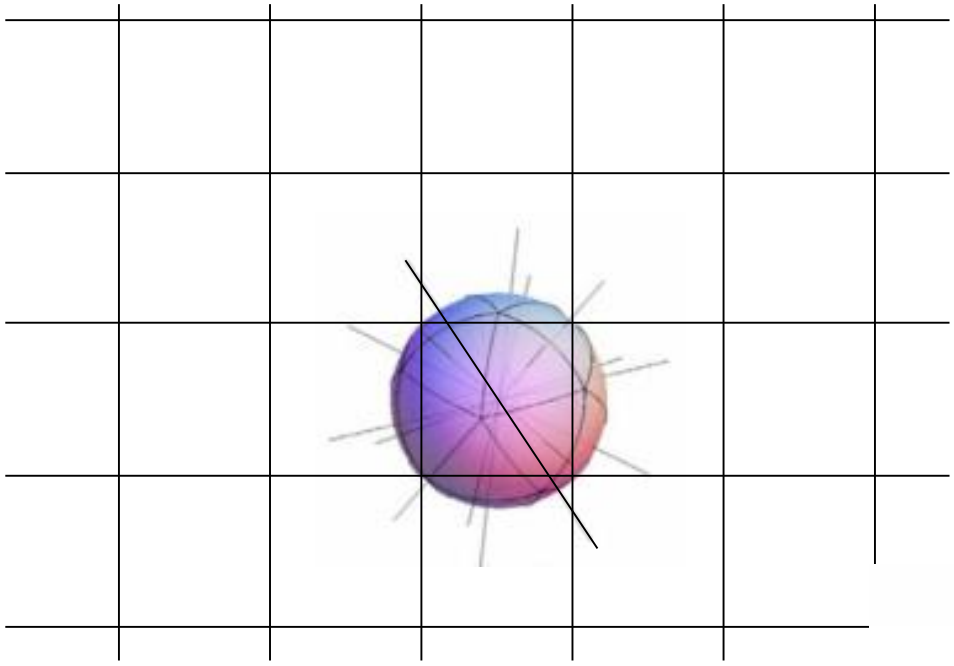

Method to define a grid of transport lines along the discretization directions

$$\Phi = \lim_{\substack{N\to\infty \\ V\to 0}} \left\{ \frac{1}{V} \sum_{i=1}^{N} l_i \right\}$$

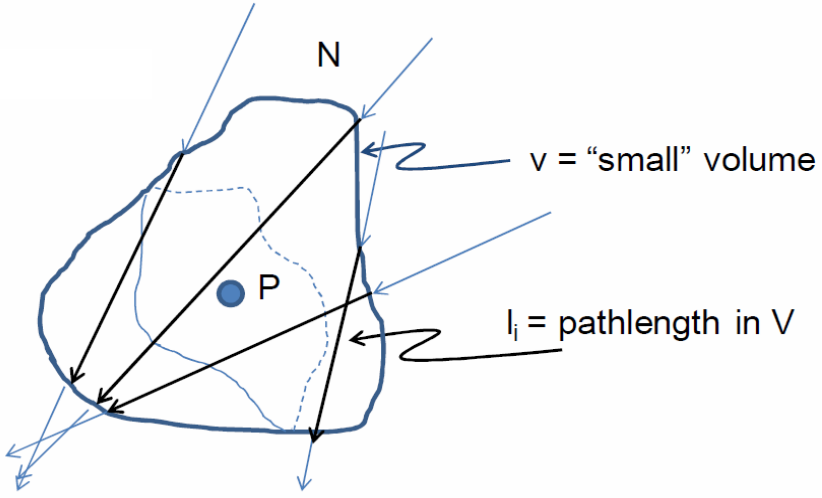

1. I need to be efficient

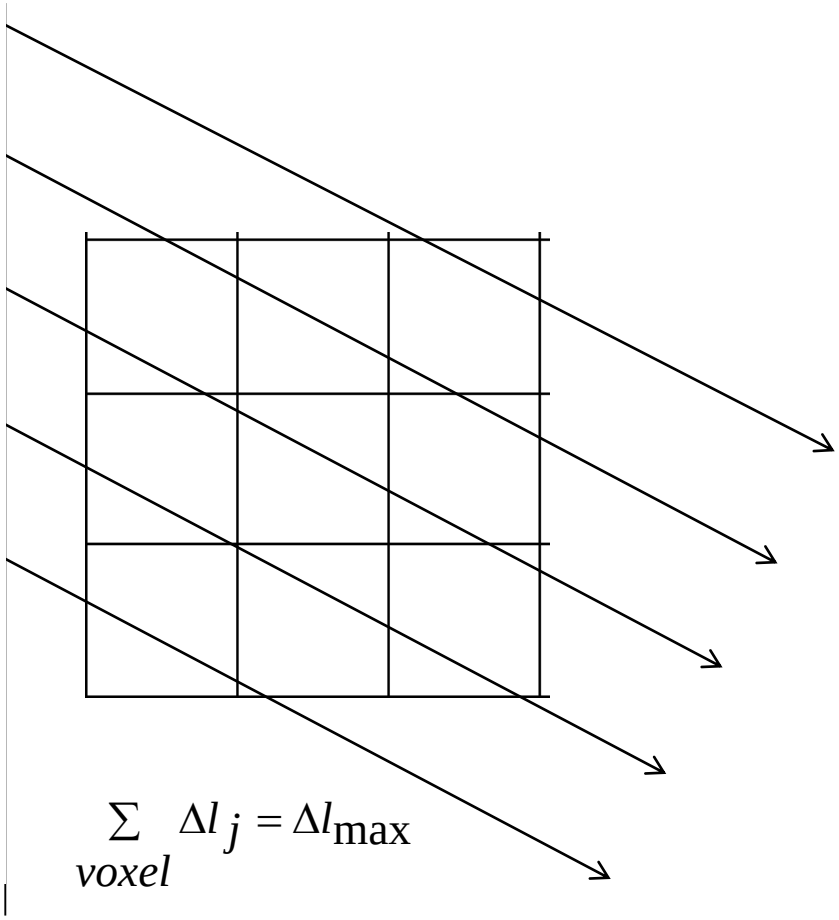

Method to define a grid of transport lines along the discretization directions

1. I need to be efficient

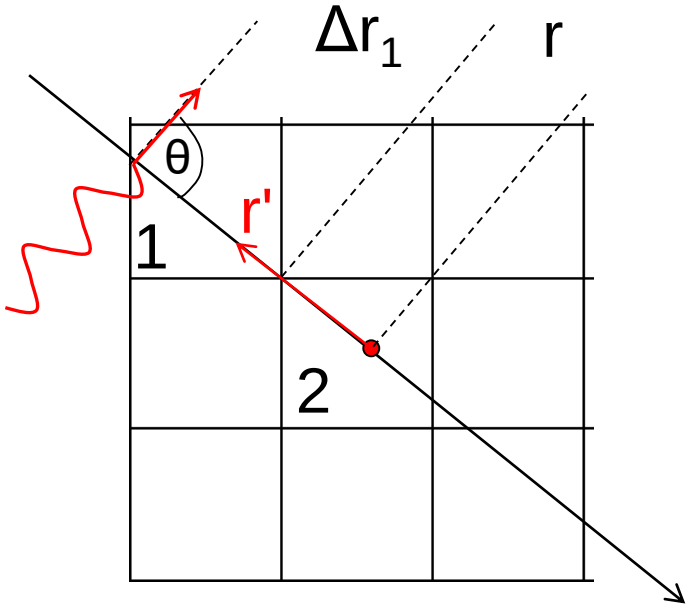

Dose **from** points along Δr1 in voxel 1, **to** a point in voxel 2 :

$$D_{1sc1\to2} = \iint_{\Delta\Omega}\int_{r'} \frac{\rho 1}{\rho 2} S_{1sc,1} B_\theta \exp(-b_\theta r')\, d\Omega\, dr' =$$

$$\Delta\Omega \frac{\rho 1}{\rho 2} S_{1sc,1} B_\theta \int_{r}^{r+\Delta r_1} \exp(-b_\theta r')\, dr' =$$

$$\Delta\Omega \frac{\rho 1}{\rho 2} S_{1sc,1} \frac{B_\theta}{b_\theta} \exp(-b_\theta r)[1-\exp(-b_\theta \Delta r_1)] = \frac{B_\theta}{\rho 2} \frac{\Delta\Omega S_{1sc,1}\, \rho 1}{b_\theta} \exp(-b_\theta r)[1-\exp(-b_\theta \Delta r_1)]$$

Mass energy absorption term [cm²/g]

Ψ_{1sc} term [J/cm²]

Attenuation term

Equations for the transport of scerma generated at each point along a transport line

Under the collapsed cone approximation:

- Scerma does not vary with θ within ΔΩ (Bθ, bθ constant along transport line) and scerma generated, emitted and absorbed along transport line

and assuming:

- Scerma generated per unit r is constant within the same voxel (scerma does not vary considerably within voxels)

1. I need to be efficient

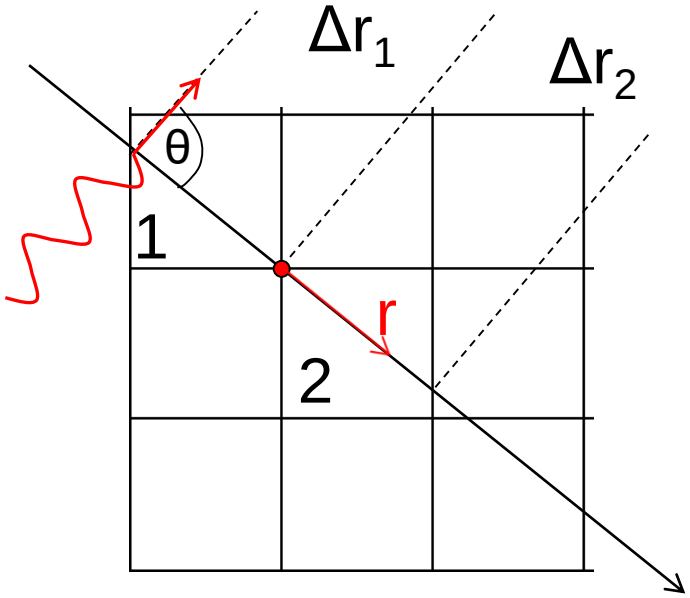

Equations for the transport of scerma generated at each point along a transport line

Under the collapsed cone approximation:

- Scerma does not vary with θ within ΔΩ (Bθ, bθ constant along transport line) and scerma generated, emitted and absorbed along transport line

and assuming:

- Scerma generated per unit r is constant within the same voxel (scerma does not vary considerably within voxels)

Averaging dose over all points **along Δr2** in voxel 2 :

$$\overline{D_{1sc1\to 2}} = \frac{\int_0^{\Delta r_2} D_{1sc1\to 2}\,dr}{\Delta r_2} = \frac{\frac{B_\theta}{\rho_2}\frac{\Delta\Omega S_{1sc,1}\,\rho_1}{b_\theta}[1-\exp(-b_\theta\,\Delta r_1)]\int_0^{\Delta r_2}\exp(-b_\theta\,r)]\,dr}{\Delta r_2} =$$

$$\frac{B_\theta}{\rho_2}\frac{\Delta\Omega S_{1sc,1}\,\rho_1}{b_\theta}\frac{[1-\exp(-b_\theta\,\Delta r_1)][1-\exp(-b_\theta\,\Delta r2)]}{b_\theta\Delta r_2}$$

1. I need to be efficient

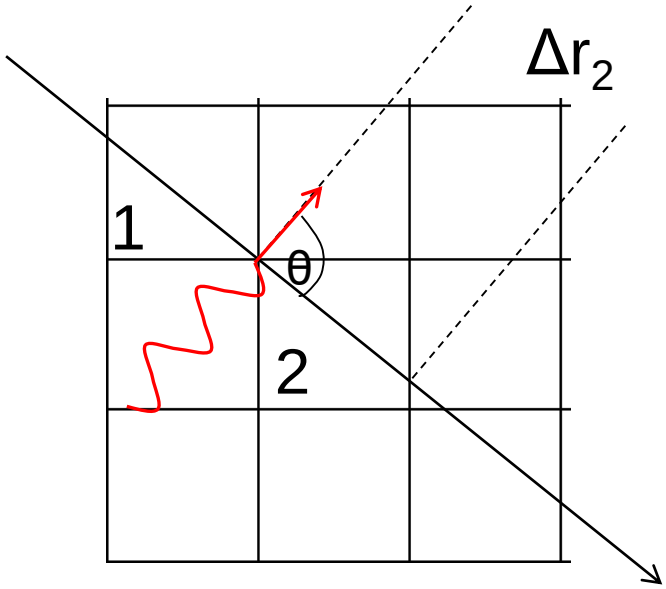

Dose **from voxel 2** points at r' along Δr2, **to a voxel 2** point at r :

$$D_{1sc2\to 2} = \iint_{\Delta\Omega}\int_{r'}\frac{\rho 2}{\rho 2}S_{1sc,2}B_\theta \exp[-b_\theta (r-r')]\, d\Omega\, dr' =$$

$$\Delta\Omega S_{1sc,2}B_\theta \int_0^r \exp[-b_\theta (r-r')]dr' =$$

$$B_\theta \Delta\Omega S_{1sc,2}\frac{[1-\exp(-b_\theta r)]}{b_\theta}$$

Equations for the transport of scerma generated at each point along a transport line

Under the collapsed cone approximation:

- Scerma does not vary with θ within ΔΩ (Bθ, bθ constant along transport line) and scerma generated, emitted and absorbed along transport line

and assuming:

- Scerma generated per unit r is constant within the same voxel (scerma does not vary considerably within voxels)

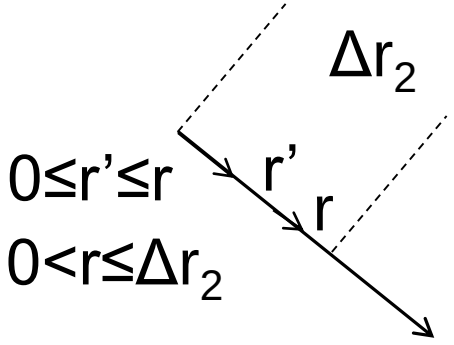

1. I need to be efficient

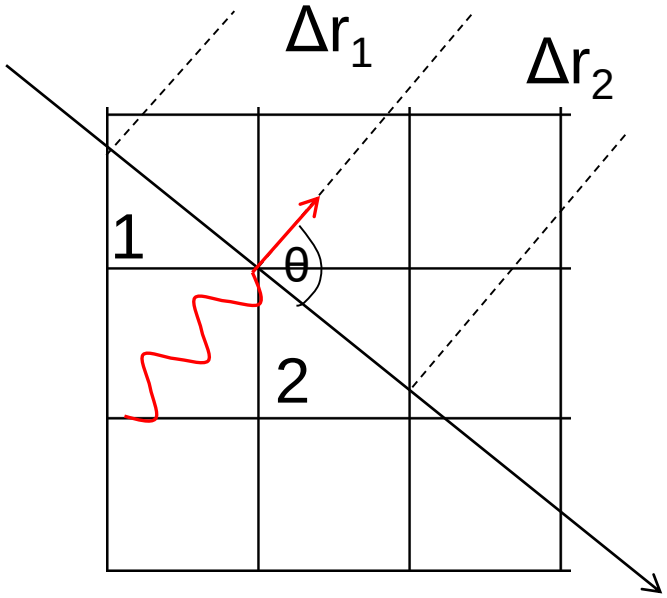

Averaging dose over all points **along Δr2** in voxel 2 :

Equations for the transport of scerma generated at each point along a transport line

Under the collapsed cone approximation:

- Scerma does not vary with θ within ΔΩ (Bθ, bθ constant along transport line) and scerma generated, emitted and absorbed along transport line

and assuming:

- Scerma generated per unit r is constant within the same voxel (scerma does not vary considerably within voxels)

$$\overline{D_{1sc2\to 2}} = \frac{\int_0^{\Delta r_2} D_{1sc2\to 2}\,dr}{\Delta r_2} = \frac{\int_0^{\Delta r_2} [1-\exp(-b_\theta r)]\,dr}{\Delta r_2} =$$

$$B_\theta \frac{\Delta\Omega S_{1sc,2}}{b_\theta} \frac{\{b_\theta \Delta r_2 - [1-\exp(-b_\theta \Delta r_2)\}}{b_\theta \Delta r_2}$$

1. I need to be efficient

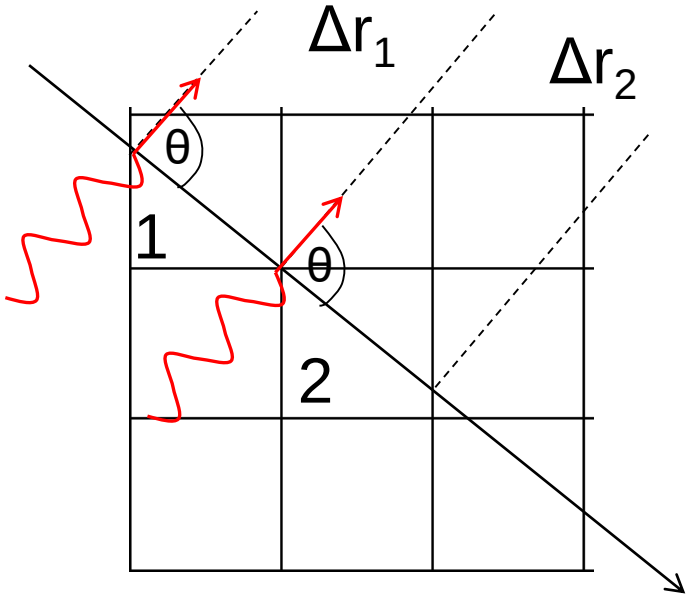

Overall, exiting voxel 2:

Equations for the transport of scerma generated at each point along a transport line

Under the collapsed cone approximation:

- Scerma does not vary with θ within ΔΩ (Bθ, bθ constant along transport line) and scerma generated, emitted and absorbed along transport line

and assuming:

- Scerma generated per unit r is constant within the same voxel (scerma does not vary considerably within voxels)

$$\overline{D_{1sc2}} = \overline{D_{1sc1\to 2}} + \overline{D_{1sc2\to 2}} =$$

$$\frac{B_\theta}{\rho_2}\frac{\Delta\Omega S_{1sc,1}\,\rho_1}{b_\theta}\frac{[1-\exp(-b_\theta\,\Delta r_1)][1-\exp(-b_\theta\,\Delta r2)]}{b_\theta\Delta r_2} + B_\theta\frac{\Delta\Omega S_{1sc,2}}{b_\theta}\frac{\{b_\theta\Delta r_2-[1-\exp(-b_\theta\,\Delta r_2)\}}{b_\theta\Delta r_2}$$

1. I need to be efficient

Equation for the transport of scerma generated at each point along a transport line

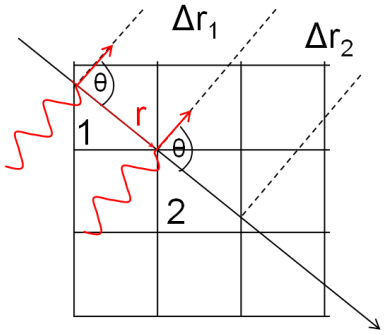

$$\overline{D_{1sc1}} = \overline{D_{1sc0\to1}} + \overline{D_{1sc1\to1}} = 0 + B_\theta \frac{\Delta\Omega S_{1sc,1}}{b_\theta} \frac{\{b_\theta \Delta r_1 - [1-\exp(-b_\theta \Delta r_1)\}}{b_\theta \Delta r_1}$$

$$\overline{D_{1sc2}} = \overline{D_{1sc1\to2}} + \overline{D_{1sc2\to2}} =$$

$$\frac{B_\theta}{\rho 2} \frac{\Delta\Omega S_{1sc,1}\,\rho 1}{b_\theta} \frac{[1-\exp(-b_\theta \Delta r_1)][1-\exp(-b_\theta \Delta r 2)]}{b_\theta \Delta r_2} + B_\theta \frac{\Delta\Omega S_{1sc,2}}{b_\theta} \frac{\{b_\theta \Delta r_2 - [1-\exp(-b_\theta \Delta r_2)\}}{b_\theta \Delta r_2}$$

$$\overline{D_{1sc3}} = \overline{D_{1sc1\to3}} + \overline{D_{1sc2\to3}} + \overline{D_{1sc3\to3}} = \ldots$$

$$\overline{D_{1sci}} = \sum_i \overline{D_{1sci-1\to i}} + \overline{D_{1sci\to i}} = \sum_1^{i-1} \frac{B_\theta}{\rho_i} \frac{\Delta\Omega S_{1sc,i-1}\rho_{i-1}}{b_\theta} \frac{[1-\exp(-b_\theta \Delta r_{i-1})][1-\exp(-b_\theta \Delta r_i)]}{b_\theta \Delta r_i} +$$

$$+ B_\theta \frac{\Delta\Omega S_{1sc,i}}{b_\theta} \frac{\{b_\theta \Delta r_i - [1-\exp(-b_\theta \Delta r_i)]\}}{b_\theta \Delta r_i}$$

1. I need to be efficient

An efficient algorithm for the calculation of dose from 1st scatter:

- Calculate S_{1sc} distr., from D_{prim} distr.
- Choose $\Delta\Omega$: optimal number of directions
- Construct lattice of transport lines (B_θ, b_θ per $\Delta\Omega$, relative to direction of primaries)
- Ray-trace along each transport line for Δr_i and iteratively calculate D_i
- Sum D_i from all transport lines

Input:

- D_{prim} distr.
- Source primary spectrum for calculating S_{1sc}
- 1st scatter kernel
- Individual voxel density data

Assumptions:

CC:

- S_{1sc} does not vary with θ within $\Delta\Omega$ (Bθ, bθ constant along transport line)
- S_{1sc} generated, emitted and absorbed along transport line

and:

- S_{1sc} generated per unit r is constant within the same voxel (scerma does not vary considerably within voxels)

$$\overline{D_{1sc}i} = \sum_{i} \overline{D_{1sc}i-1\rightarrow i} + \overline{D_{1sc}i\rightarrow i} = \sum_{1}^{i-1} \frac{B_\theta}{\rho_i} \frac{\Delta\Omega S_{1sc,i-1}\rho_{i-1}}{b_\theta} \frac{[1-\exp(-b_\theta \Delta r_{i-1})][1-\exp(-b_\theta \Delta r_i)]}{b_\theta \Delta r_i} +$$

$$+ B_\theta \frac{\Delta\Omega S_{1sc,i}}{b_\theta} \frac{\{b_\theta \Delta r_i - [1-\exp(-b_\theta \Delta r_i)]\}}{b_\theta \Delta r_i}$$

1. I need to be efficient

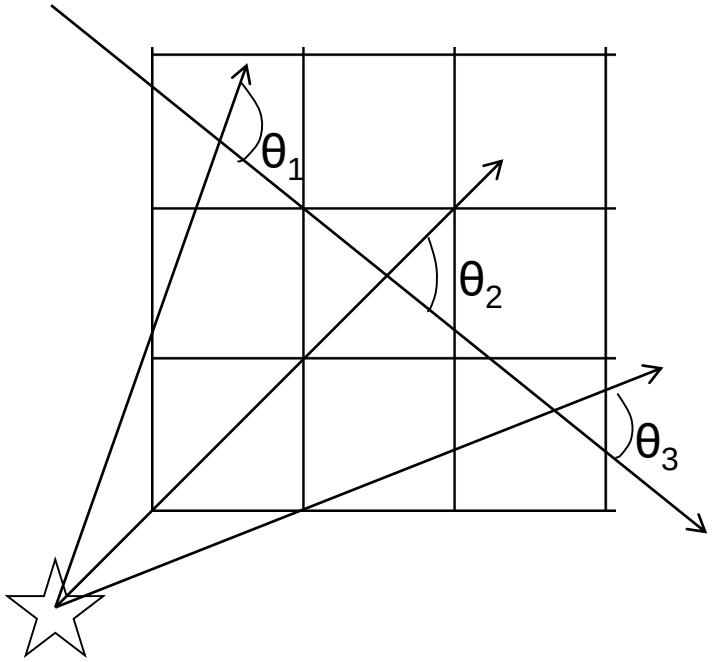

Implementation corrections:

- S_{1sc} does not vary with θ within ΔΩ (Bθ, bθ constant along transport line)

→ Kernel tilting problem less important as E decreases

→ bθ evaluated recursively as a moving average of previous and current step

- S_{1sc} generated per unit r is constant within the same voxel (scerma does not vary considerably within voxels)

→ Scerma gradient problem more important close to a source

→ in high scerma gradient regions scerma is estimated piecewise from a log-linear interpolation over r

2. inhomogeneities

Medium can be of varying density
What changes…?

Our basic equation already accounts for:

- Density @ scatter release voxel
- Density @ energy absorption voxel

$$D_{1sc\,j} = \iiint_V \frac{\rho_i}{\rho_j} S_{1sc,i}\, h_j\, dV$$

$$h_{1sc}(r,\theta) = \frac{\varepsilon(r,\theta)}{\overline{R}_{1sc}\, dV} = \frac{dR_{1sc}(\theta)}{\overline{R}_{1sc}} \frac{1}{r^2 d\Omega} \exp(-\mu_{1sc,\theta}\, r)\, \mu en_{1sc,\theta}$$

The kernel also changes …!

$$= \frac{dR_{1sc}(\theta)}{E(1-\frac{\mu_{en}}{\mu})} \frac{1}{r^2 d\Omega} \exp(-\mu_{1sc,\theta}\, r)\, \mu en_{1sc,\theta}$$

$$= \frac{B_\theta \exp(-b_\theta\, r)}{r^2}$$

$$B_\theta = \frac{dR_{1sc}(\theta)}{E(1-\frac{\mu_{en}}{\mu})} \frac{1}{d\Omega}\, \mu en_{1sc,\theta}$$

$$b_\theta = \mu_{1sc,\theta}$$

2. inhomogeneities

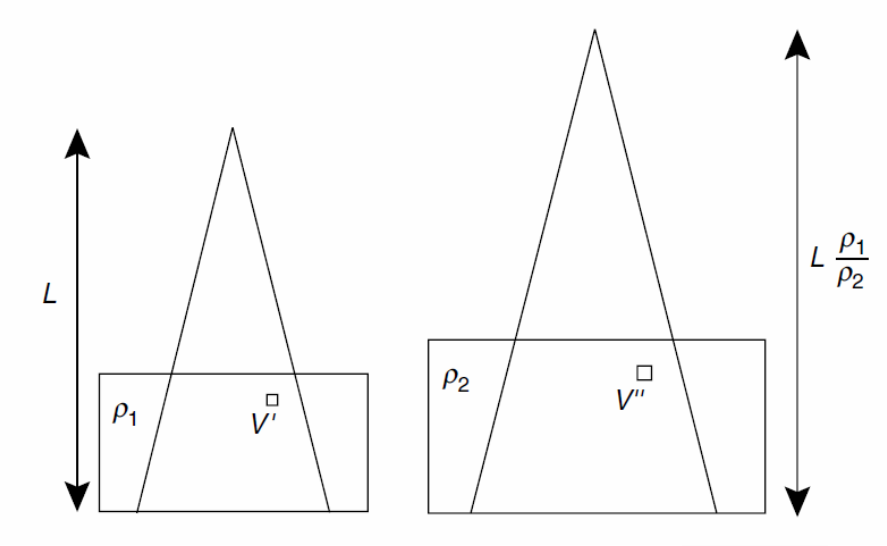

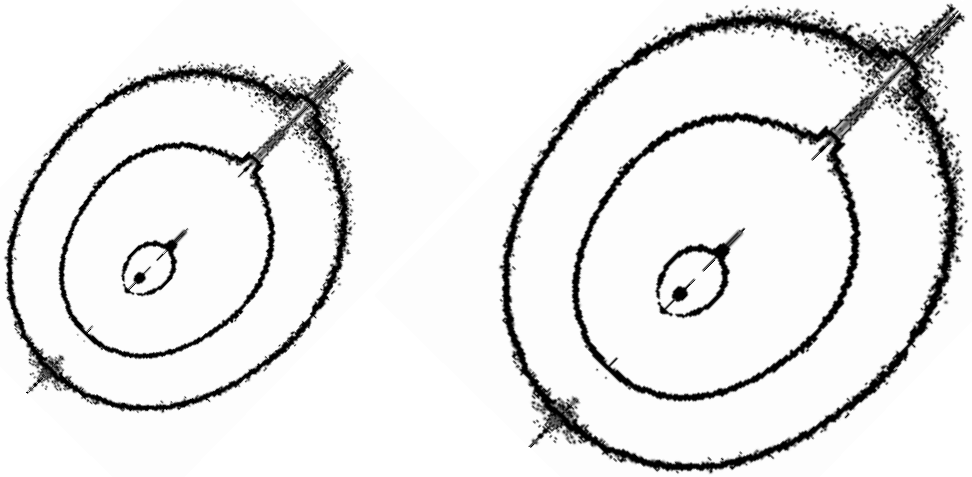

Medium can be of varying density

So if we also scale all distances with density we solve the problem and our method is in accordance with O'Connor's theorem:

When considering two media of different densities but the same atomic composition exposed to the same beam, the dose at corresponding points in the two media will be the same provided that all geometric distances in the two media are scaled inversely with density

2. inhomogeneities

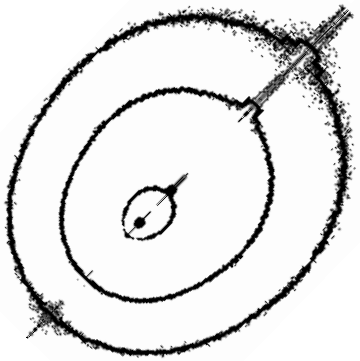

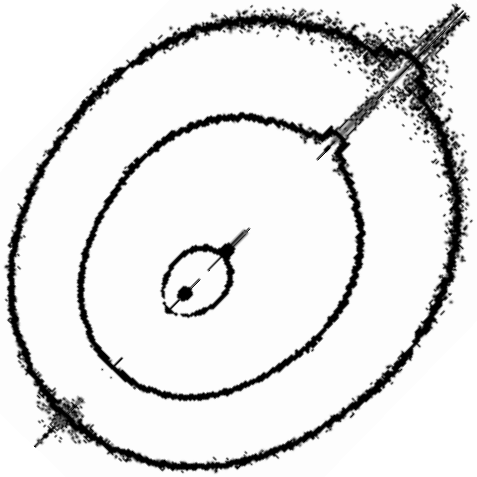

Medium can be of varying density

This affects only the exponential attenuation term in our recursive equation which now has to be:

$$\exp(-b_\theta \sum_{1}^{i-1} \rho_i \Delta r_i)$$

2. inhomogeneities

$$h_{1sc}(r,\theta) = \frac{\varepsilon(r,\theta)}{\overline{R}_{1sc}\,dV} = \frac{dR_{1sc}(\theta)}{\overline{R}_{1sc}}\frac{1}{r^2 d\Omega}\exp(-\mu_{1sc,\theta}\,r)\,\mu en_{1sc,\theta}$$

$$= \frac{dR_{1sc}(\theta)}{\mathrm{E}(1-\frac{\mu en}{\mu})}\frac{1}{r^2 d\Omega}\exp(-\mu_{1sc,\theta}\,r)\,\mu en_{1sc,\theta}$$

$$= \frac{B_\theta \exp(-b_\theta\, r)}{r^2}$$

$$B_\theta = \frac{dR_{1sc}(\theta)}{\mathrm{E}(1-\frac{\mu en}{\mu})}\frac{1}{d\Omega}\,\mu en_{1sc,\theta}$$

$$b_\theta = \mu_{1sc,\theta}$$

Medium can be of varying material (different elemental composition and Zeff)

This affects cross sections and hence B_θ,b_θ

Can't we scale the kernel?

Yes and different approaches have appeared in the literature.

ACE scales attenuation and absorption voxel-wise according to:

$$b_{\theta m} = b_\theta \frac{\rho_m}{\rho_w}\left[\frac{\overline{\mu_{1sc,\theta}}}{\rho}\right]_w^m = b_\theta\,\eta_{1sc}$$

$$B_{\theta m} = B_\theta \frac{\rho_m}{\rho_w}\left[\frac{\overline{\mu en_{1sc,\theta}}}{\rho}\right]_w^m = \mathrm{B}_\theta\,\chi_{1sc}$$

2. inhomogeneities

ACE scales attenuation and absorption voxel-wise according to:

$$b\theta_m = b\theta \frac{\rho_m}{\rho_w}\left[\frac{\overline{\mu_{1sc,\theta}}}{\rho}\right]_w^m = b\theta\, \eta_{1sc}$$

$$B\theta_m = B\theta \frac{\rho_m}{\rho_w}\left[\frac{\overline{\mu en_{1sc,\theta}}}{\rho}\right]_w^m = b\theta\, \chi_{1sc}$$

Medium can be of varying material (different elemental composition and Zeff)

The same recursive equation applies

BUT:

- additional input is required to calculate η_{1sc} , χ_{1sc} : the energy spectrum of 1sc photons generated at each point.

This is taken from calculations in water so:

- the scaling is APPROXIMATE and its accuracy deteriorates as materials yield different 1sc spectrum from water (as Z increases due to coherent & photoelectric phenomena-x ray fluorescence and S(x,Z))

3. catter

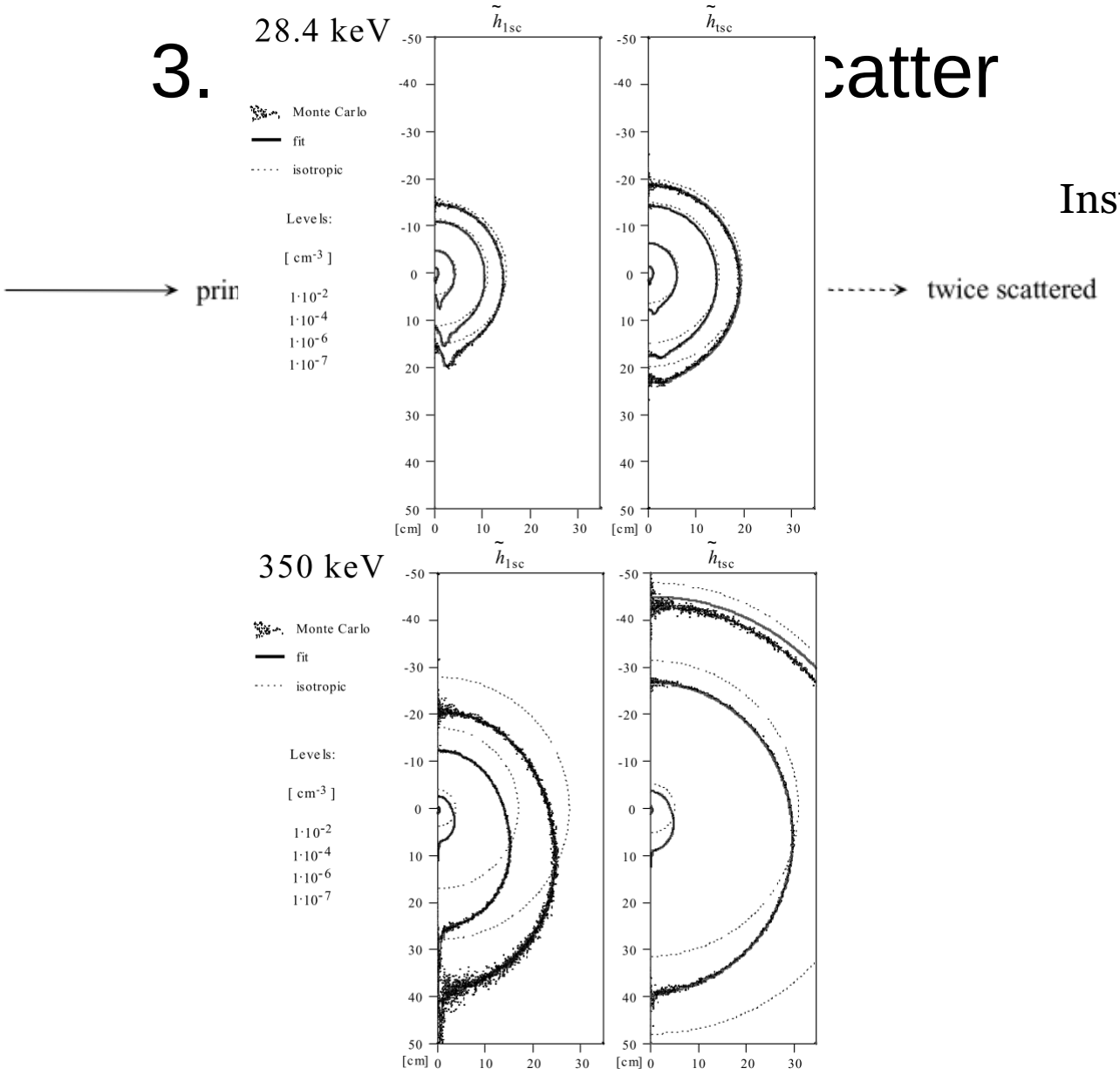

Instead of using h_{1sc} with S_{1sc} obtained from D_{prim}, to obtain D_{1sc}

couldn't I distribute S_{1sc}

due to ALL orders of scattering

in a single step

using a different kernel, i.e. h_{msc} ...?

I could, but it is NOT a good idea due to:

- h_{msc} reducing less than h_{1sc} with r → ray artefacts
- accuracy close to boundaries of finite geometries (discussed in the following)

Figures from: Carlsson & Ahnesjö Phys. Med. Biol. 45 357 (2000)

3. Higher order of scatter

I have to repeat the method 2 times:

$D_{prim} \rightarrow S_{1sc} \rightarrow$ CC with $h_{1sc} \rightarrow D_{1sc}$

$D_{1sc} \rightarrow S_{2sc} \rightarrow$ CC with $H_{msc} \rightarrow D_{msc}$

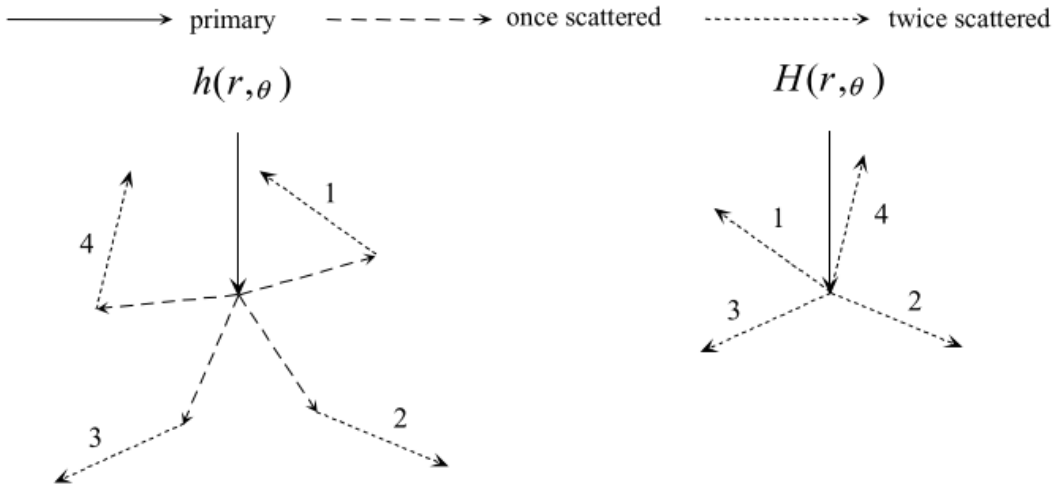

- Primary photons forced to interact
- Once scattered photons and all subsequent particles transported
- Scoring of dose mediated by
  - once-scattered photons: h_{1sc}
  - all scatter generations : h_{tsc}

- Primary photons forced to interact
- Once scattered photons started but forced to interact without transport
- Twice scattered photons and all subsequent particles transported
- Scoring of dose mediated by multiply-scattered photons: H_{msc}

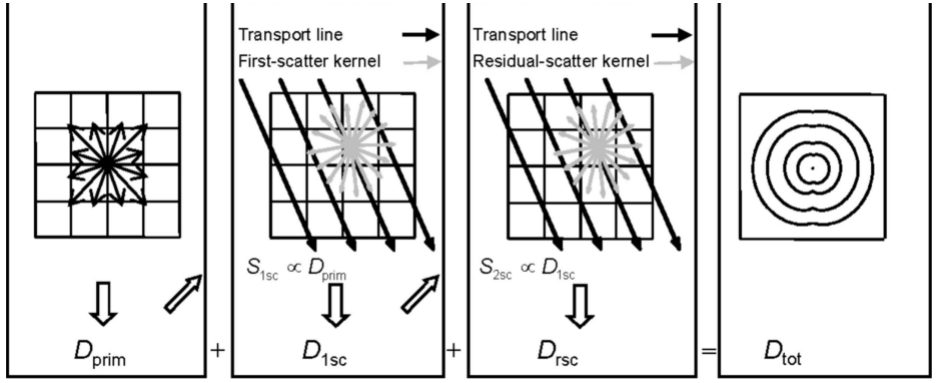

Figures from: Carlsson & Ahnesjö Phys. Med. Biol. 45 357 (2000) & Med. Phys. 35 (4) 1611 (2008)

3. Higher order of scatter

I have to repeat the method 2 times:

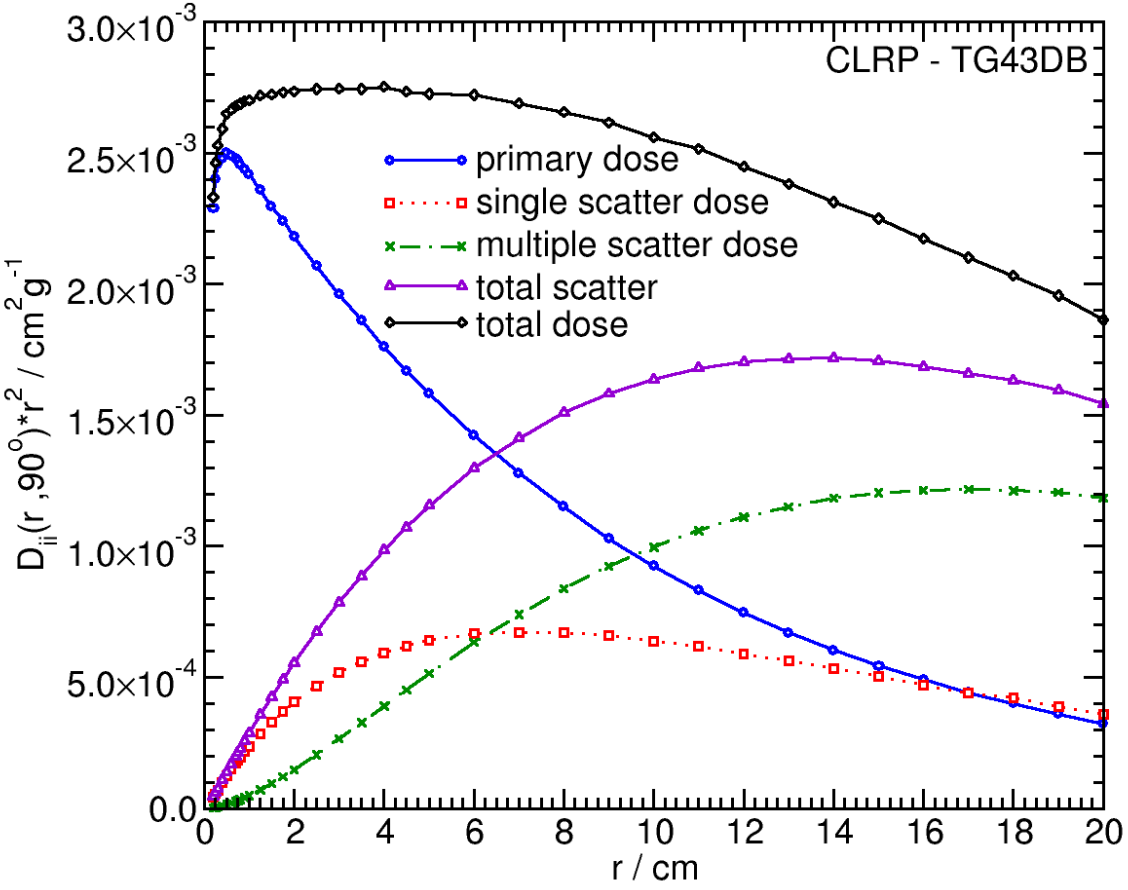

- The second step is approximate in that I do not know the orientation of H_{msc}

  I can assume it is isotropic or align it with h_{1sc}

- Calculation time increases to $(M_{1sc}+M_{msc})N^3$

- Required M_{msc} is < M_{1sc} since the gradient of D_{1sc} is considerably less than that of D_{prim}

3. Higher order of scatter

I have to repeat the method 2 times:

$D_{prim} \rightarrow S_{1sc} \rightarrow$ CC with $h_{1sc} \rightarrow D_{1sc}$

$D_{1sc} \rightarrow S_{2sc} \rightarrow$ CC with $H_{msc} \rightarrow D_{msc}$

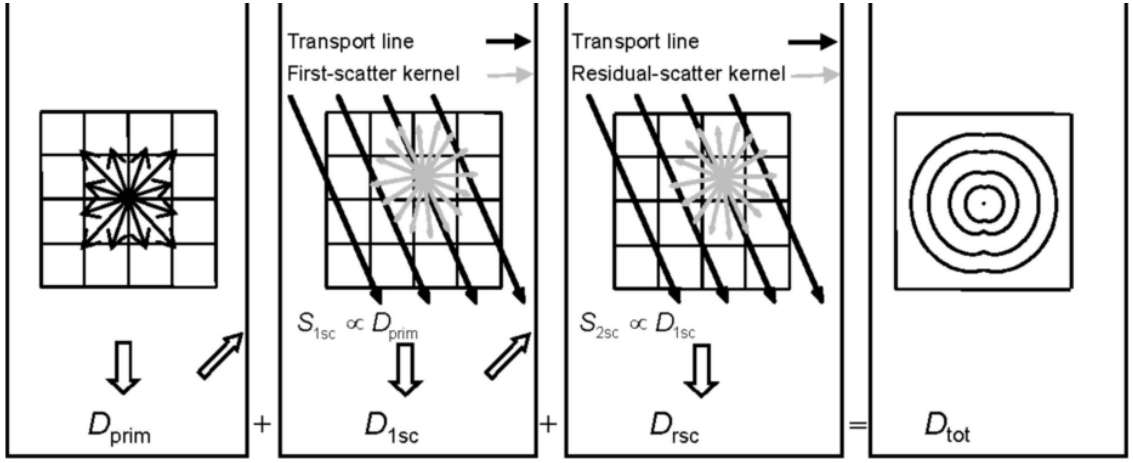

An analogous recursive equation applies with the difference that H_{msc} is better fit by a bi-exponential function

$$H_{msc}(r,\theta) = \frac{C_\theta \exp(-c_\theta r) + D_\theta \exp(-d_\theta r)}{r^2}$$

Additional input is required to calculate inhomogeneity corrections: the energy spectrum of msc photons generated at each point

4. real sources

Input must now be source specific:

- Primary dose distribution
- Distribution of primary photon energy spectrum
- Distribution of 1sc photon energy spectrum
- Distribution of msc photon energy spectrum

μ/ρ, μen/ρ data for the calculation of scerma, as well as 1sc & msc kernels, must be weighed over the appropriate energy spectra

Implementation detail:

Primary dose distribution is fit by an analytical expression

$$\frac{K_{\text{prim}}(\mathbf{x})}{R} = \gamma_C(r,\theta,v)\cdot\frac{\psi(\theta)}{4\cdot\pi\cdot r^2}\cdot\left(\frac{\bar{\mu}_{\text{en}}(\mathbf{x})}{\rho}\right)_{\text{med}}\cdot e^{-m(\theta)\cdot\sum_{i\in\text{rayline to x}}(\bar{\mu}/\rho)_i\cdot\rho_i\cdot\Delta r_i}$$

V ave. correction

Ψ_E anis. correction

Att. anis. Correction due to Ψ_E diffs over θ

This allows calculations @ resolution different than that used in the MC simulation to derive the primary dose distribution

5. finite patient dimensions

Kernel data are traditionally calculated in full scatter geometries (8mfp)

This overestimates msc dose close to the edges of a bounded geometry

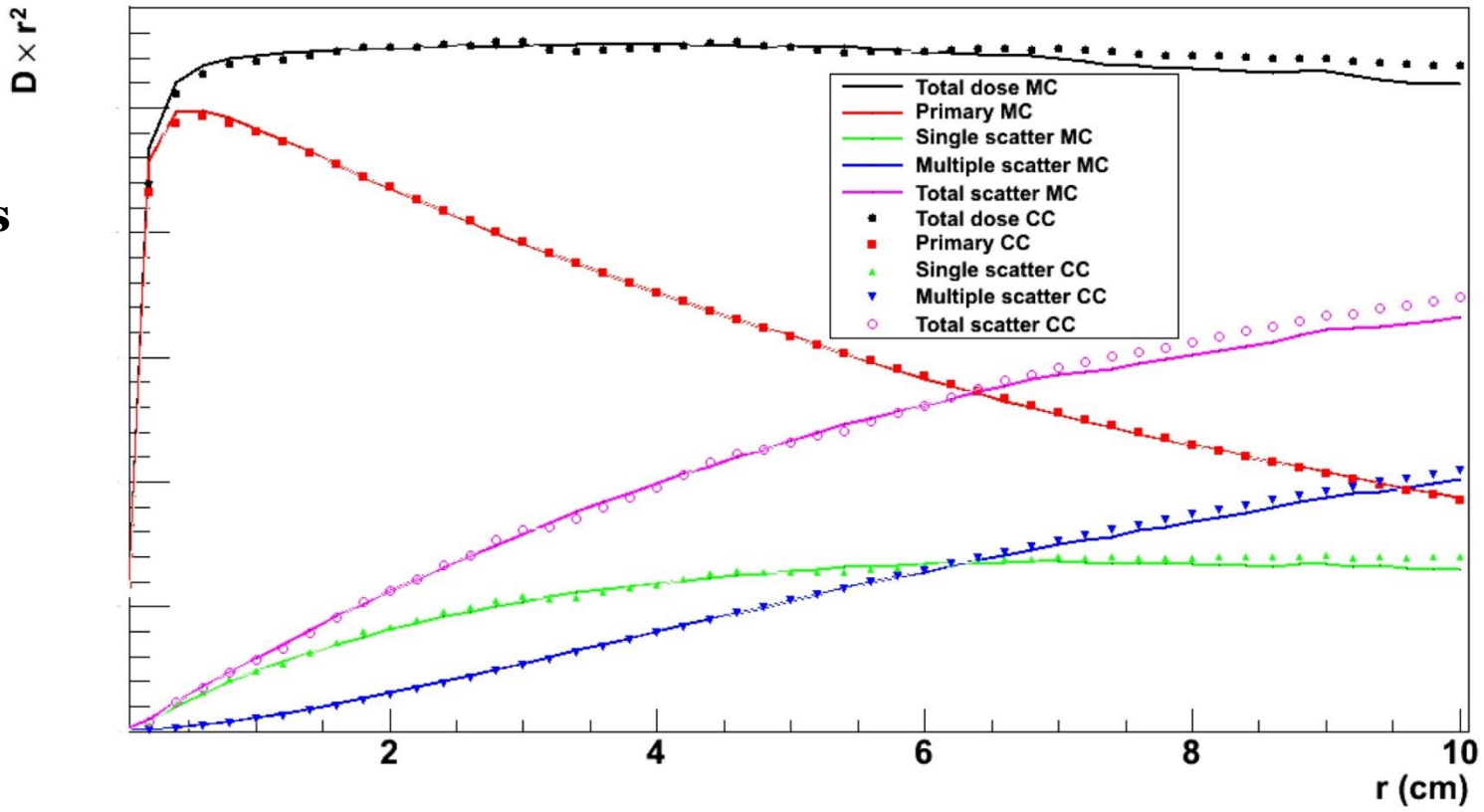

Figure : unpublished data, courtesy of L. Beaulieu

5. finite patient dimensions

Kernel data are traditionally calculated in full scatter geometries (8mfp)

This overestimates msc dose close to the edges of a bounded geometry

Differences could be lifted if a msc kernel calculated in a phantom of equal dimensions to the geometry was used.

Diff. phantoms, Hmsc in R=50cm

Diff. phantoms Hmsc in R=10cm

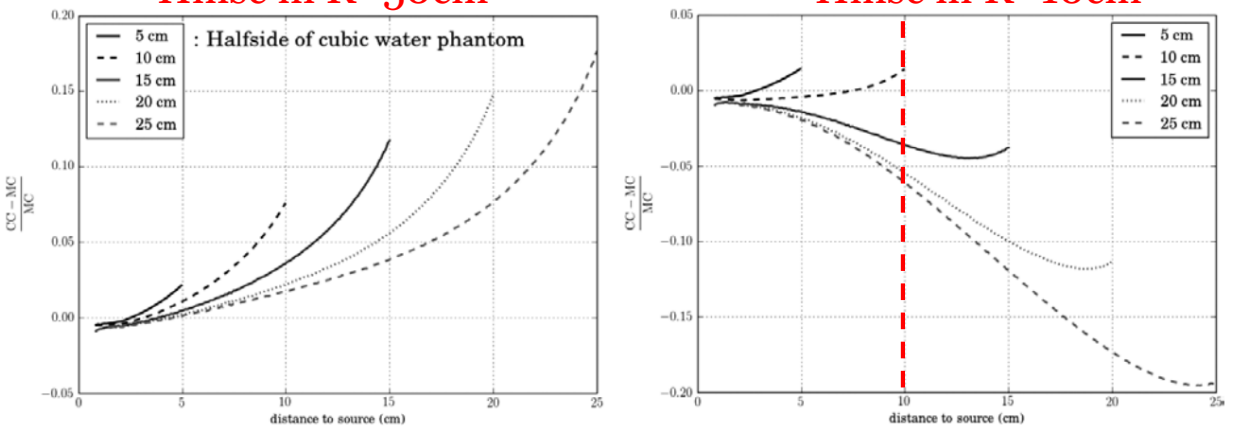

Figure 3. (left): Dose differences between CC and MC as function of the distance from a centrally positioned ^{192}Ir source obtained in cubic water phantoms of halfsides 5 cm, 10 cm, 15 cm, 20 cm and 25 cm. A multiple-scatter point kernel that was generated in a water sphere of outer radii 50 cm was used with CC for all the distributions. (right): Dose differences between CC and MC as function of the distance from a centrally positioned ^{192}Ir source obtained in cubic water phantoms of halfsides 5 cm, 10 cm, 15 cm, 20 cmm and 25 cm. A multiple-scatter point kernel that was generated in a water sphere of outer radii 10 cm was used with CC for all the distributions.

Figure from: A. C. Tedgren et al. Phys. Med. Biol. 60 5313 (2015)

Important implementation details

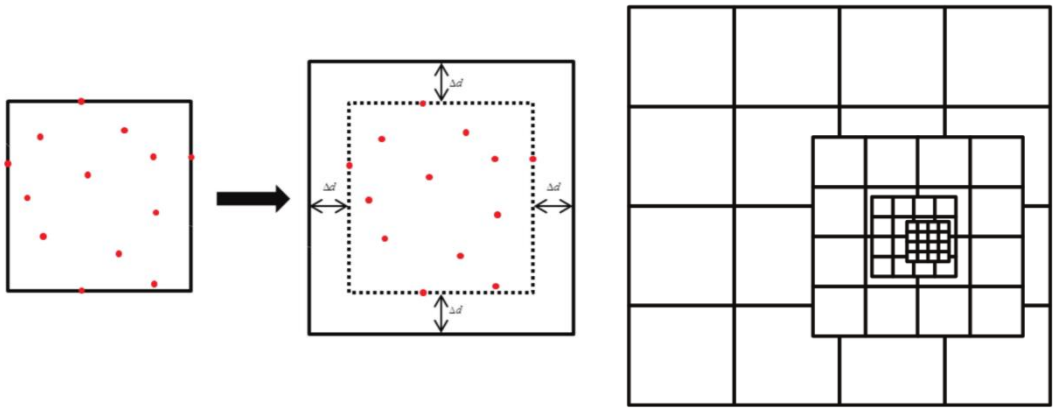

Accuracy Level	Voxel size (cm)			
	0.1	0.2	0.5	1.0
Standard	1	8	20	50
High	8	20	35	50
High (single dwell position)	10	20	50	100

Accuracy level	Number of transport directions for first and residual scatter dose calculations				
	1 dwell position	2-50 dwell positions	51-150 dwell positions	151-300 dwell positions	>300 dwell positions
Standard	320 and 180	320 and 180	240 and 128	200 and 80	180 and 72
High	1620 and 240	720 and 240	500 and 200	320 and 180	240 and 128

All calculation settings are preset!

- The user only selects between two options denoted as: standard and high accuracy levels.

These options control:

- the extent of each of the 4 regions in the multi-resolution Cartesian calculation grid used
- the number of directions for 1sc and msc dose calculations.

- Material assignment is ROI based (TG-186 + applicator materials) otherwise water is considered **within** the patient external contour
- Density can be uniform (ROI based) or HU based (ICRP 44/46 data + method in Knöös et al. Radiother. Oncol. 5, 337, 1986)

Figures from a white paper by Elekta: ACE Advanced Collapsed cone Engine, B. van Veelen, Y. Ma, L. Beaulieu

In short:

	ACE (Oncentra Brachy)
Long heritage	√
Angular discretization	adaptive (“accuracy” selection & # sources)
Spatial discretization	adaptive multi-resolution Cartesian grid (“accuracy” selection)
Pre-calculated data as input	Primary dose for source model, energy spectra, kernels
Energy discretization	-
Primary scatter separation	√
Ray-tracing for primary	√
Successive scattering	Prim. dose → 1st scatter SCERMA → multiple scatter SCERMA

In short:

	ACE (Oncentra Brachy)
Applicator libraries	√
Pre-fixed calculation settings to optimize t vs. accuracy	√
Type A uncertainty (through pre-calculated data)	√
Type B uncertainty	√ cross sections, ray effects, spectral changes in low E/high Z, approx. inhomogeneity correction, ray trace in high scatter gradients, kernel tilting, use of geometry specific kernels
Where to look for type Bs:	high gradients such as very close to the source(s), away from implant, close to geom. boundaries, high Z inhomogeneities

In short:

	ACE (Oncentra Brachy)
Material definition	User (ROI) based: Uniform or individual voxel density from CT + user defined materials from list based on TG186 (ICRU 46, Woodard & White 1986) CT based: individual voxel density from CT + material from density look up table
Dose reporting medium	local medium
Dose calculation grid	geometry defined by imaging
Use in plan optimization	X

ESTRO School

WWW.ESTRO.ORG/SCHOOL

Advanced Brachytherapy Physics

07-10 October 2018 | Valencia, Spain

Dosimetry using a Grid-Based Boltzmann equation Solver (Acuros)

P. Papagiannis, PhD
Medical Physics Laboratory
Medical School
National & Kapodistrian University of Athens

(no conflict of interest to disclose)

Dosimetry using Dosimetry using a Grid-Based Boltzmann equation Solver (Acuros)

• GBBS algorithms used primarily for neutron transport and shielding problems

• Method evaluated for brachy in the literature as early as 2000

• The first GBBS algorithm incorporated in a commercially available ^{192}Ir brachytherapy TPS was Acuros

• Acuros is based on the Attila GBBS developed at Los Alamos National Laboratory, optimized for brachytherapy and later also for external beam therapy (XB) and even CT scatter correction (CTS).

Method can be reviewed in a number of publications:

✓ Daskalov GM et al 2000 Med. Phys. 27(10):2307

✓ Daskalov GM et al, 2002 Med. Phys. 29(2): 113

✓ Gifford K A et al, 2006 Phys. Med. Biol., 51(9): 2253

✓Gifford et al 2008 Med. Phys. 35(6): 2279

+

✓ BV-Acuros user manual

Objectives/Outline:

To :

- review the basic principles of the method
- outline its implementation

so as to identify:

- strengths and weaknesses
- analogies and differences between (current/future) commercially available MBDCAs
- potential improvements over TG-43
- potential shortcomings relative to reference dose distributions

The basic idea …

Remember, if I know the energy distribution of fluence, Φ_E, at all points of a geometry, I know the dose distribution!

$$D(\boldsymbol{r}) = K(\boldsymbol{r}) = \int_E E\Phi_E(\mathbf{r})[{}^{\mu_{en}(E)}/_{\rho}]\,dE$$

Can't I formulate an equation describing Φ_E, at my simple problem (point isotropic source in infinite homogeneous medium) and solve it…?

The basic equation is the LBTE

Let $\Phi_{\Omega,E}(\vec{r},E,\hat{\Omega})$ be the angular fluence ($d\Phi/d\Omega dE=dN/dAd\Omega dE$) denoting the number of photons in phase space element $(\vec{r},E,\hat{\Omega})$, i.e. passing through a voxel of area dA normal to $\hat{\Omega}$ located at $\vec{r}$, with $\hat{\Omega}$ within Ω and $\Omega+d\Omega$ and E between E and E+dE.

At any part of this "phase space", conservation of E dictates particle density balance.

The net flow of photons through a phase space cell equals:

photons scattered in it from all others (E', Ω')

+ photons emitted by a source in it

- photons absorbed or scattered out of it

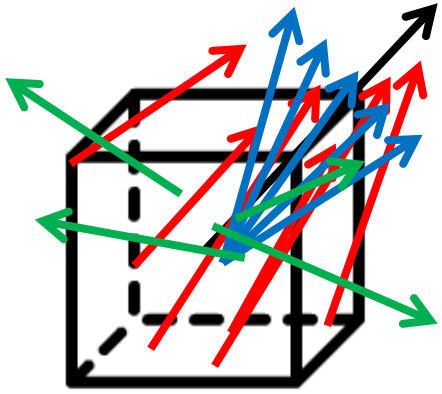

$$\hat{\Omega}\cdot\nabla\Phi_{\Omega,E}(\vec{r},E,\hat{\Omega}) =$$

$$q_{scat}(\vec{r},E,\hat{\Omega})$$

$$+\frac{q_p(E,\hat{\Omega})}{4\pi}\delta(\vec{r}-\vec{r}_p)$$

$$-\mu_t(\vec{r},E)\Phi_{\Omega,E}(\vec{r},E,\hat{\Omega})$$

L.B.T.E.

The LBTE

Rearranging the equation, and dropping notation for angular Φ and E distr. of Φ (these can be discerned by the argument):

$$\hat{\Omega}\cdot\vec{\nabla}\Phi(\vec{r},E,\hat{\Omega})+\mu_t\Phi(\vec{r},E,\hat{\Omega})=q_{scat}+\sum_{p=1}^{P}\frac{q_p}{4\pi}\delta(\vec{r}-\vec{r}_p)$$

Where:
μ_t is the total linear interaction coefficient
q_p is the primary photon density due to any of P point sources present at a phase space cell
q_{scat} is the scatter photon density

OK…!

Can I solve the LBTE for Φ …?

The LBTE

$$\hat{\Omega}\cdot\vec{\nabla}\Phi(\vec{r},E,\hat{\Omega})+\mu_t\Phi(\vec{r},E,\hat{\Omega})=q_{scat}+\sum_{p=1}^{P}\frac{q_p}{4\pi}\delta(\vec{r}-\vec{r}_p)$$

There is no analytical (closed form) solution of the LBTE.

This is because it is an equation of 6 variables which is integro-differential since the scatter source is:

$$q_{scat}(\vec{r},E,\hat{\Omega})=\int_0^{\infty}\int_{4\pi}\mu_S(\vec{r},E'\rightarrow E,\hat{\Omega}\cdot\hat{\Omega}')\Phi(\vec{r},E',\hat{\Omega}')d\hat{\Omega}'dE'$$

i.e. : I must integrate for the scatter source and this depends on the solution itself at all other (E',Ω') points of the phase space…!

The only option is to solve the equation numerically (and this is exactly what Acuros and similar algorithms do) by:

- separating variables: $\Phi(\vec{r},E,\hat{\Omega})=\Phi(\vec{r},E)Y(\hat{\Omega})=\Phi(\vec{r})\,f(E)Y(\hat{\Omega})$
- solve the LBTE iteratively:
  - make initial guess for $\Phi(\vec{r})$
  - approximate integration for the scatter source by summation over discrete E, Ω elements
  - approximate derivatives by finite differences over discrete space elements
  - correct initial guess, and continue until a convergence criterion is met

The method

Let us take a closer look at q_{scat}:

$$q_{scat}(\vec{r}, E, \hat{\Omega}) = \int_{0}^{\infty} \int_{4\pi} \mu_S(\vec{r}, E' \to E, \hat{\Omega} \cdot \hat{\Omega}') \Phi(\vec{r}, E', \hat{\Omega}') d\hat{\Omega}' dE'$$

The probability of a photon scattering from Ω' to Ω (for a given energy)
depends only on $\cos\theta \in [-1,1]$, where θ is the scattering angle
and
the number of photons scattered in a given direction (for a given energy)
depends on the solid angle element around the direction: $\sin\theta d\theta d\varphi$
or
the area on the unit sphere defined by the solid angle around the direction

Hence, I can expand q_{scat} in an infinite series of spherical harmonics.

WHAT...???!!!

The method

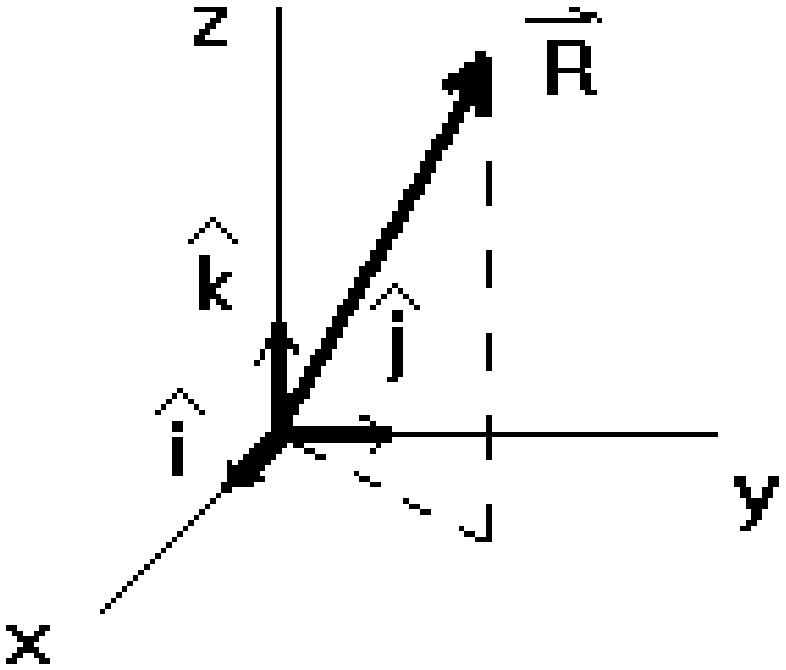

It would not strike you as odd that
any function in R^3
can be expanded as a 3 term series

provided the basis for this expansion is orthogonal, e.g.:

$$\hat{i} \bullet \hat{j} = \hat{j} \bullet \hat{k} = \hat{k} \bullet \hat{i} = 0$$

$$\hat{i} \bullet \hat{i} = \hat{j} \bullet \hat{j} = \hat{k} \bullet \hat{k} = 1$$

i, j, and k are said to form an orthogonal basis

Many orthogonal bases exist!

The method

Many orthogonal bases exist

In example:

- Legendre polynomials, $P_n(x)$, are a series of functions that exhibit orthogonality for $-1 \le x \le 1$:

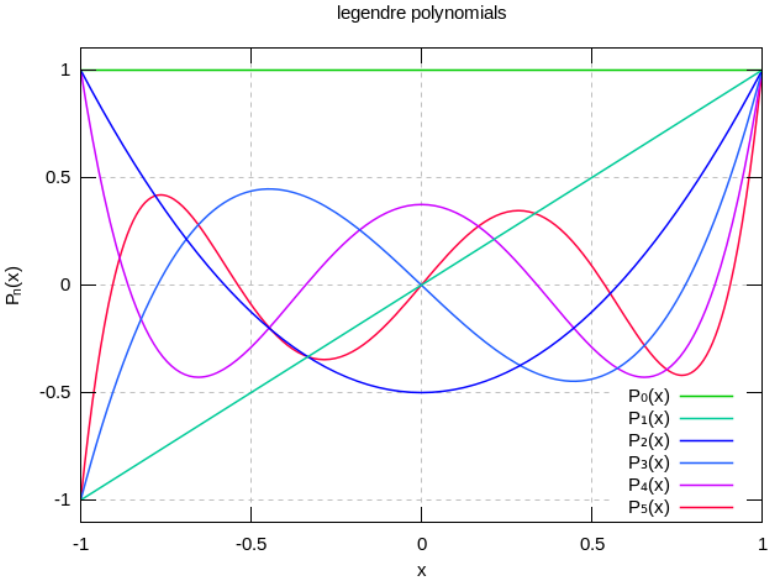

$$\int_{-1}^{1} P_m(x) P_n(x)\, dx = \frac{2}{2n+1}\delta_{mn}$$

and therefore they can be used to expand any function defined in [-1,1] in an infinite series:

$$f(x) = \sum_{n=0}^{\infty} w_n P_n(x),$$

$$w_n = \int_{-1}^{1} f(x)\, P_n(x)\, dx$$

$$\mu_s(\vec{r}, E' \to E, \hat{\Omega}\cdot\hat{\Omega}') = \sum_{n=0}^{\infty} \frac{2n+1}{4\pi} \mu_{s,n}(\vec{r}, E' \to E)\, P_n(\hat{\Omega}\cdot\hat{\Omega}'),$$

$$\mu_{s,n}(\vec{r}, E' \to E) = 1/2 \int_{-1}^{1} \mu_s(\vec{r}, E' \to E, \hat{\Omega}\cdot\hat{\Omega}')\, P_n(\hat{\Omega}\cdot\hat{\Omega}')\, d(\hat{\Omega}\cdot\hat{\Omega}')$$

The method

- We can truncate the expansion of μ_s up to N

(N=3 is adequate for ^{192}Ir anisotropic scattering)

$$\mu_S(\vec{r}, E' \to E, \hat{\Omega} \cdot \hat{\Omega}') = \sum_{n=0}^{N=3} \frac{2n+1}{4\pi} \mu_{S,n}(\vec{r}, E' \to E) P_n(\hat{\Omega} \cdot \hat{\Omega}'),$$

$$\mu_{S,n}(\vec{r}, E' \to E) = 1/2 \int_{-1}^{1} \mu_S(\vec{r}, E' \to E, \hat{\Omega} \cdot \hat{\Omega}') \; P_n(\hat{\Omega} \cdot \hat{\Omega}') \, d(\hat{\Omega} \cdot \hat{\Omega}')$$

Note that truncation pertains to the detail in the description of scatter cross section in terms of the scattering angle and that we have NOT discretized in direction

The method

Many orthogonal bases exist

In example:

- Spherical harmonics, $Y_l^m(\theta,\phi)$, are a series of functions defined on the surface of a sphere that exhibit orthogonality:

$$\int_{2\pi}\int_{\pi} Y_l^m(\theta,\phi)\bar{Y}_{l'}^{m'}(\theta,\phi)\sin\theta\,\mathrm{d}\theta\,\mathrm{d}\varphi =$$

$$\int_{2\pi}\int_{-1}^{1} Y_l^m(\theta,\phi)\bar{Y}_{l'}^{m'}(\theta,\phi)\,d(\cos\theta)\,\mathrm{d}\varphi = \delta_{mm'}\ \delta_{ll'}$$

and therefore they can be used to expand any function defined on the surface of a sphere in an infinite series:

$$f(\theta,\phi) = \sum_{l=0}^{\infty}\sum_{m=-l}^{l} C_{l,m}Y_l^m(\theta,\phi),$$

$$C_{l,m} = \iint_{\Omega} f(\theta,\phi)\,Y_l^m(\theta,\phi)\,d\Omega$$

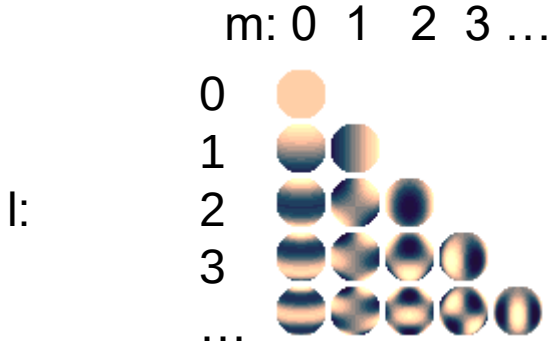

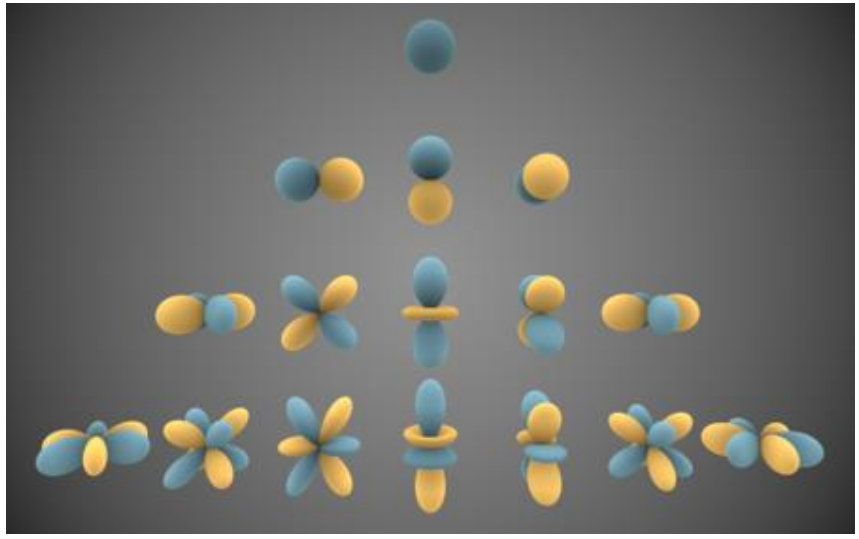

Various types of spherical harmonics are available.
A particular set, of order l=N (orthogonal basis) + the corresponding weights of a function are called a **quadrature set of order N**.

The method

Many orthogonal bases exist

In example:

- Spherical harmonics, $Y_l^m(\theta,\phi)$, are a series of functions defined on the surface of a sphere that exhibit orthogonality:

$$\int_{2\pi}\int_{\pi} Y_l^m(\theta,\phi)\bar{Y}_{l'}^{m'}(\theta,\phi)\sin\theta\,\mathrm{d}\theta\,\mathrm{d}\varphi =$$

$$\int_{2\pi}\int_{-1}^{1} Y_l^m(\theta,\phi)\bar{Y}_{l'}^{m'}(\theta,\phi)\,d(\cos\theta)\,\mathrm{d}\varphi = \delta_{mm'}\ \ \delta_{ll'}$$

and therefore they can be used to expand any function defined on the surface of a sphere in an infinite series:

$$f(\theta,\phi) = \sum_{l=0}^{\infty}\sum_{m=-l}^{l} C_{l,m}Y_l^m(\theta,\phi),$$

$$C_{l,m} = \iint_{\Omega} f(\theta,\phi)\,Y_l^m(\theta,\phi)\,d\Omega$$

$$\Phi(\vec{r},E',\hat{\Omega}') = \sum_{l=0}^{\infty}\sum_{m=-l}^{l} \Phi_{l,m}(\vec{r},E')\,Y_l^m(\hat{\Omega}'),$$

$$\Phi_{l,m}(\vec{r},E') = \iint_{4\pi} \Phi(\vec{r},E',\hat{\Omega}')\,Y_l^m(\hat{\Omega}')\,d\Omega'$$

Note we have described the energy fluence in spherical coordinates and that we have NOT discretized in direction

The method

OK.

Let us agree that instead of :

$$q_{scat}(\vec{r},E,\hat{\Omega}) = \int_0^{\infty}\int_{4\pi}\mu_S(\vec{r},E'\to E,\hat{\Omega}\cdot\hat{\Omega}')\Phi(\vec{r},E',\hat{\Omega}')d\hat{\Omega}'dE'$$

q_{scat} can be written as :

$$q_{scat}(\vec{r},E,\hat{\Omega}) = \int_0^{\infty}\sum_{l=0}^{\infty}\sum_{m=-l}^{l}\mu_{S,l}(\vec{r},E'\to E)\,\Phi_{l,m}(\vec{r},E')\,Y_l^m(\theta,\phi)\,dE',$$

$$\mu_{S,l}(\vec{r},E'\to E) = 1/2\int_{-1}^{1}\mu_S(\vec{r},E'\to E,\hat{\Omega}\cdot\hat{\Omega}')\,P_l(\hat{\Omega}\cdot\hat{\Omega}')\,d(\hat{\Omega}\cdot\hat{\Omega}')$$

$$\Phi_{l,m}(\vec{r},E') = \iint_{4\pi}\Phi(\vec{r},E',\hat{\Omega}')\,Y_l^m(\hat{\Omega}')\,d\Omega'$$

is there a benefit?

The method

- We have separated r and E, from direction variables and turned integration to summation for direction in the scatter source

$$\hat{\Omega}\cdot\vec{\nabla}\Phi(\vec{r},E,\hat{\Omega})+\mu_t\Phi\ (\vec{r},E,\hat{\Omega})=q_{scat}+\sum_{p=1}^{P}\frac{q_p}{4\pi}\delta(\vec{r}-\vec{r}_p)\quad(1)$$

$$q_{scat}(\vec{r},E,\hat{\Omega})=\int_0^{\infty}\sum_{l=0}^{\infty}\sum_{m=-l}^{l}\mu_{s,l}(\vec{r},E'\to E)\ \Phi_{l,m}(\vec{r},E')\ Y_l^m(\theta,\varphi)\,dE'\quad(2)$$

$$\mu_{s,l}(\vec{r},E'\to E)=1/2\int_{-1}^{1}\mu_s(\vec{r},E'\to E,\hat{\Omega}\cdot\hat{\Omega}')\ P_l(\hat{\Omega}\cdot\hat{\Omega}')\,d(\hat{\Omega}\cdot\hat{\Omega}')\quad(3)$$

$$\Phi_{l,m}(\vec{r},E')=\iint_{4\pi}\Phi(\vec{r},E',\hat{\Omega}')\ Y_l^m(\hat{\Omega}')\,d\Omega'\quad(4)$$

Let us continue with E …

The method

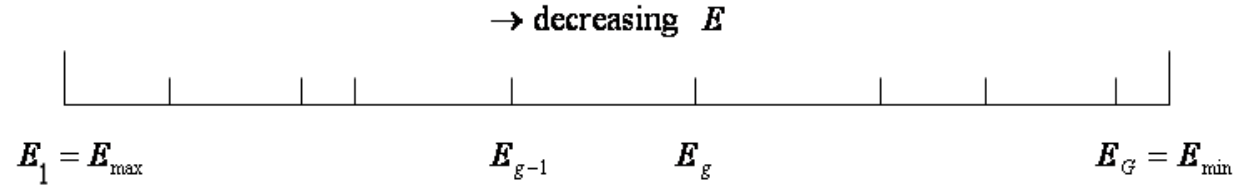

- Energy is divided in g=1,..,**G groups** of width ΔE_g so that energy decreases as group order decreases

Our equations become:

$$\hat{\Omega}\cdot\vec{\nabla}\Phi_g(\vec{r},\hat{\Omega})+\mu_{t,g}\Phi_g(\vec{r},\hat{\Omega})=q_{scat,g}+\sum_{p=1}^{P}\frac{q_{p,g}}{4\pi}\delta(\vec{r}-\vec{r}_p) \quad (1)$$

$$q_{scat,g}(\vec{r},\hat{\Omega})=\sum_{l=0}^{\infty}\sum_{m=-l}^{l}\sum_{g'=1}^{G}\mu_{s,l,g'->g}(\vec{r})\,\Phi_{l,m,g'}(\vec{r})Y_l^m(\theta,\phi) \quad (2)$$

$$\mu_{s,l,g'->g}(\vec{r})=\frac{\int_{E_{g'}}^{E_{g'-1}}\int_{E_g}^{E_{g-1}}\mu_{s,l}(\vec{r},E'\to E)\Phi(\vec{r},E')\,dE'\,dE}{\int_{E_g}^{E_{g-1}}\Phi(\vec{r},E)\,dE} \quad (3)$$

$$\Phi_{l,m,g}(\vec{r})=\int_{E_g}^{E_{g-1}}\Phi_{l,m}(\vec{r},E)dE=\int_{E_g}^{E_{g-1}}\iint_{4\pi}\Phi(\vec{r},E',\hat{\Omega}')Y_l^m(\hat{\Omega}')\,d\Omega'\,dE \quad (4)$$

$$\mu_{t,g}(\vec{r})=\frac{\int_{E_g}^{E_{g-1}}\mu_t(\vec{r},E)\Phi(\vec{r},E')\,dE}{\int_{E_g}^{E_{g-1}}\Phi(\vec{r},E)\,dE} \quad (5)$$

The method

- Up to now, our set of equations is EXACT

but we need to separate r from E to solve it iteratively

$$\hat{\Omega}\cdot\vec{\nabla}\Phi_g(\vec{r},\hat{\Omega})+\mu_{t,g}\Phi_g(\vec{r},\hat{\Omega})=q_{scat,g}+\sum_{p=1}^{P}\frac{q_{p,g}}{4\pi}\delta(\vec{r}-\vec{r}_p) \tag{1}$$

$$q_{scat,g}(\vec{r},\hat{\Omega})=\sum_{l=0}^{\infty}\sum_{m=-l}^{l}\sum_{g'=1}^{G}\mu_{s,l,g'->g}(\vec{r})\,\Phi_{l,m,g'}(\vec{r})Y_l^m(\theta,\phi) \tag{2}$$

$$\mu_{s,l,g'->g}(\vec{r})=\frac{\int_{E_{g'}}^{E_{g'-1}}\int_{E_g}^{E_{g-1}}\mu_{s,l}(\vec{r},E'\to E)\Phi(\vec{r},E')\,dE'\,dE}{\int_{E_g}^{E_{g-1}}\Phi(\vec{r},E)\,dE} \tag{3}$$

$$\Phi_{l,m,g}(\vec{r})=\int_{E_g}^{E_{g-1}}\Phi_{l,m}(\vec{r},E)dE=\int_{E_g}^{E_{g-1}}\iint_{4\pi}\Phi(\vec{r},E',\hat{\Omega}')Y_l^m(\hat{\Omega}')\,d\Omega'\,dE \tag{4}$$

$$\mu_{t,g}(\vec{r})=\frac{\int_{E_g}^{E_{g-1}}\mu_t(\vec{r},E)\Phi(\vec{r},E')\,dE'}{\int_{E_g}^{E_{g-1}}\Phi(\vec{r},E)\,dE} \tag{5}$$

The method

- if we define a spectral weighting factor: f(E) so that: $\Phi(\vec{r},E)=\Phi(\vec{r})\,f(E),\ \int_E f(E)dE=1$

Our equations become:

$$\hat{\Omega}\cdot\vec{\nabla}\Phi_g(\vec{r},\hat{\Omega})+\mu_{t,g}\Phi_g(\vec{r},\hat{\Omega})=q_{scat,g}+\sum_{p=1}^{P}\frac{q_{p,g}}{4\pi}\delta(\vec{r}-\vec{r}_p) \quad (1)$$

$$q_{scat,g}(\vec{r},\hat{\Omega})=\sum_{l=0}^{\infty}\sum_{m=-l}^{l}\sum_{g'=1}^{G}\mu_{s,l,g'->g}(\vec{r})\,\Phi_{l,m,g'}(\vec{r})Y_l^m(\theta,\phi) \quad (2)$$

$$\mu_{s,l,g'->g}(\vec{r})=\int_{E_{g'}}^{E_{g'-1}}\int_{E_g}^{E_{g-1}}\mu_{s,l}(\vec{r},E'\to E)\,f(E')\,dE\,dE' \quad (3)$$

$$\Phi_{l,m,g}(\vec{r})=\int_{E_g}^{E_{g-1}}\Phi_{l,m}(\vec{r})\,f(E)dE=\int_{E_g}^{E_{g-1}}\iint_{4\pi}\Phi(\vec{r},\hat{\Omega}')f(E)Y_l^m(\hat{\Omega}')\,d\Omega'\,dE \quad (4)$$

$$\mu_{t,g}(\vec{r})=\int_{E_g}^{E_{g-1}}\mu_t(\vec{r},E)\,f(E)\,dE \quad (5)$$

- All that is left then is to discretize direction and space and solve iteratively!

The method

$$\Phi(\vec{r},E) = \Phi(\vec{r})\, f(E), \quad \int_E f(E)dE = 1$$

The importance of f(E):

The spectral weighting factor connects photon fluence to energy fluence at any point of a geometry and hence depends on the actual geometry and its physical properties.

However, as G increases, and ΔE_G become narrow, the energy group cross sections $\mu_{t,g}$, $\mu_{s,g}$, become constant approximations of the continuous $\mu_t(E)$, $\mu_s(E)$ and do not depend heavily on f(E).

This means that generic multi group cross sections (of ΔE_G <<) are used with analytic or semi-analytic f(E) appropriate for the problem at hand.

The method

Let us make the final step:

We ask our equations to hold for a number of directions M determined by a **quadrature set S_N** of order N (Discrete Ordinates Method-DOM)

(M is linked to N in a different way for different quadrature sets)

$$\hat{\Omega}\cdot\vec{\nabla}\Phi_{g,n}(\vec{r})+\mu_{t,g}\Phi_{g,n}(\vec{r})=q_{scat,g,n}+\sum_{p=1}^{P}\frac{q_{p,g,n}}{4\pi}\delta(\vec{r}-\vec{r}_p),\qquad \Phi_{g,n}(\vec{r})=\Phi_g(\vec{r},\hat{\Omega}_n) \tag{1}$$

$$q_{scat,g,n}(\vec{r},\hat{\Omega})=\sum_{l=0}^{\infty}\sum_{m=-l}^{l}\sum_{g'=1}^{G}\mu_{s,l,g'->g}(\vec{r})\,\Phi_{l,m,g'}(\vec{r})Y_l^m(\theta,\phi) \tag{2}$$

$$\mu_{s,l,g'->g}(\vec{r})=\int_{E_{g'}}^{E_{g'-1}}\int_{E_g}^{E_{g-1}}\mu_{s,l}(\vec{r},E'\to E)\,f(E')\,dE dE' \tag{3}$$

$$\Phi_{l,m,g}(\vec{r})=\int_{E_g}^{E_{g-1}}\Phi_{l,m}(\vec{r})\,f(E)dE=\int_{E_g}^{E_{g-1}}\iint_{4\pi}\Phi(\vec{r},\hat{\Omega}')\,f(E)Y_l^m(\hat{\Omega}')\,d\Omega' dE=\int_{E_g}^{E_{g-1}}\sum_{n=1}^{N}\Phi_{g,n}(\vec{r})\,f(E)Y_l^m(\hat{\Omega}_n)w_n\,dE \tag{4}$$

$$\mu_{t,g}(\vec{r})=\int_{E_g}^{E_{g-1}}\mu_t(\vec{r},E)\,f(E)\,dE \tag{5}$$

The method … is ready

I have GxM equations of the form (1) @ each voxel (GxMxN$_{vox}$ in total)

- begin with E1 (highest energy group)
- make an initial guess for $\Phi_{1,n}(\vec{r})_{iter=0}$
- calculate cross sections from (3) & (5)
- calculate the expansion from (4)
- use these in (2) to calculate $q_{scat,1,n}$
- solve (1) for $\Phi_{1,n}(\vec{r})_{iter=1}$
- if convergence criterion not met, re-iterate
- if convergence criterion met, proceed with g=2

$$\hat{\Omega}\cdot\vec{\nabla}\Phi_{g,n}(\vec{r})+\mu_{t,g}\Phi_{g,n}(\vec{r})=q_{scat,g,n}+\sum_{p=1}^{P}\frac{q_{p,g,n}}{4\pi}\delta(\vec{r}-\vec{r}_p) \quad (1)$$

$$q_{scat,g,n}(\vec{r},\hat{\Omega})=\sum_{l=0}^{\infty}\sum_{m=-l}^{l}\sum_{g'=1}^{G}\mu_{s,l,g'->g}(\vec{r})\,\Phi_{l,m,g'}(\vec{r})Y_l^m(\theta,\phi) \quad (2)$$

$$\mu_{s,l,g'->g}(\vec{r})=\int_{E_{g'}}^{E_{g'-1}}\int_{E_g}^{E_{g-1}}\mu_{s,l}(\vec{r},E'\to E)\,f(E')\,dE\,dE' \quad (3)$$

$$\Phi_{l,m,g}(\vec{r})=\int_{E_g}^{E_{g-1}}\sum_{n=1}^{N}\Phi_{g,n}(\vec{r})f(E)Y_l^m(\hat{\Omega}_n)w_n\,dE \quad (4)$$

$$\mu_{t,g}(\vec{r})=\int_{E_g}^{E_{g-1}}\mu_t(\vec{r},E)\,f(E)\,dE \quad (5)$$

BUT…:

1. **I need to be efficient** (t~ GxMxN$_{vox}$x#iters.x order of legendre exp.) **& work with finite voxels**
2. **I need to account for inhomogeneities**
3. **I need to work with real sources**
4. **I need to account for finite patient dimensions**

1. I need to be efficient

The iterations are needed because I do not know q_{scat} within the energy group
i.e. scattering events with minimal energy transfer

When do I expect delays in convergence?

1. I need to be efficient

The iterations are needed because I do not know q_{scat} within the energy group
i.e. scattering events with minimal energy transfer

When do I expect delays in convergence?

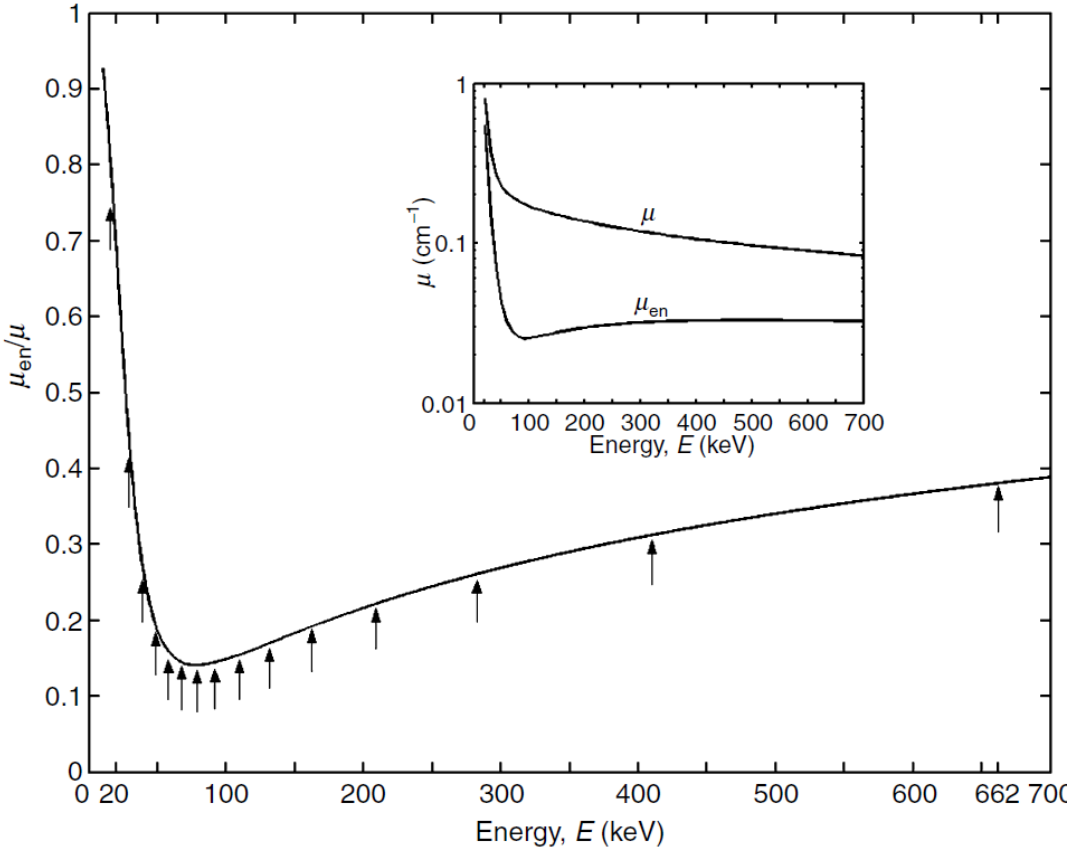

Multiple scattering with minimal energy transfer that occurs in the ^{192}Ir energy range

as well as

coherent scattering that is significant at low energies and high Z materials,

delay convergence

Algorithms to force convergence are used (DSA-Diffusion synthetic acceleration)

1. I need to be efficient

The multigroup (G), DOM (S_N), cross section expansion (P_N) method converges to an analytic solution of the LBTE for G, N →infinity

and

no volume averaging is expected for fine spatial discretization (N_{vox} →infinity)

BUT

I need to be efficient

and since t~ G x M x N_{vox} (x #iters. x order of legendre exp.),

even if I have the perfect finite differencing algorithm for solving the system of equations,

I need to reduce G, M, N_{vox} !!!

1. I need to be efficient, angular discretization

Guess what happens when I reduce M (order of S_N) …

RAY EFFECTS…!

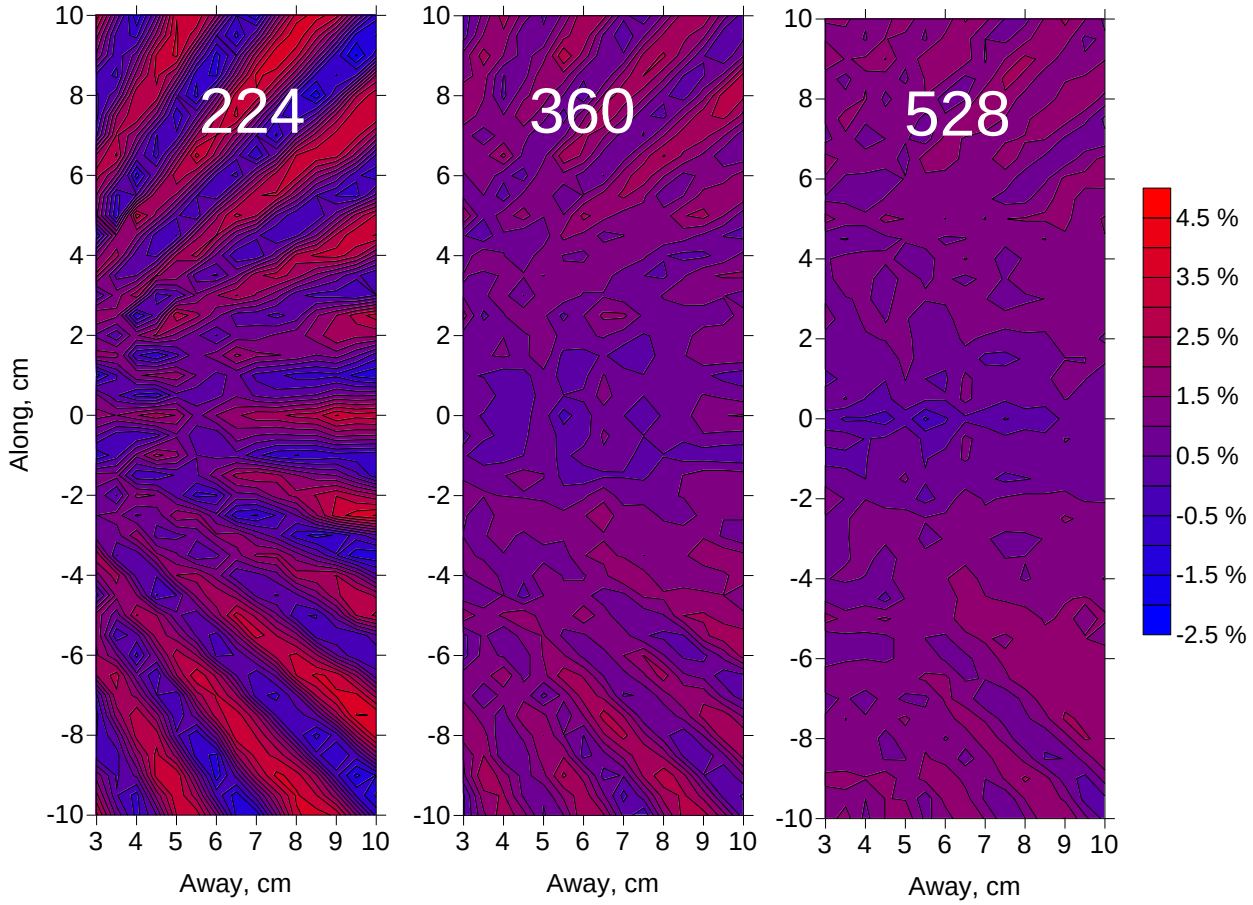

Figure from: Venselaar, Baltas, Meigooni, Hoskin (Eds), Comprehensive Brachytehrapy: physical and clinical aspects. CRC Press, Taylor & Francis, © 2013

1. I need to be efficient, angular discretization

- discretization artifacts or “rays”: an artificial buildup of particle fluence along the finite number of directions used

↑ with high gradients of scatter fluence, at points where primary dose is small

↓ with ↑ $N_{directions}$ & voxel size at the expense of calculation time and potential volume averaging

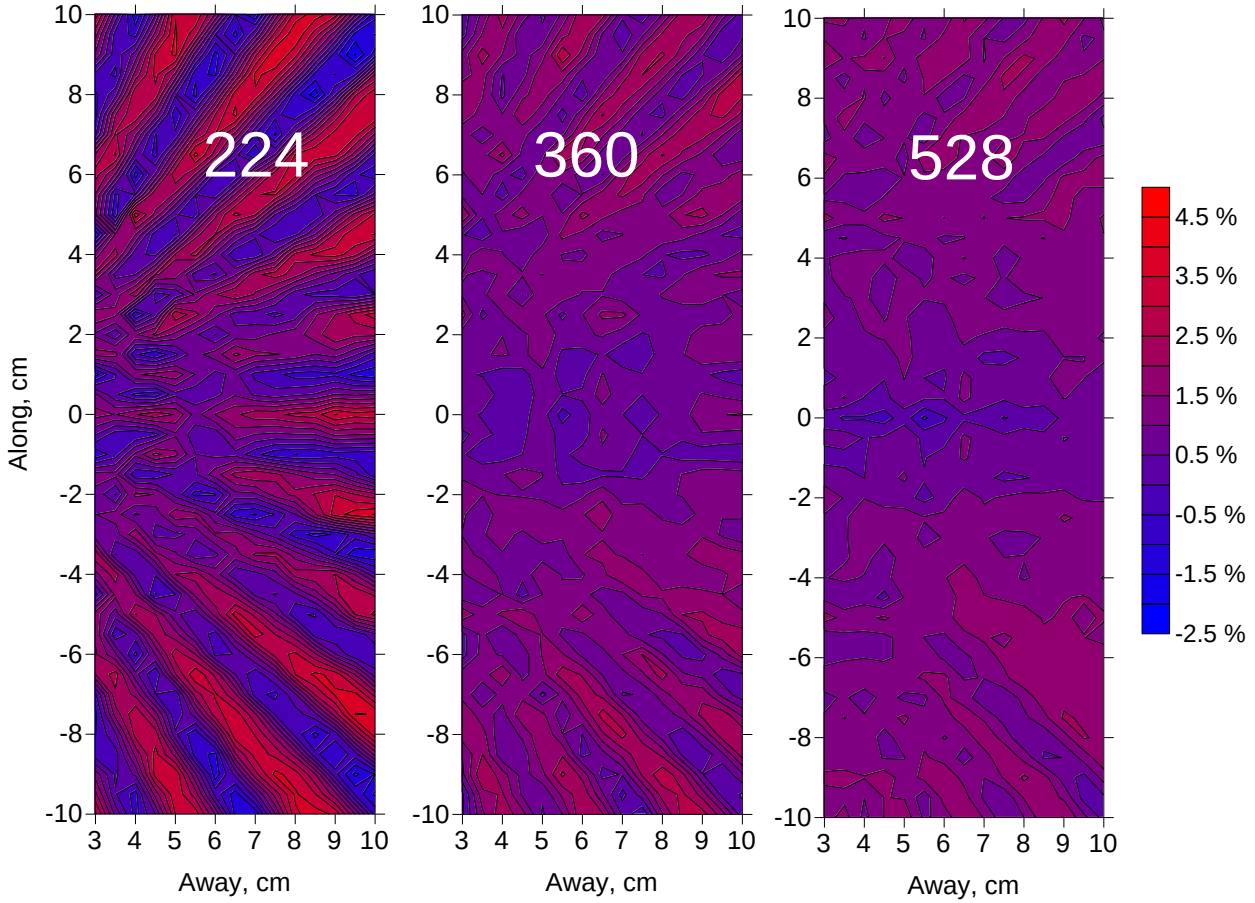

Figure from: Venselaar, Baltas, Meigooni, Hoskin (Eds), Comprehensive Brachytehrapy: physical and clinical aspects. CRC Press, Taylor & Francis, ©

1. I need to be efficient, angular discretization

How can I relax the demand on S_N without ray effects?

The LBTE is linear so assuming:

$$\Phi_g(\vec{r},\hat{\Omega}) = \sum_{p=1}^{P} \Phi_{p,g}^{unc}(\vec{r},\hat{\Omega}) + \Phi_g^{coll}(\vec{r},\hat{\Omega})$$

For any direction, we can split our system of equations in two:

$$\hat{\Omega}\cdot\vec{\nabla}\Phi_g^{unc} + \sigma_{t,g}\Phi_g^{unc} = \sum_{p=1}^{P} \frac{q_{p,g}}{4\pi}\delta(\vec{r}-\vec{r}_p) \qquad (1)$$

$$\hat{\Omega}\cdot\vec{\nabla}\Phi_g^{coll} + \sigma_{t,g}\Phi_g^{coll} = q_g^{scat,coll} + \sum_{p=1}^{P} q_{p,g}^{scat,unc} \qquad (2)$$

Equation (1) for the primary (uncolided) part of the fluence can be analytically solved!!!

I can ray-trace the solution for the spectrum of primary photons through the geometry and arrive at very quick and accurate: initial guess $\Phi_{1,n}(\vec{r})_{iter=0}$ and $q_{scat,1,n}$

Then I proceed to solve the system of equations (2) for the collided fluence to refine my solution with the higher orders of scatter

This is known as the 1st scatter source method

1. I need to be efficient, angular discretization

- Acuros uses the first scatter source method so the photon spectrum exiting a source needs to be known
- Acuros uses Triangular-Chebyshev quadrature sets for angular discretization and the integration for the generation of the scattering source
- The angular discretization scheme is adaptive with S_N order

ranging from N=4 (24 discrete directions) to 30 (960 discrete directions) varying both within an energy group (g→g) and between energy groups (g→g')

Guess which energies are given larger N …!

1. I need to be efficient, energy discretization

Remember: Energy discretization is realistic if cross sections do not vary considerably within each group and appropriate f(E) is very important

Acuros (for ^{192}Ir) uses an adaptive G=37 group cross section set.

For the uncollided component all 37 groups are used, with $f(E) = 1/\Delta E_g$

For the collided (scattered) component, this group is collapsed applying an appropriate (proprietary) energy weighting function f(E).

Acuros uses cross section generated by CEPXS, a multigroup-Legendre cross-section generating code.

CEPXS does not include coherent scattering and uses the Klein-Nishina incoherent scattering cross sections.

1. I need to be efficient, spatial discretization

For spatial discretization, Acuros partitions the computational volume (the CT image series) into variable sized Cartesian elements.

Computational element size varies based on material properties and the gradient of the scatter photon fluence.

The spatial derivatives in the LBTEs are replaced by finite differences at multiple points within each computational element

Supplementary equations are used to describe fluence variation between these points and preserve particle balance (DFEM - linear discontinuous Galerkin finite-element method)

Hence the angular fluence is known everywhere in each element, not only at the points where spatial derivatives are evaluated

BUT

spatial discretization errors can ensue at points in high fluence gradients

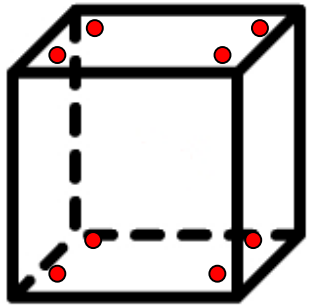

$$\frac{\partial \Phi_{m,g}(x_i)}{\partial x} = \frac{\Phi_{m,g}(x_{i+1}) - \Phi_{m,g}(x_{i-1})}{\Delta x_i}$$

2. inhomogeneities

The method inherently accounts for inhomogeneities assuming material properties are constant within each computational element (!!! restriction on computational element size !!!)

through:

- $\mu_{t,g}$, $\mu_{s,l,g}$
- primary fluence ray tracing
- dose calculation

$$D(\vec{r}) = \frac{1}{\rho(\vec{r})} \sum_{g=1}^{G} \mu_{en,g}(\vec{r}) \left\{ \sum_{p=1}^{P} \Phi_{p,g}^{unc}(\vec{r}) + \Phi_{g}^{coll}(\vec{r}) \right\} \qquad D(\vec{r}) = \frac{1}{\rho_{water}} \sum_{g=1}^{G} \mu_{en,g}^{water}(\vec{r}) \left\{ \sum_{p=1}^{P} \Phi_{p,g}^{unc}(\vec{r}) + \Phi_{g}^{coll}(\vec{r}) \right\}$$

(note that D is calculated as a post processing operation)

3. real sources

Input must now be source specific:

- Energy distribution of primary fluence (in essence the source phase space file)

Acuros uses effective sources:

pre-calculated source specific phase space file

+

a number of points within the source volume for ray tracing the primary fluence in the geometry

Brachy sources are small BUT the number of point sources used for ray tracing can be important

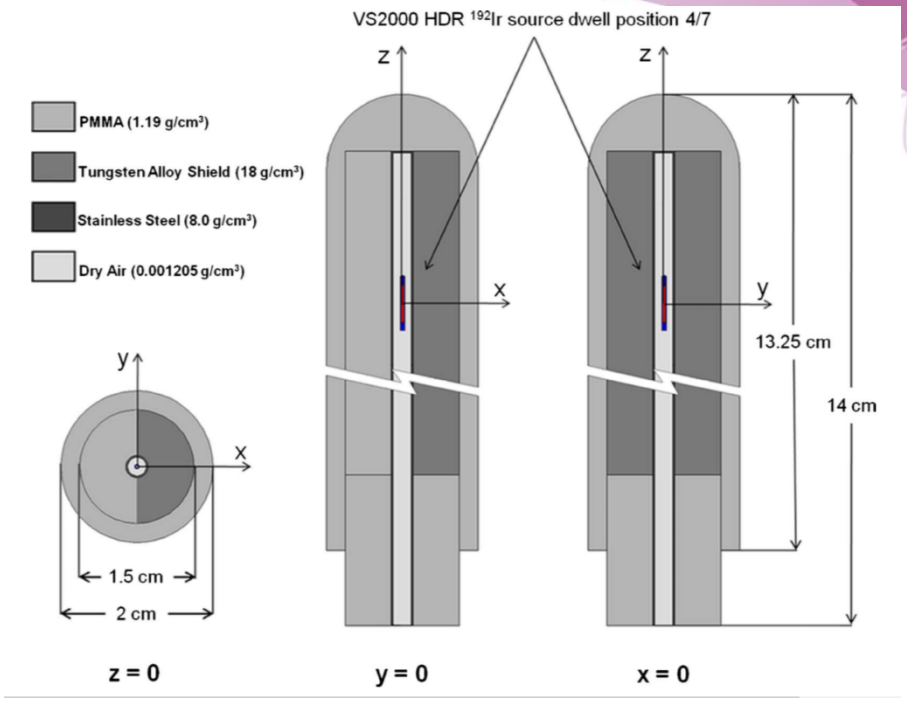

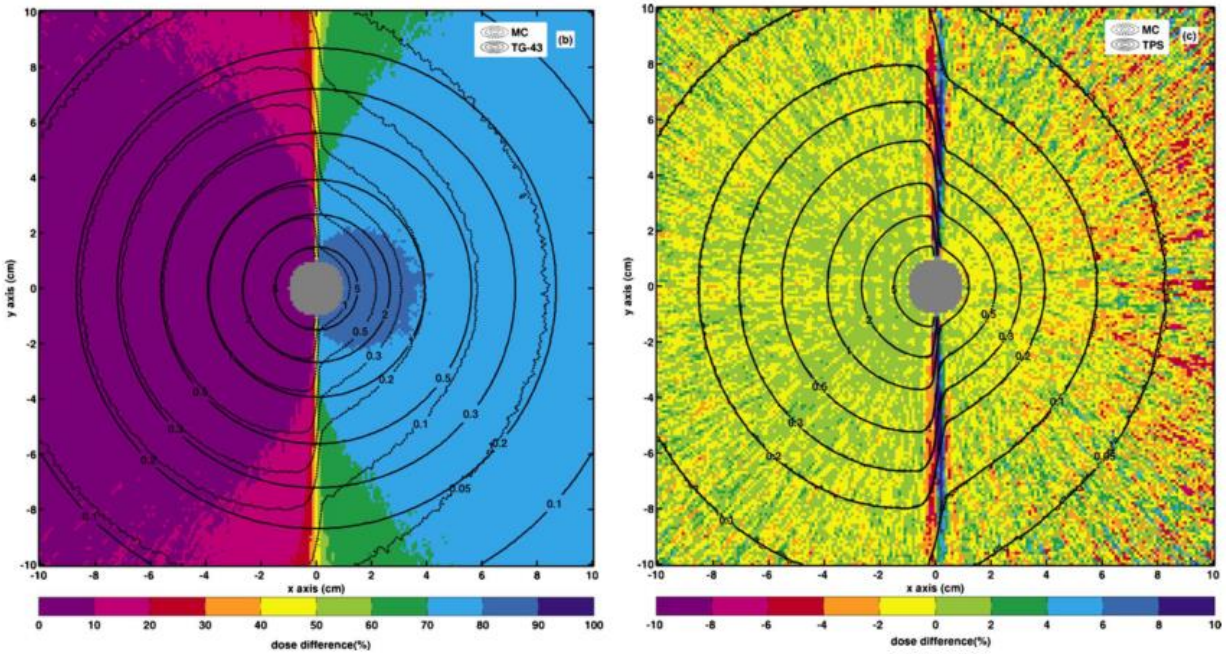

Figure from: L. Petrokokkinos et al. Med. Phys. 38 1981 (2011)

4. finite patient dimensions

Inherently taken into account

(there is no geometry specific input to the method apart from f(E) and the method accounts for geometry specific scatter conditions)

Important implementation details

All calculation settings are preset!

- user specifies D output grid (affects t) and resolution (affects t & accuracy)
- D calculation grid is automatically defined as the D output grid +10 cm in all directions, unless CT image boundary is reached
- Density is HU based through a user editable calibration
- Material assignment is based on a density lookup table and data from ICRP 23 (1975)

In short:

	ACE (Oncentra Brachy)	**Acuros (BrachyVision)**
Long heritage	√	√
Angular discretization	adaptive ("accuracy" selection & # sources)	adaptive (24 to 960 auto. varying within/between energy groups)
Spatial discretization	adaptive multi-resolution Cartesian grid ("accuracy" selection)	adaptive multi-resolution Cartesian grid (auto. based on scatter fluence gradient)
Pre-calculated data as input	Primary dose for source model, energy spectra, kernels	Phase space file for source model
Energy discretization	-	37 groups (adaptive for the scatter fluence using an appropriate energy weighting function f(E))
Primary scatter separation	√	√
Ray-tracing for primary	√	√
Successive scattering	Prim. dose →1st scatter SCERMA → multiple scatter SCERMA	Prim. fluence →1st scatter source

In short:

	ACE (Oncentra Brachy)	**Acuros (BrachyVision)**
Applicator libraries	√	√
Pre-fixed calculation settings to optimize t vs. accuracy	√	√
Type A uncertainty (through pre-calculated data)	√	√
Type B uncertainty	√ cross sections, ray effects, spectral changes in low E/high Z, approx. inhomogeneity correction, ray trace in high scatter gradients, kernel tilting, use of geometry specific kernels	√ cross sections, ray effects, E and spatial discretization, ray trace in high scatter gradients
Where to look for type Bs:	high gradients such as very close to the source(s), away from implant, close to geom. boundaries, high Z inhomogeneities	high gradients such as very close to the source(s), away from implant

In short:

	ACE (Oncentra Brachy)	**Acuros (BrachyVision)**
Material definition	User (ROI) based: Uniform or individual voxel density from CT + user defined materials from list based on TG186 (ICRU 46, Woodard & White 1986) CT based: individual voxel density from CT + material from density look up table	CT based: individual voxel density from CT + material from density look up table based on ICRP 23 1975
Dose reporting medium	local medium	originally water now both water and local medium
Dose calculation grid	geometry defined by imaging	(user defined) output grid + 10cm (unless end of CT image is met)
Use in plan optimization	X	X (?)

ESTRO School

WWW.ESTRO.ORG/SCHOOL

INTRODUCTION ON COMMISSIONING AND EVALUATION OF DOSE CALCULATION ALGORITHMS

Prof. Luc Beaulieu, Ph.D., FAAPM, FCOMP

1- Département de physique, de génie physique et d'optique, et Centre de recherche sur le cancer, Université Laval, Canada

2- Département de radio-oncologie et Centre de recherche du CHU de Québec, CHU de Québec, Canada

Valencia, Spain – Oct 7-10 2018

Report of the Task Group 186 on model-based dose calculation methods in brachytherapy beyond the TG-43 formalism: Current status and recommendations for clinical implementation

Luc Beaulieu[a)]
Département de Radio-Oncologie et Centre de Recherche en Cancérologie de l'Université Laval, Centre hospitalier universitaire de Québec, Québec, Québec G1R 2J6, Canada and Département de Physique, de Génie Physique et d'Optique, Université Laval, Québec, Québec G1R 2J6, Canada

Åsa Carlsson Tedgren
Department of Medical and Health Sciences (IMH), Radiation Physics, Faculty of Health Sciences, Linköping University, SE-581 85 Linköping, Sweden and Swedish Radiation Safety Authority, SE-171 16 Stockholm, Sweden

Jean-François Carrier
Département de radio-oncologie, CRCHUM, Centre hospitalier de l'Université de Montréal, Montréal, Québec H2L 4M1, Canada and Département de physique, Université de Montréal, Montréal, Québec H3C 3J7, Canada

Stephen D. Davis
Department of Medical Physics, University of Wisconsin-Madison, Madison, Wisconsin 53705 and Department of Medical Physics, McGill University Health Centre, Montréal, Québec H3G 1A4, Canada

Firas Mourtada
Radiation Oncology, Helen F. Graham Cancer Center, Christiana Care Health System, Newark, Delaware 19899

Mark J. Rivard
Department of Radiation Oncology, Tufts University School of Medicine, Boston, Massachusetts 02111

Rowan M. Thomson
Carleton Laboratory for Radiotherapy Physics, Department of Physics, Carleton University, Ottawa, Ontario K1S 5B6, Canada

Frank Verhaegen
Department of Radiation Oncology (MAASTRO), GROW, School for Oncology and Developmental Biology, Maastricht University Medical Center, Maastricht 6201 BN, the Netherlands and Department of Medical Physics, McGill University Health Centre, Montréal, Québec H3G 1A4, Canada

Todd A. Wareing
Transpire Inc., 6659 Kimball Drive, Suite D-404, Gig Harbor, Washington 98335

Jeffrey F. Williamson
Department of Radiation Oncology, Virginia Commonwealth University, Richmond, Virginia 23298

(Received 7 May 2012; revised 26 July 2012; accepted for publication 2 August 2012; published 25 September 2012)

The charge of Task Group 186 (TG-186) is to provide guidance for early adopters of model-based dose calculation algorithms (MBDCAs) for brachytherapy (BT) dose calculations to ensure practice uniformity. Contrary to external beam radiotherapy, heterogeneity correction algorithms have only recently been made available to the BT community. Yet, BT dose calculation accuracy is highly dependent on scatter conditions and photoelectric effect cross-sections relative to water. In specific situations, differences between the current water-based BT dose calculation formalism (TG-43) and MBDCAs can lead to differences in calculated doses exceeding a factor of 10. MBDCAs raise three major issues that are not addressed by current guidance documents: (1) MBDCA calculated doses are sensitive to the dose specification medium, resulting in energy-dependent differences between dose calculated to water in a homogeneous water geometry (TG-43), dose calculated to the local medium in the heterogeneous medium, and the intermediate scenario of dose calculated to a small volume of water in the heterogeneous medium. (2) MBDCA doses are sensitive to voxel-by-voxel interaction cross sections. Neither conventional single-energy CT nor ICRU/ICRP tissue composition compilations provide useful guidance for the task of assigning interaction cross sections to each voxel. (3) Since each patient-source-applicator combination is unique, having reference data for each possible combination to benchmark MBDCAs is an impractical strategy. Hence, a new commissioning process is required. TG-186 addresses in detail the above issues through the literature review

Report of the Task Group 186 on model-based dose calculation methods in brachytherapy beyond the TG-43 formalism: Current status and recommendations for clinical implementation

1. recommendations to MBDCA early-adopters to evaluate:
   - phantom size effect
   - inter-seed attenuation
   - material heterogeneities within the body
   - interface and shielded applicators
2. commissioning process to maintain inter-institutional consistency
3. patient-related input data
4. research is needed on:
   - tissue composition standards
   - segmentation methods
   - CT artifact removal

Approved by
ESTRO (BRAPHYQS, EIR)
AAPM (BTSC, TPC)
ABS (U.S. Phys Cmte)
ABG (Australia)

Beaulieu, et al., *Med. Phys.* 39, 6209-6236 (2012)

Specific commissioning process

- MBDCA specific tasks

  “Currently, only careful comparison to Monte Carlo with or w/o experimental measurements can fully test the advanced features of these codes”.

  - This is not sustainable for the clinical physicists.

➔ Led to a concerted international effort

Vision 20/20 Paper: 2010

TABLE I. Status of MBDCAs that can account for radiation scatter conditions and/or material heterogeneities and were useable in brachytherapy treatment planning systems as of 12 May 2010.

MBDCA system	Sponsor(s)	Radiation type	Clinical use	FDA/CE mark status	Release date
PLAQUE SIMULATOR	Astrahan	^{125}I+^{103}Pd photons	Y	N	1990
Collapsed cone	Ahnesjö, Russell, and Carlsson	^{192}Ir photons	N	N	1996
BRACHYDOSE	Yegin, Taylor, and Rogers	0.01–10 MeV photons	N	N	2004
MCPI	Chibani and Williamson	^{125}I+^{103}Pd photons	N	N	2005
GEANT4/DICOM-RT	Carrier *et al.*	Any	N	N	2007
Scatter correction	Poon and Verhaegen	^{192}Ir photons	N	N	2008
Hybrid TG-43:MC	Price and Mourtada, and Rivard *et al.*	Any	Y	Y	2009
ACUROS	Transpire/Varian	^{192}Ir photons	Y	Y	2009

V. NEEDED INFRASTRUCTURE

While MBDCAs are expected to produce more accurate dosimetric results than the current TG-43 formalism, the authors feel that the medical community should not immediately replace the current approach without careful consideration for widespread integration. Assessment of the current infrastructure is needed before assigning new resources, with opportunity for further cooperation of national and international professional societies.

V.A. Centralized dataset management

Societal recommendations and reference data do the clinical physicist no good if they cannot be readily implemented. Having quantitative data available beyond the scientific, peer-reviewed literature may be accomplished through expansion of the joint AAPM/RPC Brachytherapy Source Registry. An independent repository such as the Registry to house the reference data would facilitate this process–especially with international accessibility.

Rivard, Beaulieu, Mourtada, *Med. Phys.* 37, 2645-2658 (2010)

TG186 Commissioning Proposal

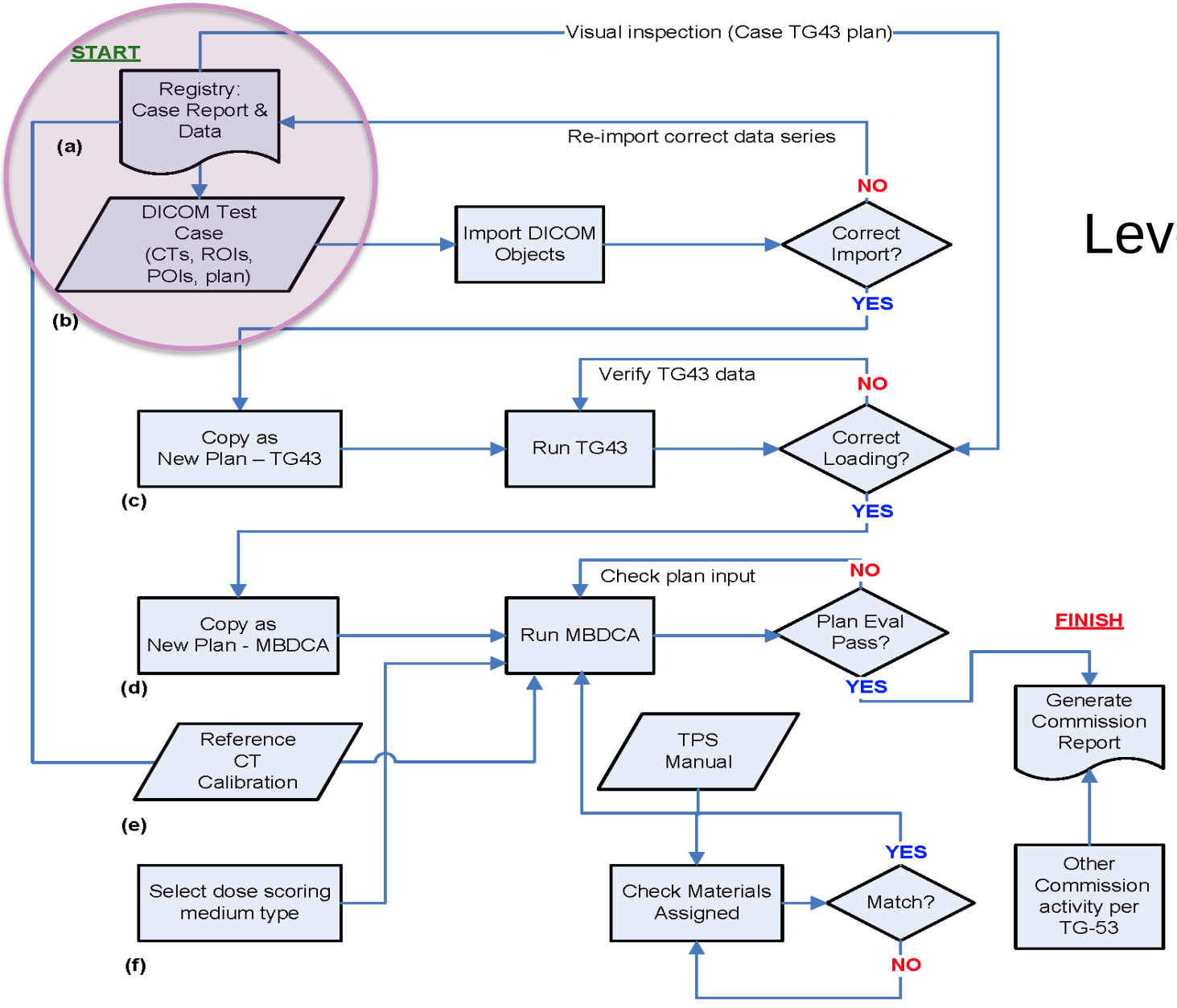

Level 1: TG43 like calc.

Level 2: Advanced dose calc.

TG186 Commissioning Proposal

- Two parts process

- Level 1: MBDCA should fall back to TG43 in well controlled conditions
  - Full scatter: R-r ≥ 5 cm or 20 cm
  - All water

^{192}Ir Test Geometry for MBDCA

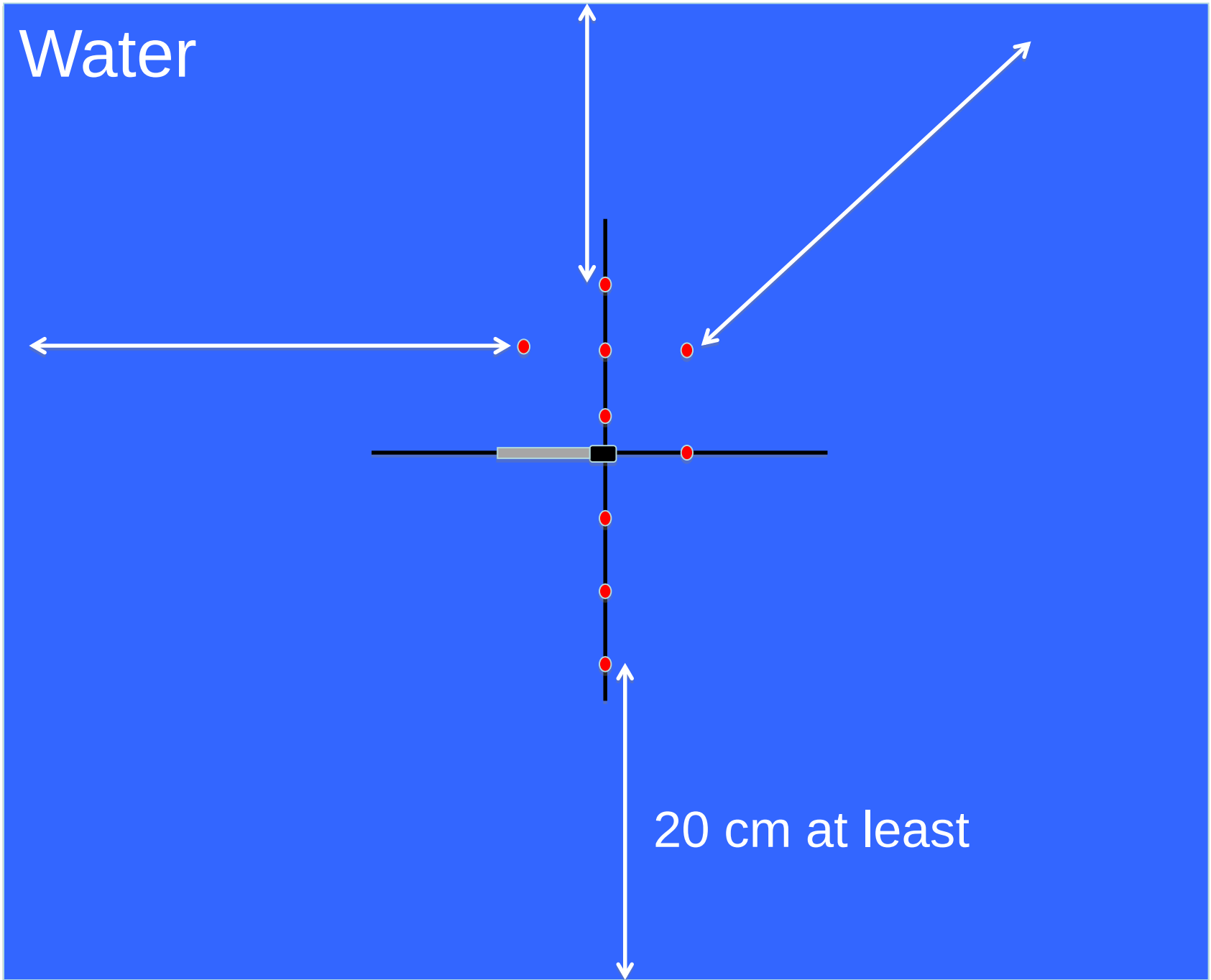

ACE vs TG43: TG-43 conditions (L1)

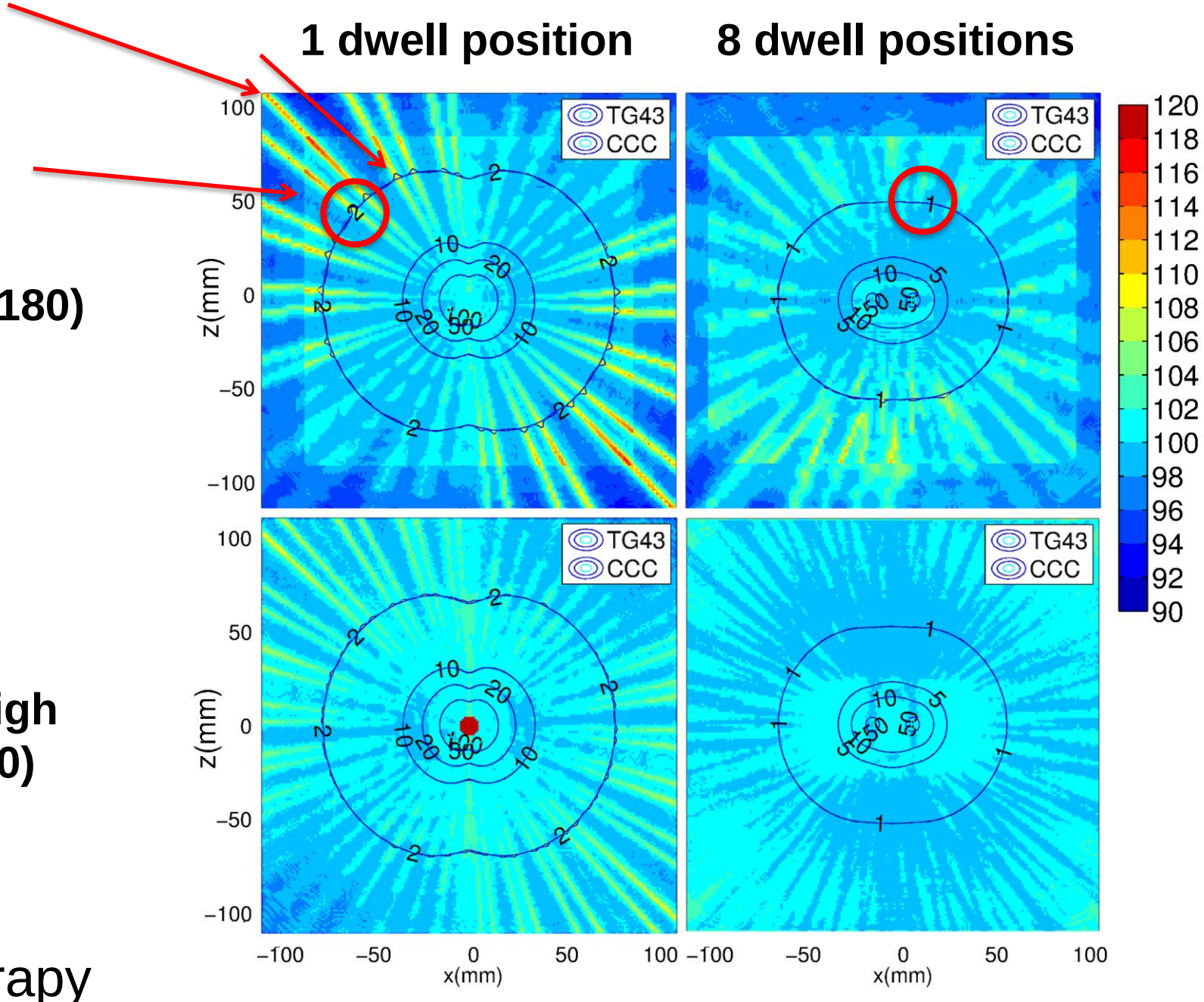

Ma *et al*. Brachytherapy

LEVEL 2

- MBDCA specific tasks
  - Monte Carlo remains the gold standard for comparison
    - Might not be appropriate for all clinics
  - Look at literature…

Need Standardized MBDCA Benchmarks

Excellent reference HDR ^{192}Ir benchmarks in *MedPhys*

- Acuros BrachyVision

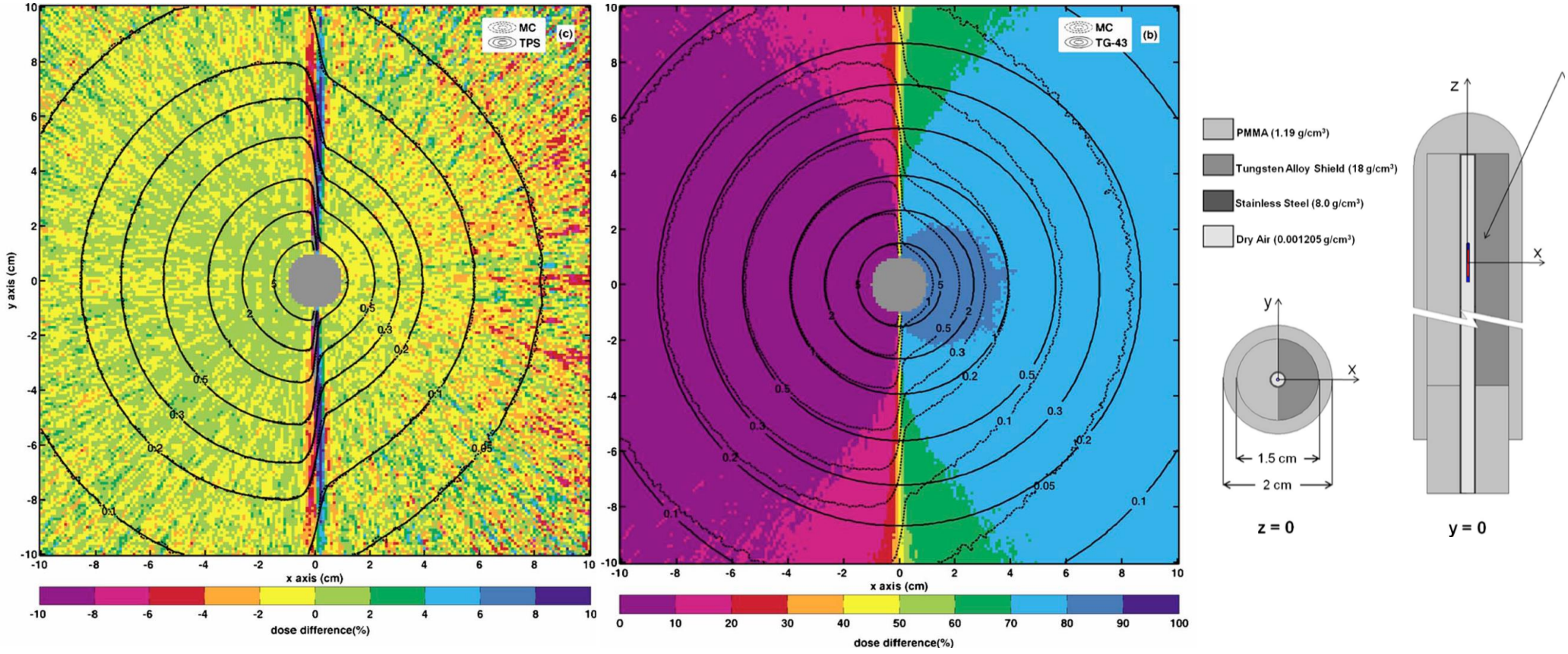

Petrokokkinos *et al*., MedPhys 38, 1981-1992 (2011)

The joint AAPM/ESTRO/ABG Working Group on Model-Based Dose Calculations Algorithms in Brachytherapy

Shirin Abbasi Nejad Enger
shirin.enger@mcgill.ca
1/1/2018 - 12/31/2020 Member

Gabriel P. Fonseca
gabriel.paivafonseca@maastro.nl
1/1/2018 - 12/31/2020 Member

Choonik Lee, PhD
choonik@umich.edu
1/1/2018 - 12/31/2020 Member

Jessica R. Lowenstein, MS
jlowenst@mdanderson.org
1/1/2014 - 12/31/2019 Member
1/1/2018 - 12/31/2020 Member

Yunzhi Ma, PhD
yunzhi7@yahoo.com
1/1/2018 - 12/31/2020 Member

Firas Mourtada, PhD
fmourtad@gmail.com
1/1/2018 - 12/31/2020 Work Group Vice Chair

Susan L. Richardson, PhD
Susan.Richardson@swedish.org
1/1/2018 - 12/31/2020 Member

Ryan L. Smith, PhD
ryan.smith@wbrc.org.au
1/1/2018 - 12/31/2020 Member

Rowan M. Thomson, PhD
rthomson@physics.carleton.ca
7/29/2012 - 12/31/2018 Member
1/1/2018 - 12/31/2020 Member

Javier Vijande, PhD
javier.vijande@uv.es
1/1/2018 - 12/31/2020 Workgroup Chair

Facundo Ballester, PhD
Facundo.Ballester@uv.es
1/1/2018 - 12/31/2018 Consultant (nonvoting)

Luc Beaulieu, PhD
beaulieu@phy.ulaval.ca
1/1/2018 - 12/31/2018 Consultant (nonvoting)

Åsa K. Carlsson Tedgren, PhD
asa.carlsson.tedgren@liu.se
1/1/2018 - 12/31/2018 Consultant (nonvoting)

Yury Niatsetski, MS
yury.niatsetski@elekta.com
9/10/2018 - 12/31/2021 Guest (nonvoting)

P. Papagiannis
ppapagi@phys.uoa.gr
1/1/2018 - 12/31/2018 Consultant (nonvoting)

Rebecca Park
Rebecca.Park@varian.com
9/10/2018 - 12/31/2021 Guest (nonvoting)

Vasiliki Peppa
vpeppa@med.uoa.gr
1/1/2018 - 12/31/2020 Member (nonvoting)

Mark J. Rivard, PhD
mark.j.rivard@gmail.com
1/1/2018 - 12/31/2018 Consultant (nonvoting)

Frank-Andre Siebert, PhD
siebert@onco.uni-kiel.de
1/1/2018 - 12/31/2018 Consultant (nonvoting)

Ronald S. Sloboda, PhD
ron.sloboda@albertahealthservices.ca
1/1/2018 - 12/31/2018 Consultant (nonvoting)

Frank Verhaegen, PhD
frank.verhaegen@maastro.nl
1/1/2018 - 12/31/2018 Consultant (nonvoting)

Todd A. Wareing, PhD
Todd.Wareing@varian.com
9/10/2018 - 12/31/2021 Guest (nonvoting)

WG Charges

- Develop a limited number (approximately 5) of well-defined test case plans and perform MBDCA dose calculations and comparisons.

- Identify the best venue for housing the reference plans/data, and put in place in collaboration with identified partners of the Registry.

- *Propose to the community well-defined prerequisites for test case plans to be submitted to the Registry.*

- *Develop a review process for evaluation as new reference data meeting the prerequisites.*

- Engage the vendors to promote uniformity of practice.

Enabling clinical use of advanced dose calculation algorithms

ESTRO School

Level 1 Dosimetry Benchmark

Medical Physics

A generic high-dose-rate ^{192}Ir brachytherapy source for evaluation of model-based dose calculations beyond the TG-43 formalism

Ballester, Carlsson Tedgren, Granero, Haworth, Mourtada, Paiva Fonseca, Zourari, Papagiannis, Rivard, Siebert, Sloboda, Smith, Thomson, Verhaegen, Vijande, Ma, and Beaulieu

Conclusions: A hypothetical, generic HDR ^{192}Ir source was designed and implemented in two commercially available TPSs employing different MBDCAs. Reference dose distributions for this source were benchmarked and used for evaluation of MBDCA calculations employing a virtual, cubic water phantom in the form of a CT DICOM image series. Implementation of a generic source of identical design in all TPSs using MBDCAs is an important step toward supporting univocal commissioning procedures and direct comparisons between TPSs.

Ballester *et al*., *Med. Phys.* 42, 3048-3062 (2015)

Level 1 Dosimetry Benchmark

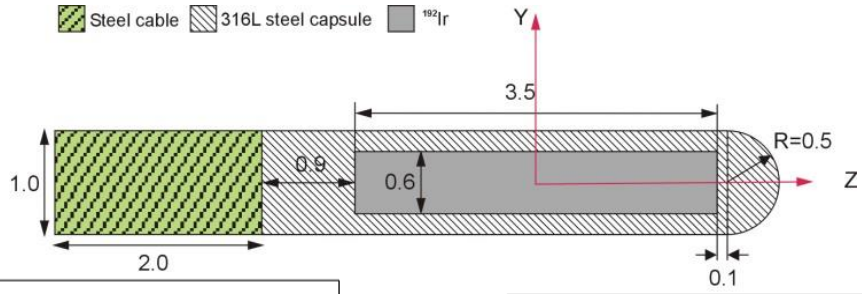

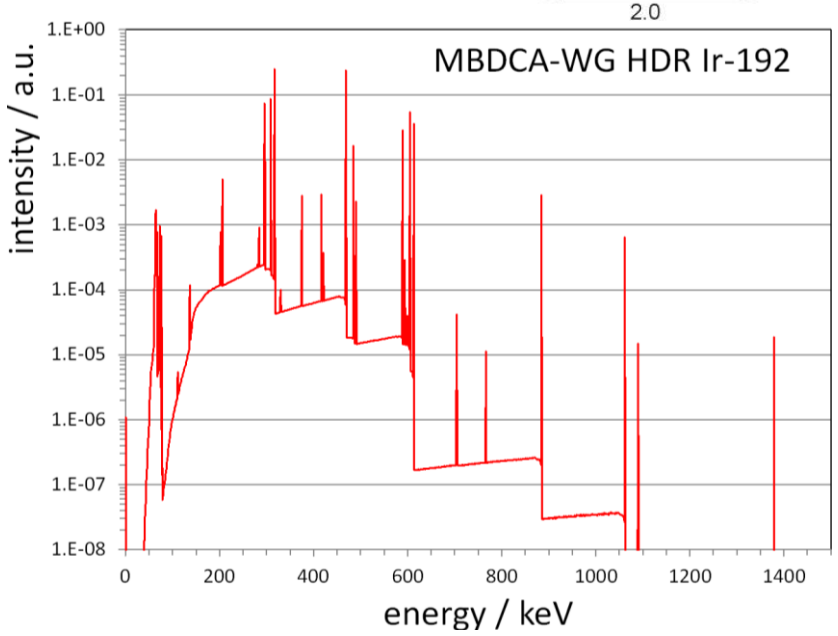

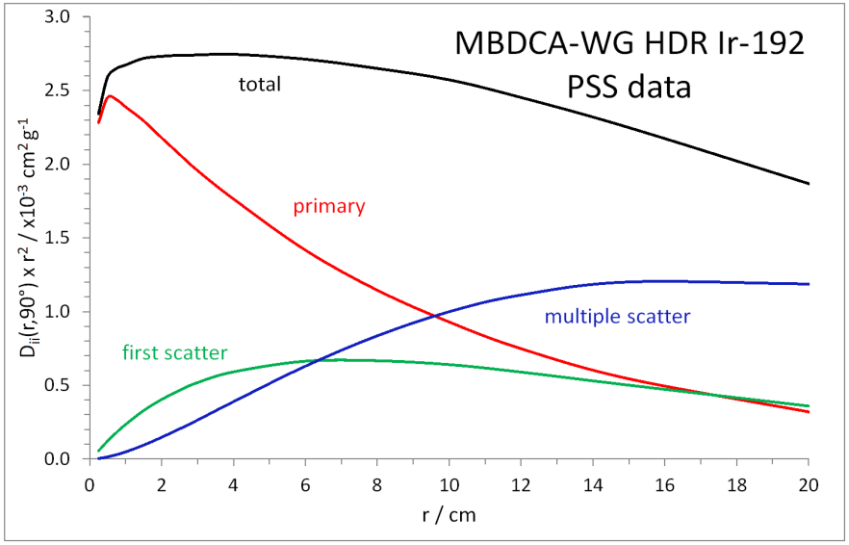

TABLE III. Air-kerma strength s_K and dose-rate constant Λ for the generic HDR ^{192}Ir source obtained with several MC methods. Reported uncertainties (absolute uncertainties in columns 2 and 4 and relative ones in columns 3 and 5) are Type A (statistical) with a coverage factor $k = 1$.

MC code	s_K ($\times 10^{-8}$ U/Bq)		Λ [cGy/(h U)]	
ALGEBRA	9.798 ± 0.006	0.06%	1.1113 ± 0.0006	0.04%
BrachyDose	9.804 ± 0.001	0.01%	1.1100 ± 0.0010	0.04%
GEANT4	9.799 ± 0.012	0.18%	1.1104 ± 0.0020	0.18%
MCNP5 v.1.60	9.797 ± 0.001	0.01%	1.1110 ± 0.0004	0.04%
MCNP5 v.1.60[a]	9.812 ± 0.006	0.06%	1.1107 ± 0.0006	0.06%
MCNP6 v.1	9.813 ± 0.006	0.06%	1.1106 ± 0.0006	0.06%
PENELOPE2008	9.784 ± 0.006	0.06%	1.1113 ± 0.0006	0.05%

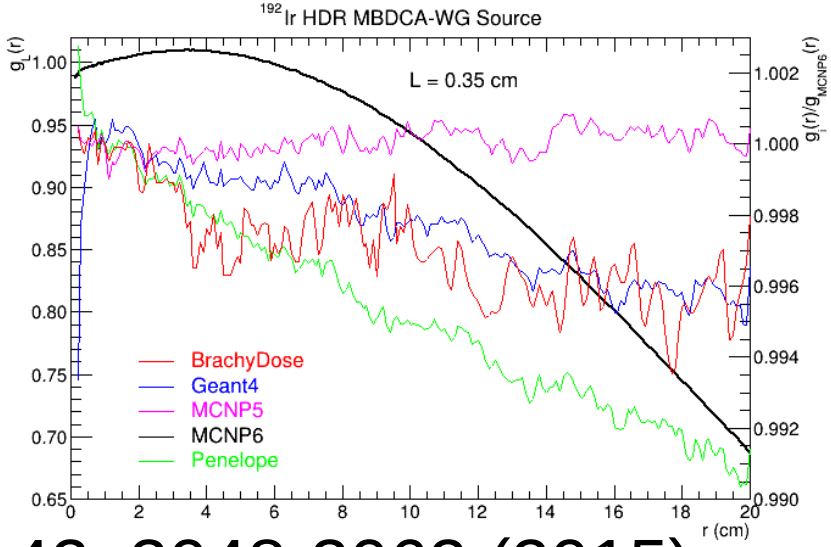

Ballester *et al.*, *Med. Phys.* 42, 3048-3062 (2015)

Level 2 Dosimetry Benchmark

Level 2: Test cases tools

DICOM $(512\ mm)^3$ $(1\ mm)^3$ voxel

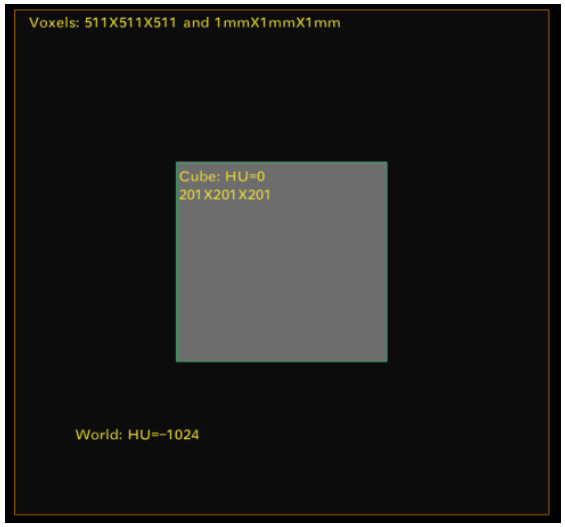

Generic HDR ^{192}Ir source

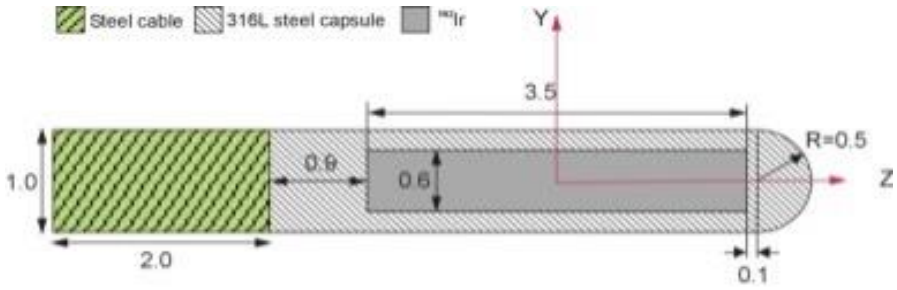

HDR ^{192}Ir model MBDCA-WG source

Shielded GYN applicator

	Material	Elemental composition	Mass Density (g/cm^3)
Body	PMMA	$C_5O_2H_8$	1.19
Shield	Densimet D176	Fe (2.5%), Ni (5%), W (92.5%)	17.6

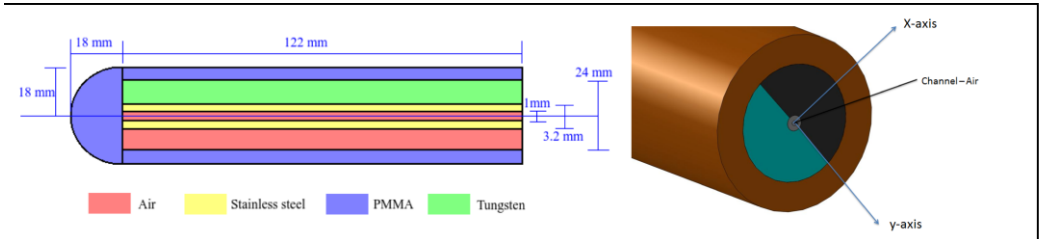

FIG. 1. The generic cylindrical HDR brachytherapy applicator with 180° shielding (lateral and bottom view). Figure not drawn to scale.

Level 2: Test cases

- Test case 1

- Test case 2

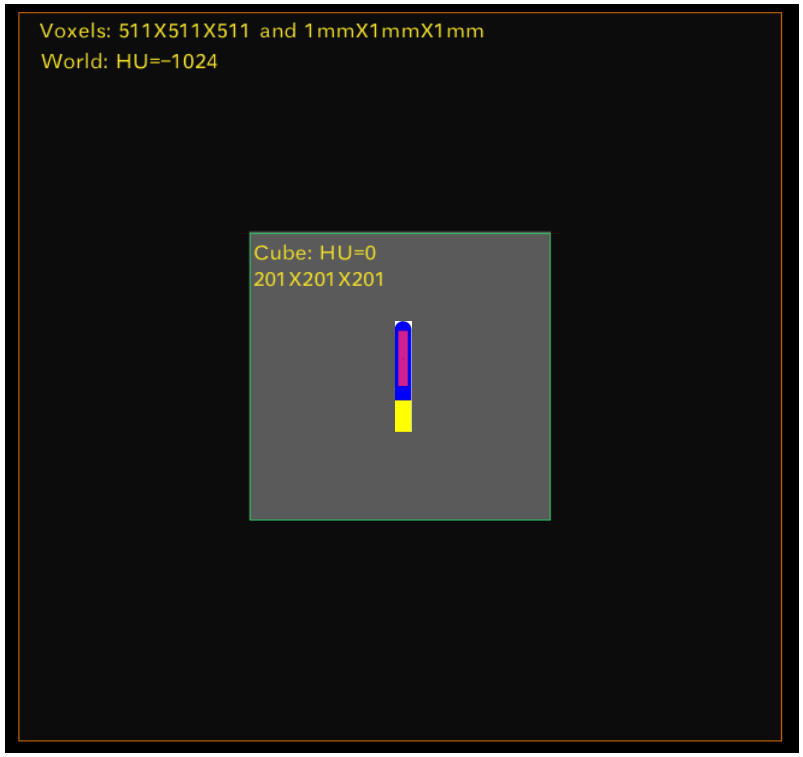

(source not to scale)

Level 2: Test cases

- Test case 3

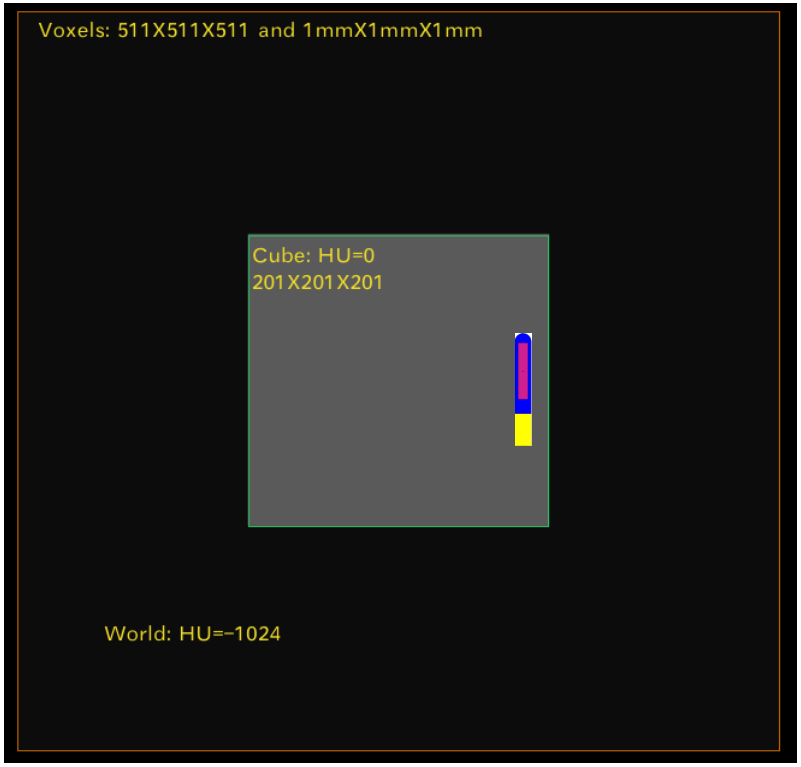

- Test case 4

(source not to scale)

Level 2: Monte Carlo

- Seven state-of-the-art MC codes have been considered:
  - MCNP6
  - Penelope
  - egs_brachy
  - BrachyDose
  - MCNP5
  - Geant4
  - Algebra b(G4-based code)

- Collisional kerma was scored using $(201)^3$ 1 mm^3 cubic voxels.

- Number of photons simulated were in the range 10^{10} – 10^{11}.

Level 2: MBDCA

- The two MBDCAs comercially available have been used
  - Oncentra Brachy with ACE (4.5)
  - BrachyVision ACUROS (13.0.23)

2D Comparisons. Results for Test case 2

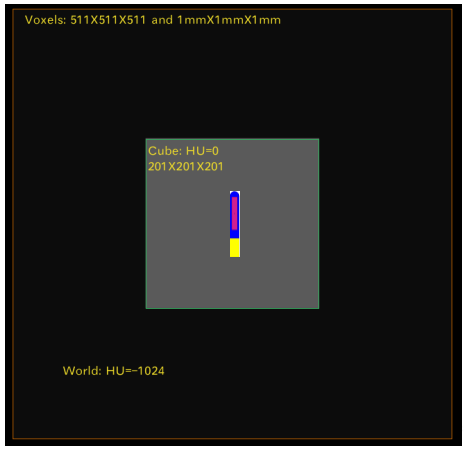

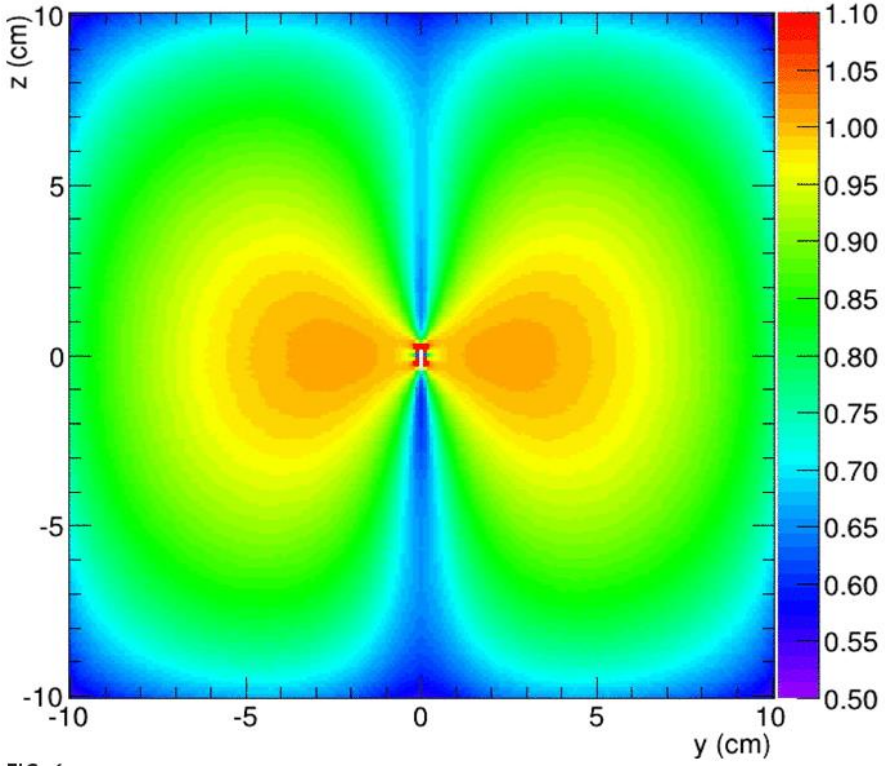

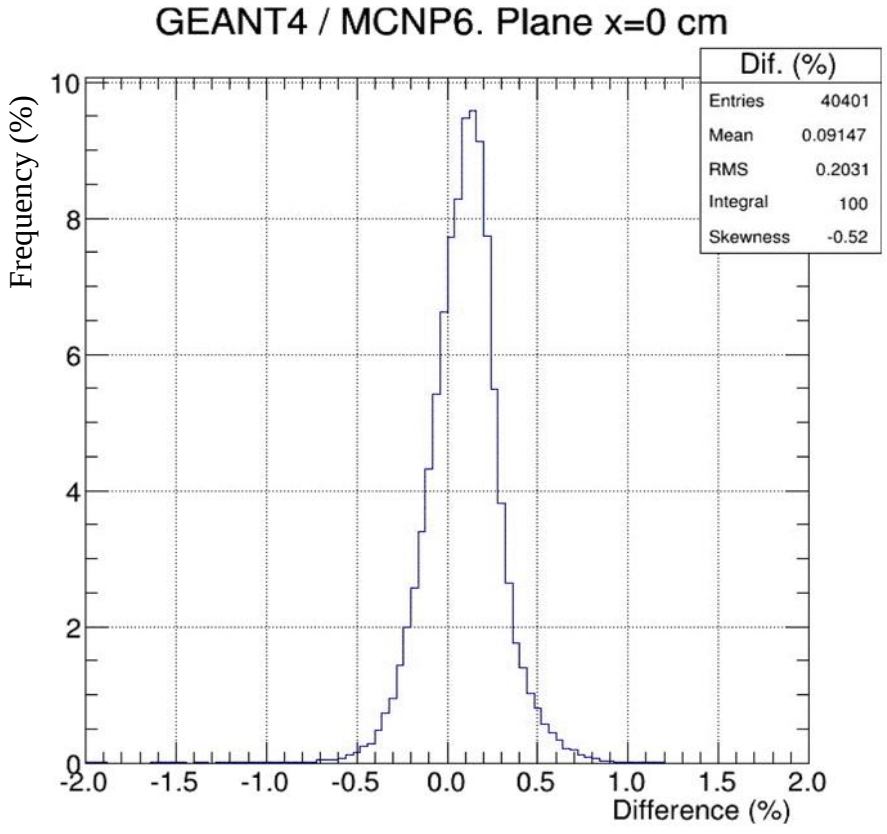

2D Comparisons. Results for Test case 3

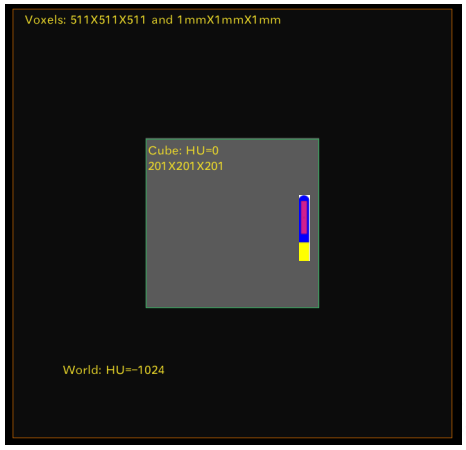

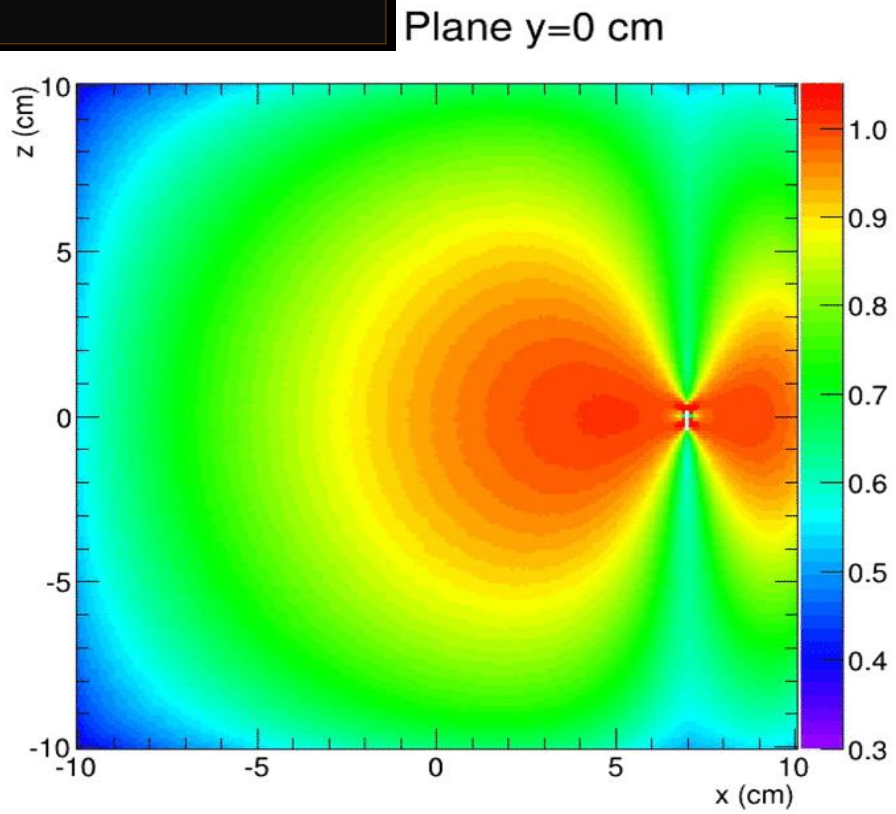

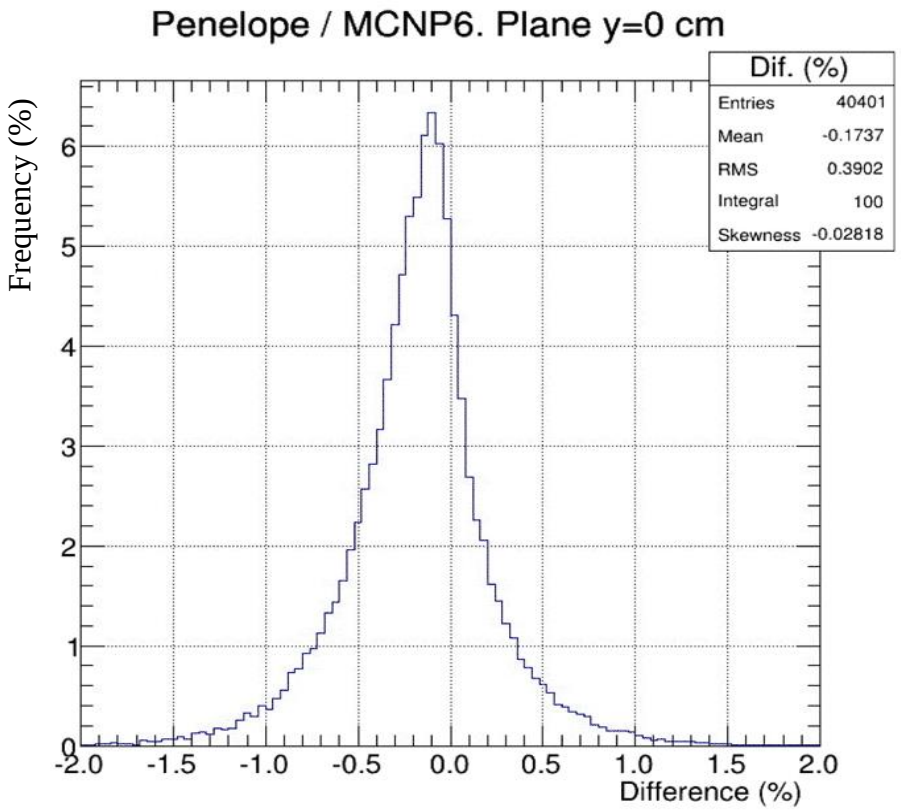

2D Comparisons. Results for Test case 3

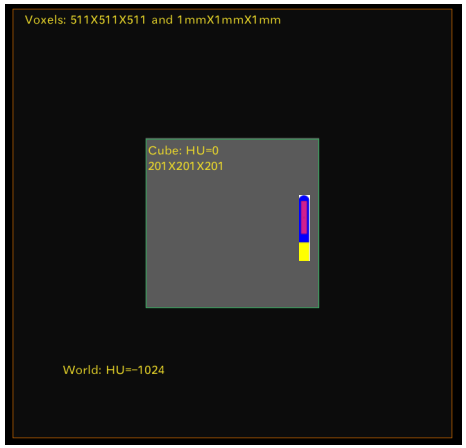

Red: 5 x 5 cm^2
Blue: 10 x 10 cm^2

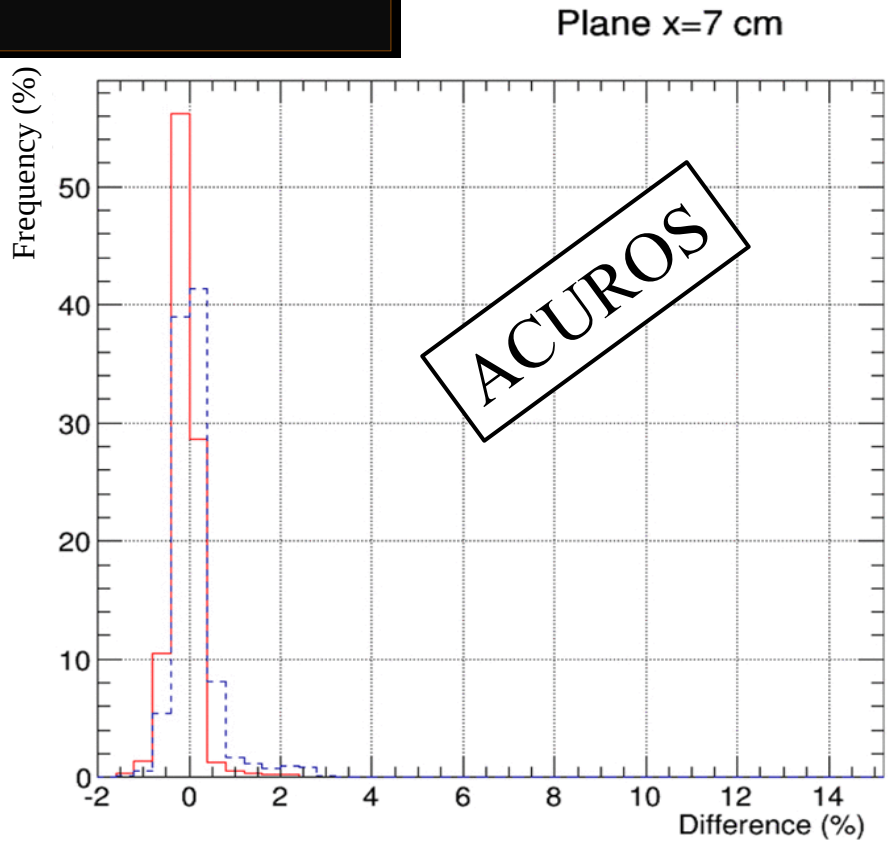

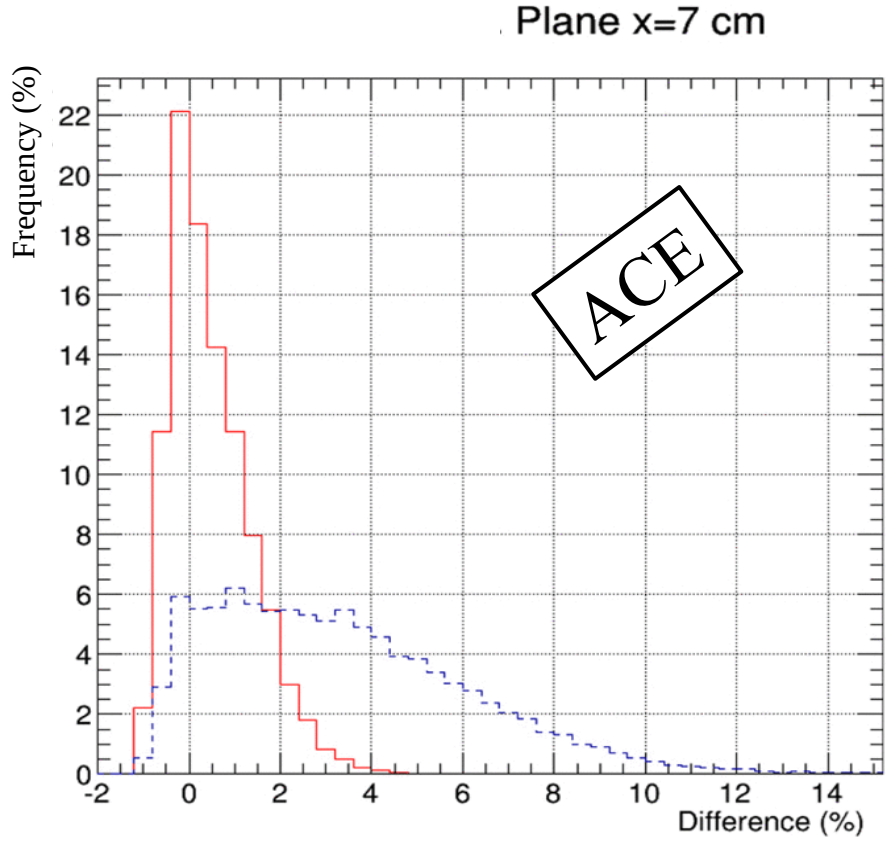

Commissioning Workflow

Commissioning Workflow

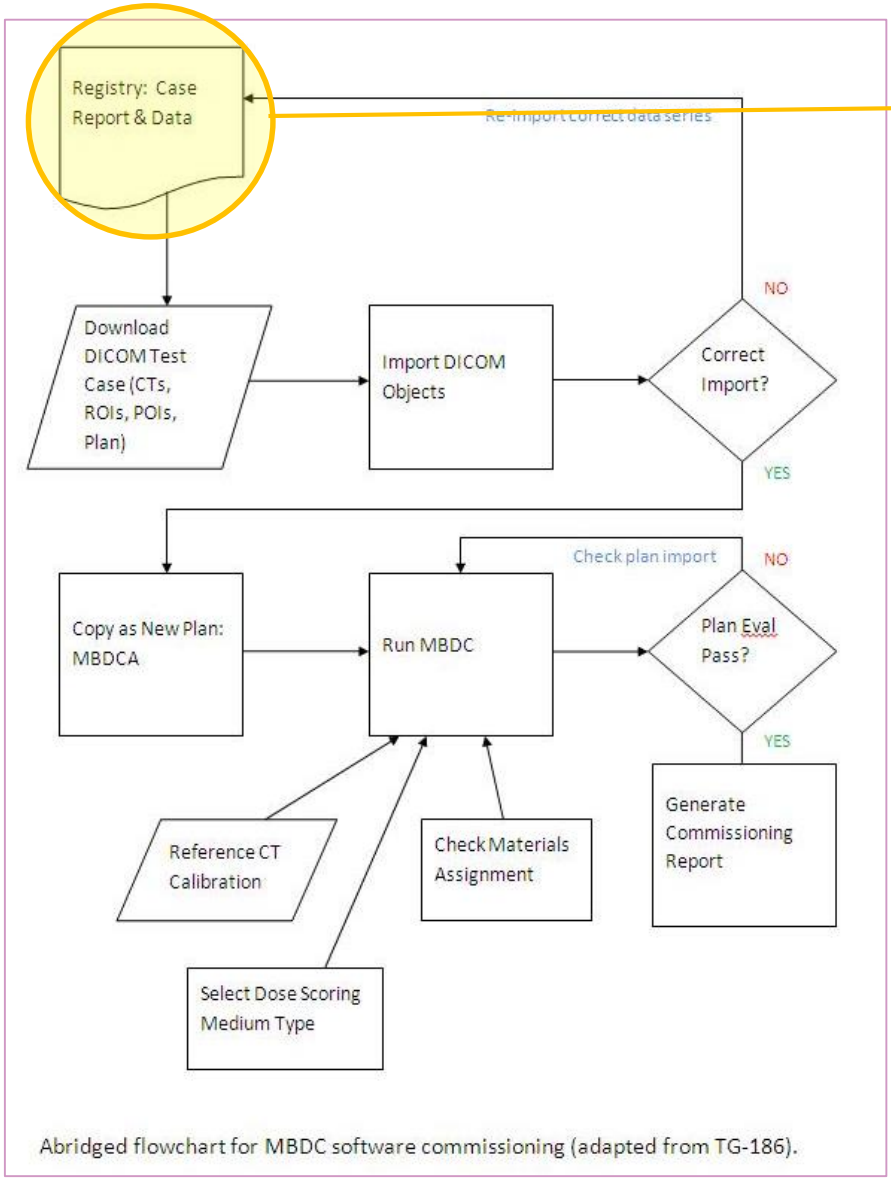

Abridged flowchart for MBDC software commissioning (adapted from TG-186).

1. Access the Registry

From R. Sloboda

1. Access the Registry @ irochouston.mdanderson.org/RPC/…

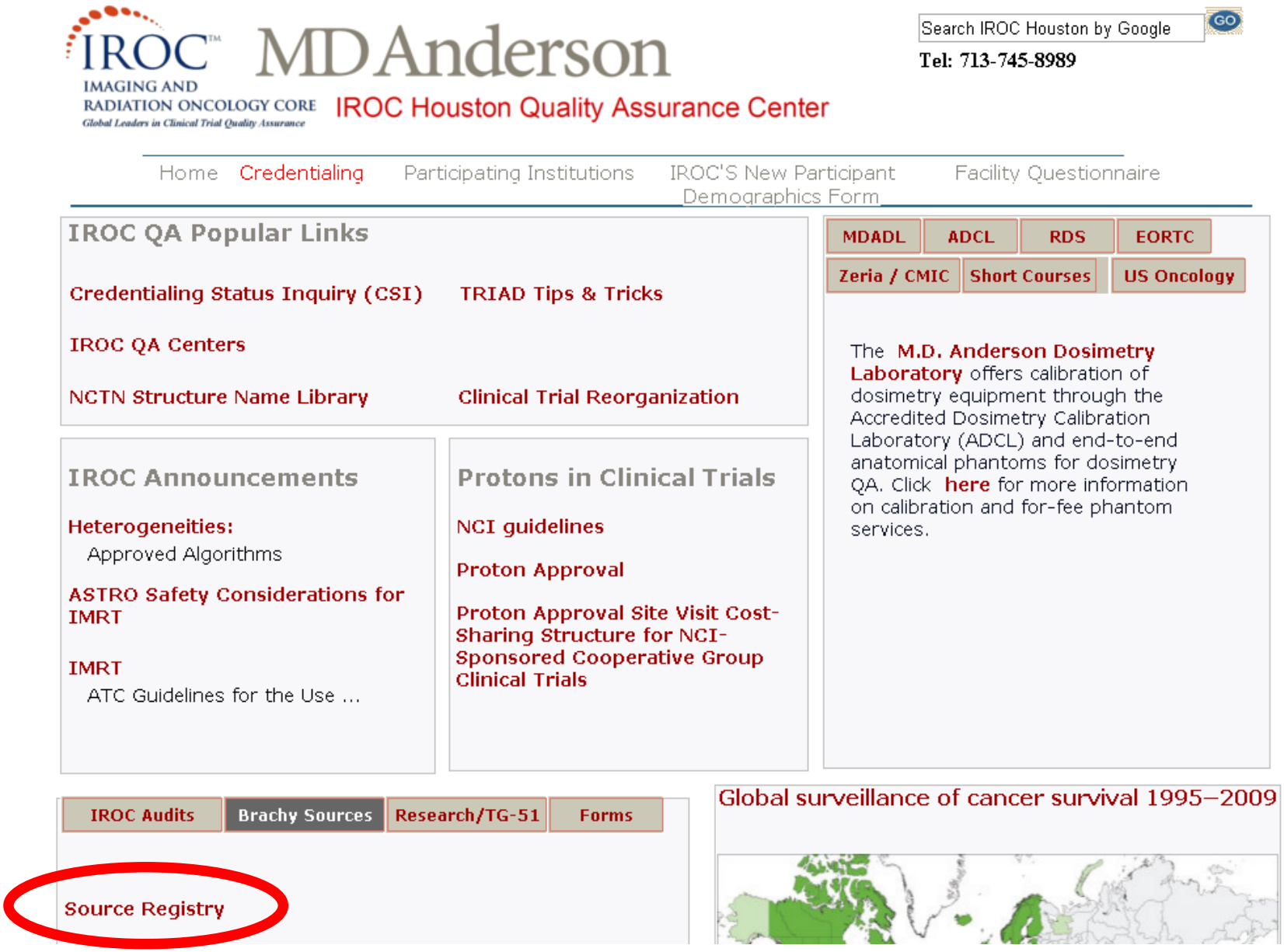

Joint AAPM/IROC Houston Registry of Brachytherapy Sources Meeting the AAPM Dosimetric Prerequisites

Source Registry	Application for Registry	Registry Policy
Prerequisites	Dosimetry Datasets	Model-Based Dose Calcs
AAPM Publications	3rd Party Checks	Disclaimer

LDR ^{125}I Sources

Manufacturer	Sources	Model
BEBIG GmbH	IsoSeed I-125	I25.S17 plus
Best Medical International Inc	Best I-125 Source	2301
BARD Medical	^{125}Implant Seeds	STM1251
IsoAid, LLC	Advantage I-125	IAI-125A
Nucletron	selectSeed I-125	130.002
Theragenics	I-Seed I-125	AgX100

LDR ^{103}Pd Sources

Manufacturer	Sources	Model
Best Medical International Inc	Best Palladium - 103	2335
IsoAid, LLC	Advantage Pd-103	IAPd-103A
Theragenics Corporation	TheraSeed	200
CivaTech Oncology	CivaString	CS10

LDR ^{131}Cs Sources

Manufacturer	Sources	Model
IsoRay Medical Inc.	Proxcelan	CS-1 Rev2

PDR ^{192}Ir Sources

Manufacturer	Sources	Model
Nucletron, an Elekta company	Nucletron	mPDR-v1 (classic)
Varian Medical Systems, Inc. USA	GammaMed	PDR 12i
Varian Medical Systems, Inc. USA	GammaMed	PDR plus
Eckert & Ziegler BEBIG GmbH	BEBIG PDR	Ir2.A85-1

HDR ^{192}Ir Sources

Manufacturer	Sources	Model
Nucletron, an Elekta company	Nucletron mHDR	mHDR-v2
Nucletron, an Elekta company	Nucletron mHDR	mHDR-v1 (“Classic”)
Varian Medical Systems, Inc.	Varian HDR	VS2000

Model-Based Dose Calculations

Source Registry	Application for Registry	Registry Policy
Prerequisites	Dosimetry Datasets	Model-Based Dose Calcs
AAPM Publications	3rd Party Checks	Disclaimer

Reference dataset (DICOM archive) generated with MC simulation. Users may import these archives into TPS for benchmarking.

- Reference Data

TPS-specific seed DICOM archive. Users may start TPS calculation simply by importing these archives. CT images, RP and RS files are contained.

- Elekta Database
- Varian Database

Google web forum for sharing user ideas and experience.

- MBDCA-BT Forum

Disclaimer for source-model definition files.

- Disclaimer

Guidance Documents

Open a TPS database to access the User Guide

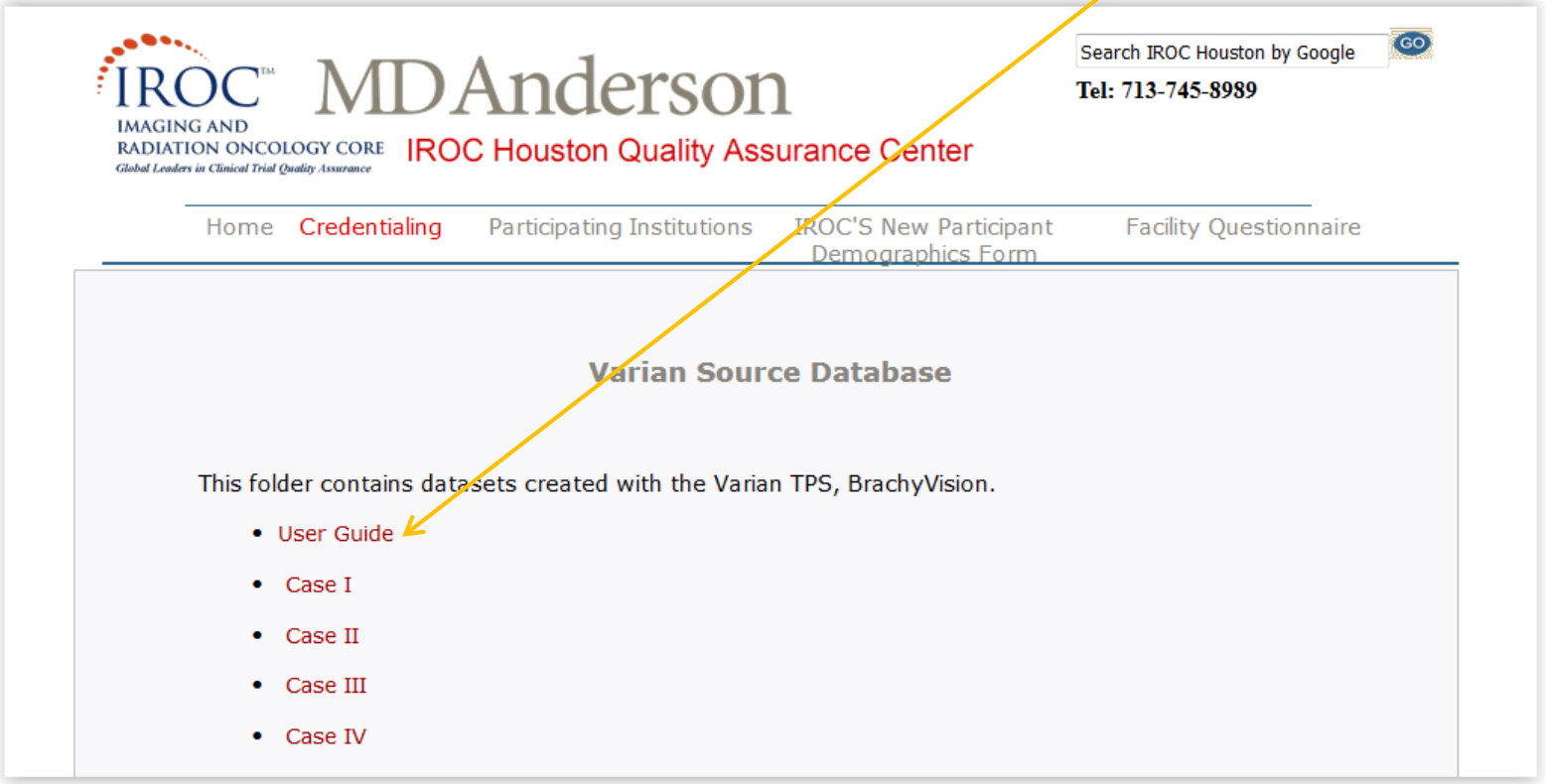

User Guide for Varian Medical Systems BrachyVision™ Algorithm Testing

Contents

Commissioning Workflow

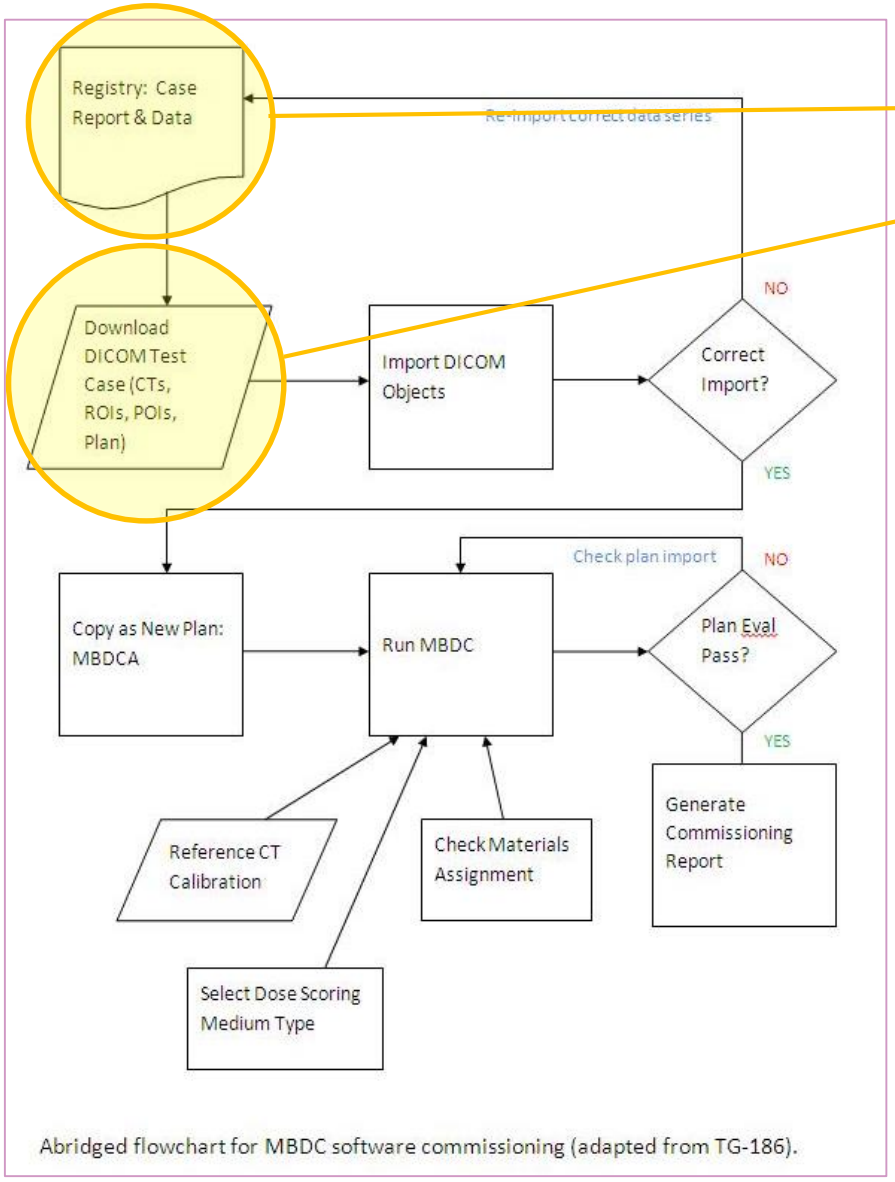

Abridged flowchart for MBDC software commissioning (adapted from TG-186).

1. Access the Registry

2. Download (a) a test plan and *(b)* MC reference dose distribution (DICOM)

From R. Sloboda

Main Steps

2.(a) Download a zipped test plan

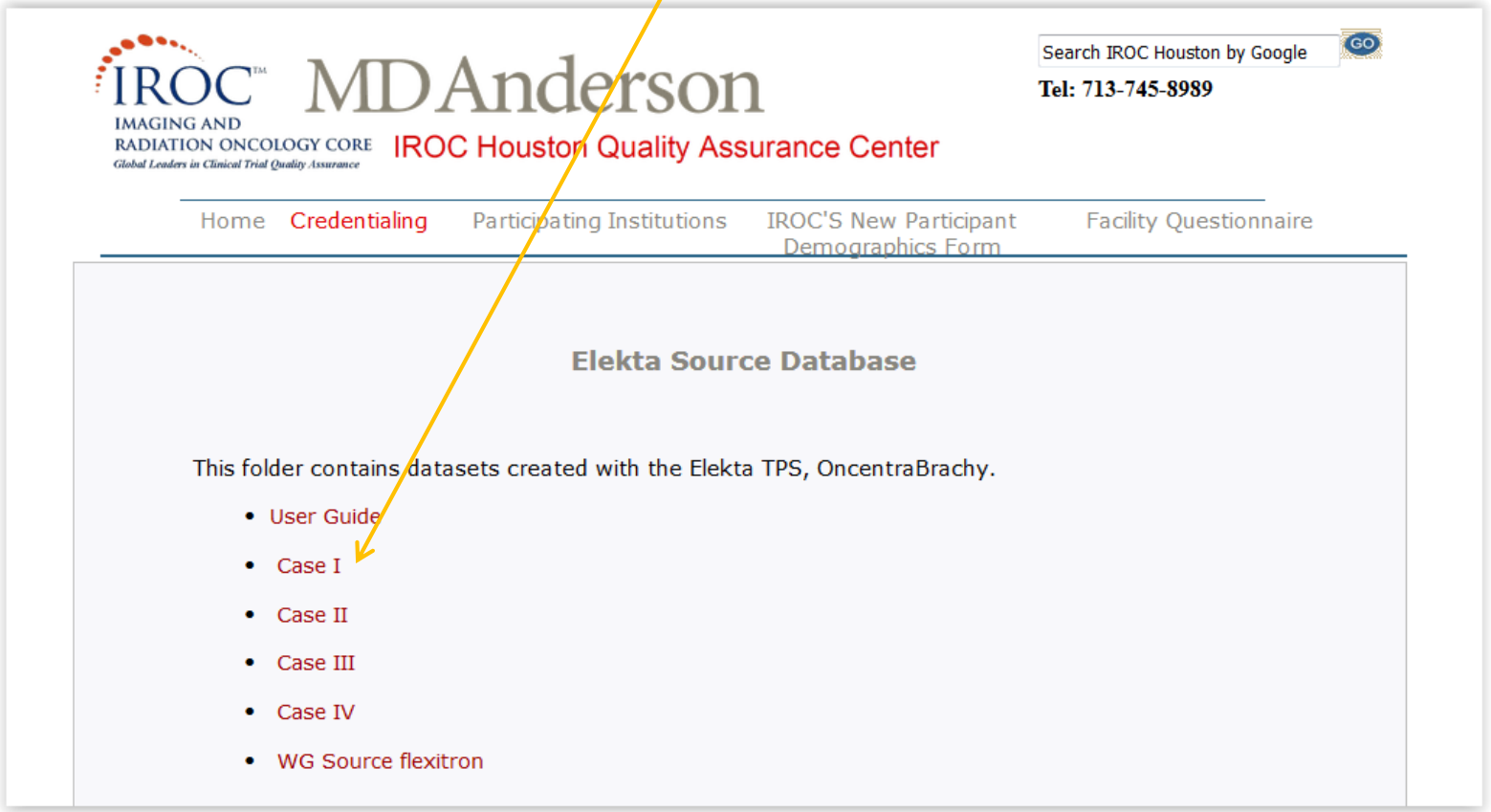

Main Steps

2.(b) Download a zipped reference dose distribution

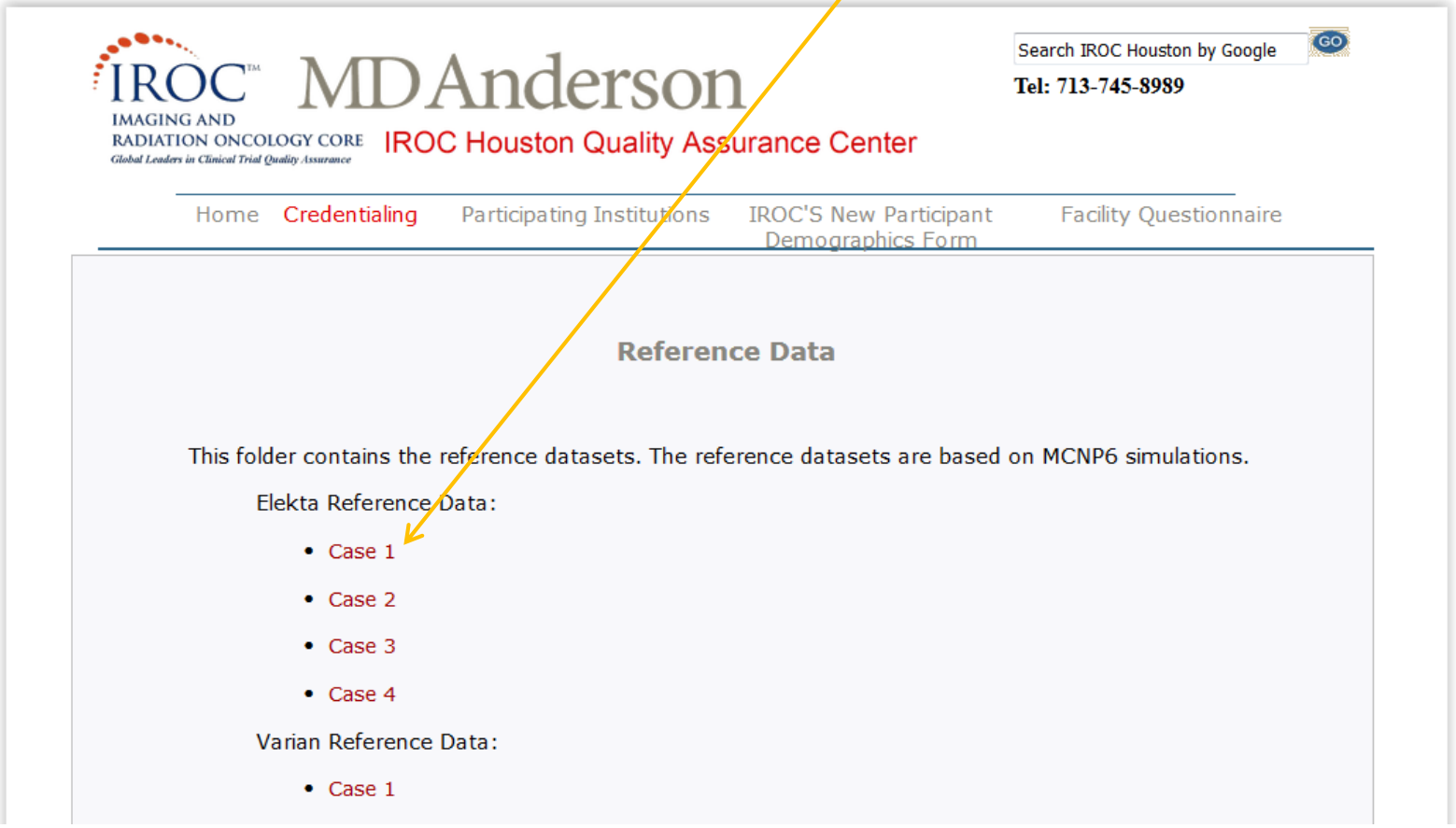

Commissioning Workflow

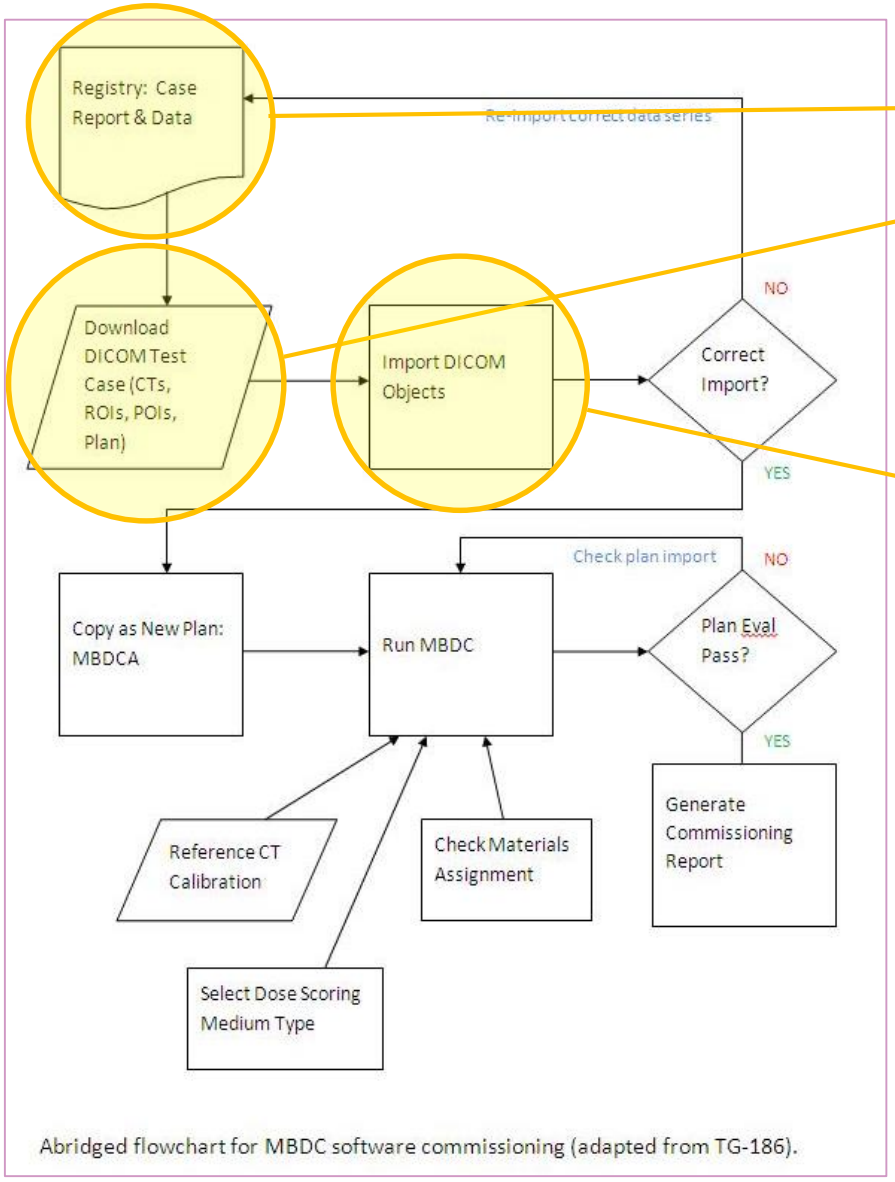

Abridged flowchart for MBDC software commissioning (adapted from TG-186).

1. *Access* the Registry
2. *Download (a)* a test plan and *(b)* MC reference dose distribution (DICOM)
3. *Import* DICOM objects

From R. Sloboda

Main Steps

3. Import DICOM objects for the test plan and reference dose distribution

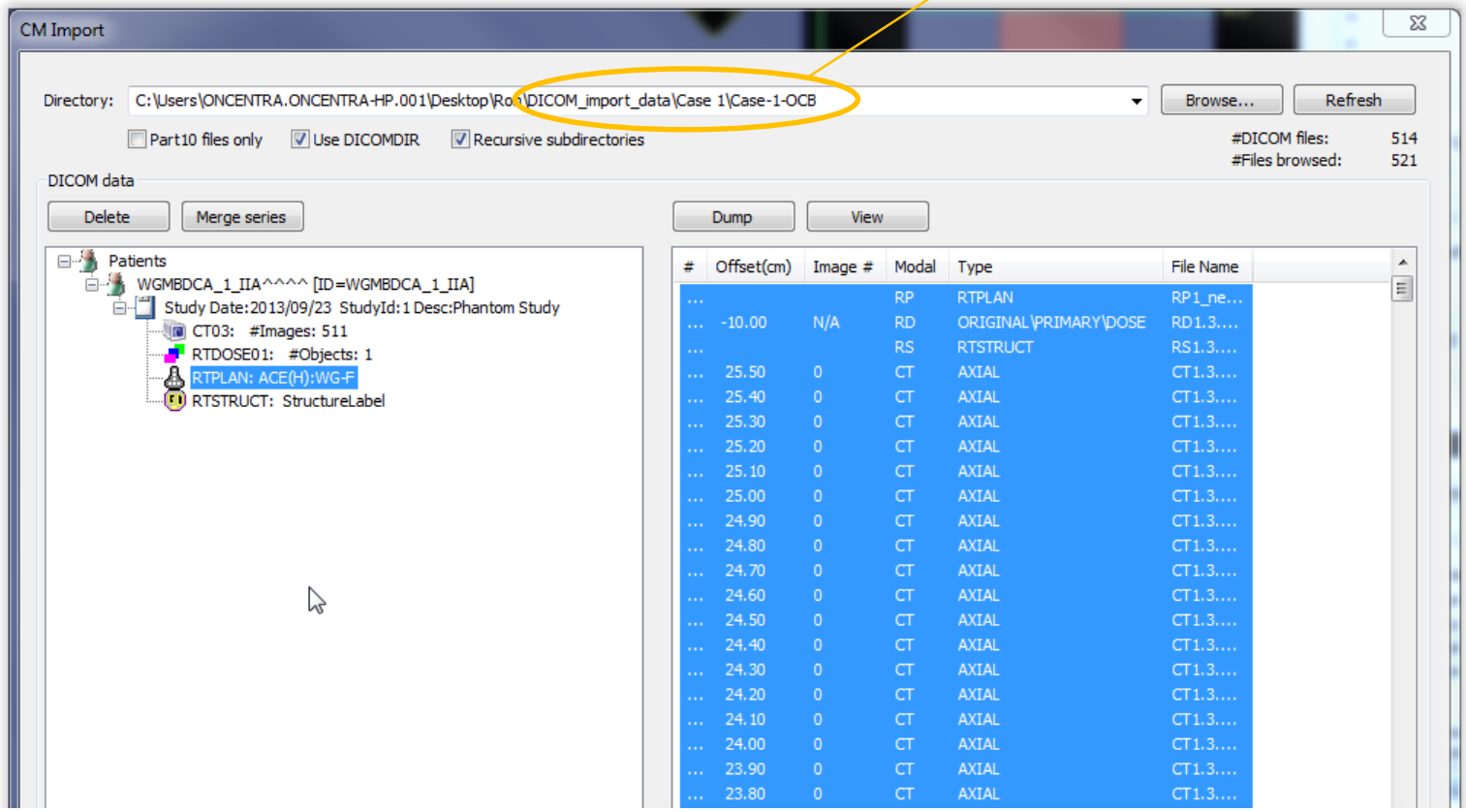

Commissioning Workflow

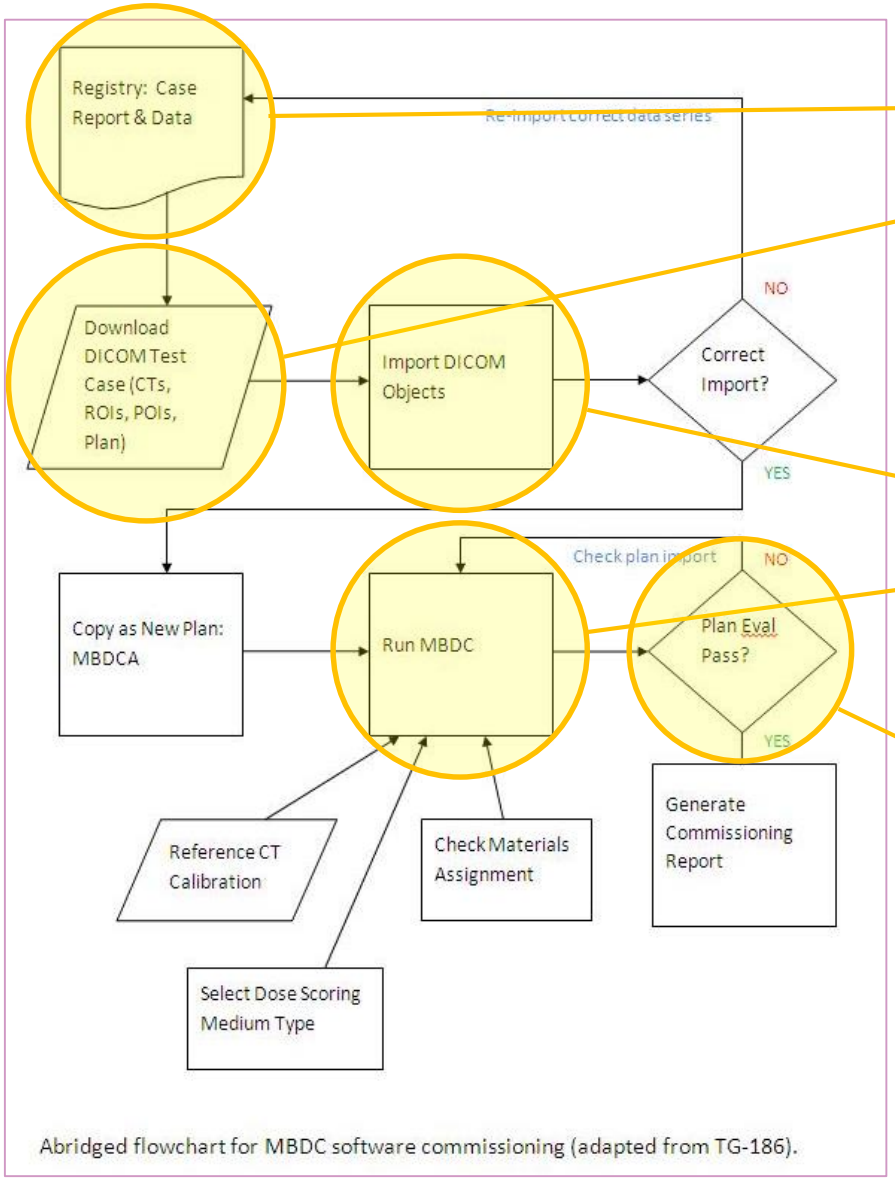

Abridged flowchart for MBDC software commissioning (adapted from TG-186).

1. *Access* the Registry
2. *Download (a)* a test plan and *(b)* MC reference dose distribution (DICOM)
3. *Import* DICOM objects
4. *Calculate* dose locally using the plan and MBDCA
5. *Compare & evaluate* MBDCA and reference dose distributions

From R. Sloboda

Main Steps

Set up for local dose calculation

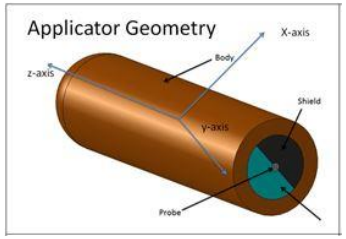

Case 4

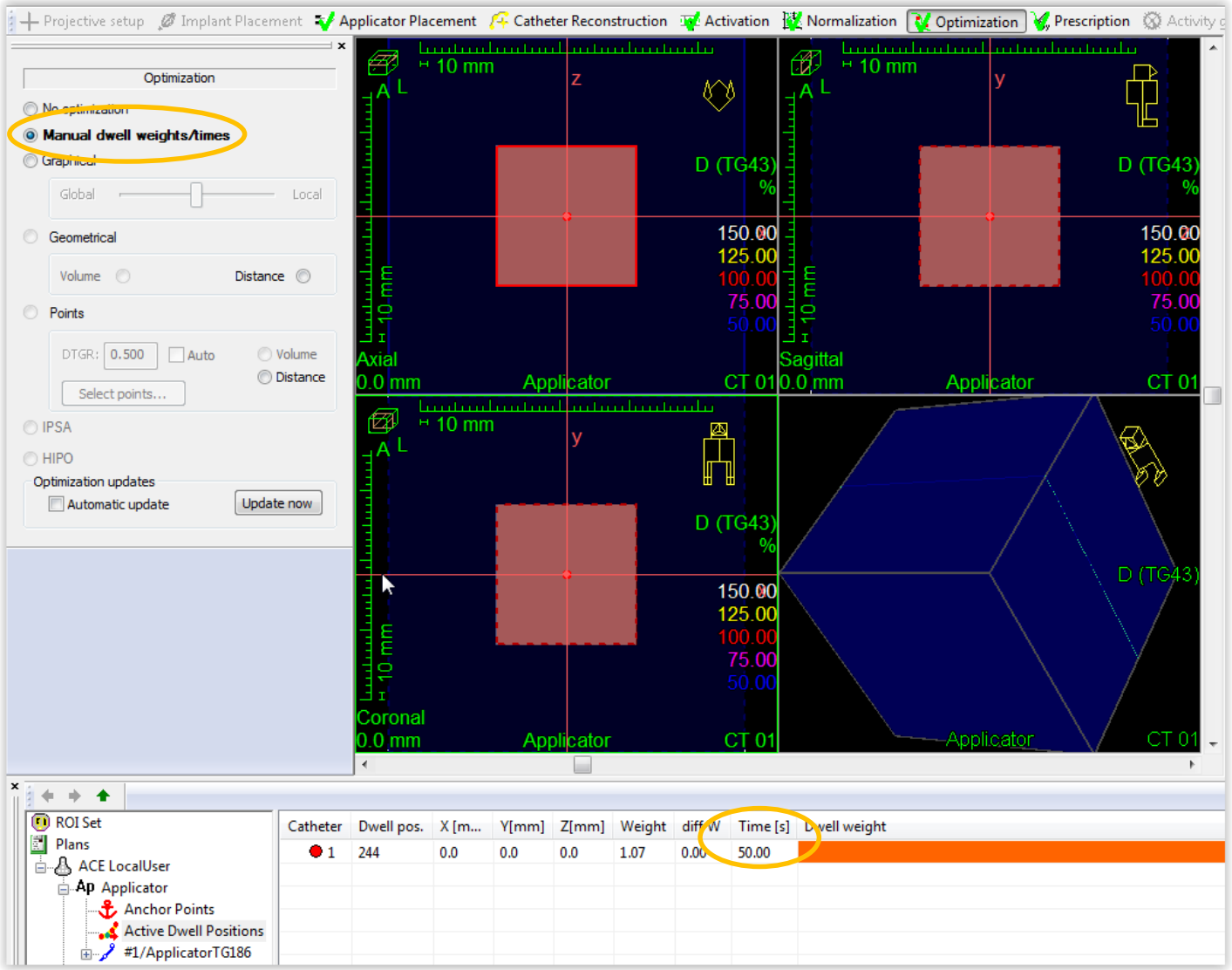

From Sloboda, 2017

Main Steps

4. Calculate dose locally using the MBDCA

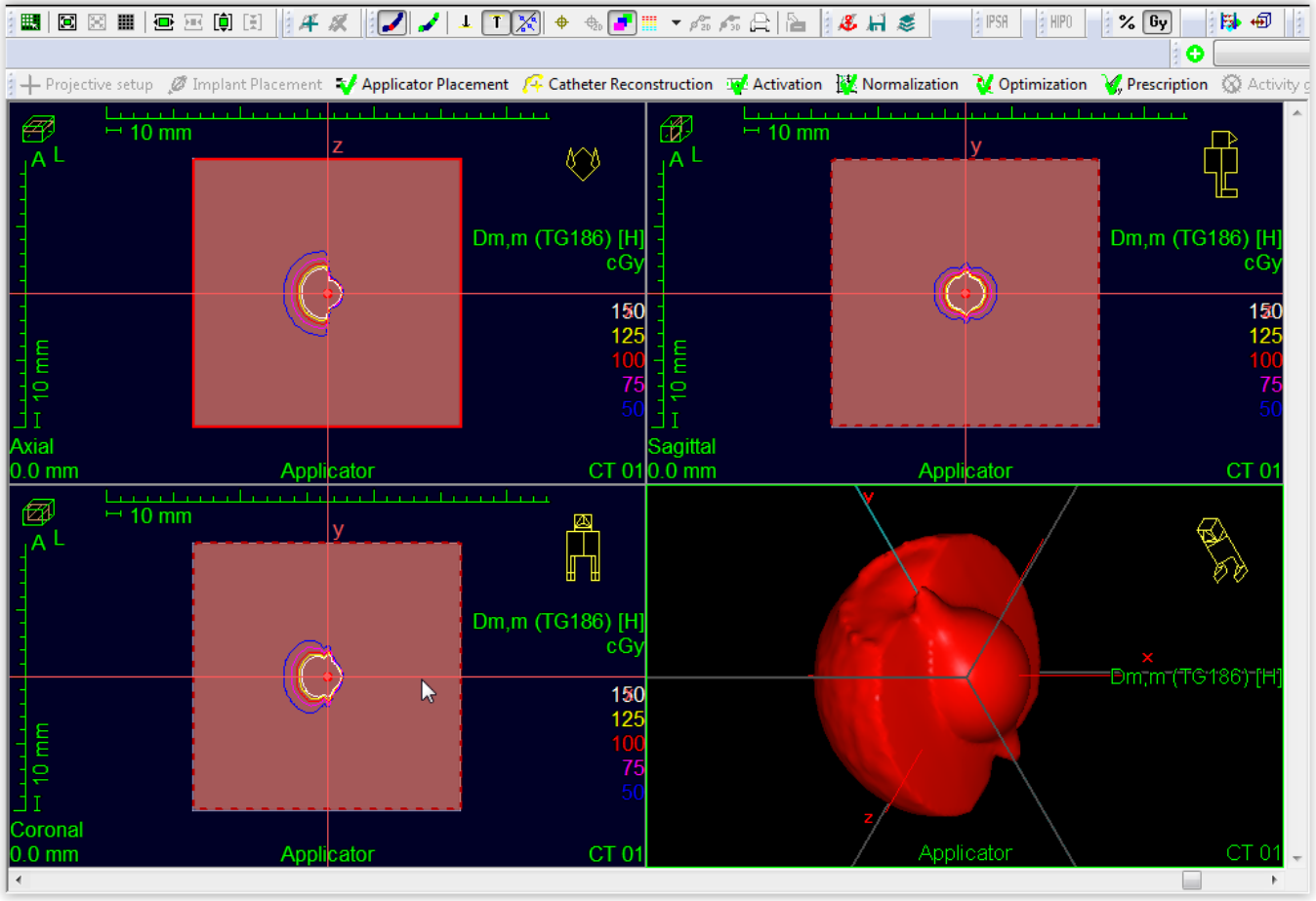

Case 4

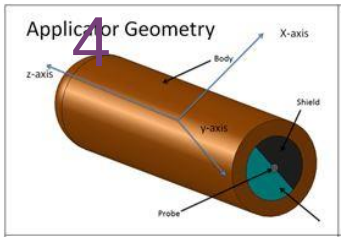

Main Steps

5. Compare & evaluate TPS and Ref. doses

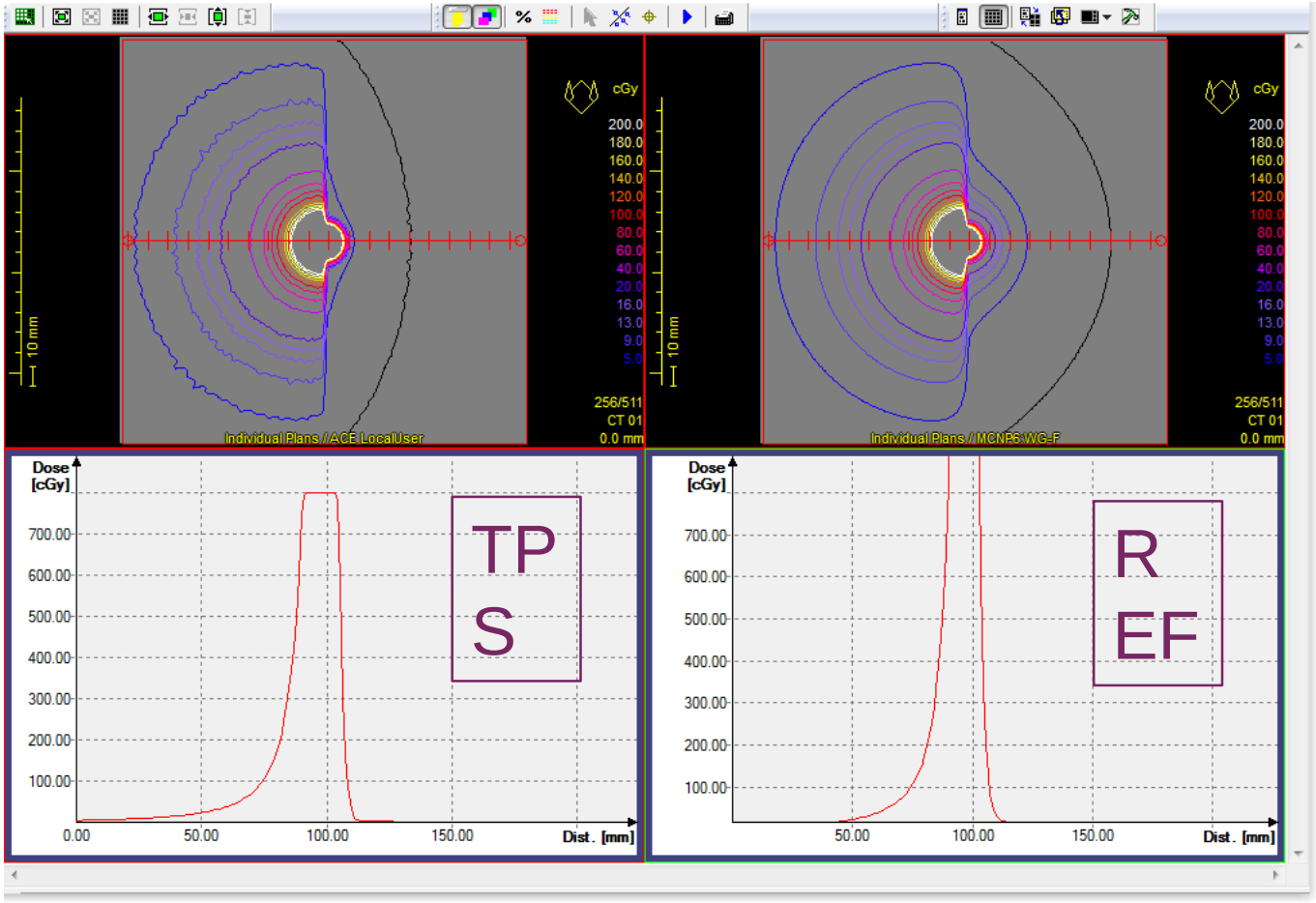

Case 4

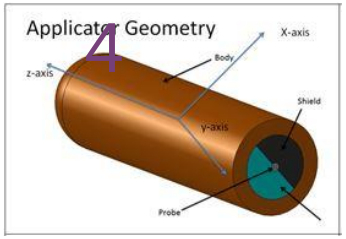

OCB dose profiles

Main Steps

OCB dose difference map, point dose query

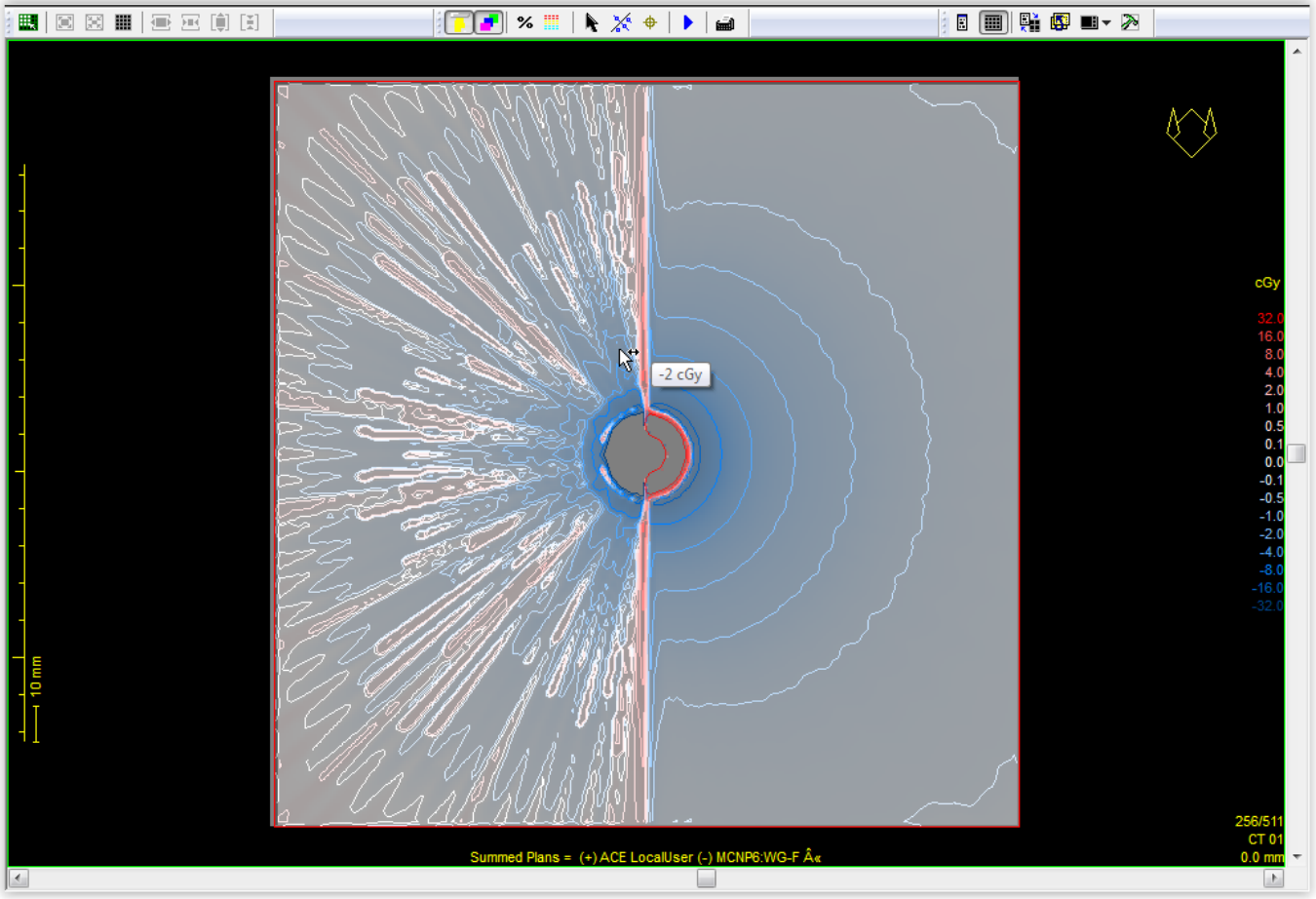

Case 4

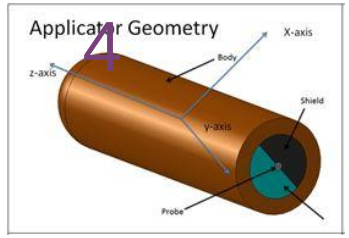

A Tested Process…

- Started in 2016
  - Alpha: Internal (to WG) testing
  - Beta:
    - 12 clinical physicists from 10 institutions
    - Over 200 physicists at the 2017 AAPM Summer School
- … probably not perfect
  - So as you implement MBDCA in your clinics, provide feedback on the dedicated Google forum (link at IROC Houston)

In the next session

- You will experience this workflow with
  - Test case #2 and #4
  - With a clinically relevant test case based on multi-catheters breast HDR.

WiP: Breast Test Case

New, clinically oriented test case

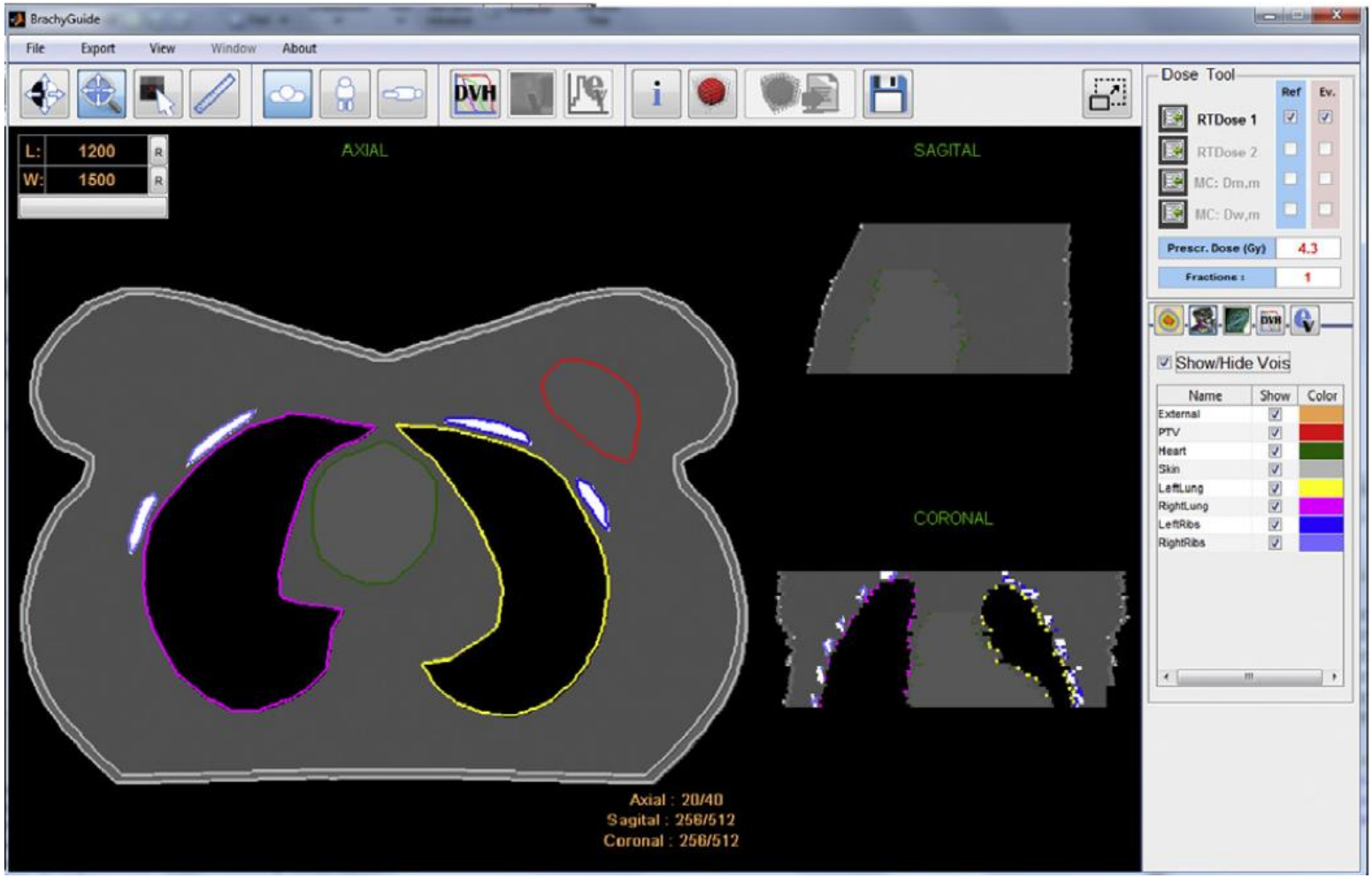

AcurosBV
ACE
MCNP6
egs_brachy

Peppa *et al*, Brachytherapy 15 (2016) 252-262

ESTRO School

WWW.ESTRO.ORG/SCHOOL

Advanced Brachytherapy Physics

07-10 October 2018 | Valencia, Spain

Close up
(Day 2)

P. Papagiannis, PhD
Medical Physics Laboratory
Medical School
National & Kapodistrian University of Athens

(no conflict of interest to disclose)

The essence of MBDCA commissioning and your practical session

In short, the commissioning procedure involves the following steps:

(0. go through the corresponding literature)

1. download test case(s) from the official test case registry
2. import test case files
3. recalculate (local) MBDCA dose for the test case plan
4. compare MBDCA, local MBDCA and reference dose for the test case plan

• Comparison between MBDCA and reference dose data establishes a reference pattern of differences, which is also useful to educate users in the principles and settings of the MBDCA.

•Comparison between local MBDCA and reference data should yield the same pattern of differences.

•If the user TPS version is later than the one used for preparing the test case (v.4.5 for Oncentra and v. 13 for BrachyVision) agreement should be equal or improved.

Let us take another look
at the test cases you worked with
from the perspective of
local % dose difference…

(using BrachyGuide distributed freely via:
www.rdl.gr)

Test case 2
ACE vs MC
(color map: ±20%)

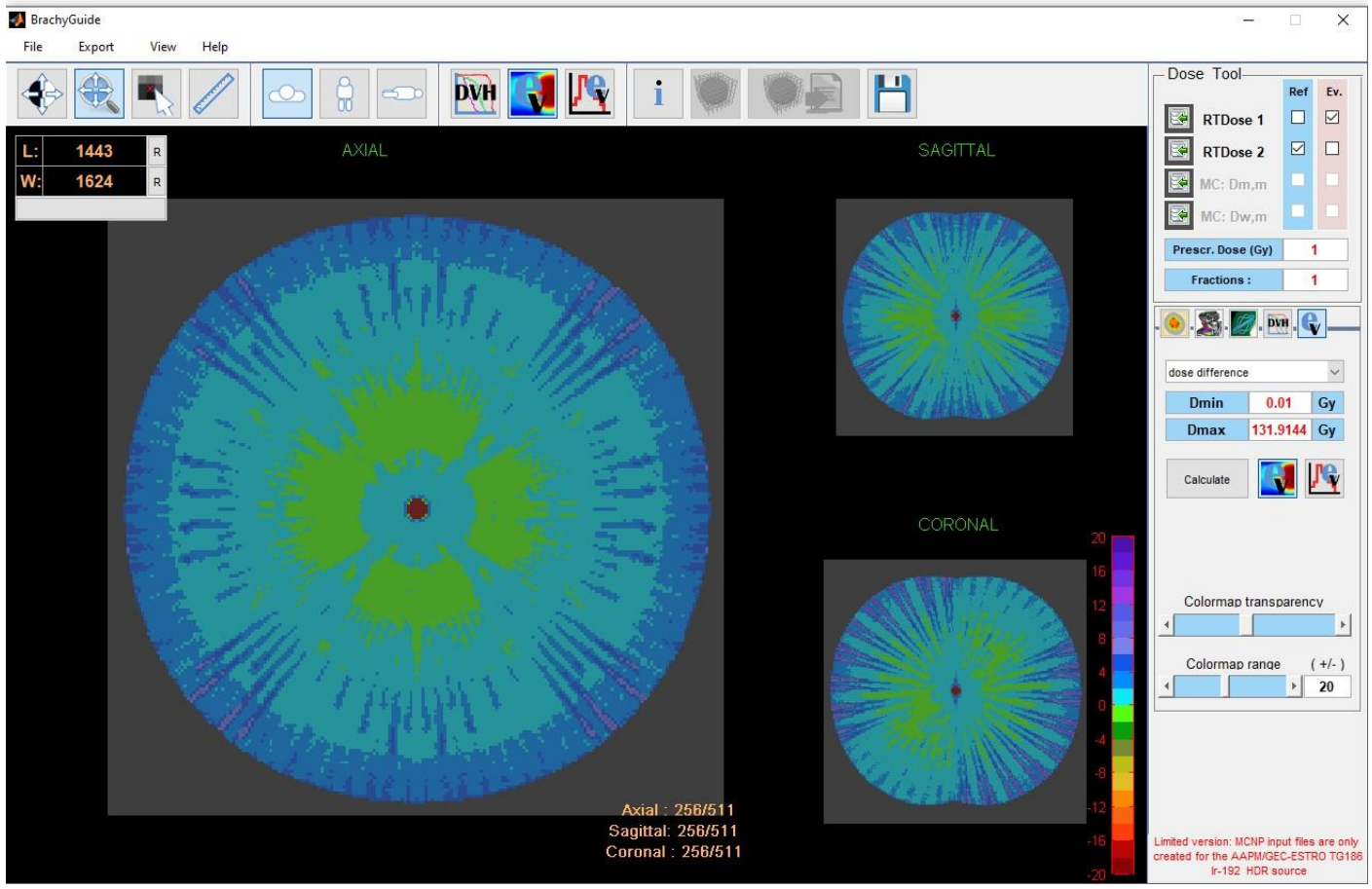

Test case 2
ACE vs MC
(color map: ±2%)

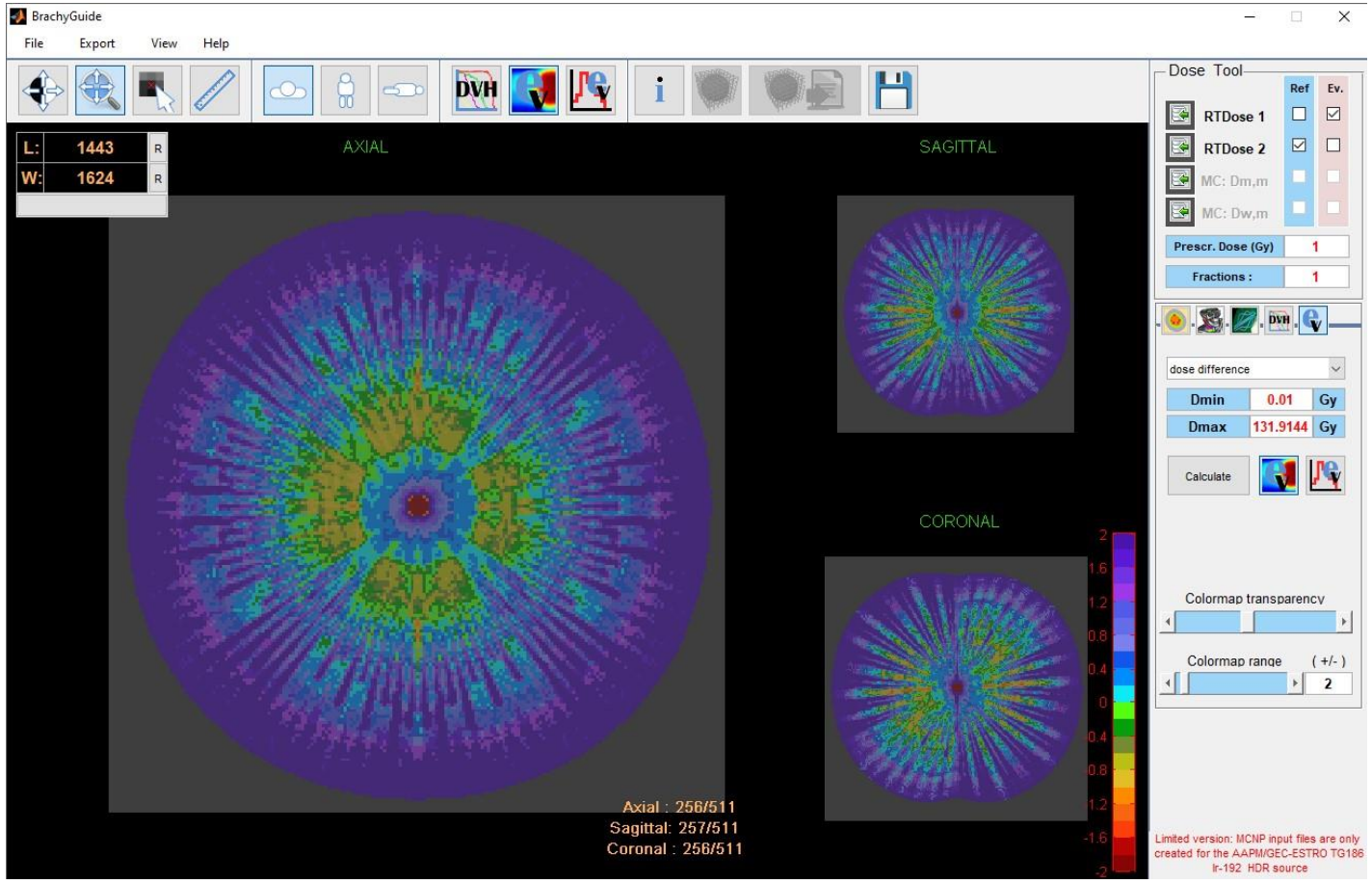

Test case 2
ACE vs MC

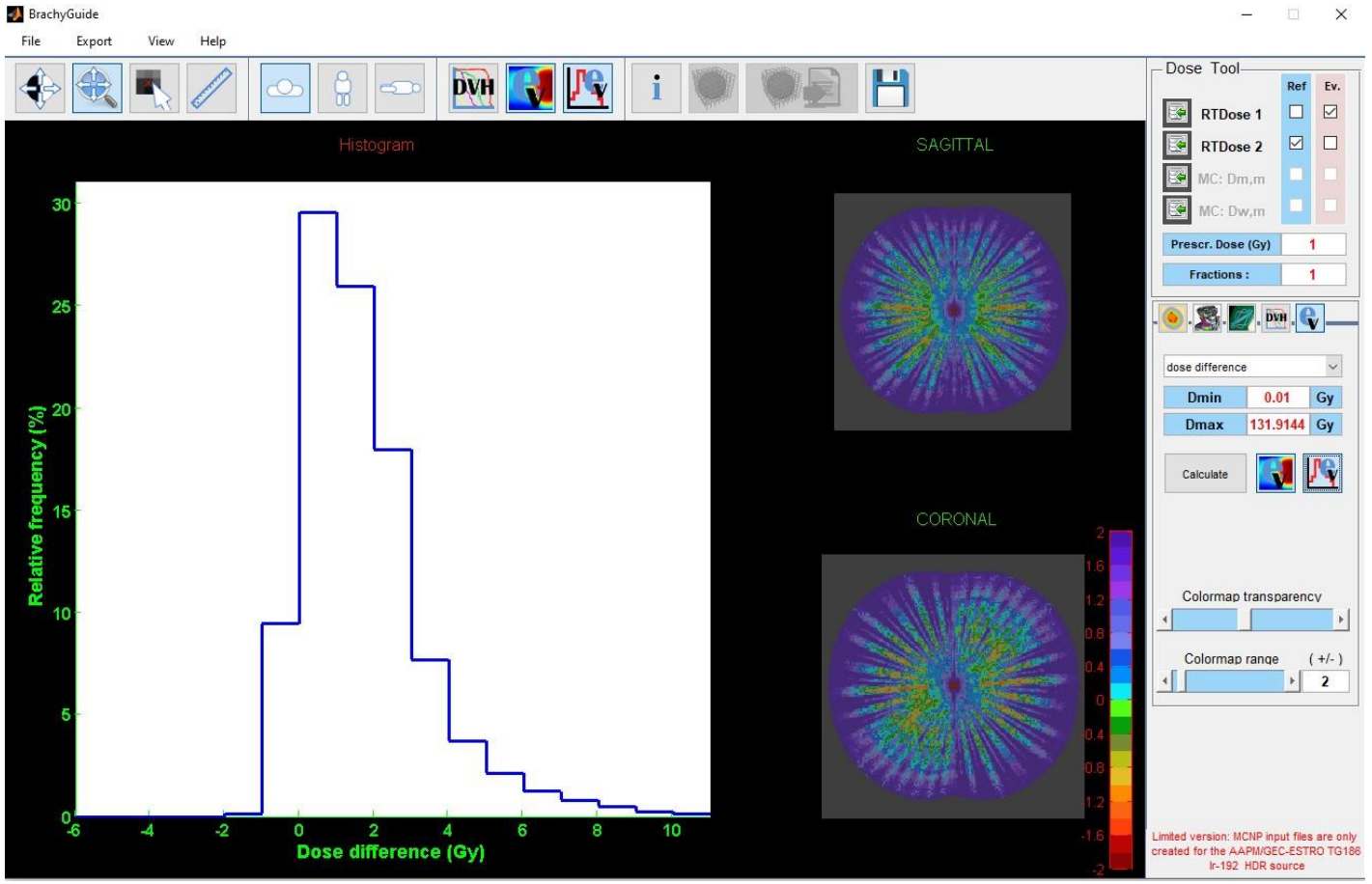

Test case 2
Acuros vs MC
(color map: ±2%)

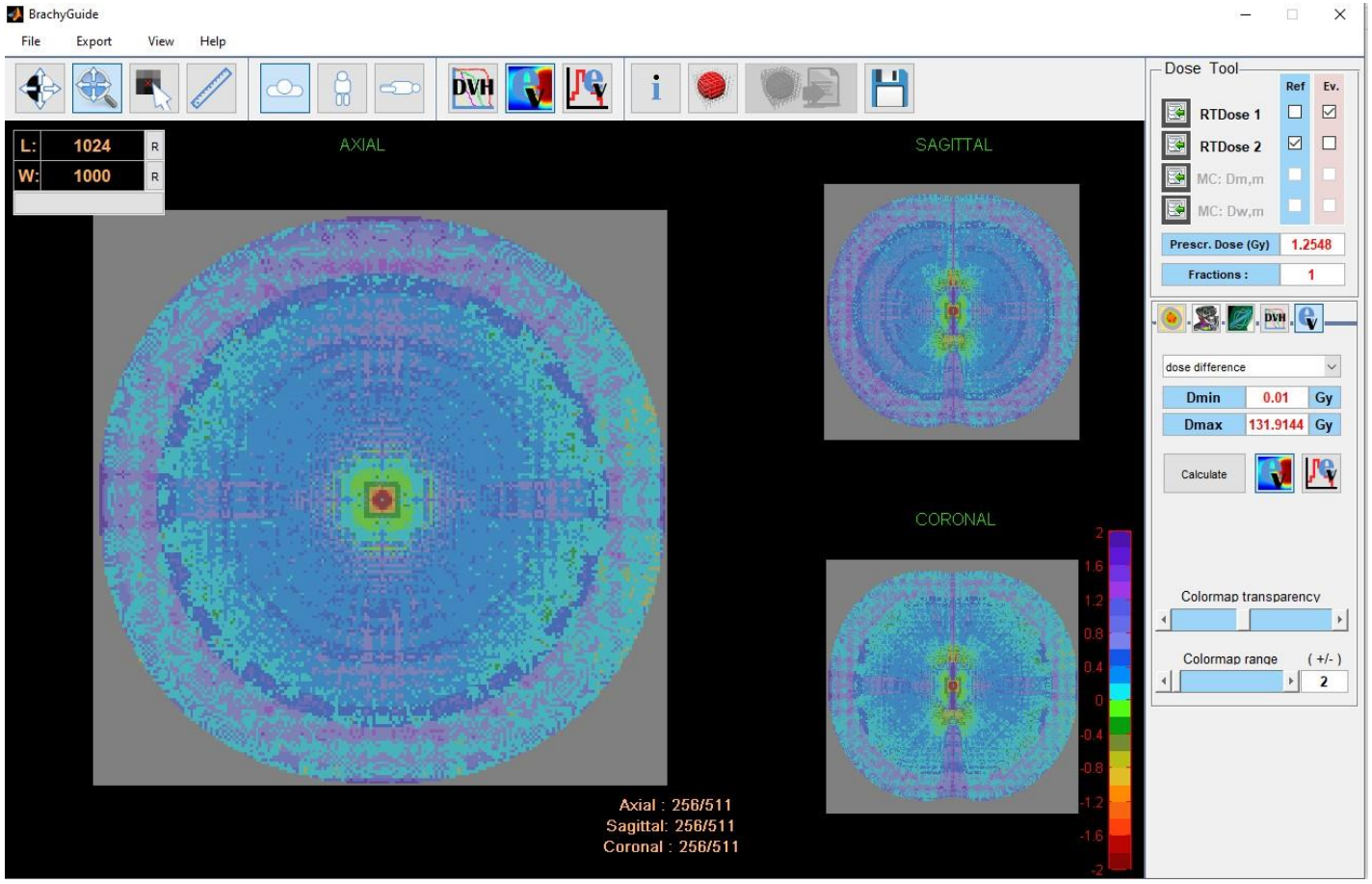

Test case 2
Acuros vs MC

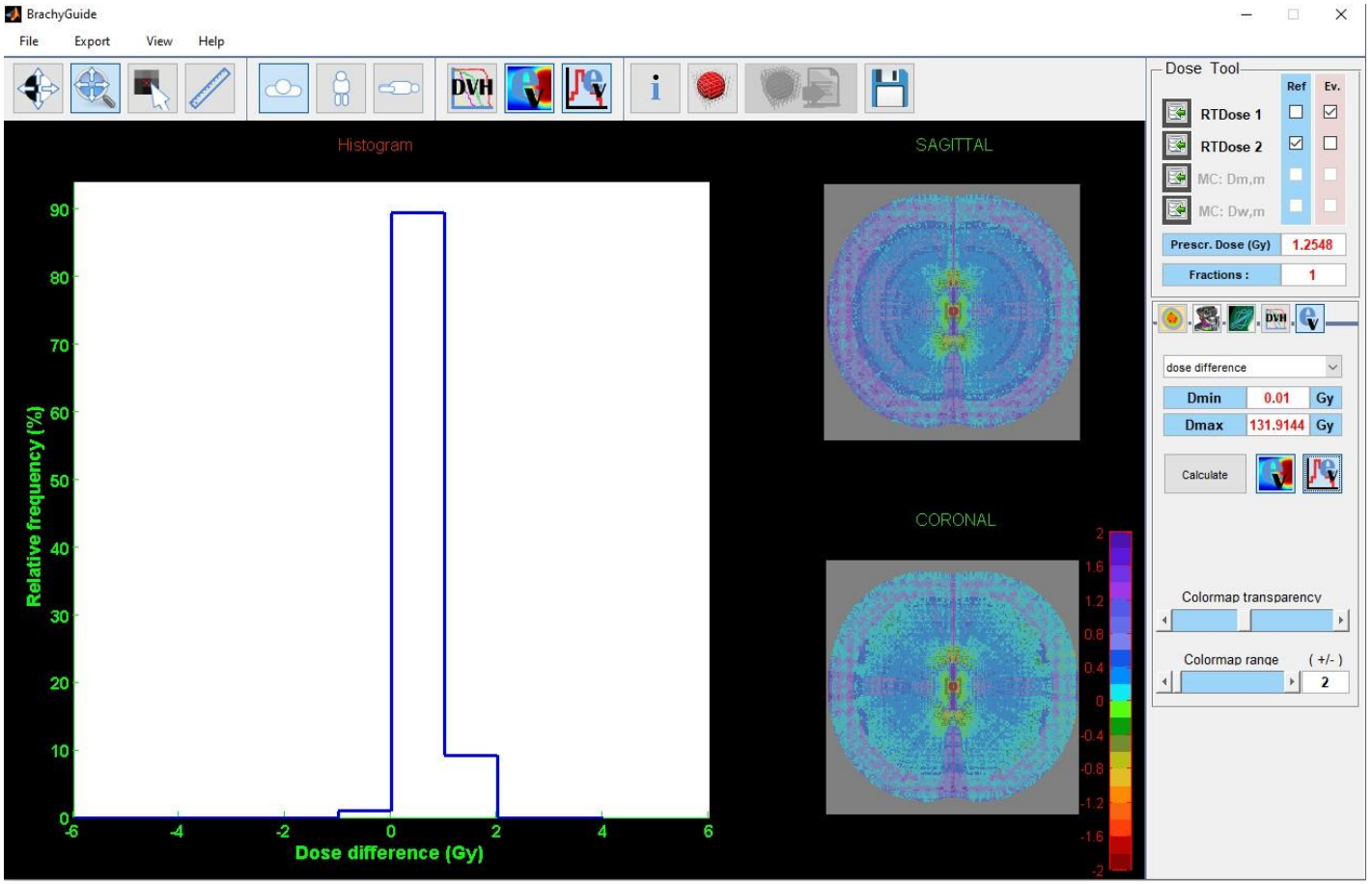

Test case 2

- MBDCAs do present differences from MC dose calculations for single source in the center of a water phantom.

- The cause of these differences should be clear from the corresponding discussion on MBDCAs.

- So maybe it is better to stick with TG-43 …?

Test case 2
TG-43 vs MC
(color map: ±20%)

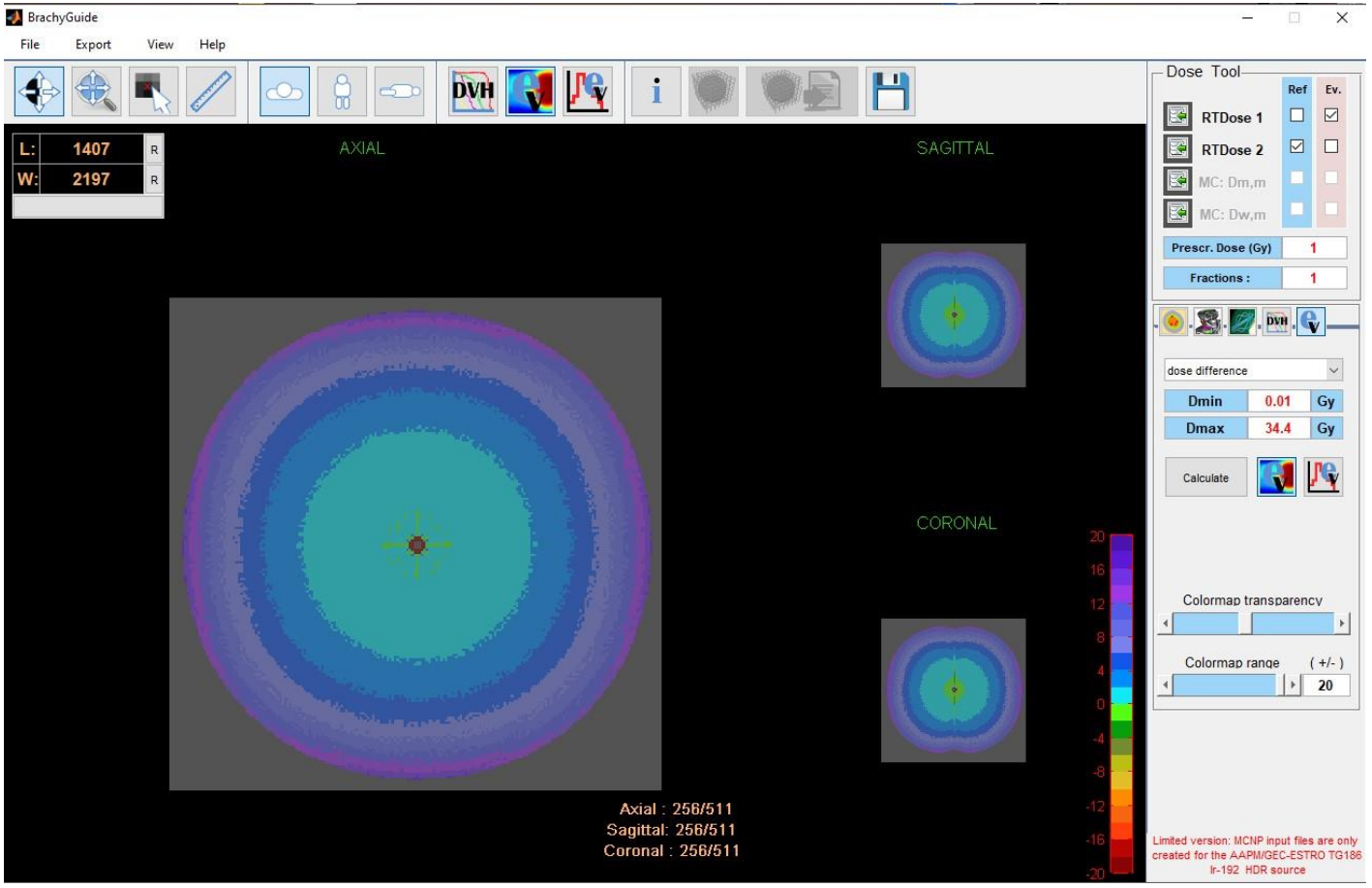

TG-43 is not free of caveats and sources of uncertainty …

Test case 4
ACE vs MC
(color map: ±20%)

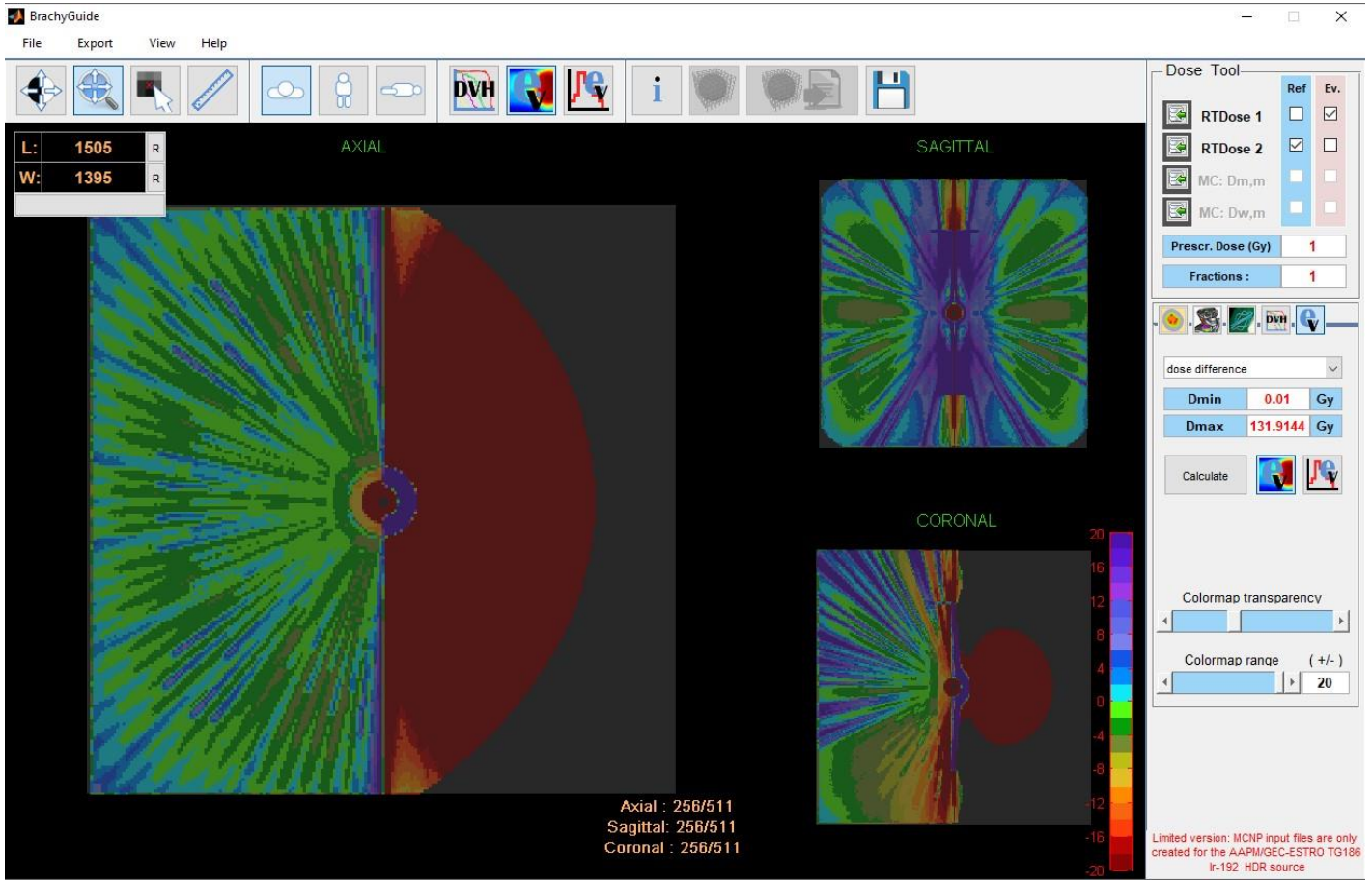

Test case 4
ACE vs MC
(color map: ±2%)

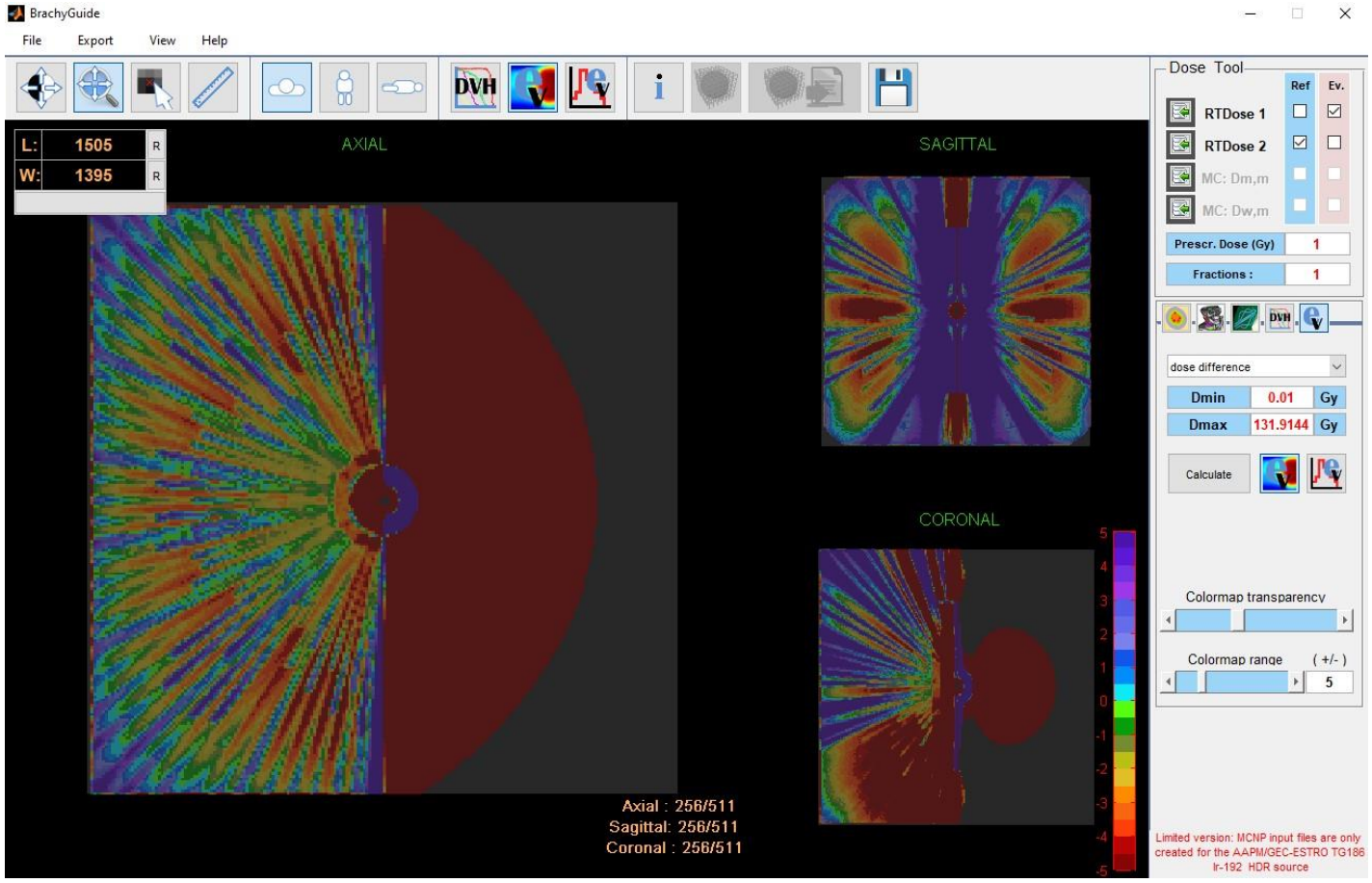

Test case 2
ACE vs MC

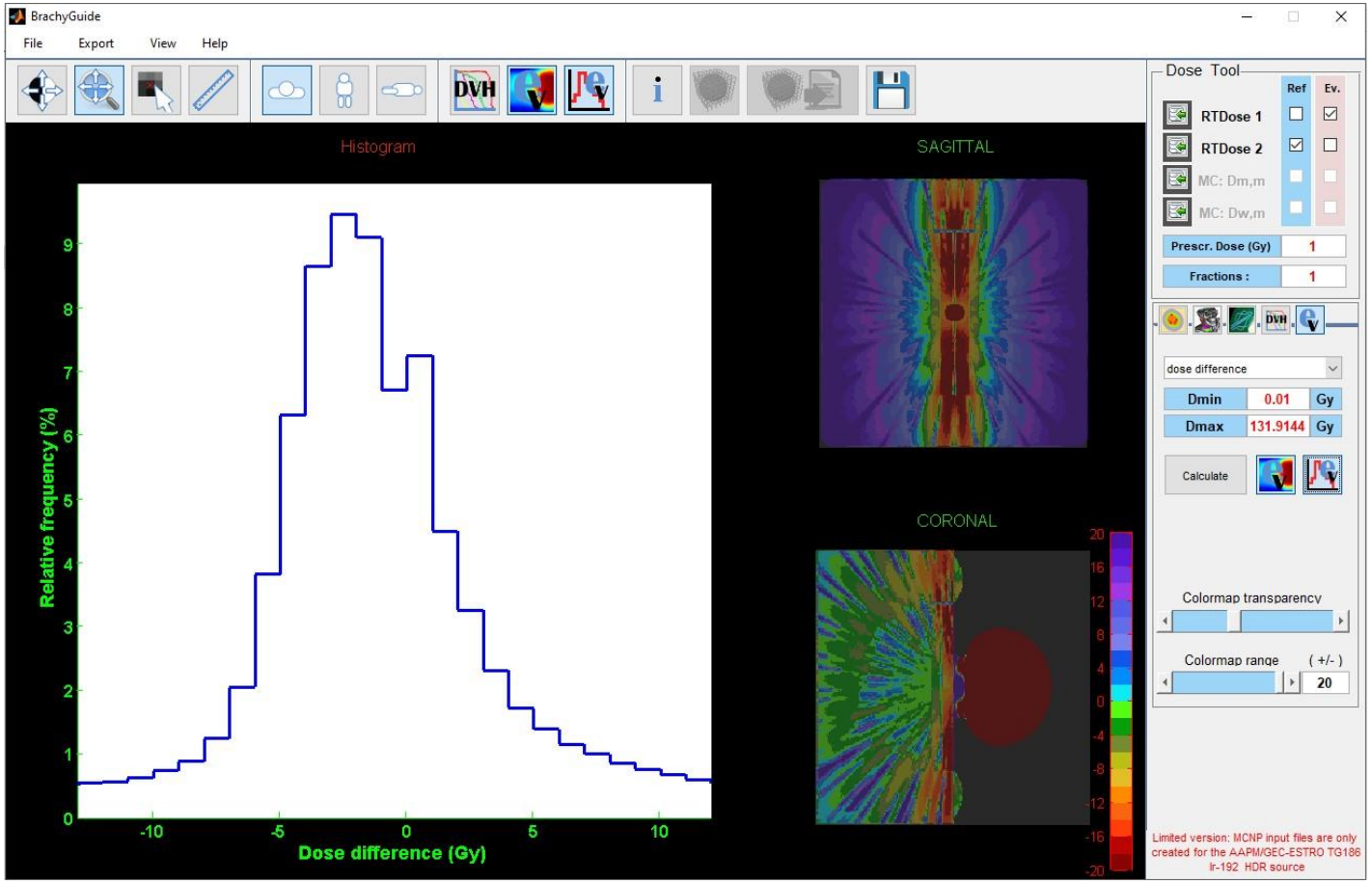

Test case 4
Acuros vs MC
(color map: ±20%)

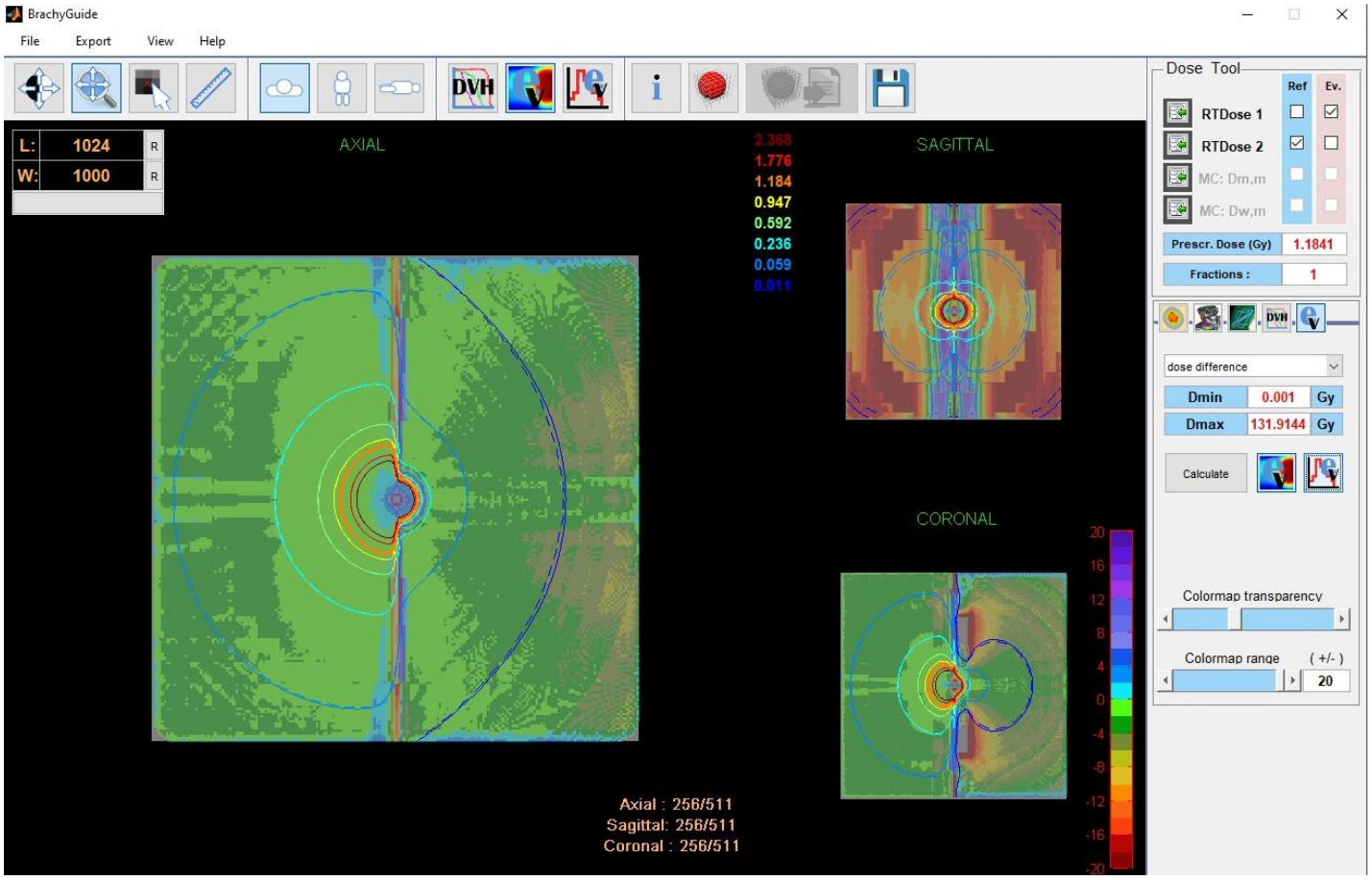

Test case 4
Acuros vs MC
(color map: ±2%)

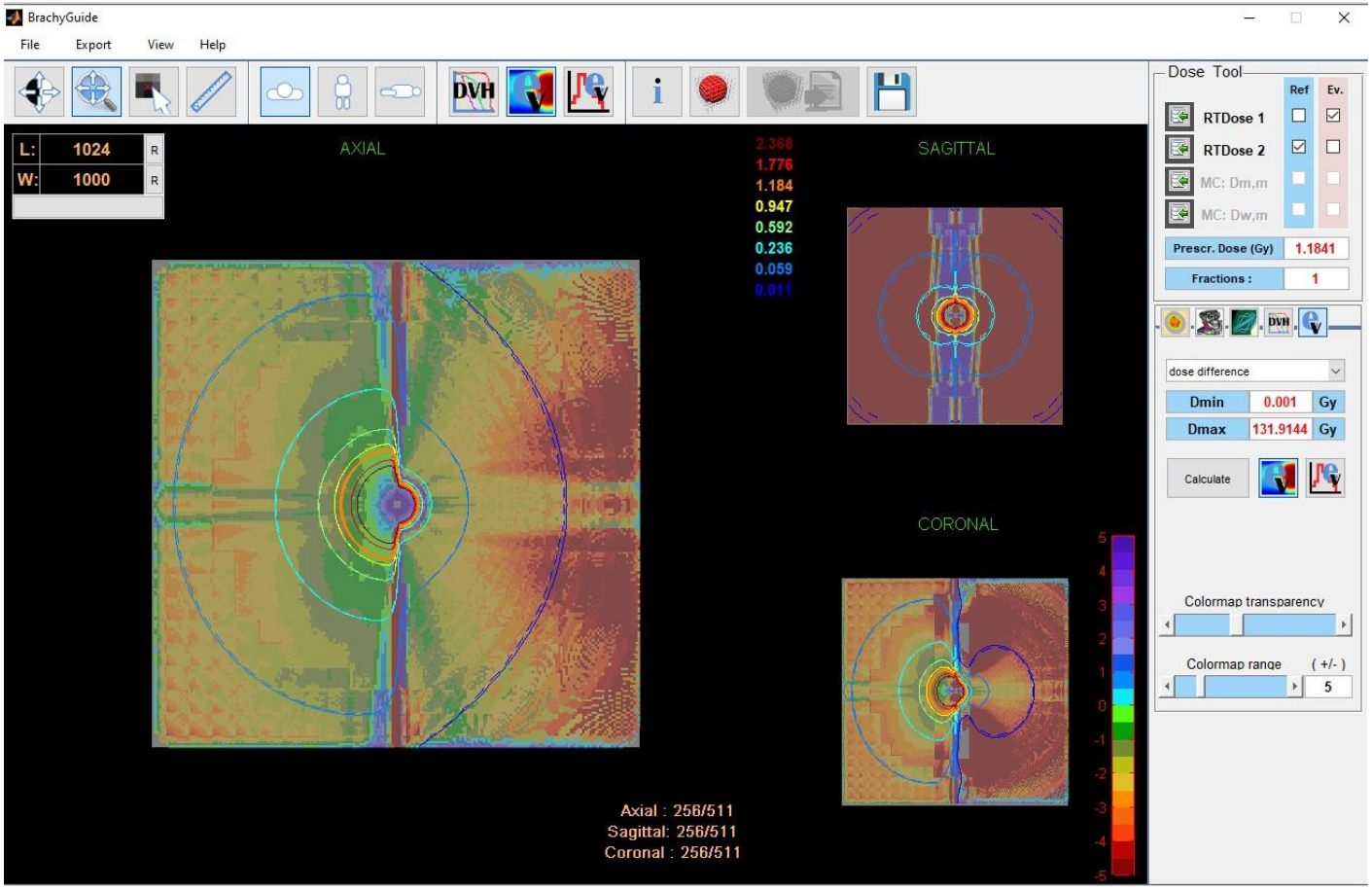

Test case 4
Acuros vs MC

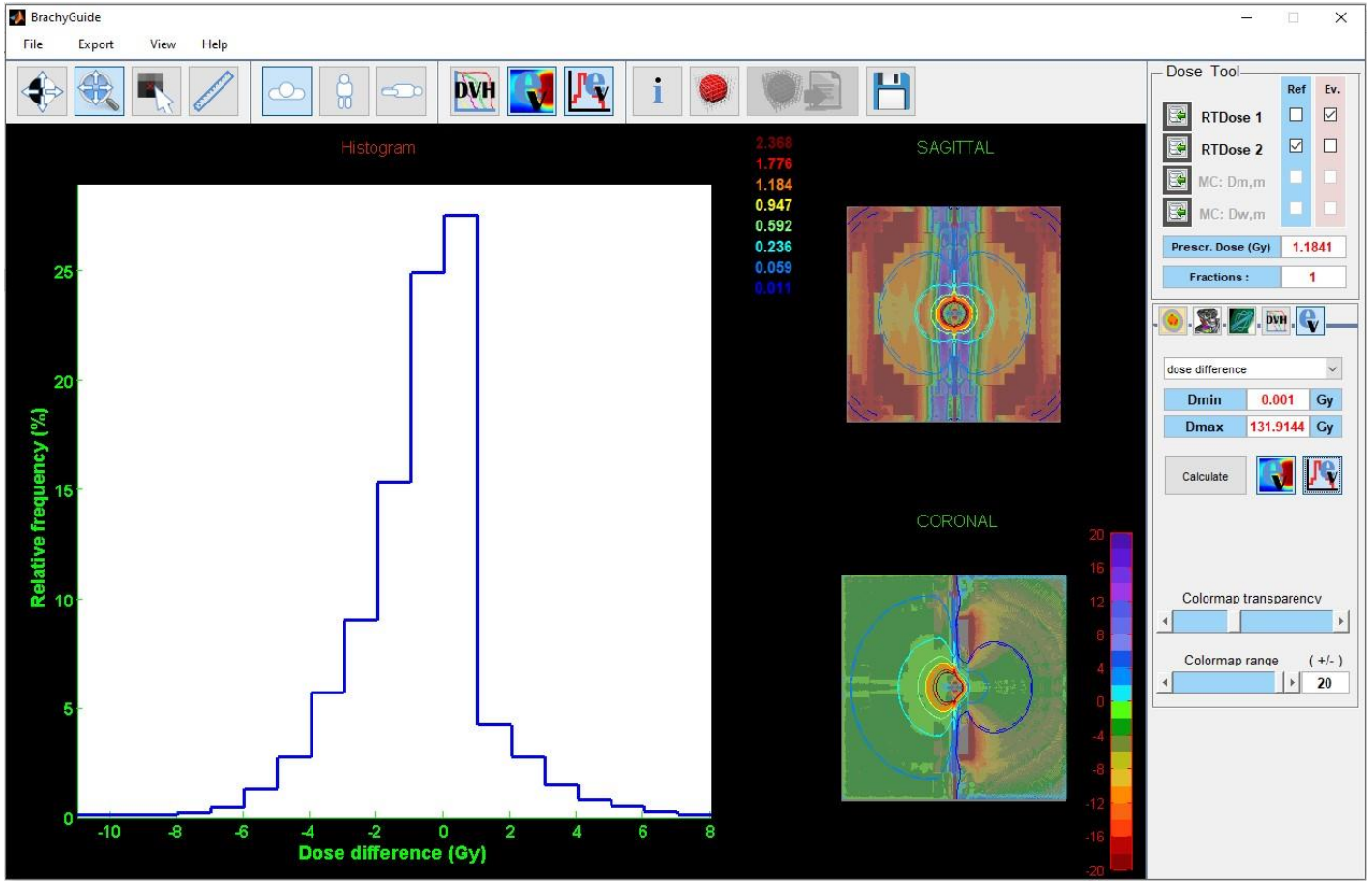

Test case 4

- MBDCAs do present differences from MC dose calculations for single source in the center of a shielded cyl. applicator.

- The cause of these differences should be clear from the corresponding discussion on MBDCAs.

- So maybe it is better to stick with TG-43 …?

Test case 4
TG-43 vs MC
(color map: ±20%)

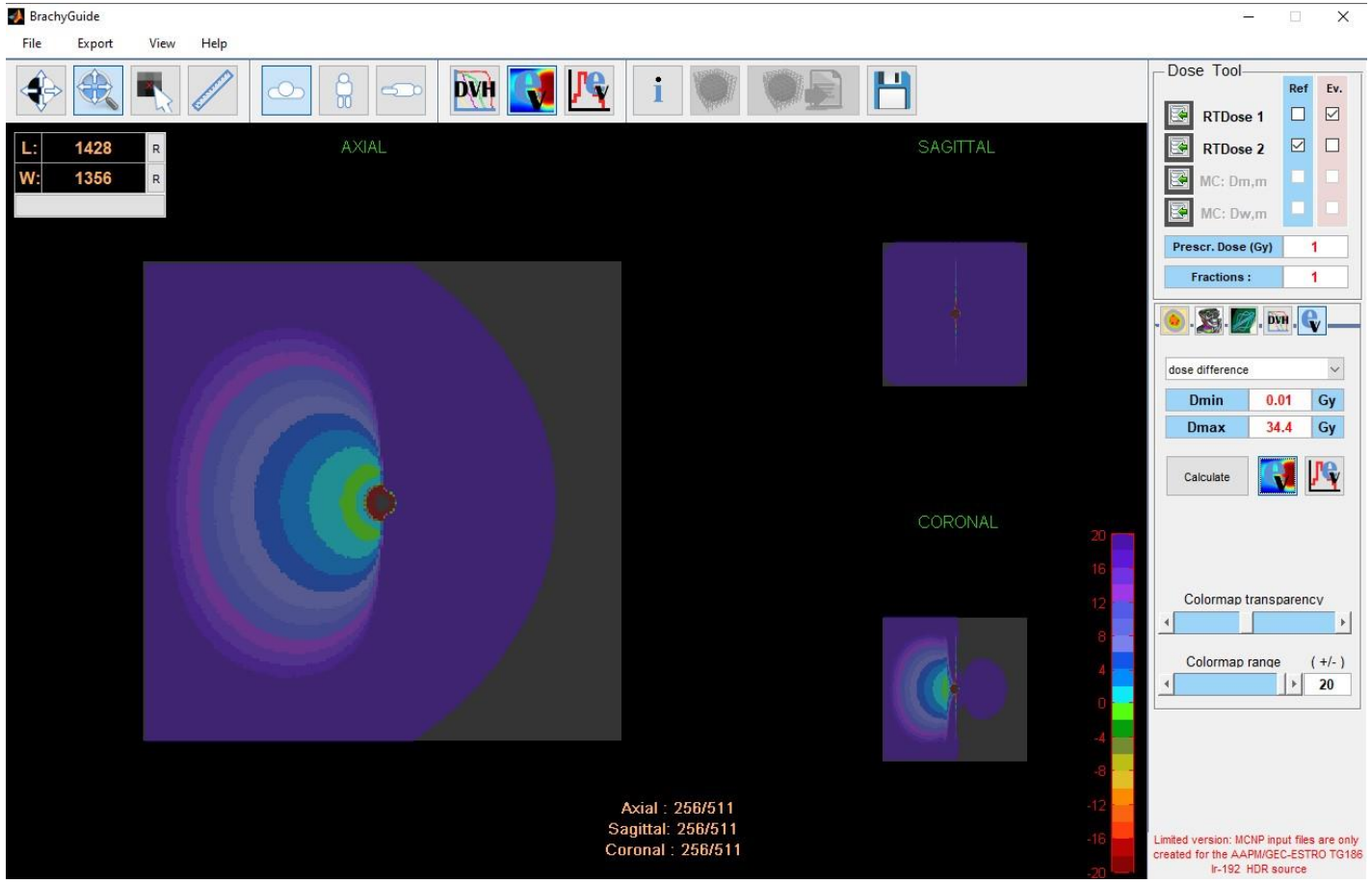

Test case 4
TG-43 vs MC
(color map: ±20%)

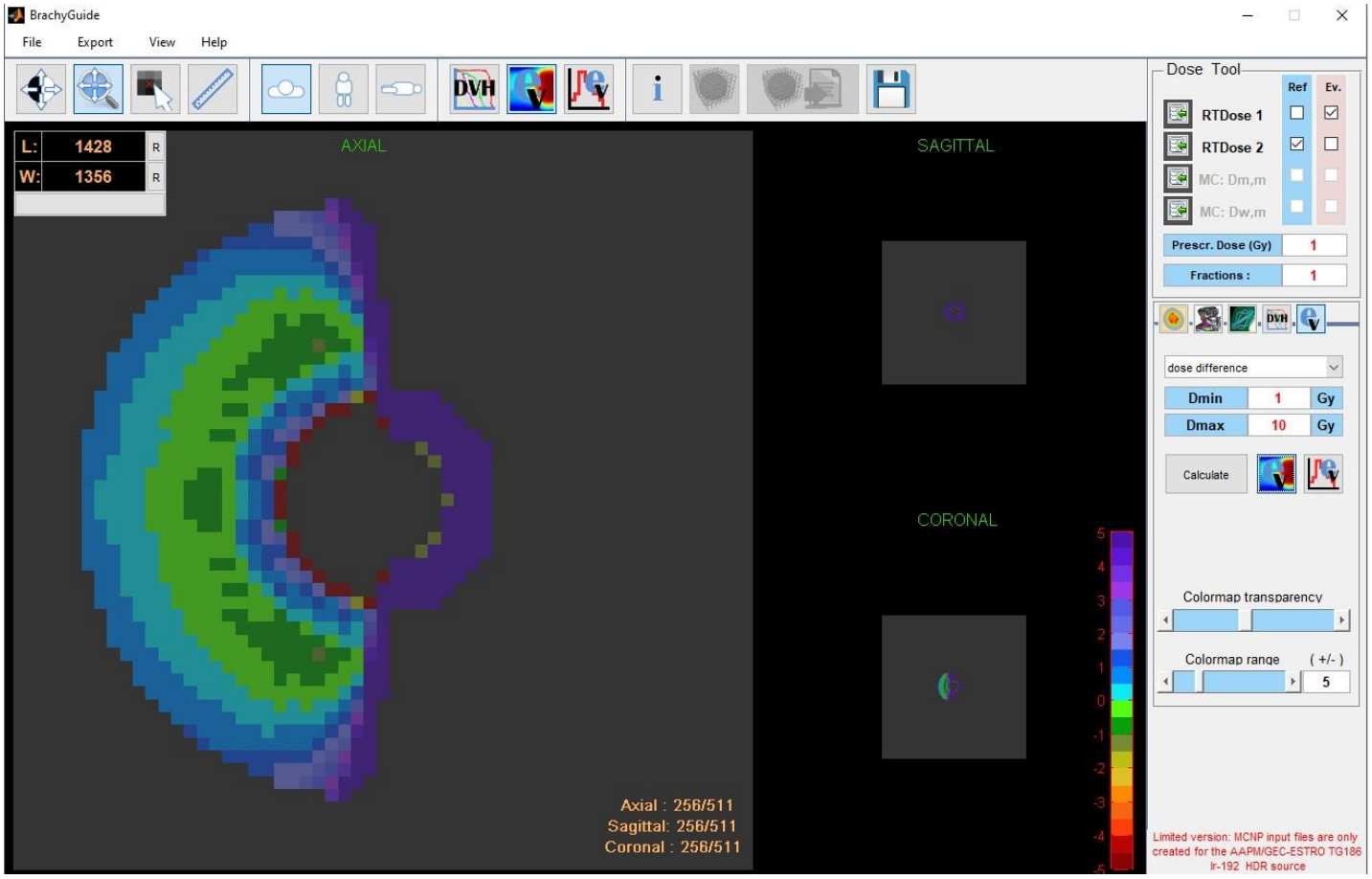

TG-43 presents a higher dose overestimation affecting the PTV

Test case breast
ACE vs MC
(color map: ±20%)

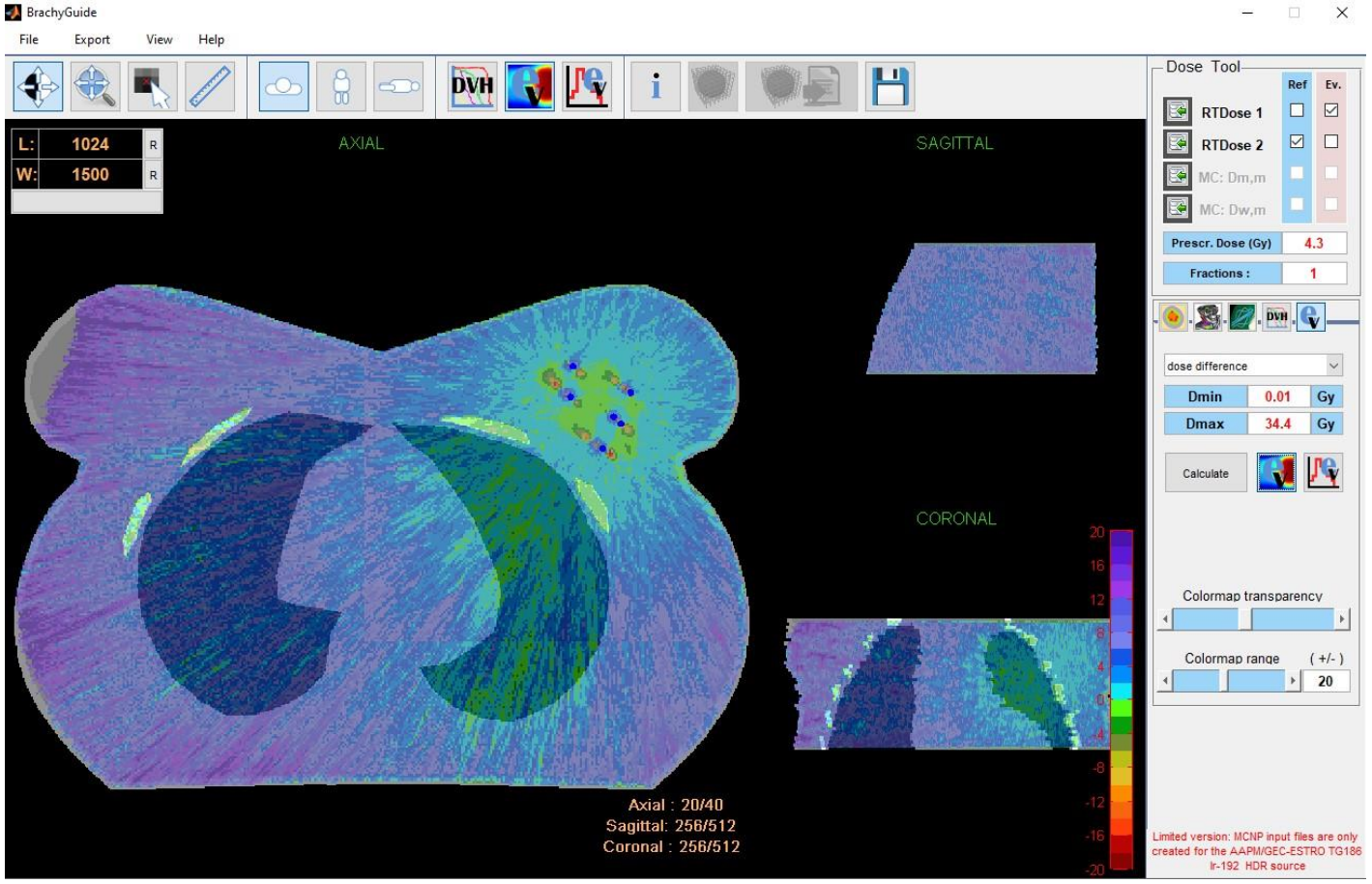

Test case breast
ACE vs MC
(color map: ±5%)

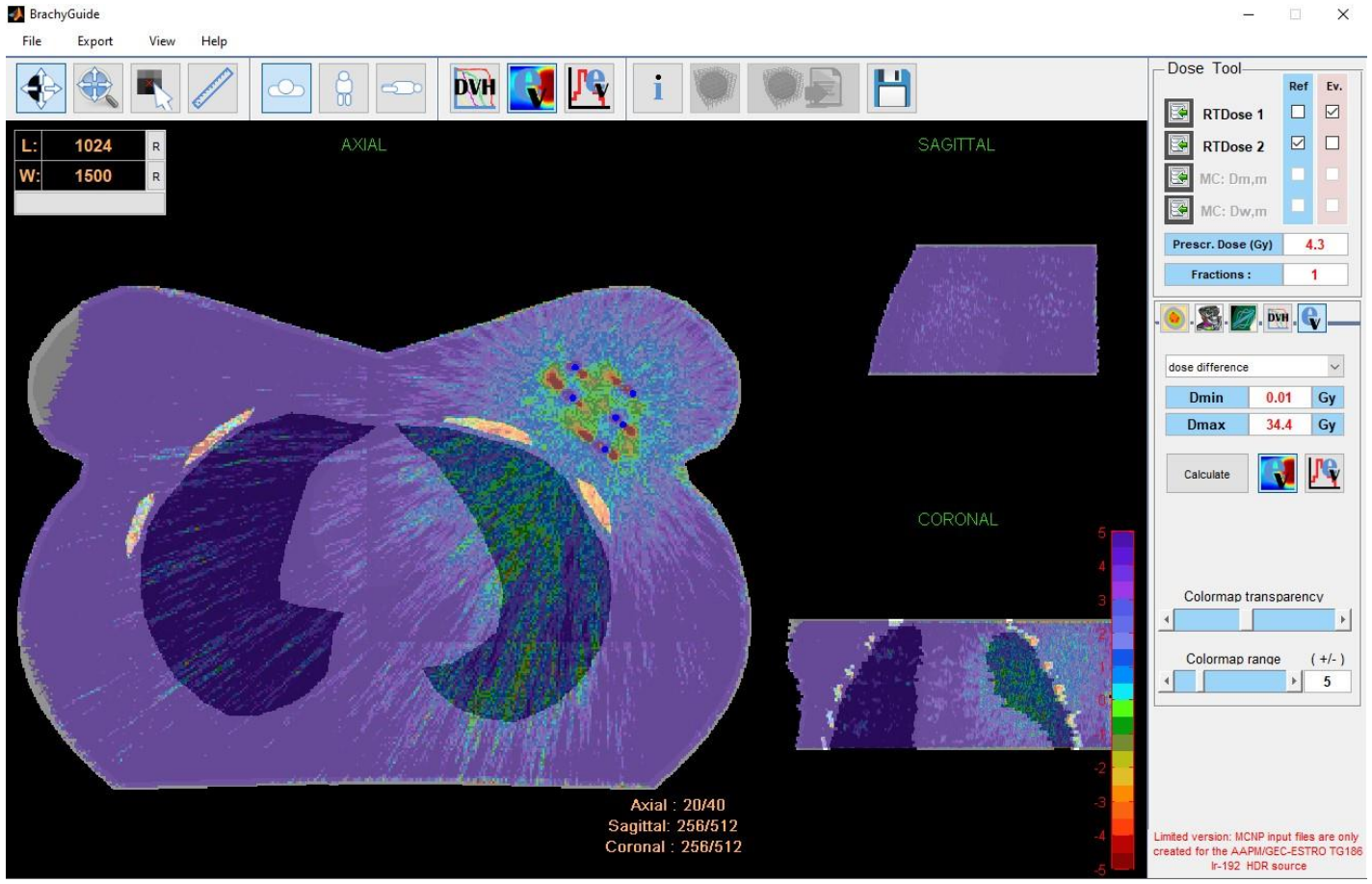

Test case breast
ACE vs MC

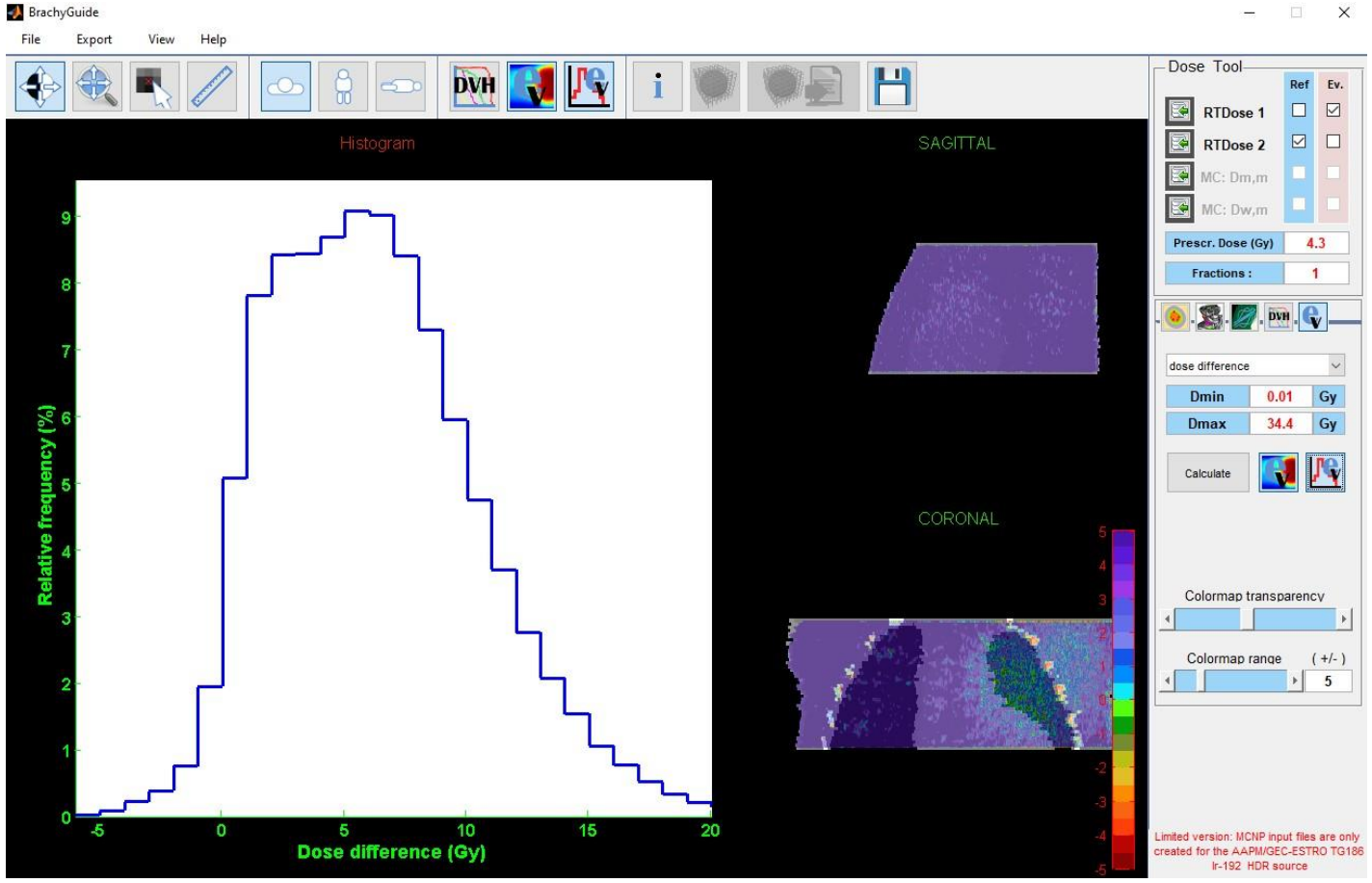

Test case breast
Acuros vs MC
(color map: ±20%)

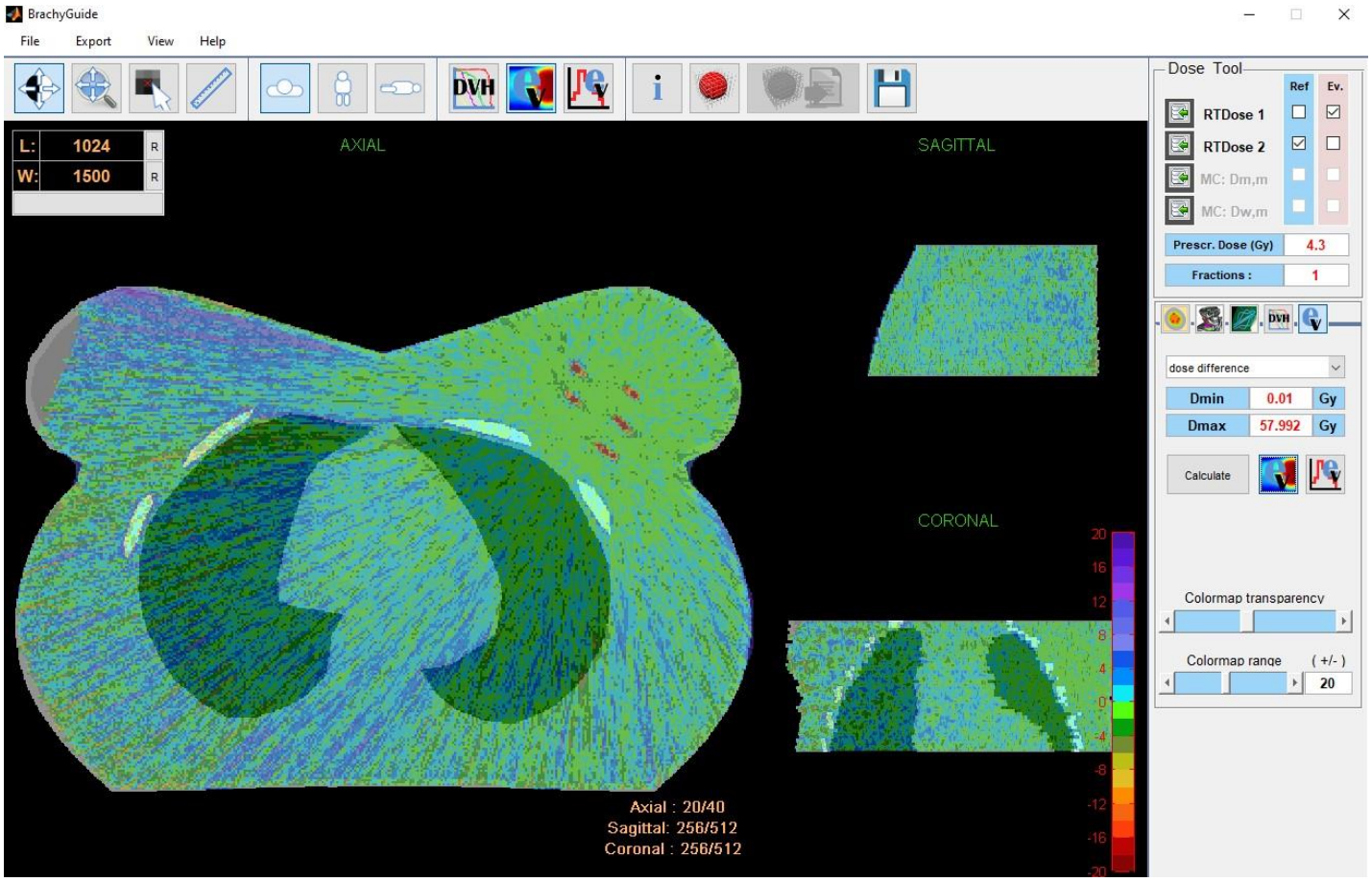

Test case breast
Acuros vs MC
(color map: ±5%)

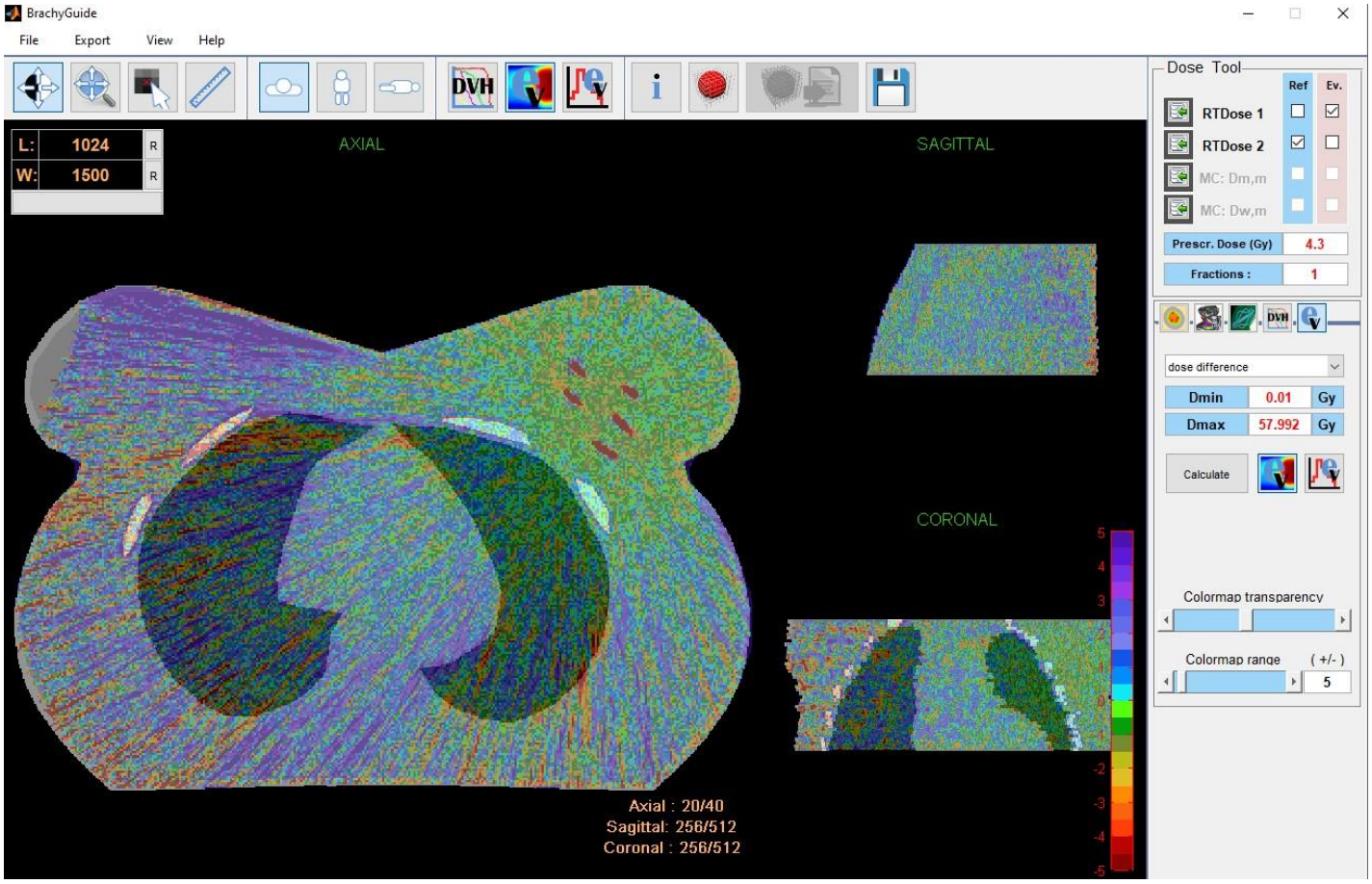

Test case breast
Acuros vs MC

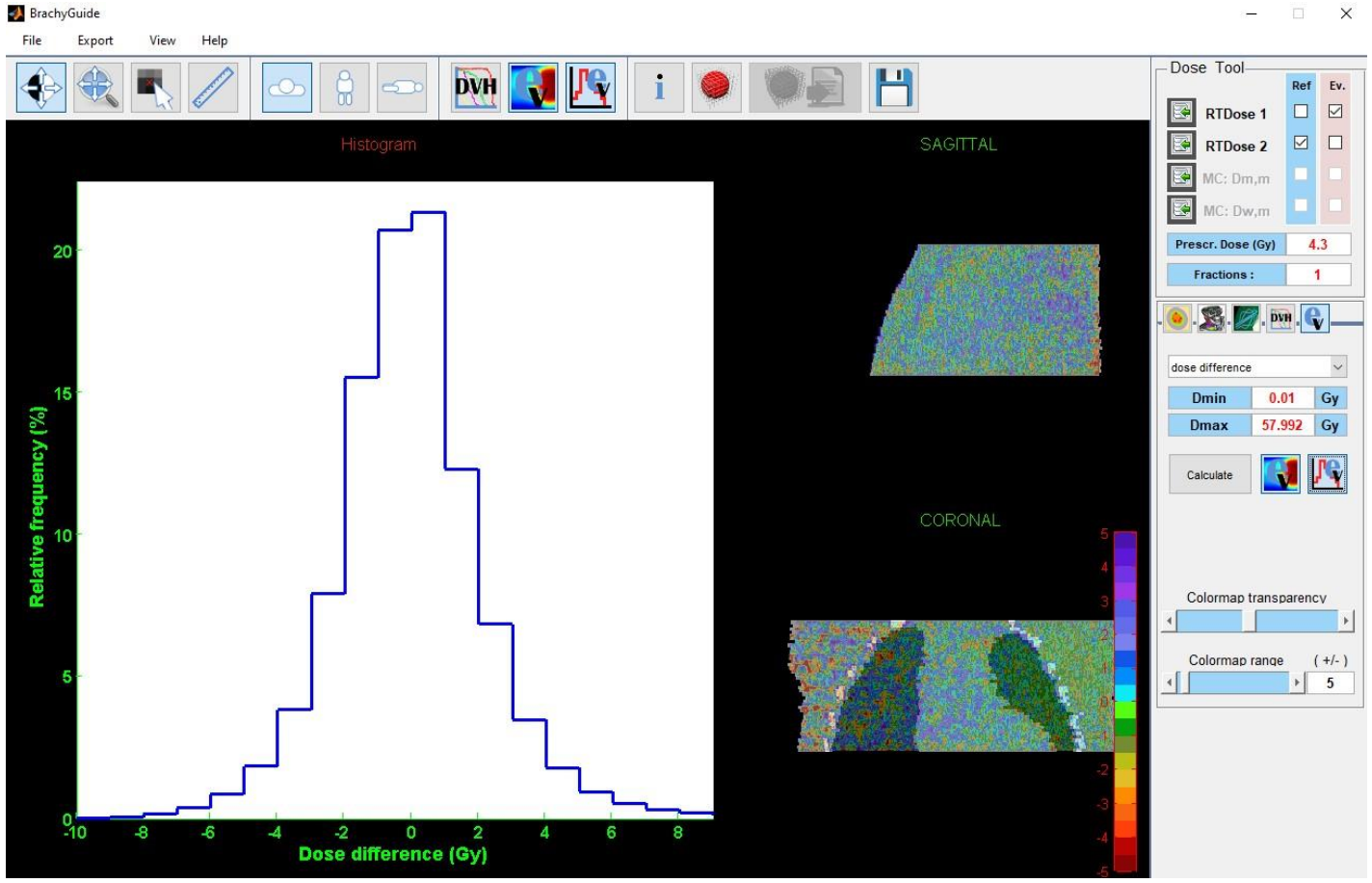

Test case breast

- MBDCAs do present differences from MC dose calculations for a breast case resembling a clinical scenario.

- The cause of these differences should be clear from the corresponding discussion on MBDCAs.

- So maybe it is better to stick with TG-43 …?

Test case breast
TG-43 vs MC
(color map: ±20%)

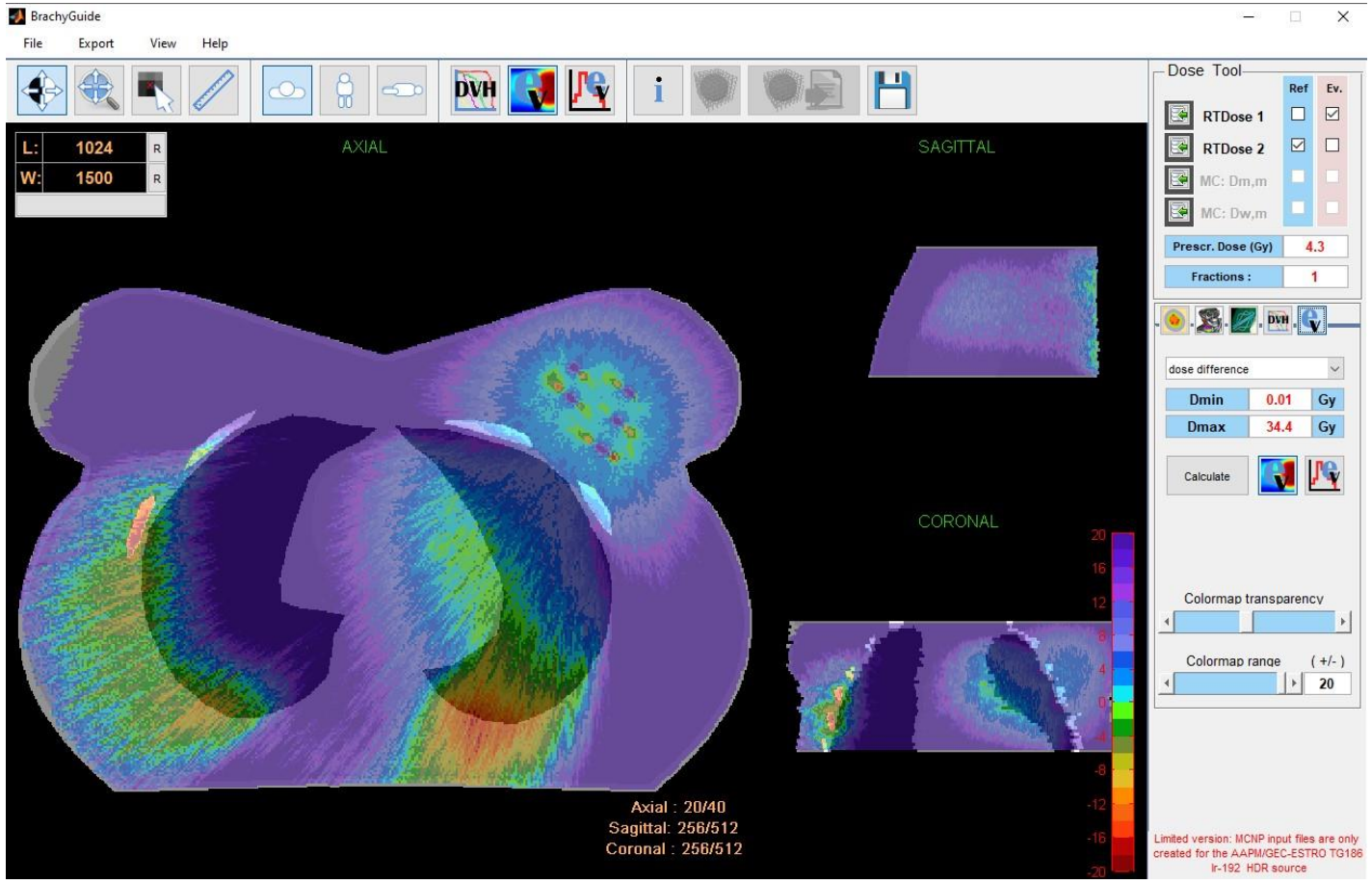

TG-43 presents higher differences from MC
but these do not appear to be clinically relevant

breast
TG-43 vs MC
(color map: ±20%)

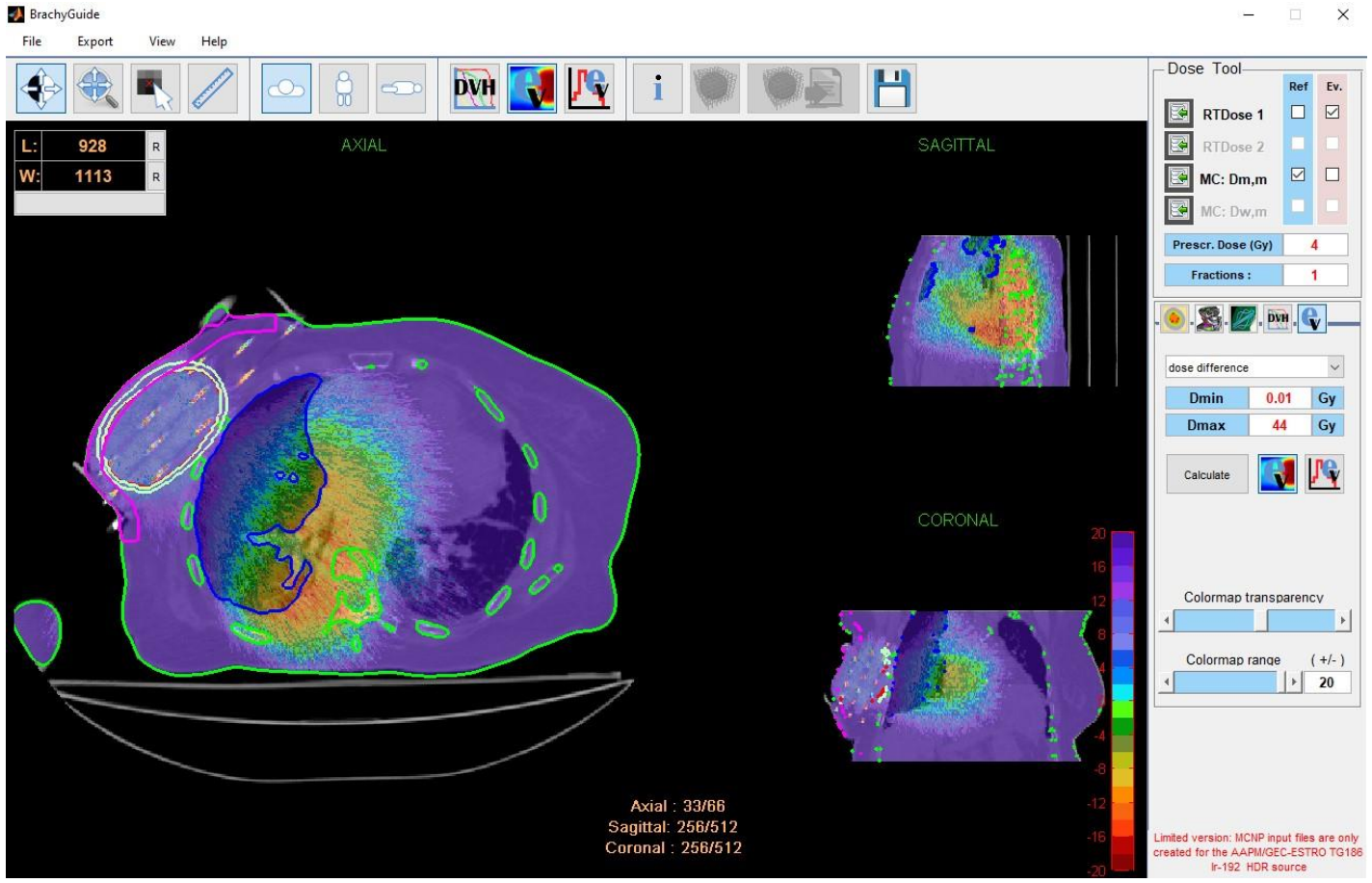

All cases are NOT the same …
All treatment sites are NOT the same …

1. MBDCAs were NOT developed for single source dosimetry.

2. Such tests are there to introduce you to MBDCA mechanics and serve as a sanity check (correct source, changes with TPS version change, etc).

3. You can review test case results as:
local D diff. (to highlight diffs)
global D dif. (to factor in their relative importance)
plan metrics such as DVH and associated indices (to review their clinical significance)

4. MBDCAs do improve dosimetric accuracy relative to TG-43

5. Potential clinical benefit is treatment site- and patient- specific.

ESTRO School

WWW.ESTRO.ORG/SCHOOL

ESTRO School

La Fe
Hospital Universitari i Politècnic

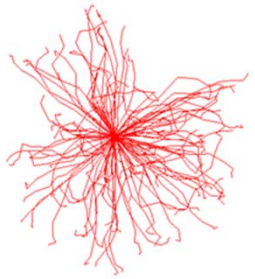

Medical Physics Group
University of Valencia
IRIMED

Dose plan evaluation in Brachytherapy

Jose Perez-Calatayud

Hospital Universitario y Politecnico La Fe. Valencia.

perez_jos@gva.es

Advanced Brachytherapy Physics. Valencia 7-10 October 2018

ESTRO School

Disclosures

- We are users of Elekta equipment (HDR Ir-192 and LDR I-125)
- Commercial products included in this presentation just for illustrative purposes

Acknowledgments

Christian Kirisits

Françoise Lliso

Vicente Carmona

José Gimeno

Rafael García

Núria Carrasco

José Richart

ESTRO School

Learning Objectives

- To identify the different aspects to be considered when a brachy dose distribution is evaluated
- To understand the required cautions
- To present the current TPS limitations in biology evaluation

Aspects to be considered for plan evaluation

- Dose points
- Dose distribution
- Dose Volume Histograms
- Global indexes
- Biology (EQD2)

Dose to points

- Points derived from traditional Brachy Systems
- Target points at CTV periphery used for polynomial optimization
- New ICRU 89 points

- Some examples and cautions 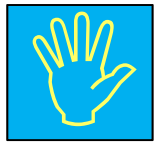

Dose to points

- Traditional Brachy Systems:
  - Manchester (Gyn cervix).
    - A points (*ICRU38*) H Points (*ABS 2000*)
    - A "universal" cervix approach to unify prescription criteria and to control the overdose volumes

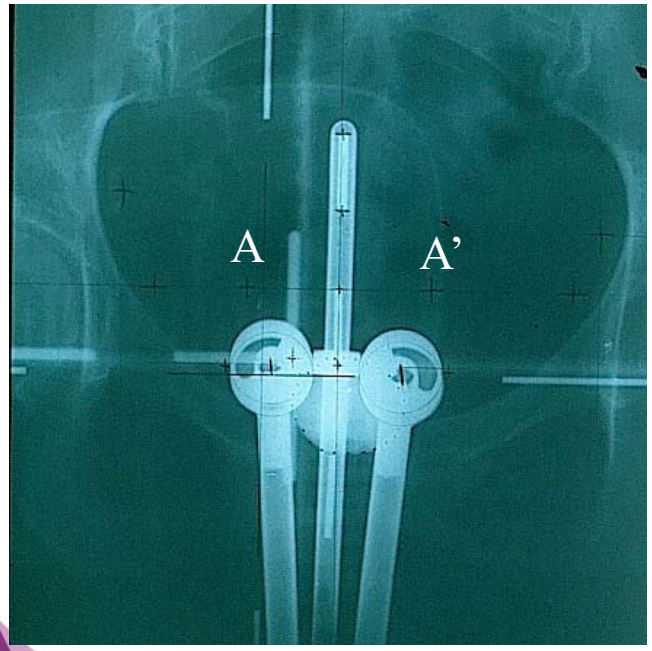

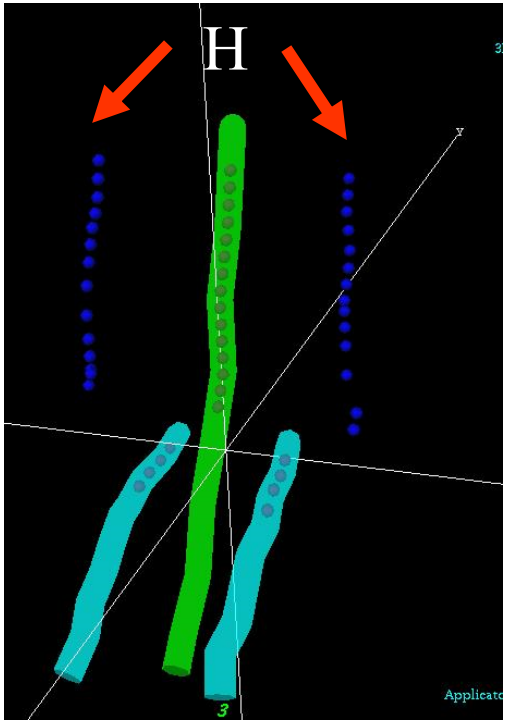

2 cm lateral

ESTRO School

Dose to points

Overdose volume

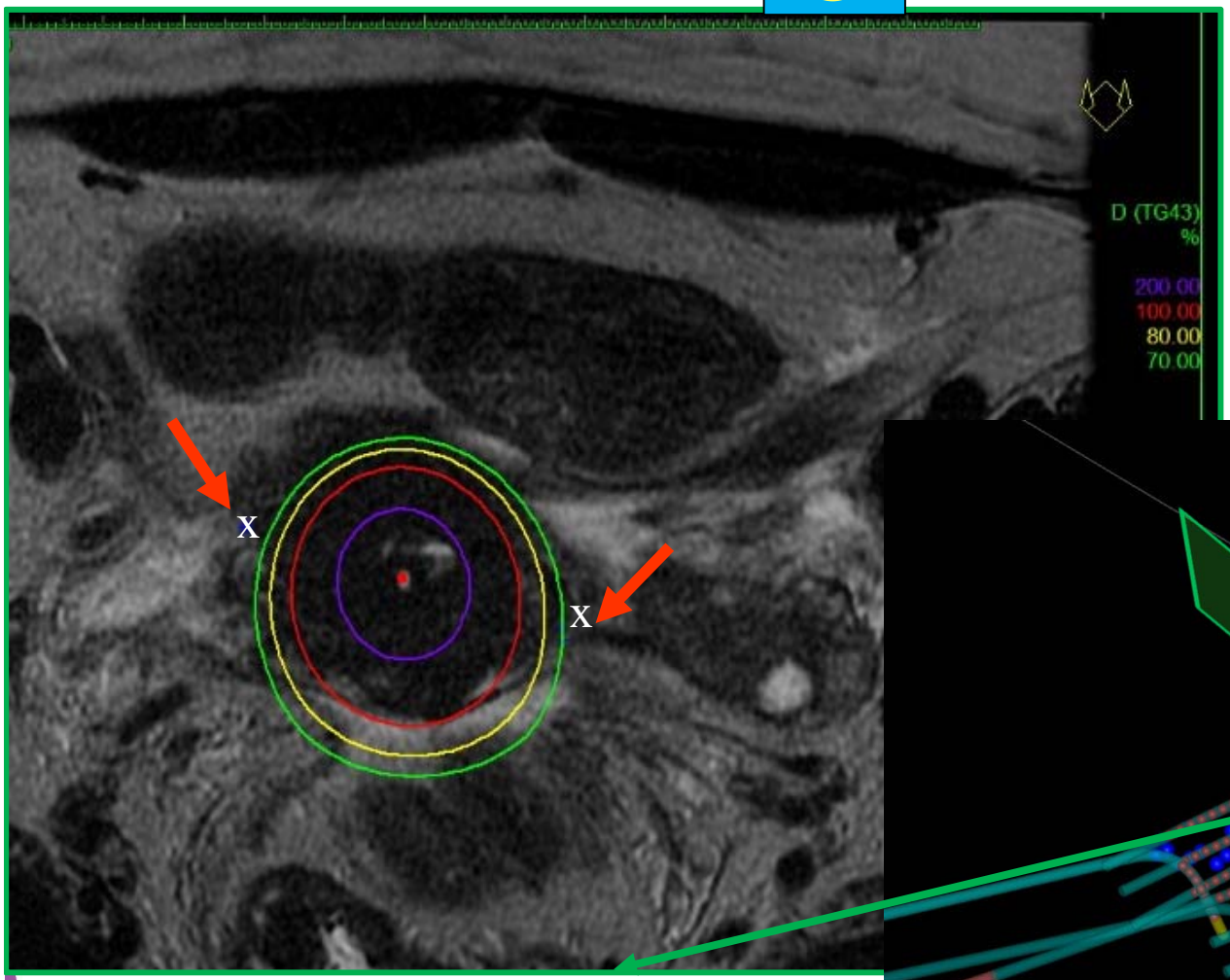

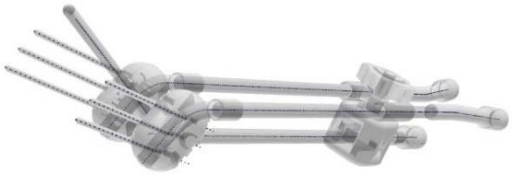

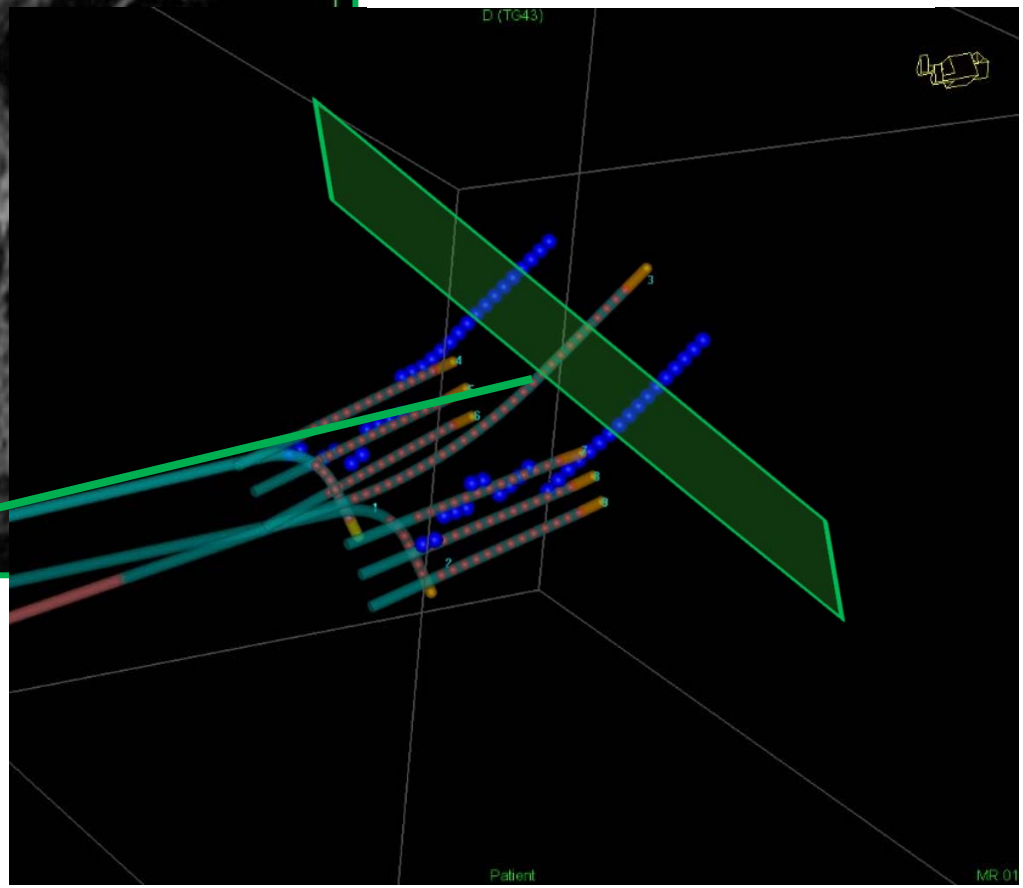

Dose to points

- Traditional Brachy Systems:
  - Paris “System”: a set of rules to obtain suitable dose distributions.
  - For different regular source patterns, basal points are defined in regions of dose plateau or minimum
  - In HDR it evolved to Steeping Source Dosimetry System (SSDS) (*Van der Laarse 1997*)
  - Adopted by *ICRU 58*

Dose to points

- SSDS basal dose or Mean Central Dose ICRU58
- Reference dose **90%** basal dose

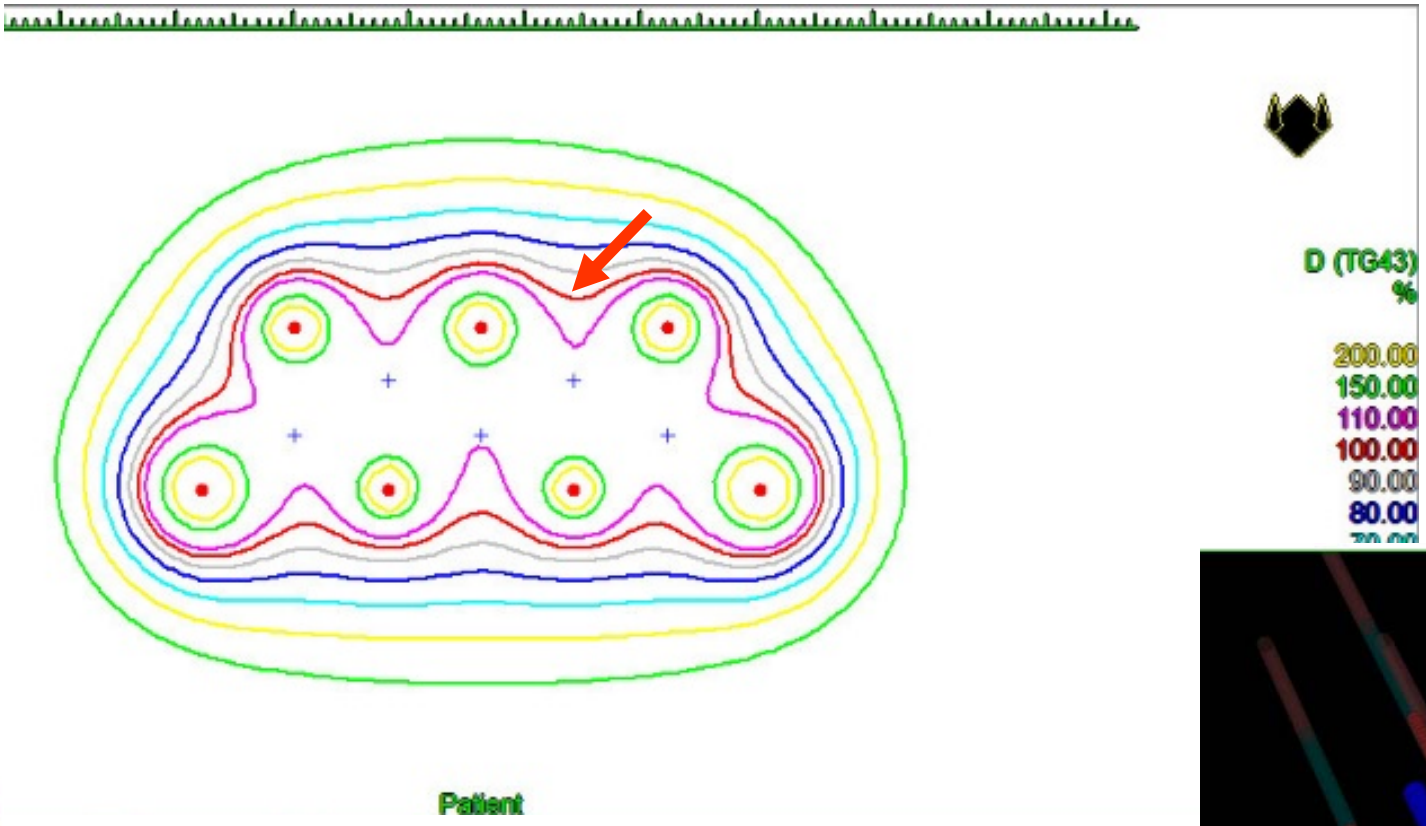

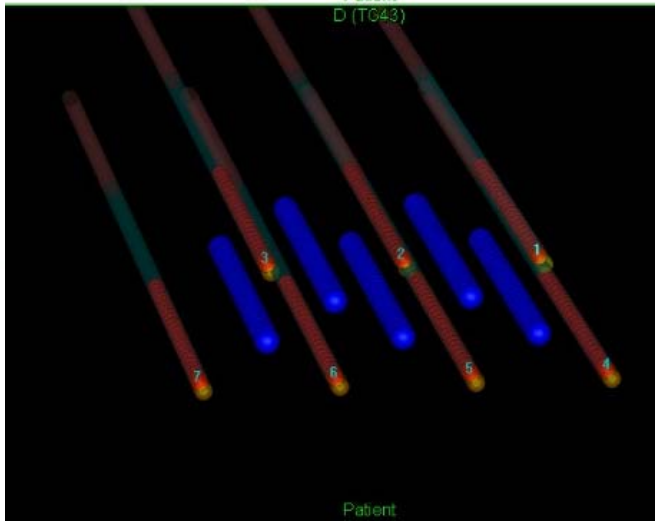

Dose to points

- Optimization using basal points
- Example: breast normalized 90%

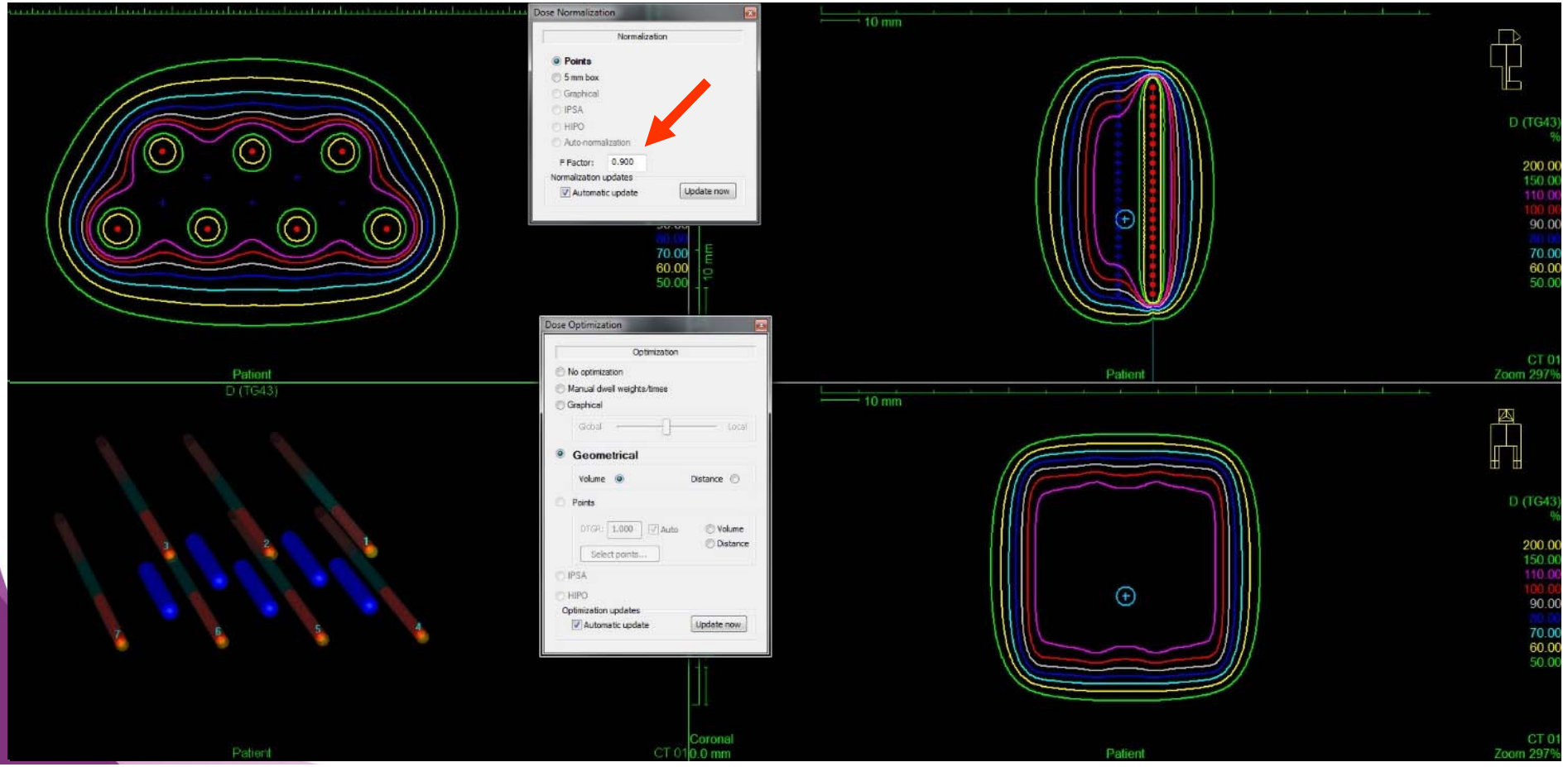

Dose to points

- Optimization using basal points
- Example: breast normalized 90%

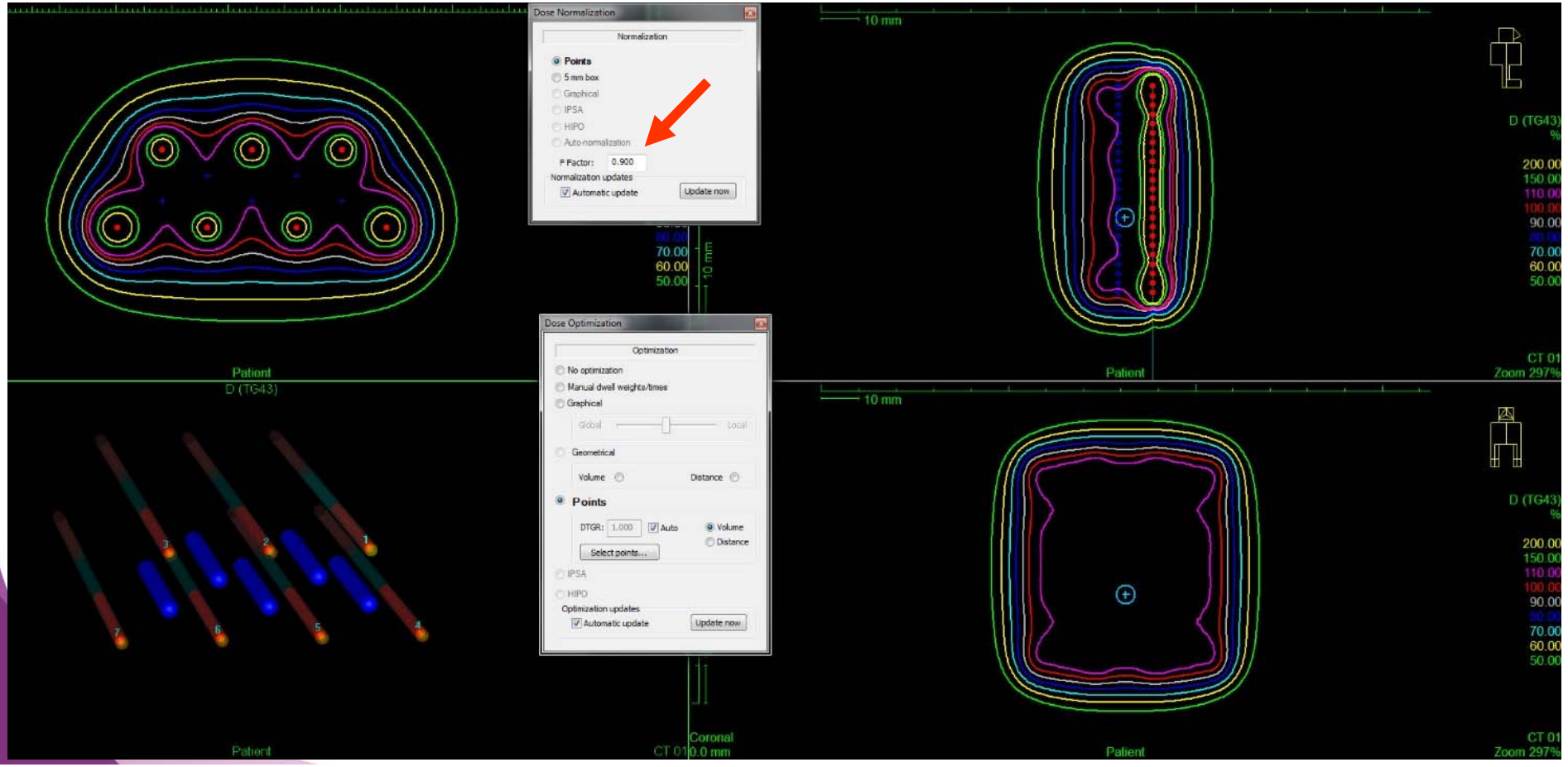

Dose to points

- Optimization using basal points
- Example: H&N normalized 90% plus graphical optimization

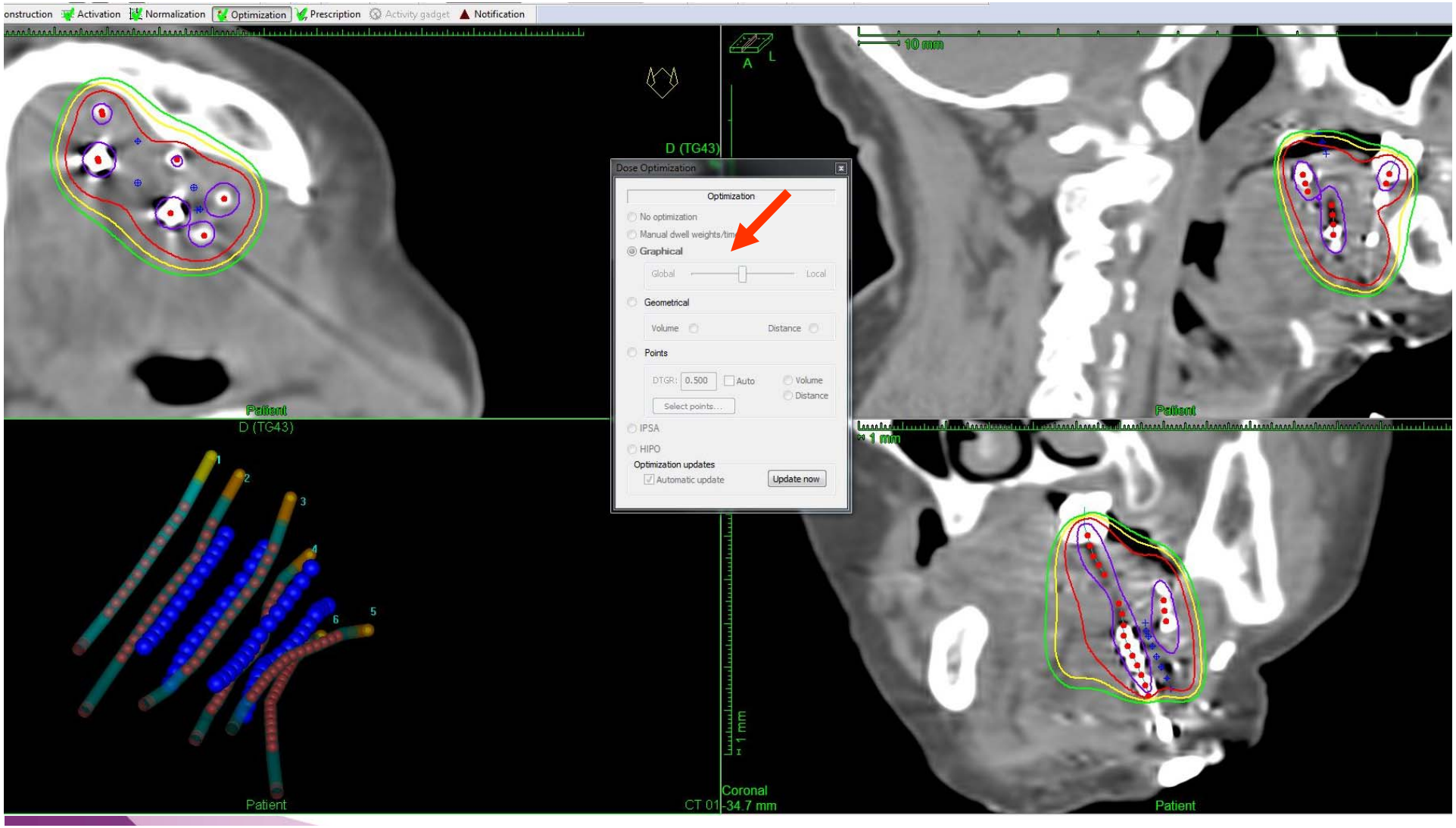

Dose to points

- Optimization using basal points
- Example: Vagina normalized 90% plus graphical optimization

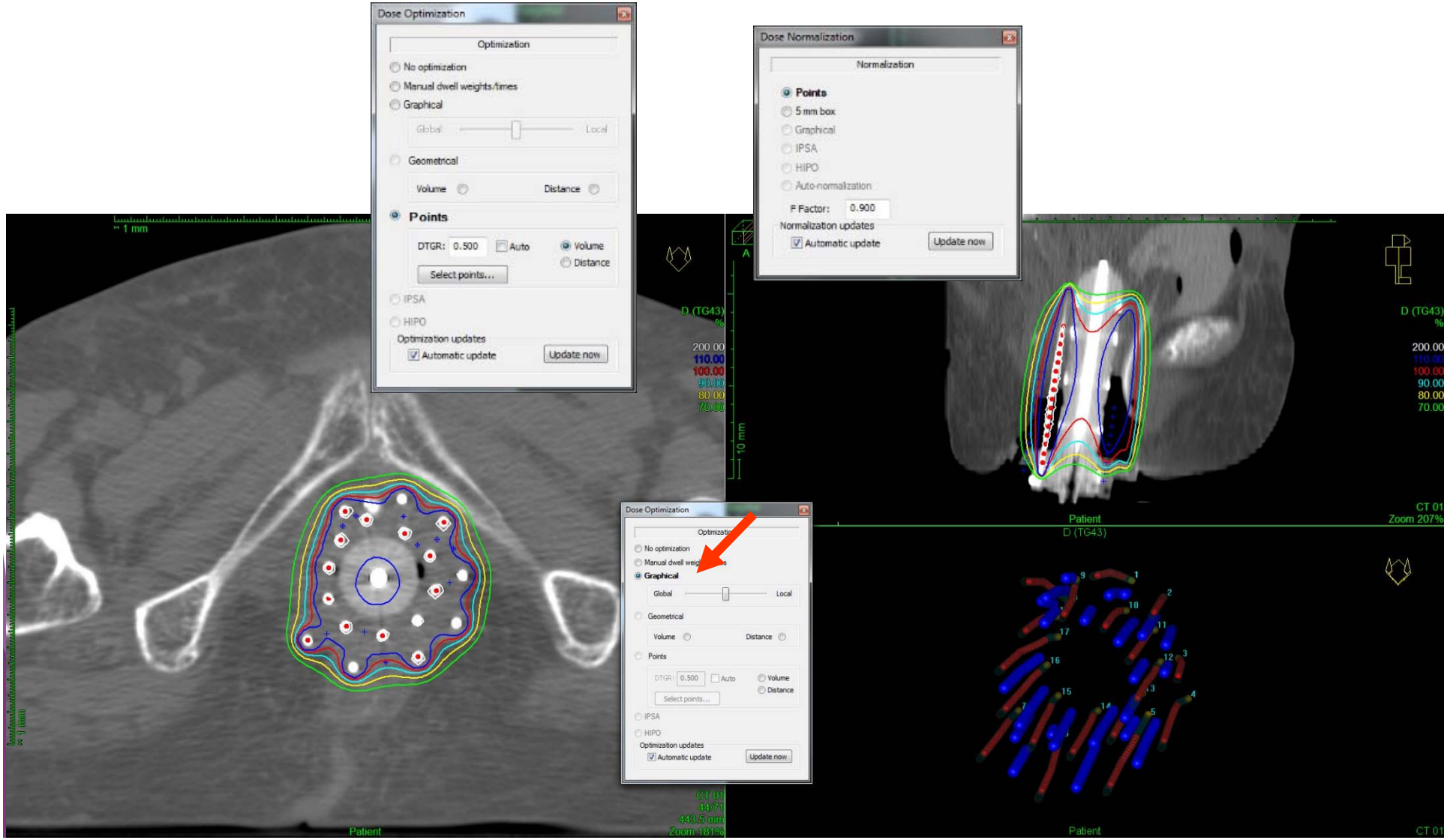

Dose to points

- Dose points at the CTV periphery to be used in HDR polynomial optimization

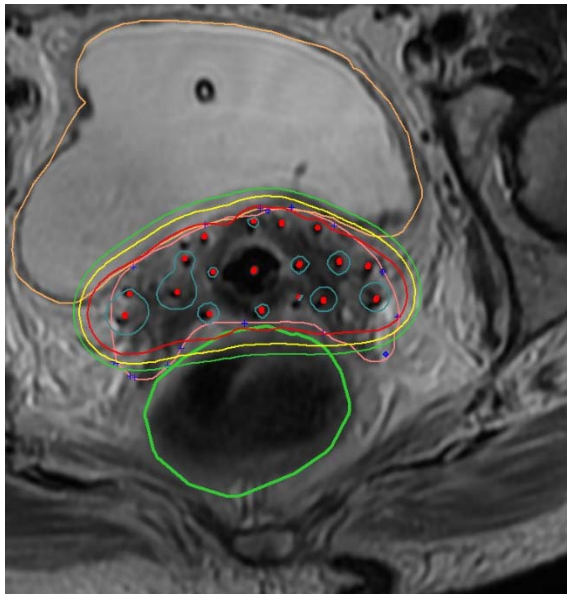

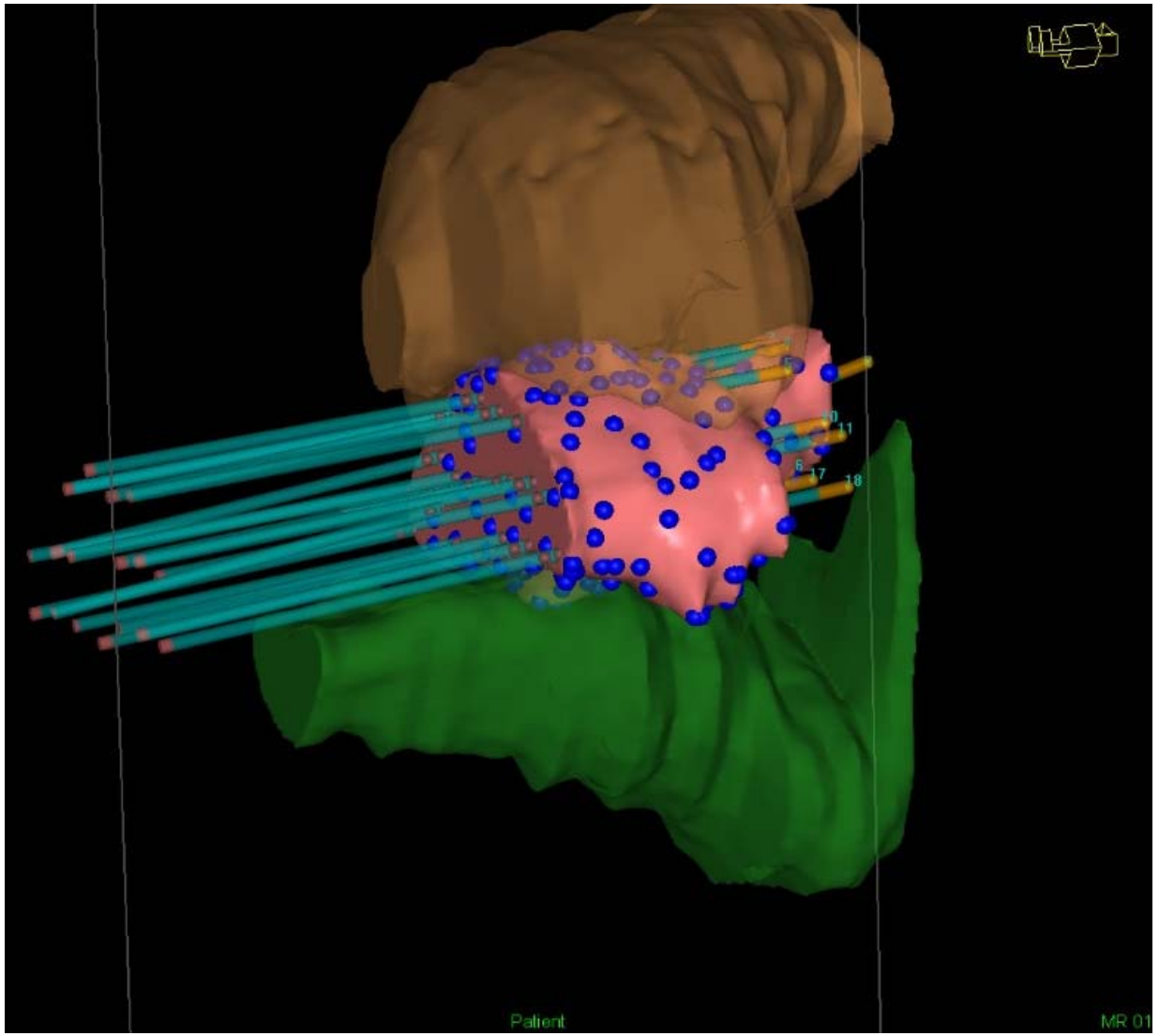

Dose to points

- Caution: Overdose volume (ie. V200%)

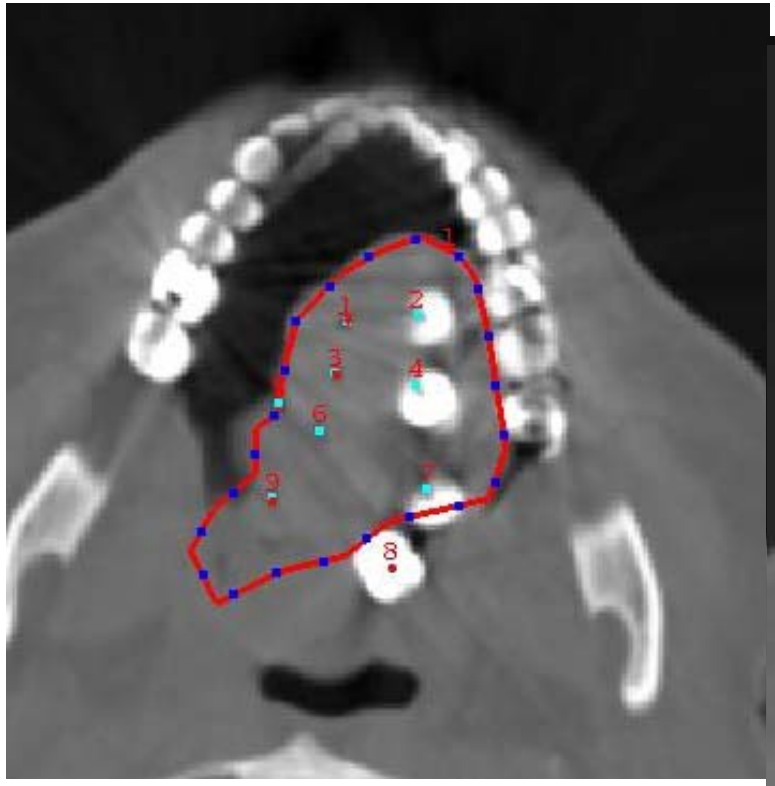

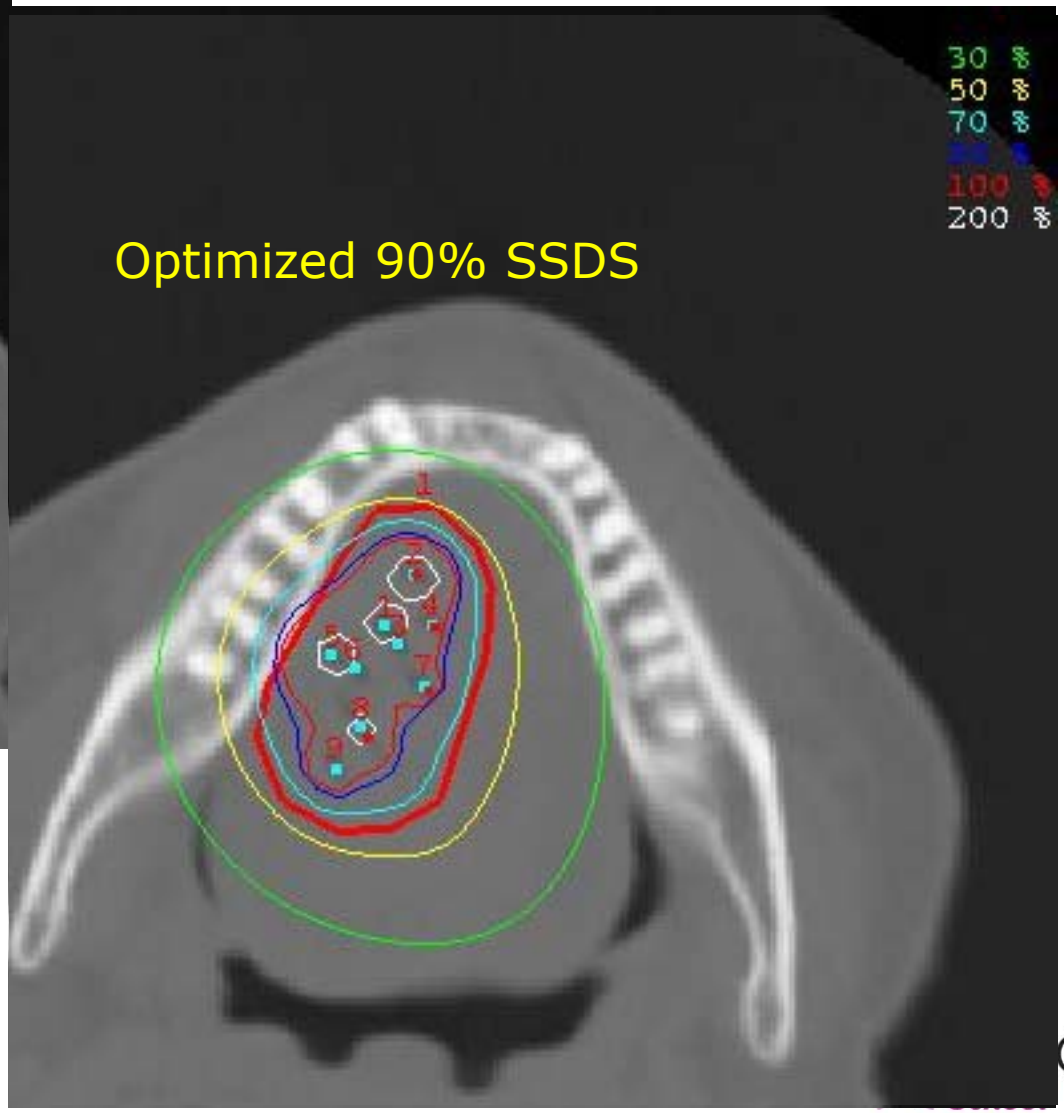

Dose to points

- Caution: Overdose volume (ie. V200%)

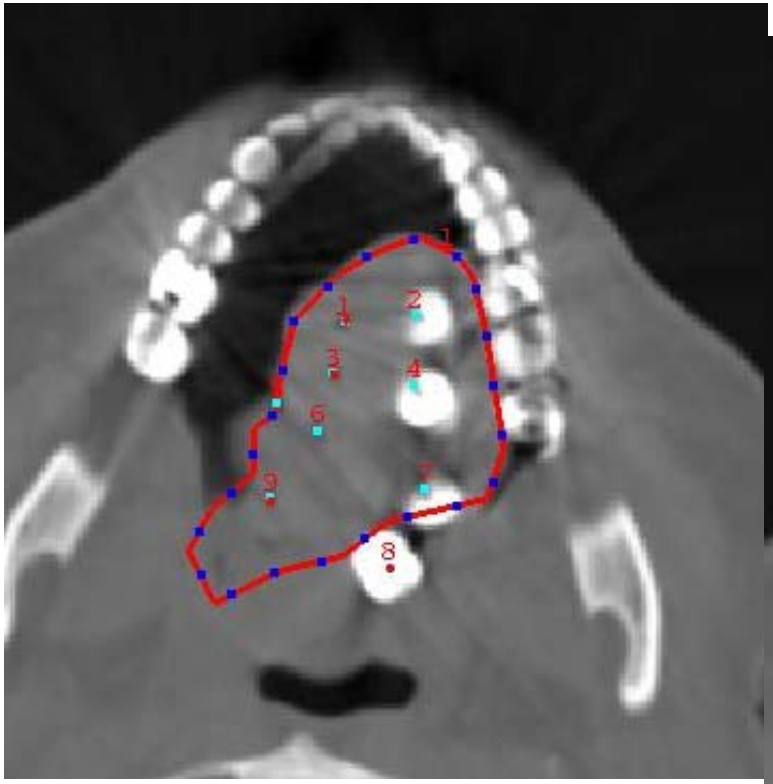

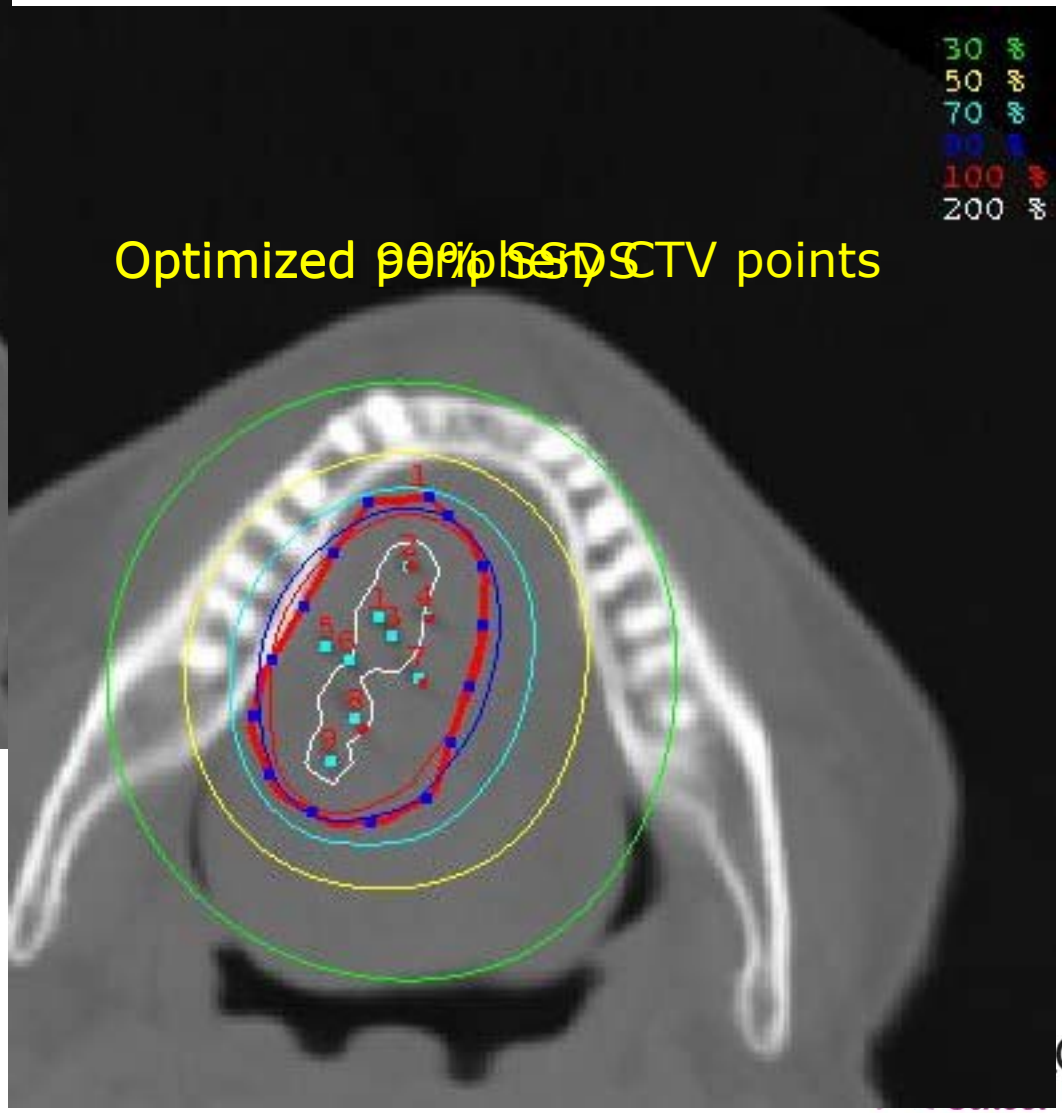

Dose to points

- Caution: Overdose volumen (ie. V200%)

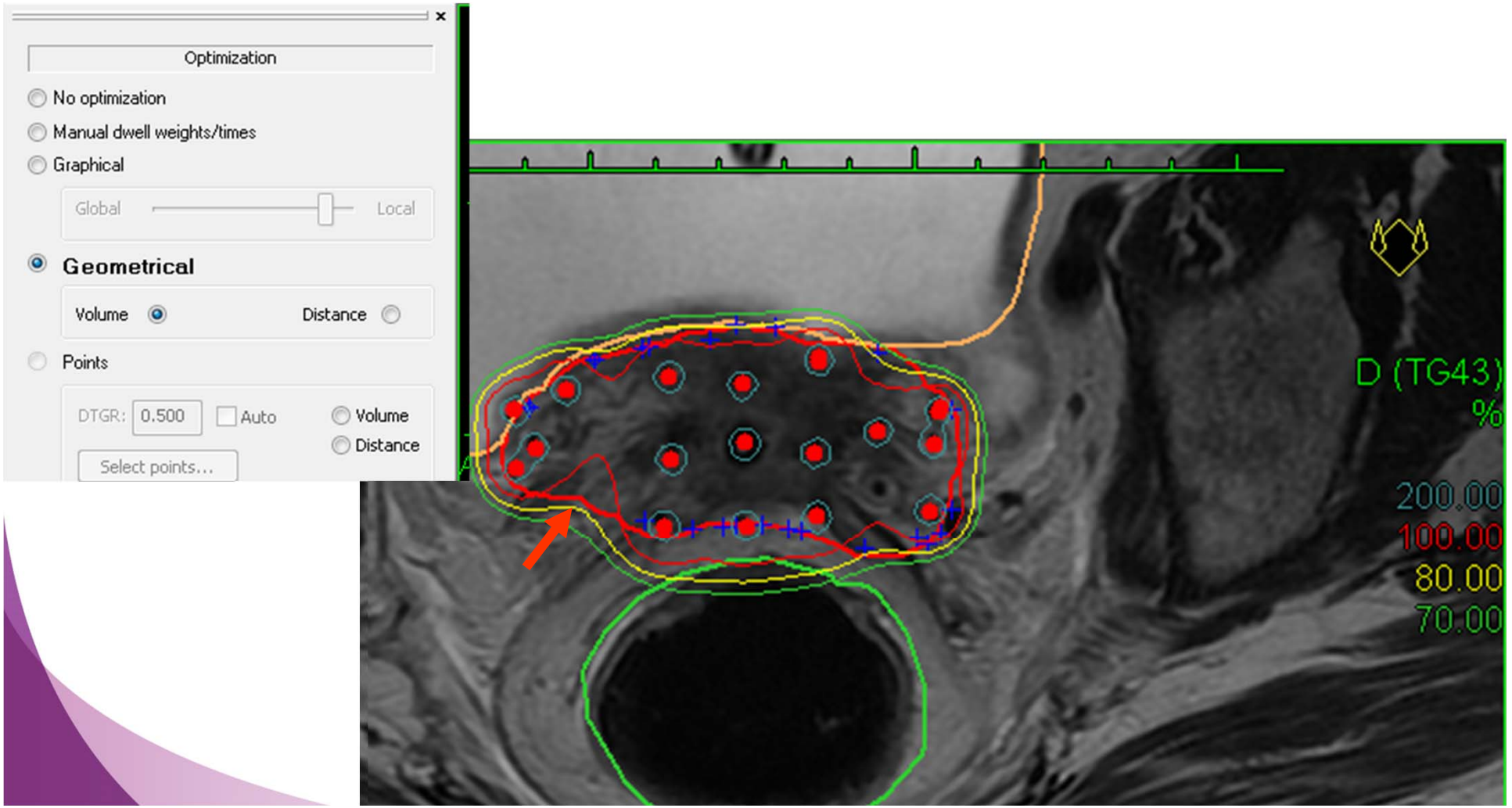

Dose to points

- Caution: Overdose volumen (ie. V200%)

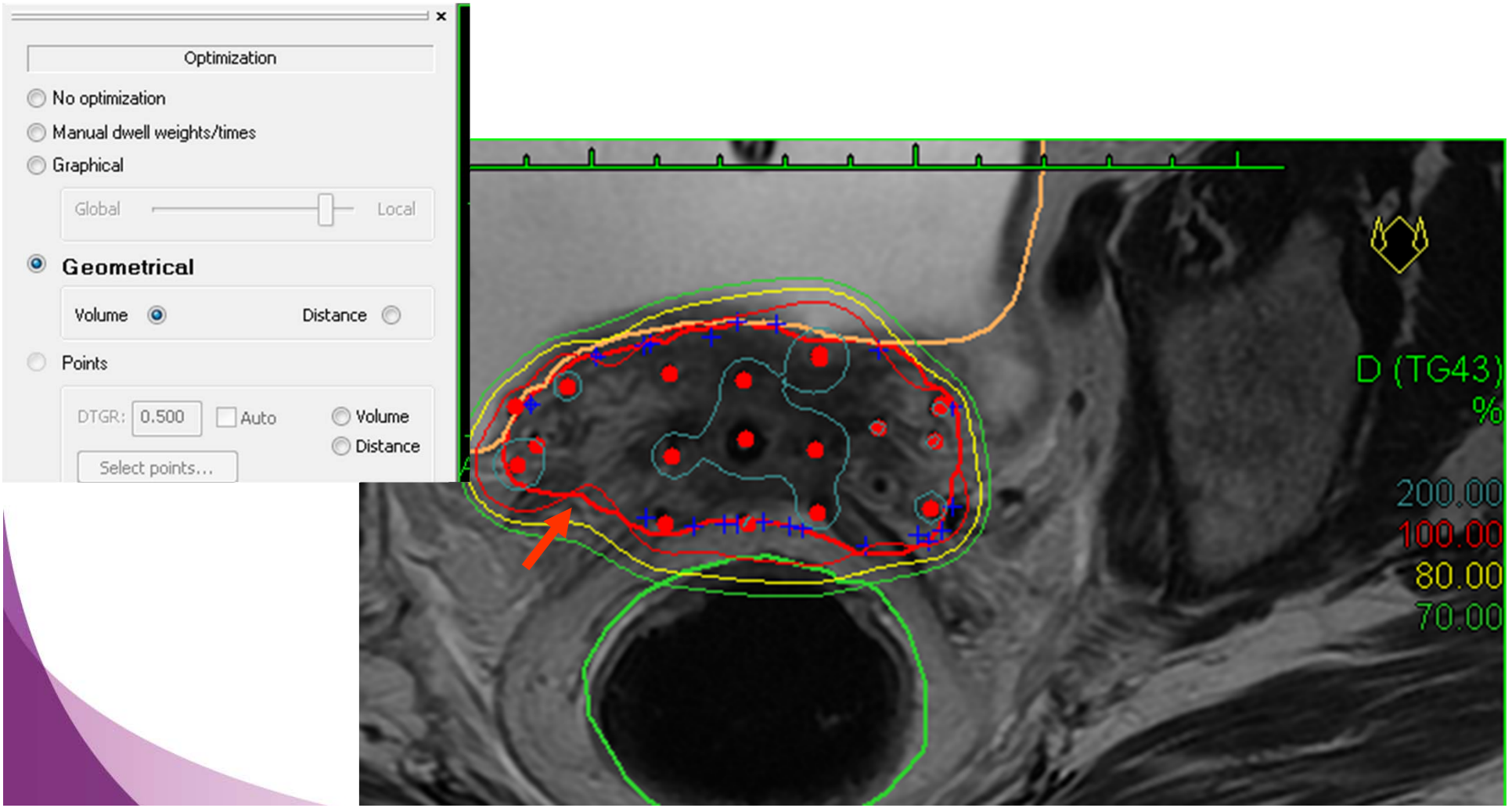

Dose to points

- Example: bronchus with prescription to a given distance

Scheme from GEC-ESTRO Handbook: Bronchus, Limberger et al 2017

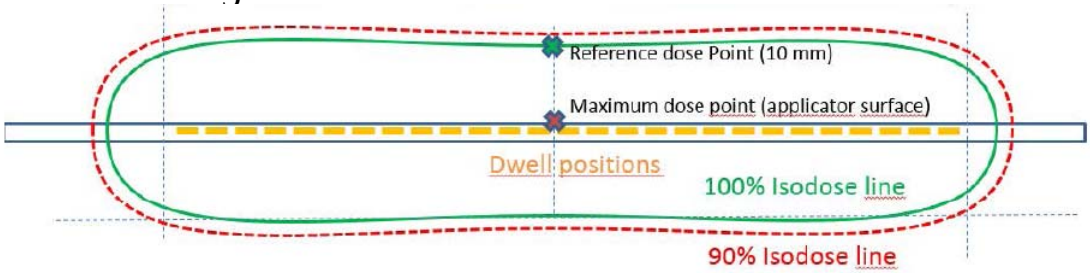

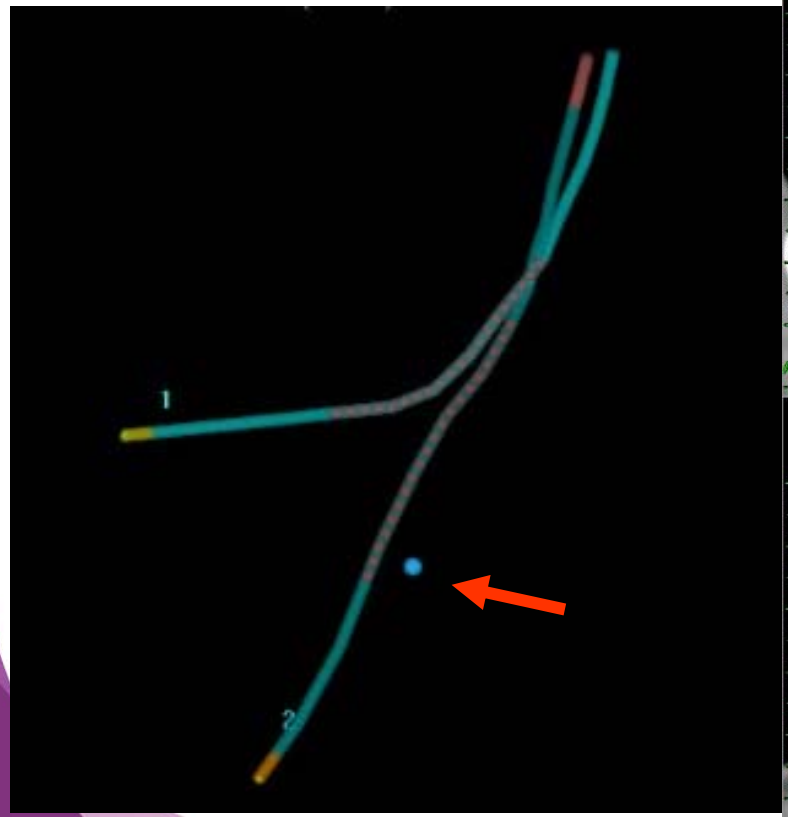

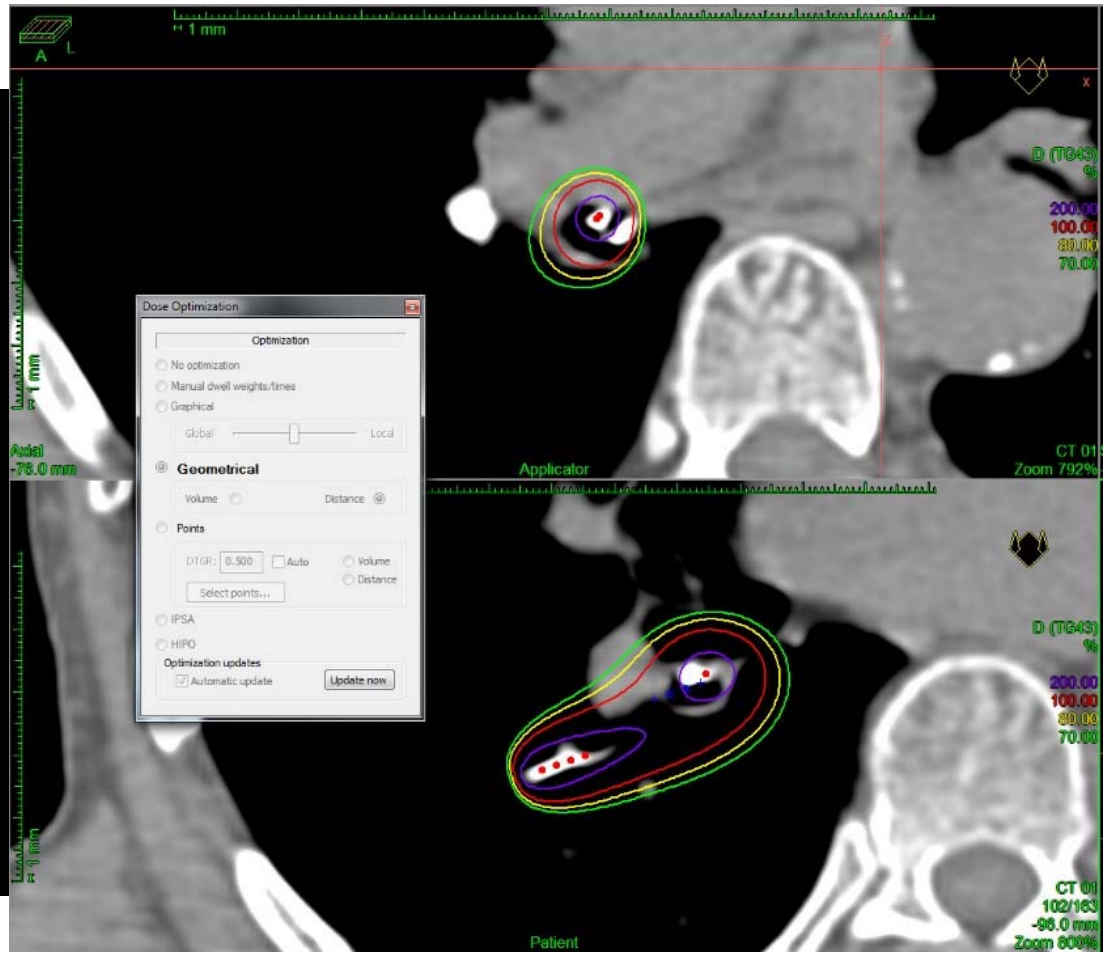

Dose to points

- Cervix Gyn ICRU89 points

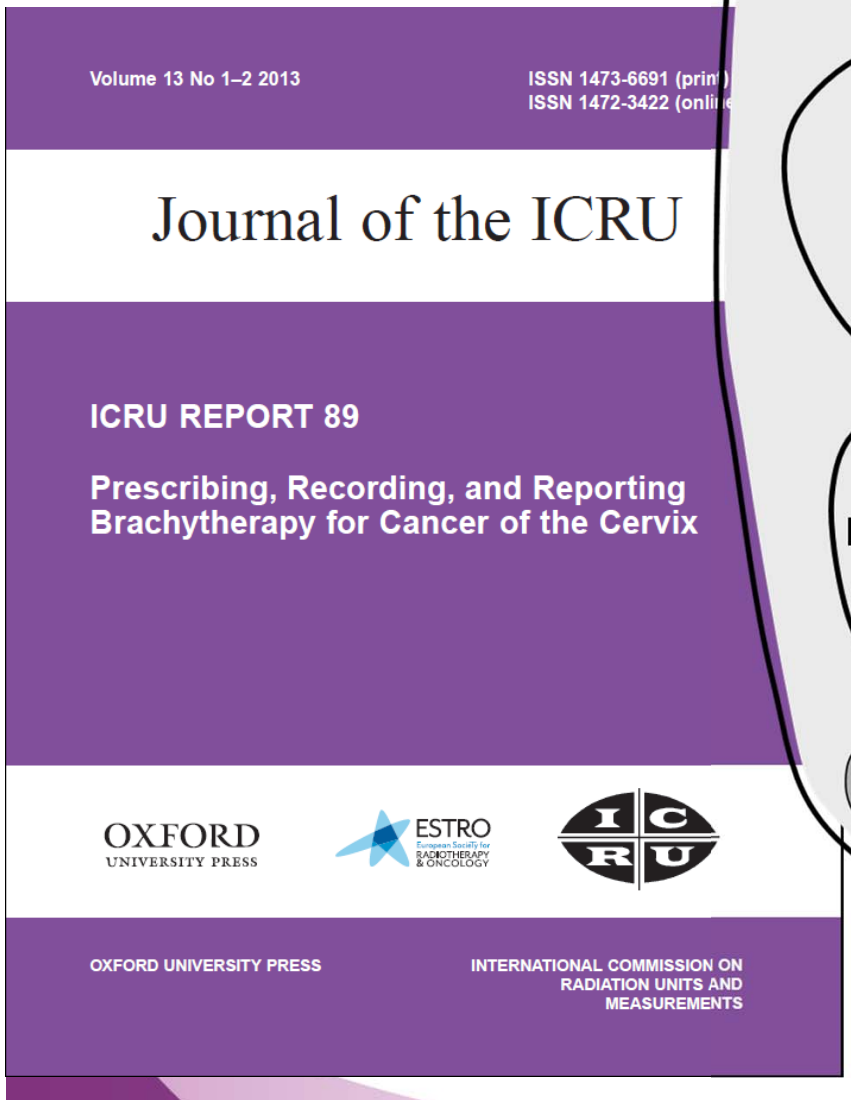

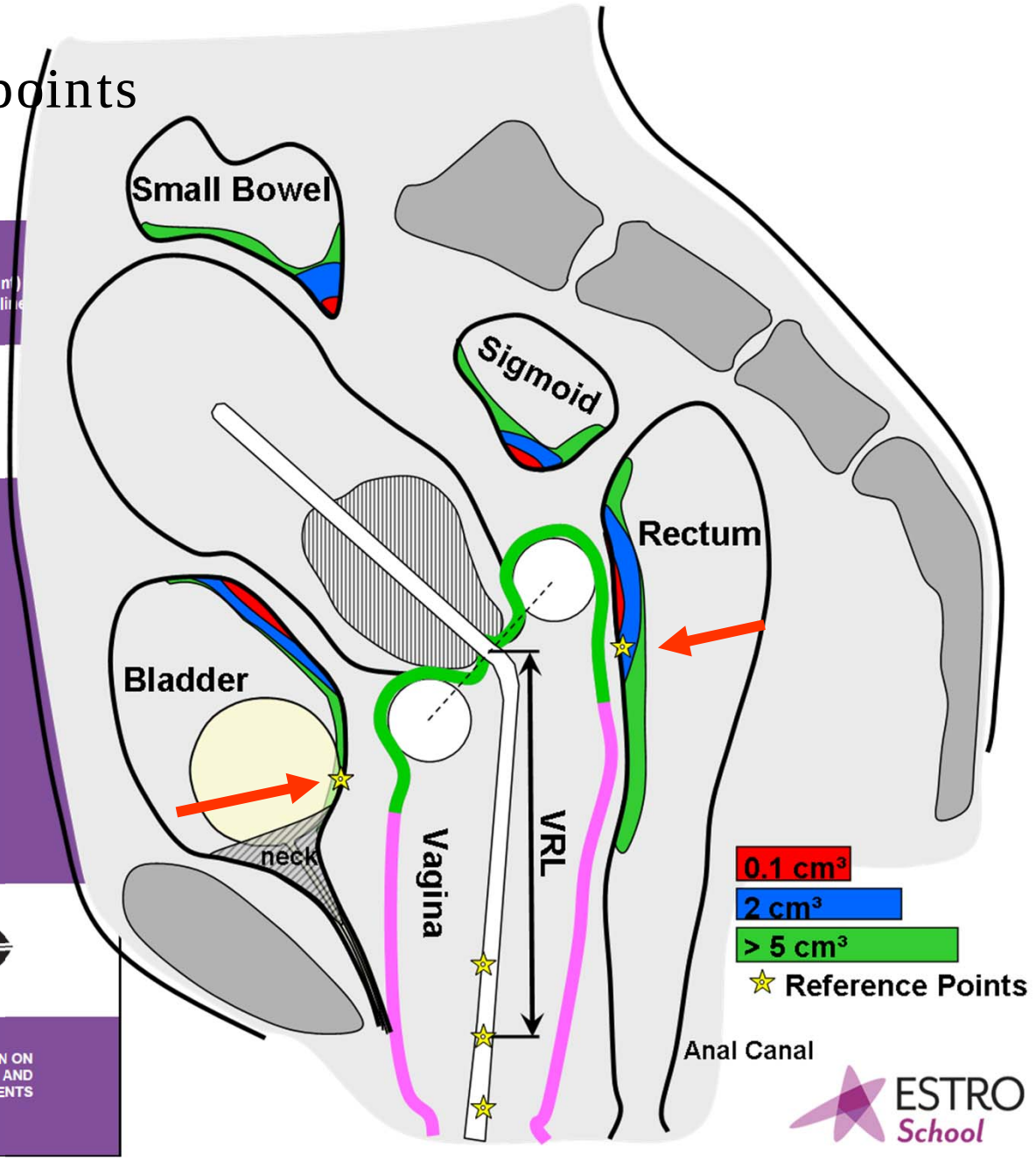

Dose to points

- Cervix Gyn ICRU89 points: vaginal points

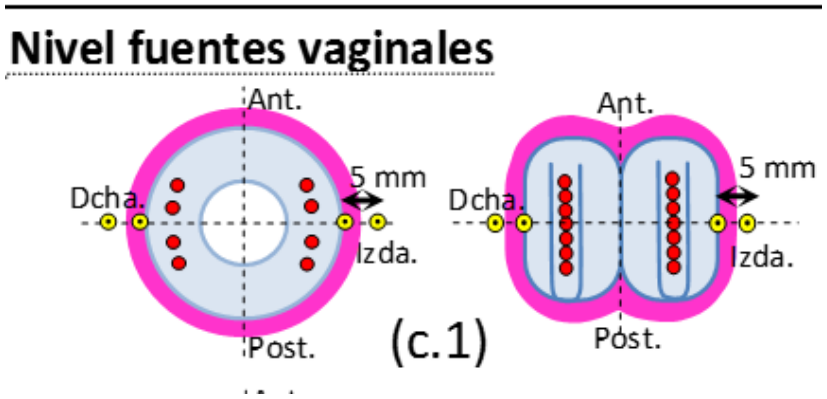

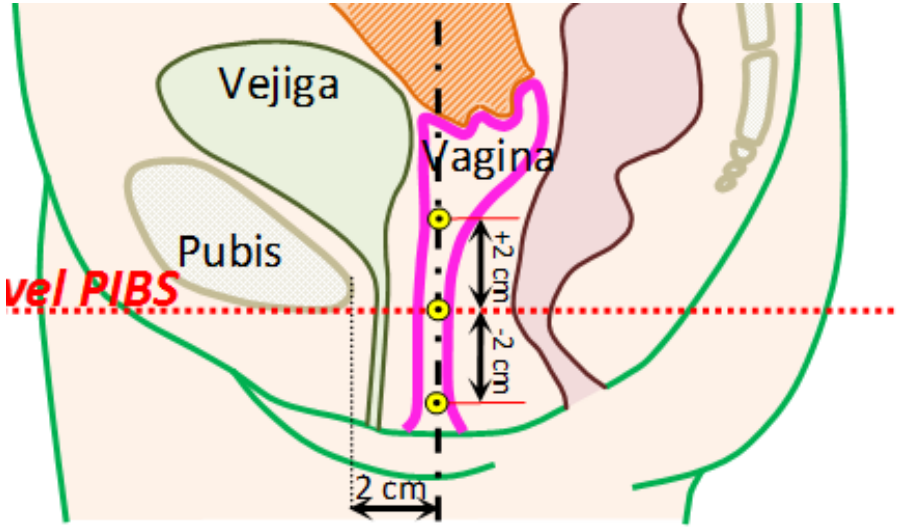

RTE

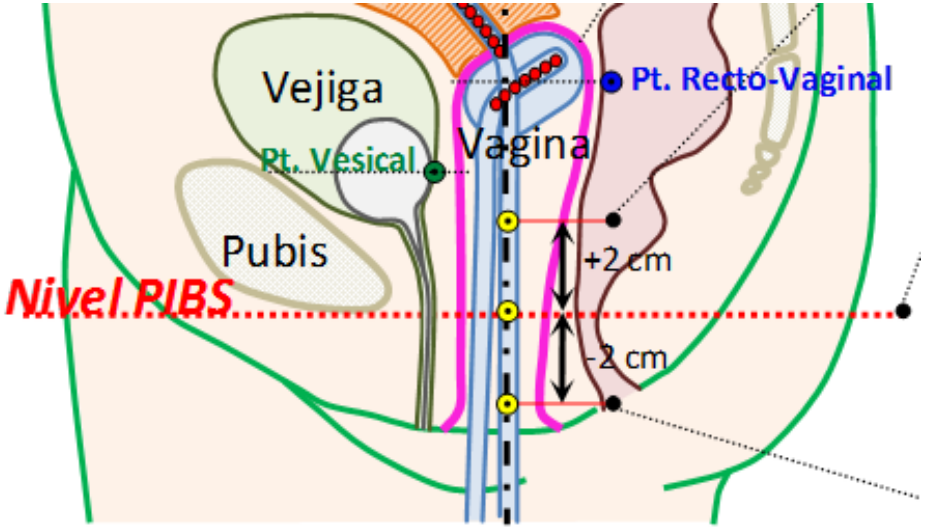

BT

Schemes from: Practical Recommendations of the Spanish Society of Medical Physics in MRI Based Cervix Brachytherapy. Perez-Calatayud, Colmenares, Garcia, Herreros, Pellejero, Richart, Tornero. In press

ESTRO School

Dose to points

- Cervix Gyn ICRU89 points: robustness evaluation

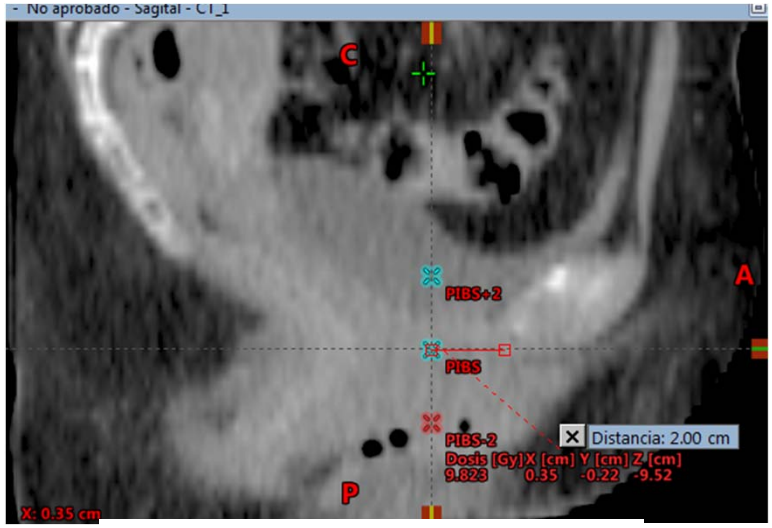

(Patient #5)	)
Point	Range (SD)
PIBS	51.3-53.2(0.8)
PIBS+2cm	69.8-115.8(19.1)
PIBS-2cm	46.7-47.5(0.3)
Vaginal top anterior	62.7-67.9(2.2)
Vaginal top anterior + 5mm	57.5-61.4(1.6)
Vaginal top posterior	82.1-89.5(3.0)
Vaginal top posterior + 5mm	72.1-78.3(2.5)
Vaginal top left	111.6-118.0(2.5)
Vaginal top left + 5mm	76.7-78.9(0.9)
Vaginal top right	108.6-122.8(5.7)
Vaginal top right + 5mm	74.6-79.6(2.0)

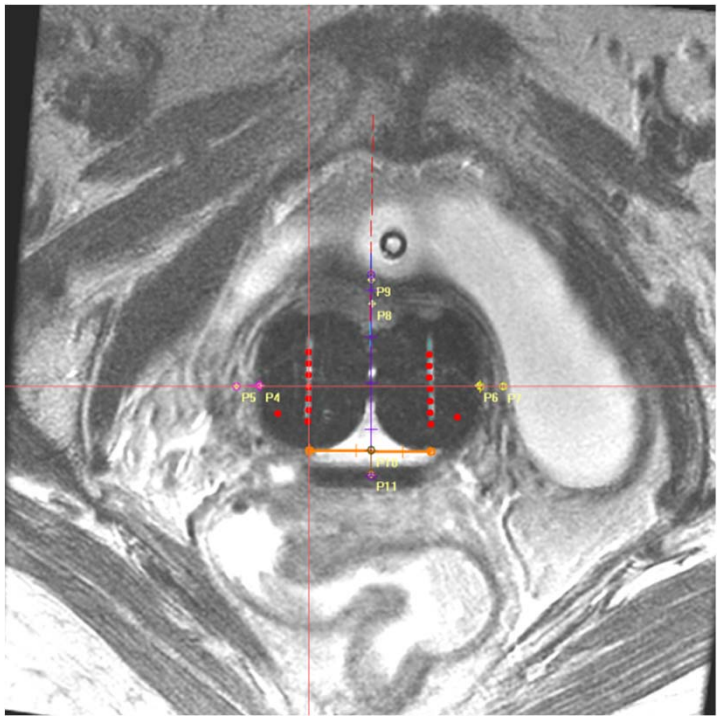

"Interobserver variability of vaginal dose points reporting in cervical cancer radiotherapy treatment". B. Ibañez, ESTRO 37. 2018

ESTRO School

Dose distribution

- CTV coverage (where under-over dose are), OAR sparing... Example: Prostate. Lobes coverage (mainly the affected one), some underdose in the anterior part is allowed, to see distribution of overdose volumes, how robust is the urethra sparing ...

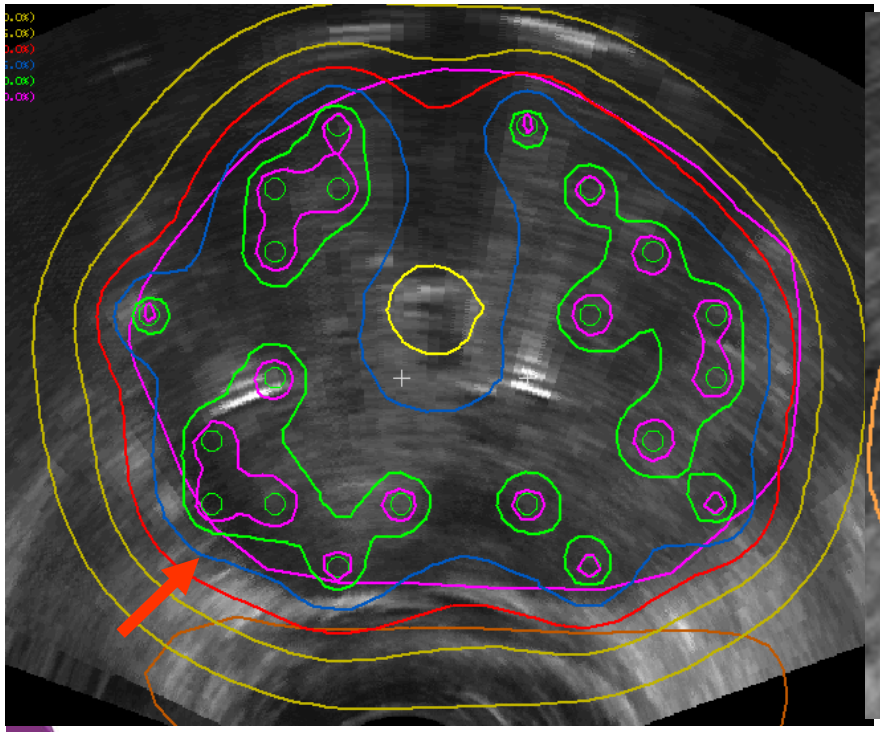

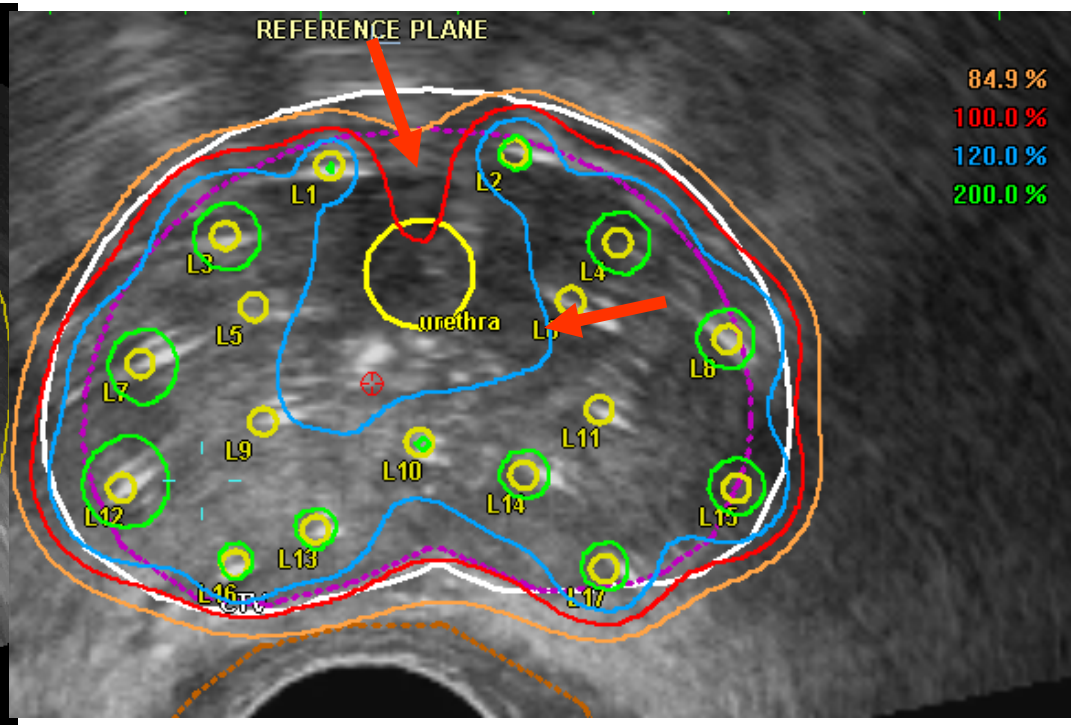

LDR I-125 seeds

HDR Ir-192

ESTRO School

DVH

- Typically absolute for OARs and relative for CTVs
- Dosimetric Recommendations (GEC-ESTRO & ABS & ICRU) based in DVH parameters
- OAR: organ or organ wall? Wall more realistic but high difficulty in contouring

DVH

- Dosimetric Recommendations based in DVH parameters

ESTRO-EAU-EORTC Salembier 2007, AAPM TG-137 Nath 2009

Prostate LDR

CTV $V_{100}\geq 95\%$, $D_{90}>100\%$, $V_{150}\leq 50\%$
Rectum: $D_{2cc}\leq 145$ Gy, $D_{0.1cc}<200$ Gy
Urethra: $D_{10}<150\%$, $D_{30}<130\%$

Postplan:
CTV-P and CTV-PM: $D_{90}, V_{100}, V_{150}, V_{200}, D_{100}$
Rectum: $D_{2cc}, D_{0.1cc}, V_{100}$
Urethra: $D_{10}, D_{0.1cc}, D_{30}, D_5$

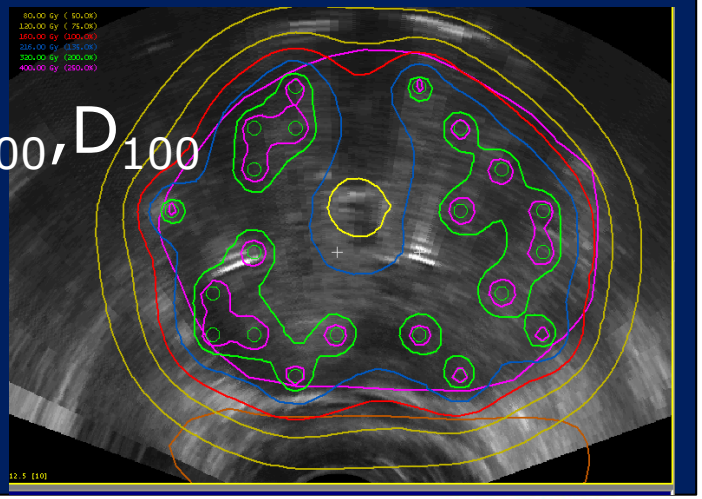

DVH

- Dosimetric Recommendations based in DVH parameters

GEC-ESTRO Hoskin 2013

Prostate HDR

CTV	D_{90}	≥ 100%
	V_{100}	≥ 95%
Rectum	D_{2cc}	≤ 75 Gy EQD_2
Urethra	$D_{0,1cc}$	≤ 120 Gy EQD_2
	D_{10}	≤ 120 Gy EQD_2
	D_{30}	≤ 105 Gy EQD_2

i i ERT + BT

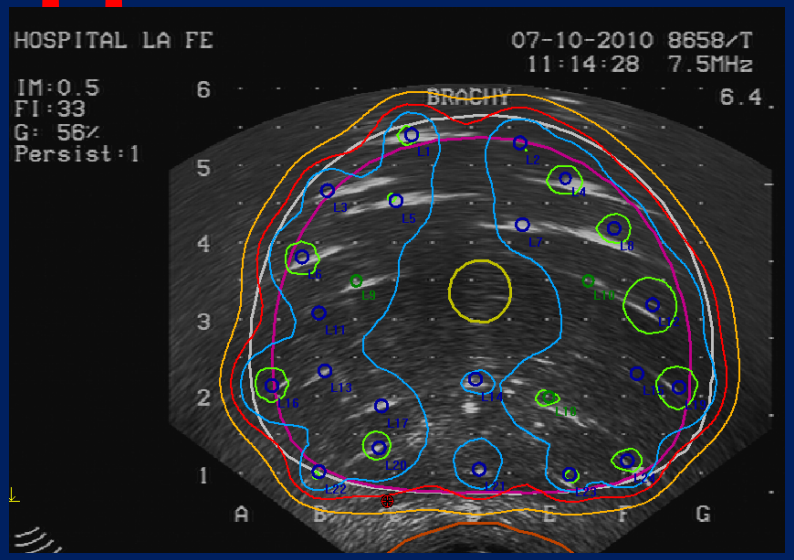

DVH

- Dosimetric Recommendations based in DVH parameters

ESTRO-ACROP Guideline Strnad 2018

Implant	$V_{PD} \leq 300cc$ $DNR \leq 0,35$
PTV	$V_{100} \geq 90\%$ $V_{150} < 65$ cc $V_{200} < 15$ cc $COIN \geq 0,65$
Skin *(5 mm shell)*	$D_{1cc} < 90\%$ $D_{0,2cc} < 100\%$
Rib	$D_{0,1cc} < 90\%$ $D_{1cc} < 80\%$

Breast HDR

Strnad 2018

DVH

- Dosimetric Recommendations based in DVH parameters

ICRU 89 2016

Level 2: *Advanced standard for reporting*
All that is reported in level 1 plus

Dose reporting for defined volumes
- $D_{98\,\%}$, $D_{90\,\%}$, $D_{50\,\%}$ for the CTV_{HR}
- ($D_{98\,\%}$, $D_{90\,\%}$ for the CTV_{IR} if used for prescription)
- $D_{98\,\%}$ for GTV_{res}
- $D_{98\,\%}$ for pathological lymph nodes

Dose reporting OARs
- Bladder reference-point dose
- $D_{0.1cm^3}$, D_{2cm^3} for the sigmoid
- D_{cm^3} for the bowel
- Intermediate- and low-dose parameters for the bladder, rectum, sigmoid, and bowel (*e.g.*, $V_{15\,Gy}$, $V_{25\,Gy}$, $V_{35\,Gy}$, $V_{45\,Gy}$, or $D_{98\,\%}$, $D_{50\,\%}$, $D_{2\,\%}$)
- Vaginal point doses at level of sources (lateral at 5 mm)[a]
- Lower and mid-vagina doses (PIBS, PIBS ± 2 cm)[a]

[a]Surrogate points for volumetric vaginal-dose assessment.

Cervix GYN

ERT + BT

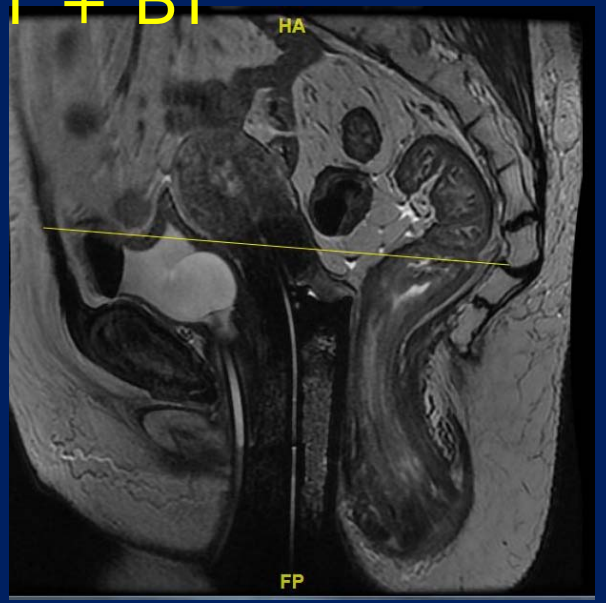

OAR total or wall?

	Wall	Total	deviation
Volume	22 cm³	34 cm³	
D_{10cc}	40.9 Gy	52.0 Gy	21.4 %
D_{5cc}	71.6 Gy	79.2 Gy	9.6 %
D_{2cc}	115.7 Gy	117.7 Gy	1.7 %
D_{1cc}	140.3 Gy	141.6 Gy	0.9 %
$D_{0.1cc}$	206.7 Gy	206.0 Gy	-0.4 %

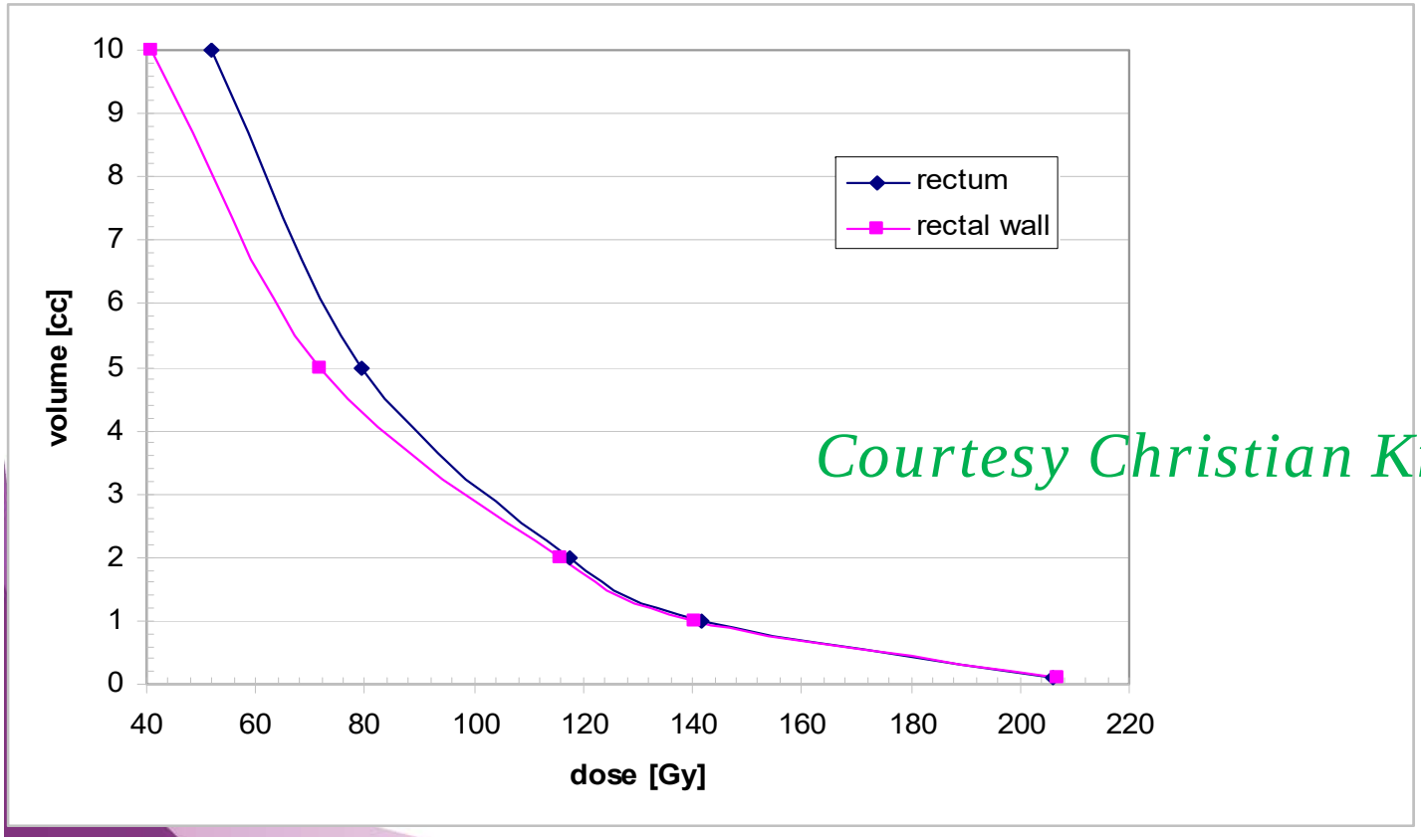

Courtesy Christian Kirisits ABP 2016

ESTRO School

DVH

Volume sampling and bar width

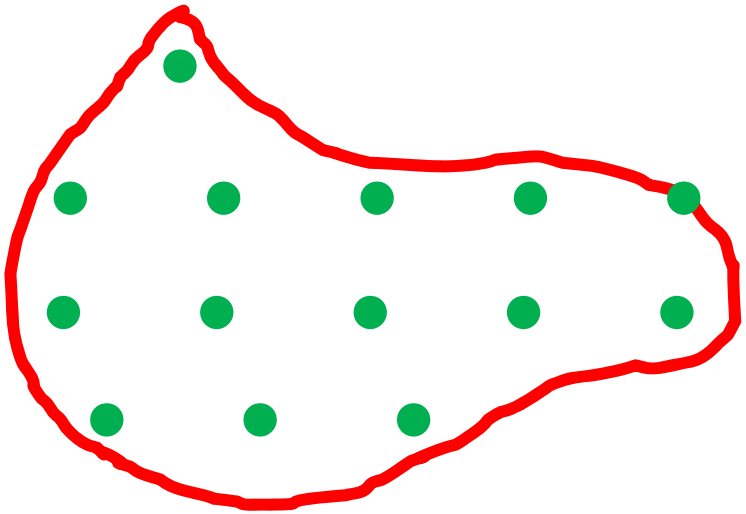

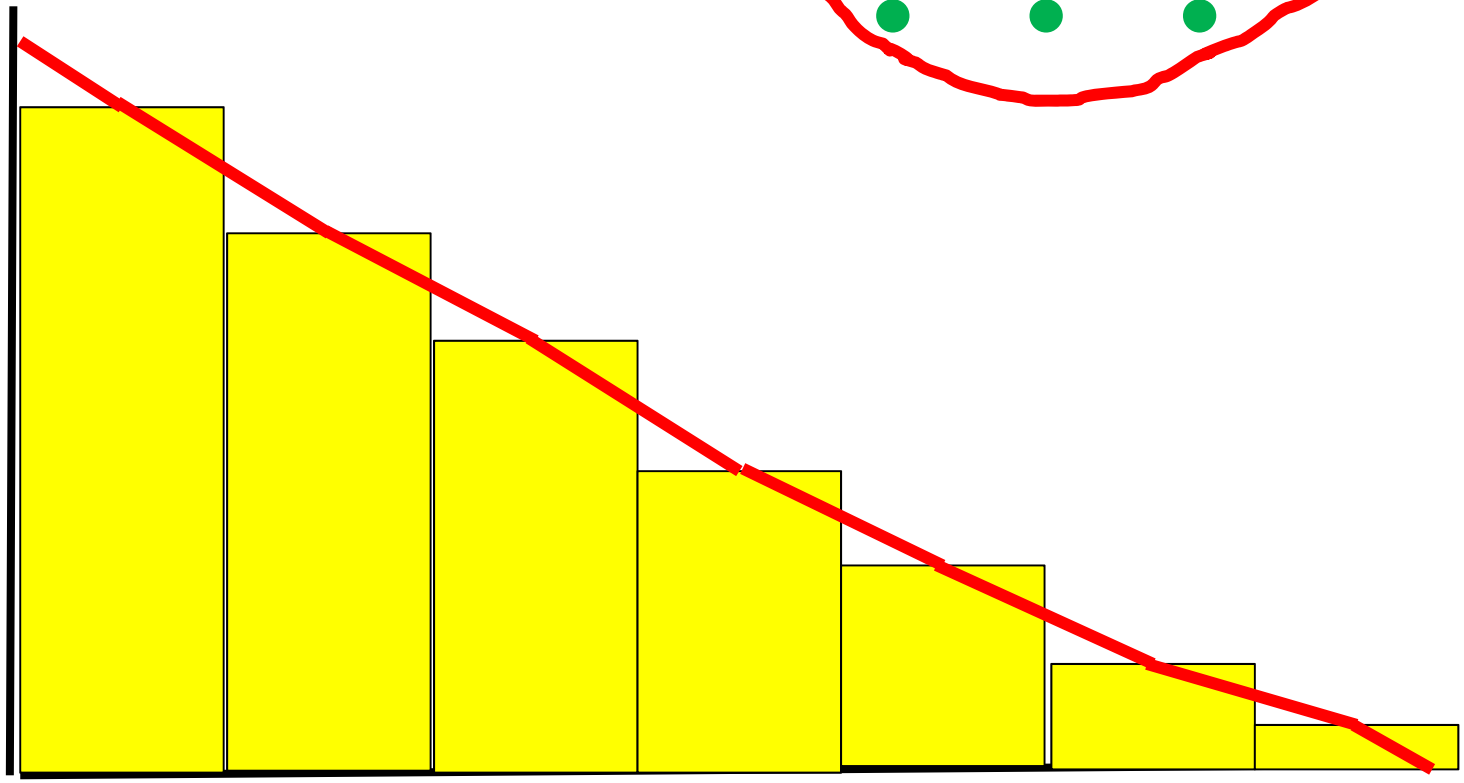

ESTRO School

DVH

Volume sampling and bar width

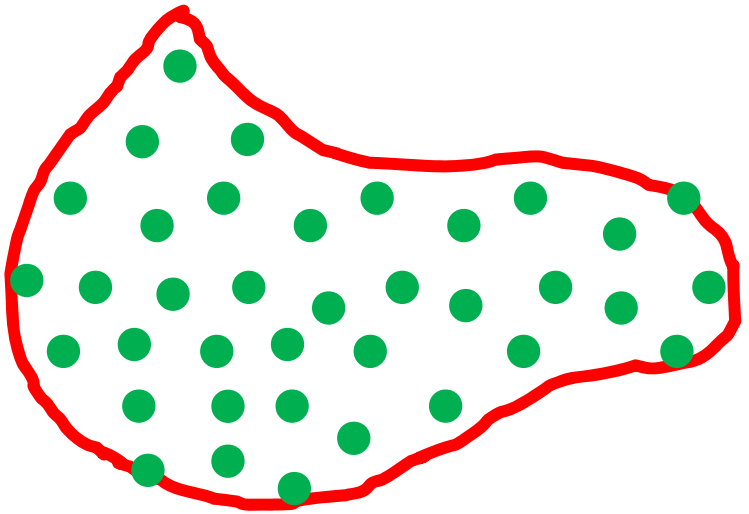

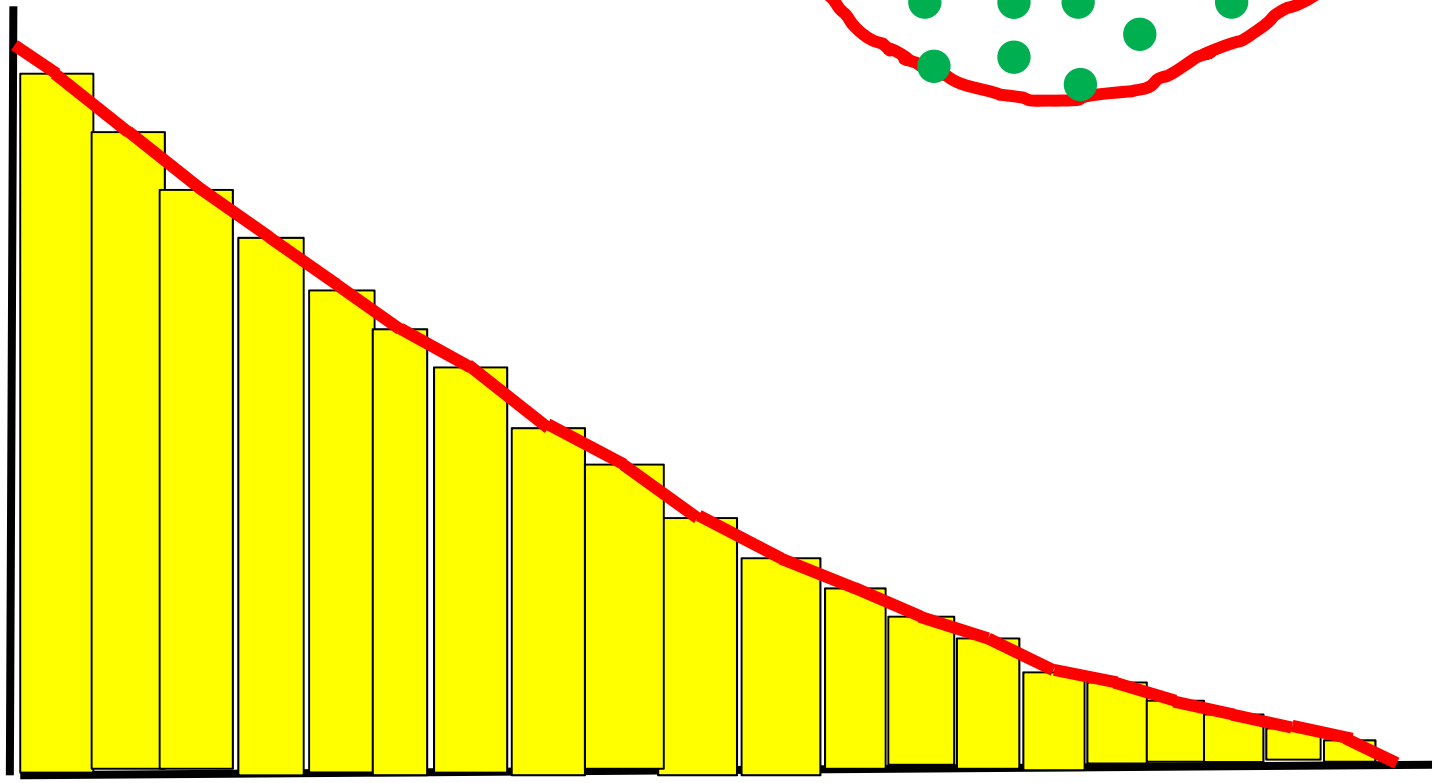

ESTRO School

DVH

ABS 2012

Volume sampling and bar width

For treatment planning systems that use sample dose points, a minimum of 5,000–10,000 sample points should be used for the calculation of each cumulative dose–volume histogram. The planner must ensure that

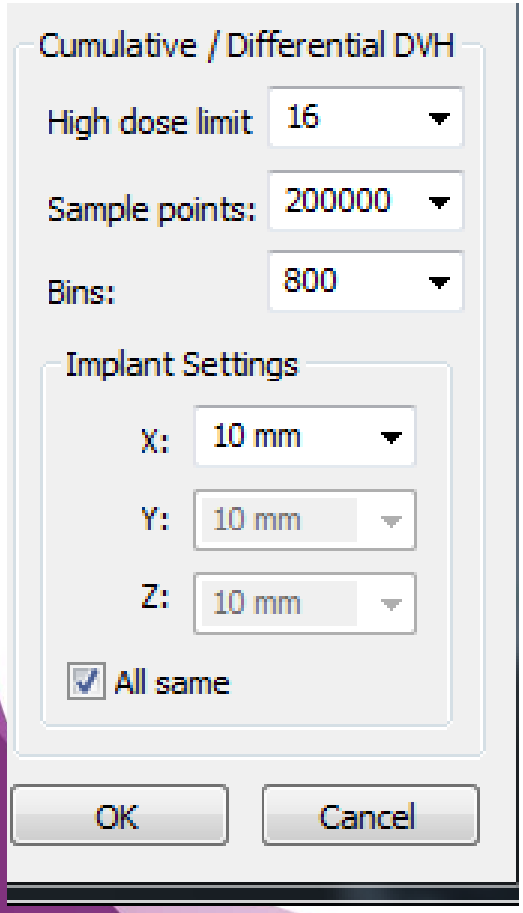

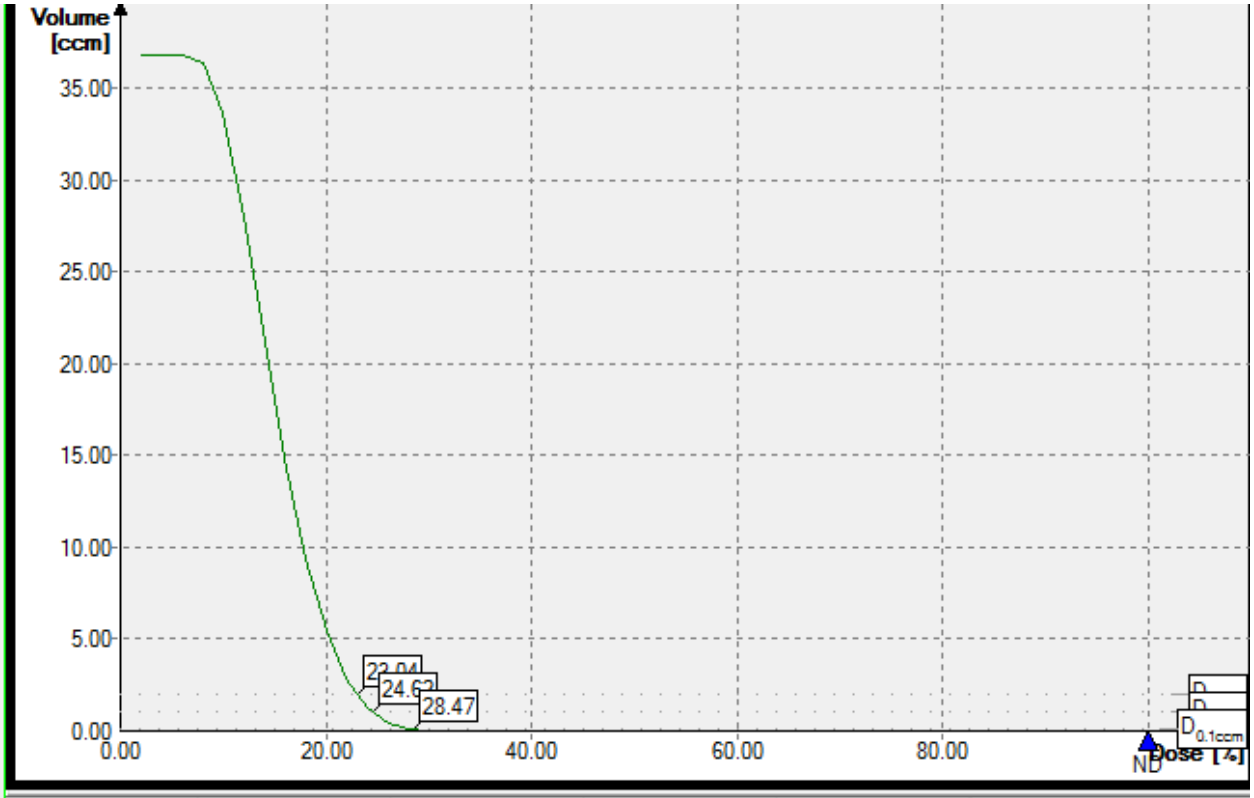

ROI	Dose [%]	Dose [Gy]	Volume [%]	Volume [ccm]
Rectum	28.47	1.9872	0.27	**0.10**
Rectum	24.62	1.7183	2.72	**1.00**
Rectum	23.04	1.6079	5.44	**2.00**

Indexes

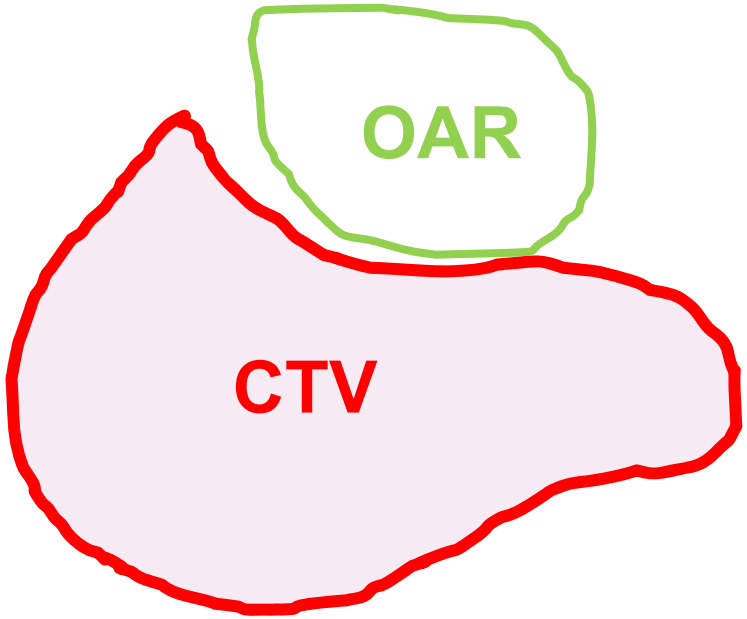

Indexes

PD —

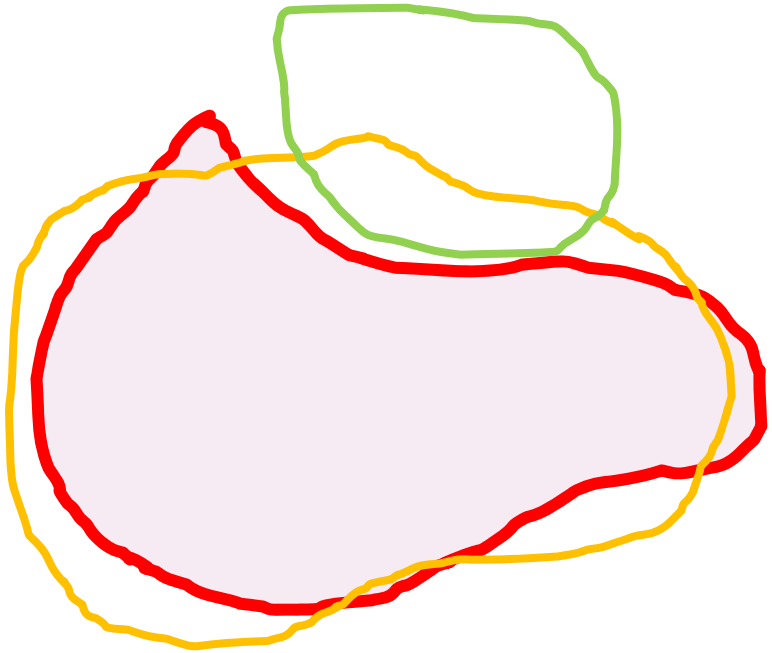

Indexes

PD —

1.5 PD —

2 PD —

ESTRO School

Indexes

PD —

1.5 PD —

2 PD —

$$DNR = \frac{V_{1.5PD}}{V_{PD}}$$

- Dose-Non-Uniformity Ratio
- Independent of CTV-OAR
- Lower DNR more homogeneous is
- Also Dose-Homogeneity-Index

$$DHI = \frac{V_{PD} - V_{1.5PD}}{V_{PD}} = 1 - DNR$$

ESTRO School

Indexes

PD —

1.5 PD —

2 PD —

$$OI = \frac{V_{2PD}}{V_{CTV}}$$

- Overdose-Volume-Index
- Characterize the dose homogeneity

Indexes

PD or V_{REF} ——

PTV_{REF}

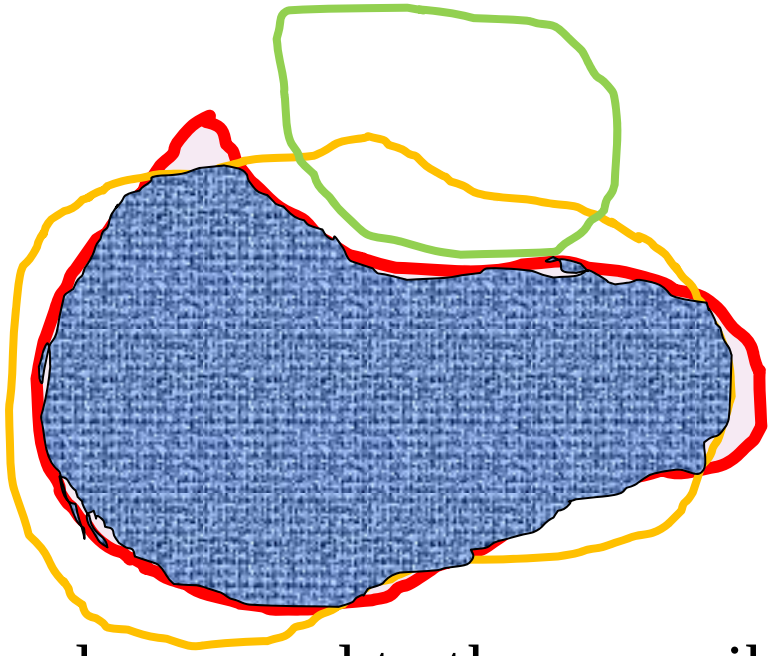

Volume of PTV-CTV that receives a dose equal to the prescribed dose or higher

- Conformity-Index
- Characterize the dose homogeneity

ESTRO School

Indexes

PD or V_{REF} ——

PTV_{REF}

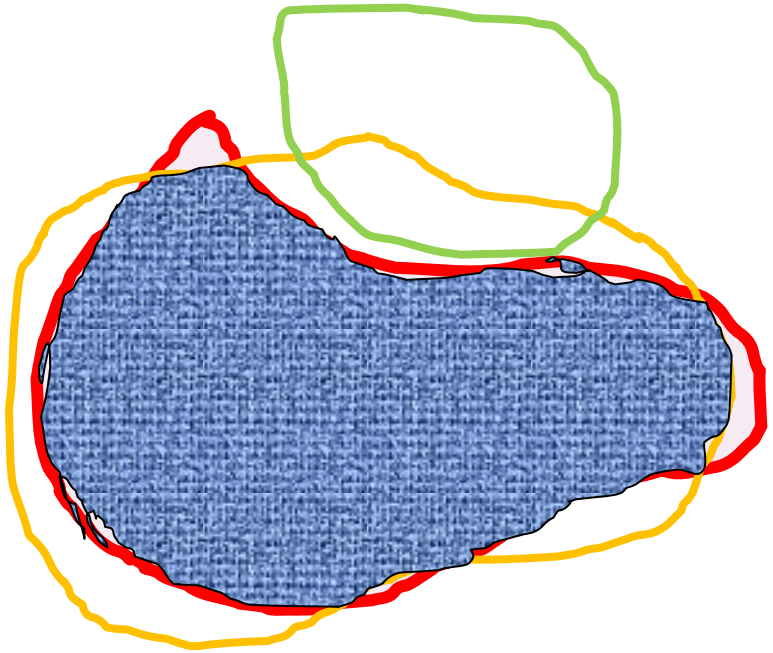

$$c_1 = \frac{PTV_{ref}}{PTV} \qquad c_2 = \frac{PTV_{ref}}{V_{ref}}$$

$$c_3 = \prod_{i=1}^{N_{OARs}} \left[1 - \frac{V_{OAR,i}(D > D_{limit,i})}{V_{OAR,i}} \right]$$

Baltas IJROBP 1998

ESTRO School

Indexes

COIN = c_1 x c_2 x c_3

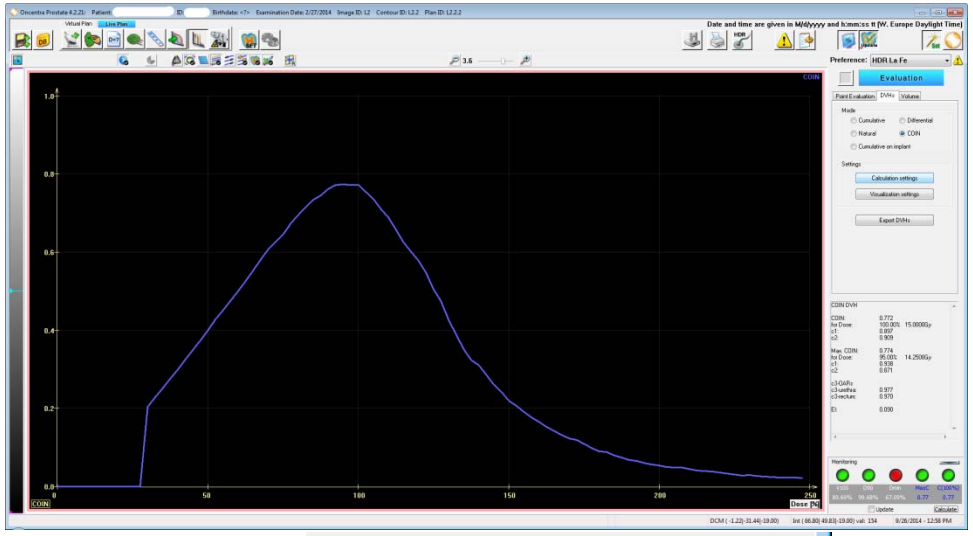

$$c_1 = \frac{PTV_{ref}}{PTV} \qquad c_2 = \frac{PTV_{ref}}{V_{ref}}$$

$$c_3 = \prod_{i=1}^{N_{OARs}} \left[1 - \frac{V_{OAR,i}(D > D_{limit,i})}{V_{OAR,i}} \right]$$

Baltas IJROBP 1998

- Conformity-Index
- Most conformal when the COIN is maximal and is as close to 1 as possible

ESTRO School

Biology

- Cervix Gyn recommended doses CTV-OARs are specified in EQD2 (*Rec GEC-ESTRO* and *ICRU 89*)
- Combining ERT with BT (typically 46-50 Gy ERT plus 2 app with 2 fx/app 7 Gy nominal)
- EQD2 CTV-OAR optimization is not included in current versions of TPSs
- In clinical practice, it is evaluated with an external spreadsheet

- Brief illustration of the Cervix GYN clinical procedure (H La Fe)

EMBRACE II v1

Tanderup, Pötter, Lindegaard, Kirisits, et al

Target	D90 CTV_{HR} $EQD2_{10}$	D98 CTV_{HR} $EQD2_{10}$	D98 GTV_{res} $EQD2_{10}$	D98 CTV_{IR} $EQD2_{10}$	Point A $EQD2_{10}$
Planning Aims	> 90 Gy < 95 Gy	> 75 Gy	>95 Gy	> 60 Gy	> 65 Gy
Limits for Prescribed Dose	> 85 Gy	-	>90 Gy	-	-
OAR	Bladder D_{2cm^3} $EQD2_3$	Rectum D_{2cm^3} $EQD2_3$	Recto-vaginal point $EQD2_3$	Sigmoid D_{2cm^3} $EQD2_3$	Bowel D_{2cm^3} $EQD2_3$
Planning Aims	< 80 Gy	< 65 Gy	< 65 Gy	< 70 Gy*	< 70 Gy*
Limits for Prescribed Dose	< 90 Gy	< 75 Gy	< 75 Gy	< 75 Gy*	< 75 Gy*

School

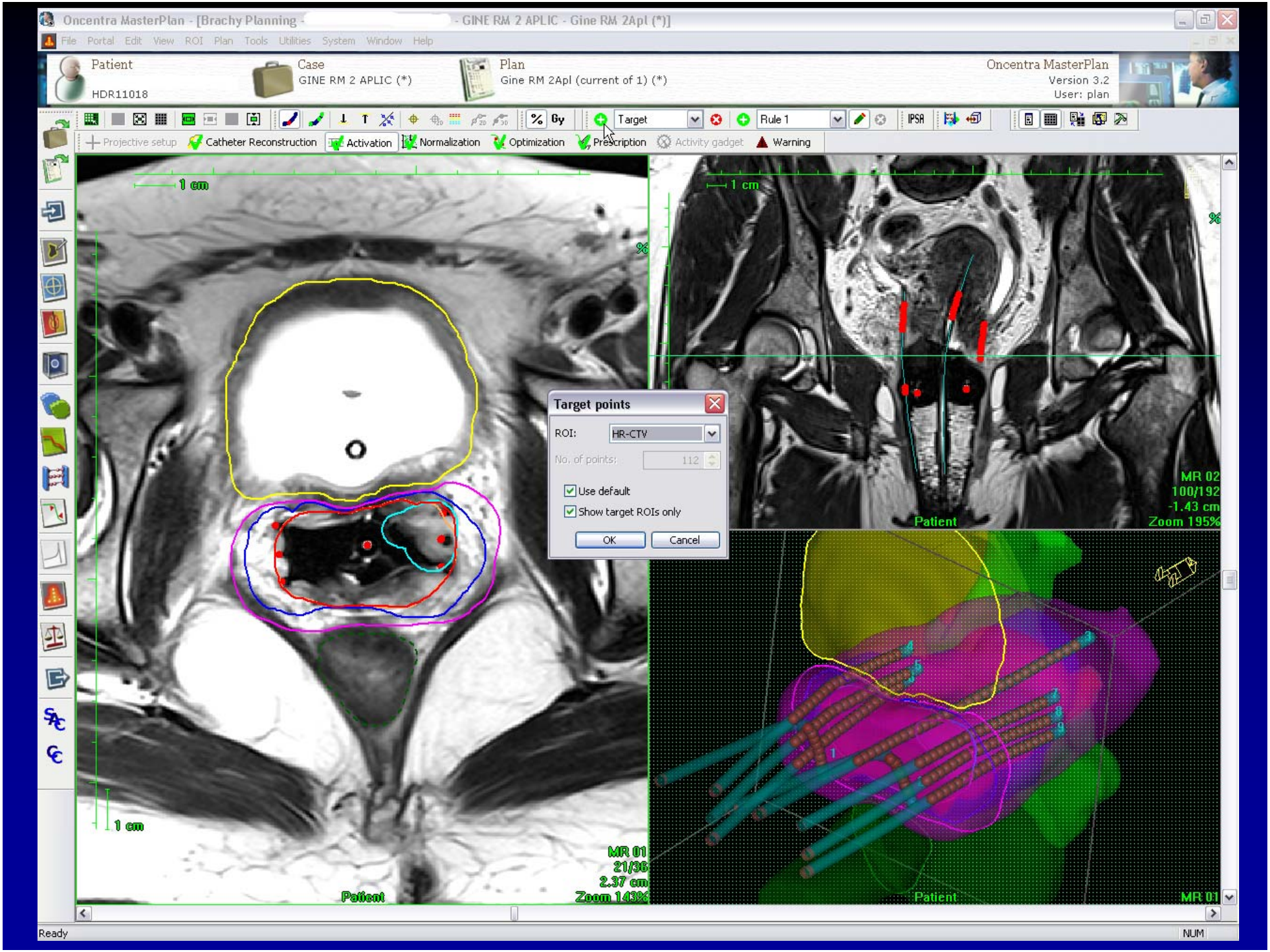
Oncentra MasterPlan - [Brachy Planning - - GINE RM 2 APLIC - Gine RM 2Apl (*)]
File Portal Edit View ROI Plan Tools Utilities System Window Help
Patient
HDR11018
Case
GINE RM 2 APLIC (*)
Plan
Gine RM 2Apl (current of 1) (*)
Oncentra MasterPlan
Version 3.2
User: plan
Target
Rule 1
IPSA
Projective setup
Catheter Reconstruction
Activation
Normalization
Optimization
Prescription
Activity gadget
Warning
1 cm
Target points
ROI:
HR-CTV
No. of points:
112
Use default
Show target ROIs only
OK
Cancel
MR 02
100/192
-1.43 cm
Zoom 195%
Patient
MR 01
21/36
2.37 cm
Zoom 143%
Ready
NUM

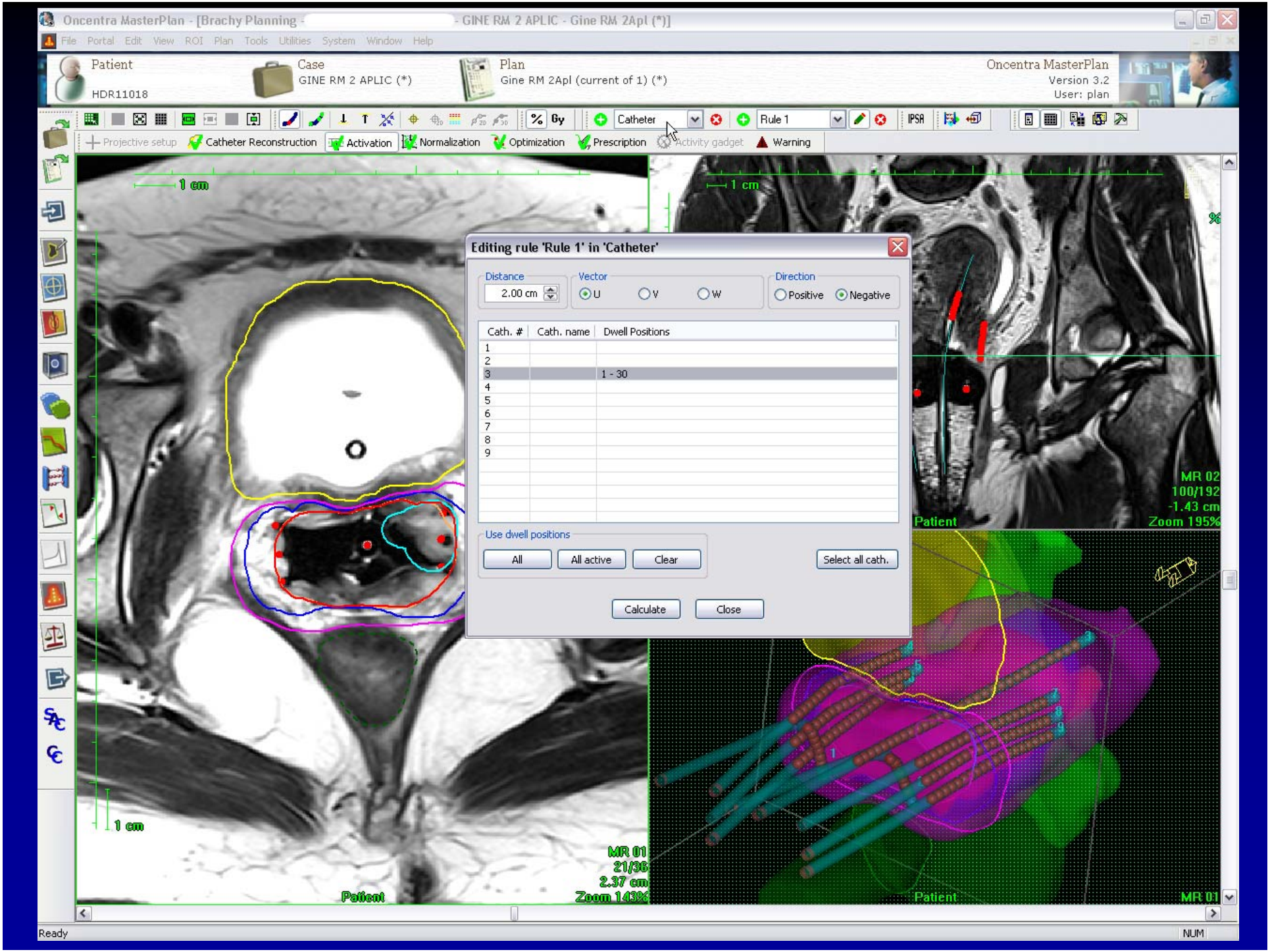
Oncentra MasterPlan - [Brachy Planning - - GINE RM 2 APLIC - Gine RM 2Apl (*)]
File Portal Edit View ROI Plan Tools Utilities System Window Help
Patient
HDR11018
Case
GINE RM 2 APLIC (*)
Plan
Gine RM 2Apl (current of 1) (*)
Oncentra MasterPlan
Version 3.2
User: plan
Catheter
Rule 1
IPSA
Projective setup
Catheter Reconstruction
Activation
Normalization
Optimization
Prescription
Activity gadget
Warning
1 cm
Editing rule 'Rule 1' in 'Catheter'
Distance
2.00 cm
Vector
U
V
W
Direction
Positive
Negative
Cath. #
Cath. name
Dwell Positions
1 - 30
Use dwell positions
All
All active
Clear
Select all cath.
Calculate
Close
MR 02
100/192
-1.43 cm
Zoom 195%
Patient
MR 01
21/36
2.37 cm
Zoom 143%
Ready
NUM

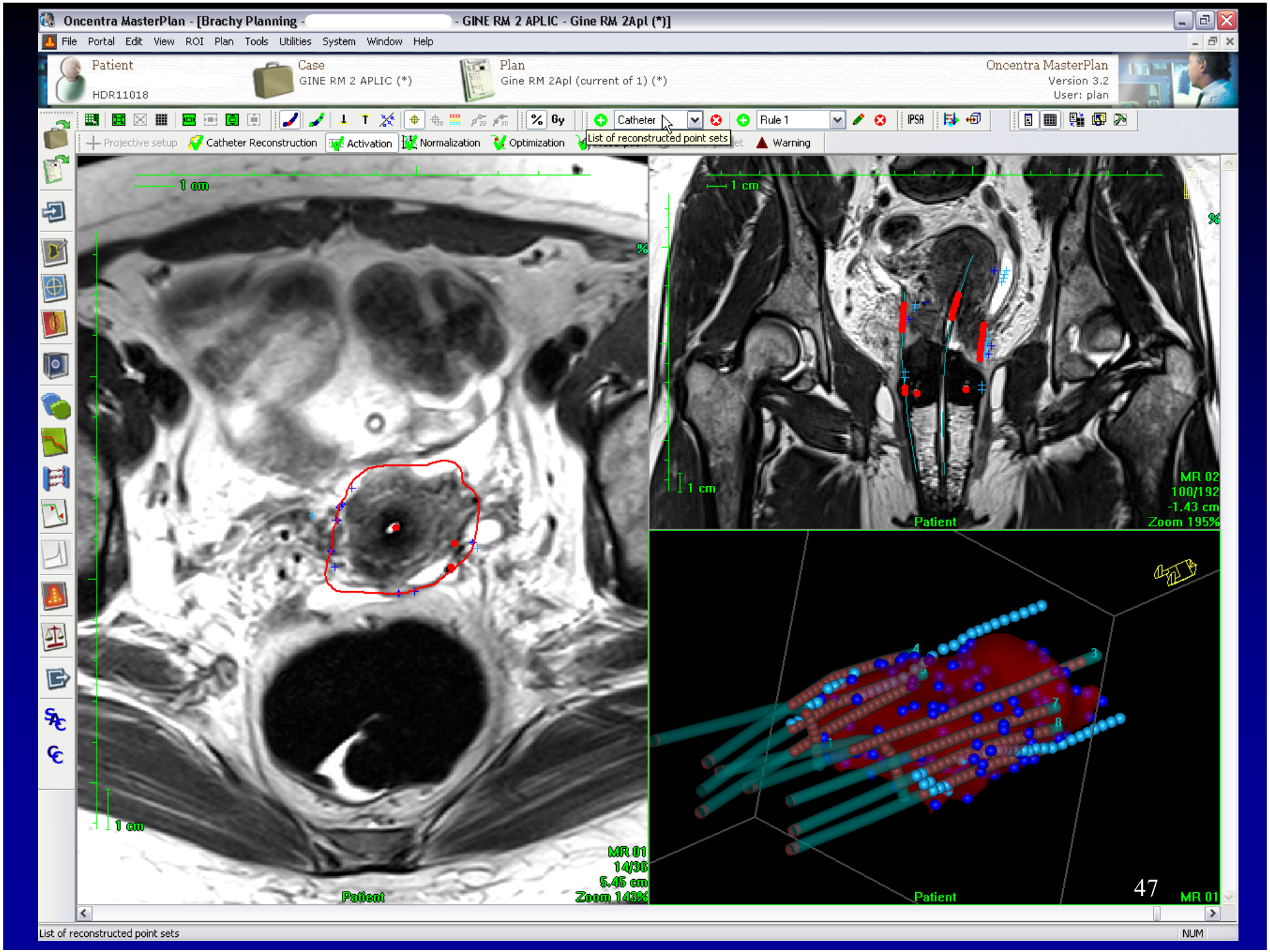
Oncentra MasterPlan - [Brachy Planning - - GINE RM 2 APLIC - Gine RM 2Apl (*)]
File Portal Edit View ROI Plan Tools Utilities System Window Help
Patient
HDR11018
Case
GINE RM 2 APLIC (*)
Plan
Gine RM 2Apl (current of 1) (*)
Oncentra MasterPlan
Version 3.2
User: plan
Catheter
Rule 1
IPSA
List of reconstructed point sets
Projective setup
Catheter Reconstruction
Activation
Normalization
Optimization
Warning
1 cm
MR 01
14/36
5.45 cm
Zoom 143%
Patient
MR 02
100/192
-1.43 cm
Zoom 195%
Patient
Patient
MR 01
47
List of reconstructed point sets
NUM

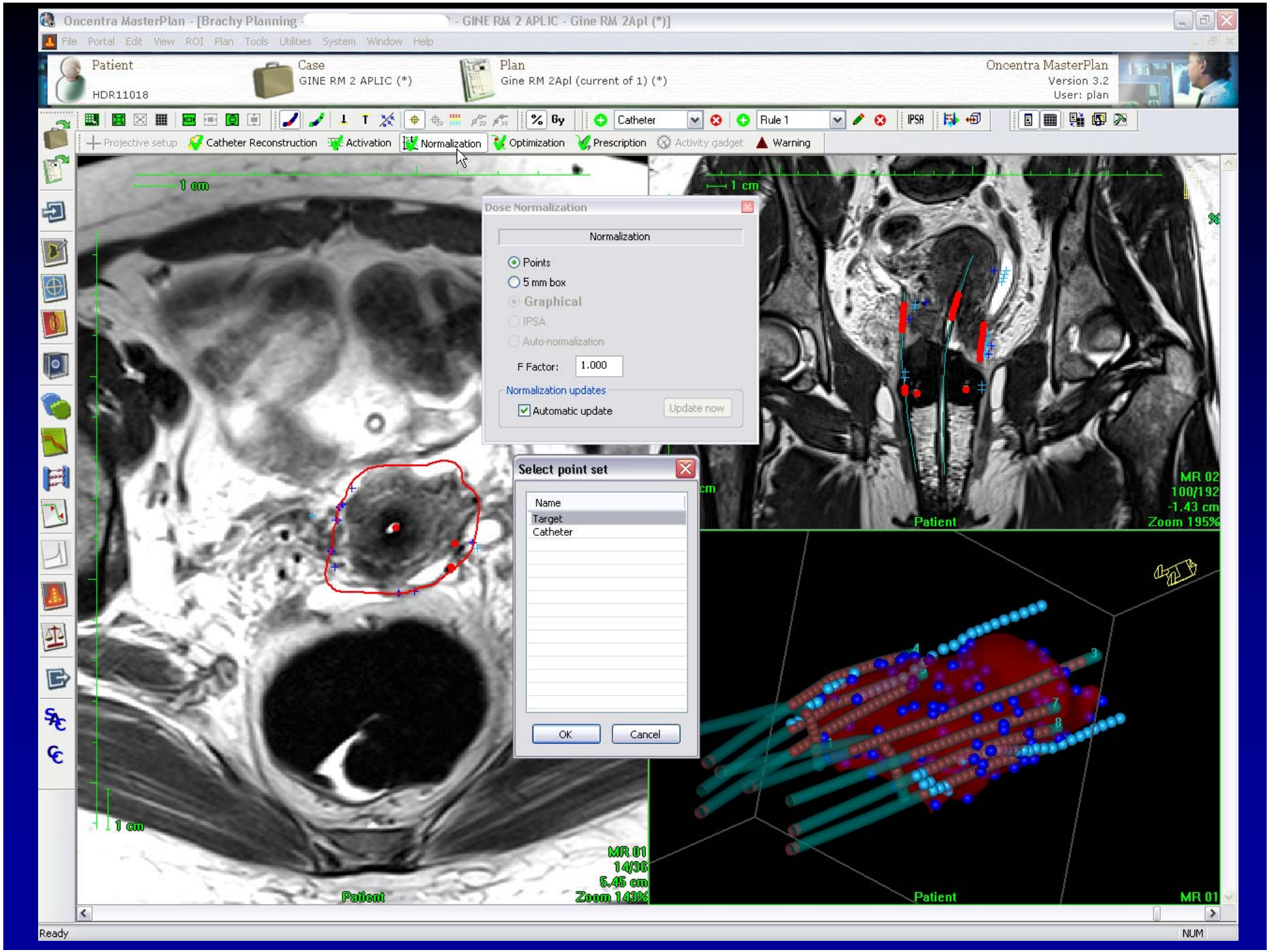
Oncentra MasterPlan - [Brachy Planning - GINE RM 2 APLIC - Gine RM 2Apl (*)]
File Portal Edit View ROI Plan Tools Utilities System Window Help
Patient
HDR11018
Case
GINE RM 2 APLIC (*)
Plan
Gine RM 2Apl (current of 1) (*)
Oncentra MasterPlan
Version 3.2
User: plan
Catheter
Rule 1
IPSA
Projective setup
Catheter Reconstruction
Activation
Normalization
Optimization
Prescription
Activity gadget
Warning
1 cm
Dose Normalization
Normalization
Points
5 mm box
Graphical
IPSA
Auto-normalization
F Factor:
1.000
Normalization updates
Automatic update
Update now
Select point set
Name
Target
Catheter
OK
Cancel
MR 02
100/192
-1.43 cm
Zoom 195%
Patient
MR 01
14/36
5.45 cm
Zoom 143%
Patient
MR 01
Ready
NUM

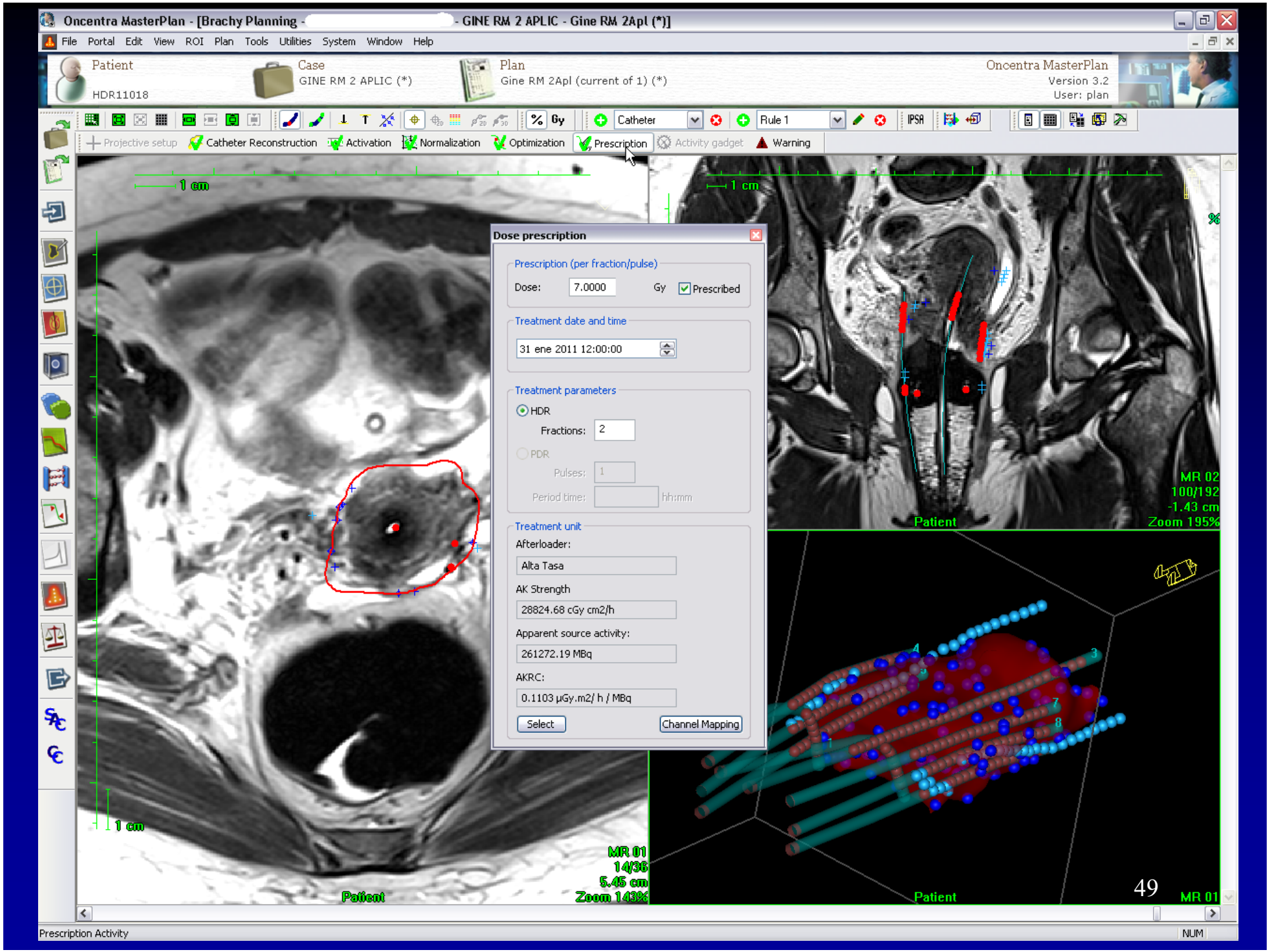
Oncentra MasterPlan - [Brachy Planning - - GINE RM 2 APLIC - Gine RM 2Apl (*)]
File Portal Edit View ROI Plan Tools Utilities System Window Help
Patient
HDR11018
Case
GINE RM 2 APLIC (*)
Plan
Gine RM 2Apl (current of 1) (*)
Oncentra MasterPlan
Version 3.2
User: plan
Catheter
Rule 1
Projective setup
Catheter Reconstruction
Activation
Normalization
Optimization
Prescription
Activity gadget
Warning
1 cm
Dose prescription
Prescription (per fraction/pulse)
Dose: 7.0000 Gy Prescribed
Treatment date and time
31 ene 2011 12:00:00
Treatment parameters
HDR
Fractions: 2
PDR
Pulses: 1
Period time: hh:mm
Treatment unit
Afterloader:
Alta Tasa
AK Strength
28824.68 cGy cm2/h
Apparent source activity:
261272.19 MBq
AKRC:
0.1103 µGy.m2/ h / MBq
Select
Channel Mapping
MR 02
100/192
-1.43 cm
Zoom 195%
Patient
MR 01
14/36
5.45 cm
Zoom 143%
Patient
Patient
MR 01
Prescription Activity
NUM

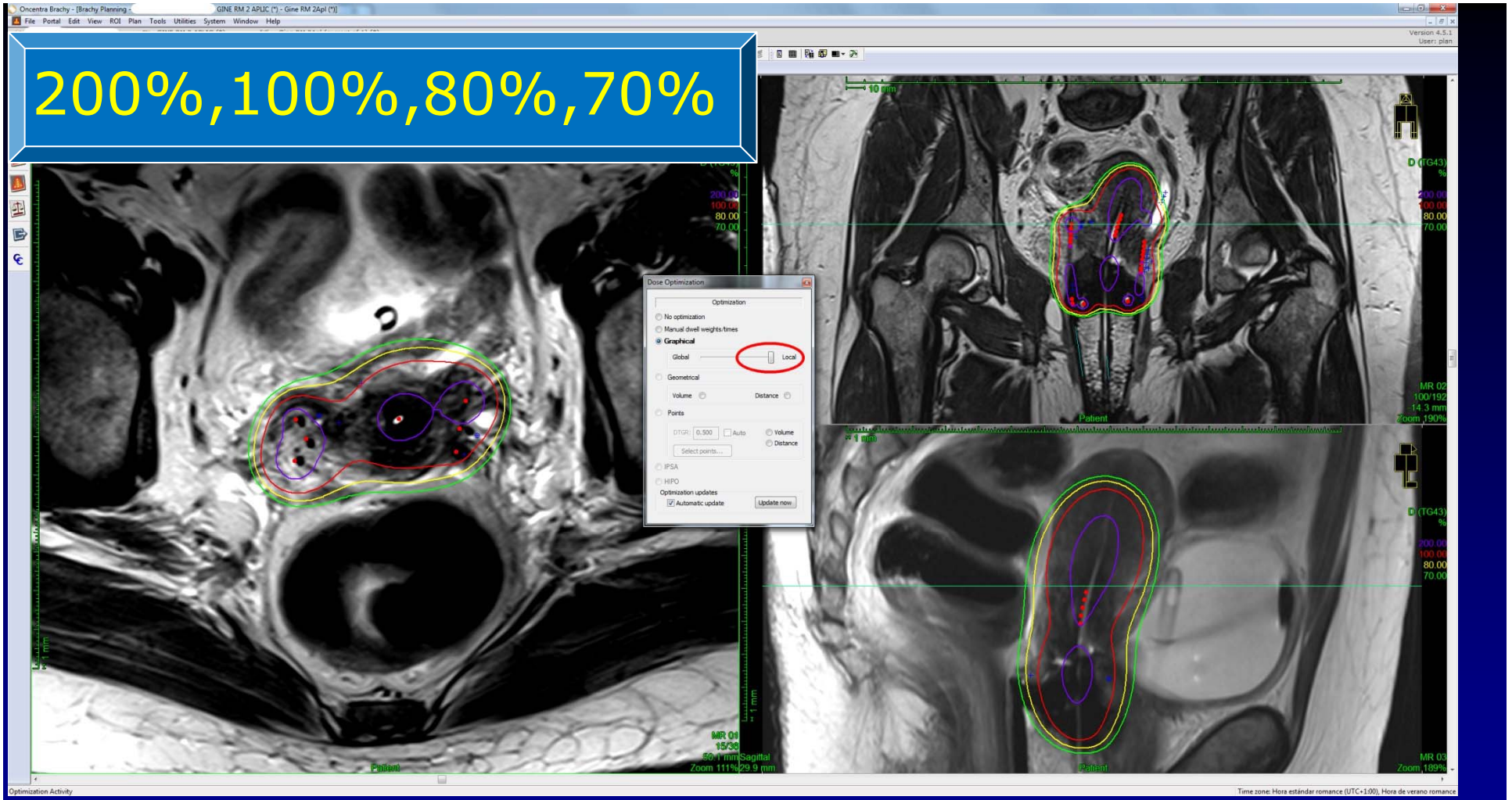

NO 15-20% limit to the interstitial component.

NO target points optimization (starting form the uniform dwell times distribution)

Fine tuning with manual graphical optimization

Caution with "local" gradients

Caution with overdose volumes

- Brief illustration of the Cervix GYN clinical procedure (H La Fe)

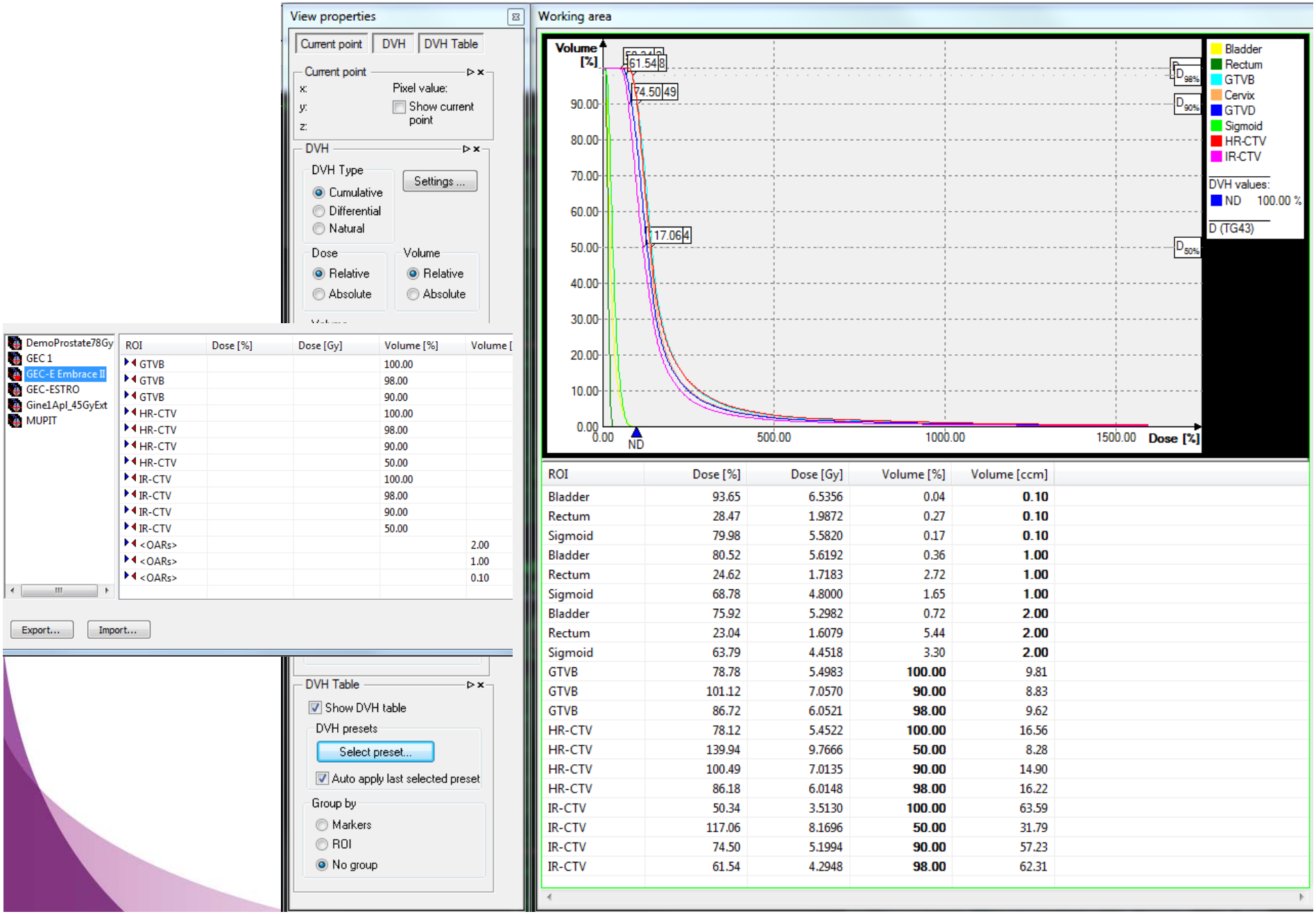

ROI	Dose [%]	Dose [Gy]	Volume [%]	Volume [ccm]
Bladder	93.65	6.5356	0.04	**0.10**
Rectum	28.47	1.9872	0.27	**0.10**
Sigmoid	79.98	5.5820	0.17	**0.10**
Bladder	80.52	5.6192	0.36	**1.00**
Rectum	24.62	1.7183	2.72	**1.00**
Sigmoid	68.78	4.8000	1.65	**1.00**
Bladder	75.92	5.2982	0.72	**2.00**
Rectum	23.04	1.6079	5.44	**2.00**
Sigmoid	63.79	4.4518	3.30	**2.00**
GTVB	78.78	5.4983	**100.00**	9.81
GTVB	101.12	7.0570	**90.00**	8.83
GTVB	86.72	6.0521	**98.00**	9.62
HR-CTV	78.12	5.4522	**100.00**	16.56
HR-CTV	139.94	9.7666	**50.00**	8.28
HR-CTV	100.49	7.0135	**90.00**	14.90
HR-CTV	86.18	6.0148	**98.00**	16.22
IR-CTV	50.34	3.5130	**100.00**	63.59
IR-CTV	117.06	8.1696	**50.00**	31.79
IR-CTV	74.50	5.1994	**90.00**	57.23
IR-CTV	61.54	4.2948	**98.00**	62.31

- Brief illustration of the Cervix GYN clinical procedure (H La Fe)

Spread sheet

Carmona et al 2011

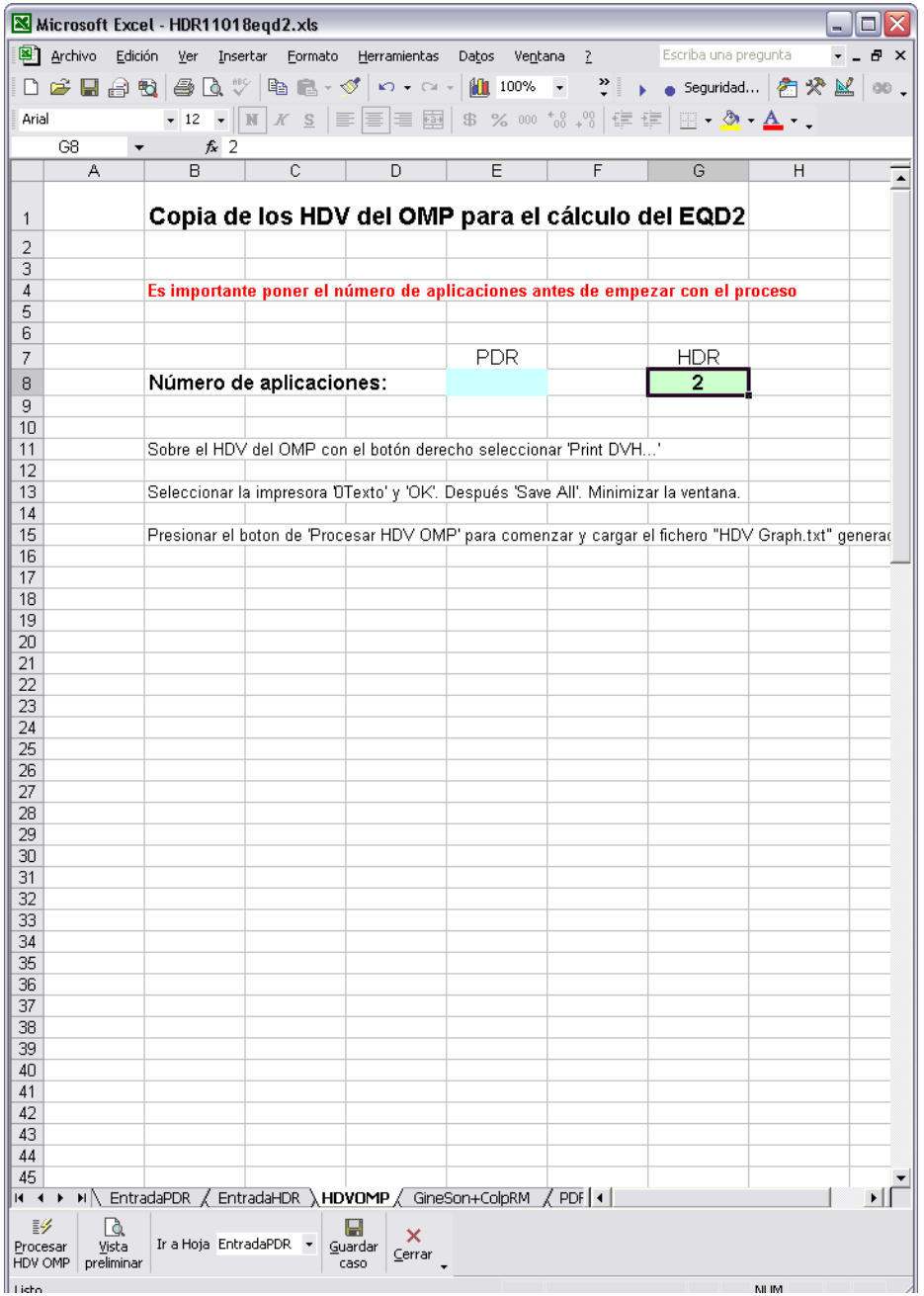

- Brief illustration of the Cervix GYN clinical procedure (H La Fe)

Spread sheet

Cálculo de EQD_2 en braquiterapia ginecológica para HDR

Radiofisica - Radioterapia - Hospital La Fe

Identificació	
Paciente:	
Historia RT	
Médico:	

Externa		
Dosis / sesión	1.80	Gy
Sesiones:	28	
Subtotal =	50.40	Gy

Número de aplicaciónes: 2

	HDR 1 Aplicación		HDR 2 Aplicación	
	Fracciones	Factor Dosis	Fracciones	Factor Dosis
	2	93.0%	2	91%
	Cálculo	Tratamiento	Cálculo	Tratamiento
osis / fracción	7.000 Gy	6.510 Gy	7.000 Gy	6.370 Gy
tal / aplicación		13.02 Gy		12.74 Gy
tal acumulada	Ext + HDR 1 =	63.42 Gy	Ant + HDR 2 =	76.16 Gy

			Dosis / fracción		Dosis / fracción		Dosis / fracción			EMBRACE II		
	α/β = 10		Cálculo	Tratamiento	Cálculo	Tratamiento	Cálculo	EQD_2 Total		Mín	Obj	Máx
		D_{100}	6.66 Gy	**6.20** Gy	7.48 Gy	**6.81** Gy		85.30 Gy				
	GTV_B	**D_{98}**	7.35 Gy	**6.83** Gy	8.91 Gy	**8.11** Gy		**93.20** Gy		> 90	> 95	
		D_{90}	8.22 Gy	**7.64** Gy	10.33 Gy	**9.40** Gy		102.40 Gy				
		D_{100}	6.40 Gy	**5.95** Gy	6.98 Gy	**6.35** Gy		82.70 Gy				
		D_{98}	7.20 Gy	**6.69** Gy	7.62 Gy	**6.93** Gy		**87.70** Gy			> 75	
	HR-CTV	**D_{90}**	8.24 Gy	**7.66** Gy	8.46 Gy	**7.69** Gy		**94.80** Gy		> 85	> 90	< 95
		D_{50}	11.62 Gy	**10.80** Gy	11.22 Gy	**10.21** Gy		121.40 Gy				
		Volumen	8.38 cc		7.72 cc							
		D_{100}	2.86 Gy	**2.66** Gy	3.01 Gy	**2.74** Gy		61.00 Gy				
	IR-CTV	**D_{98}**	3.65 Gy	**3.39** Gy	3.87 Gy	**3.52** Gy		**65.10** Gy			> 60	
		D_{90}	4.57 Gy	**4.25** Gy	5.20 Gy	**4.73** Gy		71.30 Gy				
		D_{50}	8.47 Gy	**7.88** Gy	9.06 Gy	**8.24** Gy		98.10 Gy				
	Punto A										> 65	
	α/β = 3											
	Vejiga	**2 cm^3**	4.78 Gy	**4.45** Gy	4.51 Gy	**4.10** Gy		**73.30** Gy			< 80	< 90
		1 cm^3	5.14 Gy	**4.78** Gy	4.80 Gy	**4.37** Gy		76.20 Gy				
		0.1 cm^3	5.84 Gy	**5.43** Gy	5.36 Gy	**4.88** Gy		82.10 Gy				
	Recto	**2 cm^3**	2.00 Gy	**1.86** Gy	3.66 Gy	**3.33** Gy		**60.40** Gy			< 65	< 75
		1 cm^3	2.26 Gy	**2.10** Gy	4.09 Gy	**3.72** Gy		62.70 Gy				
		0.1 cm^3	2.81 Gy	**2.62** Gy	4.81 Gy	**4.38** Gy		67.20 Gy				
	Sigmoide	**2 cm^3**	2.52 Gy	**2.34** Gy	2.59 Gy	**2.35** Gy		**58.40** Gy			< 70	< 75
		1 cm^3	2.82 Gy	**2.62** Gy	2.92 Gy	**2.66** Gy		60.30 Gy				
		0.1 cm^3	3.70 Gy	**3.44** Gy	3.59 Gy	**3.27** Gy		65.40 Gy				
	Intestino	**2 cm^3**									< 70	< 75
		1 cm^3										
		0.1 cm^3										
	Punto recto-vaginal										< 65	< 75
	V_{ICRU}											
	R_{ICRU}											

ESTRO School

- Brief illustration of the Cervix GYN clinical procedure (H La Fe)

Optimization: IPSA

Only *MIN* & *MAX* in *Surface* & *Volume are specified*
Our experience: Excessive dwell times distribution gradient

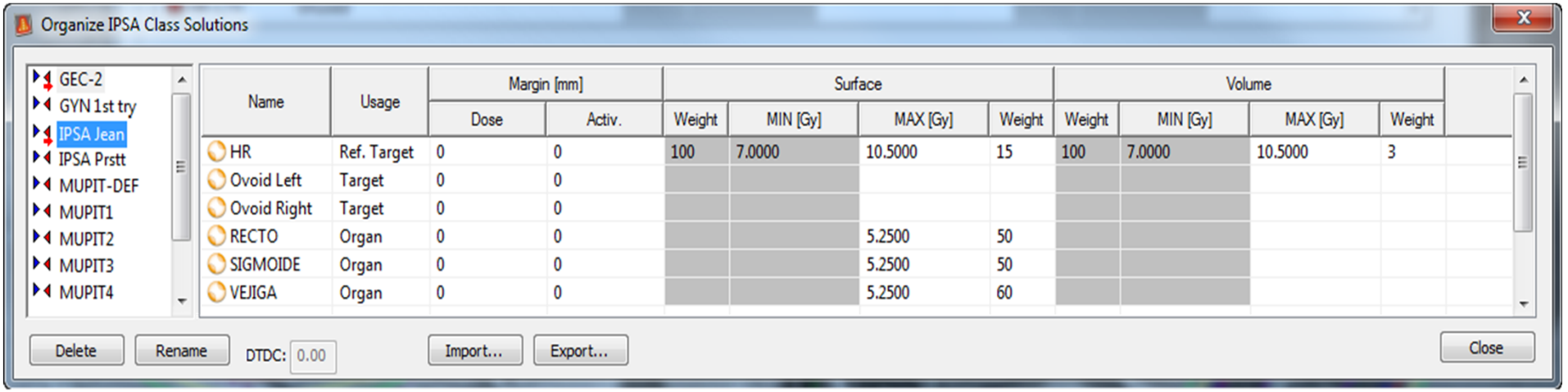

Name	Usage	Margin [mm]		Surface				Volume			
		Dose	Activ.	Weight	MIN [Gy]	MAX [Gy]	Weight	Weight	MIN [Gy]	MAX [Gy]	Weight
HR	Ref. Target	0	0	100	7.0000	10.5000	15	100	7.0000	10.5000	3
Ovoid Left	Target	0	0								
Ovoid Right	Target	0	0								
RECTO	Organ	0	0			5.2500	50				
SIGMOIDE	Organ	0	0			5.2500	50				
VEJIGA	Organ	0	0			5.2500	60				

ROI	Usage	Margin [mm]		Surface				Volume			
		Dose	Activ.	Wei...	MIN [cGy]	MAX [cGy]	Wei...	Wei...	MIN [cGy]	MAX [cGy]	Wei...
Bladder	Organ	0.0	0.0			500.00	100				
HR-CTV	Ref. Tar...	0.0	0.0	100	700.00			100	700.00	1050.00	1
IR-CTV	Target	0.0	0.0					10	350.00		
Rectum	Organ	0.0	0.0			300.00	50				
Sigmoid	Organ	0.0	0.0			300.00	5				

"Using IPSA algorithm in dose planning for cervix HDR Brachytherapy with the Utrecht applicators. First phase results" D. Krishnamurthy, AJ. Cunha, IC. Hsu, J. Pouliot, J. Perez-Calatayud, A. Tormo, V. Carmona, F. Lliso. ESTRO-GEC-ESTRO. 2011. Radiotheraphy and Oncology Vol 99 Supl 1 May 2011 S278

ESTRO School

- Cervix GYN

Typically ERT → VMAT with different volumes & doses
OAR D2cc can result very different from the low dose prescription volume

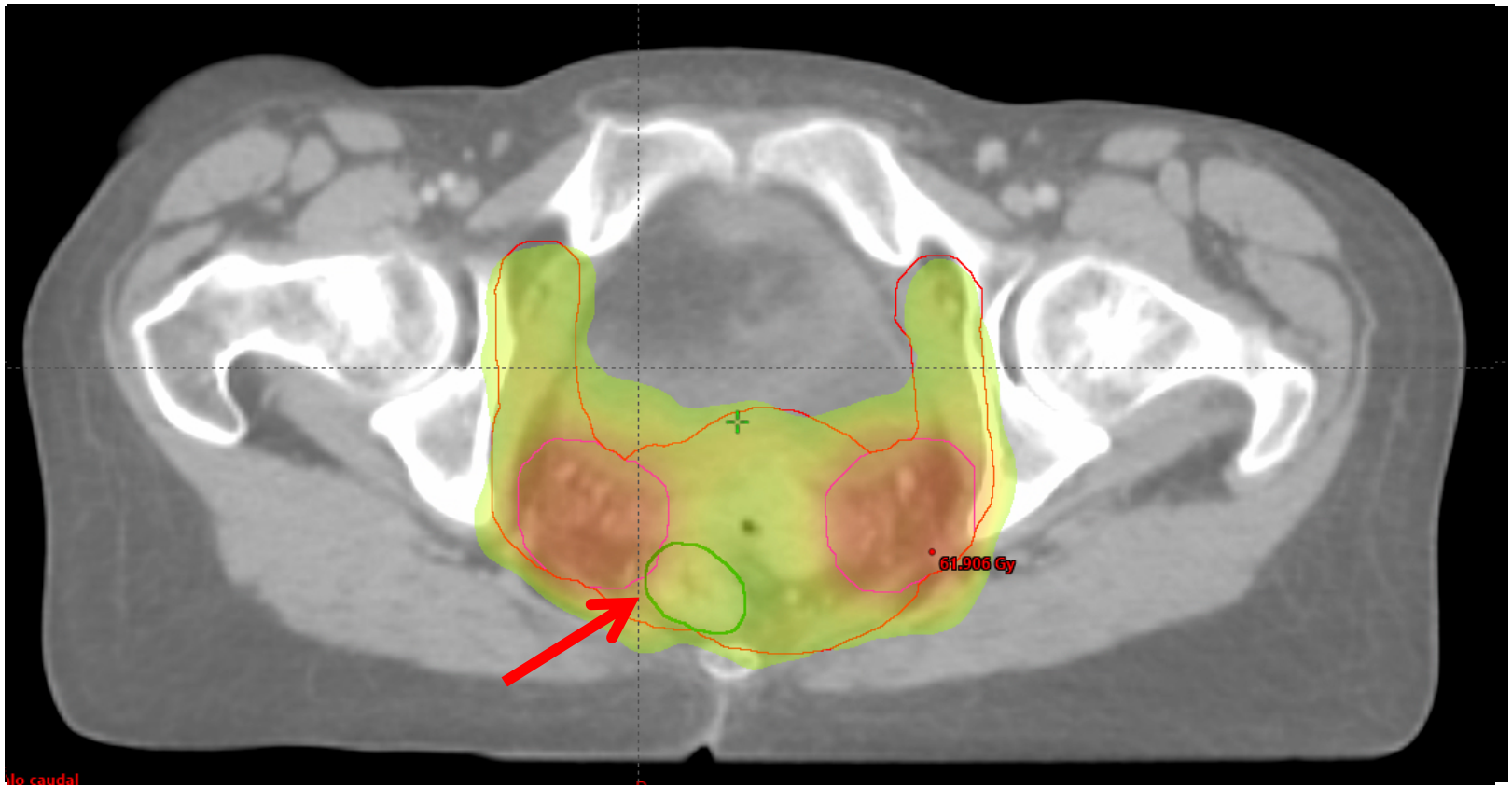

ESTRO School

Conclusions

- Brachy plan must be evaluated using **point doses** (in some cases), **DVH** parameters, **dose distribution** and global **indexes.**
- Overdose volumes due to **"target points"** based optimization must be **carefully evaluated** (more convenient "basal points").
- Resulting **under-over dose** volumes must be evaluated looking in detail at the **3D** dose distribution.
- For small volumes **whole** OAR volume subrogates well to the **wall**.
- Sampling and **histogram** bar with must be selected with **high resolution.**
- **EQD2** evaluation in cervix GYN **needs** an adequate implementation on TPSs future versions by manufacturers in order **to improve efficiency**.

ESTRO School

Thank you

perez_jos@gva.es

Valencia, 2016

ESTRO School

Advanced Brachytherapy Physics

Prescribing and reporting

Nicole Nesvacil
Medical University of Vienna

Part of the material has been kindly provided by Christian Kirisits, Vienna

ESTRO School

Summary of

Cervix recommendations
Prostate recommendations
Breast recommendations

Recommendations for gynaecological brachytherapy

GYN GEC ESTRO recommendations I (Haie-Meder et al.) - contouring

GYN GEC ESTRO recommendations II (Pötter et al.) - dose parameters

GYN GEC ESTRO recommendations III (Hellebust et al.) - reconstruction

GYN GEC ESTRO recommendations IV (Dimopoulos et al.) - imaging

ABS recommendations on GYN general (Viswanathan and Thomadsen, ABS Cervical Cancer Recommendations Committee) -general

ABS recommendations on GYN HDR (Viswanathan et al.)

ABS recommendations on GYN PDR (Lee et al.)

ICRU/GEC-ESTRO 89 report (coordinators: R. Pötter and C. Kirisits, committee members: B. Erickson, C. Haie-Meder, J. Lindegaard, E. van Limbergen, J. Rownd, K. Tanderup, B. Thomadsen)

Table of Contents for ICRU/GEC-ESTRO 89

ESTRO School

Target definition

Advanced disease, significant remission after EBRT:

Change of GTV/CTV with time (4D RT) (FIGO IIB)

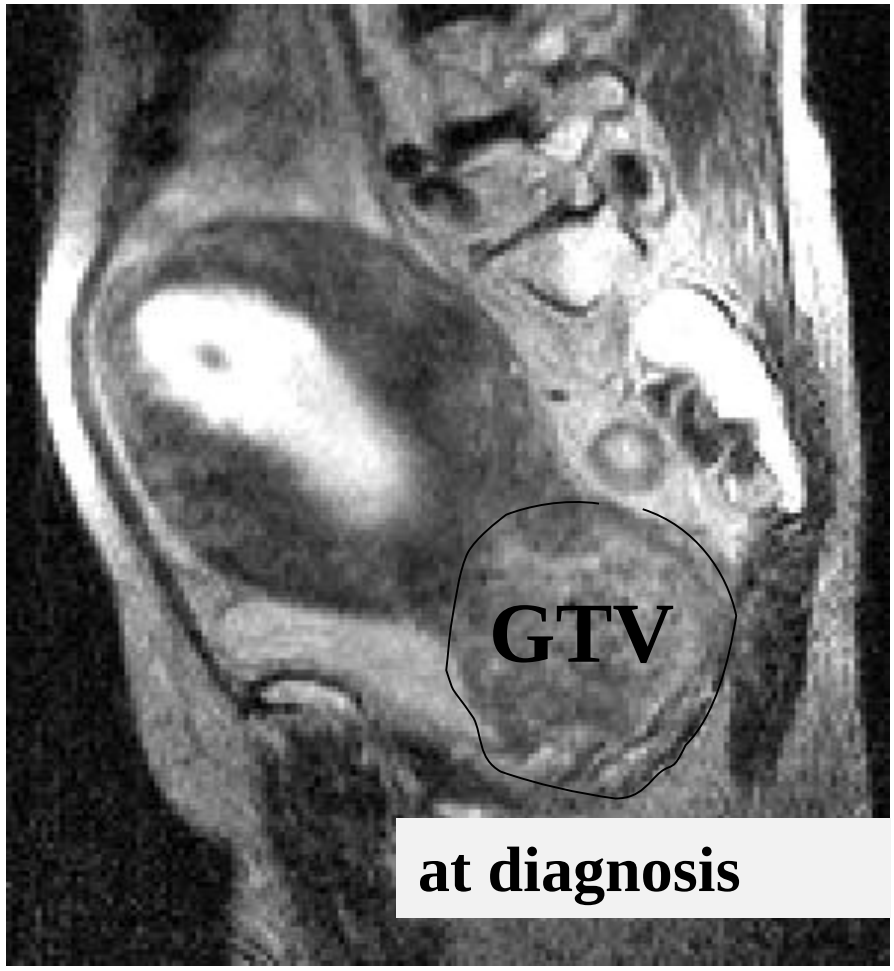

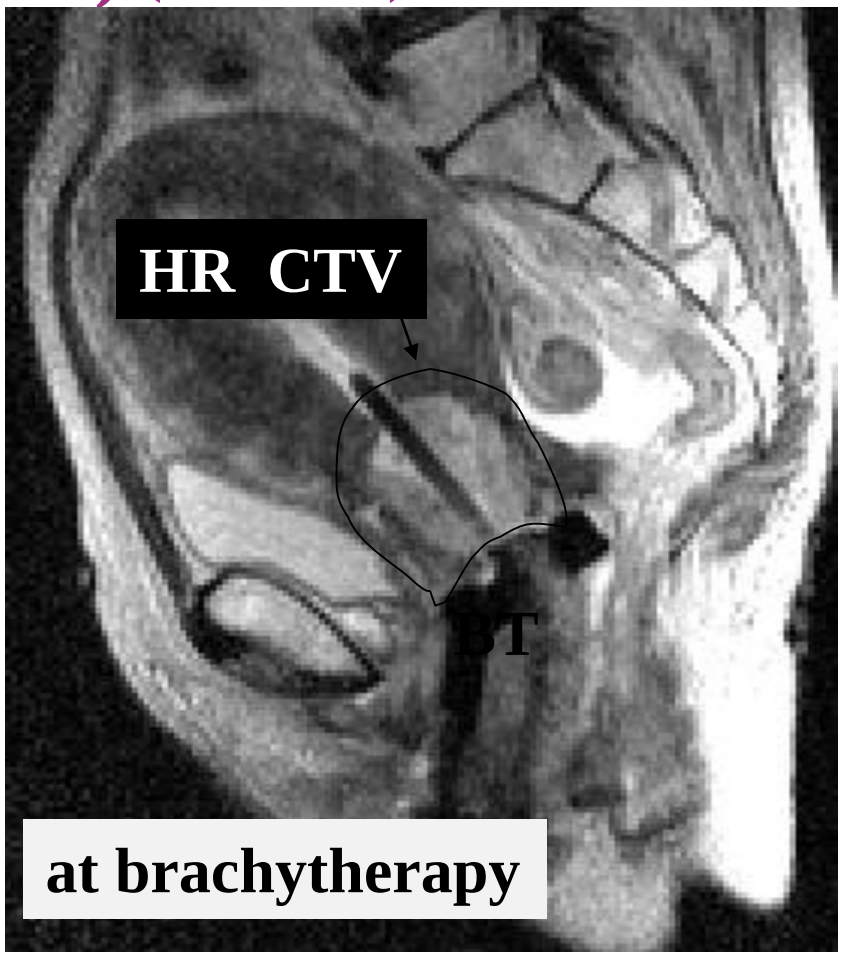

Tumor Extension before EBT

Target Volume of BT Based on dimensions and Topography at time of BT

ESTRO School

Various patterns of tumor response adapted CTV

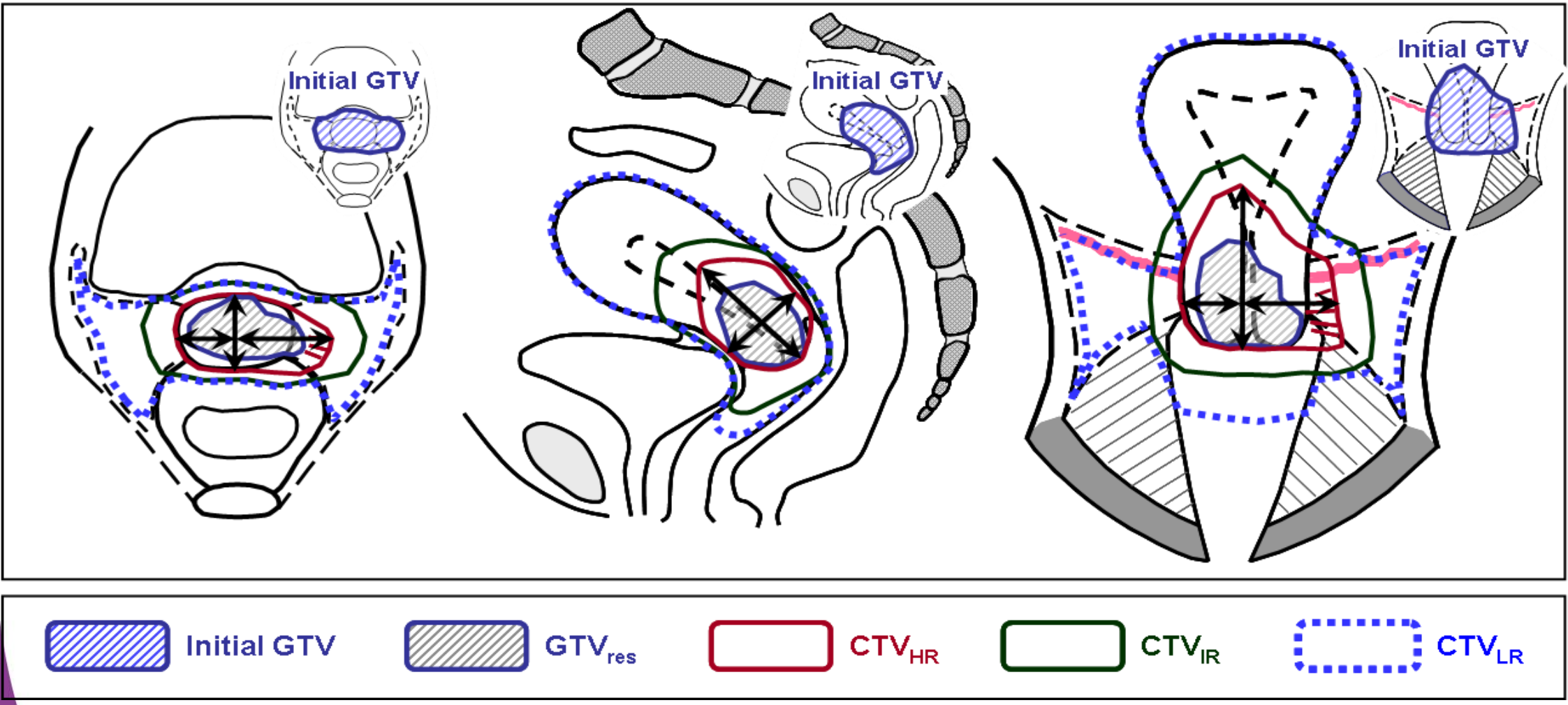

OAR concept and related volumes

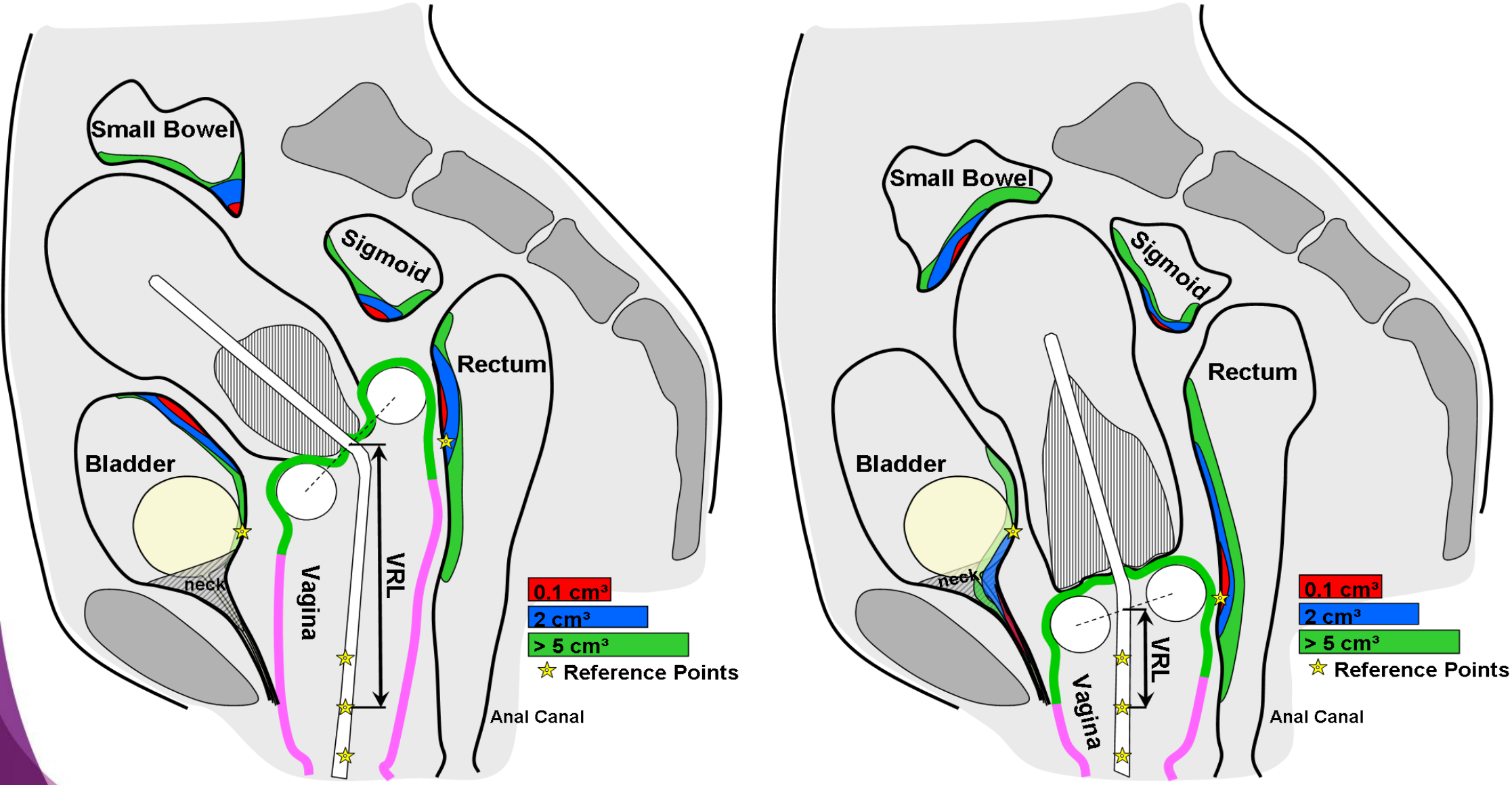

ESTRO School

Radiobiology: Time-dose pattern

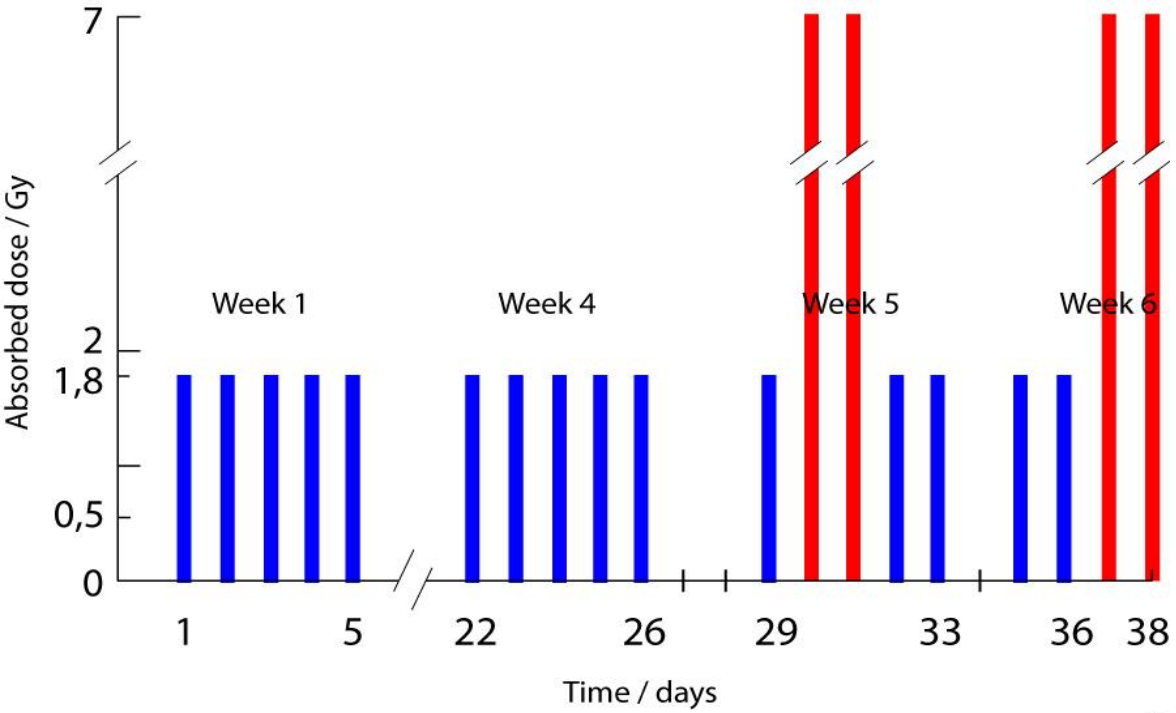

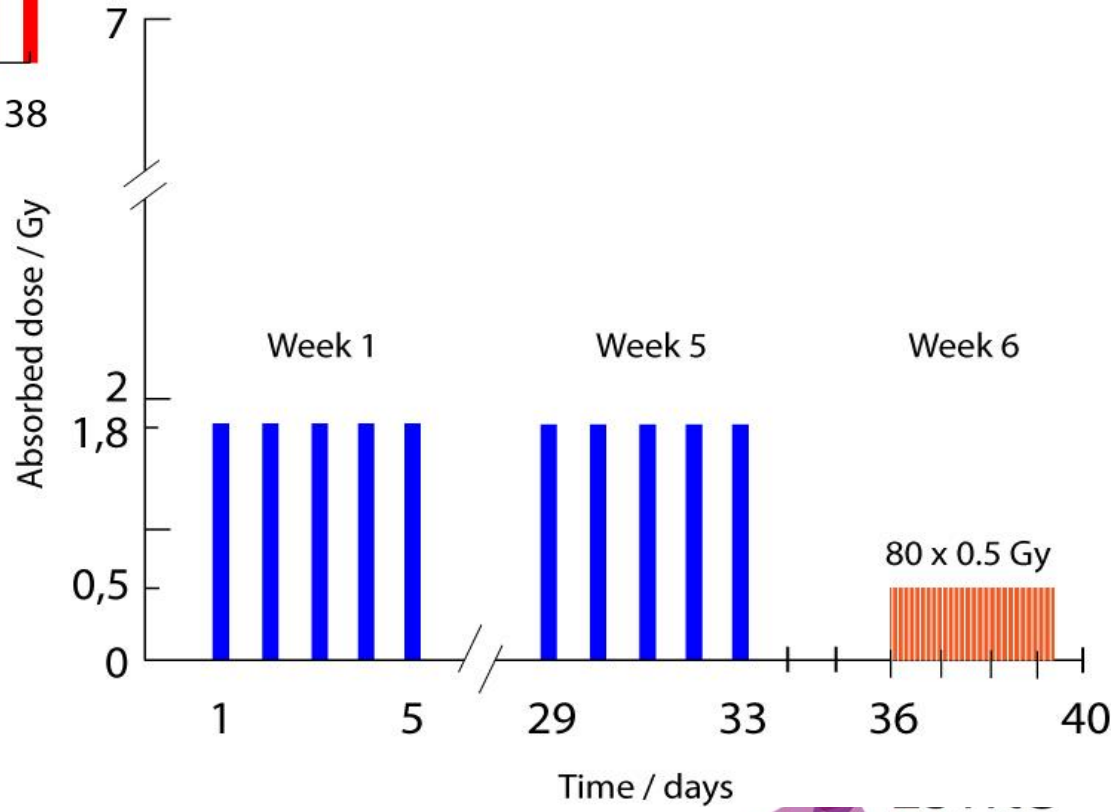

General principles for assessment and reporting of physical and equieffective EBRT and BT dose (all reporting levels)

Physical dose and number of fractions is assessed for target, OARs, dose points:

- BT
- EBRT

Total equieffective dose (EQD2) is calculated according to the linear quadratic model through the following steps:

- BT EQD2 for each fraction
- Total BT EQD2
- Total EBRT EQD2
- Accumulated total EBRT+BT EQD2*

**Based on current assumptions outlined in chapter 9*

Reporting of radiobiological parameters:

α/β values for tumour and OARs*

In addition $T_{1/2}$ and recovery model for LDR and PDR treatments*

*At present: α/β=3 Gy for late effects in OAR and 10 Gy for tumour, and $T_{1/2}$=1.5h

Radiotherapy & Oncology
Volume 105, Issue 2 , Pages 266-268, November 2012

Bioeffect modeling and equieffective dose concepts in radiation oncology – Terminology, quantities and units

Søren M. Bentzen, Wolfgang Dörr, Reinhard Gahbauer, Roger W. Howell, Michael C. Joiner, Bleddyn Jones, Dan T.L. Jones, Albert J. van der Kogel, André Wambersie, Gordon Whitmore

ESTRO School

FROM PLANNING AIMS TO PRESCRIPTION

Traditional concepts:

"when prescribing to a target, the prescription dose is the planned dose to cover this target as completely as possible."

or

prescription to a 100% isodose which is "to cover" the target volume"

Need for common terminology according to ICRU reports on proton treatment and IMRT

Planning aim dose

- Set of dose and dose/volume constraints for a treatment

Prescribed dose

- Finally accepted treatment plan (which is assumed to be delivered to an individual patient)

Delivered dose

- Actually delivered dose to the individual patient

Need for common terminology according to ICRU reports on proton treatment and IMRT

Example:

~~Previously: 4x7 Gy ~ 84 Gy EQD2 prescribed, mean D90 was 93 Gy~~

Planning aim was to deliver 4 x 7 Gy ~ 84 Gy, D_{2cm^3} for rectum, sigmoid < 70 Gy EQD2, bladder < 90 Gy EQD2

Prescribed dose was mean 93 Gy ± 13 Gy (1SD) EQD2 to D_{90} CTV_{HR}

Delivered dose ? *Depending on variations and uncertainties – on average no systematic deviation from prescribed dose*

Level 1 - *Minimum standard for reporting*

Source and dose calculation:

Radionuclide and source model

Source strength

Dose calculation algorithm

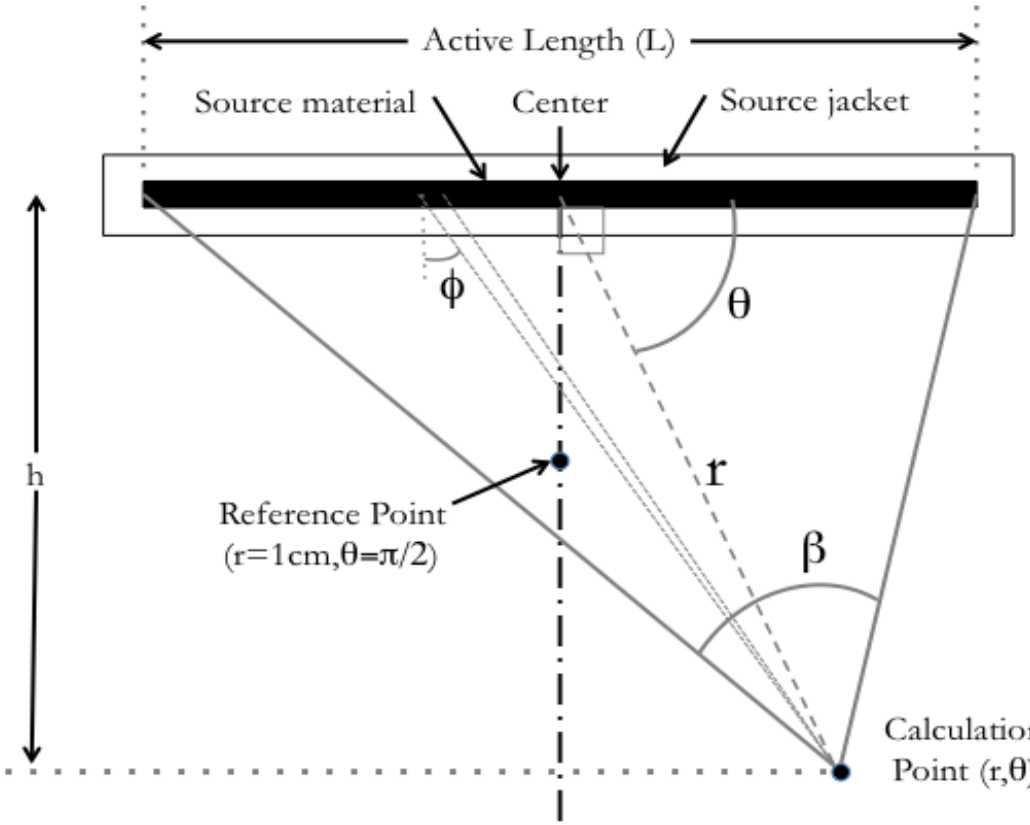

Level 1 - *Minimum standard for reporting*

Comprehensive clinical gynecologic examination

Volumetric imaging (MRI, CT, US, PET CT) at time of diagnosis and BT

FIGO/TNM stage

Baseline morbidity and QoL assessment

Schematic 3D documentation on a clinical diagram indicating dimensions and volumes for:

- GTV_{init} (GTV at diagnosis)
- GTV_{res} (GTV at brachytherapy)
- CTV_{HR} (GTV_{res} (plus residual pathologic tissue plus whole cervix)
- (CTV_{IR}: GTV_{init} and CTV_{HR} plus safefy margin if used for prescription)

Level 1 - *Minimum standard for reporting*

Dose reporting:

TRAK

Point A dose

Recto-vaginal reference point dose (=ICRU point)

$D_{0.1cm^3}$,D_{2cm^3} for bladder, rectum

or

Bladder reference point for radiographs

Chapter 8 and Chapter 10

Point A

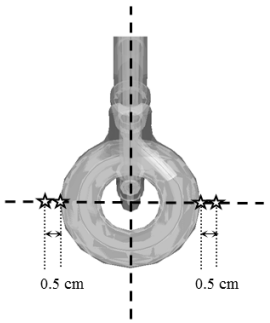

axial

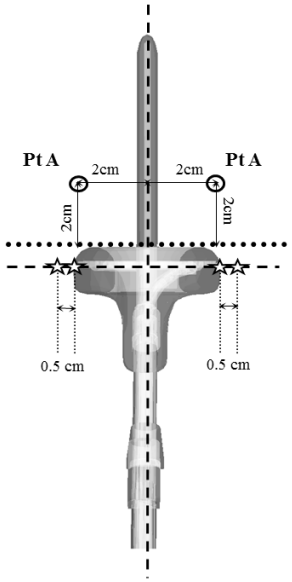

coronal

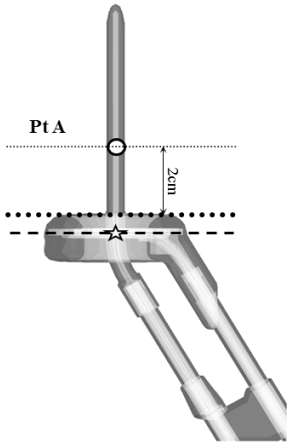

sagittal

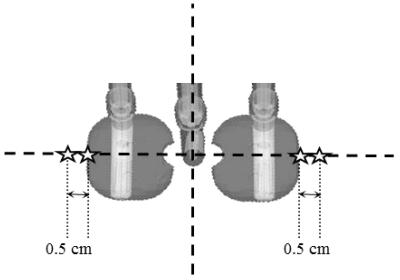

axial

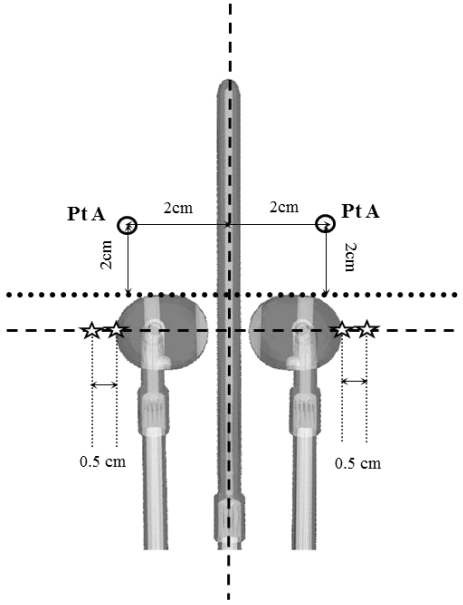

coronal

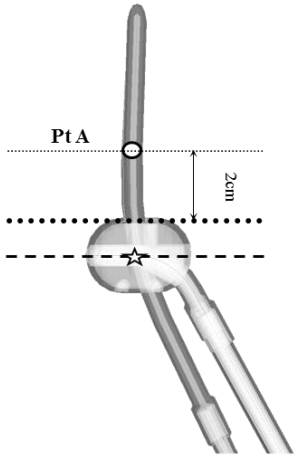

sagittal

Level 2 - *Advanced standard for reporting*
All that is reported in level 1 plus:

3D delineation of volumes (on volumetric images with applicator and on clinical diagrams):

GTV_{res}

CTV_{HR}

(CTV_{IR} if used for prescription)

With maximum width, height, thickness and with volume

Level 2 - *Advanced standard for reporting*
All that is reported in level 1 plus:

Dose reporting for defined volumes:

D_{98}, D_{90}, D_{50} for CTV_{HR}

(D_{98}, D_{90} for CTV_{IR} if used for prescription)

D_{98} for GTV_{res}

D_{98} for pathological Lymph nodes

DVH for target volumes

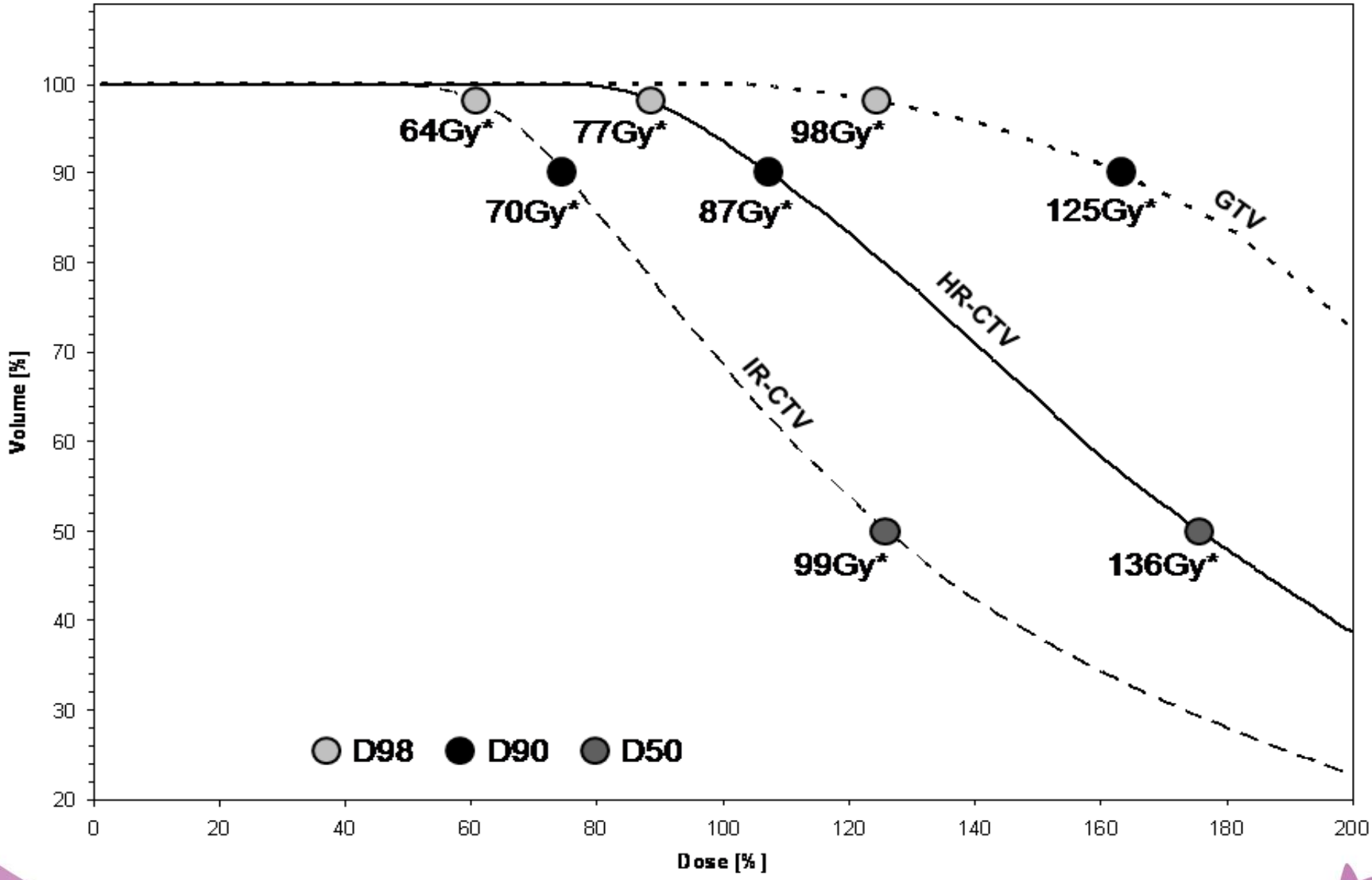

Level 2 - *Advanced standard for reporting*
All that is reported in level 1 plus:

Dose reporting OARs:

Bladder reference point dose

$D_{0.1cm^3}$,D_{2cm^3} for sigmoid*

D_{2cm^3} bowel (if fixed)*

EBRT: Intermediate and low dose parameters in bladder, rectum, sigmoid, bowel (e.g. V_{25Gy}, V_{35Gy}, V_{45Gy} or $D_{98\%}$, $D_{50\%}$, $D_{2\%}$)

Vaginal point doses at level of sources (lateral at 5 mm)**

Lower and mid vagina doses (PIBS, PIBS ±2cm)**

DVH for OAR

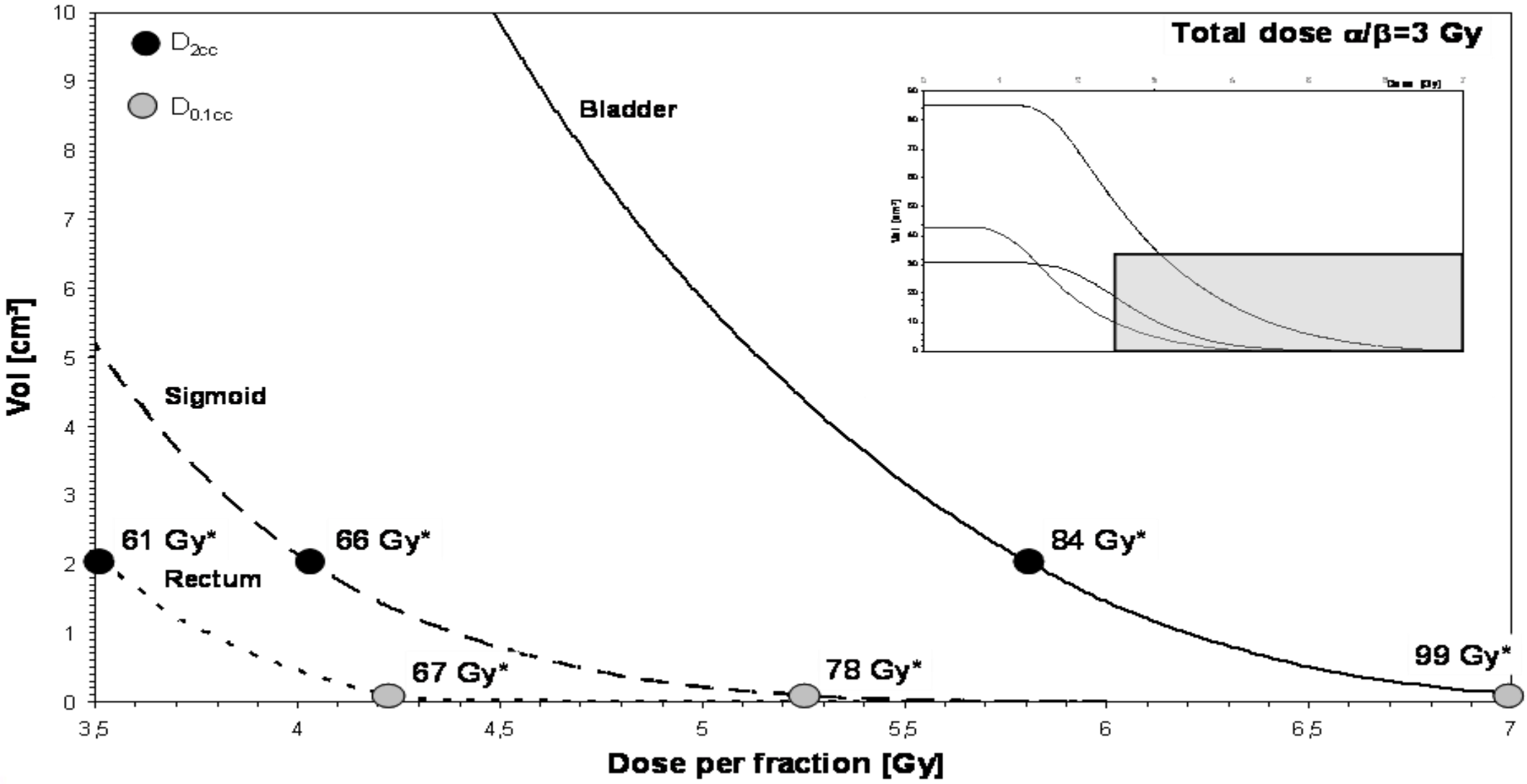
Total dose α/β=3 Gy
D2cc
D0.1cc
Bladder
Sigmoid
Rectum
61 Gy*
66 Gy*
67 Gy*
78 Gy*
84 Gy*
99 Gy*
Vol [cm³]
Dose per fraction [Gy]
0
1
2
3
4
5
6
7
8
9
10
3,5
4
4,5
5
5,5
6
6,5
7

Vaginal Reference Points

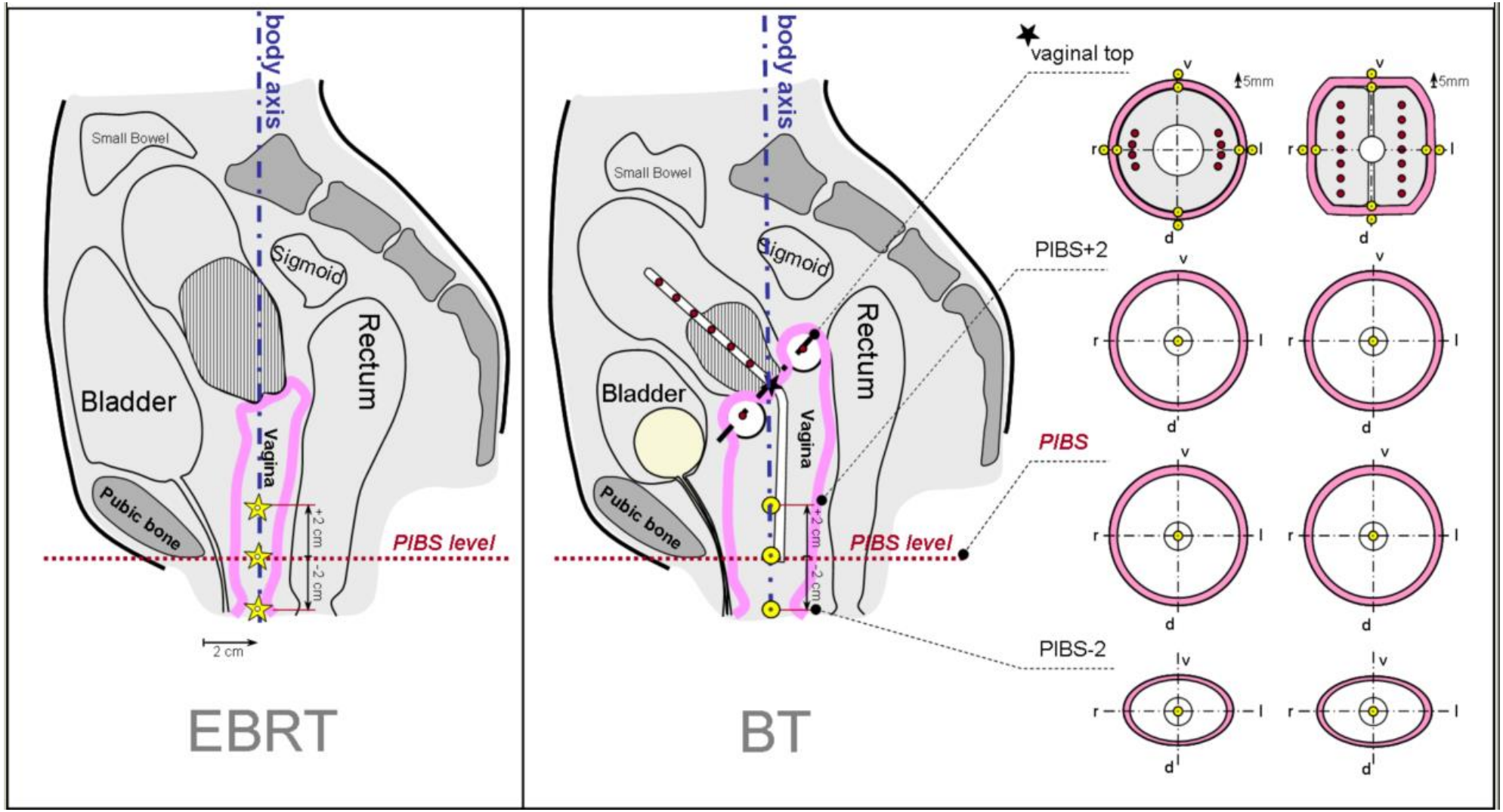

ESTRO School

Dose-response for local control

RETRO EMBRACE

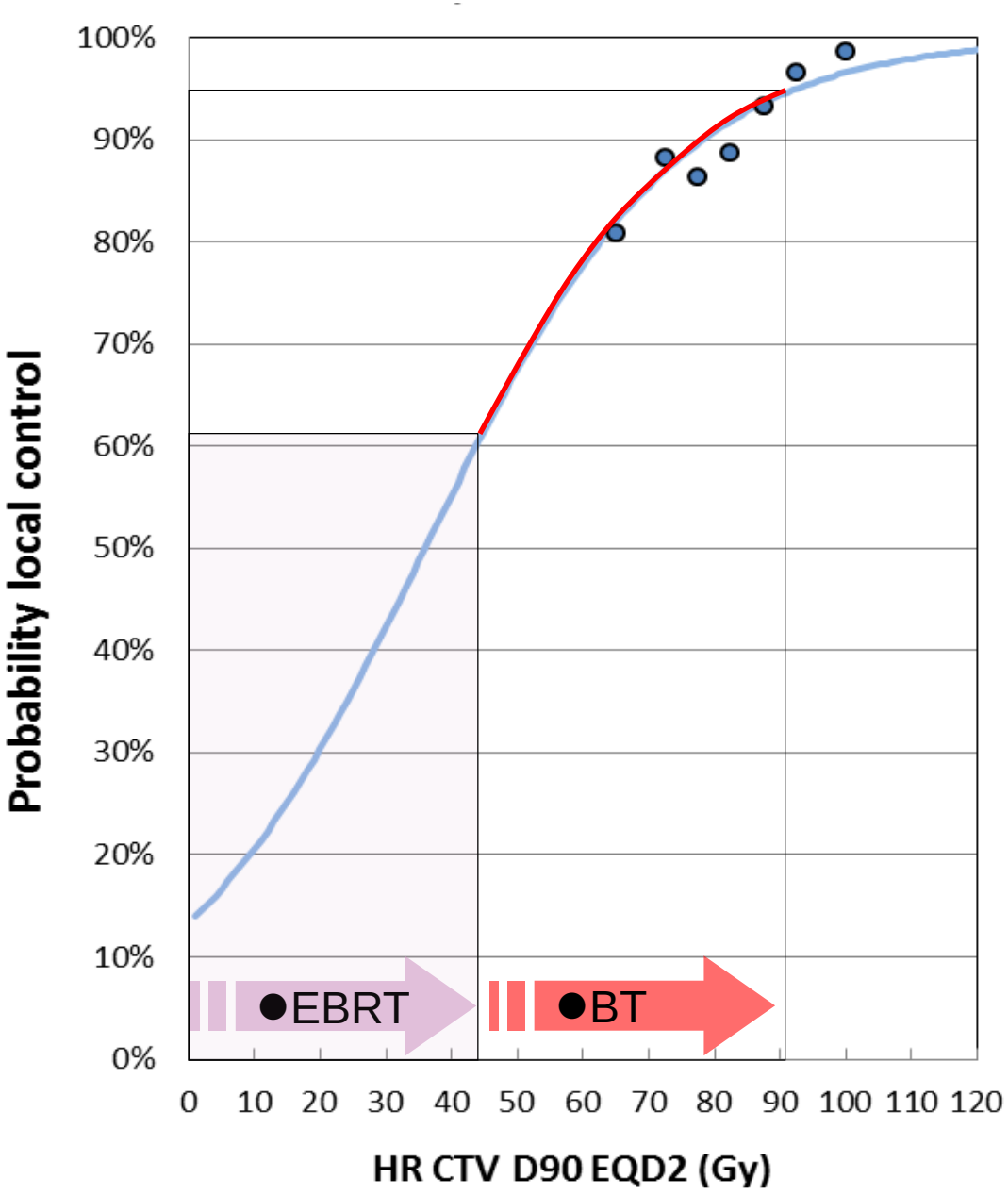

Tanderup et al.
ESTRO 2nd Forum
Geneve, 2013
& R&O2016

ESTRO School

RETRO EMBRACE

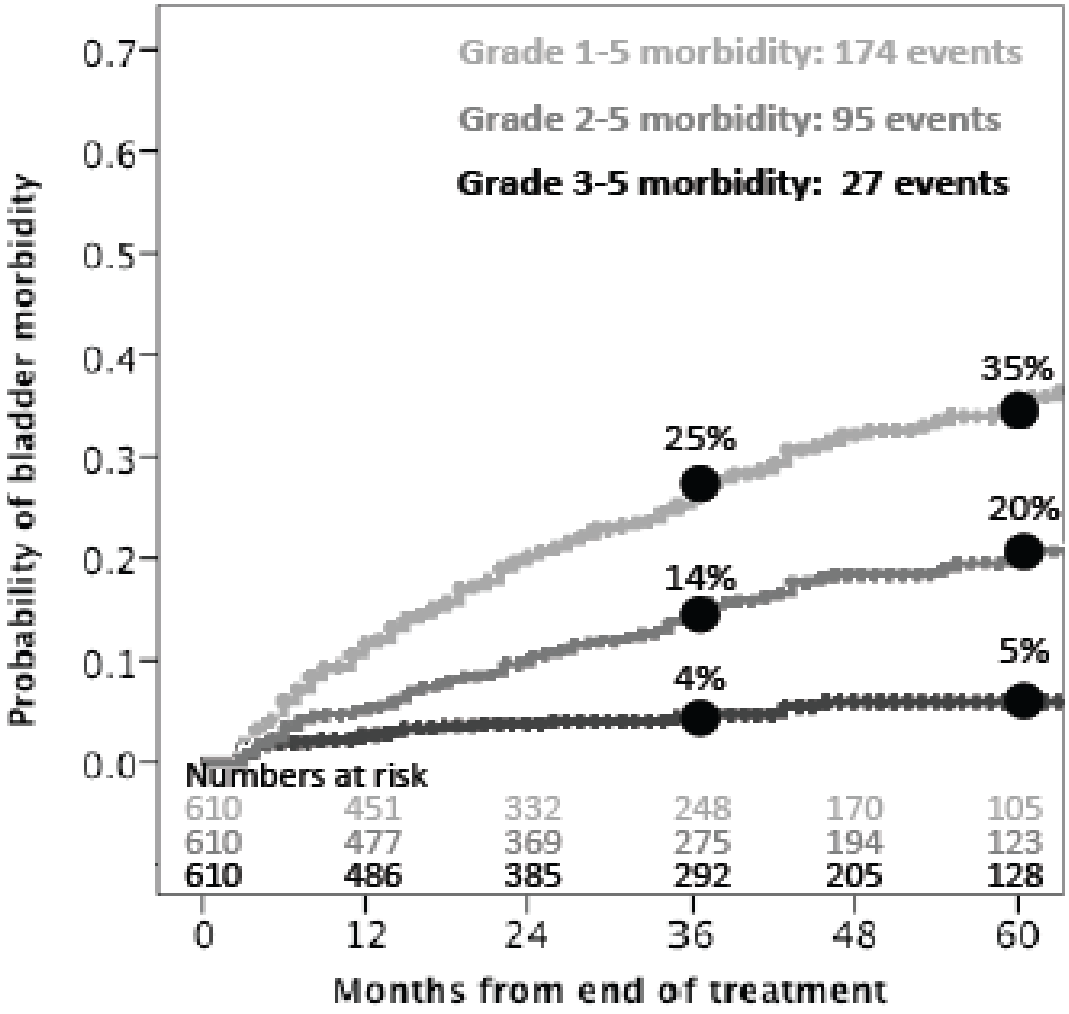

EMBRACE

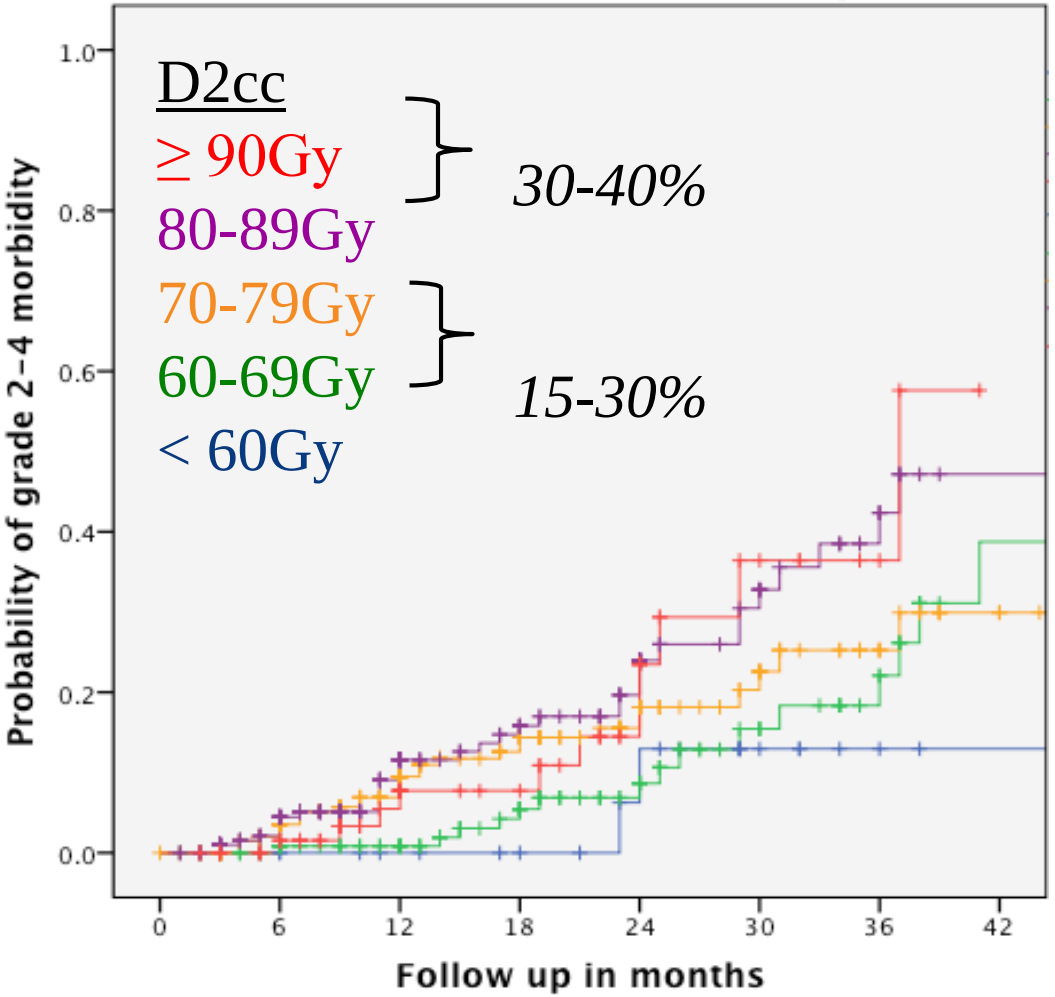

Fokdal & EMBRACE group, R&O 2018

ESTRO School

www.embracestudy.dk

EMBRACE II

RChTh + BT in < 50 days

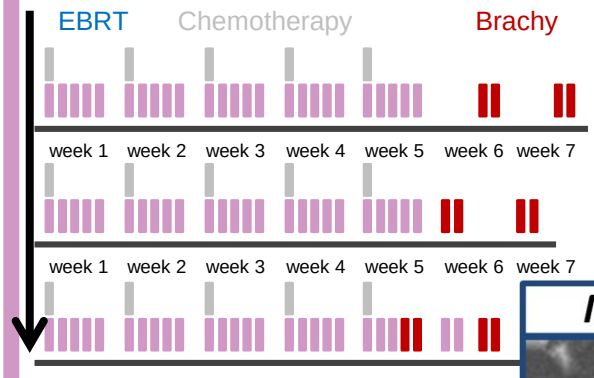

IMRT + IGRT

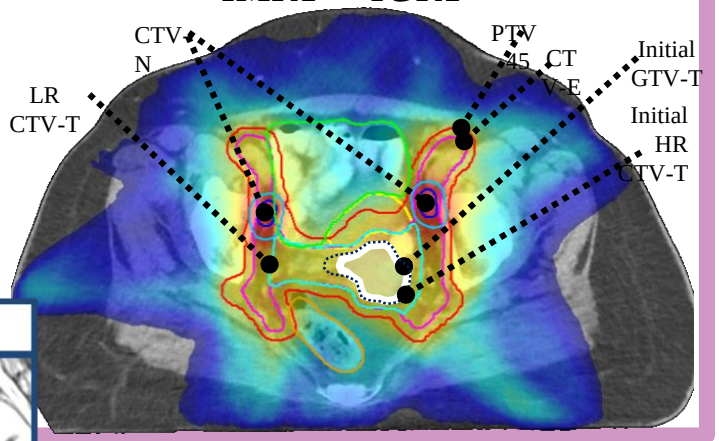

MRI guided adaptive brachytherapy (IGABT)

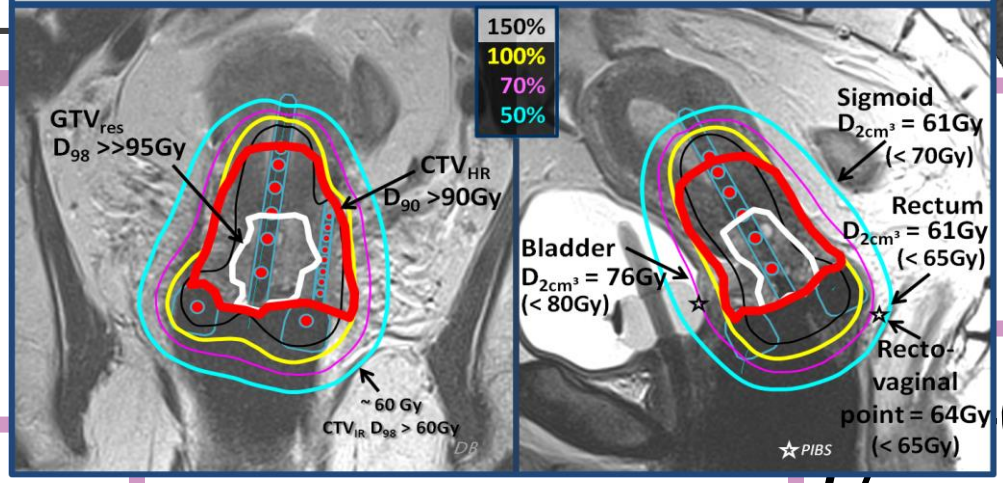

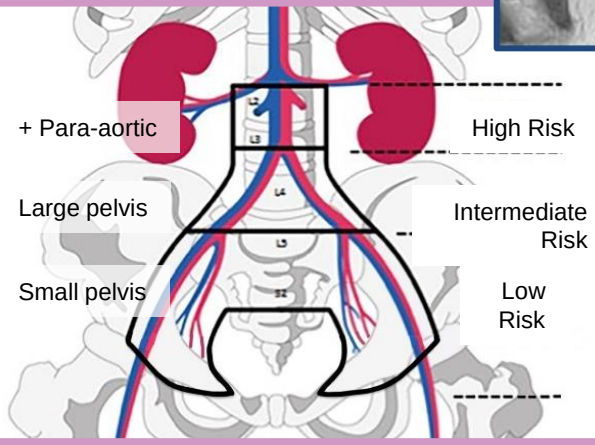

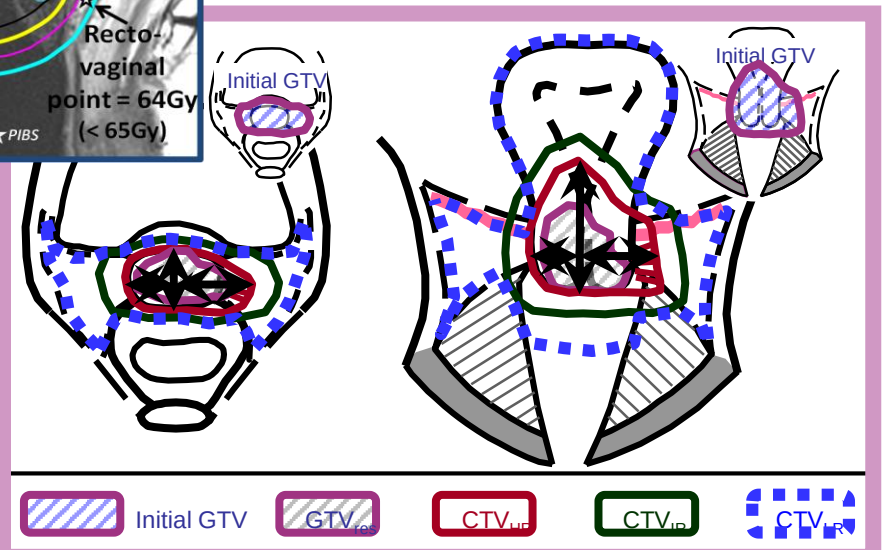

Nodal CTV-E based on Risk Group

Residual GTV-T, Adaptive HR CTV-T, IR CTV-T

ESTRO School

EMBRACE II
Prospective dose prescription protocol

Target	D90 CTV_{HR} $EQD2_{10}$	D98 CTV_{HR} $EQD2_{10}$	D98 GTV_{res} $EQD2_{10}$	D98 CTV_{IR} $EQD2_{10}$	Point A $EQD2_{10}$
Planning Aims	> 90 Gy < 95 Gy	> 75 Gy	>95 Gy	> 60 Gy	> 65 Gy
Limits for Prescribed Dose	> 85 Gy	-	>90 Gy	-	-
OAR	Bladder D_{2cm^3} $EQD2_3$	Rectum D_{2cm^3} $EQD2_3$	Recto-vaginal point $EQD2_3$	Sigmoid D_{2cm^3} $EQD2_3$	Bowel D_{2cm^3} $EQD2_3$
Planning Aims	< 80 Gy	< 65 Gy	< 65 Gy	< 70 Gy*	< 70 Gy*
Limits for Prescribed Dose	< 90 Gy	< 75 Gy	< 75 Gy	< 75 Gy*	< 75 Gy*

* for the sigmoid/bowel structures these dose constraints are valid in case of non-mobile bowel loops resulting in the situation that the most exposed volume is located at a similar part of the organ

ESTRO School

Example

			Planning aim	Prescribed dose
CTV_{HR}	D_{90}	$EQD2_{10}$	≥ 90 Gy	92.3 Gy
Bladder	D_{2cm^3}	$EQD2_3$	≤ 80 Gy	80.6 Gy
Rectum	D_{2cm^3}	$EQD2_3$	≤ 65 Gy	64.3 Gy
Sigmoid	D_{2cm^3}	$EQD2_3$	≤ 70 Gy	51.7 Gy

GEC/ESTRO recommendations on high dose rate afterloading brachytherapy for localised prostate cancer: an update.

Radiotherapy and Oncology 107 (2013) 325–332

Contents lists available at SciVerse ScienceDirect

Radiotherapy and Oncology

journal homepage: www.thegreenjournal.com

GEC/ESTRO recommendations

GEC/ESTRO recommendations on high dose rate afterloading brachytherapy for localised prostate cancer: An update

Peter J. Hoskin [a,*,1], Alessandro Colombo [b,1], Ann Henry [c,1], Peter Niehoff [d,1], Taran Paulsen Hellebust [e,1], Frank-Andre Siebert [f,1], Gyorgy Kovacs [g,1]

ESTRO School

Planning aim dose

Prescription dose

Table 3
Reporting parameters for HDR prostate brachytherapy.

1. External beam dose
2. Implant technique; number of catheters;
3. Total reference air kerma (TRAK). Total source exposure
4. Pattern of dwell times for each applicator
5. CTV: D90, V100, V150, V200
6. PTV (if defined): D90, V100, V150, V200
7. Organs at risk:
   a. Rectum: D2 cc, D0.1 cc
   b. Urethra: D0.1 cc, D10, D30

Other volumes which may be recorded but are not considered mandatory: GTV, subvolumes within CTV/PTV and Penile bulb.

Definition of target volumes / planning aim dose

CTV1 Prostate

CTV2 Peripheral zone

CTV3 Suspected tumor location (if available)

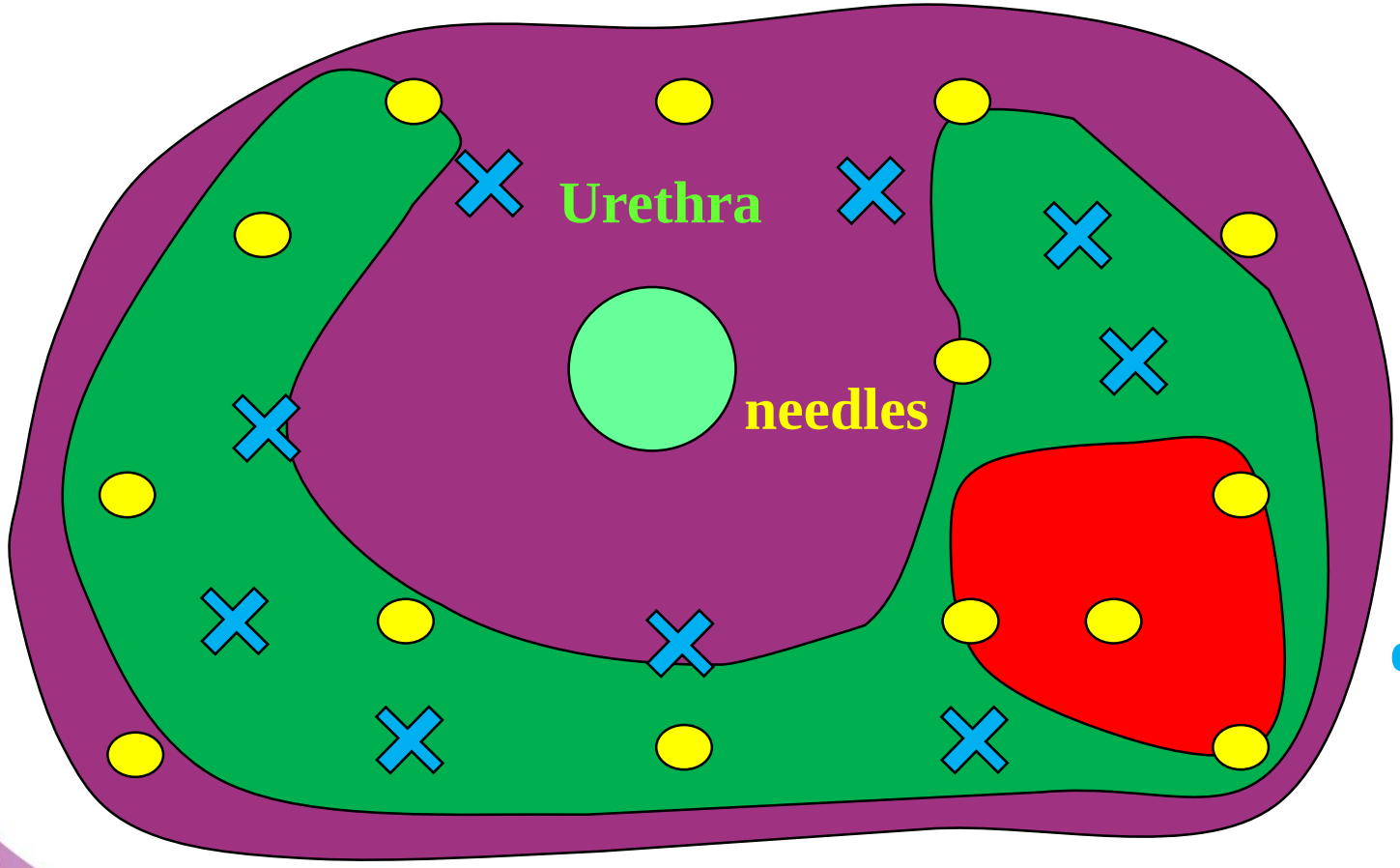

dose points

Kovacs et al. GEC-ESTRO/EAU recommendations. *Radiother Oncol* 2005

ESTRO School

MR imaging before treatment (T2)

(a) central lobe, (b) peripheral zone, (c) tumor, (d) prostate.

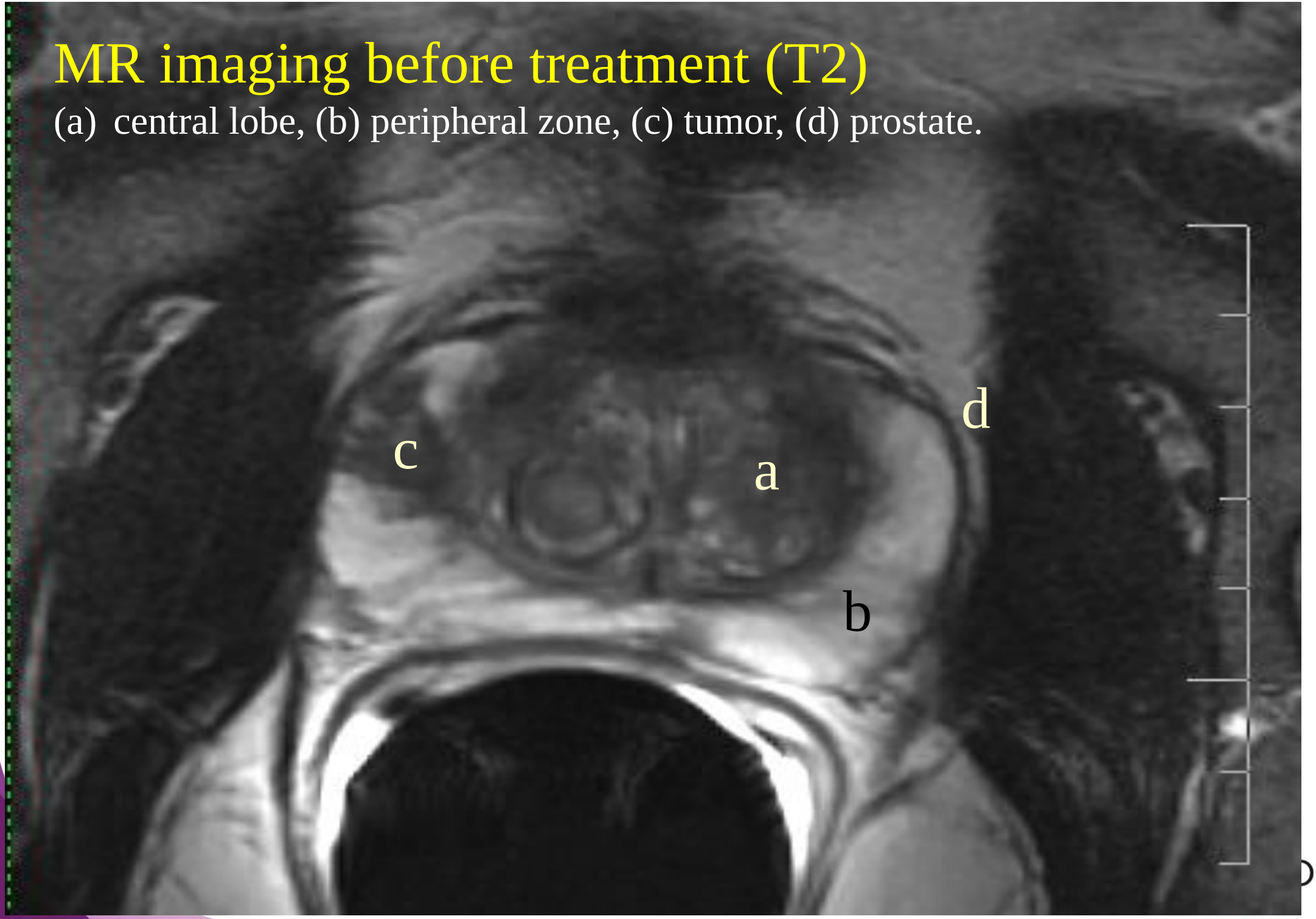

Definition of target volumes and dose

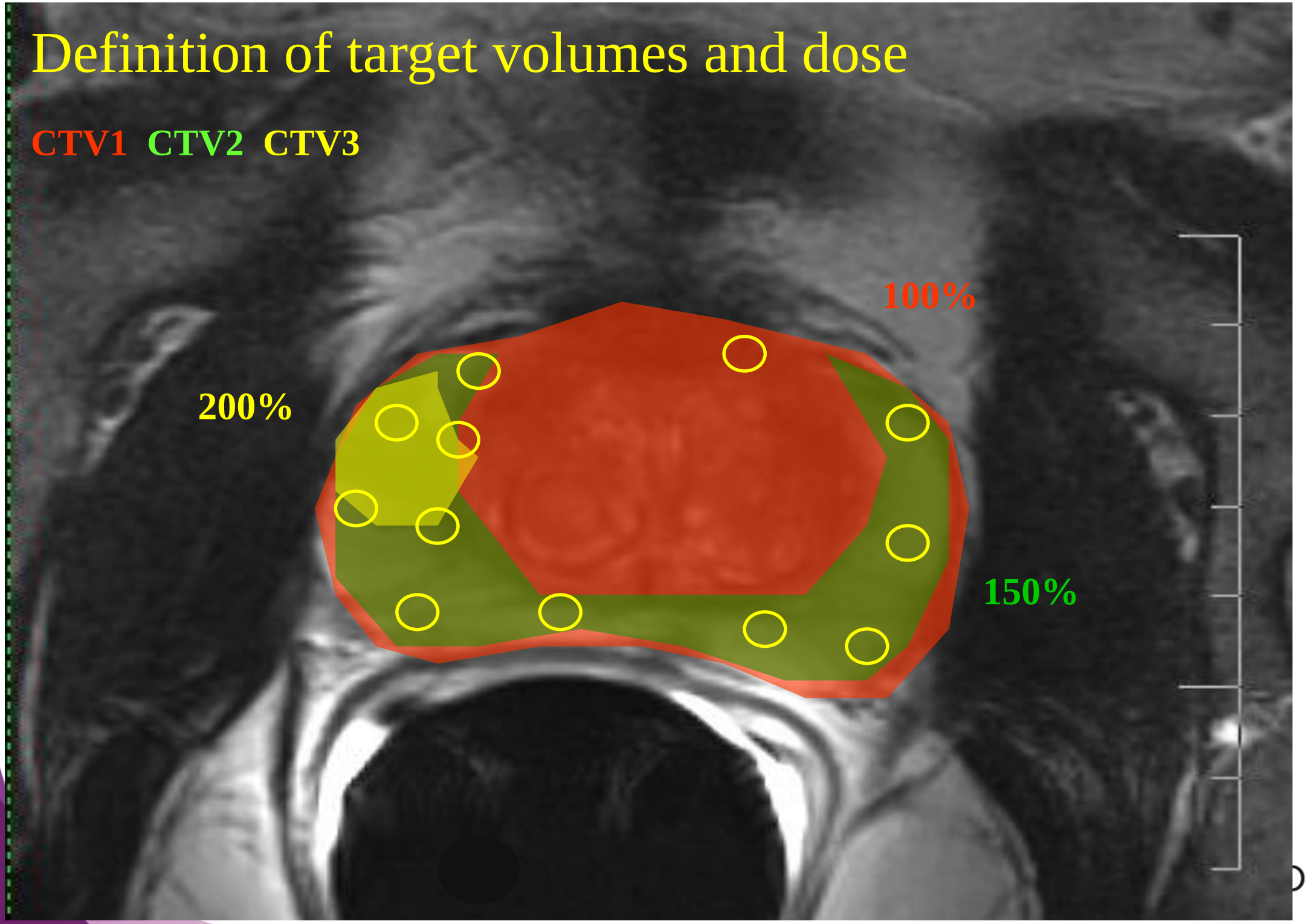

Interstitial Multicatheter Breast Brachytherapy

Radiotherapy and Oncology 128 (2018) 411–420

Contents lists available at ScienceDirect

Radiotherapy and Oncology

journal homepage: www.thegreenjournal.com

ESTRO-ACROP Guideline

ESTRO-ACROP guideline: Interstitial multi-catheter breast brachytherapy as Accelerated Partial Breast Irradiation alone or as boost – GEC-ESTRO Breast Cancer Working Group practical recommendations

Vratislav Strnad [a,*], Tibor Major [b], Csaba Polgar [c], Michael Lotter [a], Jose-Luis Guinot [c], Cristina Gutierrez-Miguelez [d], Razvan Galalae [e], Erik Van Limbergen [f], Benjamin Guix [g], Peter Niehoff [h], Kristina Lössl [i], Jean-Michel Hannoun-Levi [j]

[a] Department of Radiation Oncology, University Hospital Erlangen, Germany; [b] Center of Radiotherapy, National Institute of Oncology Budapest, Hungary; [c] Department of Radiation Oncology, Fundación Instituto Valenciano de Oncología, Valencia, Spain; [d] Department of Radiation Oncology, Catalan Institute of Oncology Barcelona, Spain; [e] Department of Radiation Therapy, Evangelische Kliniken, Gelsenkirchen, Germany; [f] Department of Radiotherapy, University Hospital Gasthuisberg, Leuven, Belgium; [g] IMOR Foundation, Medical Institute for Radiotherapy and Oncology, Barcelona, Spain; [h] Department of Radiation Therapy, Sana Hospital Offenbach, Germany; [i] Department of Radiation Oncology, University Hospital Bern, Inselspital, Switzerland; [j] Department of Radiation Oncology, Centre Antoine Lacassagne, Nice, France

Commonly reported parameters

Table 1
The most common dose–volume parameters used for reporting in interstitial breast brachytherapy.

Parameter	Definition/calculation
Implant related	
V_{PD}	Absolute volume irradiated by the prescribed dose
$V_{1.5xPD}$	Absolute volume irradiated by 1.5 x the prescribed dose
DNR – dose non-uniformity ratio	$V_{1.5xPD}/V_{PD}$
DHI – dose homogeneity index	$(V_{PD} - V_{1.5xPD})/V_{PD}$
Target related	
V_{PTV}	Volume of the PTV
V_{xx}	Percentage of PTV receiving xx% of the PD
OI – overdose volume index	V_{2xPD}/V_{PTV}
CI – coverage index	$V_{100}/100$
COIN – conformal index	$PTV_{PD}/V_{PTV} \times PTV_{PD}/V_{PD}$
D_{xx}	Percentage dose that covers xx% of the PTV
OAR related	
D_{mean}	Mean dose in organ
V_{xGy}	Relative volume receiving × Gy
V_{xx}	Percentage of organ receiving xx% of the PD
D_{xcm3}	Relative dose given to most exposed × cm^3 of organ

PD: prescribed dose, PTVPD: volume in PTV received at least the PD.

ESTRO School

Dose planning and reporting for 3D image based APBI (GEC-ESTRO trial)

Major et al. 2007, Radiother Oncol 90(1):48-55

Results for 28 pts. (mean and ranges):

volume PTV:	63.1cm³	(17.2-124cm³)
D_{90} PTV:	102 %	(99-107 %)
D_{100} PTV::	69 %	(90-96 %)
DNR:	0.33	(0.25-0.41)
skin D_{max}:	53 %	(18-75 %)
ipsilateral lung D_{max}:	42 %	(7-75 %)
V5Gy:	42.6 cm³	(0-160 cm³)
V10Gy:	4.8 cm³	(0-39.5 cm³)
V15Gy:	0.5 cm³	(0-7.9 cm³)
heart D_{max}:	21 %	(4-40 %)
V5Gy:	8 cm³	(0-33.5 cm³)
V10Gy:	0.1 cm³	(0-0.3 cm³)

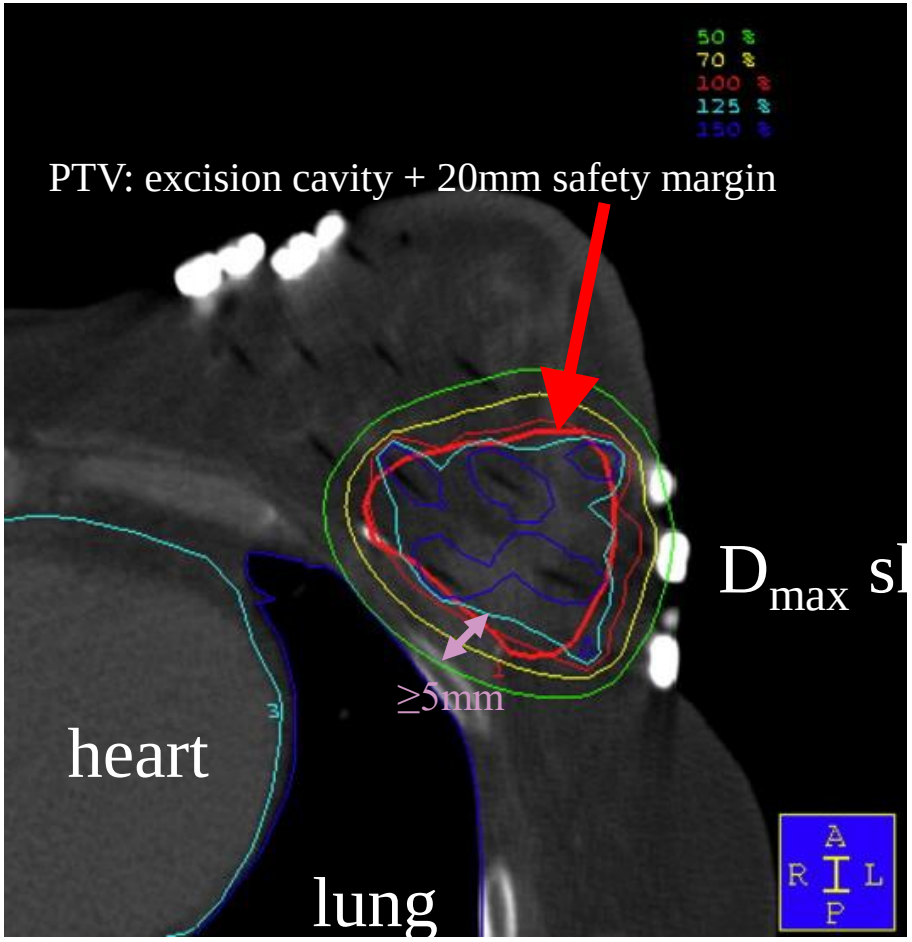

planning aim: PD = 30.1Gy (7x 4.3Gy),
V_{100} = 90%,
DNR <0.35,
implant-rib distance ≥ 5mm

ESTRO School

Recommended parameters for reporting

- nuclide, technique (HDR/PDR)
- # catheters, # planes

- method of dose optimization (manual, geometric, graphical, inverse) and normalization
- method of dose prescription: isodose line, volumetric, dose per Fx, total dose, time dose pattern
- implant-related volume parameters: VPD, DNR
- source strength, TRAK

Recommended parameters for reporting

- target-related volume parameters: V_{100}, V_{150}; V_{200}; D_{90}

- optional OAR-related parameters:
  - ipsilateral non-target breast: V_{90}, V_{50}
  - skin: D_{1cm^3}, $D_{0.2cm^3}$
  - ipsilageral lung: MLD (mean lung dose), $D_{0.1cm^3}$
  - contralateral breast: D_{1cm^3}
  - contralateral lung: D_{1cm^3}

Recommended values for prescription

Based on experience from GEC-ESTRO randomized multicenter trial *(Strnad et al. Lancet, 2016)*

Table 2
Recommended dose–volume limits for implant and PTV.

	Constraints
Implant	$V_{PD} \leq 300\ cm^3$ DNR ≤ 0.35
PTV	$V_{100} \geq 90\%$ $V_{150} < 65\ cm^3$ $V_{200} < 15\ cm^3$ COIN ≥ 0.65

Table 3
Recommended dose–volume limits for OAR-s.

Organ	Constraints
Ipsilateral non-target breast	$V_{90} < 10\%$ $V_{50} < 40\%$
Skin*	$D_{1cm3} < 90\%$ $D_{0.2cm3} < 100\%$
Rib	$D_{0.1cm3} < 90\%$ $D_{1cm3} < 80\%$
Heart**	MHD < 8% $D_{0.1cm3} < 50\%$
Ipsilateral lung	MLD < 8% $D_{0.1cm3} < 60\%$

* Skin volume is defined as a 5 mm shell below the body contour.

** Left sided lesion only, MHD: mean heart dose, MLD: mean lung dose

Need for common terminology

Planning aim dose

- Set of dose and dose/volume constraints for a treatment
  - 4 x 7 Gy to D_{90} to achieve 84 Gy EQD2 to D_{90} for HR CTV in cervix (EBRT+BT)
  - 145 Gy to D_{90} for prostate LDR
  - 8 x 4 Gy to D_{90} for breast APBI

Prescribed dose

- Finally accepted treatment plan (which is assumed to be delivered to an individual patient)

Delivered dose

- Actually delivered dose to the individual patient

From ICRU 89

PHYSICAL - BIOLOGICAL DOCUMENTATION OF GYNAECOLOGICAL HDR BT

PATIENT , ID-number

tumour entity cervix ca

EXTERNAL BEAM THERAPY

		TUMOUR	OAR
dose per fraction	1,8	D_{iso} [α/β=10Gy]	D_{iso} [α/β=3Gy]
fractions without central shield	25	44,3	43,2
fractions with central shield		0,0	0,0
total dose	**45,0**	**44,3**	**43,2**

FIGO, TNM IIB cT2b pN0

GTV at diag. 88 cm^3

chemoth. cisplatin

BRACHYTHERAPY

dose values in Gy

	F 1	F 2	F 3	F 4	F 5	F 6		
date								
TRAK [cGy at 1m]	0,54	0,49	0,47	0,44			**1,94**	
prescribed dose PD	7	7	7	7				
PD $_{iso}$ [α/β=10Gy]	9,9	9,9	9,9	9,9	0,0	0,0	39,7	**83,9**
volume of PD [cm^3]	121,1	106,9	97,7	89,5			***103,8***	*11,7*
PDx2	14,0	14,0	14,0	14,0	0,0	0,0		
PDx2 $_{iso}$ [α/β=10Gy]	28,0	28,0	28,0	28,0	0,0	0,0	112,0	156,3
volume of PDx2 [cm^3]	41,6	33	30	26,1			*32,7*	*5,7*
pres. point level (A / My / [mm])	A	A	A	A				
pres. point [mm $_{left}$ / mm $_{right}$]	22 / -22	A	A	19 / -19				
dose to + A left	7,6	7,1	6,7	6,5				
A_{left} - D_{iso} [α/β=10Gy]	11,1	10,1	9,3	8,9	0,0	0,0	39,5	**83,8**
dose to - A right	7,8	6,9	7,3	6,7				
A_{right} - D_{iso} [α/β=10Gy]	11,6	9,7	10,5	9,3	0,0	0,0	41,1	**85,4**
dose to A mean	7,7	7,0	7,0	6,6	0,0	0,0		
A_{mean} - D_{iso} [α/β=10Gy]	11,4	9,9	9,9	9,1	0,0	0,0	40,3	**84,6**
GTV [cm^3]	8,8	7,8	5,5	6,1			*7,1*	*1,3*
D 100 = MTD	9,3	8,9	6,9	6,2				
D 100 $_{iso}$ [α/β=10Gy]	15,0	14,0	9,7	8,4	0,0	0,0	47,1	91,3
D 90	13,3	12,0	11,7	10,6				
D 90 $_{iso}$ [α/β=10Gy]	25,8	22,0	21,2	18,2	0,0	0,0	87,2	**131,4**
V 100 = volume of PD [%]	100,0%	100,0%	99,9%	99,1%			***99,8%***	*0,4%*
CTV [cm^3]	53,5	51,5	40	40,4			*46,4*	*6,2*
D 100 = MTD	5,0	5,0	3,5	3,8				
D 100 $_{iso}$ [α/β=10Gy]	6,3	6,3	3,9	4,4	0,0	0,0	20,8	65,1
D 90	8,1	7,0	6,9	6,4				
D 90 $_{iso}$ [α/β=10Gy]	12,2	9,9	9,7	8,7	0,0	0,0	40,6	**84,8**
V 100 = volume of PD [%]	95,9%	90,4%	89,3%	86,8%			***90,6%***	*3,3%*
volume of mean A-dose [%]	92,7%	90,4%	89,3%	88,9%			*90,3%*	*1,5%*

LQ Model

Biological effect E of dose D:

$$E = \alpha \cdot D + \beta \cdot D^2$$

Total dose :

$$D = n \cdot d$$

n... Nr. of fractions, d... fraction dose

$$E = n \cdot (\alpha d + \beta d^2) = nd(\alpha + \beta d) =$$

$$= \alpha nd(1 + \frac{d}{\alpha / \beta})$$

=> E = α x total dose x relative dose effectiveness

Biologically effective dose:

BED = total dose x relative dose effectiveness = E / α

ESTRO School

Effective dose in EQD_{2Gy} (normalized to 2Gy fx)

$$EQD_{2Gy} = \frac{D_{(xGy)} \cdot (x + \alpha/\beta)}{(2 + \alpha/\beta)}$$

$$\alpha/\beta = 10(tumour)$$

$$\alpha/\beta = 3(OAR)$$

EBRT: $d = 1.8Gy$

$n = 25$

tumour $$EQD_{2Gy} = \frac{45_{(1.8Gy)} \cdot (1.8 + 10)}{(2 + 10)} = 44.3Gy$$

OAR $$EQD_{2Gy} = \frac{45_{(1.8Gy)} \cdot (1.8 + 3)}{(2 + 3)} = 43.2Gy$$

ESTRO School

Example for cervix cancer Brachytherapy

$$EQD_{2Gy} = \frac{D_{(xGy)} \cdot (x + \alpha/\beta)}{(2 + \alpha/\beta)}$$

$$\alpha/\beta = 10(tumour)$$

$$\alpha/\beta = 3(OAR)$$

Brachy: $d = 7Gy(tumour)$

$$d = 4.4Gy(rectum, sigmoid)$$

$$n = 4$$

tumour $$EQD_{2Gy} = \frac{28_{(7Gy)} \cdot (7+10)}{(2+10)} = 39.7Gy$$

OAR $$EQD_{2Gy} = \frac{17.6_{(4.4Gy)} \cdot (4.4+3)}{(2+3)} = 26Gy$$

ESTRO School

Conclusion

Concepts and terminology for
prescribing
recording and reporting

In a level concept:

- Level 1 - *Minimum standard for reporting*
- Level 2 - *Advanced standard for reporting*
- Level 3 - *Research oriented reporting*

Valencia, 07 – 10 October 2018

ESTRO School

Advanced Brachytherapy Physics

Optimization and Inverse Planning

Dimos Baltas, Ph.D.

Professor for Medical Physics in Radiation Oncology

Division of Medical Physics
Department of Radiation Oncology, Medical Center - University of Freiburg
Faculty of Medicine, University of Freiburg, Germany
and
German Cancer Consortium (DKTK), Partner Site Freiburg, Germany

E-mail: dimos.baltas@uniklinik-freiburg.de

ESTRO School

List of Content

- Introduction on Dose Optimisation
- Forward Planning
- Inverse Optimisation and Planning

ESTRO School

X-Ray-based / Electronic Brachytherapy (eBx)

Carl Zeiss Meditec. Inc.

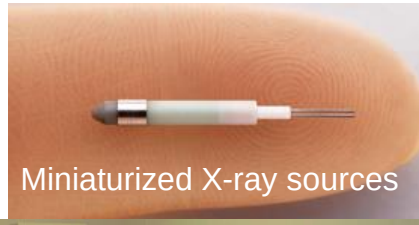

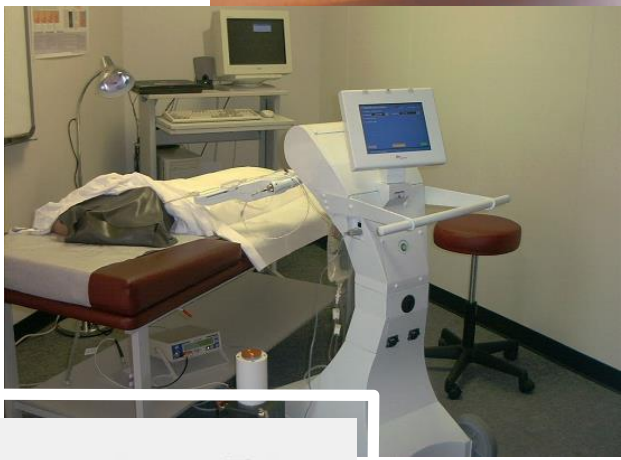

Xoft Inc.

SRT-100™
Sensus Healthcare

Ariane Medical Systems Ltd

IORT-50
WOLF-Medizintechnik

ESTRO School

Radioactive Single Source-based Brachytherapy

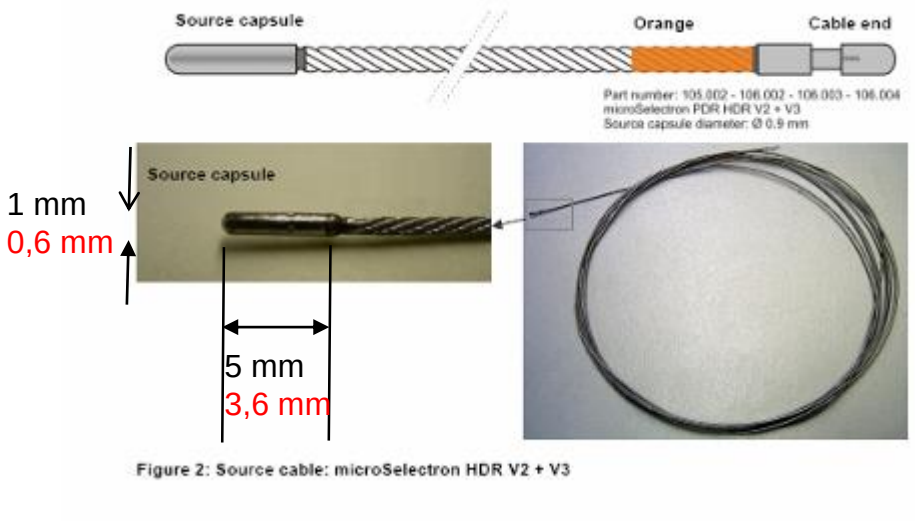

Figure 2: Source cable: microSelectron HDR V2 + V3

Introduction on Dose Optimisation

General Concept: The Mapping process or *The Dose Kernel*

From Source/ Energy Fluence Ψ

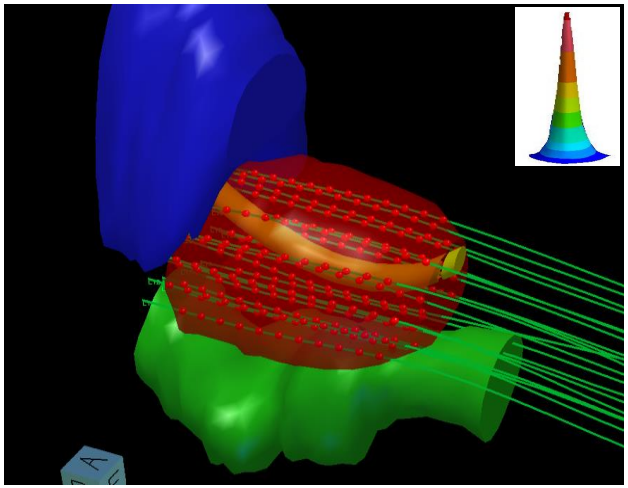

$$D = \Psi . A$$

To Dose Distribution *D*

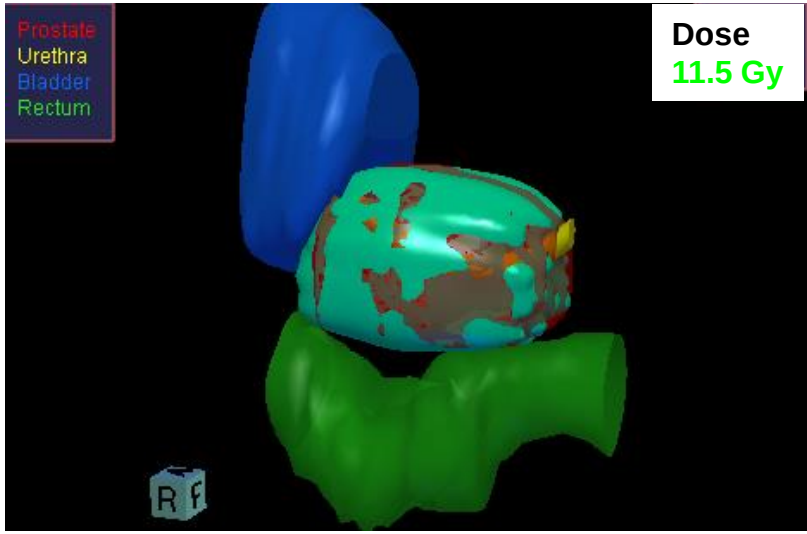

A **is the energy absorption per unit mass (dose) and unit energy fluence or the *Dose Kernel***

Ψ is the Source/Energy Fluence Function

ESTRO School

The *Dose Kernel A*

Dose rate from a single source
at a point in water-filled space
per Unit Source Strength
(in Gy min^{-1} U^{-1} or cGy min^{-1} U^{-1} or cGy h^{-1}U^{-1})
dose to water in water

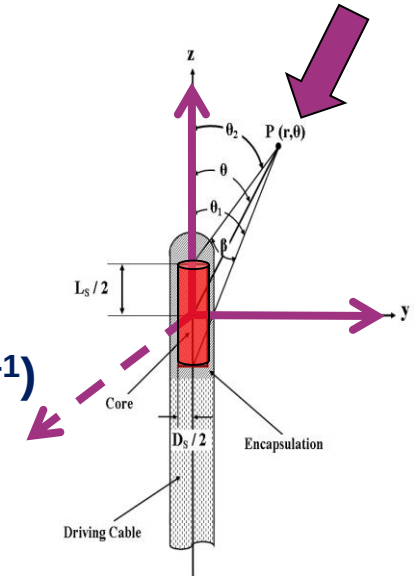

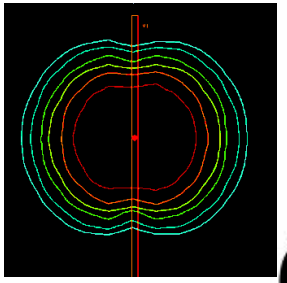

Characteristic for every Source Type

- ^{192}Ir
- ^{60}Co
- ^{169}Yb
- ^{125}I
- ^{103}Pd
- ^{131}Cs
- …

$$A(\vec{r}) = \frac{\dot{D}(\vec{r})}{S_K} = \frac{\dot{D}(r,\theta)}{S_K} = \Lambda \cdot \frac{G_L(r,\theta)}{G_L(r_0,\theta_0)} \cdot g_L(r) \cdot F(r,\theta)$$

constant

1D/2D LUTs

calculated

$$S_K = \dot{K}_\alpha(r).r^2 = \dot{\Psi}_\alpha(r).\left(\frac{\mu_{tr}}{\rho}\right)_\alpha.r^2$$

ESTRO School

Introduction on Dose Optimisation

General Concept: The Mapping process or The *Dose Kernel*

$$\{\Psi\} \rightarrow \{D\}: \qquad D = \Psi \,.\, A$$

Ψ is the Source/Energy Fluence Function

Ψ is for a single stepping source delivery system (afterloader) the *Source Propagation Function*

$$S_K = \dot{K}_\alpha(r).r^2 = \dot{\Psi}_\alpha(r).\left(\frac{\mu_{tr}}{\rho}\right)_\alpha.r^2$$

$$\Psi(\vec{r}) = \sum_{i=1}^{N_{ASDPs}} S_{K,i}.t_i.\delta(\vec{r}-\vec{r}_i)$$

$$\Psi(\vec{r}) = \sum_{i=1}^{N_{ASDPs}} \dot{\Psi}_{\alpha,i}(\vec{r}).\left(\frac{\mu_{tr}}{\rho}\right)_\alpha.r^2.t_i.\delta(\vec{r}-\vec{r}_i)$$

$\{\vec{r}_i\}$ Spatial and

$\{t_i\}$ Strength/Time Pattern

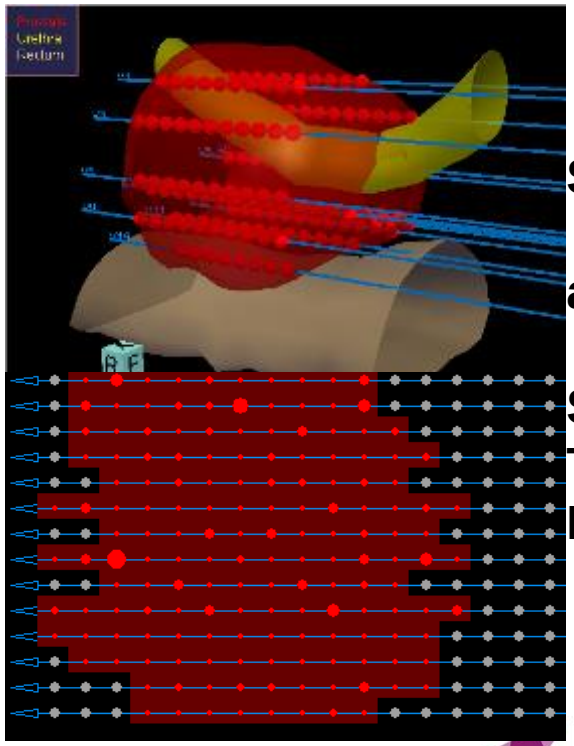

ESTRO School

Introduction on Dose Optimisation

General Concept: The Mapping process or The *Dose Kernel*

$$\{\Psi\} \rightarrow \{D\}: \qquad D = \Psi \,.\, A$$

A **is the energy absorption per unit mass (dose) and unit energy fluence or the *Dose Kernel***

Ψ **is for a single stepping source delivery system (afterloader) the *Source Propagation Function***

$$A(\vec{r}) = \frac{\dot{D}(\vec{r})}{S_K}$$

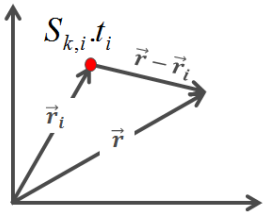

$$\Psi(\vec{r}) = \Psi(\{\vec{r}\},\{t\}) = \sum_{i=1}^{N_{ASDPs}} S_{K,i}.t_i.\delta(\vec{r}-\vec{r}_i)$$

$$D(\vec{r}) = \sum_{i=1}^{N_{ASDPs}} S_{K,i}.t_i.A(\vec{r}-\vec{r}_i)$$

or

$$D(\vec{r}) = \int_{-\infty}^{+\infty} \Psi\left(\vec{r'}\right) A(\vec{r}-\vec{r'})\, dv$$

With N_{ASDPs} the total number of source dwell positions (steps) at positions r_i and dwell times t_i.

ESTRO School

Introduction on Dose Optimisation

General Concept: The Mapping process or The *Dose Kernel*

$$\{\Psi\} \rightarrow \{D\}: \qquad D = \Psi \,.\, A$$

$$D(\vec{r}) = \sum_{i=1}^{N_{ASDPs}} S_{K,i}.t_i.A(\vec{r} - \vec{r}_i)$$

or

$$D(\vec{r}) = \int_{-\infty}^{+\infty} \Psi\left(\vec{r'}\right) A(\vec{r} - \vec{r}')\, dv$$

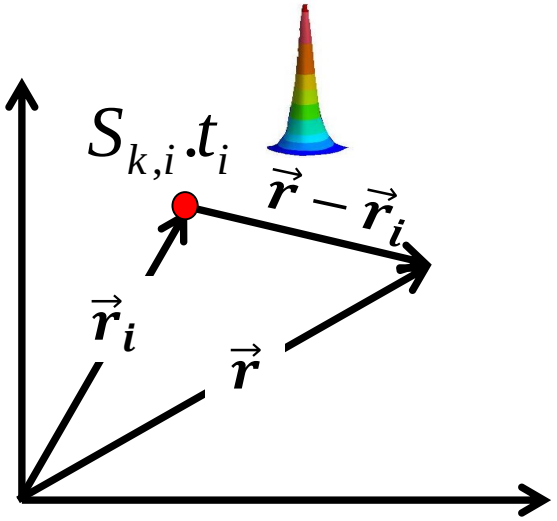

Example for the 1D simplification

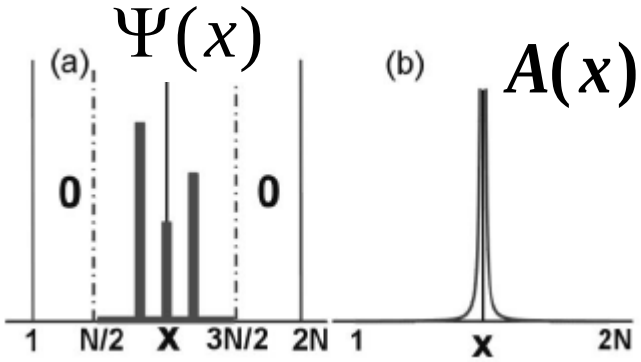

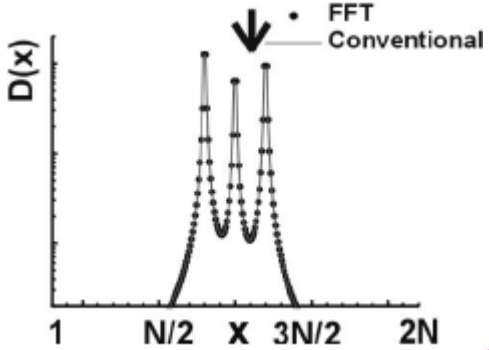

ESTRO School

Introduction on Dose Optimisation

The Mapping process or the *Dose Kernel*:

A dose distribution *D* is *achievable*, if there exist a source/ energy fluence function Ψ that is able to generate it!

- **The dose space {*D*} defines the space of all *physically achievable* dose distributions**
- **The source/energy fluence space {Ψ} defines the space of all *physically possible* source/energy fluence functions**

ESTRO School

Introduction on Dose Optimisation

While the determination of *D* from *Ψ*, the solution of the so-called forward problem, is always possible, the inverse problem, i.e. determination of *Ψ* for a specified *D* is not always possible.

The forward problem is the *dose calculation* problem for which a unique solution exists.

{Ψ*}, {D*} : all *possible*

{Ψ}, {D} : physically possible, achievable (feasible)

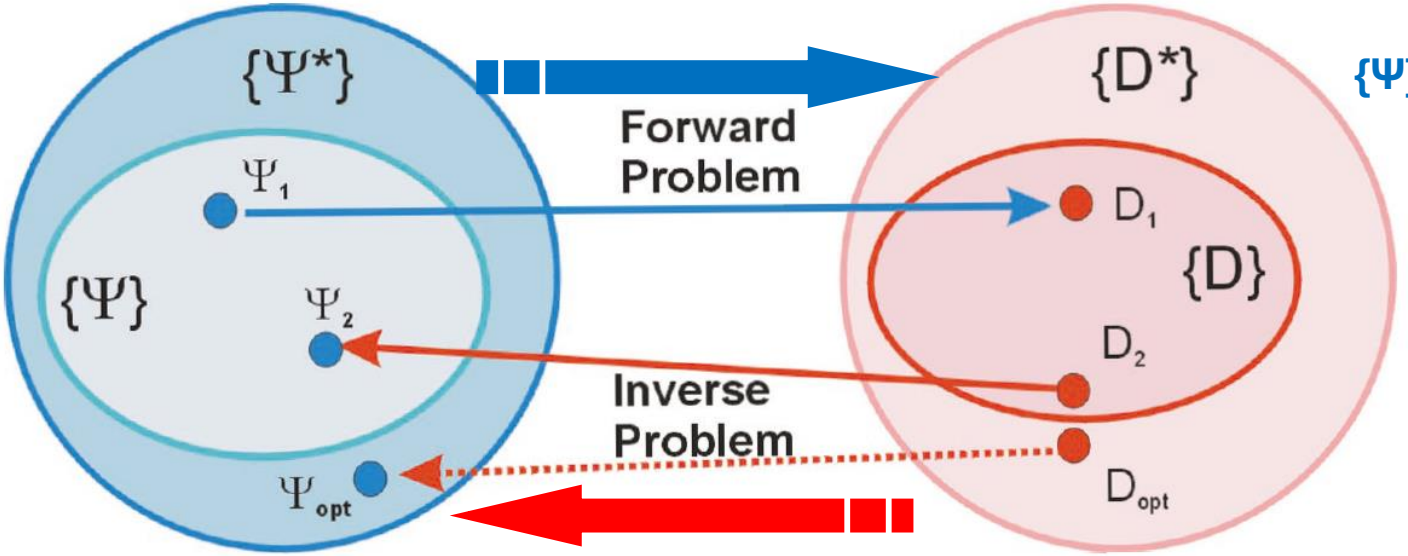

Figure 1. Forward and inverse problem in radiotherapy: The sets {Ψ*} and {D*} are all possible fluence and dose distributions respectively which include the corresponding physical possible distributions {Ψ} and {D}. The determination of a fluence distribution from a desired optimal dose distribution D_{opt} is not always possible, such as for the two physical possible dose distributions D_1 and D_2 because the corresponding fluence distribution Ψ_{opt} may not be an element of {Ψ}

ESTRO School

List of Content

- Introduction on Dose Optimisation
- Forward Planning
- Inverse Optimisation and Planning

ESTRO School

Introduction on Dose Optimisation

While the determination of *D* from *Ψ*, the solution of the so-called forward problem, is always possible, the inverse problem, i.e. determination of *Ψ* for a specified *D* is not always possible.

The forward problem is the *dose calculation* problem for which a unique solution exists.

{Ψ*}, {D*} : all *possible*

{Ψ}, {D} : physically possible (feasible)

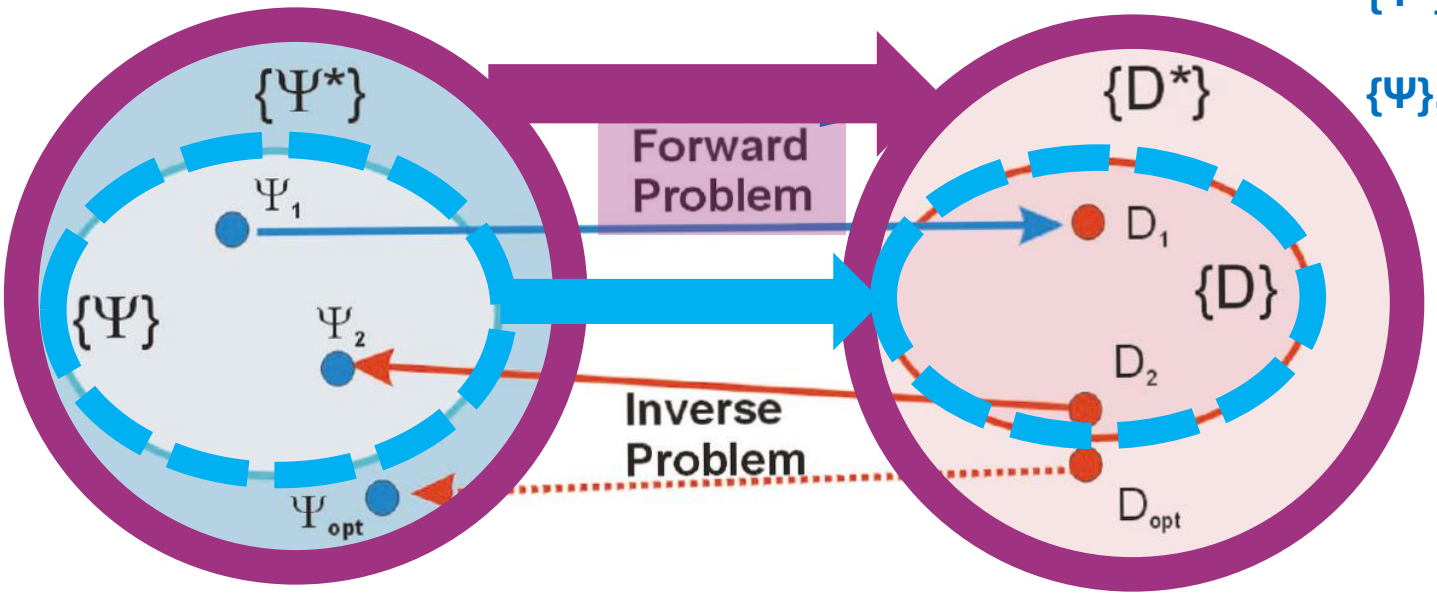

Figure 1. Forward and inverse problem in radiotherapy: The sets {Ψ*} and {D*} are all possible fluence and dose distributions respectively which include the corresponding physical possible distributions {Ψ} and {D}. The determination of a fluence distribution from a desired optimal dose distribution D_{opt} is not always possible, such as for the two physical possible dose distributions D_1 and D_2 because the corresponding fluence distribution Ψ_{opt} may not be an element of {Ψ}

ESTRO School

The "Forward Planning" in Brachytherapy (1990 – 1999)

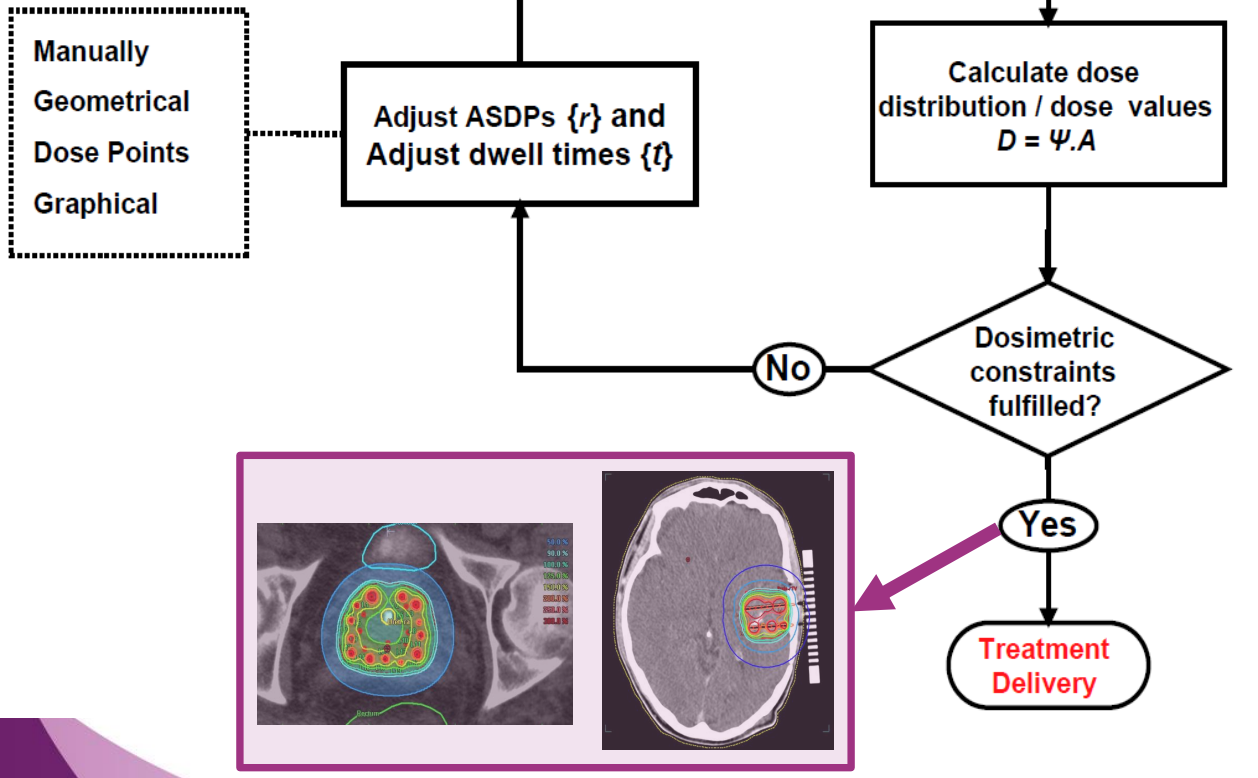

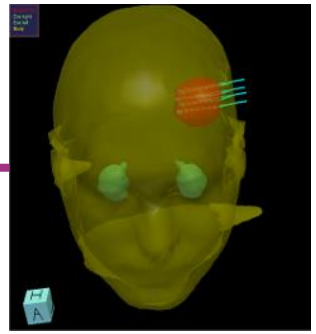

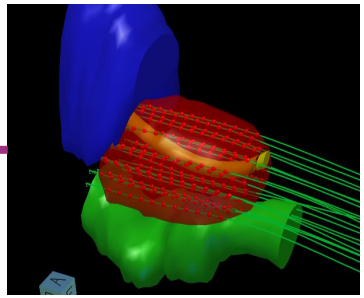

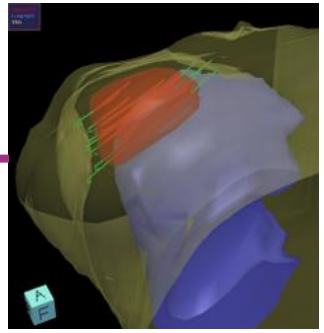

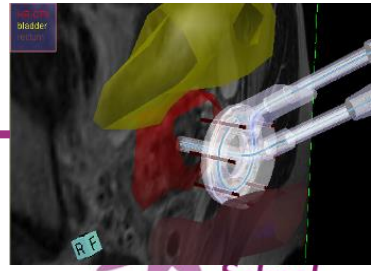

List of Content

- Introduction on Dose Optimisation
- Forward Planning
- **Inverse Optimisation and Planning**

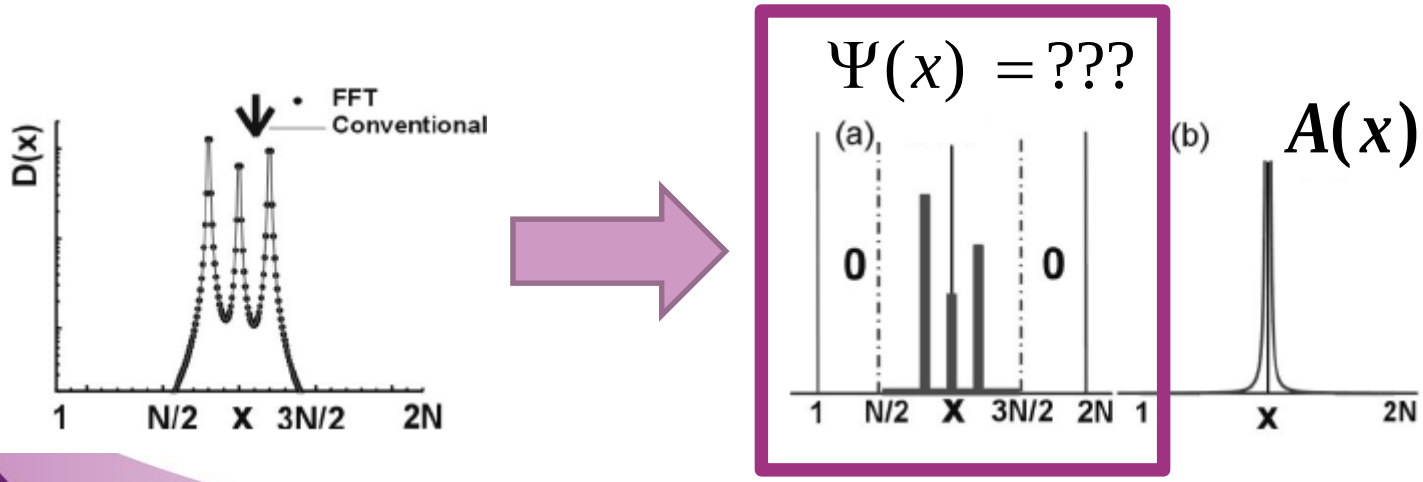

ESTRO School

Inverse Optimisation and Planning

General Concept: The *Inverse Problem*

$$\{D\} \rightarrow \{\Psi\}: \qquad D = \Psi . A$$

A **is the energy absorption per unit mass (dose) and unit energy fluence or the *Dose Kernel***

Ψ **is for a single stepping source delivery system (afterloader) the *Source Propagation Function***

$$A(\vec{r}) = \frac{\dot{D}(\vec{r})}{S_K}$$

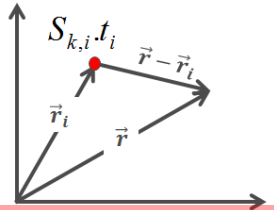

$$\Psi(\vec{r}) = \Psi(\{\vec{r}\},\{t\}) = \sum_{i=1}^{N_{ASDPs}} S_{K,i}.t_i.\delta(\vec{r}-\vec{r}_i)$$

$$D(\vec{r}) = \sum_{i=1}^{N_{ASDPs}} S_{K,i}.t_i.A(\vec{r}-\vec{r}_i)$$

or

$$D(\vec{r}) = \int_{-\infty}^{+\infty} \Psi(\vec{r}')\,A(\vec{r}-\vec{r}')\,dv$$

With N_{ASDPs} the total number of source dwell positions (steps) at ***which*** positions r_i and with ***what*** dwell times t_i?

ESTRO School

Inverse Optimisation and Planning

Preconditions:

- **Complete 3D anatomy model: Targets (GTVs), CTV/PTV, OARs** ⇨ **Morphology**
- **Implantation rules (anatomical constraints)**
- **Implantation methods, instruments, …** } **Topography**
- **Desired dose distribution $D(\vec{r})$** ⇨ **Dosimetric Result/Aims**

$$\Psi(\vec{r}) = \Psi(\{\vec{r}\},\{t\}) = \sum_{i=1}^{N_{ASDPs}} S_{K,i}.t_i.\delta(\vec{r}-\vec{r}_i) = ?$$

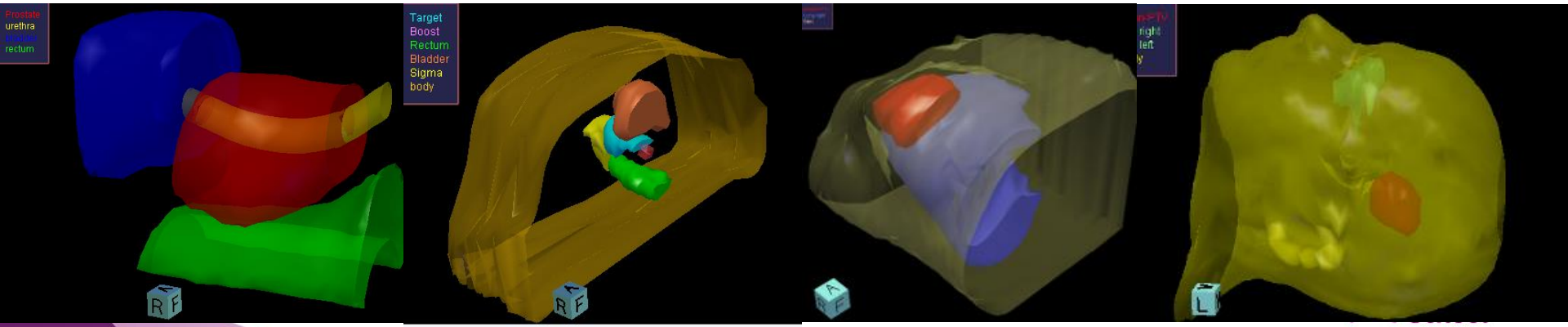

Inverse Optimisation and Planning

Preconditions:

- **Complete 3D anatomy model: Targets (GTVs), CTV/PTV, OARs** ⇨ **Morphology**
- **Implanted catheters/applicators**
- **Rules/selection of source dwell positions** } **Topography**
- **Desired dose distribution $D(\vec{r})$** ⇨ **Dosimetric Result/Aims**

$$\Psi(\vec{r}) = \Psi(\{\vec{r}\},\{t\}) = \sum_{i=1}^{N_{ASDPs}} S_{K,i}.t_i.\delta(\vec{r}-\vec{r}_i) = ?$$

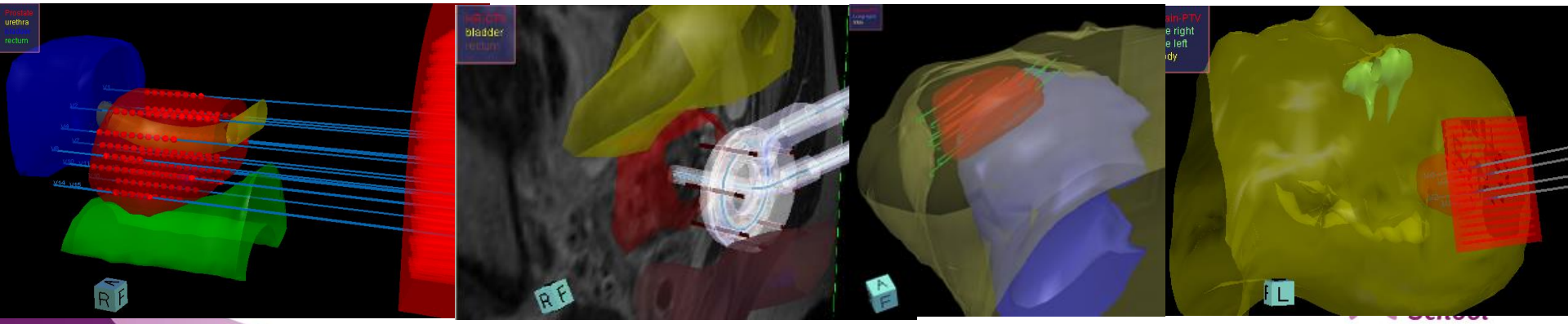

Inverse Optimisation and Planning

Desired/Aimed Dose Distribution:

Even if the "*ideal*" dose distribution can be easily decided:

$$D(\vec{r}) = \begin{cases} D_{prescription} & \forall\ \vec{r} \in \mathrm{PTV} \\ 0 & \forall\ \vec{r} \notin \mathrm{PTV} \end{cases}$$

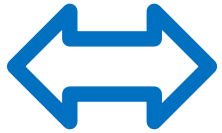

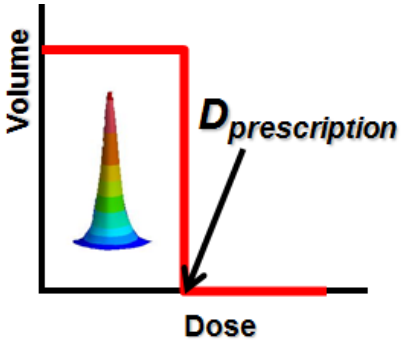

due to the "*nature*" of the dosimetric Kernel *A(r)*, *D* ∈ *{D*}* as defined here does not belong to the *Physically* achievable dose distributions *D* ∉ *{D}*.

ESTRO School

Inverse Optimisation and Planning

Desired Dose Distribution:

"Desired" Dose Distribution

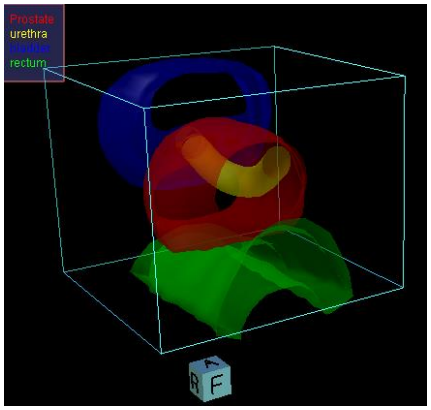

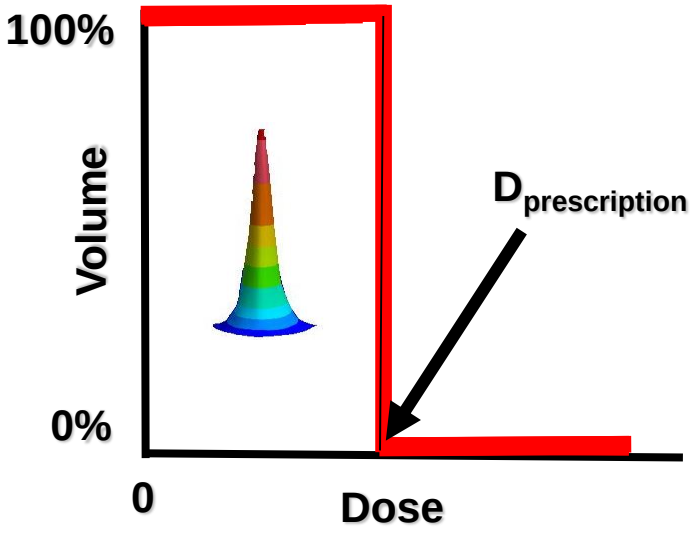

$$D(\vec{r}) = \begin{cases} D_{prescription} & \forall\ \vec{r} \in \mathrm{PTV} \\ 0 & \forall\ \vec{r} \notin \mathrm{PTV} \end{cases}$$

ESTRO School

Inverse Optimisation and Planning

Desired Dose Distribution:

"Desired" Dose Distribution ⇨ Define Dose Window for Target(s), NT & OAR(s) ⇨ *Objectives*

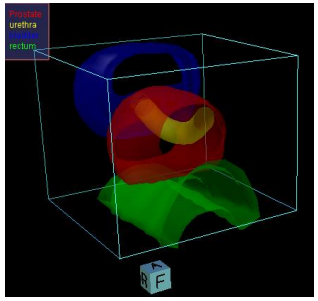

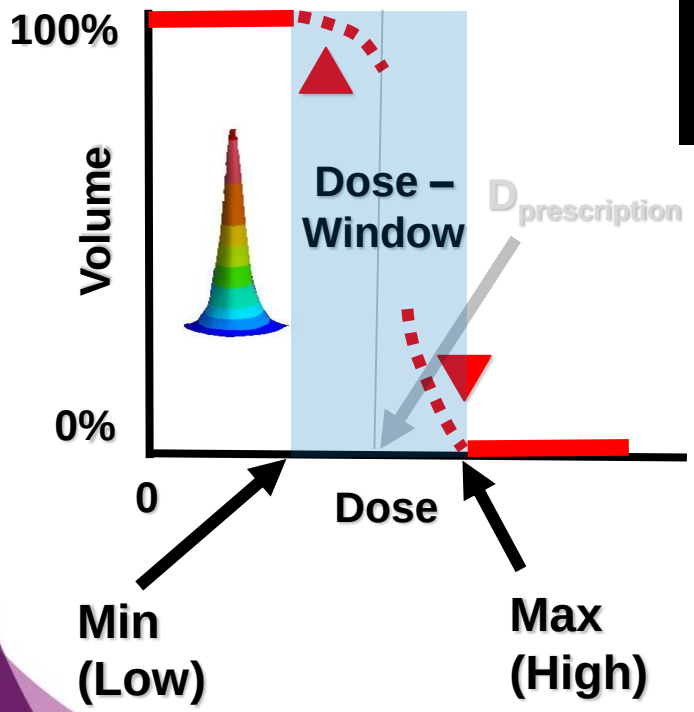

Dose - Volume – Pairs D_V for GTVs, CTV/PTV, OARs

⇨ **V = 0% => $D_{max} = D_H$**

⇨ **V = 100% => $D_{min} = D_L$**

The Desired Dose Distribution for the *Inverse Planning - Optimisation Process* is then defined as $\{D_V\}$, and/or $\{V_D\}$ *desired/aim value sets, the Objectives*.

ESTRO School

Inverse Optimisation and Planning

Objectives and Objective Functions:

The selected and defined Dose-Volume parameters, usually D_V, for the inverse optimisation process determine the *Objectives* of the optimisation.

The measure of how well these values are achieved defines the "*Metrics*" – the *Objective Functions* of the optimisation methodology (algorithm).

A natural measure quantifying the similarity of a dose distribution at N sampling points with dose values d_i to the corresponding desired dose values d_i^* is a distance measure. A common measure is the L_p norm:

$$L_p = \left\{ \sum_{i=1}^{N} \left(d_i - d_i^* \right)^p \right\}^{1/p}$$

For $p = 2$, i.e. L_2 we have the Euclidean distance.

ESTRO School

Inverse Optimisation and Planning

Desired Dose Distribution:

"Desired" Dose Distribution ⇨ Define Dose Window for Target(s), NT & OAR(s) ⇨ *Objectives* ⇨ *Objective Functions*

General Form of an *Objective Function* and DVH

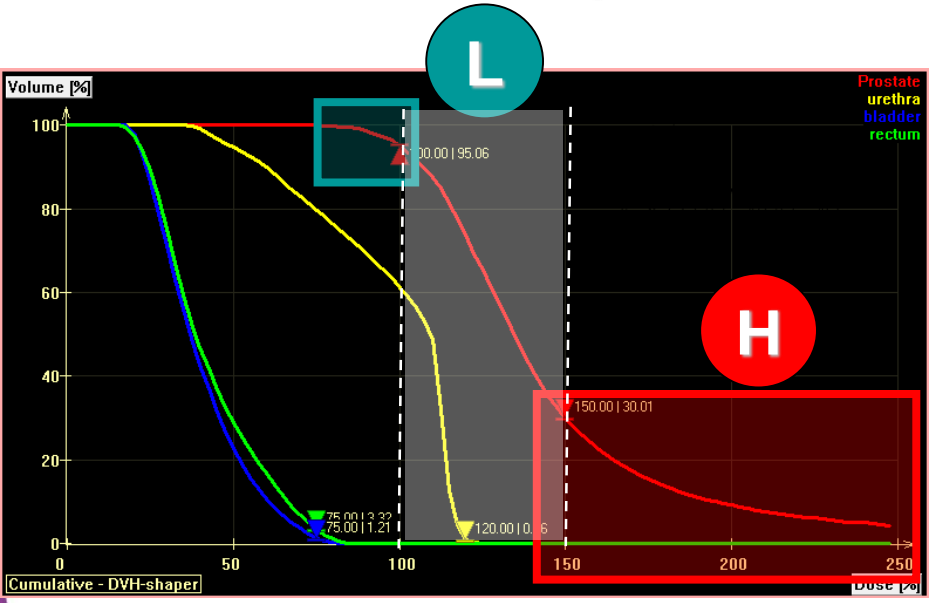

Dose window

Low dose Objective for PTV/GTVs

$D_L = D_V$ for $V_{100\%}$

$$f_i = \frac{1}{N_i}\sum_{j=1}^{N_i}\left[\Theta\left(D_L^i - d_j^i(\boldsymbol{x})\right)\left[D_L^i - d_j^i(\boldsymbol{x})\right]^p\right]$$

High dose Objective for PTV/GTVs

$D_H = D_V$ for $V_{0\%}$

$$f_i = \frac{1}{N_i}\sum_{j=1}^{N_i}\left[\Theta\left(d_j^i(\boldsymbol{x}) - D_H^i\right)\left[d_j^i(\boldsymbol{x}) - D_H^i\right]^p\right]$$

Transition Function *Θ*:

$$\Theta(y) = \begin{matrix} 0, & \forall\, y < 0 \\ 1, & \forall\, y \geq 0 \end{matrix}$$

The Norm Factor *p*

0 : Volume counting

1 : Linear penalty

2 : Quadratic penalty

ESTRO School

Inverse Optimisation and Planning

Objectives & Objective Functions

General

$$f_i = \frac{1}{N_i}\sum_{j=1}^{N_i}\left[\Theta\left(D_L^i - d_j^i(\boldsymbol{x})\right)\left[D_L^i - d_j^i(\boldsymbol{x})\right]^p\right] \Rightarrow \textit{Under-dosage (low)}$$

$$f_i = \frac{1}{N_i}\sum_{j=1}^{N_i}\left[\Theta\left(d_j^i(\boldsymbol{x}) - D_H^i\right)\left[d_j^i(\boldsymbol{x}) - D_H^i\right]^p\right] \Rightarrow \textit{Over-dosage (high)}$$

Optimising the values of the *Objective Functions* results to *Optimisation of the 3D Dose Distribution*.

Due to the fact that in general *Objective Functions* are defined as over-dosages (High-Objective) or under-dosage(s) (Low-Objective), *Optimisation of an Objective Function means Minimization of its value (ideally 0) by adjusting the independent parameter values such as catheter positions, active source dwell positions and source dwell times*.

ESTRO School

Inverse Optimisation and Planning

Objectives & Objective Functions

Define Dose Window for Target(s), NT & OAR(s) ⇒ **Objectives** ⇒ ***Objective Functions***

Low-Objective
***D_L* for V_{Low}**

$$f_i = \frac{1}{N_i}\sum_{j=1}^{N_i}\left[\Theta\left(D_L^i - d_j^i(x)\right)\left[D_L^i - d_j^i(x)\right]^p\right]$$

High-Objective
***D_H* for V_{High}**

$$f_i = \frac{1}{N_i}\sum_{j=1}^{N_i}\left[\Theta\left(d_j^i(x) - D_H^i\right)\left[d_j^i(x) - D_H^i\right]^p\right]$$

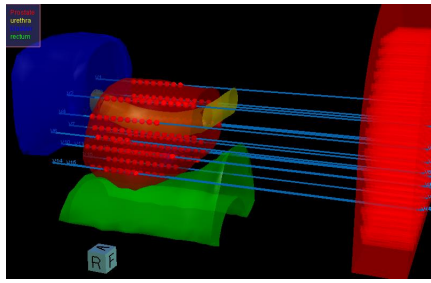

***d^i_j* is the Dose at the Sampling Point *j* for *Objective Function i*:**

$$d^i_j(x) = \sum_{k=1}^{N_{cath}}\sum_{l=1}^{N^k_{ASDP}} x^2_{lk} S_{K,lk}\,\tilde{d}^{\,i}_{jkl}$$

$$D(\vec{r}) = \int_{-\infty}^{+\infty} \Psi(\vec{r}')\, A(\vec{r} - \vec{r}')\, dv$$

- x^2_{lk} → **Implanted Catheters**
- N^k_{ASDP} → **Active SDPs**
- $S_{K,lk}$ → **Dwell time $t_{lk} = x_{lk}^2$**

ESTRO School

Inverse Optimisation and Planning

Objectives & Objective Functions

d^i_j is the dose at the j^{th}-sampling point for the i^{th}-objective function:

$$d^i_j(x) = \sum_{k=1}^{N_{cath}} \sum_{l=1}^{N^k_{ASDP}} x^2_{lk} S_{K,lk} \tilde{d}^i_{jkl}$$

Catheters — Active SDPs — Dwell times t_{lk} ?

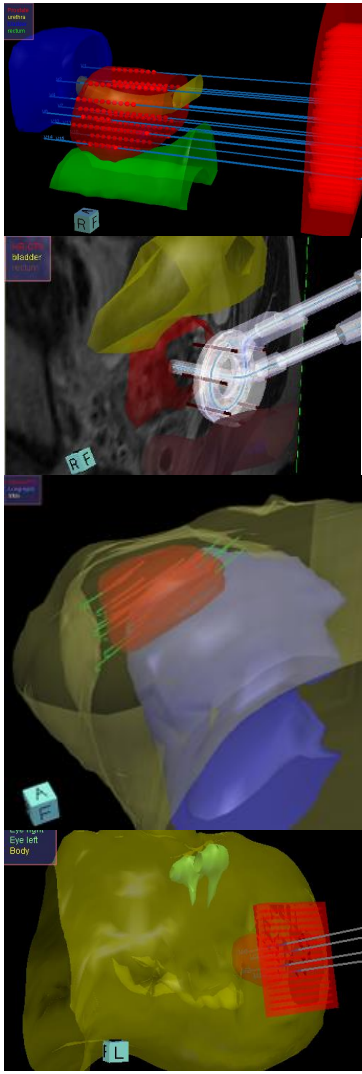

- $x^2_{lk} = t_{lk}$ to avoid negative (non-physical) dwell time values t_{lk}
- $\tilde{d}^i_{jkl}$, can (should) be calculated in a pre-processing step and are then available in a sense of *a Look-Up-Table* for the optimisation process. Implementations in this way make optimiser independent of the dose calculation engine considered (*TG 43, MC, BS, CC, other Engines*)

ESTRO School

A short Introduction into the Multiobjective Optimisation Problem

Facts

Inverse Optimisation and Planning **for brachytherapy has to consider several *Objectives* and is thus a *Multiobjective* (*MO*) problem.**
We have *competing Objectives*. Increasing the dose in the Target will increase the dose outside it.
A trade-off between the Objectives exist and we never have a situation in which all the Objectives can be in the best possible way satisfied simultaneously.

GTVs
CTV/PTV
OARs
NT

$$f_i = \frac{1}{N_i}\sum_{j=1}^{N_i}\left[\Theta\left(D_L^i - d_j^i(\boldsymbol{x})\right)\left[D_L^i - d_j^i(\boldsymbol{x})\right]^p\right] \quad \textbf{(low)}$$

$$f_i = \frac{1}{N_i}\sum_{j=1}^{N_i}\left[\Theta\left(d_j^i(\boldsymbol{x}) - D_H^i\right)\left[d_j^i(\boldsymbol{x}) - D_H^i\right]^p\right] \quad \textbf{(high)}$$

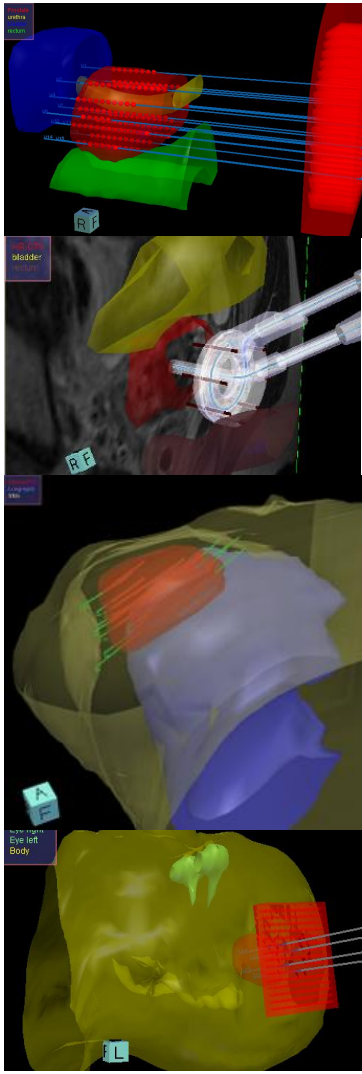

ESTRO School

Dominance & Pareto Front

A plan/solution x_1 **dominates** a plan/solution x_2 ***if and only if*** the two following conditions are true:

- x_1 **is no worse than** x_2 **in all objectives,** ***i.e.*** $f_j(x_1) \leq f_j(x_2) \;\; \forall$ j=1,...,*M.*
- x_1 **is strictly better than** x_2 **in at least one objective,**
  i.e. $f_j(x_1) < f_j(x_2)$ ***for at least one*** $j \in \{1,...,M\}$.

Among a set of solutions ***P***, the ***non-dominated set of* solutions *P'*** are those that ***are not dominated*** by any other member of the set ***P***: ***The Pareto Optimal Set P'***.
For the case that the set ***P*** *is* the entire feasible search space then the set ***P'*** is called ***the global Pareto Optimal Set***.

The image ***f(x)*** **of the** ***Pareto Optimal Set*** is called the ***Pareto Front (PF)***.
The ***Pareto Optimal Set*** is defined in the ***Parameter Space***, while the ***Pareto Front*** is defined in the ***Objective Space***.

Inverse Optimisation and Planning: A Multi-Objective (MO) Problem

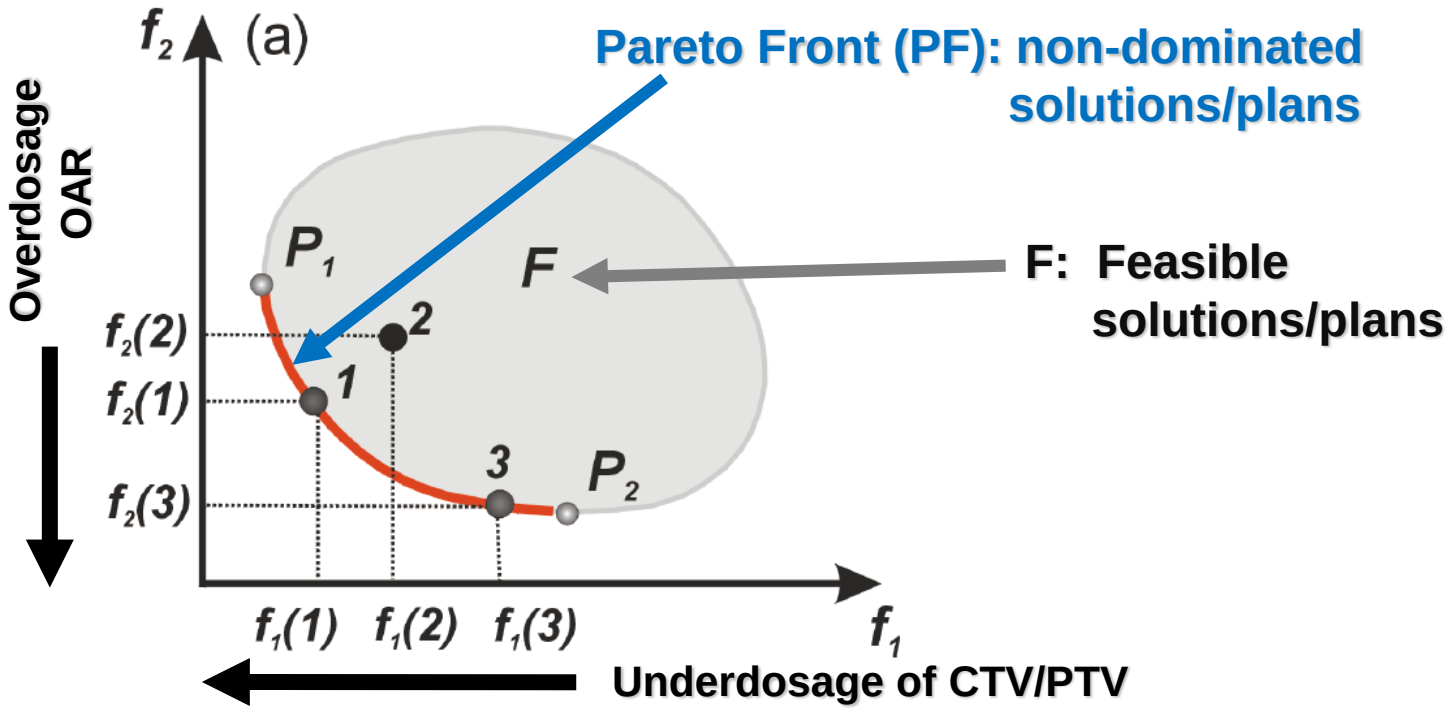

Example of ***a bi-objective space (f_1, f_2)***. *We assume as mentioned already the minimization problem.*

The ***Pareto Front*** is the boundary between the points P_1 and P_2 of the ***feasible set F***. Solutions 1 and 3 are ***non-dominated Pareto optimal solutions***. Solution 2 is ***not Pareto Optimal*** as solution 1 has simultaneously smaller values for both objectives. **There is no reason why solution 2 should be accepted rather than solution 1.**

Therefore the aim of MO optimisation is to obtain a representative set of non-dominated solutions.

ESTRO School

Inverse Optimisation and Planning: A Multi-Objective (MO) Problem

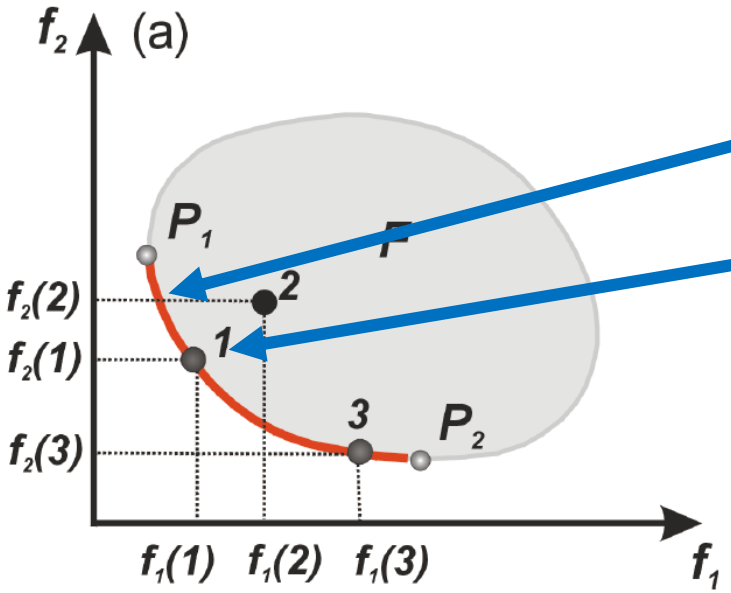

The *Multiobjective Optimisation* (*MO*) consists of two main Steps:

1. **Estimation/Localisation of the *Pareto Front* (*Optimisation*)**
2. **Selection of the *most appropriate Plan* (*Decision*)**

Some issues:

- **Computationally intensive (time)**
- **Decision Tools (expertise)**

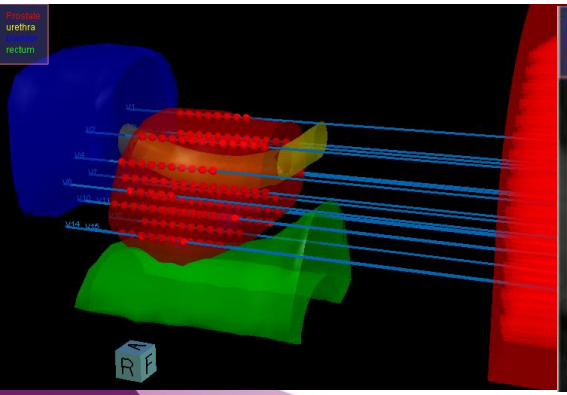

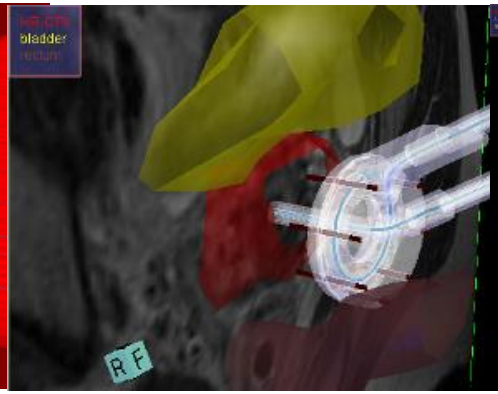

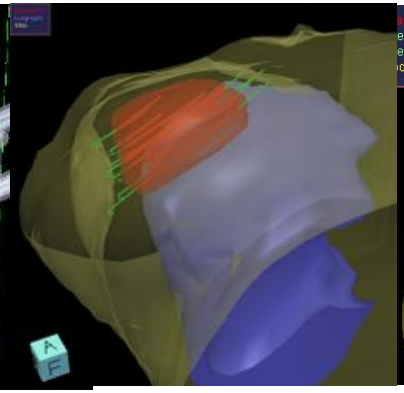

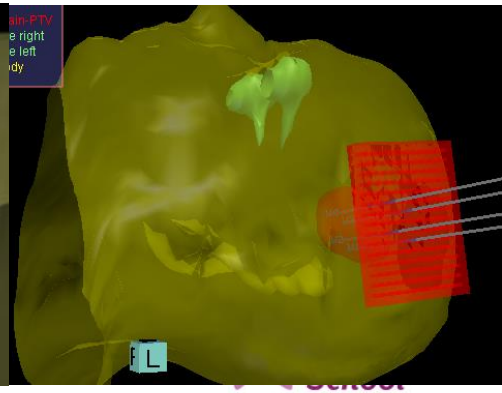

Inverse Optimisation and Planning: A Multi-Objective (MO) Problem

Strong trade-off

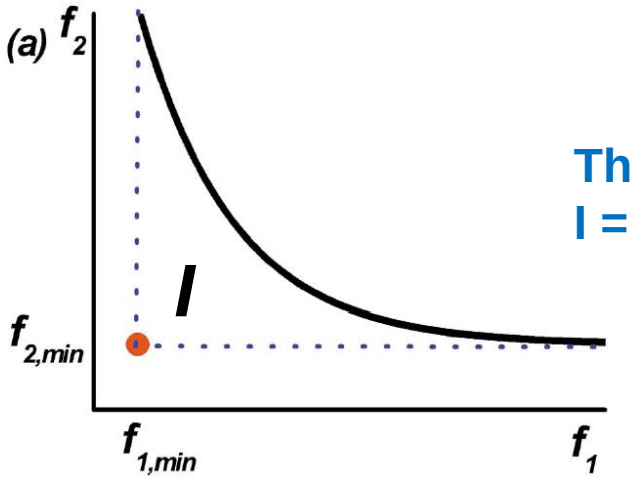

The *"ideal solution/plan" I:*
$I = (f_{1,min}, f_{2,min})$

Weak trade-off

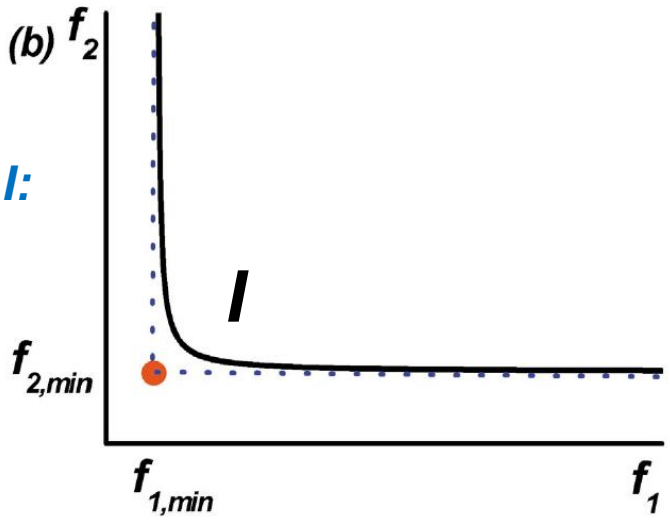

Examples of a Pareto Front

Left: there is ***a strong trade-off*** between the objectives/ objective functions f_1 *and* f_2. The smaller the f_1 value is that we want the larger is the corresponding f_2 value. The ***"ideal point/plan" I*** lies far away form the front. **There is a high dependence on the selection of the f_1 value**.

Right: there is ***a weak trade-off*** between the objectives/ objective functions f_1 *and* f_2. It is possible to optimise (minimise) the f_1 significant and close to the ***"ideal point/plan" I.*** Only very close to ***I*** we observe a rapid increase of f_2. This is a case where for a set of parameters **we can obtain simultaneously almost individual optimal values for f_1 and f_2**

ESTRO School

Inverse Optimisation and Planning: A Multi-Objective (MO) Problem

Example:

Bi-Objective Pareto Fronts obtained for **22 prostate implants**. The variety shows that a single objective optimization does not give always a good result. **In general a strong trade-off is observed. ***

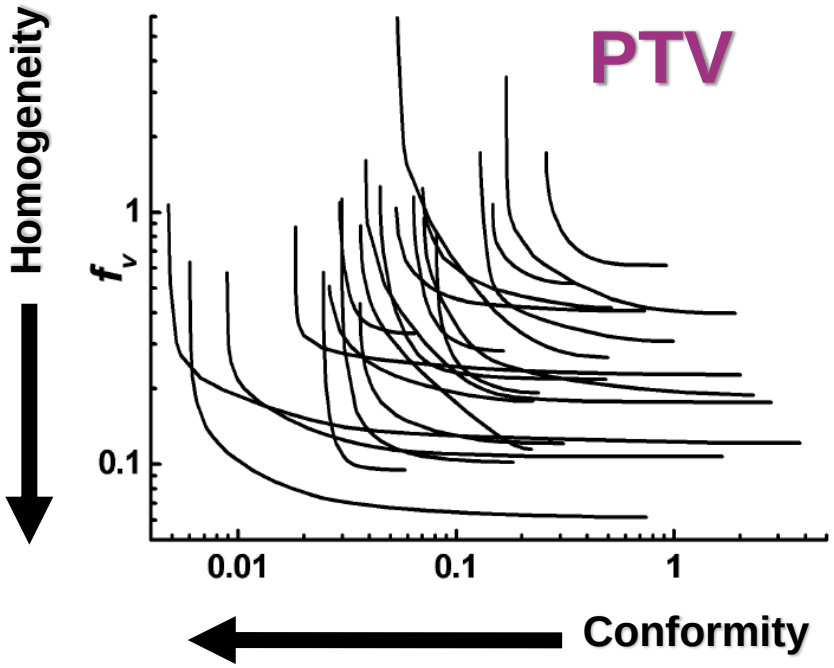

Example of a Pareto Front: there is ***a strong trade-off*** between the objectives/ objective functions f_1 *and* f_2. The smaller the f_1 value is that we want the larger is the corresponding f_2 value. The ***"ideal point/plan" I*** lies far away form the front. There is a high dependence on the selection of the f_1 *value.*

***Lahanas, Milickovic, Baltas, Zamboglou: "Application of Multiobjective Evolutionary Algorithms for Dose Optimization Problems in Brachytherapy",** EMO 2001, LNCS 1993, 574-587, 2001.

ESTRO School

Inverse Optimisation and Planning: A Multi-Objective (MO) Problem

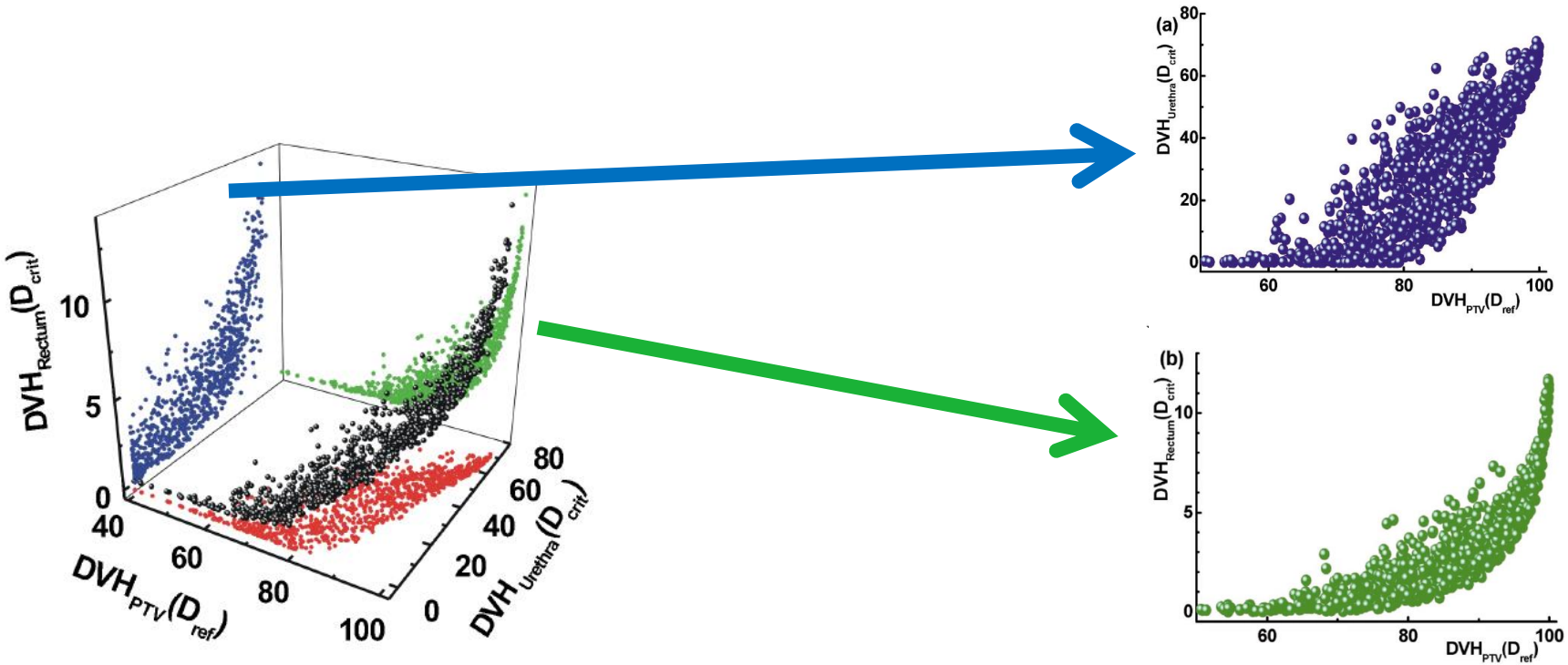

Trade-off between three objectives (objective functions) for a prostate implant:

f_1* : *PTV coverage*, *f_2* : *urethra overdose and ***f_3* : *rectum overdose***.

There resulting ***three two-dimensional projections*** are shown. These show the ***trade-off*** between two objectives in each case.

While for two objectives a solution very close to the optimal can be found, this becomes more difficult as more objectives are considered. **The complexity of the *Pareto Front* increases rapidly with the number of objectives / objective functions**.

ESTRO School

Inverse Optimisation and Planning

Objectives & Objective Functions (several: GTVs, OARs, NT,..)

Create a single Objective Function via *weighted Aggregation*

The M ***objective functions f_m*** *are* combined into a ***single objective function f***, by using a ***weighted sum (aggregation)*** of all objectives:

$$f = \sum_{m=1}^{M} w_m f_m = f(\{\vec{r}\},\{t\},\{w\})$$

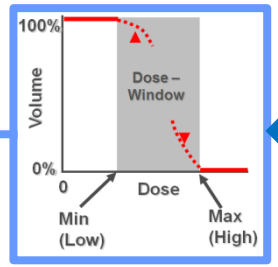

$$f_i = \frac{1}{N_i}\sum_{j=1}^{N_i}\left[\Theta\left(D_L^i - d_j^i(\boldsymbol{x})\right)\left[D_L^i - d_j^i(\boldsymbol{x})\right]^p\right]$$

$$f_i = \frac{1}{N_i}\sum_{j=1}^{N_i}\left[\Theta\left(d_j^i(\boldsymbol{x}) - D_H^i\right)\left[d_j^i(\boldsymbol{x}) - D_H^i\right]^p\right]$$

w_m : the relative *Importance Factors* (*IFs*) for the individual *Objective Functions* f_m or *Penalties* for the *penalisation* of the *violation of the individual objectives*.

These are considered as a measure of the significance of each of the *objectives/objective functions* in the optimisation process.

The optimisation process equals then the minimisation of the *Aggregated Objective Function f*.

ESTRO School

Inverse Optimisation and Planning

Create a single Objective Function via *weighted Aggregation*

The minimisation of the Aggregated Objective Function ***f*** can be interpreted as finding the value ***f*** for which the line with slope $-w_1/w_2$ just touches the boundary of ***F*** as it proceeds outwards from the origin.

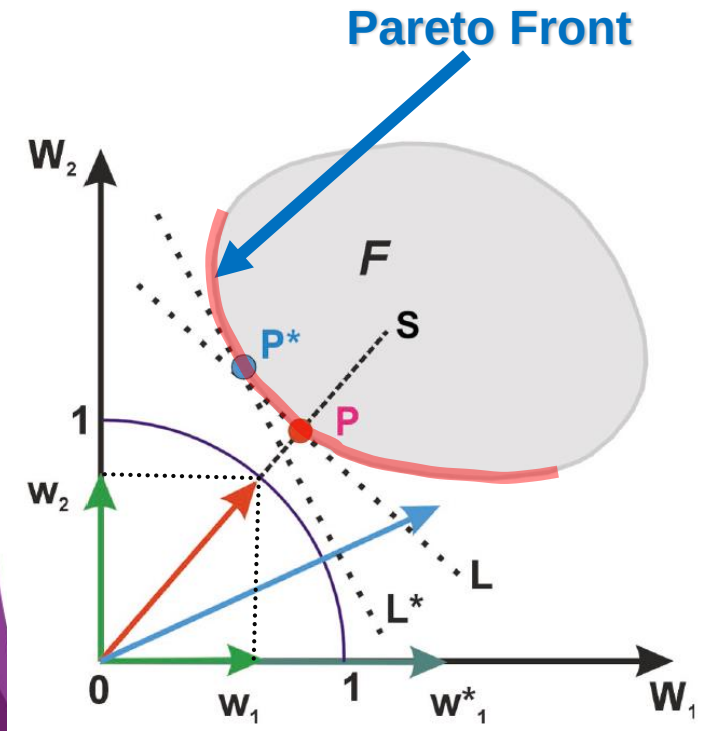

w1 f1 + w2 f2 ???

The plan/solution which is obtained in the ***Weighted Aggregation*** approach depends on the shape of the ***Pareto Front*** and the ***importance factors/penalties*** used.
Planner is not aware if there exist a better ***"choice"*** on the ***Pareto Front*** just next door!

Empirically estimated penalisation schemes, found to result to „good" dose distributions are ussually saved as ***presets / protocols / class solutions*** and can be used as starting points for the individual patient plan optimisation process.

ESTRO School

Summary – *Inverse Optimisation*

A single Objective Function via *weighted Aggregation*

Minimise $$f = \sum_{m=1}^{M} w_m f_m = f(\{\vec{r}\},\{t\},\{w\})$$

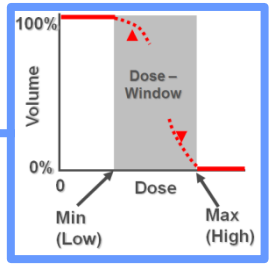

$$f_i = \frac{1}{N_i}\sum_{j=1}^{N_i}\left[\Theta\left(D_L^i - d_j^i(\boldsymbol{x})\right)\left[D_L^i - d_j^i(\boldsymbol{x})\right]^p\right]$$ ⇨ ***Under-dosage (low)***

$$f_i = \frac{1}{N_i}\sum_{j=1}^{N_i}\left[\Theta\left(d_j^i(\boldsymbol{x}) - D_H^i\right)\left[d_j^i(\boldsymbol{x}) - D_H^i\right]^p\right]$$ ⇨ ***Over-dosage (high)***

with $$d_j^i(\mathbf{x}) = \sum_{k=1}^{N_{cath}}\sum_{l=1}^{N_{ASDP}^k} x_{lk}^2 S_{K,lk}\tilde{d}_{jkl}^{\,i}$$

parameter values

ESTRO School

Summary – *Inverse Optimisation*

Diversity of Solutions regarding objective function minimisation:

- ***Exact Solver***
  - **Linear Programming (LP)** (e.g. Simplex)
- ***Deterministic***
  - **Gradient based** (e.g. Broyden-Fletcher-Goldfarb-Shanno-BFGS, L-BFGS➔ **HIPO**, Fletcher-Reeves-Polak-Ribiere-FRPR)
  - **Gradient-free** (e.g. Nelder-Mead Simplex Algorithm, …)
- ***Stochastic/Probabilistic***
  - ***Simulating Annealing (SA)*** ➔ ***IPSA***
  - ***Genetic/Evolutionary Algorithms (GA)***

Diversity of techniques of dose analysis (sampling points, where values of the objective functions are analysed)

Inverse Optimisation and Planning

Preconditions:

- **Complete 3D anatomy model: Targets (GTVs), CTV/PTV, OARs** ⇨ **Morphology**
- **Implantation rules (anatomical constraints)**
- **Implantation methods, instruments, …** } **Topography**
- **Desired dose distribution $D(\vec{r})$** ⇨ **Dosimetric Result/Aims**

$$\Psi(\vec{r}) = \Psi(\{\vec{r}\},\{t\}) = \sum_{i=1}^{N_{ASDPs}} S_{K,i}.t_i.\delta(\vec{r}-\vec{r}_i) = ?$$

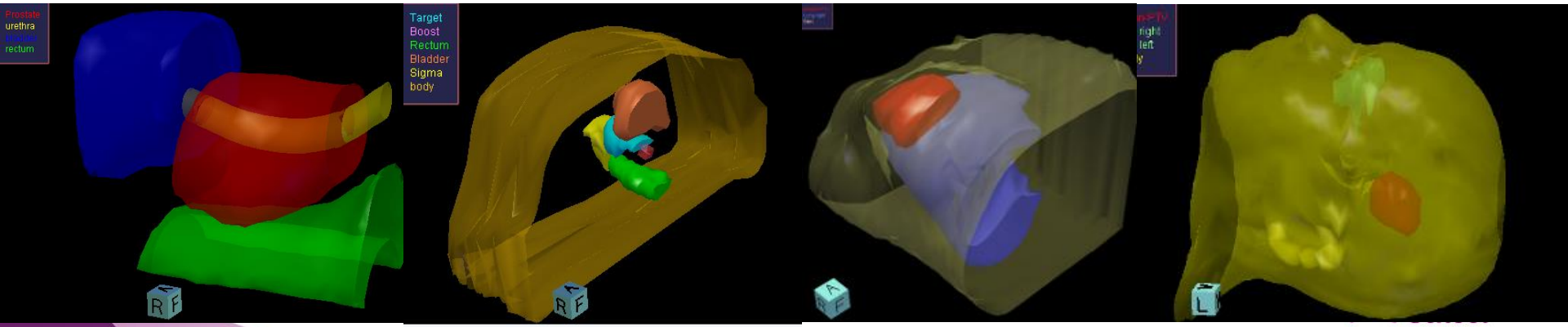

Inverse Optimisation and Planning

Objectives & Objective Functions

Define Dose Window for Target(s), NT & OAR(s) ⇨ **Objectives** ⇨ ***Objective Functions***

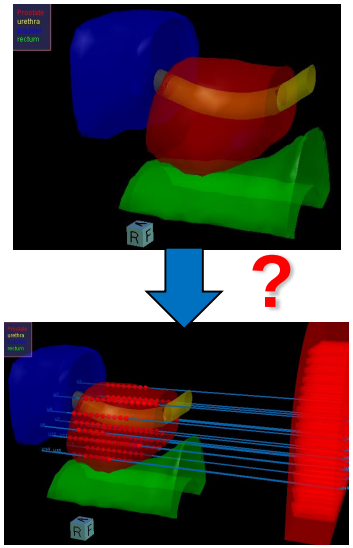

Low-Objective
D_L **for** V_{Low}

$$f_i = \frac{1}{N_i}\sum_{j=1}^{N_i}\left[\Theta\left(D_L^i - d_j^i(x)\right)\left[D_L^i - d_j^i(x)\right]^p\right]$$

High-Objective
D_H **for** V_{High}

$$f_i = \frac{1}{N_i}\sum_{j=1}^{N_i}\left[\Theta\left(d_j^i(x) - D_H^i\right)\left[d_j^i(x) - D_H^i\right]^p\right]$$

d^i_j **is the Dose at the Sampling Point** ***j*** **for** ***Objective Function i*****:**

$$d_j^i(x) = \sum_{k=1}^{N_{feasible}} \sum_{l=1}^{N_{ASDP}^k} b_k x_{lk}^2 S_{K,lk} \tilde{d}_{jkl}^{\,i}$$

$$D(\vec{r}) = \int_{-\infty}^{+\infty} \Psi(\vec{r}\,') A(\vec{r} - \vec{r}\,')\, dv$$

- **Feasible Catheters**
- **Active SDPs**
- **Binary: Catheter Selection**
- **Dwell times $t_{lk} = x_{lk}^2$**

ESTRO School

Inverse Optimisation and Planning

Objectives & Objective Functions

d^i_j is the dose at the j^{th}-sampling point for the i^{th}-objective function:

$$d^i_j(\mathbf{x}) = \sum_{k=1}^{N_{feasible}} \sum_{l=1}^{N^k_{ASDP}} b_k x^2_{lk} S_{K,lk} \tilde{d}^i_{jkl}$$

- $\sum_{k=1}^{N_{feasible}}$: feasible Catheters
- $\sum_{l=1}^{N^k_{ASDP}}$: Active SDPs
- b_k: Binary catheter Selection ?
- x^2_{lk}: Dwell times t_{lk} ?

- $x^2_{lk} = t_{lk}$ to avoid negative (non-physical) dwell time values t_{lk}
- $\tilde{d}^i_{jkl}$, can (should) be calculated in a pre-processing step and are then available in a sense of *a Look-Up-Table* for the optimisation process. Implementations in this way make optimiser independent of the dose calculation engine considered (*TG 43, MC, BS, CC, other Engines*)

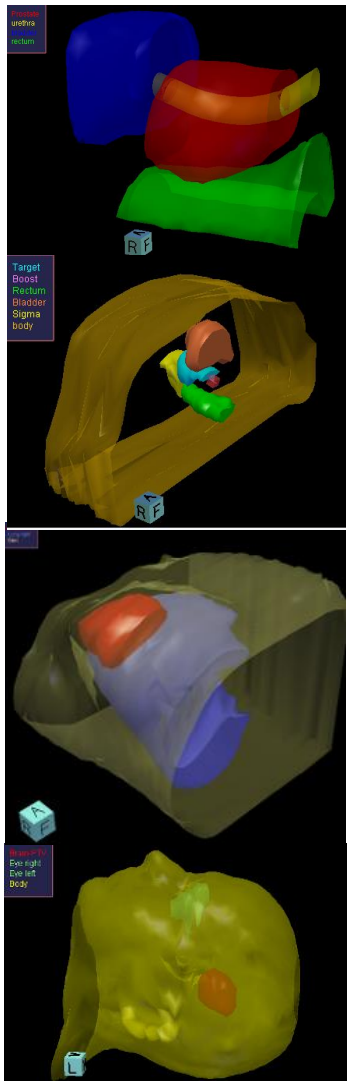

ESTRO School

Inverse Optimisation and Planning

The Inverse Planning of an adequate number of catheters/applicators / needles based on dosimetric objectives and constraints *is solvable in clinically acceptable time* only after *discretisation* $\{b_k\}$:

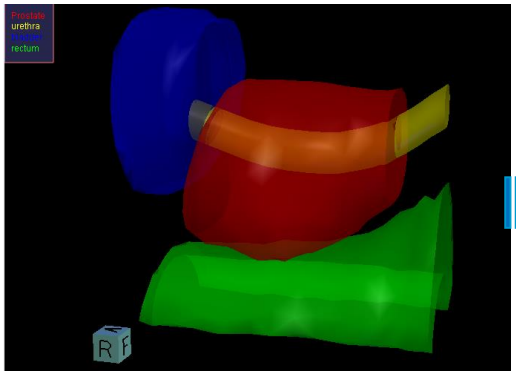

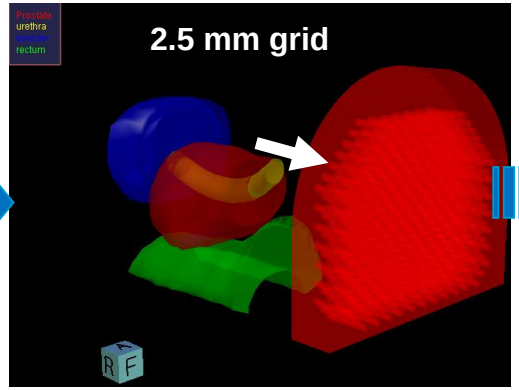

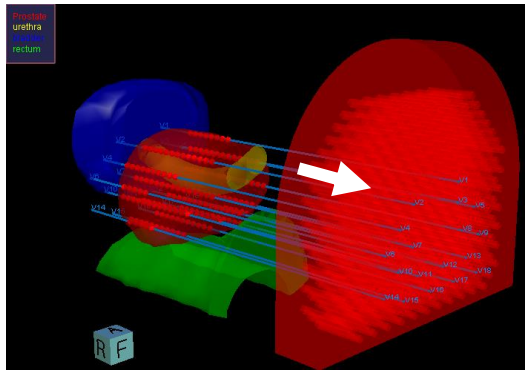

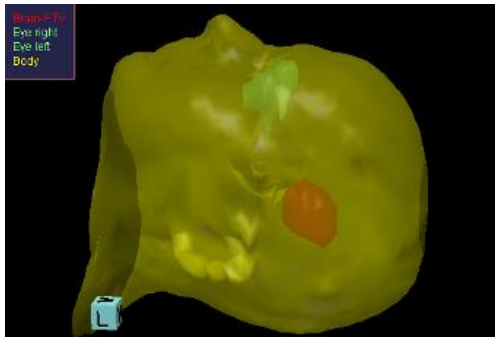

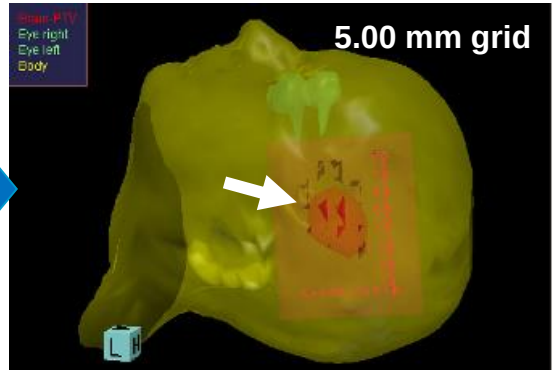

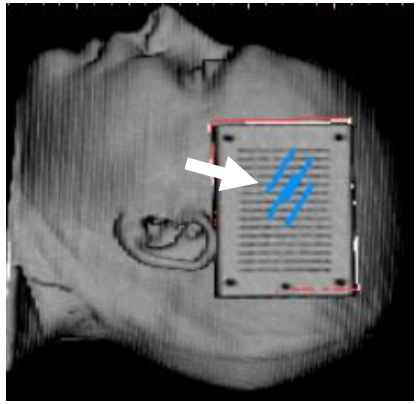

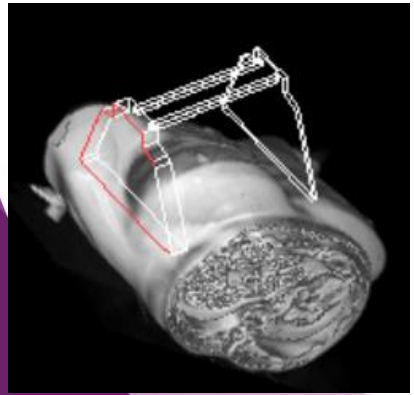

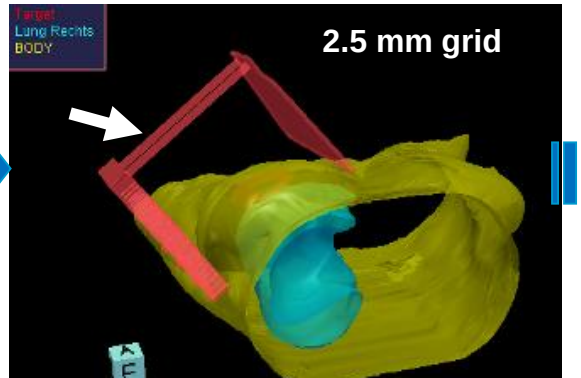

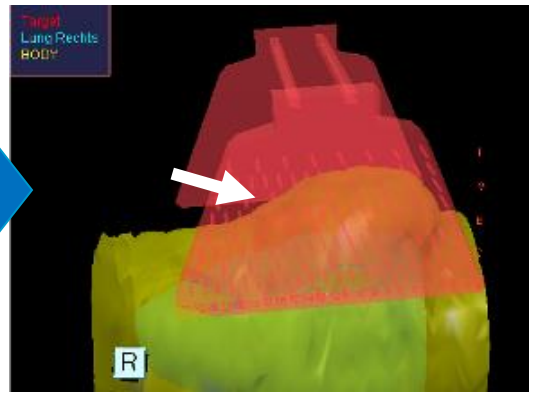

Inverse Optimisation and Planning

Objectives & Objective Functions

Grid-based discretisation ➔ Set of Feasible Catheters/Needles

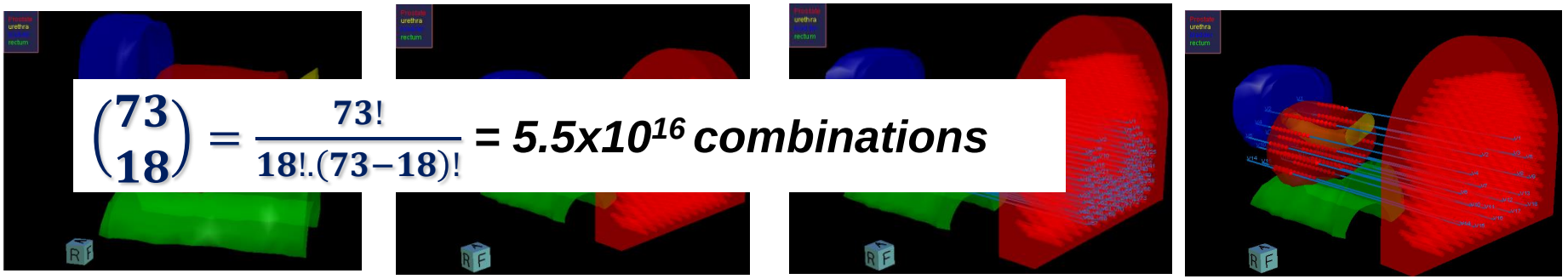

$$\binom{73}{18} = \frac{73!}{18!.(73-18)!} = 5.5x10^{16}\ combinations$$

1 x PTV
3 x OARs
NT

2.5 mm grid

73x feasible

18x clinically

$$d_j^i(\mathbf{x}) = \sum_{k=1}^{N\ feasible} \sum_{l=1}^{N_{ASDP}^k} b_k x_{lk}^2 S_{K,lk} \tilde{d}_{jkl}^{\,i}$$

$$D(\vec{r}) = \int_{-\infty}^{+\infty} \Psi\left(\vec{r'}\right) A(\vec{r} - \vec{r}')\, dv$$

feasible Catheters

Active SDPs

Binary catheter Selection ?

Dwell times t_{lk} ?

ESTRO School

Summary – *Inverse Planning*

A single Objective Function via *weighted Aggregation*

Minimise $$f = \sum_{m=1}^{M} w_m f_m = f(\{\vec{r}\},\{t\},\{w\})$$

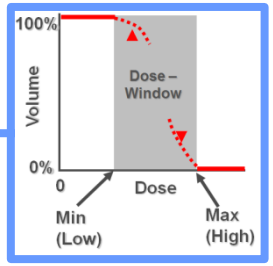

$$f_i = \frac{1}{N_i}\sum_{j=1}^{N_i}\left[\Theta\left(D_L^i - d_j^i(\boldsymbol{x})\right)\left[D_L^i - d_j^i(\boldsymbol{x})\right]^p\right]$$ ⇨ ***Under-dosage (low)***

$$f_i = \frac{1}{N_i}\sum_{j=1}^{N_i}\left[\Theta\left(d_j^i(\boldsymbol{x}) - D_H^i\right)\left[d_j^i(\boldsymbol{x}) - D_H^i\right]^p\right]$$ ⇨ ***Over-dosage (high)***

with $$d_j^i(\mathbf{x}) = \sum_{k=1}^{N\ feasible}\sum_{l=1}^{N_{ASDP}^k} b_k x_{lk}^2 S_{K,lk}\tilde{d}_{jkl}^{\,i}$$

parameter values

ESTRO School

Summary – *Inverse Planning*

$$d_j^i(\mathbf{x}) = \sum_{k=1}^{N_{feasible}} \sum_{l=1}^{N_{ASDP}^k} b_k x_{lk}^2 S_{K,lk} \tilde{d}_{jkl}^{\,i}$$

Catheter/needle selection

Source dwell time or seed position

Source strength

- $b \in \{0,1\}$ & $x \in R$
  single stepping source HDR-afterloader
  z.B.^{192}Ir
  - ➔ ***HIPO*** (in RTPs)
  - ➔ ***GA*** – based (research)
  - ➔ ***MILP*** – *based (research)*
- $b \in \{0,1\}$ & $x \in \{0,1\}$
  seeds implants permanent
  z.B. ^{125}I
  - ➔ ***IPSA*** (in RTPs)
  - ➔ ***MIP***-formulations & methods
  - ➔ ***GA*** – based

ESTRO School

Inverse Planning – using *HIPO*

Minimise $f = \sum_{m=1}^{M} w_m \; f_m = \; f(\{\vec{r}\},\{t\},\{w\})$ $\quad d_j^i(\mathbf{x}) = \sum_{k=1}^{N_{feasible}} \sum_{l=1}^{N_{ASDP}^{k}} b_k \, x_{lk}^2 \, S_{K,lk} \, \tilde{d}_{jkl}^{\,i}$

Hybrid Inverse Planning and Optimization Engine HIPO

The MINLP problem is solved by ***HIPO*** by a ***hybrid approach***:

- ***A heuristic*** combining ***SA*** & *scoring* for the binary part ***b***
- ***A quasi-Newton*** for the continuous part $\boldsymbol{t = x^2}$ (*optimisation, L-BFGS*)
- Make use of a ***non-linear*** description of the ***transition function Θ***

$$\Theta = 0.5[1 + tanh(b.y)]$$

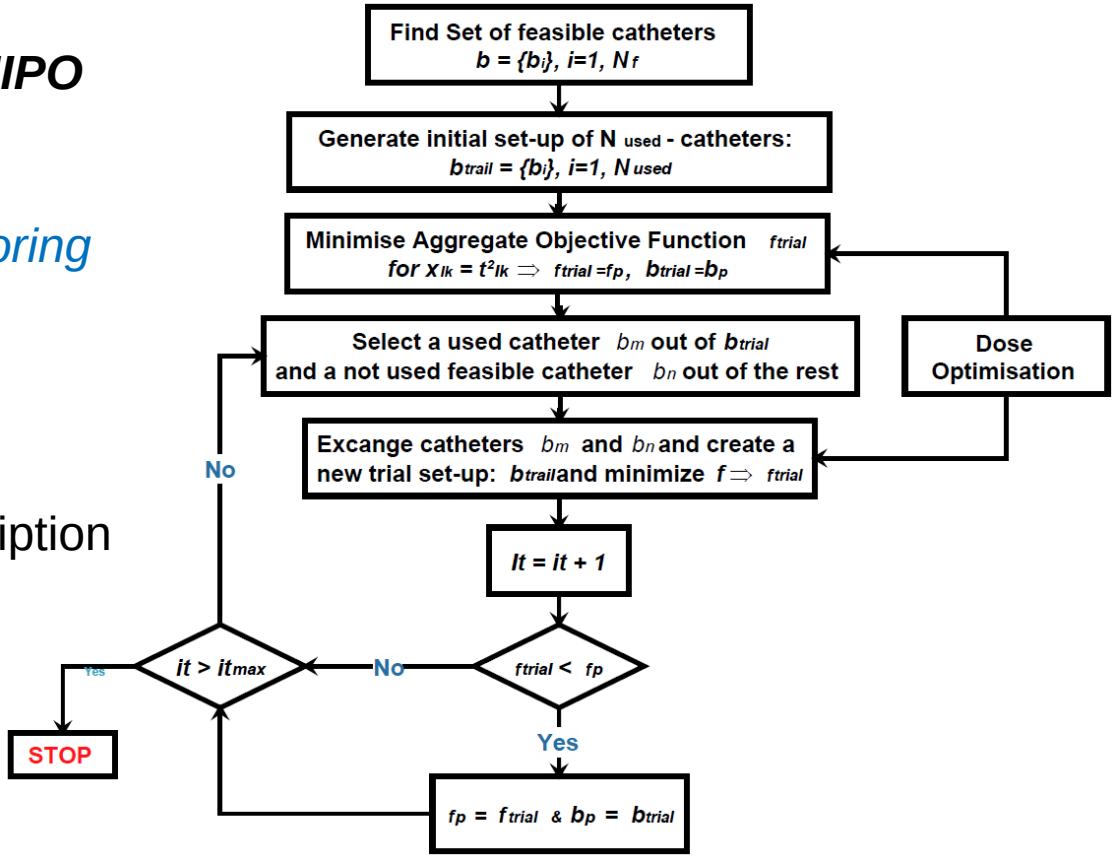

(1) Karabis A, Giannouli S, Baltas D: *Radiotherapy & Oncology*, 76, 29, 2005
(2) Karabis A, Belotti P, Baltas D: *WC 2009*

ESTRO School

Inverse Planning – using *HIPO*

Minimise $f = \sum_{m=1}^{M} w_m \; f_m = \; f(\{\vec{r}\},\{t\},\{w\})$ $\quad d_j^i(\mathrm{x}) = \sum_{k=1}^{N\ feasible} \sum_{l=1}^{N_{ASDP}^{k}} b_k \, x_{lk}^2 \, S_{K,lk} \, \tilde{d}_{jkl}^{\,i}$

- ***A heuristic*** combining SA & scoring for the binary part ***b***
- ***A quasi-Newton*** for the continuous part ***t = x²*** (optimisation)

⇨ **30s – 120s (parallelised, ...)**

⇨ **< 1.0s**

Optimization of Catheter Position and Dwell Time in Prostate HDR Brachytherapy using HIPO and Linear Programming

A. Karabis[1], P. Belotti[2] and D. Baltas[3,4]

[1]Pi-Medical Ltd., Athens, Greece
[2]Dept. of Industrial & Systems Engineering, Lehigh University, Bethlehem PA, USA
[3]Dept. of Medical Physics & Engineering, Strahlenklinik, Klinikum Offenbach GmbH, Germany
[4]Nuclear and Particle Physics Section, Physics Department, University of Athens, Greece

O. Dössel and W.C. Schlegel (Eds.): WC 2009, IFMBE Proceedings 25/I, pp. 612–615, 2009.

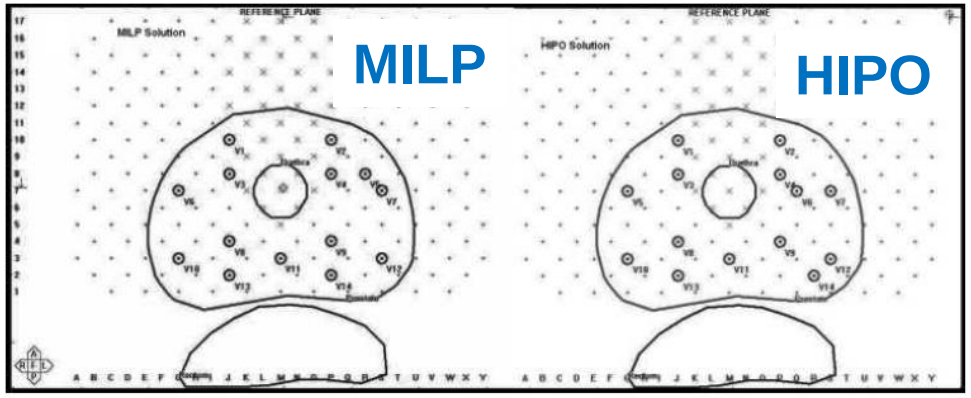

Fig. 1 Catheter configuration for Case #1. MILP upper bound on the left and HIPO solution on the right.

Table 5 Dose–volume parameters using HIPO (1) and MILP (2).

Case No		PTV			Urethra		
		V_{100}	V_{150}	D_{90}	V_{115}	D_{10}	$D_{0.1cm^3}$
# 1	(1)	93.3	32.5	104.3	24.4	119.3	123.9
	(2)	93.7	32.7	105.1	23.8	119.3	124.3
# 2	(1)	90.7	25.1	100.8	4.8	113.4	114.3
	(2)	90.1	26.5	100.1	4.6	113.0	114.1
# 3	(1)	92.3	25.3	102.4	3.0	112.6	114.9
	(2)	92.8	24.9	102.5	3.9	112.4	115.7

HIPO: < 240 s (not parallelised)
MILP solver CPLEX: ≈ 48 hrs

ESTRO School

Inverse Planning – using *HIPO*

Supported clinical scenarios

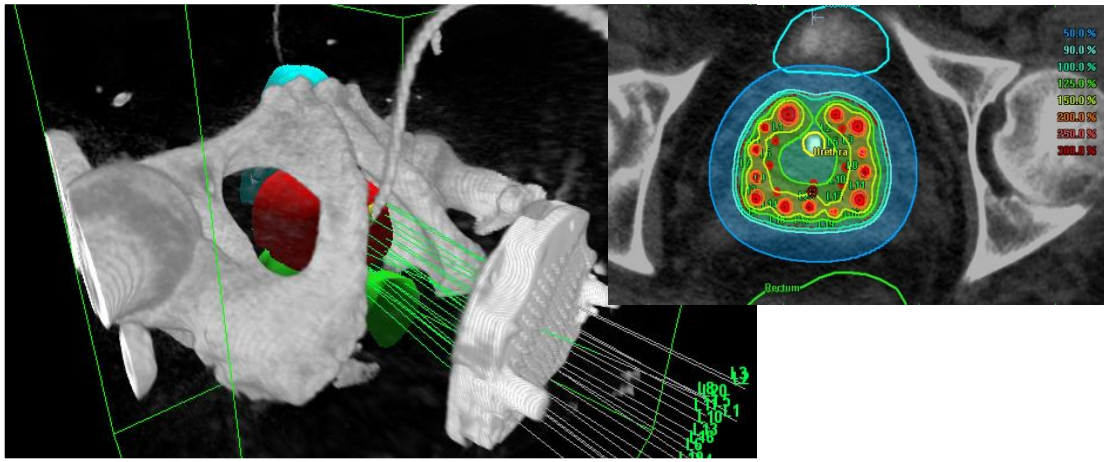

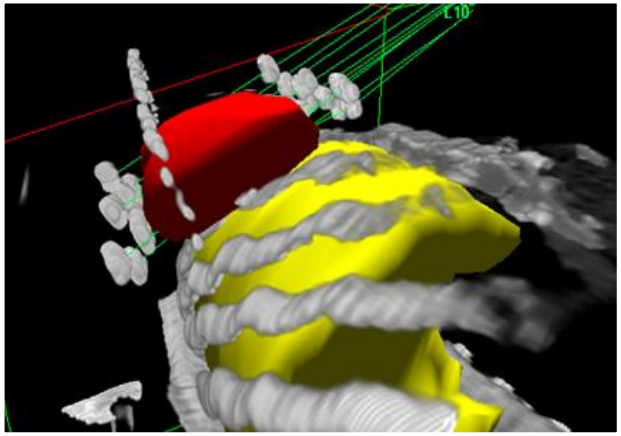

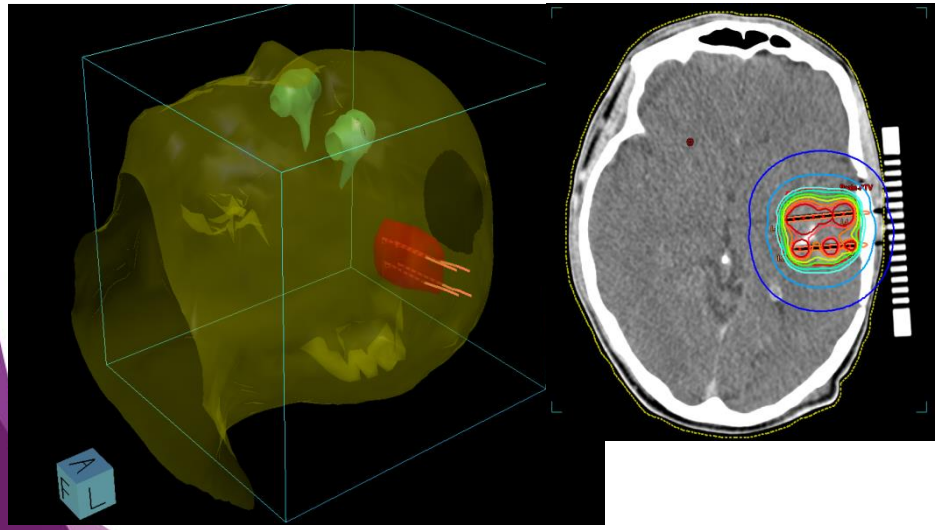

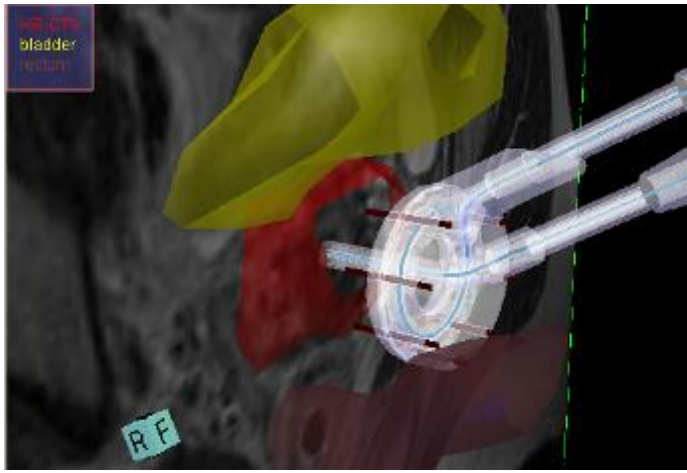

ESTRO School

Inverse Planning – using *HIPO*

Minimise $f = \sum_{m=1}^{M} w_m f_m = f(\{\vec{r}\},\{t\},\{w\})$ $\quad d_j^i(\mathrm{x}) = \sum_{k=1}^{N\ feasible} \sum_{l=1}^{N_{ASDP}^{k}} b_k x_{lk}^2 S_{K,lk} \tilde{d}_{jkl}^{\ i}$

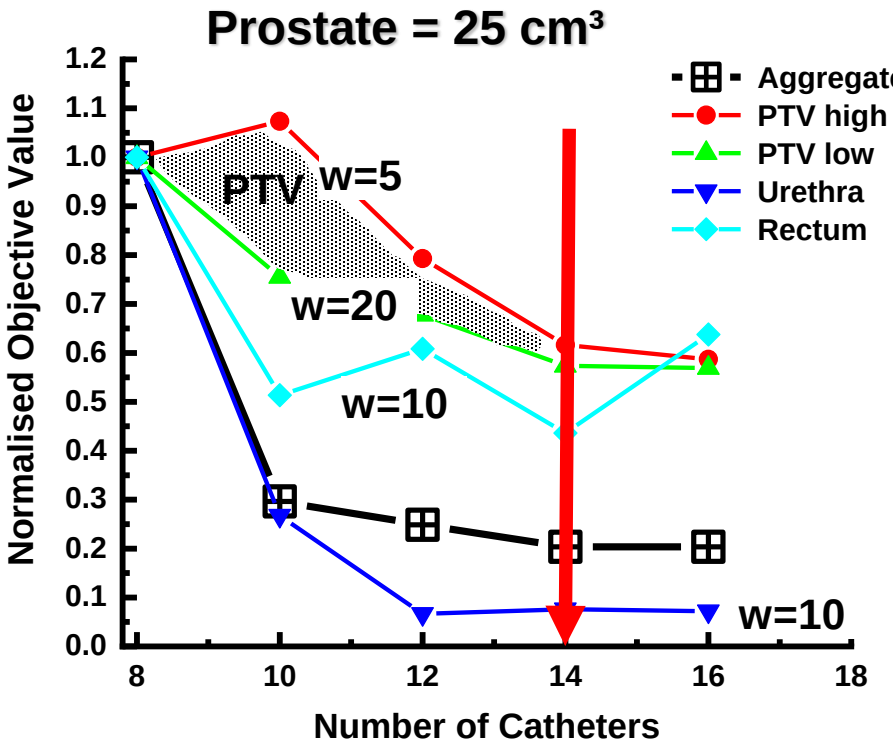

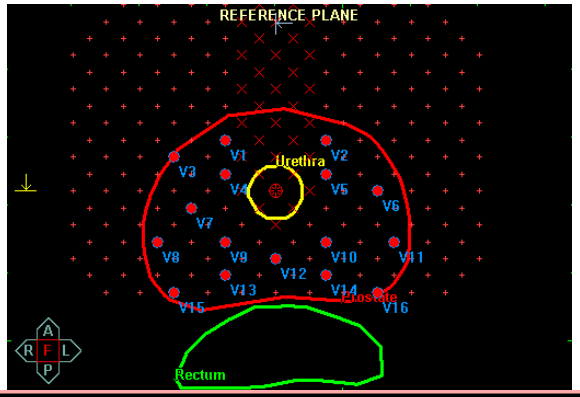

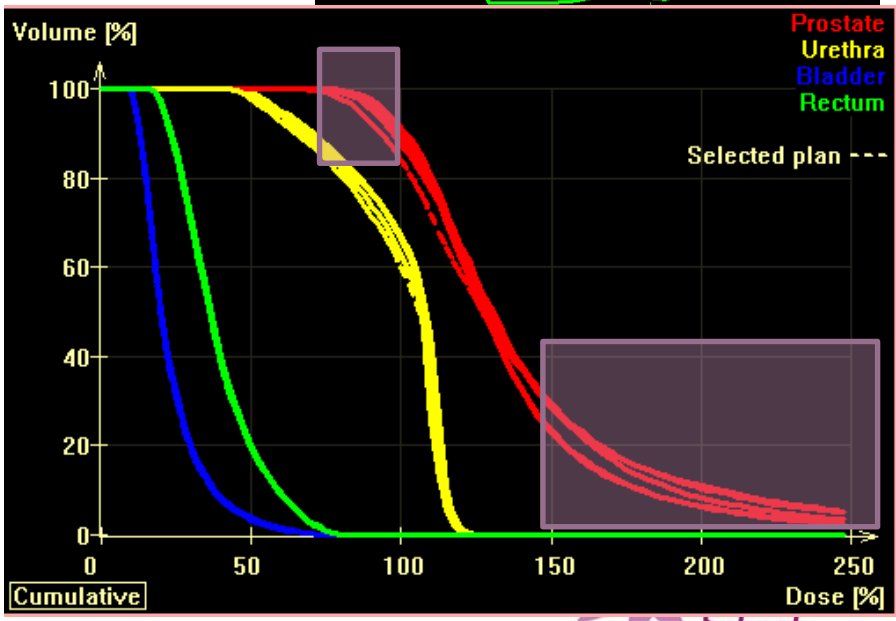

Inverse Planning – *Number of Catheters*

ELSEVIER

CrossMark

BRACHYTHERAPY

Brachytherapy 15 (2016) 102–111

Physics

Comparison of dose and catheter optimization algorithms in prostate high-dose-rate brachytherapy

Eric Poulin[1,2], Nicolas Varfalvy[2], Sylviane Aubin[2], Luc Beaulieu[1,2,*]

[1]*Département de physique, de génie physique et d'optique et Centre de recherche sur le cancer de l'Université Laval, Université Laval, Québec, Canada*
[2]*Département de radio-oncologie et Axe Oncologie du Centre de recherche du CHU de Québec, CHU de Québec, Québec, Canada*

8x cases
prostate = 37 - 65cm³

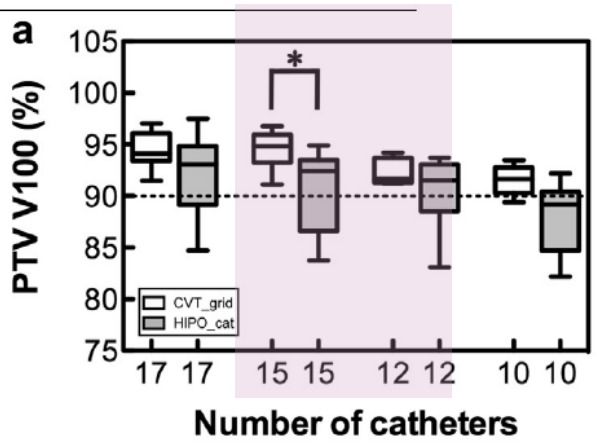

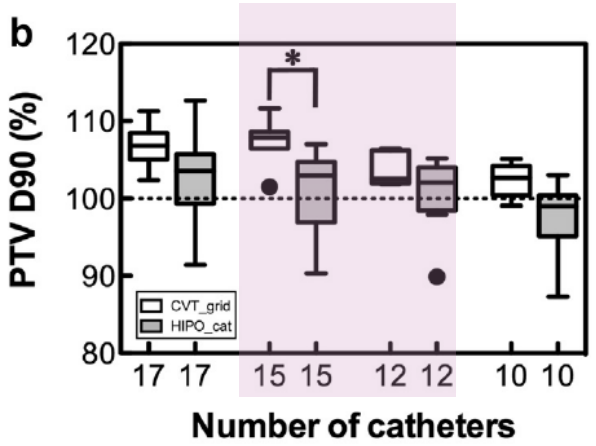

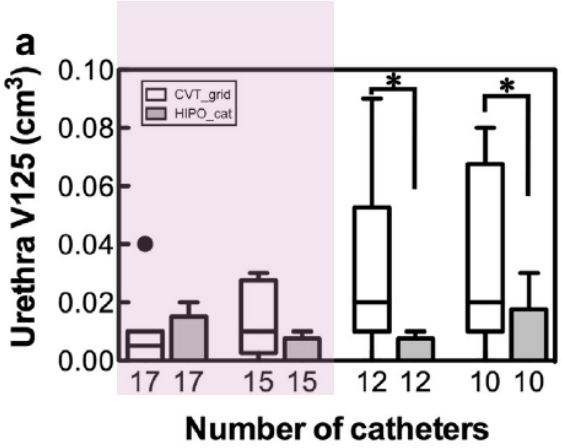

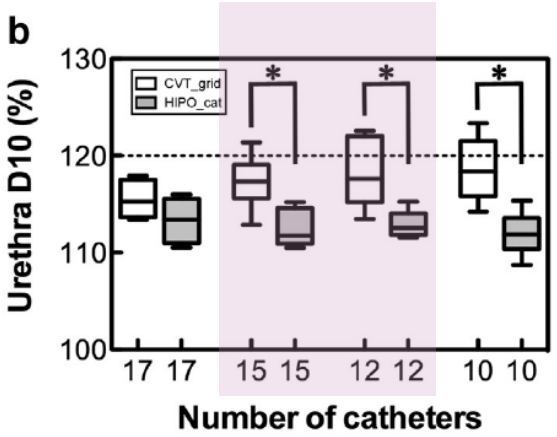

Inverse Optimisation and Planning

Topography based (TOP)

TOP: **Additional not morphology (VOIs, DVHs) based Features, and/or local History:**

- **Dwell Time Modulation Restriction (MR)**

  (Smoothness of Source Movement)

Inverse Optimisation and Planning

Topography based (TOP)

Independently of the used Inverse Optimization Algorithm it is not an uncommon result for HDR implants that there exist a few very dominating Dwell positions where the largest part of the total dwell time is spent.
This leads obviously to a *selective extension of high dose volumes* around such dwell positions. If there is *no information available* about its necessity (e.g. location of a GTV/IDL), then it is reasonable to investigate whether this can be avoided.

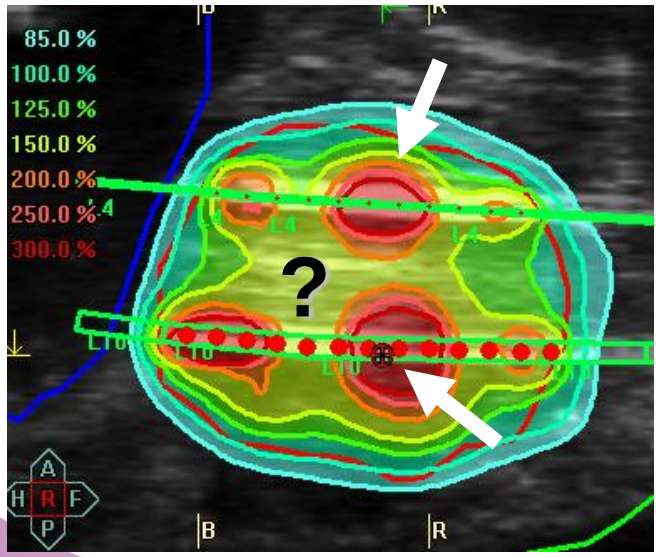

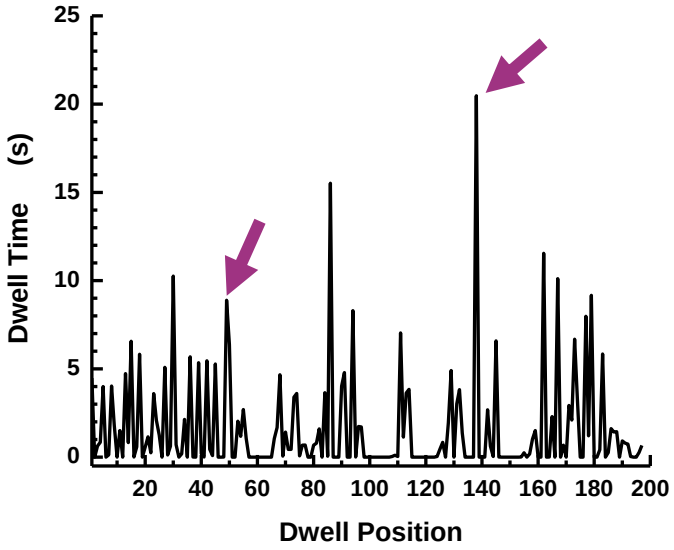

ESTRO School

Inverse Optimisation and Planning

Topography based (TOP)

Dwell Time *Modulation Restriction (MR) - Smoothness of Source Movement* - can be achieved by considering Dwell Time (Modulation) related *Objective Functions*:

- ***Smoothness* of Dwell Time Modulation within Catheters**
- ***Pseudo:* Restricting the maximal possible Dwell Time per Source Dwell Position**
- ***Overall* Dwell Time**

Topographic Optimisation (TOP)

Modulation/Gradient Restriction
Parameter = 0.0

Modulation/Gradient Restriction
Parameter = 0.12

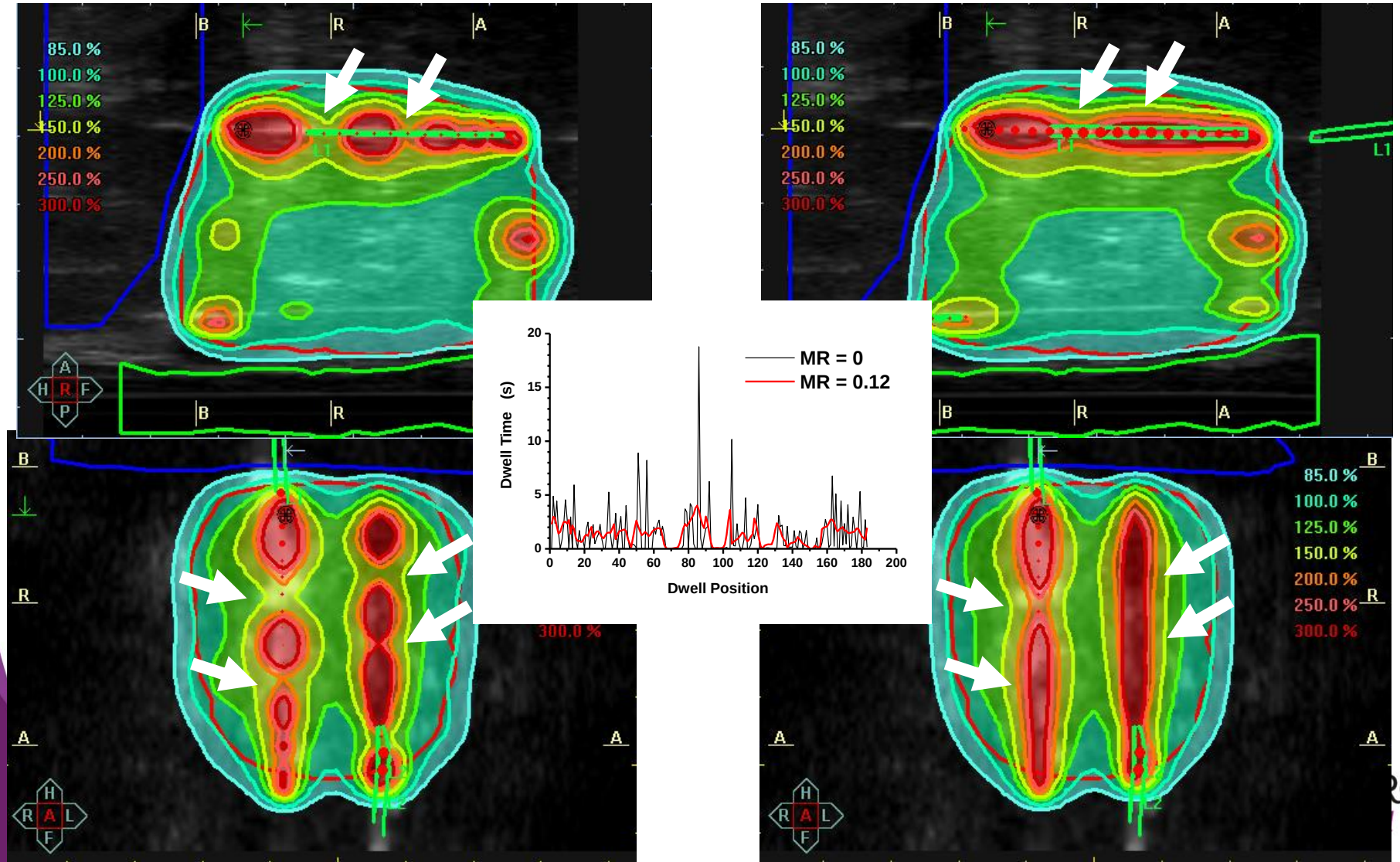

Topographic Optimisation (TOP)

MR: Modulation Restriction*

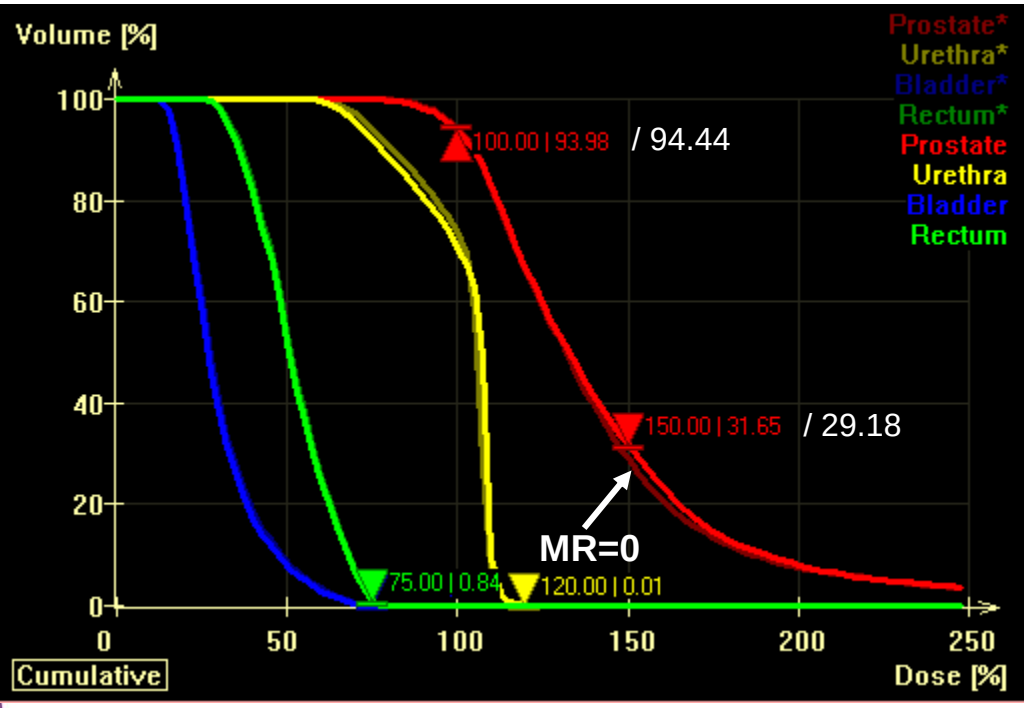

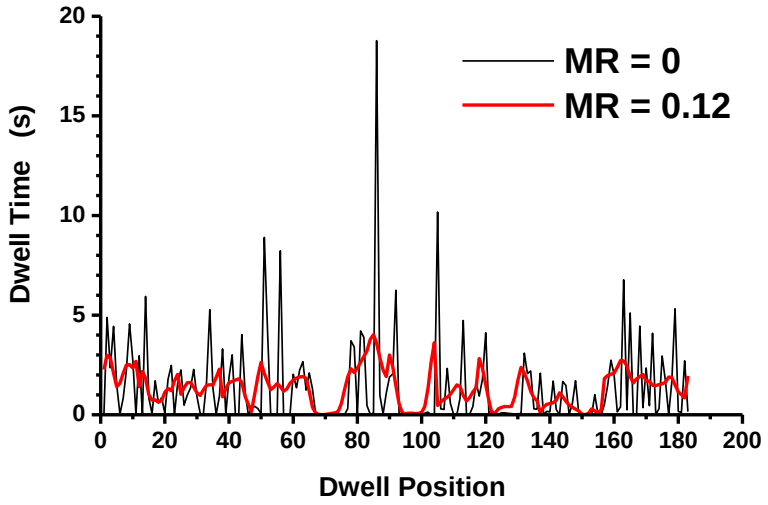

Total Dwell Time:	**686.4 s**	**=>**	**675.3 s (-1.6%)**
COIN:	**0.884**	**=>**	**0.888**

* Using HIPO (Pi-Medical Ltd) implementation in Oncentra Prostate (Elekta, Nucletron B.V.)

ESTRO School

Inverse Optimisation and Planning: Topography based (TOP)

- "..local History": Pre-delivered Dose Part of Implant

$$f_i = \frac{1}{N_i}\sum_{j=1}^{N_i}\left[\Theta\left(D_L^i - d_j^i(\mathrm{x})\right)\left[D_L^i - d_j^i(\mathrm{x})\right]^p\right]$$

$$f_i = \frac{1}{N_i}\sum_{j=1}^{N_i}\left[\Theta\left(d_j^i(\mathrm{x}) - D_H^i\right)\left[d_j^i(\mathrm{x}) - D_H^i\right]^p\right]$$

$d^i_j(x)$ has a "History".

"History":

- Pre-delivered Dose (previous Implants or ERT)
- Fixed contribution of a part of the implant (Fixed contribution form Ring + Tandem & TOP of additional interstitial needles)

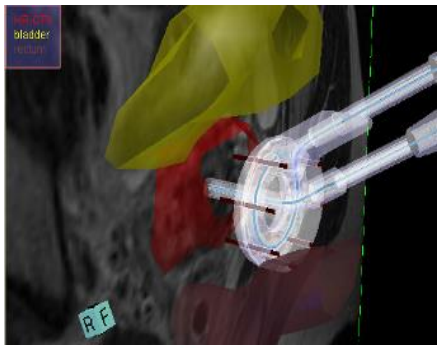

* Using HIPO (Pi-Medical Ltd) implementation in Oncentra Prostate & Oncentra Brachy (Elekta, Nucletron B.V.)

TOP: Topographic Optimisation

(A) Only 15 Catheters

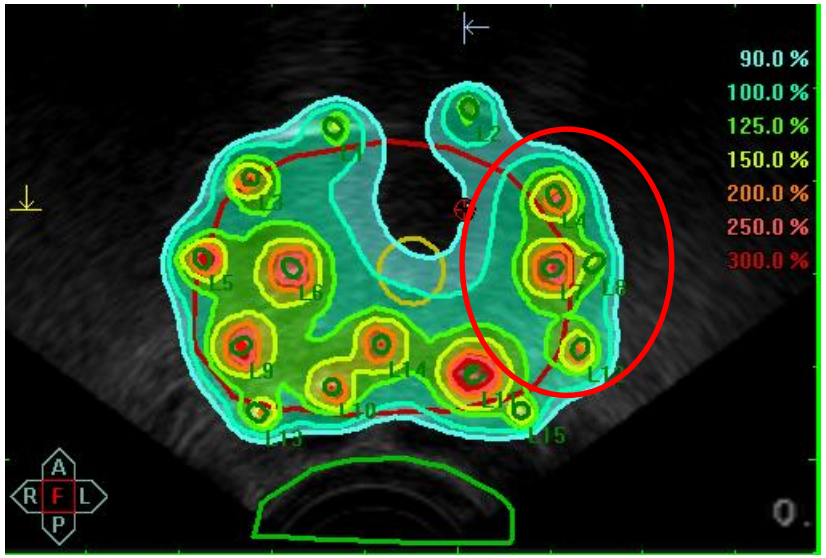

(B) 15 + 1 Catheters, freely optimized

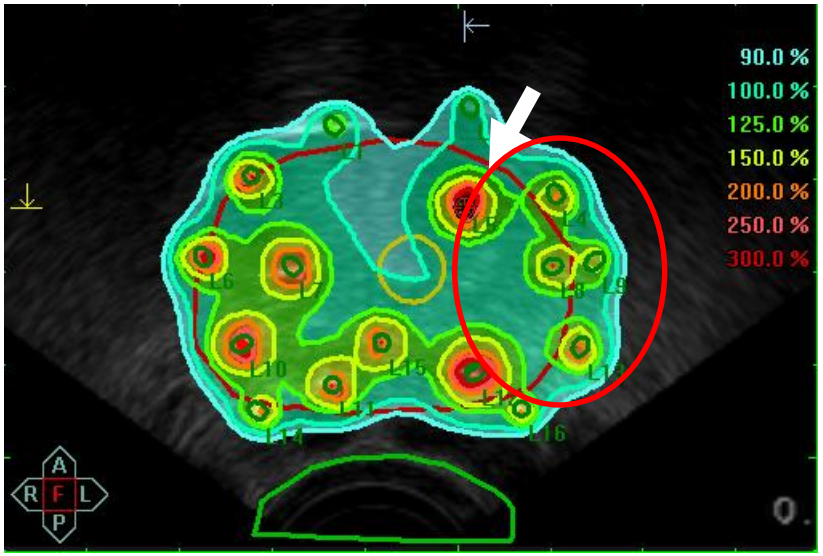

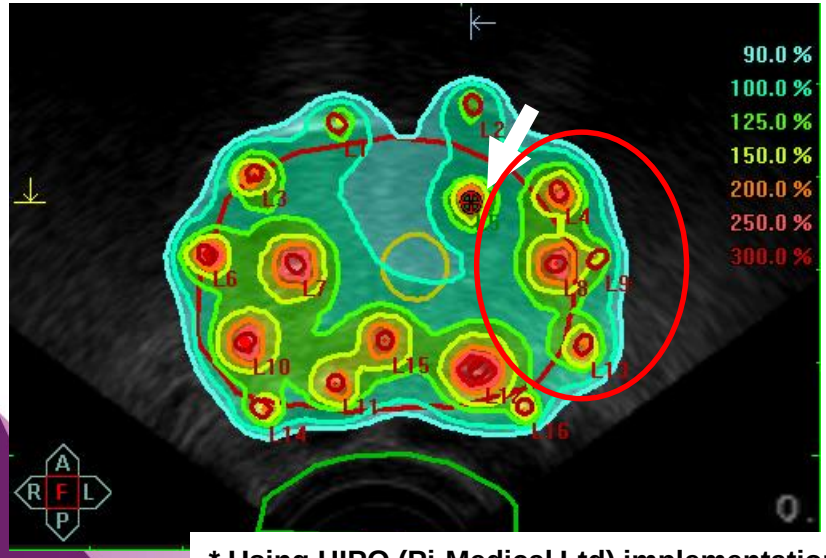

(C) 15 + 1 Catheters, TOP: Dwell times for (A) "frozen" Additional Catheter used for Local Dwell Time Adjustment

ESTRO School

*** Using HIPO (Pi-Medical Ltd) implementation in Oncentra Prostate & Oncentra Brachy (Elekta, Nucletron B.V.)**

TOP: Topographic Optimisation

(A) Only 8 Catheters

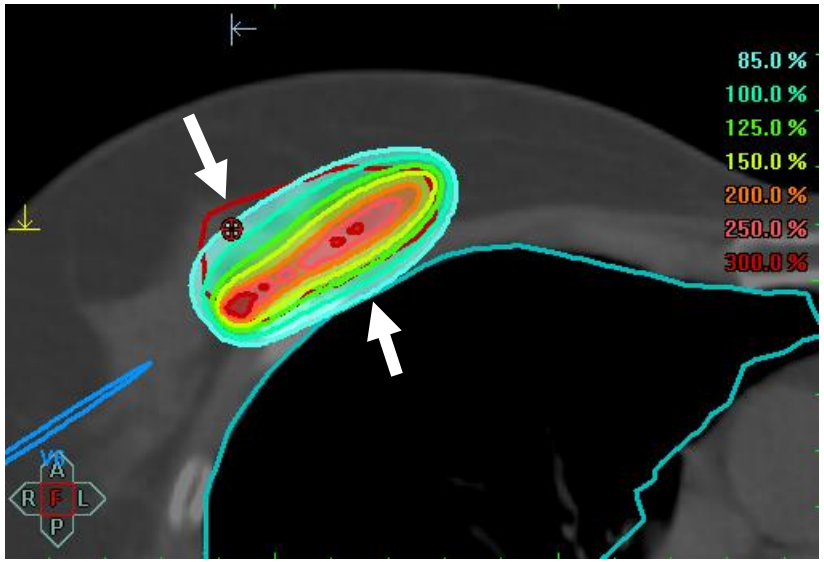

(B) 8 + 1 Catheters, freely optimized

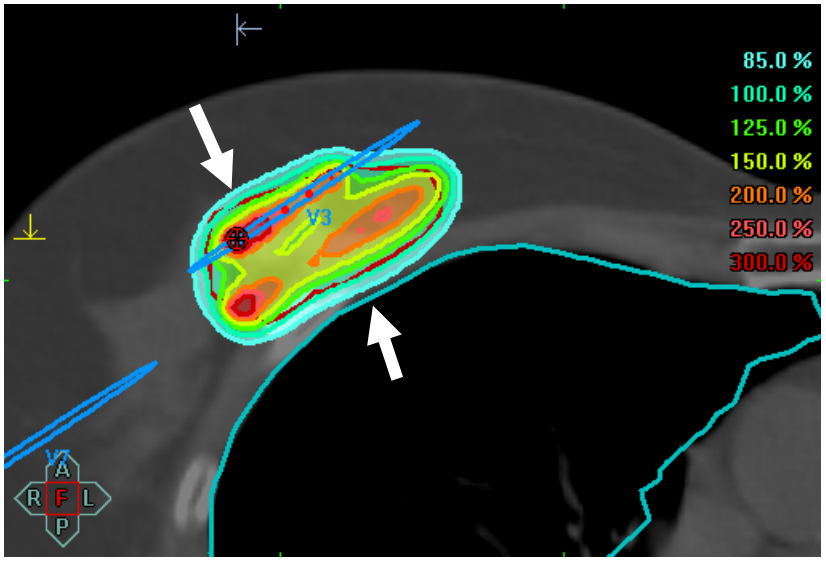

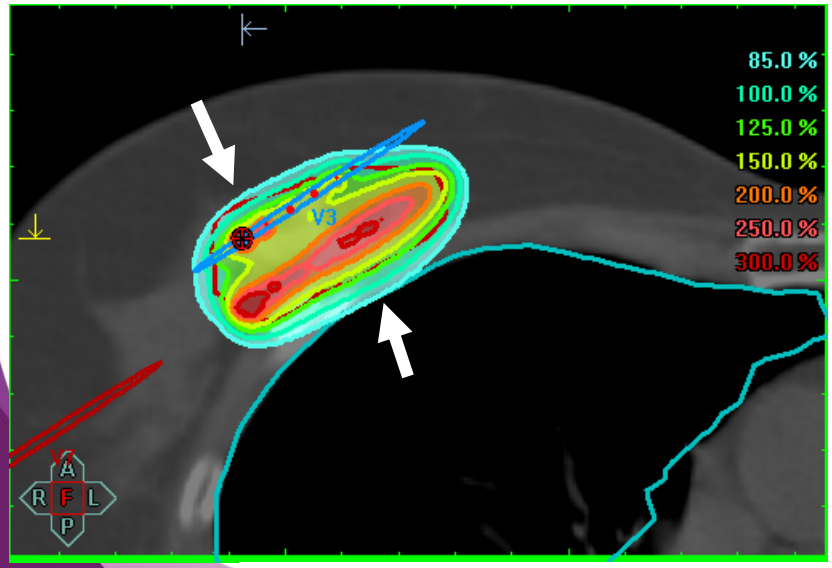

(C) 8 + 1 Catheters, TOP: Dwell times for (A) "frozen" Additional Catheter used for Local Dwell Time Adjustment

ESTRO

*** Using HIPO (Pi-Medical Ltd) implementation in Oncentra Prostate & Oncentra Brachy (Elekta, Nucletron B.V.)**

Overview of Commercially available Inverse Optimisation and Planning Tools for HDR BRT

Company RTP	Optimiser (HDR)	Objectives / Functions	Artificial VOI NT & Objective	Automatic Catheter Placement	Numerical Solver	TOP	Dwell Time (DT) Modulation Control
BEBIG HDR Plus Vs. 3.0.5	---	**Aggregation:** Low and High	only user-defined and added to OFs	No	Stochastic FSA	Yes DT	**DT** Homogeneity Error Weight & Total DT
Nucletron, ELEKTA Oncentra Brachy Vs. 4.3	IPSA	**Aggregation:** Low and High	automatically defined & added as OF	No	Stochastic FSA	Yes DT	**DT** Gradient
Nucletron, ELEKTA Oncentra Brachy Vs. 4.3 & OcP	HIPO	**Aggregation:** Low and High	automatically defined & added as OF	YES (Discretisation Case)	Deterministic L-BFGS & Heuristic/ Stochastic for Catheters	Yes DT & pre-delivered	**DT** Gradient Modulation Restriction
VARIAN Brachy-Vision Vs. 10 +	AVOL	**Aggregation:** Low and High incl. Basal Dose	automatically defined user option for OF	No	Deterministic Nelder-Mead Simplex Algorithm	Yes DT	Max./Min **DT** Constraints Gradient restriction

ESTRO School

Literature I

G. Edmundson, ‘‘Geometry based optimization for stepping source implants,’’ in Brachytherapy HDR and LDR, edited by A. A. Martinez, C. G. Orton, and R. F. Mould ~Nucletron, Columbia, 1990

Van der Laarse and T. P. E. Prins, ‘‘Introduction to HDR brachytherapy optimisation,’’ in Brachytherapy from Radium to Optimization, edited by R. F. Mould, J. Batterman, A. A. Martinez, and B. L. Speiser, Nucleotron International, Veenendaal, The Netherlands, 1994, pp. 331–351.

Y. Yu and M. C. Schell, ‘‘A genetic algorithm for the optimization of prostate implants,’’ Med. Phys. 23, 2085–2091, 1996

Kneschaurek P, Schiessl W and Wehrmann R Volume-based dose optimization in brachytherapy Int. J. Radiat. Oncol. Biol. Phys. 45 811–5,1999

Baltas, C. Kolotas, K. Geramani, R. F. Mould, G. Ioannidis, M. Kekchidi, and N. Zamboglou, ‘‘A conformal index COIN to evaluate implant quality and dose specifications in brachytherapy,’’ Int. J. Radiat.Oncol., Biol., Phys. 40, 512–524 ~1998

Lahanas, M., Baltas, D., Zamboglou, N.: Anatomy-based three-dimensional dose optimization in brachytherapy using multiobjective genetic algorithms. Med. Phys., 26, No. 9, 1904-1918, 1999.

Lahanas, M., Milickovic, N., Baltas, D., Zamboglou, N.: Application of Multiobjective Evolutionary Algorithms for Dose Optimization in Brachytherapy. E. Zitzler et al. (Eds.): EMO 2001, LNCS 1993, 574-587, 2001

Milickovic, N., Lahanas, M., Baltas, D., Zamboglou, N.: Comparison of Evolutionary and Deterministic Multiobjective Algorithms for Dose Optimization in Brachytherapy. E. Zitzler et al. (Eds.): EMO 2001, LNCS 1993, 167-180, 2001

Lessard, E., & Pouliot, J. (2001). Inverse planning anatomy-based dose optimization for HDRbrachytherapy of the prostate using fast simulated annealing algorithm and dedicated objective function. Medical Physics, 25(5), 773-779.

Milickovic, N., Lahanas, M., Papagianopoulou, M., Zamboglou, N., Baltas, D.: Multiobjective anatomy-based dose optimization for HDR-brachytherapy with constraint free deterministic algorithms. Phy.s Med. Biol., 47(13), 2263-2280, 2002

Lahanas, M., Baltas, D., Zamboglou, N.: A hybrid evolutionary algorithm for multi-objective anatomy-based optimization in high-dose-rate brachytherapy. Phys. Med. Biol., 48, 399-415, 2003.

Lahanas, M., Baltas, D., Giannouli, S.: Global convergence analysis of fast multi-objective gradient-based dose optimization algorithms for high-dose-rate brachytherapy. Phys. Med. Biol., 48, 599-617, 2003

Jozsef, G., Streeter, O. E., & Astrahan, M. A. (2003). The use of linear programming in optimization of HDR implant dose distributions. Medical Physics, 30(5), 751-760.

Lahanas, M., Karouzakis, K., Giannouli, S., Mould, R.F., Baltas, D.: Inverse planning in brachytherapy from radium to high dose rate 192Iridium afterloading. NOWOTWORY Journal of Oncology, 54 No 6, 535–546, 2004.

Karabis, A., Giannouli, S., Baltas, D.: HIPO: A hybrid inverse treatment planning optimization algorithm in HDR brachytherapy. Radiother. Oncol., 76, Supplement 2, 29, 2005.

De Witt, K. D., Hsu, I.-C. J., Speight, J., Weinberg, V. K., Lessard, E., & Pouliot, J. (2005). 3D inverse treatment planning for the tandem and ovoid applicator in cervical cancer. International Journal of Radiation Oncology, Biology, Physics, 63(4), 1270-1274.

Sumida, I., Shiomi, H., Yoshioka, Y., Inoue, T., Lessard, E., Hsu, I.-C. J., & Pouliot, J. (2006). Optimization of dose distribution for HDR brachytherapy of the prostate using attraction-repulsion model. International Journal of Radiation Oncology, Biology, Physics, 64(2), 643-649.

Alterovitz, R., Lessard, E., Pouliot, J., Hsu, I.-C. J., O'Brien, J. F., & Goldberg, K. (2006). Optimization of HDR brachytherapy dose distributions using linear programming with penalty costs. Medical Physics, 33(11), 4012-4019.

ESTRO School

Literature II

Baltas, D., & Zamboglou, N. (2006). 2D and 3D planning in brachytherapy. In W. Schlegel, T. Bortfeld, & A. L. Grosu (Eds.), New technologies in radiation oncology (pp. 237-254). New York: Springer.

Jacob, D., Raben, A., Sarkar, A., Grimm, J., & Simpson, L. (2008). Anatomy-based inverse planning simulated annealing optimization in high-dose-rate prostate brachytherapy: Significant dosimetric advantage over other optimization techniques. International Journal of Radiation Oncology, Biolology, Physics, 72(3), 820-872.

Kim, Y., Hsu, I.-C. J., Lessard, E., Kurhanewicz, J., Noworolsky, S. M., & Pouliot, J. (2008). Class solution in inverse planned HDR prostate brachytherapy for dose escalation of DIL defined by combined MRI/MRSI. Radiotherapy and Oncology, 88, 148-155.

Karabis, A., Belotti, P., & Baltas, D. (2009). Optimization of catheter position and dwell time in prostate HDR brachytherapy using HIPO and linear programming. Proceedings of the 11th International Congress of the IUPESM (World Congress on Medical Physics and Biomedical Engineering), 25 (1), 612-615, doi: 10.1007/978-3-642-03474-9 172.

Trnková, P., Pötter, R., Baltas, D., Karabis, A., Fidarova, E., Dimopoulos, J., Georg, D., Kirisits, C.: New inverse planning technology for image-guided cervical cancer brachytherapy: Description and evaluation within a clinical frame. Radiother. Oncol., 93, 331-340, 2009.

Mavroidis, P., Katsilieri, Z., Kefala, V., Milickovic, N., Papanikolaou, N., Karabis, A., Zamboglou, N., Baltas, D. Radiobiological evaluation of the influence of dwell time modulation restriction in HIPO optimized HDR prostate brachytherapy implants. J Contemp Brachyther Vol 2, No 3: 117-128, 2010.

Jamema, S. V., Kirisits, C., Mahantshetty, U., Trnková, P., Deshpande, D. D., Shrivastava, S. K., & Pötter, R. (2010). Comparison of DVH parameters and loading patterns of standard loading, manual and inverse optimization for intracavitary brachytherapy on a subset of tandem/ovoid cases. Radiotherapy and Oncology, 97, 501-506.

De Boeck Liesje, Belien Jeroen, Egyed Wendy. “Dose Optimisation in HDR brachytherapy: A literature review of quantitative models”. HUB Research Papers 2011/32, Economics & Management, December 2011.

Dinkla A.M., van der Laarse R., Koedooder K., Kok H.P., van Wieringen N., Pieters B.R., Bel A. Novel tools for stepping source brachytherapy treatment planning: Enhanced geometrical optimization and interactive inverse planning. Medical Physics 42 (1), 348-353, 2015.

Dinkla A.M., van der Laarse R., Kaljouw E., Pieters B.R., Koedooder K., van Wieringen N., Bel A. A comparison of inverse optimization algorithms for HDR/PDR prostate brachytherapy treatment planning. Brachytherapy 14, 279-288, 2015.

Poulin E, Collins Fekete CA, Létourneau M, Fenster A, Pouliot J, Beaulieu L (2013). Adaptation of the CVT algorithm for catheter optimization in high dose rate brachytherapy Med. Phys. 40 (11), 111724-1-9

Panettieri V, Schmidt RL, Mason NJ, Millar JL (2014). Comparison of IPSA and HIPO inverse planning optimization algorithms for prostate HDR brachytherapy. Journal of Applied Clinical Medical Physics, 15, No 6, 256-266.

Dinkla AM, van der Laarse R, Kaljouw E, Pieters BR, Koedooder K, van Wieringen N, Bel A (2015). A comparison of inverse optimization algorithms for HDR/PDR prostate brachytherapy treatment planning. Brachytherapy 14, 279-288.

Poulin E, Varfalvy N, Aubin S, Beaulieu (2016). Comparison of dose and catheter optimization algorithms in prostate high-dose-rate brachytherapy. Brachytherapy 15, 102-111.

Holm A, Carlson Tedgren A, Larsson T (2016). Heuristics for integrated optimization of catheter positioning and dwell time distribution in prostate HDR brachytherapy. Ann Oper Res, 236, 319–339.

ESTRO School

ESTRO School

ESTRO School

WWW.ESTRO.ORG/SCHOOL

ESTRO School

Advanced Brachytherapy Physics

Source Strength Determinations in Brachytherapy

Prof. Mark J. Rivard, Ph.D., FAAPM

Advanced Brachytherapy Physics, 29 May – 1 June, 2016

ESTRO School

Disclosures

The are no conflicts-of-interest to report.

Opinions herein are solely those of the presenter, and are not meant to be interpreted as societal guidance.

Specific commercial equipment, instruments, and materials are listed to fully describe the necessary procedures. Such identification does not imply endorsement by the presenter, nor that these products are necessarily the best available for these purposes.

ESTRO School

Learning Objectives

1. Accepted standard units for brachytherapy source strength
2. Source calibration traceability and standards labs
3. Calibration methods and techniques
4. Calibration uncertainties
5. Future calibrations

Photon Sources Examined

	High Energy	Low Energy
High Dose Rate	^{192}Ir, ^{60}Co	electronic (x rays)
Low Dose Rate	^{137}Cs	^{125}I, ^{103}Pd, ^{131}Cs

ESTRO School

2004 AAPM TG-43U1
Brachytherapy Dosimetry Formalism

RAKR nearly identical to air-kerma strength S_K (distance specification)

$$\dot{D}(r,\theta) = S_K \cdot \Lambda \cdot \frac{G_L(r,\theta)}{G_L(r_0,\theta_0)} \cdot g_L(r) \cdot F(r,\theta)$$

$\dot{D}(r,\theta)$	dose rate to water in water at point P(r,θ)
S_K	air-kerma strength
Λ	dose-rate constant
$g_L(r)$	radial dose function
$G_L(r,\theta)$	geometry function (line-source approximation)
$F(r,\theta)$	2D anisotropy function

ESTRO School

Brachytherapy Source Strength

Only the reference air kerma rate (RAKR) K_R is a quantity that is traceable to a standards laboratory (i.e., NMI or PSDL)

RAKR defined as kerma rate to air @ 1 meter
in vacuo, corrected for attenuation/scatter

RAKR defined on the source transverse-plane for photons with E > δ
δ threshold is dependent on source calibration protocol

RAKR has units Gy/s, also Gy/h or μGy/s (unit conversion - convenience)

mg Ra, mgRaEq, mCi (apparent activity), Bq are not traceable quantities

Obsolete units: mg Ra, mgRaEq, mCi (apparent activity), Bq

All Authorities Agree on Correct Unit

(1974) NCRP Report 41

(1983) French Cmte on ionizing Radiation Measurements

(1984) British Cmte on Radiation Units and Measurements

(1985) ICRU Report 38: Dose and volume specification for reporting intracavitary therapy in gynecology

(1987) AAPM TG-32: Specification of brachytherapy source strength

(1997) ICRU Report 58: Dose and volume specification for reporting interstitial brachytherapy

(2004) ESTRO Booklet 8: A practical guide to quality control of brachytherapy equipment

etc., etc., etc.

ICRU, GEC-ESTRO, and AAPM explicitly recommend against A_{app}

ESTRO School

NRC Information Notice 2009-17

"The NRC has received reports of numerous medical events caused by errors in confusing the units of source strength in the specification of sources—specifically, units of air-kerma strength and apparent activity in units of millicurie (mCi)."

"human error caused all these events"

27% overdose errors with ^{125}I

78% overdose errors with ^{192}Ir

use of apparent activity for brachytherapy sources is unsafe and inexcusable

Influence of Missing Calibration on ^{103}Pd Dosage

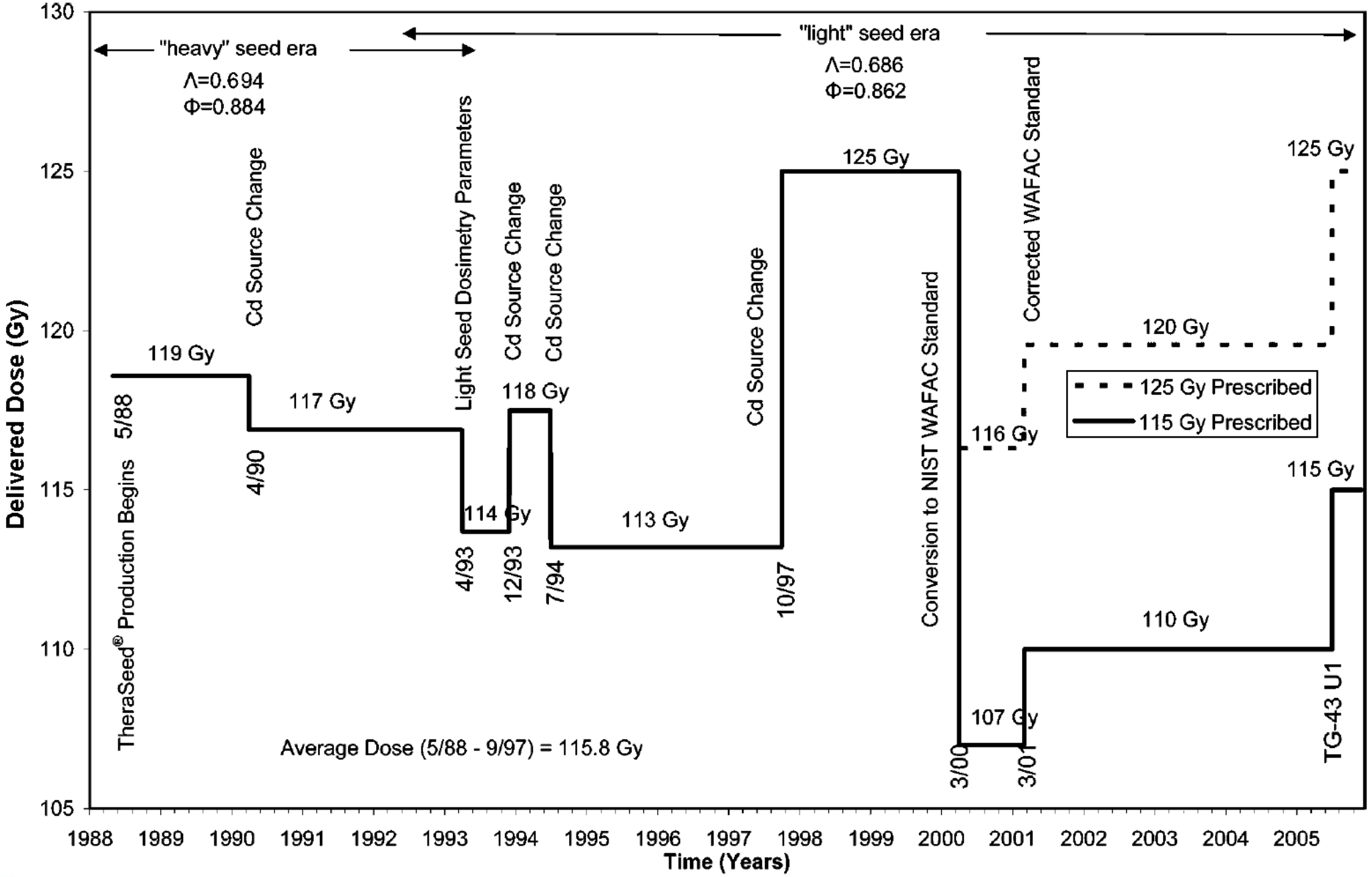

Williamson, et al., *Med. Phys.* 32, 1424-1439 (2005)

ESTRO School

Impact of Missing Time Calibration on Movies

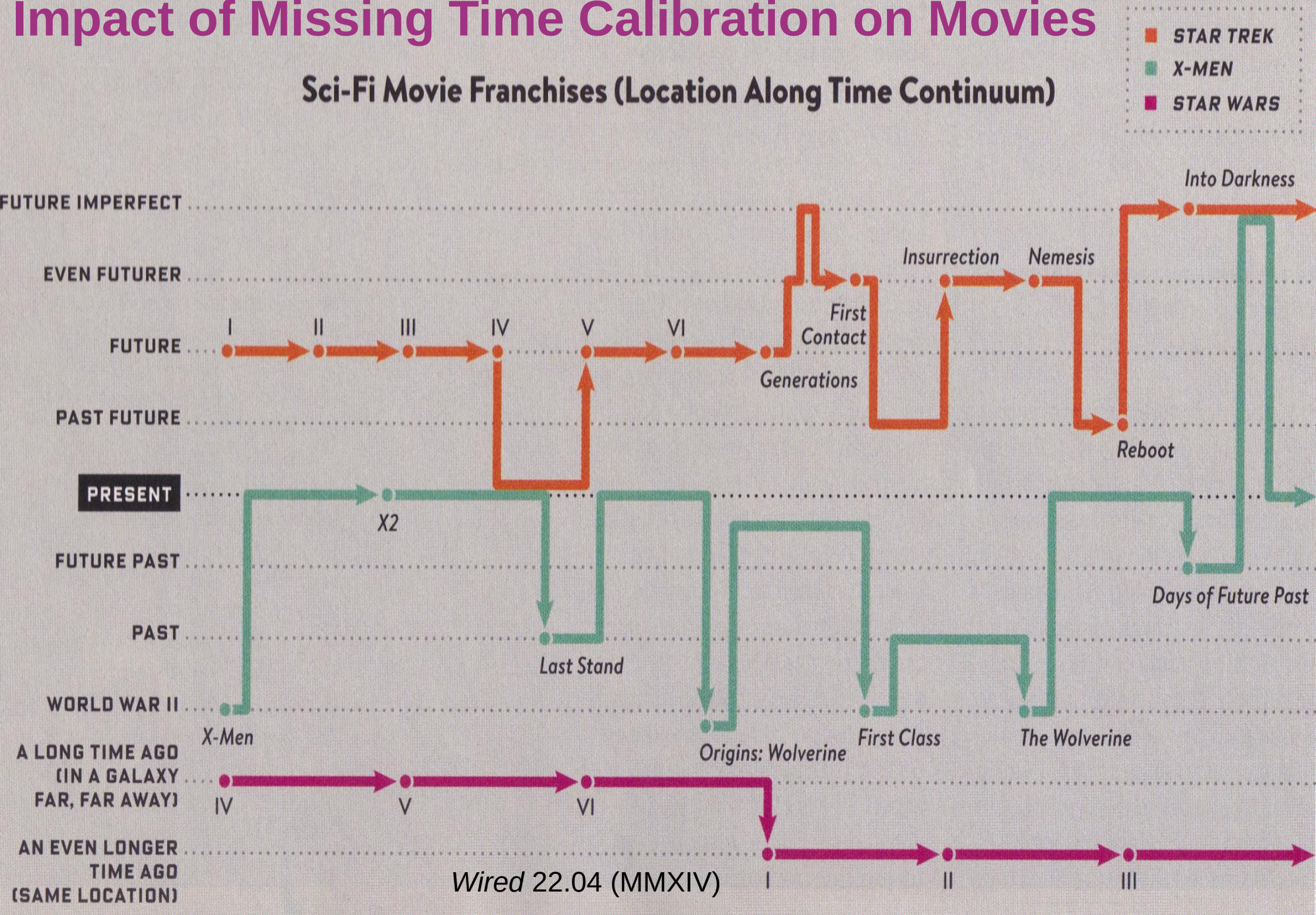

Wired 22.04 (MMXIV)

Uncertainty is a Quantitative Measure of Quality

AAPM + ESTRO TG-138 Report

Medical Physics

A dosimetric uncertainty analysis for photon-emitting brachytherapy sources: Report of AAPM Task Group No. 138 and GEC-ESTRO

This report addresses uncertainties pertaining to brachytherapy single-source dosimetry preceding clinical use. The International Organization for Standardization (ISO) Guide to the Expression of Uncertainty in Measurement (GUM) and the National Institute of Standards and Technology (NIST) Technical Note 1297 are taken as reference standards for uncertainty formalism. Uncertainties in using detectors to measure or utilizing Monte Carlo methods to estimate brachytherapy dose distributions are provided with discussion of the components intrinsic to the overall dosimetric assessment. Uncertainties provided are based on published observations and cited when available. The uncertainty propagation from the primary calibration standard through transfer to the clinic for air-kerma strength is covered first. Uncertainties in each of the brachytherapy dosimetry parameters of the TG-43 formalism are then explored, ending with transfer to the clinic and recommended approaches. Dosimetric uncertainties during treatment delivery are considered briefly but are not included in the detailed analysis. For low- and high-energy brachytherapy sources of low dose rate and high dose rate, a combined dosimetric uncertainty <5% (k=1) is estimated, which is consistent with prior literature estimates. Recommendations are provided for clinical medical physicists, dosimetry investigators, and source and treatment planning system manufacturers. These recommendations include the use of the GUM and NIST reports, a requirement of constancy of manufacturer source design, dosimetry investigator guidelines, provision of the lowest uncertainty for patient treatment dosimetry, and the establishment of an action level based on dosimetric uncertainty. These recommendations reflect the guidance of the American Association of Physicists in Medicine (AAPM) and the Groupe Européen de Curiethérapie–European Society for Therapeutic Radiology and Oncology (GEC-ESTRO) for their members and may also be used as guidance to manufacturers and regulatory agencies in developing good manufacturing practices for sources used in routine clinical treatments.

DeWerd, et al, *Med. Phys.* 38, 782-801 (2011)

Methodology for Uncertainty Estimation

Guide to Expression of Uncertainty in Measurement
ISO GUM (2010) precision ≠ accuracy

Type A (statistical: standard deviation of results)

Type B (non-Type A uncertainties)

Law of Propagation of Uncertainty (no covariations)

TG-138 applies principles for expressing brachytherapy dosimetric uncertainties

expanded uncertainty, k = 2 (95.45% confidence, 21/22)
special case for large # DOF
k = t-factor otherwise with covariations

DeWerd, et al, *Med. Phys.* 38, 782-801 (2011)

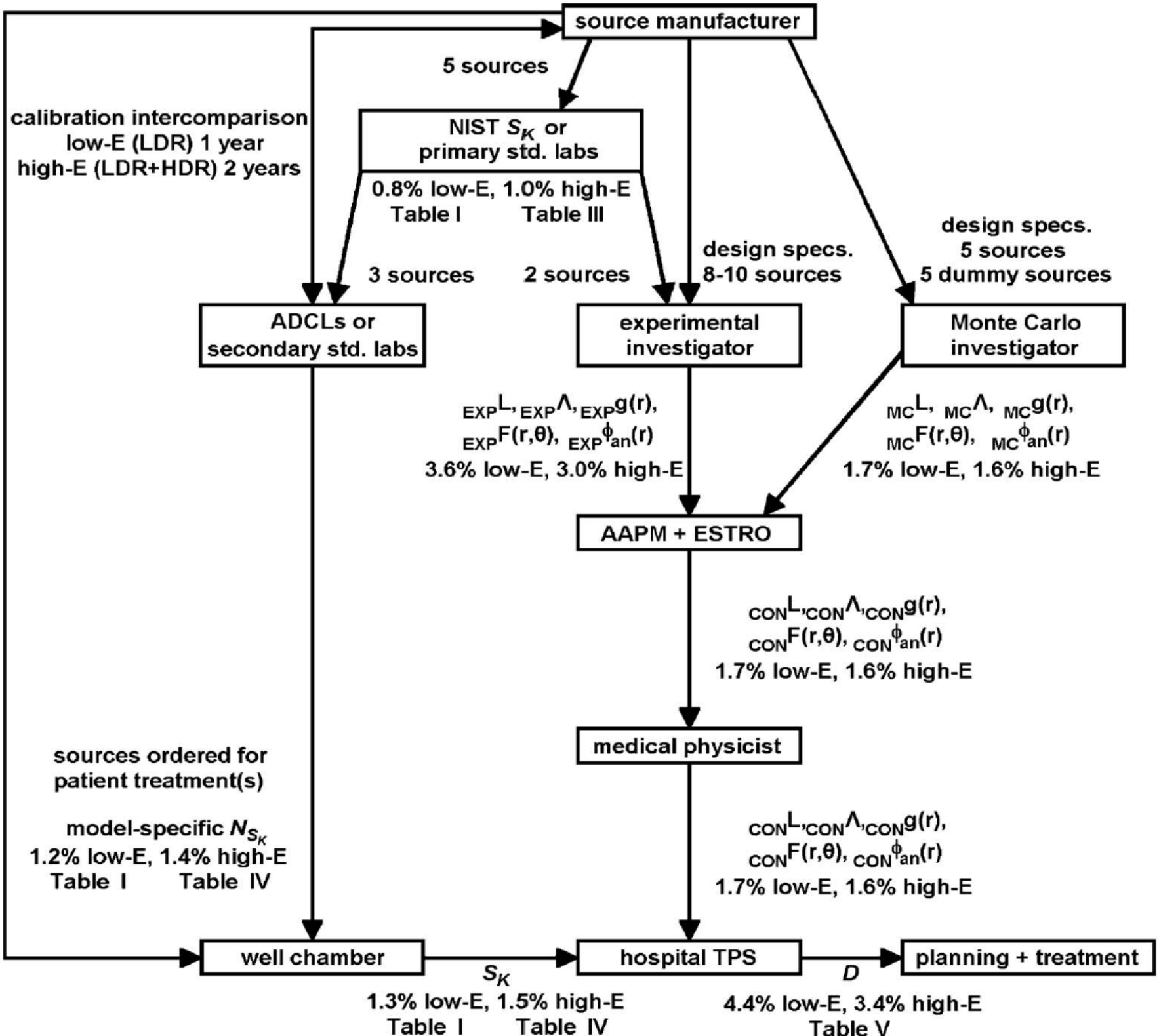
source manufacturer
5 sources
calibration intercomparison
low-E (LDR) 1 year
high-E (LDR+HDR) 2 years
NIST S_K or
primary std. labs
0.8% low-E, 1.0% high-E
Table I Table III
3 sources
2 sources
design specs.
8-10 sources
design specs.
5 sources
5 dummy sources
ADCLs or
secondary std. labs
experimental
investigator
Monte Carlo
investigator
$_{EXP}L$, $_{EXP}\Lambda$, $_{EXP}g(r)$,
$_{EXP}F(r,\theta)$, $_{EXP}\phi_{an}(r)$
3.6% low-E, 3.0% high-E
$_{MC}L$, $_{MC}\Lambda$, $_{MC}g(r)$,
$_{MC}F(r,\theta)$, $_{MC}\phi_{an}(r)$
1.7% low-E, 1.6% high-E
AAPM + ESTRO
$_{CON}L$,$_{CON}\Lambda$,$_{CON}g(r)$,
$_{CON}F(r,\theta)$, $_{CON}\phi_{an}(r)$
1.7% low-E, 1.6% high-E
medical physicist
sources ordered for
patient treatment(s)
model-specific N_{S_K}
1.2% low-E, 1.4% high-E
Table I Table IV
$_{CON}L$,$_{CON}\Lambda$,$_{CON}g(r)$,
$_{CON}F(r,\theta)$, $_{CON}\phi_{an}(r)$
1.7% low-E, 1.6% high-E
well chamber
S_K
1.3% low-E, 1.5% high-E
Table I Table IV
hospital TPS
D
4.4% low-E, 3.4% high-E
Table V
planning + treatment

Low-Energy Calibration Uncertainty

Table I Propagation of best practice uncertainties ($k = 1$ unless stated otherwise) associated with the transfer of air-kerma strength from NIST through the ADCL to the clinic for LDR low-energy brachytherapy sources.

Row	Measurement description	Quantity (units)	Relative propagated uncertainty (%)
1	NIST WAFAC calibration	$S_{K,NIST}$ (U)	0.8
2	ADCL well ion chamber calibration	$S_{K,NIST} / I_{ADCL}$ (U / A)	0.9
3	ADCL calibration of source from manufacturer	$S_{K,ADCL}$ (U)	1.1
4	ADCL calibration of clinic well ion chamber	$S_{K,ADCL} / I_{CLINIC}$ (U / A)	1.2
5	Clinic measures source air-kerma strength	$S_{K,CLINIC}$ (U)	1.3
	Expanded uncertainty ($k = 2$)	$S_{K,CLINIC}$ (U)	2.6

Table II Propagation of best practice uncertainties ($k = 1$ unless stated otherwise) associated with the transfer of the air-kerma strength standard from NIST to the manufacturer for LDR low-energy brachytherapy sources.

Row	Measurement description	Quantity (units)	Relative propagated uncertainty (%)
1	NIST WAFAC calibration	$S_{K,NIST}$ (U)	0.8
2	Manufacturer well ion chamber calibration	$S_{K,NIST} / I_M$ (U / A)	0.9
3	Manufacturer calibration of QA source	$S_{K,M}$ (U)	1.1
4	Manufacturer instrument calibration for assay	$S_{K,M} / I_M$ (U / A)	1.2
5	Manufacturer assays production sources	$S_{K,M}$ (U)	1.3
6	Manufacturer places sources in 2% or 7% bins	$S_{K,Mbin}$ (U)	1.4 or 2.4
	Expanded uncertainty ($k = 2$)	$S_{K,Mbin}$ (U)	2.8 or 4.8

DeWerd, et al, *Med. Phys.* 38, 782-801 (2011)

High-Energy Calibration Uncertainty

Table III Propagation of "best practice" uncertainties associated with the transfer of air-kerma strength from NIST through the ADCL to the clinic for **LDR high-energy** brachytherapy sources. Well chamber measurement uncertainty is estimated to be 0.5 %.

Step	Measurement description	Quantity (units)	Relative propagated uncertainty (%)
1	NIST calibration	$S_{K,NIST}$ (U)	1.0
2	ADCL well ion chamber calibration	$S_{K,NIST}$ / I_{ADCL} (U / A)	1.1
3	ADCL calibration of source from manufacturer	$S_{K,ADCL}$ (U)	1.2
4	ADCL calibration of clinic well ion chamber	$S_{K,ADCL}$ / I_{CLINIC} (U / A)	1.3
5	Clinic measures source air-kerma strength	$S_{K,CLINIC}$ (U)	1.4
	Expanded uncertainty (k = 2)	$S_{K,CLINIC}$ (U)	2.8

Table IV Propagation of "best practice" uncertainties associated with the transfer of air-kerma strength from a traceable NIST coefficient from the ADCL to the clinic for **HDR high-energy** brachytherapy sources.

Step	Measurement description	Quantity (units)	Relative propagated uncertainty (%)
1	ADCL calibration	$S_{K,NIST}$ (U)	1.1
2	ADCL well ion chamber calibration	$S_{K,NIST}$ / I_{ADCL} (U / A)	1.2
3	ADCL calibration of source from manufacturer	$S_{K,ADCL}$ (U)	1.3
4	ADCL calibration of clinic well ion chamber	$S_{K,ADCL}$ / I_{CLINIC} (U / A)	1.4
5	Clinic measures source air-kerma strength	$S_{K,CLINIC}$ (U)	1.5
	Expanded uncertainty (k = 2)	$S_{K,CLINIC}$ (U)	2.9

DeWerd, et al, *Med. Phys.* 38, 782-801 (2011)

Summary of TG-138 Report

- AAPM + ESTRO recommend GUM methods for expressing dosimetric uncertainties
- precision ≠ accuracy
- Type A (statistical: standard deviation of results)
  Type B (non-Type A uncertainties)
- low-E (8.7%, k=2) high-E (6.8%, k=2)
- expanded uncertainty, k=2 (95% confidence 21/22)
- pre-Tx recommendations: S_K, exp, MC, vendors
- clinical practice uncertainties are larger

ESTRO School

AAPM Calibration Recommendations

Medical Physics

Third-party brachytherapy source calibrations and physicist responsibilities: Report of the AAPM Low Energy Brachytherapy Source Calibration Working Group

Compiling and clarifying recommendations established by previous AAPM Task Groups 40, 56, and 64 were among the working group's charges, which also included the role of third-party handlers to perform loading and assay of sources. This document presents working group findings on the responsibilities of the institutional medical physicist and a clarification of the existing AAPM recommendations in the assay of brachytherapy sources. The AAPM leaves it to the discretion of the institutional medical physicist whether the manufacturer's or institutional physicist's measured value should be used in performing dosimetry calculations.

Butler, et al, *Med. Phys*. 35, 3860-3865 (2008)

ESTRO School

AAPM Calibration Recommendations

TABLE I. Quantities of brachytherapy sources to be assayed by the end-user physicist.

Source form	number to be assayed
All loose sources, nonsterile	⩾10% of total or 10 seeds, whichever is larger.
Nonsterile cartridges	⩾10% of total via whole cartridge assay or via single sources.
Mixture of nonsterile loose sources and sterile assemblies	Loose sources amounting to ⩾10% of the total order or ten seeds, whichever is larger.
Sterile source assemblies	⩾10% of assemblies via sterile well chamber inserts or quantitative image analysis. Alternatively, order and assay nonsterile loose seeds equal to 5% of the total or five seeds, whichever is fewer.
Strands	⩾10% of total or two strands, whichever is larger, using single-seed calibration coefficient (see Ref. 15). Alternatively, order and assay nonstranded loose seeds equal to 5% of the total or five seeds, whichever is fewer.

[a]Each source-strength grouping in an order should be sampled. If the number of sources in a strength group is <10, the entire group should be assayed.

Butler, et al, *Med. Phys*. 35, 3860-3865 (2008)

AAPM Calibration Recommendations

TABLE II. Actions to be taken by the physicist at the end-using institution based on the sample size assayed and the relative difference, ΔS_K, found between the manufacturer's source strength certificate and the assay by the physicist at the using institution.[a]

Sample size for assay of sources by end-user medical physicist	ΔS_K	action by medical physicist
Individual source as part of an order of $\geq$10 sources[b]	$\Delta S_K \leq 6\%$	Nothing further.
	$\Delta S_K > 6\%$	Consult with the radiation oncologist regarding use of the outlier source: Dependent on the radionuclide, intended target, source packaging, and the availability of extra sources.
$\geq$10% but <100% of order, or batch measurements of individual sterile strands, cartridges or preloaded needles	$\Delta S_K \leq 3\%$	Nothing further.
	$5\% \geq \Delta S_K > 3\%$	Investigate source of discrepancy or increase the sample size.
	$\Delta S_K > 5\%$	Consult with manufacturer to resolve differences or increase the sample size. For assays performed in the operating room, consult with the radiation oncologist regarding whether to use the measured source strength or to average with the manufacturer's value.
100% of order, or batch measurements of each and every individual sterile strand, cartridge or preloaded needle	$\Delta S_K \leq 3\%$	Nothing further.
	$5\% \geq \Delta S_K > 3\%$	Investigate source of discrepancy.
	$\Delta S_K > 5\%$	Consult with manufacturer to resolve differences. For assays performed in the operating room, consult with the radiation oncologist regarding the consequences of proceeding with the implant using the measured source strength.

[a]Assay results obtained at sites other than the end-user institution should not replace the source strength value on the manufacturer's certificate. The source strength value to be used in planning may be either that stated on the manufacturer's certificate or the value determined by institutional medical physicist when the difference is $\geq$5%.

[b]For orders consisting of < ten sources, the action threshold is $\Delta S_K > 5\%$ for individual sources.

Butler, et al, *Med. Phys*. 35, 3860-3865 (2008)

Calibration and Measurement Capabilities Ionizing Radiation

BIPM
Bureau International des Poids et Mesures

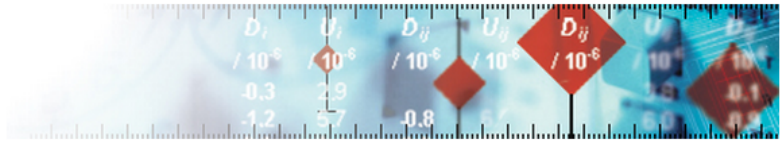

Home | Key and supplementary comparisons | Calibration and Measurement Capabilities - CMCs

Home > CMCs Search > RI search form > CMC descriptions

CMCs - Result of the search

KCDB

↘ Physics
- Acoustics, Ultrasound, Vibration
- Electricity and Magnetism
- Length
- Mass and related quantities
- Photometry and Radiometry
- Ionizing Radiation
- Thermometry
- Time and Frequency

↘ Chemistry
- Chemistry

↘ Traceability to the SI through the BIPM
- BIPM calibration and measurement services

↘ Related links
- KCDB Statistics
- KCDB FAQs
- KCDB Reports
- CIPM MRA
- JCRB
- Find my NMI
- Metrologia

↘ Contact us
- BIPM.KCDB@bipm.org

Calibration and Measurement Capabilities Ionizing Radiation

↘ Result of the search

Your selection : Dosimetry, Reference air kerma rate

17 summary CMC descriptions match your selection. Please select one or more CMCs, then click on 'view' to access more information.

Select	Quantity	Source	Country	NMI	RMO
☐	Reference air kerma rate	Cs-137	Cuba	CPHR	COOMET
☐	Reference air kerma rate	Ir-192	France	LNE	EURAMET
☐	Reference air kerma rate	Co-60	Germany	PTB	EURAMET
☐	Reference air kerma rate	Ir-192	Germany	PTB	EURAMET
☐	Reference air kerma rate	I-125	Germany	PTB	EURAMET
☐	Reference air kerma rate	Cs-137	Greece	IRCL/GAEC-EIM	EURAMET
☐	Reference air kerma rate	Ir-192	Greece	IRCL/GAEC-EIM	EURAMET
☐	Reference air kerma rate	Ir-192	Italy	ENEA-INMRI	EURAMET
☐	Reference air kerma rate	Cs-137	Korea, Republic of	KRISS	APMP
☐	Reference air kerma rate	Ir-192	Netherlands	VSL	EURAMET
☐	Reference air kerma rate	Ir-192	Russian Federation	VNIIM	COOMET
☐	Reference air kerma rate	Co-60	Slovakia	SMU	EURAMET
☐	Reference air kerma rate	Cs-137	Slovakia	SMU	EURAMET
☐	Reference air kerma rate	Cs-137	United States	NIST	SIM
☐	Reference air kerma rate	Ir-192	United States	NIST	SIM
☐	Reference air kerma rate	I-125	United States	NIST	SIM
☐	Reference air kerma rate	Pd-103	United States	NIST	SIM

ESTRO School

US: National Institute of Standards and Technology

Calibration of Low-Energy Photon Brachytherapy Sources

Summary:

Small radioactive "seed" sources used in prostate brachytherapy, containing the radionuclide ^{103}Pd, ^{125}I, or ^{131}Cs, are calibrated in terms of air-kerma strength using the NIST Wide-Angle Free-Air Chamber (WAFAC). The WAFAC is an automated, free-air ionization chamber with a variable volume, allowing corrections to be made for passage of the beam through non-air-equivalent electrodes.

Description:

Since 1999, over 1,000 seeds of more than 40 different designs from 18 manufacturers have been calibrated using the WAFAC. On-site characterization at seed manufacturing plants for quality control, as well as at therapy clinics for treatment planning, relies on well-ionization chamber measurements. Following the primary standard measurement of air-kerma strength, the responses of several well-ionization chambers to the various seed sources are determined. The ratio of air-kerma strength to well-chamber response yields a calibration coefficient for the well-ionization chamber for a given seed type. Such calibration coefficients enable well-ionization chambers to be employed at therapy clinics for verification of seed air-kerma strength, which is used to calculate dose rates to ensure effective treatment planning. To understand the relationship between well-ionization chamber response and WAFAC-measured air-kerma strength for prostate brachytherapy seeds, emergent x-ray spectra are measured with a high-purity germanium (HPGe) spectrometer.

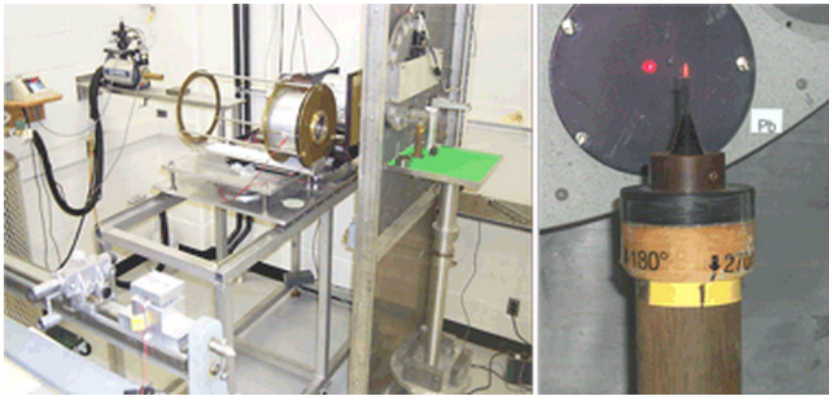

Photograph by: Michael G. M itch

Lead Organizational Unit:

PML

Staff:

Dosimetry Group

Michael G. Mitch

Jason S. Walia

ESTRO School

NIST: WAFAC (Low-E Sources)

Table 6b. Correction factors for measurements made with the automated WAFAC, assuming a source-to-aperture distance of 30 cm

Correction factor	For:	Currently implemented values		Values from the analyses presented in the text					
		^{125}I	^{103}Pd	^{125}I	^{125}I + 0.053 Ag Kx	^{125}I + 0.094 Ag Kx	^{125}I + 0.195 Ag Kx	^{125}I + 0.181 Pd Kx	^{103}Pd
1 k_{decay}	Correction to reference date, $T_{1/2}$(d)	59.43	16.991	59.40	59.40	59.40	59.40	59.40	16.991
2 k_{sat}	Recombination inside WAFAC	<1.004	<1.004	<1.004	<1.004	<1.004	<1.004	<1.004	<1.004
3 k_{foil}	Attenuation in filter	1.0295	1.0738	1.0320	1.0342	1.0358	1.0394	1.0417	1.0776
4 $k_{att\text{-}WAFAC}$	Aperture-to-WAFAC air attenuation	1.0042	1.0079	1.0048	1.0050	1.0051	1.0055	1.0057	1.0089
5 $k_{att\text{-}SA}$	Source-to-aperture air attenuation	1.0125	1.0240	1.0143	1.0149	1.0153	1.0163	1.0170	1.0267
6 k_{invsq}	Inverse-square correction for aperture	1.0089	1.0089	1.0089	1.0089	1.0089	1.0089	1.0089	1.0089
7 $k_{humidity}$	Humidity correction	0.9982	0.9981	0.9979	0.9979	0.9979	0.9979	0.9979	0.9979
8 $k_{int\text{-}scatt}$	In-chamber photon-scatter correction	0.9966	0.9962	0.9968	0.9968	0.9968	0.9967	0.9967	0.9964
9 k_{stem}	Source-holder stem-scatter correction	0.9985	0.9985	0.9985	0.9985	0.9985	0.9985	0.9985	0.9985
10 k_{elec}	In-chamber electron-loss correction	1.0	1.0	1.0	1.0	1.0	1.0	1.0	1.0
11 k_{pen}	Aperture penetration	0.9999	0.9999	0.9999	0.9999	0.9999	0.9999	0.9999	0.9997
12 $k_{ext\text{-}scatt}$	External photon-scatter correction	1.0	1.0	0.9947	0.9947	0.9947	0.9947	0.9947	0.9945
$\Pi\, k_{3\text{-}12}$		1.0489	1.1100	1.0483	1.0513	1.0535	1.0585	1.0618	1.1116
	Percent change			–0.06	+0.23	+0.44	+0.92	+1.23	+0.14

Seltzer, et al. *J Res NIST* 108, 337-358 (2003)

ESTRO School

NIST: WAFAC (Low-E Sources)

Table 7. Estimated relative standard uncertainties in the determination of air-kerma strength from prostate seeds using the WAFAC

Component	For:	Relative standard uncertainty, %		
		Type A	^{125}I	^{103}Pd
			Type B	Type B
$I_{net,diff}$	Net current	s_I [a]	0.06	0.06
W/e	Mean energy per ion pair		0.15	0.15
ρ_0	Air density		0.03	0.03
d	Source-aperture distance		0.24	0.24
V_{eff}	Effective volume	0.11	0.01	0.01
k_{decay}	Correction to reference date, $T_{1/2}$(d)		0.02[b]	0.08[b]
k_{sat}	Recombination inside WAFAC		0.05	0.05
k_{foil}	Attenuation in filter		0.61	0.51
$k_{att\text{-}WAFAC}$	Aperture-to-WAFAC air attenuation		0.08	0.10
$k_{att\text{-}SA}$	Source-to-aperture air attenuation		0.24	0.31
k_{invsq}	Inverse-square correction for aperture		0.01	0.01
$k_{humidity}$	Humidity correction		0.07	0.07
$k_{int\text{-}scatt}$	In-chamber photon scatter correction		0.07	0.07
k_{stem}	Source-holder stem-scatter correction		0.05	0.05
k_{elec}	In-chamber electron-loss correction		0.05	0.05
k_{pen}	Aperture penetration		0.02	0.08
$k_{ext\text{-}scatt}$	External photon scatter correction		0.17	0.19
Combined			0.754	0.719

[a] Determined as the standard deviation of the mean of the net current.
[b] Assuming time from the reference date is no more than ≈15 days.

Seltzer, et al. *J Res NIST* 108, 337-358 (2003)

ESTRO School

NIST: WAFAC (Low-E Sources)

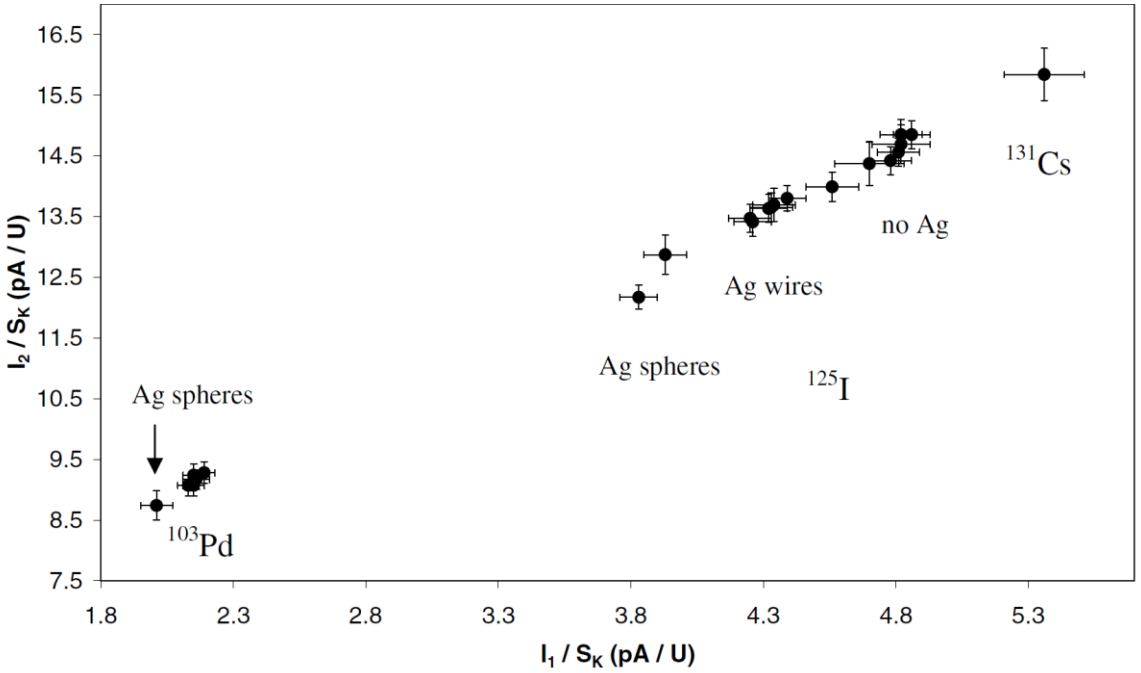

Correlation of the response coefficients of two well-ionization chambers for various ^{103}Pd, ^{125}I and ^{131}Cs source

	Value	s_i/%	u_j/%
Net current, I_{net}		s_I	0.06
$\bar{W}/e$	33.97 J C^{-1}	—	0.15
Air density, ρ_{air}	1.196 mg cm^{-3}	—	0.03
Aperture distance, d		—	0.24
Effective chamber volume, V_{eff}		0.11	0.01
Decay correction, k_1	$T_{1/2}$ = 59.43 d	—	0.02
Recombination, k_2	<1.004	—	0.05
Attenuation in filter, k_3	1.0295	—	0.61
Air attenuation in WAFAC, k_4	1.0042	—	0.08
Source–aperture attenuation, k_5	1.0125	—	0.24
Inverse-square correction, k_6	1.0089	—	0.01
Humidity, k_7	0.9982	—	0.07
In-chamber photon scatter, k_8	0.9966	—	0.07
Source-holder scatter, k_9	0.9985	—	0.05
Electron loss, k_{10}	1.0	—	0.05
Aperture penetration, k_{11}	0.9999	—	0.02
External photon scatter, k_{12}	1.0	—	0.17
Combined uncertainty			$(s_I^2 + 0.762^2)^{1/2}$

Soares, et al., *Metrologia* 46, S80-S98 (2009)

ESTRO School

NIST: Electronic Brachytherapy

Calibrations of a Miniature X-ray Source Used for Electronic Brachytherapy

Summary:

A new laboratory dedicated to establishing a national primary air-kerma rate standard for Xoft's AXXENT™ miniature x-ray source has been fabricated. The Xoft source was designed to provide low-energy xrays (< 50 keV) for use in brachytherapy.

Description:

The Xoft source was designed to provide low-energy x-rays (< 50 keV) for use in brachytherapy. The air-kerma rate is being directly realized through use of the Lamperti free-air chamber, which was compared with another national x-ray standard with these sources. A high-purity germanium (HPGe) x-ray spectrometer is used to monitor the energy spectrum of the beam in real time, as well as provide necessary input data for Monte Carlo calculations of correction factors for the free-air chamber. To account for spatial anisotropy of emissions, the free-air chamber and spectrometer are rotated about the long axis of the x-ray tube during measurements. The response of well-ionization chambers to the x-ray sources is being studied in preparation for the development of a measurement assurance program for the dissemination of the new NIST standard to Accredited Dosimetry Calibration Laboratories (ADCLs). The ADCLs are accredited by the American Association of Physicists in Medicine (AAPM), and calibrate radiation measuring instruments for use in therapy clinics.

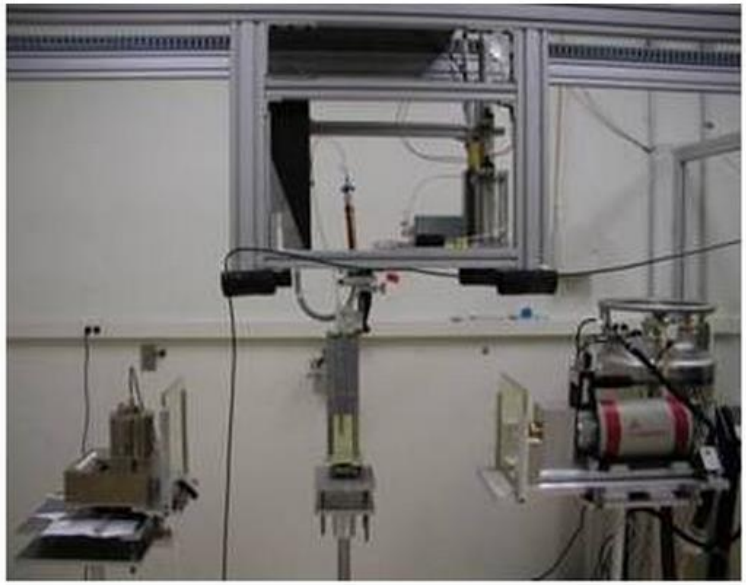

Xoft AXXENT (tm) electronic brachytherapy source in NIST Laboratory. (Photograph by: Michael G. Mitch)

ESTRO School

Germany: Physikalisch-Technische Bundesanstalt

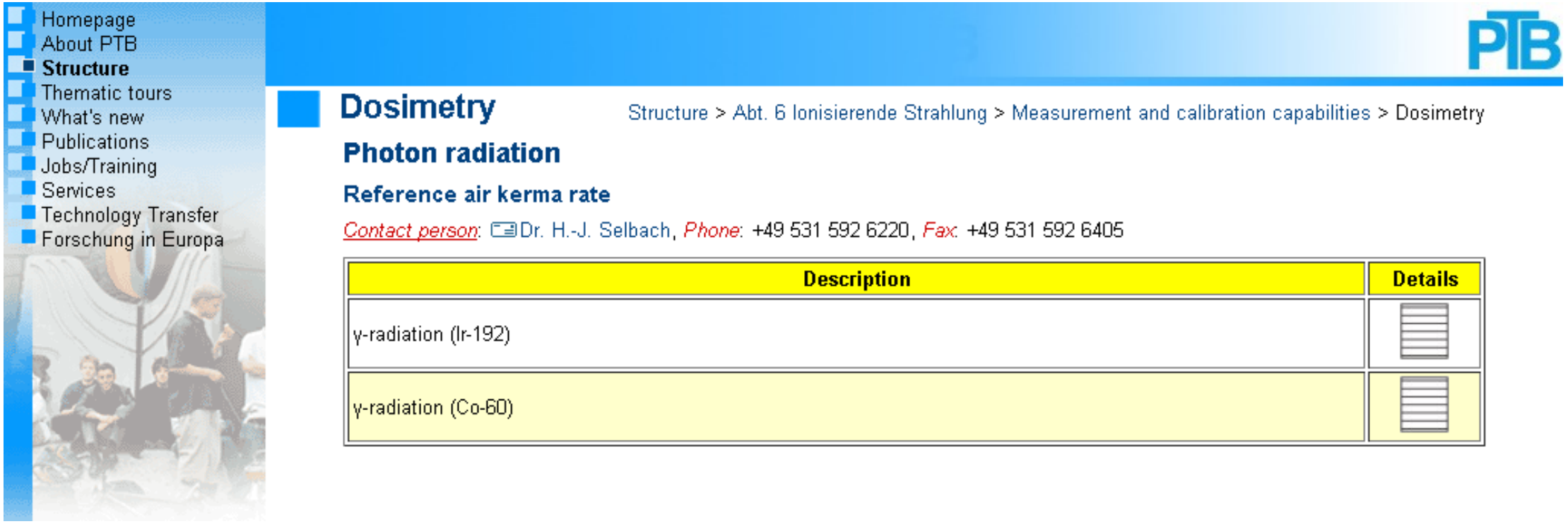

Homepage
About PTB
Structure
Thematic tours
What's new
Publications
Jobs/Training
Services
Technology Transfer
Forschung in Europa

PTB

Dosimetry

Structure > Abt. 6 Ionisierende Strahlung > Measurement and calibration capabilities > Dosimetry

Photon radiation

Reference air kerma rate

Contact person: Dr. H.-J. Selbach, *Phone*: +49 531 592 6220, *Fax*: +49 531 592 6405

Description	Details
γ-radiation (Ir-192)	
γ-radiation (Co-60)	

ESTRO School

PTB: RAKR Capabilities

3.1 Weitergabe der Einheiten im gesetzlichen Messwesen

U_r Relative erweiterte Messunsicherheit, die sich aus der Standardmessunsicherheit durch Multiplikation mit dem Erweiterungsfaktor $k = 2$ ergibt. Sie wurde gemäß dem *"Guide to the Expression of Uncertainty in Measurement"* (ISO, 1995) ermittelt. Der Wert der Messgröße liegt im Regelfall mit einer Wahrscheinlichkeit von annähernd 95 % im zugeordneten Werteintervall.

Einträge in "The BIPM key comparison database (KCDB)", http://www.bipm.org

Bezeichnung	*Calibration or Measurement Service*			Messbereich *Measurand level or range*			Messbedingungen *Measurement conditions*		U_r in %	Arbeitsanweisung	Zuständig	Aufgabe	Bemerkung
Service identification	Messgröße *Quantity*	*Instrument or Artifact*	*Instrument Type or Method*	Min *Min*	Max *Max*	Einheit *Unit*	Parameter *Parameter*	Spezifikation *Specification*		*Work instruction*	*Responsible*	*Task*	*Remark*
EUR-RAD-PTB-1001	Absorbed dose rate to water	Dosemeter	Conversion coefficient, PMMA phantom	2,0E-04	2,0E-02	Gy s^{-1}	X-rays 10 kV to 50 kV	10 kV to 40 kV DIN 6809/4 1988	2,8	AA-6200-001	6.2	09	Approved on 15 November 2010
EUR-RAD-PTB-1002	Absorbed dose rate to water	Dosemeter	Conversion coefficient, PMMA phantom	2,0E-04	2,0E-02	Gy s^{-1}	X-rays 50 kV to 420 kV	50 kV to 100 kV DIN 6809/4 1988	2,8	AA-6200-001	6.2	09	Approved on 15 November 2010
EUR-RAD-PTB-1003	Absorbed dose rate to water	Dosemeter	Secondary standard in a water phantom	2,0E-04	2,0E-03	Gy s^{-1}	X-rays 50 kV to 420 kV	100 kV to 300 kV DIN 6809/5 1996	2,1	AA-6200-001	6.2	09	Approved on 15 November 2010
EUR-RAD-PTB-1004	Absorbed dose rate to water	Dosemeter	Calibration in water phantom, reference field	2,0E-03	2,0E-02	Gy s^{-1}	Co-60	DIN 6800/2 2008	0,5	AA-6200-010	6.2	08	Approved on 15 November 2010
EUR-RAD-PTB-1005	Reference air kerma rate	Ir-192 source (HDR, PDR, wire)	Transfer chamber calibrated with primary cavity chamber	1,0E-04	1,0E-01	Gy h^{-1}	air kerma free in air at 1 m	DIN 6800/2 2008	1,8	AA-6200-022	6.2	11, 12	Approved on 15 November 2010
EUR-RAD-PTB-1006	Reference air kerma rate	Well-type chamber ionization chamber	Ir-192 reference field	1,0E-04	1,0E-01	Gy h^{-1}	air kerma free in air	DIN 6800/2 2008	2,0	AA-6200-022	6.2	11, 12	Approved on 15 November 2010
EUR-RAD-PTB-1007	Reference air kerma rate	Co-60 HDR-source	Transfer chamber calibrated with primary cavity chamber	1,0E-04	1,0E-01	Gy h^{-1}	air kerma free in air	DIN 6800/2 2008	1,5	AA-6200-022	6.2	11, 12	Approved on 15 November 2010
EUR-RAD-PTB-1008	Reference air kerma rate	Well-type chamber ionization chamber	Co-60 reference field	1,0E-04	1,0E-01	Gy h^{-1}	air kerma free in air	DIN 6800/2 2008	1,7	AA-6200-022	6.2	11, 12	Approved on 15 November 2010
EUR-RAD-PTB-1009	Reference air kerma rate	I-125	Calibration using primary standard extrapolation chamber	1,0E-06	1,0E-04	Gy h^{-1}	air kerma free in air	AAPM TG43	1,8	AA-6200-025	6.2	11, 12	Approved on 15 November 2010
EUR-RAD-PTB-1010	Reference air kerma rate	Well-type chamber	I-125 reference field	1,0E-06	1,0E-04	Gy h^{-1}	air kerma free in air	AAPM TG43	2,0	AA-6200-025	6.2	11, 12	Approved on 15 November 2010

PTB: Grossvolumen Extrapolationskammer (GROVEX)

Electrode separation	50 mm	100 mm	150 mm	200 mm
Correction factor	1.0000	1.0001	1.0002	1.0003

Cause of the uncertainty	$u \times 100$	Degree of freedom	Index
Ionization current measurement (reproducibility)	0.5	100	32.6%
Electrode separation	0.06	50	0.4%
Air density and humidity	0.05	50	0.3%
Electrode area	0.5	50	33.0%
Source-to-measurement point distance	0.035	∞	0.2%
Incomplete ion collection	0.03	∞	0.1%
Attenuation in the Al-filter	0.5	∞	27.8%
Attenuation in the entrance window	0.12	∞	1.7%
Attenuation and scatter between source and entrance window	0.12	∞	1.7%
Attenuation and scatter in the chamber volume	0.12	∞	1.7%
Source holder	0.06	∞	0.4%
Combined uncertainty ($k = 1$)	0.9		
Uncertainty U ($k = 2$)	1.8		

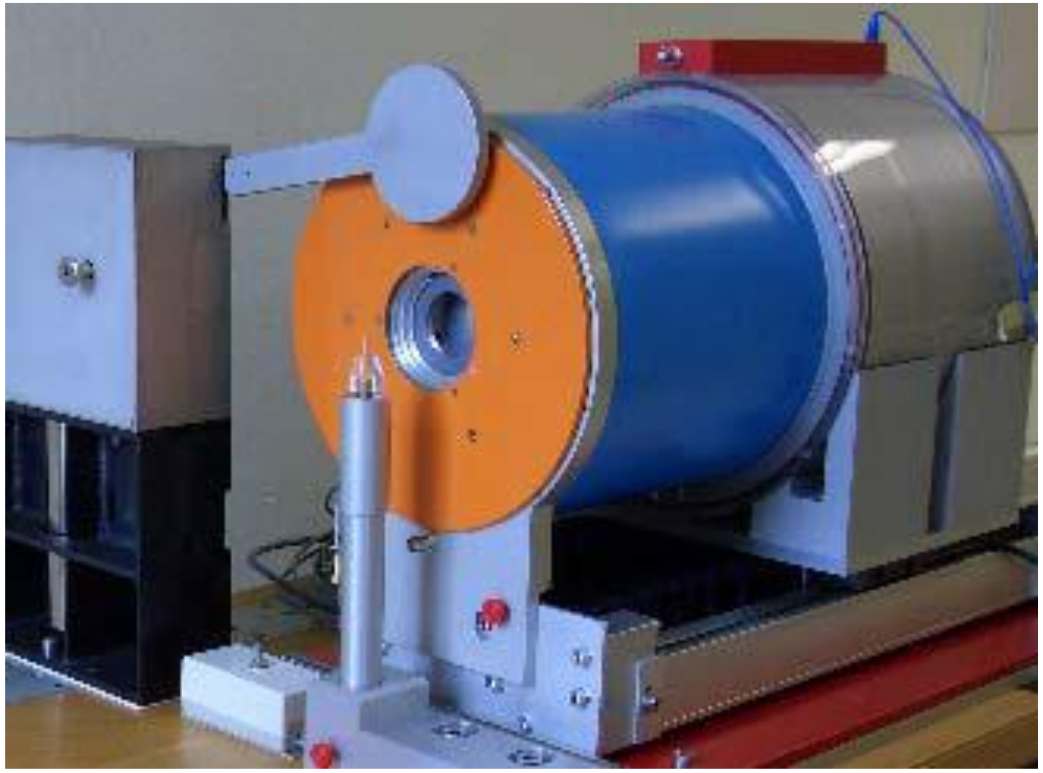

Seed	PTB GROVEX $\mu Gy\,h^{-1}$	UW VAFAC $\mu Gy\,h^{-1}$	NIST WAFAC $\mu Gy\,h^{-1}$	GROVEX / VAFAC	GROVEX / WAFAC
^{103}Pd No 1	26.307	26.389	26.4	0.997	0.997
^{103}Pd No 2	26.327	26.380	26.44	0.998	0.996
^{103}Pd No 3	27.973	26.951	26.90	1.001	1.003
^{125}I No 1	17.288	17.138	17.16	1.009	1.007
^{125}I No 2	12.191	12.226	12.25	0.997	0.995
^{125}I No 3	17.093	17.053	17.18	1.002	0.995

Selbach, et al., *Metrologia* 45, 422-428 (2008)

ESTRO School

PTB: GROVEX II (Low-E Sources)

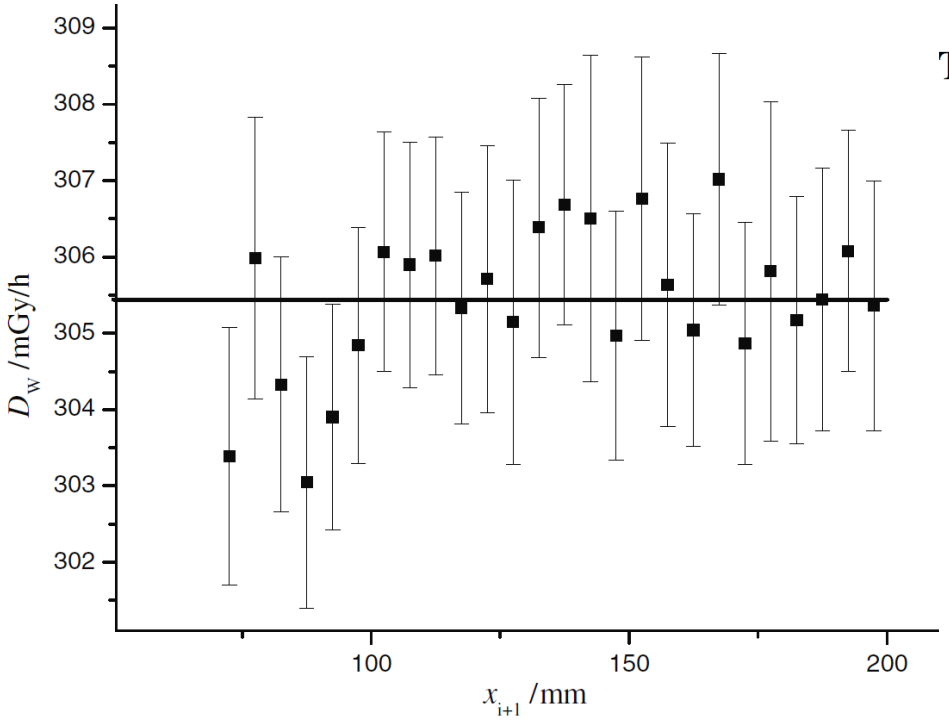

Figure 4. Results of a single extrapolation chamber measurement of an I-125 seed (BEBIG Symmetra I25.S16).

Table 2. Uncertainty budget of the absorbed-dose-rate to water $\dot{D}_w$.

Quantity	$(\Delta U/U) \times 100$	Index $\times$ 100
r	0.2	6.7
k_{div}	0.1	8.3
A	0.5	14.7
k_{inv}	0.4	9.5
SYS_{EXP}	0.9	47.6
$STAT_{EXP}$	0.3	12.1
k_{hold}	0.1	0.2
k_{sat}	0.1	0.8
Total	1.3	$k = 1$

With a value of 1.3%, the total uncertainty is well below the targeted value of 2%.

As the next step, the measuring device will be optimized for routine measurements so that a calibration service can be started in the near future.

Schneider, et al., *Metrologia* 49, S198-S202 (2012)

ESTRO School

UK: National Physical Laboratory

NPL

HDR and LDR brachytherapy

Calibration Service for ^{192}Ir High Dose Rate (HDR) Brachytherapy Dosemeters

NPL's ^{192}Ir HDR brachytherapy calibration service is for ionisation chambers used as secondary standards or instruments required for measurement of the greatest accuracy. Calibration of either an ionisation chamber alone or of a complete system including an electrometer is available.

Well chambers

Service Features

- Calibration directly against the NPL air kerma primary standard
- Reference air kerma rate (RAKR) of the ^{192}Ir source up to 50 mGy/h

Specification and Availability

- Calibration of well-type (re-entrant) chambers suitable for HDR sources
- Calibration of thimble chambers with customer provided calibration jig
- Electrometer calibration (charge or current calibration)
- Calibrations are normally carried out in spring, and are undertaken using a microSelectron ^{192}Ir HDR source
- Calibration conforms to IPEM Code of Practice (2010)

Thimble chamber calibration jig

For more information, please contact Thorsten Sander or our Radiation Dosimetry Team

Calibration Service for Low Dose Rate (LDR) Brachytherapy Sources

NPL's LDR brachytherapy service includes the calibration of ^{125}I seeds and ^{192}Ir wires and pins. The sources are calibrated with the Fidelis secondary standard radionuclide calibrator.

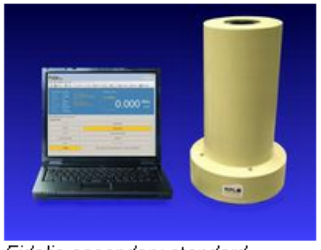

Fidelis secondary standard radionuclide calibrator

Service Features

- Source calibration traceable to the NPL air kerma primary standard

Specification and availability

- Source calibrations in terms of µGy/h at 1 m or MBq
- Calibration of ^{125}I seeds and ^{192}Ir wires and pins, including ^{125}I seeds (e.g. IMC 6711 OncoSeed™, IMC 7000 RAPIDStrand™)and ^{192}Ir wires and pins (e.g. Amersham ICW-series)
- Calibrations of other source types/configurations possible
- Calibrations are available by arrangement throughout the year

ESTRO School

NPL: HDR ^{192}Ir Graphite Calorimetry

Table 2. Uncertainty budget of the HDR brachytherapy calorimeter for quasi-adiabatic absorbed dose rate measurements.

Quantity	Relative standard uncertainties 100 × Type A	100 × Type B
Repeatability of dT_0/dt measurements	0.60	—
Thermistor calibration	—	0.10
Heat transfer correction factor, $k_{ht,q-a}$	—	0.50
Specific heat capacity of core, c_p	—	0.50
Radial source position	—	0.10
Vertical source position	—	0.10
Transient time	—	0.05
MC calculated perturbation correction factors	0.10	0.10
Graphite-to-water conversion	—	0.35
Quadratic summation	0.61	0.82
Combined relative standard uncertainty in $\dot{D}_{w,1\,cm}$	1.02	

Table 3. Uncertainty budget of the HDR brachytherapy calorimeter for quasi-isothermal absorbed dose rate measurements.

Quantity	Relative standard uncertainties 100 × Type A	100 × Type B
Repeatability of ΔP_0^{elec} measurements	0.20	—
Stability of power supplies	—	0.05
Heat transfer correction factor, $k_{ht,q-i}$	—	0.50
Mass of core, m_0	—	0.10
Radial source position	—	0.10
Vertical source position	—	0.10
MC calculated perturbation correction factors	0.10	0.10
Graphite-to-water conversion	—	0.35
Quadratic summation	0.22	0.64
Combined relative standard uncertainty in $\dot{D}_{w,1\,cm}$	0.68	

$$\dot{D}_{w,1\,cm} = -\frac{\Delta P_0^{elec}}{m_0} k_{ht,q-i} k_{gr/w} k_{volavg} k_{imp} k_{gap} k_{inh} k_{fullscat}$$

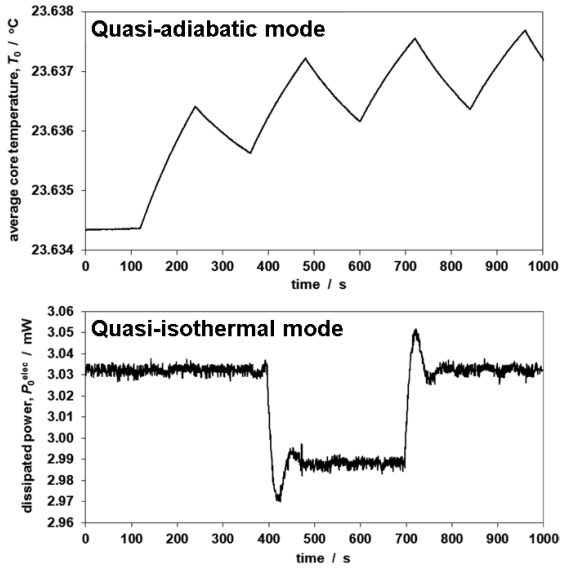

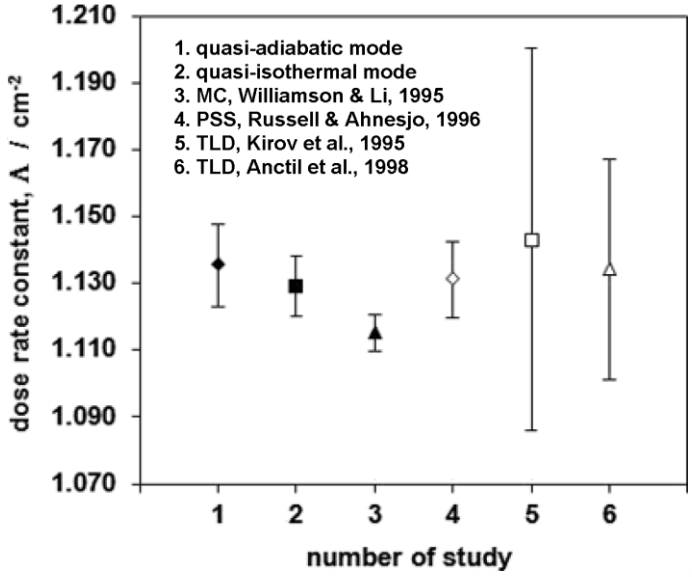

Sander, et al., *Metrologia* 49, S184-S188 (2012)

ESTRO School

Italy (ENEA-INMRI): HDR ^{192}Ir Graphite Calorimetry

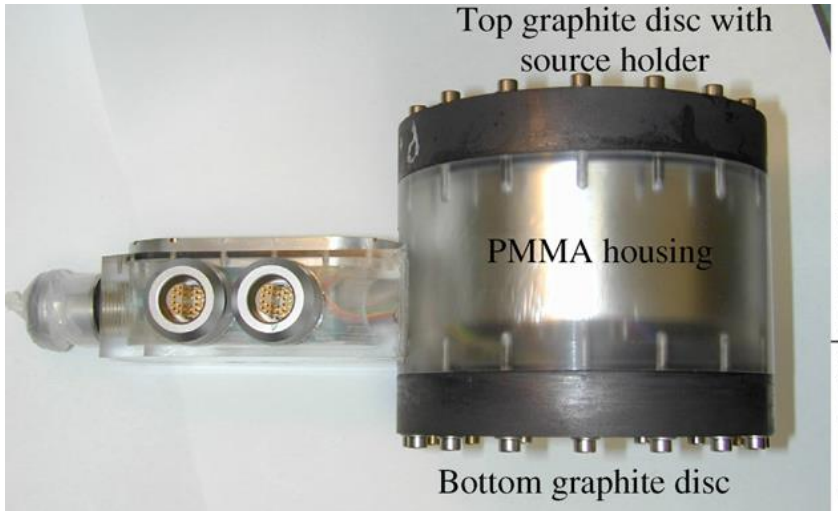

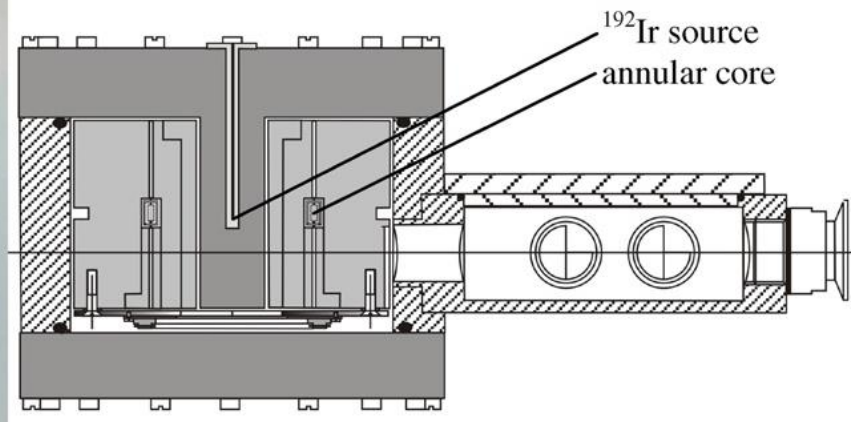

$$\dot{D}_{\mathrm{w,1\,cm}} = \frac{f_{\mathrm{c}} k_{\mathrm{qa}} k_{\mathrm{gap}} k_{\mathrm{fs}} k_{\mathrm{vol\,avg}} k_{\mathrm{gw}} k_{\mathrm{sh}}}{m}$$

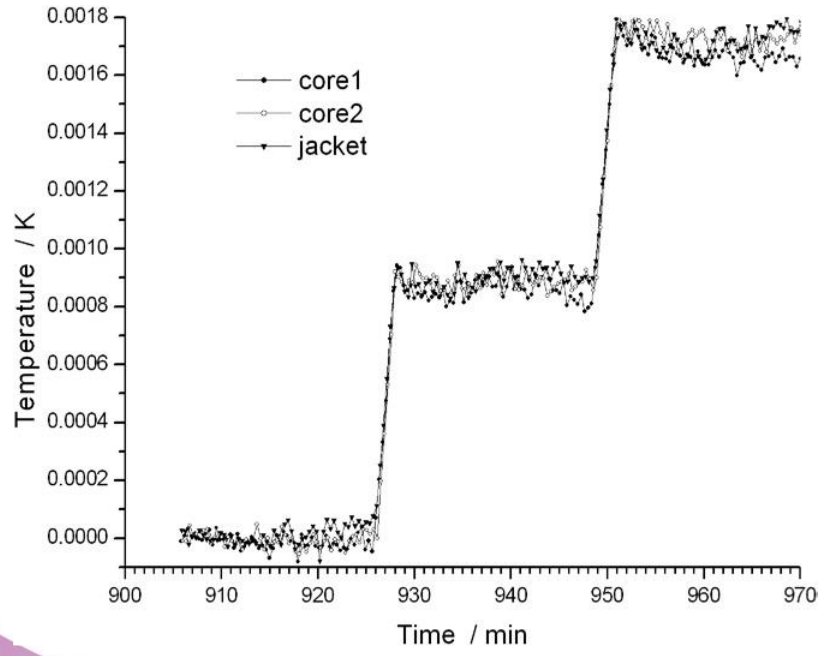

Table 1. Relative standard uncertainty for the determination of D_{w}.

Quantity	Value	Relative standard uncertainty $100\,s_i$	Relative standard uncertainty $100\,u_j$
$-f_{\mathrm{c}}/(\Delta\Omega/\Omega)\ \mathrm{s}^{-1}$	1.073×10^{-6}	1.11	0.10
$-k_{\mathrm{qa}}/(\mathrm{J}/(\Delta\Omega/\Omega))$	52.09	0.59	0.15
$-k_{\mathrm{gap}}$	0.998	0.14	0.15
$-k_{\mathrm{fs}}$	1.020	0.20	0.15
$-k_{\mathrm{vol\,avg}}$	1.004	0.15	0.15
$-k_{\mathrm{gw}}$	6.890	0.12	0.15
$-k_{\mathrm{sh}}$	0.997	—	0.10
$-m/\mathrm{g}$	2.767	—	0.15
Measurement time /s	120	—	0.2
Source positioning		—	0.18
Quadratic summation		1.30	0.48
Combined relative standard uncertainty of $\dot{D}_{\mathrm{w}}$ (1.418×10^{-1} Gy s^{-1})		1.38	

Guerra, et al., *Metrologia* 49, S179-S183 (2012)

ESTRO School

France: LNE–LNHB HDR ^{192}Ir Calibration

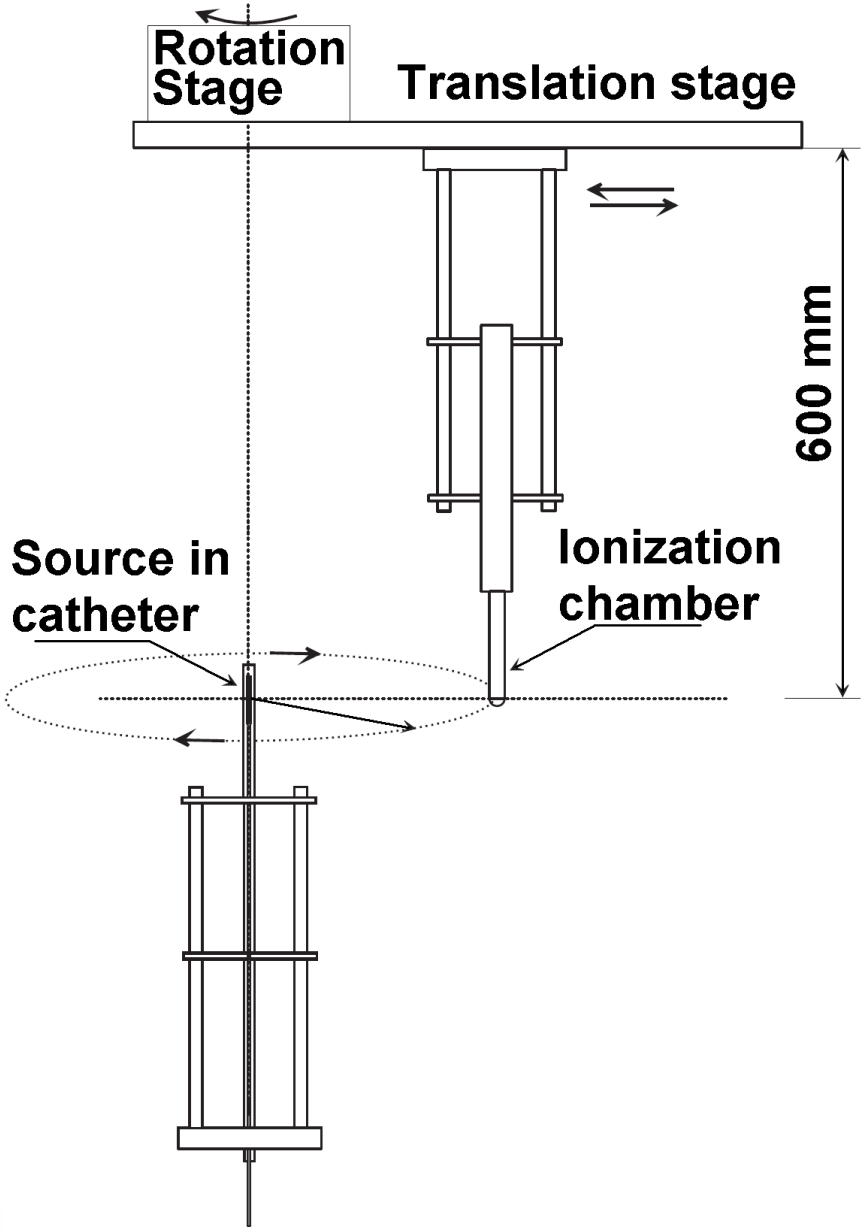

Uncertainty budget for a typical routine well-type chamber calibration (LNHB).	Value	Relative standard uncertainty (%) Type A	Type B
$\dot{K}_R(0)$(Gy h^{-1} (1 m))	3.239×10^{-2}	–	0.60
I (A)	3.1441×10^{-8}	<0.01	0.20
k_{dec}	1.07790	–	<0.01
k_{rec}	1.0005	<0.01	0.03
Combined standard uncertainty		0.63	
Expanded uncertainty ($k = 2$)		1.3	

Ionization chamber	UWADCL	LNHB	Discrepancy (%)
Nucletron 077.091 (S/N 25324)	9.421×10^5	9.432×10^5	−0.12
Standard Imaging HDR1000+ (S/N A002231)	4.652×10^5	4.665×10^5	−0.28
Standard Imaging HDR1000+ (S/N A032012)	4.659×10^5	4.669×10^5	−0.22

Douysset, et al. *Phys Med Biol* 50, 1961-1978 (2005)

ESTRO School

LNE–LNHB: ^{125}I Air-Kerma and Absorbed Dose to Water

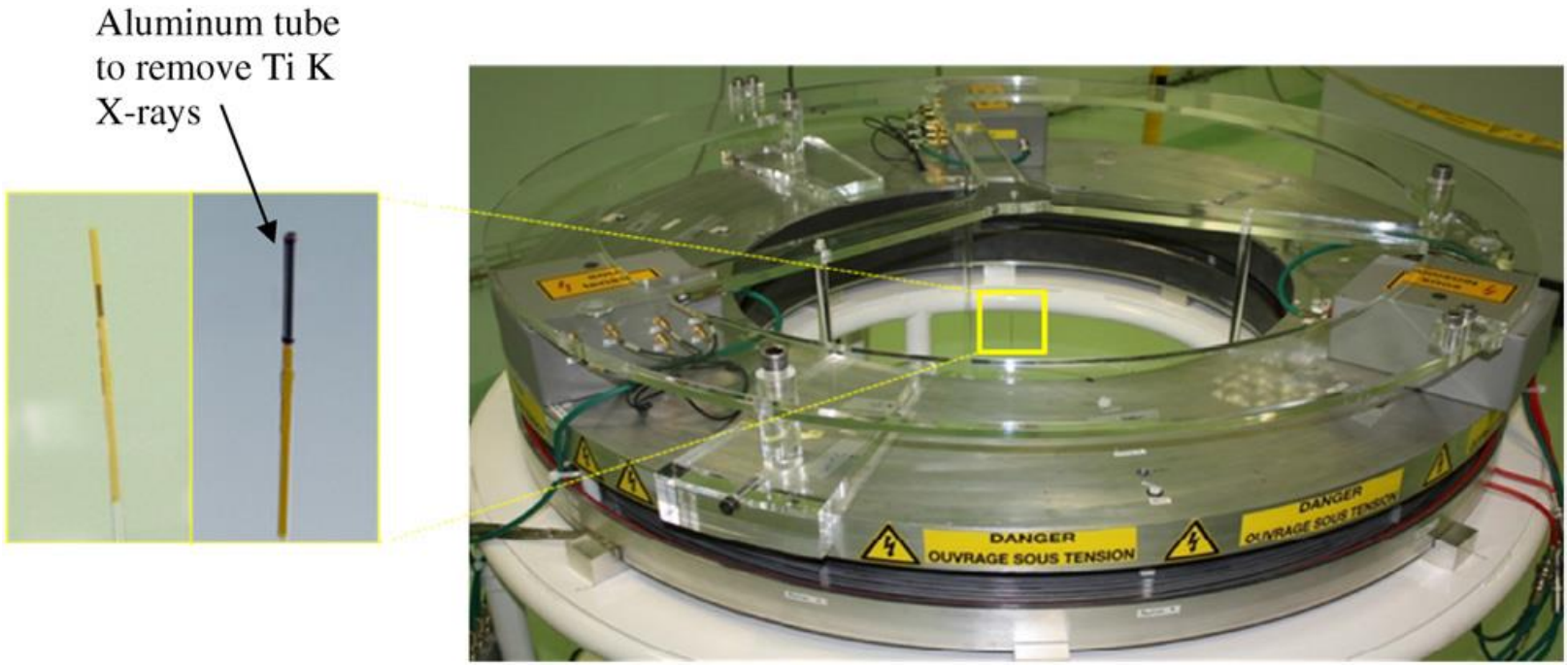

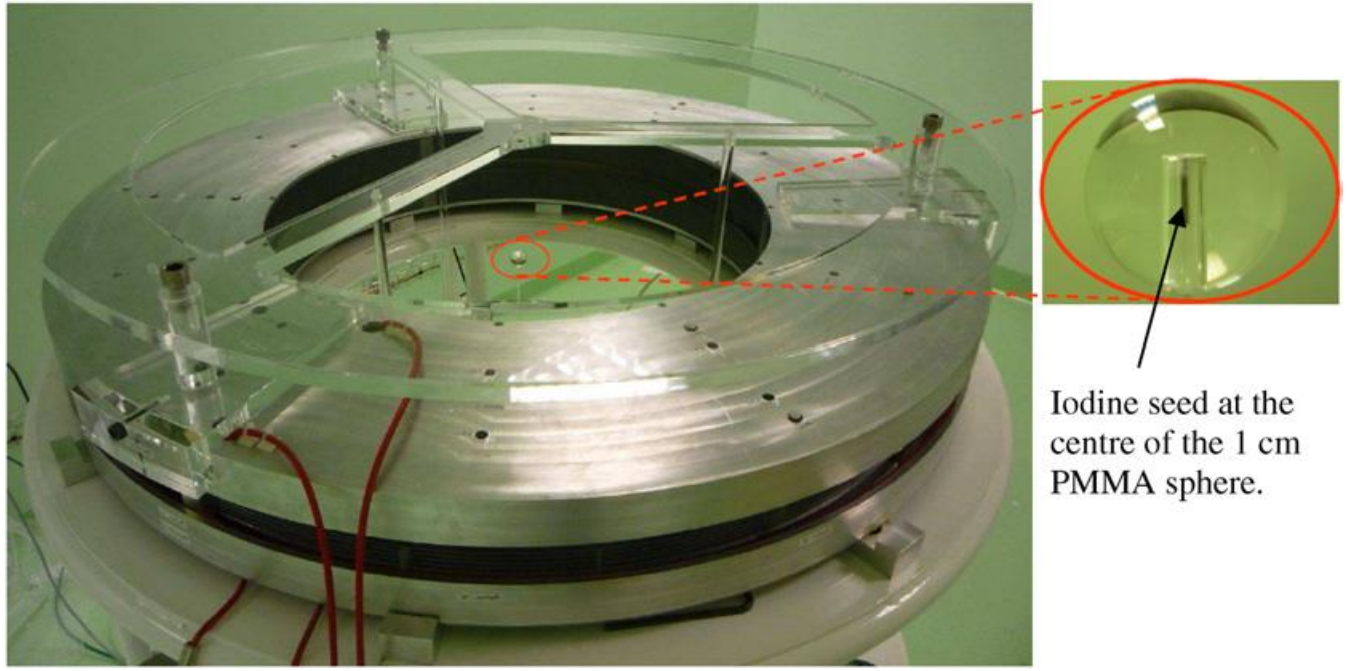

Aubineau-Lanièce, et al. *Metrologia* 49, S189-S192 (2012)

ESTRO School

Sweden: HDR ^{192}Ir Calibration Audit

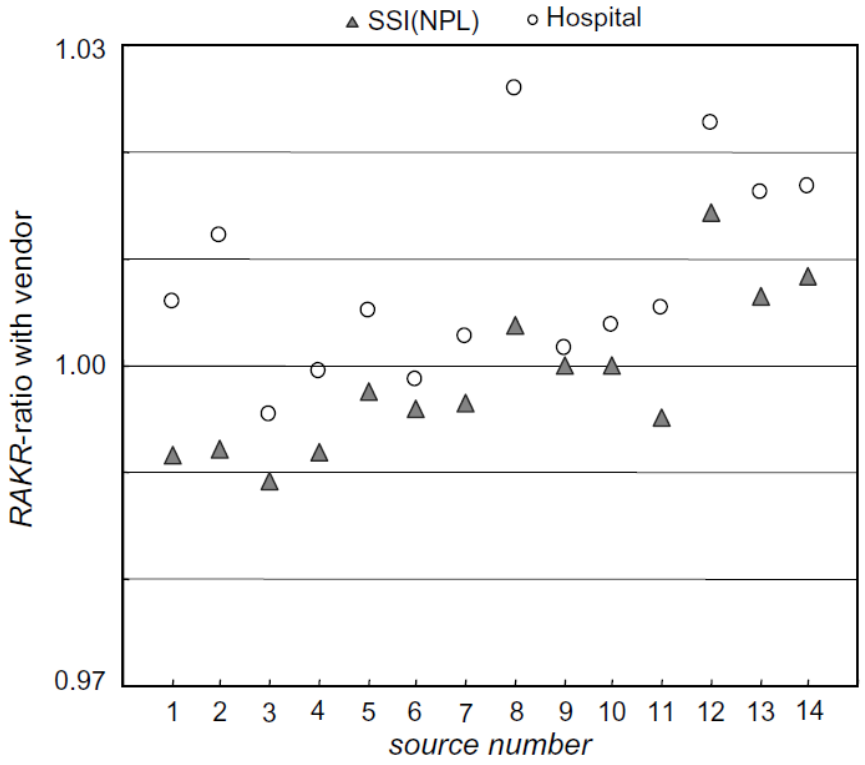

Fig. 4. Ratios of SSI- and hospital-determined *RAKR* values, respectively, to the corresponding values on vendor certificates.

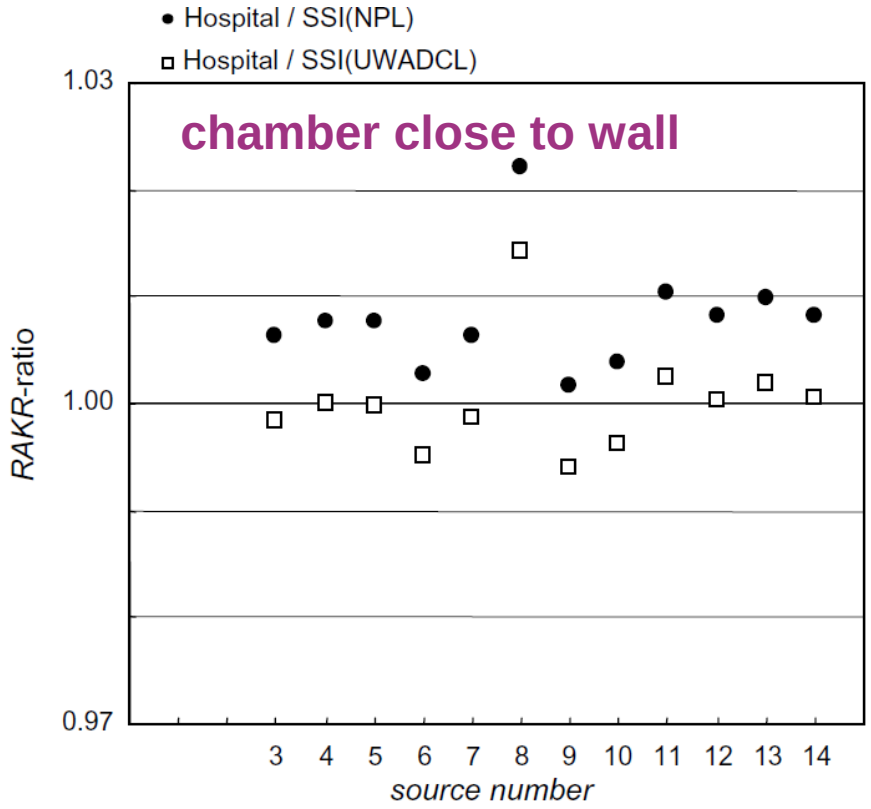

Fig. 5. Comparing ratios of the *RAKR* determined by the hospitals to those determined by SSI using either the NPL- or the UWADCL-calibration factor.

The well-type chamber of the Swedish Secondary Standard Laboratory is traceable to the HDR ^{192}Ir primary standard at NPL, and all Swedish hospitals use well-type chambers fulfilling recommendations for use in brachytherapy.

Carlsson Tedgren and Grindborg, *Radiotherapy Oncol* 86, 126-130 (2008)

ESTRO School

IAEA TECHDOC 1274

Calibration of photon and beta ray sources used in brachytherapy

Guidelines on standardized procedures at Secondary Standards Dosimetry Laboratories (SSDLs) and hospitals

INTERNATIONAL ATOMIC ENERGY AGENCY

IAEA

March 2002

ESTRO School

Chapter 5: Calibration at the SSDL and Hospital Level

5.1. Establishment of standards for photon and intravascular sources

5.1.1. Traceability in calibrations at SSDLs

The recommended detector is an appropriately calibrated well type chamber. The preferred traceability method is to have the well type chamber calibrated against the primary standard at the PSDL. Calibrations at an ADCL or the IAEA Dosimetry Laboratory can serve as an alternative. This calibration should be carried out for each radionuclide and source type to be used.

5.1.2. Traceability in calibrations at hospitals

It is recommended that for brachytherapy sources be calibrated with an appropriately calibrated well type chamber. For traceability, the well type chamber should be calibrated at the SSDL (or ADCL).

Chapter 5: Calibration at the SSDL and Hospital Level

5.2. Maintenance of standards for photon sources and intravascular sources

Well type chambers should be recalibrated regularly. SSDL recalibrations at ^{137}Cs quality can be made at a PSDL or the IAEA Dosimetry Laboratory.

5.3. Maintenance of standards for ^{192}Ir quality

Upon calibrating well type chambers every 2 years with HDR ^{192}Ir sources, some chamber types have shown calibration factor constancy to within 0.5%, and chamber-to-chamber variation of the ratio of HDR ^{192}Ir source calibration to ^{137}Cs and ^{60}Co also within 0.5%. Thus, a practical solution for checking a well chamber HDR ^{192}Ir source calibration factor is for the physicist to monitor chamber response throughout its lifetime by bracketing the ^{192}Ir average energy of 397 keV with ^{137}Cs and ^{241}Am sources.

Chapter 5: Calibration at the SSDL and Hospital Level

5.5. Guidance on constancy limits for well type chambers

Chamber output stability should be checked at least 4 times per year. If the calibration factor from ^{137}Cs re-calibrations, and periodic constancy checks, remain the same within 1% for high-energy photon sources, or within 1.5% for low-energy photon sources, it can reasonably be assumed that the calibration factor for other sources has not changed. Recalibration is recommended if it is observed that response changes by more than the limits given above.

5.6. Electrometer to be used

IEC 60731 describes desired characteristics of electrometers. They also shall be capable of measuring up to 0.2 μA for HDR sources and have a signal resolution of 0.1%. For LDR sources, signal resolution should be $\leq$ 10 fA or less; this may be achieved by charge resolution of 0.2 pC when used in charge integration mode. It may be necessary to have two electrometers to cover the full range of brachytherapy sources to be calibrated.

Chapter 6: Calibration Using Free In-air Measurements

6.1. General

The free in-air measurement technique cannot be used for low-energy sources due to air-kerma calibration factor uncertainties, low air-kerma rates, and uncertainties due to air humidity. For long-lived radionuclides, e.g., ^{137}Cs, a source can be a working standard.

$$K_R = N_K \cdot (M_u/t) \cdot k_{air} \cdot k_{scatt} \cdot k_n \, (d/d_{ref})^2$$

6.2. Formalism for reference air kerma rate

- K_R reference air kerma rate
- N_K chamber air kerma calibration factor at desired photon energy
- M_U measured charge, corrected for T, P, recombination, transit error
- t time for collecting charge
- k_{scat} correction for room scatter
- k_n correction factor for non-uniform electron fluence within the cavity
- d measurement distance from source center to chamber center
- d_{ref} reference measurement distance (i.e., 1 meter)

Chapter 6: Calibration Using Free In-air Measurements

6.3. Ionization chambers to be used

For HDR sources, chambers volumes > 0.5 cm^3 can be used (e.g. Baldwin-Farmer 0.6 cm^3 chamber). For LDR sources, chamber volumes up to 1,000 cm^3 may be used for sufficient signal, but have large non-uniformity correction factor uncertainties. For ^{192}Ir, chambers should have air-kerma calibration factors vary less than 5% between ^{60}Co and 60 keV.

6.4. Air kerma calibration of ionization chambers

6.5. Correction factors for free in-air measurements

6.6. Uncertainty of free in-air calibration

etc., etc.

Chapter 7: Calibrations Using Well Type Chambers

7.1. General guidance

7.2. Calibration of SSDL reference sources

7.3. Calibration of hospital's well type chamber

The hospital's well chamber system is calibrated at the SSDL using the SSDL reference source. The response curve, spacer and insert, ion recombination, atmospheric communication, and air kerma calibration are checked.

7.4. Calibration of hospital's non-standard ^{137}Cs sources

7.5. Guidance for some special cases

7.6. Calibration of source trains

7.7. Traceability of ^{137}Cs source calibrations

etc., etc.

2004 ESTRO Booklet 8

EUROPEAN SOCIETY FOR THERAPEUTIC RADIOLOGY AND ONCOLOGY

A PRACTICAL GUIDE TO QUALITY CONTROL OF BRACHYTHERAPY EQUIPMENT

ESTRO

Edited by
Jack Venselaar
José Pérez-Calatayud

Supported by the EU
"Europe against Cancer" Programme
Grant Agreements N°SPC.2002480 / S12.322029

A PRACTICAL GUIDE TO QUALITY CONTROL OF BRACHYTHERAPY EQUIPMENT

ESTRO School

Chapter 3: Calibration of Brachytherapy Sources

3.3 In-air measurement technique

3.4 Calibration using well type chambers

3.5 Calibration using solid phantoms

Measurements in solid phantoms are not suitable for low-energy sources.

3.6 Relative measurements

Readings of consecutive source deliveries can be compared and deviations larger than 3% or 5% should be investigated. Serious incidents may be identified before treatment.

Chapter 9.2 on TPS Commissioning

9.2.6 *Influence of shields, missing tissue, and inhomogeneities* (abridged)

Presently, only simple correction algorithms are applied in some TPS. The effect of these algorithms must be verified and documented. **yes**

Published shielding or tissue inhomogeneity data are based on MC. **yes**

Validation of these MC data should be done by comparing with measured data, such as those obtained using TLD or small ionisation chambers. **ouch!**

Algorithms are under development to account for scatter conditions and tissue inhomogeneities. **yes**

Validation of these algorithms should be done in a similar way to the method used for checking the shielding algorithms. **ouch!**

Comparison of RAKR Measurement Methods

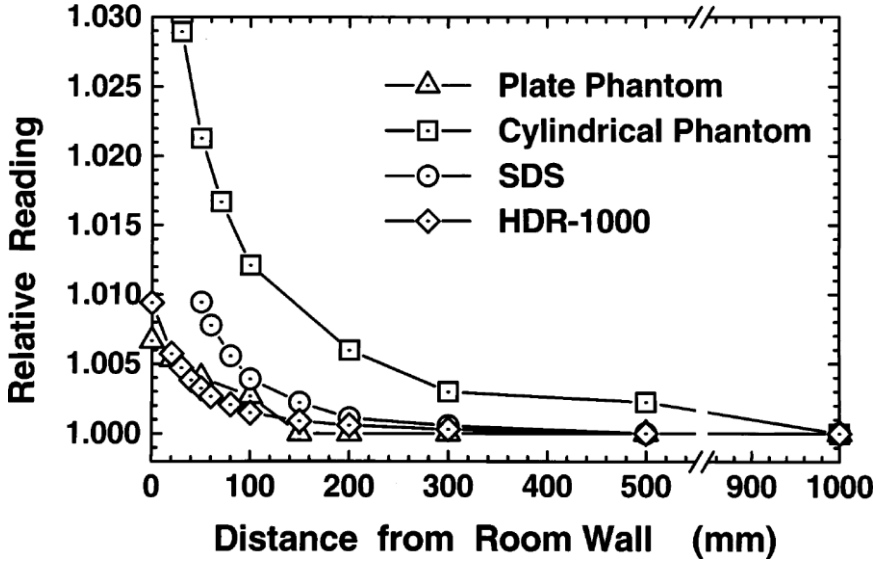

Calibration system	Reference air kerma rate mGy·h^{-1} at 1m	Deviation from PTB
PTB	19.52	0.0%
HDR-1000	19.57	+0.3%
SDS	19.60	+0.4%
Cylindrical phantom	19.56	+0.2%

Adequate measurement precision (within 0.5%) using well chambers and Farmer chambers in-air or in-plastic phantoms.

Baltas, et al., *Intl J Radiat Oncol, Biol, Phys* 43, 653-661 (1999)

ESTRO School

UK IPEM Code of Practice for HDR ^{192}Ir RAKR

$$\dot{K}_R = I_{raw} \cdot f_{elec} \cdot k_{dec} \cdot k_{Tp} \cdot k_{ion} \cdot k_{sg} \cdot N_{\dot{K}_R}$$

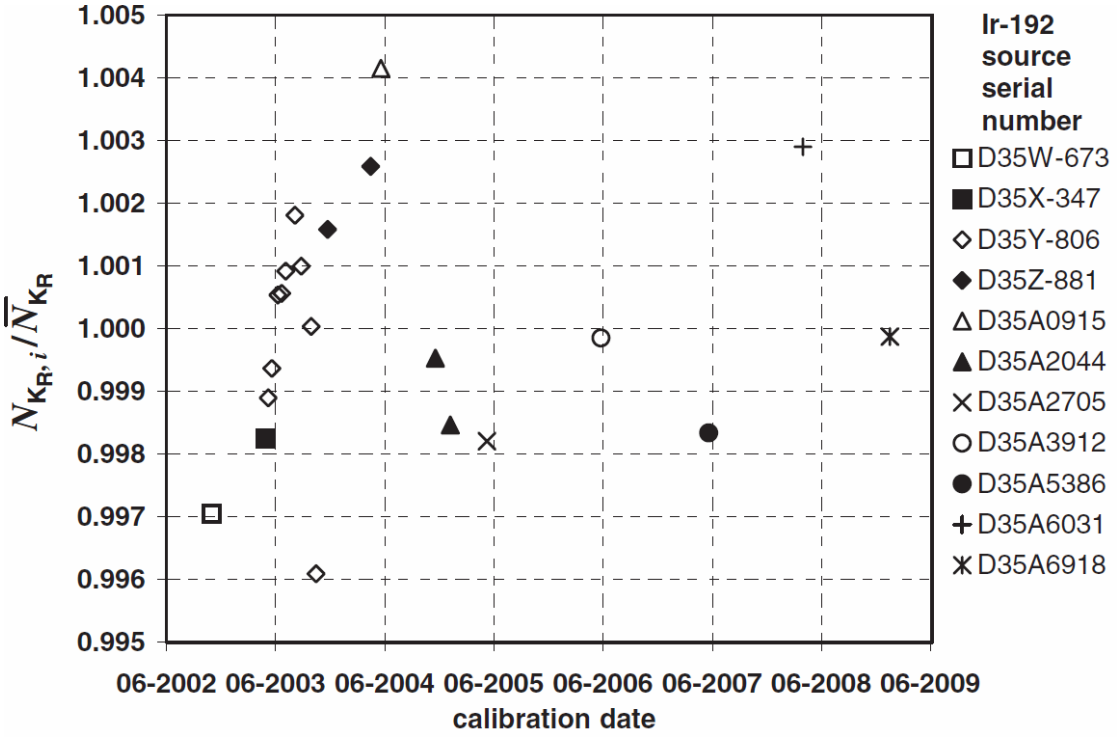

Figure 1. The graph shows the calibration history of a Standard Imaging 1000 Plus well chamber over 7 years. Calibrations were carried out with 11 different Nucletron microSelectron-v1 (classic) HDR ^{192}Ir brachytherapy sources. The maximum variation of all calibration coefficients, $N_{K_R,i}$, determined between 2002 and 2009 was found to be ±0.4% of the running mean, $\bar{N}_{K_R}$.

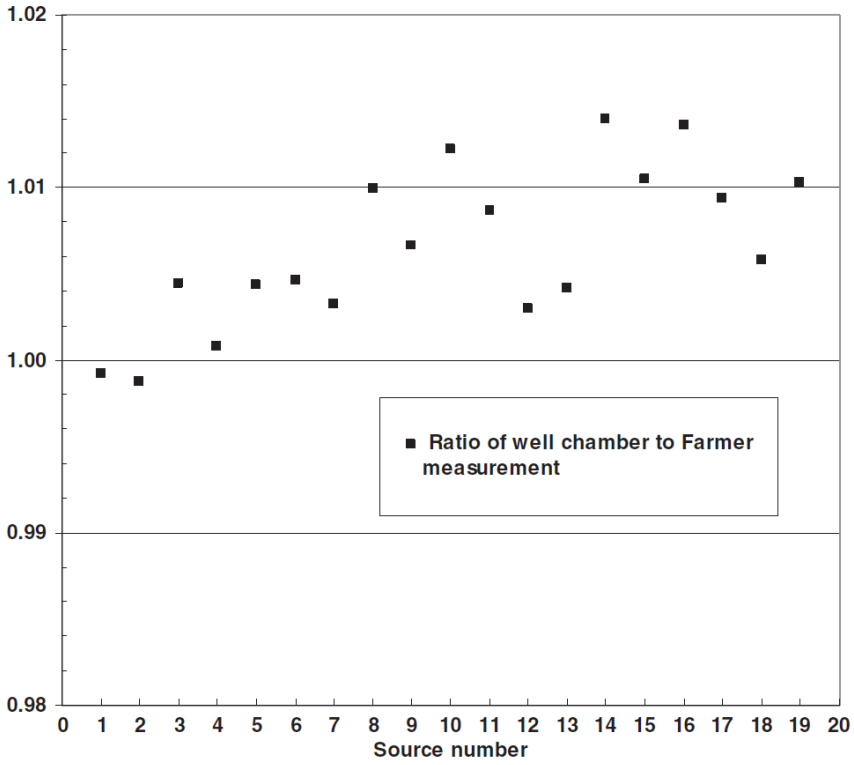

Figure B1. Reference air kerma rate (RAKR) comparison between a Standard Imaging 1000 Plus well chamber, calibrated using the new COP, and a Farmer chamber, calibrated at 280 kVp according to the old 1992 BIR/IPSM recommendations.

This COP aims to eliminate systematic differences between users, and reduce uncertainties by recommending the well chamber method of source calibration over the previously recommended (Aird *et al*., 1993) Farmer method.

Bidmead, et al., *Phys Med Biol* 55, 3145-3159 (2010)

ESTRO School

Implementation of UK IPEM Code of Practice

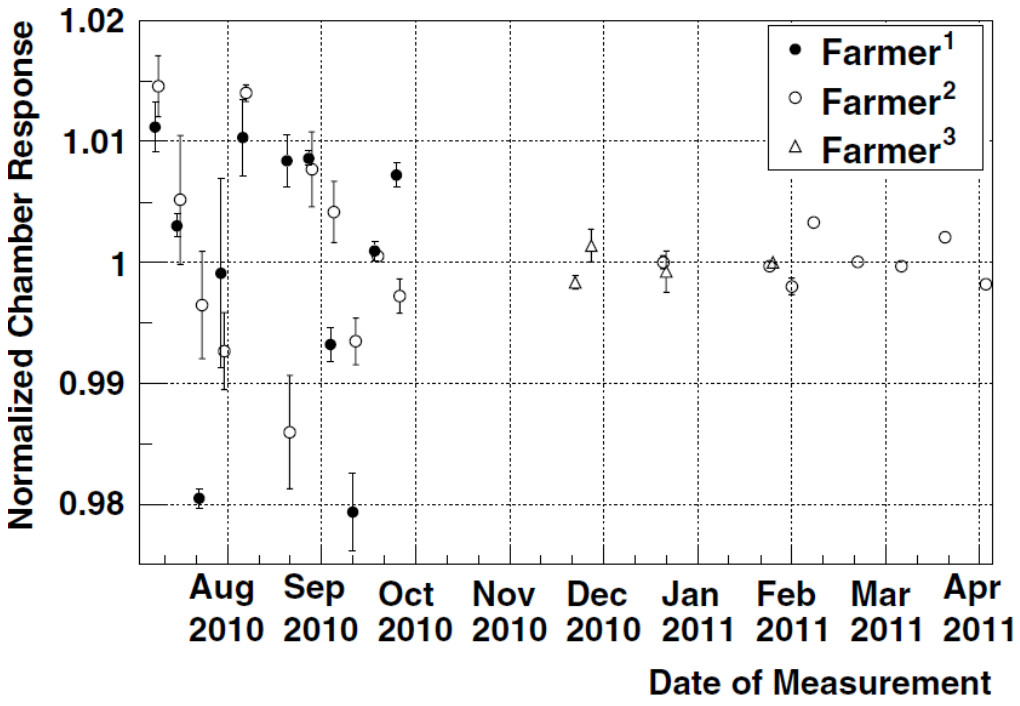

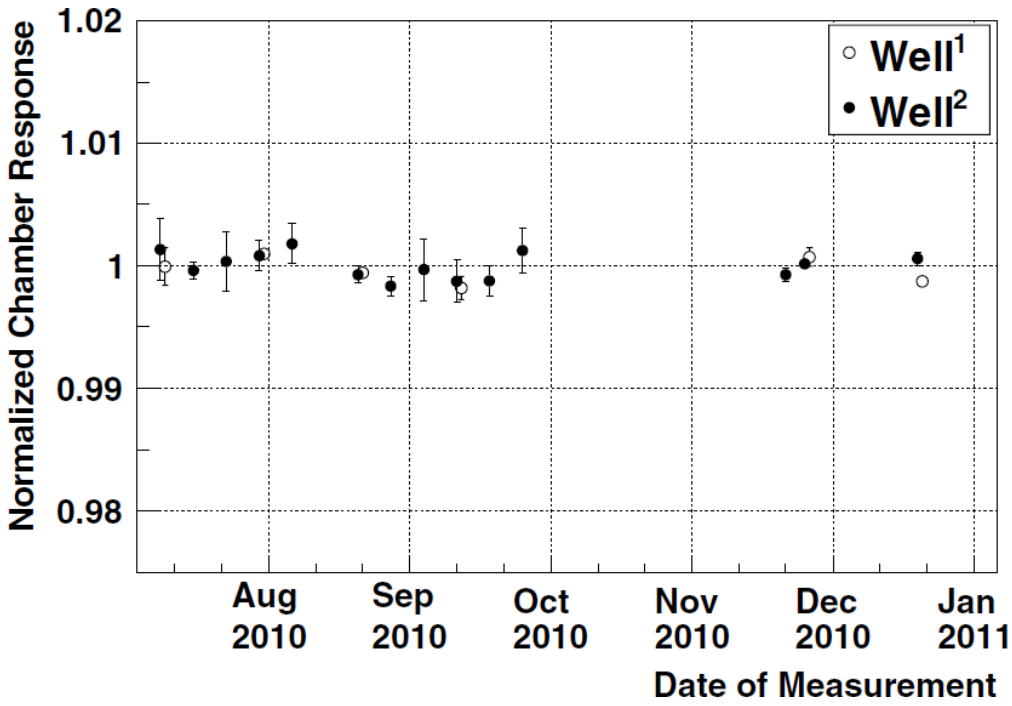

Improved measurement precision using well chambers instead of Farmer chambers.

Awunor, et al., *Phys Med Biol* 56, 5397-5410 (2011)

ESTRO School

Custom Room-Scatter Correction Factors

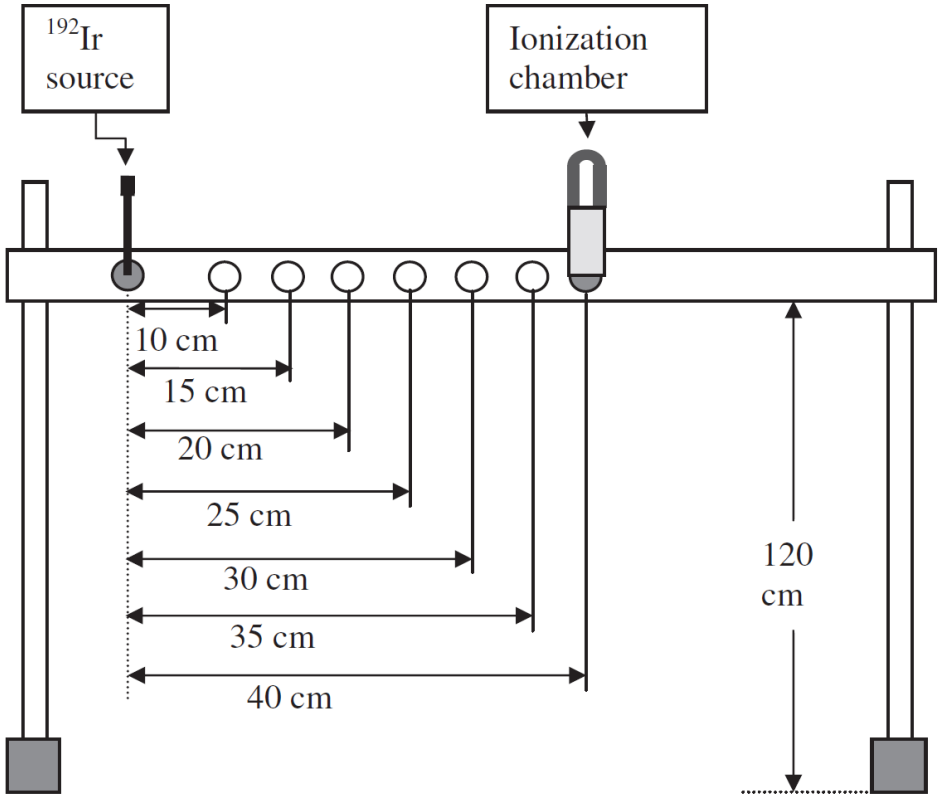

Fig. 1. Schematic cross-sectional view of the experimental arrangement used to measure the signal of the ionization chamber at seven different distances.

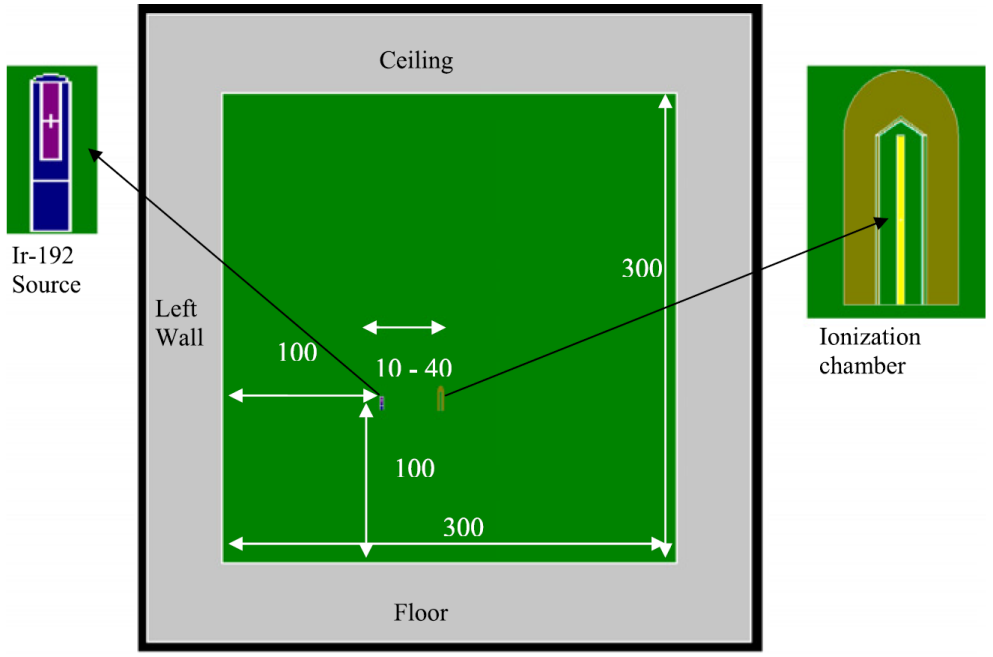

Fig. 2. MCNP Plot of the cross-sectional view of the problem geometry showing locations of the ^{192}Ir source and ionization chamber (all dimensions are in cm).

Monte Carlo calculations of K_{SC} (for *f* calculation) produced better agreement to analytical calculations than to Selvam et al. (2001).

Kumar, et al., *Appl Radiat Isot* 70, 282-289 (2012)

ESTRO School

RAKR for LDR ^{137}Cs

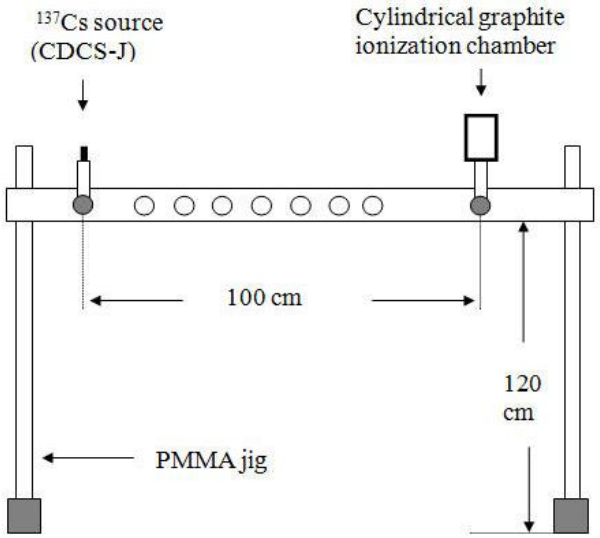

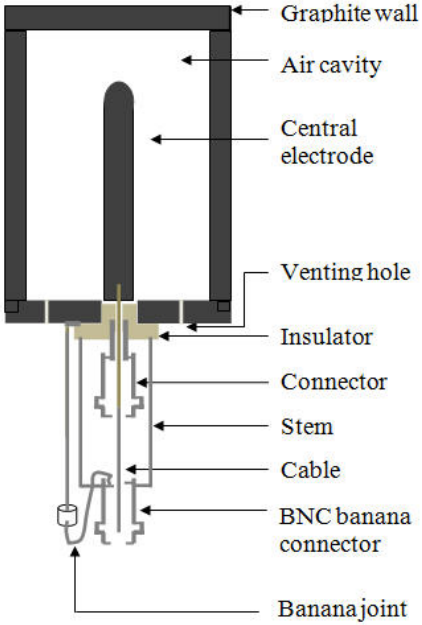

TABLE 3. Uncertainty in experimental determination of air kerma calibration coefficient (N_K) of the cylindrical graphite ionization chamber.

Uncertainty Components	*Relative Standard Uncertainty (%)* *Type A*	*Type B*
Charge collection reproducibility	0.1	
Electrometer calibration		0.2
Leakage (Chamber +electrometer)		0.05
Temperature pressure correction factor (ktp)	0.2	
Timer accuracy	0.1	
Positional accuracy and reproducibility	0.2	
Room scatter correction factor (ksc)	0.12	
Ion recombination correction factor (krecom)		0.04
Nonuniformity correction factor (kn)		0.4
Air attenuation correction factor (katt)		0.1
RAKR of the 137Cs source		1.0
Combined standard uncertainty (k = 1)	1.15 %	
Expanded uncertainty (k = 2)	2.3 %	

Good agreement (1.07%) between measured and MC-simulated N_K values.

Sharma, et al., *J Appl Clin Med Phys* 12, 275-285 (2011)

ESTRO School

US RAKR Standard for HDR ^{192}Ir

TABLE VI. HDR 1000 Plus inverse well chamber calibration coefficient Monte Carlo simulation summary.

Source model	pA/U (MCNP5)	Percent difference from existing classic Nucletron standard (%)
Classic Nucletron	2.074	—
Nucletron microSelectron V2	2.080	0.29
GammaMed	2.075	0.08
VariSource VS2000	2.114	1.79
Flexisource	2.084	0.48
Average	2.085	N/A

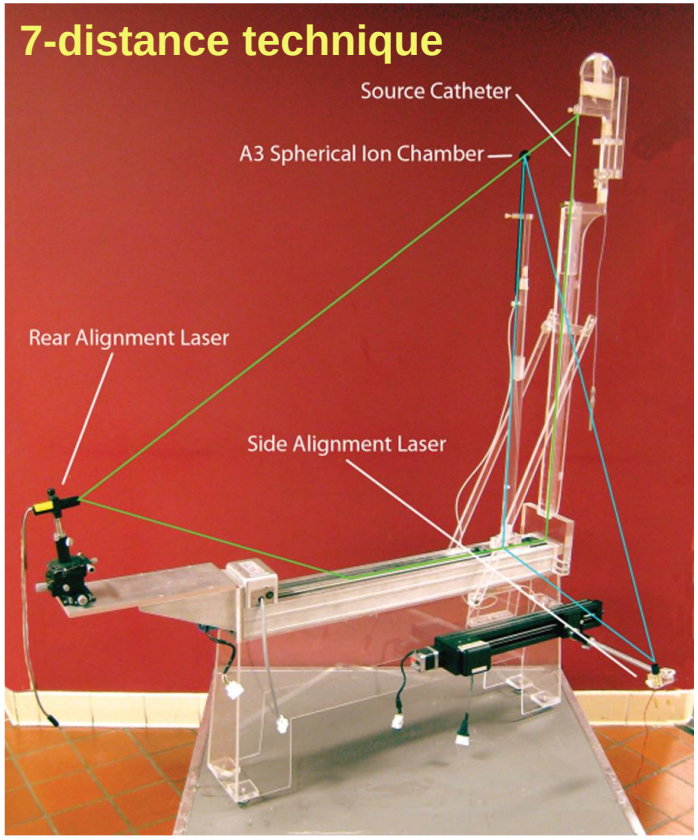

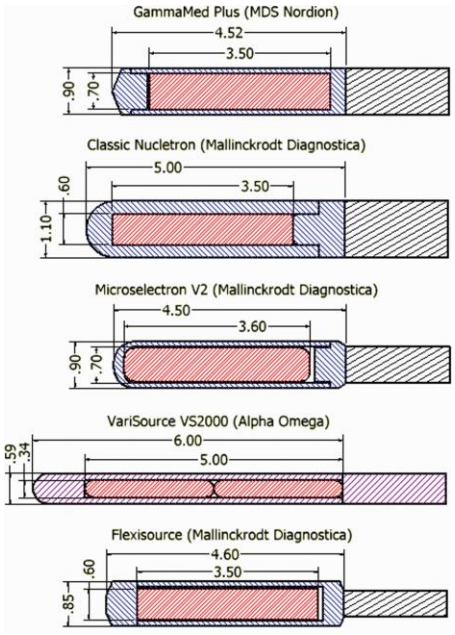

TABLE VIII. Uncertainty analysis for transfer from standard well chamber to customer well chamber. Analysis was performed using the guidelines of NIST Technical Note 1297.

Parameter	Type A (%)	Type B (%)
Exradin A3 CHAMBER		
Charge	0.05	0.05
Air density	0	0.02
Ionic recombination	0	0
Beam divergence	0	0.1
Air attenuation/scatter	0	0.04
NIST N_K calibration coefficient	0	0.7
ELECTROMETER		
Electrometer calibration coefficient	0	0.11
Timing error	0	0.005
MEASUREMENT REPRODUCIBILITY		
Independent trial standard deviation	0.43	0
CALCULATION		
Interpolation for N_K	0	0.25
Solution algorithm	0	0.2
Time (half life)	0	0.03
Quadratic sum	0.433	0.812
Seven-distance method uncertainty k = 1		0.920
Source model effects		0.96
Customer chamber k = 1		0.309
Customer electrometer k = 1		0.166
Quadratic sum ADCL calibration k = 1		1.38
Quadratic sum ADCL calibration k = 2		2.75

TABLE VII. International comparison results.

Well chamber model	UWADCL (10^2 Gy/C)	LNHB (10^2 Gy/C)	NPL (10^2 Gy/C)	Ratio UWADCL/LNHB	Ratio UWADCL/NPL
Nucletron 077.091 (S/N 25324)	2.617	2.592	2.584	1.010	1.013
Standard Imaging HDR 1000 Plus (S/N A002231)	1.294	1.285	1.280	1.006	1.010

RAKR agreement across labs within ~ 1%.

Rasmussen, et al., *Med Phys* 38, 6721-6729 (2011)

ESTRO School

Are New HDR ^{192}Ir Calibration Methods Needed?

Austerlitz, et al., Determination of absorbed dose in water at the reference point D(r_0, θ_0) for an ^{192}Ir HDR brachytherapy source using a Fricke system. *Med Phys* 35, 5360-5365 (2008).

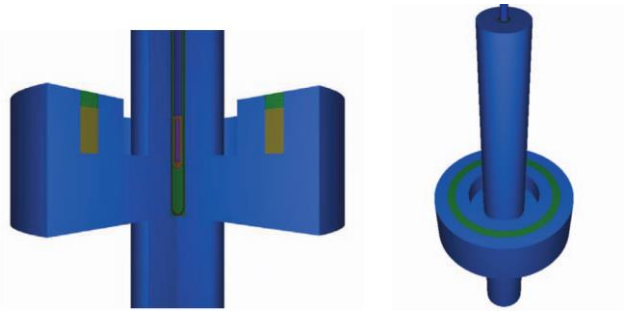

Chang, et al., An innovative method for ^{192}Ir HDR calibration by farmer chamber, V-film, and solid phantom. *NIM-A* 646, 192-196 (2011).

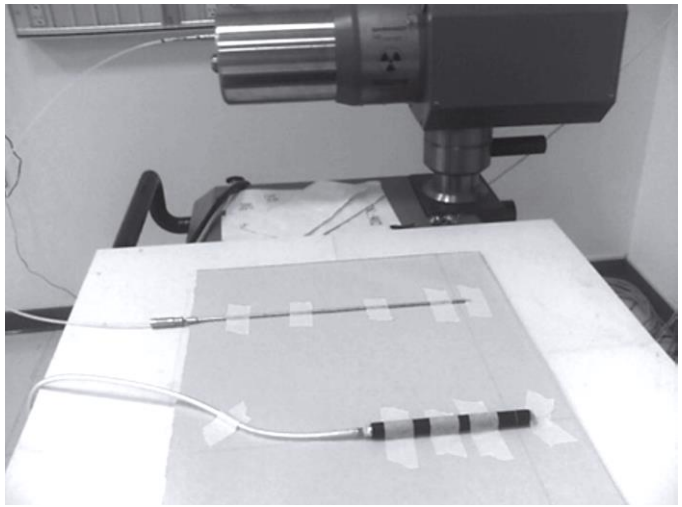

Fourie and Crabtree, A technique for calibrating a high dose rate ^{192}Ir brachytherapy source. *Australas Phys Eng Sci Med* 35, 85-92 (2012).

Kaulich, et al., Direct reference air-kerma rate calibration of ^{192}Ir for a thimble-type ionization chamber in a cylindrical solid phantom. *Metrologia* 49, S241-S245 (2012).

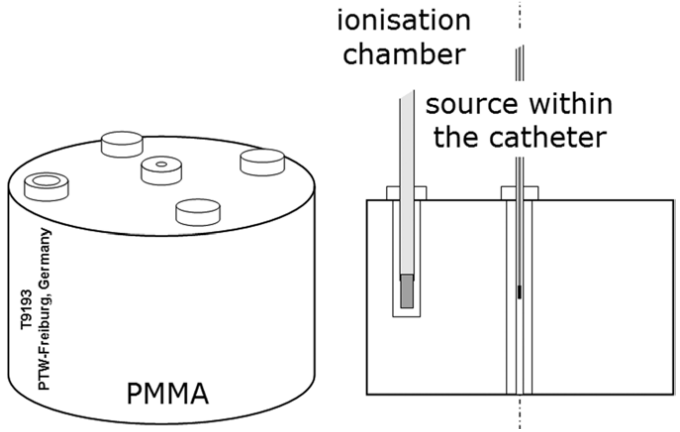

etc., etc.

ESTRO School

Take Home Message

1. Independent assay of RAKR from the manufacturer is required.

2. Calibration methods are established for all brachytherapy sources.

3. Calibration infrastructure (i.e., SSDL availability) is variable.

4. Future improvements forthcoming in calibration methods and infrastructure.

Further Reading

Aird, et al. BIR & IPSM, London, UK, 1993.
Aubineau-Lanièce, et al. Metrologia 2012;49:S189-92.
Awunor, et al. Phys Med Biol 2011;56:5397-410.
Bidmead, et al. Phys Med Biol 2010;55:3145-59.
Butler, et al. Med Phys 2008;35:3860-5.
DeWerd, et al. Med Phys 2011;38:782-801.
Douysett, et al. Phys Med Biol 2005;50:1961-78.
Douysett, et al. Phys Med Biol 2008;53:N85-97.
Goetsch, et al. Med Phys 1991;18:462-67.
Goetsch, et al. Intl J Radiat Oncol, Biol, Phys 1992;24:167-70.
IAEA, TECDOC 1079, IAEA, Vienna, Austria, 1999.
IAEA, TECDOC 1274, IAEA, Vienna, Austria, 2002.
ICRU, ICRU Report 58, Bethesda, MD, 1997.
Kumar et al. Appl Radiat Oncol 2012;70:282-9.
Mainegra-Hing and Rogers, Med Phys 2006;33:3340-7.
Nath, et al. AAPM TG-32, Melville, NY, 1987.
Rasmussen, et al. Med Phys 2008;35:1483-8.
Rasmussen, et al. Med Phys 2011;38:6721-9.
Sander, et al. Metrologia 2012;49:S184-8.
Sarfehnia, et al. Med Phys 2007;34:4957-61.
Schneider. Metrologia 2012;49:S198-202.
Selbach, et al. Metrologia 2008;45:422-8.
Seltzer, et al. J Res NIST 2003;108:337-58.
Soares, et al. Metrologia 2009;46:S80-98.
Stump, et al. Med Phys 2002;29:1483-8.

ESTRO School

ESTRO School

WWW.ESTRO.ORG/SCHOOL

Advanced Brachytherapy Physics

07-10 October 2018 | Valencia, Spain

Experimental dosimetry in brachytherapy

P. Papagiannis, PhD
Medical Physics Laboratory
Medical School
National & Kapodistrian University of Athens

(no conflict of interest to disclose)

Objectives:

After this lecture the attendants should:

- have a clear understanding of:
  - dosimeter selection criteria & brachytherapy dosimetry challenges
- be familiar with:
  - a general terminology introduced to describe dosimeter characteristics
  - a general formalism for absorbed dose measurement
  - the key properties & operational features of utilized dosimeters (mainly TLD and radiochromic Film)
- be informed of:
  - current trends
  - relevant literature
  - sources for further reading

Experimental dosimetry in brachytherapy WHY…?

"theory is an interpolation of experiment"
(J.H. Hubbell in: X-Ray Spectrom. 28(4), 215–223, 1999)

Experimental dosimetry is needed for:

• **establishing source reference dose rate distributions**
(for clinical TG43-based TP)

• **commissioning and QA testing of TPS**
(planned dose is accurate)

• **dose verification in phantom or "in-vivo"**
(planned dose is accurately delivered)

Experimental dosimetry:

Use of a detector (dosimeter) providing a measurable signal
that is of a known relationship with the absorbed dose in its volume

- The relationship between signal and dose is known for absolute dosimeters (calorimeters, ion chambers & Fricke gels)
- All other dosimeters must be **calibrated** relative to an absolute one in a beam quality Q_o, to obtain the **absorbed dose sensitivity**:

$$S_{AD,w}(Q_0) = \frac{M(Q_0)}{D_w(Q_0)}$$

or equivalently the **calibration coefficient**:

$$N_{AD,w}(Q_0) = \frac{D_w(Q_0)}{M(Q_0)}$$

- Dose to a medium in the absence of the detector (water) is of interest
- The calibration must be traceable to international standards

*** The terminology used in this lecture is that introduced in:**

Rogers & Cygler (Eds), Clinical dosimetry measurements in radiotherapy (2009 AAPM Summer School), Monograph No. 34, Medical Physics Publishing 2011

Dosimeter characteristics/requirements :

(1) Sensitivity: must be high enough for low dose rate measurements. If the sensitivity is too high, it may cause rapid saturation at high dose rate

(2) Adequate **dose range** and (preferably) **linearity of the response** as a function of accumulated dose

(3) Insensitivity of response to influence quantities (dose rate, temperature, pressure, directional effect, accumulated dose, etc.): response should be independent, or variation should be known or measurable in order to perform adequate correction

(4) Energy response: preferably independence of response as a function of energy

(5) Repeatability: stability for repeated measurements over a short period of time

& Reproducibility: stability of material, construction, etc. over a long period of time

(6) Accuracy/precision: the derivation of the dose from the dosimeter response must be possible with minimum uncertainty, but the requirements may differ for different applications

Quoted from:

Mayles, Nahum, Rosenwald (Eds): Handbook of radiotherapy physics: theory and practice,

Dose range / linearity / saturation:

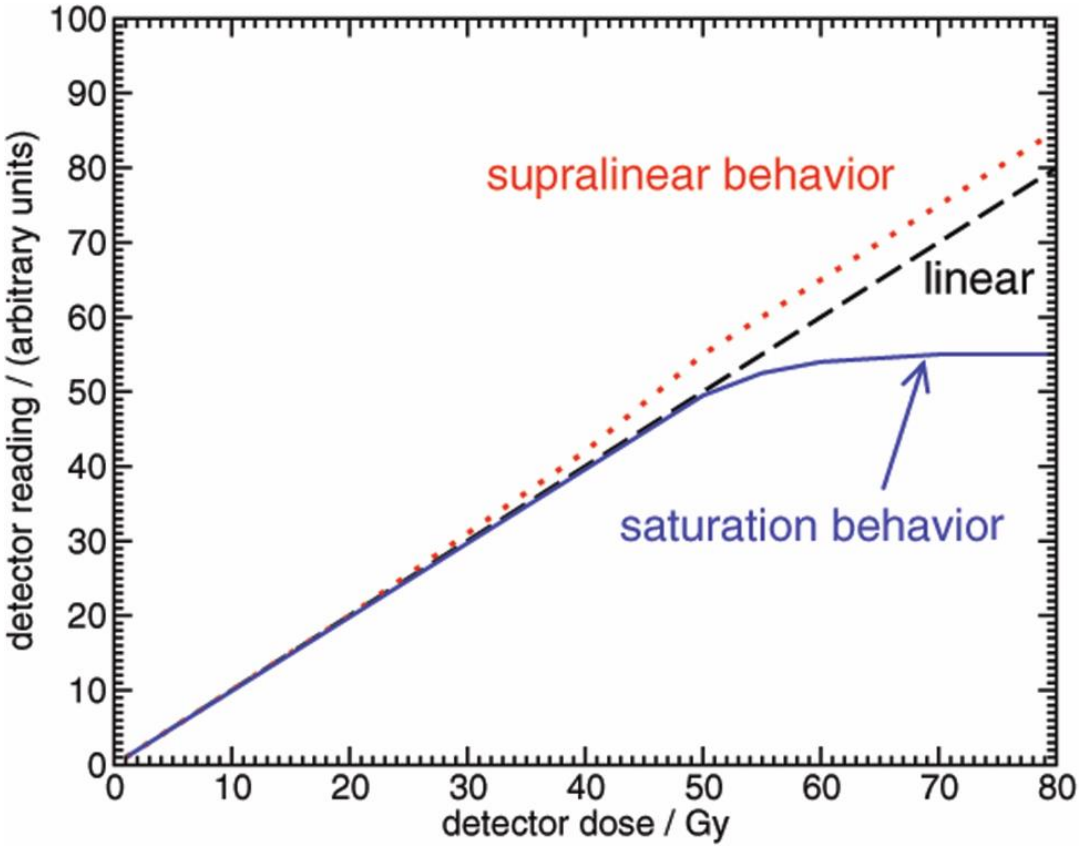

$$D_{\mathrm{det}}(D) = k_l(M(D))\ \alpha\ M(D)$$

where: k_l is the **intrinsic linearity** (normalized to 1 @ some D_o) and α relates D_o to $M(D_o)$

- Detector response is linear if k_l is 1 for any D, M(D)
- !!!This is not always the case!!!

Figure from:

Rogers & Cygler (Eds), Clinical dosimetry measurements in radiotherapy (2009 AAPM Summer School), Monograph No. 34, Medical Physics Publishing 2011

Influence quantities:

A series of correction factors must be applied (if appropriate) to correct the dosimeter reading for any measurement condition affecting it

In example:

•environmental conditions

•background correction:

$$k_{bkgd} = (1 - \frac{M_{bkgd}}{M})$$

•dose rate dependence:

$$M'(\dot{D}) = k_{dr}(M(\dot{D}))M(\dot{D})$$

Sensitivity, calibration & energy response:

Our calibration coeff. (inverse of dosimeter A.D. sensitivity)

actually comprises 2 parts:

$$N_{AD,w}(Q) = \frac{D_w(Q)}{M(Q)} = \frac{D_w(Q)}{D_{\mathrm{det}}(Q)} \frac{D_{\mathrm{det}}(Q)}{M(Q)} = f(Q) k_{bq}(Q)$$

- we define the **absorbed dose energy dependence** of the detector as the ratio of dose to water per unit dose to the detector at a given beam quality,

$$f(Q) = \frac{D_w(Q)}{D_{\mathrm{det}}(Q)}$$

- We define the **intrinsic energy dependence** of the detector as the ratio of dose required to be absorbed to produce a unit signal

$$k_{bq}(Q) = \frac{D_{\mathrm{det}}(Q)}{M(Q)}$$

Sensitivity, calibration & energy response:

Our calibration coeff. (inverse of dosimeter A.D. sensitivity)

actually comprises 2 parts:

$$N_{AD,w}(Q) = \frac{D_w(Q)}{M(Q)} = \frac{D_w(Q)}{D_{\mathrm{det}}(Q)} \frac{D_{\mathrm{det}}(Q)}{M(Q)} = f(Q) k_{bq}(Q)$$

- we define the **absorbed dose energy dependence** of the detector as the ratio of dose to water per unit dose to the detector at a given beam quality,

$$f(Q) = \frac{D_w(Q)}{D_{\mathrm{det}}(Q)}$$

This depends on physical properties and radiation quality (cross sections) and detector geometry. It can be calculated via MC!

- We define the **intrinsic energy dependence** of the detector as the ratio of dose required to be absorbed to produce a unit signal

$$k_{bq}(Q) = \frac{D_{\mathrm{det}}(Q)}{M(Q)}$$

This depends mainly on the physical process underlying the conversion of dose to the measured signal (and hence LET). It can only be measured!

Practical significance of f(Q), $k_{bq}(Q)$

- Using a detector at the same quality as calibration (Q_o) is straightforward:

$$D_w(Q_0) = M(Q_0) * \prod_i (corr.factor)_i N_{AD,w}(Q_0)$$

- Using a detector at a quality Q different than calibration (Q_o):

$$D_w(Q) = M(Q_0) * \prod_i (corr.factor)_i N_{AD,w}(Q_0) \frac{N_{AD,w}(Q)}{N_{AD,w}(Q_0)} =$$

$$= M(Q_0) * \prod_i (corr.factor)_i N_{AD,w}(Q_0) \frac{f(Q)}{f(Q_0)} \frac{k_{bq}(Q)}{k_{bq}(Q_0)} =$$

$$= M(Q_0) * \prod_i (corr.factor)_i N_{AD,w}(Q_0) f^{rel}(Q,Q_0) k_{bq}^{rel}(Q,Q_0)$$

f^{rel}, k_{bq}^{rel} cannot be generally assumed energy independent

f^{rel} must be calculated

k_{bq}^{rel} must be measured

or taken from the literature for **matching** exp. conditions (Q, Q_o, detector make, size, set up, …)

f^{rel} or k^{rel} >1 => detector under-responds …!

f^{rel} or k^{rel} <1 => detector over-responds …!

Dosimeter characteristics/requirements :

(1) Sensitivity: must be high enough for low dose rate measurements. If the sensitivity is too high, it may cause rapid saturation at high dose rate

(2) Adequate **dose range** and (preferably) **linearity of the response** as a function of accumulated dose

(3) Insensitivity of response to influence quantities (dose rate, temperature, pressure, directional effect, accumulated dose, etc.): response should be independent, or variation should be known or measurable in order to perform adequate correction

(4) Energy response: preferably independence of response as a function of energy

(5) Repeatability: stability for repeated measurements over a short period of time

& Reproducibility: stability of material, construction, etc. over a long period of time

(6) Accuracy/precision: the derivation of the dose from the dosimeter response must be possible with minimum uncertainty, but the requirements may differ for different applications

Quoted from:

Mayles, Nahum, Rosenwald (Eds): Handbook of radiotherapy physics: theory and practice,

Brachy dosimetry is challenging …

$\dot{D}(y,z)/S_K$ for an Ir-192 HDR source

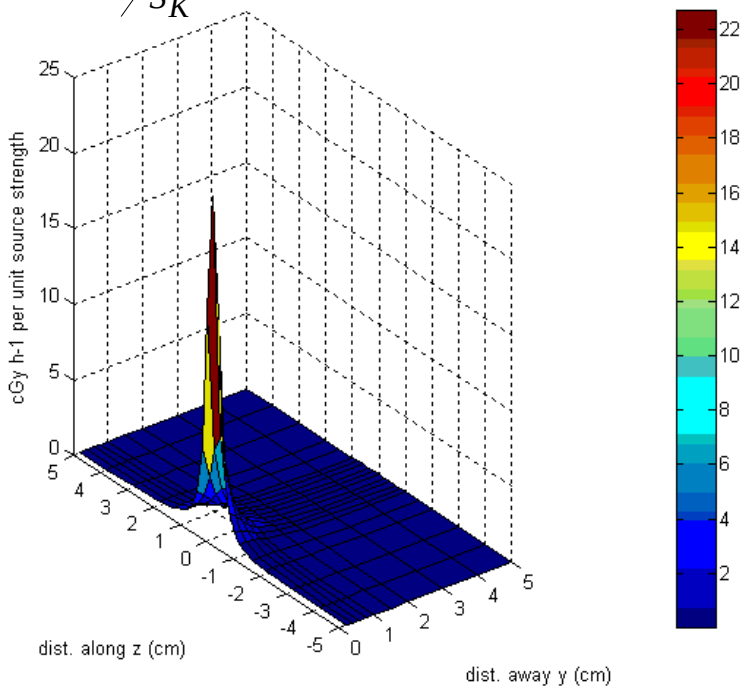

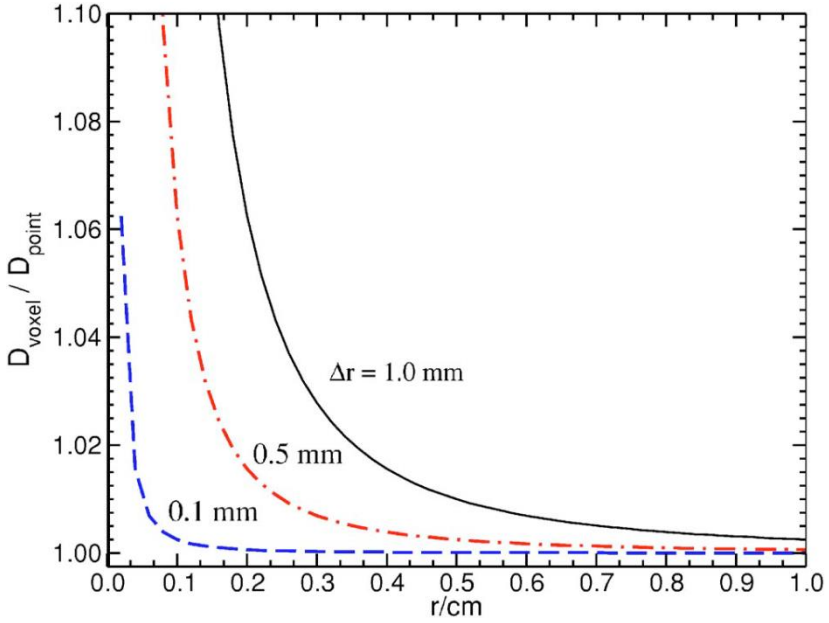

Figure from: Taylor, Yegin, Rogers, Med. Phys. 34(2) 445 (2007)

Dose rate varies from ~20 Gy/s @ (0.5cm,90°) from an Ir-192 HDR source to ~2 μGy/s @ (5cm,90°) from an I-125 LDR source

Sensitivity high for low uncertainty, dose range high, (preferably) with $k_l=k_{dr}=1$

Spatial dose gradient is high (i.e. ~25%/mm in the radial direction @ (0.5cm,90°) from an Ir-192 HDR source)

Volume must be small, positional accuracy is very important

(1% rel. uncert. in D(1cm,90°) requires 0.05mm uncertainty in r, assuming $1/r^2$ dose dependence since: $\frac{\sigma_D}{D} = 2\frac{\sigma_r}{r}$)

If solid phantoms are used to increase positional accuracy a correction is required from $D_{w,phant}$ to $D_{w,w}$ at each meas. position

Brachytherapy Q is source/position dependent…

photon fluence vs distance per starting particle emitted from a point 125I (top) and 192Ir (bottom) source centered in a 15cm radius water phantom, multiplied by distance squared

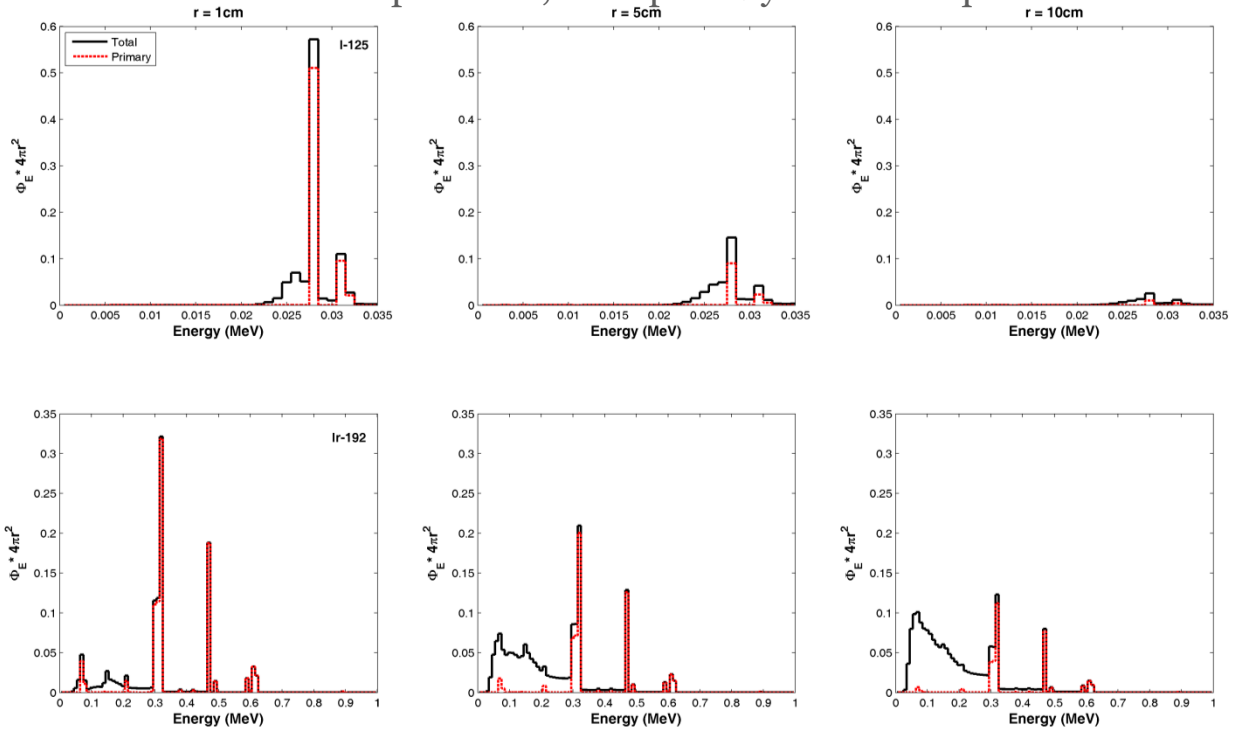

Figure from: Papagiannis, Pantelis, Karaiskos, Br J Radiol (2014) 87: 20140163

f^{rel}, k_{bq}^{rel} may be considerable (especially for low E)

BUT

- They are source dependent (source materials)
- and position dependent (source spectra vary with distance, angle)

especially for high Z detectors

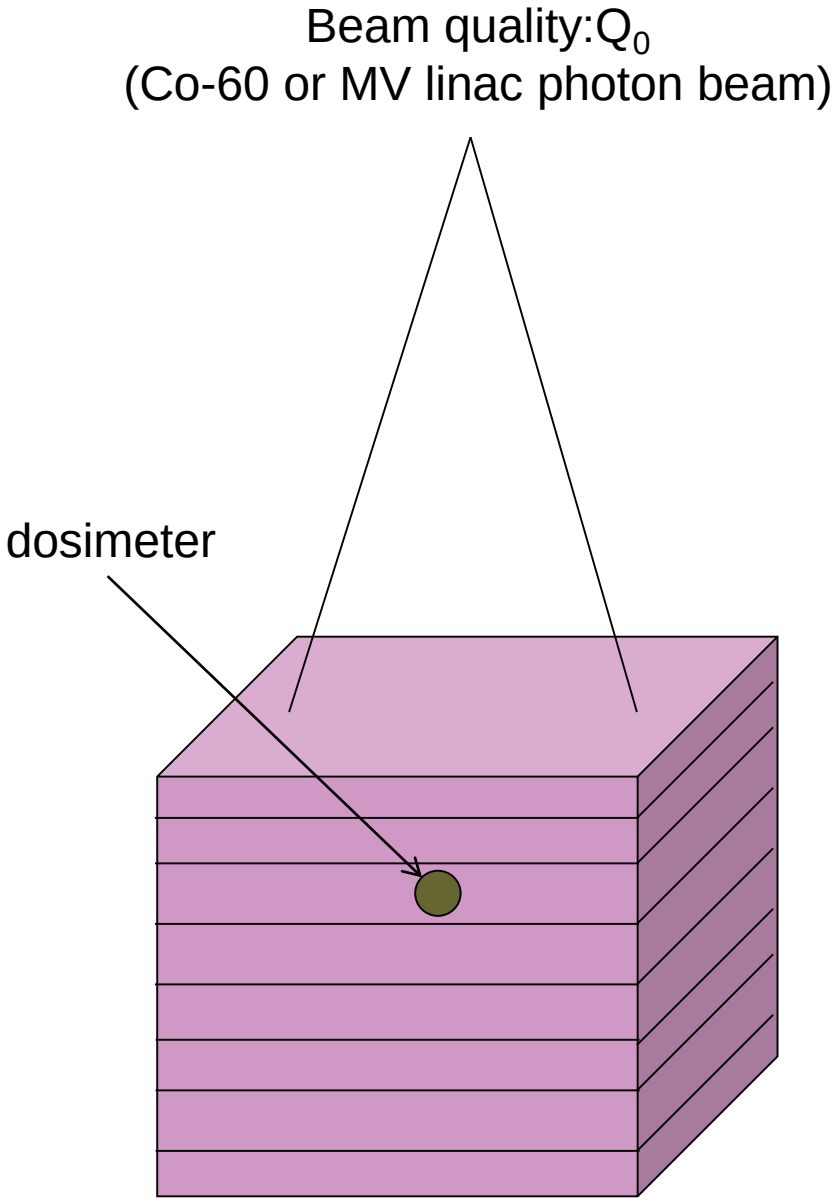

Calibration:

!!! Calibration uncertainty will be propagated as a type B unc. component to experimental results **!!!**

Absorbed dose sensitivity calibration

$$S_{AD,w}(Q_0) = \frac{M(Q_0)}{D_w(Q_0)} = \frac{1}{N_{AD,w}(Q_0)}$$

is usually performed using a Linac

where:

$M(Q_o)$ is the dosimeter reading

$D_w(Q_o)$ is dose to water at the point of measurement in the absence of the detector obtained using an established reference dosimetry protocol (e.g. TRS398) and an ion chamber with a dose to water calibration traceable to international standards

Let us do single source dosimetry (TG-43 characterization of a source) using TLD as is traditionally done in the literature.

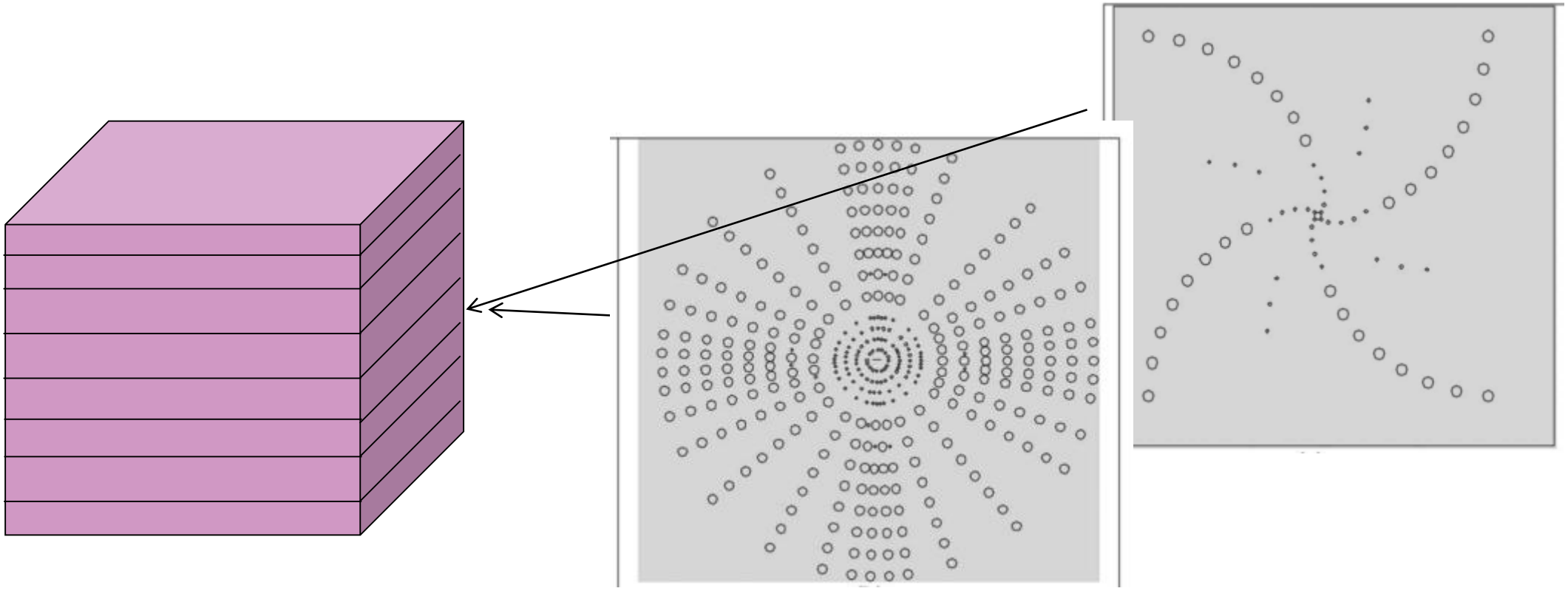

Figures from: Rogers & Cygler (Eds), Clinical dosimetry measurements in radiotherapy (2009 AAPM Summer School), Monograph No. 34, Medical Physics Publishing 2011

TLD: basic principles

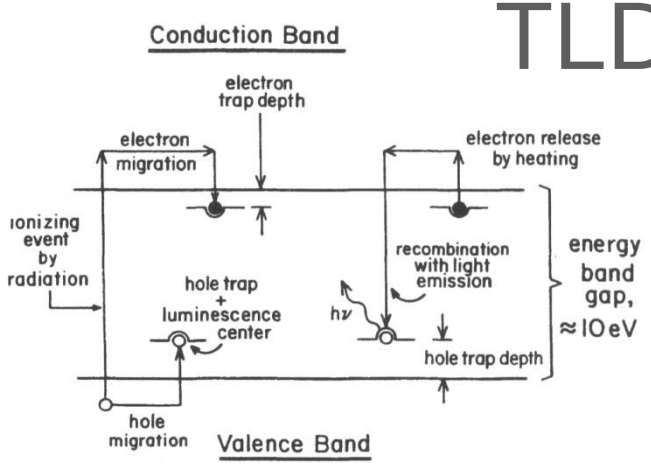

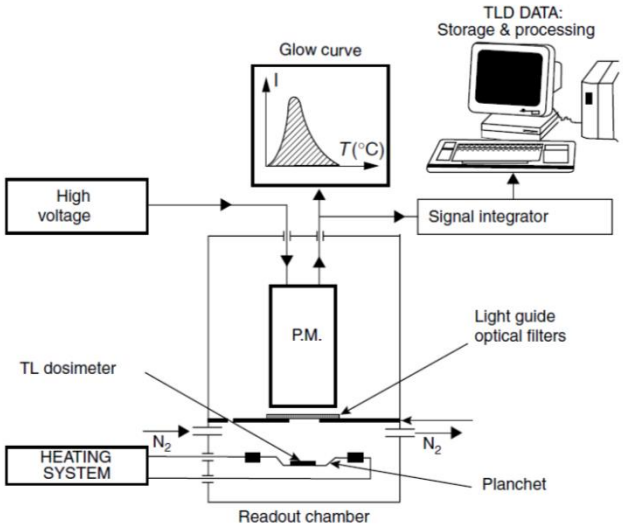

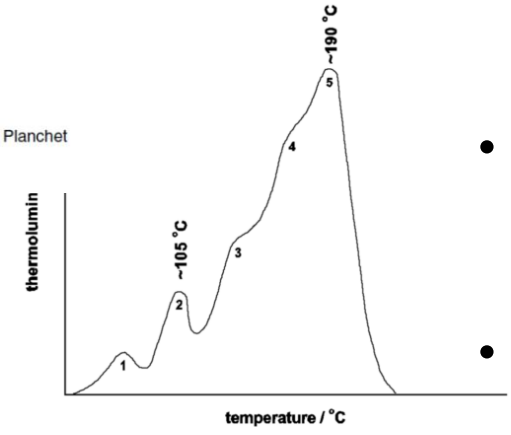

- In imperfect crystals (i.e. TLD100: LiF doped with Mg and Ti in trace amounts) part of the energy absorbed by ionising radiation is stored and re-emitted upon heating in the form of light. Light is detected and correlated to the absorbed dose.
- Stored energy is in the form of the fraction of e^- freed by irradiation, that is trapped in a metastable energy state.
- When the crystal is heated, part of these e^- recombine with holes trapped in luminescence centers and emit light (thermo-luminescence, TL)
- The curve of TL output versus temperature (glow curve) shows peaks characteristic of trap energy depths in the crystal
- Besides TL crystal, glow curve shape varies with heating rate & max temperature

TLD: sensitivity/linearity

Material	Photoelectric Effect Z_{eff}	Compton Effect e^-/g	Density g/cm^3
Silicon (diodes)[a]	14	3×10^{23}	2.33
LiF (Mg,Ti)[b]	8.14	2.79×10^{23}	2.64
LiF (Mg,Ti,Na)[b]	8.14	2.79×10^{23}	2.64
$Li_2B_4O_7$:Mn[b]	7.4	2.92×10^{23}	2.30
$Li_2B_4O_7$:Cu[c]	7.4	2.92×10^{23}	2.30
$CaSO_4$:Mn[b]	15.3	3.02×10^{23}	2.61
$CaSO_4$:Dy[b]	15.3	3.03×10^{23}	2.61
CaF_2:Mn[b]	16.3	2.95×10^{23}	3.18
CaF_2:Dy[b]	16.3	2.95×10^{23}	3.18
Air[d]	7.64	3.03×10^{23}	1.293×10^{-3}
Water[d]	7.42	3.34×10^{23}	1.00
Fat[d]	5.92	3.48×10^{23}	0.91
Muscle[d]	7.42	3.36×10^{23}	1.04
Bone[d]	14	3×10^{23}	1.01–1.60

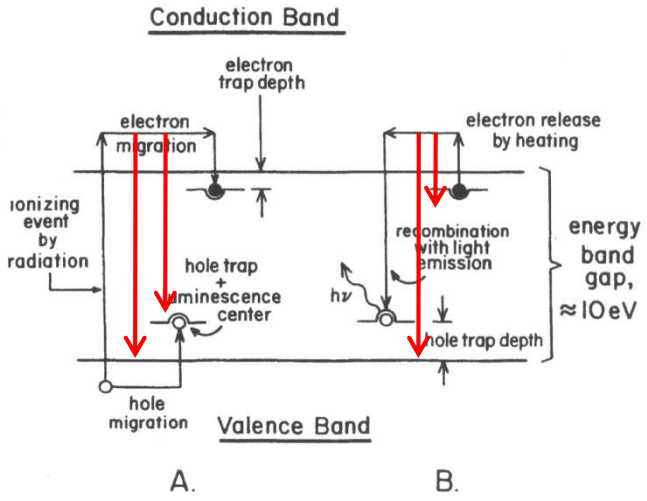

- TLD is effective in terms of interacting with photons in the brachytherapy E range
- The TL mechanism however is inefficient
- About 0.04% of TLD absorbed dose is emitted as TL energy per unit mass
- Individual TLD calibration is required as well as meticulous care in reproducible conditions of use to ensure precision/accuracy
- TLD dynamic dose range is wide. It comprises a linear D region followed by a region of supra-linearity and, eventually, saturation
- Linearity cannot be assumed and has to be measured by irradiating TLD groups in graded doses in the region of interest

Table from: Mayles, Nahum, Rosenwald (Eds): Handbook of radiotherapy physics: theory and practice,© 2007 by Taylor & Francis Group LLC

TLD: influence factors

- TLD response is not significantly affected from environmental conditions (normal room temperatures, moderate exposure to light).

BUT

Traps are not stable @ room temperatures and annealing @ 400 ^{o}C for 1 h is required to ensure trap stability.

Fading can affect low T peaks. This can be mitigated by eliminating corresponding traps (annealing @ 80 ^{o}C for 24 h pre-irradiation) or emptying them before readout (annealing @ 100 ^{o}C for 2 h pre-irradiation and 10 min post-irradiation)

- background correction is necessary for PM dark current and TL non-related to D (the latter is reduced with N_2 gas purging during readout)

- TLD response is dose rate independent

General formalism

- $$\frac{D_{w,w}(Q)}{S_K} = \frac{M(Q) * k_{bkgd} * k_l * g(t)}{S_K} * N_{AD,w}(Q_0) \frac{N_{AD,w}(Q)}{N_{AD,w}(Q_0)} * p_{phant} =$$
$$\frac{M(Q) * k_{bkgd} * k_l * g(t)}{S_K} * N_{AD,w}(Q_0) * k_{bq}^{rel} * f^{rel} * p_{phant}$$

Where: $$g(t) = \frac{\lambda}{\exp[-\lambda(t_{start} - t_{cal})][1 - \exp(-\lambda \Delta t_{\exp})]}$$

and $$p_{phant} = \frac{D_{w,w}(Q)}{D_{w,phant}(Q)}$$ can be calculated using MC

I need to measure: M, $N_{AD,w}(Q_0)$, corrections k_l , and k_{bq} ,
calculate: g(t), f, p_{phant} ,
and know: S_K ,

with as low an uncertainty as possible!

Uncertainty requirements for single source dosimetry

In their methodological recommendations for measuring dosimetry parameters:

- TG-43U1* advises on using a dosimeter system with sufficient precision and accuracy to permit dose-rate estimations with combined 1σ Type A uncertainty <5% and 1σ Type B uncertainty <7% for a total 1 σ uncertainty <9% for LE sources

- Joint AAPM-ESTRO report** advises on using a dosimeter system with sufficient precision and accuracy to permit dose-rate estimations with k=1 Type A (statistical) uncertainties 3% and k=1 Type B uncertainties 6%

* Rivard et al., 2004. Update of AAPM Task Group No. 43 Report: A revised AAPM protocol for brachytherapy dose calculations. Med. Phys. 31(3), p.633.
** Perez-Calatayud et al., 2012. Dose calculation for photon-emitting brachytherapy sources with average energy higher than 50 keV: report of the AAPM and ESTRO. Med. Phys. 39(5), p.2904

TLD: absorbed dose energy dependence

$$f^{rel}(Q,Q_0) = \frac{D_W(Q)/D_{TLD}(Q)}{D_W(Q_0)/D_{TLD}(Q_0)}$$

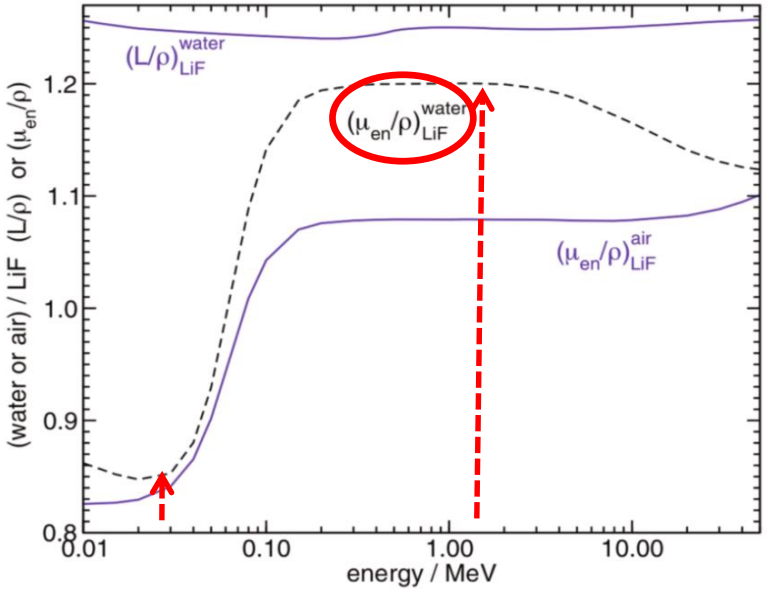

- TLD dose changes more than water at $Q << Q_0$ due to higher Z than water, so $f^{rel} < 1$
- Assuming TLD is a large cavity (dimensions large compared to max. e^- range & small compared to photon m.f.p.):

$$f^{rel}(Q,Q_0) = \frac{(\mu_{en}/\rho)^{W}_{TLD}(Q)}{(\mu_{en}/\rho)^{W}_{TLD}(Q_0)} \approx 0.7$$

for LDR sources relative to Co-60.

This is only an approximation.

MC is used to account for:

- photon spectra @ each point in Q, Q_0
- TLD attenuation,
- v. averaging
- cavity corrections, … etc.

See: Rodriguez and Rogers, Med. Phys. 41(11) p. 114301 (2014) for an excellent review…!

Figure from: Rogers & Cygler (Eds), Clinical dosimetry measurements in radiotherapy (2009 AAPM Summer School), Monograph No. 34, Medical Physics Publishing 2011

TLD: absorbed dose energy dependence

$$f^{rel}(Q,Q_0) = \frac{D_w(Q)/D_{TLD}(Q)}{D_w(Q_0)/D_{TLD}(Q_0)}$$

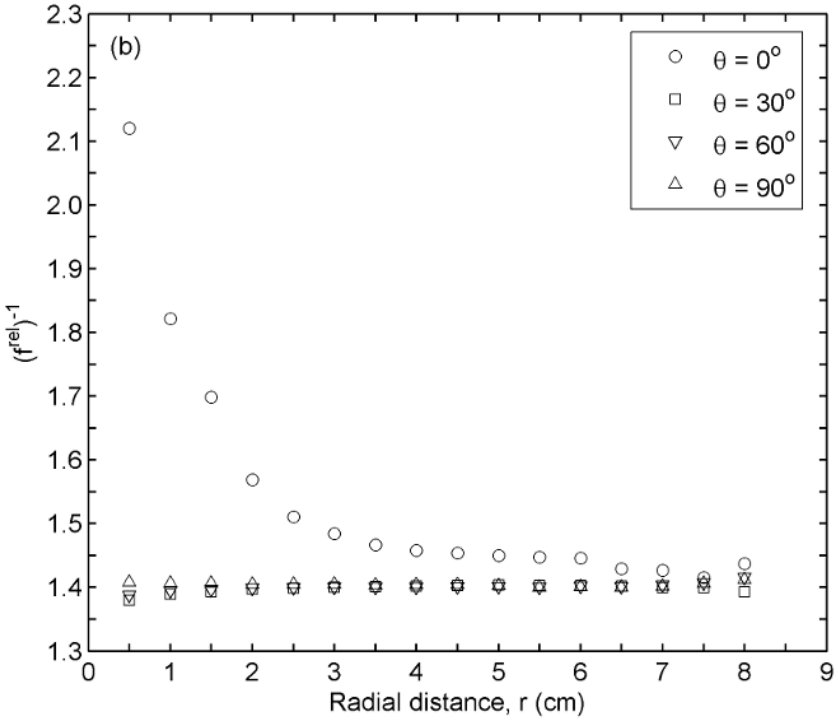

Best practice example for I-125 dosimetry with 6 MV linac calibration:

- f^{rel} is close to 0.7 but varies with point around the source
- Uncertainties: Type A=0.56%, type B=1%

<u>Neglecting f^{rel} would introduce a type B uncertainty (dose overestimation) of 40%...!</u>

Moutsatsos et al. Experimental determination of the Task Group-43 dosimetric parameters of the new I25.S17plus (125)I brachytherapy source, Brachytherapy, 13(6), 618 (2014).

TLD: intrinsic energy dependence

$$k_{bq}^{rel}(Q,Q_0) = \frac{D_{TLD}(Q)/M(Q)}{D_{TLD}(Q_0)/M(Q_0)}$$

Tochilin et al. 1968

Values normalized to Co-60

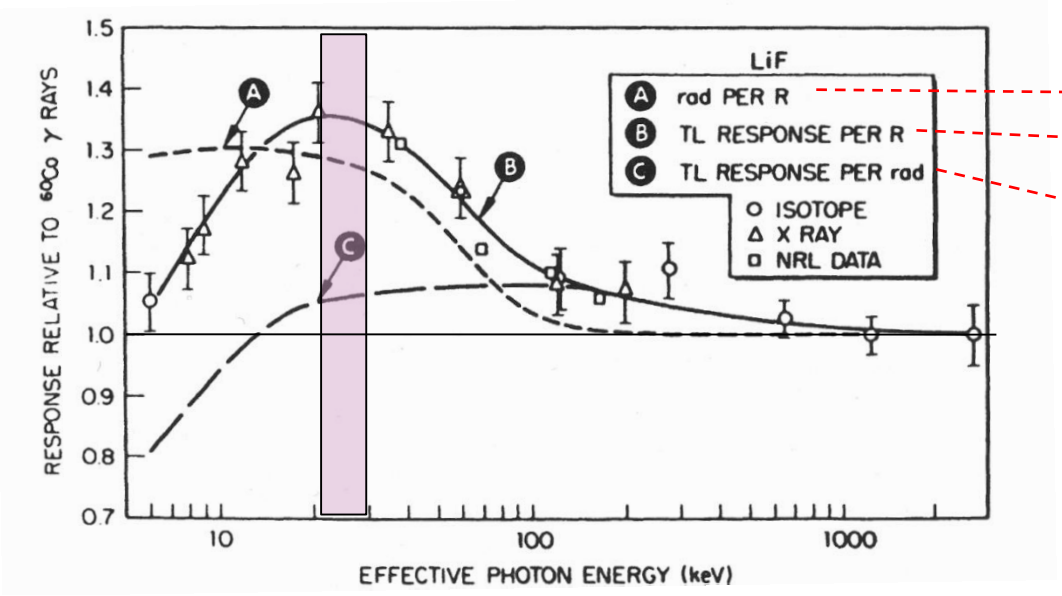

Figure from: Attix: Introduction to radiological physics and radiation dosimetry, © 2004 by Wiley-VCH Verlag GmbH & Co

$$\frac{M}{X} \rightarrow \left(\frac{D_{TLD}}{X}\right)_{large-cavity}$$

$$B/A = C \Leftrightarrow \frac{1}{k_{bq}^{rel}}$$

It was well known that dose to TLD to produce a unit signal decreases as energy decreases and LET increases

i.e.: $k_{bq}^{rel} < 1$ @ the brachy energies

or equivalently: TLD over-responds (more signal per unit dose) at lower energies due to LET increase

TLD: intrinsic energy dependence

$$k_{bq}^{rel}(Q,Q_0) = \frac{D_{TLD}(Q)/M(Q)}{D_{TLD}(Q_0)/M(Q_0)}$$

- In the light of studies indicating $k_{bq}^{rel}=1$ within experimental uncertainties (i.e. Das et al 1996) k_{bq} was disregarded by most experimentalists

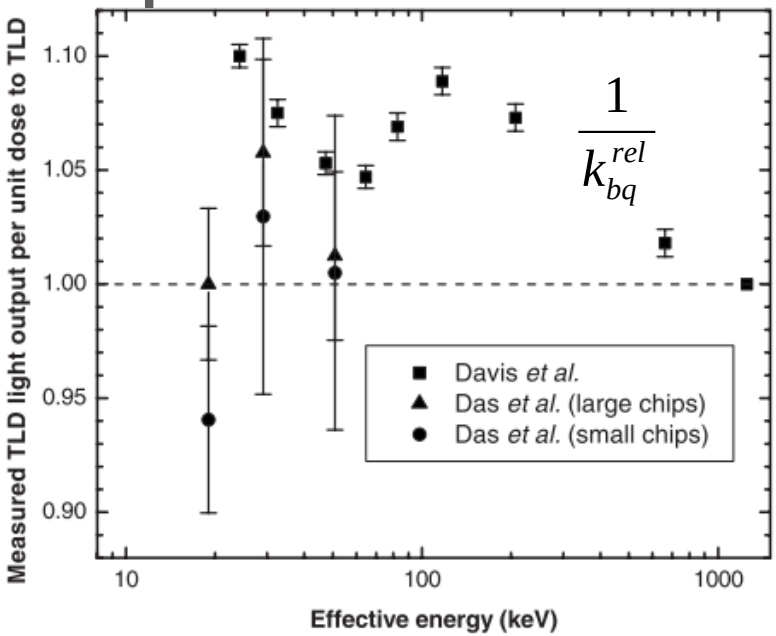

Figure from: Nunn et al, Med. Phys. 38(8) 1859 (2008)

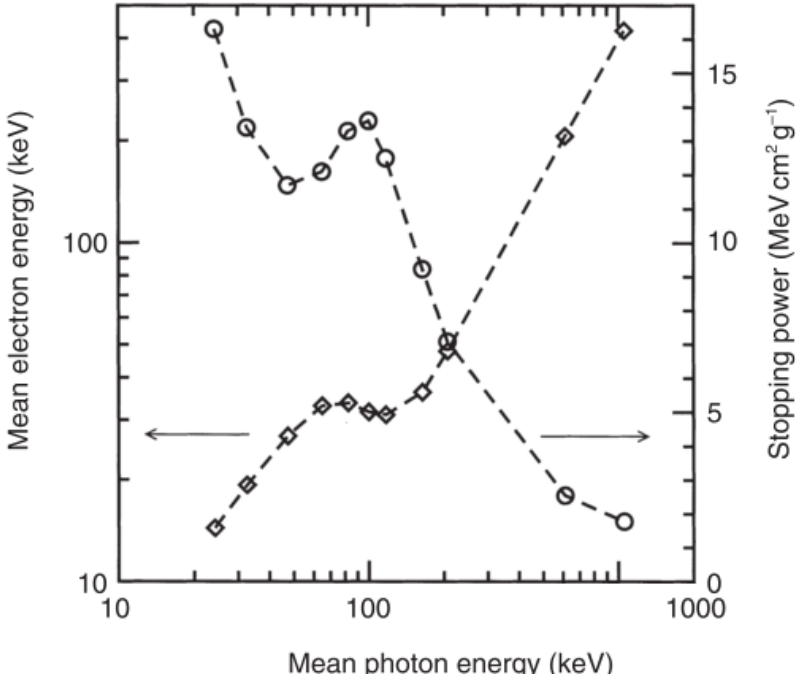

Figure from: Davis et al, Radiation Protection Dosimetry Vol. 106, No. 1, pp. 33–43 (2003)

• Until Davis et al (2003) measured TLD100 over-response at low E due to LET increase and the race to determine k_{bq} was on ...!

TLD: intrinsic energy dependence

$$k_{bq}^{rel}(Q,Q_0) = \frac{D_{TLD}(Q)/M(Q)}{D_{TLD}(Q_0)/M(Q_0)}$$

- Davis et al. k_{bq}^{rel} down to 0.9 (0.6 % Type A uncertainty, k=1, x-ray beams, LiF:Mg,Ti).
- Nunn et al. k_{bq}^{rel} down to 0.885 (3.5% combined standard uncertainty, k=1, x-ray beams, LiF:Mg,Ti).
- Carlsson Tedgren et al. k_{bq} down to 0.935 (1.9% combined standard uncertaintiy, k=1, x-ray beams, LiF:Mg,Ti). They also discussed potential differences due to TLD handling and formulation, and expressed concern regarding the applicability of determinations obtained using x-ray beams to other photon fields.
- Reed et al. k_{bq}^{rel} = 0.883±0.011 (I-125), 0.870±0.012 (I-125 w. Ag), 0.871±0.013 (Pd-103) (combined standard uncertainties, k=1 LiF:Mg,Ti).
- Rodriquez and Rogers minimized the difference between Λ measurements in the literature and MC calculations and arrived at k_{bq}^{rel} = 0.931±0.013 (I-125) and 0.922±0.022 (Pd-103).

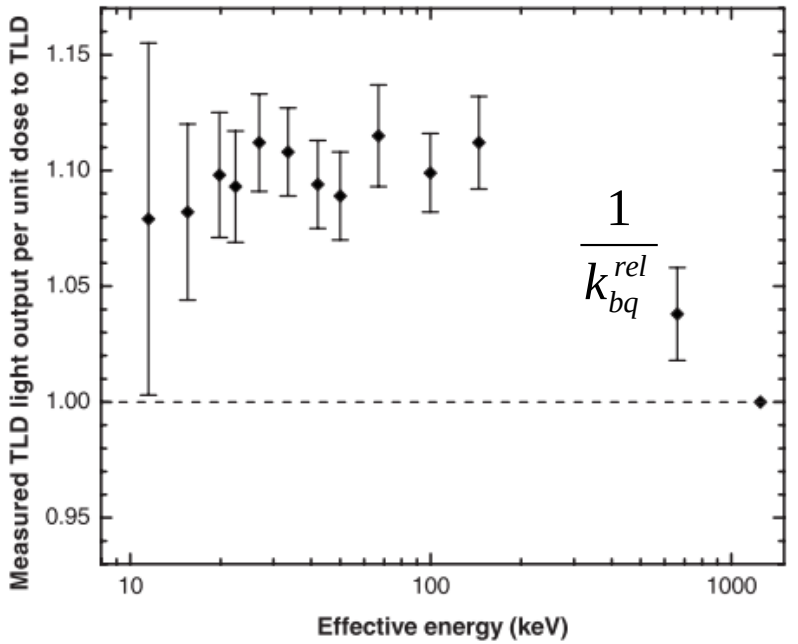

Figure from: Nunn et al, Med. Phys. 38(8) 1859 (2008)

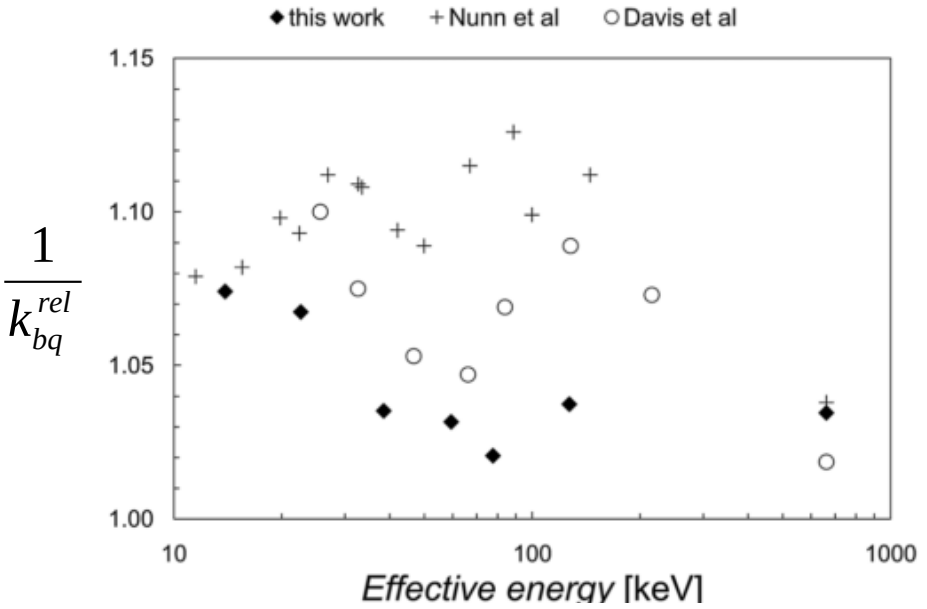

Figure from: Carlsson Tedgren et al, Med. Phys. 38(10) 3839 (2011)

TLD: intrinsic energy dependence

$$k_{bq}^{rel}(Q,Q_0)=\frac{D_{TLD}(Q)/M(Q)}{D_{TLD}(Q_0)/M(Q_0)}$$

- k_{bq}^{rel} is in the order of 0.90 ± 0.05 to 0.935 ± 0.03 for I-125 and Pd-103
- This correction appears to be protocol and TLD make specific.
- A correction might be needed for HE sources as well
  (Joint AAPM-ESTRO report suggests $k_{bq}^{rel}=1$) but for Ir-192 Carlsson et al. (Med. Phys. 39(2), 1133. 2012) suggests $k_{bq}^{rel}=0.95$ but with increased uncertainties (3.5%, k=1).

$$p_{phant} = \frac{D_{w,w}(Q)}{D_{w,phant}(Q)}$$

Phantom correction

- Plastics fabricated for water equivalence in MV beams used as phantom material (solid water 457-Gamex, white water RW3-PTW, plastic water CIRS)
- Williamson (1991) first noted the need for a p_{phant} correction

TABLE II. Percent atomic composition (by weight) and densities of phantoms.[a]

Atomic species	Water	PMMA	WT1	RW-1
H	11.2	8.0	8.1	13.2
C	···	60.0	67.2	79.4
N	···	···	2.4	···
O	88.8	32.0	19.9	3.8
Ca	···	···	2.3	2.7
Mg	···	···	···	0.9
Cl	···	···	0.1	···
Density (g cm^{-3})	1.00	1.17	1.015[b]	0.97

Table from: Luxton, Med. Phys. 21(5), 631 (1994)

$$p_{phant} = \frac{D_{w,w}(Q)}{D_{w,phant}(Q)}$$

Phantom correction

- p_{phant} increases with distance due to increased density and increased attenuation from %Ca content
- There might also be a minor θ dependence

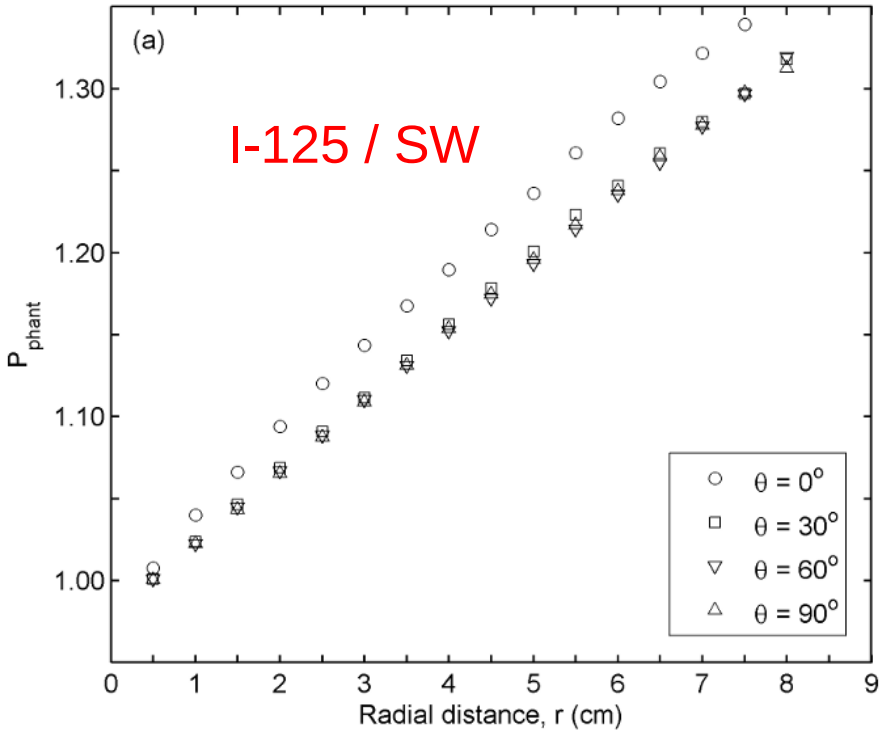

TABLE II. Percent atomic composition (by weight) and densities of phantoms.[a]

Atomic species	Water	PMMA	WT1	RW-1
H	11.2	8.0	8.1	13.2
C	···	60.0	67.2	79.4
N	···	···	2.4	···
O	88.8	32.0	19.9	3.8
Ca	···	···	2.3	2.7
Mg	···	···	···	0.9
Cl	···	···	0.1	···
Density (g cm^{-3})	1.00	1.17	1.015[b]	0.97

Table from: Luxton, Med. Phys. 21(5), 631 (1994)

Figure from: Moutsatsos et al. Brachytherapy, 13(6), 618 (2014)

$$p_{phant} = \frac{D_{w,w}(Q)}{D_{w,phant}(Q)}$$

Phantom correction

- Phantom material MUST be checked for density variation and composition (Ca or other high Z content variation that can be up to 30%) to minimize type B uncertainty.

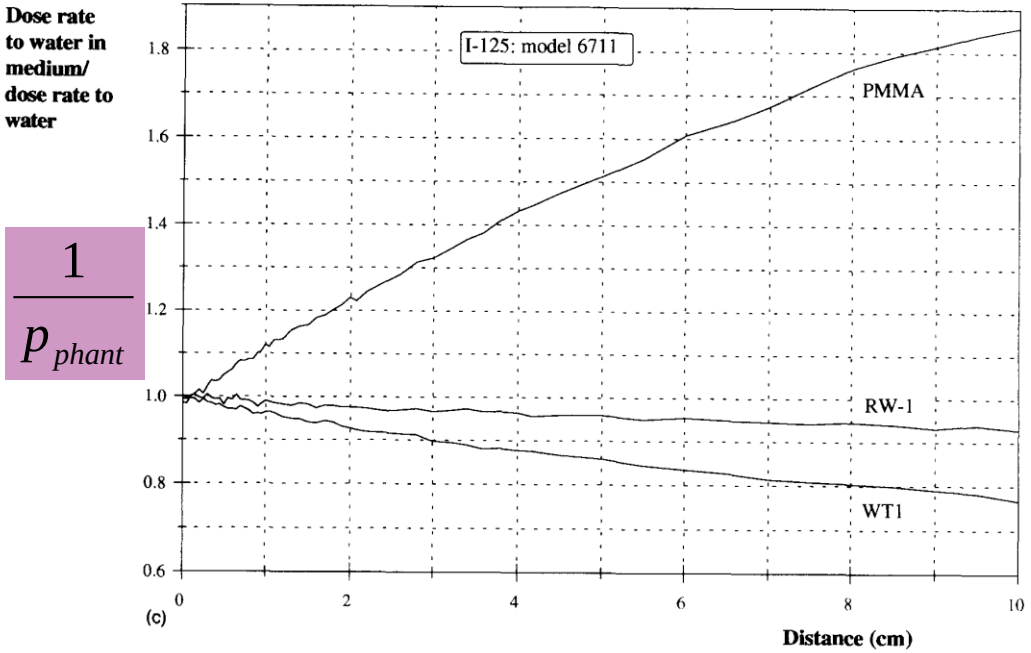

$$\frac{1}{p_{phant}}$$

Figure from: Luxton, Med. Phys. 21(5), 631 (1994)

- High purity plastics (PMMA, polystyrene) might be preferable since p_{phant} deviation from unity is greater for LE source dosimetry BUT type B uncertainty of the correction will be lower.

TLD: uncertainty budget

Table 1
Analysis of the uncertainty associated with TLD results for the dose-rate constant of the I25.S17plus brachytherapy source

Component	Type A (%)	Type B (%)
Average of repetitive measurements	3.22[a]	—
TLD dose calibration	0.48	1.21
Relative intrinsic energy dependence, k_{bq}^{rel}		2.50
Phantom material correction factor, P_{phant}	0.14	2.46
Relative absorbed dose energy dependence, f^{rel}	0.56	1.0
TLD-source relative positioning		0.6
Source strength, S_K		0.78[b]
Quadratic sum	3.31	3.97
Combined total uncertainty ($k = 1$)	5.16[c]	

TLD = thermoluminescent dosimeter.

Random or statistical effects are described with type A uncertainties, whereas type B uncertainties account for nonstatistical discrepancies. The tabulated values correspond to the National Institute of Standards and Technology–calibrated seed.

[a] 3.20%, 5.90%, and 3.44% for seed 1, 2, and 3, respectively.

[b] 1% for seed 1, 2, and 3.

[c] 5.19%, 7.18%, and 5.34% for seed 1, 2, and 3, respectively.

Moutsatsos et al. Brachytherapy, 13(6), 618 (2014)

In summary:

- TLD remains the standard method for single source exp. dosimetry (both LE,HE)
- Methodological recommendations are included in TG43U1 (Rivard et al. 2004), Joint AAPM-ESTRO report (Perez-Calatayud et al, 2012) and refs therein
- At minimum calculate your f^{rel} correction using MC and including TLD att./volume and p_{phant} as a function of (r,θ). These are significant for LE and less for HE.
- What you don't know (phantom composition, density, etc) goes in your uncertainty budget!
- Overall uncertainty for LE is high mainly due to k_{bq}^{rel} uncertainty. Dose rate constants measured are on average ~5% higher than MC and hence the recommendation for equally averaged, consensus values in TG43U1 (Rivard et al. 2004)

- A dosimeter with reduced uncertainty would be welcome!

Alternatives to TLD

- Systems used for single source dosimetry and especially QA: ion chambers, alanine, OSLDs, PSDs, film, …. i.e:

Araki, F. et al., 2013. Measurement of absorbed dose-to-water for an HDR (192)Ir source with ionization chambers in a sandwich setup. Med. Phys., 40(9), p.092101.

Sarfehnia, A., Kawrakow, I. & Seuntjens, J., 2010. Direct measurement of absorbed dose to water in HDR [sup 192]Ir brachytherapy: Water calorimetry, ionization chamber, Gafchromic film, and TG-43. Med. Phys., 37(4), p.1924.

Adolfsson, E. et al., 2010. Response of lithium formate EPR dosimeters at photon energies relevant to the dosimetry of brachytherapy. Med. Phys., 37(9), p.4946.

Schaeken, B. et al., 2011. Experimental determination of the energy response of alanine pellets in the high dose rate 192Ir spectrum. PMB, 56(20), pp.6625–34.

Kolbun, N. et al., 2010. Experimental determination of the radial dose distribution in high gradient regions around 192Ir wires: comparison of electron paramagnetic resonance imaging, films, and Monte Carlo simulations. Med. Phys., 37(10), pp.5448–55.

Chiu-Tsao, S.-T., Medich, D. & Munro, J., 2008. The use of new GAFCHROMIC EBT film for [sup 125]I seed dosimetry in Solid Water phantom. Med. Phys., 35(8), p.3787.

Aldelaijan, S. et al., 2011. Radiochromic film dosimetry of HDR (192)Ir source radiation fields. Med. Phys., 38(11), pp.6074–83.

Palmer, A.L. et al., 2013. Comparison of methods for the measurement of radiation dose distributions in high dose rate (HDR) brachytherapy: Ge-doped optical fiber, EBT3 Gafchromic film, and PRESAGE® radiochromic plastic. Med. Phys., 40(6), p.061707.

Palmer, A.L., Lee, C., et al., 2013. Design and implementation of a film dosimetry audit tool for comparison of planned and delivered dose distributions in high dose rate (HDR) brachytherapy. PMB, 58(19), pp.6623–40.

Palmer, A.L., Nisbet, A. & Bradley, D., 2013. Verification of high dose rate brachytherapy dose distributions with EBT3 Gafchromic film quality control techniques. PMB, 58(3), pp.497–511.

- Due to spatial measurement resolution, other limitations, and mainly level of development, TLD remains the method of choice for single source dosimetry.
- OSLDs, PSDs and alanines are also used for in-vivo and will be reviewed in the next lecture.
- What about 2D dosimetry using radiochromic films …?

Radiochromic films

- Self-developing films based on diacetylenes researched since the 1960s as high dose radiations dosimeters
- A more sensitive film, known as GAFchromic™, was introduced by the mid-1980s by International Specialty Products (ISP) Technology, a division of GAF Chemical Corporation (General Aniline & Film Corporation)
- ISP was acquired by Ashland Inc in 2011
- for commercial information on radiochromic films see: http://www.gafchromic.com/index.asp

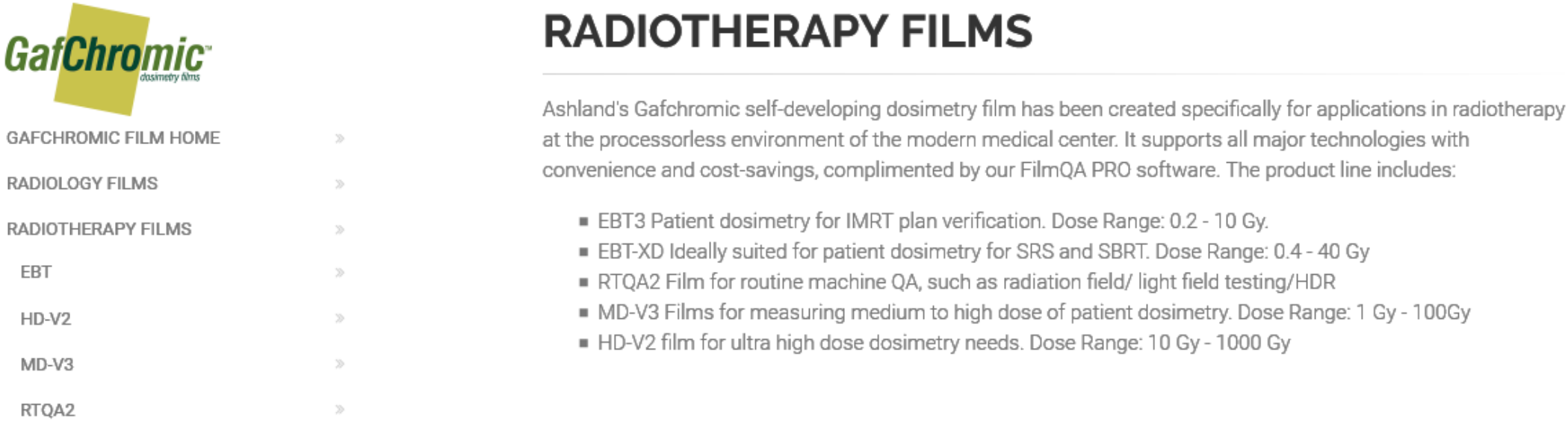

Radiochromic films: basic principles

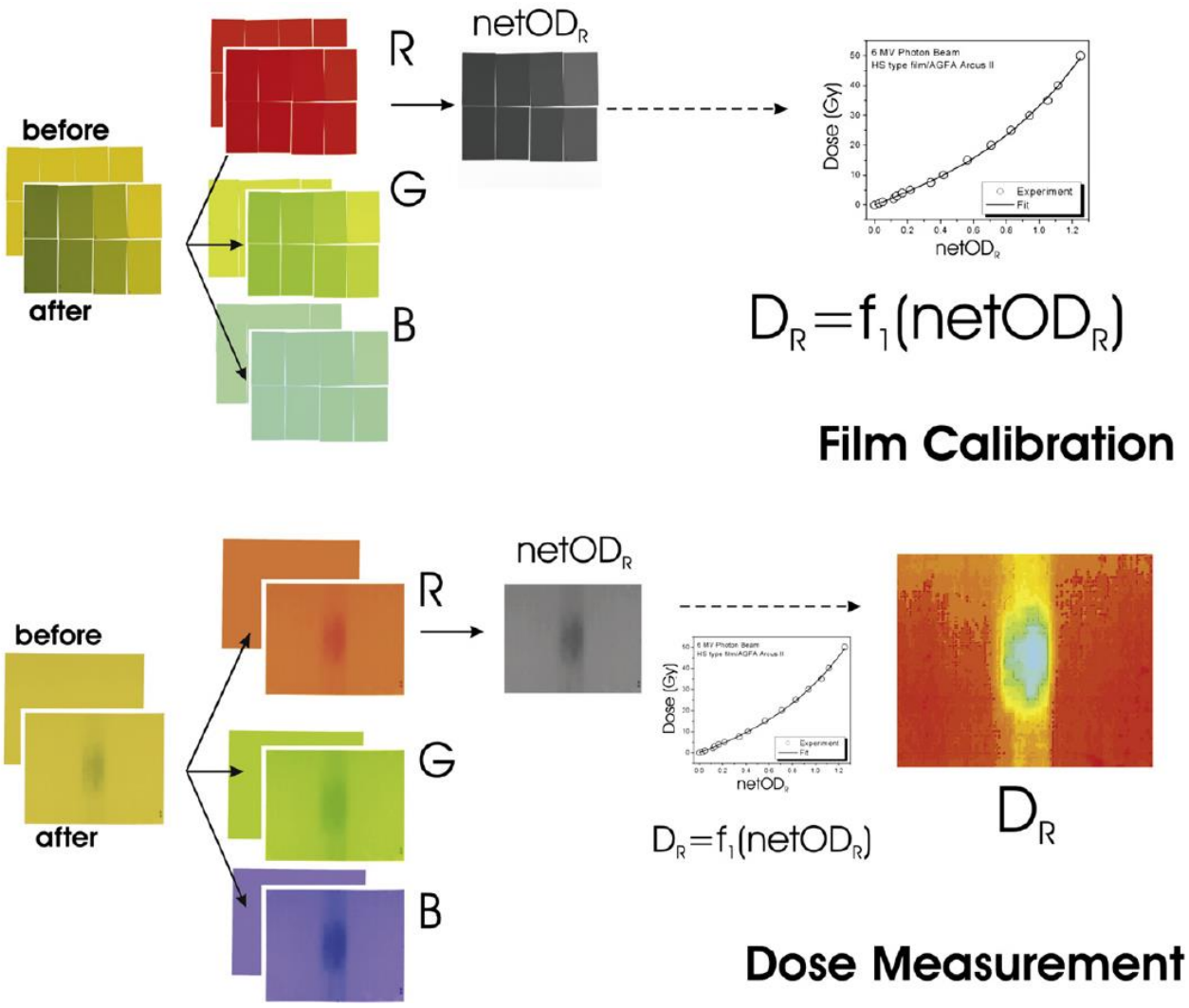

- Diacetylene molecules in a w. sol. polymer matrix coated on a polyester substrate
- Radiation induces polymerization of diacetylene molecules to form polydiacetylene dye polymers (self-developing)
- These are blue in color and cause light absorbance (mainly) in the other parts of the visible spectrum
- The change in net OD is measured using flat-bed scanners employing broad band visible light sources, and correlated to dose
- $OD=\log(1/T)=\log(I_o/I_T)$

Figure from: Devic, Physica Medica 27(3) 122 (2011)

Radiochromic films: types

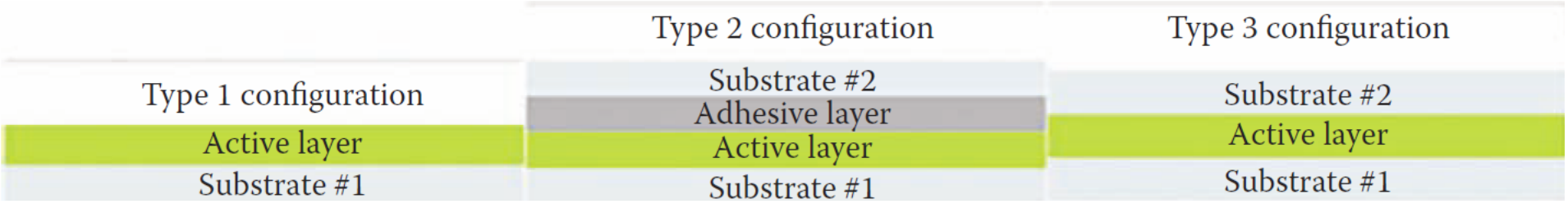

Film model	Configuration	Active layer			Substrate 1		Substrate 2		Adhesive layer	Sizes	Dose range
		Nominal thickness, (μm)	Marker dye	Alumina	Type	Nominal thickness, (μm)	Type	Nominal thickness (μm)	Nominal thickness (μm)		
HD-V3	Type 1	12	Yes	Yes	Clear transparent polyester	97	–	–	–	8″ × 10″	10–1000 Gy
MD-V3	Type 2	10	Yes	Yes	Clear transparent polyester	125	Clear transparent polyester	50	7	5″ × 5″	1–100 Gy
EBT2	Type 2	28	Yes	Yes	Clear transparent polyester	175	Clear transparent polyester	50	20	8″ × 10″ 12.8″ × 17″	0.01–40 Gy
EBT3	Type 3	28	Yes	Yes	Clear transparent polyester	125	Clear transparent polyester	125		8″ × 10″ 12.8″ × 17″	0.01–40 Gy

Data from: I.J. Das (Ed.), Radiochromic film: role and applications in radiation, © 2018 by Taylor & Francis Group, LLC

Radiochromic films: types

Type 1 configuration
Active layer
Substrate #1

Type 2 configu
Substrate
Adhesive la
Active lay
Substrate

Film model	Configuration	Active layer: Nominal thickness, (μm)	Active layer: Marker dye	Active layer: Alumina	Substrate 1: Type	Substrate 1: Nom thick (μ
HD-V3	Type 1	12	Yes	Yes	Clear transparent polyester	9
MD-V3	Type 2	10	Yes	Yes	Clear transparent polyester	12
EBT2	Type 2	28	Yes	Yes	Clear transparent polyester	175
EBT3	Type 3	28	Yes	Yes	Clear transparent polyester	125

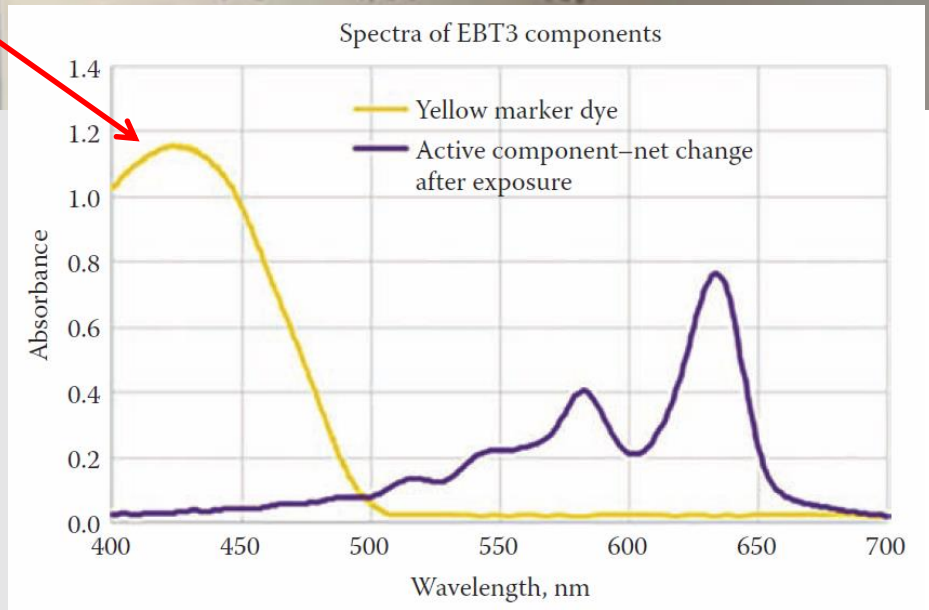

Data from: I.J. Das (Ed.), Radiochromic film: role and applications in radiation, © 2018 by Taylor & Francis Group, LLC

Radiochromic films: types

Type 1 configuration	Type 2 configuration	Type 3 configuration
	Substrate #2	
	Adhesive layer	Substrate #2
Active layer	Active layer	Active layer
Substrate #1	Substrate #1	Substrate #1

Film model	Configuration	Active layer: Nominal thickness, (μm)	Active layer: Marker dye	Active layer: Alumina	Substrate 1: Type	Substrate 1: Nominal thickness, (μm)	Substrate 2: Type	Substrate 2: Nominal thickness (μm)	Adhesive layer: Nominal thickness (μm)	Sizes	Dose range
HD-V3	Type 1	12	Yes	Yes	Clear transparent polyester	97	–	–	–	8″ × 10″	10–1000 Gy
MD-V3	Type 2	10	Yes	Yes	Clear transparent polyester	125	Clear transparent polyester				Gy
EBT2	Type 2	28	Yes	Yes	Clear transparent polyester	175	Clear transparent polyester				40 Gy
EBT3	Type 3	28	Yes	Yes	Clear transparent polyester	125	Clear transparent polyester	125		8″ × 10″ 12.8″ × 17″	0.01–40 Gy

special surface treatment containing microscopic silica particles to prevent the formation of Newton's Rings interference patterns when films are in close proximity to another reflective surface as in a flatbed scanner.

Data from: I.J. Das (Ed.), Radiochromic film: role and applications in radiation, © 2018 by Taylor & Francis Group, LLC

Radiochromic films: types

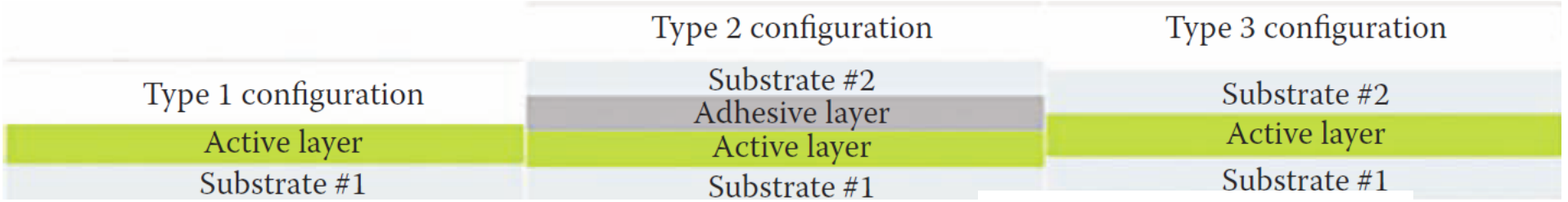

Film model	Configuration	Active layer: Nominal thickness, (µm)	Active layer: Marker dye	Active layer: Alumina	Substrate 1: Type	Substrate 1: Nominal thickness, (µm)	Substrate 2	Dose range
HD-V3	Type 1	12	Yes	Yes	Clear transparent polyester	97	–	10–1000 Gy
MD-V3	Type 2	10	Yes	Yes	Clear	125	Clear	1–100 Gy
EBT2	Type 2	28	Yes	Yes	C			
EBT3	Type 3	28	Yes	Yes	C			

Active layer composition is (**allegedly**) constant and after 2011 it contains aluminum oxide nanoparticles to minimize the energy dependence of film response from MV down to about 40 keV

Table 2.5 Specific elemental compositions, atom (%), and effective atomic numbers (Z_{eff}) of the active layer of HD-V2, MD-V3, EBT2, EBT3, EBT3 unlaminated, EBT-XD, RTQA2, and XR-QA2 radiochromic films

	Composition by element and atom (%)											
Film model	H	Li	C	N	O	Na	Al	S	Cl	Ba	Bi	Z_{eff}
HD-V2	58.2	0.6	27.7	0.4	11.7	0.5	0.3	0.1	0.6			7.63
MD-V3	58.2	0.6	27.7	0.4	11.7	0.5	0.3	0.1	0.6			7.63
EBT2	56.5	0.6	27.4	0.3	13.3	0.1	1.6	0.1	0.1			7.46
EBT3	56.5	0.6	27.4	0.3	13.3	0.1	1.6	0.1	0.1			7.46
EBT3 unlaminated	56.5	0.6	27.4	0.3	13.3	0.1	1.6	0.1	0.1			7.46
EBR-XD	57.0	0.6	28.5	0.4	11.7	1.0	1.5	0.1	0.1			7.42
RTQA2	56.5	0.6	27.4	0.3	13.3	0.1	1.6	0.1	0.1			7.46
XR-QA2	56.2	1.0	27.6	1.6	11.7	0.0			0.1		1.7	55.23

Source: Courtesy of Azam Niroomand-Rad.

Radiochromic films: influence factors

- There is post-irradiation signal growth that depends on t (log, 5% per decade) and T. A $k_{t,T}(t,T,D)$ correction must be applied OR films are kept @ stable T (store exposed and unexposed films at ambient temperature ~22 C or less) for (at least 8h) 24h before scanning.
- Background signal from an un-irradiated control film of the same batch and size, handled in the same way as the exp. films must be subtracted pixel-by-pixel to account for base OD and absorbance changes due to environmental conditions (T, visible light, humidity, scanning light, etc.) and obtain net OD change
- Film non-uniformity correction, $k_{nu}(x,y)$, is important. A double exposure technique with pixel-by-pixel subtraction must be employed.
- Alternatively, a triple channel technique has been developed (Micke et al, Multichannel film dosimetry with nonuniformity correction, *Med. Phys. 38(5)* 2523, 2011) and commercially available (FilmQA Pro software, Ashland-former ISP).
- There is also reader non-uniformity and films should always be read at the same scanner bed location to avoid application of a $k_{pos(x,y)}$ correction
- Film response is dose rate independent!
- Films can be used in water (~1mm/h water penetration)!

EBT films: sensitivity/linearity

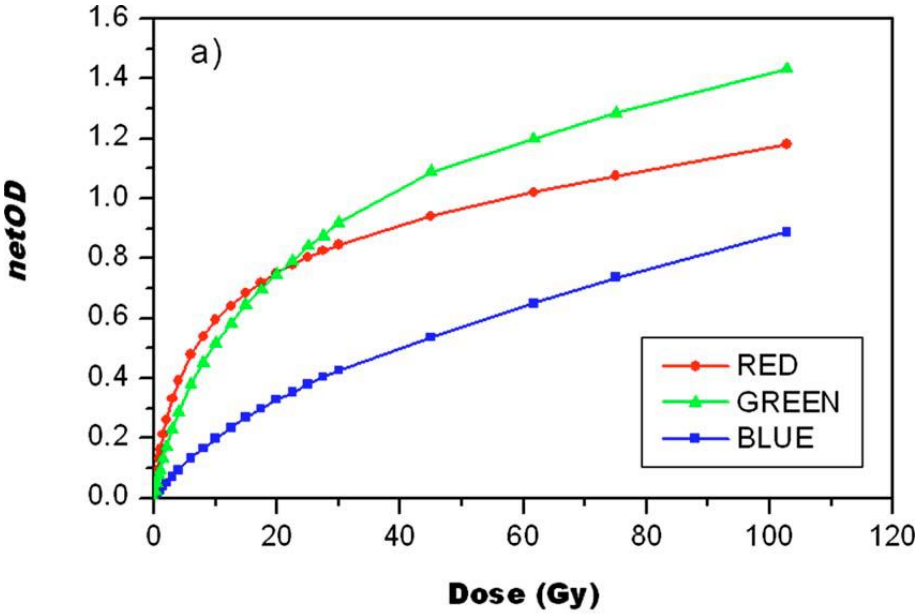

- Sensitivity is film, scanner, protocol, and dose dependent
- It is non-linear and different or all RGB channels can be used
- A variety of fitting functions has been used in literature. Popular choices are power fits and rational functions:

$$\Delta OD = -\log\frac{a+bD}{c+D} \,/\, \Delta OD = \frac{a+b}{D-c} \,/\, D = a + b\Delta OD + c\Delta OD^{n}$$

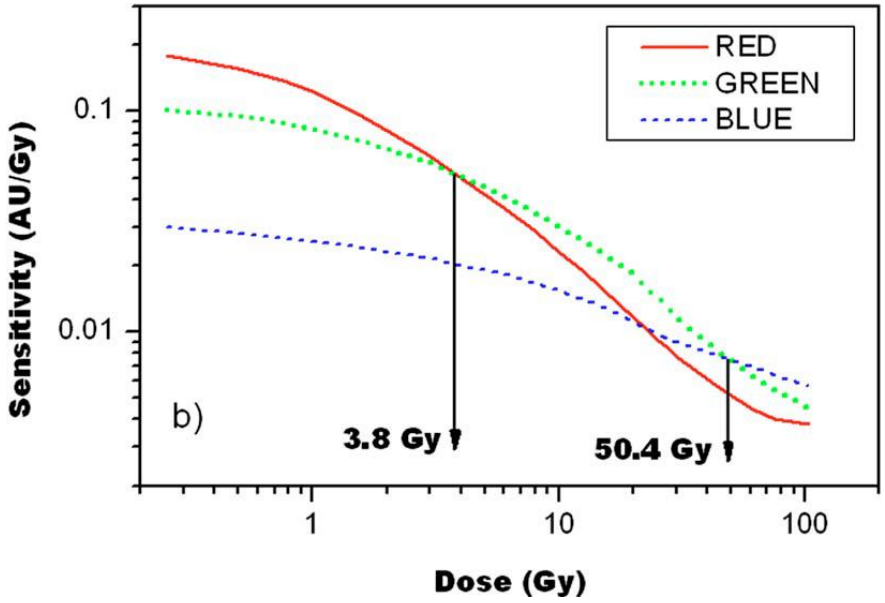

- Separate calibration recommended for each lot
- Calibration quality criterion is (of course) uncertainty

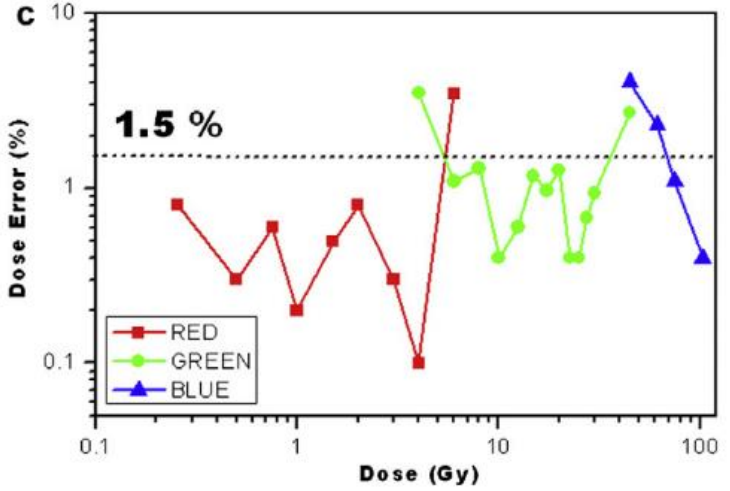

Figures from: Devic, Physica Medica 27(3) 122 (2011)

Radiochromic films: rel. E response

$$f^{rel}(Q,Q_0) = \frac{D_w(Q)/D_{TLD}(Q)}{D_w(Q_0)/D_{TLD}(Q_0)} \qquad k_{bq}^{rel}(Q,Q_0) = \frac{D_{TLD}(Q)/M(Q)}{D_{TLD}(Q_0)/M(Q_0)}$$

- Investigators reported inconsistent results of rel. E response.
- E.g.: for EBT3 Brown et al (2012) used synchrotron mono-chromatic x-rays and found up to 3% dose over-response ($f^{rel}k_{bq}^{rel} = 0.97$) at low E (25-35 keV) while Massillon-JL et al (2012) reported under-response up to 13% for 50kVp beams.

- It became apparent that manufacturing and compositional changes do take place, that are not always accompanied by updates to the film model or label (!!!)

Radiochromic films: rel. E response

$$f^{rel}(Q,Q_0) = \frac{D_w(Q)/D_{TLD}(Q)}{D_w(Q_0)/D_{TLD}(Q_0)} \qquad k_{bq}^{rel}(Q,Q_0) = \frac{D_{TLD}(Q)/M(Q)}{D_{TLD}(Q_0)/M(Q_0)}$$

- Bekerat et al (2014) indicate different marketed versions of EBT3 and report:
  - no relative energy dependence of the latest EBT3 between Ir-192 and Co-60 (albeit for 3cm film-source distance in a parallel-opposed Ir-192 HDR irradiation setup)
  - an under response ($f^{rel} k_{bq}^{rel} > 1$) at all energies <100 keV, varying from 20% ± 4% at 20 keV to ± 4% at 40 keV.

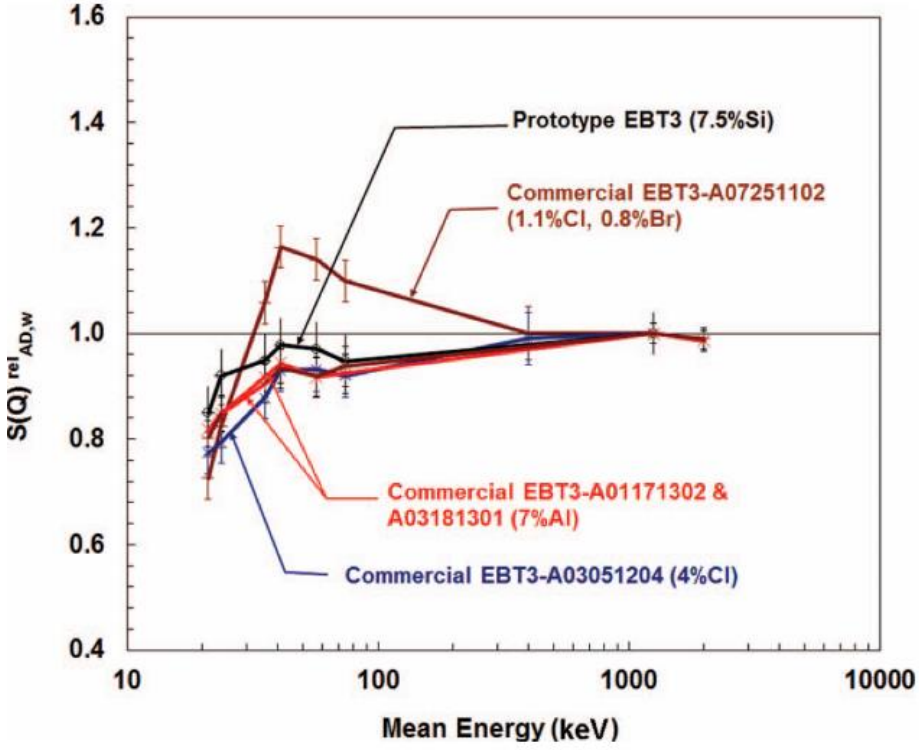

Figure from: Bekerat et al, Medical Physics 41(2) 022101 (2014)

Radiochromic films: rel. E response

$$f^{rel}(Q,Q_0) = \frac{D_w(Q)/D_{TLD}(Q)}{D_w(Q_0)/D_{TLD}(Q_0)} \qquad k_{bq}^{rel}(Q,Q_0) = \frac{D_{TLD}(Q)/M(Q)}{D_{TLD}(Q_0)/M(Q_0)}$$

- Hammer et al (2018) further elaborated on the **three versions of EBT3 marketed without notice** and yield results in agreement with Bekerat et al (2014) for the latest version
- EBT3-V1 was released in early 2011 and discontinued in October 2011 when EBT3-V2 was initially released.
- EBT3-V3 was initially released in August 2013, when EBT3-V2 was discontinued.
- EBT3-V3 is the currently available version of EBT3.

TABLE I. The material compositions of EBT2 and EBT3 film listed in mass percent (%). EBT3 film has undergone three chemical compositions (the first, second, and third versions of EBT3 are denoted here as V1, V2, and V3, respectively), with each iteration becoming more water equivalent.[12,23]

	H	Li	C	N	O	Na	S	Cl	Br	Al	Z_{eff}	Density (g/cm^3)
EBT2	9.7	0.9	58.4	0.1	28.4	0.4	0.2	1.1	0.8	-	9.38	1.2
EBT3-V1	9.7	0.9	58.4	0.1	28.4	0.4	0.2	1.1	0.8	-	9.38	1.2
EBT3-V2	8.9	1.0	61.3	0.1	23.5	0.5	0.01	4.5	-	0.1	7.99	1.2
EBT3-V3	8.8	0.6	51.1	-	32.8	-	-	-	-	6.7	7.26	1.2

Data from : Hammer et al, Medical Physics 45 (1) 448 (2018)

Radiochromic films: rel. E response

$$f^{rel}(Q,Q_0) = \frac{D_w(Q)/D_{TLD}(Q)}{D_w(Q_0)/D_{TLD}(Q_0)} \qquad k_{bq}^{rel}(Q,Q_0) = \frac{D_{TLD}(Q)/M(Q)}{D_{TLD}(Q_0)/M(Q_0)}$$

- Hammer et al (2018) further elaborate on the **three versions of EBT3 marketed without notice** and yield results in agreement with Bekerat et al (2014) for the latest version
- EBT3-V3 is the currently available version of EBT3.

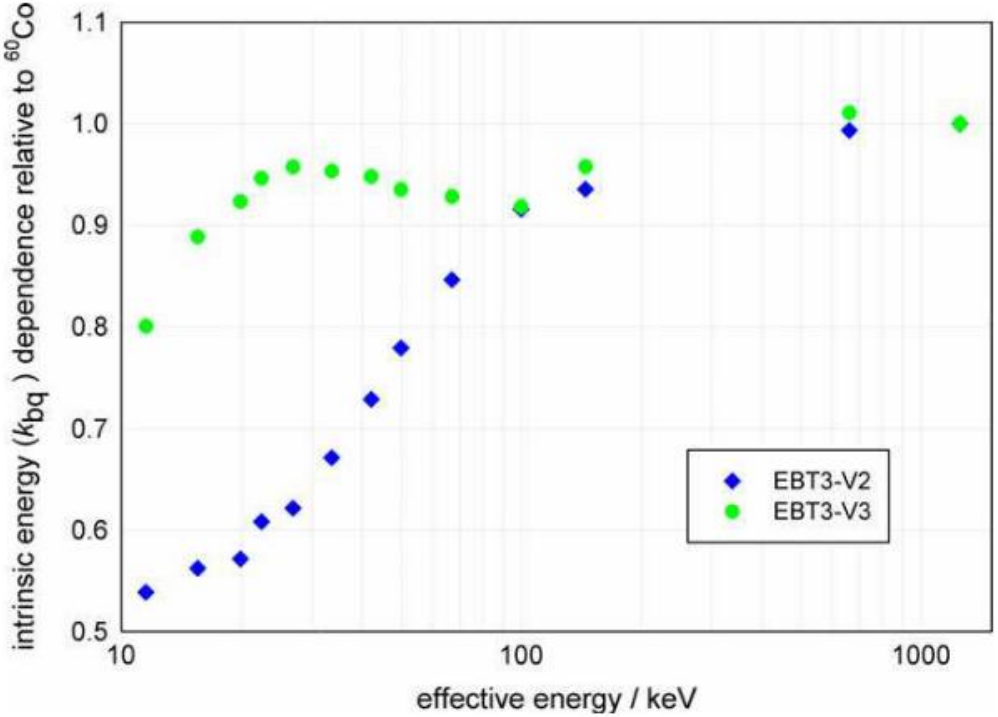

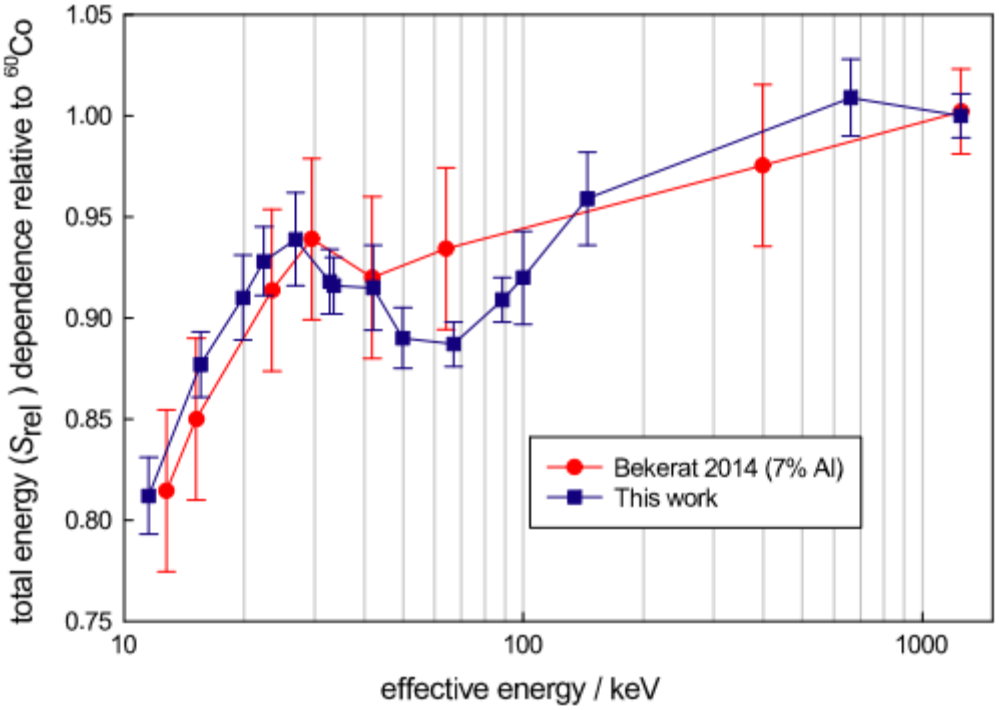

Figures from : Hammer et al, Medical Physics 45 (1) 448 (2018)

Radiochromic films: precision/accuracy

- Ignoring intrinsic E dependence, Dempsey et al. (Med. Phys. 27(10) 2462 2000) reported 1.5-4% agreement of Gafchromic MD-55-2 results around a single Ir-192 source with MC
- Chiu-Tsao et al. (Med. Phys. 35, 3787 2008) reported 6.8% (k=1) uncertainty for I-125 dose rate constant determination using EBT1 calibrated using a I-125 seed
- Ignoring intrinsic E dependence, Sarfehnia et al. (Med. Phys. 37(4) 1924 2010) reported 1.78% (k=1) uncertainty for dose rate to water determination around a single Ir-192 source using EBT-1

In summary:

- Radiochromic films mature for brachytherapy dosimetry

BUT

- (some) work still required for their accurate relative energy response characterization in brachytherapy
- Due to calibration uncertainty (rel. high and dose dependent) and influence factors they are reserved mainly for relative dosimetry in QA and D verification

3D dosimeters…?

- radiation-induced chemical change in a gel matrix can be mapped in 3D using MRI or optical CT

Figure from: Baltas, Sakelliou, Zamboglou (Eds), The Physics of modern brachytherapy for oncology, Taylor & Francis Books Inc, 2006

Figure from: Rogers & Cygler (Eds), Clinical dosimetry measurements in radiotherapy (2009 AAPM Summer School), Monograph No. 34, Medical Physics Publishing 2011

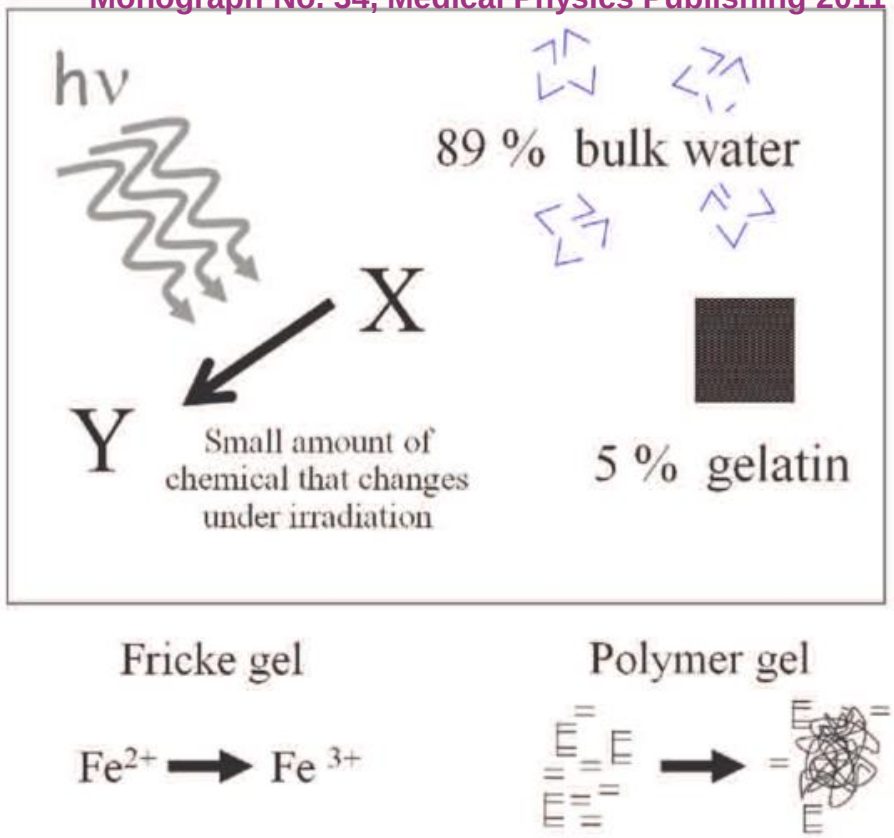

- polymer gels: Custom made with organic co-monomers
- PRESAGE (Heuris Inc.): color forming leucodye (LMG) + initiator within a polyurethane matrix (not a gel)
- Radiochromic gels: FXG, tetrazolium salt, or leucodye based (e.g. Truview/Clearview gels by Modus Medical devices Inc.)

3D dosimeters

Advantages

- Dosimeter is the phantom (negligible to small p_{phant} depending on type)
- 3D character facilitates concurrent measurements and processing for minimizing positional and type A uncertainty
- negligible to small f^{rel} (depending on type)
- No dose rate dependence (except for methacrylic acid based gels-MAGIC & PRESAGE at very low dose rates)

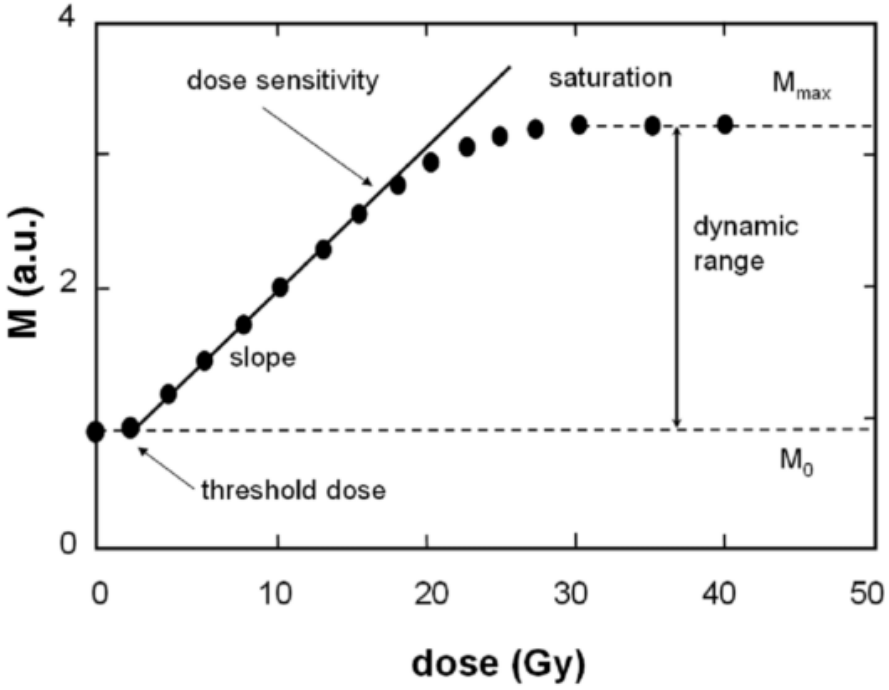

Disadvantages

- Sensitivity varies with type and batch
- k^{rel}_{bq} can be significant for some dosimeters @ low E
- 3D character augments influences and problems similar to that of films increasing type B uncertainty

Figure from: Rogers & Cygler (Eds), Clinical dosimetry measurements in radiotherapy (2009 AAPM Summer School), Monograph No. 34, Medical Physics Publishing 2011

Example polymer gels

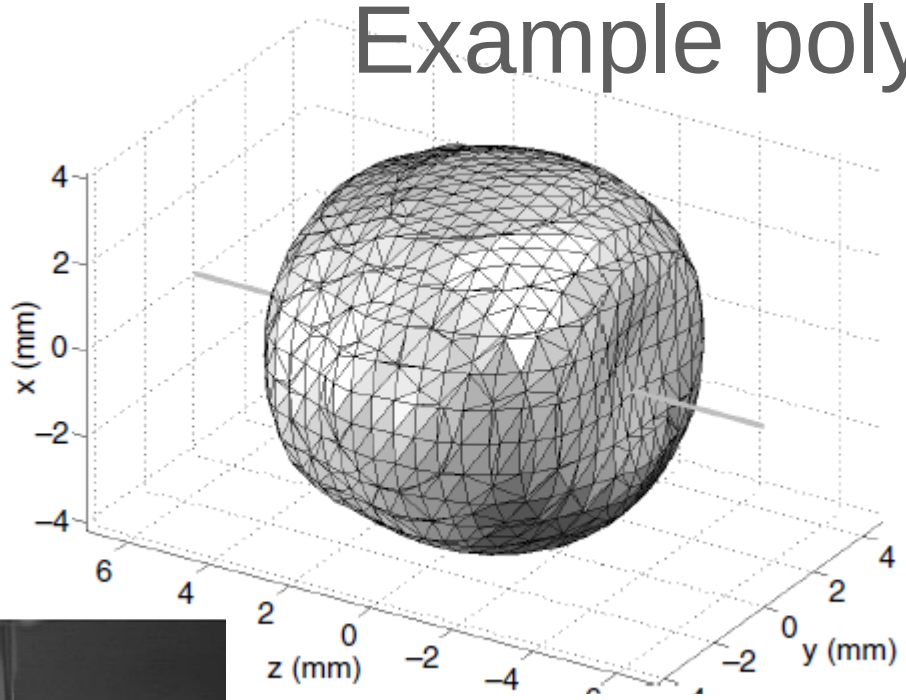

Fig. 1. A picture of the PABIG gel irradiated with two seeds (top: I25.S17, bottom: I25.S06) for a time period of 26 days.

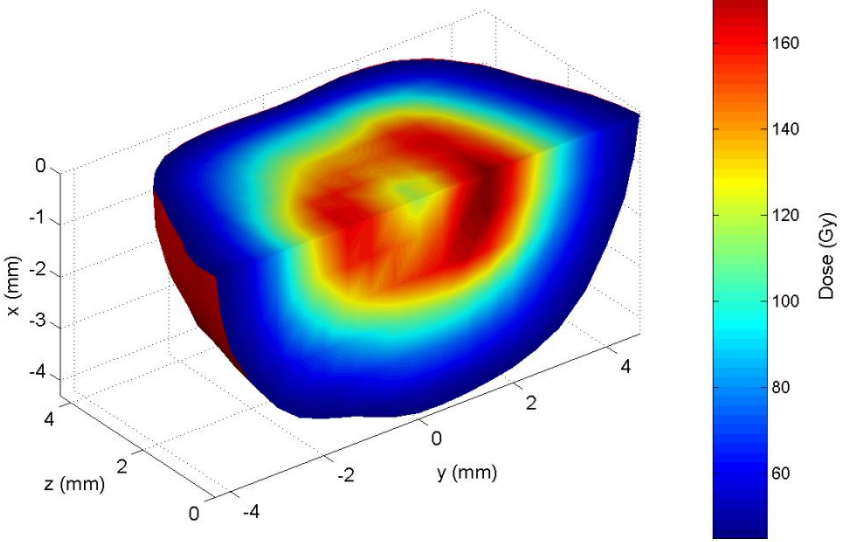

Figures from: Baltas, Sakelliou, Zamboglou (Eds), The Physics of modern brachytherapy for oncology, Taylor & Francis Books Inc, 2006

Example PRESAGE

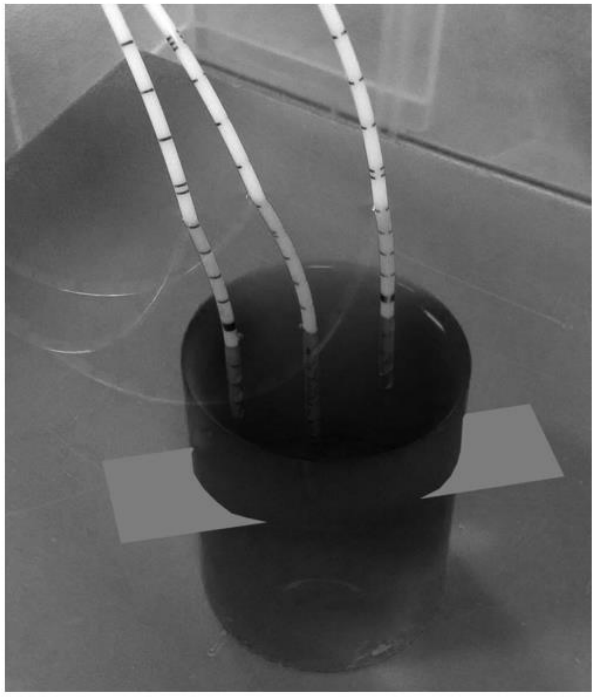

- Palmer et al. Ir-192 HDR dosimetry in TG-43 conditions

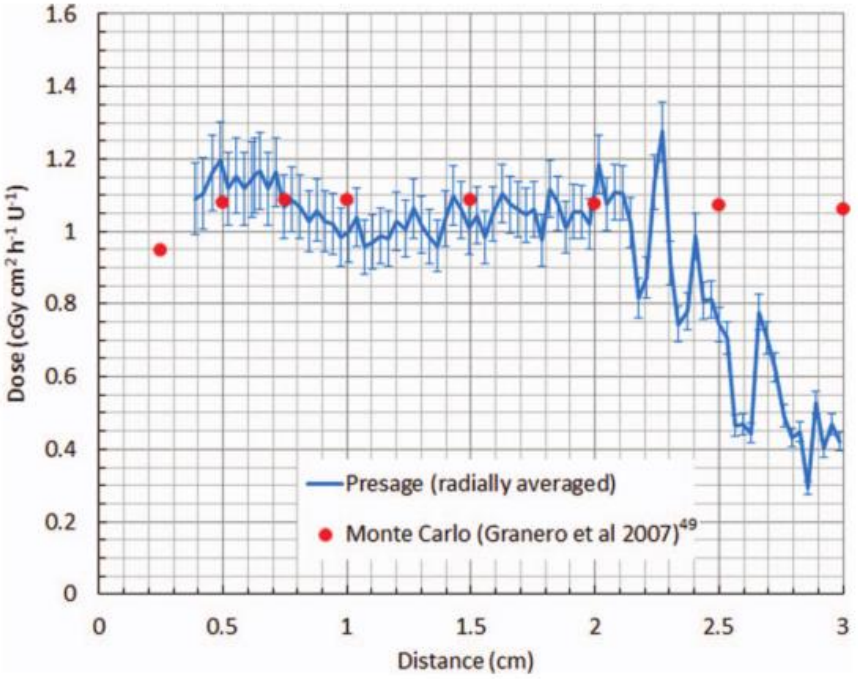

Pictures from: Palmer et al, Med. Phys. 40, 061707 (2013)

Example Truview

calibration

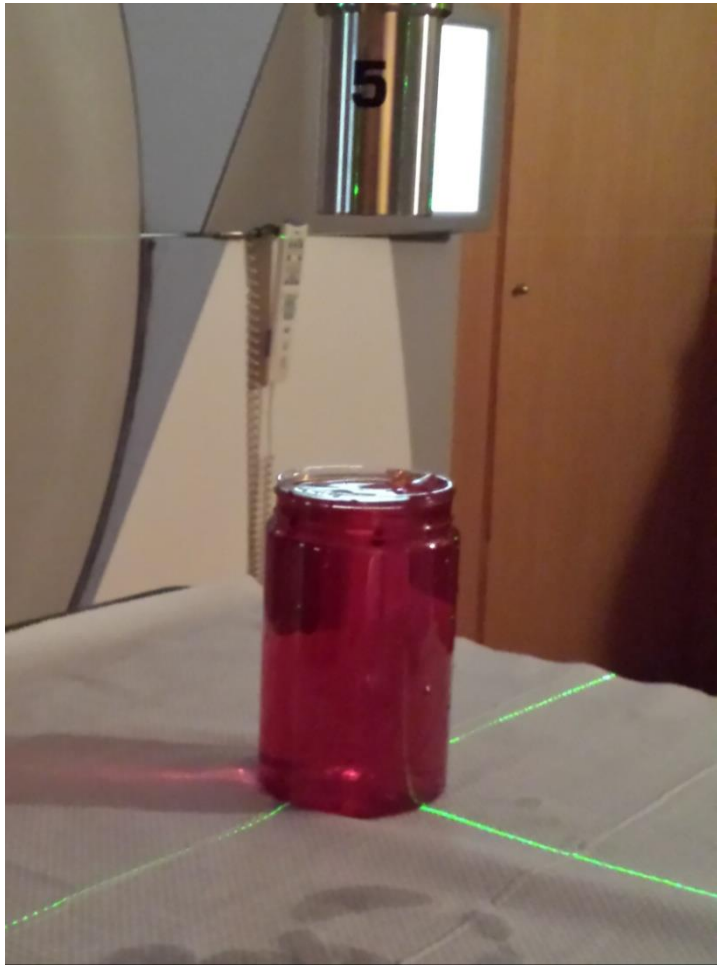

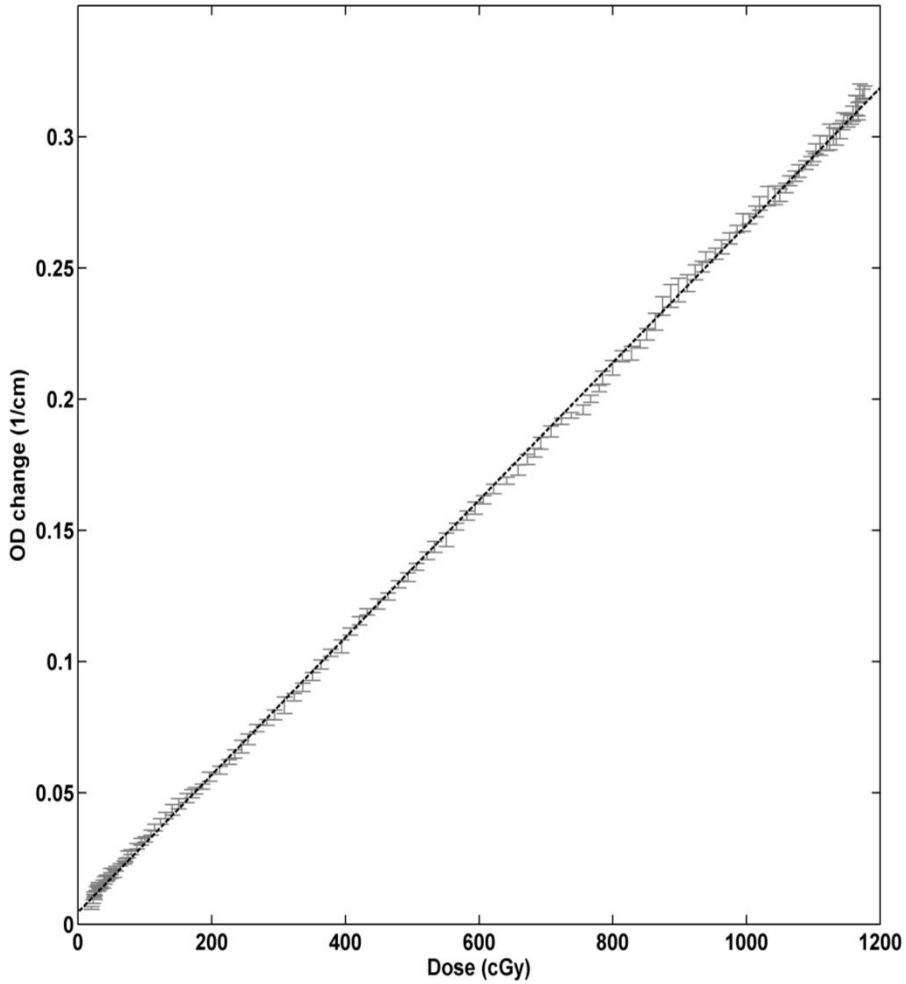

Pappas et al, Phys. Medica 45, 162 (2018)

Example Truview

Set up and planning

(8 Gy to an arbitrary PTV using geometrical optimization)

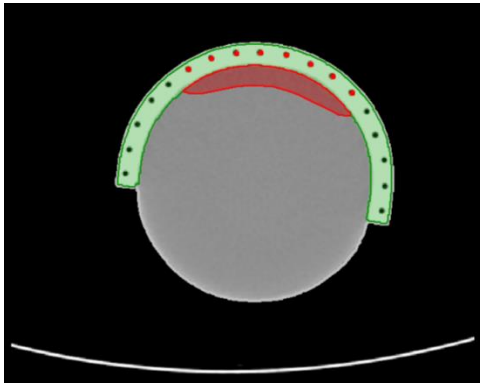

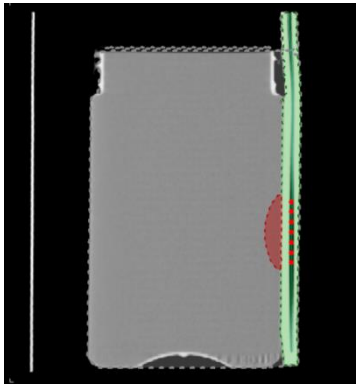

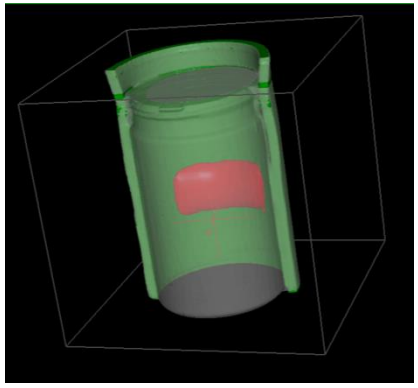

Pappas et al, Phys. Medica 45, 162 (2018)

Example Truview

Source of Uncertainty	Type	Spatial Uncertainty (mm)	Dosimetric Uncertainty (%)
Spatial registration	B	1.5	
Catheter reconstruction	B	0.5	
Calibration linear fitting	B		0.9
Linear accelerator calibration	B		2.1
Source Air Kerma Strength	B		1.5
Temperature variations (± 1.5 °C)	B		3.75
OD change reproducibility	A		1.5
Total standard ($k = 1$)		1.8	4.9
Total expanded ($k = 2$)		–	9.8

Pappas et al, Phys. Medica 45, 162 (2018)

Gamma index maps (2mm/5%) :

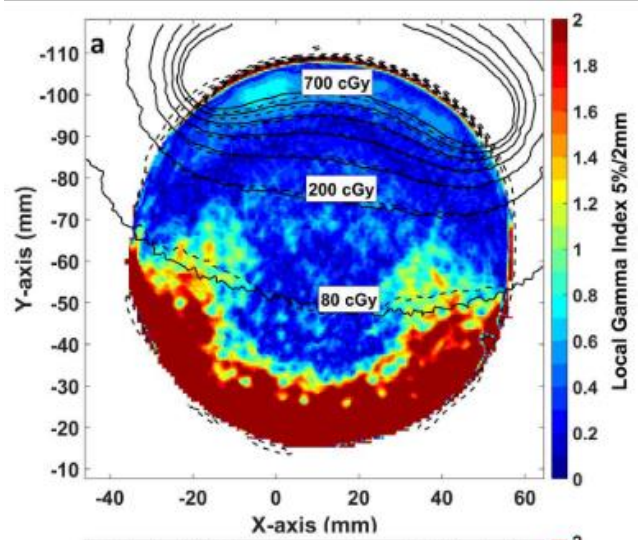

MC versus Truview

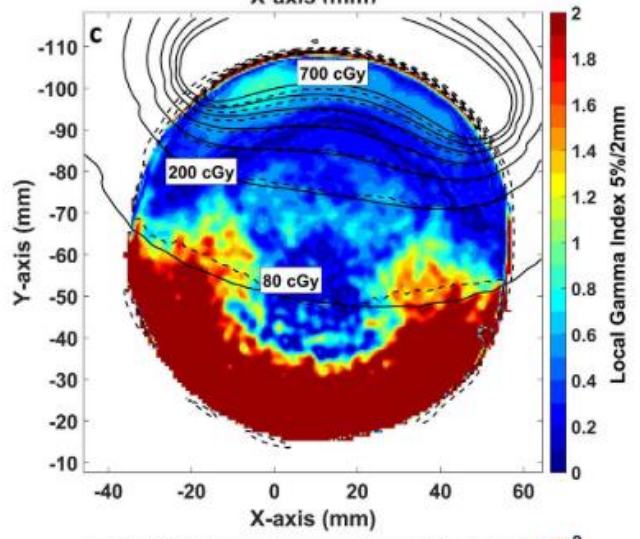

ACE versus Truview

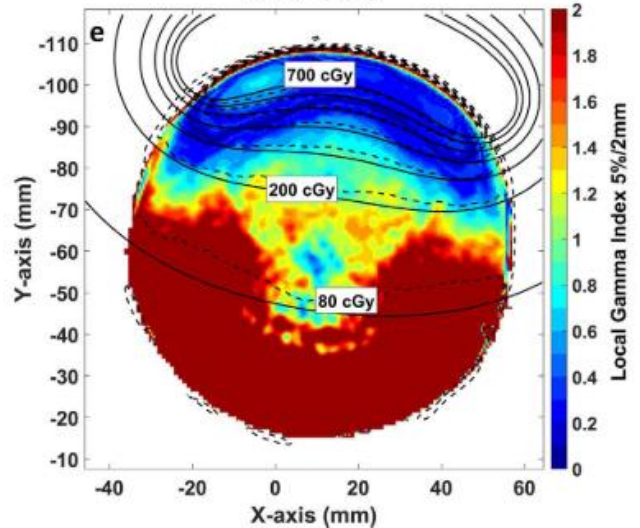

TG-43 vs Truview

Example Truview

Pappas et al, Phys. Medica 45, 162 (2018)

Example commissioning/dose verification

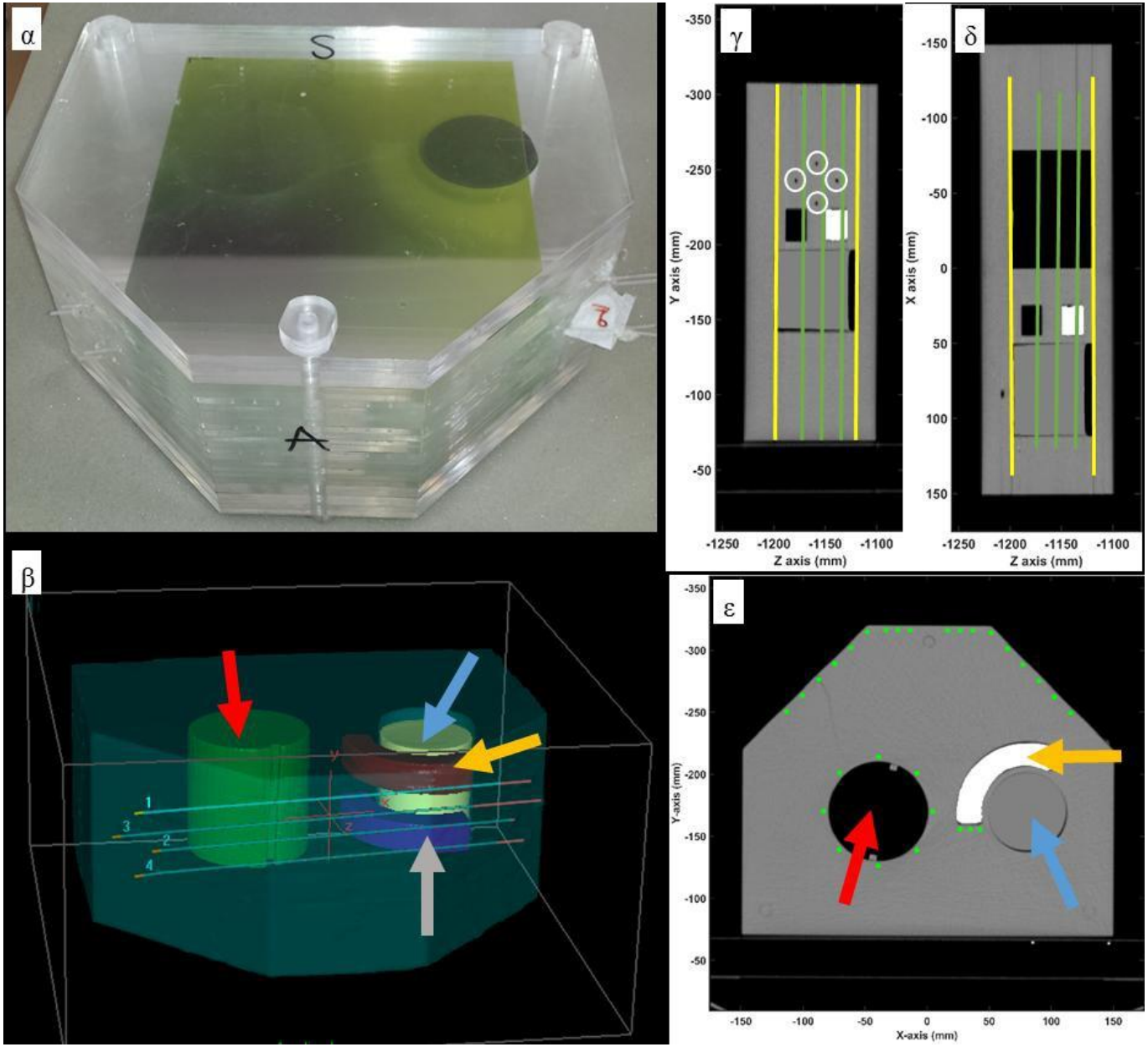

experimental dosimetry for the validation of MBDCA results for Ir-192 HDR

Pappas et al., Phys. Med. Biol. 62(10), 4160 (2017)

Example commissioning/dose verification

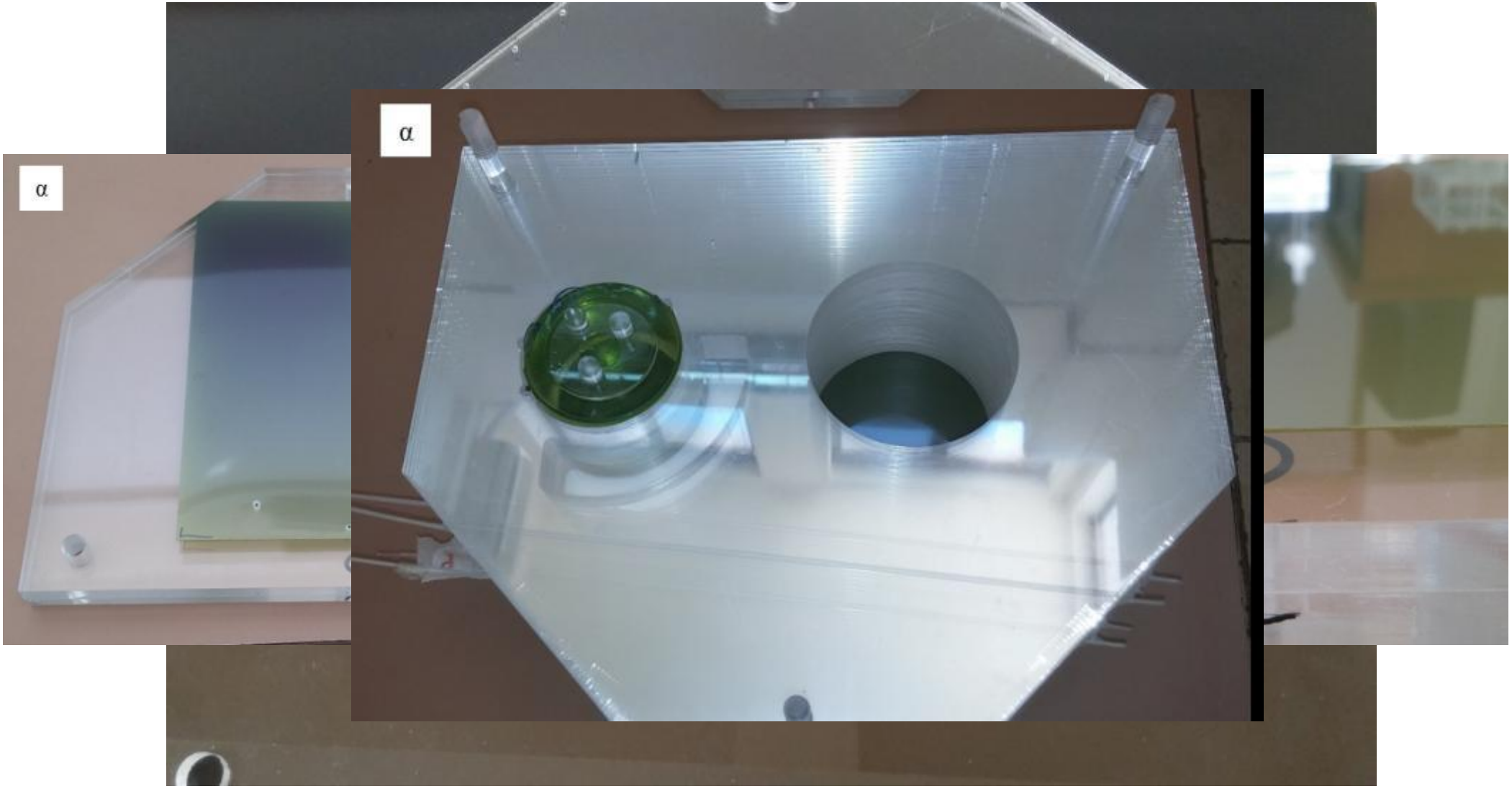

Pappas et al., Phys. Med. Biol. 62(10), 4160 (2017)

Example commissioning/dose verification

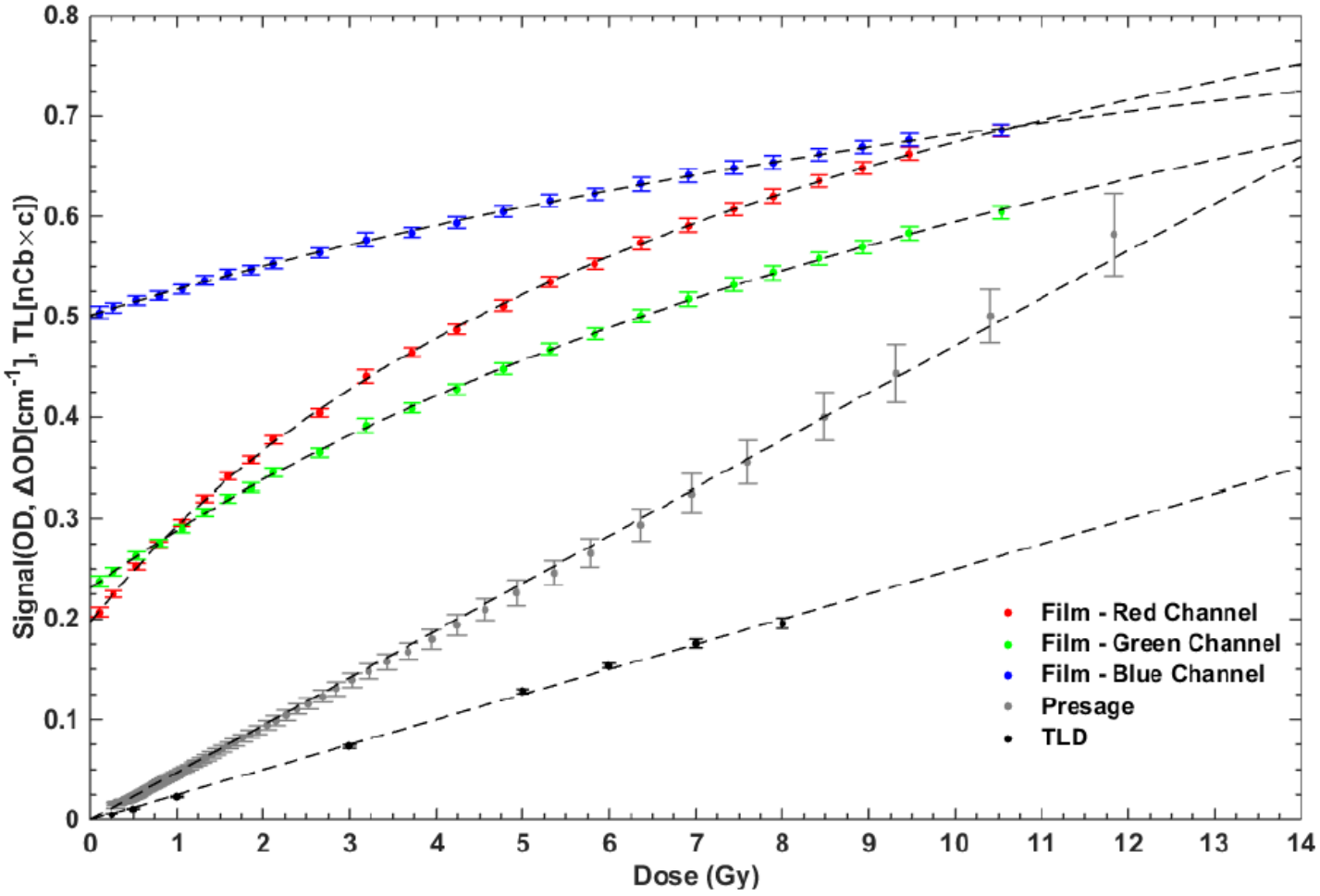

Figure 2: Absorbed dose sensitivity calibration data and calibration curves for the three dosimetric systems used in this work. TLD readings were scaled using a factor $c=52x10^3$.

Pappas et al., Phys. Med. Biol. 62(10), 4160 (2017)

Dosimetric System	Source of Uncertainty	Spatial Uncertainty (mm)	Dosimetric Uncertainty (%)		Ref.
		Type B	Type A	Type B	
TLDs	Detector position	0.5			
	Catheter reconstruction	0.5			
	Calibration			1.51	
	Reference light correction factor		1.81		
	Absorbed dose sensitivity correction		4.28		
	f^{rel}		Position dependent: 1.8 - 3.8		
	Source air kerma strength			1.50	37
	Combined Uncertainty (k=1)	0.71	4.98 - 6.00	2.13	
	Total standard (*k=1*)	0.71	5.4 - 6.4		
	Total expanded (*k=2*)	-	10.8 - 12.7		
EBT3 films	Registration	1.5			
	Catheter reconstruction	0.5			
	Scanner reproducibility		0.25		38, 39
	OD measurement reproducibility		0.30		
	Scanner homogeneity			0.20	38, 39
	Film calibration			Dose dependent: 1.9 - 6.2	
	Source air kerma strength			1.50	37
	$(\bar{S}_{col}/\rho)_{PMMA,w}$			0.5	16
	Combined Uncertainty (k=1)	1.58	0.39	2.48 - 6.40	
	Total standard (*k=1*)	1.58	2.5 - 6.4		
	Total expanded (*k=2*)	-	5.0 - 12.8		
PRESAGE	Registration	2.5			
	Catheter reconstruction	0.5			
	Optical-CT readout reproducibility		2.50		
	Calibration			1.54	
	Source air kerma strength			1.50	37
	Temperature variations (±0.5 °C)			0.85	22
	Temporal stability			2.00	22
	Intradosimeter consistency			2.00	23
	Intrabatch reproducibility			2.00	22
	Combined Uncertainty (k=1)	2.55	2.50	4.16	
	Total standard (k=1)	2.55	4.85		
	Total expanded (k=2)	-	9.7		

Example commissioning /dose verification

Pappas et al., Phys. Med. Biol. 62(10), 4160 (2017)

Example commissioning/dose verification

Table 2: Gamma Index test pass rates for the comparison of calculations and corresponding TLD measurements using the latter as the reference data, as a function of TLD position in the phantom. Distance-to-agreement and dose difference passing criteria were 6% local reference dose and 1 mm, respectively.

Proximal inhomogeneity	**GI pass rate**	
	ACE	**MC**
Phantom boundary	39/ 54	54/54
Air cylinder	20 / 23	21/23
Teflon insert	3 / 3	3/3
Air insert	3 / 3	3/3

Pappas et al., Phys. Med. Biol. 62(10), 4160 (2017)

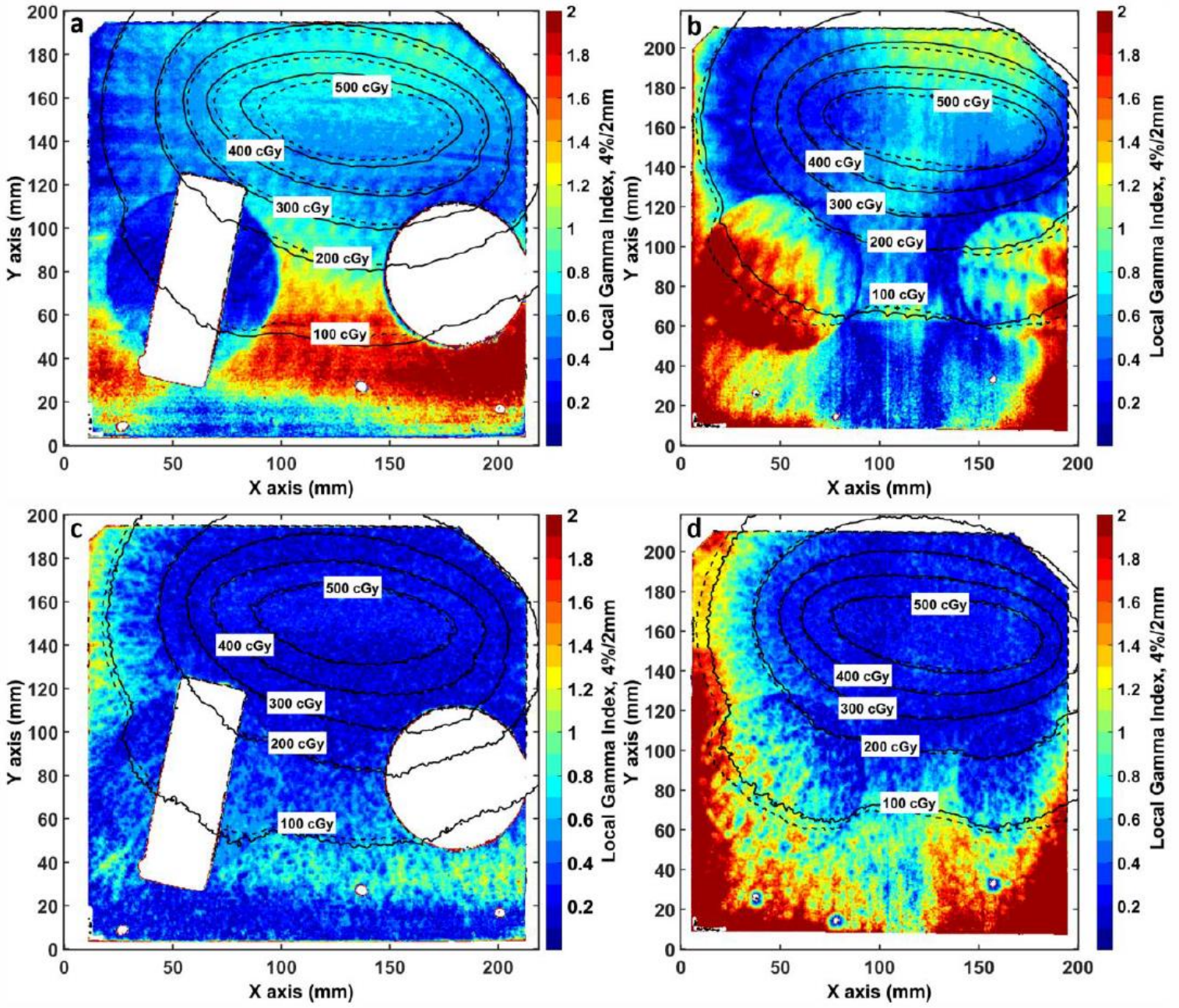

Figure 3: Gamma index maps (4%, 2mm) for Film1 (right) and Film2 (left) with measured (dashed lines) and calculated (solid lines) isodoses. (a-b) , Film – ACE, (c-d) Film – MC.

Example commissioning /dose verification

Pappas et al., Phys. Med. Biol. 62(10), 4160 (2017)

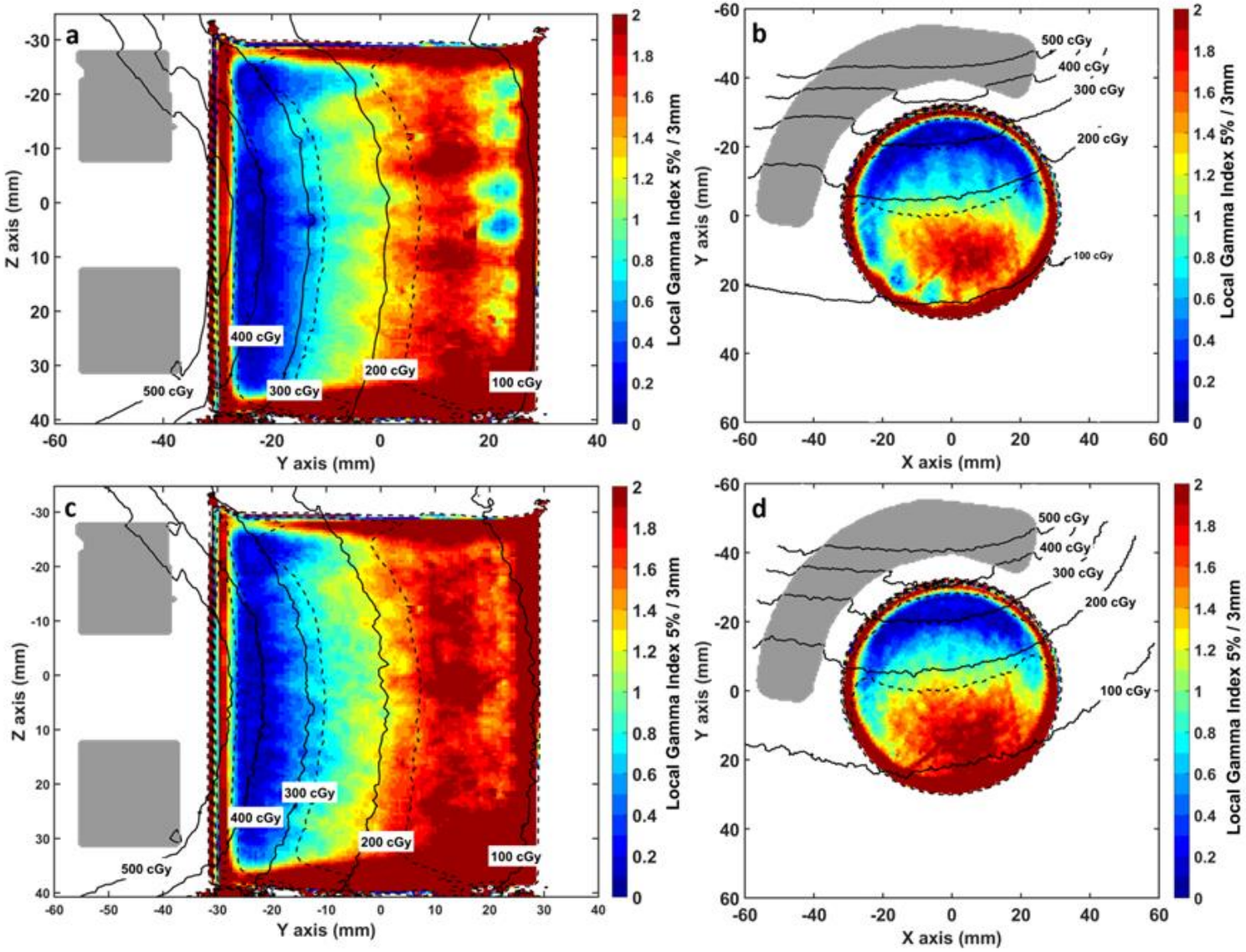

Figure 4: Sagittal (left) and axial (right) slices of gamma index maps (5%, 3mm) for PRESAGE with measured (dashed lines) and calculated (solid lines) isodoses. (a-b) PRESAGE – ACE, (c-d) PRESAGE – MC.

Example commissioning /dose verification

Pappas et al., Phys. Med. Biol. 62(10), 4160 (2017)

Example PRESAGE

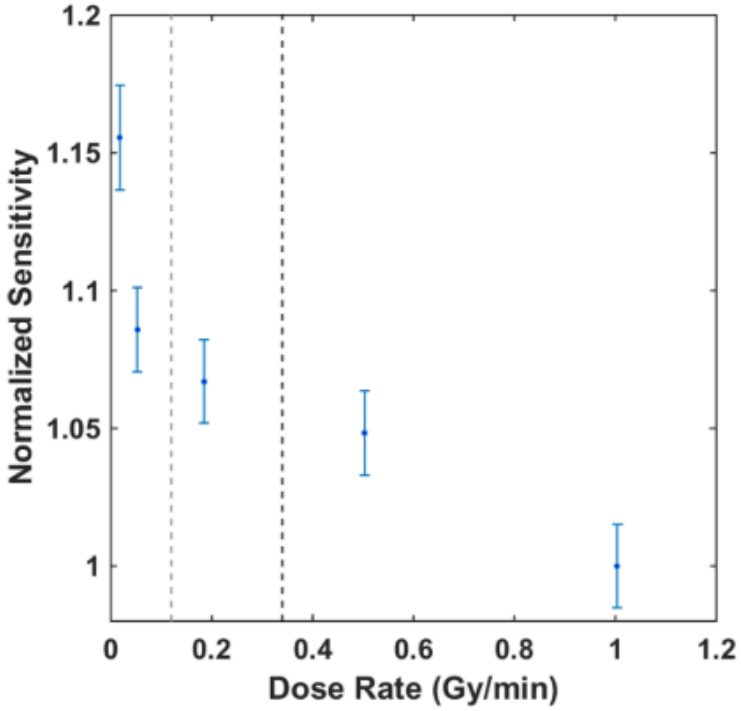

Figure 5. Normalized dose sensitivity as a function of dose rate, measured using PRESAGE cuvette samples from the same batch as the experimental and calibration PRESAGE dosimeters of this work. Data presented for each dose rate correspond to the average relative signal from the 2 cuvettes. Uncertainty bars correspond to the total combined uncertainty at $k = 1$. The gray and black dashed lines correspond to the maximum average dose rate in the experimental PRESAGE irradiation (0.12 Gy min^{-1}) and the minimum dose rate considered from the calibration PRESAGE irradiation (range of 0.34–13.79 Gy min^{-1}), respectively.

relative response variation with dose rates encountered outside the PTV in HDR brachy, measured with PRESAGE cuvvettes

Pappas et al., Phys. Med. Biol. 62(10), 4160 (2017)

Commissioning/dose verification

- Laborious…!
- No single, ideal, system exists
- Registration of measured and calculated dose distributions comes into play

Still there is a way to verify calculations,
albeit,
within the experimental uncertainties

Can’t we do it like the EBRT colleagues do it…?
(active detectors, software support, automation, …)

Further reading …

• Rogers & Cygler (Eds), Clinical dosimetry measurements in radiotherapy (2009 AAPM Summer School), Monograph No. 34, Medical Physics Publishing 2011

• Rivard, M.J. et al., 2004. Update of AAPM Task Group No. 43 Report: A revised AAPM protocol for brachytherapy dose calculations. Medical Physics, 31(3), p.633.

• Perez-Calatayud, J. et al., 2012. Dose calculation for photon-emitting brachytherapy sources with average energy higher than 50 keV: report of the AAPM and ESTRO. Medical physics, 39(5), pp.2904–29.

and references cited herein

Valencia, 07 – 10 October 2018

ESTRO School

Advanced Brachytherapy Physics

WWW.ESTRO.ORG/SCHOOL

Treatment Delivery Verification

Dimos Baltas, Ph.D.

Professor for Medical Physics in Radiation Oncology

Division of Medical Physics
Department of Radiation Oncology, Medical Center - University of Freiburg
Faculty of Medicine, University of Freiburg, Germany
and
German Cancer Consortium (DKTK), Partner Site Freiburg, Germany

E-mail: dimos.baltas@uniklinik-freiburg.de

Modern Brachytherapy: Treatment Verification – An Example

- **The planned treatment delivery**

CT-Verification

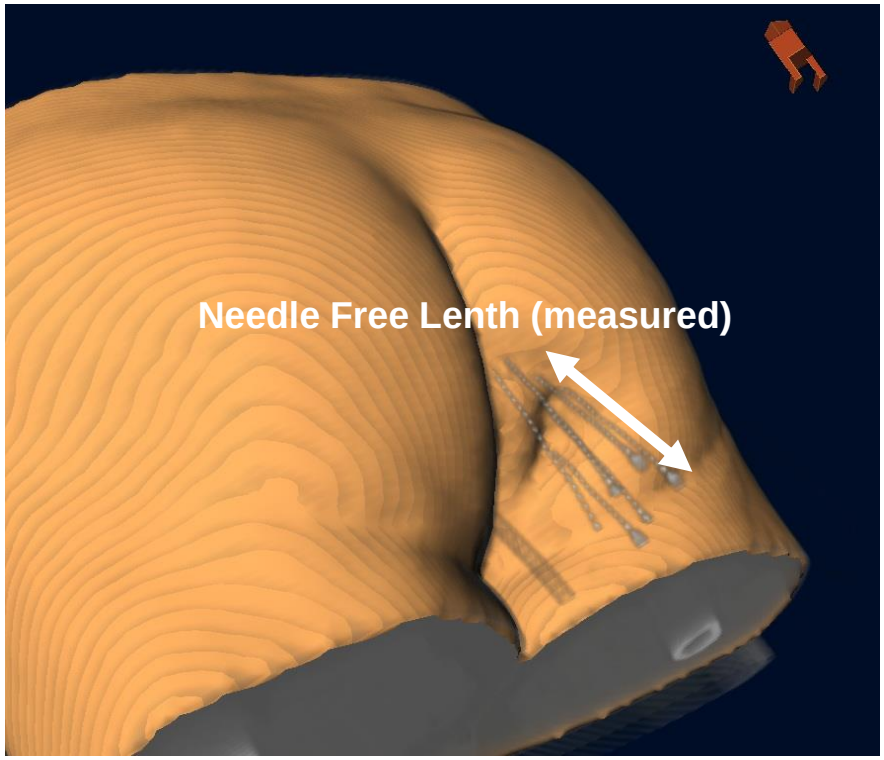

CT-Planning

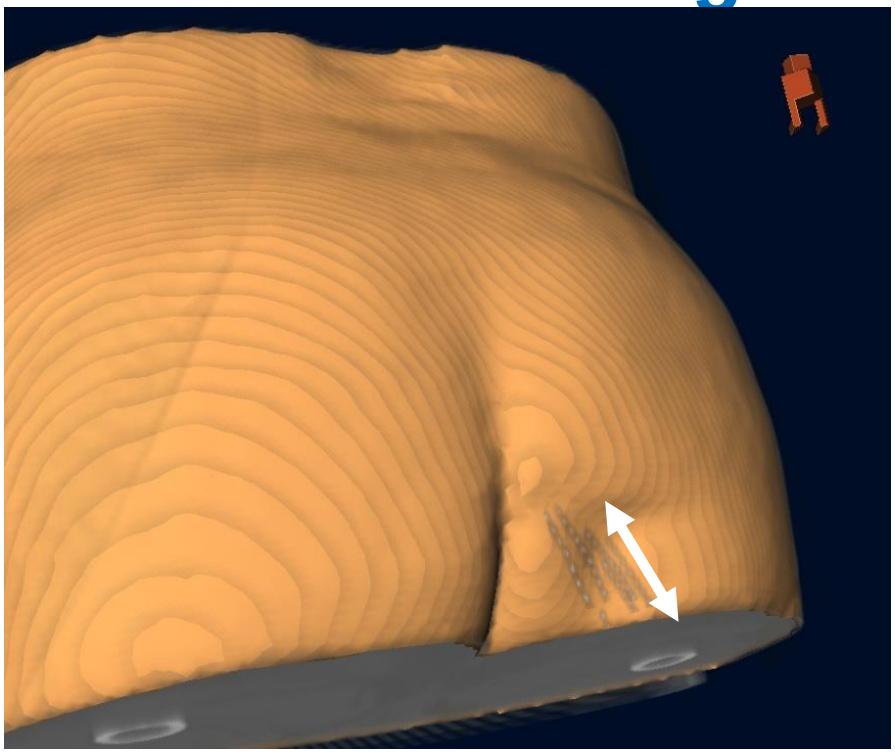

Needle free length

- **measured after implantation and before CT-imaging**
- **controlled before each fraction**

Modern Brachytherapy: Treatment Verification – An Example

- *Delivered* Treatment versus *Planned* Treatment

CT-Verification I **CT-Verification II** **CT-Planning**

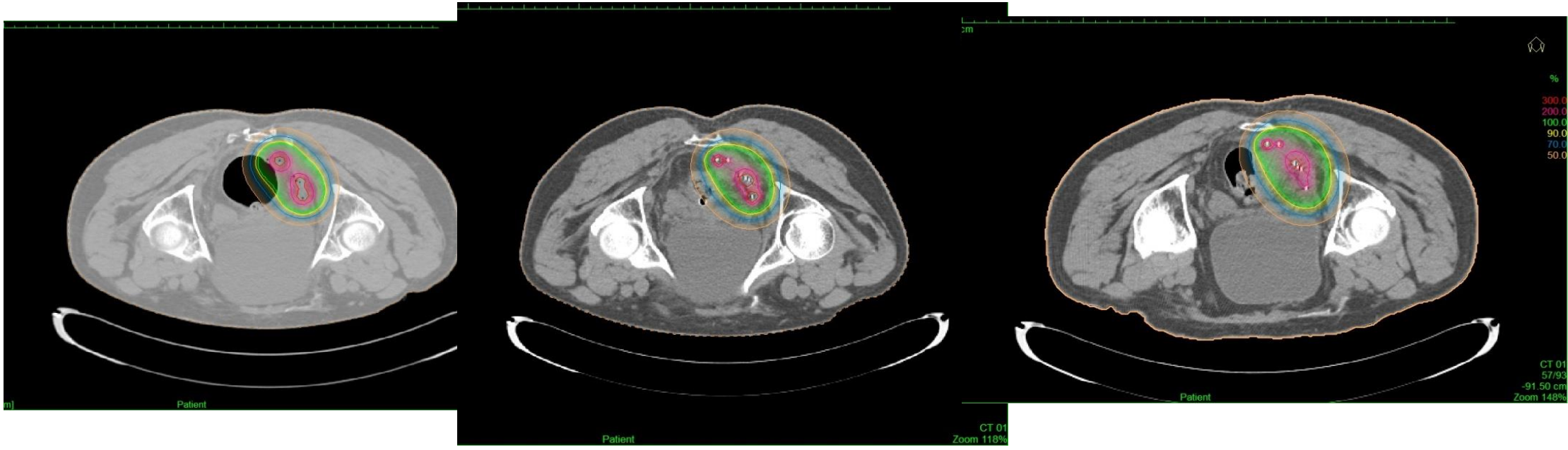

Modern Brachytherapy: Treatment Delivery Verification

- *Delivered* Treatment versus *Planned* Treatment

Currently we assume that:

- The **geometry** and **location** of the implanted catheters
- The connection of **channels** to implanted catheters
- The length of the channels
- The source movement patterns (**dwell positions and dwell times**) within the implanted catheters
- The patient **anatomy** at the relevant **location**

are during treatment delivery exact as considered and planned in the RTP.

BRT *versus* EBRT ***Similarities*** and Differences

Dosimetric Kernel → **Particles** ✓
(Spot)

Delivery Technology → **IMRT (X, P)** ✓
(Modulation, Dose-Volume-Prescription)

Dose Distribution → **SRS / SBRT** ✓
(Inhomogeneity)

BRT *versus* EBRT Similarities and *Differences*

- **Beam Delivery System in BRT**

Beam	**=**	**Implanted Catheter/Needle/Applicator**
MLC Settings	**=**	**Source moving patterns within implanted Catheter/ Needle/Applicator**
Monitor Units	**=**	**Dwell Times**

Thus "beams" become for BRT *patient-dependent parameters*, that requires 3D reconstruction (Localization: Imaging, …) and registration to anatomy

BRT *versus* EBRT Similarities and *Differences*

- **Verification**

  We mean the *process* of proof that we deliver the dose we planned to the tissue (3D) within a specific accuracy and precision level.

- **BRT (HDR)**

  In opposite to EBRT our dose delivery system (stepping source within implanted catheters) *depends on the specific patient implant geometry (anatomy)*.

  This is not the case for EBRT, where the performance of the dose delivery system itself (MLC, Dose Rate, Energy, Gantry Angle, Collimator Angle & Couch Settings) is independent of the specific patient.

Where are we today in EBRT?

- Verification of individual RT-Plan via 2D/3D measurements:
  RTP(Phantom) + Machine as an Off-Line Pre-Treatment-Procedure
- Dose Reconstruction in Patient Anatomy utilising Off-Line 3D-measurements: RTP + Machine
- 3D-Dose Verification in Patient-customized Phantom
  Off-Line 3D-measurement: RTP + Machine + Set-Up
- Real-Time Fluence Measurement during Treatment and Dose Reconstruction: RTP + Machine + Set-Up + Patient
- ...

Where are we today in EBRT?

Example of a PCA-IMRT Offline Pre-Treatment Procedure: *RTP (Phantom) + Machine*

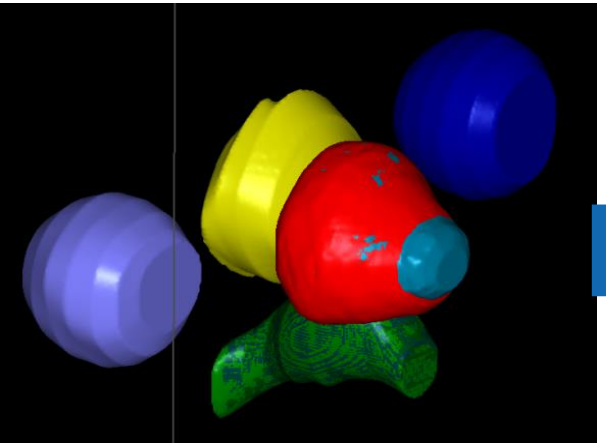

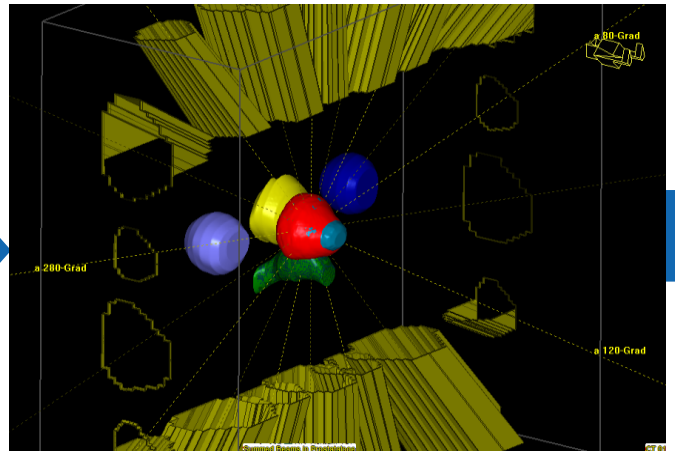

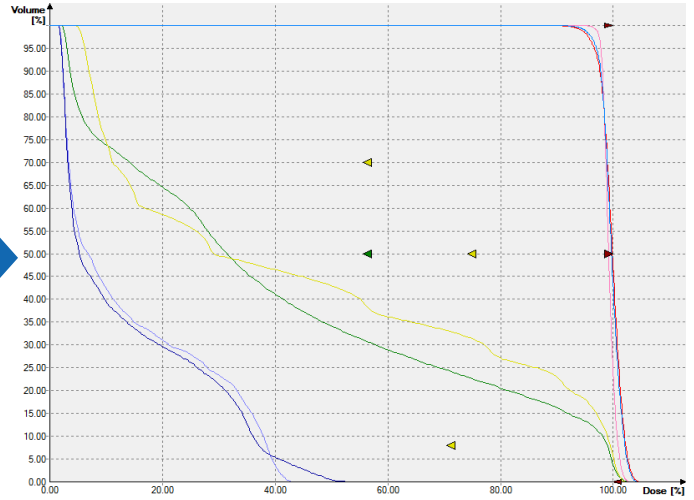

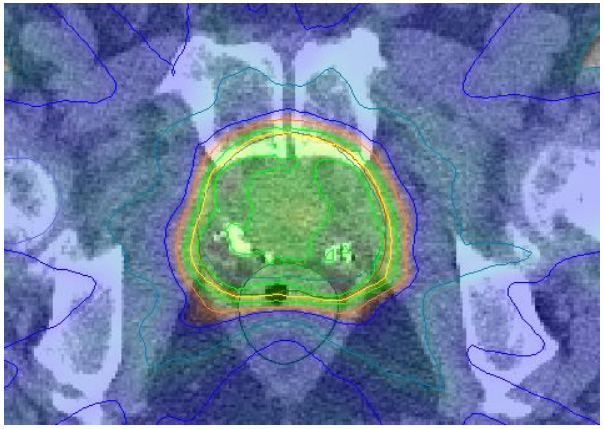

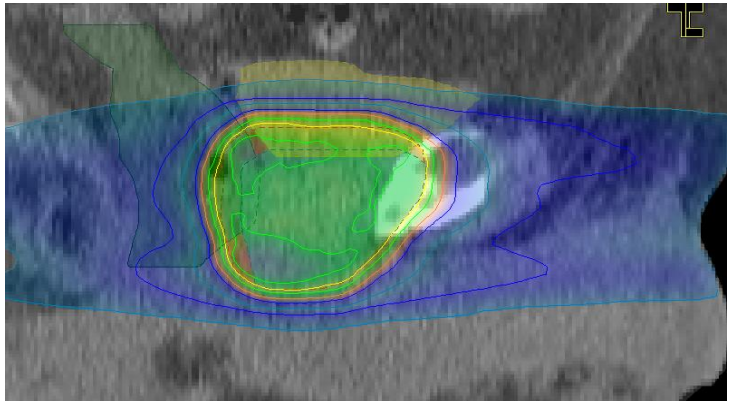

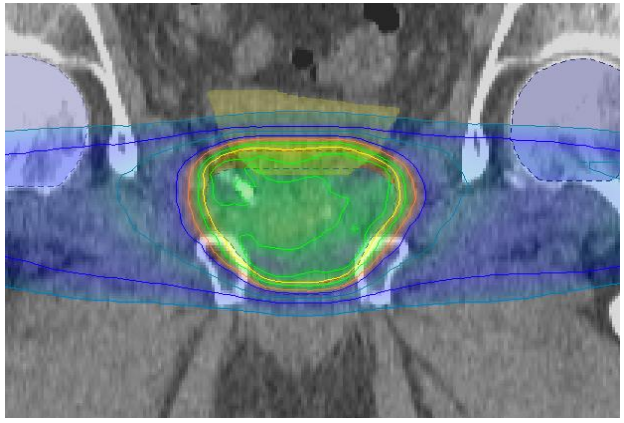

Where are we today in EBRT?

Example of a PCA-IMRT Offline Pre-Treatment Procedure: *RTP (Phantom) + Machine*

RTP: Automatic transfer to phantom geometry

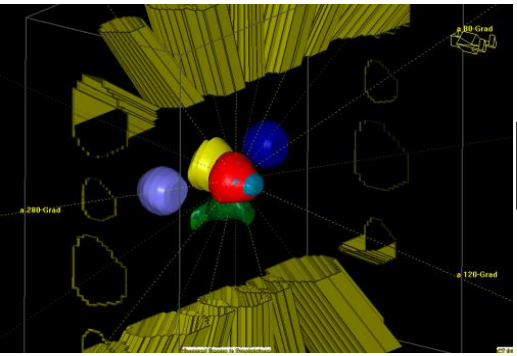

RTP

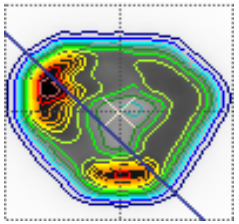

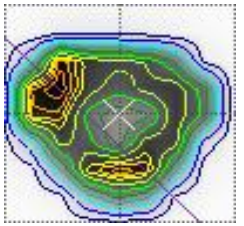

Meas.

Compare

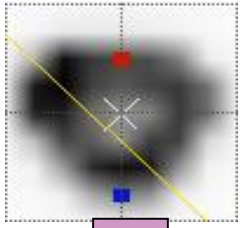

Gamma-3D

RTP + Machine: Individual Plan

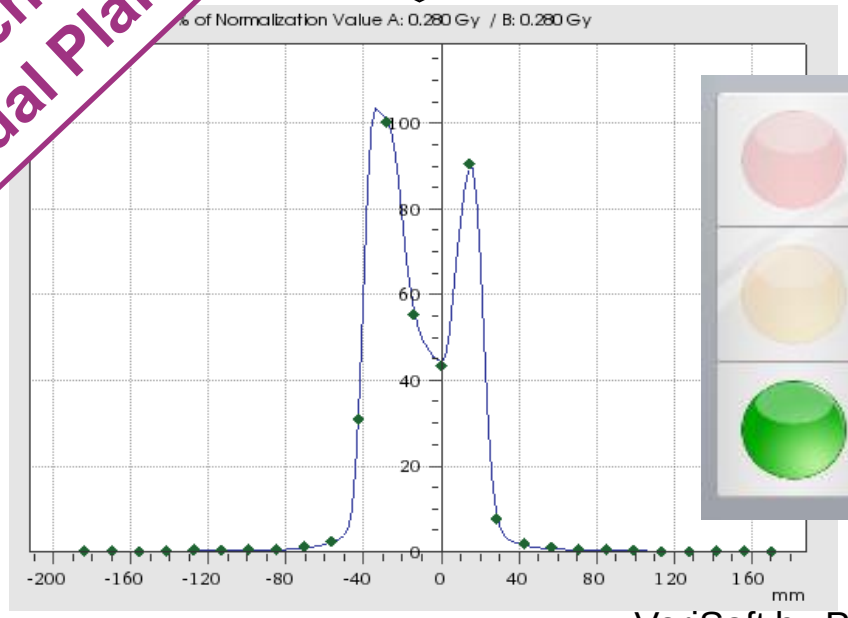

Decision

VeriSoft by PTW

Fluence / Intensity Maps

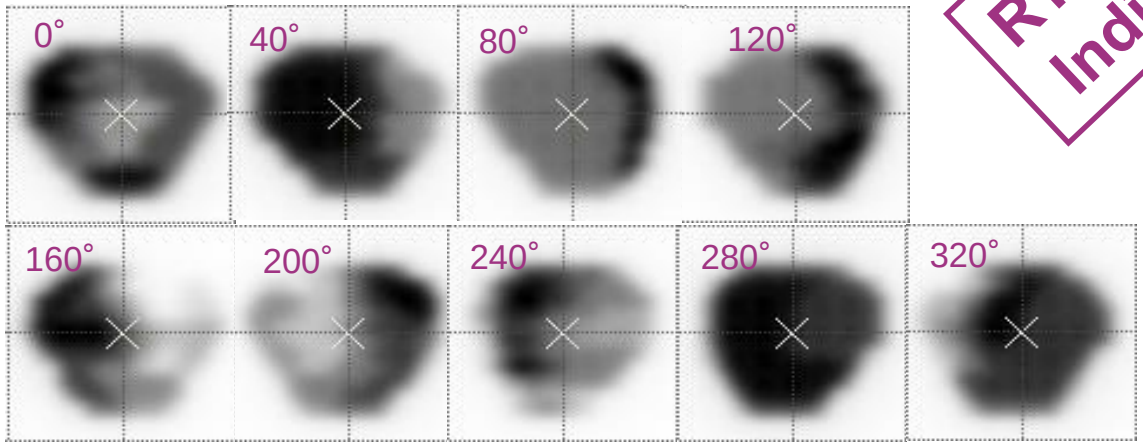

Where are we today in EBRT?

Example of Dose Reconstruction in Patient Anatomy utilising Off-Line 3D-measurements: *RTP + Machine*

White Paper October 2013 D913.200.06/00

Dose reconstruction in the OCTAVIUS 4D phantom and in the patient without using dose information from the TPS

B. Allgaier, E. Schüle, J. Würfel

PTW-Freiburg Physikalisch-Technische Werkstätten Dr. Pychlau GmbH
Lörracher Straße 7, 79115 Freiburg, Germany

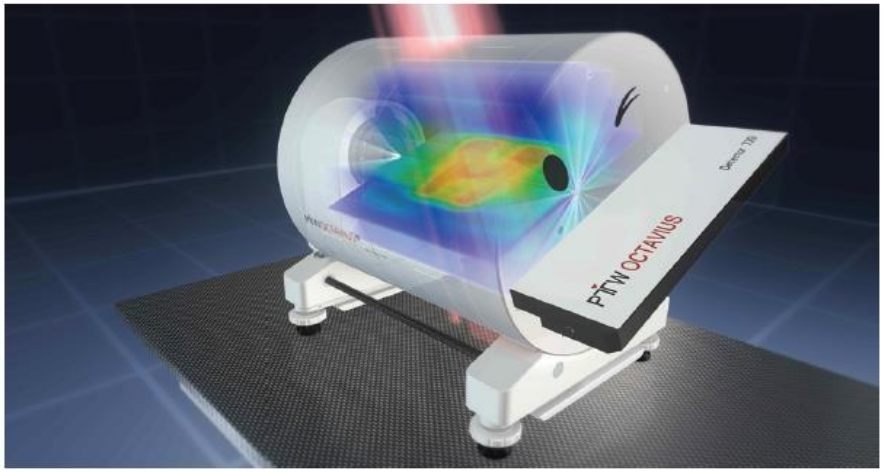

Fig. 1 *The OCTAVIUS 4D system. The detector panel is inserted in a cylindrical phantom that rotates synchronously with the gantry. Detector panels with different spatial resolutions are available. The Detector 729 features 10 mm resolution, the central region of the Detector 1000^{SRS} features 2.5 mm.*

Where are we today in EBRT?

Example of Dose Reconstruction in Patient Anatomy utilising Off-Line 3D-measurements: *RTP + Machine*

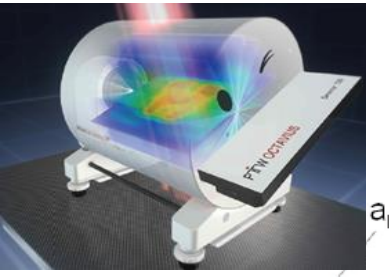

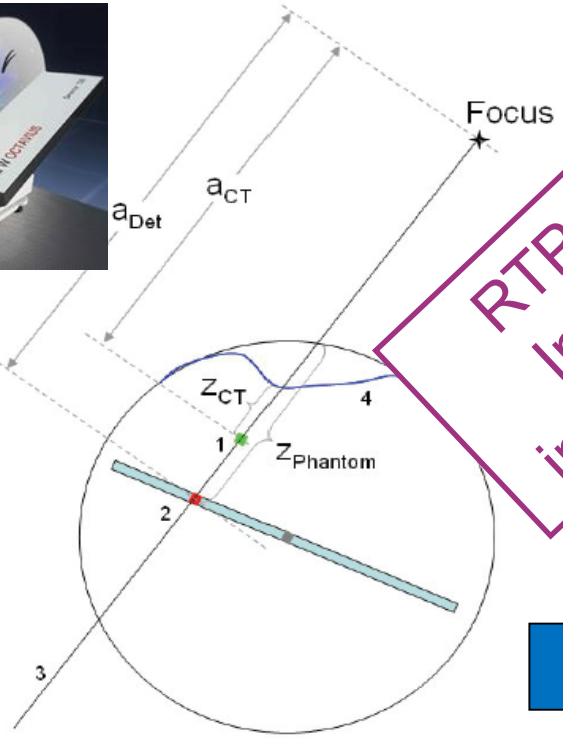

RTP + Machine: Individual Plan in Patient Geometry

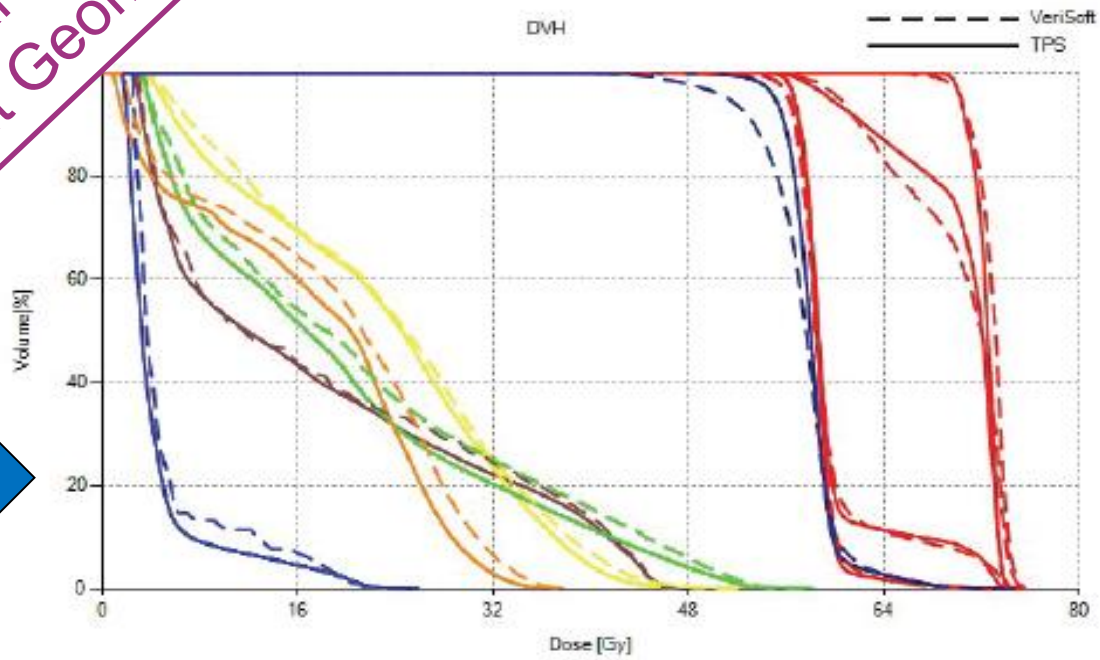

Fig. 2 *OCTAVIUS 4D phantom with ray line (3) through focus and current detector (2), not to scale. The contour (4) is the patient surface from the CT image. The current detector measures the dose D_{Det} at the water-equivalent depth $z_{Phantom}$. The algorithm reconstructs the dose D_{CT} for the current voxel (1) at the water-equivalent depth z_{CT} in the CT image. a_{Det} and a_{CT} are geometrical distances from the focus to the current detector and to the current voxel, respectively.*

Fig. 3 *Dose volume histograms in the patient's geometry determined by OCTAVIUS 4D (dashed lines) and by the TPS (solid lines)*

Where are we today in EBRT?

Example of 3D-Dose Verification in
Patient-customized Phantom:
Off-Line 3D-measurement: *RTP + Machine + Set-Up*

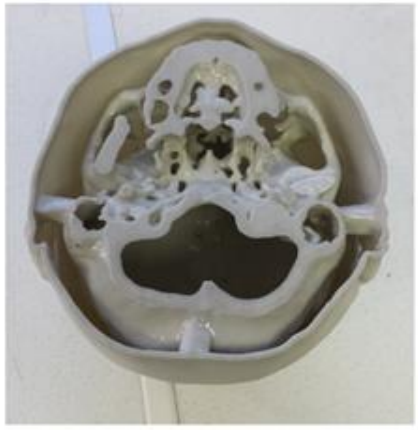

Where are we today in EBRT?

Example of 3D-Dose Verification in Patient-customized Phantom:
Off-Line 3D-measurement: *RTP + Machine + Set-Up*

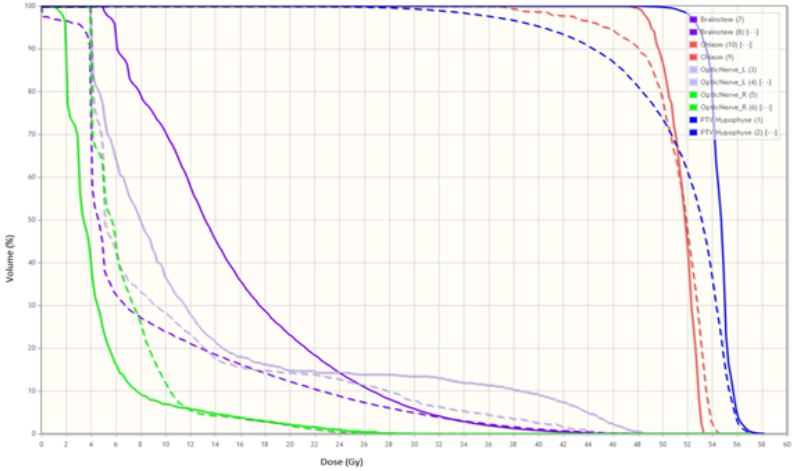

RTP + Machine + Set-Up:
Individual Plan
in Patient Geometry

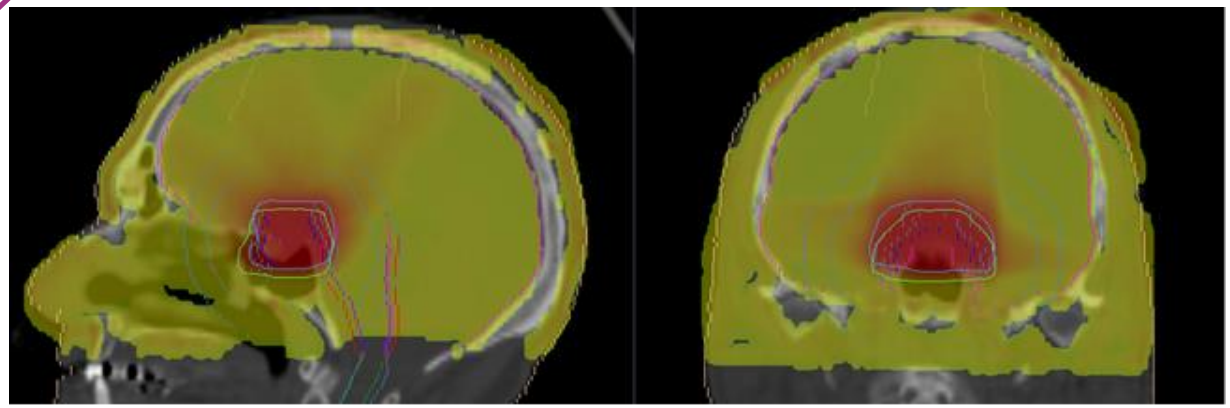

RTsafe

Where are we today in EBRT?

Example of Real-Time Fluence Measurement during Treatment and Dose Reconstruction:

RTP + Machine + Set-Up + Patient

**Two Years of Clinical Experience with DAVID –
A Translucent Multi-Wire Detector for On-Line Verification of Patient Treatments**

B. Poppe[1+2], H.K. Looe[1+2], A. Rühmann[1+2], Y. Upphoff[2], K. Willborn[2] and D. Harder[3]
[1]WG Medical Radiation Physics, Carl von Ossietzky University,Oldenburg Germany
[2]Pius-Hospital, Oldenburg, Germany
[3]Prof. emer., University of Göttingen, Germany

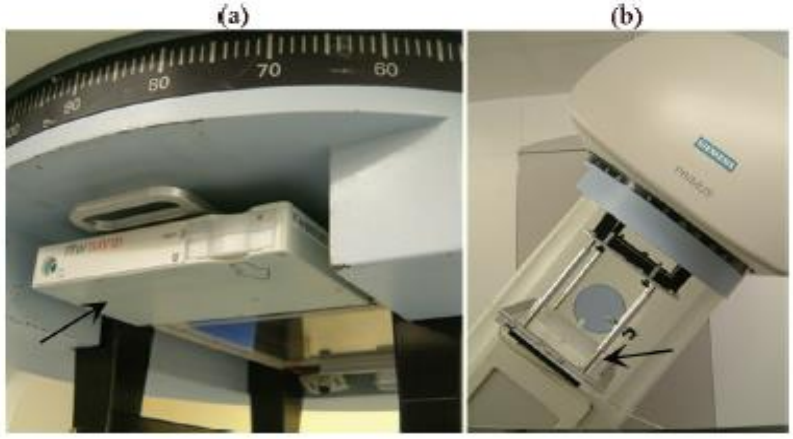

Fig. 1. (a) The DAVID transmission detector array, serving for permanent supervision of the MLC, at its operation position in the accessory holder of the Siemens PRIMUS accelerator. (b) The 2D-ARRAY, serving for daily accelerator checks and dosimetric plan verification, at its operation position in the gantry mount of the Siemens PRIMUS accelerator.

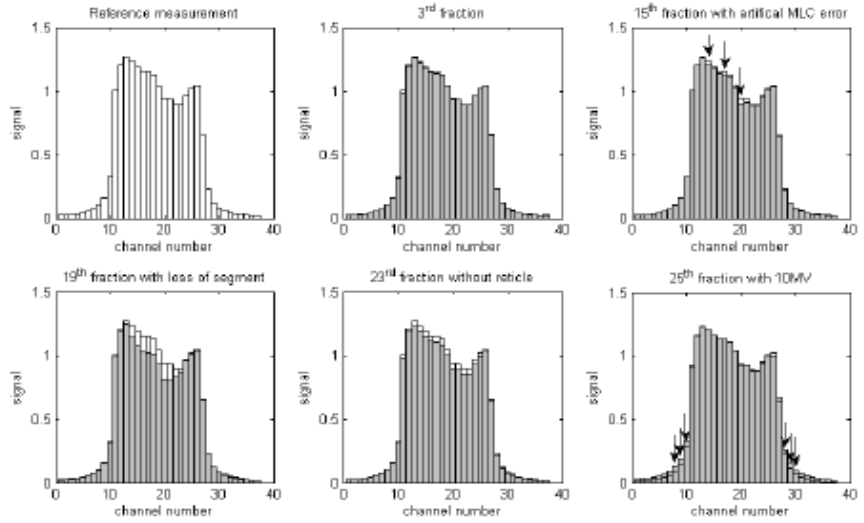

Fig. 2 Examples of the measured DAVID channel signals at gantry angle 0° for some selected fractions. Artificial errors, introduced in the 15th, 19th, 23rd and 25th fraction, were detected as deviations from the reference signals. Figure taken from (3).

Where are we today in EBRT?

Example of Real-Time Fluence Measurement during Treatment and Dose Reconstruction:

RTP + Machine + Set-Up + Patient

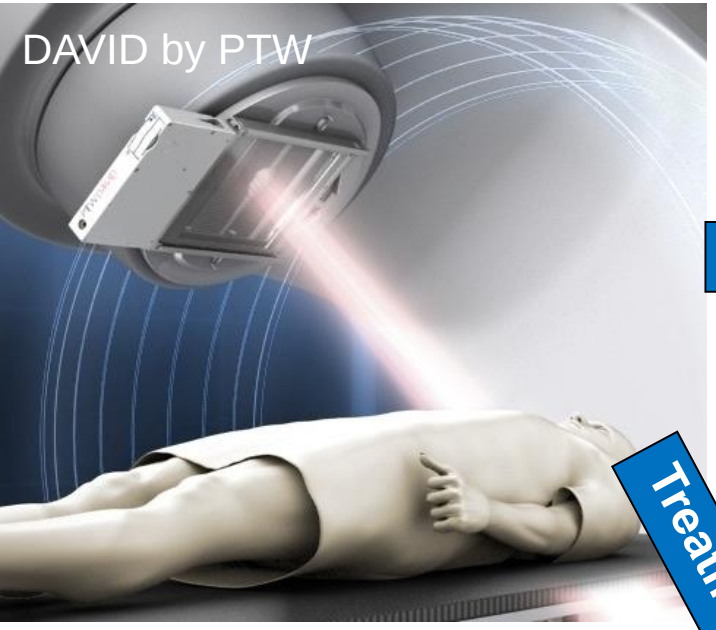

delivered

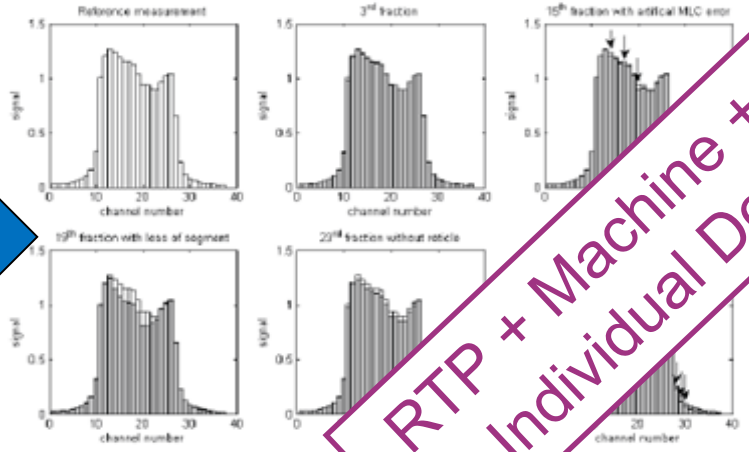

RTP + Machine + Set-Up + Patient:
Individual Delivered Treatment

Treatment

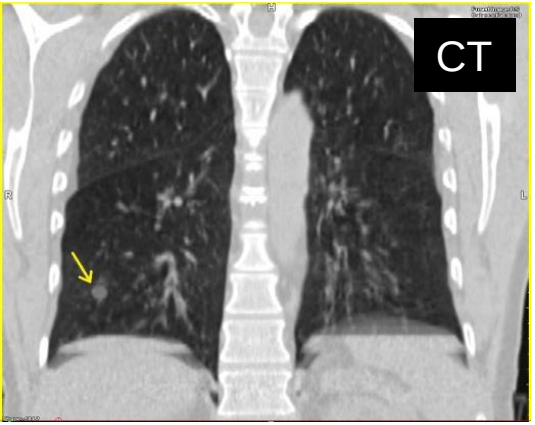

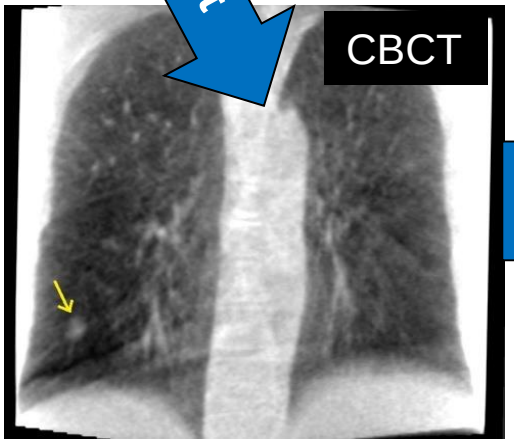

RTP

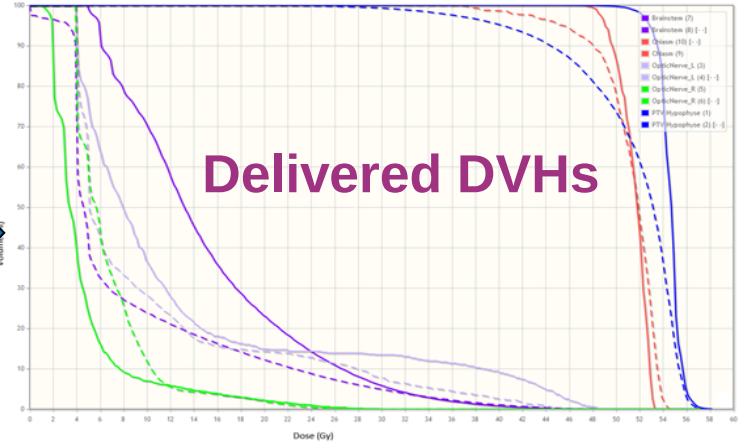

Where are we today in EBRT?

Example of Anatomy (Target) based Verification of Positioning:

Patient (PTV) + Machine + Set-Up + ... (Targeting)

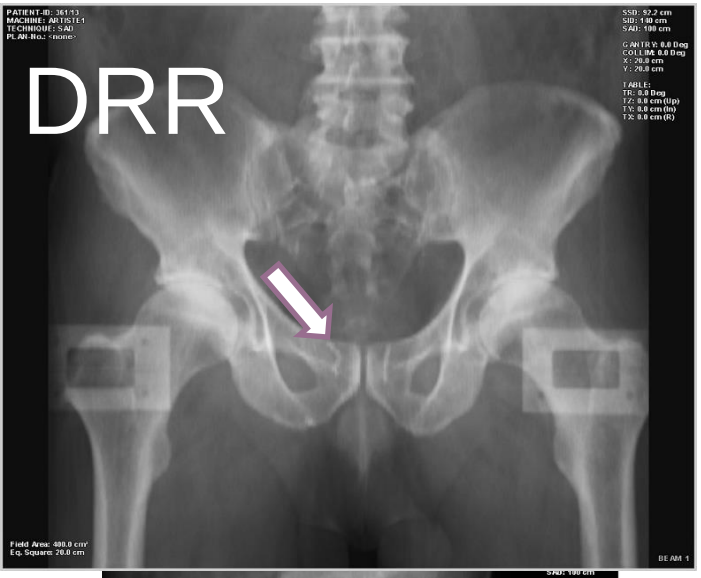

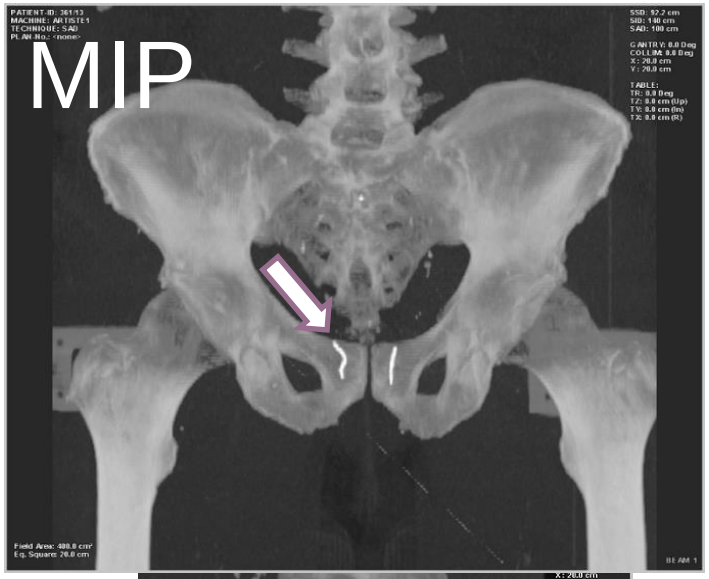

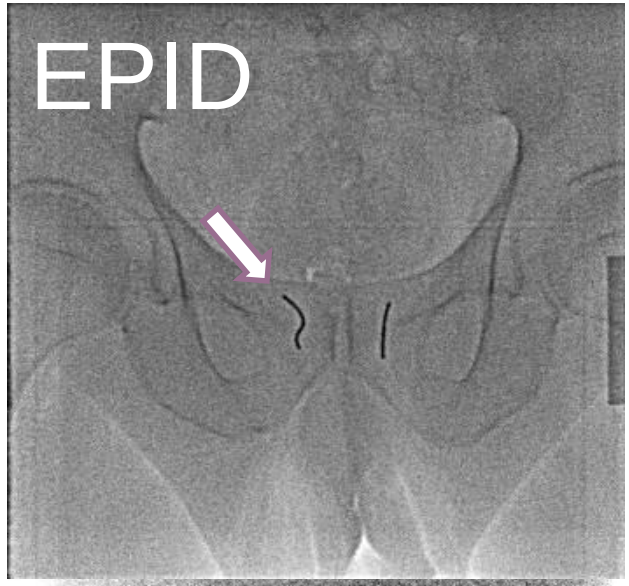

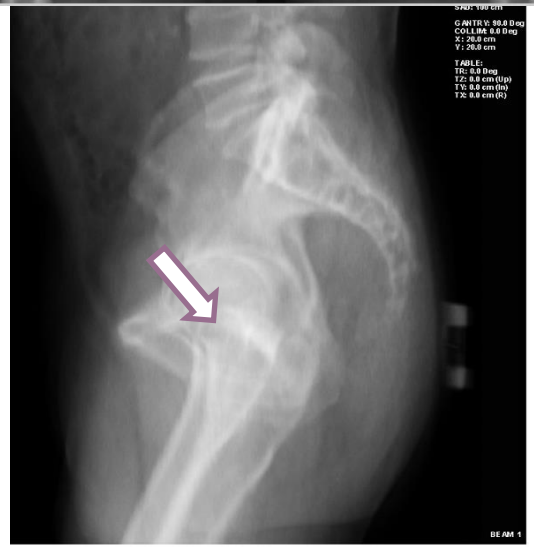

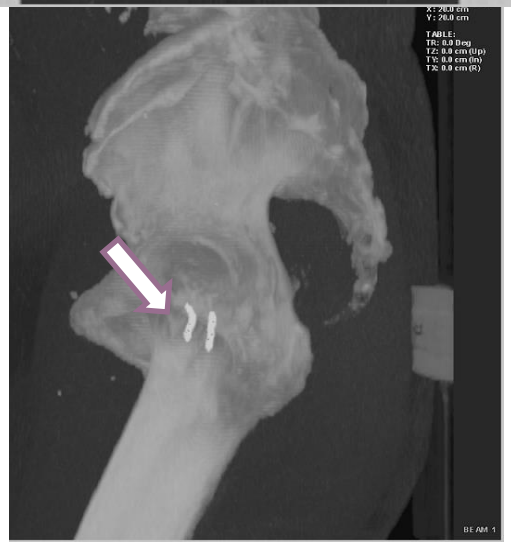

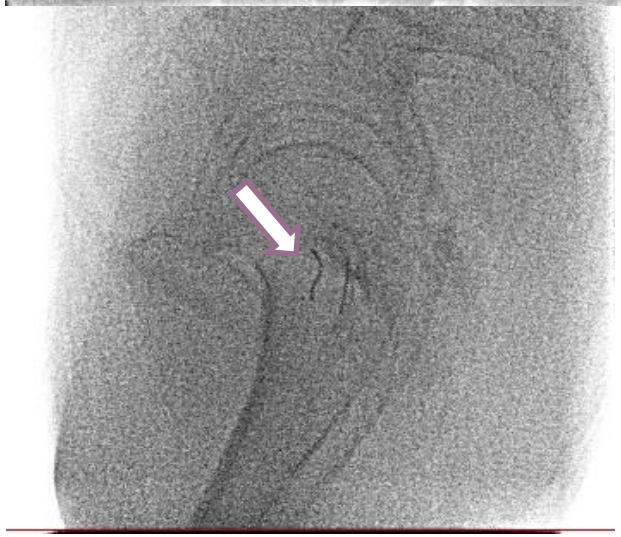

BRT *versus* EBRT Similarities and Differences

- The Verification Process
  - What is the "DRR" in BRT?
  - What is the "BEV" in BRT?
  - What is the "EPID" in BRT?
  - What is the "Fiducial" in BRT?
  - What is the "measurable Beam Fluence" in BRT?
  - What is the "Fingerprint" of a "Beam-Delivery" in BRT?
  - What is the "individual plan verification process" in BRT?
  - ???

BRT *versus* EBRT Similarities and Differences

- The Verification Process

  The majority of those tools and/or processes *are not defined at all and are not implemented / are not part* of the current clinical treatment planning and treatment delivery procedure (RTP)!

Modern Brachytherapy: Treatment Delivery Verification

- *Delivered* Treatment versus *Planned* Treatment

Currently we assume that:

- The geometry and location of the implanted catheters
- The connection of channels to implanted catheters
- The length of the channels
- The source movement patterns (dwell positions and dwell times) within the implanted catheters
- The patient anatomy at the relevant location

are during treatment delivery exact as considered and planned in the RTP.

Modern Brachytherapy: Treatment Delivery Verification

Educational Activity Corner

Review paper

Electromagnetic tracking for treatment verification in interstitial brachytherapy

Prof. Christoph Bert, PhD[1], Markus Kellermeier, PhD[1], Prof. Kari Tanderup, PhD[2,3]

[1]Department of Radiation Oncology, Universitätsklinikum Erlangen, Friedrich-Alexander-Universität Erlangen-Nürnberg, Erlangen, [2]Department of Oncology, Department of Medical Physics, Aarhus University Hospital, Aarhus, Denmark, [3]Institute of Clinical Me Aarhus University, Aarhus, Denmark

Abstract

Electromagnetic tracking (EMT) is used in several medical fields to determine the position and orientatio ed sensors, e.g., attached to surgical tools. Recently, EMT has been introduced to brachytherapy for implan tion and error detection. The manuscript briefly summarizes the main issues of EMT and error detection in apy. The potential and complementarity of EMT as treatment verification technology will be discussed i *in vivo* dosimetry and imaging.

J Contemp Brachytherapy 2016;
DOI: 10.5114/j

Table 1. Errors and variations in brachytherapy along with the potential of detectability by real-time *in vivo* dosimetry (IVD), real-time imaging (each according to [19,22,23]), and real-time electromagnetic tracking (EMT). The probability of error and the potential effect were reported by Kertzscher *et al.* [23], i.e. only the classification of detectability by real-time EMT and the needed EMT coordinate systems is original in this manuscript. The EMT coordinate systems refer to: «E», the intrinsic coordinate system of the EMT device; «F» fiducial markers visible in imaging and EMT reproducibly placed during each treatment fraction; «A» an absolute cross-calibration between EMT and imaging as, e.g., reported by Bharat *et al.* for transrectal ultrasound and EMT [24]. A schematic drawing of the coordinate system options is shown in Figure 2. (✓) refers to partially applicable

Quality item	Detectability			EMT coordinate system	Error probability and effect [23]	
	IVD	Imaging	EMT		Probability of error	Effect
Source calibration	✓	✗	✗	–	Low	Low-high
Afterloader source positioning and dwell time (non-patient specific)	✓	✗	(✓)	E	–	–
Afterloader malfunction	✓	✗	(✓)	E	Low	Low-high
Patient identification	✗	✓	(✓)	E/F	Low	High
Correct treatment plan	✓	✗	✓	E	Low	High
Intra- and interfraction organ/applicator movement	✓	✓	✓	E/F/A	–	–
Applicator reconstruction	✓	✓	✓	E	Intermediate	Low-intermediate
Applicator length/source indexer length	✓	✗	✓	E/F	Intermediate	Low-high
Source step size (patient specific)	✓	✗	✓	E	Low	High
Interchanged guide tubes	✓	✗	✓	E/F	Intermediate	Low-high
Recording of dose	✓	✗	✗	–	–	–

Off-line procedures / Non-patient specific

Towards Dose-Reconstruction

3D Dose reconstruction/delivery

A Concept of Verification in BRT: Computational Verification CoVer

Dose Planned = Dose Delivered ? can not completely be answered w/o incorporating in-situ imaging and 3D-localization techniques!

If the *performance* of our BRT-MLC, thus the correct stepping with the correct dwell time pattern (fluence) at the correct geometrical configuration (the analogue of Gantry, Collimator, Couch Set-Up) is the appropriate (planned) can be most probably answered by applying *Computational Techniques*.

***Computational*, since in BRT we have to compute firstly and on the top issues similar to a DRR, an EPID, or a Fluence profile (the Finger-Print ?), which currently are not part of our standard RTP-procedure (as it is the case in ERT-RTP-Process).**

A Concept of Verification in BRT:

- **Computational Methods (*Software*)**
- **System Implementation (*Hardware*)**
- **Integration (*Brainware*)**

A Concept of Verification in BRT: Computational Verification - CoVer

- **Dedicated DRRs for Localisation and Verification purposes**

N x different ?

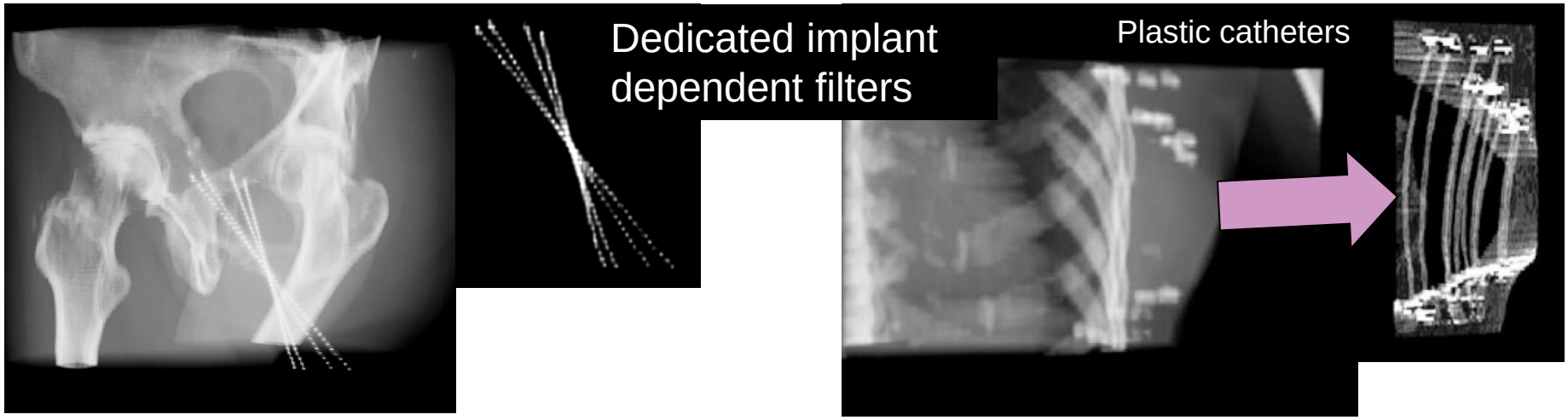

Milickovic N., Baltas D, et al. “CT imaging based digitally reconstructed radiographs and their application in brachytherapy“, Phys. Med. Biol. 45, 2000

Integrated in the **RTPs + DICOM Export (SC) to Imaging-based Verification Systems**

- **The “finger print” or the measurable fluence of a treatment**

Compute time-resolved information (dose-rate, dose, etc..)

Time-resolved *in vivo* luminescence dosimetry for online error detect in pulsed dose-rate brachytherapy

Claus E. Andersen[a)]
Radiation Research Division, Risø National Laboratory for Sustainable Energy, Technical University of Denmark, DK-4000 Roskilde, Denmark

Søren Kynde Nielsen
Department of Medical Physics, Aarhus University Hospital, DK-8000 Århus C, Denmark

Jacob Christian Lindegaard
Department of Oncology, Aarhus University Hospital, DK-8000 Århus C, Denmark

Kari Tanderup
Department of Medical Physics, Aarhus University Hospital, DK-8000 Århus C, Denmark

(Received 7 May 2009; revised 17 August 2009; accepted for publication 5 September 2009; published 6 October 2009)

In vivo dosimetry in brachytherapy

Kari Tanderup[a)]
Department of Oncology, Aarhus University Hospital, Aarhus 8000, Denmark and Department of Clinical Medicine, Aarhus University, Aarhus 8000, Denmark

Sam Beddar
Department of Radiation Oncology, The University of Texas MD Anderson Cancer Center, Houston, Texas 77030

Claus E. Andersen and Gustavo Kertzscher
Center of Nuclear Technologies, Technical University of Denmark, Roskilde 4000, Denmark

Joanna E. Cygler
Department of Physics, The Ottawa Hospital Cancer Centre, Ottawa, Ontario K1H 8L6, Canada

(Received 15 January 2013; revised 12 April 2013; accepted for publication 16 April 2013; published 25 June 2013)

In vivo dosimetry (IVD) has been used in brachytherapy (BT) for decades with a number of different detectors and measurement technologies. However, IVD in BT has been subject to certain difficulties and complexities, in particular due to challenges of the high-gradient BT dose distribution and the large range of dose and dose rate. Due to these challenges, the sensitivity and specificity toward error detection has been limited, and IVD has mainly been restricted to detection of gross errors. Given these factors, routine use of IVD is currently limited in many departments. Although the impact of potential errors may be detrimental since treatments are typically administered in large fractions and with high-gradient-dose-distributions, BT is usually delivered without independent verification of the treatment delivery. This Vision 20/20 paper encourages improvements within BT safety by developments of IVD into an effective method of independent treatment verification. © *2013 American Association of Physicists in Medicine*. [http://dx.doi.org/10.1118/1.4810943]

Key words: *in vivo* dosimetry, brachytherapy, treatment errors, quality assurance

A phantom study of an *in vivo* dosimetry system using plastic scintillation detectors for real-time verification of ^{192}Ir HDR brachytherapy

Francois Therriault-Proulx
Department of Radiation Physics, The University of Texas MD Anderson Cancer Center, Houston, Texas 77030 and Département de Physique, de Génie Physique et d' Optique, Université Laval, Québec, Québec G1K 7P4, Canada

Tina M. Briere and Firas Mourtada
Department of Radiation Physics, The University of Texas MD Anderson Cancer Center, Houston, Texas 77030

Sylviane Aubin
Département de Radio-Oncologie, Hôtel-Dieu de Québec, Centre Hospitalier Universitaire de Québec, Québec, Québec G1R 2J6, Canada

Sam Beddar[a)]
Department of Radiation Physics, The University of Texas MD Anderson Cancer Center, Houston, Texas 77030

Luc Beaulieu
Département de Physique, de Génie Physique et d'Optique, Université Laval, Québec, Québec G1K 7P4, Canada and Département de Radio-Oncologie, Hôtel-Dieu de Québec, Centre Hospitalier Universitaire de Québec, Québec, Québec G1R 2J6, Canada

(Received 3 October 2010; revised 22 February 2011; accepted for publication 9 March 2011; published 5 May 2011)

Adaptive error detection for HDR/PDR brachytherapy: Guidance for decision making during real-time *in vivo* point dosimetry

Gustavo Kertzscher[a)] and Claus E. Andersen[b)]
Centre for Nuclear Technologies, Technical University of Denmark, DTU Nutech, Frederiksborgvej 399, DK-4000 Roskilde, Denmark

Kari Tanderup[c)]
Department of Oncology, Aarhus University Hospital and Institute of Clinical Medicine, Aarhus University, Nørrebrogade 44, DK-8000 Aarhus, Denmark

(Received 15 October 2013; revised 5 March 2014; accepted for publication 23 March 2014; published 14 April 2014)

The “finger print” or the measurable fluence of a treatment

Compute time-resolved information (dose-rate, dose, etc..)

ELSEVIER

CrossMark

BRACHYTHERAPY

Brachytherapy 17 (2018) 122–132

Treatment Delivery Verification in Brachytherapy

Time-resolved *in vivo* dosimetry for source tracking in brachytherapy

Jacob Graversen Johansen[1,*], Susanne Rylander[1], Simon Buus[1], Lise Bentzen[1], Steffen Bjerre Hokland[1], Christian Skou Søndergaard[1], Anders Karl Mikael With[2], Gustavo Kertzscher[3], Kari Tanderup[1]

[1]*Department of Oncology, Aarhus University Hospital, Aarhus C, Denmark*
[2]*Department of Medical Physics, Örebro University Hospital, Örebro, Sweden*
[3]*Department of Radiation Physics, The University of Texas MD Anderson Cancer Center, Houston, TX*

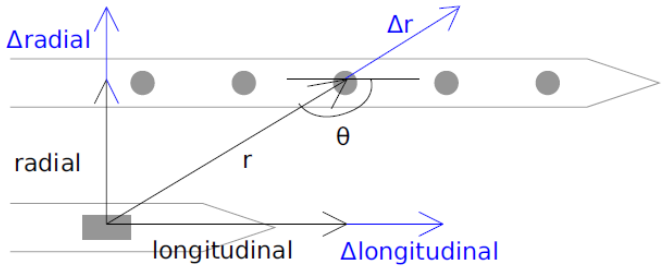

Fig. 1. Schematic representation of a treatment needle with five dwell positions (circles) and the needle with dosimeter (square). The coordinates used in the analysis are also shown. Free parameters are shown in blue. (For interpretation of the references to color in this figure legend, the reader is referred to the Web version of this article.)

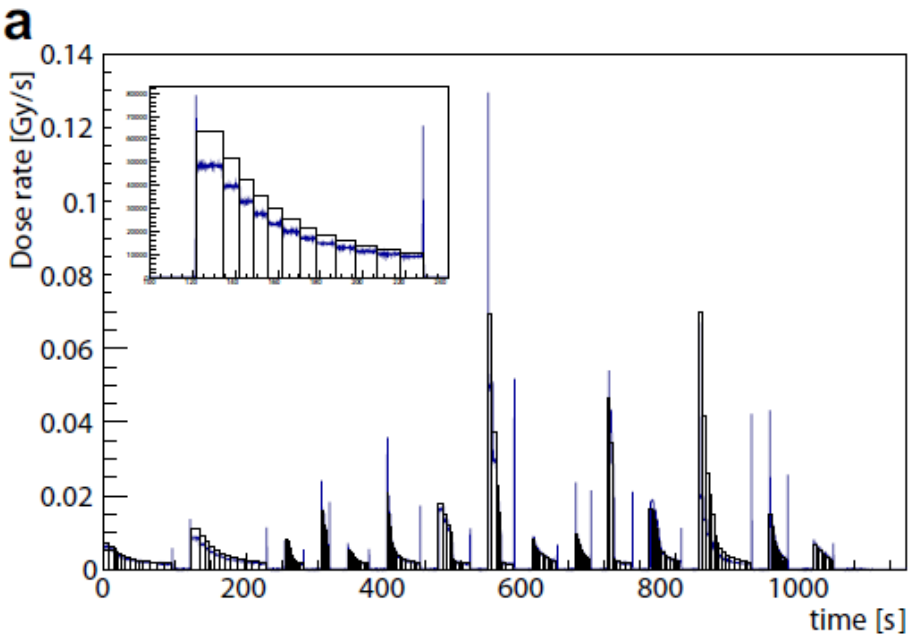

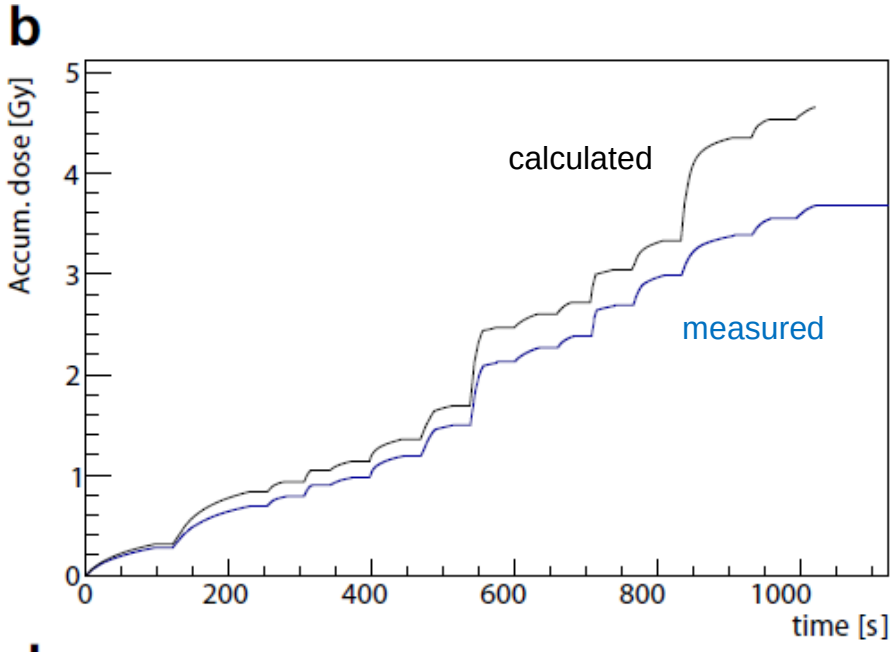

CONCLUSION: Time-resolved in vivo dosimetry can be used to provide geometric information about the treatment progression of afterloading brachytherapy. This information may provide a clear indication of errors and uncertainties during a treatment and, therefore, enables real-time treatment monitoring.

A Concept of Verification in BRT: Computational Verification - Cover

- **The “finger print” or the measurable fluence of a treatment**

(1) Compute time-resolved information (dose-rate, dose, etc..)

that can be considered as the ***reference*** information for an ***on-line*** (in-vivo) verification process. This could be the ***analogon*** to DRR or fluence profile in ERT and could be considered as the “Finger-Print” of the treatment delivery **(?)**:

- **per channel / catheter**
- **whole treatment plan**
- **including uncertainties**
  - **Implant-specific**
  - **Treatment Device-specific**
  - **Measurement system-specific**
  - **???**

Integrated in the **RTPs + Export to Measurement-based Verification Systems**

A Concept of Verification in BRT: Computational Verification - Cover

(2a) Where to be computed?

- Single position *versus* Multiple Positions (IVD)
- 1D-Array
- 2D-Array
- Measuring System-dependent

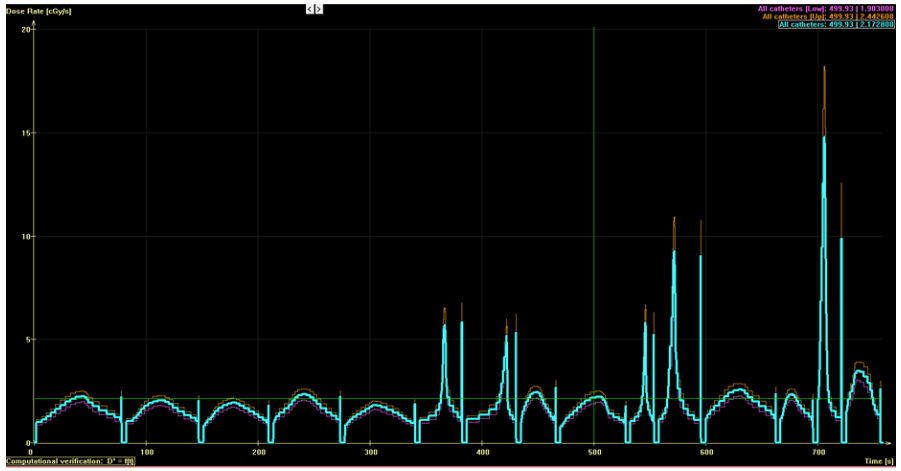

(2b) How to be computed?

- Time-resolved
- Channel & Dwell Position resolved
- Whole Treatment Plan (Monitoring)
- Dedicated Verification Plan
- Workflow & Verification System-dependent

A Concept of Verification in BRT: Computational Verification Cover – A Prototype

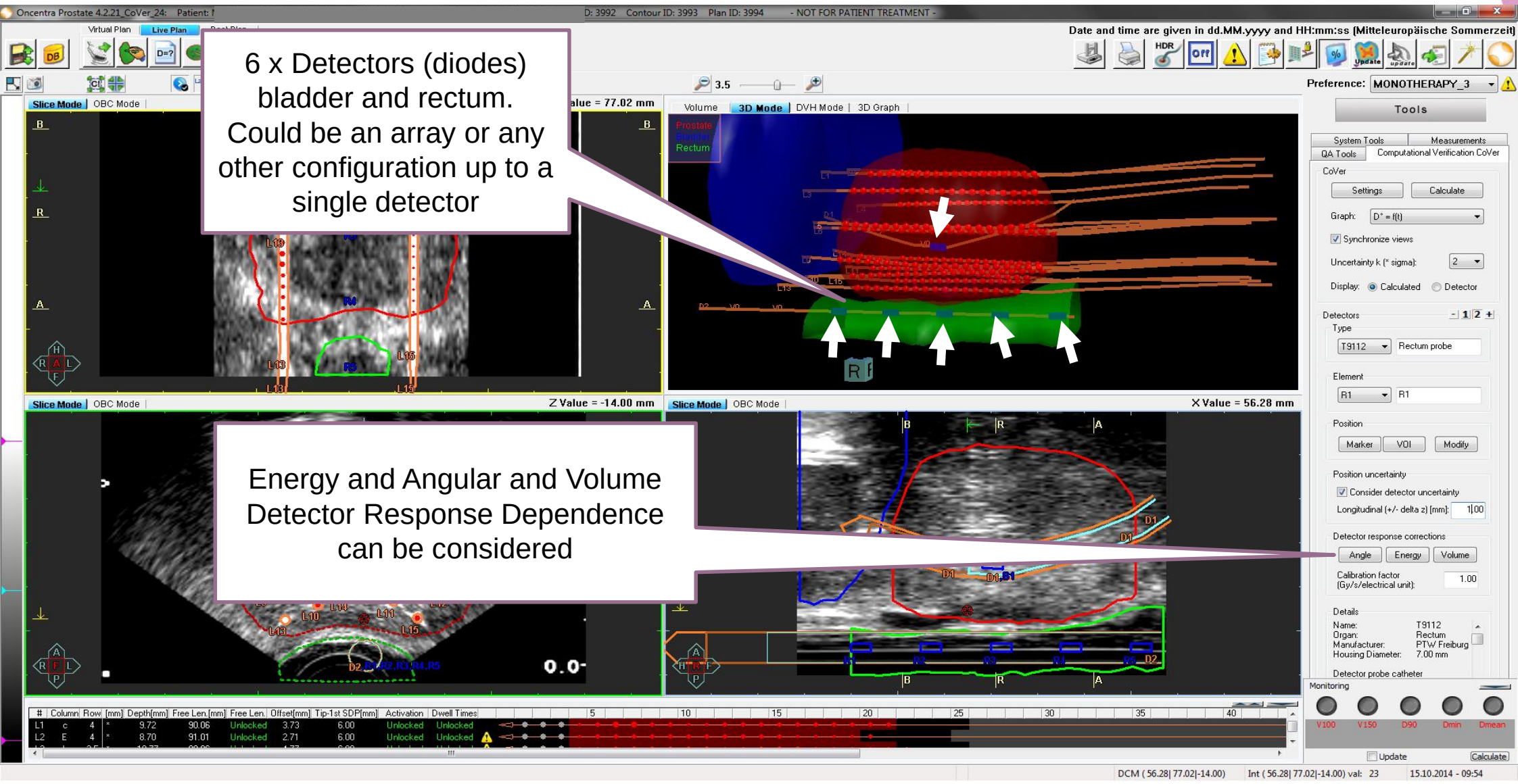

A Concept of Verification in BRT: Computational Verification Cover – A Prototype

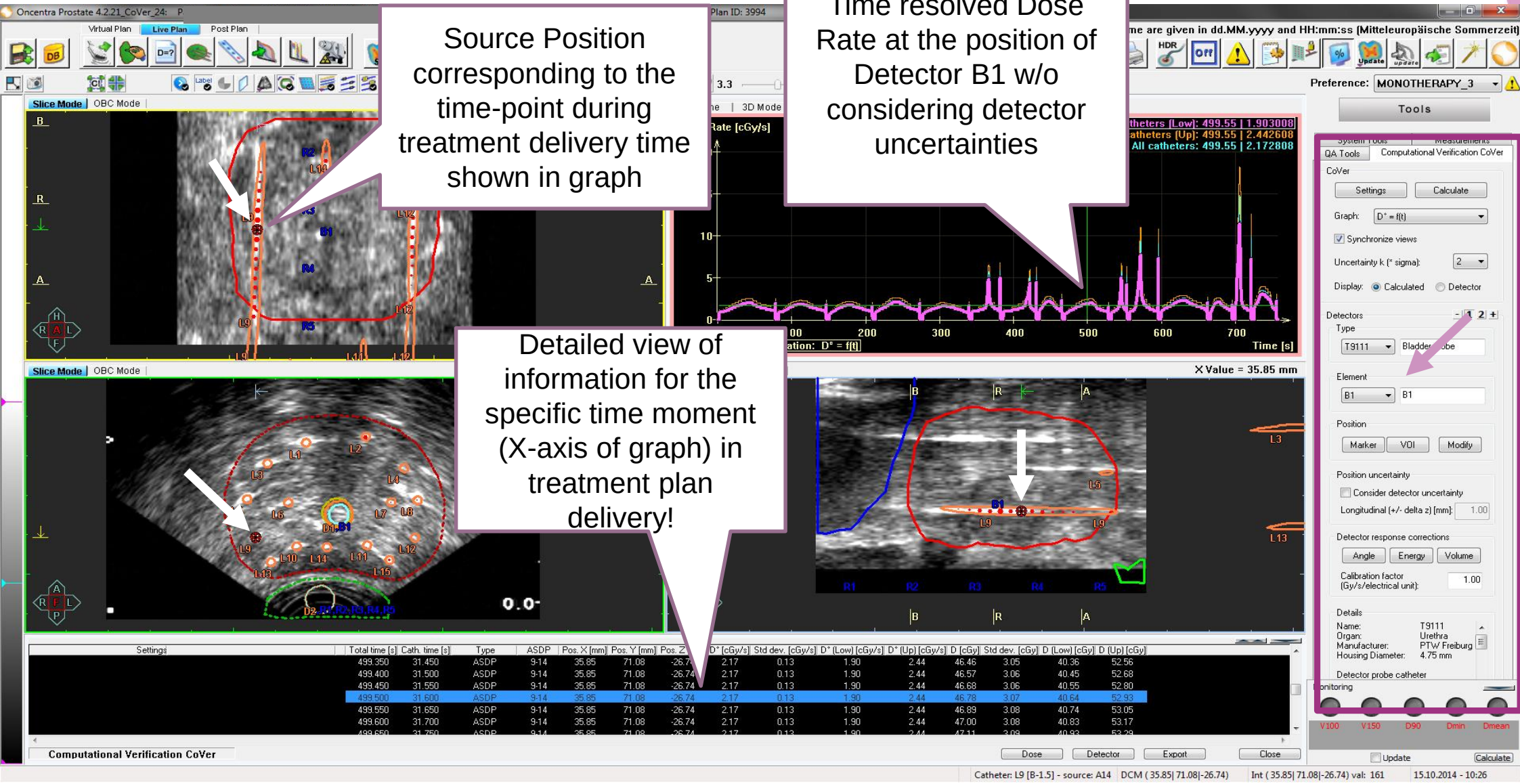

A Concept of Verification in BRT:

- **Computational Methods (*Software*)**
- **System Implementation (*Hardware*)**
- **Integration (*Brainware*)**

A Concept of Verification in BRT: Hardware - Detectors

TABLE III. Characteristics of detectors and dosimetry systems of importance for precise routine IVD in brachytherapy. The items are rated according to: advantageous (++), good (+), and inconvenient (−).

	TLD	Diode	MOSFET	Alanine	RL	PSD
Size	+	+/−	+/++	−	++	++
Sensitivity	+	++	+	−	++	+/++
Energy dependence	+	−	−	+	−	++
Angular dependence	++	−	+	+	++	++
Dynamic range	++	++	+	−	++	++
Calibration procedures, QA, stability, robustness, size of system, ease of operation	+	++	++	−	−/+	+/++
Commercial availability	++	++	++	++	−	+
Online dosimetry	−	++	+	−	++	++
Main advantages	No cables, well studied system	Commercial systems at reasonable price, well studied system	Small size, commercial system at reasonable price	Limited energy dependence, no cables	Small size, high sensitivity	Small size, no angular and energy dependence, sensitivity
Main disadvantages	Tedious procedures for calibration and readout, not online dosimetry	Angular and energy dependence	Limited life of detectors, energy dependence	Not sensitive to low doses, tedious procedures for calibration and readout, not online dosimetry, expensive readout equipment not available in clinics	Needs frequent recalibration, stem effect, not commercially available	Stem effect

Energy-, Angular-, Temperature-, Volume-dependence: Computational methods in RTP !

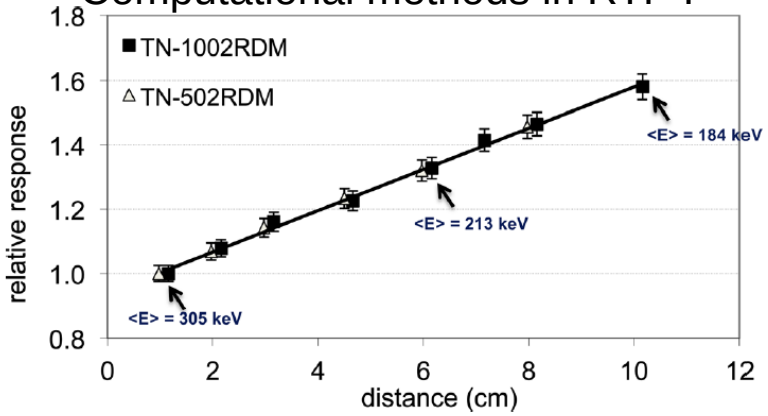

FIG. 6. Variation of the MOSFET response with distance for two detectors, normalized to 1 cm distance. The mean photon energies in PMMA are given for distance of 1, 6, and 10 cm.

B. Reniers, G. Landry, R. Eichner, A. Hallil, F. Verhaegen, Med. Phys. 39 (4), 1925-1935, 2012

Most probably it is a sufficient requirement for the time-resolved –based systems:
Have a stable response/behaviour over the period of signal acquisition (usually 10-30 min)
Be small enough to be entered into catheters/applicators/ ….

A Concept of Verification in BRT: System Implementation – Hardware: Imaging / EPID

A method for verification of treatment delivery in HDR prostate brachytherapy using a flat panel detector for both imaging and source tracking

Ryan L. Smith[a)]
Alfred Health Radiation Oncology, The Alfred Hospital, Melbourne, VIC 3004, Australia and School of Science, RMIT University, Melbourne, VIC 3000, Australia

Annette Haworth
School of Science, RMIT University, Melbourne, VIC 3000, Australia and Physical Sciences, Peter MacCallum Cancer Centre, East Melbourne, VIC 3002, Australia

Vanessa Panettieri
Alfred Health Radiation Oncology, The Alfred Hospital, Melbourne, VIC 3004, Australia

Jeremy L. Millar and Rick D. Franich
Alfred Health Radiation Oncology, The Alfred Hospital, Melbourne, VIC 3004, Australia and School of Science, RMIT University, Melbourne, VIC 3000, Australia

(Received 13 January 2016; revised 21 March 2016; accepted for publication 3 April 2016; published 20 April 2016)

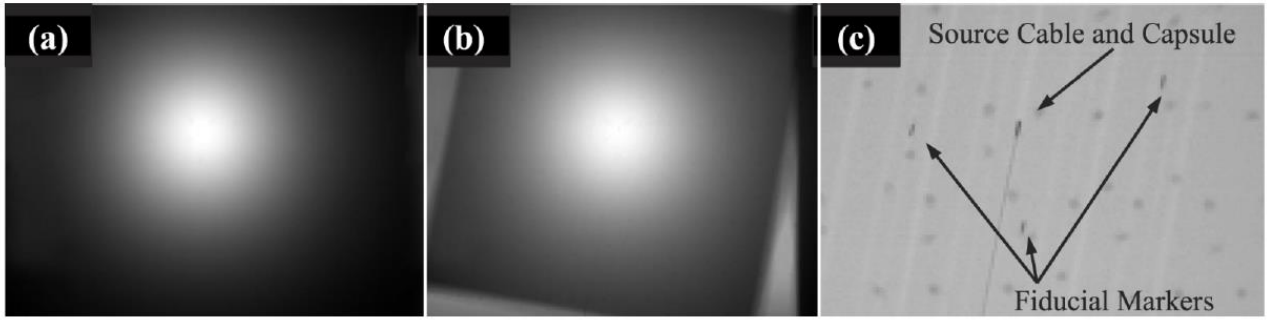

FIG. 5. (a) The captured exposure of the ^{192}Ir source using the FPD. (b) The simultaneous FPD exposure of the ^{192}Ir source and the projection image of the phantom. (c) The result of subtraction of (a) from (b), magnified view to show the physical source capsule used for independent position verification. The source cable, voids from the other empty catheters, and fiducial markers are also visible.

ELSEVIER
CrossMark
BRACHYTHERAPY
Brachytherapy 17 (2018) 111–121

Treatment Delivery Verification in Brachytherapy

An integrated system for clinical treatment verification of HDR prostate brachytherapy combining source tracking with pretreatment imaging

Ryan L. Smith[1,2,*], Max Hanlon[2], Vanessa Panettieri[1], Jeremy L. Millar[1,2,3], Bronwyn Matheson[1], Annette Haworth[2,4], Rick D. Franich[2]

[1]Alfred Health Radiation Oncology, Alfred Health, Melbourne, VIC, Australia
[2]School of Science, RMIT University, Melbourne, VIC, Australia
[3]Central Clinical School, Monash University, Melbourne, VIC, Australia
[4]School of Physics, University of Sydney, Camperdown, NSW, Australia

1. (a) The custom designed couch assembly to support the FPD under the patient, mounted to our HDR brachytherapy treatment couch. The carbon fiber
ch top supports the weight of the patient above the sensitive region of the FPD and improves reproducible patient positioning. (b) The lasers in the HDR
hytherapy treatment bunker projected on to the skin marks of the patient at treatment fraction 2. The blue skin marks from fraction 1 are also visible.
roducible patient positioning at treatment improves the agreement with the treatment plan when performing treatment verification. FPD = flat panel
ctor; HDR = high-dose-rate. (For interpretation of the references to color in this figure legend, the reader is referred to the Web version of this article.)

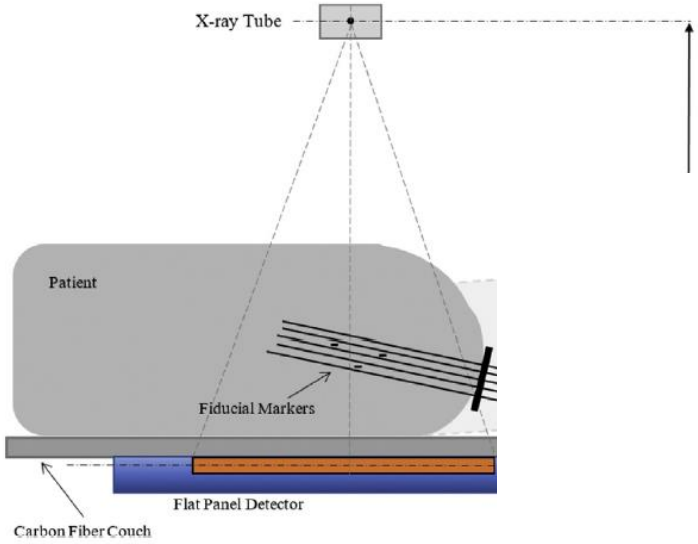

Fig. 2. A diagram showing the setup used to acquir
patient immediately before treatment delivery. The
tioned above the patient at a known focus to image
fiducial markers implanted in the prostate are used
the TPS, enabling comparison of planned catheter pc
catheter positions. A-P = anterior–posterior; TPS
system.

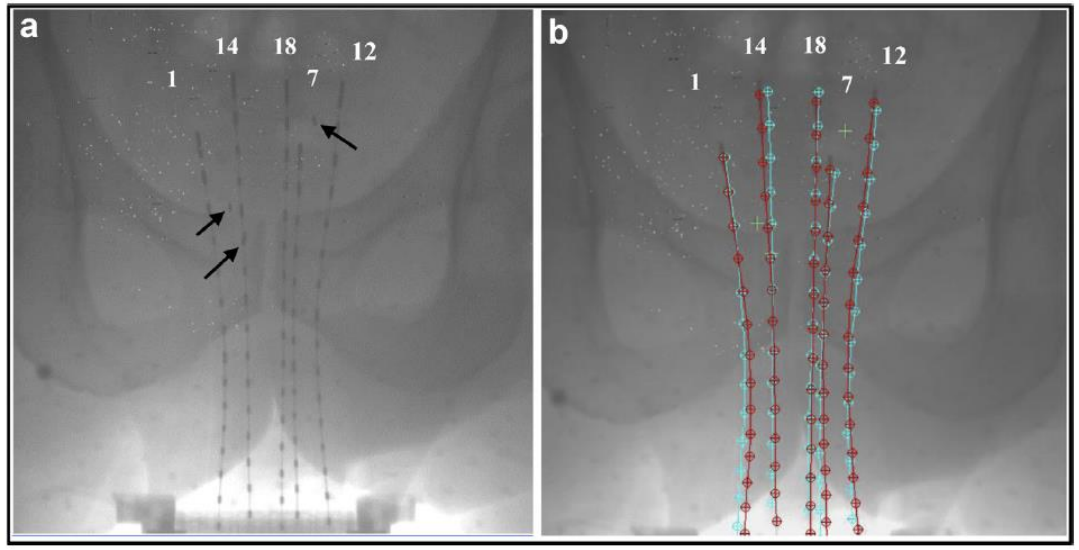

Fig. 3. (a) A pretreatment A-P image acquired with the catheter position markers inserted into the specified catheters. The BB array and the three gold fiducial markers (black arrows) implanted into the prostate are also visible (b) A comparison of the planned (TPS) catheter positions (cyan) and the measured catheter paths immediately prior to treatment (red) overlaid on the A-P image. BB array = ball-bearing array; A-P = anterior–posterior; TPS = treatment planning system. (For interpretation of the references to color in this figure legend, the reader is referred to the Web version of this article.)

A Concept of Verification in BRT: System Implementation – Hardware: Imaging / EPID

IOP Publishing | Institute of Physics and Engineering in Medicine
Physics in Medicine & Biology
Phys. Med. Biol. 62 (2017) 5440–5461
https://doi.org/10.1088/1361-6560/aa7028

Online pretreatment verification of high-dose rate brachytherapy using an imaging panel

Gabriel P Fonseca[1], Mark Podesta[1], Murillo Bellezzo[1], Michiel R Van den Bosch[1], Ludy Lutgens[1], Ben G L Vanneste, Robert Voncken[1], Evert J Van Limbergen[1], Brigitte Reniers[2] and Frank Verhaegen[1]

[1] Department of Radiation Oncology (MAASTRO), GROW—School for Oncology and Developmental Biology, Maastricht University Medical Center, Dr. Tanslaan 12, Maastricht 6229 ET, Netherlands
[2] Research group NuTeC, CMK, Hasselt University, Agoralaan Gebouw H, B-3590 Diepenbeek, Belgium

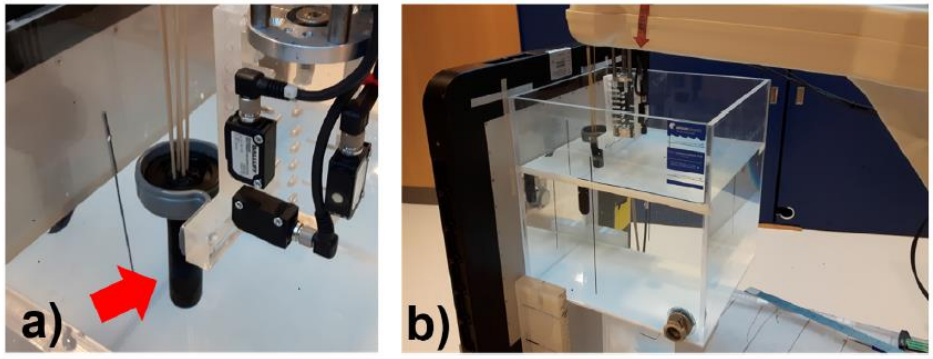

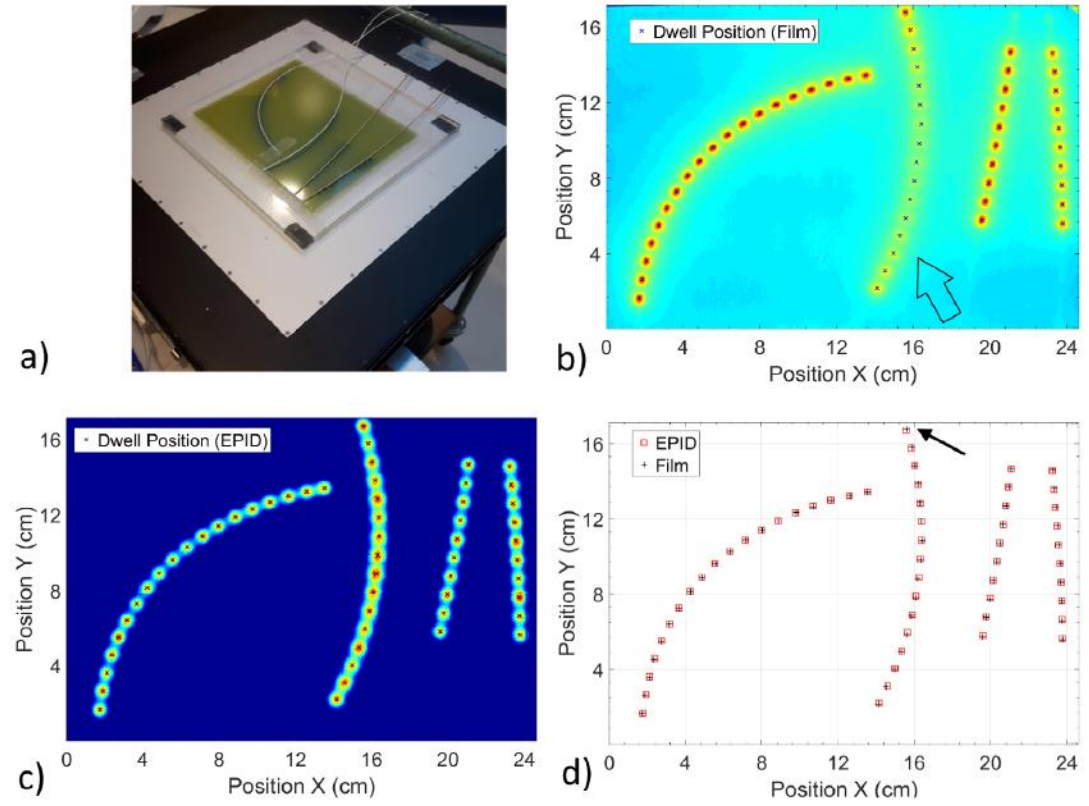

Patient Specific QA using a high resolution 2D-Array

- Analogue to Patient-specific QA in EBRT

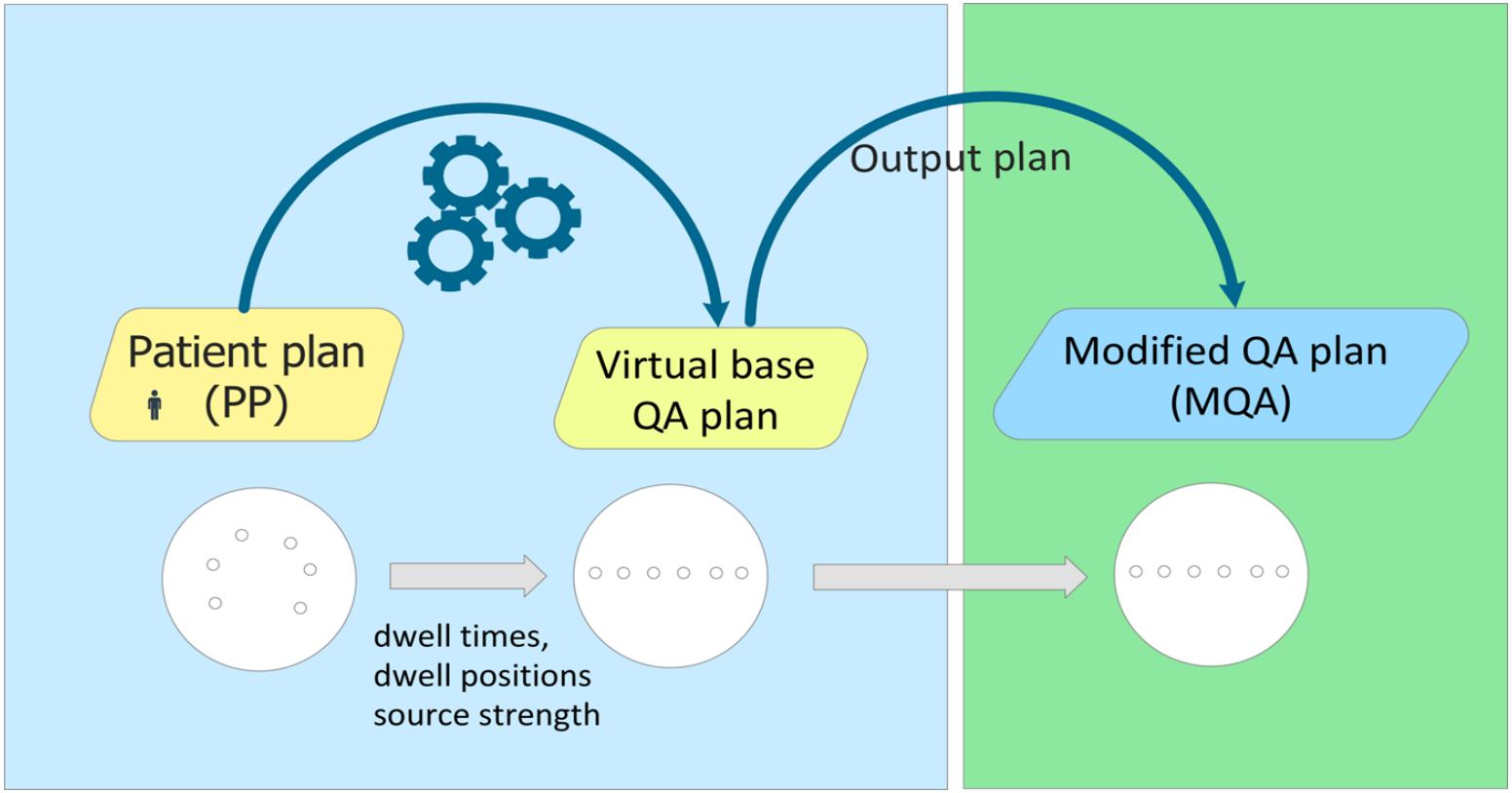

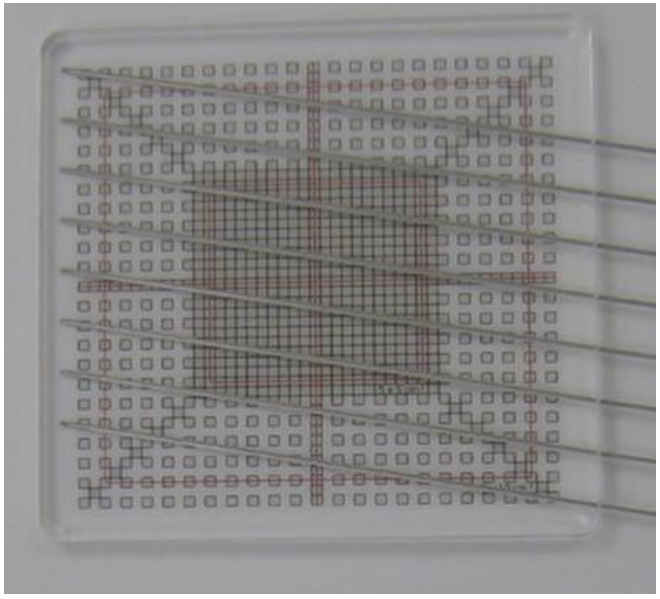

977 Iso-octan 0.693 gcm^{-3} filled chamber
SRS1000 by PTW-Freiburg, Germany

Patient Specific QA using a high resolution 2D-Array

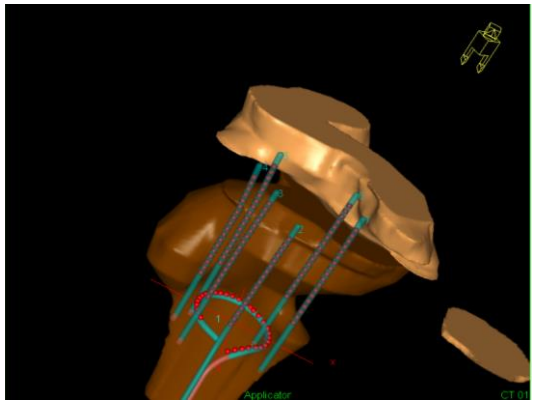

Plan Transfer

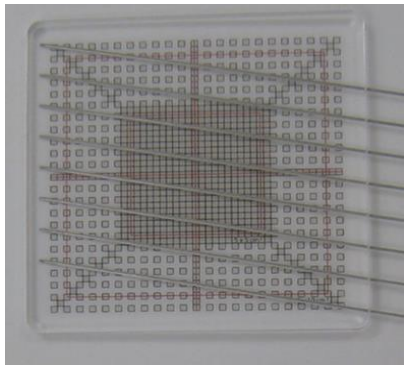

Patient

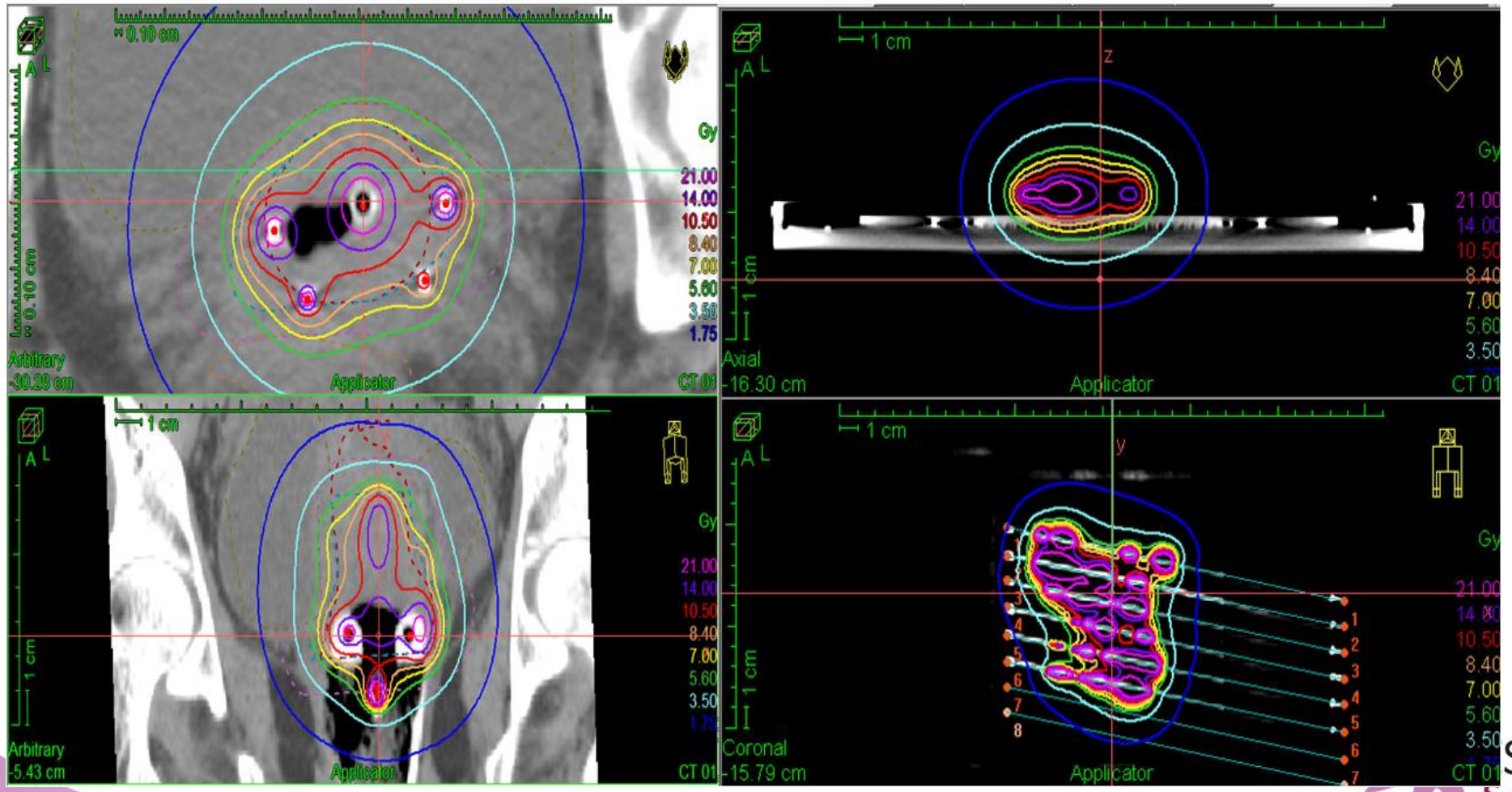

QA-Phantom

Patient Specific QA using a high resolution 2D-Array

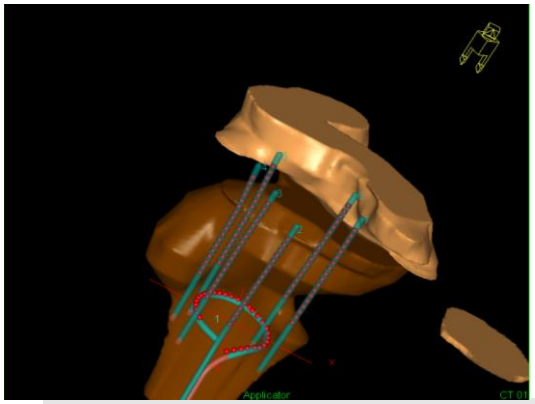

Plan Transfer

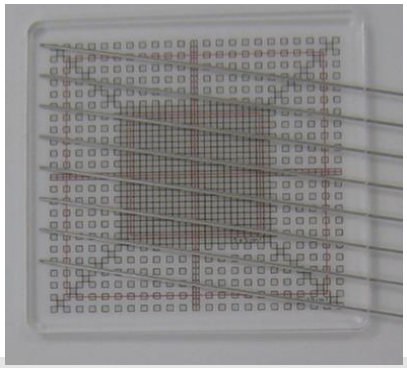

Measurement

RTP: QA-Phantom

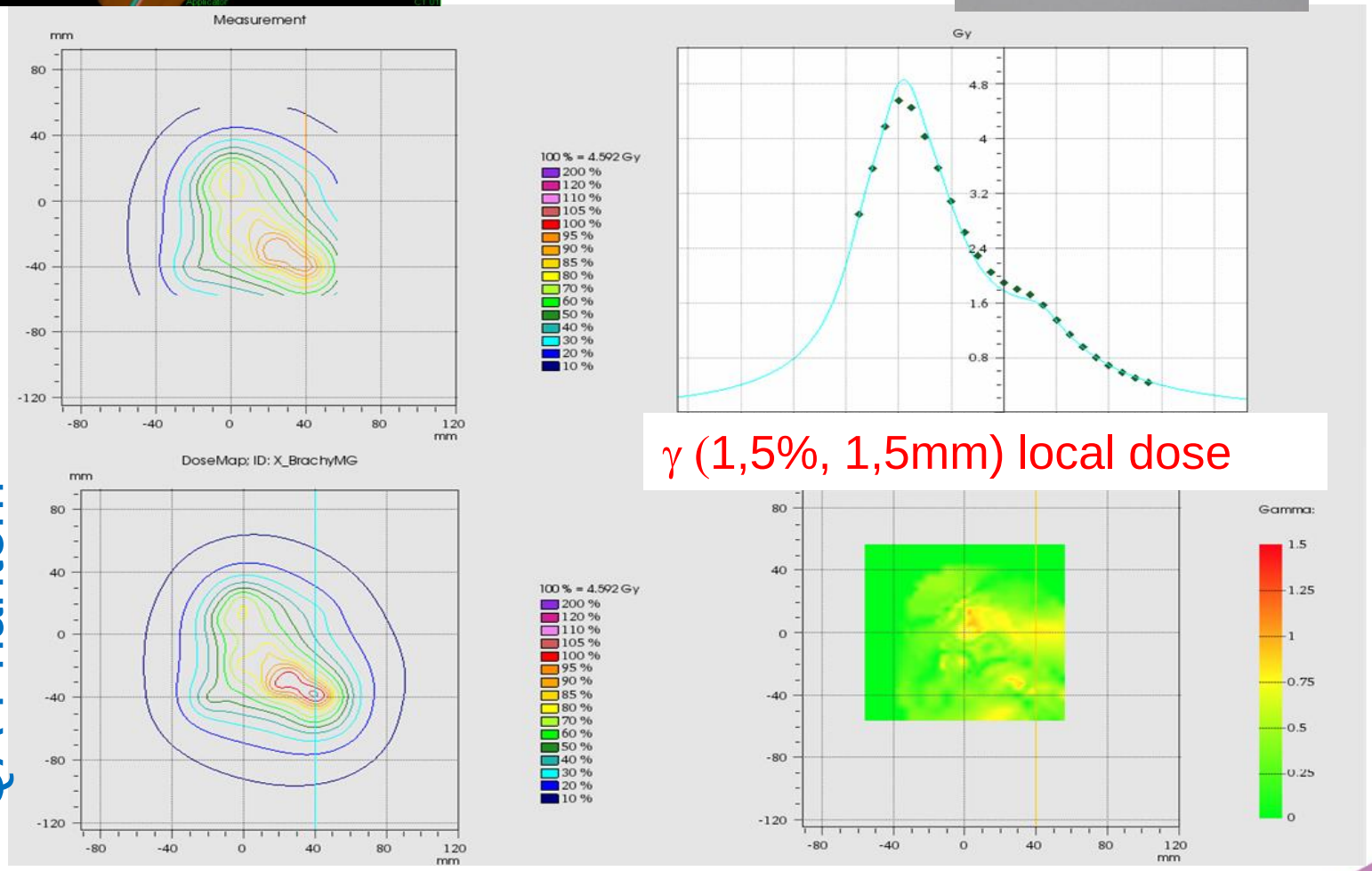

γ (1,5%, 1,5mm) local dose

ESTRO School

Modern Brachytherapy: Treatment Delivery Verification

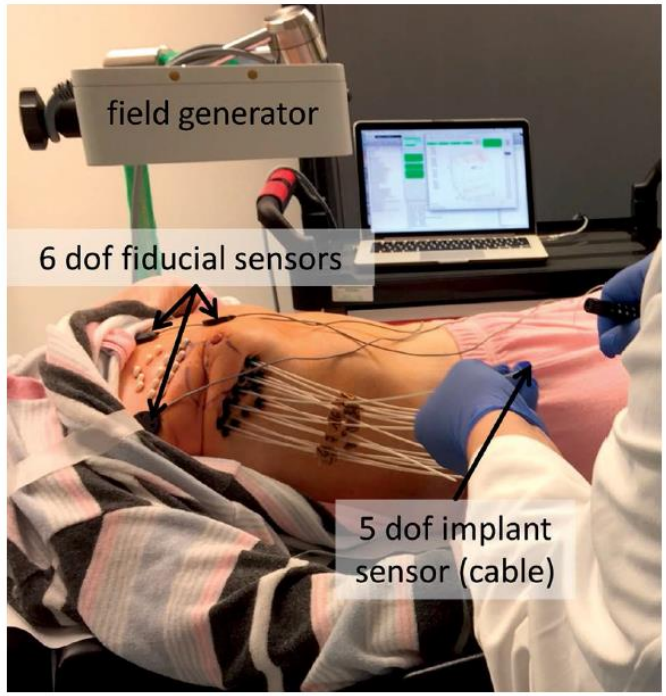

Educational Activity Corner

Review paper

Electromagnetic tracking for treatment verification in interstitial brachytherapy

Prof. Christoph Bert, PhD[1], Markus Kellermeier, PhD[1], Prof. Kari Tanderup, PhD[2,3]

[1]Department of Radiation Oncology, Universitätsklinikum Erlangen, Friedrich-Alexander-Universität Erlangen-Nürnberg, Erlangen, [2]Department of Oncology, Department of Medical Physics, Aarhus University Hospital, Aarhus, Denmark, [3]Institute of Clinical Me Aarhus University, Aarhus, Denmark

Abstract

Electromagnetic tracking (EMT) is used in several medical fields to determine the position and orientatio ed sensors, e.g., attached to surgical tools. Recently, EMT has been introduced to brachytherapy for implan tion and error detection. The manuscript briefly summarizes the main issues of EMT and error detection in apy. The potential and complementarity of EMT as treatment verification technology will be discussed i *in vivo* dosimetry and imaging.

J Contemp Brachytherapy 2016;
DOI: 10.5114/j

Table 1. Errors and variations in brachytherapy alo h t dosimetry (IVD), real-time imaging (each according t 2,2 The probability of error and the potential effect we rte tion of detectability by real-time EMT and the nee T markers visible in imaging and EMT reproducibly pl in calibration between EMT and imaging as, e.g., repo A schematic drawing of the coordinate system option s sho

Quality item	Detectability			EMT coordinate system	Error probability and effect [23]	
	IVD	Imaging	EMT		Probability of error	Effect
Source calibration	✓	✗	✗	–	Low	Low-high
Afterloader source positioning and dwell time (non-patient specific)	✓	✗	(✓)	E	–	–
Afterloader malfunction	✓	✗	(✓)	E	Low	Low-high
Patient identification	✗	✓	(✓)	E/F	Low	High
Correct treatment plan	✓	✗	✓	E	Low	High
Intra- and interfraction organ/applicator movement	✓	✓	✓	E/F/A	–	–
Applicator reconstruction	✓	✓	✓	E	Intermediate	Low-intermediate
Applicator length/source indexer length	✓	✗	✓	E/F	Intermediate	Low-high
Source step size (patient specific)	✓	✗	✓	E	Low	High
Interchanged guide tubes	✓	✗	✓	E/F	Intermediate	Low-high
Recording of dose	✓	✗	✗	–	–	–

Off-line procedures / Non-patient specific

Towards Dose-Reconstruction

3D Dose reconstruction/delivery

A Concept of Verification in BRT

Implant / Set-Up*

Implant / Set-Up* + Anatomy?

Implant / Set-Up* + Anatomy

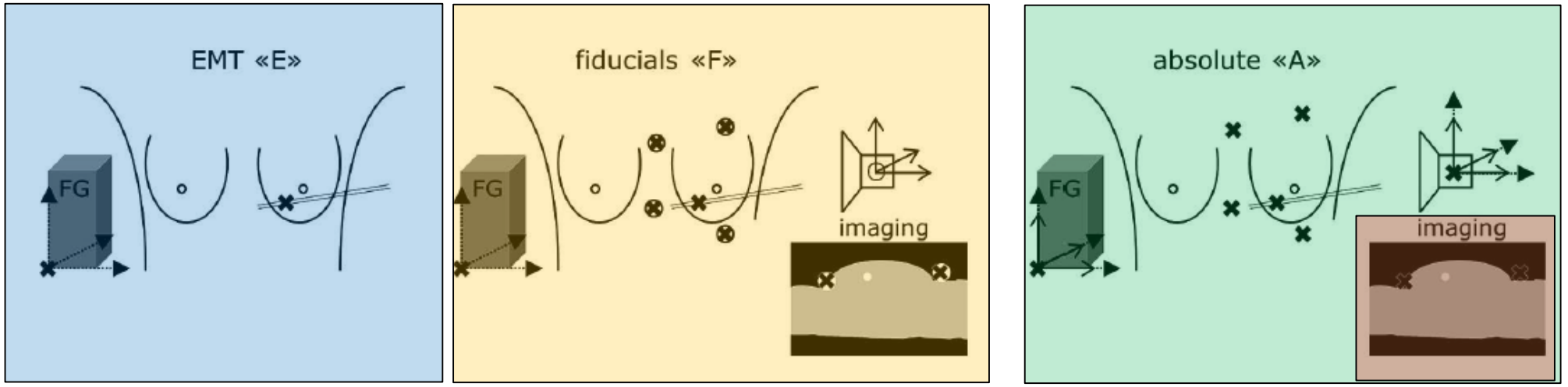

Fig. 2. Schematic of electromagnetic tracking usage in breast cancer treatments. Electromagnetic tracking can either be used standalone (×, method «E»), in combination with fiducials visible in electromagnetic tracking and an alternative imaging system (⊗, method «F»), or fully integrated to an imaging modality by an absolute cross-calibration (method «A»)

*EM independent of source driving system – Off-Line

*EM independent of source driving system – Off-Line

*EM independent of source driving system – Off-Line

EM in source driving system:
Machine – Source Stepping – On-Line

A Concept of Verification in BRT

ELSEVIER

CrossMark

BRACHYTHERAPY

Brachytherapy 17 (2018) 94–102

Treatment Delivery Verification in Brachytherapy

Assessment of the implant geometry in fractionated interstitial HDR breast brachytherapy using an electromagnetic tracking system

Markus Kellermeier, Rainer Fietkau, Vratislav Strnad, Christoph Bert*

Department of Radiation Oncology, Universitätsklinikum Erlangen, Friedrich-Alexander-Universität Erlangen-Nürnberg, Erlangen, Germany

PURPOSE: During the partial-breast treatment course by interstitial brachytherapy, electromagnetic tracking (EMT) was applied to measure the implant geometry. Implant-geometry variation, choice of reference data, and three registration methods were assessed.

METHODS AND MATERIALS: The implant geometry was measured in 28 patients after catheter implantation (EMT_{bed}), during CT imaging (EMT_{CT}), and in each of up to $n = 9$ treatment fractions ($EMT_{F(k),\ k\ =\ 1,\ 2,\ldots\ n}$). $EMT_{F(k)}$ were registered to the planned implant reconstruction (CT_{plan}) by using all dwell positions (DPs), the button centers, or three fiducial sensors on the patient's skin. Variation in implant geometry obtained from $EMT_{F(k)}$ was assessed for EMT_{bed}, EMT_{CT}, and CT_{plan}.

RESULTS: EMT was used to measure 3932 catheters. A duration of 6.5 ± 1.7 min was needed for each implant measurement (mean, 17 catheters) plus setup of the EMT system. Data registration based on the DP deviated significantly lower than registration on button centers or fiducial sensors. Within a registration group, there was a <0.5-mm difference in the choice of reference data. Using CT_{plan} as reference for registration, the mean residual distance of DPs on EMT-derived DPs was found at 2.1 ± 1.6 mm (EMT_{bed}), 1.3 ± 0.9 mm (EMT_{CT}), and 2.5 ± 1.5 mm ($EMT_{F(k)}$).

CONCLUSIONS: EMT can assess the implant geometry in high-dose-rate interstitial brachytherapy breast treatments. EMT_{bed}, EMT_{CT}, and CT_{plan} data can serve as reference for assessment of implant changes.

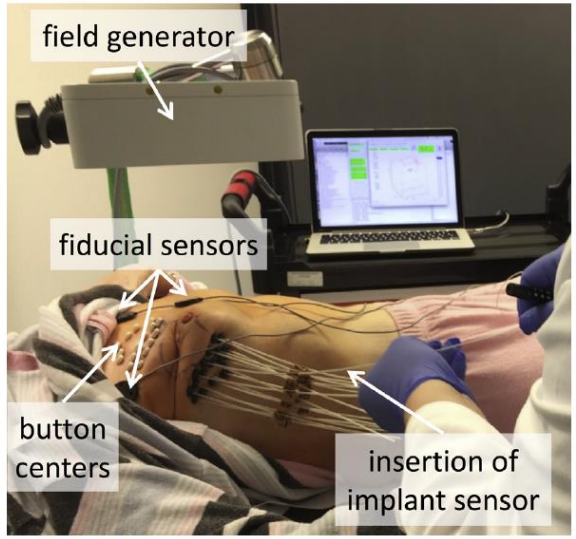

Fig. 2. Patient in treatment position in the HDR treatment room. The 5DoF implant sensor is manually inserted in each catheter of the implant. EMT is performed using the field generator (FG) and the three 6DoF fiducial sensors on the patient's chest to correct for breathing motion. DoF = degree of freedom; EMT = electromagnetic tracking; HDR = high-dose-rate.

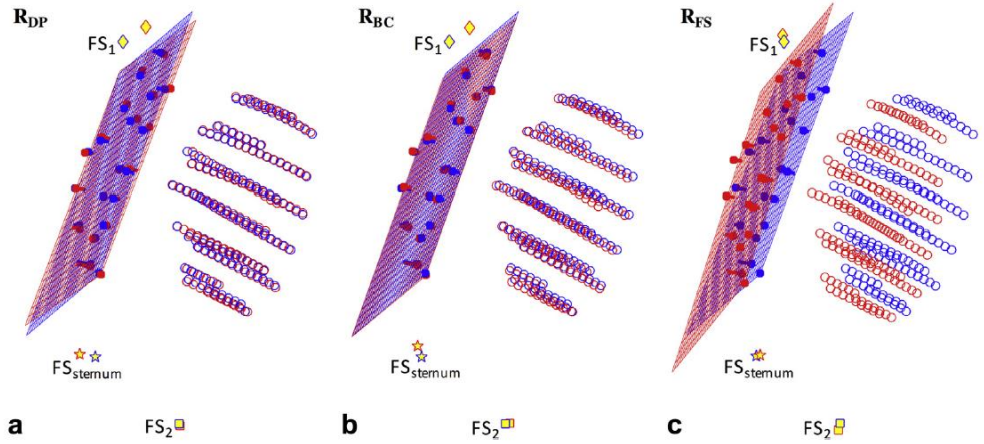

Fig. 3. Example data from Patient ID 20. The data indicate the differences of the registration methods that use (a) all dwell positions (R_{DP}, open circles), (b) the centers of the distal buttons (R_{BC}, filled circles), or (c) the three fiducial sensor positions (FS_1, diamond; FS_2, star; and $FS_{sternum}$, square) on the skin for the minimization of the distances between reference data set (blue) and a data set (red) for comparison (here: EMT_{bed}). EMT = electromagnetic tracking; FS = fiducial sensor. (For interpretation of the references to color in this figure legend, the reader is referred to the Web version of this article.)

A Concept of Verification in BRT

Dose Planned = Dose Delivered ? can not completely be answered w/o incorporating in-situ imaging and 3D-localization techniques!

If the *performance* of our BRT-MLC, thus the correct stepping with the correct dwell time pattern (fluence) at the correct geometrical configuration (the analogue of Gantry, Collimator, Couch Set-Up) is the appropriate (planned) can be most probably answered by applying *Computational Techniques*.

Computational, since in BRT we have to compute firstly and on the top issues similar to a DRR, an EPID, or a Fluence profile (the Finger-Print ?), which currently are not part of our standard RTP-procedure (as it is the case in ERT-RTP-Process).

Intra-operative 3D-Imaging

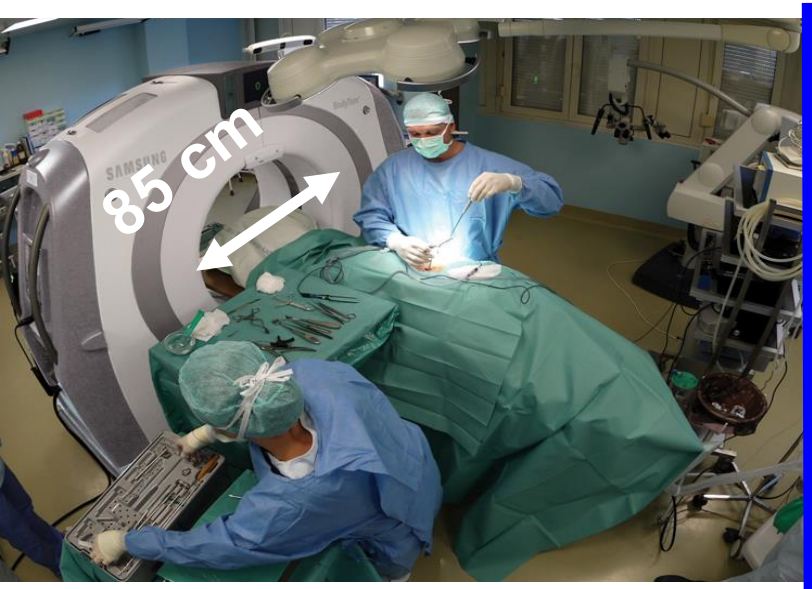

BodyTom® by SAMSUNG

- **Rel. small clearance**
- **FOV 60 cm**
- **Range 90 cm**
- **Axial, Helical**
- **3D**
- **HUs**
- **Flexible - radiolucent table**

- **Large clearance**
- **FOV 50 cm**
- **Range 100 cm**
- **Helical**
- **3D**
- **HUs ???**
- **Specific – table Trumpf TruSystem 7500**

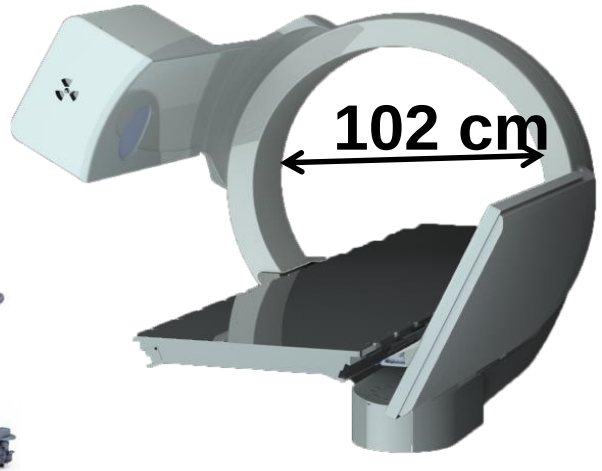

MedPhoton GmbH, Salzburg, Austria

- Large clearance
- FOV 22 – 42 (76) cm
- Range 26 cm
- 2D (fluoroscopy)
- 3D - CBCT
- Dual Energy
- HUs
- Flexible: radiolucent table / rail

ESTRO School

A Concept of Verification in BRT:

- **Computational Methods (*Software*)**
- **System Implementation (*Hardware*)**
- **Integration - Workflow (*Brainware*)**

A Concept of Verification in BRT: Integration - Workflow

To Do

- **Interface to Afterloading device**
  - **Synchronization of “time-axis” - Triggering**
  - **Synchronization of “system-status”**
  - **Interlock-Interface**
  - **???**

- **Standardized Interface to:**
  - **Afterloaders**
  - **Detectors / Detector Systems**

- **Interface to BRT-RTP-Systems**

A Concept of Verification in BRT: Integration - Workflow

To Do …

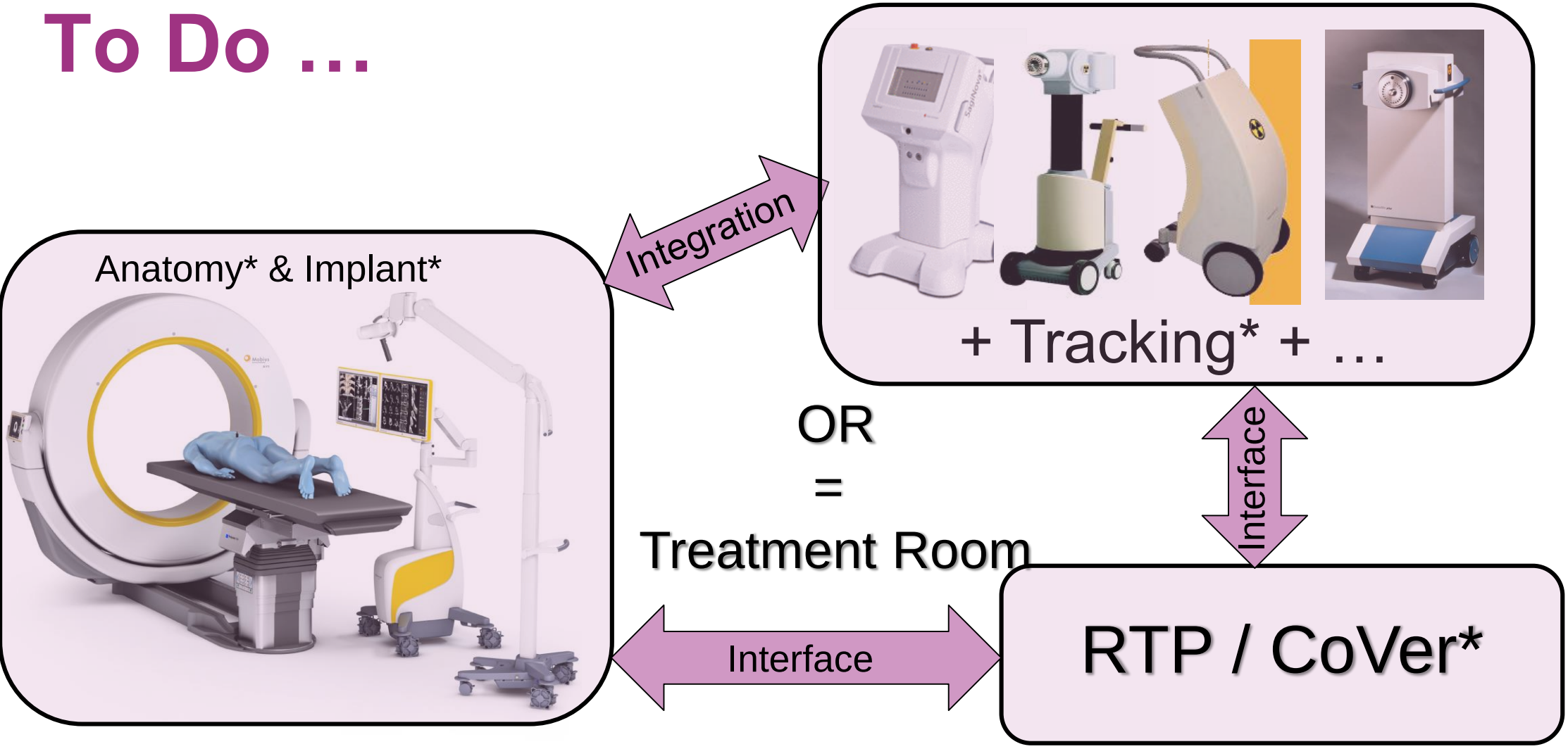

*Just before or/and during delivery

Brachytherapy

Articles in press | Latest issue | Special issues | All issues | About the journal ↗ | Follow journal

Treatment Delivery Verification in Brachytherapy: Prospects of Technology Innovation

Edited by Kari Tanderup, Christian Kirisits, Antonio L. Damato
Volume 17, Issue 1, Pages A1-A6, 1-250 (January–February 2018)

Thank you very much for your Attention

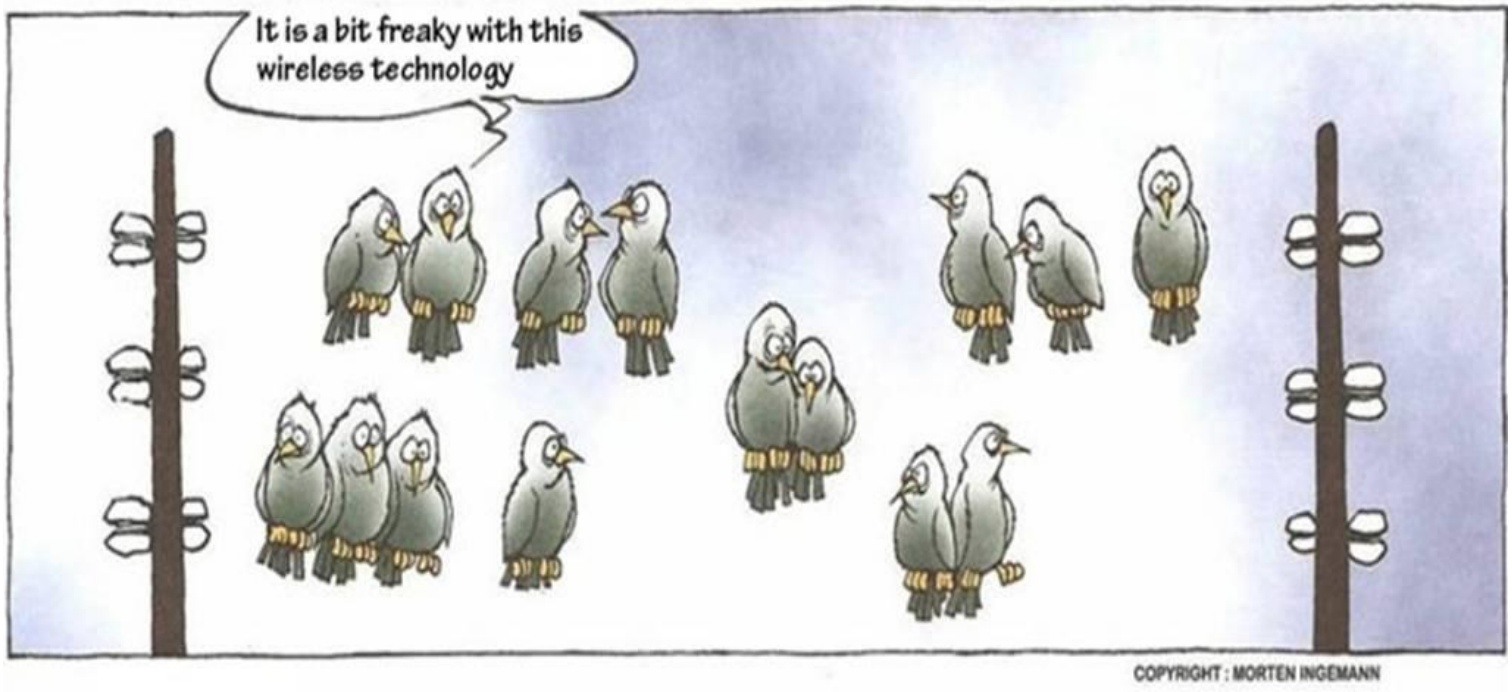

ESTRO School

WWW.ESTRO.ORG/SCHOOL

In Vivo Dosimetry (IVD)

Prof. Luc Beaulieu, Ph.D., FAAPM, FCOMP

1- Département de physique, de génie physique et d'optique, et Centre de recherche sur le cancer, Université Laval, Canada

2- Département de radio-oncologie et Centre de recherche du CHU de Québec, CHU de Québec, Canada

Valencia, Spain – Oct 7-10 2018

Disclosures

- I am leading a research effort to develop scintillator-based dosimeters
- I hold patents related to scintillation dosimetry
- My institution has a licensing agreement with Standard Imaging

Learning Objectives

- Context surrounding IVD in brachytherapy.
- Overview of the tools available and use for clinical IVD in brachytherapy.
- Know the key challenges associated with IVD in brachytherapy.
  - ✓ and possible solutions and NextGEN tools…
- Provide a “skeleton framework” to set-up an IVD in your clinic ➔ Pointers

ESTRO School

In-Vivo Dosimetry

- Dose measurement(s) performed while the Tx. is proceeding
  - Within catheters
  - Intracavity
  - Surface

  - Not necessarily in real-time…

In-Vivo Dosimetry

"In vivo dosimetry (IVD) is in use in external beam radiotherapy (EBRT) to detect major errors, to assess clinically relevant differences between planned and delivered dose, to record dose received by individual patients, and to fulfill legal requirements"

- In vivo dosimetry in external beam radiotherapy. Mijnheer et al, Med. Phys 2013 (Vision 20/20)

In-Vivo Dosimetry

“The initial motivation for performing IVD in BT was mainly to assess doses to organs at risk (OAR) by direct measurements, because precise evaluation of OAR doses was difficult without 3D dose treatment planning.”

- In vivo dosimetry in brachytherapy. Tanderup et al, Med. Phys 2013 (Vision 20/20)

ESTRO School

June 20, 2009

Failed Prostate Procedures at the Philadelphia V.A.

Investigators from the Nuclear Regulatory Commission have found that from 2002 to 2008, a cancer unit at the Philadelphia V.A. botched 92 of 116 brachytherapy procedures. A look at how the procedure is commonly performed.

What went wrong at the Philadelphia V.A.

These computer-generated images, part of a presentation produced by the Nuclear Regulatory Commission, show two specific patients who received the treatment. The images show the major organs, with the surrounding tissue rendered as white. Seeds that are implanted in or near the bladder or rectum can cause undue damage to otherwise healthy organs.

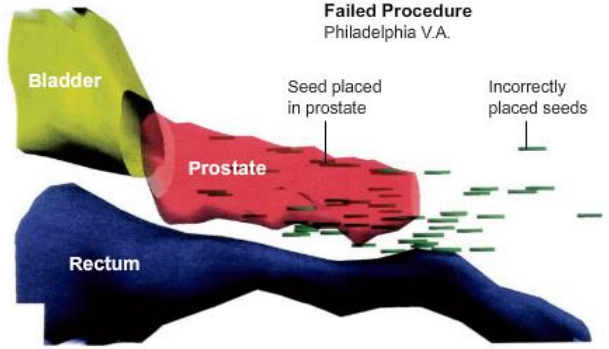

Here some of the radioactive seeds were implanted near the patient's rectum, potentially causing damage to that organ. In addition, the patient's prostate received only 43 gray of the 160 prescribed by the doctor.

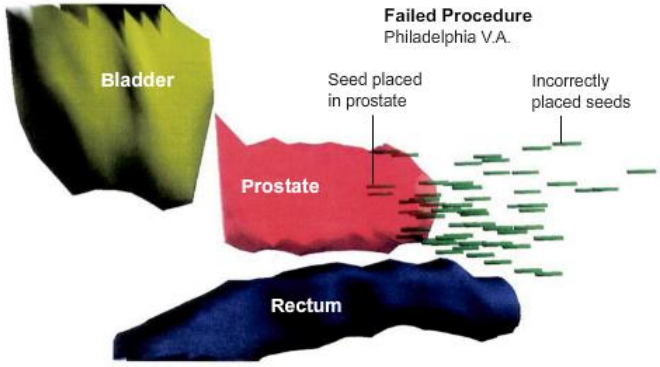

In this case, nearly all of the seeds have been placed outside of the prostate, in the perineum. Of the prescribed dose of 160 gray, the prostate received only 24. This means that the patient's prostate cancer was only minimally treated by the procedure.

Sources: Dr. Adam P. Dicker and Dr. Yan Yu, Jefferson Medical College of Thomas Jefferson University; The Nuclear Regulatory Commission

Graham Roberts/The New York Times

Why in vivo dosimetry?

- Prevent, rare but major accidents
  - *Brachytherapy procedures are performed without the safeguards of Record and Verify systems.*

- Human errors are the main cause of inadequate brachytherapy dose delivery, although mechanical failures occur as well. Examples are:
  - exchanged guide tubes;
  - misadjusted applicators;
  - reconstruction errors;
  - mechanical errors.

ESTRO School

Why in vivo dosimetry?

- About 1/3 of the reported incidents in this IAEA booklet refer to brachytherapy!

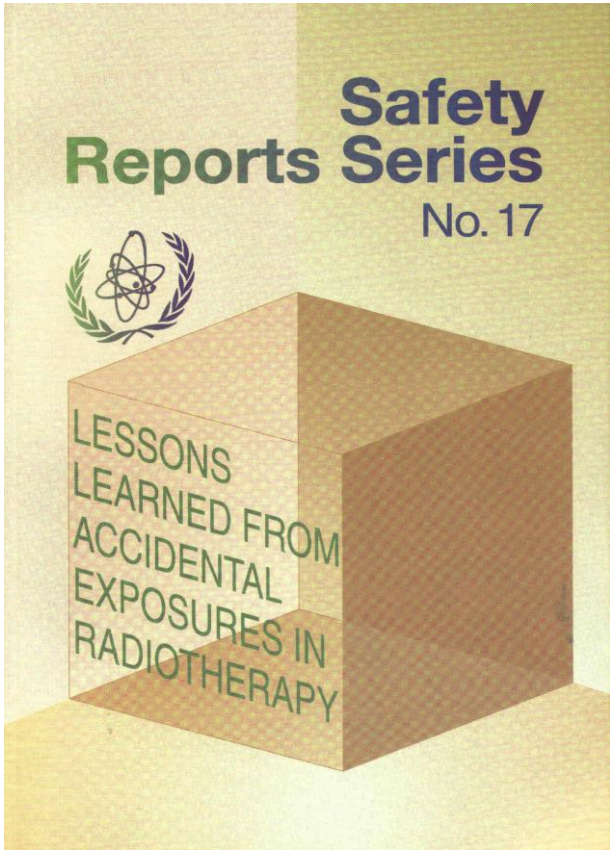

ESTRO School

Why in vivo dosimetry?

- Planned = delivered ?
  - Learning curve
  - Small number of fractions with increasing doses
    - Organ movement or deformation during treatment delivery
    - Organ swelling (LDR/PDR) or relative organ-catheter motion (HDR – multiple fractions)

Why in vivo dosimetry?

- Commissioning of new treatment technique – “in vivo” in phantom;
- Quality control of patient treatments;
- Confirmation of delivered dose (proof of good Tx);
- Used for inter-comparisons and audit systems.

Why in vivo dosimetry?

- Support for the use of in-vivo dosimetry by (inter-) national bodies

- Legal obligation in many countries

Key questions!

- What do we want to know?
- What do we need to measure?

ESTRO School

Incidents in brachytherapy

Uncertainties - Position

- 2mm uncertainty accepted for tip of the needle.
- 0.2mm freedom for the source.
- **In total Δpos $\approx$ 2mm.**

GEC ESTRO survey (2005) - 15/18 responded they encountered incidents

- Incorrect guide tube connection (5 clinics) - Position
- Wrong reconstruction of catheter orientation (tip vs. end) - Position
- Swapped reconstruction of ring and intrauterine applicator - Position
- Uncertain catheter reconstruction - Position
- Wrong catheter length - Position
- Wrong source offset in TPS - Position
- Software bug: wrong definition of template position - Position
- New computer: default dose prescription not updated - Dose rate
- Wrong protocol followed - Position
- Shielding in treatment plan - no shielding in treatment Dose/dose rate
- Shifts (small) of vaginal applicator (due to patient transfer) - Position
- Wrong date change $\rightarrow$ source activity 1 month off - Dose rate
- Mis-typed RAKR value in source certificate by vendor - Dose rate
- Wrong patient in fractionated scheme - Position

Most incidents are due to wrong positioning!

source: Jacob Johansen

Societal Guidance

- ESTRO- the basic philosophy includes routine in-vivo dosimetry as an important chain in Quality Control of radiotherapy including brachytherapy;

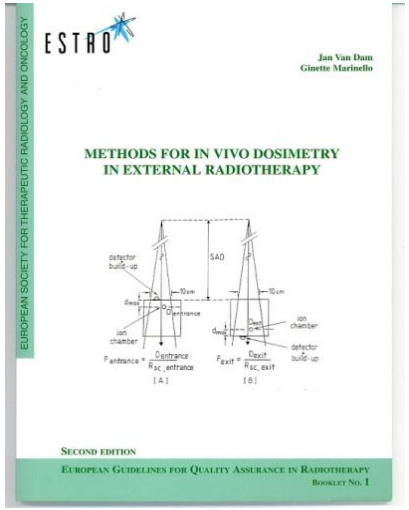

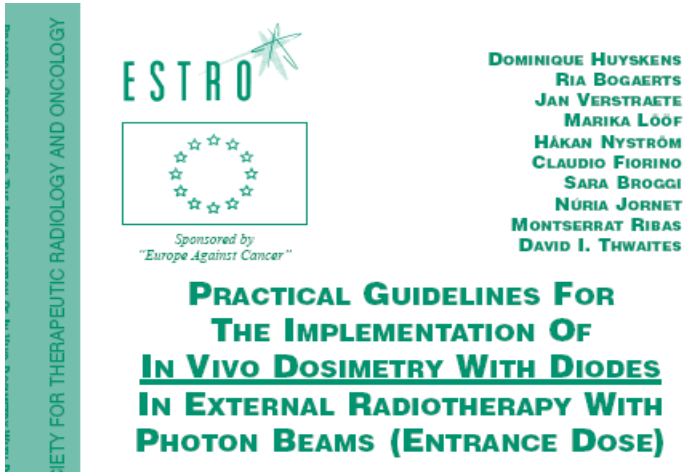

- IAEA – in a mission to improve the accuracy and safety of radiotherapy in developing countries;
- AAPM – TG-62 in a recommendation on the use of diode dosimetry in external beam radiotherapy (AAPM 2005).

ESTRO School

What about Brachytherapy?

Key References

- Work is currently being done by a group within ESTRO to provide a pair of white papers on IVD for EBRT and Brachytherapy.

Key References

- Comprehensive Brachytehrapy: physical and clinical aspect. JLM Venselaar, D Baltas, AS Meigooni and P.J. Hoskin. CRC Press, Taylor & Francis, 2013.
  - In particular Chapters 25: In Vivo Dosimetry in Brachytherapy by Cygler J. et al
- Brachytherapy physics, 2ed, AAPM monograph #31, 2005.
- In vivo dosimetry in brachytherapy. Tanderup K, Beddar S, Andersen C E, Kertzscher G and Cygler J E. Med. Phys. 40 (2013) 070902 - Vision 20/20 manuscript
- In vivo dosimetry: trends and prospects for brachytherapy. Kertzscher G, Rosenfeld A, Beddar S, Tanderup K and Cygler J E. Br. J. Radiol. 87 (2014) 20140206
- **Time-resolved in vivo luminescence dosimetry for online error detection in pulsed dose-rate brachytherapy. Andersen C E, Nielsen S K, Lindegaard J C and Tanderup K. Med. Phys. 36 (2009) 5033–43**
- A dosimetric uncertainty analysis for photon-emitting brachytherapy sources: Report of AAPM Task Group No. 138 and GEC-ESTRO. DeWerd L A, Ibbott G S, Meigooni A S, Mitch M G, Rivard M J, Stump K E, Thomadsen B R and Venselaar J L M 2011 *Med. Phys.* **38** 782–801

Tools and clinical experiences

ESTRO School

TABLE III. Characteristics of detectors and dosimetry systems of importance for precise routine IVD in brachytherapy. The items are rated according to: advantageous (++), good (+), and inconvenient (−).

	TLD	Diode	MOSFET	Alanine	RL	PSD
Size	+	+/−	+/++	−	++	++
Sensitivity	+	++	+	−	++	+/++
Energy dependence	+	−	−	+	−	++
Angular dependence	++	−	+	+	++	++
Dynamic range	++	++	+	−	++	++
Calibration procedures, QA, stability, robustness, size of system, ease of operation	+	++	++	−	−/+	+/++
Commercial availability	++	++	++	++	−	+
Online dosimetry	−	++	+	−	++	++
Main advantages	No cables, well studied system	Commercial systems at reasonable price, well studied system	Small size, commercial system at reasonable price	Limited energy dependence, no cables	Small size, high sensitivity	Small size, no angular and energy dependence, sensitivity
Main disadvantages	Tedious procedures for calibration and readout, not online dosimetry	Angular and energy dependence	Limited life of detectors, energy dependence	Not sensitive to low doses, tedious procedures for calibration and readout, not online dosimetry, expensive readout equipment not available in clinics	Needs frequent recalibration, stem effect, not commercially available	Stem effect

Tanderup et al, Vision 20/20, Med Phys 2013

The Dosimeters

- Diodes (real-time)
  - e.g. PTW 9112 (five diodes array)

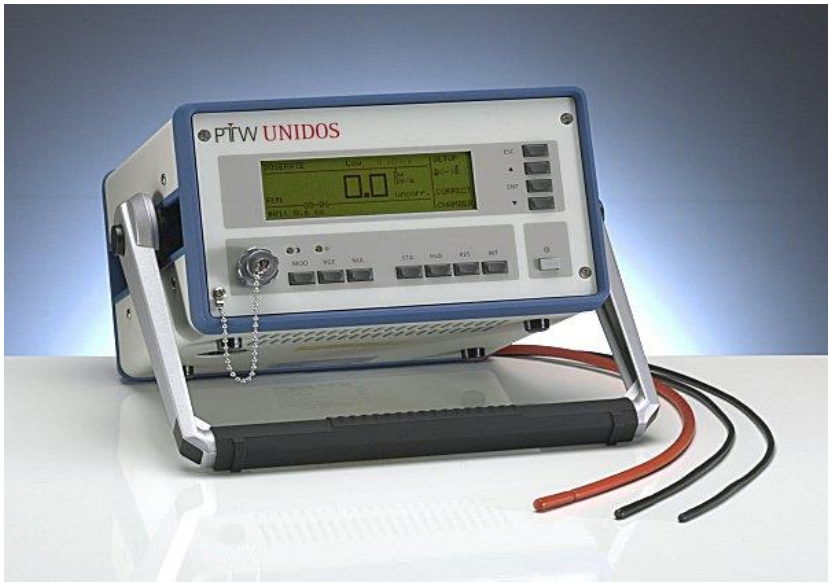

ESTRO School

The Dosimeters

- Diodes: PTW 9112 (5) and 9113 (1)
  - Cervix
    - Alecu R and Alecu M. Med Phys 26 (1999)
      - Agreement with TPS within 15%
    - Waldhäusl C et al., Rad Onc 77 (2005)
      - Phantom: uncertainty of diode measurements of 7% (1σ)
      - Clinical action level of ±10%
      - 36 out of 55 cases need further investigation
        - » 19 > 20% rectal dose
        - » 6 > 20% bladder dose

The Dosimeters

- Diodes

  "...diodes allow performing in-vivo measurements, provided that the position of the diodes relative to the reference points are determined accurately"

  - Waldhäusl C et al., Rad Onc 77 (2005)

Summary of Clinical IVD Studies

Table 9.1. A summary of clinical brachytherapy in vivo dosimetry studies.

Dosimeter	Study	Site	Action Level / Comment	Uncertainty (1 σ)
TLD	Brezovich et al(Brezovich *et al* 2000) Anagnostopoulos et al(Anagnostopoulos *et al* 2003) Das et al(Das *et al* 2007) Toye W et al(Toye *et al* 2008)	Prostate, Urethra, rectal dose,	Action level: 20% generally,	8-10%;
	Raffi et al(Raffi *et al* 2010)	skin (breast)		<3% (TLD uncertainty budget)
MOSFET	Cygler et al(Cygler *et al* 2006) Bloemen-van Gurp et al(Bloemen-van Gurp *et al* 2009a)	Urethra (prostate seed implants)	Action level: 16%	8%
Alanine /ESR	Schultka et al(Schultka *et al* 2006)	GYN (^{137}Cs)	Detector volume too large; Difference with planning 10+%	None provided
	Anton et al(Anton *et al* 2009)	Urethra (prostate HDR)		5% (excl. source strength uncertainty)
Diodes	Alecu and Alecu(Alecu and Alecu 1999)	Cervix	Agreement with TPS within 15%	None provided
	Waldhäusl C et al(Waldhäusl *et al* 2005)	Cervix	Action level: 10% (36/55 cases needs further investigation)	7%
	Seymour et al(Seymour *et al* 2011)	Rectum (Prostate HDR)	95% measurements within 20%	9.8% (meas. only)

Beaulieu et al. Chapter 9

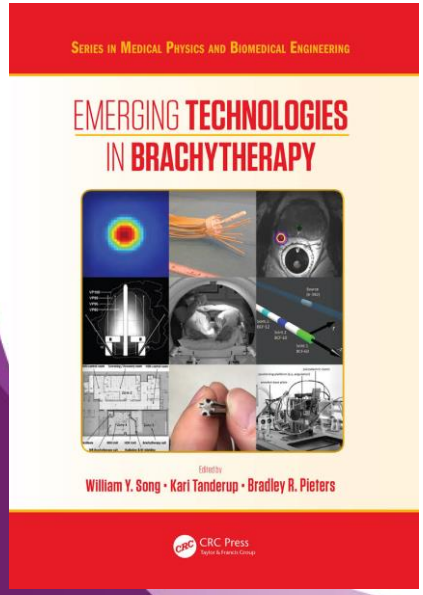

STRO School

Glass Dosimeters	Takayuki et al(Nose *et al* 2008) Hsu et al(Hsu *et al* 2008) Takayuki et al(Nose *et al* 2008) Takayuki et al(Nose *et al* 2005)	Prostate GYN H&N	Deviations of more than 20% seen.	None provided
OSLD "NanoDot"	Sharma and Jursinic(Sharma and Jursinic 2013)	GYN,Breast	-4.4% to 6.5% difference to AcurosBV	None provided
Real-time OSL	Andersen et al(Andersen *et al* 2009)	Cervix (PDR)	Errors detection are distance dependent; Time-resolved measurements are better	5%
Plastic Scintilla-tion	Suchowerska et al(Suchowerska *et al* 2011)	Urethra (prostate HDR)	Maximum deviation without imaging 67%;	None provided
Dosimeters			maximum deviation with imaging 9%	
MOSkin	Carrara et al(Carrara *et al* 2016) Qi et al(Qi *et al* 2012)	Rectum (Prostate HDR) Nasopharynx	Action level: 20%	None provided 2.5% (MOSkin uncertainty budget)

Beaulieu et al. Chapter 9

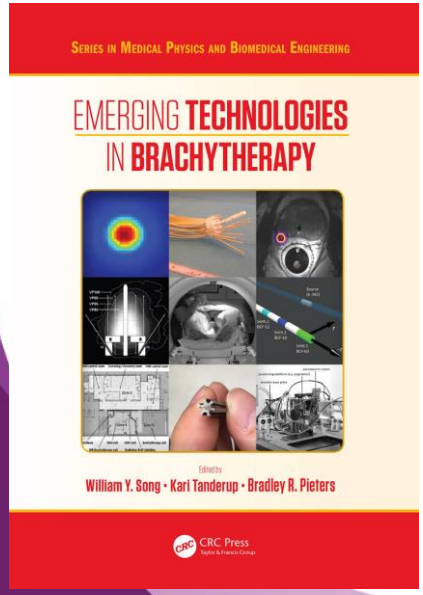

ESTRO School

Lesson learned

- IVD in brachytherapy has only demonstrated its ability to detect gross (dose) errors
  - Above 10 (warning) to 20% (action) depending on sites (dosimeters, isotopes, TPS, …)

Challenges

or

“the physics is killing me” problem

You cannot beat the house

DeWerd et al, AAPM/ESTRO TG138

TABLE IV. Propagation of best practice uncertainties ($k=1$ unless stated otherwise) associated with the transfer of air-kerma strength from a traceable NIST coefficient from the ADCL to the clinic for HDR high-energy brachytherapy sources.

Row	Measurement description	Quantity (units)	Relative propagated uncertainty (%)
1	A		
2	ADCL wel		
3	ADCL calibratio		
4	ADCL calibrati		
5	Clinic measur		
	Expand		

TABLE V. Propagation of best practice uncertainties ($k=1$ unless stated otherwise) in dose at 1 cm on the transverse plane associated with source-strength measurements at the clinic, brachytherapy dose measurements or simulation estimates, and treatment planning system dataset interpolation for low-energy (*low-E*) and high-energy (*high-E*) brachytherapy sources as relating to values presented in Fig. 1.

		Relative propagated uncertainty (%)	
Row	Uncertainty component	*low-E*	*high-E*
1	S_K measurements from row 5 of Tables I and IV	1.3	1.5
2	Measured dose	3.6	3.0
3	Monte Carlo dose estimate	1.7	1.6
4	TPS interpolation uncertainties	3.8	2.6
5	Total dose calculation uncertainty	4.4	3.4
	Expanded uncertainty ($k=2$)	8.7	6.8

School

Tanderup et al.
Vision 20/20.
Med. Phys. 2013

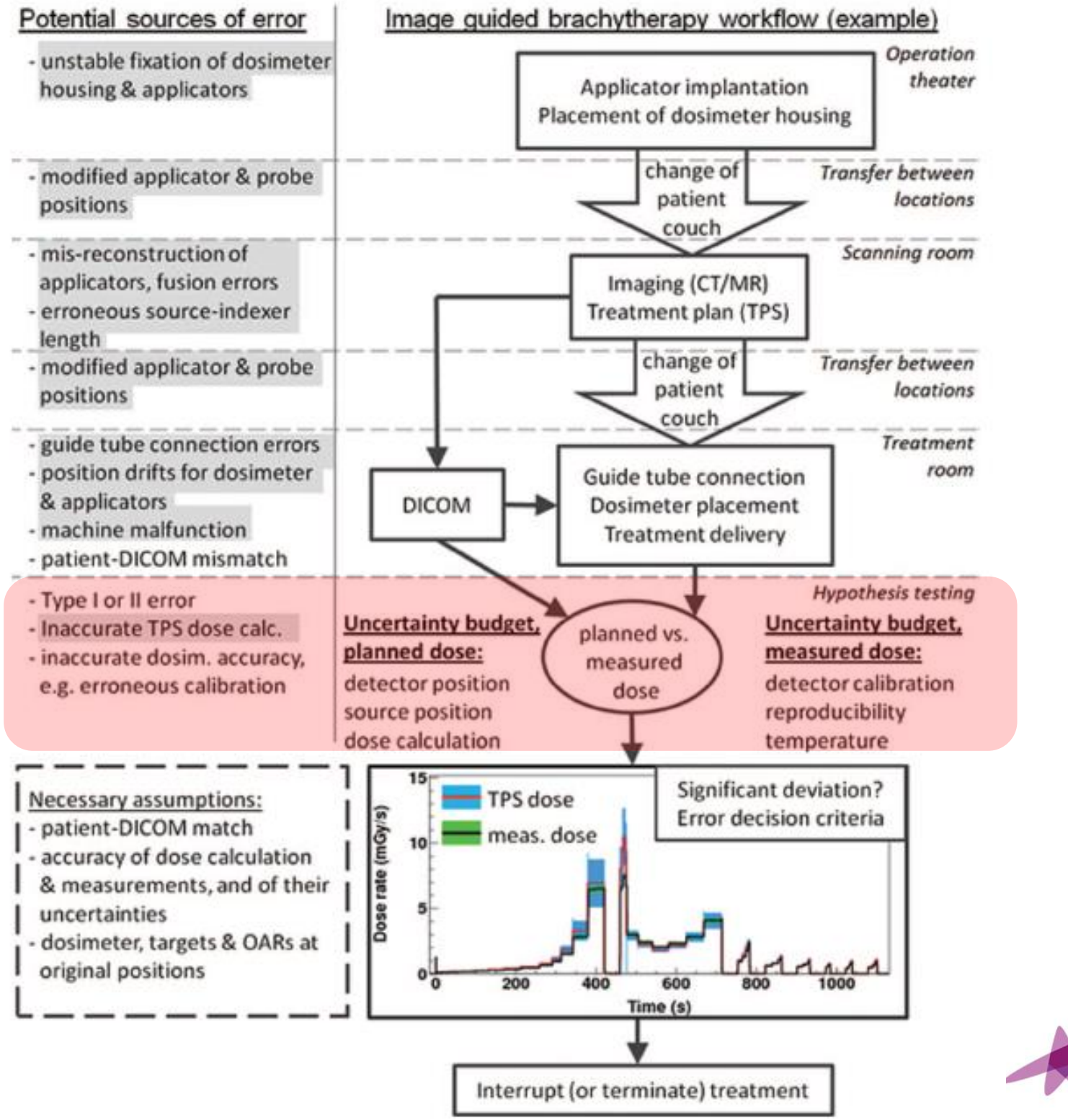

ESTRO School

On uncertainty, detector position and the like…

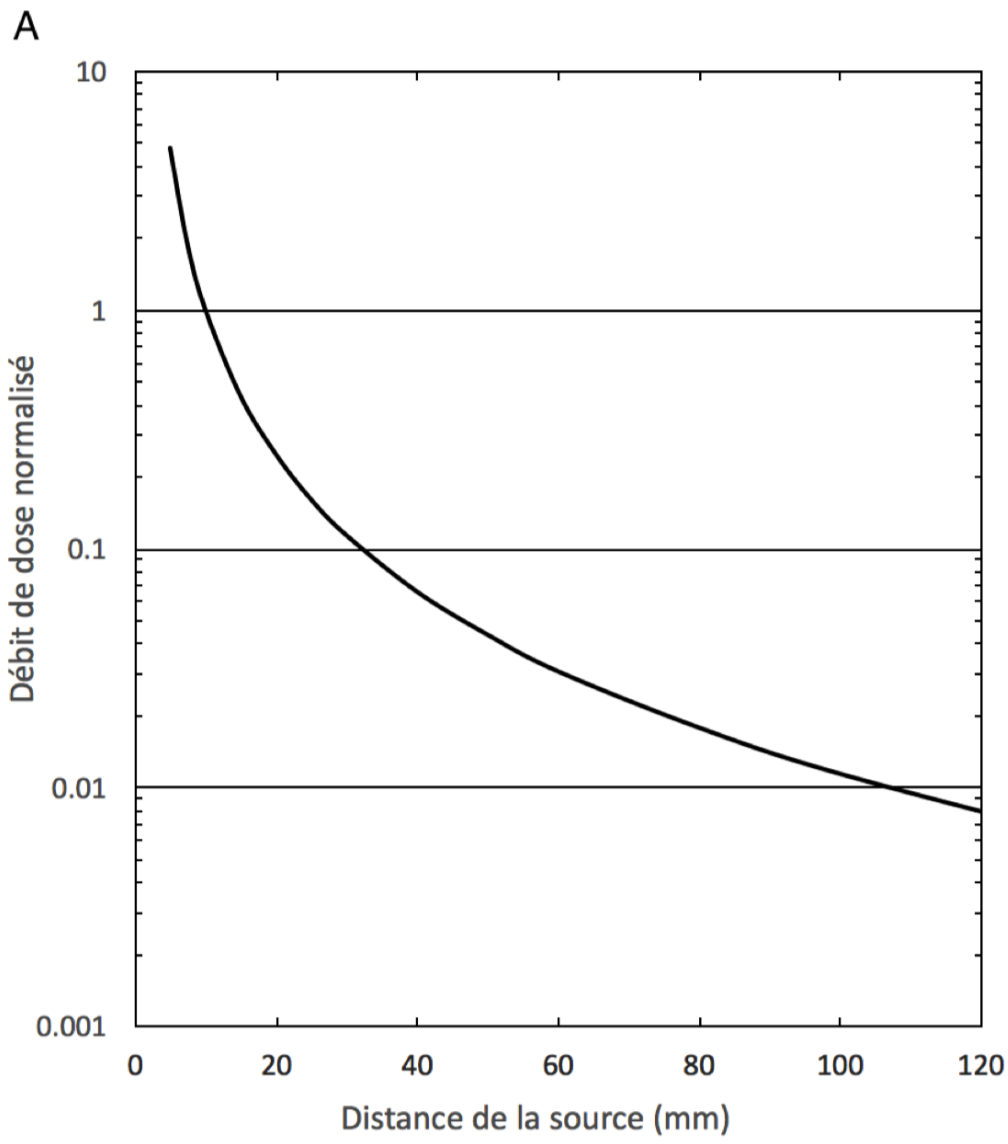

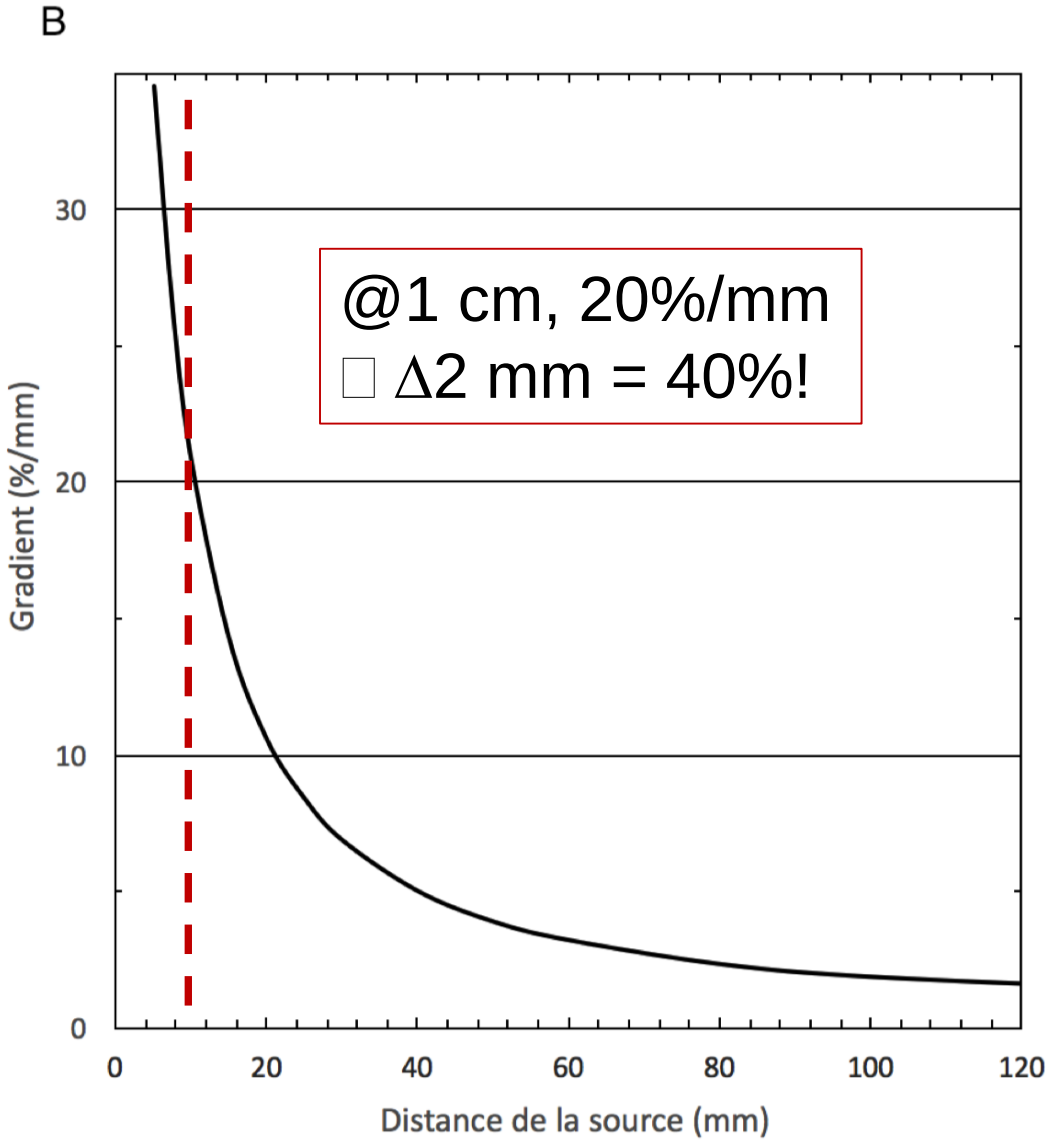

ESTRO School

On uncertainty, detector position and the like…

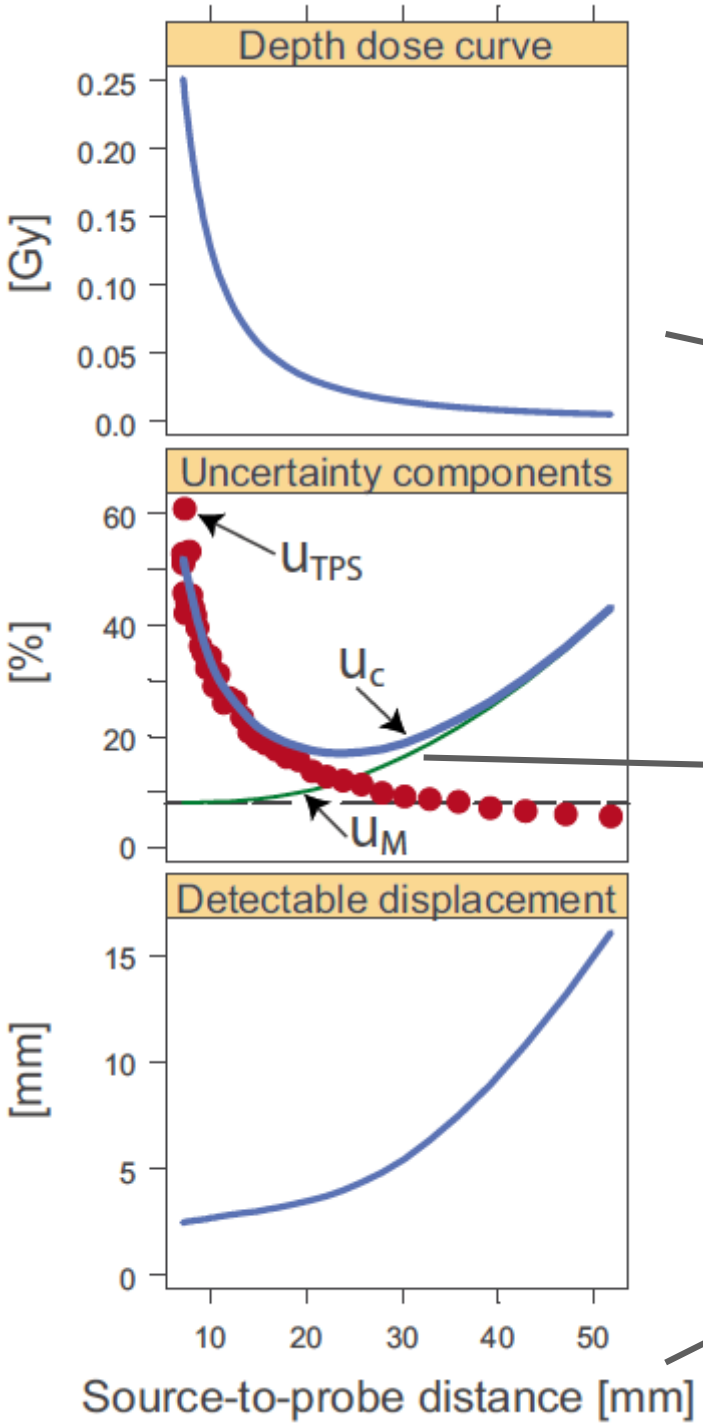

Dose gradient

Dosimeter response

Source-Detector Distance

Andersen et al. *Med. Phys.* **36** (2009) 5033–43

ESTRO School

Source-Detector Distance “problem”

1. Displacement of the dosimeter relative to plan position
    a) Organ-induced displacement
    b) Manipulation error (digitization, displacement before measurements…)
2. Displacement of source position(s) relative to plan position(s)
    a) Displacement of one or more catheters or an applicator, including rotation for certain applicators.
    b) Organ-induced displacement
    c) Manipulation error (wrong transfer tube connection…)
3. Combination of the above two i.e. source and sensor displacements
    a) Perfectly in sync: no effect on dose measured but effect on dose delivered
    b) Out of sync
4. Organ-related change that does not impact the relative distances but organ dosimetry (e.g. swelling, deformation, …)

ESTRO School

Integrated vs Time-Resolved IVD?

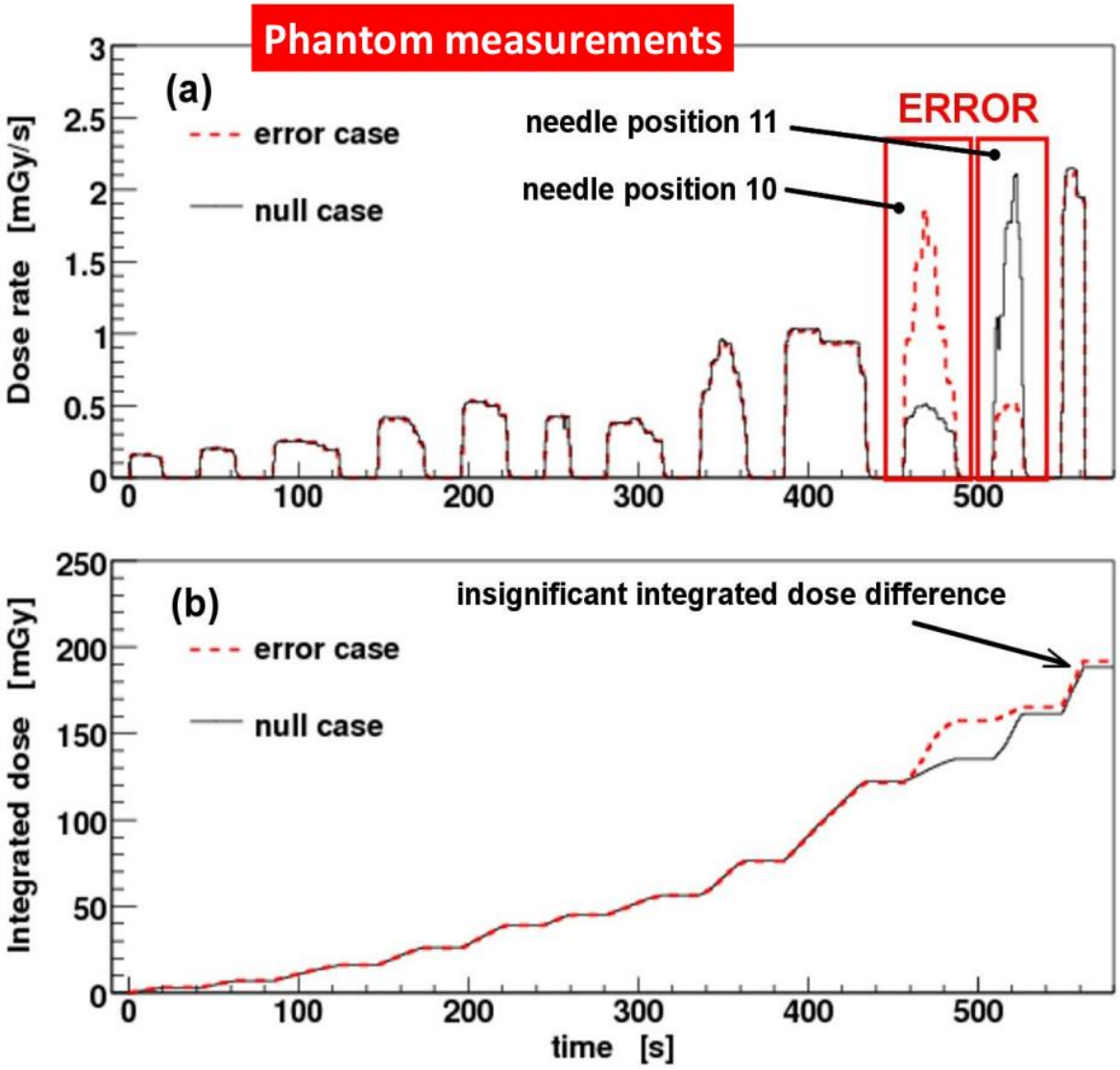

Swap of two needles

- Undetected in total dose
- Clearly seen on a needle or dwell position level

Kertzscher K. et al. Med Phys. 41, 052102 (2014)

ESTRO School

Time-Resolved IVD!

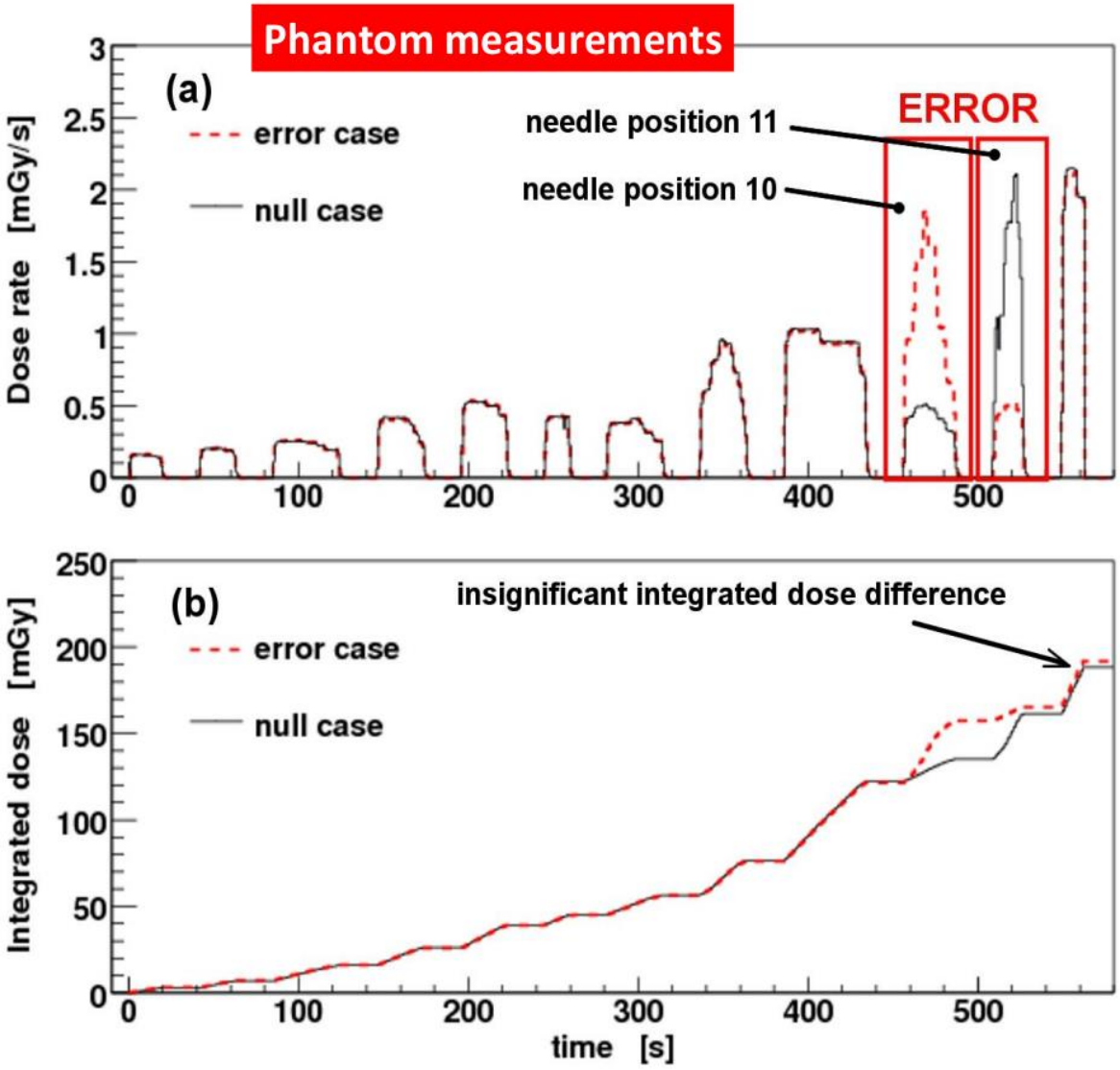

Swap of two needles

- Undetected in total dose
- Clearly seen on a needle or dwell position level

Kertzscher K. et al. Med Phys. 41, 052102 (2014)

ESTRO School

Potential Solutions
and
NextGen IVD tools

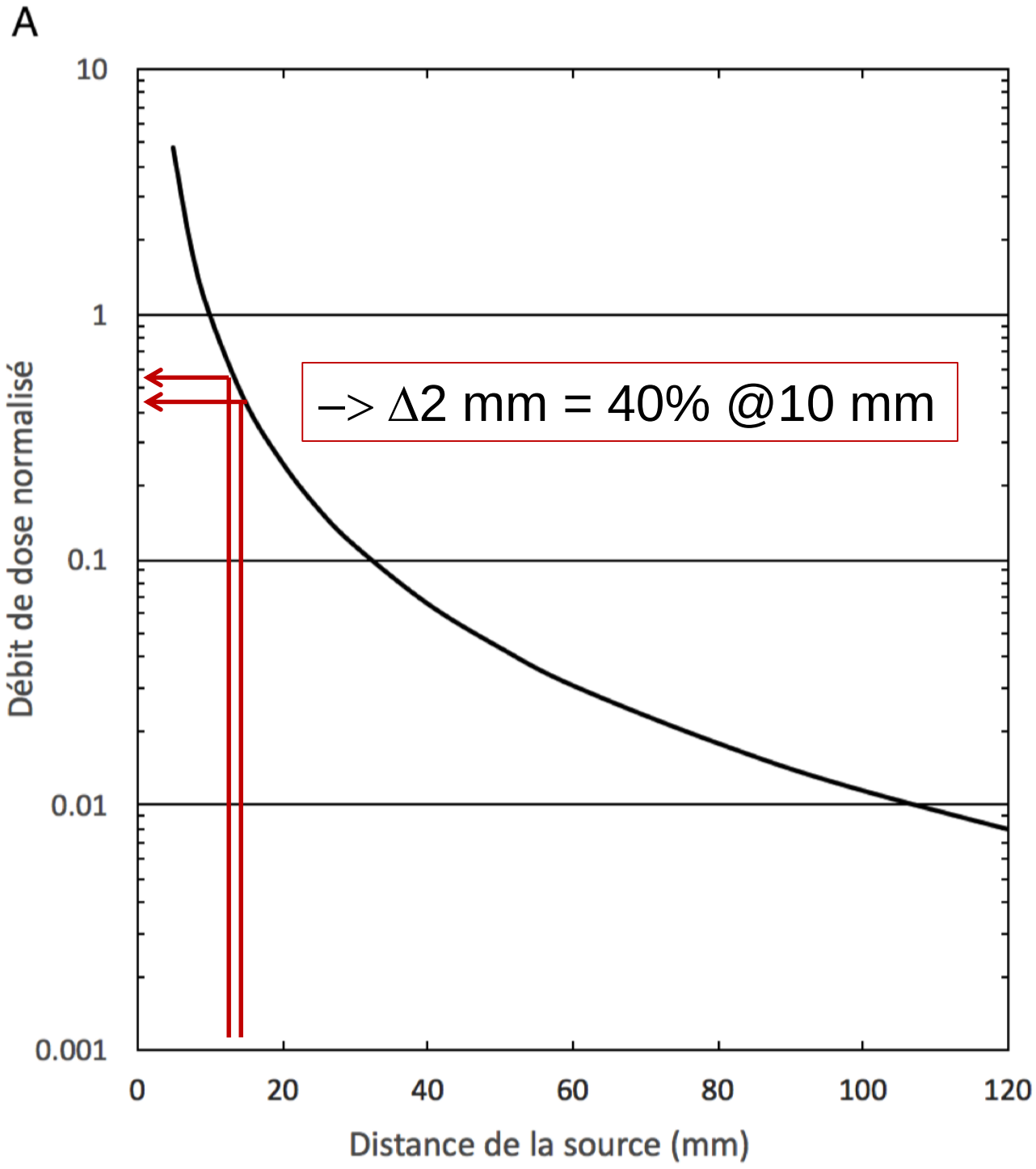

$$\dot{D} \propto \frac{S_K}{r^2}$$

$$\frac{\Delta \dot{D}}{\dot{D}} = 2\frac{\Delta r}{r}$$

ESTRO School

Changing our point of view

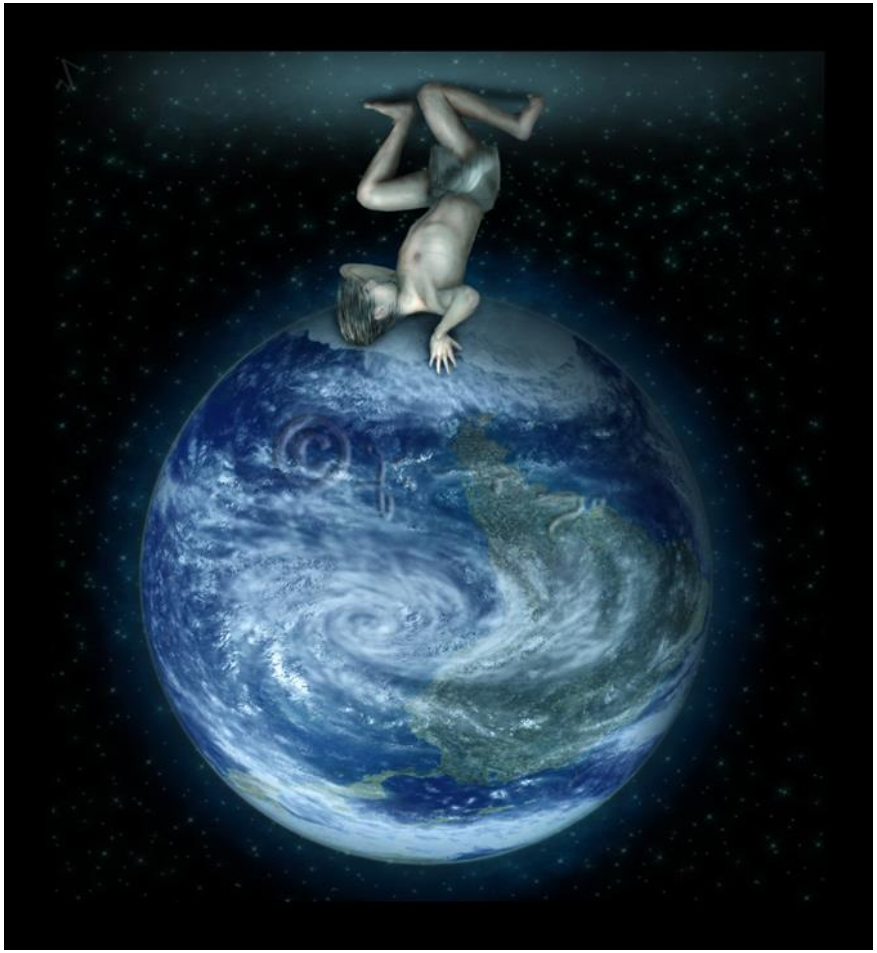

Kertzscher, *Johansen et al.*

ESTRO School

Source tracking

$$\frac{\sigma(\dot{D})}{\dot{D}} \leq 1\% \ (5\%)$$

$$s(r) < 0.05\ mm\ (\square\ 0.15\ mm)\ @1\ cm$$

$$s(r) < 0.25\ mm\ (\square\ 1.4\ mm)\ @5\ cm$$

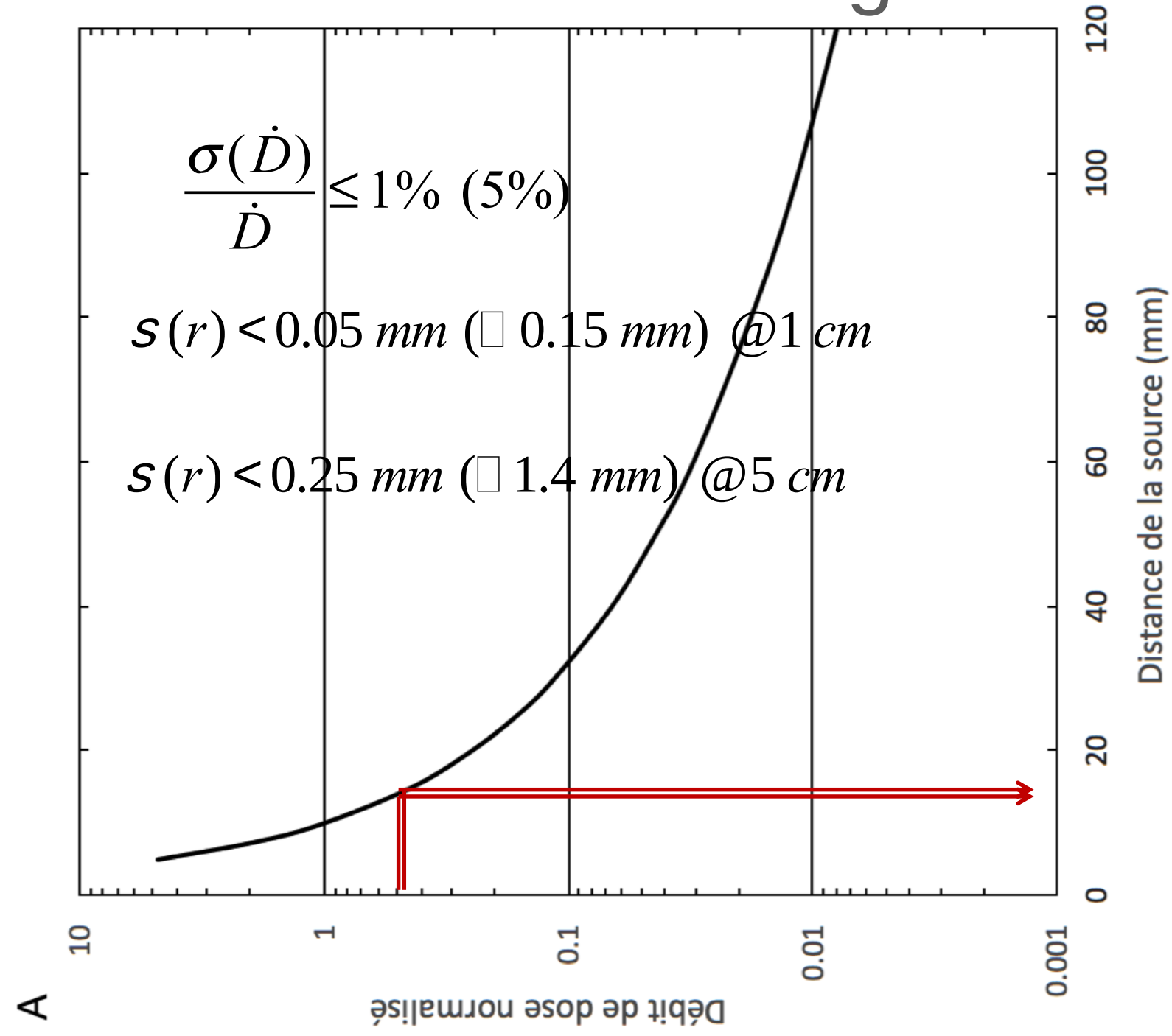

ESTRO School

High SNR IV Dosimeter

- BCF-60
- BCF-12
- Ruby
- Y_2O_3:Eu
- YVO_4:Eu
- **ZnSe:O**
- CsI:Tl

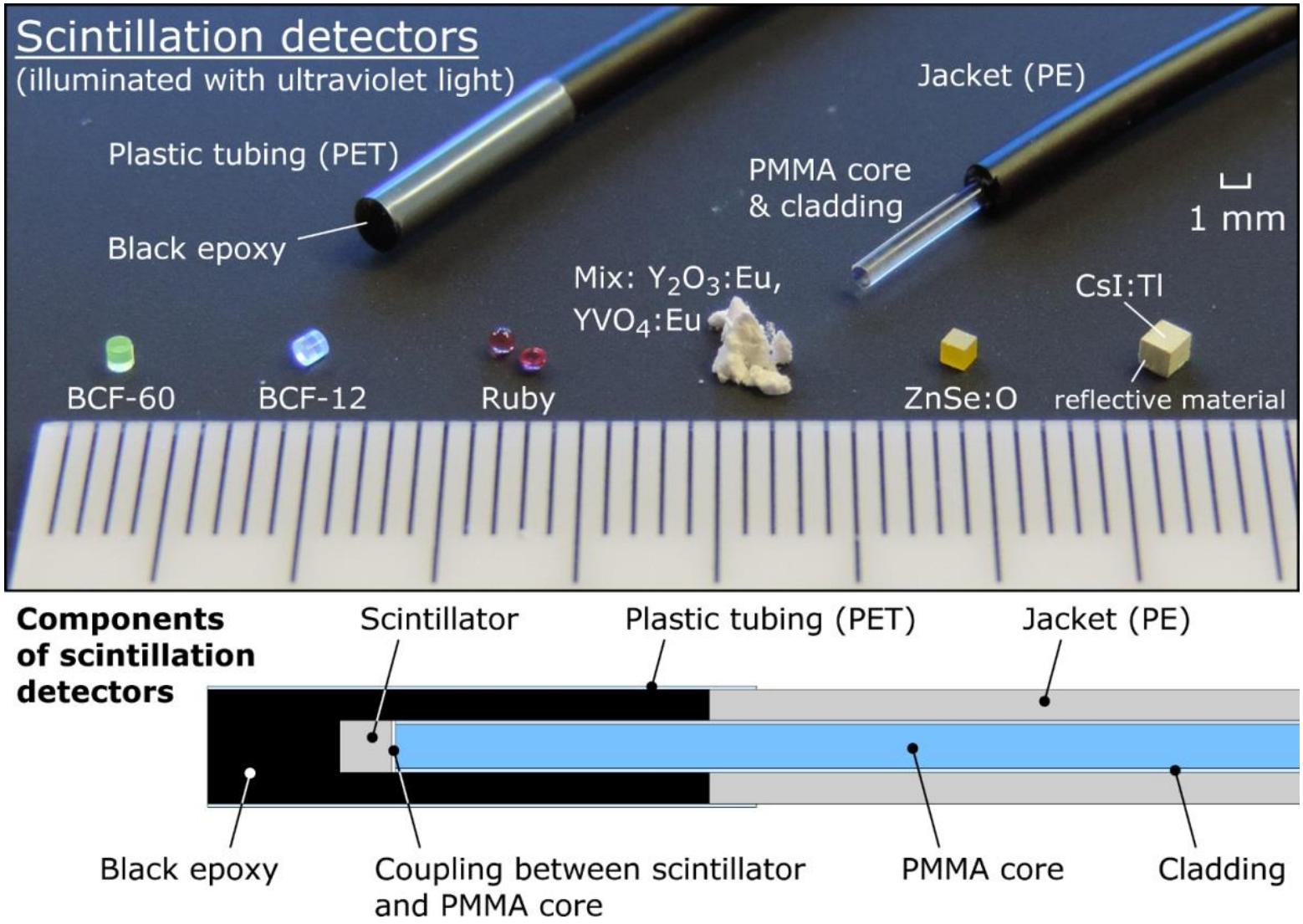

Kertzscher and Beddar. PMB 61 2016; PMB 62 2017,
J of Physics 2017; Physica Medica 52 2018

ESTRO School

High SNR IV Dosimeter

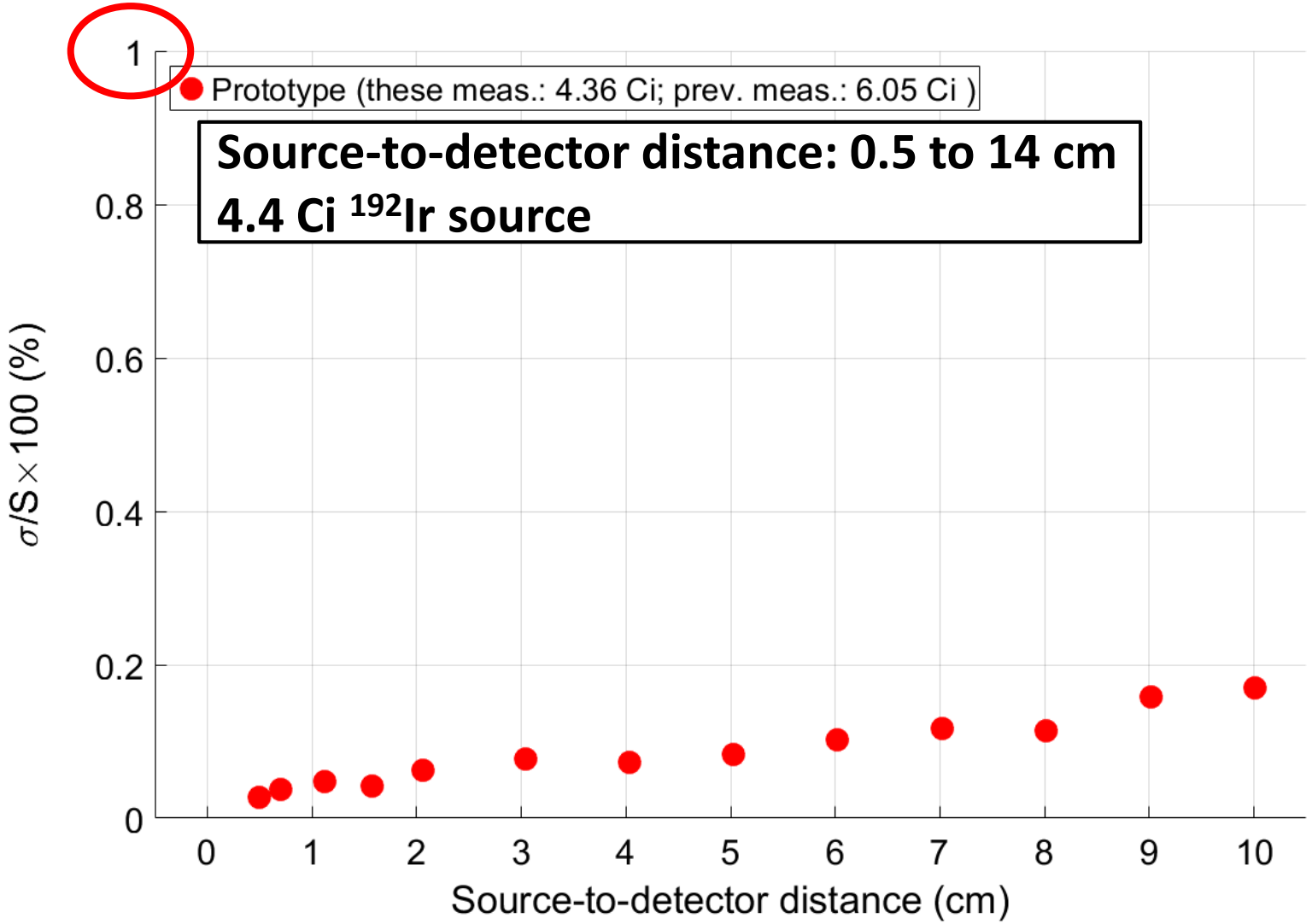

Kertzscher and Beddar. PMB 61 2016; PMB 62 2017,
J of Physics 2017; Physica Medica 52 2018

ESTRO School

Source Tracking

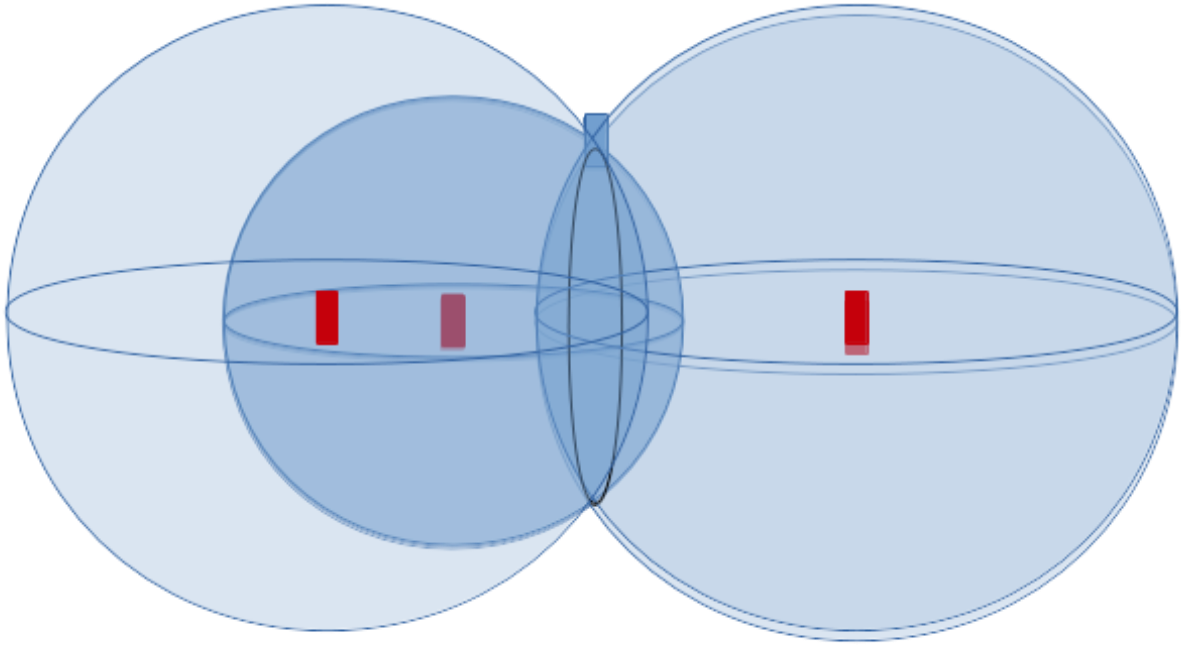

Johansen J.G. et al. Brachy. 17 122-132 (2018)

ESTRO School

Source Tracking

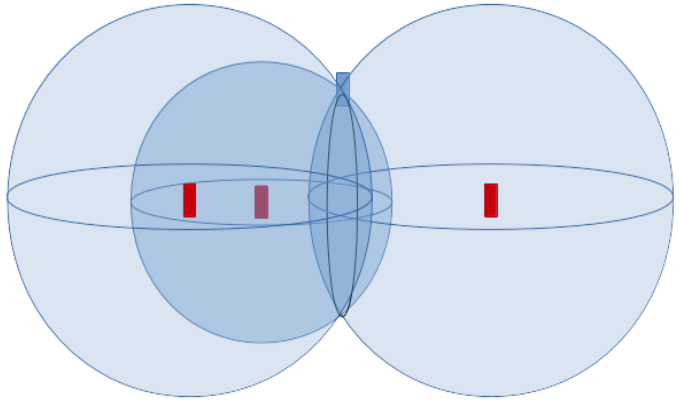

- 1 IV dosimeter and at least 3 dwell positions
  - ➢ Or 3 dosimeters and 1 dwell positions
    - ✓ +1 on a separate line removes solution degeneracies
- Knowledge of source channel: catheter(s) / applicator
- Knowledge of expected dose at the dosimeter position from each dwell position
  - ➢ High SNR/SBR dosimeter
  - ➢ Energy/temperature/angle independent or corrected
- Express any deviation in measured dose as a positional deviation along the channel axis (Δz) and radial distance from it (Δr)

Johansen J.G. et al. Brachy. 17 122-132 (2018)

ESTRO School

Source tracking with one point dosimeter

$\Delta r = \Delta z = 0$

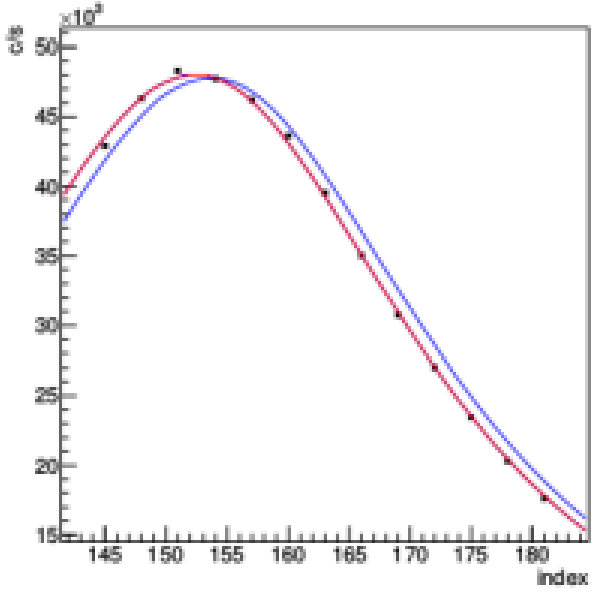

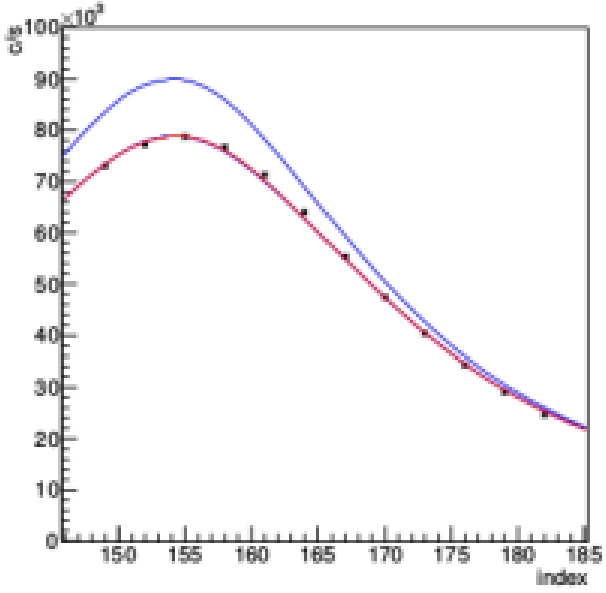

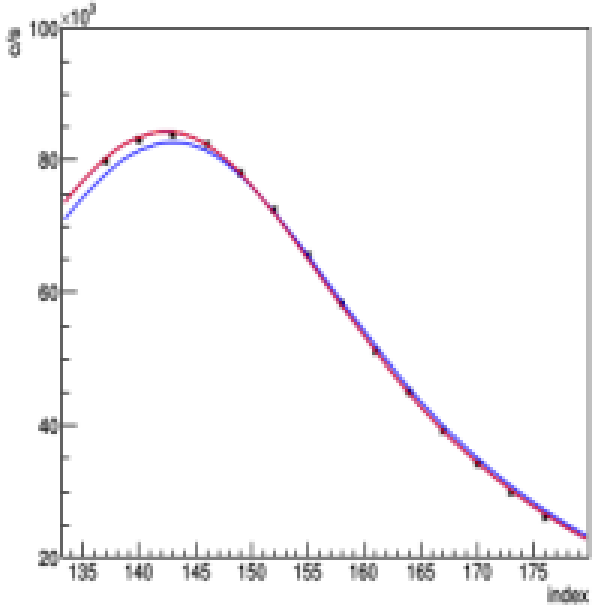

Δz: 1.29mm

Δr: -0.06mm

Δz: -0.25mm

Δr: 1.31mm

Δz: -0.23mm

Δr: 0.65mm

- Δz shifts the curve along the x-axis.
- Δr increases maximum and decreases width.

Johansen J.G. et al. Brachy. 17 122-132 (2018)

ESTRO School

Results from 20 HDR treatments

Δr vs Δz (~300 Needles)

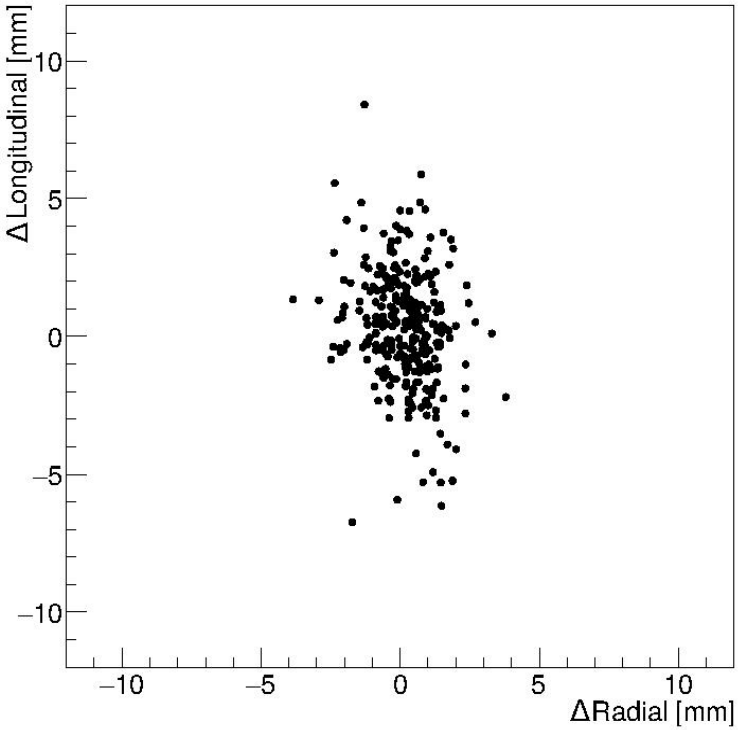

Projections and fits to Gaussian:

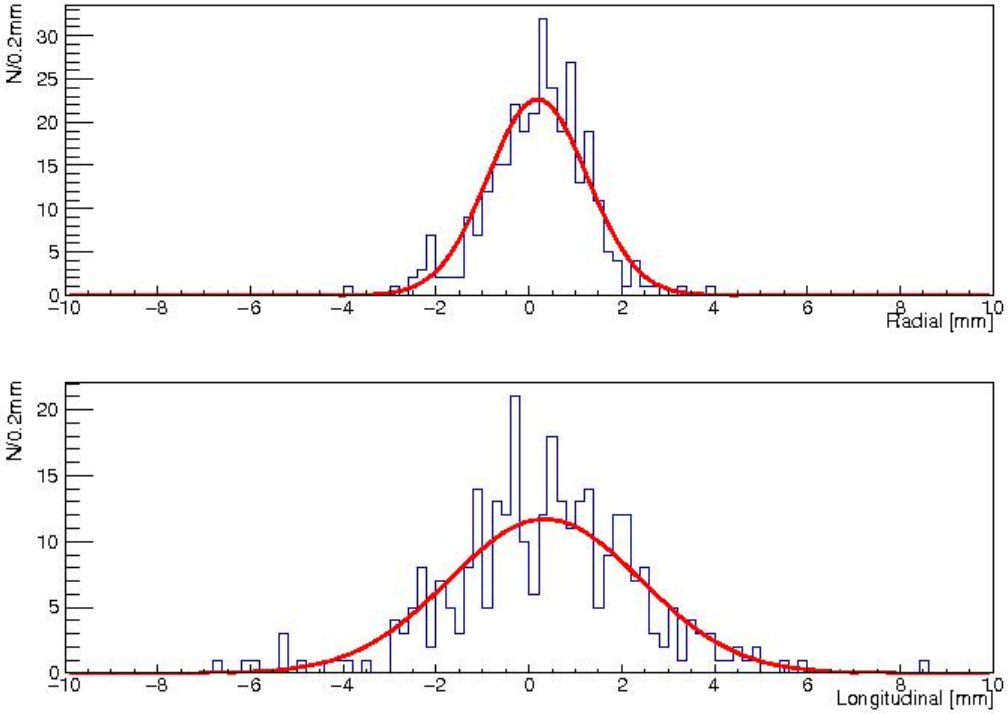

Δr:
Mean = 0.19 mm
1SD = 1.1 mm

Δz:
Mean = 0.34 mm
1SD = 2.0 mm

Johansen J.G. et al. Brachy. 17 122-132 (2018)

Johansen J.G. et al. Brachy. 17 122-132 (2018)

ESTRO School

Results from 20 HDR treatments + 2

Δr vs Δz (~300 Needles)

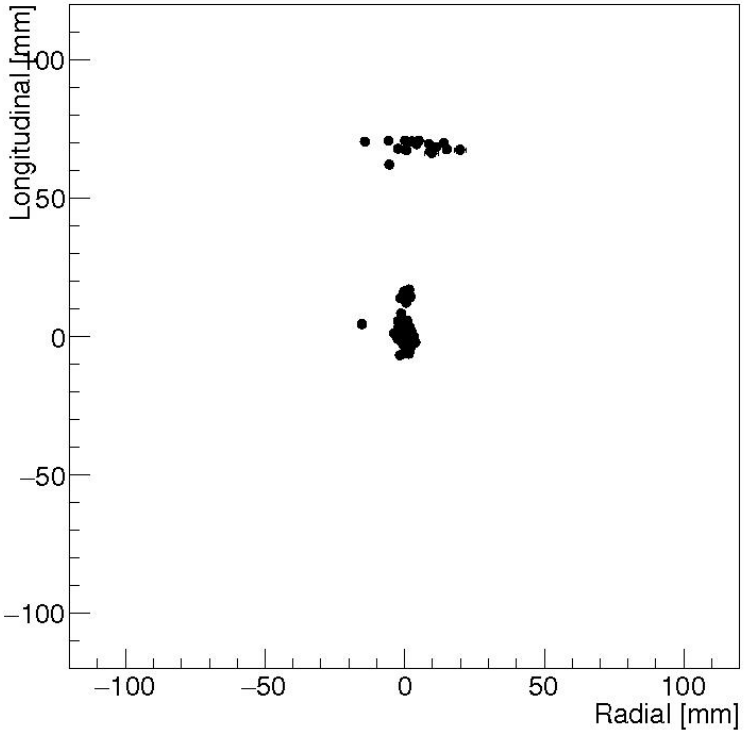

Projections and fits to Gaussian:

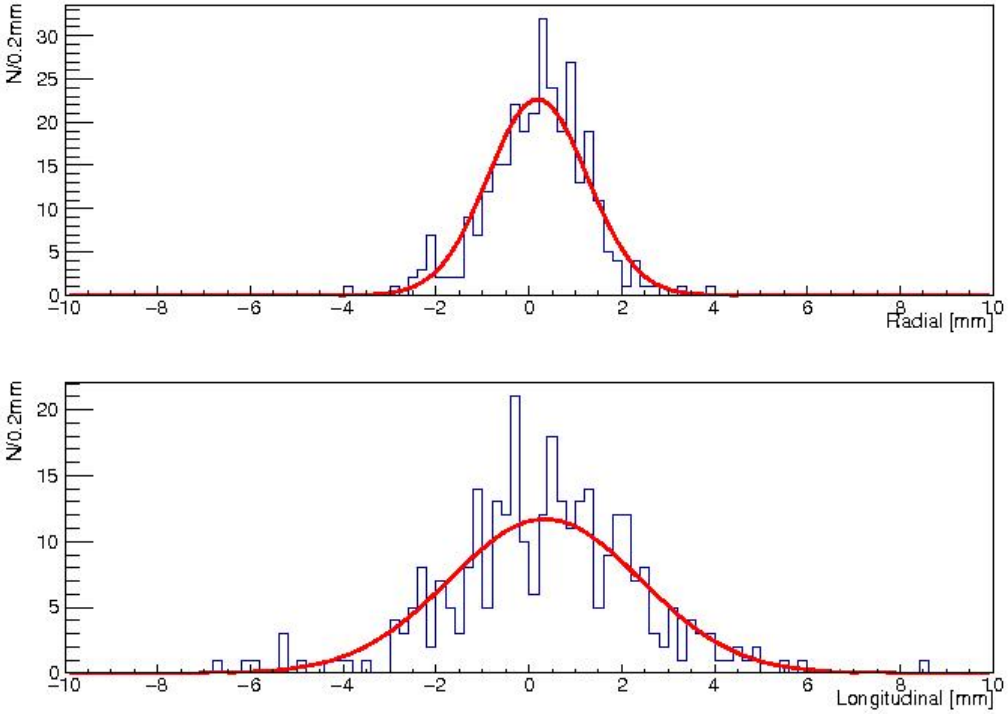

- All needles in a single treatment shifted ~70 mm
  - ➔ Dosimeter drifted 70 mm

Δz:
Mean = 0.34 mm
1SD = 2.0 mm

Johansen J.G. et al. Brachy. 17 122-132 (2018)

ESTRO School

Multi-points IV Dosimeter

- *Archambault et al, PMB 2012*
- *Therriault-Proulx et al, PMB 2012*
- *Therriault-Proulx et al, Med Phys 2013*
- ***H. Linares-Rosales et al., Submited Med Phys 2018.***

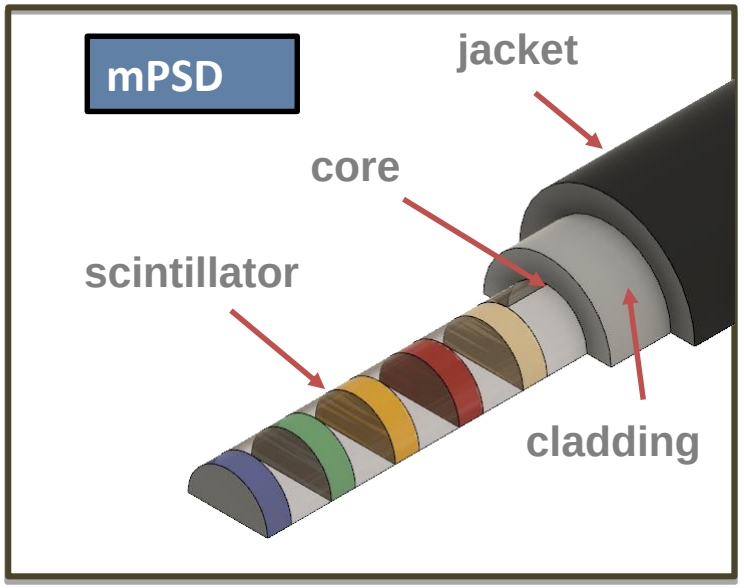

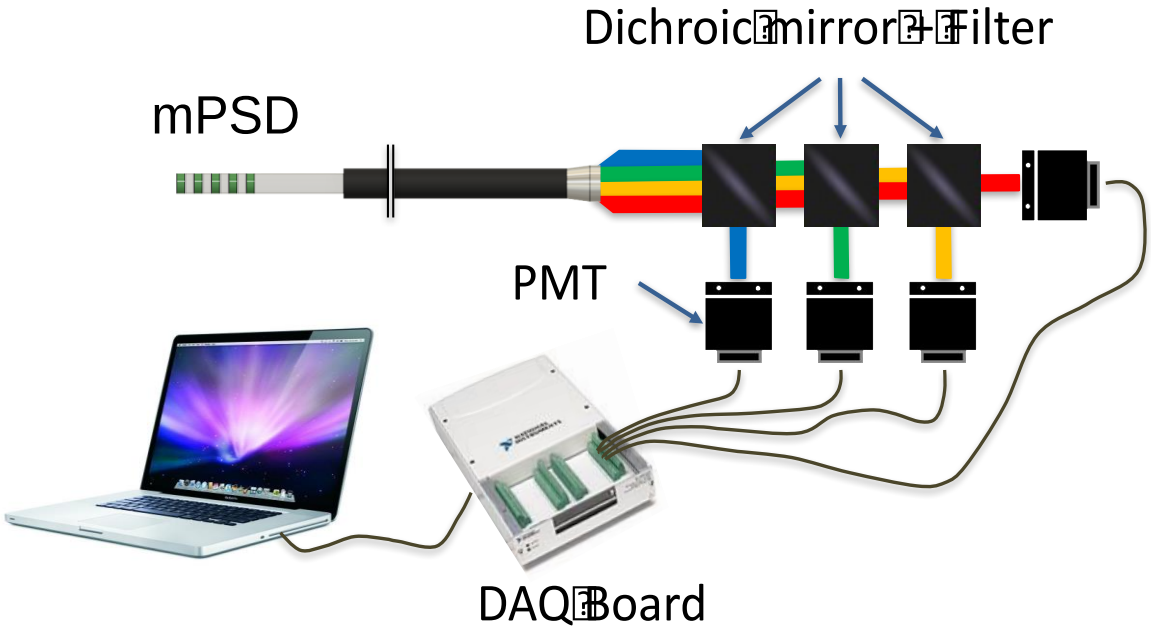

ESTRO School

Multi-points IV Dosimeter

Preliminary

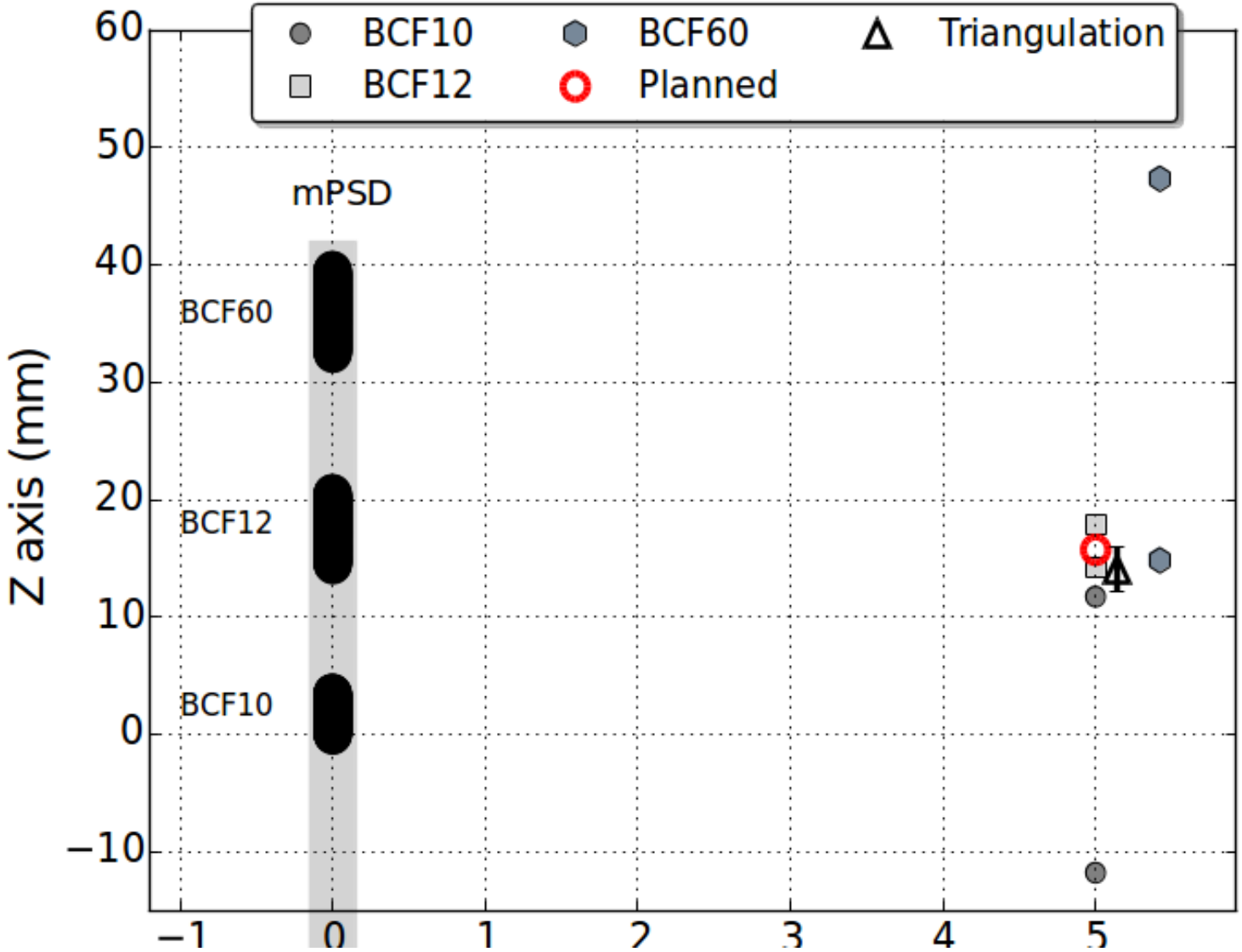

Source: Linares-Rosales

ESTRO School

Next Generation Tools

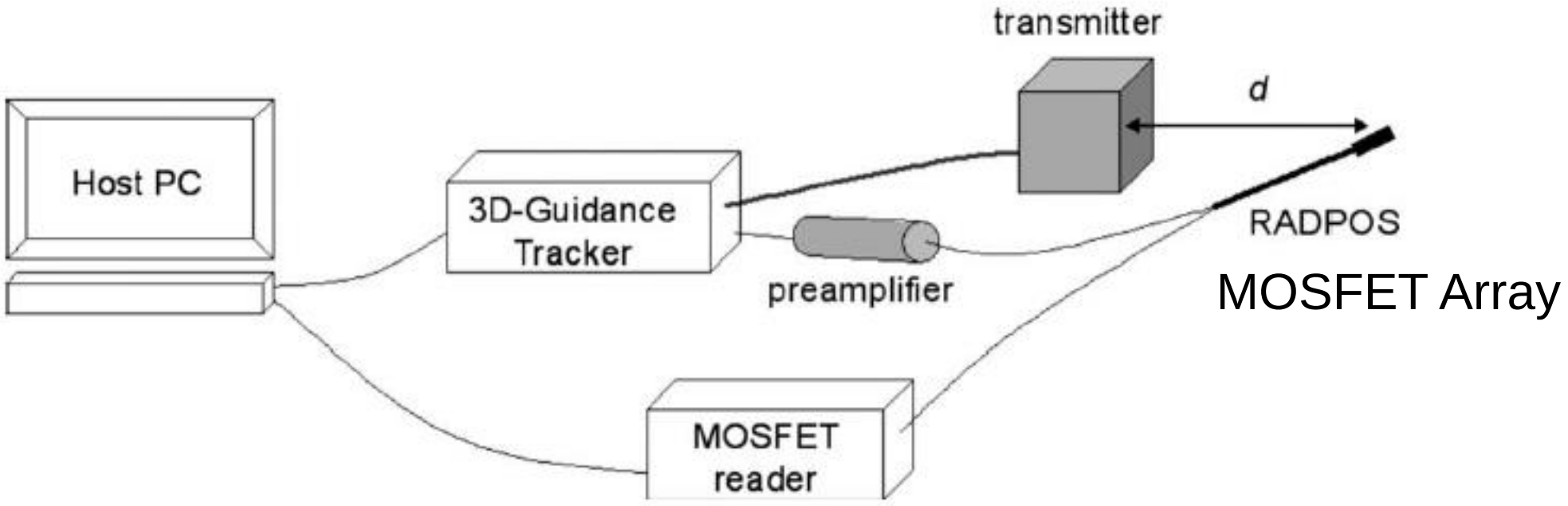

MORE ON TRACKING TECHNOLOGY TOMORROW

Cherpak A J, Cygler J E, E C and Perry G 2014 Real-time measurement of urethral dose and position during permanent seed implantation for prostate brachytherapy. - PubMed - NCBI Brachytherapy 13 169–77

Cherpak A, Ding W, Hallil A and Cygler J E 2009 Evaluation of a novel 4D in vivo dosimetry system Med. Phys. 36 1672

ESTRO School

Next Generation Tools

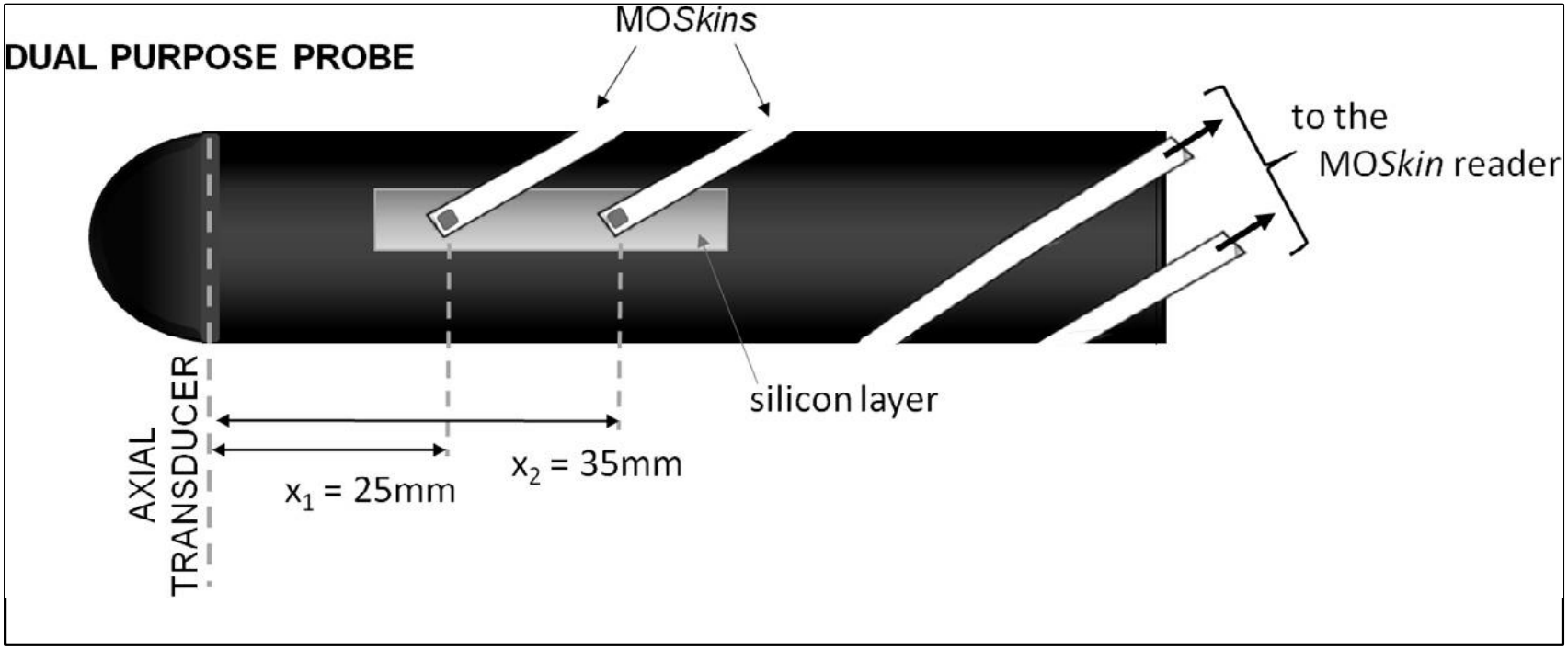

Carrara et al 2016 In vivo rectal wall measurements during HDR prostate brachytherapy with MOSkin dosimeters integrated on a trans-rectal US probe: Comparison with planned and reconstructed doses. *Radiother. Oncol.* **118** 148–53

ESTRO School

Next Generation Tools

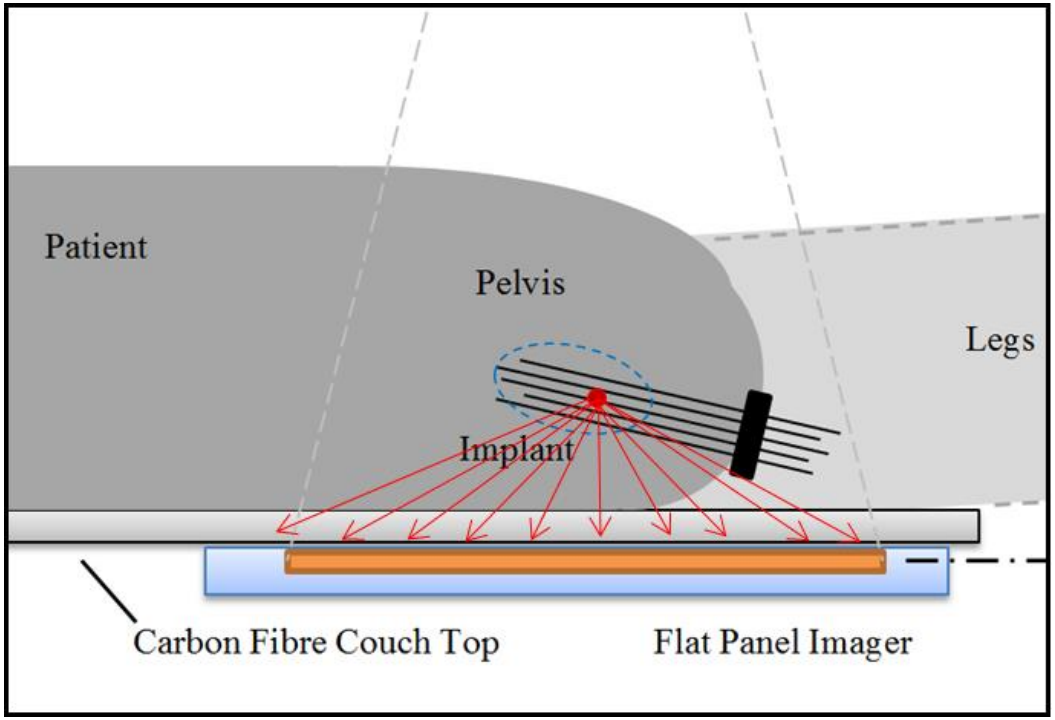

Smith R L, Taylor M L, McDermott L N, Haworth A, Millar J L and Franich R D 2013 Source position verification and dosimetry in HDR brachytherapy using an EPID. Med. Phys. 40 111706

Smith R L, Haworth A, Panettieri V, Millar J L and Franich R D 2016 A method for verification of treatment delivery in HDR prostate brachytherapy using a flat panel detector for both imaging and source tracking. Med. Phys. 43 2435–42

Some pointers…

To do before usage!

- Get to know your IVD tool(s)
  - No dosimeters is perfect
  - Expected performance in controlled conditions
    - Establish the uncertainty budget
  - Limitations
    - Explore characteristics (dependence): energy, angular, temperature, …
    - Detection thresholds (dose, dose rate, known displacements)
    - …

To do before usage!

- Plan to use imaging – think position(s)
  - IV Dosimeters have no direct relation to patient anatomy.
- Take into account TPS limitation
  - Use MBDCA if available.

Consider the following:

- Use time-resolved measurements whenever possible
  - Use more than 1 measurement points if possible
    - Nakano T, Suchowerska N, Bilek M M, McKenzie D R, Ng N and Kron T 2003 High dose-rate brachytherapy source localization: positional resolution using a diamond detector. Phys. Med. Biol. 48 2133–46
  - Track your IV dosimeters in real-time if possible

Back to our key questions…

- Is IVD really the most appropriate tools for the task(s) you are trying to achieve?

Table 9.3 Table adapted from Tanderup *et al.* (2013) recast in term of potentially appropriate technology for the test to be performed.

Quality item	Typical quality test	Appropriate technology
Source calibration	Independent source calibration in the department	Well chamber
Afterloader source positioning and dwell time (nonpatient specific)	Autoradiography, commissioning of applicators, other source stepping and dwell time QA	- Films (position) - Well Chamber (time) - Flat Panel (possible for both)

Afterloader malfunction	Unpredictable afterloader malfunction is
	difficult to target with general QA.
		- Real-time feedback
		  o IVD
		  o Flat Panel

Patient identification	Manual check	Not relevant
Correct treatment plan	Manual check	Checksum and similar independent software validation tools is the more efficient
Intra- and interfraction organ/applicator movement	Reimaging performed just before treatment delivery can in some cases be used to assess organ or tumor dose in image-guided BT.	- For organ motion: real-time imaging if possible - Applicator motion: real-time tracking of the applicator or 3D source tracking within the applicator (EM, optical, Flat Panel) - IVD could be relevant depending on decoupling between applicator and dosimeters
Applicator reconstruction and fusion errors	Manual check	- IVD relevant to catch error during treatment - Pre-delivery or real-time imaging - Independent applicator/channel reconstruction technology (e.g. EM tracking)
Applicator length/source-indexer length	Manual check	- IVD relevant to catch error during treatment - Flat Panel technology - EM tracking (if link to the afterloader drive wire)
Source step size (patient specific)	Manual check	- IVD relevant to catch error during treatment - Flat Panel technology
Interchanged guide tubes	Manual check	- IVD relevant to catch error during treatment - Flat Panel technology - EM tracking (if link to the afterloader drive wire)
Recording of dose	General QA related to dose calculation in the TPS	- IVD only direct mean to measure the real delivered dose - Flat Panel (dose engine needed, not direct)

Beaulieu et al.
Chapter 9

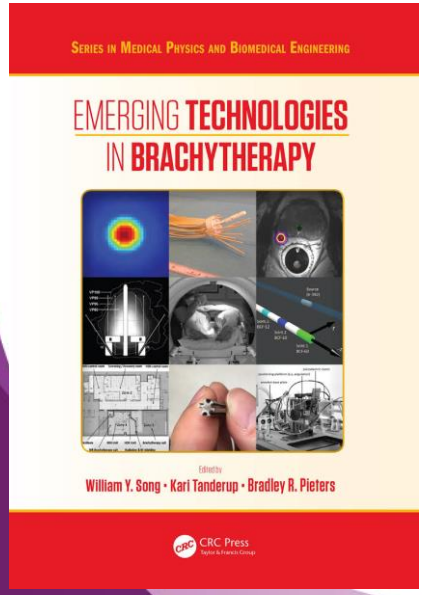

ESTRO School

Conclusion

- IVD has a role in brachytherapy
  - Remains the only way to measure the delivered dose to OARs and target.
- Execution in a clinical setting requires a high level expertise and background preparation
  - It is more difficult than measuring S_k using you well chamber!
- Commercial implementation of appropriate tools needed
  - Tracking
  - Better software (Intelligent, variable action level)

ESTRO School

Valencia, 2018

ESTRO School

Advanced Brachytherapy Physics

Clinical impact of uncertainties

Nicole Nesvacil
Medical University of Vienna

with material by Christian Kirisits, Vienna

ESTRO School

Clinical impact of uncertainties

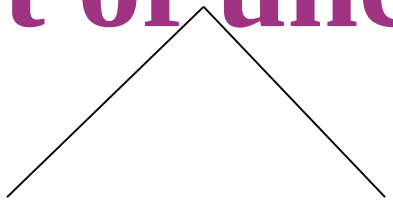

reduction of

Nicole Nesvacil
Medical University of Vienna

with material by Christian Kirisits, Vienna

Terminology

Planning aim dose

- Set of dose and dose/volume constraints for a treatment
  - 4 x 7 Gy to D90 to achieve 84 Gy EQD2 to D90 for HR CTV in cervix (EBRT+BT)
  - 145 Gy to D90 for prostate LDR
  - 8 x 4 Gy to D90 for breast APBI

Prescribed dose = reported dose (input dose for dose-response analysis)

- Finally accepted treatment plan (which is assumed to be delivered to an individual patient)

Delivered dose = dose that produces observable effect (input effect for dose-response analysis)

- Actually delivered dose to the individual patient

From ICRU 89

Example for fractionated brachytherapy

A center performs 4 fractions with the same treatment plan.

The mean prescribed D_{90} is 7 Gy per fraction.

What is the uncertainty in dose delivery due to target volume and OAR changes compared to the treatment plan?

ESTRO School

Raw data

Prescribed D_{90} values in Gy

	Fraction 1	Fraction 2	Fraction 3	Fraction 4
Patient 1	7,0	7,0	7,0	7,0
Patient 2	6,5	6,5	6,5	6,5
Patient 3	7,9	7,9	7,9	7,9
Patient 4	6,7	6,7	6,7	6,7
Patient 5	6,8	6,8	6,8	6,8
Patient 6	8,1	8,1	8,1	8,1
Patient 7	7,5	7,5	7,5	7,5
Patient 8	6,4	6,4	6,4	6,4
Patient 9	6,2	6,2	6,2	6,2
Patient 10	7,0	7,0	7,0	7,0

Raw data

Delivered D_{90} values in Gy

	Fraction 1	Fraction 2	Fraction 3	Fraction 4
Patient 1	7,0	5,4	6,1	6,2
Patient 2	6,5	6,9	7,0	6,5
Patient 3	7,9	7,8	7,7	8,5
Patient 4	6,7	8,3	8,5	10,2
Patient 5	6,8	7,1	5,9	5,5
Patient 6	8,1	8,3	6,5	7,4
Patient 7	7,5	7,1	7,3	6,5
Patient 8	6,4	6,7	6,7	6,0
Patient 9	6,2	4,7	5,8	5,4
Patient 10	7,0	7,9	8,5	10,1

Results - Study 1 – Total physical dose

The mean prescribed D90 is

28 Gy (4 x 7 Gy)

The mean delivered D90 is

28.3 Gy

<u>This means on average a 1 % deviation.</u>

Results - Study 2 – Difference per fraction

The mean difference of prescribed dose and delivered dose per fraction is

0.1 Gy

<u>This means on average a 1 % deviation.</u>

Results – Study 3 – Difference per fraction

The mean difference of prescribed dose to delivered dose per fraction is

0.1 Gy (1%) systematic uncertainty

One standard deviation

0.9 Gy (13 %) random uncertainty

Results – Study 4 – Difference in total EQD2

The total prescribed dose including 45 Gy EBRT in EQD2

is

84.2 Gy EQD2

The delivered dose is

84.8 Gy EQD2

Mean difference is 0.6 Gy (< 1%)

Results - Study 5 – Difference in total EQD2

The total prescribed dose including 45 Gy EBRT in EQD2

is

84.2 Gy EQD2

The delivered dose is

84.8 Gy EQD2

Mean difference is 0.6 Gy (< 1%)

One standard deviation is 3.5 %

ESTRO School

Radiotherapy and Oncology

Volume 110, Issue 1, January 2014, Pages 199–212

Guidelines

Review of clinical brachytherapy uncertainties: Analysis guidelines of GEC-ESTRO and the AAPM ☆

Christian Kirisits[a], Mark J. Rivard[b], Dimos Baltas[c], Facundo Ballester[d], Marisol De Brabandere[e], Rob van der Laarse[f], Yury Niatsetski[g], Panagiotis Papagiannis[h], Taran Paulsen Hellebust[i, j], Jose Perez-Calatayud[k], Kari Tanderup[l], Jack L.M. Venselaar[m], Frank-André Siebert[n]

Show more

doi:10.1016/j.radonc.2013.11.002

Get rights and content

Open Access funded by Austrian Science Fund (FWF)

"A substantial reduction of uncertainties in clinical brachytherapy should result in improved outcome in terms of increased local control and reduced side effects. Types of uncertainties have to be identified, grouped, and quantified."

- Comprehensive literature review of uncertainty components in Brachytherapy for different clinical sites, and their relative importance to the combined overall dosimetric uncertainty.
- Examples for gyn, prostate, breast BT that can be used as templates for future dose and uncertainty reporting.

ESTRO School

Need for common terminology

Errors

- Mainly resulting in systematic deviations
  - Wrong source strength in afterloader unit
  - Wrong offset for applicator tip to first dwell position
  - Wrong catheter connections, etc…

Need for common terminology

Uncertainties

- Type A (statistical)
- Type B (everything else)

Analyze and present systematic effects

(target volume shrinkage, edema causing applicator shifts)

Analyze and present normally distributed effects

(random catheter shifts, reconstruction with finite slice thickness)

Need for common terminology

Variations

- Known effects which can be predicted.
  - E.g. bladder filling can have an impact on dose to bladder or bowel
  - Prostate swelling influences the D90 – if the variations over time are known the delivered dose can be predicted

Systematic set-up uncertainties

- Same error in every fraction
- Examples
  - ➢ Incorrect reconstruction procedures (source path commissioning)
  - ➢ Systematic misinterpretation of images

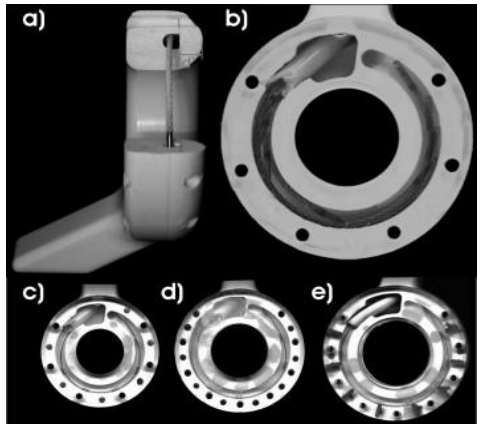

Berger et al. 2009, R&O 93

CT MR

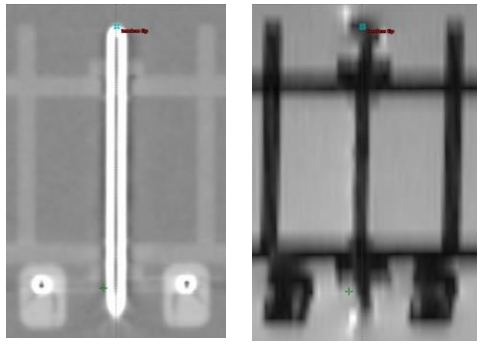

Hellebust et al 2007, PMB 52

Random set-up uncertainties

- Different in every fraction
- Visibility of applicator (dependent on slice thickness)
- Uncertainties of image fusion
- Pronounced in longitudinal direction (perpendicular to slice orientation)

Sagittal reconstruction from para-transverse MR

Sagittal reconstruction from transverse MR

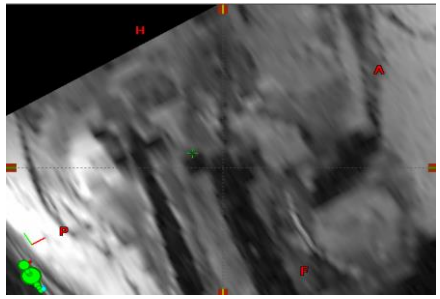

Examples for setup uncertainties in BT:

Gyn: Mean DVH shifts (%) due to uncertainties in tandem/ring applicator position (mm) (reconstruction or movement)

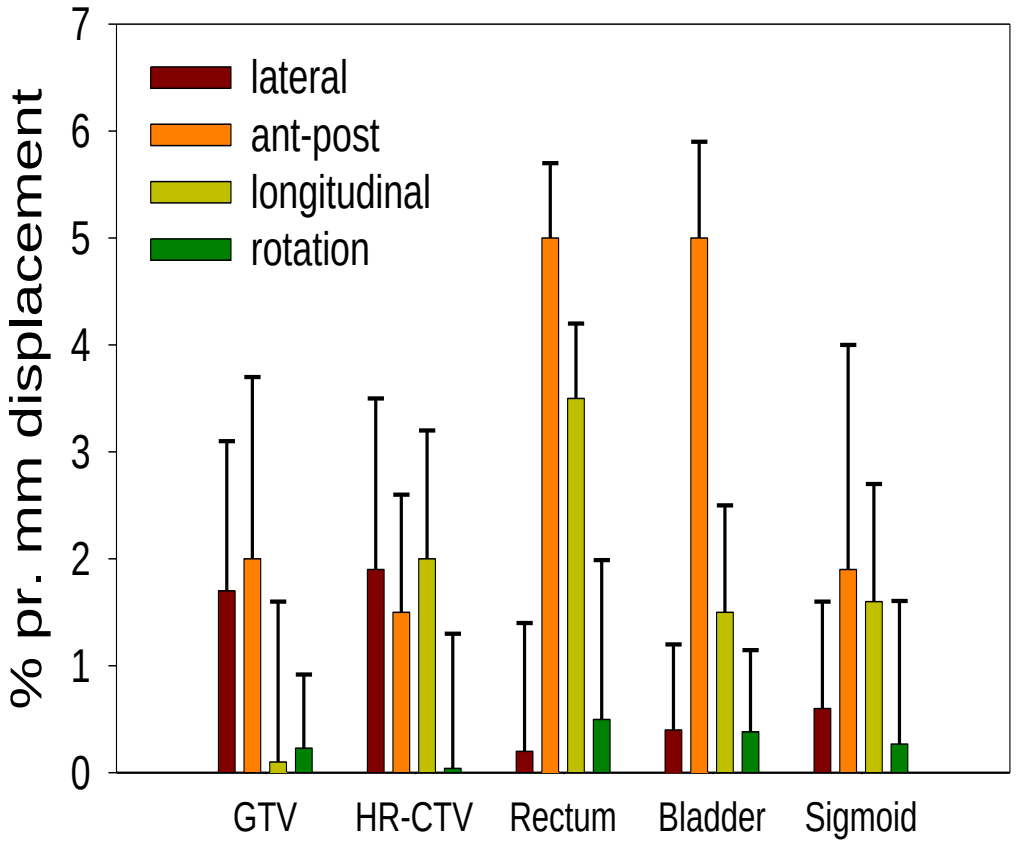

Tanderup et al. 2008, Radiother Oncol 89

Prostate: Variations of target dose during HDR treatment due to catheter and gland movement

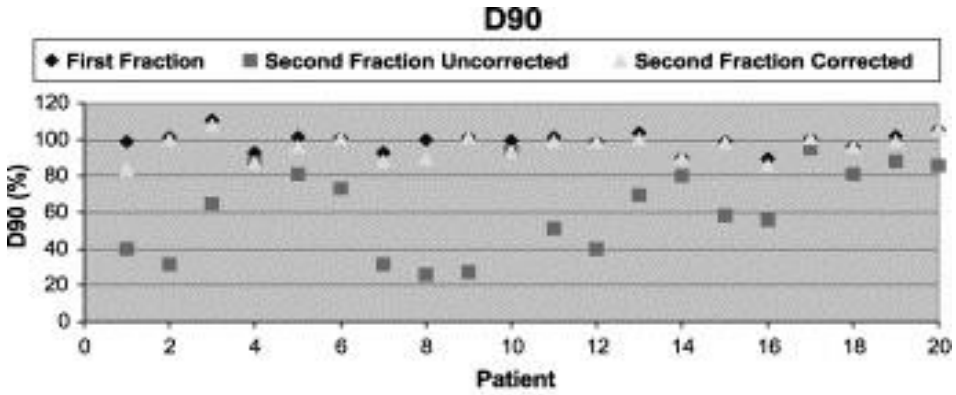

Hoskin et al. 2003, Radiother Oncol 68

Breast: variations of maximum skin dose and high dose volumes of breast tissue (Mammo Site applicator)

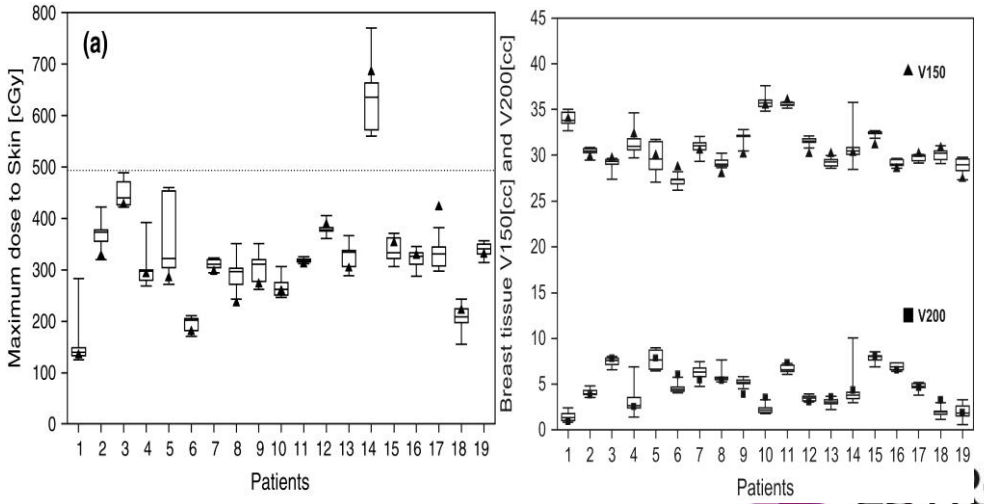

Kim Y. et al 2008, IJROBP 71

Deviations of DVH parameters

Inter-TPS variation

	Large Cylinder	Cone
$D_{0.1cc}$ 1 SD	**3%**	**3%**
D_{2cc} 1 SD	**1%**	**5%**

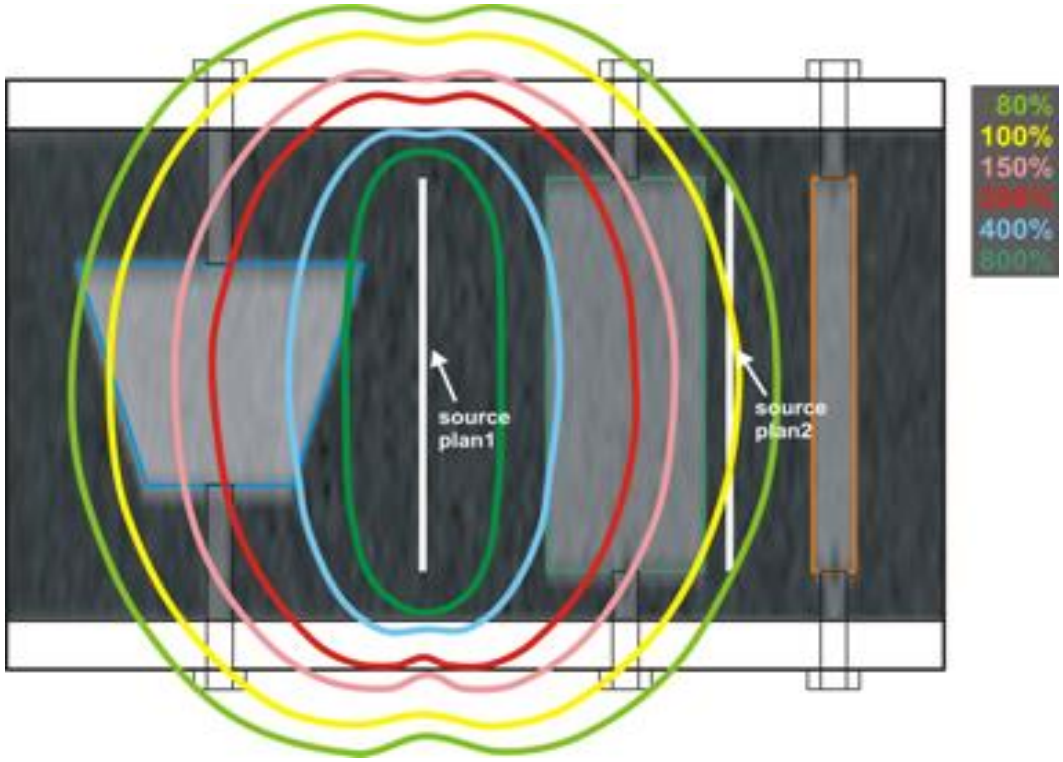

ESTRO BRAPHYQS DVH subgroup

Kirisits et al. R&O 2007

ESTRO School

Accuracy of source localisation

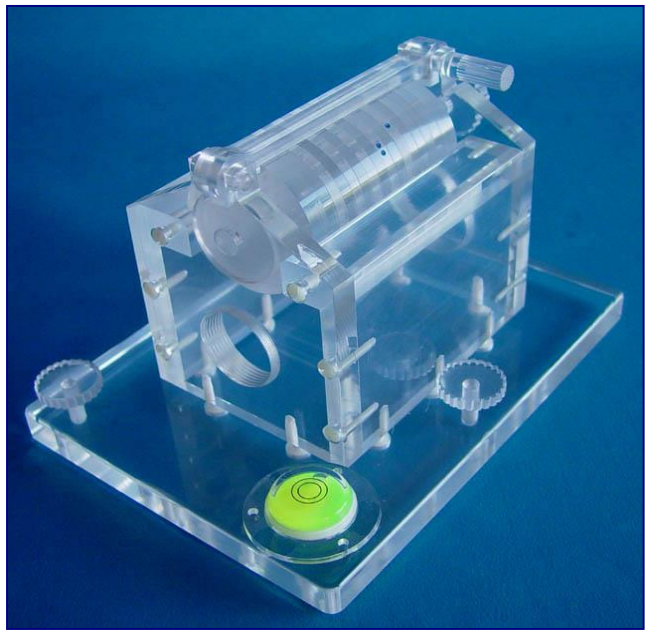

CT phantom (solid)

Siebert et al. R&O 2007

- reconstruction uncertainty (1 SD)
  - < **1.4 mm** for 4-5 mm scans
  - < **1.0 mm** for 2-3 mm scans

MRI / CT phantom (agarose gel)

De Brabandere et al. R&O 2006

- uncertainties for MRI slightly larger than for CT
- reconstruction uncertainty
  - < **2 mm** for 3-5 mm scans

See also DeBrabandere et al. 2011,

Contouring uncertainties CTV_{HR} on MRI

- CTV_{HR}:
  - Mean deviation <4mm
- GTV, CTV_{IR}:
  - Mean deviation <6-7mm

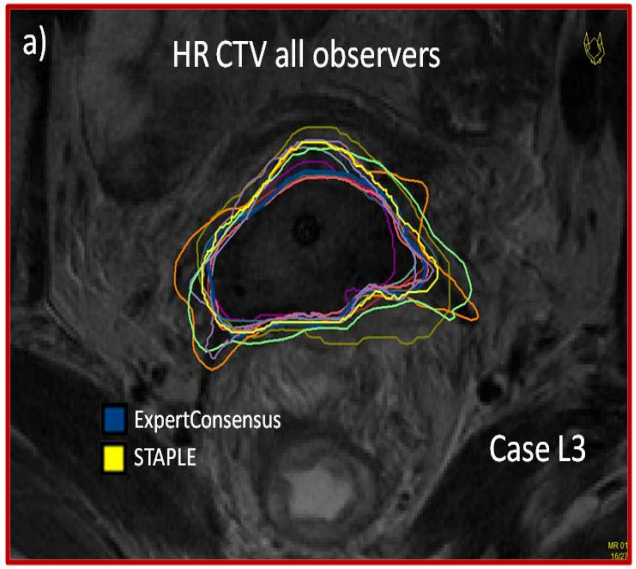

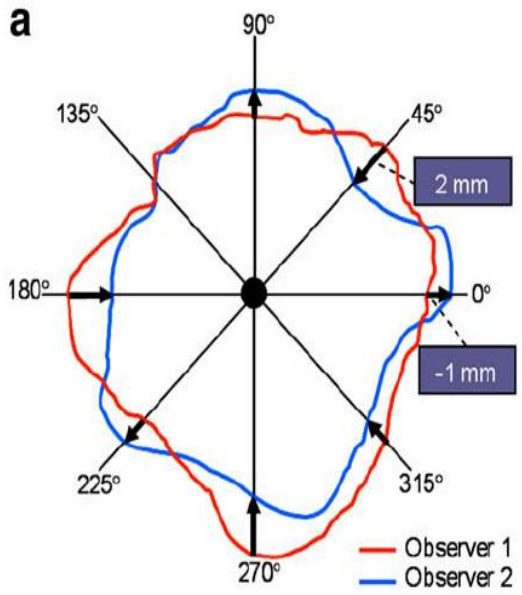

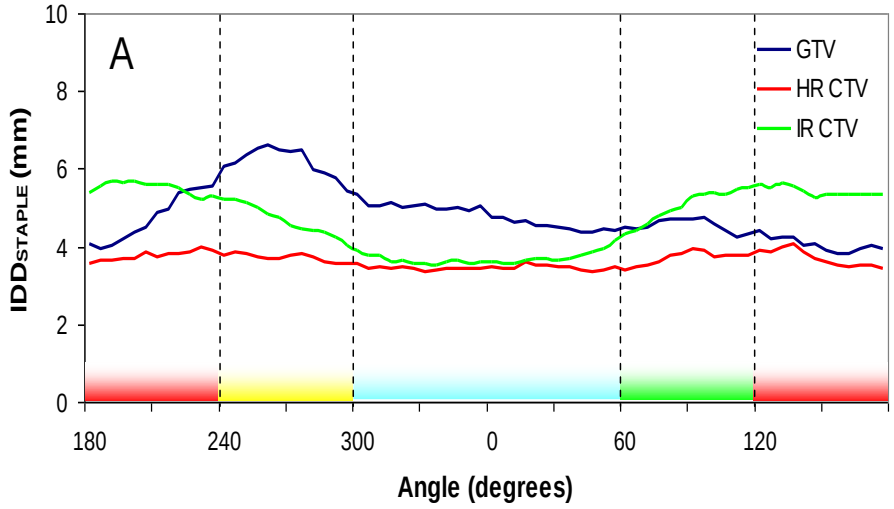

Petric et al. 2013 R&O

ESTRO School

Impact of contouring uncertainties on dose: random uncertainty (SD)

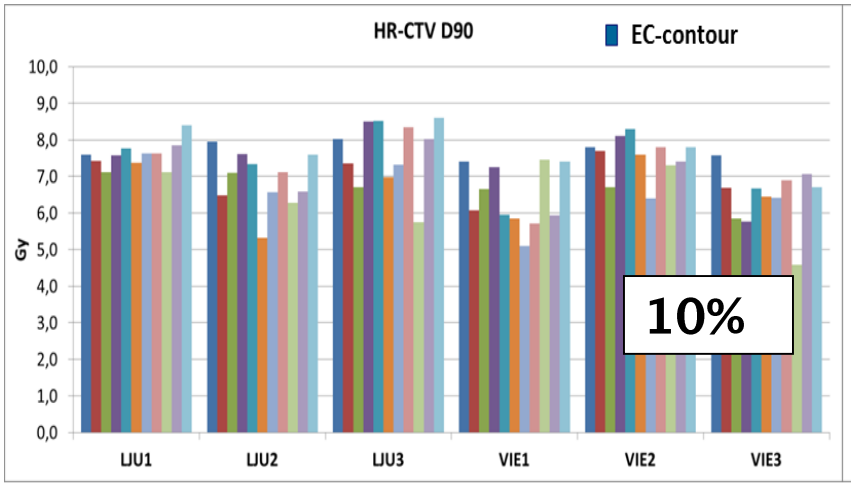

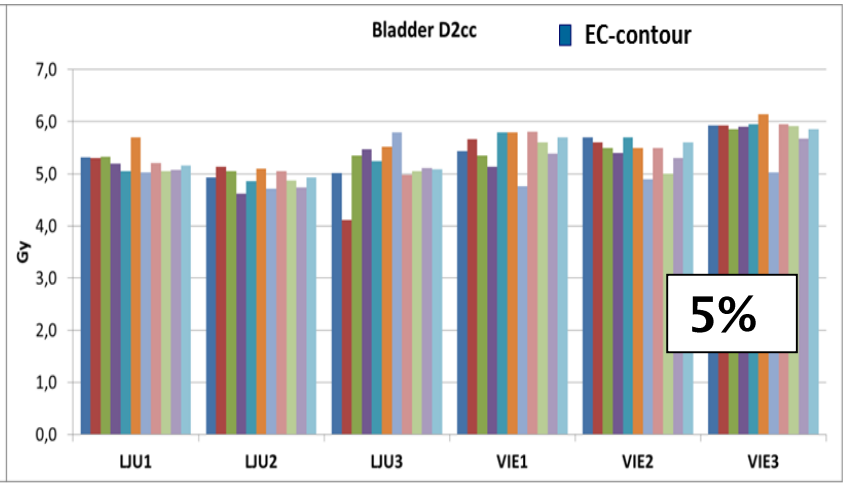

Mean (Gy)	7,59	6,80	7,61	6,34	7,51	6,31
SD (Gy)	0,38	0,70	0,95	0,81	0,59	0,74
Rel.SD (%)	5,0	10,3	12,5	12,7	7,9	11,7

Mean (Gy)	5,21	4,91	5,17	5,5	5,4	5,82
SD (Gy)	0,20	0,18	0,45	0,34	0,26	0,30
Rel.SD (%)	3,9	3,6	8,7	6,2	4,9	5,2

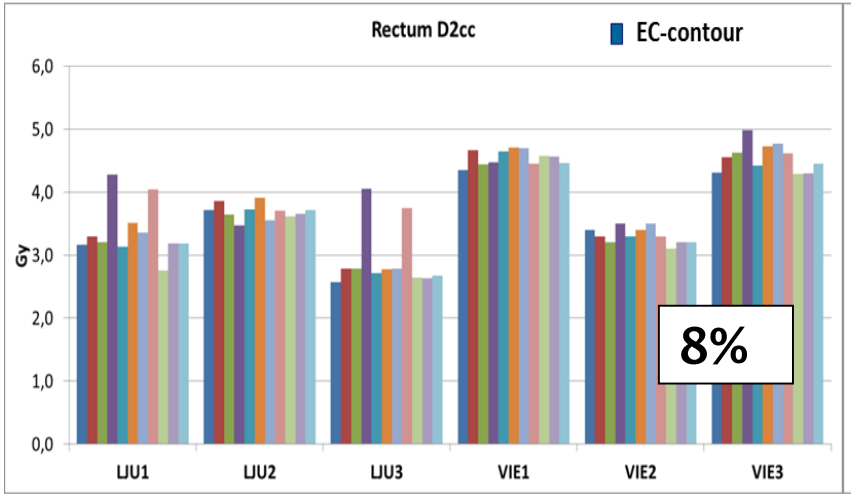

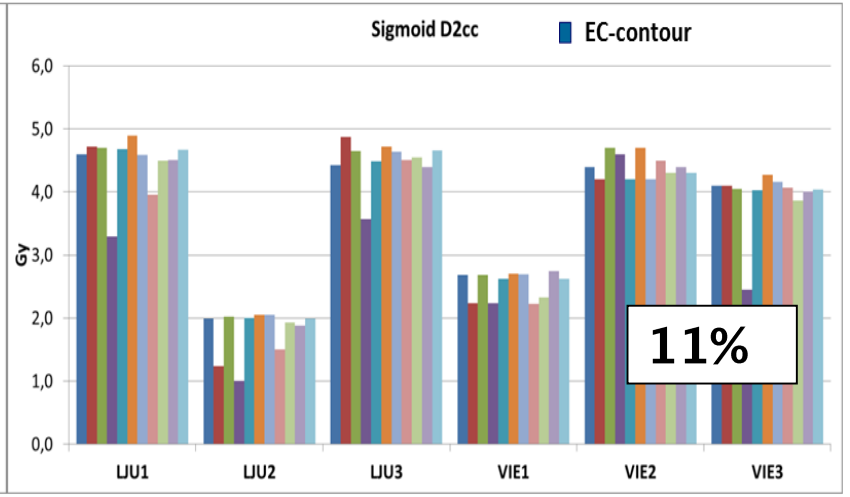

Mean (Gy)	3,39	3,68	2,96	4,57	3,30	4,57
SD (Gy)	0,45	0,13	0,51	0,11	0,13	0,22
Rel.SD (%)	13,3	3,6	17,1	2,4	4,0	4,8

Mean (Gy)	4,45	1,77	4,51	2,51	4,41	3,91
SD (Gy)	0,47	0,38	0,35	0,22	0,20	0,52
Rel.SD (%)	10,6	21,6	7,9	8,9	4,6	13,4

Hellebust & Petric et al. 2013 R&O

ESTRO School

Expected interfraction variations for cervix BT

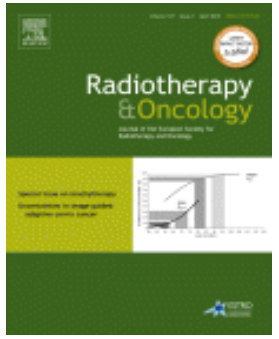

Radiother Oncol 107

Target
should remain fixed relative to applicator

Rectum:
may slightly change in location and fill with gas

Bladder:
use of bladder filling protocols

Sigmoid:
might change its location

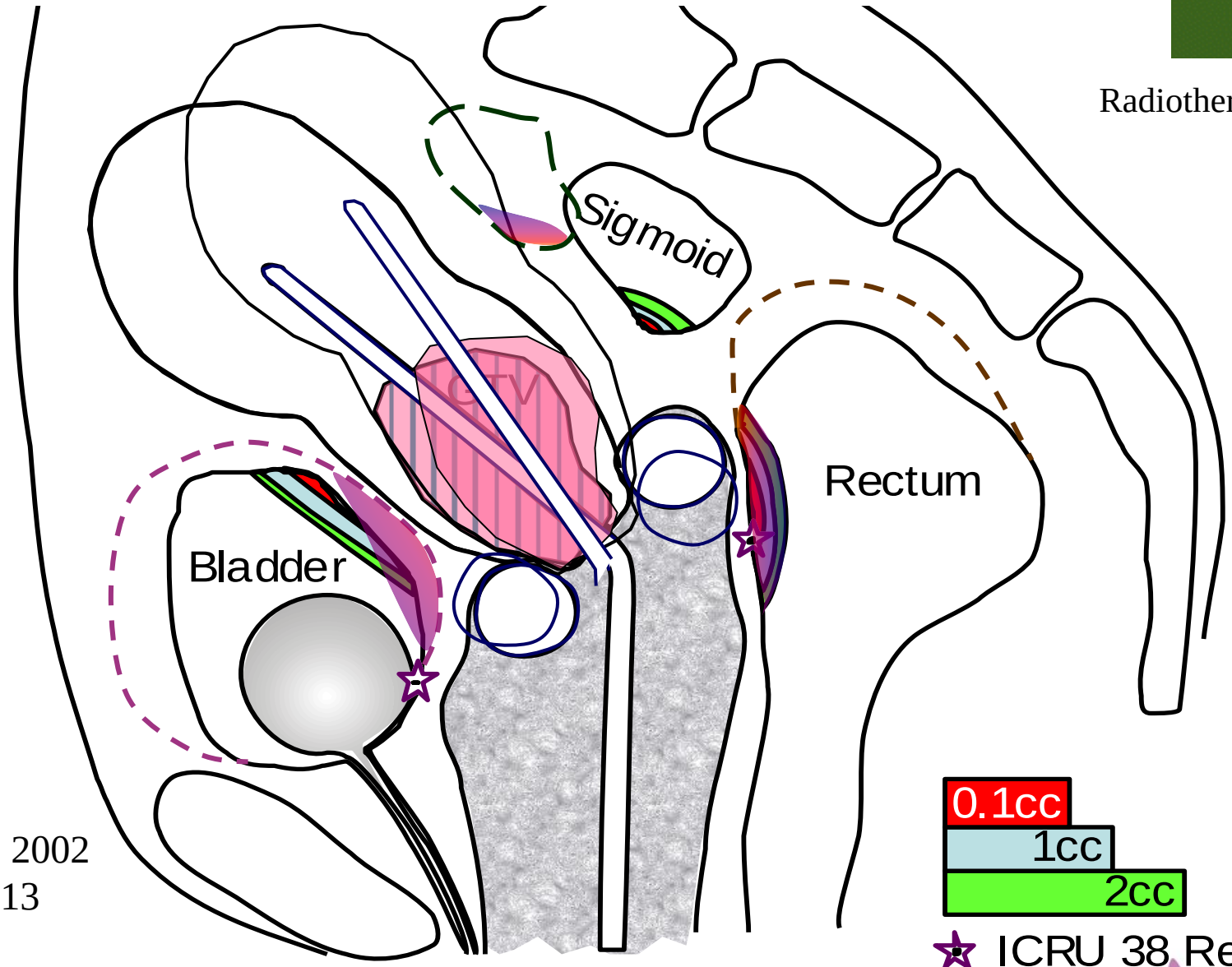

Hellebust et al. R&O 60, 2002
Lang et al. R&O 107, 2013
Kirisits et al. R&O 2006
Nesvacil et al. R&O 107, 2013
Tanderup et al. R&O 107, 2013 (and references therein)

ESTRO School

Inter-/intrafraction variation in cervix cancer BT

1 plan evaluated for images at different time points.
Anatomical changes between irradiations may lead to large random dosimetric uncertainties

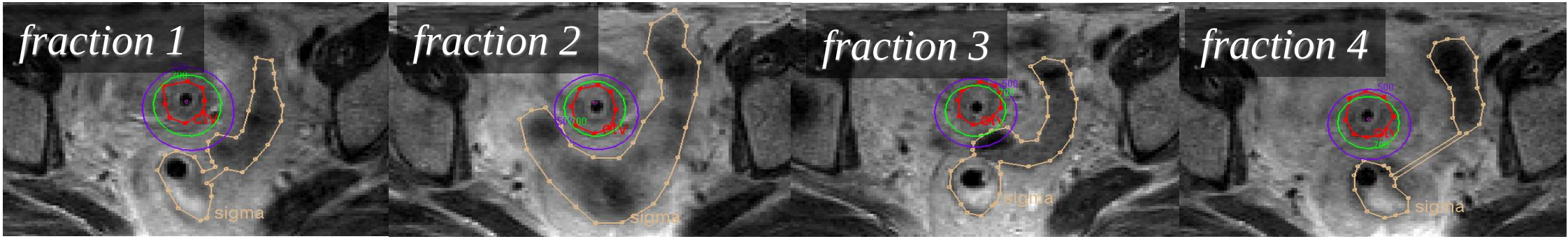

#	patients	treatment	fractions	time range	Image type	images	variation
1	21	HDR	4	18-20 hrs	MRI	84	Intra-app.
2	21	HDR	3	5 hrs	MRI	72	Intra-app.
3	9	PDR	2 x 29 / 32	22 hrs	MRI	36	Intra-app.
4	14	HDR	5	1-22 days	CT	69	Inter-app.
5	27	HDR	4	7-10 days	MRI	54	Inter-app.
6	31	PDR	2 x 20	1 week	MRI	62	Inter-app.

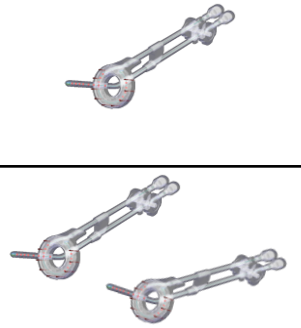

123 patients 5 h – 3 weeks 377 3 + 3

Nesvacil et al. 2013, Radiother Oncol 107

ESTRO School

Multicenter Center study of inter-/intrafraction variations for target and OARs in cervix BT

	Δ D_{2cm^3} between 2 acquisitions [%] (fixed plan, variable anatomy)									Δ D_{90} [%] (fixed plan, variable anatomy)		
	bladder			rectum			sigmoid/bowel			HR CTV		
	Mean	median	SD	mean	median	SD	mean	median	SD	mean	median	SD
total	2.7	1.5	**20.3%**	4.5	4.1	**22.0%**	1.6	-0.9	**26.8%**	-1.1	-1.7	**13.1%**
Intraaplication	1.3	1.5	**17.7**	3.8	2.3	**20.5**	-2.3	-3.7	**23.5**	-2.5	-4.3	**10.8**
interapplication	3.9	0.0	**22.3**	5.8	5.2	**23.2**	6.8	3.7	**30.2**	0.4	-0.8	**15.1**

Random uncertainties (1SD) of physical dose per BT fraction can be

~ 10% for HR CTV D90
(contouring uncertainty (Petric, Hellebust R&O 2013))
~ 20% for bladder, rectum D_{2cm^3}
~ 30% for sigmoid D_{2cm^3}

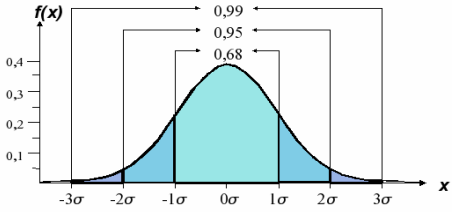

No correlation with time between images was detected!

Conclusion: As long as there is no direct imaging and dose reporting at the time of irradiation (online imaging, verification), we have to expect 20-30% dosimetric uncertainty for D_{2cm^3} for OARs for each fraction, between prescribed and delivered dose.

Radiotherapy and Oncology

Volume 110, Issue 1, January 2014, Pages 199–212

Guidelines

Review of clinical brachytherapy uncertainties: Analysis guidelines of GEC-ESTRO and the AAPM ☆

Christian Kirisits[a], Mark J. Rivard[b], Dimos Baltas[c], Facundo Ballester[d], Marisol De Brabandere[e], Rob van der Laarse[f], Yury Niatsetski[g], Panagiotis Papagiannis[h], Taran Paulsen Hellebust[i, j], Jose Perez-Calatayud[k], Kari Tanderup[l], Jack L.M. Venselaar[m], Frank-André Siebert[n]

Show more

doi:10.1016/j.radonc.2013.11.002

Get rights and content

Open Access funded by Austrian Science Fund (FWF)

"A substantial reduction of uncertainties in clinical brachytherapy should result in improved outcome in terms of increased local control and reduced side effects. Types of uncertainties have to be identified, grouped, and quantified."

- Comprehensive literature review of uncertainty components in Brachytherapy for different clinical sites, and their relative importance to the combined overall dosimetric uncertainty.
- Examples for gyn, prostate, breast BT that can be used as templates for future dose and uncertainty reporting.

ESTRO School

Example for HDR intracavitary Cervix brachytherapy – per fraction

Category	Optimum level	Assumptions
Source strength	2%	PSDL traceable calibrations
Treatment planning	3%	Reference data with the appropriate bin width is used
Medium dosimetric corrections	1%	Applicator without shielding and CTV inside pelvis (concerning for scatter)
Dose delivery including registration of applicator geometry to anatomy	4%	Accurate QA concept for commissioning and constancy checks, especially for source positioning and applicator/source path geometry, appropriate imaging techniques, applicator libraries
Interfraction/Intrafraction changes	11%	For one treatment plan per applicator insertion but several subsequent fractions – check for major deviations in subsequent fractions
Total dosimetric uncertainty for one single fraction	12%	

ESTRO School

Difference on uncertainty per fraction to uncertainty for total dose

For normal distributions the number of subsequent fractions (observations) results in compensation of variations

$$1 / \sqrt{N}$$

including constant EBRT results in

$$1 / 2$$

So 13% per fraction can be 3.5% for total dose

ESTRO School

Example for HDR intracavitary Cervix brachytherapy – total dose 4 fractions

Category	Optimum level		Assumptions
Source strength	2%		PSDL traceable calibrations
Treatment planning	3%		Reference data with the appropriate bin width is used
Medium dosimetric corrections	1%		Applicator without shielding and CTV inside pelvis (concerning for scatter)
Dose delivery including registration of applicator geometry to anatomy	4%	$1 / \sqrt{N}$ → 2%	Accurate QA concept for commissioning and constancy checks, especially for source positioning and applicator/source path geometry, appropriate imaging techniques, applicator libraries
Interfraction/Intrafraction changes	11%	$1 / \sqrt{N}$ → 6%	For one treatment plan per applicator insertion but several subsequent fractions –
Total dosimetric uncertainty for entire BT		7%	

ESTRO School

Example for LDR prostate brachytherapy

Category	Optimum level	Assumptions
Source strength	3%	PSDL traceable calibrations
Treatment planning	4%	Reference data with the appropriate bin width is used
Medium dosimetric Corrections	5%	A general prostate tissue is considered, but no consideration is given for calcifications (or their composition) in the patient
Inter-seed attenuation	4%	An advanced dose calculation formalism may indicate source models and orientations cause the largest effects
Treatment delivery imaging	2%	US QA performed according to AAPM TG-128
Anatomy changes between dose delivery and post-implant imaging	7%	Post-implant (day 0) imaging using CT, with a scalar correction factor for edema correction
Total dosimetric uncertainty	11%	

ESTRO School

Example for US-based HDR prostate brachytherapy

Category	Optimum level	Assumptions
Source strength	2%	PSDL traceable calibrations.
Treatment planning	3%	Reference data with the appropriate bin width.
Medium corrections	1%	Full scatter conditions in the pelvic region and for the prostate location are assumed.
Catheter reconstruction and source positioning accuracy	2%	Assuming usage of dedicated catheter reconstruction tools (0.7 mm) and 1.0 mm source positioning accuracy
US-imaging overall effect	2%	US QA performed according to AAPM TG-128 report.
Changes of catheter geometry	2%	Assuming that new image acquisition and treatment plan calculation before each fraction.
Total dosimetric uncertainty	5%	For treatment delivery without patient movement and changes in the lithotomic set-up and with the US probe at the position of the acquisition

Example for HDR ^{192}Ir BT source for breast balloon applicator

Category	Optimum level	Assumptions
Source strength	2%	PSDL traceable calibrations.
Treatment planning	3%	Reference data with the appropriate bin width.
Medium dosimetric corrections	3%	Balloon filled with standard level of contrast agent, no consideration or composition of chestwall, lung, or breast.
Scatter dosimetric corrections	7%	A non-scalar correction for skin dose is needed, and will require an advanced dose calculation formalism to properly account for radiation scatter conditions in the patient.
Dose delivery including registration of applicator geometry to anatomy	7%	Accurate QA concept for commissioning and constancy checks, especially for source positioning and applicator/ source path geometry, appropriate imaging techniques (either small slice thickness, 3D sequences or combination of different slice orientations), applicator characterization.

Example for HDR ^{192}Ir BT source for breast balloon applicator

Category	Optimum level	Assumptions
Interfraction/Intrafraction changes between imaging and dose delivery	7%*	For one treatment plan per applicator insertion and measures to detect major variations for subsequent fractions.
Total dosimetric uncertainty	13%	For treatment delivered with the same BT source.

*Estimated value based on expert discussion

Dosimetric uncertainties and dose-response relationships

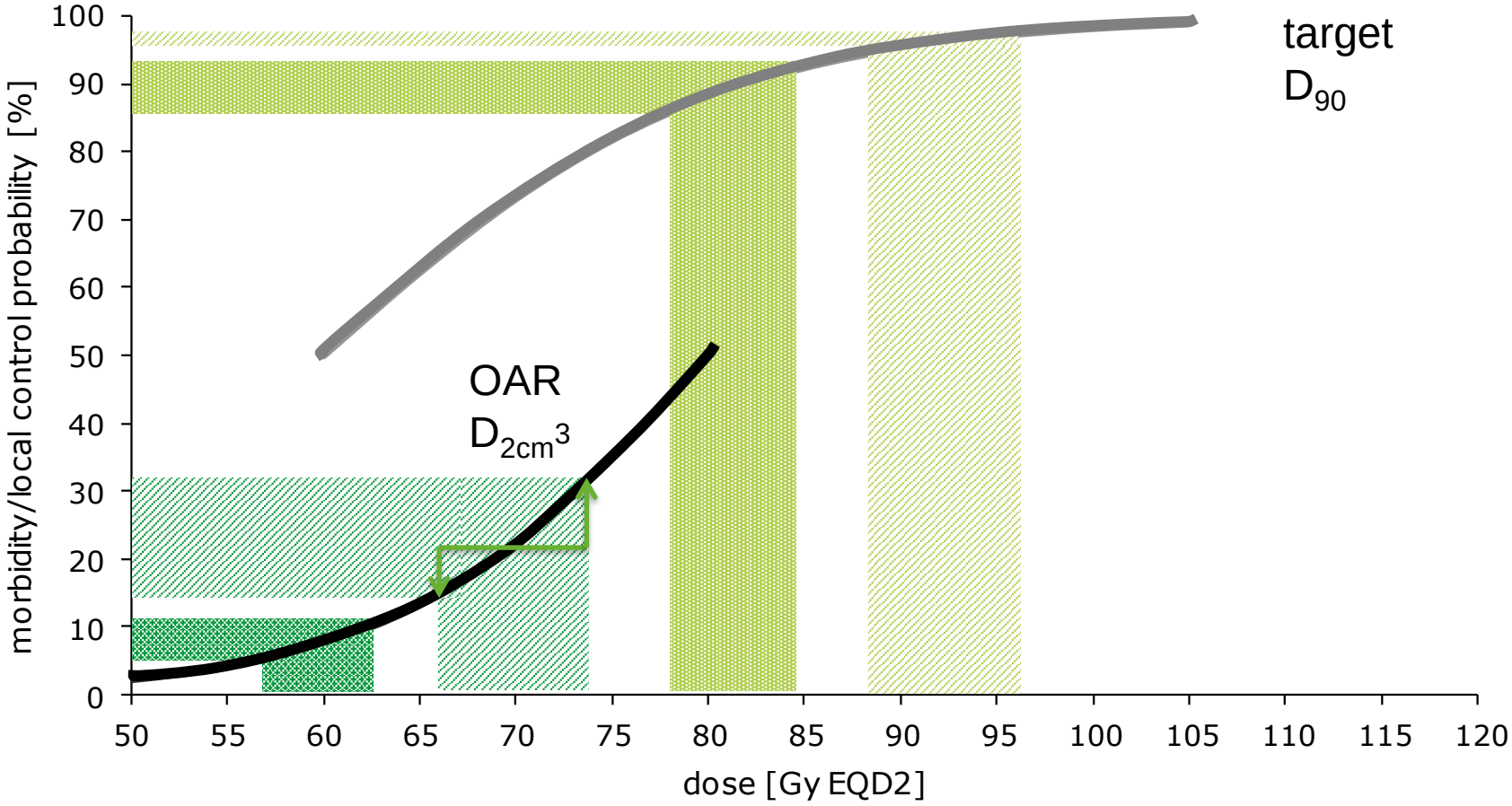

Schematic illustration of the effect of dosimetric ucertainties of prescribed vs. delivered dose on response probabilities

Tanderup et al. 2013, Radiother Oncol 107

ESTRO School

Translating random uncertainties to EQD2: single fraction dose

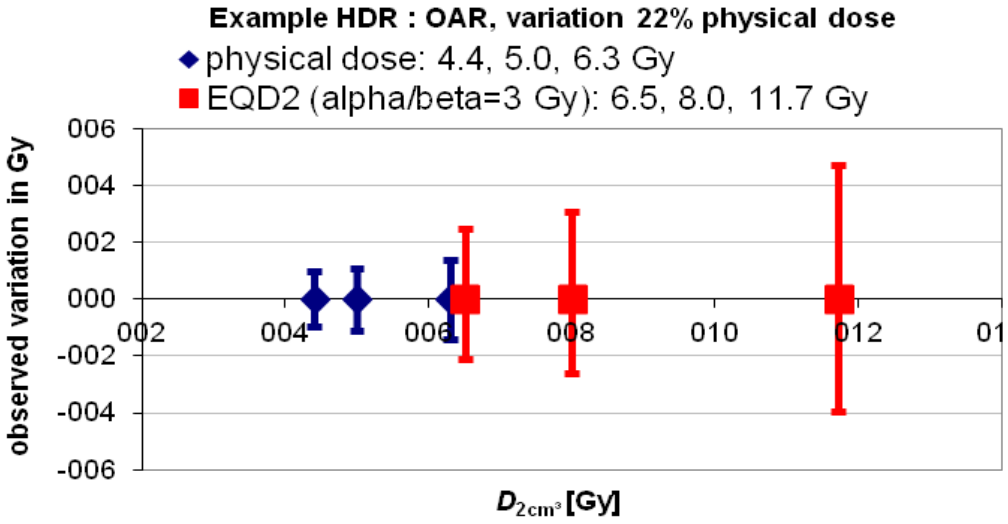

OAR
(SD 22%)

asymmetrical EQD2 error bars

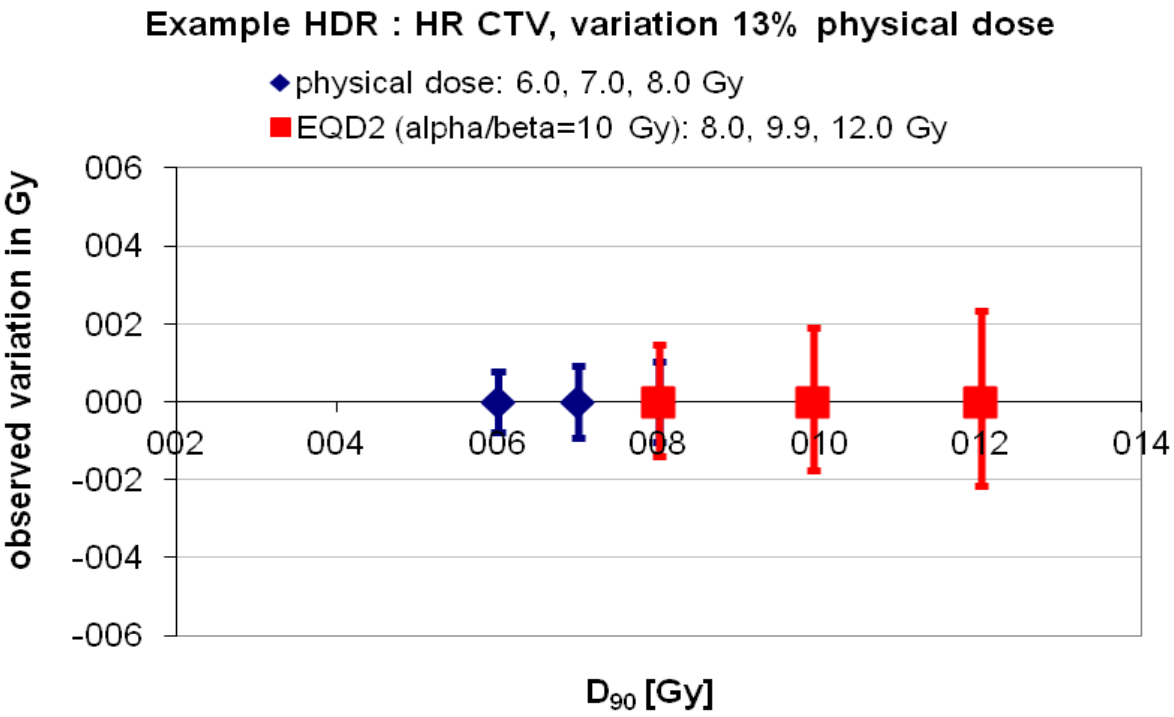

CTV_{HR}
(SD 13%)

The effect on the total treatment dose depends on the fractionation scheme!
The PDR uncertainties per pulse are currently unknown because of low time resolution of observations.

Translating random uncertainties to EQD2:

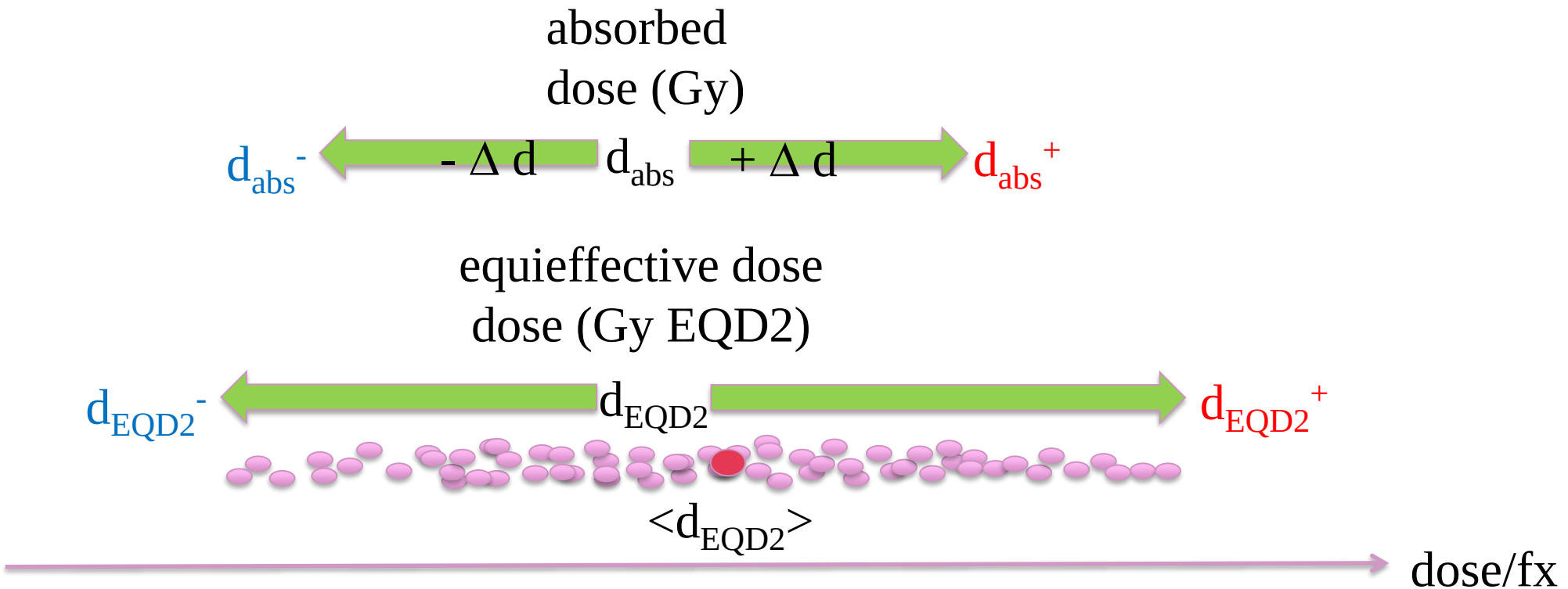

e.g. n~500 with same prescribed dose and SD 30% / fx:
mean of delivered doses $<d_{EQD2}>$ from 500 patients > prescribed dose in EQD2

d_{abs} …… prescribed dose (Gy)
d_{EQD2} ……. d_{abs} converted to (Gy EQD2)

Δd ……. … e.g. 30% d_{abs} (Gy)

$d_{abs}^{-/+}$ ……. prescribed dose –/+ Δd (Gy) = delivered dose in Gy
$d_{EQD2}^{-/+}$…… $d_{abs}^{-/+}$ converted to Gy EQD2

$d_{abs} - d_{abs}^- = d_{abs}^+ - d_{abs}$ $\qquad$ $d_{EQD2} - d_{EQD2}^- < d_{EQD2}^+ - d_{EQD2}$

ESTRO School

Dose-response relationships (published examples for cervix BT)

OAR

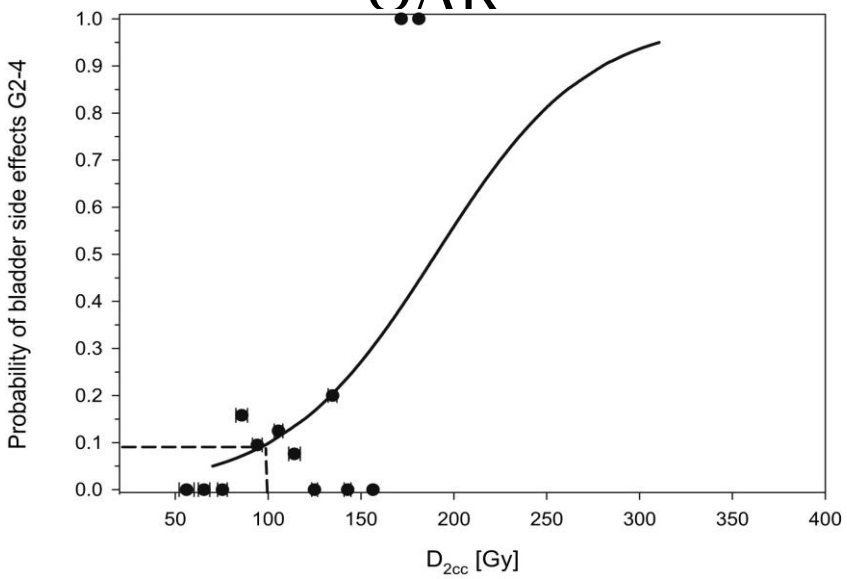

urinary bladder G2-4: *Georg et al. 2012, IJROBP 82*

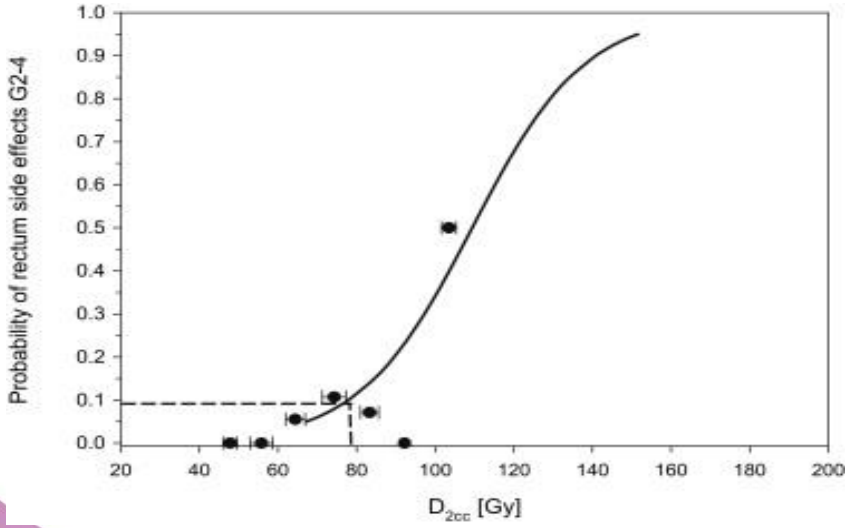

rectum G2-4: *Georg et al. 2012, IJROBP 82*

CTV_{HR}

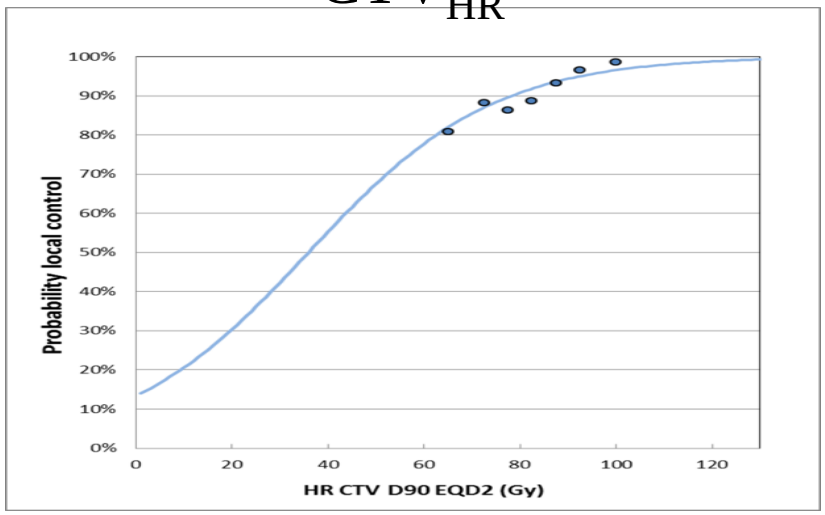

Relationship between EBRT-C+BT dose and local control from retroEMBRACE patients (*Tanderup et al, GEC-ESTRO workshop, Brussels, 2013*)

Other OARs for cervix: sigmoid, vagina, and upcoming dose response curves from EMBRACE study (www.embracestudy.dk)

Clinical outcome reports for prostate: e.g. *Martinez A. et al. 2011 IJROBP 79, Ghilezan et al. 2012, IJROBP 83, Martinez E. et al. 2015, Brachytherapy 14, …*

Dose response for breast (APBI): e.g. *Herskind & Wenz 2010, Strahlentherapie und Onkologie 186*

ESTRO School

Effect of uncertainties on observed dose response relationships

Comparison of model dose response curve (based on published curves, see previous slides), and simulated „observed“ dose response curves assuming different systematic and random uncertainties.

systematic dosimetric uncertainty
e.g. rectum D_{2cm^3} (+3,+5,+10,+15 % / fx)

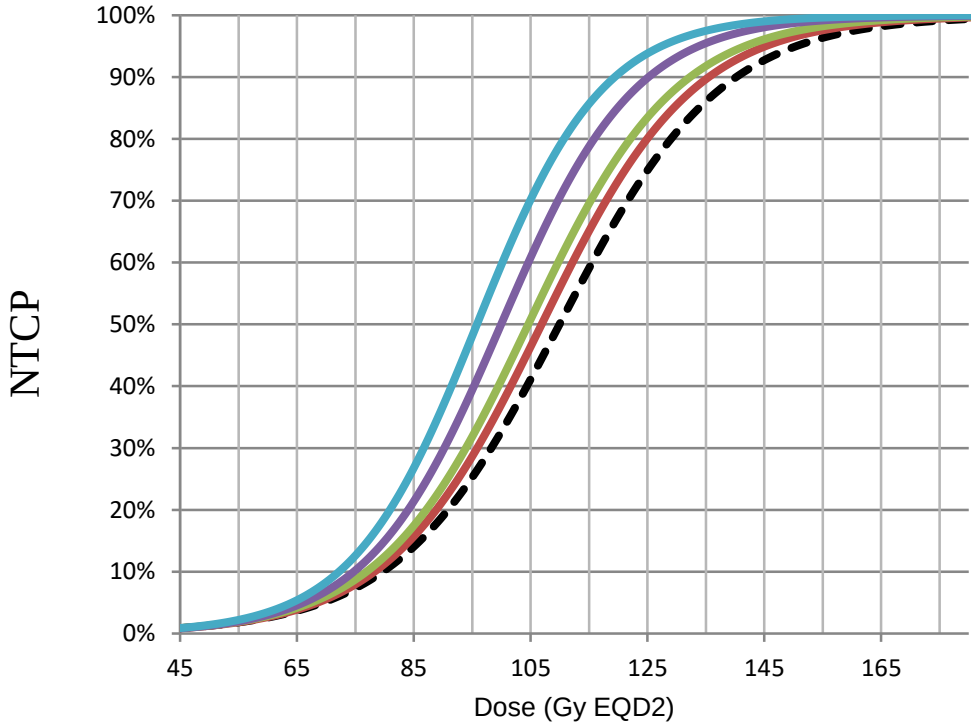

random dosimetric uncertainty
e.g. rectum D_{2cm^3} (±10, ±20, ±30 % / fx)

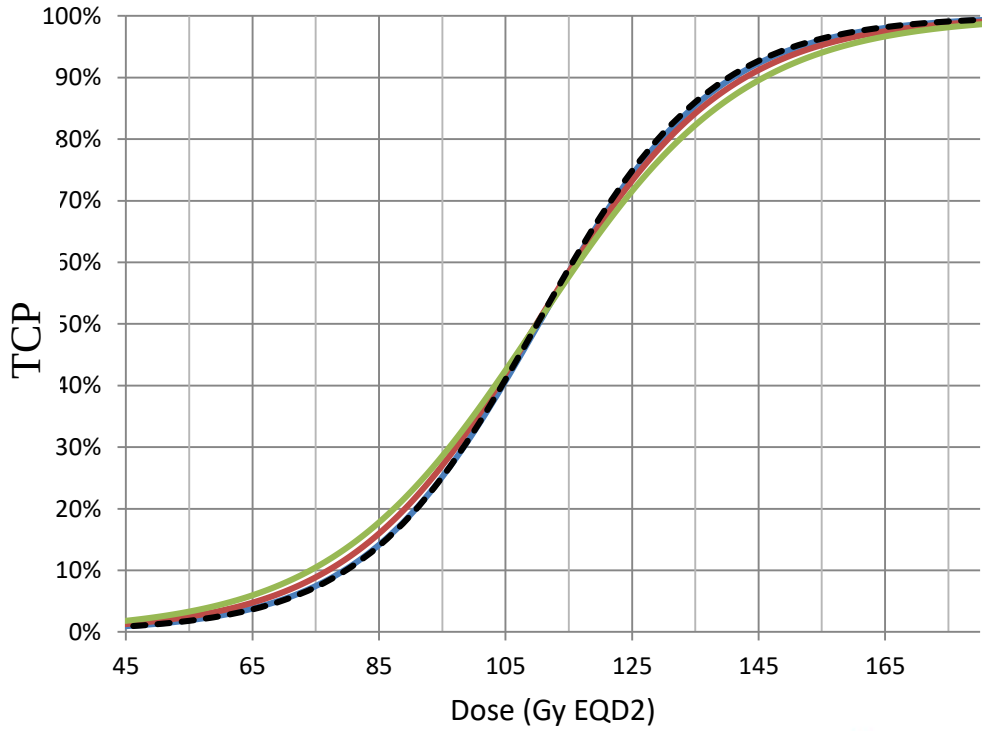

n=10000 patients per dose level, total dose = 45Gy EBRT + 4 fx BT (equal PD for each fx)
model based on *Georg er al. 2012, IJROBP*

Nesvacil et al., ESTRO33, 2014

Example: systematic uncertainties for target

effect of systematic underestimation of target D_{90} on observed dose-response

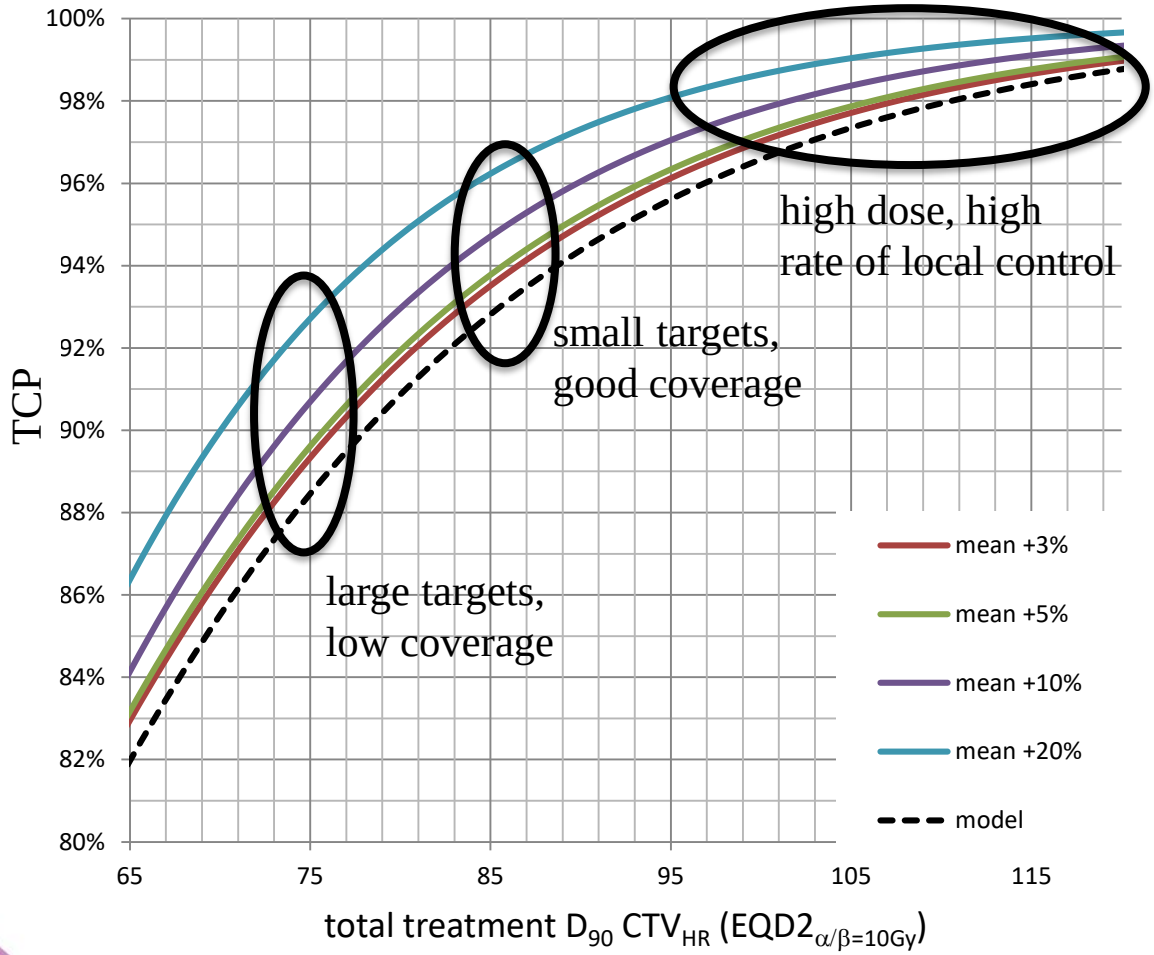

Systematic 1.5 mm applicator reconstruction uncertainty for MRI- based cervix BT *(Tanderup et al., R&O 2008):*

e.g. $\Delta D90 \leq +3\%/fx$ => „observed" local control @85 Gy <1% higher than model prediction

Systematically larger contours on CT vs. MRI => underestimation of D90 by CT contours *(e.g. Viswanathan et al. 2007, IJROBP 68):*

e.g. i) $\Delta D_{90} = +10\%/fx$ => 2% overestimation of local control @ 85 Gy

ii) $\Delta D_{90} = +20\%/fx$ => 3.5% overestimation of local control @ 85 Gy

(model based on preliminary retroEMBRACE data:*Tanderup et al, GEC-ESTRO workshop, Brussels, 2013*)

ESTRO School

Example: random uncertainties for target + OAR

effect of random intra-/interfraction variation on D_{90}, D_{2cm^3} and dose-response

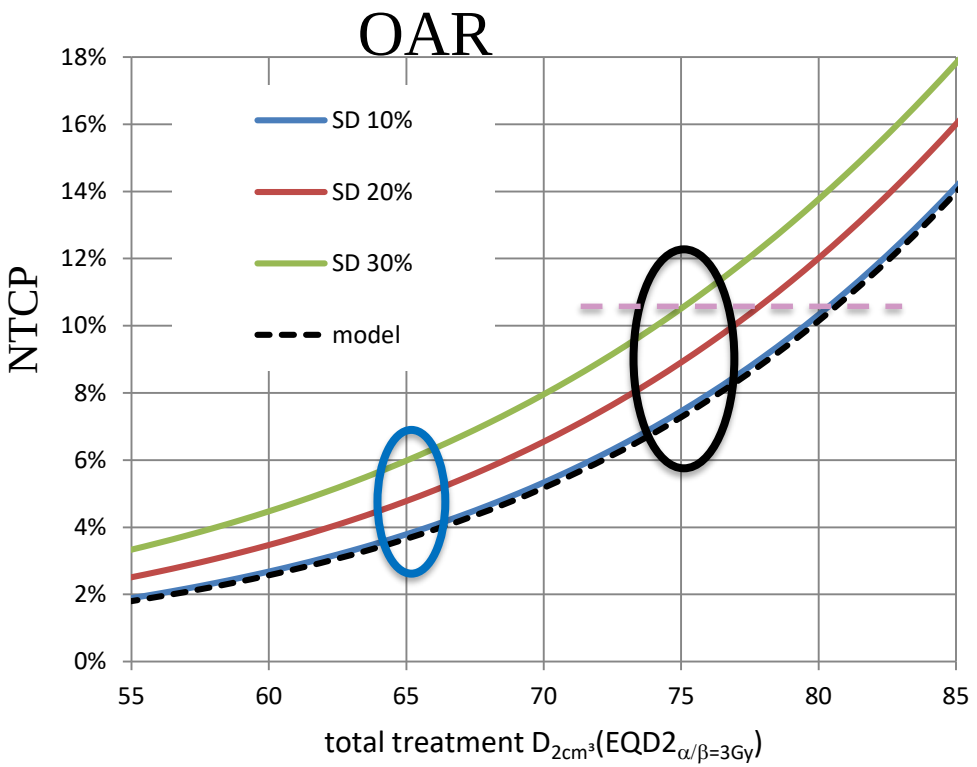

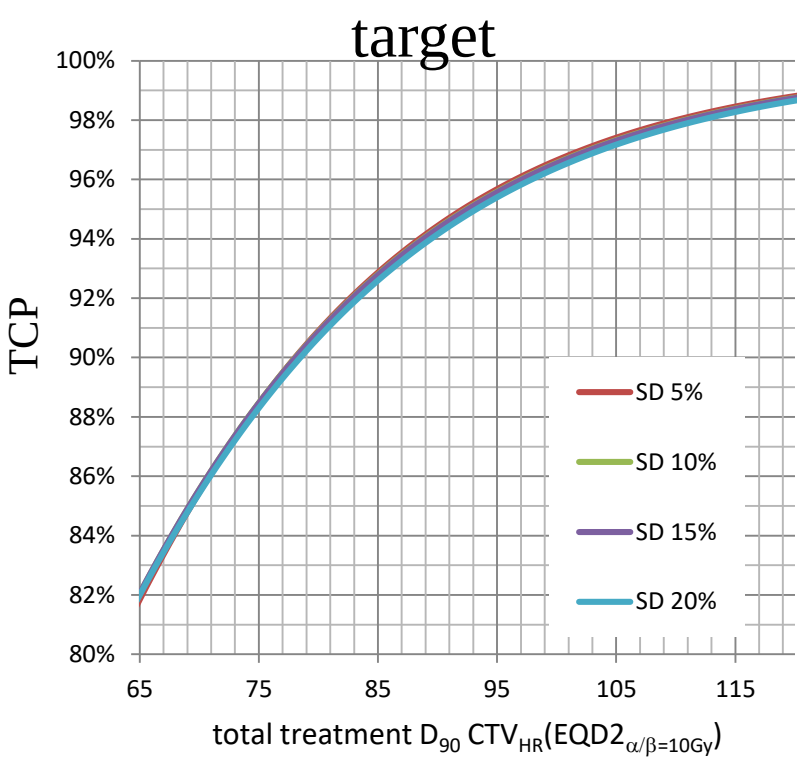

Example: 75Gy, **random variation of rectum D_{2cm^3}**:

- $\Delta D_{2cm^3} = \pm 10\%$/fx -> observed NTCP 7.5 %
  (vs 7.3% model prediction)
- $\Delta D_{2cm^3} = \pm 20\%$/fx -> observed NTCP 8.9 %
- $\Delta D_{2cm^3} = \pm 30\%$/fx -> observed NTCP 10.5 %
- Model predicts 10.5% morbidity NTCP @ 80Gy EQD2!

For target – differences in TCP < 0.5%

ESTRO School

Example: influence of the number of BT Fx

Random uncertainties and dose response for different fractionation schemes

OAR

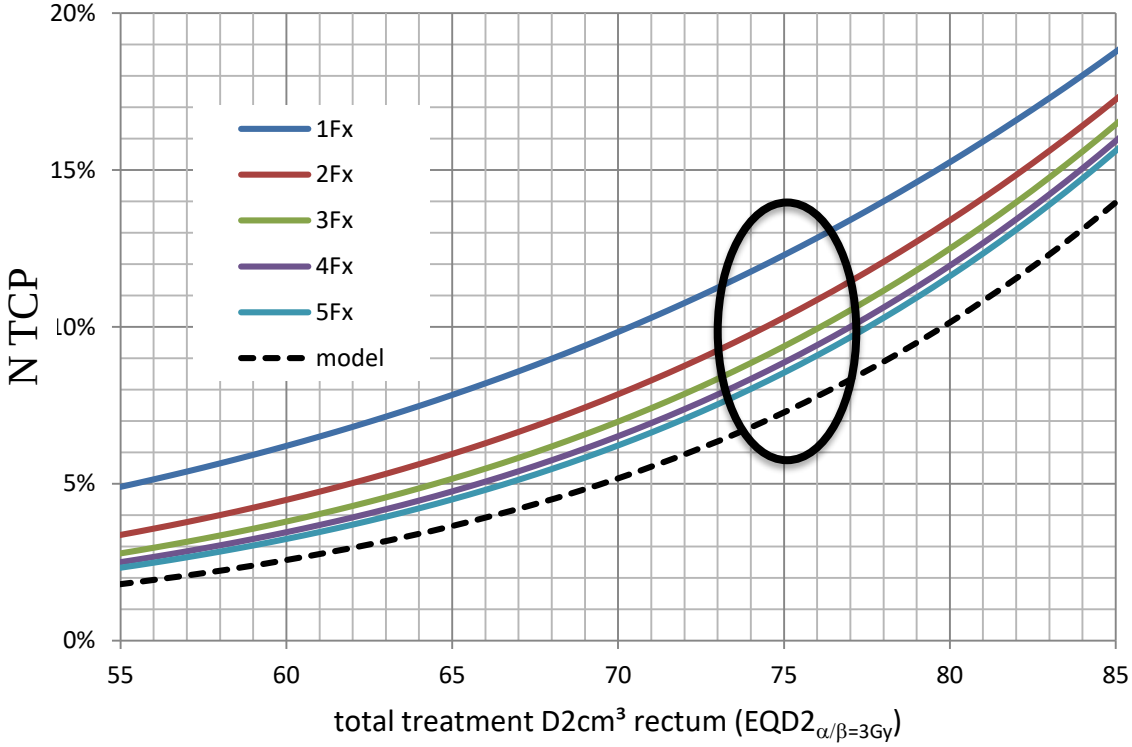

target

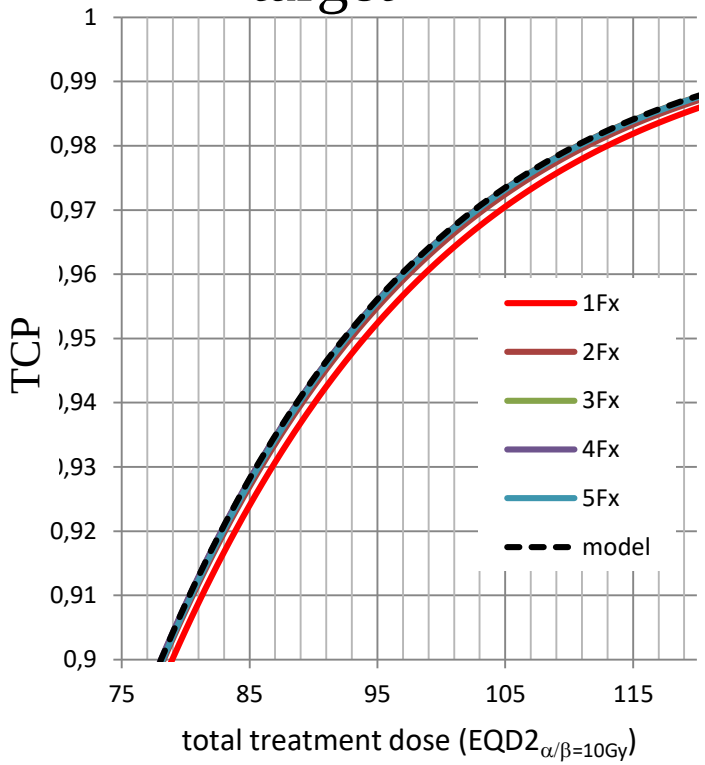

Example: random uncertainty $\Delta D_{2cm^3} = \pm 20\%/fx$:

- nFx=5 => observed morbidity @75Gy 8.5%
- nFx=4 => observed morbidity @75Gy 8.9%
- nFx=3 => observed morbidity @75Gy 9.4%
- nFx=2 => observed morbidity @75Gy 10.3%
- nFx=1 => observed morbidity @75Gy 12.3%

For target: using 1 fx vs 2-5 fx results in ~0.5% lower response probability than predicted by model

ESTRO School

Difference between models and simulated (TCP and NTCP) dose-response

	dose	systematic	random		
	(Gy $EQD2_{\alpha/\beta=10Gy}$)	U_s 5%	U_r 10%	U_r 20%	
Δ TCP	75	1.0%	-0.1%	-0.3%	
	90	0.8%	-0.1%	-0.3%	
	(Gy $EQD2_{\alpha/\beta=3Gy}$)	U_s 5%	U_r 10%	U_r 20%	U_r 30%
Δ NTCP	65	0.5%	0.1%	1.1%	2.3%
	75	1.4%	0.2%	1.6%	3.2%

"Can reduction of uncertainties in cervix cancer brachytherapy potentially improve clinical outcome?" Nesvacil et al. 2016, submitted to R&O

ESTRO School

Increasing OAR dose constraints by reducing uncertainties

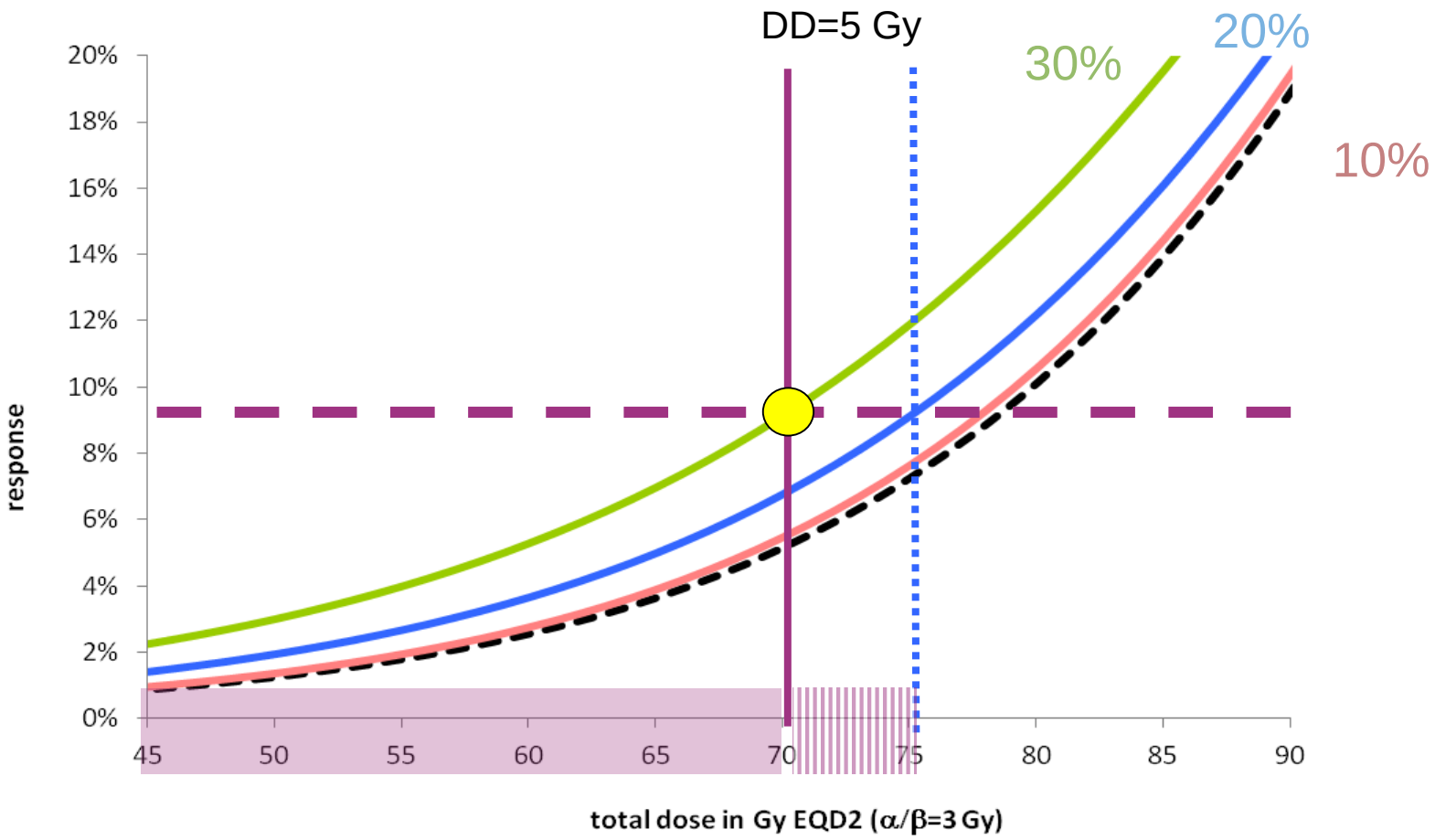

If uncertainty can be reduced by 10%, clinicans could think about relaxing their dose constraint.in this case

Nesvacil et al. 2016, R&O

ESTRO School

TAKE HOME MESSAGES

- Investigate your uncertainty budgets for your specific clinical workflows and report them
- Clinical impact depends on dose level (EQD2, α/β) and shape of the dose-response curve
- Observed dose-response curves in the literature are subject to (unreported) uncertainties
- Uncertainty reduction can help in individual cases near OAR dose limits and below target planning aims

ESTRO School

TAKE HOME MESSAGES

- reducing random uncertainties can change the slope of the dose-response relationship observed in a patient cohort
  - Online image-based treatment delivery verification (reduce time between treatment simulation and treatment)
  - Advanced in vivo treatment dose verification

- reduction of large systematic uncertainties should be a goal for OAR and target structures
  - Contouring uncertainties
  - Large dose calculation uncertainties (see Luc‘s presentation on clinical outcome vs. dose calculation algorithm)
  - Systematic OAR filling changes during treatment (filling protocols!)

Impact of geometrical uncertainties in extreme hypo with brachytherapy

Nicole Nesvacil[1]

C. Kirisits[1], K. Tanderup[2], R. Pötter[1]

[1]Department of Radiotherapy, Comprehensive Cancer Center, Medical University of Vienna, and Christian Doppler laboratory for Medical Radiation Research for Radiation Oncology, Austria,

[2]Aarhus University Hospital, Denmark

MEDICAL UNIVERSITY OF VIENNA

COMPREHENSIVE CANCER CENTER VIENNA

RAD ONC
A Christian Doppler Laboratory

ESTRO School

Examples for hypofractionation schedules in Brachytherapy

- Cervix:
  - 4 x 7 Gy
  - 2 x 9 Gy
- Bronchus: 4 x 7.5 Gy
- Breast:
  - APBI: 8 x 4 Gy, 6 x 6 Gy
  - Boost: 1 x 10Gy
- Prostate: up to 20 Gy in 1 fraction

ESTRO School

Geometrical uncertainties in brachytherapy

- Reconstruction uncertainties
  - Specification of sources relative to anatomy
  - Equivalent to EBRT set-up uncertainties

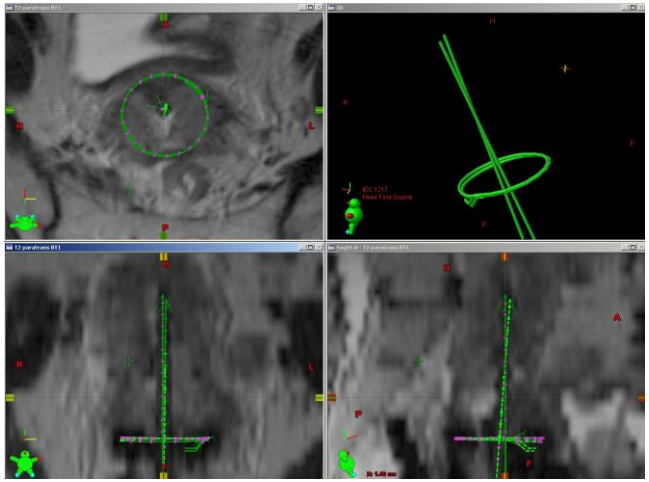

© K Tanderup

- Internal movement (relative to applicator)
  - Target: depends on applicator
    - Intracavitary cervix BT: applicator moves with cervix?
    - Prostate (and breast) needle implant: movement along needles
  - OAR: volume and location changes relative to BT implant

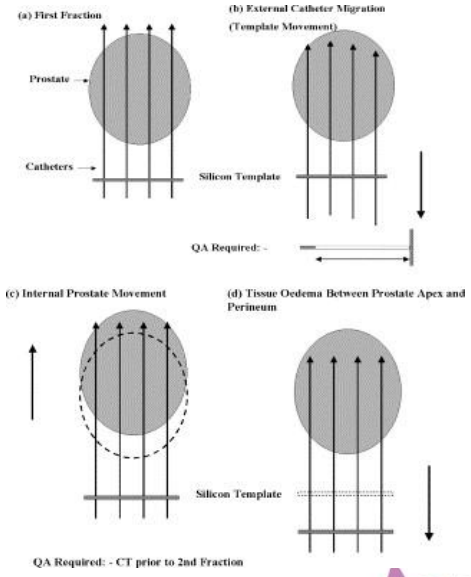

- Translating geometric uncertainties to dosimetric uncertainties for D_{90} target, D_{2cm^3} OAR

Hoskin et al 2003, R&O 68

Radiotherapy and Oncology

Volume 110, Issue 1, January 2014, Pages 199–212

Guidelines

Review of clinical brachytherapy uncertainties: Analysis guidelines of GEC-ESTRO and the AAPM ☆

Christian Kirisits[a], Mark J. Rivard[b], Dimos Baltas[c], Facundo Ballester[d], Marisol De Brabandere[e], Rob van der Laarse[f], Yury Niatsetski[g], Panagiotis Papagiannis[h], Taran Paulsen Hellebust[i, j], Jose Perez-Calatayud[k], Kari Tanderup[l], Jack L.M. Venselaar[m], Frank-André Siebert[n]

Show more

doi:10.1016/j.radonc.2013.11.002

Open Access funded by Austrian Science Fund (FWF)

"A substantial reduction of uncertainties in clinical brachytherapy should result in improved outcome in terms of increased local control and reduced side effects. Types of uncertainties have to be identified, grouped, and quantified."

- Comprehensive literature review of uncertainty components in Brachytherapy for different clinical sites, and their relative importance to the combined overall dosimetric uncertainty.
- Examples for gyn, prostate, breast BT that can be used as templates for future dose and uncertainty reporting.

ESTRO School

Example: overview of optimum level of uncertainties for different clinical sites (*BRAPHYQS AAPM guidelines 2014, Radiother Oncol 110)*

BT application	HDR ^{192}Ir gyn vaginal	HDR ^{192}Ir ic cervix	HDR ^{192}Ir breast balloon*	LDR ^{125}I prostate	HDR ^{192}Ir prostate
Source strength	2%	2%	2%	3%	2%
Treatment planning	3%	3%	3%	4%	3%
Medium dosimetric corrections	1%	1%	3%	5%	1%
Dose delivery including registration of applicator geometry to anatomy	5%	4%	7%	4%**	2%
Interfraction/Intrafraction changes	5%	11%	7%	7%	2%
…					
Total dosimetric uncertainty (for one fraction)	**~8%**	**~12%**	**~13%**	**~11%**	**~5%**

*additional scatter dosimetric corrections (skin, surface): 7%
** inter-seed attenuation
*** additional imaging and planning based uncertainties, see original publication

ESTRO School

Systematic set-up uncertainties

- Same error in every fraction
- Examples
  - ➢ Incorrect reconstruction procedures (source path commissioning)
  - ➢ Systematic misinterpretation of images

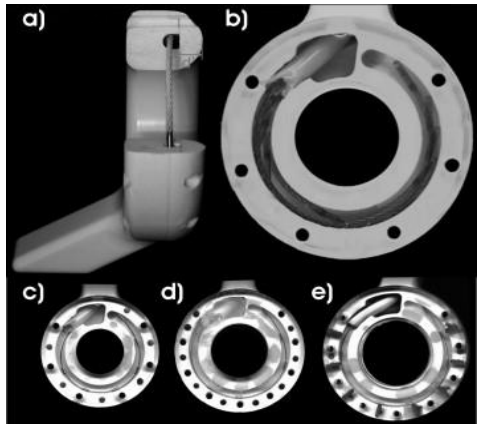

Berger et al. 2009, R&O 93

CT

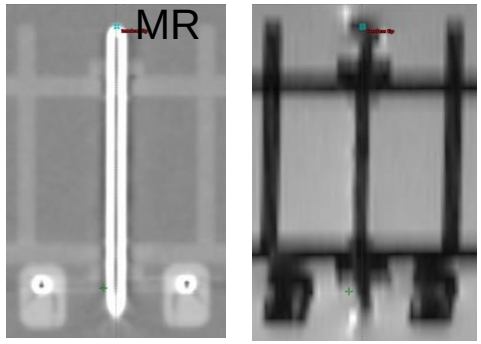

Hellebust et al 2007, PMB 52

Random set-up uncertainties

- Different in every fraction
- Visibility of applicator (dependent on slice thickness)
- Uncertainties of image fusion
- Pronounced in longitudinal direction (perpendicular to slice orientation)

Sagittal reconstruction from para-transverse MR

Sagittal reconstruction from transverse MR

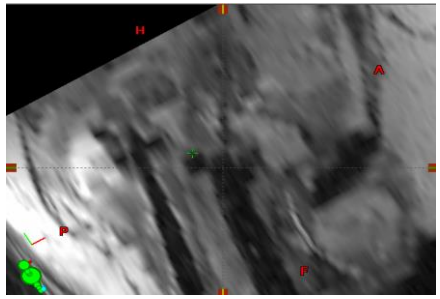

Examples for setup uncertainties in BT:

Gyn: Mean DVH shifts (%) due to uncertainties in tandem/ring applicator position (mm) (reconstruction or movement)

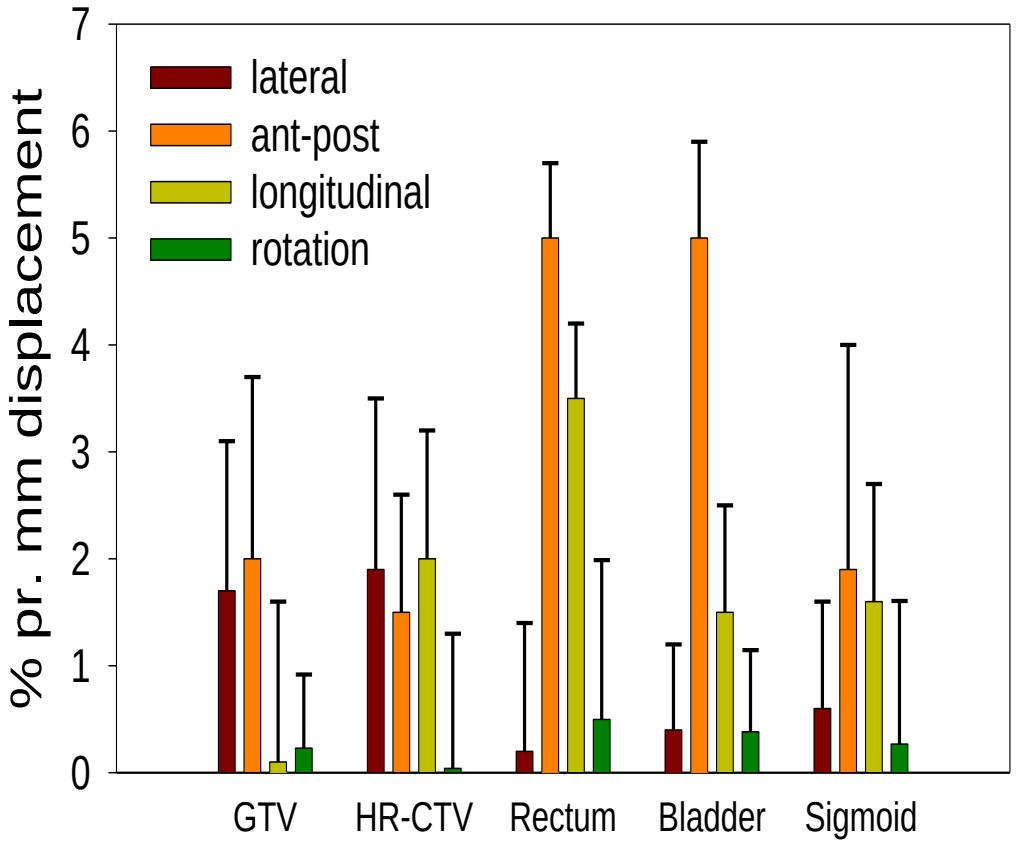

Tanderup et al. 2008, Radiother Oncol 89

Prostate: Variations of target dose during HDR treatment due to catheter and gland movement

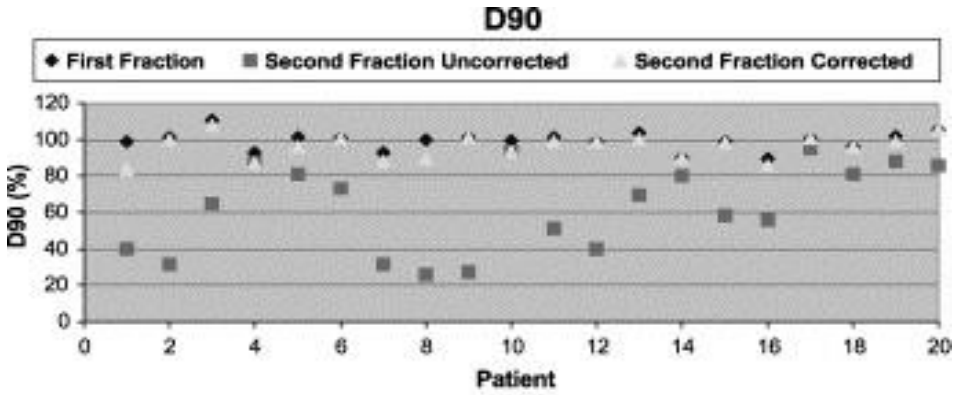

Hoskin et al. 2003, Radiother Oncol 68

Breast: variations of maximum skin dose and high dose volumes of breast tissue (Mammo Site applicator)

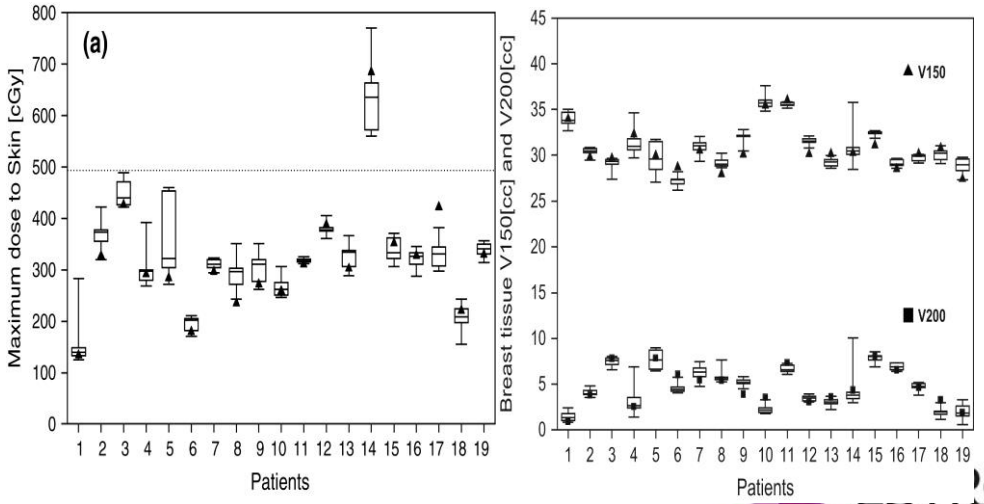

Kim Y. et al 2008, IJROBP 71

Expected interfraction variations for cervix BT

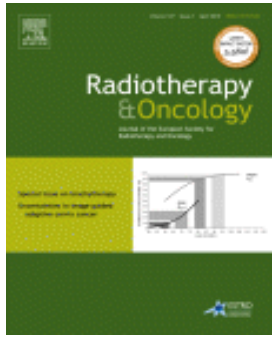

Radiother Oncol 107

Target

should remain fixed relative to applicator

Rectum:

may slightly change in location and fill with gas

Bladder:

use of bladder filling protocols

Sigmoid:

often changes its location

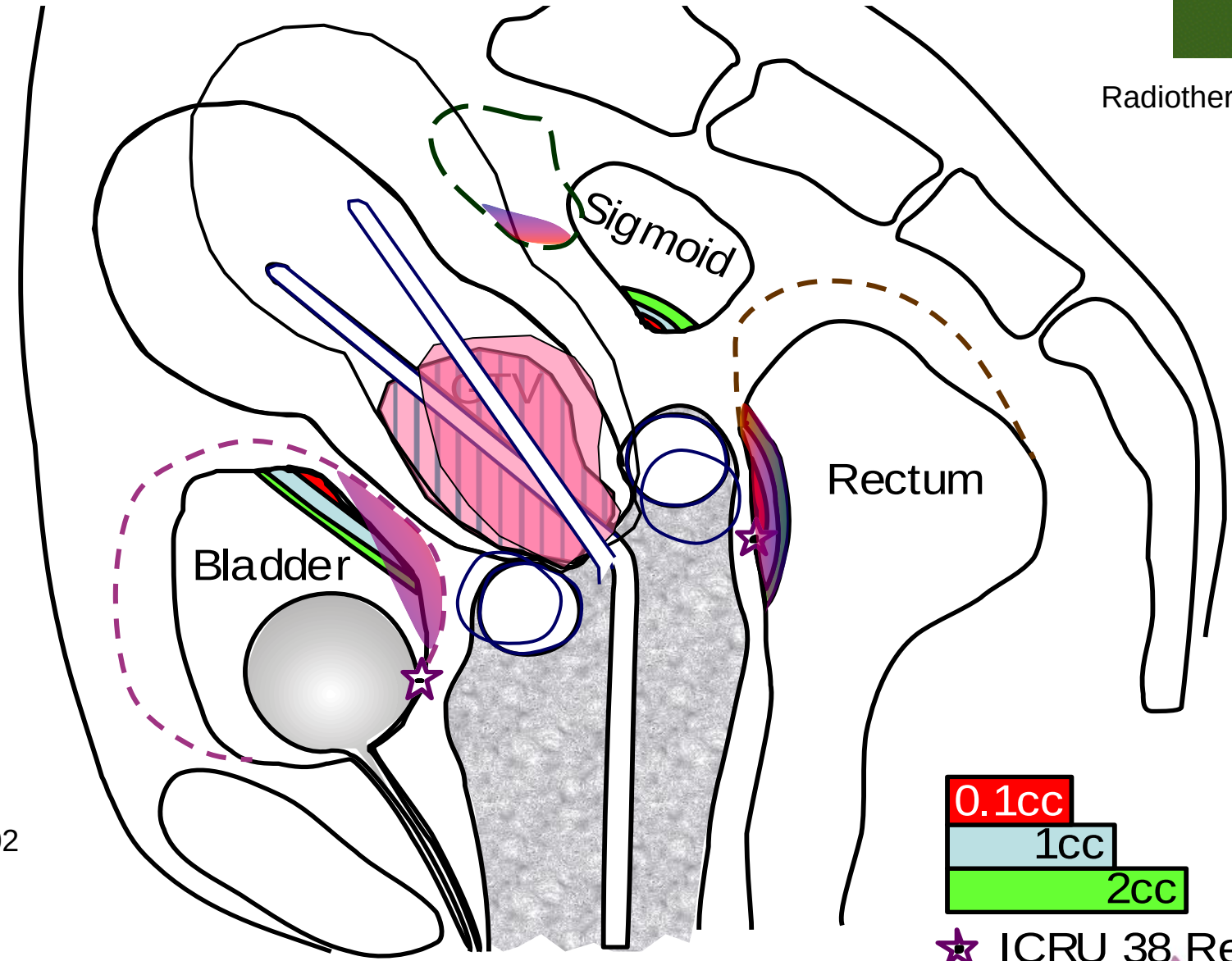

Hellebust et al. R&O 60, 2002
Lang et al. R&O 107, 2013
Kirisits et al. R&O 2006
Nesvacil et al. R&O 2013
Tanderup et al. R&O 107, 2013 (and references therein)

ESTRO School

Inter-/intrafraction variation in cervix cancer BT

1 plan evaluated for images at different time points in a multicenter study *(Nesvacil et al. 2013, Radiother Oncol 107)*

	Δ D_{2cm^3} between 2 acquisitions [%] (fixed plan, variable anatomy)									Δ D_{90} [%] (fixed plan, variable anatomy)		
	bladder			**rectum**			**sigmoid/bowel**			**CTV_{HR}**		
	Mean	median	SD	mean	median	SD	mean	median	SD	mean	median	SD
Total (123 pts, 377 images)												
Intraaplication												
interapplication												

No correlation with time between images was detected!
Random inter-intrafraction uncertainties (1SD) of absorbed dose can be

- **~ 10%** for HR CTV D90 / fx
- **~ 20%** for bladder, rectum D_{2cm^3} /fx
- **~ 30%** for sigmoid D_{2cm^3} / fx

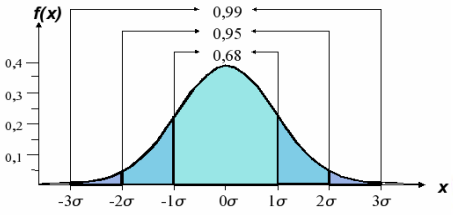

ESTRO School

Translating random uncertainties to EQD2:

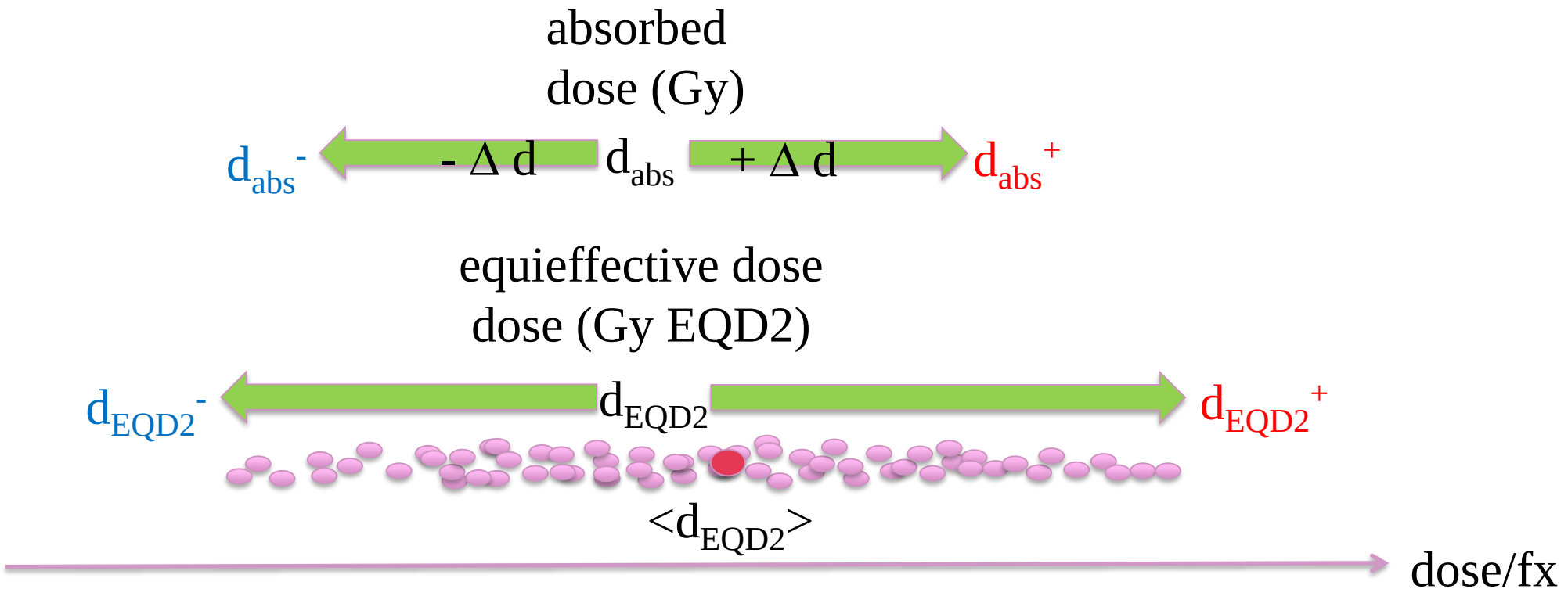

e.g. n~500 with same prescribed dose and SD 30% / fx:
mean of delivered doses $<d_{EQD2}>$ from 500 patients > prescribed dose in EQD2

d_{abs} …… prescribed dose (Gy)
d_{EQD2} ……. d_{abs} converted to (Gy EQD2)

Δd ……. … e.g. 30% d_{abs} (Gy)

$d_{abs}^{-/+}$ ……. prescribed dose –/+ Δd (Gy) = delivered dose in Gy
$d_{EQD2}^{-/+}$…… $d_{abs}^{-/+}$ converted to Gy EQD2

$d_{abs} - d_{abs}^- = d_{abs}^+ - d_{abs}$ $\qquad$ $d_{EQD2} - d_{EQD2}^- < d_{EQD2}^+ - d_{EQD2}$

ESTRO School

Dosimetric uncertainties and dose-response relationships

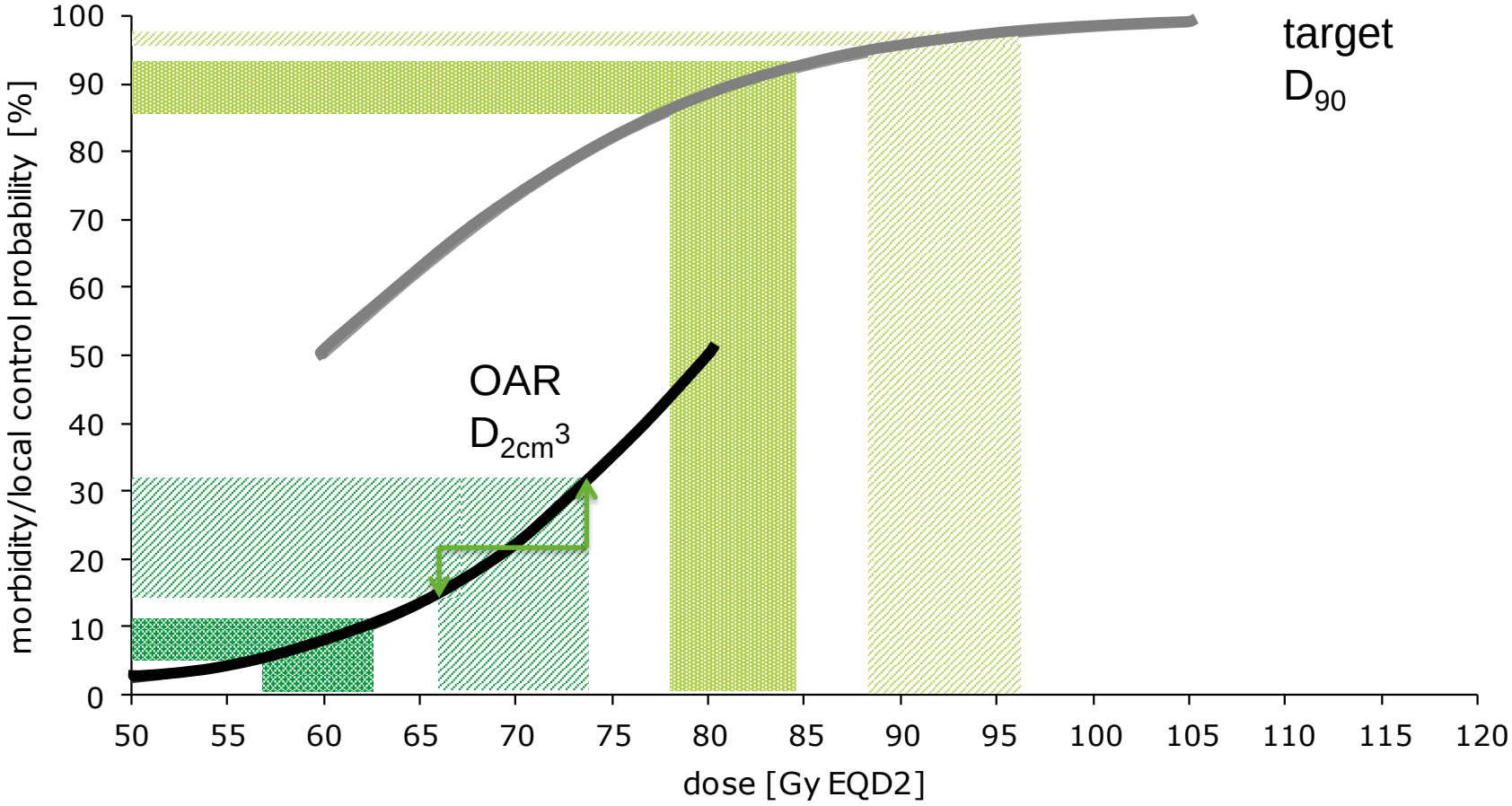

Schematic illustration of the effect of dosimetric ucertainties of prescribed vs. delivered dose on response probabilities

Tanderup et al. 2013, Radiother Oncol 107

ESTRO School

Dose-response relationships (published examples for cervix BT)

OAR

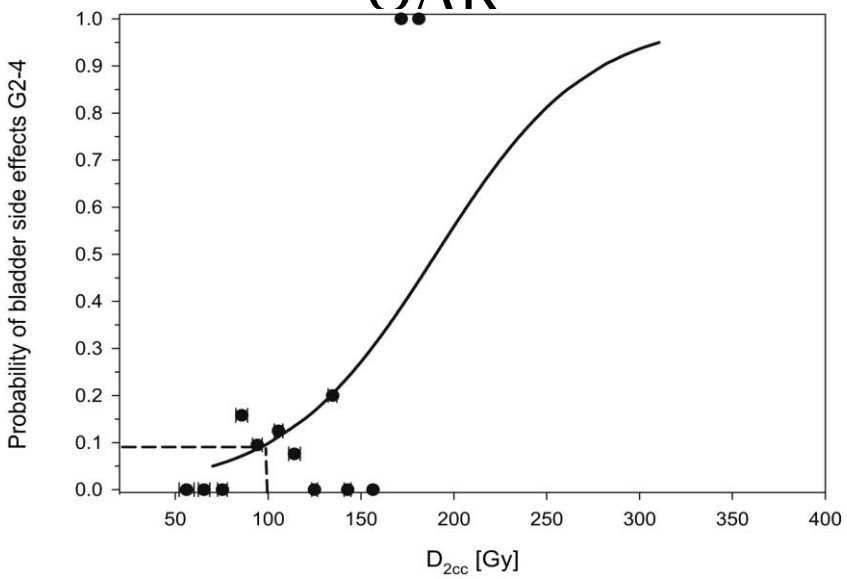

urinary bladder G2-4: *Georg et al. 2012, IJROBP 82*

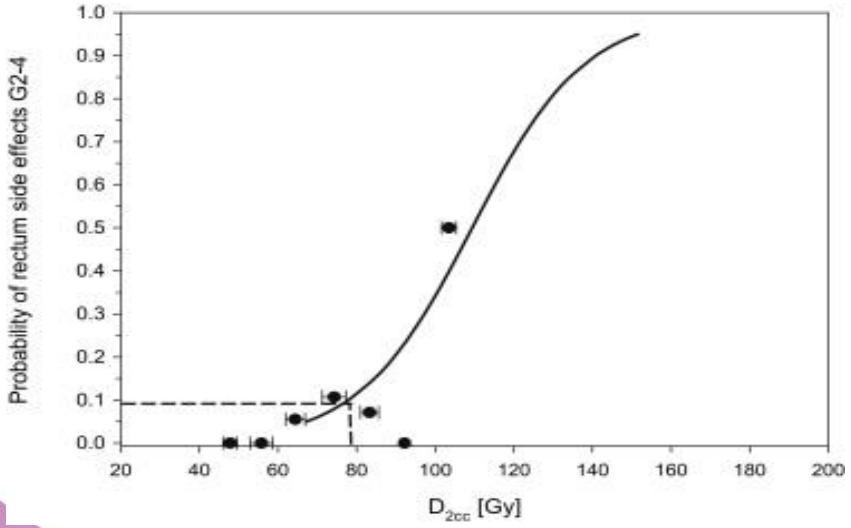

rectum G2-4: *Georg et al. 2012, IJROBP 82*

CTV_{HR}

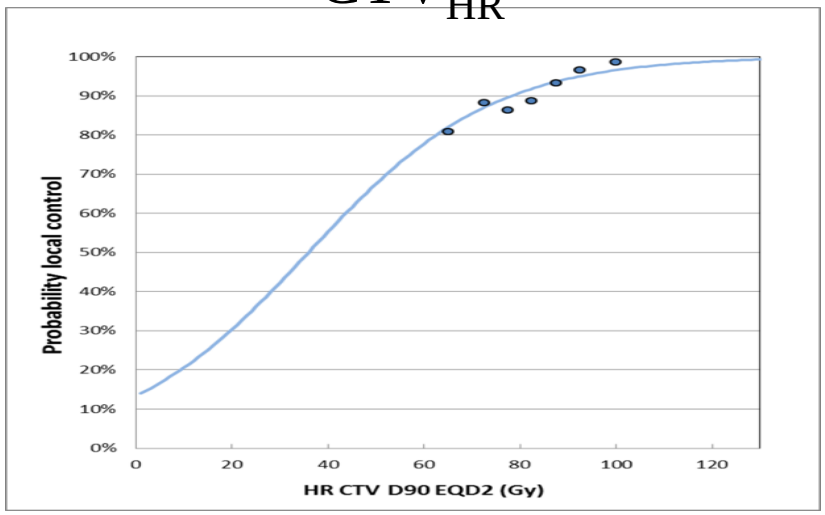

Relationship between EBRT-C+BT dose and local control from retroEMBRACE patients (*Tanderup et al, GEC-ESTRO workshop, Brussels, 2013*)

Other OARs for cervix: sigmoid, vagina, and upcoming dose response curves from EMBRACE study (www.embracestudy.dk)

Clinical outcome reports for prostate: e.g. *Martinez A. et al. 2011 IJROBP 79, Ghilezan et al. 2012, IJROBP 83, Martinez E. et al. 2015, Brachytherapy 14, …*

Dose response for breast (APBI): e.g. *Herskind & Wenz 2010, Strahlentherapie und Onkologie 186*

ESTRO School

Effect of uncertainties on observed dose response relationships

Comparison of model dose response curve (based on published curves, see previous slides), and simulated „observed“ dose response curves assuming different systematic and random uncertainties.

systematic dosimetric uncertainty
e.g. rectum D_{2cm^3} (+3,+5,+10,+15 % / fx)

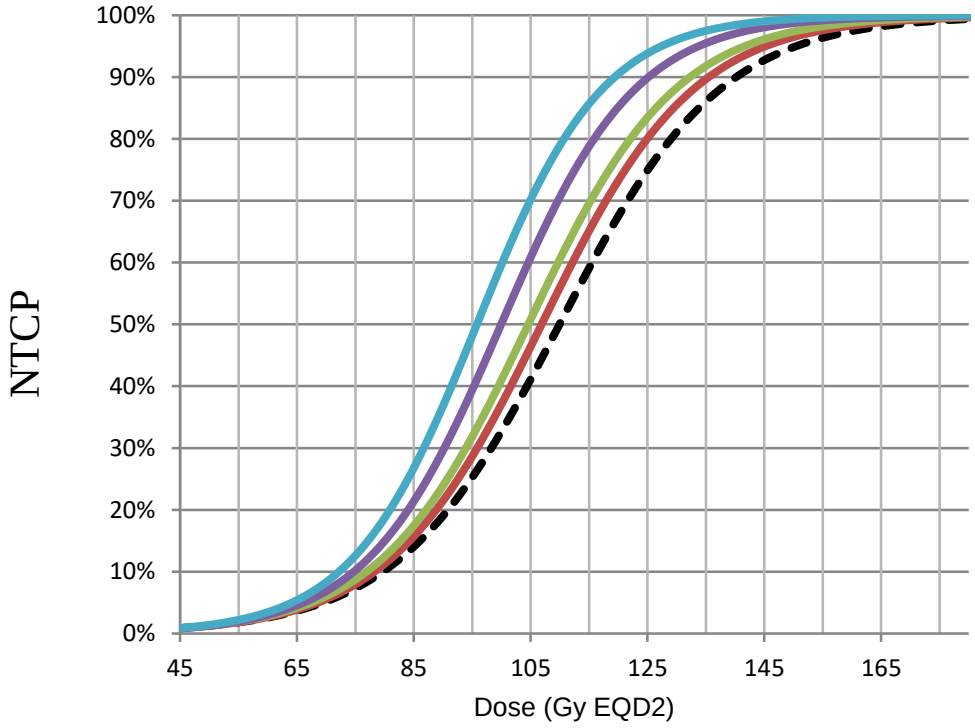

random dosimetric uncertainty
e.g. rectum D_{2cm^3} (±10, ±20, ±30 % / fx)

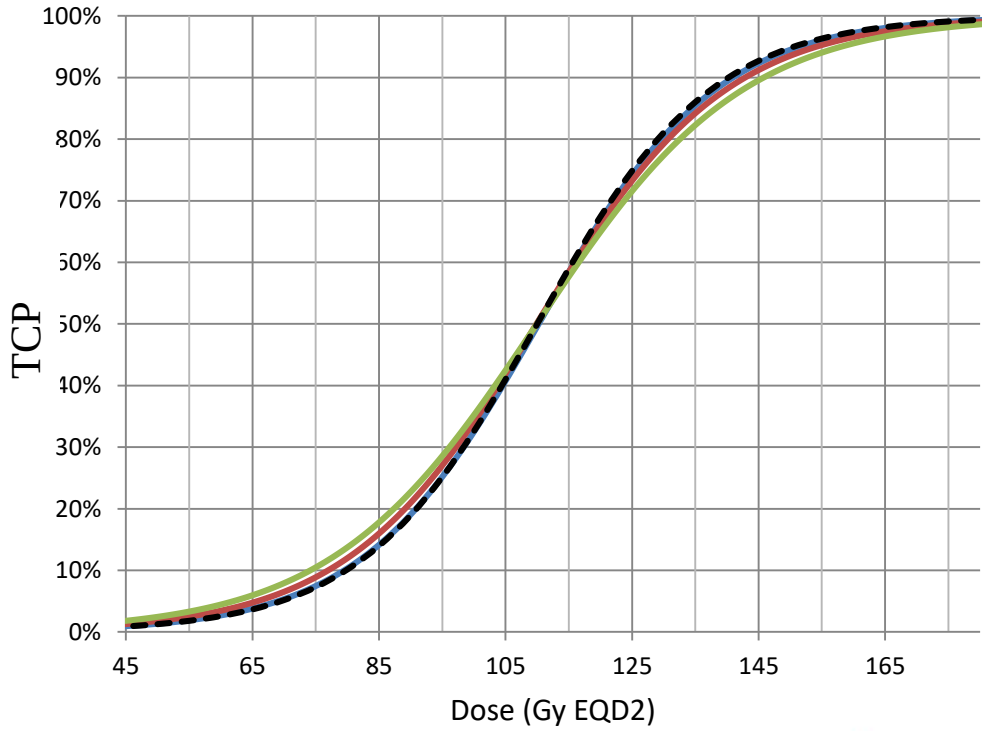

n=10000 patients per dose level, total dose = 45Gy EBRT + 4 fx BT (equal PD for each fx)
model based on *Georg er al. 2012, IJROBP*

Nesvacil et al., ESTRO33, 2014

Example: systematic uncertainties for target

effect of systematic underestimation of target D_{90} on observed dose-response

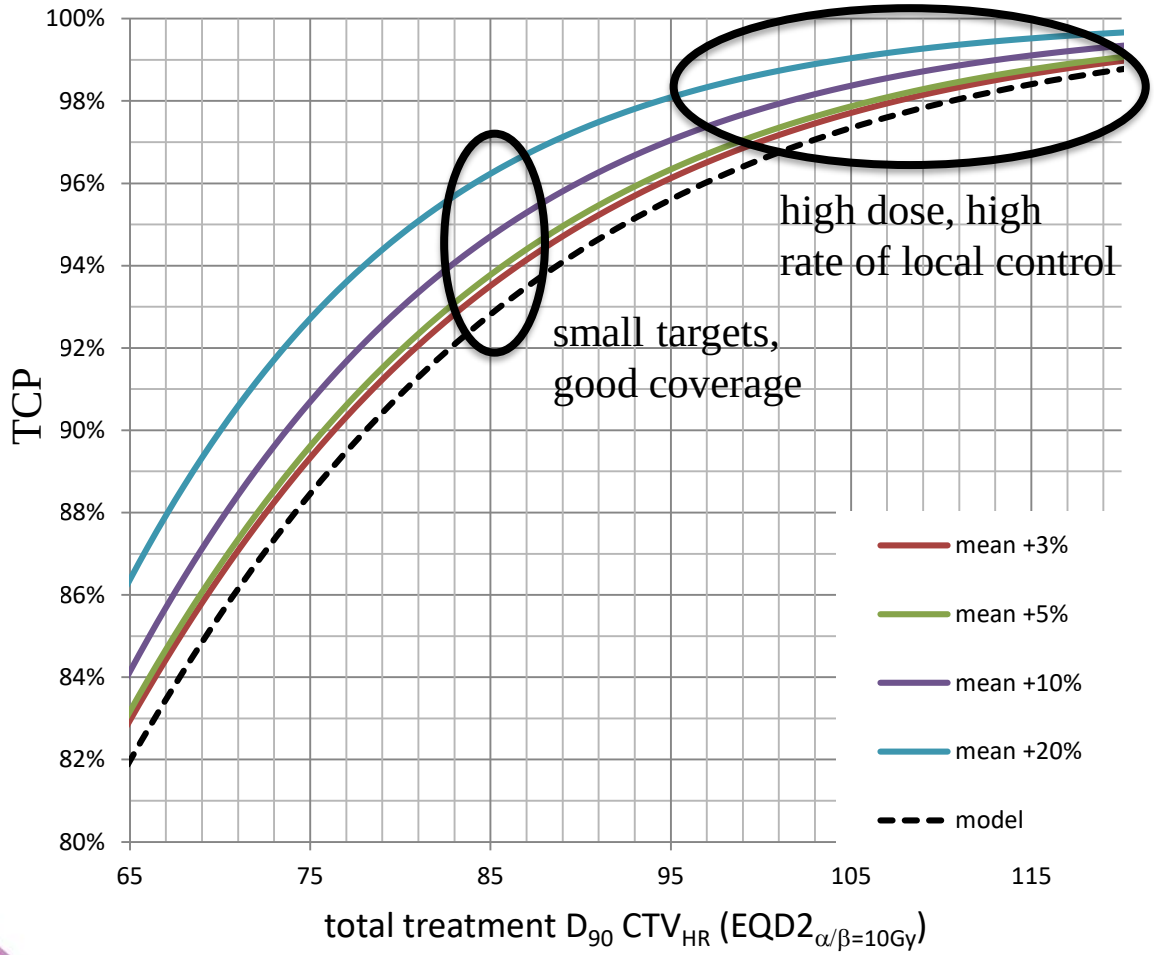

Systematic 1.5 mm applicator reconstruction uncertainty for MRI- based cervix BT *(Tanderup et al., R&O 2008):*

e.g. $\Delta D90 \leq +3\%/fx$ => „observed" local control @85 Gy <1% higher than model prediction

Systematically larger contours on CT vs. MRI => underestimation of D90 by CT contours *(e.g. Viswanathan et al. 2007, IJROBP 68):*

e.g. i) $\Delta D_{90} = +10\%/fx$ => 2% overestimation of local control @ 85 Gy

ii) $\Delta D_{90} = +20\%/fx$ => 3.5% overestimation of local control @ 85 Gy

(model based on preliminary retroEMBRACE data:*Tanderup et al, GEC-ESTRO workshop, Brussels, 2013*)

ESTRO School

Example: random uncertainties for target + OAR

effect of random intra-/interfraction variation on D_{90}, D_{2cm^3} and dose-response

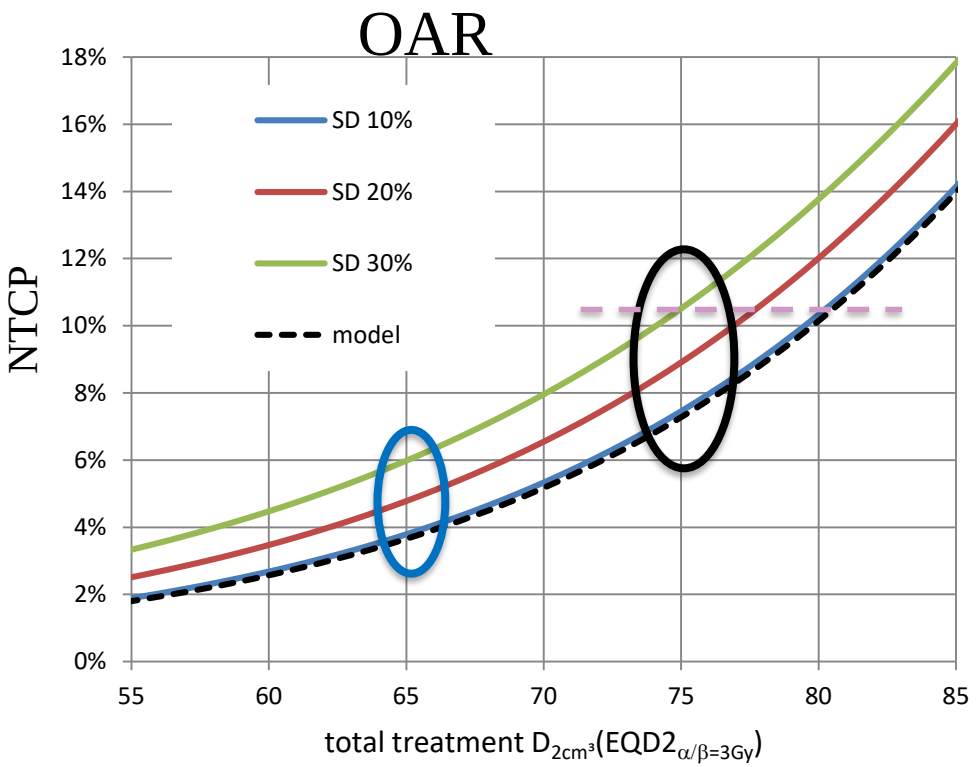

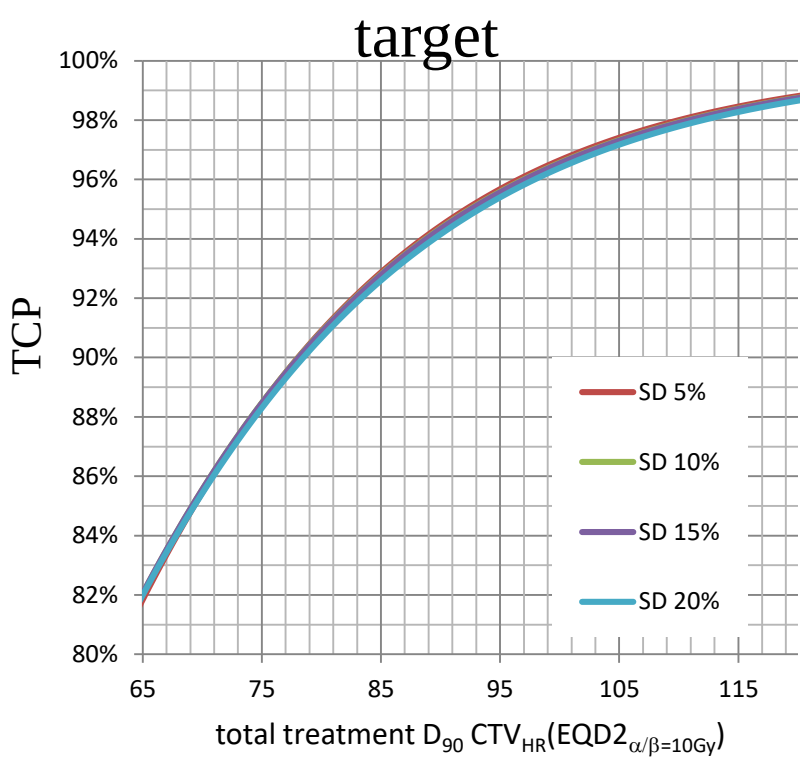

Example: 75Gy, **random variation of rectum D_{2cm^3}**:

- $\Delta D_{2cm^3} = \pm 10\%$/fx -> observed NTCP 7.5 %
  (vs 7.3% model prediction)
- $\Delta D_{2cm^3} = \pm 20\%$/fx -> observed NTCP 8.9 %
- $\Delta D_{2cm^3} = \pm 30\%$/fx -> observed NTCP 10.5 %
- Model predicts 10.5% morbidity NTCP @ 80Gy EQD2!

For target – differences in TCP < 0.5%

ESTRO School

Example: influence of the number of BT Fx

Random uncertainties and dose response for different fractionation schemes

OAR

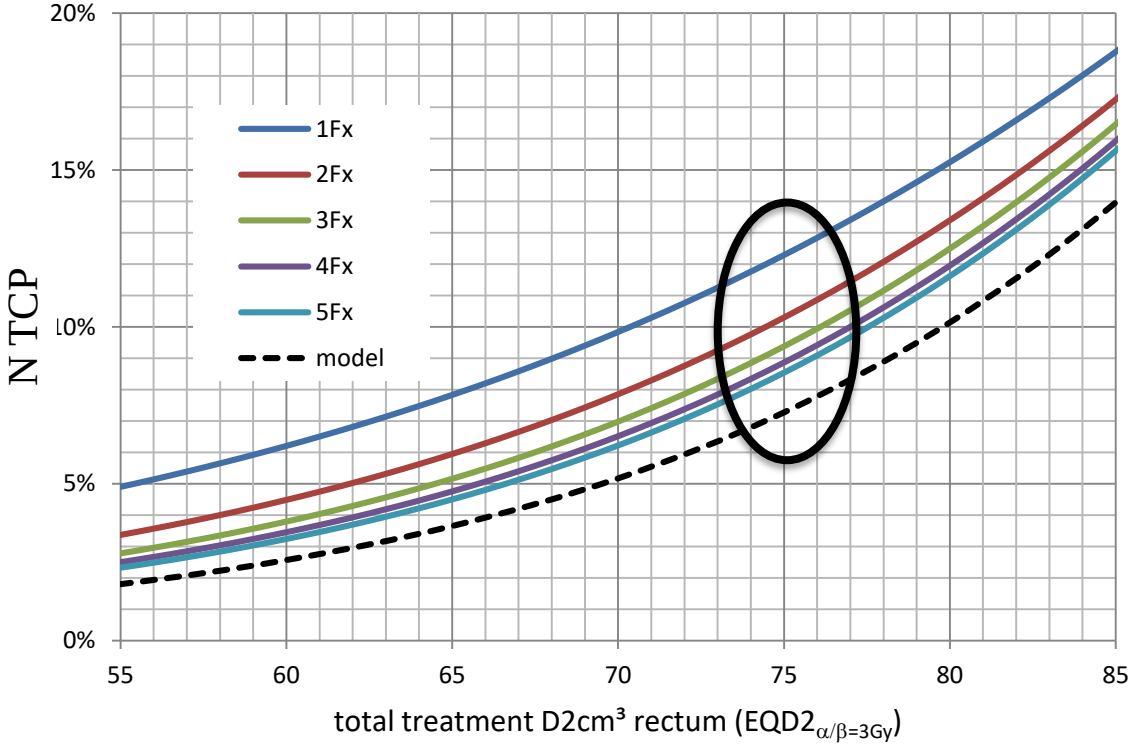

target

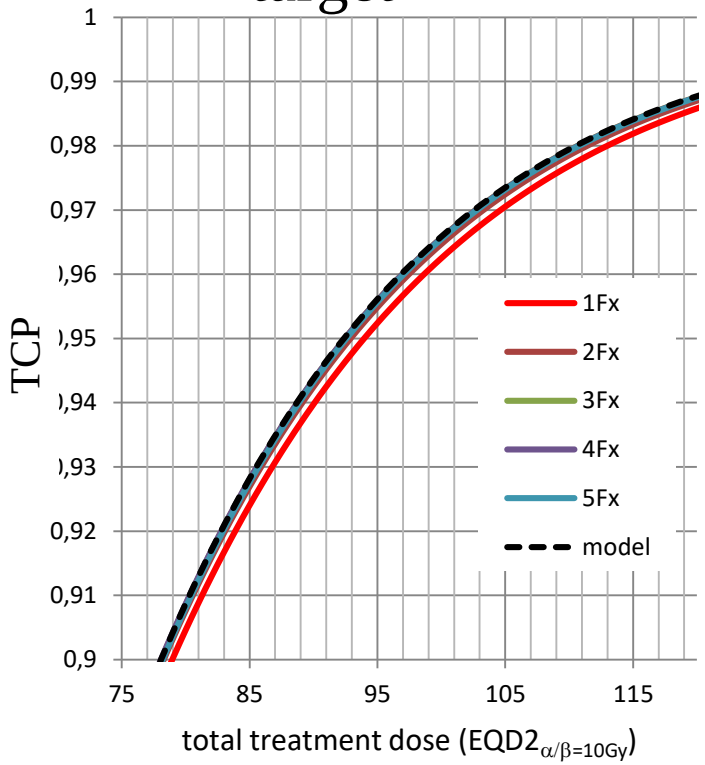

Example: random uncertainty $\Delta D_{2cm^3} = \pm 20\%/fx$:

- nFx=5 => observed morbidity @75Gy 8.5%
- nFx=4 => observed morbidity @75Gy 8.9%
- nFx=3 => observed morbidity @75Gy 9.4%
- nFx=2 => observed morbidity @75Gy 10.3%
- nFx=1 => observed morbidity @75Gy 12.3%

For target: using 1 fx vs 2-5 fx results in ~0.5% lower response probability than predicted by model

ESTRO School

Strategies to reduce uncertainties for brachytherapy planning and treatment

- Organ filling protocols
- Optimize target contouring (MRI, US, …)
- Adaptive planning to reduce large systematic/random variations between fractions (online planning, plan of the day)
- Advanced in vivo dosimetry (dose rate time profiles)
- Online imaging in treatment room (comparable to CBCT in EBRT) – limited by infrastructure of the BT suite (imaging in treatment room)
  - CBCT, in-room MRI/CT, 3D ultrasound, …

Conclusions

- Extreme hypo with BT bears large dosimetric uncertainties, and benefits from high target dose per fraction: flat part of dose response curve is less sensitive to uncertainties in dose

- Future development of BT fractionation schemes should take into account

  - Existing/missing knowledge about dose response relationships
    - For target and OARs!

  - Existing/missing knowledge about uncertainty budget of the specific treatment technique and workflow

  - All these combined will help to improve safety of predicting the optimal therapeutic window

ESTRO School

ESTRO School

WWW.ESTRO.ORG/SCHOOL

ESTRO School

Advanced Brachytherapy Physics

Elements for a Quality Management Program in Brachytherapy

Prof. Mark J. Rivard, Ph.D., FAAPM

Advanced Brachytherapy Physics, 29 May – 1 June, 2016

ESTRO School

Disclosures

The are no conflicts-of-interest to report.

Opinions herein are solely those of the presenter, and are not meant to be interpreted as societal guidance.

Specific commercial equipment, instruments, and materials are listed to fully describe the necessary procedures. Such identification does not imply endorsement by the presenter, nor that these products are necessarily the best available for these purposes.

Special thanks is extended to Bruce Thomadsen as the source for many of the slides in this presentation.

Learning Objectives

1. Definitions, terminology, and accepted nomenclature
2. Pre-purchase preparations and installation
3. Acceptance testing requires formalization
4. Commissioning a brachytherapy program
5. Example forms for clinical practice

Learning Objectives

1. Definitions, terminology, and accepted nomenclature
2. Pre-purchase preparations and installation
3. Acceptance testing requires formalization
4. Commissioning a brachytherapy program
5. Example forms for clinical practice

ESTRO School

QMP Schema

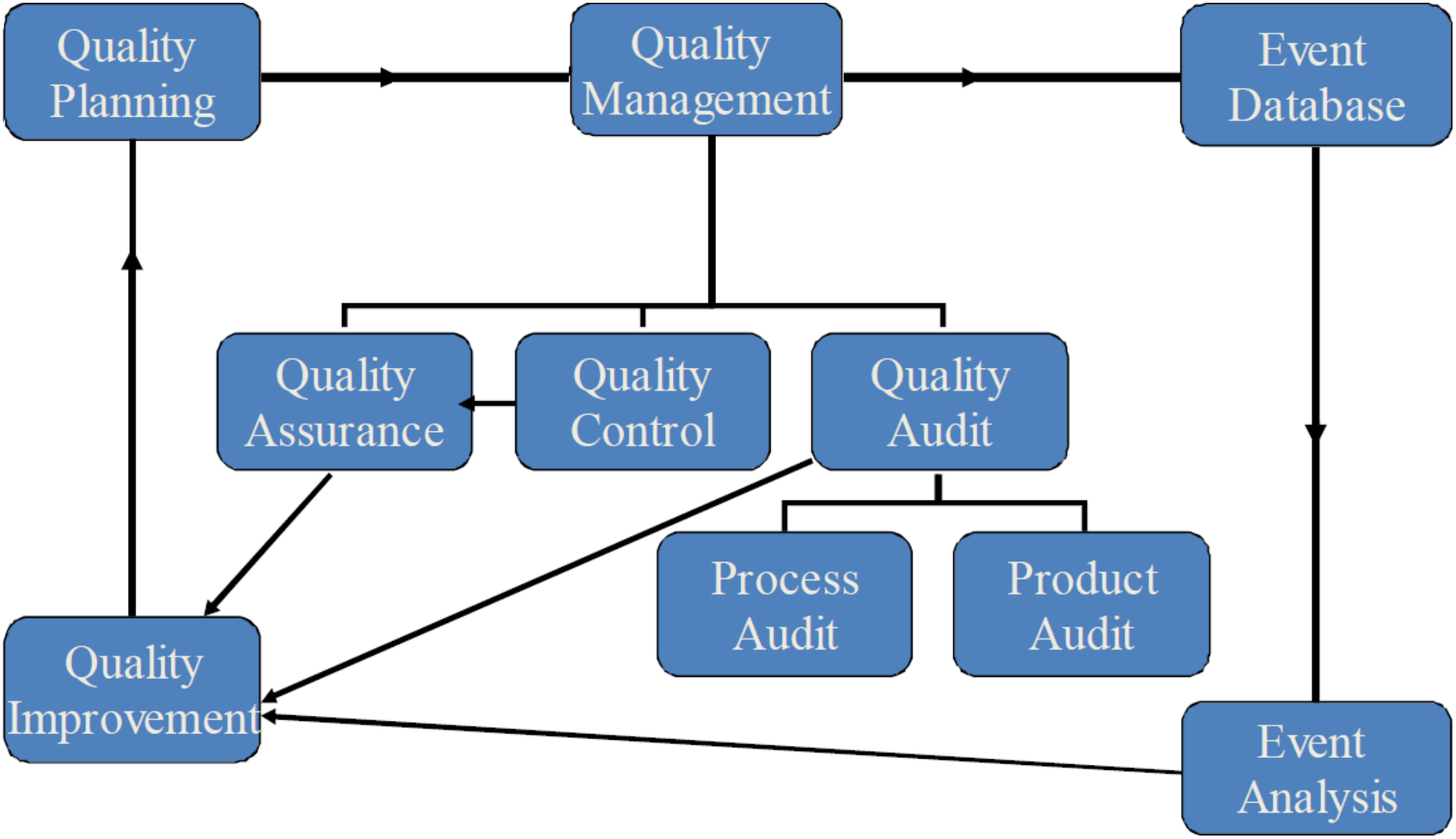

slide courtesy of Bruce Thomadsen

QMP Presentation Focus

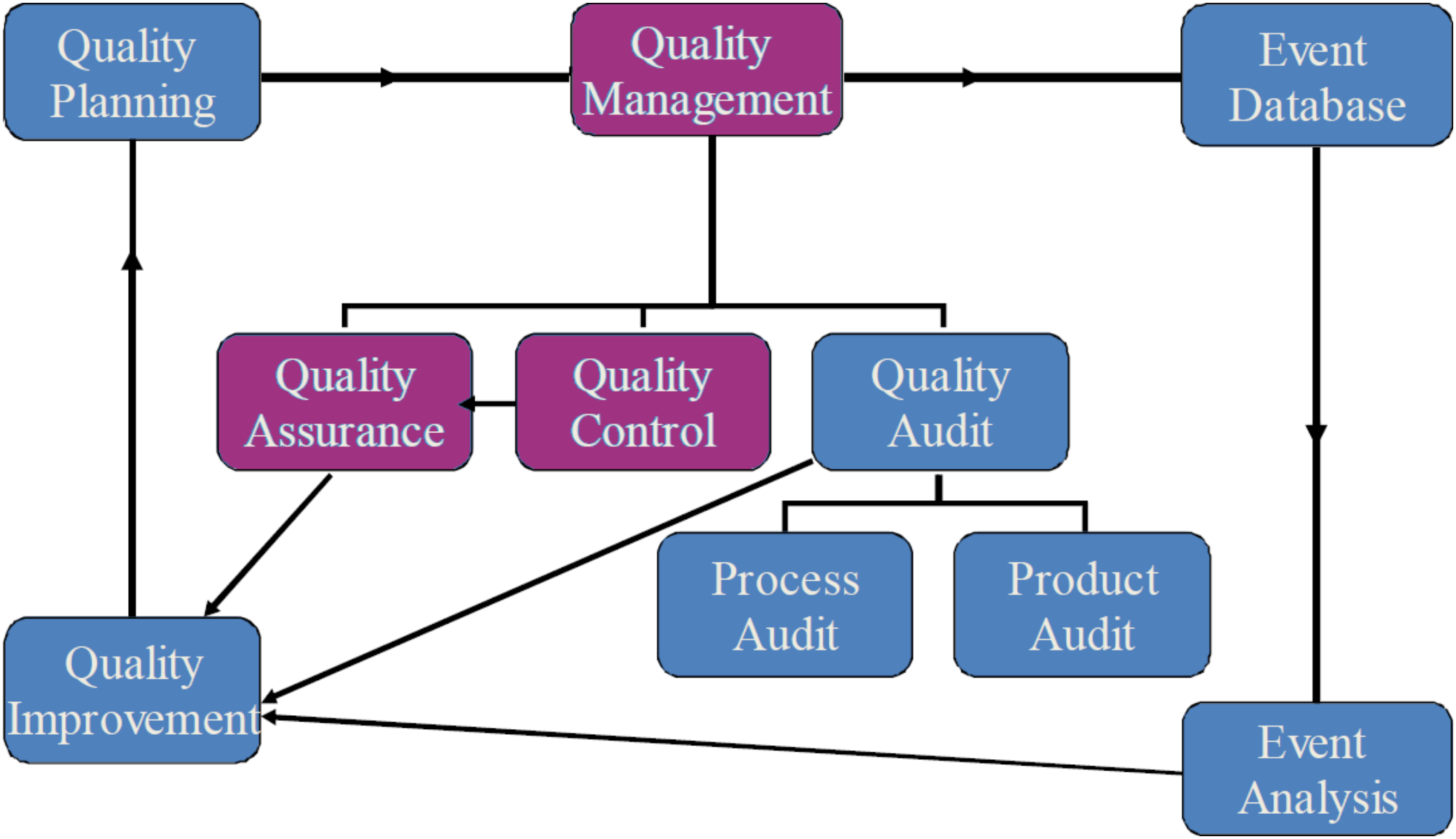

ESTRO School

QMP Philosophy

- Devise the QMP mission

patients will be treated safely, accurately, and efficiently
as defined by Rx, regulations, and societal standards

equipment + patient + staff + culture = success

Shewhart: Father of Statistical Quality Control

Walter Andrew Shewhart (1891–1967)

1917: Ph.D. in Physics, University of California, Berkeley

1918: Joined Western Electric Company (supplier to AT&T)

1924: Invented the Control Diagram

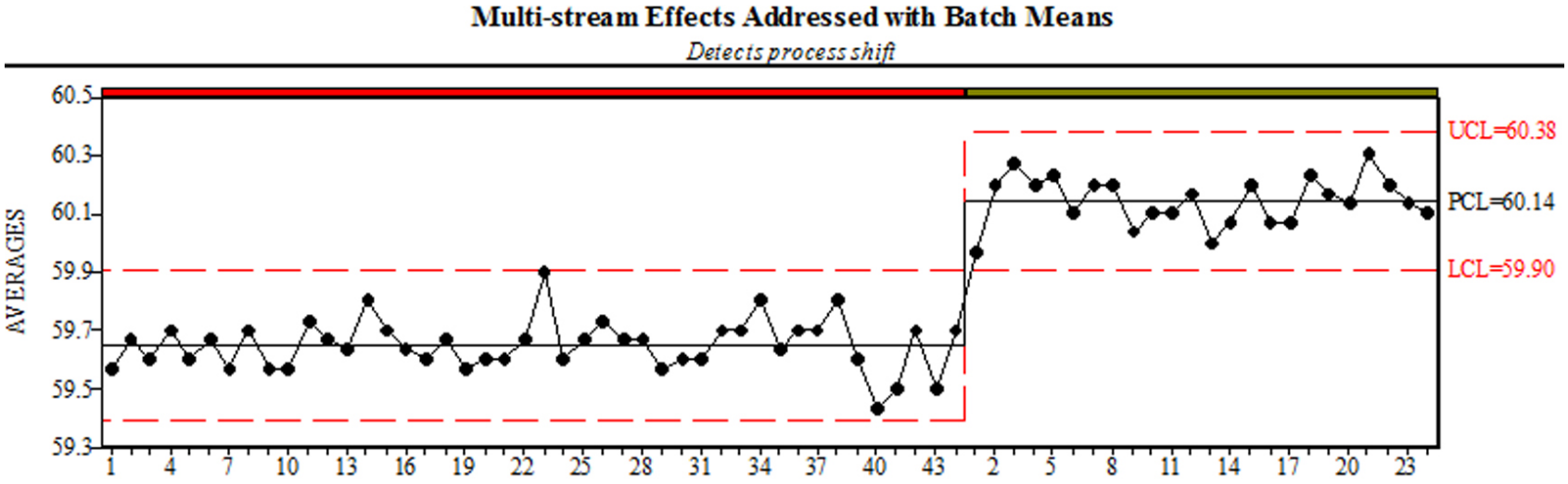

1924-1932: Initiated study on sensitivity of worker productivity to light

Improvements were later attributed to management attention

ESTRO School

Deming: Father of PDSA

William Edwards Deming (1900–1996)

1926: Ph.D. in Mathematical Physics, Yale University

1927: Employed by USDA and met Walter Shewhart
Applied statistics to industrial production methods

A system must be managed. It will not manage itself.

1943: Deming Cycle
Plan or design an experiment
Do the experiment by performing the steps
Study the results by analyzing the information
Act on decisions based upon the analyzed results

Fault Tree Analysis

Developed in 1961 at Bell Laboratories by H. A. Watson

Launch Control Safety Study for Intercontinental Ballistic Missile

Translation of system failure behavior into visual diagram and logic model

Visual model portrays system relationships and root cause pathways

Logic model provides qualitative & quantitative system evaluation

Utilizes Boolean algebra and probability theory

FTA popularized by US tragedies: Apollo 1 fire (1967), Three Mile Island nuclear meltdown (1979), Space Shuttle Challenger (1986)

FTA provides top-down risk assessment, FMEA is a bottom-up approach

US Military Procedures

assistdocs.com
U.S. Department of Defense

Database Last Updated: 02-MAY-2014 | New Search | What's New | Site Overview | ASSIST

Basic Search → Results → Document Details

Document ID: MIL-P-1629

Overview

Title:	PROCEDURES FOR PERFORMING A FAILURE MODE, EFFECTS AND CRITICALITY ANALYSIS
Scope:	Scope information has not been recorded for this document
Document Status:	Canceled
Doc Date:	09-NOV-1949
FSC/Area:	8405
Dist Stmt:	See below
Doc Category:	Detail Specification

Responsibilities

Lead Standardization Activity:	CT	DLA Troop Support - Clothing & Textile Items of Supply
Preparing Activity:	GL	U.S. Army Soldier Systems Center
Army Custodian:	GL	U.S. Army Soldier Systems Center

ESTRO School

US Space Agency

RA-006-013-1A

OFFICE OF MANNED SPACE FLIGHT

APOLLO PROGRAM

PROCEDURE FOR FAILURE MODE, EFFECTS, AND CRITICALITY ANALYSIS (FMECA)

AUGUST 1966

NATIONAL AERONAUTICS AND SPACE ADMINISTRATION
WASHINGTON, D.C. 20546

ESTRO School

First Known Paper on Brachytherapy Risk Analysis

Intl. J. Radiation Oncology, Biology, Physics

Analysis of treatment delivery errors in brachytherapy using formal risk analysis techniques

Purpose: To identify hazardous situations in treatments, analyze the nature of errors committed, and assess the value of several analysis techniques.

Methods and Materials: The study applied several risk analysis techniques to brachytherapy events (misadministrations) reported to the U.S. Nuclear Regulatory Commission and the International Atomic Energy Agency.

Results:

(1) Events usually have multiple causes.

(2) Failure to consider human performance in the design of equipment led to a large fraction of the events.

(3) Verification procedures often were ineffectual.

(4) Many events followed the failure of persons involved to detect that the situation was abnormal, often even though many indications pointed to that fact. Once the event was identified, the response often included actions appropriate for normal conditions, but inappropriate for the conditions of the event.

(5) Events tended to happen most with actions having the least time available.

(6) Lack of training and procedures covering unusual conditions frequently contributed to events.

(7) New procedures or new persons joining a case in the middle present increased hazards.

Conclusion: Risk analysis tools common in industry provide useful information for error reduction in medical settings, although not as effectively, and modification of such techniques could improve their efficacy.

Thomadsen, et al, *Intl. J. Radiat. Oncol., Biol., Phys.* 57, 1492-1508 (2003)

Numerous Opportunities for Errors

Table 3. Summary of the branches of the fault tree for high-dose-rate brachytherapy misadministrations, tracing backward to the initiating errors, with the frequency of errors along each branch indicated

Result of error	Major process	General category	Subcategory	Type of initial error
Wrong dose distribution or site 0.98 (43/44)	Treatment planning error 0.30 (13/44)	Localization 0.07 (3/44)		Improper simulation: >Marker misinterpretation 0.05 (2/44) Digitization error: >Entry error: Localization 0.07 (3/44) ≫Digitization not follow protocol 0.02 (1/44) Calculation error: >Wrong input data 0.02 (1/44)
		Dosimetry error 0.23 (10/44)	Source strength 0.07 (3/44)	Erroneous source strength data: >Failure to enter or alter data 0.07 (3/44)
			Dose calculation 0.16 (7/44)	Incorrect data entry for calculation 0.02 (1/44) Wrong dose: >Incorrect dose entry 0.05 (2/44) Wrong position of dose distribution: >Inaccurate source position entry 0.05 (2/44) Dose specified to the wrong point 0.05 (2/44)
	Treatment implementation 0.68 (30/44)	Applicator shifted in patient 0.07 (3/44)	Applicator shifts >Patient movement ≫Failure of securing mechanism 0.07 (3/44)	Poor techniques 0.05 (2/44) Equipment failure 0.02 (1/44)
		Applicator connection 0.05 (2/44)	Incorrect guide tubes 0.02 (1/44)	Applicator connected to through the wrong transfer tube type 0.02 (1/44)
			Wrong channel 0.02 (1/44)	Applicator connected incorrectly 0.02 (1/44)
		Treatment programming error 0.48 (21/44)	Manual programming error 0.48 (21/44)	Transcription error 0.41 (17/44) Data transposition 0.02 (1/44) Interpretation error 0.07 (3/44)
		Treatment delivery error: >Source fails to progress 0.10 (4/44)	Drive mechanism fails 0.05 (2/44)	Mechanical malfunction 0.02 (1/44) Kink in catheter 0.02 (1/44)
Wrong patient treated 0.02 (1/44)			Source disconnect 0.05 (2/44)	

Thomadsen, et al, *Intl. J. Radiat. Oncol., Biol., Phys.* 57, 1492-1508 (2003)

ESTRO School

Recent Paper on Brachytherapy FMEA

Failure modes and effects analysis applied to high-dose-rate brachytherapy treatment planning

D. Allan Wilkinson*, Matthew D. Kolar

Department of Radiation Oncology, Cleveland Clinic, Cleveland, OH

PURPOSE: To apply failure modes and effects analysis to high-dose-rate treatment planning to identify the most likely and significant sources of error in the process.

METHODS: We have made a list of 25 failure modes grouped into six categories (imaging, catheter reconstruction, dwell position activity, dose points/normalization, optimization/dose, and evaluation). Each mode was rated on a one to five scale for severity, likelihood of occurrence, and probability of escaping detection. An overall ranking was formed from the product of the three scores. The authors assigned scores independently and the resulting rankings were averaged. We also analyzed 44 reported medical events related to high-dose-rate treatment planning listed on the Nuclear Regulatory Commission Web site and compared them with our own rankings.

RESULTS: Failure modes associated with image sets, catheter reconstruction, indexer length, and incorrect dose points had the highest ranking in our analysis (scores higher than 20). The most often cited failure modes in the Nuclear Regulatory Commission reports examined were indexer length (20/44) and incorrect dose points (6/44). Several of our high-ranking modes are not associated with reported events.

CONCLUSION: It is a useful exercise to identify failure modes locally and analyze the efficacy of the local quality assurance program. Comparison with nationally reported failures can help direct the local analysis, but the absence or small number of reports for failure modes with a high score may be owing to low detectability. Such modes obviously cannot be ignored.

Keywords: Failure modes; High-dose-rate brachytherapy; Treatment planning

Wilinson and Kolar, *Brachytherapy* 12, 382-386 (2013)

ESTRO School

Further Adoption of FMEA

1960s US civil aviation, automotive, and food industries

1970s Petroleum, plastics, waste water, and software industries

1980s …

1990s …

2000s Radiation oncology (brachytherapy)

Key Concepts

- Quality Management Program (QMP)
  - *ALL* activities **designed to contribute to process quality**
- Quality Assurance (QA) non-patient tests
  - activities that **measure the quality level** of a process
- Quality Control (QC) patient treatment checks
  - activities that **force specific qualities** onto a process

Quality Controls vs. Quality Assurance

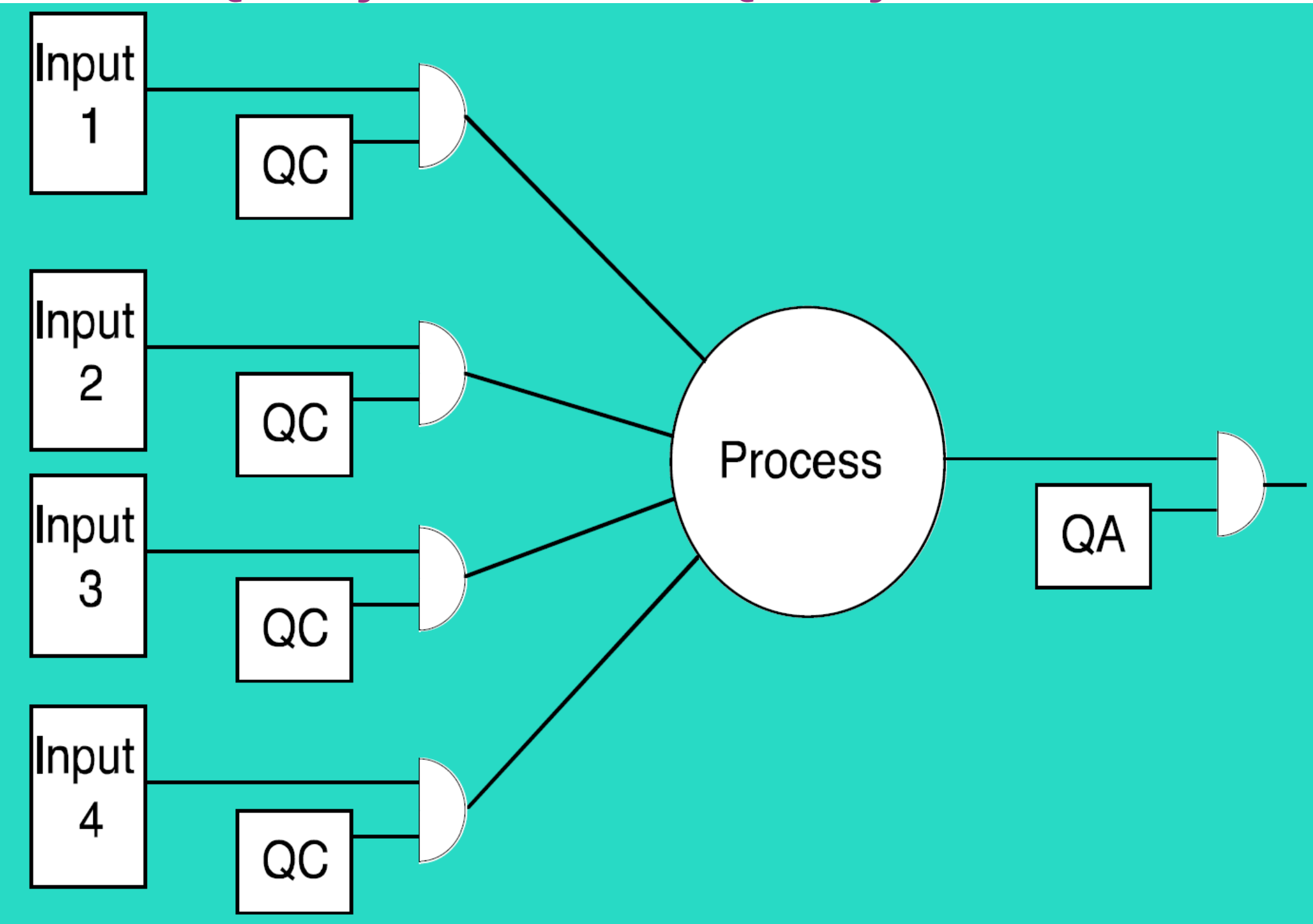

ISO 900X and Quality Management

ISO 9000

A series of standards that define, establish, and maintain an effective QA system for manufacturing and service industries.

ISO 9001

Requirements for organizations wishing to meet the ISO 9000 standard

Reported benefits

1. Improve efficiencies and effective operations
2. Increases customer satisfaction and retention
3. Reduces audits
4. Enhances marketing
5. Improves employee motivation, awareness, and morale
6. Promotes international trade
7. Increases profit
8. Reduces waste and increases productivity
9. Common tool for standardization

Appropriate for large scale industries, not individual clinics

ESTRO School

Learning Objectives

1. Definitions, terminology, and accepted nomenclature
2. Pre-purchase preparations and installation
3. Acceptance testing requires formalization
4. Commissioning a brachytherapy program
5. Example forms for clinical practice

Pre-Installation Preparations

- Assist administrators to create a realistic business plan
  - prepare for reimbursement fluctuations
  - include QA equipment and dummy markers
  - budget for regular training for new staff and facility upkeep
- Plan disease site(s): GYN, breast, prostate, skin, etc.
  - consider future potential for treating additional disease sites
  - balance desires for growth with a dash of realism
- Review potential manufacturer system specifications, installation requirements, and clinical integration
- RAU-to-R&V connectivity is available with newer systems

Pre-Installation Preparations

- Physical layout
  - location of electrical/telephone/network connections, interconnectivity with linac interlocks, special gases, closed loop AV system
  - consider imaging proximity and position RAU near imaging (dept CT, US, MRI?) or OR, maybe not in RadOnc center proper

- Regulatory aspects
  - vault design (primary/scatter/maze/door) ala NCRP 147/151/155, acceptable exposure levels, workflow
  - enhanced security measures, source controls, staff bkgnd checks
  - approval for *n* sources and max individual/total Ci (not RAKR)
  - broadscope license need not name individuals

- Visit established centers, contact colleagues, phone a friend

Learning Objectives

1. Definitions, terminology, and accepted nomenclature
2. Pre-purchase preparations and installation
3. Acceptance testing requires formalization
4. Commissioning a brachytherapy program
5. Example forms for clinical practice

ESTRO School

Acceptance Testing: General

- Acceptance testing results set baseline for clinical use
- Usually no formal ATP form as for linacs
- Performance evaluation of system within manu. specs
- Re-perform annually to ensure system stability

Acceptance Testing: Applicators & Source

- Make electronic inventory of all hardware and disposables

- Applicators
  - confirm dimensions and serial numbers
  - confirm applicator shielding magnitude and shape
  - check connecting tubes and other ancillary equipment

- Source
  - validate source-to-dummy marker coincidence
  - superposition: transmission radiograph & autoradiograph
  - use electronic imaging tools if no radiochromic film

- Determine source strength (covered on Day 3)

Acceptance Testing: TPS

- AAPM TG-53 and TG-43 reports are good resources
- Verify functionality of dose, dwell time, and Tx time calculations
- High-level check of single-source isodose distributions
- Understanding of plan rotation matrix and coordinate recon

Acceptance Testing: TPS

- Accuracy of electronic data transfer to TCS/RAU
- Evaluate optimization software
  - develop reference dataset for accuracy & constancy
- DVH and implant figures of merit
- End-to-end testing
  - general functionality of entire system
  - identify QMP weaknesses by using items incorrectly

ideas courtesy of Bruce Thomadsen

Acceptance Testing: General

- Field service engineer provides system familiarization
- Test all components and features the time is now
- Ignore pressure to hurry and sign form
- Technical understanding of equipment is your responsibility

Learning Objectives

1. Definitions, terminology, and accepted nomenclature
2. Pre-purchase preparations and installation
3. Acceptance testing requires formalization
4. Commissioning a brachytherapy program
5. Example forms for clinical practice

ESTRO School

References for Brachytherapy Commissioning

- Consider AAPM Task Group Reports and Guidance
  - TG-41 Remote Afterloading Technology (1993)
  - TG-43 Brachytherapy Dosimetry Formalism (1995)
  - TG-56 Code of Practice for Brachytherapy (1997)
  - TG-59 High Dose Rate Tx Delivery (1998)
  - AAPM/ESTRO HEBD Report #229 (2012)

- Consider AAPM Summer School texts
  - 1994 Chapters 28, 30, 31, 32
  - 2005 Chapters 6, 7, 11, 22, 32, 48

- Consider Bruce Thomadsen's 1999 text
  "Achieving Quality in Brachytherapy"

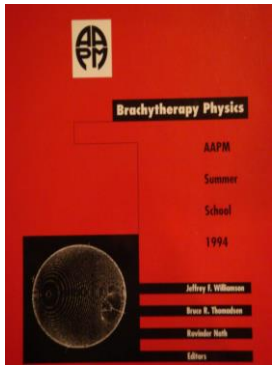

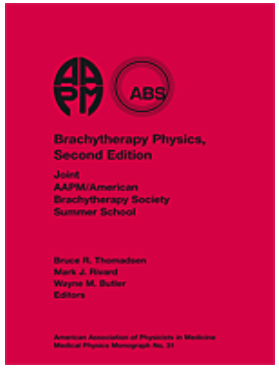

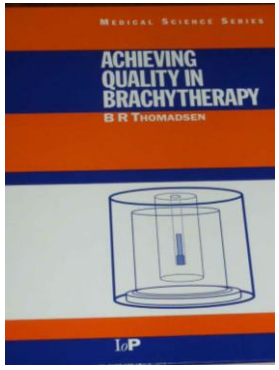

ESTRO School

Commissioning: General

- Medical Event notification plan and action levels
- Patient/personnel radiation safety plan
- Patient positioning standards and contingencies
- Use of dummy markers, contrast agents, and imaging system settings to visualize disease/applicator/markers
- Form creation
  - WD (disease-site specific)
  - daily QA (performed by therapist under physicist supervision)
  - Tx runsheet QC
  - new source QA (TPS backup, TCS backup)
  - annual QA, rigorously check applicators and TPS data

Commissioning: General

- Establish disease-specific clinical standards to minimize “medical arts” and to follow ABS/ESTRO guidelines
- Create policies-and-procedures, have staff read, provide feedback, and document understanding (annually)
- Establish workflow for all processes: identify tasks, frequency, needed resources, responsible party(s)
- Develop safety standards and clinic-specific FMEAs, share results with all stakeholders
- Staff training on HDR system (RAU, applicators, and TPS) usage, emergency procedures, and common expectations

Commissioning: RAU

- Master all aspects of TCS functionality
- Document logic chain of RAU safety interlocks
- Determine timer linearity
- Understand emergency buttons, warnings, and error codes
- Demonstrate well chamber stability

Commissioning: Source

- Absorbed dose measurements not performed in the clinic
  - detector response sensitive to photon spectrum
  - dose falloff sensitive to medium composition
  - influence of positioning, attenuation, and scatter
  - no AAPM protocol for absorbed dose measurements
- Source form, inventory, wipe test documentation
- Understand eBT output variations for same source model

Commissioning: Source

- Validate source/dummy marker coincidence
- Source positional accuracy
- eBT source output stability
  - overall / global
  - spatial dependence (spectral changes)
- Demonstrate well chamber stability

Source Strength Measurements

- All HDR ^{192}Ir sources can have RAKR measured by physicist
- Using PSDL traceably-calibrated equipment for RAKR measurement
- For the eBT sources, only the Axxent has direct traceability to PSDL
- INTRABEAM and esteya sources do not yet have direct traceability
  - physicist may use AAPM TG-61 calibration method if they know the electron scatter/absorber thickness and the HVL for their device

Commissioning: Applicators

- Inventory all applicators
- Document sterilization procedures/responsibilities
- Determine intra-applicator source positioning
- Determine source/marker congruence in applicator

Commissioning: Applicators

- Validate dimensions (c.f., TPS applicator library info)
- Applicator performance evaluation (e.g., T&R)
- Confirm applicator/marker compatibility
- Establish standard imaging protocols (Day 2)

Commissioning: TPS

- Establish dose calc methods
  - imaging slice thickness, dummy marker usage, step size, optimization type and parameter ranges
- Compare TPS TG-43 dosimetry parameters to reference dataset or publication(s)
- Compare TPS dose calcs to TG-43 hand calcs
  - devise independent (secondary) dose calculation method
  - MBDCA covered on Day 1
- Commission source over required radii and polar angles

Commissioning: TPS

- AAPM TG-53 and TG-43 reports are good resources
- Evaluate data transfer between TPS and TCS/RAU
- Compare system performance range with TPS data
- Recommission TPS following all upgrades
- For advanced dose calculation modules, read carefully the TG-186 report for specific commissioning tasks (Day 1)

Commissioning: TPS

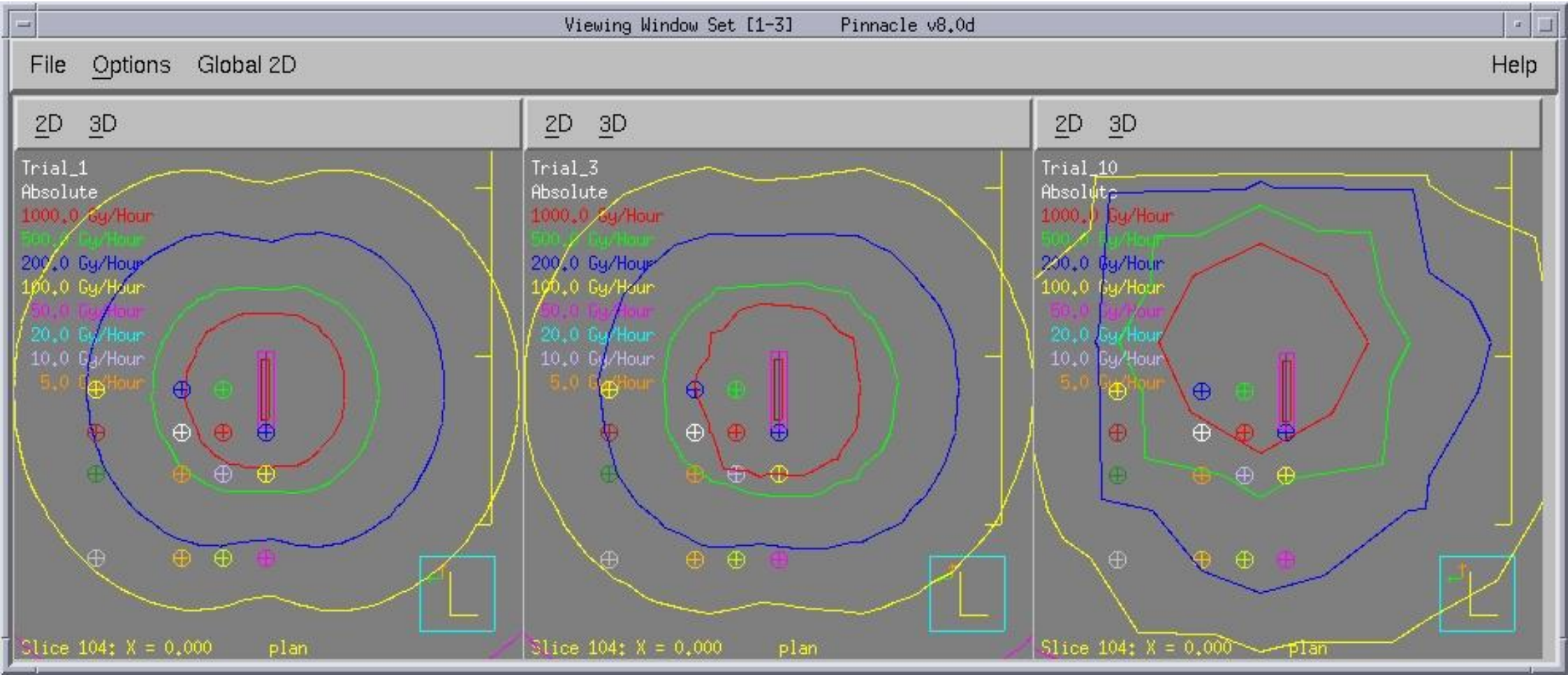

ESTRO School

eBT Commissioning Specifics

- Consider AAPM Task Group Reports and Guidance
  TG-43 Brachytherapy Dosimetry Formalism
  TG-56 Code of Practice for Brachytherapy
  TG-59 High Dose Rate Tx Delivery
  TG-182 Recommendations on eBT Quality Management
  2008 AAPM (Butler *et al*.) Low-energy Source Calibrations
  2008 ASTRO Emerging Technology Cmte: Electronic Brachytherapy

- Need comparisons of measured and calculated dose distributions, and consensus datasets

- HDR breast commissioning by Hiatt et al. JACMP (2008)

Learning Objectives

1. Definitions, terminology, and accepted nomenclature
2. Pre-purchase preparations and installation
3. Acceptance testing requires formalization
4. Commissioning a brachytherapy program
5. Example forms for clinical practice

ESTRO School

Philosophy on Forms

- Forms should be dynamic, constant improvements
- Use electronic forms, minimize paper usage (scan the paper!)
- Use mathematical tools (e.g., Excel) for non-patient data
- Data mining permits analysis across broad timescales
- Consider action levels beyond societal guidance
- Take high-level perspective on why to perform QA tasks

Example Daily HDR ^{192}Ir QA Form (upper)

Nucletron V2 MicroSelectron Remote Afterloader, Model # 105.088-03 Serial # 31743
Source is manufactured by QSA Global, model 105.002.

On each treatment day, the treating therapist will test the following system components and initial at the right indicating that the test was performed and that the result was within normal ranges. Any deviations must be promptly reported to a physicist.

1. Are the TV monitors at the control console operational (focus/zoom/pan)? _____
2. Is the intercom operational (2-way communications)? _____
3. Does the radiation survey meter function (battery check)? _____
4. Is the emergency basket stocked and the emergency storage container in place?
   [forceps/tongs, scissors, suture removal kit, and "CAUTION RADIATION AREA" tape] _____
5. Are the source guide tubes free of kinks, etc? _____
6. Did control console pass self-diagnostic checks when key switch is first turned? _____
7. Is the emergency STOP button in the treatment room (near emergency basket) operational?
   [verify illumination of the red "***Reset***" light , lower left of console] _____
8. Is the emergency STOP button on the HDR unit operational?
   [verify illumination of the red "***Reset***" light , lower left of console] _____

Attach source position check ruler to channel 2 (**incorrect channel**). Turn on ceiling light and adjust TV camera so that check ruler is clearly visible. Run: Daily QA, DQA patient to set the dummy source end to 1435 mm, and active source end to 1330 and 1430 mm. On the left side of the screen will be depicted a pre-Treatment Record

9. Are the date and time correct (within 5 minutes compared to local PC)? _____
10. Is the source strength on the printout within 0.020 cGy m^2/h of the logbook activity? _____

Example Daily HDR ^{192}Ir QA Form (lower)

11. Confirm program and dwell times, press START to initiate treatment, and verify that Error Code 14 appears on the screen and that the source is not extended out of the safe. _____

Attach the source position check ruler to channel 1 (**correct channel**). Press START to initiate treatment.

12. Does the distal end of the dummy source goto 1435 ±1 mm, and active source end goto 1330 ±1 mm (dwell position 35) and 1430 ±1 mm (dwell position 15)? _____

While the source is dwelling at dwell position 15 (nominally 1430 mm), check the door light, door interlock, interrupt button, and console emergency stop button. The source end should return to dwell position 15 after each restart.

13. Is the "HDR IN USE" door light on, and does the radiation area monitor function (red light)? _____
14. Is the door interlock operational? _____
15. Does the interrupt button on the console function properly? _____
16. Does the emergency STOP button on the treatment console promptly retract the source and emit an audible alarm and display the status on the screen?
    [verify illumination of the red "***Reset***" light , lower left of console] _____

Name: _____ Signature: _____ Date: _____

Example HDR ^{192}Ir Treatment QC Form (upper)

Patient Name: _____ Treatment Date: _____
Medical Record #: _____ Fraction #: _____
Radiation Oncologist: _____ RTT name: _____

****

Pre-Treatment Time Out

	initials	generally performed by
1. Daily check performed on Nucletron microSelectron HDR unit.	_____	RTT
2. Confirm the presence of Emergency Source Storage Safe (Pb bailout pig).	_____	RTT
3. Connect catheters to treatment device and LOCK WHEELS to V2 unit.	_____	RTT
4. Informed Consent signed & dated, confirm Patient ID using 2 approved methods.	_____	RTT
5. Verification of radionuclide, treatment site & side, and total fraction dose.	_____	RTT
6. Written Directive completed and signed by physician Authorized User.	_____	RTT
7. Treatment plan and isodose plan signed by physician Authorized User.	_____	RTT
8. Confirm that calculations were checked by an Authorized Medical Physicist.	_____	RTT
9. Physician Authorized User and Physicist sign & date the Pre-Treatment Record.	_____	RTT
10. Perform radiation survey of patient body surface near proposed treatment site. _____mR/h	_____	MP
11. Agreement of catheter-to-indexer routing sequence with the treatment plan.	_____	MP
12. Time Out Completed	_____	RTT
13. Confirm Authorized Physician and Physicist are within audible range of normal speech.	_____	RTT

****

Example HDR ^{192}Ir Treatment QC Form (lower)

****

During Treatment

14. Confirm radiation area monitor function (flash red) during treatment. _____RTT

****

After Treatment

15. Physician Authorized User and Physicist sign & date the Treatment Record. _____RTT

16. Using the Ludlum, model 14C serial # 99941, survey the following locations (a through e):
    a) Background reading outside the treatment room _____mR/h
    b) Treatment unit external surface, at the trefoil (radioactive material) symbol _____mR/h
    c) Connector and applicator apparatus _____mR/h
    d) Full length of the catheter guide tube _____mR/h
    e) Patient body surface near the treatment site prior to removal from the room _____mR/h

    Radiation surveys performed by authorized Medical Physicist. _____ MP

17. Compare pre- and post-treatment surveys to assess possibility of contamination.
    Does comparison of readings (items 10 & 16e) indicate contamination? (YES or NO) _____ MP
    If YES, ask RTT to contact Health Physics and start Emergency Procedures

18. Record patient radiation survey information in the HDR Patient Survey Logbook. _____ MP

19. Were there any unintended deviations from the Written Directive ? (YES or NO) _____ MP
    If YES, explain in detail (greater than 10% deviation is a recordable event):

20. QMP Reviewer Name _____ Signature/Date _____ MP

21. File this form in the patient's RadOnc paper chart and complete the billing. _____ MP

Example HDR ^{192}Ir Patient Survey Form

microSelectron V2 HDR ^{192}Ir model no. 105-088-03 serial no. 31743

Date	Patient Name	Site / Applicator	Survey meter model 12C s# 99941 enter √ or other info	Bkgnd (mR/h)	Patient Pre-Tx (mR/h)	Bkgnd (mR/h)	Patient Post-Tx (mR/h)	Physicist initials

Example HDR ^{192}Ir Source Exchange Form (a)

1			date: ##########				medical physicist(s): Mark Rivard					
2	rentional (not MR/CT) GYN connectors and ACD device L=1286mm											
3	5	9	13	17	21	25	29	33	37	41	45	10 mm stepsize
4	1.0	1.0	1.0	1.0	1.0	1.0	1.0	1.0	1.0	1.0	1.0	
5	1.0	1.0	1.0	1.0	1.0	1.0	1.0	1.0	1.0	1.0	1.0	
6	1.0	1.0	1.0	1.0	1.0	1.0	1.0	1.0	1.0	1.0	1.0	
7	GOOD	NA	Update daily check program, treatment plans for ongoing patients, and 2 decay tables with new length L.									
8	omogeneity on film GOOD or BAD?					GOOD						
9	hanical integrity of all applicators, connectors, and guide tubes based on visual inspection											
10	Notes:	start	stop									
11	110.7%	27:24.8	29:26.9									
12	time	122.17	GOOD	Nucletron TCS time		121.6	seconds (> 100 s)					
13	22.5	'C	press.	1000	mbar	1.015	C_{TP}	20 s				
14	2	0.2	20	2	0.2	t_{OFFSET}	-0.407	GOOD				
15	0.10673	0.05232	1.00037	0.10752	0.04725	R^2	0.99999	GOOD				
16	8:43 AM	reproducibility		0.1%	0.3%	GOOD	GOOD					
17	21	20	19	18	17	16	15	14				
18	1450.0	1452.5	1455.0	1457.5	1460.0	1462.5	1465.0	1467.5				
19	77.95	78.19	78.36	78.47	78.52	78.49	78.41	78.27				
20	timum reading	78.52	[nA]		HDR-1000 + C_{WELL} (cal'd 8/19/2010)		0.5047	mGy m^2 h^{-1} nA^{-1}				
21	decay factor	1.0034	F_{HEMC}		6517A electrometer#2 C_{EL} (cal'd 7/9/2010)		1.000	A/Rdg	200 nA scale			
22					...S$_k$ = ...Rdg x ...F x C$_{...}$ x C$_{...}$ x C$_{...}$		40.4	mGy m^2 h^{-1}				
23					measured air kerma strength		4.0358	cGy m^2 h^{-1}				
24			Manu. cal date	January 17, 2012			43.84	mGy m^2 h^{-1}				
25	F_{MANU}	done?				Cal ratio	1.010	GOOD				
26		YES	update source strength ($_{HEMC}S_K$) in microSelectron treatment console (Maintenance, Source Calibration)									
27		YES	make 2 new decay tables and post at the planning workstation and in HDR console logbook									
28		YES	update source strength (NEMCS$_K$) in the PLATO v.14.3 planning system (passwd=platobps)									
29		YES	end-to-end test using VagCyl.xls file with new S$_K$ and Tx time									
30												
31												
32	R Cs-137 insert, HDR-1000+, +300.0V, Filter(100)											
33		speed: HIACCURACY										
34												
35				-0.2136	20 nA	(same C_{EL} for all nA settings)						
36												
37	H.L. (days)		leakage	+0.00025	nA							
38												
39	...S$_k$ = Rdg x C$_{...}$ x C$_{...}$ x C$_{...}$			118.31	mGy m^2 h^{-1}							
40												
41	days	decay	calc'd	ratio	C_{WELL}							
42	0	1.000	118.31	100.0%	-5.457E+11							
43	95	0.994	119.01	100.5%	-5.457E+11							
44	169	0.989	119.57	100.6%	-5.457E+11							
45	186	0.988	119.70	100.7%	-5.457E+11							
46	1901	0.887	133.34	99.7%	-5.484E+11							
47	2072	0.878	134.78	99.2%	-5.484E+11							
48	2349	0.863	137.15	100.2%	-5.484E+11							

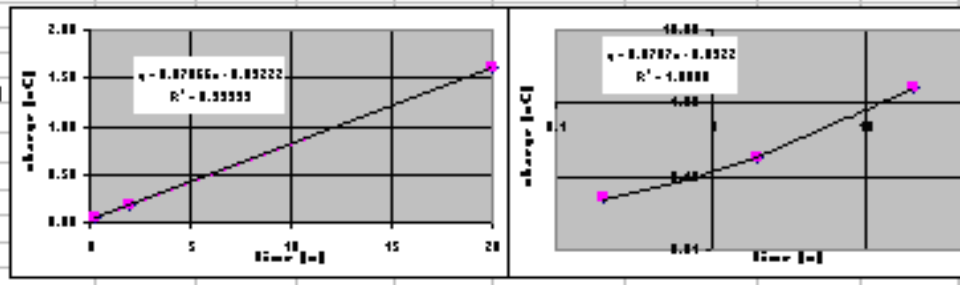

	t_{OFFSET}	R^2	
February-07	-0.452	0.99999	
May-07	-0.430	0.99999	
August-07	-0.438	0.99998	
########	-0.442	0.99998	
February-08	-0.440	0.99999	
May-08	-0.445	0.99998	
########	-0.451	0.99998	
March-09	-0.438	0.99999	
May-09	-0.449	0.99999	
August-09	-0.421	1.00000	
########	-0.408	1.00000	
	-0.438	0.99999	AVG
	0.013	0.00001	STDEV
-0.424	-0.408	0.99998	MIN
-0.451	-0.452	1.00000	MAX
	0.0403223	0.00002	3 SIGMA
	-0.031		

output / safety / daily / DECAY

Example HDR ^{192}Ir Source Exchange Form (a1)

	A	B	C	D	E	F	G	H	I	J	K	L	M	N	O	P
1	**HDR Quarterly QA**				date:	**1/27/12 8:43 AM**		medical physicist(s):	Mark Rivard							
2	**LOCALIZATION**	with 3 conventional (not MR/CT) GYN connectors and ACD device L=1286mm														
3	Position	1	5	9	13	17	21	25	29	33	37	41	45	10 mm stepsize		
4	CATH1 Shift [X mm]	1.0	1.0	1.0	1.0	1.0	1.0	1.0	1.0	1.0	1.0	1.0	1.0			
5	CATH2 Shift [X mm]	1.0	1.0	1.0	1.0	1.0	1.0	1.0	1.0	1.0	1.0	1.0	1.0			
6	CATH3 Shift [X mm]	1.0	1.0	1.0	1.0	1.0	1.0	1.0	1.0	1.0	1.0	1.0	1.0			
7	$Shift_{AVG}$ [X.X mm]	1.0	GOOD	NA	Update daily check program, treatment plans for ongoing patients, and 2 decay tables with new length											
8	**AUTORADIOGRAPH**	Is source homogeneity on film **GOOD** or **BAD**?	**GOOD**													
9		Check mechanical integrity of all applicators, connectors, and guide tubes based on visual inspection													**OK**	
12						**start**	**stop**									
13						**27:24.8**	**29:26.9**									
14	**TIMER ACCURACY**	Measured time				**122.17**	GOOD	**Nucletron TCS time**					**121.6**	**seconds (> 100 s)**		
15	**TIMER LINEARITY**	temp	22.5	'C			press.	1000	mbar				1.015	C_{TP}	20 s	
16	t_{DWELL} [s]	20	2	0.2	20	2	0.2						t_{OFFSET}	-0.407	GOOD	
17	Reading [uC]	1.60416	0.18673	0.05232	1.60697	0.18752	0.04725						R^2	0.99999	GOOD	
18				ratios to first reading		99.8%		99.6%		110.7%						
20	**SOURCE STRENGTH**	time	8:43 AM		**reproducibility**		0.1%		0.3%	GOOD	GOOD					
21	position	22	21	20	19	18		17		16	15	14				
22	Length [mm]	1447.5	1450.0	1452.5	1455.0	1457.5		1460.0		1462.5	1465.0	1467.5				
23	Reading [nA]	77.54	77.95	78.19	78.36	78.47		78.52		78.49	78.41	78.27				
24			maximum reading	78.52	[nA]			HDR-1000 + C_{WELL} (cal'd 8/19/2010)					0.5047	$mGy\ m^2\ h^{-1}\ nA^{-1}$		
25			decay factor	1.0034	F_{NEMC}			6517A electrometer#2 C_{EL} (cal'd 7/9/2010)					1.000	A/Rdg	200 nA scale	
26						$_{NEMC}S_K$ = $_{MAX}$Rdg x $_{NEMC}F$ x C_{TP} x C_{WELL} x C_{EL}							40.4	$mGy\ m^2\ h^{-1}$		
27	**S_K COMPARISON**							measured air kerma strength					4.0358	$cGy\ m^2\ h^{-1}$		
28	Source ID	D36E-0374		Manu. cal date	January 17, 2012								43.84	$mGy\ m^2\ h^{-1}$		
29	decay factor	0.912	F_{MANU}	done?							Cal ratio		1.010	GOOD		
30				YES	update source strength ($_{NEMC}S_K$) in microSelectron treatment console (Maintenance, Source Calibration)											
31				YES	make 2 new decay tables and post at the planning workstation and in HDR console logbook											
32				YES	update source strength ($NEMCS_K$) in the PLATO v.14.3 planning system (passwd=platobps)											
33				YES	end-to-end test using VagCyl.xls file with new S_K and Tx time											

Example HDR ^{192}Ir Source Exchange Form (a2)

32	**Cs-137 constancy check, LDR Cs-137 insert, HDR-1000+, +300.0V, Filter(100)**						
33	align dots, eyelet/color face up		speed: HIACCURACY				
34	s# 3M 25 01554						
35	LDR Cs-137					-0.2136	20 nA setting
36	$\mu Gy.m^2/h/A$						
37	-5.457E+11	11,018	H.L. (days)		leakage	**+0.00025**	nA
38	C_{WELL} cal'd 8/24/2010						
39	$_{NEMC}S_K$ = Rdg x C_{TP} x C_{WELL} x C_{EL}					118.31	mGy m^2 h^{-1}
40							
41		S_K	days	decay	calc'd	ratio	C_{WELL}
42	1/27/2012	118.31	0	1.000	118.31	100.0%	-5.457E+11
43	10/24/2011	118.38	95	0.994	119.01	100.5%	-5.457E+11
44	8/11/2011	118.90	169	0.989	119.57	100.6%	-5.457E+11
45	7/25/2011	118.88	186	0.988	119.70	100.7%	-5.457E+11
46	11/13/2006	133.80	1901	0.887	133.34	99.7%	-5.484E+11
47	5/26/2006	135.90	2072	0.878	134.78	99.2%	-5.484E+11
48	8/22/2005	136.90	2349	0.863	137.15	100.2%	-5.484E+11
49						100.1%	avg
50						0.6%	stdev
51							

output / safety / daily / DECAY /

Example HDR ^{192}Ir Source Exchange Form (b)

		SAFETY CHECKS	YES or NO	
1				
2	1	HDR RAL ^{192}Ir alarms activate following AC power failure simulation (error code 104)?	YES	
3	2	Door Primalert functions with AC power off using extended HDR ^{192}Ir source?	YES	covers Daily #14
4	3	Interrupt button on the console functions with display of elapsed treatment time?	YES	covers Daily #15
5	4	Emergency STOP (on console) functions with display of elapsed treatment time?	YES	covers Daily #17
6	5	Door interlock functions with display of elapsed treatment time?	YES	covers Daily #16
7	6	Survey meter battery check and constancy check OK?	YES	covers Daily #4
8	7	Was survey meter calibrated within 365 days ? (If not, notify Health Physics)	YES	
9	8	Are Emergency Procedures in the HDR Manual?	YES	
10	9	Is error 13 detected when indexer ring is not latched?	YES	
11	10	Is error 14 detected when interstitial interconnect tube is not inserted?	YES	covers Daily #12
12	11	Is error 33 detected when interstitial interconnect tube is installed without catheter present?	YES	
13	12	Review of daily checks since last physics QA?	YES	
14				
15		Additional Notes (if needed):		
16				
17				
18		date:	1/27/2012	
19		inits:	MJR	
20				
21				
22				
23				
24				
25				

output | **safety** | daily | DECAY

Example HDR ^{192}Ir Source Exchange Form (c)

		DAILY CHECKS	YES or NO	
1				
2	1	Are the TV monitors at the control console operational?	YES	
3	2	Is the intercom (audio) operational?	YES	
4	3	Does the radiation area monitor function?	YES	
5	4	Does the radiation survey meter (s# 99941) function?	YES	do prior page, 6
6	5	Is the emergency basket stocked and the emergency storage container in place?	YES	
7	6	Are the source guide tubes free of kinks, etc?	YES	
8	7	Did control console pass self-diagnostic tests when key switch is first turned?	YES	
9	8	Is the emergency STOP button in the treatment room operational?	YES	
10	9	Is the emergency STOP button on the HDR unit operational?	YES	
11	10	Is the Tx console date (exact) and time (within 5 minutes) correct?	YES	
12	11	Is the source strength on the printout within 0.020 cGy m^2/h of the posted activity?	YES	
13	12	Confirm program and dwell times, press START to initiate treatment, and verify that Error Code 14 appears on the screen and that the source is not extended out of the	YES	do prior page, 10
14	13	For L=1498 and 5 mm step size, does the distal end of the dummy source goto 1435 mm, and the active source end to 1330 mm (dwell 35) and 1430 mm (dwell 15) within 1 mm?	YES	
15	14	Is the "HDR IN USE" door light on?	YES	do prior page, 2
16	15	Does the interrupt button on the console function properly?	YES	do prior page, 3
17	16	Is the door interlock operational?	YES	do prior page, 5
18	17	Is the emergency STOP button on the treatment console operational?	YES	do prior page, 4
19				
20		date:	1/27/2012	
21		inits:	MJR	
22				
23				
24				
25				

output | safety | **daily** | DECAY

Example HDR ^{192}Ir Source Exchange Form (d)

1		HDR ^{192}Ir source D36E-0374				
2	73.83 day HL	Strength (cGy m^2/h)			Strength (cGy m^2/h)	
3	date	MIDNIGHT	NOON	date	MIDNIGHT	NOON
4	1/27/2012	4.036	4.017	3/17/2012	2.524	2.512
5	1/28/2012	3.998	3.979	3/18/2012	2.500	2.489
6	1/29/2012	3.961	3.942	3/19/2012	2.477	2.465
7	1/30/2012	3.924	3.905	3/20/2012	2.454	2.442
8	1/31/2012	3.887	3.869	3/21/2012	2.431	2.419
9	**2/1/2012**	3.851	3.833	3/22/2012	2.408	2.397
10	2/2/2012	3.815	3.797	3/23/2012	2.386	2.374
11	2/3/2012	3.779	3.761	3/24/2012	2.363	2.352
12	2/4/2012	3.744	3.726	3/25/2012	2.341	2.330
13	2/5/2012	3.709	3.691	3/26/2012	2.319	2.308
14	2/6/2012	3.674	3.657	3/27/2012	2.298	2.287
15	2/7/2012	3.640	3.623	3/28/2012	2.276	2.266
16	2/8/2012	3.606	3.589	3/29/2012	2.255	2.244
17	2/9/2012	3.572	3.555	3/30/2012	2.234	2.223
18	2/10/2012	3.539	3.522	3/31/2012	2.213	2.203
19	2/11/2012	3.506	3.489	**4/1/2012**	2.192	2.182
20	2/12/2012	3.473	3.457	4/2/2012	2.172	2.162
21	2/13/2012	3.440	3.424	4/3/2012	2.152	2.141
22	2/14/2012	3.408	3.392	4/4/2012	2.131	2.121
23	2/15/2012	3.376	3.361	4/5/2012	2.112	2.102
24	2/16/2012	3.345	3.329	4/6/2012	2.092	2.082
25	2/17/2012	3.314	3.298	4/7/2012	2.072	2.063

output | safety | daily | **DECAY**

Example Manufacturer Calibration Form: HDR ^{192}Ir

Certificate For Sealed Sources

Issue Date: 2012-01-16 (1)

Product Code: REF 105002
Serial Number: SN D36E-0374
Production Code: LOT HDR011312

Serial no. Transport Container: 2392C6
Serial no. Check Cable: N/A
Certificate Number: FUwNz U0J0r v3V6G ad2vp 60

Source Specification

Reference Air Kerma Rate: 43.84 mGy h^{-1} +/- 5% at 1m (2)
Measurement Reference Date: 2012-01-17 18:00 CET (1)
Apparent Activity: 398 GBq (10.8 Ci) at measurement reference date. (3,4)

Source Type: MICROSELECTRON-HDR
Capsule dimensions: 0.9 mm diameter, 4.5 mm length
Source pellet dimensions: 0.6 mm diameter, 3.5 mm length
Source pellet form: Solid Iridium
Radionuclide: Ir-192
Encapsulation: single
Capsule material: stainless steel, AISI 316L
ISO Classification: ISO/99/C63211
Special form certificate number: D/0070/S-96

Quality Control

Laser Weld Visual Check: Passed
Source Capsule Integrity (15 N pull test): Passed
Leakage Test: Passed (5)
Surface Contamination test: < 185 Bq (5 nCi) (6)

The undersigned, authorized officer of QSA Global, Inc. certifies that this source complies with the requirements of ISO2919 and that all of the information given in this certificate is true and correct.

Quality Assurance

(1) Date Format yyyy-mm-dd.
(2) Confidence level of 99.7%.
(3) The apparent activity is determined by applying a conversion factor (0.110 mGy $m^2 h^{-1} GBq^{-1}$) to the measured gamma radiation output of the sealed source determined with a calibrated instrument. The instrument is traceable to the National Institute of Standards & Technology. (NIST)
(4) The apparent activity is the Iridium-192 activity; other radionuclides not detectable.
(5) Leakage test method according to ISO9978 method Liquid nitrogen bubble test (6.2.4).
(6) Surface contamination test according to ISO9978 method Wet wipe test (5.3.1).
(7) The quality assurance system of QSA Global Inc. is certified by Lloyd's Register Quality Assurance (LRQA) according to ISO 9001 and ISO 13485.

QSA GLOBAL

40 North Avenue Burlington, MA 01803 1(781) 272-2000

Example Manufacturer Calibration Form: HDR ^{192}Ir

Source Specification

Reference Air Kerma Rate:	43.84 mGy h^{-1} +/- 5% at 1m	(2)
Measurement Reference Date:	2012-01-17 18:00 CET	(1)
Apparent Activity:	398 GBq (10.8 Ci) at measurement reference date.	(3,4)

Quality Assurance

(1) Date Format yyyy-mm-dd.

(2) Confidence level of 99.7%. **$k = 3$**

(3) The apparent activity is determined by applying a conversion factor (0.110 mGy $m^2 h^{-1} GBq^{-1}$) to the measured gamma radiation output of the sealed source determined with a calibrated instrument. The instrument is traceable to the National Institute of Standards & Technology. (NIST)

ESTRO School

Take Home Message

- QMP is a complex, systems concept
- QMP contains many familiar items – coordination is key
- Many societal guidelines available for brachytherapy QMP elements
- QMP should be specific to equipment and department
  - no “template” QMP, only guidance
  - regular, independent departmental review is desirable
- Forms help formalize QMP goals and make tasks consistent
- e-forms provide robust documentation, but can be altered
- Balance tension of form constancy and form advancements
- TG-100 and international error databases may alter current QMP focus

Further Reading

Nath, et al. Med Phys 1997;24:1557-98.

Thomadsen, 1999. Achieving Quality in Brachytherapy

Thomadsen, Williamson, Rivard, and Meigooni. Med Phys 2008;35:4708-23.

Thomadsen, et al. Prac Radiat Oncol 2014;4:65-70.

Venselaar and Perez-Calatayud, 2004. ESTRO Booklet 8.

ESTRO School

Acknowledgements

Bruce Thomadsen, University of Wisconsin, USA

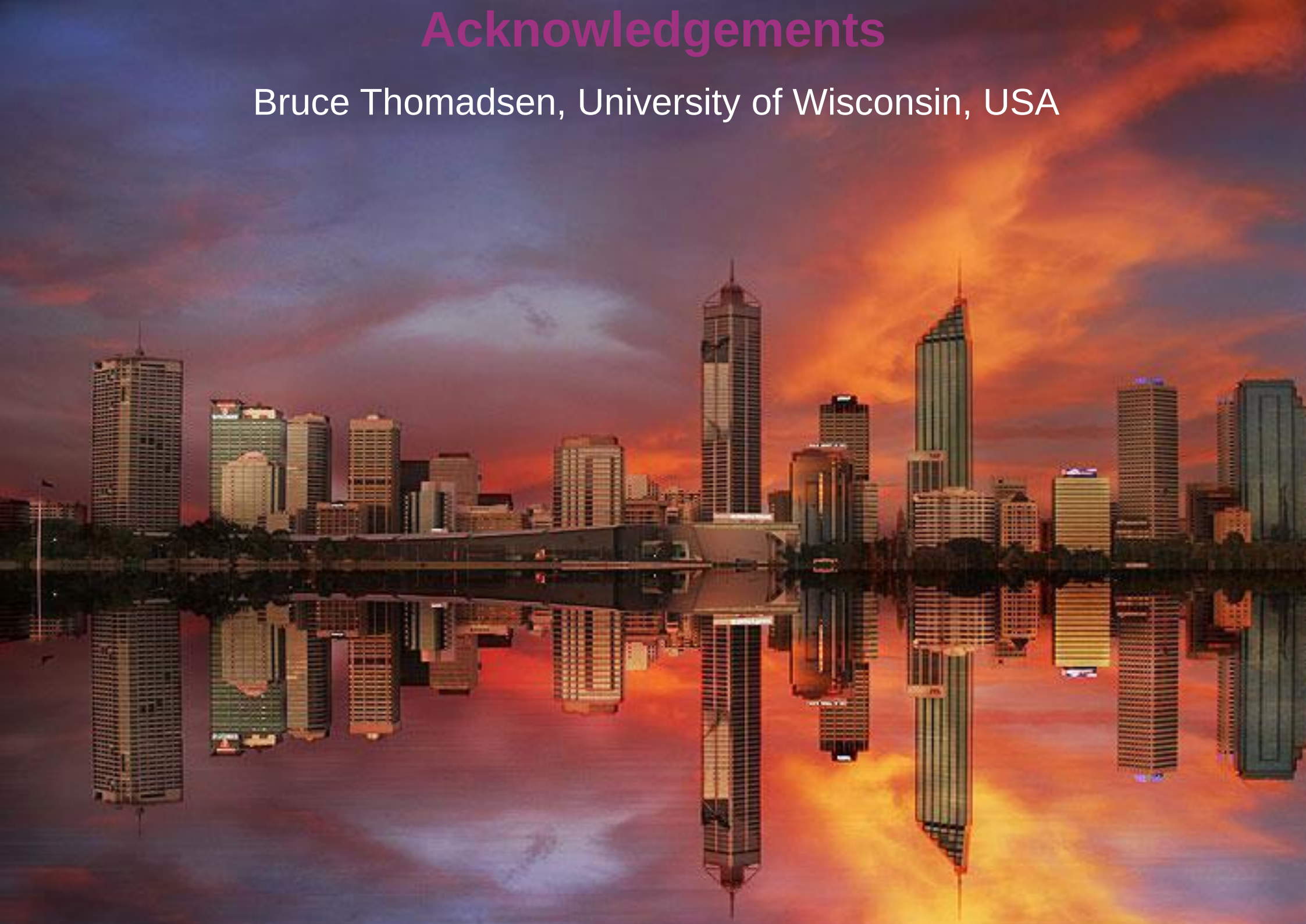

ESTRO School

WWW.ESTRO.ORG/SCHOOL

Future Perspectives I:
Tracking Technologies in Brachytherapy

Prof. Luc Beaulieu, Ph.D., FAAPM, FCOMP

1- Département de physique, de génie physique et d'optique, et Centre de recherche sur le cancer, Université Laval, Canada

2- Département de radio-oncologie et Centre de recherche du CHU de Québec, CHU de Québec, Canada

Valencia, Spain – Oct 7-10 2018

Disclosures

- I am actively involved in the development of tracking systems for brachytherapy

- I hold research contracts and grants with:
  - Canada's NSERC Industrial Research Chair
  - Elekta
  - Philips

Learning Objectives

- Tracking technologies for brachytherapy
  - What are they?
  - How they work?
- Provide examples of use
- Discuss other potential applications

Acknowledgements

Quebec's Team
Samir Boutaleb
William Foster
Louis Jay
Marie-Claude Lavallée
Fanny Monéger
Éric Poulin
Emmanuel Racine
Daline Tho
Éric Vigneault

UCSF
Adam Cunha
I-Chow J Hsu
Jean Pouliot

Erlangen
Christoph Bert
and his team: K. Kallis, V. Strnad, M. Lotter, S. Kreppner, M. Kellermeier, T. Götz, J. Herbolzheimer, D. Elz, B. Hofmann

Elekta
F. de Vries, Y. Niatsetski, J. de Becker, A. Klount, E. Neijhus, B. van Veelen

B&W – Havard
Robert Cormack

Utrecht
M.A. Morland
M. Borot de Battisti

Philips
Dirk Binnekamp
Antonio Bonilas
Roelof Feikema
Jack Geraats
Gilion Hauvast
Luc Koch
Jacek Kustra
Dave Senden

CRSNG NSERC

ELEKTA

PHILIPS

Medical Physics RESEARCH TRAINING NETWORK

ESTRO School

Tracking ➔ Real-time Guidance

ESTRO School

Real-time Guidance ➔ Augmented Reality

Daniel Burrus, LinkedIn 2013

ESTRO School

Tracking in RT

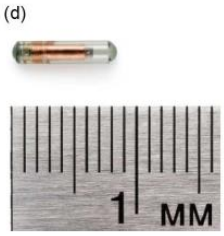

ESTRO School

Tracking in Brachytherapy?

- Position of needle, catheter or applicator in real-time
  - Angulation/rotation
  - On the fly decision -> replanning
- Automated, fast and accurate channel reconstruction
  - Wrong connection between transfer tube and afterloader
- Potentially tracking organ motion/deformation
- Enabling new brachytherapy and interventional procedures

ESTRO School

Potential Technologies

- Image-based tracking: CT, MR or US

Accuracy of Catheter Reconstruction?

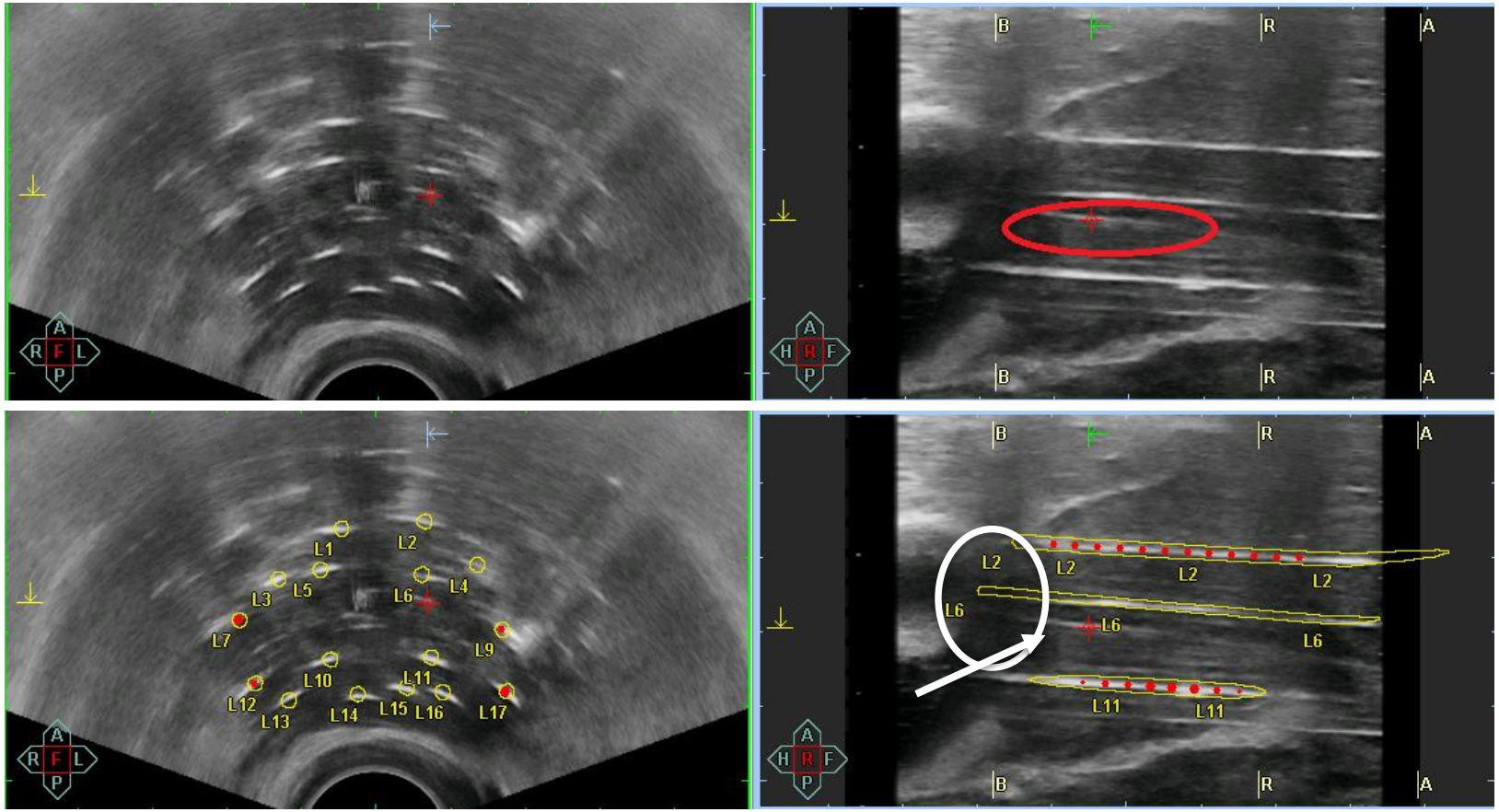

See e.g. F.-A. Siebert et al, Med Phys 36 (2009) 3406-3412.

ESTRO School

Potential Technologies

- Image-based tracking: CT, MR or US

- Real-time tracking
  - Optical IR tracking
  - Camera-based (Xbox style!)
  - Passive EM tracking
  - Active EM tracking
  - Optical Fiber Shape Sensing (Bragg Grating)

- …

IR/Optical Tracking

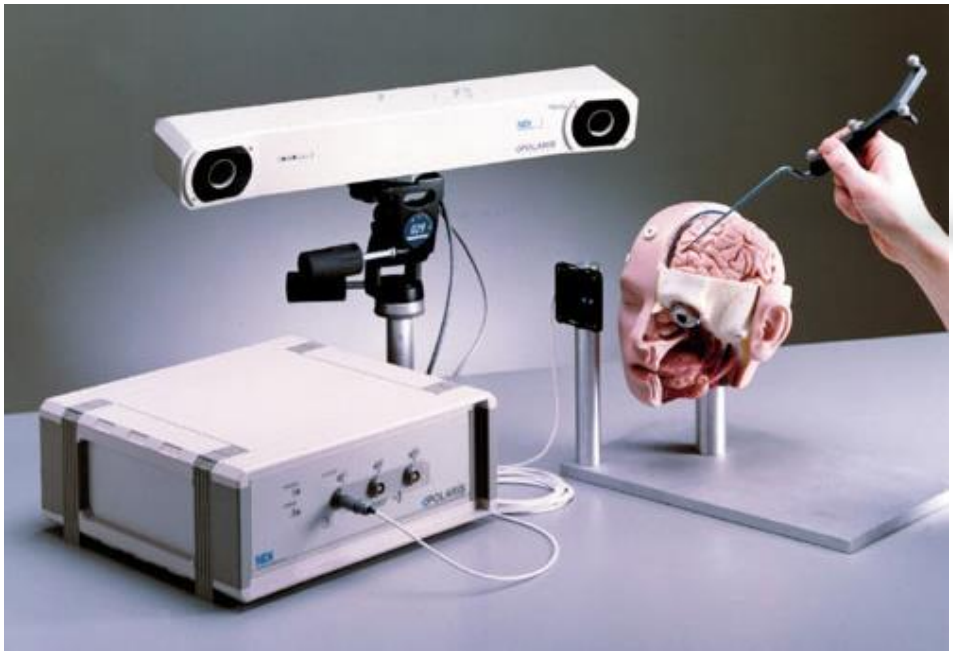

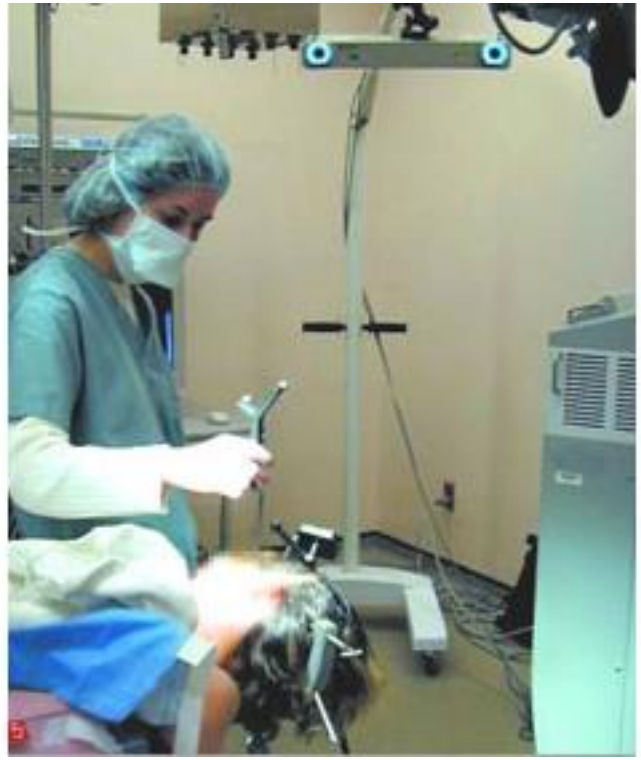

Limited to line of sight

- Same for white light camera

Overview of the technologies

Potential Technologies

- Real-time tracking – no line of sight needed
  - Passive EM tracking (CT and US compatible)
  - Active EM tracking (MR compatible)
  - Optical Fiber Bragg Grating (CT, US and MR-compatible)
    - **https://www.nasa.gov/feature/fiber-optic-sensing**

Electromagnetic tracking system (EMTS)

- **Electromagnetic Tracking in Medicine—A Review of Technology, Validation, and Applications**. Franz et al., IEEE Transactions on Medical Imaging **33** (2014)
- **Electromagnetic tracking for catheter reconstruction in ultrasound-guided high-dose-rate brachytherapy of the prostate**. Bharat S, Kung C, Dehghan E, Ravi A, Venugopal N, Bonillas A, Stanton D and Kruecker J. Brachytherapy 13 (2014) 640–50
- **EM-Navigated Catheter Placement for Gynecologic Brachytherapy: An Accuracy Study**. Mehrtash A, Damato A, Pernelle G, Barber L, Farhat N, Viswanathan A, Cormack R and Kapur T. Proc Soc Photo Opt Instrum Eng (2014) 9036 90361F
- **A system to use electromagnetic tracking for the quality assurance of brachytherapy catheter digitization**. Damato A L, Viswanathan A N, Don S M, Hansen J L and Cormack R A. Med. Phys. 41 (2014) 101702
- **Fast, automatic, and accurate catheter reconstruction in HDR brachytherapy using an electromagnetic 3D tracking system**. Poulin E, Racine E, Binnekamp D and Beaulieu L. Med. Phys. **42** (2015) 1227–32
- **Performance and suitability assessment of a real-time 3D electromagnetic needle tracking system for interstitial brachytherapy**. Boutaleb S, Racine E, Filion O, Bonillas A, Hauvast G, Binnekamp D and Beaulieu L. J Contemp Brachytherapy 7 (2015) 280–9

...And many more since 2016

ESTRO School

Electromagnetic tracking system (EMTS)

Example: Aurora® V2 from Northen Digital Inc. (Ontario, Canada)

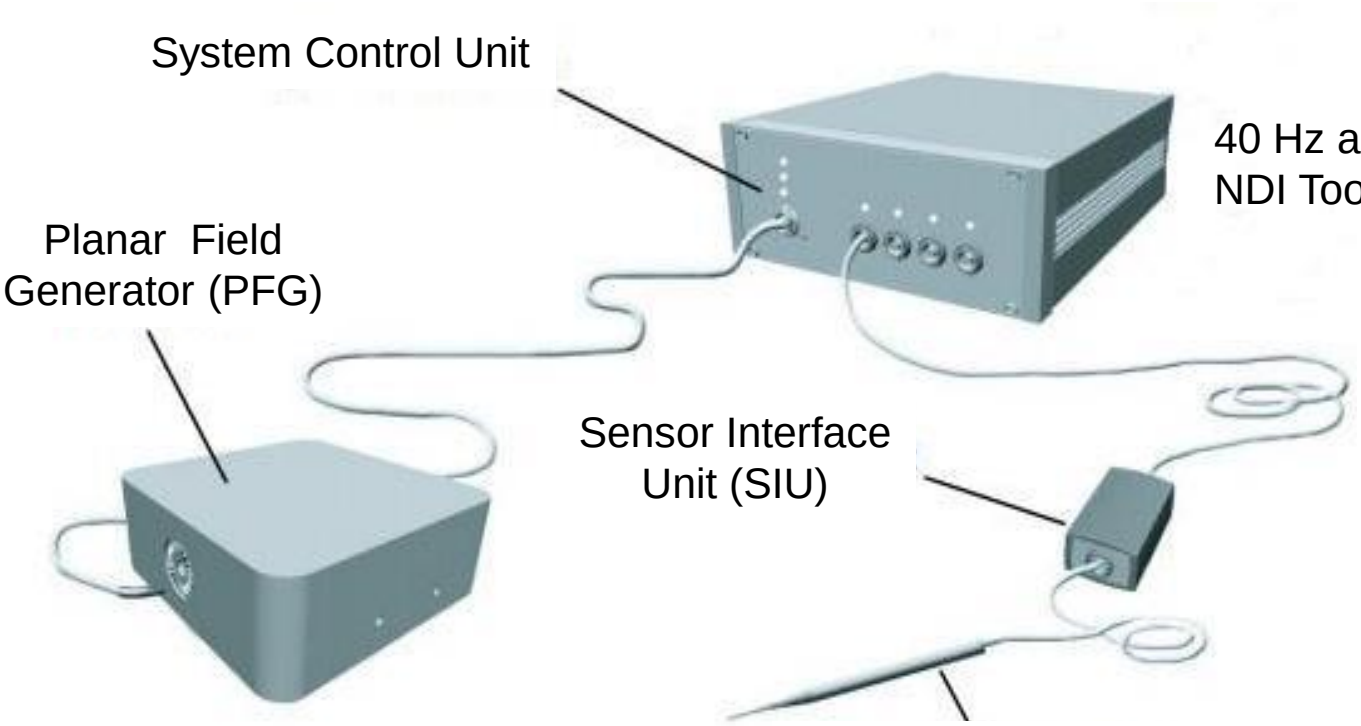

40 Hz acquisition:
NDI ToolBox v.4.002.006

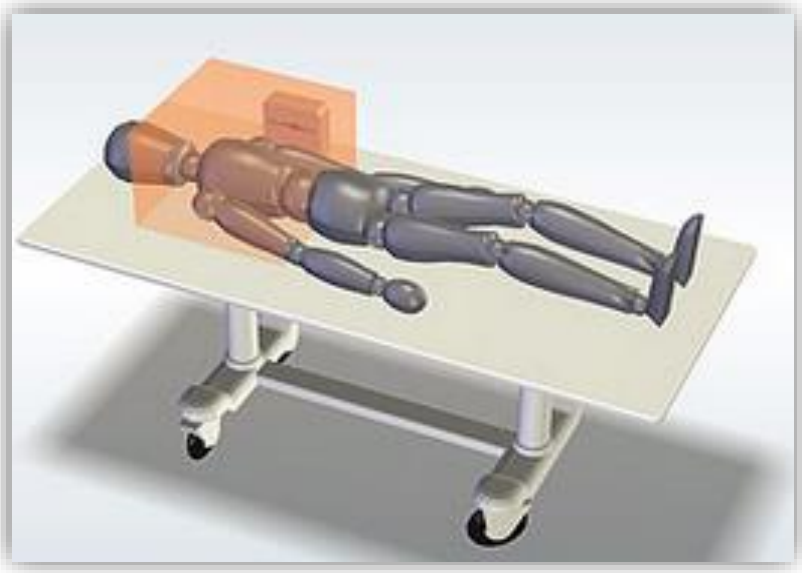

http://www.ndigital.com/msci/products/aurora/

ESTRO School

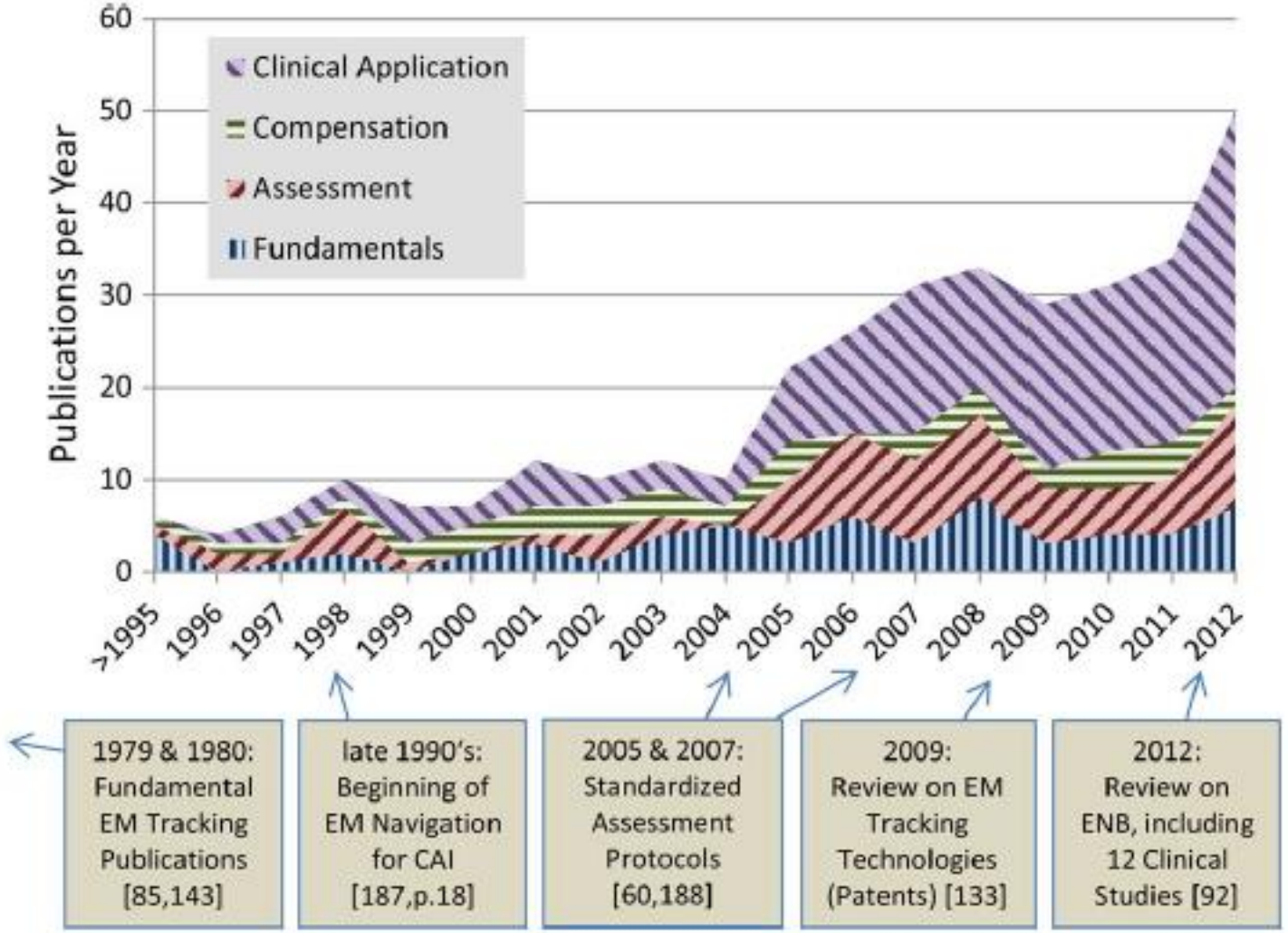

From Franz et al, 2014

ESTRO School

EMTS Technologies

TABLE I
TYPES OF FIELD GENERATORS

Type	Typical Properties	Examples
Standard	Range: ca. 1 m, Size: cube-shaped, ca. 10–30 cm	NDI Tetrahedon FG [34], NDI Planar FG [117, p.6], Ascension Mid Range [117], Polhemus Standard FG [34], Medtronic AxiEM FG [146]
Flat	Range: ca. 1 m, Size: flat, ca. 50×40 cm	NDI Tabletop FG [102], NDI Window FG [207], Ascension Flat FG [117, p.5], SuperDimension location board [145], Biosense Webster location pad [144]
Mobile	Range: ca. 0.2 m, Size: small, < ca. 10 cm	NDI Compact FG [39], NDI Handheld FG [142], Ascension Short Range FG [143], Polhemus Short Ranger [147], Smith&Nephew Donut FG [58], Cortrak Receiver Unit [81]
Long Range	Range: ca. 5 m, Size: ca. 50×50 cm	Polhemus Long Ranger [147]

From Franz et al, 2014

ESTRO School

Planar field generator - AC

- NDI Aurora system (théorie Seiler *et al*. PMB 2000)

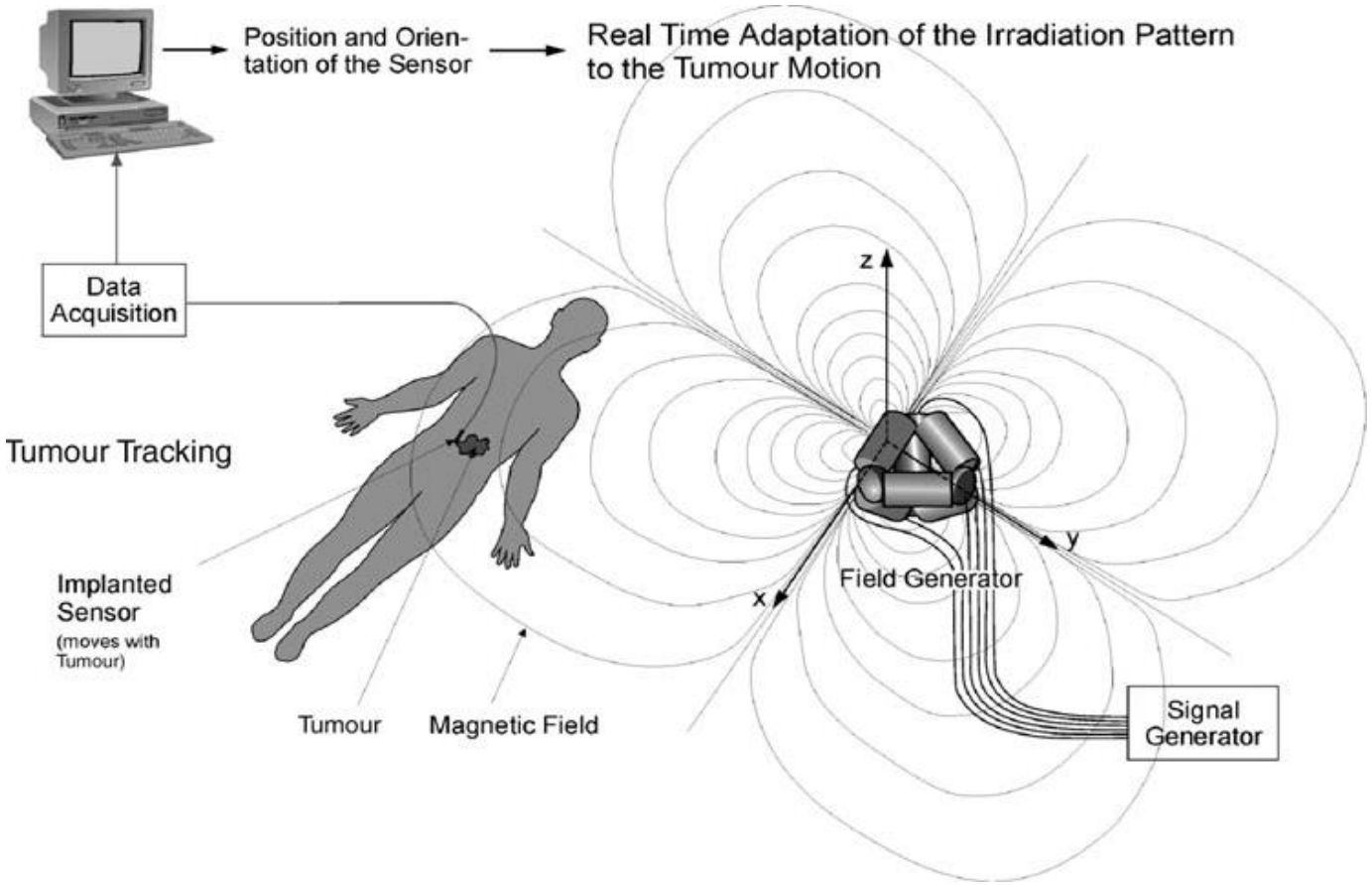

S-N-N-S ⟷ N-S-S-N
12kHz

Six differential coils

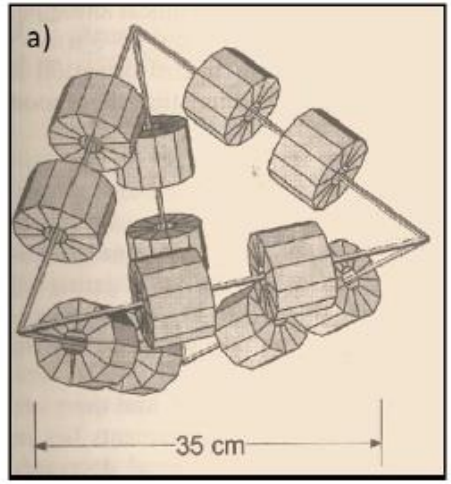

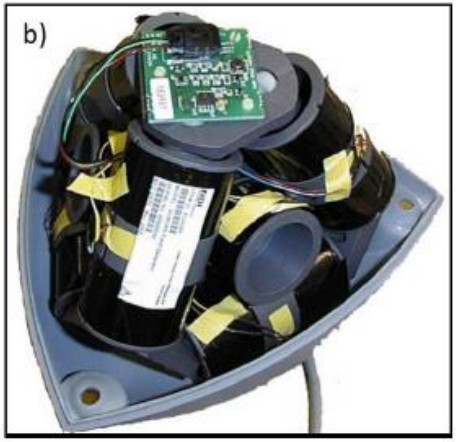

ESTRO School

Planar field generator - AC

- Sensor = induction coil
- Alternating current of ± 2 A at 12 kHz for 3.3 ms each differential coil will create 6 different voltages at the sensor
- If 5DOF needle: 6 measurements and 5 unknown
- If 6DOF: 2 sensor coils

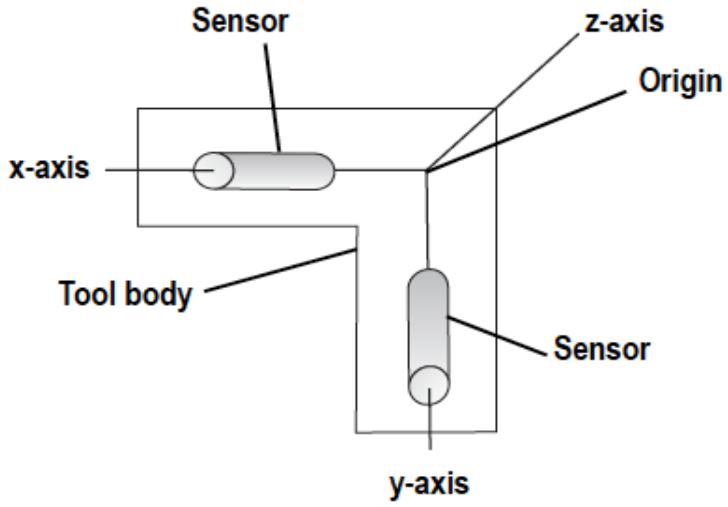

Figure 5-5 Sample 6DOF Tool

ESTRO School

TABLE III
ASSESSMENT STUDY RESULTS

(a) **Standardized assessment according to Hummel *et al.* [61]**: Shows the mean RMS error over 90 positions as precision (Prec.) and the mean error of 161 measured 5 cm distances between these points as positional accuracy (Acc.). The rotational accuracy (Rot.) is given as the mean error of thirty-one 11.5° measurements for two axes, because 5 DoF sensors were used for most assessments.

System FG	Environment	Ref.	Pos. [mm] Prec.	Acc.	Rot. [°]
NDI Aurora					
Planar FG	Laboratory	[59]	0.17	0.25	0.2/0.9
	Laboratory	[102]	0.20	0.80	1.2/1.0
	CT Suite	[102]	0.18	4.40	1.2/1.0
	X-Ray Suite	[15]	-	1.31	-
Tabletop FG	Laboratory	[102]	0.05	0.30	0.8/0.7
	CT Suite	[102]	0.05	0.90	0.8/0.7
Compact FG	Laboratory	[102]	0.05	0.50	1.0/0.8
	CT Suite	[102]	0.06	0.50	1.0/0.8
	US probes	[39]	<0.2	<2.5	<3
Ascension microBird					
Mid Range FG	Laboratory	[61]	0.14	0.69	0.04
Ascension 3D Guidance					
Mid Range FG	Laboratory	[117]	0.15	0.24	.05/.06
Flat FG	Laboratory	[117]	0.20	0.18	.02/.02

Detection Volume

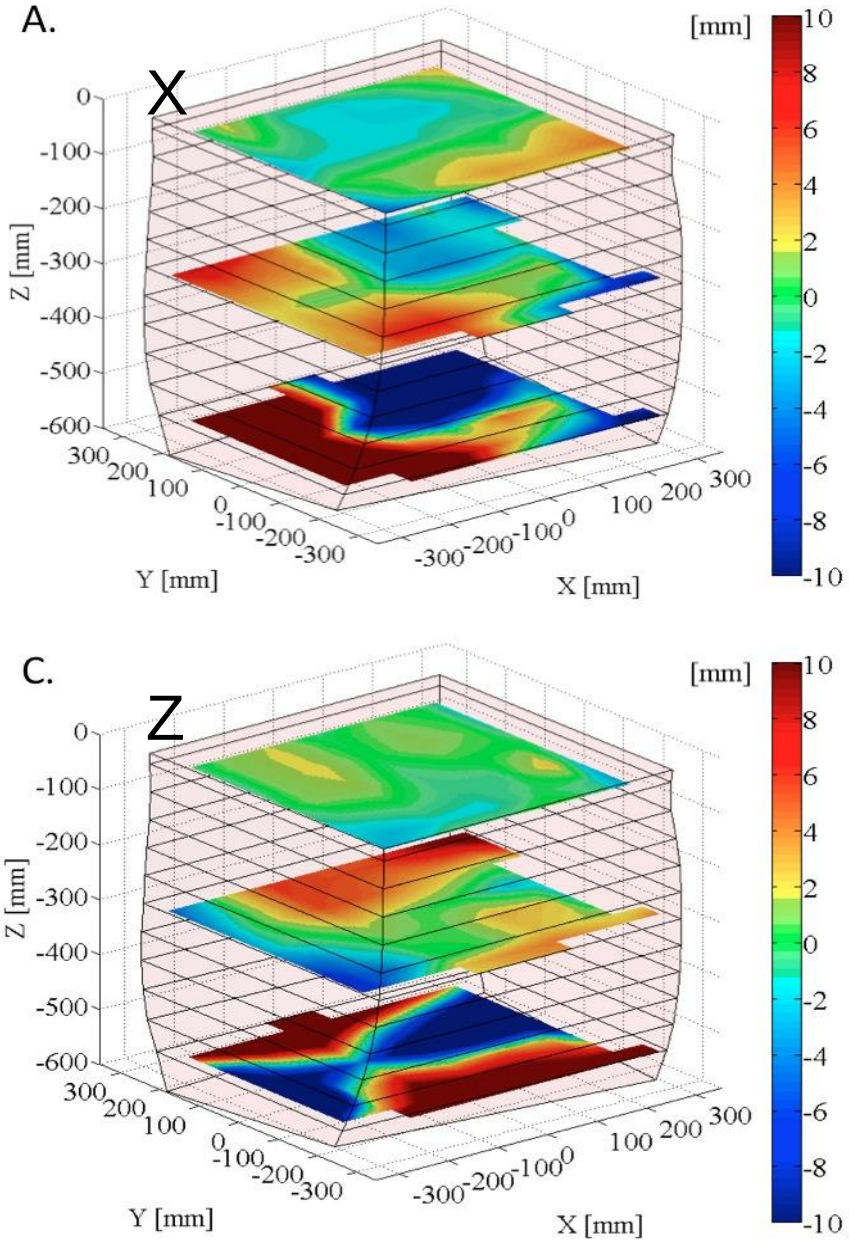

- Detection volume if not perfectly cubic
- Deviation from expected positions increase with distance (Z) and close to edges (X,Y plane)
  - ±1 mm in the first 30 cm
  - ±10 mm at 55 cm
  - Angle < 2% first 30 cm
    - +8 to -10% at 55 cm

Boutaleb et al. *J Contemp Brachytherapy* **7** 280–9

ESTRO School

Brachytherapy Clinical Settings

Electromagnetic tracking for catheter reconstruction in ultrasound-guided high-dose-rate brachytherapy of the prostate

Shyam Bharat[1,*], Cynthia Kung[1], Ehsan Dehghan[1], Ananth Ravi[2], Niranjan Venugopal[2], Antonio Bonillas[1], Doug Stanton[1], Jochen Kruecker[1]

[1]*Department of Ultrasound Imaging and Interventions, Philips Research North America, Briarcliff Manor, NY*
[2]*Department of Radiation Oncology, Sunnybrook Health Sciences Center, Toronto, ON, Canada*

Brachytherapy **13** 640–50

ESTRO School

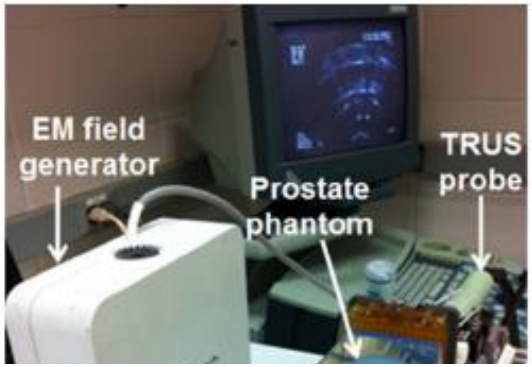

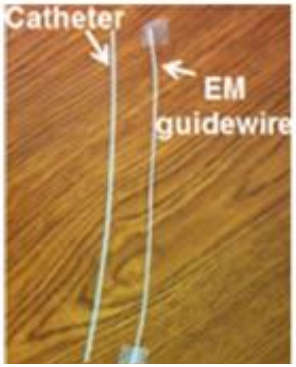

Table 6
Performance accuracy of EM catheter mapping system in the OR environment

	In-plane discrepancy (mm)			Out-of-plane discrepancy (mm)		
EM vs. TRUS (in OR)	Mean	Standard deviation	Maximum	Mean	Standard deviation	Maximum
Calibrating and testing in a "low distortion" environment	0.4	0.2	1	0.8	0.4	1.7
Calibrating in a "low distortion" environment and testing in distorting environment	1	0.2	1.5	1.1	0.8	1.9
Calibrating in a "low distortion" environment and testing in distorting environment, after updating the calibration in the distorting environment	0.3	0.2	1.1	1.1	0.8	1.9
Calibrating and testing in distorting environment	0.6	0.3	1.5	0.4	0.2	0.6

EM = electromagnetic; OR = operating room; TRUS = transrectal ultrasound.

In the OR, a "low distortion" environment refers to the absence of clinical equipment other than the treatment table and the ultrasound system near the testing area. A distorting environment refers to an environment that includes the presence of other clinically used brachytherapy equipment, such as leg stirrups, stepper holder, treatment planning computer, treatment afterloader, instrument table, and others, in their typical positions.

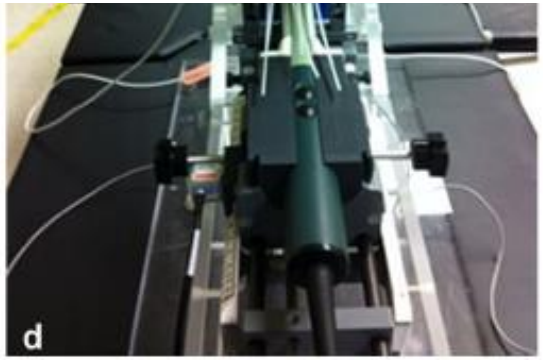

Interim Summary

- Needs to be used within the first 30 cm of the field generator
- Needle parallel to the field generator yield better angular accuracy
- Field generator generate heat: not under the patient
- Interference seen only for CRT monitor and bulky metalic arms (not shown)
  - Insensitive to US probe and needles/catheters

What can you do with this?

- Follow needles, catheters or an applicators in space (up to 6 DOF) in real-time (40 Hz)
  - Insertion guidance
  - Automatically reconstruct catheter/ applicator channels
    - Error detection
  - Workflow optimization
    - Direct link to real-time imaging
    - Direct link to a optimization engine (background replanning)
  - …

Auto. Catheter/Applicator Channel Reconstruction

Fast, automatic, and accurate catheter reconstruction in HDR brachytherapy using an electromagnetic 3D tracking system

Eric Poulin and Emmanuel Racine
Département de physique, de génie physique et d'optique et Centre de recherche sur le cancer de l'Université Laval, Université Laval, Québec, Québec G1V 0A6, Canada and Département de radio-oncologie et Axe Oncologie du Centre de recherche du CHU de Québec, CHU de Québec, 11 Côte du Palais, Québec, Québec G1R 2J6, Canada

Dirk Binnekamp
Integrated Clinical Solutions & Marketing, Philips Healthcare, Veenpluis 4-6, Best 5680 DA, The Netherlands

Luc Beaulieu[a)]
Département de physique, de génie physique et d'optique et Centre de recherche sur le cancer de l'Université Laval, Université Laval, Québec, Québec G1V 0A6, Canada and Département de radio-oncologie et Axe Oncologie du Centre de recherche du CHU de Québec, CHU de Québec, 11 Côte du Palais, Québec, Québec G1R 2J6, Canada

(Received 8 May 2014; revised 9 January 2015; accepted for publication 26 January 2015; published 18 February 2015)

Purpose: In high dose rate brachytherapy (HDR-B), current catheter reconstruction protocols are relatively slow and error prone. The purpose of this technical note is to evaluate the accuracy and the robustness of an electromagnetic (EM) tracking system for automated and real-time catheter reconstruction.
Methods: For this preclinical study, a total of ten catheters were inserted in gelatin phantoms with different trajectories. Catheters were reconstructed using a 18G biopsy needle, used as an EM stylet and equipped with a miniaturized sensor, and the second generation Aurora® Planar Field Generator from Northern Digital Inc. The Aurora EM system provides position and orientation value with precisions of 0.7 mm and 0.2°, respectively. Phantoms were also scanned using a μCT (GE Healthcare) and Philips Big Bore clinical computed tomography (CT) system with a spatial resolution of 89 μm and 2 mm, respectively. Reconstructions using the EM stylet were compared to μCT and CT. To assess the robustness of the EM reconstruction, five catheters were reconstructed twice and compared.
Results: Reconstruction time for one catheter was 10 s, leading to a total reconstruction time inferior to 3 min for a typical 17-catheter implant. When compared to the μCT, the mean EM tip identification error was 0.69 ± 0.29 mm while the CT error was 1.08 ± 0.67 mm. The mean 3D distance error was found to be 0.66 ± 0.33 mm and 1.08 ± 0.72 mm for the EM and CT, respectively. EM 3D catheter trajectories were found to be more accurate. A maximum difference of less than 0.6 mm was found between successive EM reconstructions.
Conclusions: The EM reconstruction was found to be more accurate and precise than the conventional methods used for catheter reconstruction in HDR-B. This approach can be applied to any type of catheters and applicators. © *2015 American Association of Physicists in Medicine.* [http://dx.doi.org/10.1118/1.4908011]

Medical Physics 2015;42(3):1227–32.

- EM reconstructions at 40 Hz
- µCT reconstruction (GE) at 89 µm (reference)
- CT reconstructions (Philips BigBore) at 2 mm
- Reconstructions using the EM stylet were compared to µCT and CT (3D distances used; tips as reference).

ESTRO School

Auto. Catheter reconstruction

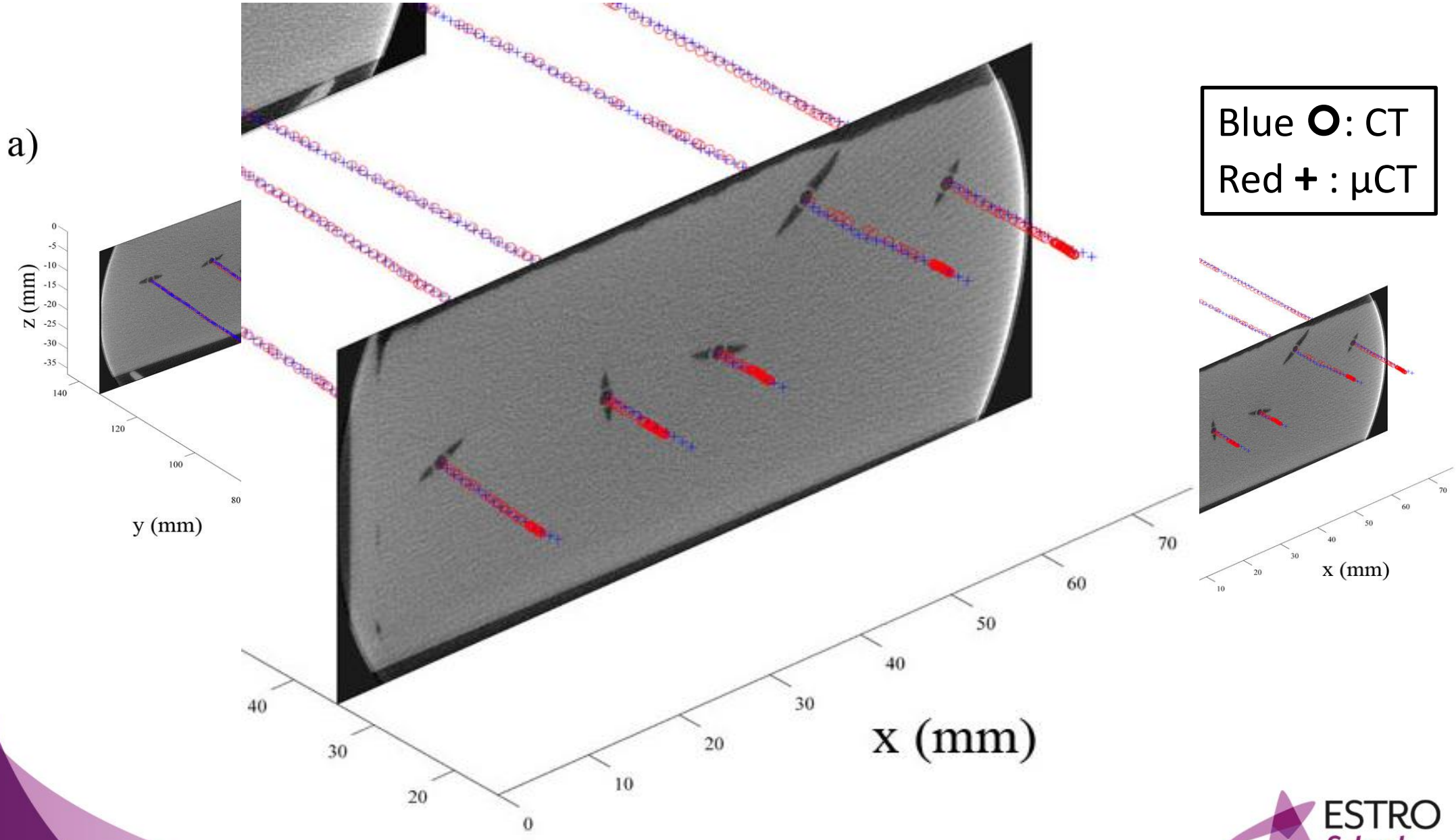

ESTRO School

Auto. Channel reconstruction

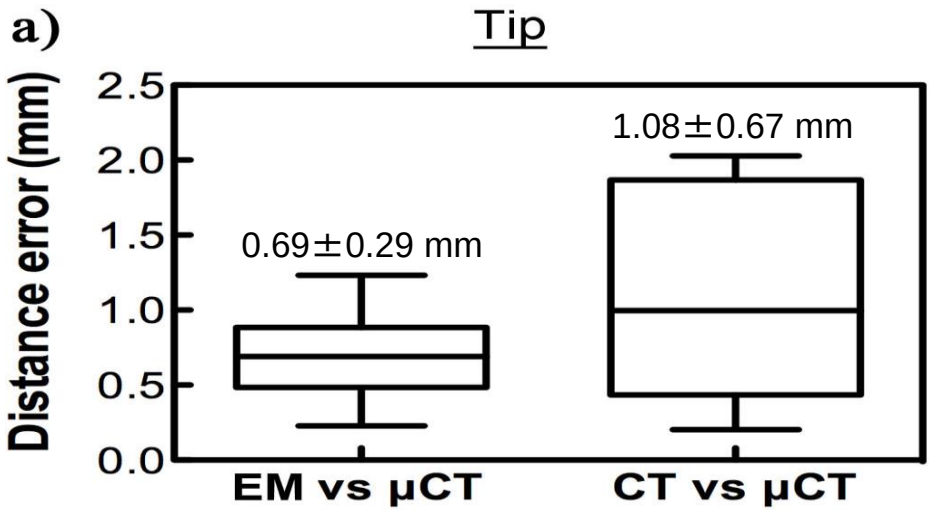

US vs EM
2.73±2.28 mm

Unpaired Student t-test show statistically significance difference

Poulin et al, Medical Physics 2015;42(3):1227–32.

* Comparison between EM vs US-only reconstruction, Brachytherapy **15** S194–5 (2016)

Seed drop position

A hollow brachytherapy electromagnetic needle prototype was recently developed by Philips Healthcare.

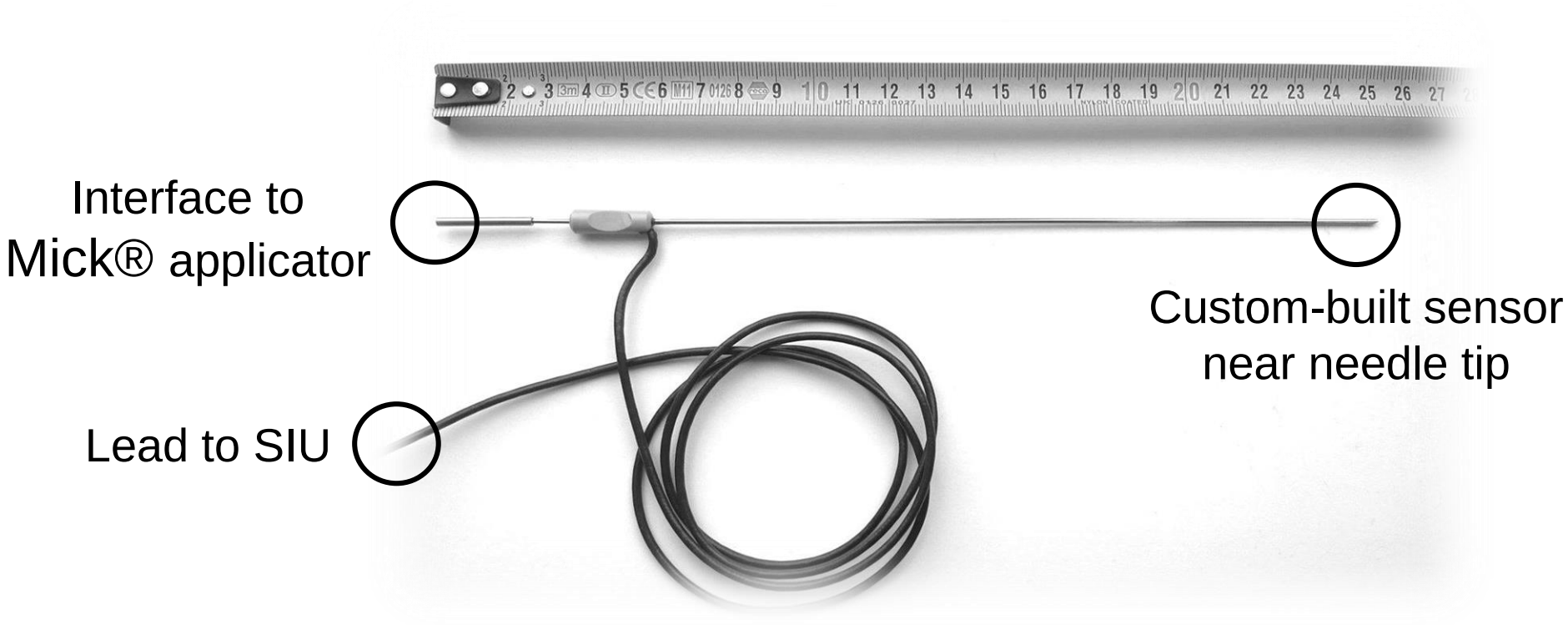

- ✓ Detects seed drops by exploiting local changes of electromagnetic properties in the medium.
- ✓ Preserves standard tacking capabilities.

Seed drop position

Registration of detected seed distributions. True seed positions were obtained from a μCT scan (GE, 89 μm slice thickness).

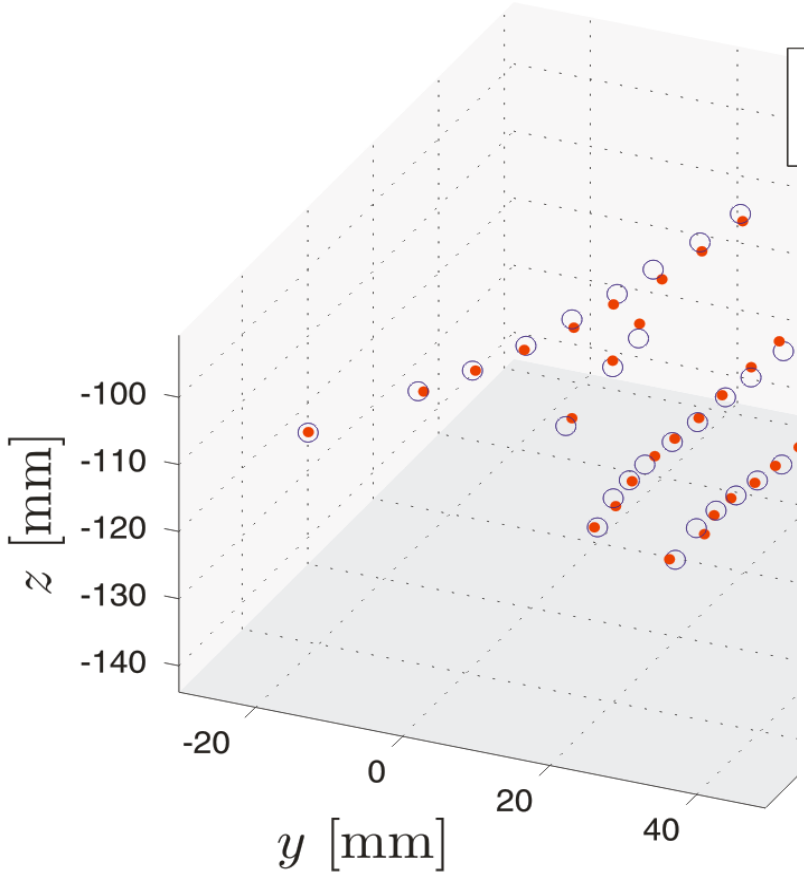

TABLE III. Statistics of the seed drop position estimates for the 3D characterization experiment.

	Error measurements [mm]			
	Minimum	Maximum	Average	Std dev.
$\lvert e_x \rvert$	$0.0^{+0.1}_{-0.0}$	$0.6^{+0.5}_{-0.1}$	$0.2^{+0.5}_{-0.2}$	$0.1^{+0.3}_{-0.1}$
$\lvert e_y \rvert$	$0.0^{+0.2}_{-0.0}$	$0.7^{+0.5}_{-0.2}$	$0.2^{+0.5}_{-0.2}$	$0.1^{+0.3}_{-0.1}$
$\lvert e_z \rvert$	$0.1^{+1.0}_{-0.1}$	$2.1^{+1.0}_{-1.1}$	$0.4^{+1.0}_{-0.4}$	$0.4^{+0.5}_{-0.2}$
e_{3D}	$0.1^{+1.0}_{-0.1}$	$2.1^{+1.1}_{-0.8}$	$0.6^{+1.2}_{-0.5}$	$0.4^{+0.7}_{-0.2}$

Racine et al, AAPM 2015; In preparation for Medical Physics

ESTRO School

Error Simulations – 15 catheters

Swap

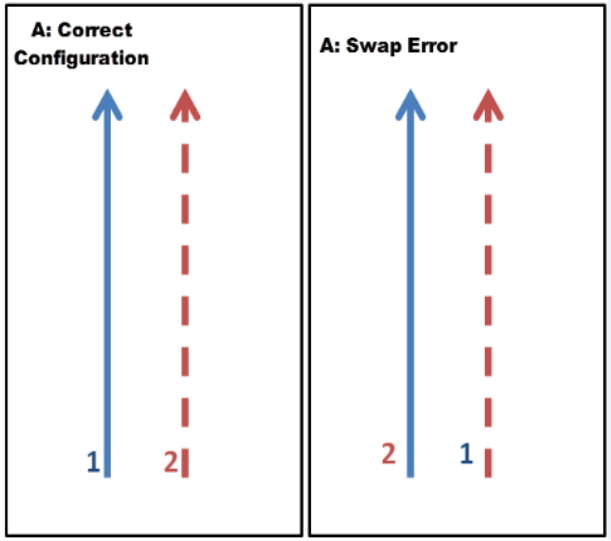

105 possible swap errors

Mix

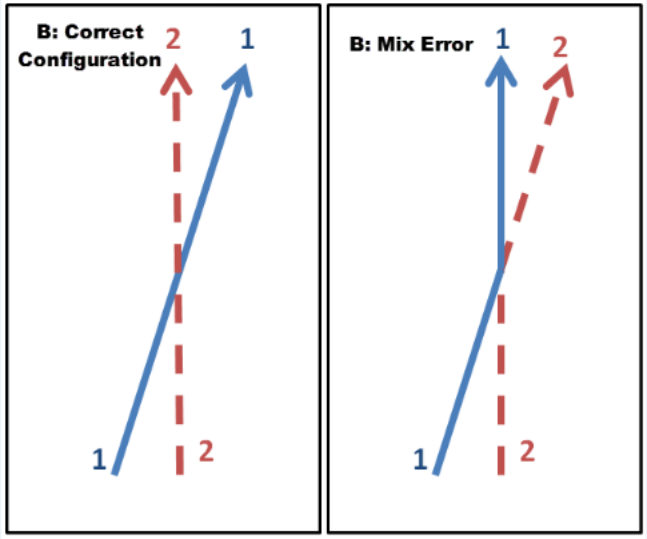

105 possible mix errors

Shift

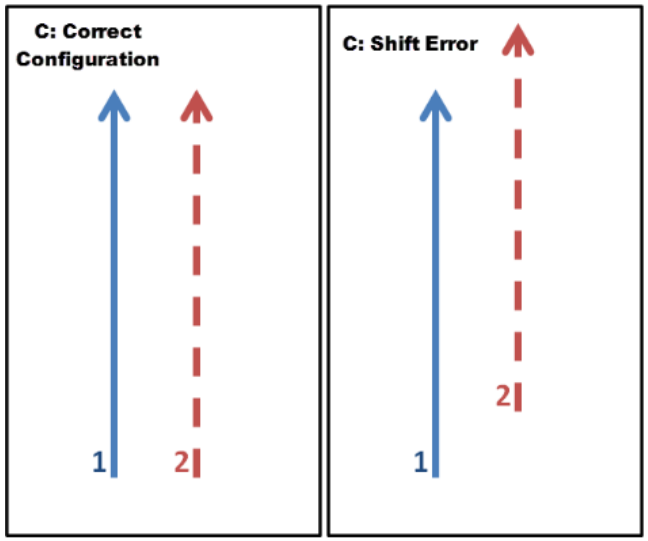

from 0 to 3 mm shifts
(in 0.1 mm increments)

↓

465 possible shift errors

Damato et al. *Med. Phys.* **41** 101702

ESTRO School

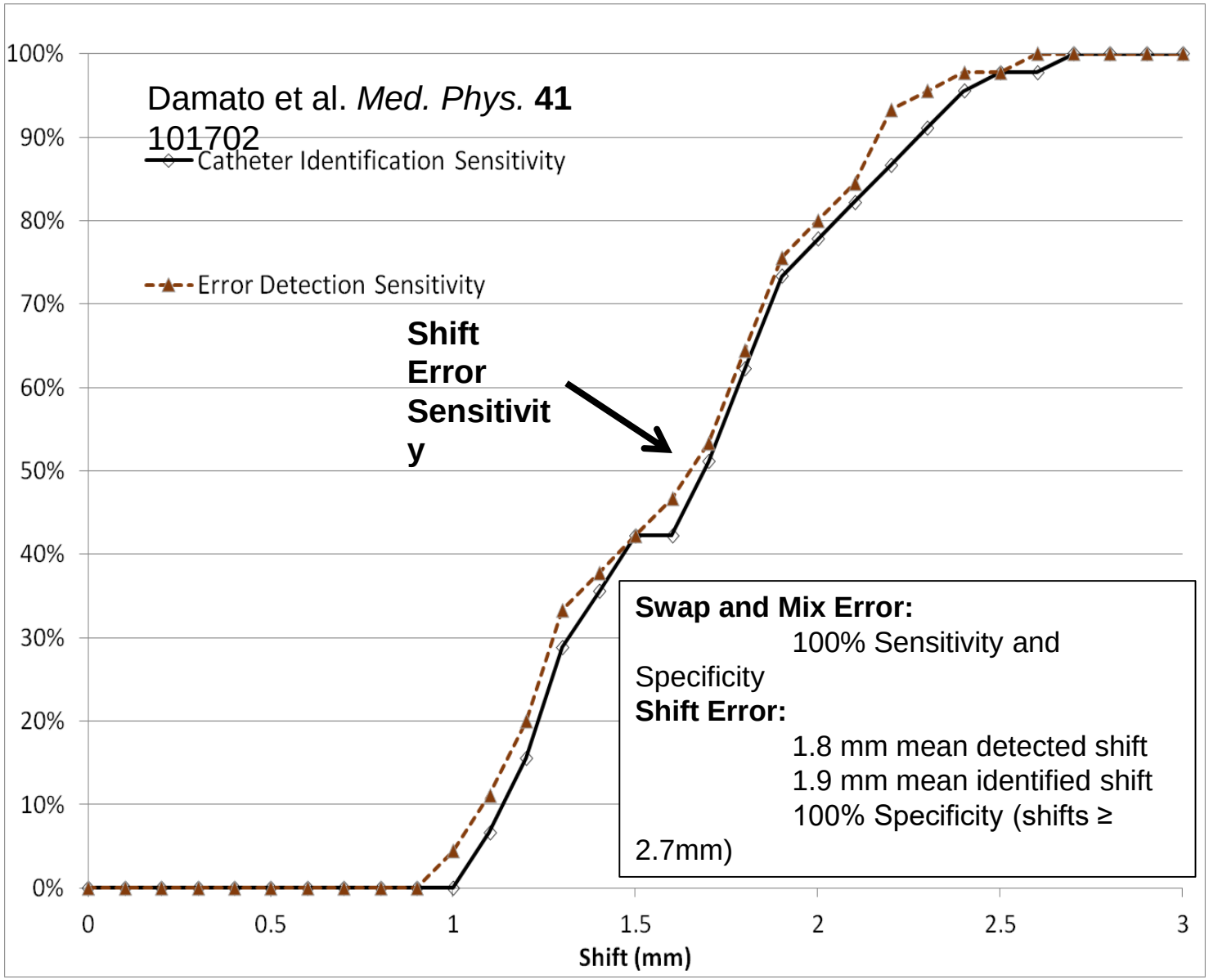
Damato et al. *Med. Phys.* **41** 101702
Catheter Identification Sensitivity
Error Detection Sensitivity
Shift Error Sensitivity
Swap and Mix Error:
100% Sensitivity and Specificity
Shift Error:
1.8 mm mean detected shift
1.9 mm mean identified shift
100% Specificity (shifts ≥ 2.7mm)
100%
90%
80%
70%
60%
50%
40%
30%
20%
10%
0%
0
0.5
1
1.5
2
2.5
3
Shift (mm)

Next slides various commercial as well as research/investigational devices

NeuroNavigation – AxiEM™

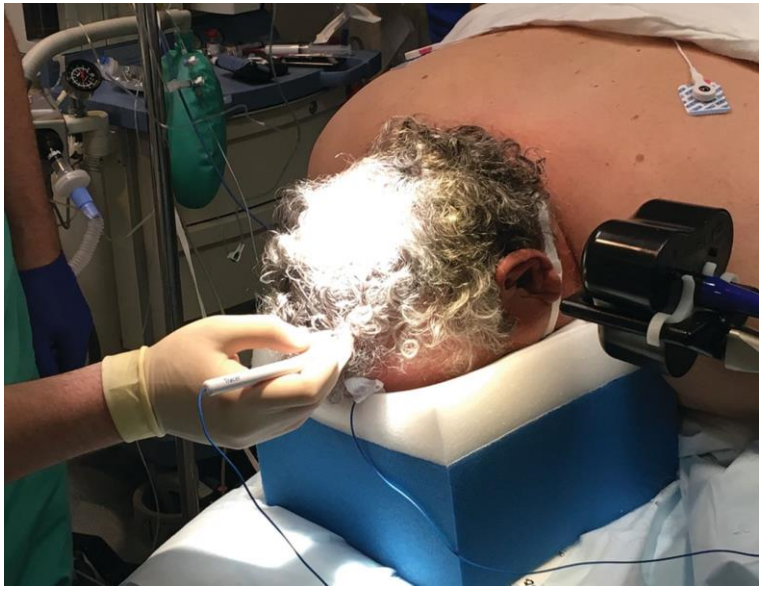

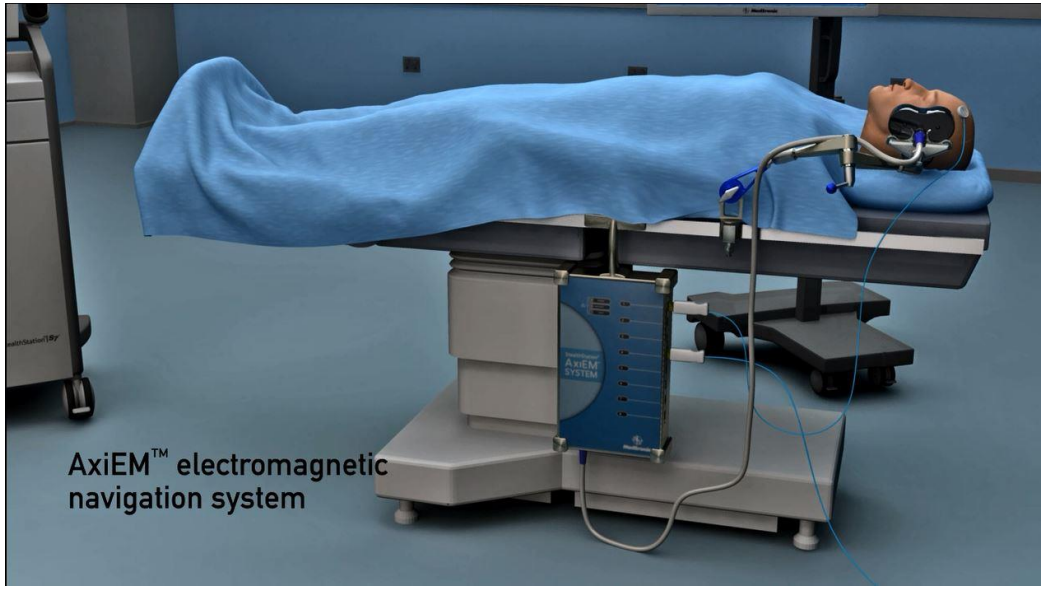

Medtronics.com

ESTRO School

Prostate Biopsy - UnoNav ™

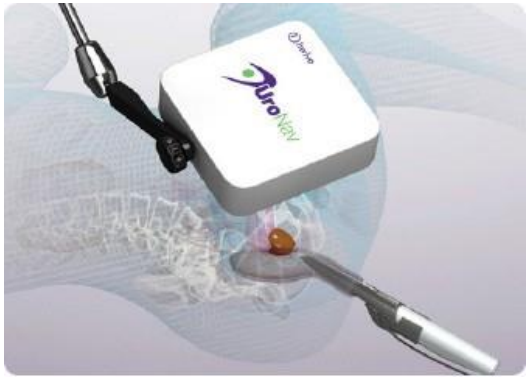

Philips InVivo

Lung procedures – Spin Drive ™

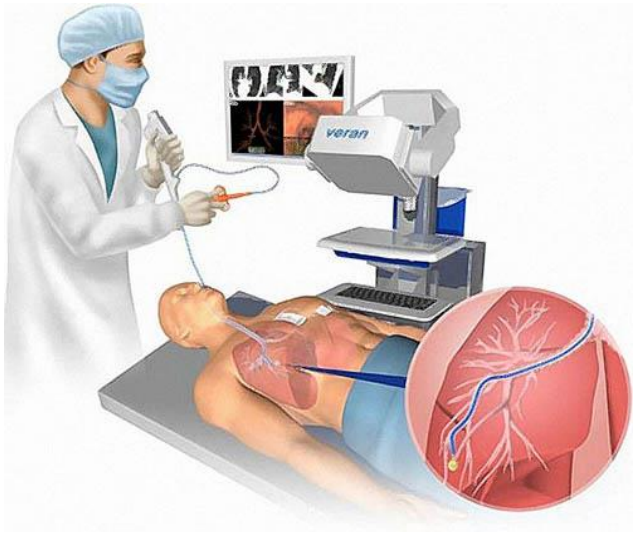

VeranMedical.com

ESTRO School

Real-time EM Tracking System: Prototype

Beaulieu *et al.* Brachytherapy **17** (2017) 103–10

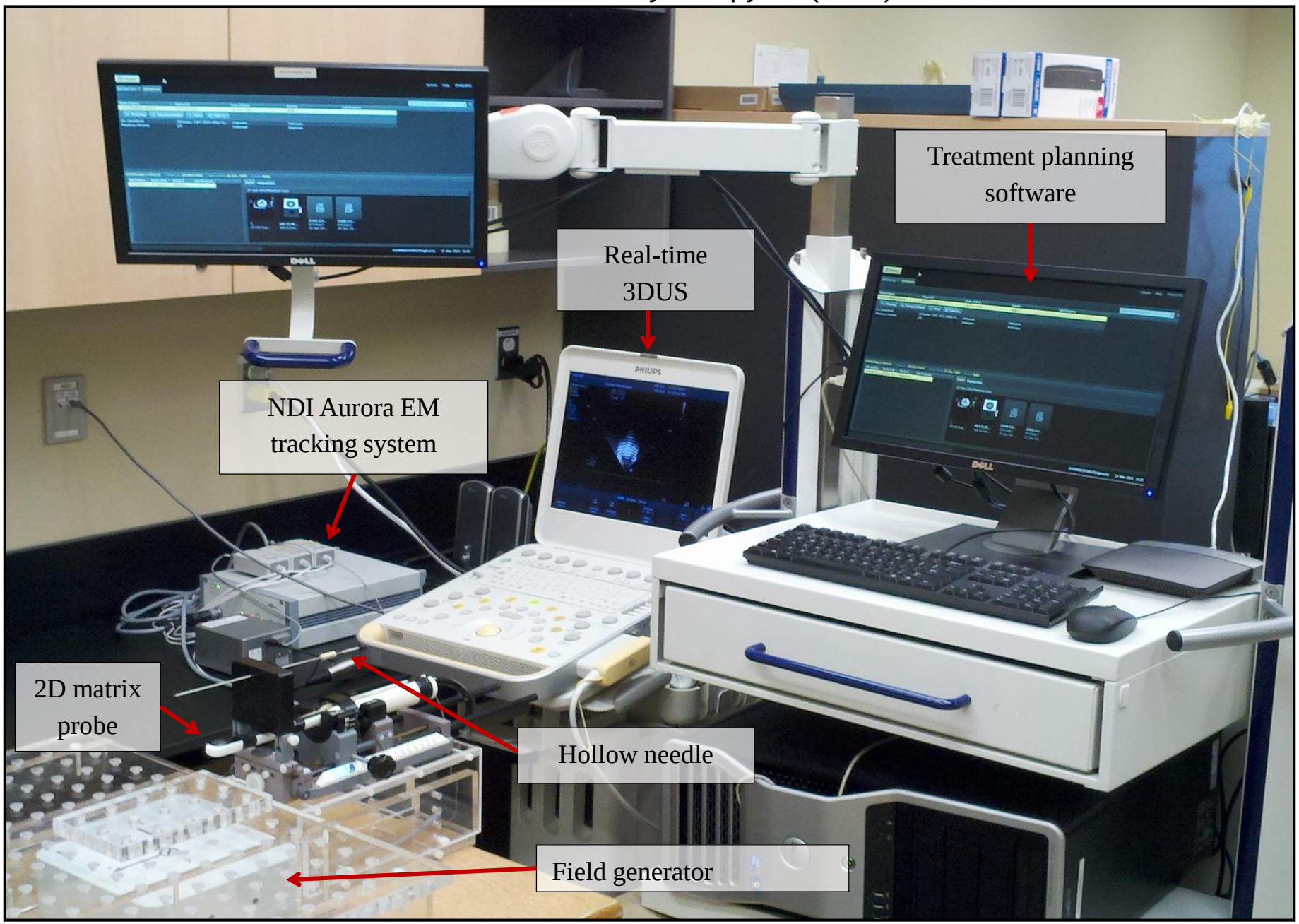

Dynamical Planning Workflow

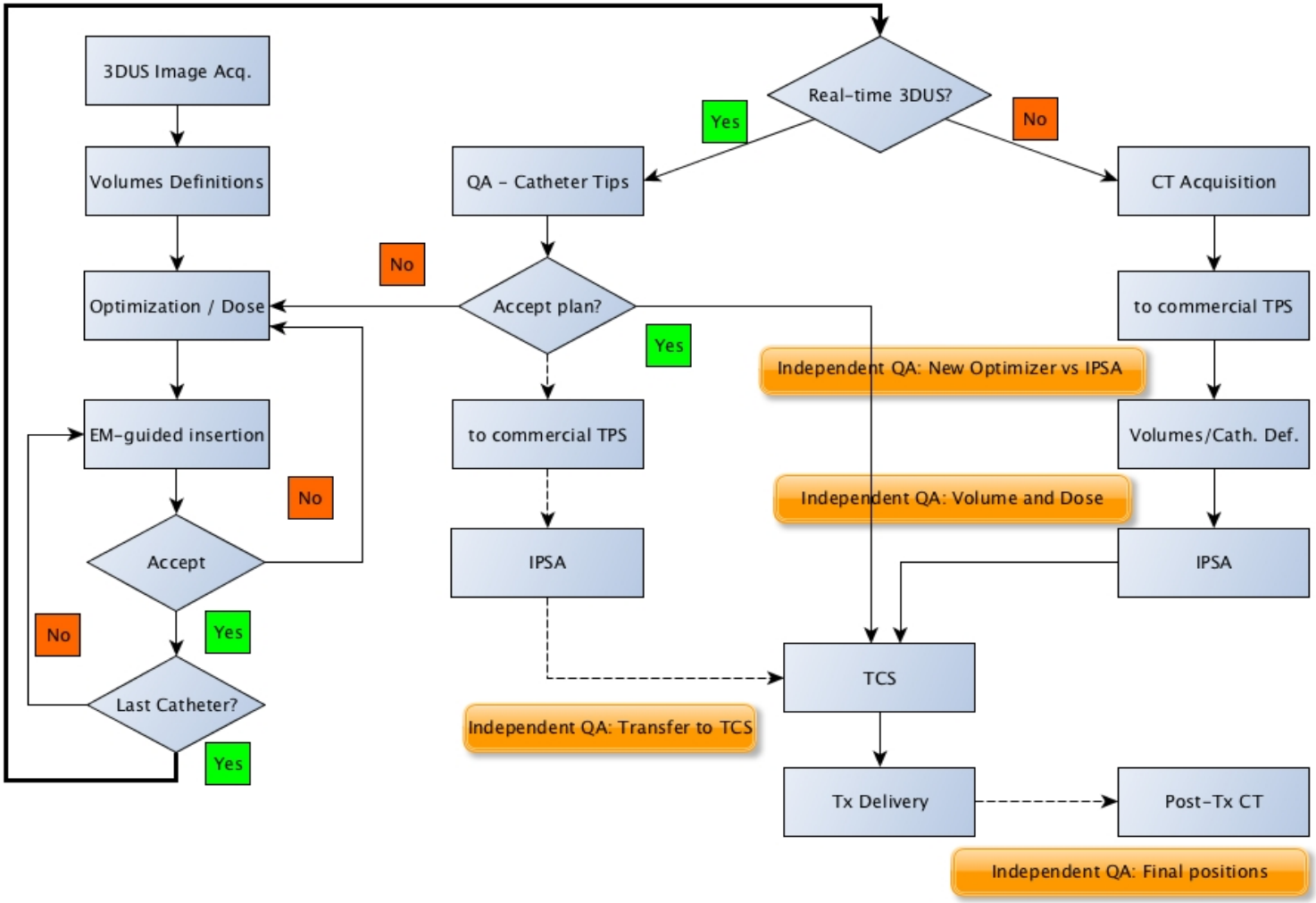

Beaulieu *et al.* Brachytherapy **17** (2017) 103–10

ESTRO School

Workflow Efficiency

Running time (min)
5-15
10-20
26-36
30-40

- Image acquisition: 1 sec
- *Contouring: 5-15 min*
- Planning: 7.6±2.5 sec ➔ more time reviewing/rerun!
- Insertion:
  - *27.6*±6.7 sec/catheter or needle on phantom
  - *≈ 60 sec/catheter or needle* expected for actual patient
- Catheter/Tip Reconstruction:
  - First one included with insertion time (free!)
  - Additional: 10.5±3.1 sec/catheter or needle

Complete procedure under 1 hour potentially feasible

ESTRO School

Beaulieu *et al.* Brachytherapy **17** (2017) 103–10

Real-time EMT Prostate HDR System: UroNav Therapy

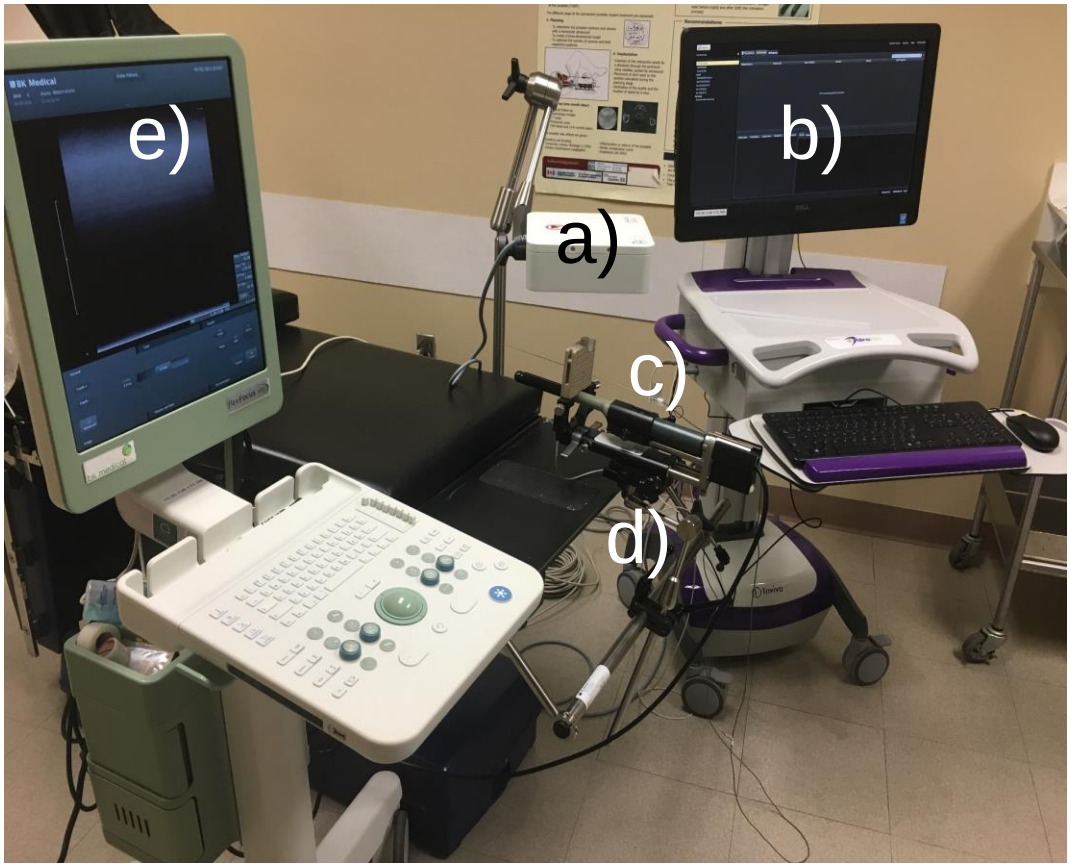

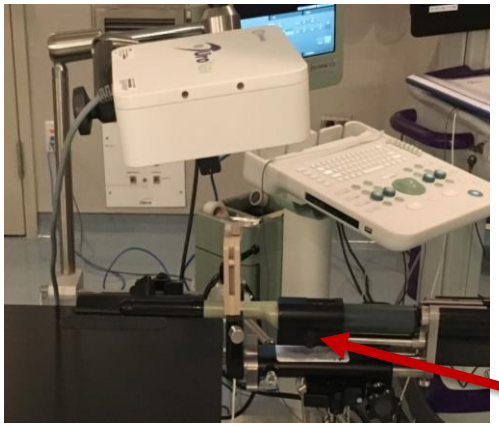

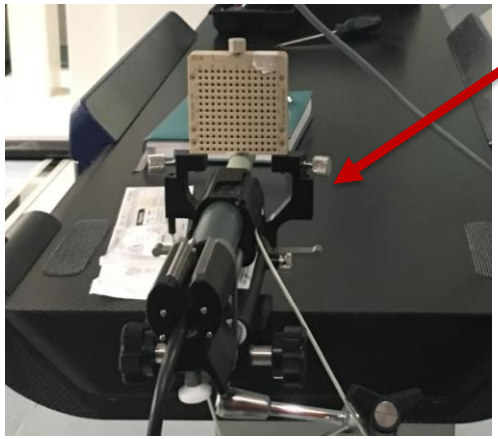

f) EM sensors

UronavTherapy system: a) EM generator fixed on the articulated arm, b) UronavTherapy cart, c) US probe mounted on the stepper, with the DK template in place and two EM sensors, d) stepper, e) BK 400 ultrasound, f) EM sensors, one on the side of the template and the other one on the right side of the stepper.

ESTRO School

Integration with an Afterloader

- Automated applicator/catheter reconstruction
- Online channel set-up QA

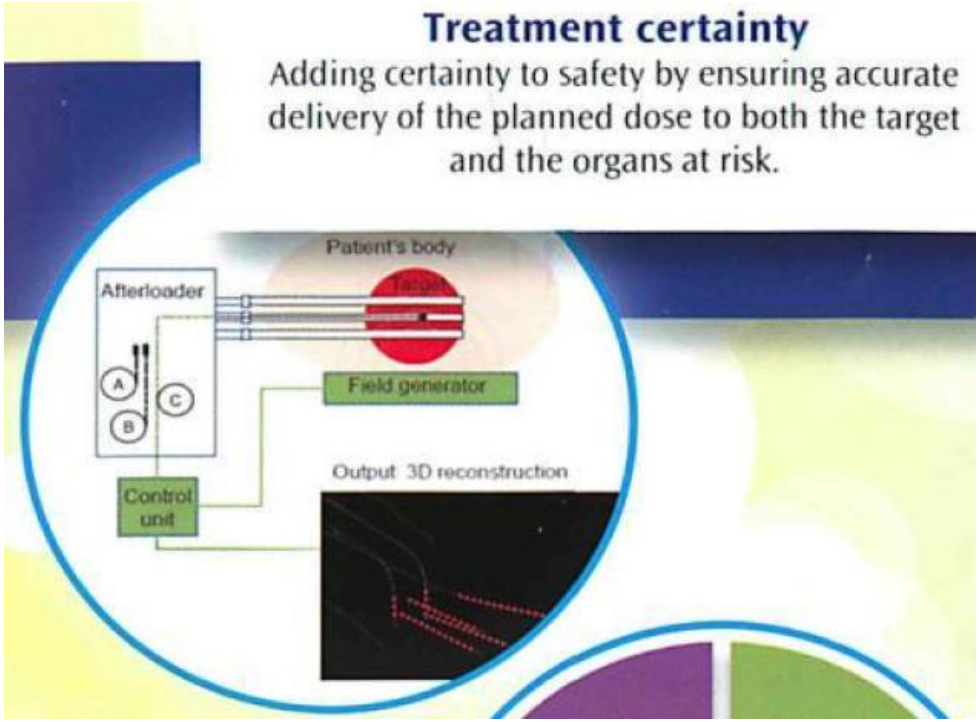

Elekta Vision 2020BrachyNext Meeting, Miami 2014

ESTRO School

Example: Flexitron with integrated EMT

- EMT data of ~50 patients collected since 2015
- 07/2016: Flexitron with EMT sensor on additional drive
- New acquisition workflow and algorithms
- Integration of sensor position data from afterloader feasible

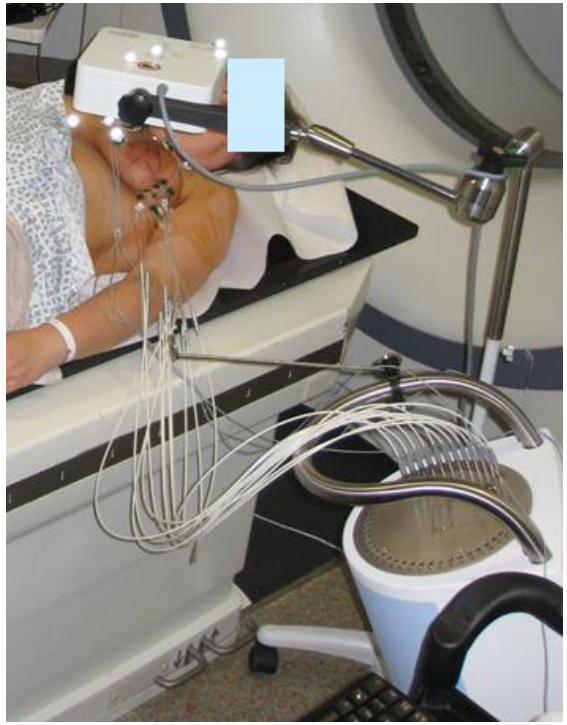

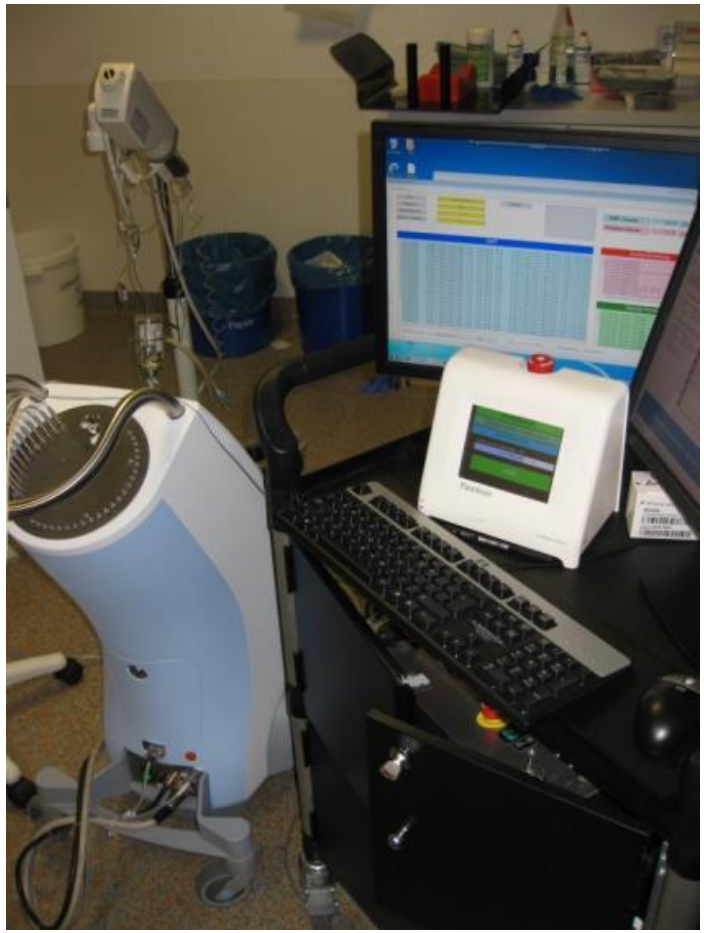

Courtesy: C. Bert

Karoline Kallis et al. Phys. Med. Biol. 2018

ESTRO School

Breast Data Collection

- Treatment: microSelectron
- EMT measurements: Flexitron prototype
- Improved sensor placement on skin
  - Compensation for breathing motion by three 6 dof sensors on breast

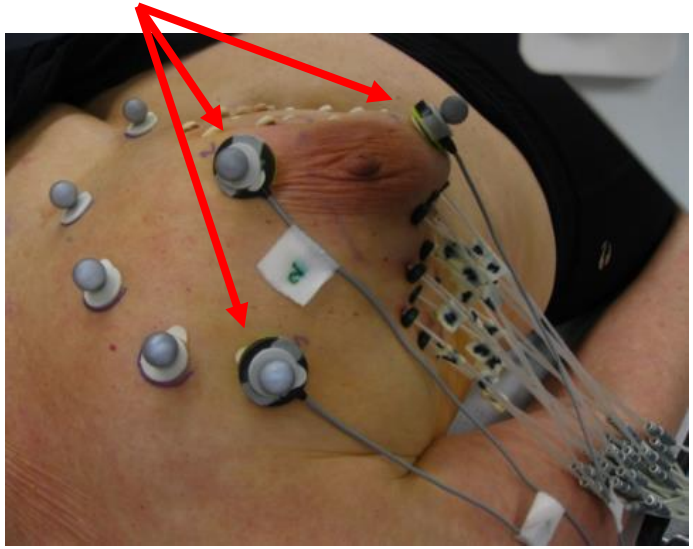

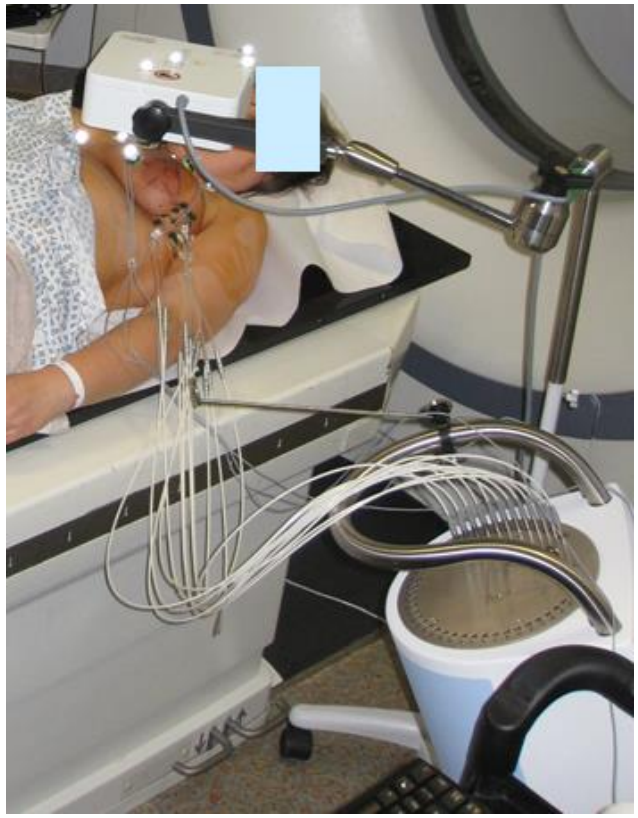

Courtesy: C. Bert

Karoline Kallis et al. Phys. Med. Biol. 2018

ESTRO School

Example data

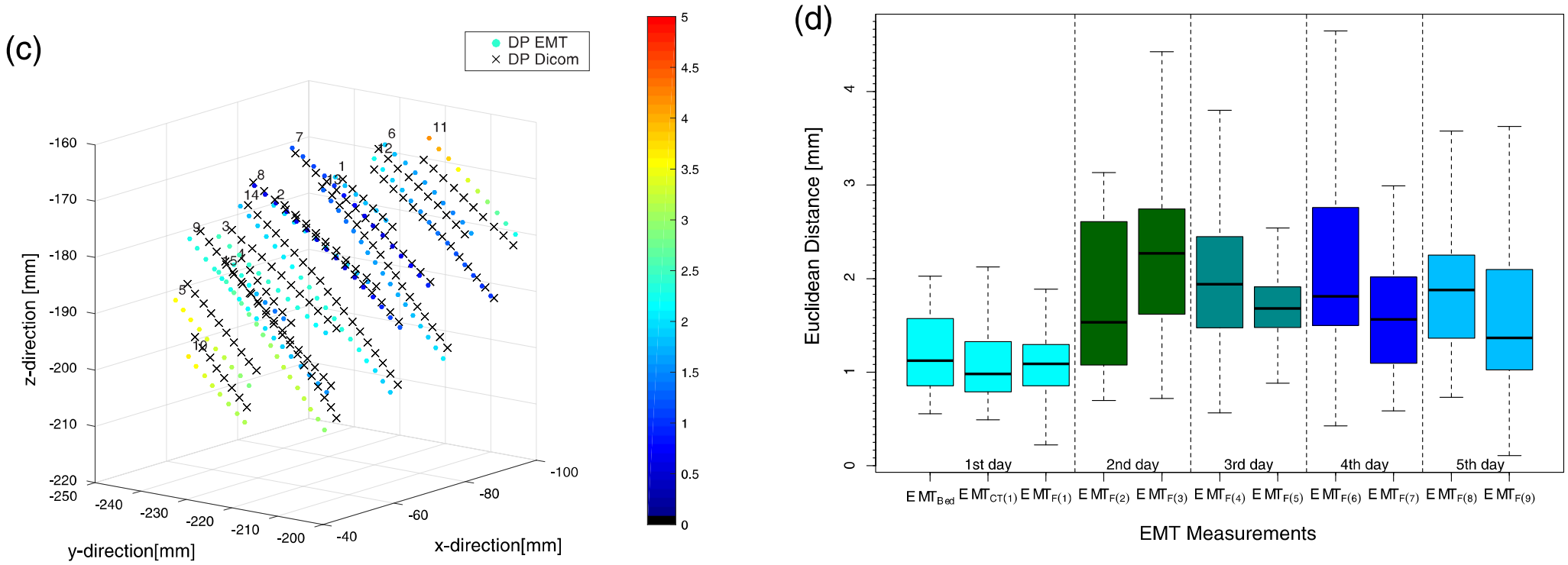

Figure 6. Exemplary comparison of DP CT to DP EMT for patient 15. Figure (a) shows the EMT measurement after the third fraction of irradiation. The colored stars represent the superficial reference sensors. Figure (b) presents the DP (colored points) and catheter traces, indicated by the black crosses, defined in the planning CT image, which served as reference. Figure (c) shows the deviations of the DPs at the 4th fraction. Figure (d) presents the course of the DP deviations within the week of treatment. In the boxplots outliers are not presented. Outliers are defined as points 1.5 times the interquartile range above the upper (3rd) quartile and below the lower (1st) quartile. The bottom and the top of the whisker represent the 75th percentile and 25th percentile. The band inside of the box indicates the median value.

Karoline Kallis et al. Phys. Med. Biol. 2018

Active MR micro-coils

- Use the MR as an intrinsic field generator.
- Sensors are active micro-coils
- Sensors positions are *de facto* in the imager reference frame!

Magnetic Resonance in Medicine 73:1803–1811 (2015)

Real-Time Active MR-Tracking of Metallic Stylets in MR-Guided Radiation Therapy

Wei Wang,[1,2]* Charles L. Dumoulin,[3] Akila N. Viswanathan,[2] Zion T.H. Tse,[4] Alireza Mehrtash,[1] Wolfgang Loew,[3] Isaiah Norton,[1] Junichi Tokuda,[1] Ravi T. Seethamraju,[5] Tina Kapur,[1] Antonio L. Damato,[2] Robert A. Cormack,[2] and Ehud J. Schmidt[1]

Purpose: To develop an active MR-tracking system to guide placement of metallic devices for radiation therapy.
Methods: An actively tracked metallic stylet for brachytherapy was constructed by adding printed-circuit micro-coils to a commercial stylet. The coil design was optimized by electromagnetic simulation, and has a radio-frequency lobe pattern extending ~5 mm beyond the strong B_0 inhomogeneity region near the metal surface. An MR-tracking sequence with phase-field dithering was used to overcome residual effects of B_0 and B_1 inhomogeneities caused by the metal, as well as from inductive coupling to surrounding metallic stylets. The tracking system was integrated with a graphical workstation for real-time visualization. The 3 Tesla MRI catheter-insertion procedures were tested in phantoms and ex vivo animal tissue, and then performed in three patients during interstitial brachytherapy.
Results: The tracking system provided high-resolution (0.6 × 0.6 × 0.6 mm^3) and rapid (16 to 40 frames per second, with three to one phase-field dithering directions) catheter localization in phantoms, animals, and three gynecologic cancer patients.
Conclusion: This is the first demonstration of active tracking of the shaft of metallic stylet in MR-guided brachytherapy. It holds the promise of assisting physicians to achieve better targeting and improving outcomes in interstitial brachytherapy.
Magn Reson Med 73:1803–1811, 2015. © 2014 Wiley Periodicals, Inc.

Key words: active MR-tracking; metallic device; radiation therapy; phase-field dithering

INTRODUCTION

Gynecologic malignancies (endometrial, ovarian, cervical, and vagina/vulva cancers) accounted for over 91,000 new cancer cases and approximately 28,000 deaths in 2013 in the United States (1). Brachytherapy places radioactive sources directly into the tumor-bearing tissues to achieve high doses of radiation to the tumor, while minimizing the dose to surrounding normal tissue. Brachytherapy is considered standard-of-care for many gynecologic cancer patients and improves survival (2). MRI is often used in gynecologic brachytherapy, due to its higher accuracy in evaluating the extent of disease in the primary tumor, as well as adjacent tissue spread. Its capacity to detect the morphology of the tumor can also be beneficial for interventional brachytherapy procedures, assisting in the navigation and targeting the lesion. Recently, real-time rather than postinsertion MRI has been integrated into radiation treatment planning to aid the insertion of interstitial implants and treatment planning (3). The initial study demonstrated that real-time MRI guidance during insertion of interstitial catheters, followed by three-dimensional (3D) planning, maximized opportunities for tumor targeting as well as the sparing of normal tissues (4).

In MRI-guided brachytherapy, multiple (10–30) catheters are typically placed into the tumor (Fig. 1). Each catheter consists of a hollow tip-sealed plastic tube into which radioactive sources are later temporarily loaded, and a metallic needle ("stylet") constructed from tungsten alloy to provide the mechanical strength needed to drive the catheter to its desired position. As a result, reliable tracking of a metallic device is crucial to the success of interventional brachytherapy procedures. Currently, MRI-guided brachytherapy is conducted by passively visualizing the magnetic susceptibility image artifact created by the metallic stylet (5). Metal itself does not generate MR signals and the presence of metal can result in severe distortion to the static magnetic field (B_0) around it because of the large susceptibility differences with surrounding tissues. The signal voids created by the metal in MR images are used as a negative contrast to identify the device, but the accurate location and size of the device is difficult to determine because the susceptibility artifact on MR images depends on the shape and material properties, the device's orientation relative to B_0, and pulse sequence parameters (6). High-resolution image-based passive tracking methods are typically time-consuming (0.5–2 tracking frames per minute) and may also compromise the contrast-to-noise ratio of anatomic images. Furthermore, this approach becomes more difficult in MR-guided brachytherapy, where the individual paths of multiple catheters need to be tracked, because catheters are close to each other (<10 mm apart) or cross paths during insertion. Various

[1]Radiology, Brigham and Women's Hospital, Boston, Massachusetts, USA.
[2]Radiation Oncology, Brigham and Women's Hospital, Boston, Massachusetts, USA.
[3]Radiology, Cincinnati Children's Hospital Medical Center, Cincinnati, Ohio, USA.
[4]Engineering, the University of Georgia, Athens, Georgia, USA.
[5]MR R&D, Siemens Healthcare, Boston, Massachusetts, USA.
Grant sponsor: American Heart Association; Grant number: 10SDG2610139; Grant sponsor: NIH; Grant numbers: 1R21CA158987-01A1; R21 CA 167800.
*Correspondence to: Wei Wang, Ph.D., Brigham and Women's Hospital, 75 Francis Street, Boston, MA 02115. E-mail: wwang21@partners.org
Received 25 February 2014; revised 1 May 2014; accepted 2 May 2014
DOI 10.1002/mrm.25300
Published online 5 June 2014 in Wiley Online Library (wileyonlinelibrary.com).

Active MR-Tracking System

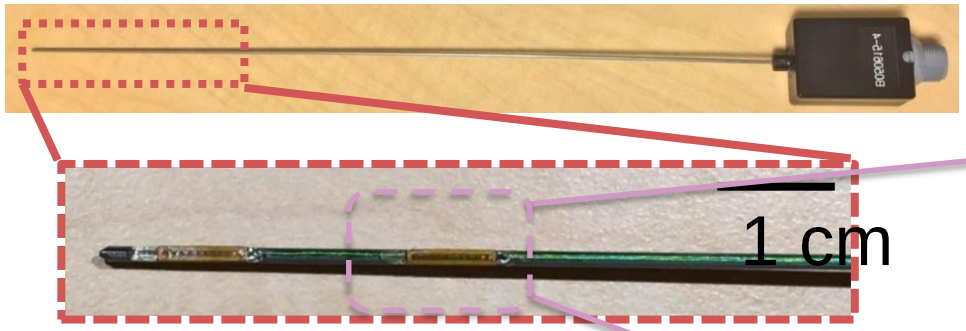

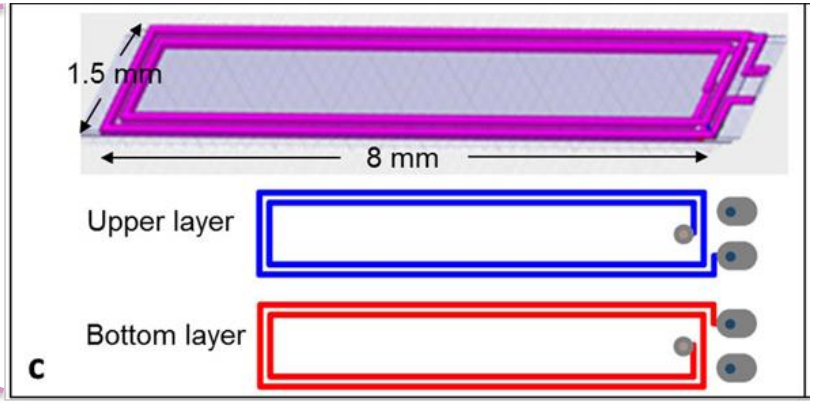

MR Tracking Sequence

- High Spatial Resolution: 0.6 × 0.6 × 0.6 mm^3
- High Temporal Resolution: 40 updates/sec
- Heating < 0.6 ° C increase for a 15-min scan (3.3 W/kg)
- Two mode: tracking only, tracking-imaging

Wang, W. et al, Magn Reson Med (2015), 73: 1803-1811

MR Tracking (quantitative): Catheter Localization

- Tracker stylet placed and withdrawn
- Closely space needles resolved
- Resolves ambiguity of crossed needles
- Accuracy sufficient for planning

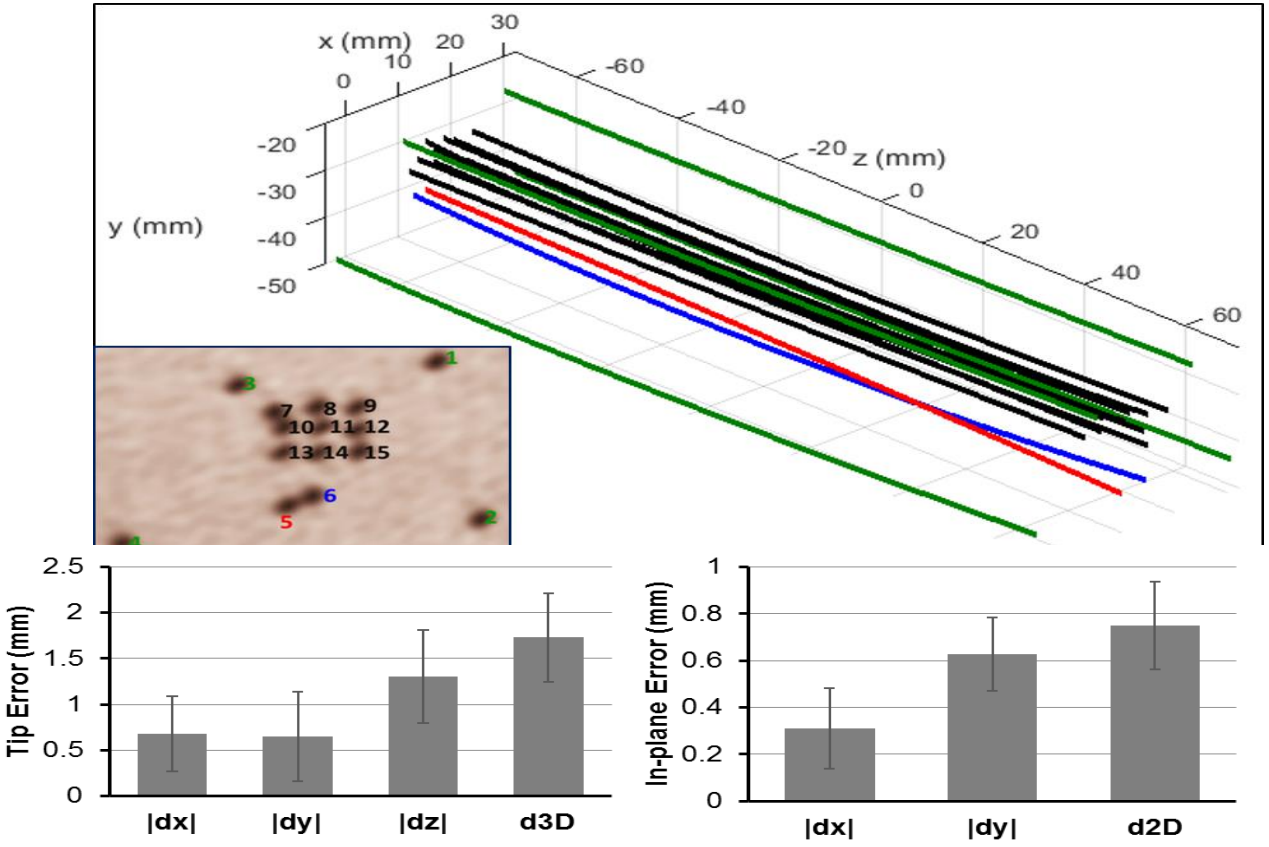

Possibilities / Limitations

Quality item	Detectability			EMT coordinate system	Error probability and effect [23]	
	IVD	Imaging	EMT		Probability of error	Effect
Source calibration	✓	✗	✗	–	Low	Low-high
Afterloader source positioning and dwell time (non-patient specific)	✓	✗	(✓)	E	–	–
Afterloader malfunction	✓	✗	(✓)	E	Low	Low-high
Patient identification	✗	✓	(✓)	E/F	Low	High
Correct treatment plan	✓	✗	✓	E	Low	High
Intra- and interfraction organ/applicator movement	✓	✓	✓	E/F/A	–	–
Applicator reconstruction	✓	✓	✓	E	Intermediate	Low-intermediate
Applicator length/source indexer length	✓	✗	✓	E/F	Intermediate	Low-high
Source step size (patient specific)	✓	✗	✓	E	Low	High
Interchanged guide tubes	✓	✗	✓	E/F	Intermediate	Low-high
Recording of dose	✓	✗	✗	–	–	–

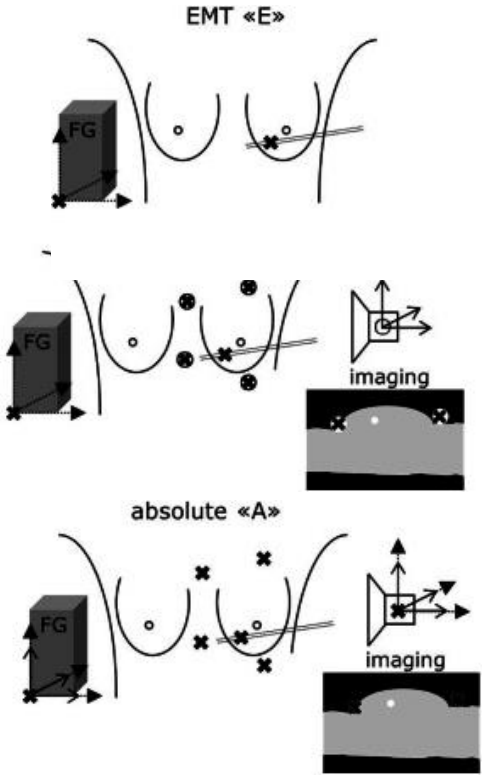

Courtesy: C. Bert

Bert et al. JCM 2016

ESTRO School

Fiber Shape Sensing

Fiber Shape Sensing

- **REVIEW ARTICLE: In-fibre Bragg grating sensors *Measurement Science and Technology***. Rao Y-J. **8** (1997) 355–75
- **Optical Fiber-Based MR-Compatible Sensors for Medical Applications: An Overview**. Fabrizio Taffoni , Domenico Formica , Paola Saccomandi, Giovanni Di Pino and Emiliano Schena. Sensors 13 (2013), 14105-14120
- **Optical in-fiber bragg grating sensor systems for medical applications.** Y. J. Rao, D. J. Webb, D. A. Jackson, L. Zhang, and I. Bennion. Journal of biomedical optics 3 (1998), 38–44
- **3D flexible needle steering in soft-tissue phantoms using Fiber Bragg Grating sensors**. Abayazid M, Kemp M and Misra S. *ICRA (2013)* 5843–9
- **Real-Time Estimation of Three-Dimensional Needle Shape and Deflection for MRI-Guided Interventions**. Yong-Lae Park, Santhi Elayaperumal, Bruce Daniel, Seok Chang Ryu, Mihye Shin, Joan Savall, Richard J. Black, Behzad Moslehi, and Mark R. Cutkosky. IEEE/ASME Transactions on Mechatronics 15 (2010) 906 – 915

ESTRO School

Fiber-optics Shape Sensing

Fiber Bragg Grating (FBG)

- Down to 80 um diameter fiber
- Femtoseconds laser
- 3 or more FBG etched within the fiber at various location along the needle or catheter or …

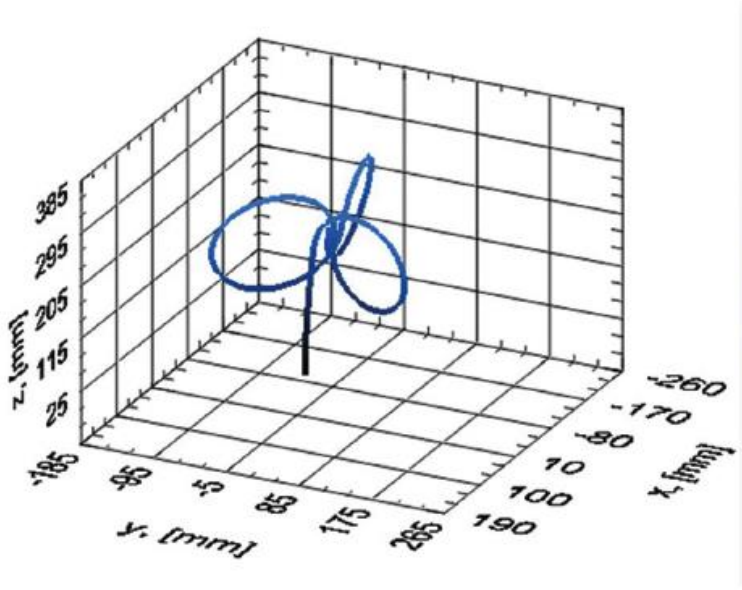

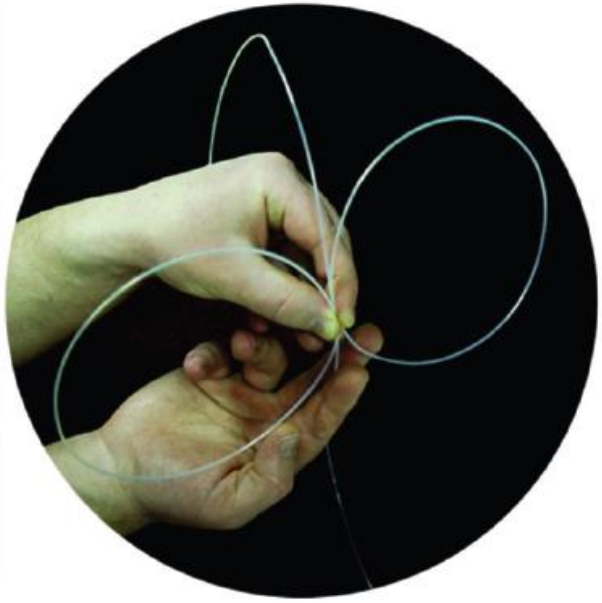

Credit: NASA

ESTRO School

Fiber-optics Shape Sensing

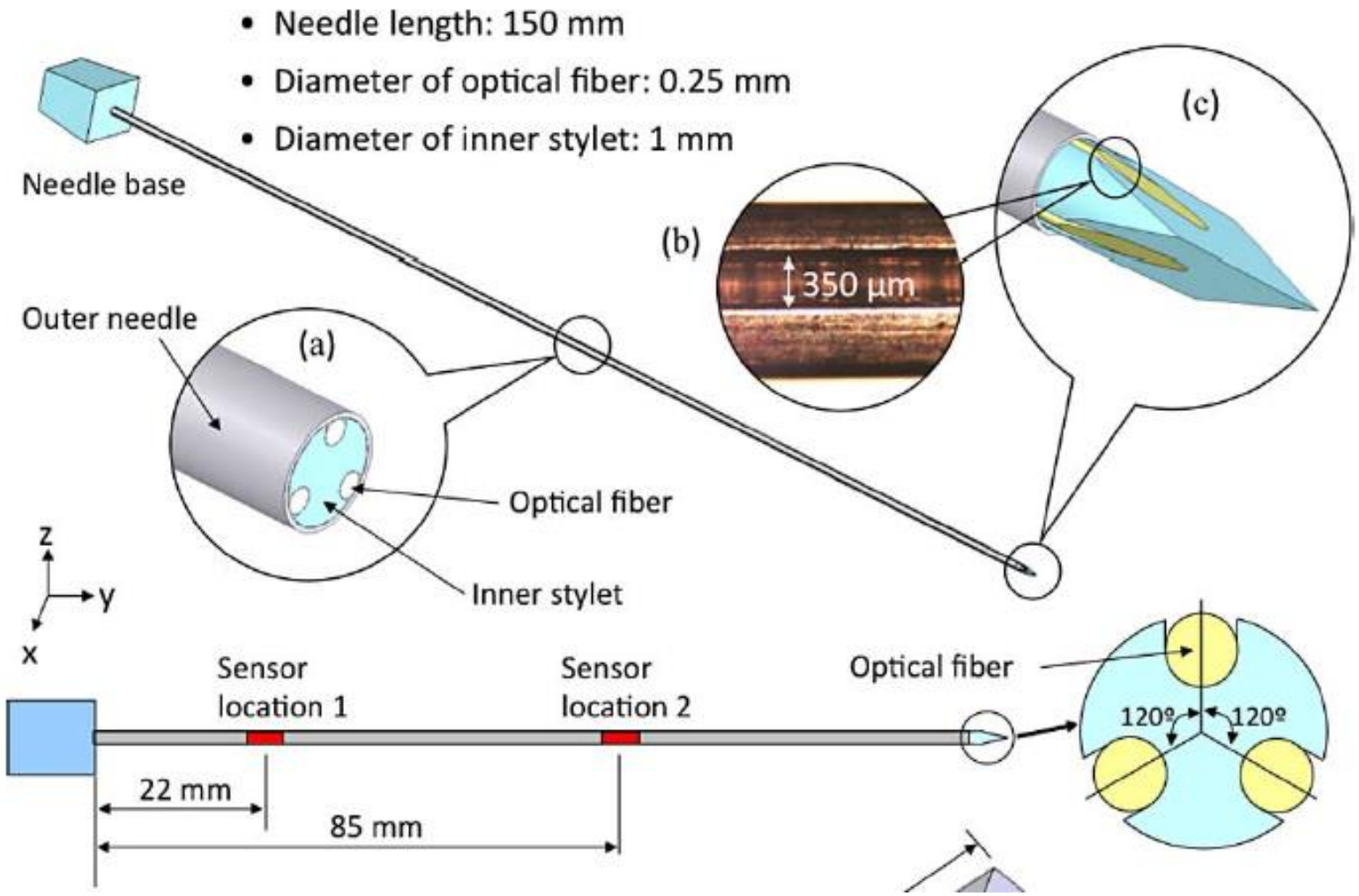

Park et al, IEEE/ASME (2010); Tiffoni et al, Sensor (2013)

ESTRO School

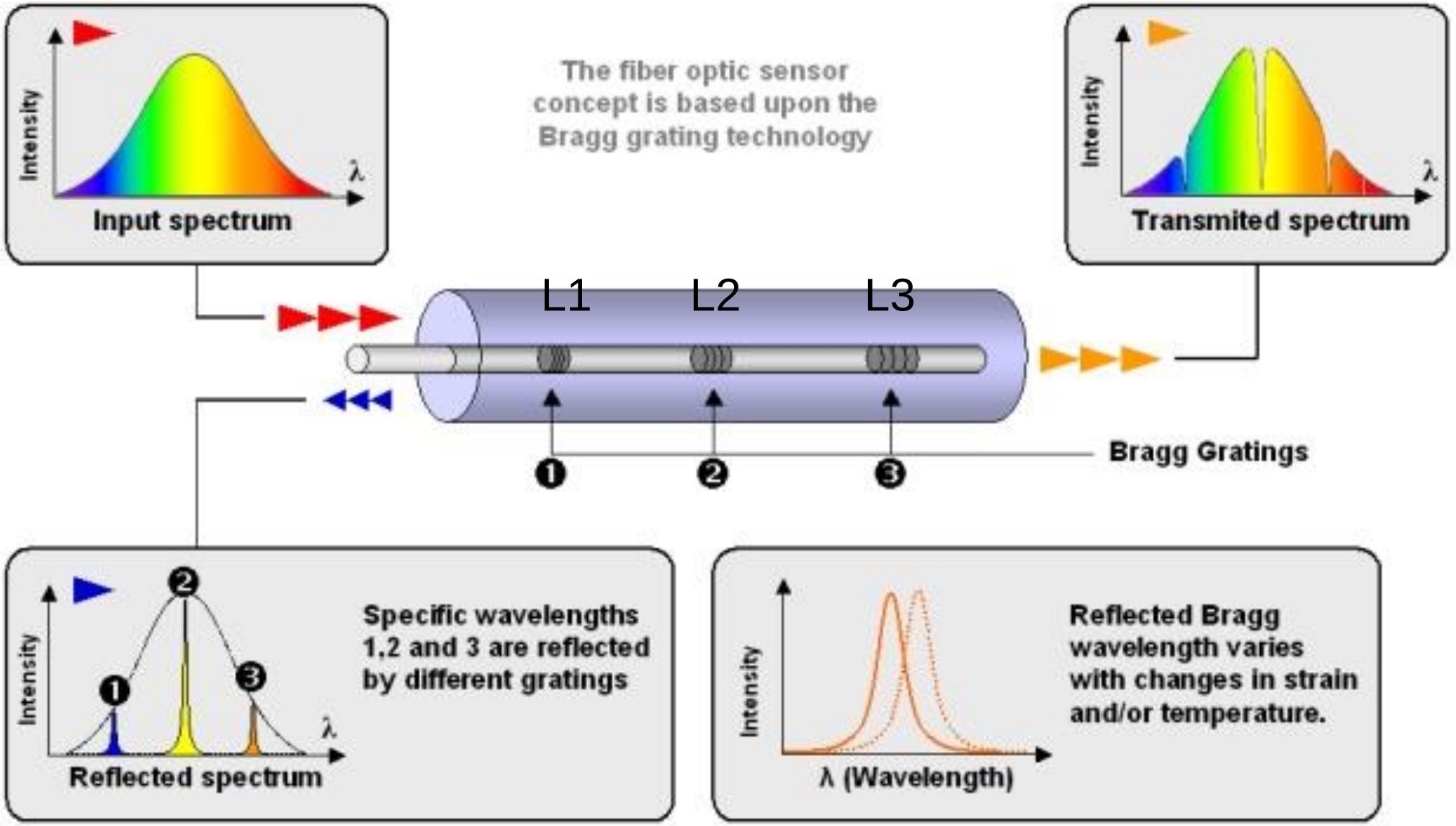

$$\frac{\Delta I_i}{I_i} = k_s e + k_T \Delta T$$

e : *strain*

ΔT : *temperature change*

k : *coefficients*

http://www.windkraft-journal.de/

ESTRO School

Table 1. Performances and medical applications for MR-compatible FBG sensors.

Reference	Sensing Element	Measurand	Application Field	Characteristics
Rao *et al.*, 1998 [18]	FBG	Temperature	Hyperthermic treatment	Accuracy ≈ 0.8 °C, range 20 °C–60 °C, Resolution ≈ 0.2 °C
Webb *et al.*, 2000 [20]	FBG	Temperature	Hyperthermic treatment	Resolution ≈ 0.2 °C
Saccomandi *et al.*, 2012–2013 [21,22]	FBG	Temperature	Hyperthermic treatment	Range up to 80 °C
Schena *et al.*, 2013 [23]	FBG	Temperature	Hyperthermic treatment	Range 20 °C–80 °C, sensitivity ≈ 8.4 pm·°C^{-1}
Gowardhan *et al.*, 2007 [24]	FBG	Temperature	Cryotherapy	Minimum value ≈ −60 °C
Samset *et al.*, 2005 [25]	FBG	Temperature	Cryotherapy	Range −195 °C–100 °C
Weherle *et al.*, 2001 [26]	FBG	Inspiratory volume	Respiratory monitoring	Range 60 mL–500 mL, Frequency up to 10 Hz
Witt *et al.*, 2012 [27]	FBG	Thoracic movements	Respiratory monitoring	/
De jonckheere *et al.*, 2007 [28]	FBG	Strain	Respiratory monitoring	/
D'Angelo *et al.*, 2008 [29]	FBG	Strain	Respiratory monitoring	/
Grillet *et al.*, 2007–2008 [30,31]	FBG	Strain	Respiratory monitoring	Strain up to 41.2%, Sensitivity ≈ 0.35 nm·%$^{-1}$ Accuracy ≈ 0.1%
Silva *et al.*, 2011 [32]	FBG	Respiratory/heart rate (HR)/(RR)	Respiratory and cardiac monitoring	

Courtesy of
Maxence Borot de Battisti
Borot de Battisti et al, Med. Phys., 2016, *in press*

UMC Utrecht

MR compatibility of Fiber Bragg Gratings (FBG)-based sensing for real-time needle tracking

M. Borot de Battisti[1], B. Denis de Senneville[2,3], M. Maenhout[1], G. Hautvast[4], D. Binnekamp[4], J.J.W. Lagendijk[1], M. van Vulpen[1], M.A. Moerland[1]

[1]University Medical Center Utrecht, Dept. of Radiotherapy, Utrecht, The Netherlands
[2]University Medical Center Utrecht, Imaging Division, Utrecht, The Netherlands
[3]University of Bordeaux, UMR 5251 CNRS, Bordeaux, France
[4]Philips Group Innovation - Biomedical Systems, Eindhoven, The Netherlands

Courtesy of
Maxence Borot de Battisti
Borot de Battisti et al, Med. Phys., 2016, *in press*

Description of prototype

- Length: 195mm, diameter: 1.15mm
- 3 optic fibers separated by an angle of 120 degree
- 9 sets of FBGs embedded separated by intervals of 20mm

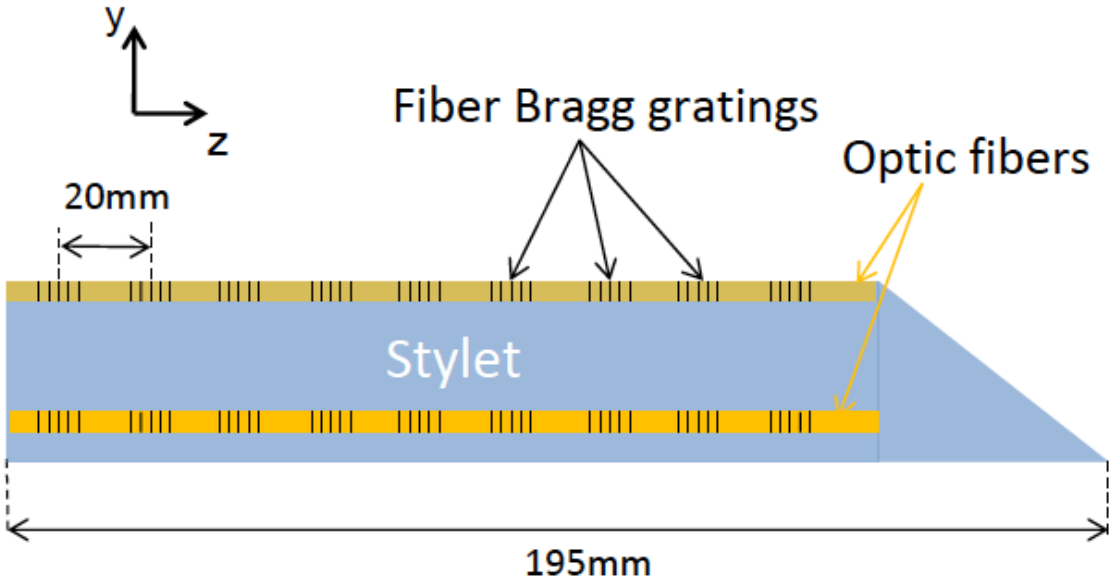

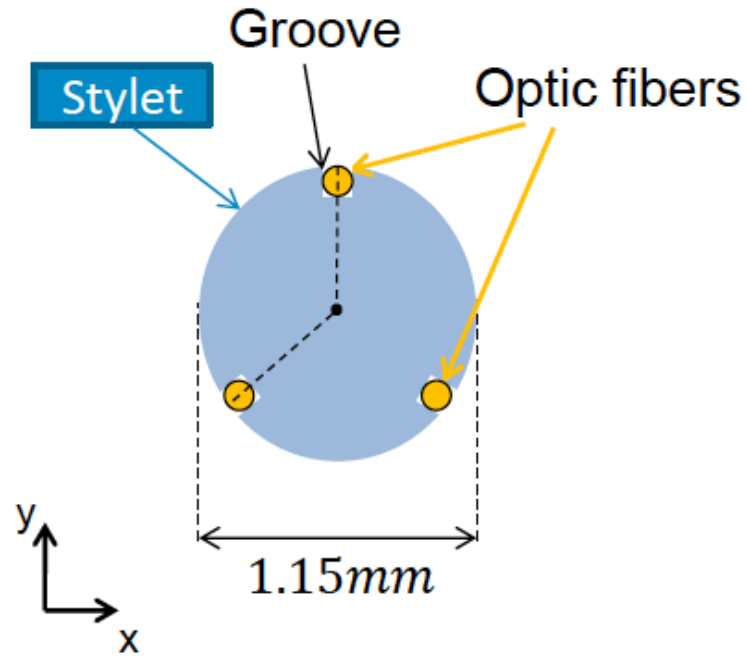

Courtesy of
Maxence Borot de Battisti
Borot de Battisti et al, Med. Phys., 2016, *in press*

Description of prototype (2)

- Broadband LED Source, Reflected wavelength measured by spectrum analyzer
- Determination of strain along the stylet

When the stylet is inserted into the needle → Measurement of the 3D needle's deflection

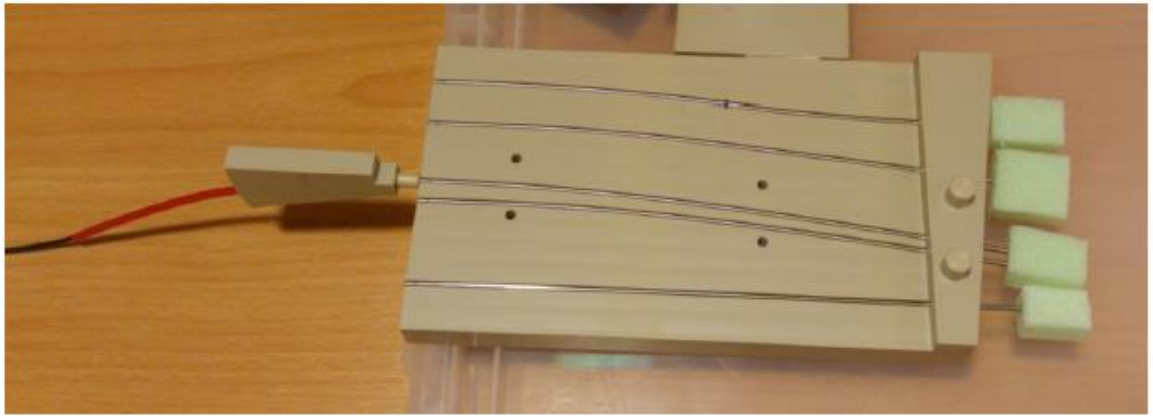

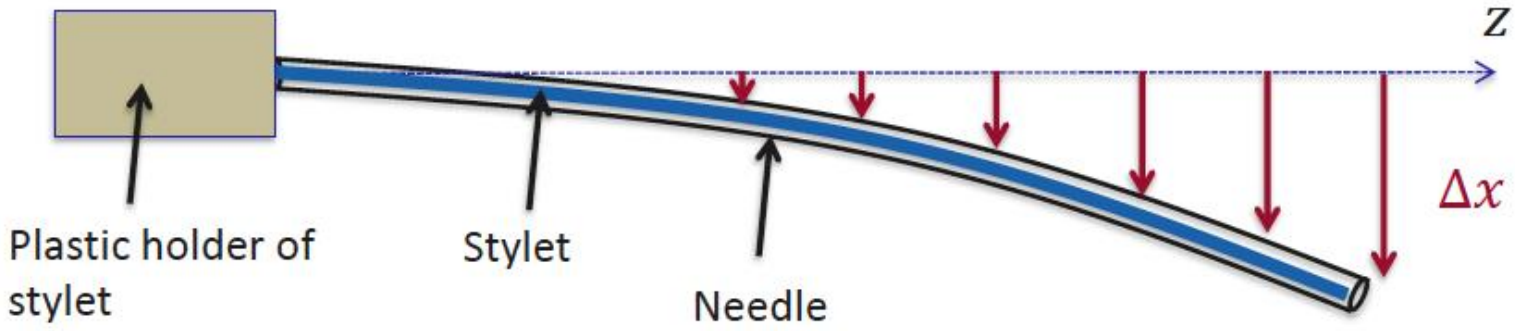

Courtesy of
Maxence Borot de Battisti
Borot de Battisti et al, Med. Phys., 2016, *in press*

Result experiment #2: Comparison with MR-based measurement

- Typical example

MR- and FBG-based measurements

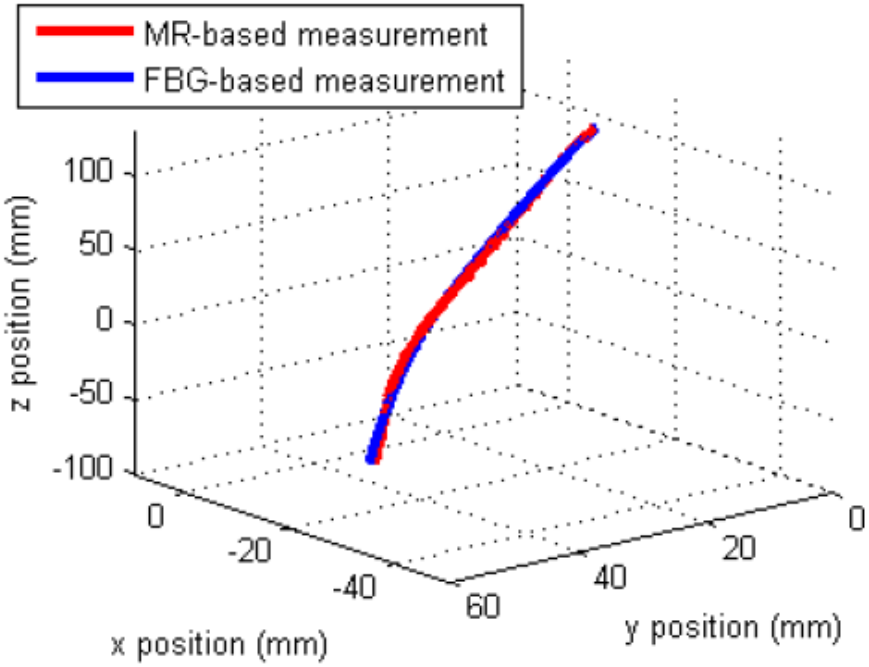

Euclidean distance between MR- and FBG-based measurements

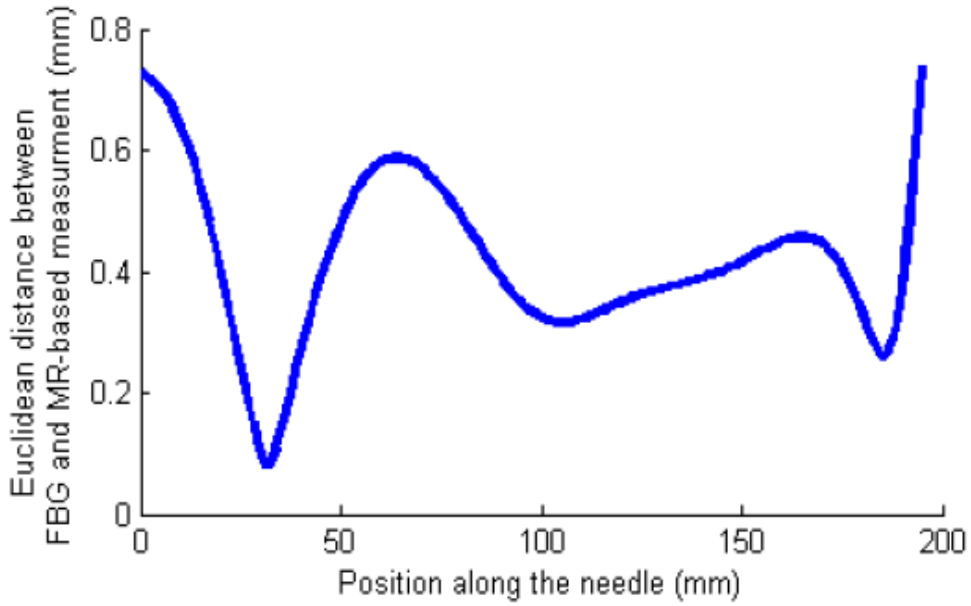

- Overall catheters:

Error<0.9mm

Average error: 0.42mm

Key Issue: Calibration to a **Relevant Reference Frame**

- Sensor to needle/stylet tip or relevant applicator ref. position
- Template (if used) to EM coordinate system
- Clinical images (target+OARs) to EM coordinate system
  - US and/or CT to EM

Each of the above will have an impact on the overall accuracy of the clinical system

Joint AAPM-ESTRO TG

Task Group No. 317 - Task Group on Catheter, Needle, and Applicator Tracking Technology in Brachytherapy (TG317)

- bookmark this page (bookmarks show under "My AAPM" in the menu to left)

No Website on file. | **Directory:** Committee | Membership

Email You may send email to this group now using gmail or outlook.
- or -
You may save the address *2018.TG317@aapm.org* to your local address book. This alias updates hourly from the AAPM Directory.

Charge View charge

Bylaws: Not Referenced. **Rules:** Not Referenced.

Approved Date(s) 12/31/2020

Committee Keywords: TG317

Most recent status update: No status update on file. Click to update.

[TG317] ⊞ Board of Directors [Status]
⊞ Science Council [Status]
⊞ Therapy Physics [Status]
⊞ Brachytherapy SC [Status]
Working Group on Brachytherapy Clinical Applications [Status]
TG317 - Task Group on Catheter, Needle, and Applicator Tracking Technology in... [Status]
» Status Reports from AAPM Groups

COI=complete and up-to-date, COI=incomplete conflict of interest statement.

VOTING Appointments

There are 4 voting members.

Luc Beaulieu, PhD
beaulieu@phy.ulaval.ca
3/25/2018 - 12/31/2020 Committee Chair

Robert A. Cormack, PhD
rcormack@lroc.harvard.edu
3/25/2018 - 12/31/2020 Member

J. Adam M. Cunha, PhD
Adam.Cunha@UCSF.Edu
3/25/2018 - 12/31/2020 Committee Vice Chair

Antonio L. Damato
antonio.damato@gmail.com
3/25/2018 - 12/31/2020 Member

NON-VOTING Appointments

There are 8 non-voting members and guests.

Christoph Bert
christoph.bert@uk-erlangen.de
3/25/2018 - 12/31/2018 Consultant (nonvoting)

Maxence Borot
maxence.borot@gmail.com
3/25/2018 - 12/31/2018 Consultant (nonvoting)

Gilion Hautvast
gilion.hautvast@philips.com
3/25/2018 - 12/31/2018 Consultant (nonvoting)

I-Chow Hsu
IChow.Hsu@ucsf.edu
3/25/2018 - 12/31/2018 Member (nonvoting)

Marinus A. Moerland, PhD
m.a.moerland@umcutrecht.nl
3/25/2018 - 12/31/2018 Consultant (nonvoting)

Yury Niatsetski, MS
yury.niatsetski@elekta.com
3/25/2018 - 12/31/2020 Consultant (nonvoting)

Kari Tanderup
karitand@rm.dk
3/25/2018 - 12/31/2018 Consultant (nonvoting)

Robert Weersink
robert.weersink@rmp.uhn.ca
3/25/2018 - 12/31/2018 Consultant (nonvoting)

ESTRO School

Real-time Tracking Technologies

They already in hospitals being use clinically

They are coming to brachytherapy

- Real-time position/angulation of needle, catheter or applicator
- Fast and accurate HDR channel reconst. and tips

Could be incorporated in specific workflows

- Automated imaging plane display
- Real-time continuous dosimetry and replanning (Seed)
- QA of channel (reconstr., swapped, …)

ESTRO School

WWW.ESTRO.ORG/SCHOOL

ESTRO School

Advanced Brachytherapy Physics

Perspective on Future Progress for Brachytherapy Physics and Technological Advancements: Radionuclides and Novel Applicators

Prof. Mark J. Rivard, Ph.D., FAAPM

Advanced Brachytherapy Physics, 29 May – 1 June, 2016

ESTRO School

Disclosures

Dr. Rivard serves as a consultant to CivaTech Oncology and a minor shareholder to Advanced Radiation Therapy, LLC

Opinions herein are solely those of the presenter, and are not meant to be interpreted as societal guidance.

Specific commercial equipment, instruments, and materials are listed to fully describe the necessary procedures. Such identification does not imply endorsement by the presenter, nor that these products are necessarily the best available for these purposes.

Learning Objectives

1. Examine radiological properties of current and potential radionuclides. Consider if these differences will be clinically meaningful.

2. Learn about current novel BT sources and applicators and possibilities. Consider if these differences will be clinically meaningful.

ESTRO School

New BT Radionuclides: Mean Photon Energy

- How sensitive is dosimetry for novel radionuclides and eBT to material heterogeneities (and general differences with TG-43)?

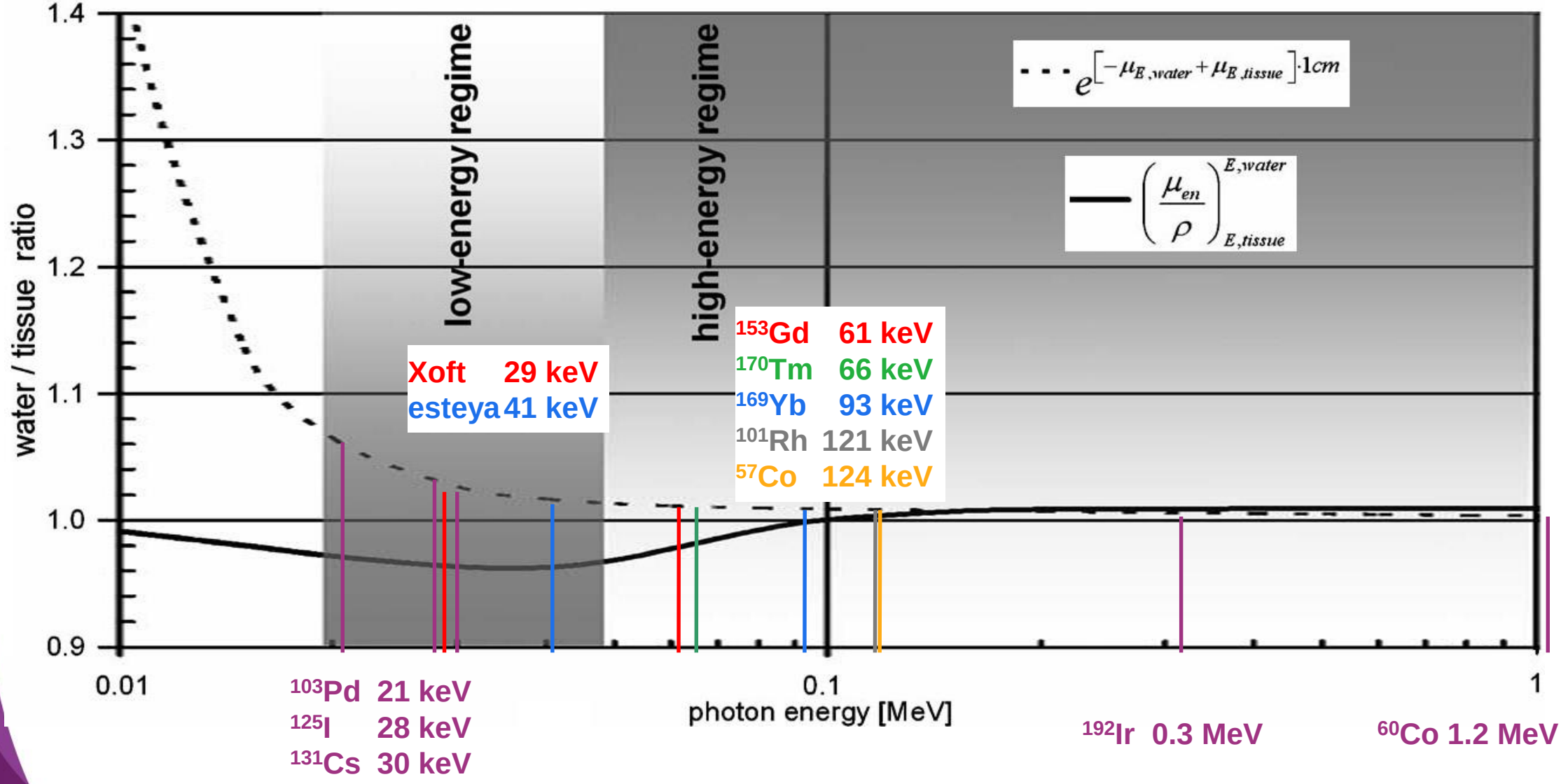

Rivard, Venselaar, Beaulieu, *Med. Phys.* 36, 2136-2153 (2009)

ESTRO School

New BT Radionuclides

established low-E sources

^{103}Pd	21 keV
^{125}I	28 keV
^{131}Cs	30 keV

"Dose-rate falloff differences" as a FN of E

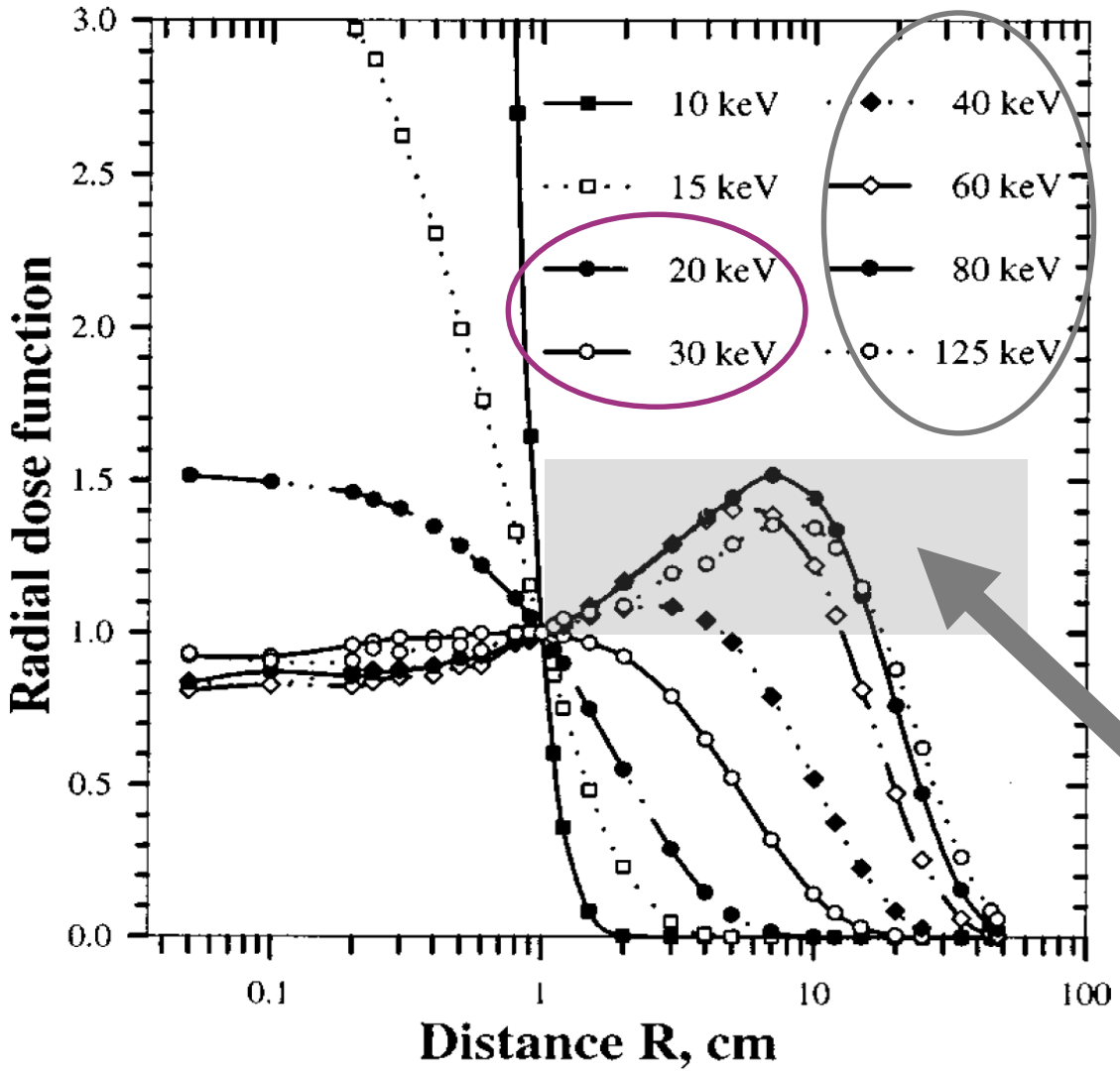

dose increase due to radiation scatter

novel sources

Xoft	29 keV
esteya	41 keV
^{153}Gd	61 keV
^{170}Tm	66 keV
^{169}Yb	93 keV
^{101}Rh	121 keV
^{57}Co	124 keV

Luxton and Jozsef, *Med. Phys.* 26, 2531-2538 (1999)

ESTRO School

Extreme BT Shielding: LDR ^{125}I

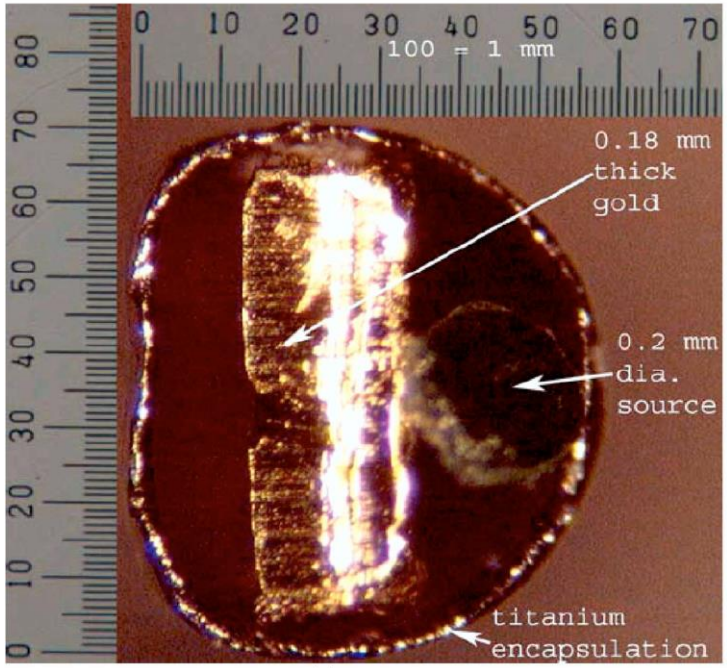

(a)

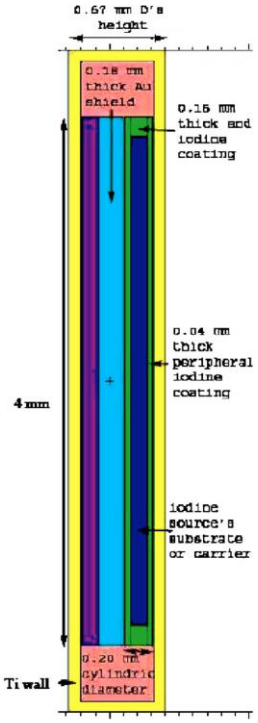

(b)

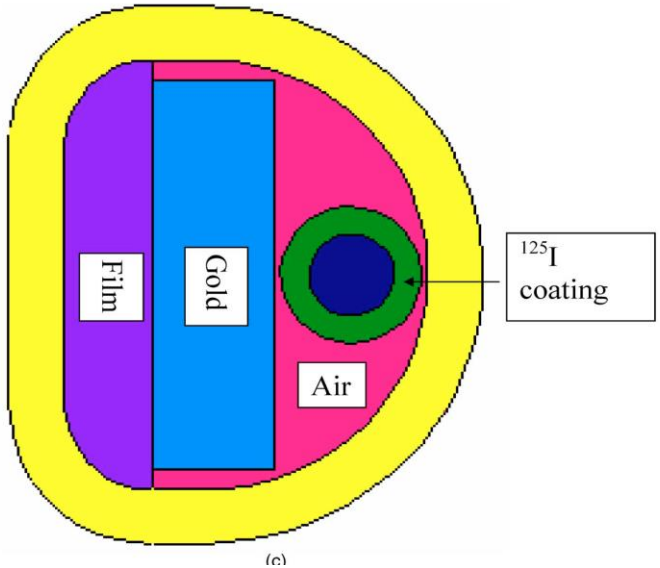

(c)

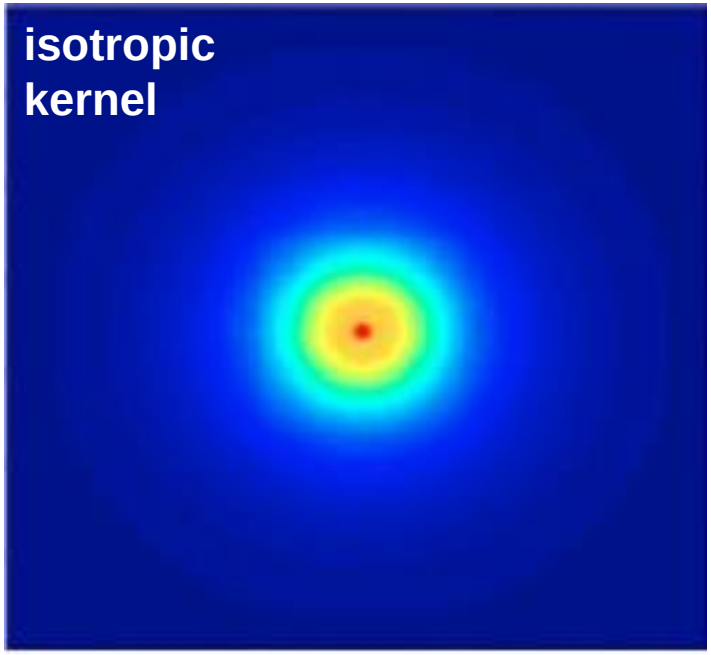

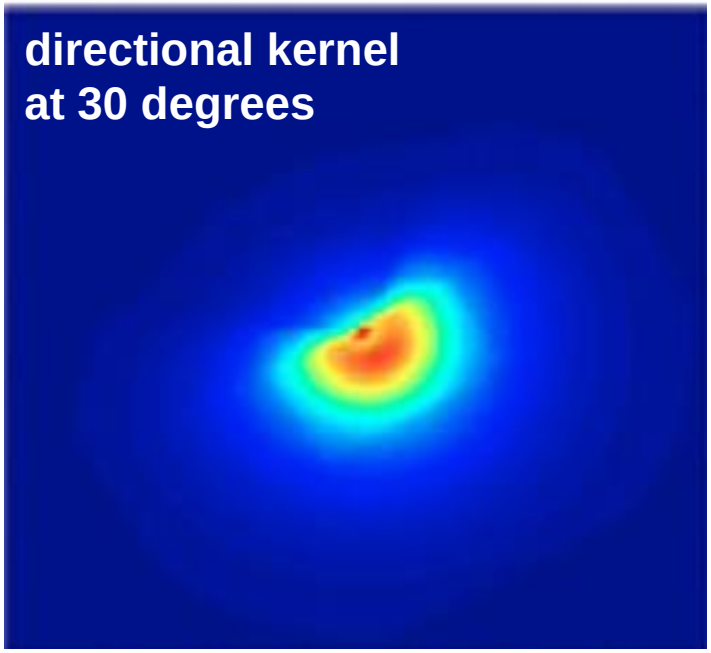

Lin, et al., *Med. Phys.* 35, 240-247 (2008)

Chaswal, et al., *Phys. Med. Biol.* 57, 963-982 (2012)

Extreme BT Shielding: LDR ^{125}I

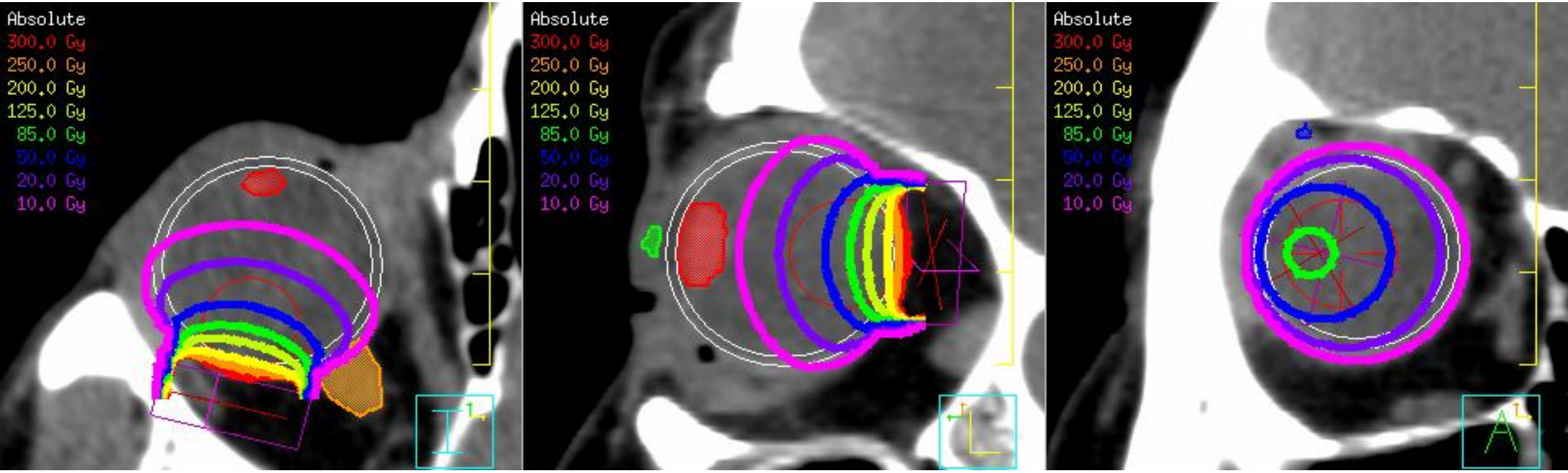

Rivard, et al., *Med. Phys.* 36, 1968-1975 (2009)

ESTRO School

Extreme BT Shielding: LDR ^{103}Pd

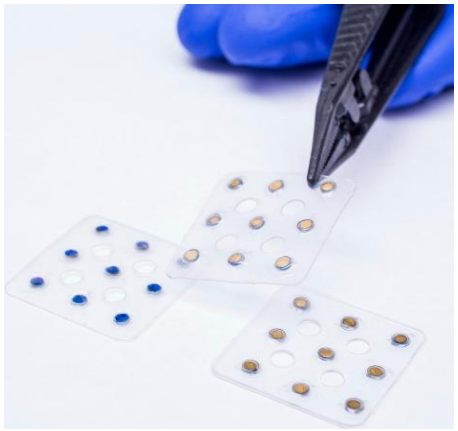

CivaSheet

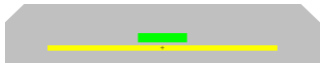

2.5 mm diam.

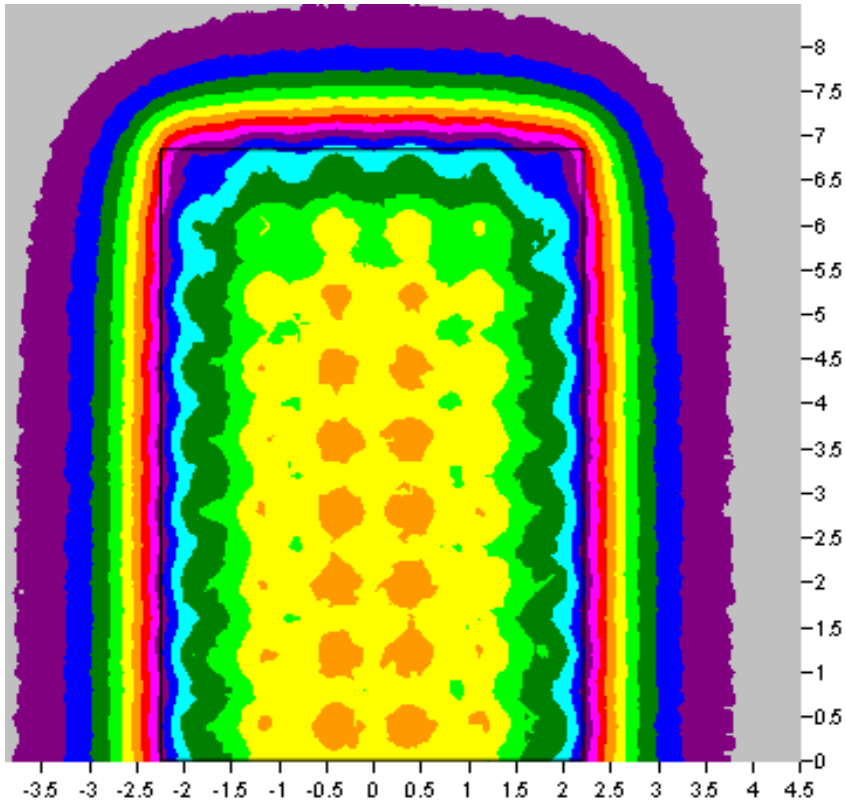

0.5 cm from front surface

Dose

160-170
150-160
140-150
130-140
120-130
110-120
100-110
90-100
80-90
70-80
60-70
50-60
40-50
30-40
20-30
10-20
0-10

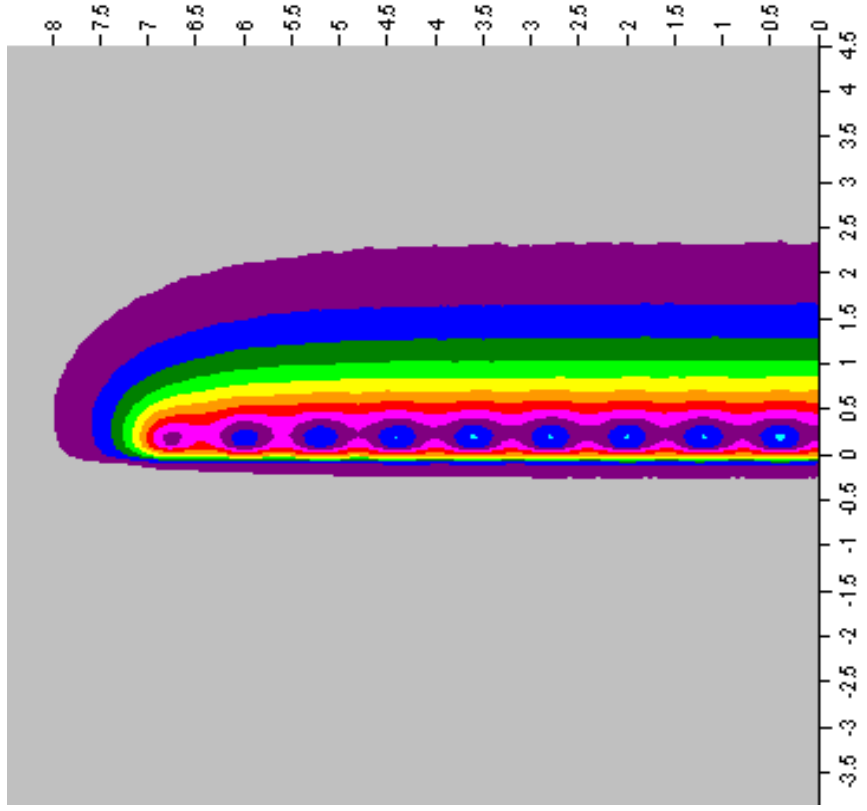

lateral view

Rivard, et al., work in progress

ESTRO School

Extreme BT Shielding: LDR ^{103}Pd

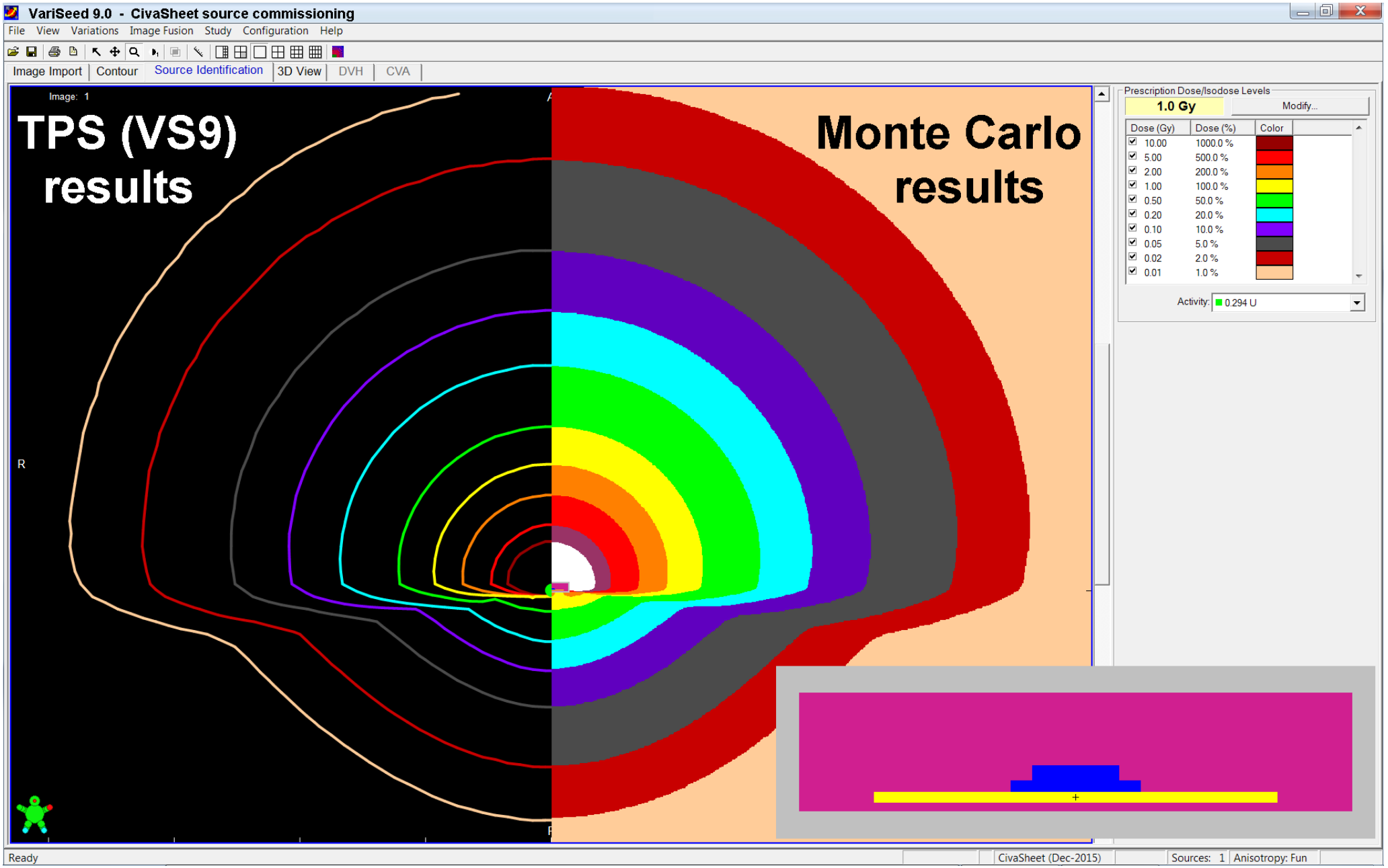

Rivard, et al., work in progress

ESTRO School

Extreme BT Shielding: HDR ^{192}Ir

AccuBoost: non-invasive breast BT

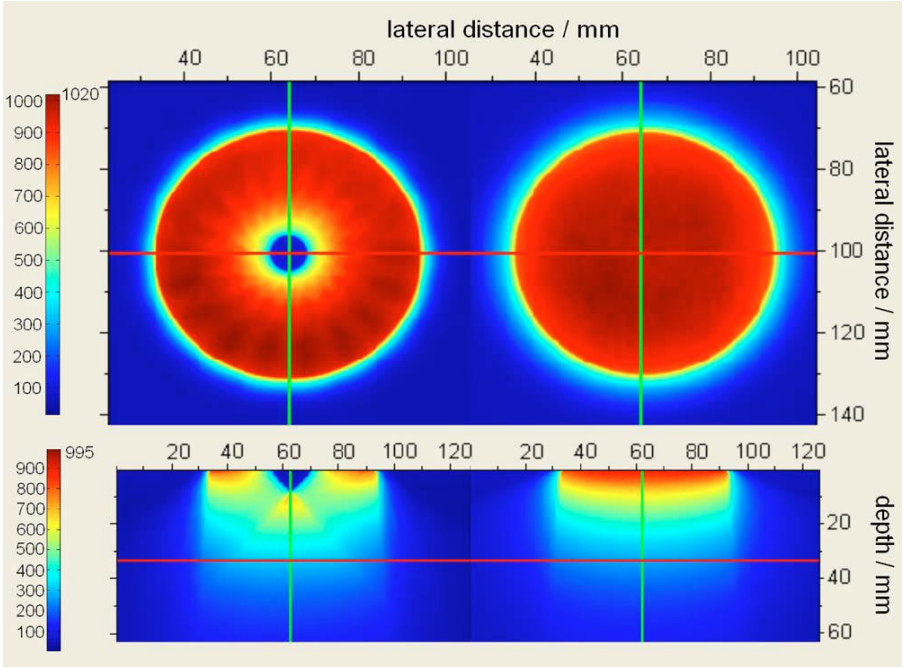

Yang, et al., *Med. Phys.* 38, 1519-1525 (2011) Yang and Rivard, *Med. Phys.* 37, 5665-5671 (2010)

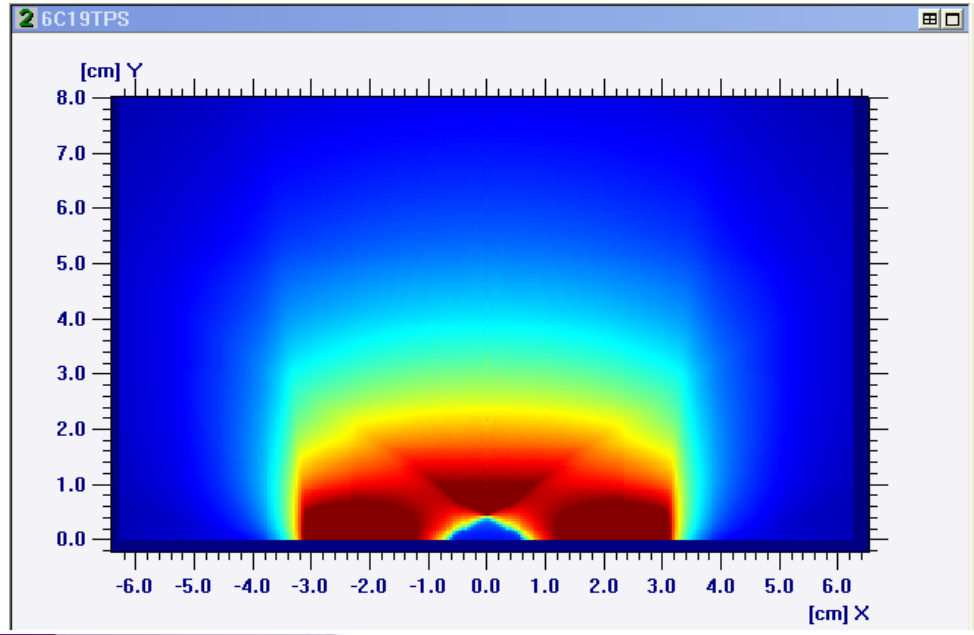

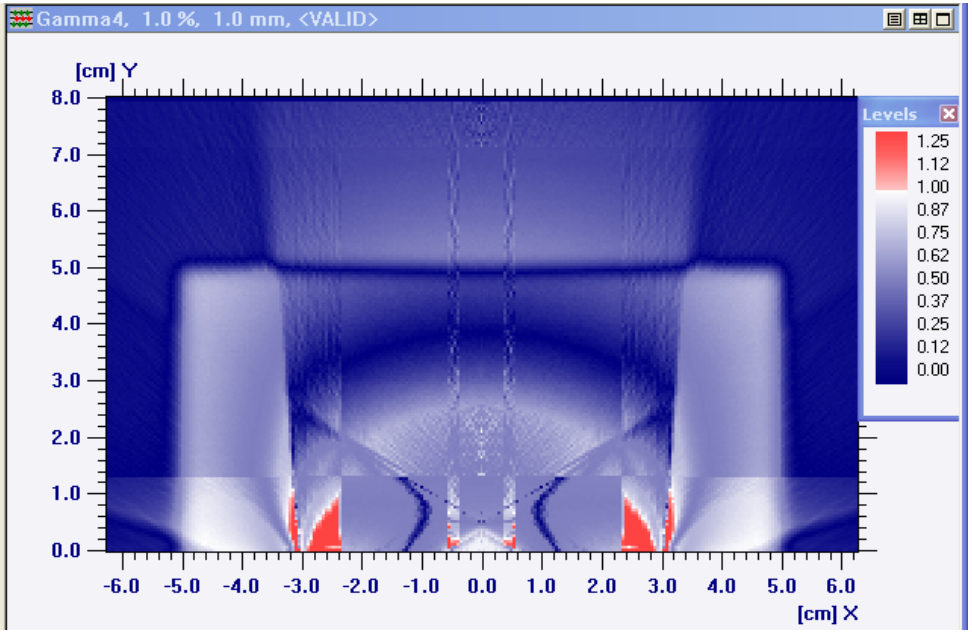

Extreme BT Shielding: HDR ^{192}Ir

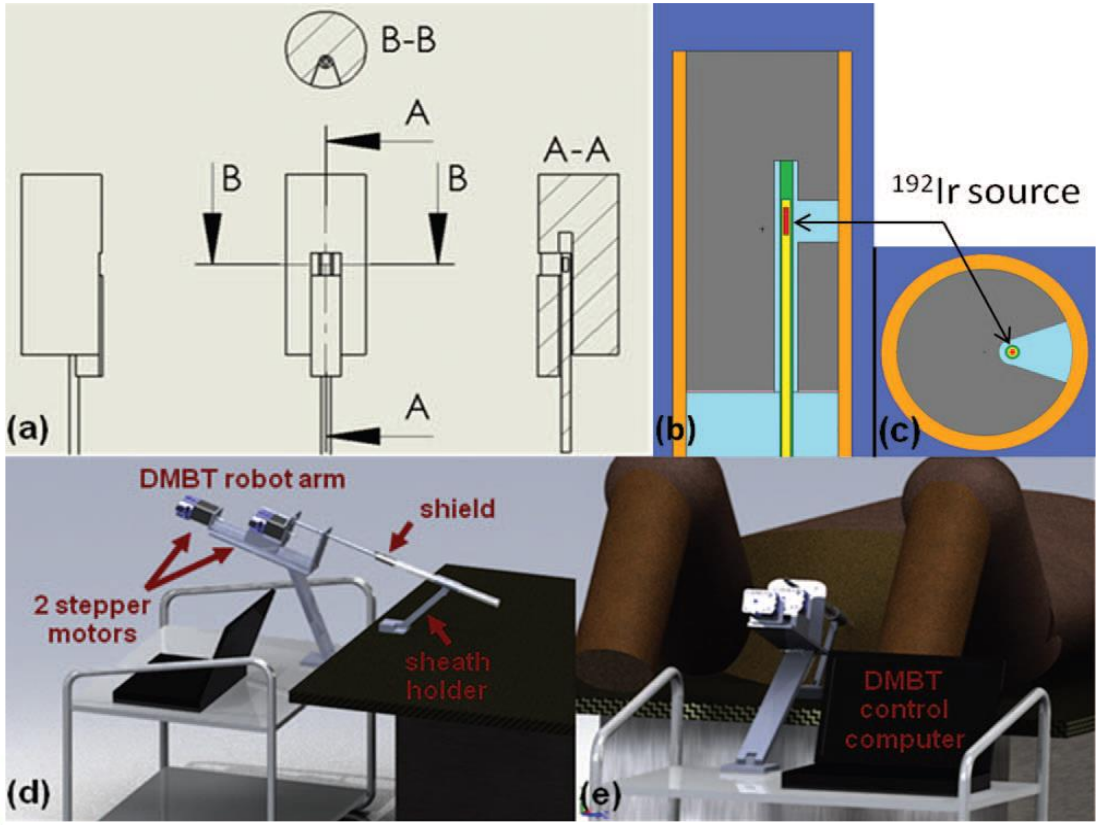

Webster, et al., *Med. Phys.* 40, 011718 (2013)

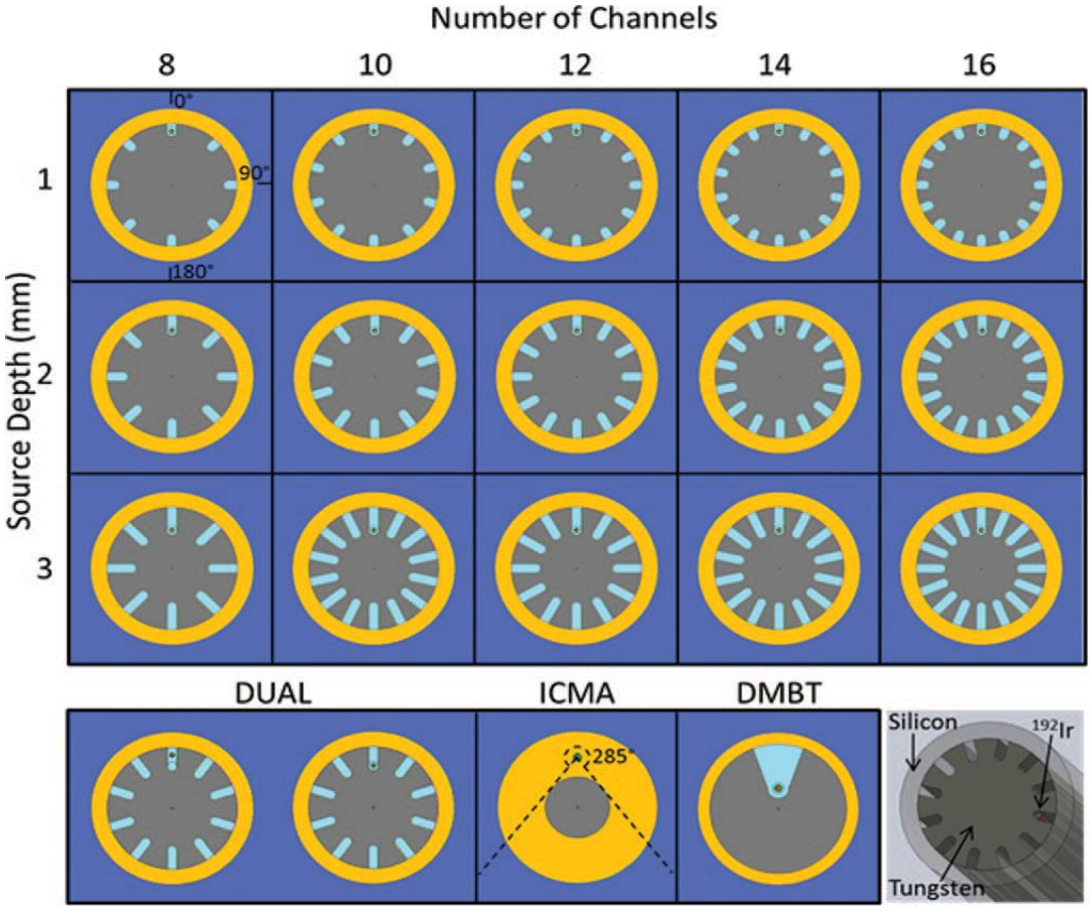

Webster, et al., *Med. Phys.* 40, 091704 (2013)

ESTRO School

Extreme BT Shielding: HDR ^{192}Ir or ^{153}Gd

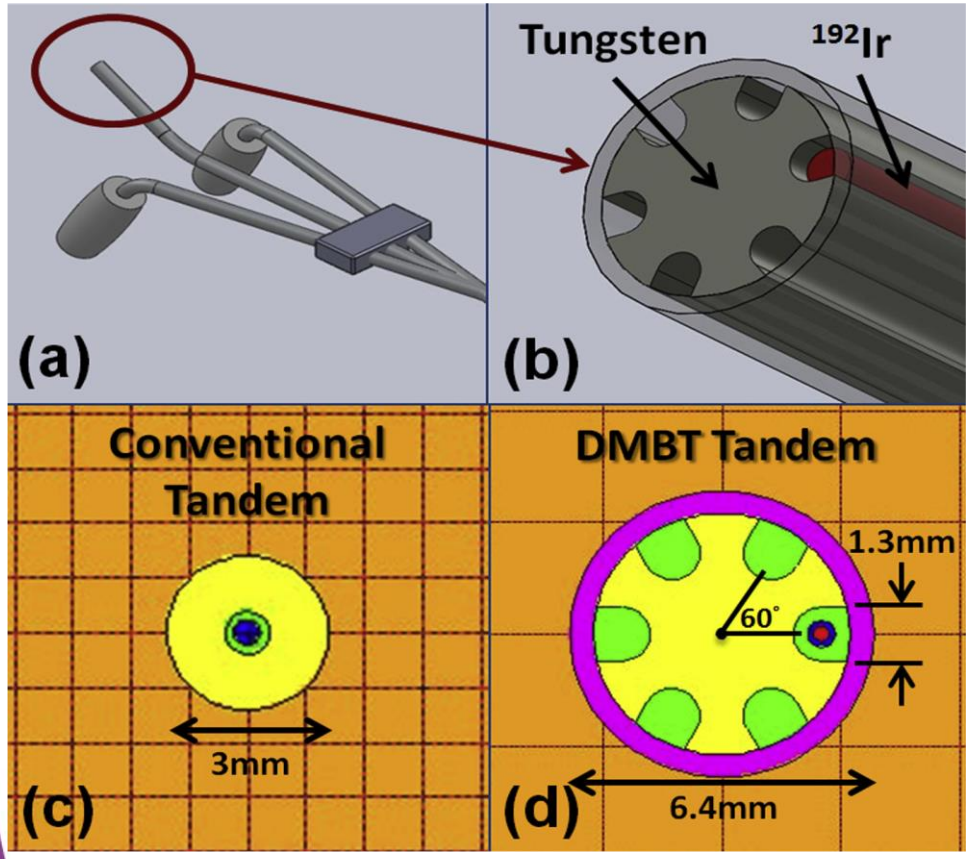

Han, et al., *IJROBP* 89, 666-673 (2014)

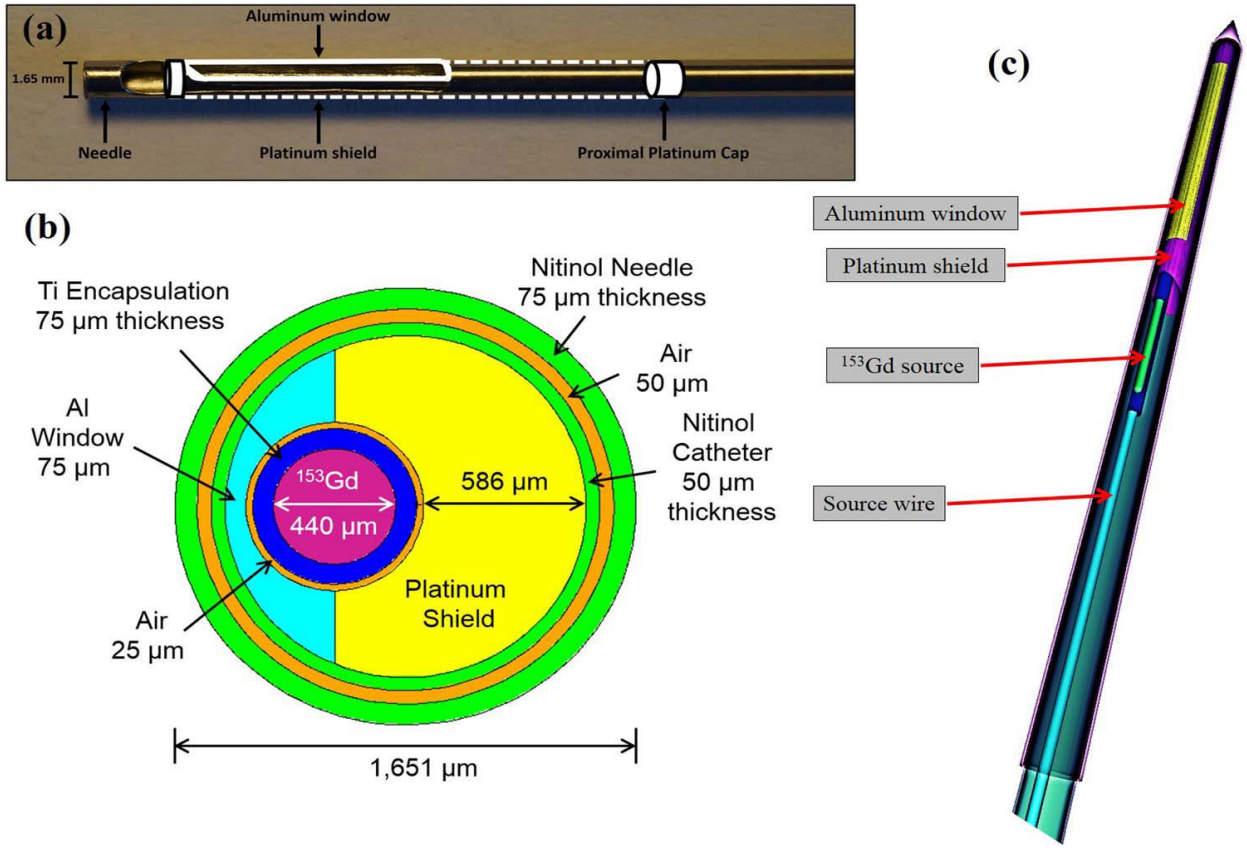

Adams, et al., *Med. Phys.* 41, 051703 (2014)

ESTRO School

Need New TPS Evaluation Criteria

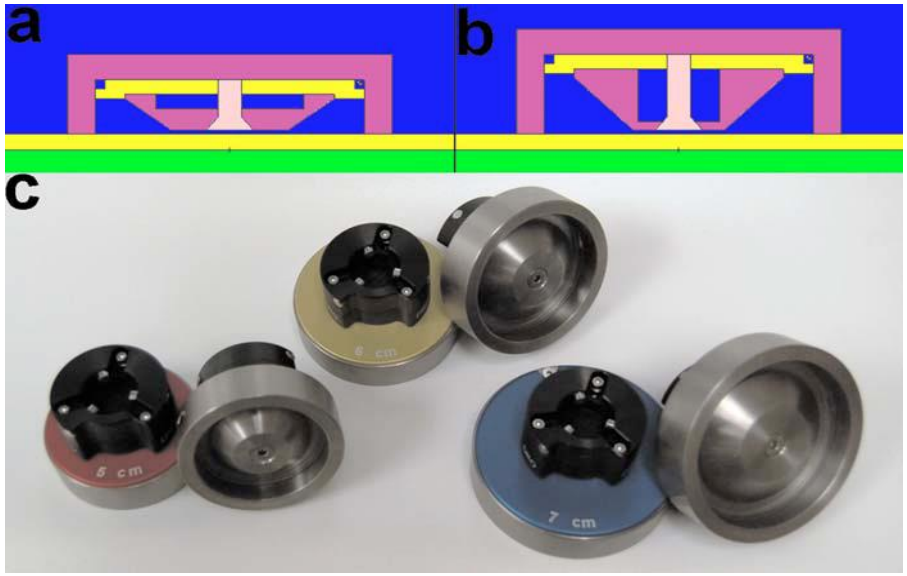

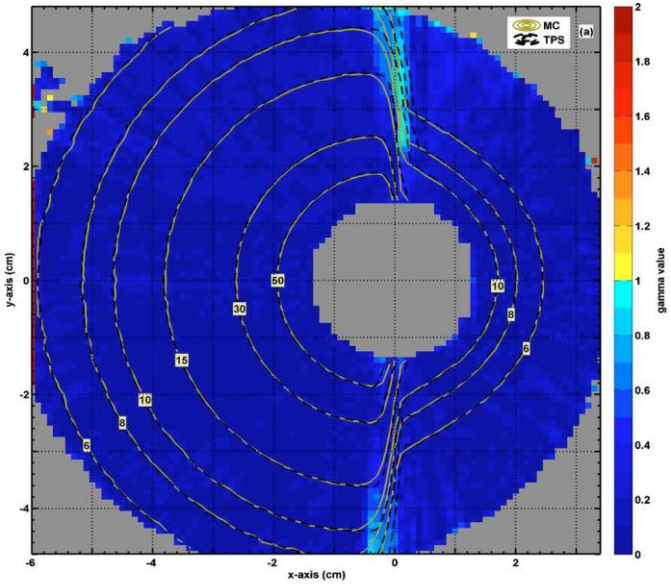

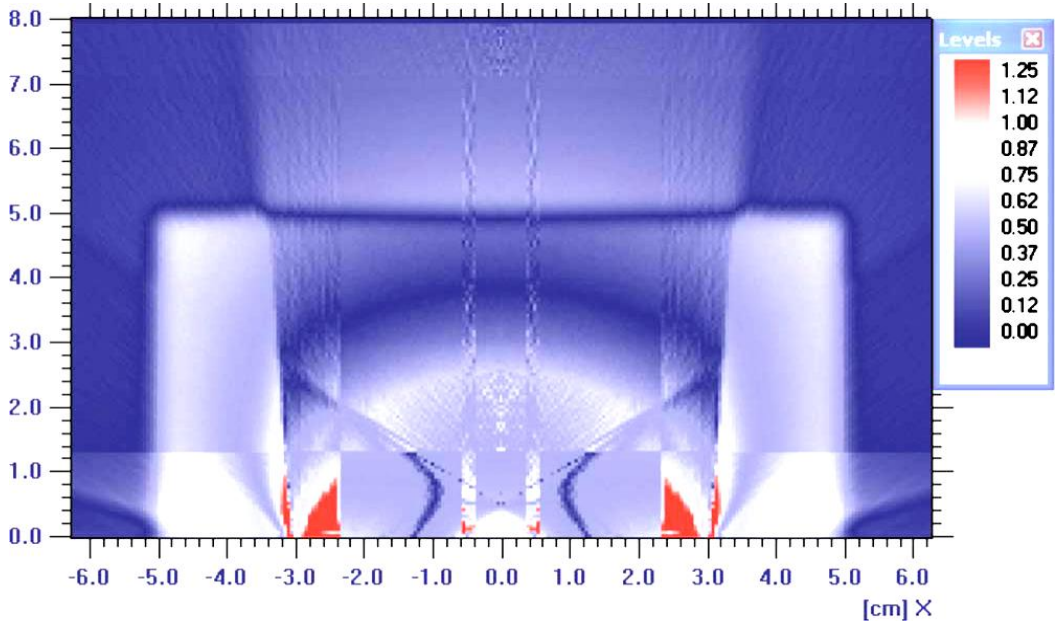

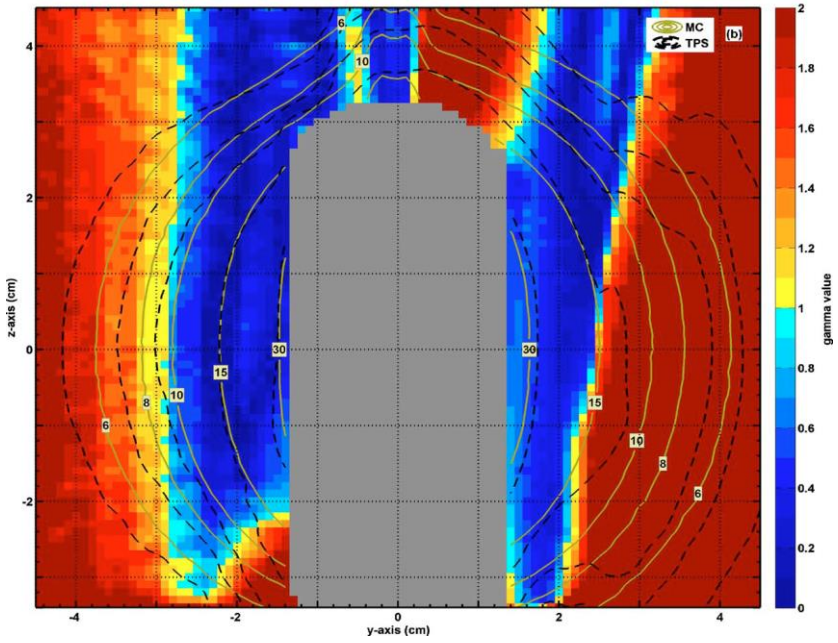

1% and 1 mm

Yang, *et al*., *Med. Phys*. (2011)

5% and 2 mm

Petrokokkinos, *et al*., *Med. Phys*. (2011)

What Would Olaf Do?

Summary

- new sources (radionuclides and eBT) fall in the energy range sensitive to scatter, requiring advanced BT dose calculations
- new sources and applicators have significant shielding, not compatible with current TPS based on simple TG-43
- commercially available (Acuros BV and Oncentra ACE) for ^{192}Ir (and academic-based TPS) can accurately calculate BT dose
- current and ongoing societal guidance for advanced BT dose calcs

... earn their trust

ESTRO School